

NASA  
CR  
3434  
c.1

NASA Contractor Report 3434

TECH LIBRARY KAFB, NM  
0062041

# Transonic Pressure Measurements and Comparison of Theory to Experiment for Three Arrow-Wing Configurations

## Summary Report

Marjorie E. Manro

LOAN COPY RETURN TO  
AFWL TECHNICAL LIBRARY  
KIRTLAND AFB, NM

CONTRACT NAS1-14962  
FEBRUARY 1982

**NASA**



NASA Contractor Report 3434

**Transonic Pressure  
Measurements and Comparison  
of Theory to Experiment for  
Three Arrow-Wing Configurations  
Summary Report**

**Marjorie E. Manro**  
*Boeing Commercial Airplane Company*  
*Seattle, Washington*

Prepared for  
Langley Research Center  
under Contract NAS1-14962



National Aeronautics  
and Space Administration

**Scientific and Technical  
Information Branch**

1982



# CONTENTS

	Page
SUMMARY .....	1
INTRODUCTION .....	2
SYMBOLS .....	3
EXPERIMENTAL TASK .....	5
Wind Tunnel Models .....	5
Flat Wing .....	5
Twisted Wing .....	5
Cambered-Twisted Wing .....	5
Body .....	7
Relative Wing and Body Location .....	7
Wing Fin .....	7
Pressure Orifice Locations .....	9
Design and Construction .....	9
Wind Tunnel Capabilities .....	18
Data System .....	18
Mach Number .....	19
Dynamic Pressure .....	19
Angle of Attack .....	19
Model Pressures .....	20
Tests and Data Acquisition .....	20
Tests .....	20
Data Repeatability .....	22
Data Acquisition and Initial Processing .....	22
Data Tape Description .....	22
Experimental Data .....	23
Cambered-Twisted Wing .....	23
Comparison of Flat, Twisted, and Cambered-Twisted Wing .....	27
Effect of Wing Twist .....	27
Effect of Wing Camber .....	27
Effect of Wing Camber and Twist .....	27
Comparison of Flat, Twisted, and Cambered-Twisted Wings With	
Full-Span Trailing-Edge Control Surface Deflection .....	27
Cambered-Twisted Wing, Fin On .....	28
Effect of Wing Fin, Undelected Trailing-Edge Control Surface .....	28
Effect of Trailing-Edge Control Surface Deflection .....	28
Flat Wing .....	28
Twisted Wing .....	30
Cambered-Twisted Wing, Fin Off .....	30
Cambered-Twisted Wing, Fin On .....	30
Effect of Wing Fin, Full-Span Trailing-Edge Control-	
Surface Deflection .....	30



## CONTENTS (Concluded)

	Page
THEORY COMPARISON TASK .....	31
Attached-Flow Theoretical Methods .....	31
FLEXSTAB .....	31
PAN AIR .....	32
Theory-to-Experiment Comparisons .....	34
Theory-to-Experiment Comparison for Undelected	
Trailing-Edge Control Surface .....	36
Prediction of Increments Due to Change in Shape .....	36
Prediction of Increment Due to Wing Fin .....	39
Body Pressure Distributions .....	39
Prediction of Data for Full-Span Trailing-Edge	
Control Surface Deflection .....	39
CONCLUDING REMARKS .....	40
APPENDIX A. DETAILED TEST LOG .....	41
APPENDIX B. SUMMARY OF PREVIOUS RELATED CONTRACTS .....	60
APPENDIX C. DATA REDUCTION AND PRESENTATION .....	79
REFERENCES .....	90

The following pages were left intentionally blank:

128  
138  
148  
154  
156  
188  
202  
210  
218  
220  
252  
262  
268  
290  
302  
304  
326  
328  
350  
352  
374  
376

## LIST OF TABLES

	Page
1. Wing Half-Thickness Distribution, Percent Chord .....	6
2. Wing Section Camber Definition, Percent Chord .....	8
3. Wing Pressure Orifice Locations, Percent Local Chord .....	10
4. Body Pressure Orifice Locations .....	17
5. Summary of Test Conditions by Run Number .....	21
6. Summary of Experimental Data Presentations in This Document .....	24
7. Summary of Additional Experimental Data Presentations .....	25
8. Summary of Presentations of Trailing-Edge Configurations by Document Number .....	29
9. Summary of FLEXSTAB Conditions by Run Number .....	33
10. Summary of PAN AIR Conditions by Run Number .....	35
11. Summary of Theory-to-Experiment Data Presentations in This Document .....	37
12. Summary of Additional Theory-to-Experiment Comparisons (NASA CR-165703) .....	38
A-1. Experimental Data Test Point Log. Twisted Wing, Fin Off .....	42
A-2. Experimental Data Test Point Log. Cambered-Twisted Wing, Fin Off .....	46
A-3. Experimental Data Test Point Log. Cambered-Twisted Wing, Fin On .....	50
A-4. FLEXSTAB Test Point Log. Twisted Wing, Fin Off .....	54
A-5. FLEXSTAB Test Point Log. Cambered-Twisted Wing, Fin Off .....	56
A-6. PAN AIR Test Point Log. Flat Wing, Fin Off, T.E. Deflection, Full Span = 0.0° .....	58
A-7. PAN AIR Test Point Log. Twisted Wing, Fin Off; T.E. Deflection, Full Span = 0.0° .....	58
A-8. PAN AIR Test Point Log. Cambered-Twisted Wing, Fin Off; T.E. Deflection, Full Span = 0.0° .....	59
A-9. PAN AIR Test Point Log. Cambered-Twisted Wing, Fin On; T.E. Deflection, Full Span = 0.0° .....	59
B-1. Summary of Subsonic/Transonic Test Conditions by Run Number (NASA Contract NAS1-12875) .....	61
B-2. Summary of Subsonic/Transonic FLEXSTAB Conditions by Run Number (NASA Contract NAS1-12875) .....	64
B-3. Summary of TEA-230 Conditions by Run Number (NASA Contract NAS1-12875) .....	68
B-4. Summary of Test Conditions by Run Number (NASA Contract NAS1-14141) .....	69
B-5. Summary of FLEXSTAB Conditions by Run Number (NASA Contract NAS1-14141) .....	70
C-1. Integration Constants .....	88

## LIST OF FIGURES

	Page
1. General Arrangement and Characteristics .....	92
2. Spanwise Twist Distribution for the Model Wing .....	93
3. Cambered-Twisted Wing Section Geometry .....	94
4. Fin Geometry, Section at 0.725 Semispan .....	95
5. Pressure Orifice Locations .....	96
6. Control Surface Bracket Details .....	97
7. Boeing Transonic Wind Tunnel .....	98
8. Variation of Reynolds Number and Dynamic Pressure with Mach Number .....	99
9. Data Acquisition and Reduction System - Boeing Transonic Wind Tunnel .....	100
10. Wind Tunnel Photographs - Twisted Wing; T.E. Deflection, Full Span = $0.0^\circ$ .....	101
11. Wind Tunnel Photographs - Cambered-Twisted Wing, Fin Off; T.E. Deflection, Full Span = $0.0^\circ$ .....	102
12. Wind Tunnel Photographs - Cambered-Twisted Wing, Fin On; T.E. Deflection, Full Span = $0.0^\circ$ .....	103
13. Wind Tunnel Photograph - Cambered-Twisted Wing, Fin On; T.E. Deflection, Full Span = $8.3^\circ$ .....	104
14. Model Installation Diagram .....	105
15. Wing Experimental Data - Comparison of Data From Two Wind Tunnel Tests; Twisted Wing; T.E. Deflection, Full Span = $0.0^\circ$ ; $M = 0.85$ .....	106
16. Body Experimental Surface Longitudinal Pressure Distributions - Comparison of Data From Two Wind Tunnel Tests; Twisted Wing, T.E. Deflection, Full Span = $0.0^\circ$ ; $M = 0.85$ .....	118
17. Wing Experimental Data - Effect of Angle of Attack; Cambered-Twisted Wing; Fin Off; T.E. Deflection, Full Span = $0.0^\circ$ ; $M = 0.40$ .....	120
18. Wing Experimental Data - Effect of Angle of Attack; Cambered-Twisted Wing; Fin Off; T.E. Deflection, Full Span = $0.0^\circ$ ; $M = 0.85$ .....	130
19. Wing Experimental Data - Effect of Angle of Attack; Cambered-Twisted Wing; Fin Off; T.E. Deflection, Full Span = $0.0^\circ$ ; $M = 1.05$ .....	140
20. Wing Experimental Data - Effect of Angle of Attack and Mach Number; Cambered-Twisted Wing; Fin Off; T.E. Deflection, Full Span = $0.0^\circ$ .....	150
21. Wing Experimental Data - Effect of Wing Shape; T. E. Deflection, Full Span = $0.0^\circ$ ; $M = 0.85$ .....	157
22. Body Experimental Data - Effect of Wing Shape; T.E. Deflection, Full Span = $0.0^\circ$ ; $M = 0.85$ .....	190
23. Wing Experimental Data - Effect of Incremental Twist; T.E. Deflection, Full Span = $0.0^\circ$ ; $M = 0.85$ .....	196
24. Wing Experimental Data - Effect of Incremental Camber; T.E. Deflection, Full Span = $0.0^\circ$ ; $M = 0.85$ .....	204
25. Wing Experimental Data - Effect of Incremental Camber and Twist; T.E. Deflection, Full Span = $0.0^\circ$ ; $M = 0.85$ .....	212
26. Wing Experimental Data - Effect of Wing Shape; T.E. Deflection, Full Span = $8.3^\circ$ ; $M = 0.85$ .....	221
27. Wing Experimental Data - Effect of Angle of Attack; Cambered-Twisted Wing; Fin On; T.E. Deflection, Full Span = $0.0^\circ$ ; $M = 0.85$ .....	254
28. Wing Experimental Data - Effect of Angle of Attack and Mach Number; Cambered-Twisted Wing; Fin On; T.E. Deflection, Full Span = $0.0^\circ$ .....	264

# LIST OF FIGURES (Continued)

	Page
29. Wing Experimental Data - Effect of a Wing Fin and Angle of Attack; Cambered-Twisted Wing; T.E. Deflection, Full Span = $0.0^\circ$ ; $M = 0.85$ .....	270
30. Wing Experimental Data - Incremental Effect of a Wing Fin; Cambered-Twisted Wing; T.E. Deflection, Full Span = $0.0^\circ$ ; $M = 0.85$ .....	284
31. Wing Experimental Data - Effect of Full- and Partial-Span Trailing Edge Control Surface Deflection; Flat Wing; $M = 0.85$ .....	292
32. Wing Experimental Data - Effect of Full- and Partial-Span Trailing Edge Control Surface Deflection on Chordwise Segments; Flat Wing; $M = 0.85$ .....	305
33. Wing Experimental Data - Effect of Full- and Partial-Span Trailing Edge Control Surface Deflection; Twisted Wing; $M = 0.85$ .....	316
34. Wing Experimental Data - Effect of Full- and Partial-Span Trailing Edge Control Surface Deflection on Chordwise Segments; Twisted Wing; $M = 0.85$ .....	329
35. Wing Experimental Data - Effect of Full- and Partial-Span Trailing Edge Control Surface Deflection; Cambered-Twisted Wing; Fin Off; $M = 0.85$ .....	340
36. Wing Experimental Data - Effect of Full- and Partial-Span Trailing Edge Control Surface Deflection on Chordwise Segments; Cambered-Twisted Wing; Fin Off; $M = 0.85$ .....	353
37. Wing Experimental Data - Effect of Full- and Partial-Span Trailing Edge Control Surface Deflection; Cambered-Twisted Wing; Fin On; $M = 0.85$ .....	364
38. Wing Experimental Data - Effect of Full- and Partial-Span Trailing Edge Control Surface Deflection on Chordwise Segments; Cambered-Twisted Wing; Fin On; $M = 0.85$ .....	377
39. Wing Experimental Data - Effect of a Wing Fin and Angle of Attack; Cambered-Twisted Wing; T.E. Deflection, Full Span = $8.3^\circ$ ; $M = 0.85$ .....	388
40. Paneling for FLEXSTAB Computer Program .....	402
41. Paneling for PAN AIR Computer Program .....	403
42. Networks for PAN AIR Computer Program, Cambered-Twisted Wing, Fin On .....	407
43. Effect of Compressibility Axis on Body Pressures Predicted by PAN AIR .....	408
44. Wing Theory-to-Experiment Comparison; Flat Wing; T.E. Deflection, Full Span = $0.0^\circ$ ; $M = 0.85$ .....	410
45. Wing Theory-to-Experiment Comparison; Twisted Wing; T.E. Deflection, Full Span = $0.0^\circ$ ; $M = 0.85$ .....	426
46. Wing Theory-to-Experiment Comparison; Cambered-Twisted Wing; Fin Off; T.E. Deflection, Full Span = $0.0^\circ$ ; $M = 0.85$ .....	442
47. Wing Theory-to-Experiment Comparison; Cambered-Twisted Wing; Fin On; T.E. Deflection, Full Span = $0.0^\circ$ ; $M = 0.85$ .....	460
48. Wing Theory-to-Experiment Comparison-Effect of Incremental Twist; T.E. Deflection, Full Span = $0.0^\circ$ ; $M = 0.40$ .....	476

## LIST OF FIGURES (Concluded)

	Page
49. Wing Theory-to-Experiment Comparison-Effect of Incremental Camber; T.E. Deflection, Full span = $0.0^\circ$ ; $M = 0.40$ .....	486
50. Wing Theory-to-Experiment Comparison-Effect of Incremental Camber and Twist; T.E. Deflection, Full Span = $0.0^\circ$ ; $M = 0.40$ .....	496
51. Wing Theory-to-Experiment Comparison-Incremental Effect of a Wing Fin; Cambered-Twisted Wing; T.E. Deflection, Full Span = $0.0^\circ$ ; $M = 0.40$ .....	506
52. Body Theory-to-Experiment Comparison; Flat Wing; T.E. Deflection, Full Span = $0.0^\circ$ ; $M = 0.40$ .....	516
53. Wing Theory-to-Experiment Comparison; Cambered-Twisted Wing; Fin Off; T.E. Deflection, Full Span = $8.3^\circ$ ; $M = 0.40$ .....	524
54. Body Theory-to-Experiment Comparison; Cambered-Twisted Wing; Fin Off; T.E. Deflection, Full Span = $8.3^\circ$ ; $M = 0.40$ .....	540
 B-1. Model in Boeing Transonic Wind Tunnel (NASA Contract NAS1-12875) .....	 71
B-2. Paneling for TEA-230 Computer Program-Flat Wing, Rounded Leading Edge, 1106 Singularities .....	73
B-3. Schematic of 9-by-7-ft Leg of NASA Ames Unitary Wind Tunnel .....	75
B-4. Data Acquisition and Reduction System - 9-by-7-ft Leg of NASA Ames Unitary Wind Tunnel .....	76
B-5. Wind Tunnel Model-Flat Wing, Rounded L.E (NASA Contract NAS1-14141) .....	77
B-6. Wind Tunnel Model-Twisted Wing (NASA Contract NAS1-14141) .....	77
B-7. Model Installation in 9-by-7-ft Leg of NASA Ames Unitary Wind Tunnel .....	78
C-1. Codes Used to Interpolate and Extrapolate .....	80

## **SUMMARY**

Wind tunnel tests of arrow-wing body configurations consisting of flat, twisted, and cambered-twisted wings, as well as a variety of leading- and trailing-edge control surface deflections, have been conducted at Mach numbers from 0.4 to 1.05 to provide an experimental pressure data base for comparison with theoretical methods. Theory-to-experiment comparisons of detailed pressure distributions have been made using current state-of-the-art and advanced attached-flow methods. The purpose of these comparisons was to delineate conditions under which these theories are valid for these wings.

This report summarizes the results of the entire program. NASA CR-165701 presents more detailed results of the experimental phase of the program for the basic data and comparison of the effect of wing shape - twist, camber, and combined camber and twist. The effects of trailing-edge control surface deflection and of the wing fin are presented in NASA CR-165702. NASA CR-165703 presents, in more detail, the comparisons of the predictions of attached-flow theory to experimental data.

These reports supplement those from earlier test programs using this model which cover a range of Mach numbers from 0.40 to 2.50. Only the flat wing and the twisted wing were available for these earlier test programs. These data have been reported in NASA CR-2610, NASA CR-132727, NASA CR-132728, NASA CR-132729, and NASA CR-145046 (refs. 1 through 5).

## INTRODUCTION

A program has been underway for the past seven years to examine the ability of state-of-the-art and advanced theoretical methods to predict aeroelastic loads on highly-swept wings. A parallel objective has been to obtain an experimental data base of the type best suited for such a task. Three wing models were chosen for the test program; all had the same planform and airfoil section but one was flat, one twisted, and one had both camber and twist. With this combination, the incremental effects of twist, camber, and camber-twist, as predicted by theory, could be correlated with experiment. Other geometric variables included in the program are wing leading-edge radius, leading- and trailing-edge control surface deflections, and an outboard fin. Most of the data have been obtained at subsonic and transonic speeds in the Boeing Transonic Wind Tunnel; however, the flat and twisted wings were also tested in the 9-by 7-foot supersonic portion of the NASA Ames Unitary Wind Tunnels in order to fully examine existing and newly formulated panel methods, which apply for both subsonic and supersonic flows.

This document will concentrate mainly on the data obtained in recent wind-tunnel tests of the cambered-twisted wing and some comparisons with a newly developed attached-flow advanced-panel method. With the aid of the newly acquired data, the incremental effects of twist, camber, twist and camber, control surface deflection, and outboard fin on wing pressure distributions may be illustrated.

Preliminary results for the cambered-twisted wing were presented at the NASA Supersonic Cruise Research '79 Conference held at the NASA Langley Research Center in November 1979. Results of the subsonic-transonic program for the flat and twisted wings are summarized in NASA SP-347 (ref. 6) and discussed in more detail in references 1 through 4. The supersonic data for these two wings are available in references 5, 7, and 8.

PAN AIR advanced-panel attached-flow method calculations made in this contract were obtained with the assistance of James L. Thomas of the NASA Langley Research Center and Forrester T. Johnson and Edward N. Tinoco of the Boeing Military Airplane Company.

Use of trade names or names of manufacturers in this report does not constitute an official endorsement of such products or manufacturers, either expressed or implied, by the National Aeronautics and Space Administration.

## SYMBOLS

$b$	wing span, cm
$BL$	buttock line, cm; distance outboard from model plane of symmetry
$c$	section chord length, cm
$\bar{c}$ , M.A.C.	mean aerodynamic chord length, cm
$C_B$	surface bending moment coefficient referenced to $y_{ref}$ ; positive wingtip up
$C_C$	surface chord force coefficient; positive aft
$C_c$	section chord force coefficient; positive aft
$C_M$	surface pitching moment coefficient, referenced to 0.25 M.A.C.; positive leading edge up
$C_m$	section pitching moment coefficient referenced to section leading edge; positive leading edge up
$C_{m.25c}$	section pitching moment coefficient referenced to section 0.25c; positive leading edge up
$C_N$	surface normal force coefficient; positive up
$C_n$	section normal force coefficient; positive up
$C_p$	pressure coefficient = $\frac{\text{measured pressure} - \text{reference pressure}}{q}$
$D$	body diameter, cm
$M$	Mach number
$MS$	model station, cm; measured aft along the body centerline from the nose
$p_s$	static pressure, kN/m <sup>2</sup>
$p_t$	total pressure, kN/m <sup>2</sup>
$q$	dynamic pressure, kN/m <sup>2</sup>
$S$	reference area used for surface coefficients, cm <sup>2</sup>
$S_h$	area of streamwise strip associated with a pressure station, cm <sup>2</sup> ; used in summation of section force coefficients (app. C)
$x,y,z$	general coordinates for distances in the longitudinal, lateral, and vertical directions respectively



$y_{ref}$	distance outboard of model centerline of the bending moment reference point, cm
$\alpha$	corrected angle of attack, degrees; the angle between the wing root chord and the relative wind measured in the model plane of symmetry; includes compensation for sting deflection, tunnel flow angularities, and wall effects; positive nose up with respect to relative wind
$\alpha_{sec}$	wing twist angle relative to wing reference plane, degrees; positive leading edge up
$\beta$	angle of sideslip, degrees; positive nose left with respect to relative wind
$\Delta C_p$	increment between adjacent lines on isobars
$\delta$	control surface deflection, degrees; positive leading edge down for leading edge (see exception in app. C) and trailing edge down for trailing edge
$\eta$	fraction of wing semispan, $y/(b/2)$
$\Lambda$	sweep angle, degrees; measured from a line perpendicular to the model centerline, positive aft
$\phi$	angle defining location of pressure orifices on the surface of the cylindrical body at a constant MS, degrees; measured from the top of the body

#### **Subscripts:**

c	compressibility axis
L.E.	leading-edge control surface
r	wing root
s	referenced to segment of local chord
T.E.	trailing-edge control surface

## EXPERIMENTAL TASK

### WIND TUNNEL MODELS

The configuration chosen for this study was a thin, low aspect-ratio, highly-swept wing mounted below the centerline of a high fineness-ratio body. The general arrangement and characteristics of the model are shown in figure 1. Two complete wings were constructed for contract NAS1-12875, one with no camber or twist and one with no camber but with a spanwise twist variation. A third wing with camber and twist was constructed for the current contract. Deflectable control surfaces were available on all three of these wings.

#### FLAT WING

The mean surface of the flat wing is the wing reference plane. The nondimensional wing thickness distributions, shown in table 1, deviate slightly from a constant for all streamwise sections to maintain a finite thickness of 0.0254 cm (0.01 in.) at the trailing edge (a manufacturing requirement). The wing was designed with a full-span, 25 percent chord, trailing-edge control surface. Sets of fixed angle brackets allowed streamwise deflections of  $\pm 4.1^\circ$ ,  $\pm 8.3^\circ$ ,  $\pm 17.7^\circ$ , and  $\pm 30.2^\circ$ , as well as  $0.0^\circ$ . A removable full-span leading-edge control surface (15 percent of streamwise chord) could be placed in an undeflected position and also drooped  $5.1^\circ$  and  $12.8^\circ$  with fixed angle brackets. Both the leading- and trailing-edge control surfaces extended from the side of the body ( $0.087 b/2$ ) to the wingtip and were split near midspan ( $0.570 b/2$ ). The inboard and outboard portions of the control surfaces could be deflected separately and were rotated about points in the wing reference plane. An additional leading-edge control surface for this wing was constructed with a sharp ( $20^\circ$  included angle) leading edge to examine the effects of leading-edge shape. The surface ordinates and slopes of this leading-edge segment were continuous with those of the flat wing at the leading-edge hingeline (table 1). The sharp leading edge was smoothly faired from  $0.180 b/2$  into the fixed portion of the rounded leading edge at  $0.090 b/2$ .

#### TWISTED WING

The mean surface of the twisted wing was generated by rotating the streamwise section chord lines about the 75 percent local chord points (trailing-edge control surface hingeline). The spanwise variation of twist is shown in figure 2. The hingeline was straight and located in the wing reference plane at its inboard end ( $0.087 b/2$ ) and 2.261 cm (0.890 in.) above the wing reference plane at the wingtip. The airfoil thickness distribution (table 1) and the trailing-edge control surface location and available deflections were identical to those of the flat wing.

#### CAMBERED-TWISTED WING

The mean surface of the cambered-twisted wing was generated by superimposing a camber on the twisted wing definition but keeping the coordinates of the leading edge and trailing edge of the cambered-twisted wing the same as those of the twisted wing. The camber is defined analytically in two parts - a typical cruise airfoil (basic) camber and an estimate of the aeroelastic deformation at a moderate positive angle of attack. The aeroelastic deformation was based on calculations - for a typical configuration - of deformation under load. This definition was modified slightly to provide zero camber at the model centerline so this wing would fit on the existing model body. This was

Table 1.—Wing Half-Thickness Distribution, Percent Chord

x/c, percent chord	0 b/2	0.09 b/2	0.20 b/2	0.35 b/2	0.50 b/2	0.65 b/2	0.80 b/2	0.93 b/2	1.00 b/2
Flat wing with rounded leading edge, twisted wing, and cambered-twisted wing									
.0000	.0000	.0000	.0000	.0000	.0000	.0000	.0000	.0000	.0000
.1250	.3359	.3359	.3359	.3359	.3360	.3360	.3360	.3362	.3364
.2500	.4506	.4506	.4506	.4506	.4507	.4507	.4508	.4509	.4512
.5000	.6064	.6064	.6064	.6064	.6065	.6065	.6066	.6068	.6072
.7500	.7247	.7247	.7247	.7248	.7248	.7249	.7250	.7253	.7258
1.0000	.8182	.8182	.8182	.8183	.8183	.8184	.8185	.8188	.8194
1.5000	.9520	.9520	.9520	.9521	.9522	.9523	.9525	.9530	.9538
2.5000	1.1191	1.1191	1.1192	1.1192	1.1194	1.1195	1.1199	1.1206	1.1219
5.0000	1.3448	1.3448	1.3449	1.3450	1.3453	1.3456	1.3462	1.3475	1.3497
8.5000	1.4809	1.4809	1.4811	1.4813	1.4816	1.4822	1.4832	1.4855	1.4892
10.0000	1.5195	1.5196	1.5197	1.5200	1.5204	1.5210	1.5222	1.5250	1.5293
12.5000	1.5444	1.5445	1.5447	1.5450	1.5456	1.5463	1.5479	1.5514	1.5568
15.0000	1.5630	1.5631	1.5634	1.5638	1.5644	1.5654	1.5673	1.5715	1.5781
17.5000	1.5720	1.5722	1.5724	1.5729	1.5737	1.5748	1.5770	1.5821	1.5898
20.0000	1.5813	1.5815	1.5818	1.5823	1.5832	1.5845	1.5871	1.5929	1.6018
30.0000	1.6214	1.6217	1.6222	1.6230	1.6242	1.6262	1.6301	1.6389	1.6522
40.0000	1.6398	1.6402	1.6408	1.6419	1.6435	1.6462	1.6514	1.6630	1.6807
45.0000	1.6282	1.6286	1.6293	1.6305	1.6324	1.6354	1.6413	1.6544	1.6742
50.0000	1.5901	1.5906	1.5914	1.5927	1.5948	1.5981	1.6046	1.6192	1.6412
60.0000	1.4344	1.4350	1.4359	1.4375	1.4400	1.4440	1.4518	1.4692	1.4956
65.0000	1.3121	1.3127	1.3137	1.3155	1.3181	1.3225	1.3310	1.3498	1.3784
70.0000	1.1627	1.1634	1.1644	1.1663	1.1692	1.1739	1.1831	1.2034	1.2341
72.5000	1.0792	1.0799	1.0810	1.0830	1.0860	1.0908	1.1003	1.1213	1.1532
75.0000	.9921	.9928	.9940	.9960	.9991	1.0041	1.0139	1.0357	1.0686
77.5000	.9006	.9013	.9025	.9046	.9078	.9129	.9231	.9456	.9796
80.0000	.8069	.8077	.8089	.8111	.8143	.8197	.8302	.8534	.8885
85.0000	.6132	.6140	.6153	.6176	.6211	.6268	.6379	.6626	.6999
90.0000	.4156	.4165	.4178	.4203	.4240	.4300	.4418	.4679	.5074
95.0000	.2153	.2162	.2177	.2202	.2241	.2305	.2430	.2706	.3122
100.0000	.0113	.0123	.0138	.0165	.0206	.0273	.0405	.0695	.1134
Sharp leading edge									
.0000	.0000	.0000	.0000	.0000	.0000	.0000	.0000	.0000	.0000
.1250	.3359	.3359	.0293	.0307	.0329	.0364	.0433	.0585	.0815
.2500	.4506	.4506	.0557	.0580	.0614	.0670	.0781	.1024	.1392
.5000	.6064	.6064	.0998	.1021	.1055	.1111	.1222	.1465	.1833
.7500	.7247	.7247	.1439	.1462	.1496	.1552	.1663	.1906	.2274
1.0000	.8182	.8182	.1880	.1903	.1937	.1993	.2103	.2347	.2715
1.5000	.9520	.9520	.2761	.2784	.2818	.2875	.2985	.3229	.3596
2.5000	1.1191	1.1191	.4524	.4547	.4581	.4638	.4748	.4992	.5359
5.0000	1.3448	1.3448	.8933	.8956	.8990	.9046	.9156	.9400	.9768
8.5000	1.4809	1.4809	1.3413	1.3429	1.3453	1.3493	1.3570	1.3741	1.4001
10.0000	1.5195	1.5196	1.4547	1.4559	1.4578	1.4609	1.4669	1.4803	1.5007
12.5000	1.5444	1.5445	1.5203	1.5210	1.5221	1.5238	1.5272	1.5347	1.5461
15.0000	1.5630	1.5631	1.5634	1.5638	1.5644	1.5654	1.5673	1.5715	1.5781

achieved by using a factor  $k$  (fig. 3) on the basic camber term which provides a transition from no camber at the model centerline to the definition camber at  $0.25 b/2$ . The defined wing is smoother than indicated in this figure as section geometry was directly calculated at only those sections marked in figure 3. The full equation for the camber is:

$$\frac{z}{c} = \left(\frac{z}{c}\right)_{\text{Basic}} + \left(\frac{z}{c}\right)_{\text{Aero}}$$

$$\left(\frac{z}{c}\right)_{\text{Basic}} = k \left(\frac{4.0}{3.0}\right) \left(0.078 + \frac{\alpha_{\text{sec}}}{57.3}\right) \left(\frac{x}{c}\right) \left(\frac{x}{c} - 1.0\right) \left(\frac{x}{c} - 0.75 - \frac{1.0}{4.0} \left(\frac{2y}{b}\right)\right)$$

$$k = \left(\frac{2y}{b}\right) \left(1.0 + 12.0 \left(\frac{2y}{b}\right)\right) \quad \text{for } \left(\frac{2y}{b}\right) \leq 0.25$$

$$k = 1.0 \quad \text{for } \left(\frac{2y}{b}\right) \geq 0.25$$

$$\left(\frac{z}{c}\right)_{\text{Aero}} = -\frac{57.3}{3.0} \left(\frac{9.0}{4.0}\right) \left(\frac{2y}{b}\right) \left(1.0 - 0.75 \left(\frac{2y}{b}\right)^2\right) \left(\sec\left(\frac{3.0}{57.3}\right) - \sec\left(\frac{3.0 \left| 1.0 - 2.0 \left(\frac{x}{c}\right) \right|}{57.3}\right)\right)$$

The resulting nondimensional camber is shown in table 2. The camber at the tip is approximately a  $6^\circ$  arc of a circle with the leading and trailing edges up. Sections at the root, mid-span, and tip (fig. 3) show not only the camber but the position of the sections of the cambered-twisted wing and the twisted wing, relative to the wing reference plane (flat wing). The airfoil thickness distribution (table 1) and the trailing-edge control surface location and available deflections were identical to those of the flat wing.

## BODY

The body was circular in cross section and had a straight centerline. The body geometry is shown in figure 1. The sting was an integral part of the model body.

## RELATIVE WING AND BODY LOCATION

The wing reference plane was located 3.149 cm (1.240 in.) below and parallel to (zero incidence) the body centerline. The apex (extension of the wing leading edge to the centerline) of the wing was located 33.496 cm (13.187 in.) aft of the model nose.

## WING FIN

The wing fin is a 3 percent biconvex airfoil placed streamwise and perpendicular to the wing reference plane on the upper surface of the cambered-twisted wing at 0.725 semispan. The dimensions of the fin and its relationship to the wing are shown in figure 4. For configurations with the outboard trailing-edge control surface deflected, the fin is extended down to touch the surface of the control surface (see fig. 4).

*Table 2.—Wing Section Camber Definition, Percent Chord*

[illegible]

## PRESSURE ORIFICE LOCATIONS

All pressure orifices were located on the left side of the model and distributed as shown in figure 5 and tables 3 and 4. The flat wing with rounded leading edge, the twisted wing, and the cambered-twisted wing each had 214 orifices, distributed in streamwise pressure stations of 31 or 30 orifices at each of seven spanwise locations. One of these orifices was located at the leading edge; the remainder were distributed so that upper and lower surface orifices were located at the same chordwise locations. The orifice locations on the sharp leading edge were identical except that the leading-edge orifice at each spanwise station was omitted. The 83 orifices on the body were located at 15 stations along the length of the model. At each station, orifices were located at angles of  $0^\circ$ ,  $45^\circ$ ,  $90^\circ$ ,  $135^\circ$ , and  $180^\circ$  measured from the top of the body. In the area of the wing-body intersection, the orifices that are nominally identified as being at  $135^\circ$  and  $180^\circ$  were located on the wing lower surface at the same lateral location as the orifices at  $45^\circ$  and  $0^\circ$ , respectively. Eight additional orifices were placed close to the juncture of the body with the wing upper surface.

## DESIGN AND CONSTRUCTION

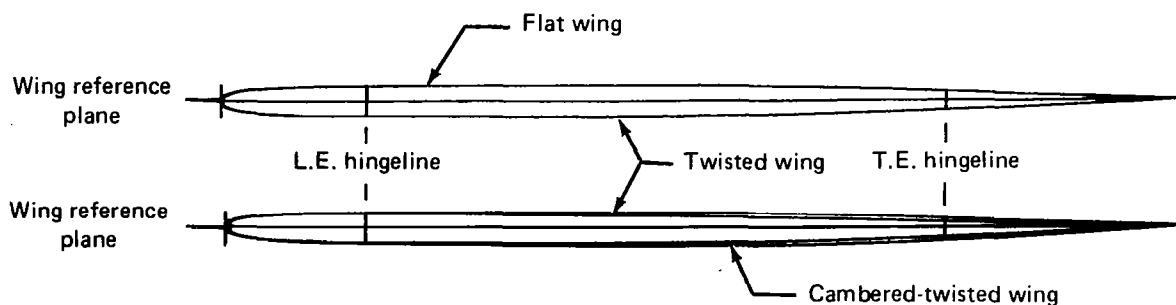
The objectives of this study dictated that the contours and physical characteristics of the flat wing, the twisted wing, and the cambered-twisted wing be as nearly identical as possible. The model was constructed of steel to minimize aeroelastic deflections and to provide strength for testing to a Mach number of 3.0. The aft body was flared approximately  $4^\circ$  from 194.310 cm (76.500 in.) aft of the nose to provide the required safety factor on predicted loads (see fig. 1). The model size was selected as the best compromise between potential tunnel blockage and adequate room to install orifices in the model.

A computerized lofting program was used to provide the wing definition. This definition was then used to machine the model components using numerically controlled machines. The tolerance on the contour was  $+0.1524$ ,  $-0.0$  mm ( $+0.006$ ,  $-0.0$  in.). The leading- and trailing-edge control surfaces were cut from the wings after they had been machined to final contour. A cut along the 15 percent chord line of the twisted wing removed enough material to simulate the elastic characteristics of the flat wing (see fig. 6). As a result of the previous tests it was determined that it was not necessary to remove this material on the cambered-twisted wing as the wings were very rigid. Fixed angle brackets, arranged as shown in figure 6, were used to obtain the required control surface deflections with all pivot points located midway between the upper and lower surfaces at the hingelines. The brackets were also machined on numerically controlled machines. The same sets of trailing-edge brackets were used on all three wings, and the same sets of leading-edge brackets were used for both the rounded and sharp leading edges.

Pressure tubing used in this model was 1.016 mm (0.040 in.) o.d. Monel with a 0.1524 mm (0.006 in.) wall thickness. The major channels for wing pressure tubing were machined into the surface. The detailed grooves required to route tubing from the orifices to these channels were cut by hand. The pressure orifices were installed normal to and flush with the local surface. After installation of the pressure tubing, the grooves were filled with solder and brought back to contour by hand-filing to match templates prepared by numerically-controlled machining.

Table 3.—Wing Pressure Orifice Locations, Percent Local Chord

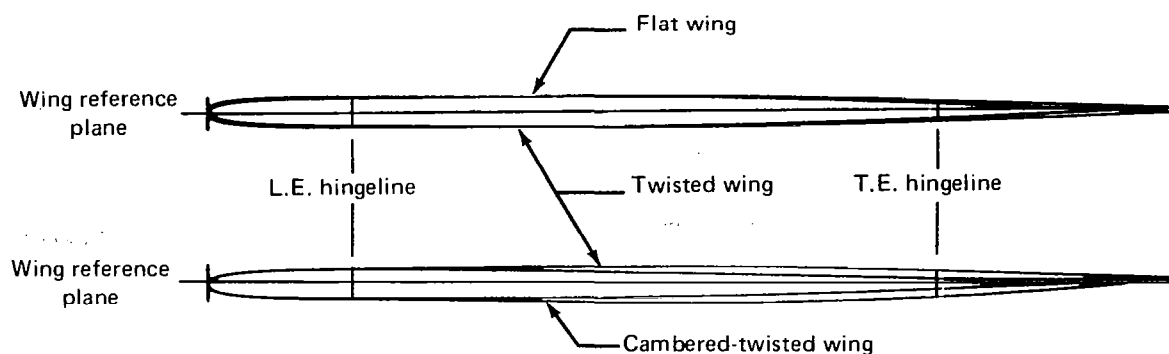
(a) Section at  $0.09 \frac{b}{2}$ , chord = 102.89 cm



Nominal	Flat wing, $\alpha_{\text{sec}} = 0.0^\circ$				Twisted wing, $\alpha_{\text{sec}} = -0.01^\circ$		Cambered-twisted wing, $\alpha_{\text{sec}} = -0.01^\circ$	
	Rounded leading edge		Sharp leading edge		Rounded leading edge		Rounded leading edge	
	Upper surface	Lower surface	Upper surface	Lower surface	Upper surface	Lower surface	Upper surface	Lower surface
0.00	0.00		—	—	0.00		0.00	
2.50	2.45	2.59	2.61	2.54	2.26	2.26	2.58	2.51
5.00	4.95	5.07	5.06	5.03	4.76	4.76	5.10	5.04
8.50	8.45	8.53	8.59	8.58	8.40	8.26	8.64	8.56
11.30	—	—	—	11.31	—	—	—	—
12.25	—	—	—	—	12.23	12.27	—	—
12.50	12.45	12.55	12.58	—	—	—	12.63	12.54
17.50	17.49	17.62			17.59	17.66	17.64	17.55
20.00	19.94	20.08			20.03	20.03	20.14	20.00
30.00	29.92	30.09			29.98	29.89	30.14	30.00
45.00	45.00	45.07			44.96	44.89	45.12	45.03
60.00	59.98	60.08			60.01	59.97	60.11	60.00
70.00	70.03	70.13			70.05	69.95	70.09	70.04
72.50	72.55	72.60			72.58	72.51	72.62	72.54
77.50	77.53	77.62			77.56	77.51	77.63	77.52
85.00	85.11	85.14			85.03	85.00	85.12	85.04
90.00	90.10	90.10			90.04	89.98	90.12	90.00
95.00	95.09	95.05			94.96	94.98	95.10	95.03

Table 3.—(Continued)

(b) Section at  $0.20 \frac{b}{2}$ , chord = 91.80 cm

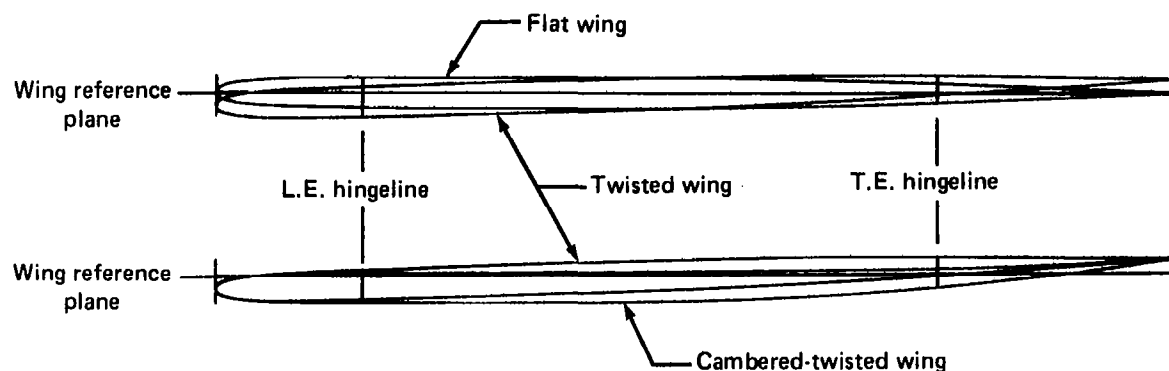


Nominal	Flat wing, $\alpha_{\text{sec}} = 0.0^\circ$				Twisted wing, $\alpha_{\text{sec}} = -0.47^\circ$		Cambered-twisted wing, $\alpha_{\text{sec}} = -0.47^\circ$	
	Rounded leading edge		Sharp leading edge		Rounded leading edge		Rounded leading edge	
	Upper surface	Lower surface	Upper surface	Lower surface	Upper surface	Lower surface	Upper surface	Lower surface
0.00	0.00		—	—	0.00		0.00	
2.50	2.59	2.69	2.62	2.65	2.52	2.42	2.63	2.59
5.00	5.05	5.00	5.14	5.14	5.00	4.93	5.09	5.05
8.50	8.54	8.59	8.67	8.62	8.52	8.40	8.61	8.64
11.40	—	—	—	11.37	—	—	—	—
12.50	12.54	12.49	12.63	—	12.53	12.42	12.51	12.62
17.50	17.63	17.61			17.65	17.52	17.59	17.63
20.00	20.08	20.07			20.00	19.90	19.95	20.05
30.00	30.04	30.09			30.02	29.89	30.05	29.97
45.00	45.08	45.09			45.03	44.92	45.04	45.01
60.00	60.02	60.13			60.03	59.91	60.02	60.06
70.00	70.11	70.13			70.06	69.96	70.03	70.01
72.50	72.63	72.61			72.55	72.50	72.59	72.67
77.50	77.59	77.65			77.59	77.52	77.53	77.57
85.00	85.07	85.13			85.02	85.00	85.09	85.10
90.00	90.14	90.11			90.07	89.97	90.04	89.98
95.00	95.14	95.10			95.05	95.08	95.06	94.98



Table 3.—(Continued)

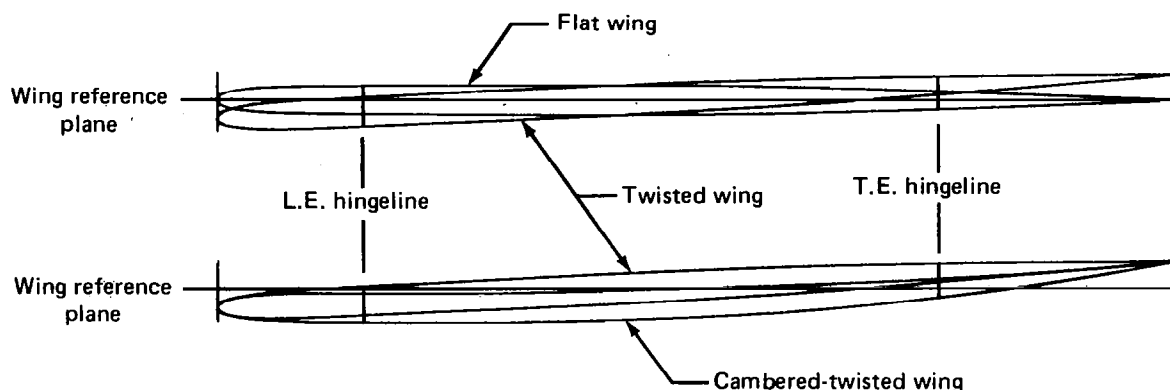
(c) Section at  $0.35 \frac{b}{2}$ , chord = 76.69 cm



Nominal	Flat wing, $\alpha_{\text{sec}} = 0.0^\circ$				Twisted wing, $\alpha_{\text{sec}} = -1.70^\circ$		Cambered-twisted wing, $\alpha_{\text{sec}} = -1.70^\circ$	
	Rounded leading edge		Sharp leading edge		Rounded leading edge		Rounded leading edge	
	Upper surface	Lower surface	Upper surface	Lower surface	Upper surface	Lower surface	Upper surface	Lower surface
0.00	0.00		—	—	0.00		0.00	
2.50	2.45	2.59	2.59	2.58	2.39	2.33	2.76	2.60
5.00	4.93	5.07	5.11	5.04	5.12	4.78	5.05	5.10
8.50	8.60	8.54	8.65	8.63	8.49	8.32	8.68	8.70
10.50	—	—	—	10.46	—	—	—	—
11.00	—	11.03	—	—	—	—	—	—
12.50	12.37	—	12.57	—	12.50	12.33	12.59	12.68
17.50	17.64	17.63			17.54	17.53	17.64	17.62
20.00	20.00	20.09			19.94	19.84	20.03	20.07
30.00	30.01	30.10			29.88	29.87	30.00	29.93
45.00	44.99	45.09			44.96	44.79	45.00	45.13
60.00	60.03	60.08			59.97	59.89	60.00	60.10
70.00	70.07	70.08			70.03	69.90	70.04	70.03
72.50	72.55	72.58			72.56	72.44	72.61	72.52
77.50	77.60	77.61			77.54	77.51	77.50	77.60
85.00	85.11	85.14			85.08	84.96	85.09	84.93
90.00	90.06	90.09			89.89	89.89	89.98	90.04
95.00	95.07	95.09			94.95	94.86	94.98	95.10

Table 3.—(Continued)

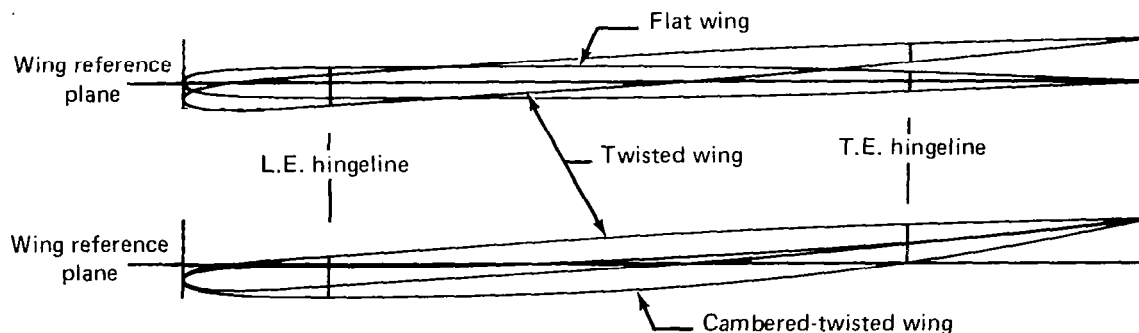
(d) Section at  $0.50 \frac{b}{2}$ , chord = 61.57 cm



Nominal	Flat wing, $\alpha_{\text{sec}} = 0.0^\circ$				Twisted wing, $\alpha_{\text{sec}} = -2.85^\circ$		Cambered-twisted wing, $\alpha_{\text{sec}} = -2.85^\circ$	
	Rounded leading edge		Sharp leading edge		Rounded leading edge		Rounded leading edge	
	Upper surface	Lower surface	Upper surface	Lower surface	Upper surface	Lower surface	Upper surface	Lower surface
0.00	0.00		—	—	0.00		0.00	
2.50	2.47	2.53	2.69	2.60	2.44	2.38	2.78	2.62
5.00	4.99	4.95	5.13	5.06	4.92	4.80	5.13	5.15
8.50	8.48	8.38	8.66	8.61	8.46	8.38	8.64	8.56
10.10	—	—	—	10.14	—	—	—	—
11.10	—	11.08	—	—	—	—	—	—
12.50	12.39	—	12.61	—	12.50	12.31	12.71	12.55
17.50	17.64	17.52			17.54	17.24	17.71	17.44
20.00	19.98	19.97			19.92	19.83	20.15	19.89
30.00	30.07	30.06			29.91	29.85	30.04	29.72
45.00	44.98	45.06			45.00	44.85	44.95	44.97
60.00	59.97	60.00			59.95	59.92	59.96	59.94
70.00	70.07	70.10			70.03	69.88	69.93	69.86
72.50	72.65	72.61			72.56	72.44	72.53	72.34
77.50	77.66	77.65			77.61	77.43	77.58	77.43
85.00	85.19	85.18			84.85	84.90	84.96	84.92
90.00	90.22	90.12			89.93	89.93	89.94	89.91
95.00	95.05	94.94			94.88	94.93	94.98	94.88

Table 3.—(Continued)

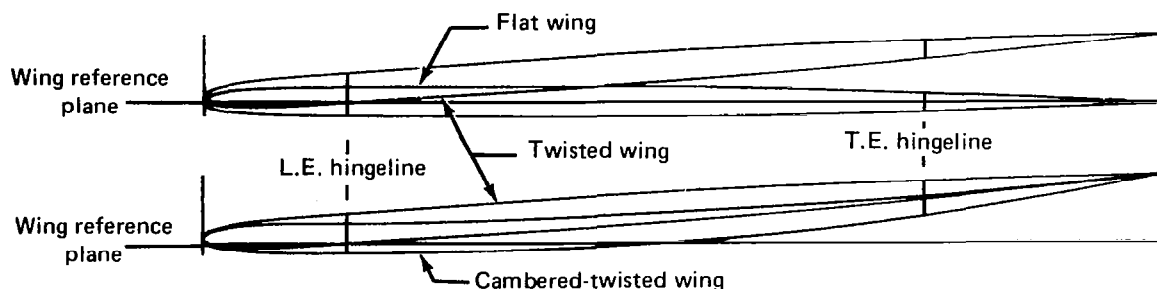
(e) Section at  $0.65 \frac{b}{2}$ , chord = 46.46 cm



Nominal	Flat wing, $\alpha_{\text{sec}} = 0.0^\circ$				Twisted wing, $\alpha_{\text{sec}} = -3.59^\circ$		Cambered-twisted wing, $\alpha_{\text{sec}} = -3.59^\circ$	
	Rounded leading edge		Sharp leading edge		Rounded leading edge		Rounded leading edge	
	Upper surface	Lower surface	Upper surface	Lower surface	Upper surface	Lower surface	Upper surface	Lower surface
0.00	0.00		—	—	0.00		0.00	
2.50	2.56	2.66	2.49	2.38	2.18	2.49	2.76	2.79
5.00	5.06	5.12	4.94	4.95	4.76	5.01	5.35	5.40
8.50	8.55	8.55	8.46	8.40	8.32	8.45	8.85	8.74
12.20	—	—	12.12	—	12.21	—	—	—
12.60	12.57	—	—	—	—	—	12.71	12.77
17.50	17.60	17.65			17.24	17.44	17.74	17.58
20.00	20.17	20.11			19.70	19.88	20.19	19.96
30.00	30.05	30.11			30.26	29.73	30.13	29.85
45.00	45.16	45.23			44.75	44.89	45.03	44.75
60.00	60.13	60.13			59.81	59.87	60.02	59.99
70.00	69.89	70.12			69.92	69.90	70.09	69.88
72.50	72.59	72.69			72.38	72.49	72.83	72.15
77.50	77.74	77.76			77.22	77.49	77.56	77.43
85.00	85.25	85.32			84.79	84.93	84.93	84.76
90.00	90.22	90.21			89.70	89.92	89.95	89.98
95.00	95.13	95.27			95.12	94.86	94.97	94.98

Table 3.—(Continued)

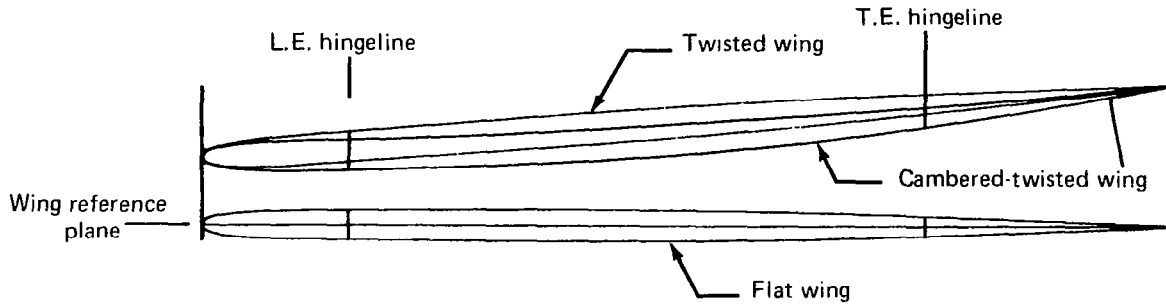
(f) Section at  $0.80\frac{b}{2}$ , chord = 31.35 cm



Nominal	Flat wing, $\alpha_{\text{sec}} = 0.0^\circ$				Twisted wing, $\alpha_{\text{sec}} = -3.84^\circ$		Cambered-twisted wing, $\alpha_{\text{sec}} = -3.84^\circ$	
	Rounded leading edge		Sharp leading edge		Rounded leading edge		Rounded leading edge	
	Upper surface	Lower surface	Upper surface	Lower surface	Upper surface	Lower surface	Upper surface	Lower surface
0.00	0.00		—	—	0.00		0.00	
2.50	2.55	2.47	2.50	2.46	2.33	2.43	2.76	2.62
5.00	5.01	5.02	5.01	4.93	4.86	4.74	5.27	5.21
8.50	8.55	8.59	8.58	8.41	8.32	—	8.78	8.54
12.50	12.50	—	12.58	—	12.47	12.43	12.69	12.58
17.50	17.53	17.57			17.36	17.47	17.83	17.34
20.00	20.16	20.13			19.79	19.82	20.11	19.79
30.00	30.00	30.11			29.83	29.83	30.15	29.48
45.00	44.91	45.15			44.81	44.91	44.81	44.75
60.00	59.94	60.10			59.80	59.92	59.84	59.79
70.00	70.06	70.11			69.89	69.87	69.77	69.94
72.50	72.61	72.60			72.22	72.39	72.50	72.33
77.50	77.73	77.72			77.29	77.41	77.22	77.40
85.00	85.25	85.18			84.80	84.95	84.92	84.92
90.00	90.20	90.34			90.62	90.03	90.19	90.09
95.00	95.41	95.49			95.71	95.00	95.05	94.94

Table 3.—(Concluded)

(g) Section at  $0.93\frac{b}{2}$ , chord = 18.25 cm



Nominal	Flat wing, $\alpha_{\text{sec}} = 0.0^\circ$				Twisted wing, $\alpha_{\text{sec}} = -4.14^\circ$		Cambered-twisted wing, $\alpha_{\text{sec}} = -4.14^\circ$	
	Rounded leading edge		Sharp leading edge		Rounded leading edge		Rounded leading edge	
	Upper surface	Lower surface	Upper surface	Lower surface	Upper surface	Lower surface	Upper surface	Lower surface
0.00	0.00		—	—	0.00		0.00	
2.51	1.70	1.81	2.12	1.86	1.74	2.59	2.77	2.26
5.00	4.38	4.68	4.72	4.52	4.41	4.65	5.11	4.79
8.50	7.89	8.24	8.21	8.06	7.92	8.23	8.64	8.13
11.59	—	—	—	—	11.59	—	—	—
12.25	12.33	—	12.19	—	—	—	12.64	12.16
17.50	17.36	16.60			16.60	17.49	18.03	16.83
20.00	19.78	19.81			19.58	19.96	19.94	19.44
30.00	29.67	29.00			29.17	29.62	30.22	28.66
45.00	44.70	44.80			44.12	44.44	44.33	44.77
60.00	59.68	59.47			59.18	59.71	59.47	59.38
70.00	69.69	70.33			68.99	69.31	69.10	70.07
72.50	72.15	71.89			71.59	72.01	71.78	72.74
77.50	77.38	77.31			76.80	77.12	76.49	77.36
85.00	84.62	84.90			84.54	84.82	84.93	85.29
90.00	89.51	89.81			89.21	89.74	90.72	90.35
95.00	94.46	94.68			94.41	94.56	95.26	94.87

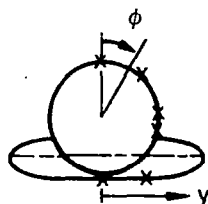


Table 4.—Body Pressure Orifice Locations

	x/L, percent body length														
Normal locations	4.5	7.5	11.0	14.5	21.8	25.0	33.0	39.0	50.0	55.0	60.0	64.0	70.0	75.5	80.0
$\phi = 0.0^\circ$	0.0	0.0	0.0	0.0	0.0	0.0	0.0	0.0	0.0	0.0	0.0	0.0	0.0	0.0	0.0
$\phi = 45.0^\circ$	44.3	44.3	44.5	44.7	44.4	44.8	45.0	44.8	45.0	44.8	44.8	45.0	44.8	45.0	44.8
$\phi = 90.0^\circ$	90.0	89.9	90.5	90.3	90.4	89.9	90.1	90.2	90.2	90.0	89.9	89.9	89.8	90.1	89.8
$\phi \approx 110.0^\circ$	---	---	---	---	110.2	110.0	110.1	110.1	110.2	116.8	119.9	124.2	---	---	---
Body, $\phi = 135.0^\circ$ Flat wing, $y = 3.094$ cm Twisted wing, $y = 3.094$ cm Cambered-twisted wing, $y = 3.094$ cm	136.1	135.3	135.0	135.2	3.025 3.132 3.040	3.028 3.106 3.056	3.028 3.048 3.075	3.056 3.048 3.072	3.071 3.005 3.079	3.056 2.926 3.067	3.043 3.094 3.084	3.045 3.094 3.069	134.6	134.5	134.8
Body, $\phi = 180.0^\circ$ Flat wing, $y = 0.0$ cm Twisted wing, $y = 0.0$ cm Cambered-twisted wing, $y = 0.0$ cm	180.0	180.0	180.0	180.0	-.018 .020 -.046	-.030 -.008 -.060	-.064 -.041 -.027	.081 -.043 .002	-.048 -.056 -.032	180.0	180.0	180.0	180.0	180.0	180.0

To facilitate model changes for the three wings, quick disconnects were used at the wing body junction. Unfortunately, by the time the cambered-twisted wing was installed in the test section, one quick disconnect block had become worn out as a result of the two previous tests and model checkout. This connection did not seal properly and measurements at a series of orifices ( $x/c$  from 0.125 through 0.600) on the lower surface at 0.80  $b/2$  were not sufficiently accurate to use. Data values to use in the integration were obtained by linear spanwise interpolation between adjacent sections.

The tubing for body pressure orifices was run through the hollow center of the model body rather than in grooves in the outside contour. Tubing from all the orifices was routed through the hollow body to the scanivalves located in the body nose. Wiring from the scanivalves was routed through the body to the sting.

The nose portion of the body was removable to provide access to the fifteen 24-position scanivalves. Figure 1 shows the aft body location of the strain gages used to measure normal force and pitching moment.

### WIND TUNNEL CAPABILITIES

The Boeing Transonic Wind Tunnel (BTWT) is a continuous-flow, closed-circuit, single-return facility with an operating range of Mach number from 0.0 to nearly 1.1. The test section is 2.438 by 3.658 by 4.420 m (8 by 12 by 14.5 ft) with 11.0 percent of the wall area in slots.

The tunnel layout is shown in figure 7. The tunnel stagnation pressure is atmospheric with a total temperature range of 300 K to 356 K (540° to 640° R). The variation with Mach number of Reynolds number based on the mean aerodynamic chord (M.A.C.) of this model is shown in figure 8, which also shows the variation of dynamic pressure with Mach number. The 26 856-kW (36 000-hp) wound-rotor induction motor in tandem with a 13 428-kW (18 000-hp) synchronous motor provides the power to drive a 7.315-m (24-ft) diameter fan up to a maximum speed of 470 rpm. The fan is made up of a 5.486-m (18-ft) diameter hub with 72 fixed-pitch fiberglass blades 0.914 m (36 in.) long in two stages and directs circuit air through two stages of 67 hollow steel stators.

### DATA SYSTEM

The Boeing wind tunnel data system provides the capabilities of real-time test data acquisition, feedback control computation, and display. The data system consists of an Astrodata acquisition subsystem and a computing subsystem which uses a Xerox data system (XDS 9300) digital computer. The Astrodata system acquires signals from the sensors, conditions them, and passes them directly to the computer. Test data, averaged from up to 256 samples per test point, are recorded on a rapid-access data drum. As final computations are performed, selected on-line displays are provided on analog X-Y plotters and teletypewriters. Real-time computations and displays are performed every 200 milliseconds for control and test monitoring functions. Any test data may be retrieved from rapid-access drum storage and displayed on an oscilloscope. On-line programs also provide for preparation of magnetic tapes for plotting or interfacing with off-line programs. Figure 9 is a schematic of the data acquisition and reduction system.

## MACH NUMBER

Mach number in the BTWT is referenced to the horizontal and lateral center of the test section at tunnel station 1000 which was the pitch point of this model (40 percent M.A.C.).

The pressures used to determine Mach number,  $p_s$ , and  $p_t$ , are measured through permanently positioned sensors. Static pressure  $p_s$  is measured by a 103.42-kN/m<sup>2</sup> (15-psi) absolute transducer. A 103.42-kN/m<sup>2</sup> (15-psi) differential transducer is used to obtain total pressure by measuring  $(p_t - p_s)$ . These transducers are temperature compensated in addition to being in a  $\pm 1.11^\circ\text{C}$  ( $\pm 2^\circ\text{F}$ ) environment. Transducer performance is checked periodically, and both the static and differential transducers have shown a maximum deviation of  $\pm 0.02$  percent of full scale.

The static pressure tap is located out of the test section above the ceiling in the pressure cap plenum. A correction is made to adjust this static pressure reading to the measured test section centerline static pressure determined during calibrations at station 1000. The tunnel total pressure is obtained from a total pressure probe mounted near the tunnel ceiling in the bellmouth throat (see fig. 7).

Signals from the pressure sensors are fed to the XDS 9300 computer. The XDS system computes and updates the Mach display five times per second. Accounting for the entire system, calculated Mach number is accurate within  $\pm 0.002$ . Data are recorded only when the tunnel is within a preselected Mach tolerance. For this test, a tolerance of  $\pm 0.003$  was used.

## DYNAMIC PRESSURE

The dynamic pressure  $q$  is computed from the Mach number and the corrected static pressure. The estimated tolerance on dynamic pressure is  $\pm 95.8\text{ N/m}^2$  ( $\pm 2.0\text{ psf}$ ).

## ANGLE OF ATTACK

The angle of attack of the reference point (0.25 M.A.C. for this model) for a sting-mounted model is determined from several increments. The input angle of attack is determined by an encoder mounted in the strut. This angle is accurate within  $\pm 0.02^\circ$ . This angle is then modified by the effects of sting deflection, up-flow, and wall corrections.

Sting deflections due to load were determined during the calibration of the strain gages mounted on the integral sting body of the model. These deflections are known within  $\pm 0.02^\circ$ . The corrections for sting deflection are based on the normal force and pitching moment loads obtained during wind-on data acquisition. The sting deflection was taken into account when setting test angles of attack to minimize the variation in final angle of attack for the various model configurations. The strain gages attached to the sting body of this model have an estimated accuracy of  $\pm 5$  percent of full-scale reading. This means that the sting deflections based on maximum model loads were known within  $\pm 0.11^\circ$ .

The wiring for the pitching moment gage broke during run 55, affecting both the normal force and pitching moment measurements and therefore the calculation of sting



deflection under load. For the remainder of the test, the model angle was set using the angle of attack as determined by the encoder for the most similar previously run configuration. After the test, the normal force and pitching moment obtained by integrating the pressure data were used to correct the final angle of attack. To verify this procedure, a comparison was made using these two methods on data obtained prior to run 55; the results matched within  $\pm 0.01^\circ$ .

Up-flow corrections were made based on data obtained from upright and inverted runs on a calibration model of similar span. These corrections were less than  $0.2^\circ$ . It is generally accepted that the up-flow values are known within  $\pm 0.05^\circ$ .

A correction to model angle was made for the effect of lift interference for 11 percent slotted walls. The lift interference is a function of the ratio of model-to-test section size, test section shape,  $C_N$ , and wall geometry. For  $C_N = 1.0$ , this correction is on the order of  $-0.48^\circ$ . Due to the limited amount of experimental substantiation, the wall correction could be in error by  $\pm 20$  percent.

## MODEL PRESSURES

The model was instrumented with fifteen 24-position scanivalves. Each scanivalve contained a  $103.42\text{-kN/m}^2$  (15-psi) differential Statham, variable resistance, unbonded strain gage transducer. These transducers are calibrated against a high accuracy standard and, if placed in a temperature-controlled environment, will read within an accuracy of 0.1 percent of full scale. For this test, the transducers were located inside the model and subjected to large temperature excursions. Temperatures recorded at the scanivalves indicate that the accuracy of readout was 0.75 percent of full-scale capability based on the calibration data.

## TESTS AND DATA ACQUISITION

### TESTS

Table 5 shows the 12 configurations that were tested in this contract. Two of these configurations were also tested in the previous contract (NAS1-12875), and were tested here to ensure that data from the two tests are consistent. Photographs of some configurations are shown in figures 10 through 13 and a diagram of the model installation in the BTWT is shown in figure 14. Pressure and total force data were obtained at Mach numbers of 0.40, 0.85, 0.95, and 1.05 for all configurations and at Mach numbers of 0.70 and 1.00 for selected configurations. Test angles of attack were from  $-8^\circ$  to  $+16^\circ$  in  $2^\circ$  increments. Table 5 shows the run numbers for each Mach number and configuration for which these data were obtained. A detailed listing of all test points is shown in appendix A. A summary of the previously tested data is in appendix B.

A trip strip of No. 60 carborundum grit was used throughout the test. On the body, the trip strip was 0.32 cm (0.125 in.) wide and placed 2.54 cm (1 in.) from the nose. On the wing, it was 0.32 cm (0.125 in.) wide from the side of body to the midspan control surface break ( $0.57\text{ b}/2$ ), and tapered to 0.16 cm (0.0625 in.) wide at the wingtip. On the upper surface of the wing, the trip strip was placed at 15 percent chord; and on the lower surface, it was placed just aft of the location of the leading-edge control surface brackets on the flat wing (see fig. 6). Density of the grit was 4 to 5 grains per quarter-inch of trip strip length.

**Table 5.—Summary of Test Conditions by Run Number**

Mach number	Trailing-edge deflection, degrees			
	Full span		Outboard (inbd=0.0)	Inboard (outbd=0.0)
	0.0	8.3	8.3	8.3
Twisted wing				
0.40	15	25	30	20
0.70	14	24	29	19
0.85	13	23	28	18
0.95	12	22	27	17
1.00	11			
1.05	10	21	26	16
Cambered-twisted wing, fin off				
0.40	43	65	80	57
0.70	41			
0.85	40	62	78	59
0.95	39	64	79	58
1.00	38			
1.05	37	61	77	55
Cambered-twisted wing, fin on				
0.40	49	70	75	54
0.70	45			
0.85	48	68	73	52
0.95	47	69	74	53
1.00	46			
1.05	44	67	72	51

## DATA REPEATABILITY

The twisted wing with undeflected trailing-edge control surfaces was tested in the previous contract (test - BTWT 1415) and again in this contract (test - BTWT 1627). These data for Mach 0.85 are compared in figure 15 for the wing and figure 16 for the body. On the wing, the data from the two tests are within the tolerance expected for repeat runs in a single test. The discrepancies between the two tests in the body data are primarily due to a change in status of the orifices, that is, some repaired and some lost. It does not indicate a difference in the flow. Based on these comparisons, data from other configurations in both tests are compared in the remainder of this document without regard to the test in which the data were obtained.

## DATA ACQUISITION AND INITIAL PROCESSING

The pressure data were recorded through the use of fifteen 24-position scanivalves located in the fore body of the model. Pressure transducers in the scanivalves measured the differential pressure between the local surface pressures and tunnel total pressure. Signals from the scanivalves, force and moment data, tunnel parameters, and model attitude angle were recorded on the Astrodata system and reduced using the XDS 9300 computer.

Final data (pressure coefficients, tunnel parameters, and model attitude) were merged on magnetic tapes, with appropriate configuration and test point identification for integration and plotting of these data.

A detailed description of the data editing and integration procedure and the data presentation are included in appendix C.

## DATA TAPE DESCRIPTION

The experimental data were recorded on nine-track unlabeled tapes written by the Boeing Computer Services CDC 6600 computer. The tapes were written in binary (odd parity) mode at a density of 1600 cpi. The first file of each tape and any program files are BCD (formatted) information. The data files are binary.

A description of each of the tape files follows:

- o First file of each tape (BCD format with 80-column records) - This file contains an identification of the test and model and describes the content of the remaining files.
- o Program files (BCD) - These files contain the source code of FORTRAN IV programs that may be used to provide listings of user-selected items in the data files.
- o Data files (binary) - The first record contains geometry pertinent to the data that will follow (i.e., for pressure data, the spanwise location of each section and arrays of  $x/c$  for which  $C_p$ s are listed; for integrated data, geometric constants used in the integrations). The remaining records each contain data for one test point. A list defining all test points is shown in appendix A.

Questions regarding the availability of these data should be addressed to Percy J. Bobbitt of the NASA Langley Research Center.

## EXPERIMENTAL DATA

The experimental data are summarized and discussed in this section. The data shown here are primarily for Mach 0.85 with data for other Mach numbers shown in the other documents. The effect on loading of wing twist, camber, combined camber and twist, a wing fin, and both full-span and partial-span trailing-edge control surface deflection are shown in figures 17 through 39. Many of these figures include data obtained under a previous contract, NAS1-12875, summarized in appendix B. Table 6 summarizes the data presented in this document. A more detailed presentation of the basic experimental data and the effect of wing shape - twist, camber, and combined camber and twist - are shown in NASA CR-165701 and of the effect of trailing-edge control surface deflection and a wing fin in NASA CR-165702. Table 7 shows the data available in these documents. The presentations include:

- o Wing upper and lower surface isobars
- o Wing upper and lower surface chordwise pressure distributions
- o Wing net chordwise pressure distributions
- o Wing spanload distributions
- o Wing section aerodynamic characteristics
- o Wing aerodynamic characteristics
- o Body longitudinal pressure distributions

### CAMBERED-TWISTED WING

The data in this report are intended to complement the data previously obtained on the flat and twisted wings and reported in NASA CR-2610, NASA CR-132727, NASA CR-132728, and NASA CR-132729. Figures 17 through 20 show data at representative Mach numbers for the cambered-twisted wing with the trailing-edge control surface undeflected and the wing fin off. The data include wing isobars, chordwise pressure distributions, spanload distributions, section aerodynamic characteristics, and total surface aerodynamic characteristics.

An examination of the isobars\* and chordwise pressure distributions show the same phenomena as seen on the flat and twisted wings. The flow on the wing upper surface separates near the leading edge and forms a spiral vortex at low angles of attack (approximately  $6^\circ$ ). The camber of this wing is leading and trailing edges up and the twist is the same as that of the twisted wing, therefore, the effects of twist and camber on leading edge angle of attack are compensating. The development of the vortex flow on this wing is more like the flat wing than the twisted wing, indicating that the local leading-edge angle of attack is the controlling feature.

---

\*The  $\Delta C_p$  noted on each of the isobars refers to the increment in pressure level between adjacent isobar lines. These  $\Delta C_p$  increments are automatically selected within the plot program based on maximum and minimum pressure levels. These increments should be carefully noted when comparing the plots for several angles of attack since they may vary.

Table 6.—Summary of Experimental Data Presentations in This Document

Type of data	T.E. deflection, deg			Mach number						
	Full Span	Inb'd	Outb'd	0.40	0.70	0.85	0.95	1.00	1.05	Several
Wing										
Twisted wing, repeatability	0.0	—	—			15				
Cambered-twisted wing										
Fin off	0.0	—	—	17		18			19	20
Fin on	0.0	—	—			27				28
Effect of wing fin, cambered-twisted wing										
	0.0	—	—			29,30				
	8.3	—	—			39				
Effect of wing shape										
	0.0	—	—			21				
	8.3	—	—			26				
Incremental twist	0.0	—	—			23				
Incremental camber	0.0	—	—			24				
Incremental camber and twist	0.0	—	—			25				
Effect of trailing edge deflection										
Flat wing						31,32				
Twisted wing						33,34				
Cambered-twisted wing, fin off						35,36				
Cambered-twisted wing, fin on						37,38				
Body										
Twisted wing, repeatability	0.0	—	—			16				
Effect of wing shape	0.0	—	—			22				

Table 7.—Summary of Additional Experimental Data Presentations

(a) Experimental Data Presented in NASA CR-165701

Type of data	T.E. deflection, deg			Mach number						
	Full Span	Inb'd	Outb'd	0.40	0.70	0.85	0.95	1.00	1.05	Several
Wing										
Flat wing	—	8.3	0.0			X				X
	—	0.0	8.3			X				X
Twisted wing										
Repeatability	0.0	—	—	X		X*			X	
	—	8.3	0.0			X				X
	—	0.0	8.3			X				X
Cambered-twisted wing, fin off										
	0.0	—	—	X*	X	X*	X	X	X*	X*
	8.3	—	—	X		X			X	X
	—	8.3	0.0			X				X
	—	0.0	8.3			X				X
Cambered-twisted wing, fin on										
	0.0	—	—	X	X	X*	X	X	X	X*
	8.3	—	—	X		X			X	X
	—	8.3	0.0			X				X
	—	0.0	8.3			X				X
Effect of wing shape										
	0.0	—	—	X		X*			X	
	8.3	—	—			X*				
Incremental twist	0.0	—	—	X		X*			X	
Incremental camber	0.0	—	—	X		X*			X	
Incremental camber and twist	0.0	—	—	X		X*			X	
Body										
Twisted wing, repeatability	0.0	—	—	X		X*			X	
Cambered-twisted wing										
Fin off	0.0	—	—	X	X	X	X	X	X	
Fin on	0.0	—	—	X	X	X	X	X	X	
Effect of wing shape	0.0	—	—	X		X*			X	

\*Included in summary document, NASA CR-3434

Table 7.—(Concluded)

(b) Experimental Data Presented in NASA CR-165702

Type of data	T.E. deflection, deg			Mach number						
	Full Span	Inb'd	Outb'd	0.40	0.70	0.85	0.95	1.00	1.05	Several
Wing										
Effect of trailing edge deflection										
Flat wing				X,X		X*,X*			X,X	
Twisted wing				X,X		X*,X*			X,X	
Cambered-twisted wing, fin off				X,X		X*,X*			X,X	
Cambered-twisted wing, fin on				X,X		X*,X*			X,X	
Incremental effect of trailing edge deflection										
Flat wing										
8.3	8.3	—	—			X				
—	—	8.3	0.0			X				
—	—	0.0	8.3			X				
Twisted wing										
8.3	8.3	—	—			X				
—	—	8.3	0.0			X				
—	—	0.0	8.3			X				
Cambered-twisted wing, fin off										
8.3	8.3	—	—			X				
—	—	8.3	0.0			X				
—	—	0.0	8.3			X				
Cambered-twisted wing, fin on										
8.3	8.3	—	—			X				
—	—	8.3	0.0			X				
—	—	0.0	8.3			X				
Effect of a wing fin, cambered-twisted wing										
0.0	0.0	—	—	X		X*			X	
8.3	8.3	—	—	X		X*			X	
—	—	8.3	0.0			X				
—	—	0.0	8.3			X				
Incremental effect of a wing fin, cambered-twisted wing										
0.0	0.0	—	—	X		X*			X	
Body										
Effect of a wing fin, cambered-twisted wing										
0.0	0.0	—	—	X		X			X	
8.3	8.3	—	—	X		X			X	

\*Included in summary document, NASA CR-3434

This vortex moves inboard across the wing as the angle of attack increases, greatly changing the load distribution on the outboard wing (similarly, the flow on the lower surface separates at negative angles of attack). At high angles of attack, this vortex is the predominant influence over the majority of the wing. The effects of the vortex are also obvious in the section characteristics but are not evident in the total integrated surface coefficients (fig. 20(c)). These results confirm once again that the large nonlinear wing loading characteristics which occur are not discernable from force measurements alone.

## **COMPARISON OF FLAT, TWISTED, AND CAMBERED-TWISTED WINGS**

Plots of the data for all three wing shapes with the trailing-edge control surface undeflected are shown in figure 21. At the inboard stations, examination of the surface pressure distributions (parts b through h) indicates a small but definite change for the three wings. At the outboard stations, where the difference in wing shape is more significant, the difference in the pressures is also more noticeable.

Longitudinal pressure distributions on the body for these three wing configurations are shown in figure 22 for a representative Mach number.

### **EFFECT OF WING TWIST**

Figure 23 shows the incremental pressures due to twist which were obtained by subtracting the data for the flat wing from data for the twisted wing at each combination of Mach number and angle of attack. This increment, particularly near the leading edge, changes with angle of attack even where there is no vortex flow.

### **EFFECT OF WING CAMBER**

The increment due to camber alone is obtained by subtracting the data for the twisted wing from that of the cambered-twisted wing. These data are shown in figure 24. There is again a marked change with angle of attack due to the difference in the position of the vortex on the two wings.

### **EFFECT OF WING CAMBER AND TWIST**

Figure 25 shows data for the combined camber-twist increment (subtracting flat wing data from cambered-twisted wing data). This increment tends to be a little more consistent because the vortex development on the cambered-twisted wing is more like that on the flat wing than either is like that on the twisted wing.

## **COMPARISON OF FLAT, TWISTED, AND CAMBERED-TWISTED WINGS WITH FULL-SPAN TRAILING-EDGE CONTROL SURFACE DEFLECTION**

Comparisons of data for the flat wing, twisted wing, and cambered-twisted wing are shown in figure 26 with all wings having the trailing-edge control surface deflected full-span  $8.3^\circ$ . The differences between the data for the three wings are similar to the differences when the trailing-edge control surfaces are undeflected (fig. 21).



## CAMBERED-TWISTED WING, FIN ON

Figures 27 and 28 show data for the cambered-twisted wing with the trailing-edge control surfaces undeflected but with a wing fin at 0.725  $b/2$ . Examination of the isobars\*\* and chordwise pressure distributions for this configuration and comparing them to the data plots in figure 18 for this wing with the fin off show that the flow is not particularly affected by the presence of the fin at low angles of attack (up to  $6^\circ$ ). However, at  $8^\circ$ , the pressures just outboard of the fin indicate that the fin has reduced the influence of the vortex off the wing apex in this area. There is some indication that a second vortex is forming off the apex of the fin. This blocking effect becomes more pronounced at the higher angles of attack.

## EFFECT OF WING FIN, UNDEFLECTED TRAILING-EDGE CONTROL SURFACE

The effect of placing a wing fin on the cambered-twisted wing at 0.725 semispan is shown in figure 29. The spanwise loading at  $4^\circ$  angle of attack is the same for both fin off and fin on, as is the loading on the inboard 70 percent of the wing at  $8^\circ$ . At higher angles of attack, when the fin is off, the load on the outboard quarter of the wing remains the same as it was at  $8^\circ$ , while the load inboard increases. With the fin on, however, it is only directly inboard of the fin ( $2y/b = 0.65$ ) that the load remains at the  $8^\circ$  angle of attack level. The load increases as angle of attack increases on the rest of the wing.

Incremental chordwise pressure distributions and spanload distributions at constant angle of attack (obtained by subtracting data for the fin off configuration from that for the fin on) are shown in figure 30. These figures emphasize the local nature of the change in loading.

## EFFECT OF TRAILING-EDGE CONTROL SURFACE DEFLECTION

The effect on wing loading of full- or partial-span deflection of the trailing-edge control surface as affected by angle of attack and wing shape is very important. Table 8 shows the document in which plots of the basic data for these configurations can be found. There is data for full-span undeflected, full-span deflected  $8.3^\circ$ , the inboard segment only deflected  $8.3^\circ$ , and the outboard segment only deflected  $8.3^\circ$ . The comparisons are discussed in the following sections and are shown in figures 31 through 38.

### Flat Wing

Figure 31 allows us to compare the spanload distribution, and section and total aerodynamic coefficients for these four trailing-edge control surface configurations on the flat wing. At all the angles of attack shown, the effect on the inboard wing loads is almost all due to the deflection of the inboard portion of the control surface. On the

\*\*The isobars for the cambered-twisted wing, fin on, were drawn after the spanwise pressure distributions were modified to add data just inboard and outboard of the fin on the upper surface. The data just inboard of the fin (0.724  $b/2$ ) were obtained by extrapolating from the two measured stations inboard of the fin. Data just outboard of the fin (0.726  $b/2$ ) was set equal to the data at 0.80  $b/2$ . Data at the corresponding locations on the lower surface were obtained by a linear interpolation on the data at adjacent stations.

*Table 8.—Summary of Presentations of Trailing-Edge Configurations by Document Number*

Wing	Fin	Trailing-edge deflection, degrees			
		Full Span		Inboard/Outboard	
		0.0	8.3	8.3/0.0	0.0/8.3
Flat	Off	NASA CR-132727	NASA CR-132728	NASA CR-165701	NASA CR-165701
Twisted	Off	NASA CR-132727	NASA CR-132728	NASA CR-165701	NASA CR-165701
Cambered-twisted	Off	NASA CR-165701	NASA CR-165701	NASA CR-165701	NASA CR-165701
Cambered-twisted	On	NASA CR-165701	NASA CR-165701	NASA CR-165701	NASA CR-165701

outboard wing the incremental load is just as great, or greater, when only the inboard portion is deflected, as it is when only the outboard control surface is deflected. This effect is noticeably greater at  $12^\circ$  angle of attack. The relative effect of these deflections on the leading-edge segment, the wing box, and the trailing-edge segment are shown in figure 32. Chordwise pressure distributions at constant angle of attack for the incremental effect of full-span, inboard only, and outboard only trailing-edge control surface deflections are shown in NASA CR-165702.

### **Twisted Wing**

For the twisted wing, comparisons of data for these four control-surface configurations are shown in figure 33, and the relative distribution by segment in figure 34. The incremental chordwise pressure distributions are shown in NASA CR-165702 for the full span, inboard only, and outboard only trailing-edge control surface deflection. The effects are very similar to that on the flat wing with only the total load level changing due to the locally lower angle of attack outboard and the resulting position of the vortex.

### **Cambered-Twisted Wing, Fin Off**

Comparisons of the integrated coefficients for these four control surface configurations on the cambered-twisted wing without fin are shown in figure 35 with the relative effect on the normal force of each segment shown in figure 36. The incremental effect on chordwise pressure distributions is shown in NASA CR-165702 for the full-span, inboard-only, and outboard-only deflection. The effect of deflecting the trailing-edge control surface on this wing is very similar to that on the other two wings.

### **Cambered-Twisted Wing, Fin On**

The fourth major configuration is the cambered-twisted wing with a wing fin. Comparisons of spanload distributions, and section and total aerodynamic coefficients for these four control-surface configurations are shown in figure 37. The relative effect on each of the segments is shown in figure 38. The incremental chordwise pressure distributions at constant angle of attack are shown in NASA CR-165702 for the full-span, inboard-only, and outboard-only trailing edge control surface deflection.

## **EFFECT OF WING FIN, FULL-SPAN TRAILING-EDGE CONTROL-SURFACE DEFLECTION**

Comparisons of data for both the fin off and fin on configurations with the trailing-edge control surface deflected full span are shown in figure 39. The effect of the fin is again only evident at the station just inboard of the fin and at those stations outboard. At  $2y/b = 0.65$  (the station just inboard of the fin), the loading increases with angle of attack throughout the angle of attack range when the fin is off, but remains at about the  $8^\circ$  angle of attack level in the presence of the wing fin. Outboard of the fin location, the reverse is true, there is no change in loading at angles of attack greater than  $8^\circ$  when the fin is off but a steady increase in load when the fin is on.

# THEORY COMPARISON TASK

## ATTACHED-FLOW THEORETICAL METHODS

The attached-flow theoretical calculations carried out in this study are based on potential-flow theories. Results from three attached-flow panel methods which satisfy the classical Prandtl-Glauert equation for linearized compressible flow are shown. The first method, FLEXSTAB, uses the constant-pressure-panel formulation, is valid for both supersonic and subsonic analysis, and satisfies only planar boundary conditions. The second method, TEA-230, is a lower order panel method (constant strength sources and doublets) which is limited to subsonic flow but can satisfy boundary conditions on the exact configuration surface. The third method, PAN AIR, is a higher order panel method using bi-quadratic doublet and bi-linear source panels, valid for both supersonic and subsonic flow, and capable of satisfying exact boundary conditions.

All three methods provided detailed surface pressure distributions and therefore the analytical results were interpolated to the orifice locations on the model and then integrated with the methods described for the experimental data (see app. C). A listing of all available data points from this contract is included in appendix A.

Additional details of the analytical methods FLEXSTAB and PAN AIR are discussed below. The second method TEA-230 was not used in this contract, i.e., the cambered-twisted wing investigation. The results obtained in connection with the previous contract are included, however, and this method is described in appendix B.

### FLEXSTAB

The primary analysis method used for pressure calculations in this study was the unified subsonic/supersonic panel technique of FLEXSTAB, which was developed by Boeing under NASA Ames sponsorship (ref. 9). The FLEXSTAB system of digital computer programs uses linear theory to evaluate the static and dynamic stability, the inertial and aerodynamic loading, and the resulting elastic deformations of aircraft configurations. The aerodynamic module contained in the FLEXSTAB system is based on the constant-pressure-panel method developed by Woodward (refs. 10 and 11) to solve the linearized potential-flow equations for supersonic and subsonic speeds with planar boundary conditions. The method can also produce answers for transonic speeds, although the nonlinear terms not accounted for become important as sonic speed is approached.

In the FLEXSTAB system (ref. 12), the flow about a configuration is simulated by a three-dimensional array of singularities. Each singularity is a solution to the governing potential flow equation. The singularities are placed on a mean surface instead of the actual configuration surface. The boundary condition that the flow is tangent to the surface is satisfied at a discrete set of points on the mean surface. This results in a linear set of equations that may be solved to yield the singularity strengths necessary to satisfy the specified boundary conditions. From knowledge of these singularity strengths, the velocities, pressures, and aerodynamic loads on the configuration may be calculated.

Figure 40 shows the distribution of panels used in this analysis. Line sources and doublets are distributed along the longitudinal axis of the body to simulate its thickness and lifting effects. Similarly, source and vortex panels are placed in the plane of the

wing to simulate its thickness and lifting effects. To account for the interference effects between the wing and body, constant-pressure vortex panels are placed on a shell around the body. This "interference" shell serves to cancel the normal velocity components on the body that are induced by the wing.

At subsonic Mach numbers and the high supersonic Mach numbers, 50 line singularities, 168 interference panels, and 160 wing panels were used to represent the configuration. For the very low supersonic Mach numbers (1.05 and 1.11), the number of interference panels had to be greatly increased (to 330) to overcome instabilities associated with the solution. The edges of the wing panels were chosen to coincide with the control-surface hingelines and breaklines. Note on figure 40 that the panels are of nearly equal width and, in the chordwise direction, panel edges are at constant percent chord with closer spacing near the leading edge and the hingelines. The same wing paneling arrangement was used at all Mach numbers. The linearized boundary conditions employed by the method permitted twist and camber changes, as well as control-surface deflection to be treated as boundary-condition changes and did not require repaneling. Table 9 summarizes the configurations and Mach numbers for which solutions were obtained in this contract. Previously obtained solutions are shown in appendix B.

## PAN AIR

The third and most recently developed attached-flow method is the higher-order panel method developed by Ehlers, Epton, Johnson, Magnus, and Rubbert (refs. 13 through 17) which uses bi-quadratic doublet and bi-linear source panels. This method, known as PAN AIR (Panel Aerodynamics), was still under development when this study was undertaken; therefore the current predictions were made using the pilot code. The method will solve a variety of boundary-value problems in steady subsonic and supersonic inviscid flow. The solutions are governed by the classical Prandtl-Glauert equation for linearized compressible flow. Boundary conditions are satisfied on the configuration surface so that new paneling is required for each configuration.

The panels are grouped into networks to represent the wetted surface of each component - wing, body, fin - of the configuration. In addition, abutting networks must abut along complete edges with the corner points coinciding. This typically results in separate networks for upper and lower body and wing, and separate networks on the body in front of and behind the wing. For the configuration in this study, a division of the upper surface of the wing into four networks was required because of the placement of the fin, and this in turn required a division of the upper body into two networks in this region. For convenience, the lower wing and body were also divided in this manner.

As the wing tip is very thin, the gap between the upper and lower surface networks at the tip was not initially filled. Whereas this would seem to be insignificant, the surface pressures at the tip station were erratic, apparently because the surface was open. The addition of two networks to fill in this gap improved the results. These additional networks would have required the lower surface of the wing (and also the lower body) to be divided into at least two networks each to maintain proper network abutment.

Figure 41 shows the paneling for the cambered-twisted wing with the fin attached. The wing was represented by 476 panels, the body by 232, and the fin by 60. In addition, wake networks shed from all trailing edges extend more than 56 meters behind the

**Table 9.—Summary of FLEXSTAB Conditions by Run Number**

Mach number	Trailing-edge deflection, degrees			
	Full span		Outboard (inbd=0.0)	Inboard (outbd=0.0)
	0.0	8.3	8.3	8.3
Twisted wing				
0.40	(15)	(25)	(30)	(20)
0.70	14	24	29	19
0.85	(13)	(23)	(28)	(18)
0.95	12	22	27	17
1.00	11			
1.05	(10)	(21)	(26)	(16)
Cambered-twisted wing, fin off				
0.40	(43)	(65)	(80)	(57)
0.70	41			
0.85	(40)	(62)	(78)	(59)
0.95	39	64	79	58
1.00	38			
1.05	(37)	(61)	(77)	(55)
Cambered-twisted wing, fin on				
0.40	49	70	75	54
0.70	45			
0.85	48	68	73	52
0.95	47	69	74	53
1.00	46			
1.05	44	67	72	51

○ FLEXSTAB solution available

**Note:** On the data tapes and in the tables of appendix A, the above run numbers have been incremented by 1000 to give the FLEXSTAB results unique identification.

configuration, but for clarity are not shown. A diagram of the networks (i.e. grouping of panels) is shown in figure 42. The flat wing, the twisted wing, and the cambered-twisted wing without fin have the same paneling and network arrangement for the wing and body and associated wakes as the cambered-twisted wing with fin. These panelings are also shown in figure 41. The configurations without fin each have 18 networks to represent the wetted surfaces and 8 wake networks for a total of 26 networks. The fin adds one wetted surface and two wakes for a total of 29 networks for the cambered-twisted wing with fin. The pressures are evaluated at panel centroids. Prior to interpolation to the orifice locations of the model, wing pressures at constant BL were grouped and body pressures at constant MS were grouped.

The results of an execution of this code for a given configuration depend not only on the Mach number and angles of attack and sideslip, but on the compressibility axes ( $\alpha_c$  and  $\beta_c$ ) relative to the body-fixed axes. The compressibility axes are defined so that the x-axis is aligned with the undisturbed flow. For the cases run in this study, the sideslip angle was zero, therefore agreeing exactly with the compressibility axis in this direction. For the majority of cases, however, the compressibility axis angle of attack was  $4^\circ$  and condition angles of attack were  $0^\circ$ ,  $4^\circ$  (except  $4.5^\circ$  for twisted wing),  $8^\circ$ , and  $12^\circ$ . The difference between these angles (i.e.,  $\alpha - \alpha_c$ ) is regarded as a contribution to the perturbation flow. To determine the effect of the compressibility angle (equal to condition angle is best), another set of conditions were run for the cambered-twisted wing with fin off. The compressibility axis was  $12^\circ$  and angles of attack of  $4^\circ$ ,  $8^\circ$ ,  $12^\circ$ , and  $16^\circ$  were run.

Comparison of the pressure data at those angles of attack -  $4^\circ$ ,  $8^\circ$ , and  $12^\circ$  - run with both compressibility axis angles of attack, shows that at Mach numbers of 0.40 and 0.85 the difference in pressures between the two solutions is not plottable for either the wing or the body. At Mach 1.05, there is also no significant difference in the wing data. On the body, however, there is a definite difference between the two solutions in the region of the wing. The comparisons are shown in figure 43. In the comparisons of theory-to-experiment shown for the cambered-twisted wing without fin, PAN AIR data have  $\alpha_c = 4^\circ$  for angles of attack of  $0^\circ$ ,  $4^\circ$ , and  $8^\circ$ ;  $\alpha_c = 12^\circ$  for angles of attack of  $12^\circ$  and  $16^\circ$ .

Pressures are calculated in PAN AIR using the isentropic pressure formula; but are not allowed to exceed vacuum pressure. Table 10 summarizes the configuration and Mach numbers for which solutions were obtained.

### THEORY-TO-EXPERIMENT COMPARISONS

The usefulness of any aerodynamic theory is determined by its ability to accurately predict flight or wind-tunnel results. The predictive methods available as production tools, as well as newly developed methods, must be tested against experimental data for those configurations and flight conditions which will figure in the design analysis. With this in mind, and recognizing the limited amount of detailed pressure data available for arrow-wing configurations over the entire subsonic-supersonic speed regimes, the present experimental and associated theoretical-methods evaluation were undertaken.

Theory-to-experiment comparisons were made over a range of Mach numbers from 0.40 to 2.50 using the FLEXSTAB system, at Mach numbers of 0.40 and 0.85 with the TEA-230 program, and at Mach numbers of 0.40, 0.85, and 1.05 using the PAN AIR pilot code. All configurations (except the cambered-twisted wing with fin on), including

Table 10.—Summary of PAN AIR Conditions by Run Number

Mach number	Trailing-edge deflection, degrees			
	Full span		Outboard (inbd=0.0)	Inboard (outbd=0.0)
	0.0	8.3	8.3	8.3
Twisted wing				
0.40	15 (450)	25	30	20
0.70	14	24	29	19
0.85	13 (449)	23	28	18
0.95	12	22	27	17
1.00	11			
1.05	10 (446)	21	26	16
Cambered-twisted wing, fin off				
0.40	(43)	65	80	57
0.70	41			
0.85	(40)	62	78	59
0.95	39	64	79	58
1.00	38			
1.05	(37)	61	77	55
Cambered-twisted wing, fin on				
0.40	(49)	70	75	54
0.70	45			
0.85	(48)	68	73	52
0.95	47	69	74	53
1.00	46			
1.05	(44)	67	72	51
Flat wing, rounded leading edge				
0.40	(269)	46	275	259
0.70	263	43	271	255
0.85	(267)	45	274	258
0.95	266	44	273	257
1.00	268			
1.05	(264)	42	272	256
1.11	262	40	270	254



PAN AIR solution available

Note: On the data tape and in the tables of appendix A, the above run numbers have been incremented by 3000 to give the PAN AIR results unique identification.



many with deflected control surfaces, were analyzed with FLEXSTAB. The flat and twisted wings, including some deflected control surfaces, were analyzed at subsonic speeds using TEA-230. The three wings without deflected control surfaces, but including the effect of the wing fin on the cambered-twisted wing, were analyzed using PAN AIR. Table 11 summarizes the theory-to-experiment comparisons shown in this document. More comparisons are shown in NASA CR-165703 as summarized in table 12.

While not the prime concern, the ability of the theories to predict forces and moments was of interest. Initial trade studies in the process of designing aircraft are often limited to experimental force data, if in fact any experimental data is available at this stage. Even with the availability of pressure data, force and moment data are required for performance and stability evaluations. Force and moment coefficients presented in subsequent figures are obtained by integrating the pressure data. Figures 44(i), 45(i), 46(j), and 47(i) show comparisons, at Mach 0.85, of attached-flow method predictions of wing normal force and pitching moment coefficients to the experimental data. At low and moderate angles of attack the predictions are quite good. At the higher angles of attack FLEXSTAB appears to be better than the other methods, although as we have seen there is strong vortex flow at these angles and FLEXSTAB does not include this phenomena. This apparent agreement is fortuitous; detailed comparisons of surface pressures (figs. 44 through 47) are necessary to evaluate the adequacy of these theoretical solutions in describing the load distribution.

#### **THEORY-TO-EXPERIMENT COMPARISONS FOR UNDEFLECTED TRAILING-EDGE CONTROL SURFACE**

A good test of a theoretical tool is whether or not the pressure change due to a change in twist and/or camber can be accurately predicted. Figures 44 through 46 show comparisons of experimental data with results from the theoretical methods at several angles of attack and Mach 0.85. At low angles of attack the predictions for the flat wing (fig. 44) are quite good for all theories. Figure 45 shows the twisted wing, where it is clear that PAN AIR and TEA-230 are much better than FLEXSTAB. Even at 8° angle of attack, the comparison on this wing is quite good, although a vortex has started to form on the outboard section.

The cambered-twisted wing, fin off, is shown in figure 46. The predictions are again very good. It seems as if the change in pressures for this smooth continuous type of deformation are adequately predicted in the region where the flow is still attached.

Data for the cambered-twisted wing with the wing fin on are shown in figure 47. The predictions are very good at low angles of attack (up to 4°) and at higher angles of attack on the inboard wing, where the flow is still attached. Again, as this is an attached-flow theory, the pressures due to the vortex are not predicted.

#### **PREDICTION OF INCREMENTS DUE TO CHANGE IN SHAPE**

As attached-flow theories are inadequate to predict the pressure distributions at moderate angles of attack, it is important to determine whether theory could be used to predict the aeroelastic increment to use in combination with rigid experimental data. Figures 48 through 50 show the incremental distributions due to change in shape at constant angle of attack at Mach 0.40.

The data for figure 48 were obtained by subtracting the flat-wing data from the twisted-wing data at each combination of angle of attack and Mach number. For this

*Table 11.—Summary of Theory-to-Experiment Data Presentations in This Document*

Type of data	T.E. deflection, deg			Mach number						
	Full Span	Inb'd	Outb'd	0.40	0.70	0.85	0.95	1.00	1.05	Several
<b>Wing</b>										
Flat wing	0.0	—	—			44				
Twisted wing	0.0	—	—			45				
Cambered-twisted wing										
Fin off	0.0	—	—			46				
	8.3	—	—			53				
Fin on	0.0	—	—			47				
Incremental twist	0.0	—	—	48						
Incremental camber	0.0	—	—	49						
Incremental camber and twist	0.0	—	—	50						
Increment due to wing fin	0.0	—	—	51						
<b>Body</b>										
Flat wing	0.0	—	—			52				
Cambered-twisted wing, fin off	8.3	—	—			54				

Table 12.—Summary of Additional Theory-to-Experiment Comparisons (NASA CR-165703)

Type of data	T.E. deflection, deg			Mach number						
	Full Span	Inb'd	Outb'd	0.40	0.70	0.85	0.95	1.00	1.05	Several
Wing										
Flat wing	0.0	—	—	X		X*			X	
Twisted wing	0.0	—	—	X		X*			X	
Cambered, twisted wing, fin off	0.0	—	—	X		X*			X	
	8.3	—	—	X		X*			X	
Cambered-twisted wing, fin on	0.0	—	—	X		X*			X	
Incremental twist	0.0	—	—	X*		X			X	
Incremental camber	0.0	—	—	X*		X			X	
Incremental camber and twist	0.0	—	—	X*		X			X	
Incremental effect of a wing fin, cambered-twisted wing	0.0	—	—	X*		X			X	
Body										
Flat wing	0.0	—	—	X		X*			X	
Cambered-twisted wing, fin off	8.3	—	—	X		X*			X	

\*Included in summary document, NASA CR-3434

increment at  $M = 0.40$ , all three attached-flow theories can be evaluated. At  $\alpha = 0^\circ$  they all predict the increment very well. FLEXSTAB, being a linear theory, predicts the same increment at all angles of attack, which is not the case in the experimental data, even on the lower surface. PAN AIR and TEA-230, with their exact on-the-surface boundary conditions, predict the lower surface pressure increments quite well at all angles of attack shown. The difference in the position of the vortex on the upper surface of the two wing shapes is apparent in the incremental experimental data; none of the attached-flow theories predict this.

The increment due to camber alone is obtained by subtracting the data for the twisted wing from that of the cambered-twisted wing. These data are shown in figure 49. FLEXSTAB and PAN AIR (TEA-230 data not available) predict the increment very well at  $\alpha = 0^\circ$ , as would be expected from examining the data at  $\alpha = 0^\circ$  in figures 45 and 46 (predictions at all Mach numbers were similar). At  $\alpha = 8^\circ$ , although the lower surface predictions are good, the shift in vortex position on the upper surface is not predicted.

Figure 50 shows the combined camber-twist increment (subtracting flat-wing data from cambered-twisted-wing data). The predictions at  $\alpha = 0^\circ$  are again good. The mid-span station at  $\alpha = 8^\circ$  tends to look a little better for the combined increment than it did for either twist or camber alone. This is because the position of the vortex on the flat and cambered-twisted wings is more nearly the same, while the position on the twisted wing is shifted.

These data clearly show that the attached-flow methods are no better at predicting incremental pressures due to aeroelastic deformation when the flow is separated than they are in predicting the absolute pressure level. The use of attached-flow methods is clearly restricted to conditions, or at least regions of the wing, where attached flow exists.

## **PREDICTION OF INCREMENT DUE TO WING FIN**

In addition to the increments due to change in wing shape, the effect of adding a vertical fin to the cambered-twisted wing was obtained and is shown in figure 51. Theoretical predictions of the pressures with the fin on are limited to the PAN AIR method. These figures show that there is no change in pressure on the inboard portion of the wing due to adding the fin, either experimentally or as shown by PAN AIR. For the Mach number angle-of-attack combinations where the flow is still attached, PAN AIR predicts the increment well. The fin, however has a large effect on the position and strength of the vortex. It is evident from figure 51 that the vortex has started at  $8^\circ$  angle of attack and that the predictions would no longer be useful at this or larger angles of attack.

## **BODY PRESSURE DISTRIBUTIONS**

Longitudinal pressure distributions on the body are shown in figure 52 for the flat wing configuration. At angles of attack up to and including  $8^\circ$ , the theoretical predictions of PAN AIR and TEA-230 are very good. Even at  $12^\circ$  the predictions on the side and bottom of the body are very good at this Mach number (0.40).

## **PREDICTION OF DATA FOR FULL-SPAN TRAILING-EDGE CONTROL SURFACE DEFLECTION**

Prediction of pressure distributions for the cambered-twisted wing (fin off) with the trailing-edge control surface deflected full span  $8.3^\circ$  are shown in figure 53 for the wing and figure 54 for the body.

## CONCLUDING REMARKS

The experimental data obtained in this contract add to the original data base accumulated in previous contracts. This data base allows testing of current theoretical methods as well as newly-formulated ones. As the leading-edge vortex is well formed on this configuration, the data base is particularly valuable for testing separated-flow theories.

The previous discussion has shown that the arrow-wing configuration of this study is dominated by leading-edge vortex flow at moderate and high angles of attack. Attached-flow methods are very good at low angles of attack typical of cruise conditions (load factor one). At critical structural and control design conditions, which involve large angles of attack and/or large control surface deflections, the attached-flow theories are inadequate. Examination of the theoretical incremental load caused by a change in shape, shows that attached-flow theories can be used to provide an aeroelastic increment to the rigid experimental data only at small angles of attack.

Boeing Commercial Airplane Company

P.O. Box 3707

Seattle, Washington 98124

July 1980

## **APPENDIX A**

### **DETAILED TEST LOG**

All test points for which pressure and force data were recorded are listed in tables A-1 through A-3. These tables include normal force and pitching moment coefficients obtained from strain gage measurements and by integrating the pressure data. Each test point is identified as a unique number within the test by the analysis number, where:

$$\text{ANALYSIS NUMBER} = 100 (\text{RUN NUMBER}) + \text{POSITION IN RUN}$$

Tables A-4 and A-5 list the points at which predicted pressure data are available from FLEXSTAB. For convenience, 1000 has been added to the run number of the corresponding experimental condition to obtain the theoretical test point number. An increment of 2000 has been added to obtain the run number for the TEA-230 results. Tables A-6 through A-9 are listings for PAN AIR data. An increment of 3000 has been added to obtain the run number for the PAN AIR results.

Table A-1.—Experimental Data Test Point Log. Twisted Wing, Fin Off

(a) T.E. Deflection, Full Span = 0.0°

Analysis number	Mach number	Dynamic pressure, kN/m <sup>2</sup> (psf)	Angle of attack, deg	Normal force coefficient, bal (integ press.)	Pitching moment coefficient, bal (integ press.)
1007	1.05	39.0(814)	-7.76	-.414(-.402)	.117(.110)
1008	1.05	39.0(814)	-5.84	-.330(-.317)	.101(.093)
1009	1.05	38.9(813)	-3.85	-.241(-.230)	.081(.073)
1010	1.05	39.0(815)	-1.89	-.154(-.149)	.058(.053)
1011	1.05	39.0(814)	-.05	-.076(-.075)	.036(.031)
1012	1.05	39.0(814)	2.01	.002(.001)	.016(.011)
1013	1.05	39.0(815)	4.00	.074(.069)	-.001(-.003)
1014	1.05	39.0(815)	4.51	.093(.086)	-.005(-.007)
1015	1.05	39.0(815)	6.01	.152(.145)	-.021(-.023)
1016	1.05	39.0(814)	7.97	.244(.232)	-.046(-.046)
1017	1.05	39.0(815)	9.95	.342(.324)	-.068(-.065)
1018	1.05	39.1(816)	11.87	.433(.411)	-.085(-.078)
1019	1.05	39.0(815)	13.82	.520(.500)	-.099(-.090)
1020	1.05	39.0(814)	15.81	.609(.584)	-.115(-.103)
1101	1.00	37.5(783)	-7.83	-.417(-.405)	.116(.106)
1102	1.00	37.5(784)	-5.84	-.329(-.315)	.099(.089)
1103	1.00	37.6(784)	-3.88	-.239(-.229)	.078(.069)
1104	1.00	37.6(785)	-1.87	-.150(-.144)	.054(.048)
1105	1.00	37.6(785)	.05	-.071(-.067)	.033(.027)
1106	1.00	37.6(785)	2.05	.003(.003)	.016(.011)
1107	1.00	37.6(785)	4.08	.074(.071)	.001(-.002)
1108	1.00	37.5(783)	4.57	.092(.088)	-.003(-.005)
1110	1.00	37.6(784)	6.00	.147(.142)	-.017(-.019)
1111	1.00	37.5(784)	7.92	.237(.228)	-.041(-.043)
1112	1.00	37.5(784)	9.87	.334(.321)	-.063(-.063)
1113	1.00	37.6(784)	11.84	.428(.409)	-.080(-.074)
1114	1.00	37.6(785)	13.78	.519(.502)	-.094(-.088)
1115	1.00	37.6(785)	15.73	.606(.583)	-.106(-.098)
1201	.95	35.9(751)	-7.81	-.412(-.400)	.107(.099)
1202	.95	35.9(749)	-5.84	-.321(-.309)	.090(.083)
1203	.95	35.9(750)	-3.89	-.234(-.223)	.072(.064)
1204	.95	35.9(750)	-1.90	-.147(-.141)	.051(.046)
1205	.95	35.9(751)	-.01	-.072(-.069)	.032(.027)
1206	.95	35.9(750)	2.03	.001(.000)	.015(.012)
1207	.95	36.0(751)	4.01	.069(.066)	.002(-.000)
1208	.95	35.9(749)	4.51	.086(.082)	-.001(-.004)
1209	.95	35.9(750)	5.98	.141(.135)	-.014(-.016)
1210	.95	35.9(749)	7.93	.226(.218)	-.035(-.036)
1211	.95	35.9(749)	9.88	.321(.308)	-.055(-.054)
1212	.95	35.9(750)	11.88	.418(.398)	-.072(-.067)
1214	.95	35.9(750)	13.86	.515(.495)	-.088(-.081)
1215	.95	35.9(750)	15.74	.606(.583)	-.102(-.093)

Analysis number	Mach number	Dynamic pressure, kN/m <sup>2</sup> (psf)	Angle of attack, deg	Normal force coefficient, bal (integ press.)	Pitching moment coefficient, bal (integ press.)
1310	.85	32.0(668)	-7.75	-.390(-.375)	.095(.088)
1311	.85	32.0(668)	-5.81	-.306(-.291)	.081(.074)
1312	.85	32.0(668)	-3.85	-.222(-.209)	.066(.071)
1313	.85	32.0(669)	-1.88	-.140(-.136)	.047(.044)
1314	.85	32.0(669)	.11	-.065(-.062)	.028(.024)
1315	.85	32.0(669)	2.07	.003(.003)	.013(.011)
1316	.85	32.0(668)	4.02	.069(.065)	.001(.000)
1317	.85	32.0(668)	4.50	.085(.080)	-.002(-.003)
1318	.85	32.0(668)	6.02	.137(.130)	-.013(-.013)
1319	.85	32.0(668)	7.97	.218(.209)	-.034(-.033)
1320	.85	32.0(669)	9.91	.310(.294)	-.052(-.050)
1321	.85	32.0(668)	11.92	.403(.382)	-.064(-.062)
1322	.85	32.0(669)	13.92	.499(.476)	-.077(-.071)
1323	.85	32.0(669)	15.82	.589(.566)	-.088(-.079)
1324	.85	32.1(670)	.12	-.063(-.060)	.027(.024)
1401	.70	25.1(524)	-7.75	-.376(-.360)	.090(.084)
1402	.70	25.0(523)	-5.79	-.293(-.278)	.077(.070)
1403	.70	25.1(524)	-3.85	-.212(-.205)	.062(.058)
1404	.70	25.1(523)	-1.90	-.134(-.130)	.044(.042)
1405	.70	25.1(524)	.11	-.062(-.059)	.026(.023)
1406	.70	25.1(524)	2.06	.004(.003)	.013(.012)
1407	.70	25.1(524)	4.05	.068(.064)	.002(.000)
1408	.70	25.1(524)	4.50	.083(.079)	-.001(-.002)
1409	.70	25.1(524)	5.99	.133(.126)	-.011(-.011)
1410	.70	25.1(524)	8.01	.210(.204)	-.029(-.033)
1411	.70	25.1(524)	9.91	.301(.287)	-.050(-.049)
1412	.70	25.1(524)	11.92	.392(.373)	-.063(-.060)
1413	.70	25.1(525)	13.93	.484(.464)	-.074(-.070)
1414	.70	25.1(525)	15.86	.575(.552)	-.083(-.076)
1501	.40	10.2(212)	-7.75	-.362(-.350)	.087(.081)
1502	.40	10.2(213)	-5.79	-.279(-.277)	.074(.074)
1503	.40	10.1(211)	-3.81	-.200(-.197)	.058(.057)
1504	.40	10.1(212)	-1.84	-.126(-.124)	.039(.039)
1505	.40	10.1(212)	.15	-.058(-.057)	.024(.022)
1506	.40	10.1(212)	2.10	.006(.003)	.012(.011)
1507	.40	10.1(210)	4.10	.069(.064)	.001(.001)
1508	.40	10.1(212)	4.49	.081(.077)	-.002(-.002)
1509	.40	10.1(212)	6.07	.132(.124)	-.011(-.010)
1510	.40	10.2(214)	8.01	.198(.189)	-.025(-.027)
1511	.40	10.2(212)	10.04	.288(.272)	-.049(-.045)
1512	.40	10.2(213)	11.95	.381(.358)	-.067(-.062)
1513	.40	10.1(210)	13.93	.470(.445)	-.079(-.072)
1514	.40	10.2(214)	15.92	.564(.537)	-.090(-.083)

Table A-1.—(Continued)

(b) T.E. Deflection, Inboard = 8.3°, Outboard = 0.0°

Analysis number	Mach number	Dynamic pressure, kN/m <sup>2</sup> (psf)	Angle of attack, deg	Normal force coefficient, bal (integ press.)	Pitching moment coefficient, bal (integ press.)
1613	1.05	39.1(816)	-7.75	-.279(-.270)	.042(.038)
1614	1.05	39.1(816)	-5.80	-.196(-.183)	.025(.019)
1615	1.05	39.1(816)	-3.86	-.111(-.105)	.007(.004)
1616	1.05	39.0(815)	-1.91	-.027(-.025)	-.014(-.016)
1617	1.05	39.0(815)	.05	.050(.047)	-.034(-.035)
1618	1.05	39.0(815)	2.01	.120(.114)	-.050(-.049)
1619	1.05	39.1(816)	4.01	.193(.184)	-.068(-.068)
1620	1.05	39.0(815)	4.50	.212(.203)	-.074(-.072)
1621	1.05	39.1(816)	6.00	.272(.263)	-.091(-.091)
1622	1.05	39.0(815)	7.96	.358(.342)	-.111(-.106)
1623	1.05	39.0(815)	9.91	.446(.425)	-.125(-.119)
1624	1.05	39.1(816)	11.87	.532(.508)	-.139(-.131)
1625	1.05	39.0(815)	13.82	.610(.591)	-.147(-.141)
1626	1.05	39.0(815)	15.82	.689(.663)	-.156(-.145)
1701	.95	35.9(750)	-7.80	-.266(-.255)	.034(.027)
1702	.95	36.0(752)	-5.84	-.182(-.171)	.022(.015)
1703	.95	36.0(751)	-3.89	-.100(-.095)	.009(.004)
1704	.95	36.0(751)	-1.19	.009(.011)	-.017(-.021)
1705	.95	35.9(750)	.06	.051(.052)	-.026(-.030)
1706	.95	36.0(752)	2.01	.118(.113)	-.040(-.041)
1707	.95	36.0(752)	4.01	.188(.182)	-.055(-.056)
1708	.95	35.9(751)	4.51	.206(.200)	-.061(-.062)
1709	.95	36.0(751)	5.97	.262(.252)	-.075(-.074)
1710	.95	36.0(752)	7.92	.348(.340)	-.098(-.100)
1711	.95	36.0(751)	9.87	.444(.432)	-.120(-.119)
1712	.95	36.0(751)	11.88	.536(.513)	-.134(-.127)
1713	.95	36.0(751)	13.84	.622(.603)	-.146(-.139)
1714	.95	35.9(751)	15.74	.700(.673)	-.151(-.140)
1801	.85	32.1(670)	-7.74	-.253(-.243)	.033(.027)
1802	.85	32.1(670)	-5.80	-.174(-.163)	.023(.015)
1803	.85	32.1(671)	-3.85	-.096(-.095)	.010(.007)
1804	.85	32.1(671)	-1.89	-.019(-.017)	-.008(-.012)
1805	.85	32.1(669)	.02	.046(.046)	-.021(-.025)
1806	.85	32.1(670)	2.06	.113(.110)	-.034(-.036)
1807	.85	32.1(671)	4.01	.179(.172)	-.047(-.048)
1808	.85	32.1(671)	4.51	.197(.190)	-.052(-.053)
1809	.85	32.1(671)	6.01	.253(.245)	-.066(-.067)
1810	.85	32.1(671)	7.97	.334(.321)	-.086(-.085)
1811	.85	32.1(670)	9.92	.430(.413)	-.108(-.105)
1812	.85	32.0(669)	11.91	.528(.505)	-.125(-.121)
1813	.85	32.1(671)	13.88	.623(.596)	-.140(-.131)
1814	.85	32.1(670)	15.84	.709(.682)	-.148(-.137)

Analysis number	Mach number	Dynamic pressure, kN/m <sup>2</sup> (psf)	Angle of attack, deg	Normal force coefficient, bal (integ press.)	Pitching moment coefficient, bal (integ press.)
1901	.70	25.1(524)	-7.75	-.245(-.233)	.035(.029)
1902	.70	25.1(524)	-5.80	-.167(-.160)	.025(.020)
1903	.70	25.1(524)	-3.85	-.091(-.089)	.012(.009)
1904	.70	25.1(524)	-1.90	-.018(-.016)	-.006(-.010)
1906	.70	25.1(525)	.02	.045(.044)	-.018(-.022)
1907	.70	25.1(525)	2.05	.111(.106)	-.030(-.032)
1908	.70	25.1(525)	4.06	.176(.168)	-.043(-.043)
1909	.70	25.2(525)	4.50	.191(.182)	-.046(-.046)
1910	.70	25.1(525)	6.01	.245(.236)	-.059(-.062)
1911	.70	25.1(525)	8.01	.322(.308)	-.078(-.077)
1912	.70	25.1(525)	9.91	.414(.397)	-.098(-.097)
1913	.70	25.1(525)	11.91	.512(.491)	-.116(-.113)
1914	.70	25.1(525)	13.92	.607(.582)	-.129(-.124)
1915	.70	25.1(525)	15.87	.698(.664)	-.140(-.128)
2001	.40	10.2(213)	-7.75	-.236(-.229)	.043(.033)
2002	.40	10.2(213)	-5.80	-.159(-.163)	.032(.027)
2003	.40	10.2(214)	-3.80	-.084(-.089)	.017(.014)
2004	.40	10.2(213)	-1.85	-.016(-.016)	.000(-.008)
2005	.40	10.2(213)	.16	.048(.045)	-.012(-.019)
2006	.40	10.2(213)	2.11	.109(.103)	-.023(-.028)
2007	.40	10.2(213)	4.11	.172(.162)	-.034(-.038)
2008	.40	10.2(213)	4.50	.182(.174)	-.037(-.041)
2009	.40	10.2(213)	6.06	.234(.226)	-.048(-.054)
2010	.40	10.2(213)	8.01	.303(.295)	-.064(-.072)
2011	.40	10.2(213)	10.01	.392(.376)	-.087(-.089)
2012	.40	10.2(213)	11.94	.488(.468)	-.107(-.109)
2013	.40	10.2(214)	13.92	.582(.557)	-.120(-.121)
2014	.40	10.2(212)	15.92	.677(.649)	-.132(-.131)



Table A-1.—(Continued)

(c) T.E. Deflection, Full Span = 8.3°

Analysis number	Mach number	Dynamic pressure, kN/m <sup>2</sup> (psf)	Angle of attack, deg	Normal force coefficient, bal (integ press.)	Pitching moment coefficient, bal (integ press.)
2113	1.05	39.2(818)	-7.75	-.262(-.255)	.027(.024)
2114	1.05	39.1(817)	-5.80	-.175(-.163)	.008(.000)
2115	1.05	39.1(817)	-3.85	-.087(-.082)	-.014(-.017)
2116	1.05	39.2(818)	-1.90	-.002(.001)	-.036(-.041)
2117	1.05	39.2(818)	.05	.075(.073)	-.057(-.059)
2118	1.05	39.2(818)	2.01	.143(.139)	-.072(-.073)
2119	1.05	39.2(818)	4.00	.216(.209)	-.089(-.091)
2120	1.05	39.1(817)	4.50	.234(.228)	-.094(-.095)
2121	1.05	39.2(818)	6.02	.293(.284)	-.110(-.110)
2122	1.05	39.2(818)	7.96	.371(.355)	-.123(-.117)
2123	1.05	39.1(817)	9.92	.455(.436)	-.134(-.130)
2124	1.05	39.1(817)	11.86	.538(.516)	-.145(-.137)
2125	1.05	39.1(817)	13.83	.616(.595)	-.153(-.144)
2126	1.05	39.1(817)	15.82	.694(.666)	-.160(-.146)
2201	.95	36.0(752)	-7.79	-.247(-.238)	.017(.012)
2202	.95	36.1(753)	-5.84	-.159(-.149)	.002(-.005)
2203	.95	36.1(753)	-3.89	-.075(-.069)	-.014(-.019)
2204	.95	36.0(753)	-1.90	.011(.014)	-.036(-.039)
2205	.95	36.0(753)	.06	.081(.082)	-.052(-.055)
2206	.95	36.0(752)	2.01	.146(.143)	-.065(-.066)
2207	.95	36.0(753)	4.02	.215(.210)	-.080(-.080)
2208	.95	36.0(753)	4.52	.233(.227)	-.084(-.085)
2209	.95	36.0(753)	5.97	.287(.279)	-.097(-.097)
2210	.95	36.1(753)	7.93	.369(.365)	-.117(-.120)
2211	.95	36.0(752)	9.87	.455(.444)	-.130(-.129)
2212	.95	36.0(752)	11.87	.541(.521)	-.140(-.134)
2213	.95	36.0(752)	13.83	.623(.607)	-.148(-.144)
2214	.95	36.0(752)	15.74	.700(.675)	-.152(-.142)
2301	.85	32.2(672)	-7.74	-.232(-.223)	.015(.011)
2302	.85	32.2(672)	-5.79	-.148(-.137)	.001(-.006)
2303	.85	32.1(670)	-3.85	-.066(-.063)	-.015(-.018)
2304	.85	32.2(672)	-1.90	.012(.015)	-.034(-.038)
2305	.85	32.1(670)	-.00	.077(.077)	-.048(-.051)
2306	.85	32.2(672)	2.06	.144(.142)	-.061(-.063)
2307	.85	32.1(670)	4.01	.210(.203)	-.074(-.073)
2308	.85	32.1(671)	4.51	.227(.220)	-.078(-.078)
2309	.85	32.2(672)	6.02	.282(.273)	-.090(-.091)
2310	.85	32.1(671)	7.97	.359(.348)	-.107(-.108)
2311	.85	32.1(671)	9.92	.449(.432)	-.123(-.120)
2312	.85	32.2(671)	11.92	.537(.515)	-.132(-.129)
2313	.85	32.2(672)	13.87	.622(.600)	-.141(-.134)
2314	.85	32.1(671)	15.83	.703(.683)	-.144(-.138)

Analysis number	Mach number	Dynamic pressure, kN/m <sup>2</sup> (psf)	Angle of attack, deg	Normal force coefficient, bal (integ press.)	Pitching moment coefficient, bal (integ press.)
2401	.70	25.3(528)	-7.75	-.221(-.209)	.015(.011)
2405	.70	25.2(526)	-5.80	-.138(-.132)	.001(-.002)
2406	.70	25.2(526)	-3.85	-.060(-.057)	-.014(-.017)
2407	.70	25.1(525)	-1.91	.015(.018)	-.033(-.036)
2408	.70	25.2(526)	.01	.078(.078)	-.046(-.048)
2409	.70	25.2(527)	2.05	.143(.140)	-.058(-.059)
2410	.70	25.2(527)	4.05	.208(.200)	-.069(-.069)
2411	.70	25.2(527)	4.51	.223(.215)	-.073(-.073)
2412	.70	25.2(527)	6.01	.275(.268)	-.084(-.087)
2413	.70	25.1(525)	8.00	.350(.337)	-.101(-.100)
2414	.70	25.2(526)	9.91	.439(.422)	-.118(-.115)
2416	.70	25.2(527)	11.91	.527(.506)	-.129(-.124)
2417	.70	25.2(526)	13.92	.613(.591)	-.134(-.130)
2418	.70	25.1(525)	15.87	.694(.668)	-.136(-.131)
2501	.40	10.2(214)	-7.75	-.208(-.203)	.020(.013)
2502	.40	10.2(214)	-5.80	-.127(-.130)	.005(.003)
2503	.40	10.2(214)	-3.80	-.052(-.052)	-.010(-.014)
2504	.40	10.2(213)	-1.85	.017(.018)	-.027(-.034)
2505	.40	10.2(212)	.15	.080(.080)	-.038(-.045)
2506	.40	10.2(213)	2.11	.141(.139)	-.049(-.055)
2507	.40	10.2(213)	4.10	.202(.195)	-.060(-.065)
2508	.40	10.2(212)	4.50	.215(.209)	-.063(-.068)
2509	.40	10.2(213)	6.06	.264(.260)	-.072(-.080)
2510	.40	10.2(213)	8.01	.330(.324)	-.086(-.095)
2511	.40	10.3(214)	10.02	.418(.407)	-.108(-.112)
2512	.40	10.2(213)	11.95	.512(.490)	-.125(-.125)
2513	.40	10.2(213)	13.92	.597(.573)	-.132(-.132)
2514	.40	10.3(214)	15.93	.685(.659)	-.138(-.138)

Table A-1.—(Concluded)

(d) T.E. Deflection, Inboard =  $0.0^\circ$ , Outboard =  $8.3^\circ$ 

Analysis number	Mach number	Dynamic pressure, kN/m <sup>2</sup> (psf)	Angle of attack, deg	Normal force coefficient, bal (integ press.)	Pitching moment coefficient, bal (integ press.)
2613	1.05	39.2(818)	-7.75	-.403(-.392)	.108(.100)
2614	1.05	39.2(818)	-5.80	-.313(-.302)	.087(.079)
2615	1.05	39.3(820)	-3.85	-.219(-.210)	.063(.054)
2616	1.05	39.2(819)	-1.90	-.129(-.123)	.035(.027)
2617	1.05	39.2(819)	.06	-.046(-.046)	.010(.006)
2618	1.05	39.2(819)	2.00	.028(.025)	-.009(-.012)
2619	1.05	39.2(819)	4.00	.100(.094)	-.024(-.026)
2620	1.05	39.2(819)	4.51	.118(.111)	-.028(-.029)
2621	1.05	39.2(819)	6.00	.178(.169)	-.044(-.045)
2622	1.05	39.2(818)	7.97	.265(.251)	-.064(-.063)
2623	1.05	39.2(818)	9.90	.349(.324)	-.079(-.073)
2624	1.05	39.2(819)	11.87	.444(.420)	-.095(-.088)
2625	1.05	39.2(818)	13.82	.533(.511)	-.110(-.101)
2626	1.05	39.2(818)	15.82	.624(.597)	-.127(-.116)
2701	.95	36.0(752)	-7.80	-.398(-.389)	.097(.089)
2702	.95	36.0(752)	-5.84	-.302(-.289)	.074(.065)
2703	.95	36.1(753)	-3.89	-.209(-.199)	.051(.043)
2704	.95	36.1(753)	-1.89	-.119(-.113)	.027(.021)
2705	.95	36.1(753)	.06	-.040(-.037)	.006(.001)
2706	.95	36.1(753)	2.01	.029(.028)	-.009(-.013)
2707	.95	36.1(754)	4.02	.098(.093)	-.022(-.025)
2708	.95	36.1(754)	4.52	.115(.110)	-.025(-.027)
2709	.95	36.1(755)	5.97	.168(.161)	-.037(-.039)
2710	.95	36.1(754)	7.92	.251(.241)	-.056(-.058)
2711	.95	36.1(754)	9.87	.339(.324)	-.070(-.068)
2712	.95	36.1(754)	11.87	.429(.404)	-.081(-.073)
2713	.95	36.0(753)	13.83	.524(.501)	-.095(-.087)
2714	.95	36.0(752)	15.74	.618(.593)	-.110(-.101)
2801	.85	32.2(672)	-7.75	-.375(-.363)	.083(.076)
2802	.85	32.1(671)	-5.79	-.283(-.270)	.064(.056)
2803	.85	32.1(671)	-3.84	-.196(-.191)	.045(.041)
2804	.85	32.2(672)	-1.89	-.111(-.107)	.023(.019)
2805	.85	32.2(672)	-.09	-.042(-.039)	.005(.000)
2806	.85	32.2(672)	2.07	.032(.031)	-.010(-.014)
2807	.85	32.2(673)	4.01	.096(.092)	-.021(-.024)
2808	.85	32.2(673)	4.52	.113(.108)	-.025(-.027)
2809	.85	32.2(671)	6.01	.165(.158)	-.035(-.038)
2810	.85	32.2(671)	7.97	.244(.235)	-.054(-.056)
2811	.85	32.2(673)	9.92	.330(.314)	-.067(-.066)
2812	.85	32.2(673)	11.92	.416(.393)	-.074(-.070)
2813	.85	32.3(674)	13.87	.506(.480)	-.084(-.077)
2814	.85	32.1(671)	15.83	.600(.576)	-.095(-.087)

Analysis number	Mach number	Dynamic pressure, kN/m <sup>2</sup> (psf)	Angle of attack, deg	Normal force coefficient, bal (integ press.)	Pitching moment coefficient, bal (integ press.)
2901	.70	25.2(527)	-7.75	-.357(-.343)	.076(.070)
2902	.70	25.1(525)	-5.80	-.268(-.255)	.059(.051)
2903	.70	25.3(528)	-3.85	-.183(-.179)	.040(.035)
2904	.70	25.3(528)	-1.90	-.104(-.102)	.021(.017)
2905	.70	25.3(528)	.01	-.034(-.032)	.003(-.001)
2906	.70	25.3(528)	2.06	.032(.032)	-.009(-.014)
2907	.70	25.3(528)	4.05	.098(.093)	-.021(-.024)
2908	.70	25.2(526)	4.50	.112(.107)	-.024(-.026)
2909	.70	25.2(527)	6.01	.163(.156)	-.034(-.036)
2910	.70	25.2(526)	8.01	.237(.231)	-.051(-.056)
2911	.70	25.3(529)	9.92	.324(.309)	-.067(-.066)
2912	.70	25.3(528)	11.91	.408(.387)	-.075(-.071)
2913	.70	25.3(528)	13.93	.497(.475)	-.082(-.078)
2914	.70	25.2(526)	15.87	.586(.560)	-.090(-.083)
3001	.40	10.2(214)	-7.75	-.338(-.329)	.074(.064)
3002	.40	10.2(213)	-5.80	-.251(-.250)	.056(.052)
3003	.40	10.1(212)	-3.80	-.170(-.166)	.038(.032)
3004	.40	10.2(213)	-1.85	-.094(-.093)	.020(.014)
3005	.40	10.2(212)	.15	-.025(-.024)	.004(-.003)
3006	.40	10.2(213)	2.11	.037(.033)	-.007(-.013)
3007	.40	10.1(212)	4.11	.100(.095)	-.018(-.024)
3008	.40	10.2(213)	4.51	.112(.107)	-.020(-.025)
3010	.40	10.2(212)	6.05	.161(.154)	-.029(-.035)
3011	.40	10.2(212)	8.01	.228(.221)	-.044(-.052)
3012	.40	10.2(212)	10.02	.316(.302)	-.066(-.068)
3014	.40	10.2(212)	11.96	.403(.382)	-.080(-.080)
3015	.40	10.3(214)	13.92	.489(.464)	-.087(-.084)
3016	.40	10.3(215)	15.92	.579(.552)	-.095(-.091)

Table A-2.—Experimental Data Test Point Log. Cambered-twisted Wing, Fin Off

(a) T.E. Deflection, Full Span = 0.0°

Analysis number	Mach number	Dynamic pressure, kN/m <sup>2</sup> (psf)	Angle of attack, deg	Normal force coefficient, bal (integ press.)	Pitching moment coefficient, bal (integ press.)
3704	1.05	39.1(817)	-7.74	-.450(-.435)	.160(.149)
3705	1.05	39.1(817)	-5.78	-.367(-.351)	.146(.133)
3706	1.05	39.1(817)	-3.84	-.284(-.281)	.126(.124)
3707	1.05	39.1(817)	-1.88	-.204(-.212)	.104(.108)
3709	1.05	39.1(817)	.07	-.125(-.128)	.081(.079)
3710	1.05	39.1(817)	2.02	-.048(-.052)	.061(.059)
3711	1.05	39.1(817)	3.99	.033(.025)	.040(.038)
3712	1.05	39.1(818)	4.51	.056(.048)	.033(.031)
3714	1.05	39.1(817)	6.03	.128(.117)	.013(.012)
3715	1.05	39.1(817)	7.95	.220(.208)	-.011(-.009)
3716	1.05	39.1(817)	9.89	.316(.300)	-.034(-.034)
3717	1.05	39.2(818)	11.86	.410(.387)	-.053(-.052)
3718	1.05	39.1(817)	13.81	.501(.478)	-.071(-.064)
3719	1.05	39.1(817)	15.84	.596(.571)	-.090(-.080)
3801	1.00	37.7(787)	-7.81	-.458(-.437)	.160(.143)
3802	1.00	37.6(786)	-5.80	-.369(-.347)	.144(.125)
3803	1.00	37.6(786)	-3.88	-.285(-.275)	.122(.113)
3804	1.00	37.6(786)	-1.89	-.206(-.210)	.101(.101)
3805	1.00	37.7(787)	-.01	-.133(-.134)	.082(.077)
3806	1.00	37.7(788)	2.02	-.056(-.060)	.064(.060)
3807	1.00	37.7(788)	4.02	.023(.018)	.045(.041)
3808	1.00	37.7(787)	4.52	.045(.040)	.039(.035)
3809	1.00	37.7(788)	5.91	.111(.103)	.022(.020)
3810	1.00	37.6(786)	7.93	.207(.193)	-.002(-.001)
3811	1.00	37.7(787)	9.87	.305(.293)	-.025(-.026)
3814	1.00	37.7(787)	11.81	.403(.383)	-.046(-.047)
3817	1.00	37.6(786)	13.80	.500(.476)	-.064(-.059)
3819	1.00	37.7(788)	15.84	.597(.575)	-.082(-.077)
3905	.95	36.0(752)	-7.79	-.460(-.439)	.157(.143)
3907	.95	36.0(751)	-5.85	-.367(-.341)	.135(.117)
3908	.95	36.0(752)	-3.88	-.281(-.270)	.114(.108)
3909	.95	35.9(750)	-1.90	-.202(-.207)	.093(.098)
3910	.95	36.0(751)	.06	-.127(-.125)	.074(.070)
3911	.95	36.0(751)	1.99	-.056(-.058)	.058(.056)
3912	.95	36.0(753)	4.00	.018(.010)	.042(.042)
3913	.95	36.0(752)	4.53	.041(.034)	.036(.036)
3914	.95	36.0(751)	5.96	.105(.094)	.021(.022)
3915	.95	36.0(752)	7.93	.193(.179)	.002(.004)
3916	.95	35.9(751)	9.87	.285(.277)	-.016(-.015)
3917	.95	36.1(753)	11.87	.387(.363)	-.035(-.033)
3918	.95	36.0(752)	13.83	.486(.460)	-.054(-.047)
3919	.95	36.0(752)	15.73	.585(.562)	-.074(-.067)

Analysis number	Mach number	Dynamic pressure, kN/m <sup>2</sup> (psf)	Angle of attack, deg	Normal force coefficient, bal (integ press.)	Pitching moment coefficient, bal (integ press.)
4001	.85	32.1(670)	-7.74	-.441(-.421)	.143(.132)
4002	.85	32.1(671)	-5.78	-.348(-.330)	.125(.112)
4003	.85	32.0(669)	-3.83	-.267(-.263)	.105(.105)
4004	.85	32.0(669)	-1.89	-.193(-.197)	.087(.090)
4005	.85	32.1(671)	.12	-.120(-.118)	.070(.065)
4006	.85	32.1(671)	2.06	-.052(-.054)	.055(.053)
4007	.85	32.1(670)	4.02	.017(.011)	.041(.041)
4008	.85	32.1(670)	4.52	.036(.028)	.037(.037)
4009	.85	32.2(672)	6.00	.099(.090)	.021(.021)
4010	.85	32.1(671)	7.96	.184(.171)	.003(.004)
4011	.85	32.2(671)	9.91	.274(.265)	-.014(-.012)
4012	.85	32.1(671)	11.92	.370(.347)	-.029(-.028)
4013	.85	32.1(670)	13.87	.463(.431)	-.042(-.037)
4014	.85	32.1(671)	15.83	.561(.534)	-.057(-.051)
4101	.70	25.2(526)	-7.75	-.425(-.394)	.138(.120)
4102	.70	25.1(524)	-5.79	-.332(-.311)	.116(.105)
4103	.70	25.1(524)	-3.86	-.258(-.262)	.099(.105)
4104	.70	25.2(526)	-1.89	-.185(-.188)	.081(.083)
4105	.70	25.2(526)	.09	-.118(-.116)	.066(.063)
4106	.70	25.2(526)	2.05	-.050(-.052)	.053(.050)
4107	.70	25.2(526)	4.05	.018(.013)	.040(.038)
4108	.70	25.1(525)	4.51	.033(.027)	.036(.035)
4109	.70	25.3(527)	6.01	.093(.085)	.021(.021)
4110	.70	25.3(528)	8.02	.179(.168)	.004(.004)
4111	.70	25.2(527)	9.91	.266(.248)	-.013(-.013)
4112	.70	25.1(525)	11.92	.357(.343)	-.027(-.025)
4113	.70	25.2(527)	13.94	.453(.429)	-.040(-.039)
4114	.70	25.2(527)	15.88	.546(.512)	-.051(-.049)
4301	.40	10.2(214)	-7.75	-.400(-.369)	.130(.110)
4302	.40	10.2(214)	-5.81	-.314(-.322)	.107(.116)
4303	.40	10.2(213)	-3.80	-.241(-.251)	.090(.097)
4304	.40	10.2(212)	-1.84	-.177(-.171)	.075(.070)
4305	.40	10.1(212)	.15	-.112(-.111)	.063(.059)
4306	.40	10.2(212)	2.11	-.048(-.049)	.050(.047)
4307	.40	10.2(212)	4.11	.019(.014)	.037(.036)
4308	.40	10.1(211)	4.51	.032(.026)	.034(.034)
4309	.40	10.2(213)	6.07	.091(.083)	.021(.020)
4310	.40	10.2(213)	8.00	.169(.159)	.003(.003)
4311	.40	10.2(212)	9.99	.255(.240)	-.013(-.012)
4312	.40	10.2(213)	10.00	.254(.239)	-.013(-.012)
4313	.40	10.2(212)	11.97	.345(.326)	-.029(-.026)
4314	.40	10.1(212)	13.90	.436(.413)	-.042(-.039)
4315	.40	10.2(213)	15.93	.534(.506)	-.054(-.050)

Table A-2.—(Continued)

(b) T.E. Deflection, Inboard = 8.3°, Outboard = 0.0°

Analysis number	Mach number	Dynamic pressure, kN/m <sup>2</sup> (psf)	Angle of attack, deg	Normal force coefficient, bal (integ press.)	Pitching moment coefficient, bal (integ press.)
5513	1.05	39.0(815)	-7.75	-.309(-.298)	.083( .077)
5514	1.05	39.0(814)	-5.81	-.224(-.212)	.067( .059)
5515	1.05	39.0(815)	-3.86	-.143(-.143)	.048( .049)
5516	1.05	39.0(815)	-1.92	-.065(-.063)	.027( .022)
5517	1.05	39.0(815)	.06	.007( .008)	.010( .006)
5518	1.05	39.0(814)	2.00	.078( .074)	-.007(-.009)
5519	1.05	39.0(815)	4.02	.159( .152)	-.030(-.030)
5520	1.05	39.0(815)	4.49	.178( .170)	-.036(-.036)
5521	1.05	39.0(814)	6.00	.247( .233)	-.055(-.052)
5522	1.05	39.0(815)	7.96	.338( .326)	-.077(-.075)
5523	1.05	39.0(813)	9.92	.429( .407)	-.097(-.090)
5524	1.05	39.0(814)	11.86	.515( .487)	-.111(-.105)
5526	1.05	39.0(814)	13.82	.595( .572)	-.122(-.116)
5528	1.05	39.1(816)	14.82	.610( .609)	.273(-.119)
5702	.40	10.1(211)	-7.75	-.271(-.248)	.125( .065)
5703	.40	10.2(214)	-5.81	-.190(-.196)	.088( .064)
5704	.40	10.2(212)	-3.83	-.123(-.113)	.057( .034)
5705	.40	10.2(213)	-1.87	-.063(-.058)	.029( .025)
5706	.40	10.2(213)	.13	-.000(-.002)	.000( .015)
5707	.40	10.1(212)	2.09	.062( .061)	-.029( .004)
5708	.40	10.1(212)	4.09	.129( .120)	-.060(-.008)
5709	.40	10.2(212)	4.47	.142( .133)	-.066(-.011)
5710	.40	10.1(211)	6.02	.199( .184)	-.092(-.022)
5711	.40	10.2(214)	7.98	.276( .264)	-.128(-.040)
5712	.40	10.2(212)	9.97	.365( .347)	-.170(-.056)
5713	.40	10.1(212)	11.91	.468( .434)	-.389(-.073)
5714	.40	10.1(211)	13.86	.835( .522)	-4.962(-.086)
5715	.40	10.2(213)	15.87	.928( .617)	-4.876(-.100)
5801	.95	35.9(749)	-7.74	-.227(-.282)	-1.107( .067)
5802	.95	35.9(749)	-5.77	-.139(-.198)	-1.168( .056)
5803	.95	35.9(749)	-3.87	-.058(-.137)	-1.207( .048)
5804	.95	35.8(748)	-1.18	.039(-.033)	-1.228( .018)
5805	.95	35.8(749)	.08	.084( .008)	-1.262( .010)
5806	.95	35.8(748)	2.04	.152( .071)	-1.286(-.002)
5807	.95	35.8(748)	4.04	.231( .143)	-1.340(-.019)
5808	.95	35.8(749)	4.56	.251( .165)	-1.336(-.025)
5809	.95	35.9(749)	6.00	.314( .223)	-1.352(-.039)
5810	.95	35.9(749)	7.97	.406( .310)	-1.369(-.061)
5811	.95	35.9(749)	9.91	.505( .411)	-1.469(-.083)
5812	.95	35.8(748)	11.90	.602( .490)	-1.484(-.097)
5813	.95	35.9(749)	13.86	.695( .583)	-1.548(-.111)
5814	.95	35.9(749)	16.11	.793( .677)	-1.616(-.119)

Analysis number	Mach number	Dynamic pressure, kN/m <sup>2</sup> (psf)	Angle of attack, deg	Normal force coefficient, bal (integ press.)	Pitching moment coefficient, bal (integ press.)
5901	.85	31.9(667)	-7.69	-.205(-.272)	-1.293( .067)
5902	.85	32.0(668)	-5.75	-.121(-.194)	-1.312( .058)
5903	.85	32.0(668)	-3.85	-.047(-.134)	-1.338( .046)
5904	.85	32.0(668)	-1.89	.022(-.058)	-1.388( .023)
5905	.85	32.0(668)	.04	.087( .004)	-1.395( .012)
5906	.85	32.0(668)	2.09	.156( .067)	-1.421( .000)
5907	.85	32.0(668)	4.04	.231( .134)	-1.486(-.014)
5908	.85	32.0(668)	4.55	.252( .155)	-1.495(-.020)
5909	.85	32.0(668)	6.03	.314( .211)	-1.530(-.033)
5910	.85	32.0(668)	8.03	.402( .296)	-1.552(-.052)
5911	.85	32.0(668)	9.96	.493( .391)	-1.604(-.070)
5912	.85	32.0(668)	11.91	.593( .474)	-1.637(-.088)
5913	.85	32.0(668)	13.91	.692( .561)	-1.668(-.097)
5914	.85	32.0(667)	15.86	.789( .658)	-1.756(-.110)

Table A-2.—(Continued)

(c) T.E. Deflection, Full Span = 8.3°

Analysis number	Mach number	Dynamic pressure, kN/m <sup>2</sup> (psf)	Angle of attack, deg	Normal force coefficient, bal (integ press.)	Pitching moment coefficient, bal (integ press.)
6107	1.05	38.9(812)	-7.68	-.292(-.281)	.136(.063)
6108	1.05	38.9(813)	-5.74	-.202(-.185)	.094(.036)
6109	1.05	39.0(814)	-3.80	-.115(-.111)	.054(.021)
6110	1.05	38.9(813)	-1.87	-.038(-.031)	.017(-.004)
6111	1.05	38.9(812)	.11	.036(.036)	-.017(-.019)
6112	1.05	38.9(813)	2.04	.107(.102)	-.050(-.034)
6113	1.05	38.9(813)	4.03	.187(.178)	-.087(-.054)
6114	1.05	38.9(813)	4.53	.208(.197)	-.097(-.059)
6116	1.05	38.9(812)	6.05	.277(.258)	-.129(-.070)
6117	1.05	38.9(813)	8.02	.362(.343)	-.168(-.088)
6118	1.05	38.9(812)	9.96	.449(.418)	-.209(-.098)
6119	1.05	38.9(812)	11.89	.532(.497)	-.247(-.112)
6121	1.05	38.9(812)	13.86	.613(.577)	-.285(-.118)
6201	.85	32.0(667)	-7.68	-.266(-.248)	.124(.049)
6202	.85	31.9(667)	-5.65	-.172(-.160)	.080(.032)
6203	.85	31.9(667)	-3.83	-.101(-.100)	.047(.019)
6204	.85	31.9(667)	-1.88	-.030(-.026)	.014(-.002)
6205	.85	31.9(667)	.01	.034(.033)	-.016(-.013)
6206	.85	32.0(668)	2.10	.103(.098)	-.048(-.025)
6207	.85	31.9(667)	4.04	.175(.164)	-.081(-.039)
6208	.85	32.0(668)	4.55	.195(.183)	-.091(-.044)
6209	.85	31.9(667)	6.05	.255(.238)	-.119(-.054)
6210	.85	31.9(667)	8.00	.338(.317)	-.157(-.069)
6211	.85	31.9(667)	9.95	.423(.404)	-.197(-.080)
6221	.85	31.9(667)	8.00	.338(.316)	-.157(-.068)
6222	.85	31.9(667)	9.98	.424(.405)	-.197(-.080)
6223	.85	31.9(667)	11.95	.516(.481)	-.240(-.092)
6224	.85	31.9(667)	13.89	.605(.562)	-.282(-.099)
6225	.85	32.0(668)	15.84	.694(.653)	-.323(-.106)
6401	.95	35.8(748)	-7.73	-.280(-.262)	.130(.050)
6402	.95	35.9(749)	-5.79	-.189(-.170)	.088(.031)
6403	.95	35.8(748)	-3.86	-.106(-.106)	.049(.021)
6404	.95	35.8(748)	-1.87	-.031(-.027)	.014(-.003)
6405	.95	35.8(748)	.09	.038(.038)	-.018(-.016)
6406	.95	35.8(749)	2.03	.106(.101)	-.050(-.027)
6407	.95	35.8(748)	4.05	.183(.172)	-.085(-.044)
6408	.95	35.8(749)	4.56	.204(.193)	-.095(-.049)
6409	.95	35.8(747)	5.99	.264(.248)	-.123(-.060)
6410	.95	35.8(748)	7.96	.352(.328)	-.164(-.076)
6411	.95	35.8(748)	9.91	.439(.420)	-.204(-.091)
6412	.95	35.8(749)	11.90	.531(.498)	-.247(-.104)
6413	.95	35.7(747)	13.87	.620(.587)	-.288(-.114)
6414	.95	35.8(748)	15.75	.701(.664)	-.326(-.118)

Analysis number	Mach number	Dynamic pressure, kN/m <sup>2</sup> (psf)	Angle of attack, deg	Normal force coefficient, bal (integ press.)	Pitching moment coefficient, bal (integ press.)
6501	.40	10.1(211)	-7.77	-.243(-.219)	.113(.042)
6502	.40	10.1(211)	-5.82	-.162(-.167)	.075(.040)
6503	.40	10.2(212)	-3.85	-.092(-.088)	.043(.013)
6504	.40	10.2(213)	-1.90	-.030(-.028)	.014(.000)
6505	.40	10.1(212)	.11	.034(.034)	-.016(-.011)
6506	.40	10.1(211)	2.07	.096(.090)	-.045(-.020)
6507	.40	10.2(213)	4.07	.164(.155)	-.076(-.035)
6508	.40	10.1(212)	4.46	.177(.166)	-.082(-.037)
6509	.40	10.1(211)	6.02	.233(.218)	-.108(-.046)
6511	.40	10.1(212)	7.96	.306(.290)	-.142(-.061)
6513	.40	10.2(213)	9.97	.390(.370)	-.181(-.073)
6514	.40	10.1(210)	11.70	.470(.442)	-.218(-.083)
6515	.40	10.2(212)	13.86	.569(.534)	-.264(-.093)
6516	.40	10.2(212)	15.88	.664(.625)	-.309(-.101)

Table A-2.—(Concluded)

(d) T.E. Deflection, Inboard =  $0.0^\circ$ , Outboard =  $8.3^\circ$ 

Analysis number	Mach number	Dynamic pressure, kN/m <sup>2</sup> (psf)	Angle of attack, deg	Normal force coefficient, bal (integ press.)	Pitching moment coefficient, bal (integ press.)
7704	1.05	38.8(810)	-7.69	-.444(-.426)	.207(.141)
7705	1.05	38.9(812)	-5.74	-.349(-.330)	.162(.115)
7706	1.05	38.8(810)	-3.82	-.262(-.251)	.122(.097)
7707	1.05	38.8(811)	-1.87	-.178(-.182)	.083(.082)
7708	1.05	38.8(811)	.10	-.095(-.096)	.044(.050)
7709	1.05	38.8(811)	2.05	-.019(-.021)	.009(.032)
7710	1.05	38.8(811)	4.03	.063(.055)	-.029(.013)
7711	1.05	38.8(811)	4.55	.087(.077)	-.040(.006)
7712	1.05	38.8(810)	6.05	.156(.143)	-.073(-.009)
7713	1.05	38.9(811)	8.01	.244(.228)	-.114(-.026)
7714	1.05	38.8(810)	9.94	.337(.312)	-.157(-.042)
7715	1.05	38.8(811)	11.88	.431(.397)	-.201(-.059)
7716	1.05	38.8(810)	13.85	.527(.493)	-.245(-.076)
7801	.85	31.8(665)	-7.70	-.422(-.401)	.197(.118)
7802	.85	31.8(665)	-5.76	-.323(-.301)	.150(.089)
7803	.85	31.8(665)	-3.81	-.239(-.229)	.111(.077)
7804	.85	31.9(666)	-1.87	-.162(-.161)	.075(.060)
7805	.85	31.8(664)	-.07	-.094(-.091)	.044(.040)
7806	.85	31.9(667)	2.09	-.017(-.019)	.008(.025)
7807	.85	31.9(666)	4.02	.051(.043)	-.024(.014)
7808	.85	31.9(665)	4.51	.070(.060)	-.032(.010)
7809	.85	31.9(666)	6.04	.133(.122)	-.062(-.004)
7810	.85	31.9(665)	8.01	.217(.199)	-.101(-.017)
7811	.85	31.9(666)	9.96	.302(.287)	-.140(-.027)
7812	.85	31.9(666)	11.93	.393(.358)	-.183(-.035)
7813	.85	31.8(665)	13.87	.488(.444)	-.227(-.045)
7814	.85	31.9(666)	15.83	.588(.548)	-.274(-.060)
7901	.95	35.7(746)	-7.76	-.450(-.427)	.210(.133)
7902	.95	35.7(745)	-5.79	-.345(-.314)	.161(.096)
7903	.95	35.7(746)	-3.86	-.257(-.238)	.120(.081)
7904	.95	35.7(745)	-1.88	-.173(-.174)	.080(.070)
7905	.95	35.7(746)	.08	-.095(-.093)	.044(.043)
7906	.95	35.7(746)	2.03	-.023(-.027)	.011(.030)
7907	.95	35.8(747)	4.04	.052(.043)	-.024(.016)
7908	.95	35.7(746)	4.52	.073(.064)	-.034(.011)
7909	.95	35.8(747)	6.00	.138(.124)	-.064(-.002)
7910	.95	35.7(746)	7.96	.223(.204)	-.104(-.016)
7911	.95	35.7(745)	9.90	.310(.293)	-.144(-.028)
7912	.95	35.7(745)	11.90	.409(.372)	-.190(-.038)
7913	.95	35.7(746)	13.85	.511(.474)	-.237(-.056)
7914	.95	35.7(745)	15.76	.612(.577)	-.284(-.076)

Analysis number	Mach number	Dynamic pressure, kN/m <sup>2</sup> (psf)	Angle of attack, deg	Normal force coefficient, bal (integ press.)	Pitching moment coefficient, bal (integ press.)
8001	.40	10.0(210)	-7.74	-.377(-.341)	.176(.089)
8002	.40	10.2(212)	-5.80	-.291(-.291)	.136(.094)
8003	.40	10.1(210)	-3.79	-.212(-.212)	.099(.067)
8004	.40	10.2(212)	-1.88	-.145(-.140)	.067(.045)
8005	.40	10.1(212)	.14	-.075(-.074)	.035(.032)
8006	.40	10.1(211)	2.08	-.012(-.016)	.006(.021)
8007	.40	10.0(210)	4.09	.055(.046)	-.025(.011)
8008	.40	10.2(212)	4.47	.068(.059)	-.031(.009)
8009	.40	10.1(211)	6.05	.128(.115)	-.060(-.005)
8010	.40	10.1(211)	7.97	.201(.188)	-.094(-.021)
8011	.40	10.1(211)	9.98	.285(.265)	-.132(-.032)
8012	.40	10.1(210)	11.92	.370(.343)	-.171(-.041)
8013	.40	10.1(210)	13.88	.458(.427)	-.212(-.049)
8014	.40	10.1(211)	15.89	.553(.518)	-.256(-.057)

Table A-3.—Experimental Data Test Point Log. Cambered-twisted Wing, Fin On

(a) T.E. Deflection, Full Span = 0.0°

Analysis number	Mach number	Dynamic pressure, kN/m <sup>2</sup> (psf)	Angle of attack, deg	Normal force coefficient, bal (integ press.)	Pitching moment coefficient, bal (integ press.)
4413	1.05	39.1(816)	-7.75	-.458(-.444)	.163(.154)
4414	1.05	39.0(815)	-5.80	-.373(-.355)	.147(.135)
4416	1.05	39.1(816)	-3.83	-.289(-.284)	.129(.125)
4417	1.05	39.0(815)	-1.90	-.207(-.215)	.105(.109)
4418	1.05	39.1(816)	.05	-.127(-.130)	.082(.077)
4419	1.05	39.1(816)	2.01	-.050(-.051)	.062(.056)
4420	1.05	39.1(816)	3.95	.029(.021)	.042(.040)
4421	1.05	39.0(815)	4.46	.051(.044)	.036(.034)
4422	1.05	39.1(816)	5.94	.118(.114)	.018(.012)
4423	1.05	39.1(816)	7.95	.213(.201)	-.007(-.007)
4424	1.05	39.1(816)	9.90	.315(.291)	-.035(-.029)
4425	1.05	39.1(817)	11.89	.414(.387)	-.058(-.054)
4427	1.05	39.1(816)	13.84	.504(.484)	-.074(-.072)
4428	1.05	39.0(815)	15.81	.589(.573)	-.087(-.088)
4501	.70	25.2(526)	-7.94	-.433(-.408)	.139(.122)
4502	.70	25.1(525)	-5.79	-.335(-.316)	.119(.107)
4503	.70	25.2(527)	-3.86	-.260(-.260)	.101(.101)
4504	.70	25.1(524)	-1.90	-.187(-.181)	.083(.075)
4505	.70	25.1(524)	.10	-.118(-.116)	.067(.063)
4506	.70	25.2(526)	2.07	-.050(-.052)	.053(.050)
4507	.70	25.2(526)	4.07	.019(.013)	.040(.037)
4508	.70	25.2(527)	4.51	.033(.026)	.037(.035)
4509	.70	25.2(526)	6.10	.094(.087)	.023(.020)
4510	.70	25.1(524)	8.10	.176(.173)	.007(-.001)
4511	.70	25.3(527)	9.92	.256(.238)	-.009(-.011)
4512	.70	25.2(526)	11.92	.351(.328)	-.027(-.021)
4513	.70	25.2(526)	13.91	.451(.418)	-.047(-.041)
4514	.70	25.2(527)	15.88	.554(.516)	-.065(-.059)
4602	1.00	37.6(785)	-7.81	-.464(-.445)	.160(.146)
4603	1.00	37.6(786)	-5.87	-.377(-.355)	.144(.128)
4604	1.00	37.7(786)	-3.89	-.290(-.281)	.122(.116)
4605	1.00	37.6(785)	-1.90	-.210(-.214)	.100(.102)
4606	1.00	37.7(787)	.01	-.134(-.132)	.080(.075)
4607	1.00	37.7(787)	2.10	-.054(-.057)	.061(.059)
4608	1.00	37.6(785)	4.01	.018(.014)	.046(.043)
4609	1.00	37.6(785)	4.51	.040(.036)	.041(.037)
4610	1.00	37.6(786)	5.93	.104(.102)	.024(.019)
4611	1.00	37.7(786)	7.93	.199(.190)	.001(-.002)
4613	1.00	37.6(786)	9.88	.297(.277)	-.023(-.017)
4614	1.00	37.6(786)	11.84	.400(.372)	-.048(-.042)
4615	1.00	37.6(786)	13.77	.495(.476)	-.067(-.063)
4616	1.00	37.6(785)	13.77	.495(.474)	-.066(-.062)
4617	1.00	37.6(785)	15.75	.583(.570)	-.078(-.080)

Analysis number	Mach number	Dynamic pressure, kN/m <sup>2</sup> (psf)	Angle of attack, deg	Normal force coefficient, bal (integ press.)	Pitching moment coefficient, bal (integ press.)
4701	.95	36.0(751)	-7.78	-.465(-.446)	.159(.146)
4702	.95	35.9(751)	-5.84	-.371(-.347)	.138(.120)
4703	.95	35.9(749)	-3.89	-.285(-.271)	.116(.107)
4706	.95	35.9(751)	-1.89	-.205(-.207)	.095(.096)
4707	.95	35.9(750)	.08	-.128(-.125)	.075(.069)
4708	.95	36.0(751)	2.01	-.056(-.059)	.059(.056)
4709	.95	36.0(752)	4.03	.018(.010)	.044(.042)
4710	.95	36.0(752)	4.51	.037(.029)	.039(.038)
4711	.95	35.9(750)	5.95	.099(.094)	.025(.020)
4712	.95	36.0(752)	7.94	.187(.176)	.006(.002)
4713	.95	35.9(751)	9.88	.281(.264)	-.016(-.010)
4714	.95	36.0(751)	11.89	.387(.359)	-.040(-.035)
4715	.95	36.0(751)	13.83	.488(.462)	-.061(-.055)
4716	.95	36.0(751)	15.75	.582(.565)	-.075(-.075)
4801	.85	32.0(668)	-7.75	-.444(-.427)	.144(.134)
4802	.85	32.1(670)	-5.81	-.352(-.336)	.126(.114)
4803	.85	32.0(669)	-3.83	-.269(-.263)	.107(.102)
4804	.85	32.1(670)	-1.89	-.195(-.197)	.088(.087)
4805	.85	32.0(669)	.09	-.122(-.121)	.070(.066)
4806	.85	32.0(669)	.09	-.122(-.121)	.070(.066)
4807	.85	32.0(669)	2.05	-.053(-.054)	.056(.052)
4808	.85	32.1(670)	4.03	.017(.011)	.042(.039)
4809	.85	32.1(671)	4.53	.036(.027)	.038(.036)
4810	.85	32.1(669)	6.21	.102(.097)	.023(.018)
4811	.85	32.1(670)	7.97	.178(.172)	.007(.000)
4812	.85	32.0(669)	9.94	.269(.255)	-.013(-.009)
4813	.85	32.0(669)	11.92	.367(.338)	-.032(-.028)
4814	.85	32.1(671)	13.87	.467(.434)	-.051(-.047)
4815	.85	32.0(669)	15.85	.565(.539)	-.066(-.062)
4901	.40	10.3(215)	-7.73	-.404(-.375)	.136(.112)
4902	.40	10.2(212)	-5.79	-.319(-.325)	.115(.117)
4903	.40	10.1(212)	-3.79	-.243(-.248)	.095(.092)
4904	.40	10.2(213)	-1.84	-.178(-.176)	.081(.071)
4905	.40	10.2(213)	.17	-.111(-.112)	.067(.059)
4906	.40	10.2(213)	2.12	-.046(-.049)	.054(.047)
4907	.40	10.2(212)	4.12	.022(.014)	.041(.035)
4908	.40	10.2(213)	4.51	.035(.027)	.038(.032)
4909	.40	10.1(211)	6.06	.090(.082)	.025(.019)
4910	.40	10.2(214)	8.01	.161(.158)	.011(.001)
4911	.40	10.3(215)	10.03	.244(.237)	-.005(-.014)
4912	.40	10.2(212)	10.03	.244(.236)	-.005(-.014)
4913	.40	10.2(214)	11.97	.331(.308)	-.021(-.023)
4914	.40	10.2(212)	13.94	.421(.389)	-.037(-.033)
4915	.40	10.3(214)	15.95	.521(.485)	-.054(-.048)

Table A-3.—(Continued)

(b) T.E. Deflection, Inboard = 8.3°, Outboard = 0.0°

Analysis number	Mach number	Dynamic pressure, kN/m <sup>2</sup> (psf)	Angle of attack, deg	Normal force coefficient, bal (integ press.)	Pitching moment coefficient, bal (integ press.)
5101	1.05	39.0(814)	-7.76	-.312(-.303)	.084(.060)
5102	1.05	39.0(814)	-5.78	-.224(-.215)	.066(.061)
5103	1.05	39.0(815)	-3.84	-.143(-.143)	.047(.049)
5104	1.05	39.0(815)	-1.91	-.064(-.064)	.025(.022)
5105	1.05	39.0(815)	.07	.009(.007)	.008(.006)
5106	1.05	39.0(814)	2.02	.079(.075)	-.008(-.009)
5107	1.05	39.0(814)	4.03	.158(.151)	-.029(-.030)
5108	1.05	39.0(814)	4.52	.177(.171)	-.034(-.035)
5109	1.05	38.9(813)	6.02	.245(.242)	-.052(-.056)
5110	1.05	38.9(813)	7.96	.337(.325)	-.077(-.075)
5111	1.05	39.0(814)	9.93	.434(.408)	-.103(-.093)
5112	1.05	39.0(814)	11.88	.522(.492)	-.120(-.112)
5113	1.05	39.0(814)	13.82	.595(.570)	-.126(-.118)
5201	.85	32.1(670)	-7.75	-.289(-.276)	.076(.069)
5202	.85	32.0(669)	-5.79	-.205(-.196)	.063(.057)
5203	.85	32.0(667)	-3.84	-.129(-.132)	.044(.045)
5204	.85	32.0(668)	-1.89	-.061(-.058)	.028(.023)
5205	.85	32.0(669)	.11	.007(.005)	.015(.011)
5206	.85	32.0(668)	2.07	.072(.067)	.002(-.000)
5207	.85	32.0(669)	4.02	.141(.133)	-.013(-.015)
5208	.85	32.0(669)	4.53	.160(.152)	-.018(-.019)
5209	.85	32.0(669)	6.03	.218(.213)	-.029(-.035)
5210	.85	32.0(669)	7.96	.300(.295)	-.048(-.055)
5211	.85	31.9(667)	9.92	.390(.372)	-.067(-.061)
5212	.85	32.0(668)	11.90	.489(.453)	-.087(-.077)
5213	.85	32.0(668)	13.87	.587(.551)	-.106(-.098)
5214	.85	31.9(667)	15.85	.681(.650)	-.120(-.112)
5303	.95	35.9(750)	-5.83	-.214(-.201)	.063(.055)
5304	.95	35.9(749)	-3.89	-.134(-.138)	.044(.047)
5305	.95	35.9(749)	-1.89	-.060(-.058)	.025(.022)
5307	.95	35.9(749)	.07	.008(.008)	.011(.009)
5308	.95	35.8(749)	2.03	.076(.071)	-.002(-.003)
5309	.95	35.9(749)	4.01	.149(.141)	-.019(-.019)
5310	.95	35.9(749)	4.51	.168(.163)	-.024(-.025)
5311	.95	35.9(749)	5.96	.227(.226)	-.037(-.043)
5312	.95	35.9(750)	7.94	.316(.308)	-.059(-.061)
5313	.95	35.9(750)	9.88	.411(.392)	-.081(-.073)
5314	.95	35.9(750)	11.88	.509(.478)	-.102(-.093)
5315	.95	35.9(750)	13.85	.596(.568)	-.114(-.105)
5316	.95	35.8(749)	15.74	.673(.650)	-.119(-.113)

Analysis number	Mach number	Dynamic pressure, kN/m <sup>2</sup> (psf)	Angle of attack, deg	Normal force coefficient, bal (integ press.)	Pitching moment coefficient, bal (integ press.)
5401	.40	10.1(211)	-7.74	-.269(-.251)	.089(.065)
5402	.40	10.2(213)	-5.81	-.187(-.199)	.065(.064)
5403	.40	10.2(213)	-3.79	-.118(-.115)	.049(.034)
5404	.40	10.2(212)	-3.78	-.118(-.116)	.049(.034)
5405	.40	10.1(211)	-1.86	-.058(-.057)	.037(.024)
5406	.40	10.1(211)	.15	.004(.004)	.025(.014)
5407	.40	10.1(211)	2.11	.065(.061)	.013(.003)
5408	.40	10.1(211)	4.11	.131(.120)	-.002(-.008)
5409	.40	10.1(212)	4.51	.145(.134)	-.005(-.012)
5410	.40	10.2(213)	6.06	.198(.187)	-.016(-.024)
5411	.40	10.2(213)	8.03	.267(.263)	-.029(-.042)
5413	.40	10.2(212)	10.04	.351(.346)	-.047(-.057)
5415	.40	10.2(213)	11.96	.436(.412)	-.062(-.064)
5416	.40	10.2(214)	13.92	.525(.489)	-.078(-.072)
5417	.40	10.1(211)	15.93	.621(.578)	-.092(-.083)



Table A-3.—(Continued)

(c) T.E. Deflection, Full Span = 8.3°

Analysis number	Mach number	Dynamic pressure, kN/m <sup>2</sup> (psf)	Angle of attack, deg	Normal force coefficient, bal (integ press.)	Pitching moment coefficient, bal (integ press.)
6704	1.05	38.9(811)	-7.68	-.294(-.282)	.137( .063)
6705	1.05	38.9(812)	-5.74	-.202(-.187)	.094( .036)
6706	1.05	38.9(812)	-3.82	-.116(-.109)	.054( .020)
6707	1.05	38.9(812)	-1.86	-.036(-.034)	.017(-.004)
6708	1.05	38.9(812)	.10	.038( .039)	-.017(-.022)
6709	1.05	38.9(811)	2.05	.108( .104)	-.050(-.036)
6710	1.05	38.9(812)	4.06	.186( .175)	-.087(-.051)
6711	1.05	38.9(812)	4.55	.206( .195)	-.096(-.057)
6712	1.05	38.9(812)	6.06	.273( .266)	-.127(-.079)
6713	1.05	38.9(812)	8.02	.364( .350)	-.169(-.096)
6721	1.05	38.9(813)	9.95	.454( .422)	-.212(-.106)
6722	1.05	38.9(812)	11.86	.537( .499)	-.250(-.118)
6723	1.05	38.9(812)	13.85	.615( .579)	-.286(-.124)
6801	.85	32.0(667)	-7.70	-.266(-.247)	.124( .047)
6802	.85	32.0(667)	-5.64	-.171(-.158)	.080( .029)
6803	.85	32.0(668)	-3.81	-.099(-.098)	.046( .017)
6804	.85	32.0(667)	-1.88	-.030(-.025)	.014(-.004)
6805	.85	32.0(668)	.03	.035( .036)	-.016(-.015)
6806	.85	32.0(668)	2.09	.105( .100)	-.049(-.027)
6807	.85	32.0(667)	4.03	.175( .164)	-.081(-.040)
6808	.85	32.0(667)	4.54	.194( .185)	-.090(-.045)
6809	.85	32.0(668)	6.04	.252( .243)	-.117(-.059)
6810	.85	31.9(667)	7.99	.333( .323)	-.155(-.077)
6811	.85	31.9(666)	9.94	.419( .396)	-.195(-.080)
6812	.85	31.9(667)	11.93	.513( .472)	-.239(-.090)
6813	.85	31.9(667)	13.87	.604( .557)	-.281(-.101)
6814	.85	31.9(666)	15.85	.697( .655)	-.324(-.112)
6903	.95	35.8(747)	-7.74	-.280(-.262)	.130( .049)
6904	.95	35.8(747)	-5.82	-.190(-.170)	.089( .028)
6905	.95	35.7(746)	-3.85	-.106(-.104)	.049( .018)
6908	.95	35.8(747)	-1.90	-.031(-.026)	.015(-.005)
6909	.95	35.8(747)	.08	.039( .040)	-.018(-.018)
6910	.95	35.7(746)	2.04	.108( .104)	-.050(-.030)
6911	.95	35.8(747)	4.06	.182( .172)	-.085(-.043)
6912	.95	35.7(747)	4.54	.201( .193)	-.093(-.050)
6913	.95	35.8(747)	5.99	.260( .256)	-.121(-.067)
6914	.95	35.8(747)	7.94	.345( .333)	-.161(-.082)
6915	.95	35.7(746)	9.89	.434( .410)	-.202(-.088)
6916	.95	35.8(747)	11.91	.527( .486)	-.245(-.097)
6917	.95	35.8(747)	13.86	.612( .573)	-.285(-.106)
6918	.95	35.7(747)	15.76	.690( .653)	-.321(-.111)

Analysis number	Mach number	Dynamic pressure, kN/m <sup>2</sup> (psf)	Angle of attack, deg	Normal force coefficient, bal (integ press.)	Pitching moment coefficient, bal (integ press.)
7007	.40	10.1(211)	-7.77	-.242(-.218)	-.113( .041)
7008	.40	10.1(212)	-5.82	-.163(-.165)	.076( .037)
7009	.40	10.1(212)	-3.84	-.092(-.086)	.043( .011)
7010	.40	10.1(211)	-1.89	-.030(-.025)	.014(-.001)
7011	.40	10.1(211)	.11	.034( .035)	-.016(-.012)
7012	.40	10.1(212)	2.08	.098( .093)	-.045(-.022)
7013	.40	10.1(210)	4.07	.165( .157)	-.077(-.036)
7014	.40	10.1(211)	4.47	.178( .169)	-.083(-.038)
7015	.40	10.1(211)	6.01	.233( .222)	-.108(-.050)
7016	.40	10.1(211)	7.97	.299( .294)	-.139(-.066)
7017	.40	10.1(211)	9.96	.379( .370)	-.176(-.078)
7018	.40	10.2(213)	11.69	.453( .429)	-.210(-.083)
7019	.40	10.2(213)	13.86	.552( .512)	-.256(-.087)
7020	.40	10.1(211)	15.85	.646( .598)	-.300(-.096)

Table A-3.—(Concluded)

(d) T.E. Deflection, Inboard = 0.0°, Outboard = 8.3°

Analysis number	Mach number	Dynamic pressure, kN/m <sup>2</sup> (psf)	Angle of attack, deg	Normal force coefficient, bal (integ press.)	Pitching moment coefficient, bal (integ press.)
7204	1.05	38.8(811)	-7.71	-.447(-.429)	.208( .139)
7205	1.05	38.9(812)	-5.75	-.351(-.330)	.163( .112)
7206	1.05	38.9(811)	-3.82	-.262(-.250)	.122( .095)
7207	1.05	38.9(812)	-1.86	-.177(-.182)	.082( .080)
7208	1.05	38.9(812)	.09	-.095(-.098)	.044( .051)
7209	1.05	38.9(813)	2.03	-.018(-.021)	.008( .030)
7210	1.05	38.9(812)	4.02	.062( .052)	-.029( .013)
7211	1.05	38.8(811)	4.53	.084( .076)	-.040( .007)
7212	1.05	38.9(811)	6.05	.153( .145)	-.071(-.013)
7213	1.05	38.9(812)	8.00	.242( .227)	-.113(-.029)
7214	1.05	38.9(813)	9.91	.340( .310)	-.159(-.047)
7215	1.05	38.9(813)	11.86	.440( .403)	-.205(-.069)
7216	1.05	38.9(813)	13.83	.536( .506)	-.249(-.093)
7301	.85	31.9(666)	-7.73	-.422(-.403)	.197( .115)
7302	.85	31.9(666)	-5.78	-.324(-.302)	.151( .087)
7303	.85	31.9(665)	-3.82	-.239(-.226)	.111( .073)
7304	.85	31.9(666)	-1.90	-.162(-.160)	.075( .057)
7305	.85	31.9(666)	-.07	-.094(-.090)	.044( .038)
7306	.85	31.9(666)	-.07	-.094(-.091)	.044( .038)
7307	.85	31.9(666)	2.08	-.017(-.019)	.008( .023)
7308	.85	31.9(667)	4.02	.052( .045)	-.024( .012)
7309	.85	31.9(666)	4.51	.070( .061)	-.033( .009)
7310	.85	31.9(666)	6.03	.131( .124)	-.061(-.008)
7311	.85	31.9(666)	8.00	.213( .204)	-.099(-.025)
7312	.85	31.9(667)	9.95	.301( .281)	-.140(-.031)
7313	.85	31.9(666)	11.91	.399( .360)	-.186(-.046)
7315	.85	31.9(665)	13.84	.496( .450)	-.231(-.060)
7316	.85	31.9(666)	15.81	.596( .555)	-.277(-.074)
7401	.95	35.7(747)	-7.76	-.450(-.428)	.209( .131)
7402	.95	35.7(746)	-5.81	-.346(-.316)	.161( .095)
7403	.95	35.7(746)	-3.89	-.257(-.233)	.119( .075)
7404	.95	35.8(747)	-1.89	-.174(-.173)	.081( .067)
7405	.95	35.8(747)	.06	-.095(-.092)	.044( .041)
7406	.95	35.8(747)	2.03	-.023(-.024)	.010( .027)
7407	.95	35.7(746)	4.02	.052( .045)	-.025( .014)
7408	.95	35.8(747)	4.52	.072( .064)	-.034( .010)
7409	.95	35.8(747)	5.98	.135( .128)	-.063(-.006)
7410	.95	35.7(746)	7.93	.220( .206)	-.103(-.022)
7411	.95	35.8(748)	9.90	.313( .290)	-.146(-.032)
7412	.95	35.7(747)	11.87	.416( .377)	-.193(-.050)
7413	.95	35.7(746)	13.82	.519( .477)	-.241(-.068)
7414	.95	35.7(745)	15.74	.620( .592)	-.289(-.097)

Analysis number	Mach number	Dynamic pressure, kN/m <sup>2</sup> (psf)	Angle of attack, deg	Normal force coefficient, bal (integ press.)	Pitching moment coefficient, bal (integ press.)
7501	.40	10.2(212)	-7.76	-.373(-.342)	.173( .088)
7502	.40	10.1(211)	-5.81	-.291(-.287)	.135( .089)
7503	.40	10.2(212)	-3.80	-.212(-.208)	.098( .063)
7504	.40	10.2(212)	-1.87	-.144(-.138)	.067( .044)
7505	.40	10.0(210)	.14	-.076(-.073)	.035( .031)
7506	.40	10.1(211)	2.10	-.011(-.013)	.005( .019)
7507	.40	10.2(212)	4.09	.055( .049)	-.026( .008)
7508	.40	10.1(211)	4.49	.069( .062)	-.032( .006)
7509	.40	10.1(212)	6.02	.125( .116)	-.058(-.008)
7510	.40	10.2(213)	7.96	.195( .192)	-.091(-.026)
7511	.40	10.2(212)	9.96	.275( .263)	-.128(-.037)
7512	.40	10.1(211)	11.70	.349( .327)	-.162(-.045)
7513	.40	10.1(212)	13.87	.451( .415)	-.210(-.054)
7514	.40	10.0(210)	15.88	.551( .510)	-.255(-.066)

Table A-4.—FLEXSTAB Test Point Log. Twisted Wing, Fin Off

(a) T.E. Deflection, Full Span = 0.0°

Analysis number	Mach number	Dynamic pressure, kN/m <sup>2</sup> (psf)	Angle of attack, deg	Normal force coefficient, bal (integ press.)	Pitching moment coefficient, bal (integ press.)
101007	1.05		-7.76	(-.366)	(.098)
101008	1.05		-5.84	(-.292)	(.081)
101009	1.05		-3.85	(-.216)	(.064)
101010	1.05		-1.89	(-.141)	(.046)
101011	1.05		-.05	(-.071)	(.030)
101012	1.05		2.01	(.008)	(.012)
101013	1.05		4.00	(.084)	(-.005)
101014	1.05		4.51	(.104)	(-.010)
101015	1.05		6.01	(.161)	(-.023)
101016	1.05		7.97	(.236)	(-.040)
101017	1.05		9.95	(.312)	(-.057)
101018	1.05		11.87	(.385)	(-.074)
101019	1.05		13.82	(.460)	(-.091)
101020	1.05		15.81	(.536)	(-.109)
101310	.85		-7.75	(-.343)	(.080)
101311	.85		-5.81	(-.274)	(.067)
101312	.85		-3.85	(-.203)	(.053)
101313	.85		-1.88	(-.133)	(.039)
101314	.85		-.11	(-.062)	(.025)
101315	.85		2.07	(.008)	(.011)
101316	.85		4.02	(.078)	(-.003)
101317	.85		4.50	(.095)	(-.006)
101318	.85		6.02	(.149)	(-.017)
101319	.85		7.97	(.219)	(-.031)
101320	.85		9.91	(.289)	(-.045)
101321	.85		11.92	(.360)	(-.059)
101322	.85		13.92	(.432)	(-.073)
101323	.85		15.82	(.500)	(-.087)
101324	.85		.12	(-.061)	(.025)
101501	.40		-7.75	(-.321)	(.068)
101502	.40		-5.79	(-.255)	(.057)
101503	.40		-3.81	(-.189)	(.045)
101504	.40		-1.84	(-.123)	(.033)
101505	.40		.15	(-.056)	(.022)
101506	.40		2.10	(.009)	(.010)
101507	.40		4.10	(.076)	(-.002)
101508	.40		4.49	(.089)	(-.004)
101509	.40		6.07	(.142)	(-.013)
101510	.40		8.01	(.207)	(-.025)
101511	.40		10.04	(.275)	(-.037)
101512	.40		11.95	(.339)	(-.048)
101513	.40		13.93	(.405)	(-.060)
101514	.40		15.92	(.472)	(-.071)

(b) T.E. Deflection, Inboard = 8.3°, Outboard = 0.0°

Analysis number	Mach number	Dynamic pressure, kN/m <sup>2</sup> (psf)	Angle of attack, deg	Normal force coefficient, bal (integ press.)	Pitching moment coefficient, bal (integ press.)
101613	1.05		-7.75	(-.181)	(.006)
101614	1.05		-5.80	(-.107)	(-.011)
101615	1.05		-3.86	(-.033)	(-.028)
101616	1.05		-1.91	(.042)	(-.045)
101617	1.05		.05	(.117)	(-.062)
101618	1.05		2.01	(.192)	(-.079)
101619	1.05		4.01	(.268)	(-.097)
101620	1.05		4.50	(.287)	(-.101)
101621	1.05		6.00	(.344)	(-.114)
101622	1.05		7.96	(.419)	(-.131)
101623	1.05		9.91	(.494)	(-.148)
101624	1.05		11.87	(.569)	(-.166)
101625	1.05		13.82	(.644)	(-.183)
101626	1.05		15.82	(.720)	(-.200)
101801	.85		-7.74	(-.185)	(.011)
101802	.85		-5.80	(-.115)	(-.002)
101803	.85		-3.85	(-.046)	(-.016)
101804	.85		-1.89	(.024)	(-.030)
101805	.85		.02	(.093)	(-.044)
101806	.85		2.06	(.166)	(-.058)
101807	.85		4.01	(.235)	(-.072)
101808	.85		4.51	(.253)	(-.075)
101809	.85		6.01	(.307)	(-.086)
101810	.85		7.97	(.377)	(-.100)
101811	.85		9.92	(.446)	(-.114)
101812	.85		11.91	(.518)	(-.128)
101813	.85		13.88	(.588)	(-.142)
101814	.85		15.84	(.658)	(-.156)
102001	.40		-7.75	(-.180)	(.012)
102002	.40		-5.80	(-.115)	(.001)
102003	.40		-3.80	(-.048)	(-.011)
102004	.40		-1.85	(.017)	(-.023)
102005	.40		.16	(.084)	(-.034)
102006	.40		2.11	(.150)	(-.046)
102007	.40		4.11	(.217)	(-.058)
102008	.40		4.50	(.230)	(-.060)
102009	.40		6.06	(.282)	(-.069)
102010	.40		8.01	(.347)	(-.081)
102011	.40		10.01	(.414)	(-.092)
102012	.40		11.94	(.479)	(-.104)
102013	.40		13.92	(.545)	(-.116)
102014	.40		15.92	(.612)	(-.127)

Table A-4.—(Concluded)

(c) T.E. Deflection, Full Span =  $8.3^\circ$ 

Analysis number	Mach number	Dynamic pressure, $\text{kN/m}^2$ (psf)	Angle of attack, deg	Normal force coefficient, bal (integ press.)	Pitching moment coefficient, bal (integ press.)
102113	1.05		-7.75	(-.139)	(-.030)
102114	1.05		-5.80	(-.065)	(-.047)
102115	1.05		-3.85	(.010)	(-.064)
102116	1.05		-1.90	(.085)	(-.081)
102117	1.05		.05	(.159)	(-.099)
102118	1.05		2.01	(.234)	(-.116)
102119	1.05		4.00	(.310)	(-.133)
102120	1.05		4.50	(.330)	(-.138)
102121	1.05		6.02	(.388)	(-.151)
102122	1.05		7.96	(.462)	(-.168)
102123	1.05		9.92	(.537)	(-.185)
102124	1.05		11.86	(.611)	(-.202)
102125	1.05		13.83	(.686)	(-.219)
102126	1.05		15.82	(.763)	(-.237)
102301	.85		-7.74	(-.139)	(-.025)
102302	.85		-5.79	(-.069)	(-.038)
102303	.85		-3.85	(-.000)	(-.052)
102304	.85		-1.90	(.070)	(-.066)
102305	.85		-.00	(.138)	(-.079)
102306	.85		2.06	(.211)	(-.094)
102307	.85		4.01	(.281)	(-.108)
102308	.85		4.51	(.299)	(-.111)
102309	.85		6.02	(.353)	(-.122)
102310	.85		7.97	(.423)	(-.136)
102311	.85		9.92	(.492)	(-.150)
102312	.85		11.92	(.564)	(-.164)
102313	.85		13.87	(.633)	(-.178)
102314	.85		15.83	(.704)	(-.192)
102501	.40		-7.75	(-.137)	(-.021)
102502	.40		-5.80	(-.071)	(-.032)
102503	.40		-3.80	(-.004)	(-.044)
102504	.40		-1.85	(.061)	(-.055)
102505	.40		.15	(.128)	(-.067)
102506	.40		2.11	(.193)	(-.079)
102507	.40		4.10	(.260)	(-.090)
102508	.40		4.50	(.273)	(-.093)
102509	.40		6.06	(.326)	(-.102)
102510	.40		8.01	(.391)	(-.114)
102511	.40		10.02	(.458)	(-.125)
102512	.40		11.95	(.523)	(-.137)
102513	.40		13.92	(.589)	(-.148)
102514	.40		15.93	(.656)	(-.160)

(d) T.E. Deflection, Inboard =  $0.0^\circ$ , Outboard =  $8.3^\circ$ 

Analysis number	Mach number	Dynamic pressure, $\text{kN/m}^2$ (psf)	Angle of attack, deg	Normal force coefficient, bal (integ press.)	Pitching moment coefficient, bal (integ press.)
102613	1.05		-7.75	(-.323)	(.061)
102614	1.05		-5.80	(-.249)	(.044)
102615	1.05		-3.85	(-.174)	(.027)
102616	1.05		-1.90	(-.099)	(.010)
102617	1.05		.06	(-.024)	(-.007)
102618	1.05		2.00	(.050)	(-.024)
102619	1.05		4.00	(.127)	(-.042)
102620	1.05		4.51	(.146)	(-.046)
102621	1.05		6.00	(.203)	(-.059)
102622	1.05		7.97	(.279)	(-.077)
102623	1.05		9.90	(.352)	(-.094)
102624	1.05		11.87	(.428)	(-.111)
102625	1.05		13.82	(.502)	(-.128)
102626	1.05		15.82	(.579)	(-.146)
102801	.85		-7.75	(-.297)	(.045)
102802	.85		-5.79	(-.227)	(.031)
102803	.85		-3.84	(-.157)	(.017)
102804	.85		-1.89	(-.088)	(.003)
102805	.85		-.09	(-.023)	(-.010)
102806	.85		2.07	(.054)	(-.025)
102807	.85		4.01	(.123)	(-.039)
102808	.85		4.52	(.142)	(-.043)
102809	.85		6.01	(.195)	(-.053)
102810	.85		7.97	(.265)	(-.067)
102811	.85		9.92	(.335)	(-.081)
102812	.85		11.92	(.406)	(-.095)
102813	.85		13.87	(.476)	(-.109)
102814	.85		15.83	(.546)	(-.123)
103001	.40		-7.75	(-.277)	(.036)
103002	.40		-5.80	(-.212)	(.024)
103003	.40		-3.80	(-.145)	(.012)
103004	.40		-1.85	(-.079)	(.001)
103005	.40		.15	(-.012)	(-.011)
103006	.40		2.11	(.053)	(-.023)
103007	.40		4.11	(.120)	(-.035)
103008	.40		4.51	(.134)	(-.037)
103010	.40		6.05	(.185)	(-.046)
103011	.40		8.01	(.251)	(-.058)
103012	.40		10.02	(.318)	(-.069)
103014	.40		11.96	(.383)	(-.081)
103015	.40		13.92	(.449)	(-.092)
103016	.40		15.92	(.516)	(-.104)

Table A-5.—FLEXSTAB Test Point Log. Cambered-twisted Wing, Fin Off

(a) T.E. Deflection, Full Span = 0.0°

Analysis number	Mach number	Dynamic pressure, kN/m <sup>2</sup> (psf)	Angle of attack, deg	Normal force coefficient, bal (integ press.)	Pitching moment coefficient, bal (integ press.)
103704	1.05		-7.74	(-.440)	(.156)
103705	1.05		-5.78	(-.365)	(.139)
103706	1.05		-3.84	(-.290)	(.122)
103707	1.05		-1.88	(-.215)	(.105)
103709	1.05		.07	(-.141)	(.088)
103710	1.05		2.02	(-.066)	(.070)
103711	1.05		3.99	(.010)	(.053)
103712	1.05		4.51	(.030)	(.049)
103714	1.05		6.03	(.088)	(.035)
103715	1.05		7.95	(.161)	(.018)
103716	1.05		9.89	(.236)	(.001)
103717	1.05		11.86	(.311)	(-.016)
103718	1.05		13.81	(.386)	(-.033)
103719	1.05		15.84	(.464)	(-.051)
104001	.85		-7.74	(-.414)	(.131)
104002	.85		-5.78	(-.343)	(.117)
104003	.85		-3.83	(-.274)	(.103)
104004	.85		-1.89	(-.204)	(.090)
104005	.85		.12	(-.132)	(.075)
104006	.85		2.06	(-.063)	(.061)
104007	.85		4.02	(.007)	(.047)
104008	.85		4.52	(.025)	(.044)
104009	.85		6.00	(.078)	(.033)
104010	.85		7.96	(.148)	(.019)
104011	.85		9.91	(.218)	(.006)
104012	.85		11.92	(.290)	(-.009)
104013	.85		13.87	(.360)	(-.023)
104014	.85		15.83	(.430)	(-.037)
104301	.40		-7.75	(-.385)	(.112)
104302	.40		-5.81	(-.320)	(.100)
104303	.40		-3.80	(-.252)	(.088)
104304	.40		-1.84	(-.187)	(.077)
104305	.40		.15	(-.120)	(.065)
104306	.40		2.11	(-.054)	(.053)
104307	.40		4.11	(.013)	(.042)
104308	.40		4.51	(.026)	(.039)
104309	.40		6.07	(.079)	(.030)
104310	.40		8.00	(.143)	(.018)
104311	.40		9.99	(.210)	(.007)
104312	.40		10.00	(.210)	(.007)
104313	.40		11.97	(.276)	(-.005)
104314	.40		13.90	(.341)	(-.016)
104315	.40		15.93	(.409)	(-.028)

(b) T.E. Deflection, Inboard = 8.3°, Outboard = 0.0°

Analysis number	Mach number	Dynamic pressure, kN/m <sup>2</sup> (psf)	Angle of attack, deg	Normal force coefficient, bal (integ press.)	Pitching moment coefficient, bal (integ press.)
105513	1.05		-7.75	(-.256)	(.065)
105514	1.05		-5.81	(-.182)	(.048)
105515	1.05		-3.86	(-.107)	(.031)
105516	1.05		-1.92	(-.033)	(.013)
105517	1.05		.06	(.043)	(-.004)
105518	1.05		2.00	(.118)	(-.021)
105519	1.05		4.02	(.195)	(-.039)
105520	1.05		4.49	(.213)	(-.043)
105521	1.05		6.00	(.271)	(-.056)
105522	1.05		7.96	(.346)	(-.073)
105523	1.05		9.92	(.421)	(-.091)
105524	1.05		11.86	(.495)	(-.108)
105526	1.05		13.82	(.570)	(-.125)
105528	1.05		14.82	(.609)	(-.134)
105702	.40		-7.75	(-.245)	(.056)
105703	.40		-5.81	(-.179)	(.044)
105704	.40		-3.83	(-.113)	(.032)
105705	.40		-1.87	(-.047)	(.021)
105706	.40		.13	(.020)	(.009)
105707	.40		2.08	(.085)	(-.003)
105708	.40		4.09	(.152)	(-.015)
105709	.40		4.47	(.165)	(-.017)
105710	.40		6.02	(.217)	(-.026)
105711	.40		7.98	(.283)	(-.038)
105712	.40		9.97	(.350)	(-.049)
105713	.40		11.92	(.415)	(-.061)
105714	.40		13.86	(.480)	(-.072)
105715	.40		15.87	(.547)	(-.084)
105901	.85		-7.69	(-.254)	(.062)
105902	.85		-5.75	(-.184)	(.048)
105903	.85		-3.85	(-.116)	(.034)
105904	.85		-1.89	(-.046)	(.020)
105905	.85		.04	(.023)	(.007)
105906	.85		2.09	(.096)	(-.008)
105907	.85		4.04	(.166)	(-.022)
105908	.85		4.55	(.184)	(-.025)
105909	.85		6.03	(.237)	(-.036)
105910	.85		8.03	(.309)	(-.050)
105911	.85		9.96	(.378)	(-.064)
105912	.85		11.91	(.448)	(-.078)
105913	.85		13.91	(.519)	(-.092)
105914	.85		15.86	(.589)	(-.106)

Table A-5.—(Concluded)

(c) T.E. Deflection, Full Span = 8.3°

Analysis number	Mach number	Dynamic pressure, kN/m <sup>2</sup> (psf)	Angle of attack, deg	Normal force coefficient, bal (integ press.)	Pitching moment coefficient, bal (integ press.)
106107	1.05		-7.68	(-.211)	(.028)
106108	1.05		-5.74	(-.137)	(.011)
106109	1.05		-3.80	(-.062)	(-.007)
106110	1.05		-1.87	(.012)	(-.024)
106111	1.05		.11	(.088)	(-.041)
106112	1.05		2.04	(.162)	(-.058)
106113	1.05		4.03	(.238)	(-.076)
106114	1.05		4.53	(.257)	(-.080)
106116	1.05		6.05	(.315)	(-.093)
106117	1.05		8.01	(.390)	(-.111)
106118	1.05		9.96	(.465)	(-.128)
106119	1.05		11.89	(.539)	(-.145)
106121	1.05		13.86	(.615)	(-.162)
106201	.85		-7.68	(-.208)	(.026)
106202	.85		-5.65	(-.135)	(.011)
106203	.85		-3.83	(-.070)	(-.002)
106204	.85		-1.88	(-.000)	(-.016)
106205	.85		.01	(.067)	(-.029)
106206	.85		2.10	(.142)	(-.044)
106207	.85		4.04	(.212)	(-.058)
106208	.85		4.54	(.230)	(-.062)
106209	.85		6.05	(.284)	(-.072)
106210	.85		8.00	(.354)	(-.086)
106211	.85		9.95	(.423)	(-.100)
106221	.85		8.00	(.354)	(-.086)
106222	.85		9.98	(.425)	(-.100)
106223	.85		11.95	(.495)	(-.114)
106224	.85		13.89	(.565)	(-.128)
106225	.85		15.84	(.634)	(-.142)
106501	.40		-7.77	(-.201)	(.023)
106502	.40		-5.82	(-.136)	(.011)
106503	.40		-3.84	(-.070)	(-.000)
106504	.40		-1.90	(-.005)	(-.012)
106505	.40		.11	(.063)	(-.024)
106506	.40		2.07	(.129)	(-.035)
106507	.40		4.07	(.196)	(-.047)
106508	.40		4.46	(.209)	(-.050)
106509	.40		6.02	(.261)	(-.059)
106511	.40		7.96	(.326)	(-.070)
106513	.40		9.97	(.394)	(-.082)
106514	.40		11.70	(.452)	(-.093)
106515	.40		13.86	(.524)	(-.105)
106516	.40		15.88	(.592)	(-.117)

(d) T.E. Deflection, Inboard = 0.0°, Outboard = 8.3°

Analysis number	Mach number	Dynamic pressure, kN/m <sup>2</sup> (psf)	Angle of attack, deg	Normal force coefficient, bal (integ press.)	Pitching moment coefficient, bal (integ press.)
107704	1.05		-7.69	(-.396)	(.119)
107705	1.05		-5.74	(-.321)	(.102)
107706	1.05		-3.82	(-.247)	(.085)
107707	1.05		-1.87	(-.173)	(.068)
107708	1.05		.10	(-.097)	(.051)
107709	1.05		2.05	(-.022)	(.034)
107710	1.05		4.03	(.054)	(.016)
107711	1.05		4.55	(.074)	(.012)
107712	1.05		6.05	(.131)	(-.002)
107713	1.05		8.01	(.206)	(-.019)
107714	1.05		9.94	(.280)	(-.036)
107715	1.05		11.88	(.355)	(-.053)
107716	1.05		13.85	(.430)	(-.070)
107801	.85		-7.70	(-.367)	(.095)
107802	.85		-5.75	(-.297)	(.081)
107803	.85		-3.81	(-.227)	(.067)
107804	.85		-1.87	(-.158)	(.053)
107805	.85		-.07	(-.093)	(.040)
107806	.85		2.09	(-.016)	(.025)
107807	.85		4.02	(.053)	(.011)
107808	.85		4.51	(.071)	(.008)
107809	.85		6.04	(.126)	(-.003)
107810	.85		8.01	(.196)	(-.017)
107811	.85		9.96	(.266)	(-.031)
107812	.85		11.93	(.336)	(-.045)
107813	.85		13.87	(.406)	(-.059)
107814	.85		15.83	(.476)	(-.073)
108001	.40		-7.74	(-.341)	(.079)
108002	.40		-5.80	(-.276)	(.067)
108003	.40		-3.79	(-.208)	(.056)
108004	.40		-1.88	(-.144)	(.044)
108005	.40		.14	(-.076)	(.032)
108006	.40		2.08	(-.011)	(.021)
108007	.40		4.09	(.056)	(.009)
108008	.40		4.47	(.069)	(.006)
108009	.40		6.05	(.122)	(-.003)
108010	.40		7.97	(.186)	(-.014)
108011	.40		9.98	(.254)	(-.026)
108012	.40		11.92	(.319)	(-.038)
108013	.40		13.88	(.385)	(-.049)
108014	.40		15.89	(.452)	(-.061)

*Table A-6.—PAN AIR Test Point Log. Flat Wing,  
Fin Off, T.E. Deflection, Full Span = 0.0°*

Analysis number	Mach number	Dynamic pressure, kN/m <sup>2</sup> (psf)	Angle of attack, deg	Normal force coefficient, bal (integ press.)	Pitching moment coefficient, bal (integ press.)
326405	1.05		.08	(.007)	(-.007)
326407	1.05		3.99	(.146)	(-.039)
326409	1.05		7.87	(.267)	(-.063)
326411	1.05		11.82	(.369)	(-.079)
326705	.85		.07	(.001)	(-.002)
326707	.85		3.99	(.133)	(-.029)
326709	.85		7.92	(.253)	(-.050)
326711	.85		11.87	(.355)	(-.065)
326905	.40		.14	(.003)	(-.001)
326907	.40		4.10	(.130)	(-.025)
326910	.40		8.00	(.250)	(-.047)
326913	.40		11.91	(.361)	(-.066)

*Table A-7.—PAN AIR Test Point Log. Twisted Wing,  
Fin Off; T.E. Deflection, Full Span = 0.0°*

Analysis number	Mach number	Dynamic pressure, kN/m <sup>2</sup> (psf)	Angle of attack, deg	Normal force coefficient, bal (integ press.)	Pitching moment coefficient, bal (integ press.)
344608	1.05		.07	(-.058)	(.022)
344612	1.05		7.95	(.217)	(-.041)
344614	1.05		11.85	(.328)	(-.062)
344620	1.05		4.51	(.102)	(-.016)
344906	.85		.09	(-.060)	(.023)
344910	.85		7.98	(.202)	(-.029)
344912	.85		11.88	(.313)	(-.049)
344920	.85		4.50	(.090)	(-.007)
345006	.40		.17	(-.054)	(.021)
345010	.40		8.05	(.196)	(-.025)
345012	.40		11.96	(.312)	(-.046)
345020	.40		4.49	(.084)	(-.005)

Table A-8.—PAN AIR Test Point Log. Cambered-twisted Wing,  
Fin Off; T.E. Deflection, Full Span = 0.0°

Analysis number	Mach number	Dynamic pressure, kN/m <sup>2</sup> (psf)	Angle of attack, deg	Normal force coefficient, bal (integ press.)	Pitching moment coefficient, bal (integ press.)
303709	1.05		.07	(-.133)	(.081)
303711	1.05		3.99	(.006)	(.049)
303715	1.05		7.95	(.135)	(.020)
303717	1.05		11.86	(.242)	(.000)
303731	1.05		3.99	(.006)	(.050)
303735	1.05		7.95	(.136)	(.022)
303737	1.05		11.86	(.242)	(.003)
303739	1.05		15.84	(.332)	(-.012)
304005	.85		.12	(-.133)	(.075)
304007	.85		4.02	(-.003)	(.049)
304010	.85		7.96	(.122)	(.024)
304012	.85		11.92	(.229)	(.006)
304027	.85		4.02	(-.003)	(.050)
304030	.85		7.96	(.122)	(.025)
304032	.85		11.92	(.230)	(.008)
304034	.85		15.83	(.317)	(-.004)
304305	.40		.15	(-.123)	(.066)
304307	.40		4.11	(.003)	(.043)
304310	.40		8.00	(.123)	(.021)
304313	.40		11.97	(.239)	(.001)
304327	.40		4.11	(.003)	(.043)
304330	.40		8.00	(.124)	(.021)
304333	.40		11.97	(.239)	(.001)
304335	.40		15.93	(.343)	(-.015)

Table A-9.—PAN AIR Test Point Log. Cambered-twisted Wing,  
Fin On; T.E. Deflection, Full Span = 0.0°

Analysis number	Mach number	Dynamic pressure, kN/m <sup>2</sup> (psf)	Angle of attack, deg	Normal force coefficient, bal (integ press.)	Pitching moment coefficient, bal (integ press.)
304418	1.05		.05	(-.136)	(.082)
304420	1.05		3.95	(.005)	(.048)
304423	1.05		7.95	(.137)	(.018)
304425	1.05		11.89	(.245)	(-.002)
304806	.85		.09	(-.137)	(.077)
304808	.85		4.03	(-.003)	(.049)
304811	.85		7.97	(.123)	(.024)
304813	.85		11.92	(.231)	(.006)
304905	.40		.17	(-.124)	(.067)
304907	.40		4.12	(.004)	(.043)
304910	.40		8.01	(.125)	(.021)
304913	.40		11.97	(.239)	(.002)



## **APPENDIX B**

### **SUMMARY OF PREVIOUS RELATED CONTRACTS**

Prior to the present contract, directly related work has been done under two other contracts using the same wind tunnel models. The flat and twisted wings were constructed under NASA contract NAS1-12875. In addition, these wings were tested at subsonic/transonic Mach numbers and theoretical predictions of pressure distributions were made and evaluated. This contract is summarized in NASA CR-2610 (ref. 1) with a more detailed report of these data available in references 2 through 4.

Testing of these wings at supersonic Mach numbers and prediction of pressure distributions using the linearized theory FLEXSTAB was conducted under the second NASA contract NAS1-14141. These data were reported in detail in reference 5, including a comparison of the data over the entire Mach number range for which data are available - 0.40 through 2.50. A brief summary of these two contracts follows.

#### **NASA CONTRACT NAS1-12875**

This contract was divided into two tasks. The experimental task was to obtain a comprehensive data base not only for use in the associated theoretical task, but also for use as new theories are developed. The theoretical task was to predict pressure distributions using existing attached- and detached-flow theories and to delineate conditions under which these theories are valid for both the flat and twisted wings.

#### **EXPERIMENTAL TASK**

The model is described in detail in the main portion of this document. The body, the flat wing (including two sets of leading edges, sharp as well as rounded), and the twisted wing were constructed as a part of this contract.

The testing was conducted in the Boeing Transonic Wind Tunnel (see main documentation). Table B-1 shows the 54 configurations that were tested. Photographs of the flat wing and the twisted wing are shown in figure B-1. Pressure and total force data were obtained throughout the test at Mach numbers of 0.40, 0.70, 0.85, 0.95, and 1.05 for all configurations and at Mach numbers of 1.00 and 1.11 for selected configurations. The angle of attack varied from  $-8^\circ$  to  $+16^\circ$  in  $2^\circ$  increments.

#### **THEORETICAL TASK**

Predictions of pressure distributions were made using two attached flow methods: FLEXSTAB and TEA-230. The FLEXSTAB method is described in the main documentation. Table B-2 shows the combinations of Mach number and configuration for which data are available.

The second attached-flow method used was the general method of Rubbert and Saaris (refs. 18 through 20) for the numerical solution of nonplanar, three dimensional boundary-value problems. The method solves the exact incompressible potential-flow equation (Laplace's equation), with compressibility effects incorporated via the Gothert rule. In contrast to FLEXSTAB, the Rubbert-Saaris solution (hereafter referred to as TEA-230) is not encumbered by the small perturbation approximation and is capable of treating problems of far more detail and generality than the linearized theories.

**Table B-1.—Summary of Subsonic/Transonic Test Conditions by Run Number  
(NASA Contract NAS1-12875)**

Leading-edge deflection, deg	Mach no.	Trailing-edge deflection, deg																
		Full Span									Outboard (inboard = 0.0)				Inboard (outboard = 0.0)			
		30.2	17.7	8.3	4.1	0.0	-4.1	-8.3	-17.7	-30.2	17.7	8.3	-8.3	-17.7	17.7	8.3	-8.3	-17.7
Flat wing, rounded leading-edge, trip strip off																		
Full span = 0.0	0.40					10												
	0.70					15												
	0.85					7												
	0.95					16												
	1.05					14												
	1.11					9												
Flat wing, rounded leading-edge, trip strip on																		
Full span=0.0	0.40	37	32	46	48	21,269	55	78	66	75	280	275			252	259		
	0.70	34	29	43	50	23,263	57	80	63	72	277	271			248	255		
	0.85	36	31	45	52	25,267	59	82	65, 69	74	279	274			250	258		
	0.95	35	30	44	51	24,266	58	81	64, 68	73	278	273			249	257		
	1.00					268												
	1.05	33	28	42	49	22,264	56	79	62	71	276	272			247	256		
	1.11			40	47	20,262	54	77				270				254		
Inboard =0.0 Outboard=5.1	0.40					223					215	209	196	202	246	241	235	229
	0.70					218					211	205	192	198	243	237	231	228
	0.85					221					214	208	195	201	245	240	233	227
	0.95					220					213	207	194	200	244	239	232	226
	1.05					219					212	206	193	199	242	238	230	224
	1.11					217					210	204	191	197		236		



Table B-1.—(Concluded)

Leading-edge deflection, deg	Mach no.	Trailing-edge deflection, deg															
		Full span								Outboard (inboard = 0.0)				Inboard (outboard = 0.0)			
		30.2	17.7	8.3	4.1	0.0	-4.1	-8.3	-17.7	-30.2	17.7	8.3	-8.3	-17.7	17.7	8.3	-8.3
Flat wing, sharp leading-edge, trip strip on																	
Full span=0.0	0.40					368											
	0.70					366											
	0.85					372											
	0.95					374											
	1.00					373											
	1.05					367											
	1.11					365											
Flat wing, twisted trailing-edge, rounded leading-edge, trip strip on																	
Full span=0.0	0.40		352	347	342	337		358	363								
	0.70		349	344	339	333		354	360								
	0.85		351	346	341	336		356	362								
	0.95		350	345	340	335		357	361								
	1.05		348	343	338	334		353	359								
	1.11					332											
	Twisted wing, rounded leading edge, trip strip on																
Full span=0.0	0.40	427	422	416	411	450		435	442								
	0.70	424	419	413	408	445		432	439								
	0.85	426	421	415	410	449		434	441								
	0.95	425	420	414	409	447		433	440								
	1.00					448											
	1.05	423	418	412	407	446		431	438								
	1.10					444											

**Table B-2.—Summary of Subsonic/Transonic FLEXSTAB Conditions by Run Number**  
(NASA Contract NAS1-12875)

Leading-edge deflection, deg	Mach no.	Trailing-edge deflection, deg															
		Full span								Outboard (inboard = 0.0)				Inboard (outboard = 0.0)			
		30.2	17.7	8.3	4.1	0.0	-4.1	-8.3	-17.7	-30.2	17.7	8.3	-8.3	-17.7	17.7	8.3	-8.3
Flat wing, rounded leading-edge, trip strip off																	
Full span = 0.0	0.40					10											
	0.70					15											
	0.85					7											
	0.95					16											
	1.05					14											
	1.11					9											
Flat wing, rounded leading-edge, trip strip on																	
Full span = 0.0	0.40	37	(32)	(46)	48	21(269)	55	(78)	(66)	75	280	275			252	259	
	0.70	34	(29)	(43)	50	23(263)	57	(80)	(63)	72	277	271			248	255	
	0.85	36	(31)	(45)	52	25(267)	59	(82)	(65)	69	74	(279)	(274)		(250)	(258)	
	0.95	35	(30)	(44)	51	24(266)	58	(81)	(64)	68	73	278	273		249	257	
	1.00					(268)											
	1.05	33	(28)	(42)	49	22(264)	56	(79)	(62)	71	276	272			247	256	
1.11			(40)	47	20(262)	54	(77)				270				254		
Inboard = 0.0 Outboard = 5.1	0.40					223					215	209	196	202	246	241	235
	0.70					218					211	205	192	198	243	237	231
	0.85					(221)					(214)	(208)	(195)	(201)	(245)	(240)	(233)
	0.95					220					213	207	194	200	244	239	232
	1.05					219					212	206	193	199	242	238	230
	1.11					217					210	204	191	197		236	229

○ FLEXSTAB solution available

Note: On the data tapes and in the tables of appendix A, the above run numbers have been incremented by 1 000 to give the FLEXSTAB results unique identification.

Table B-2.—(Continued)

Leading-edge deflection, deg	Mach no.	Trailing-edge deflection, deg																
		Full span								Outboard (inboard = 0.0)				Inboard (outboard = 0.0)				
		30.2	17.7	8.3	4.1	0.0	-4.1	-8.3	-17.7	-30.2	17.7	8.3	-8.3	-17.7	17.7	8.3	-8.3	-17.7
Flat wing, rounded leading-edge, trip strip on																		
Inboard = 5.1 Outboard = 0.0	0.40					319					286	313			329	324		
	0.70					315					283	311			326	321		
	0.85					318					285	312			328	323		
	0.95					317					284	310			327	322		
	1.05					316					282	308			325	320		
	1.11					314												
Full span = 5.1	0.40		177	149	138	183		189	132									
	0.70		173	145	140	179		185	134									
	0.85		175	148	142	182		188	136									
	0.95		174	147	141	181		187	135									
	1.05		172	146	139	180		186	133									
	1.11			144	137	178		184	131									
Full span = 12.8	0.40		118	115	109	98		85	126									
	0.70		121	112	105	100		87	128									
	0.85		123	114	108	102		89	130									
	0.95		122	113	107	101		88	129									
	1.05		120	111	106	99		86	127									
	1.11		116		104	97		84	124									

○ FLEXSTAB solution available

Note: On the data tapes and in the tables of appendix A, the above run numbers have been incremented by 1 000 to give the FLEXSTAB results unique identification.

Table B-2.—(Concluded)

Leading-edge deflection, deg	Mach no.	Trailing-edge deflection, deg															
		Full span									Outboard (inboard = 0.0)				Inboard (outboard = 0.0)		
		30.2	17.7	8.3	4.1	0.0	-4.1	-8.3	-17.7	-30.2	17.7	8.3	-8.3	-17.7	17.7	8.3	-8.3
Flat wing, sharp leading-edge, trip strip on																	
Full span=0.0	0.40					368											
	0.70					366											
	0.85					372											
	0.95					374											
	1.00					373											
	1.05					367											
	1.11					365											
Flat wing, twisted trailing-edge, rounded leading-edge, trip strip on																	
Full span=0.0	0.40		(352)	(347)	342	(337)		(358)	(363)								
	0.70		349	344	339	333		354	360								
	0.85		(351)	(346)	341	(336)		(356)	(362)								
	0.95		350	345	340	335		357	361								
	1.05		(348)	(343)	338	(334)		(353)	(359)								
	1.11					332											
	Twisted wing, rounded leading-edge, trip strip on																
Full span=0.0	0.40	427	(422)	(416)	411	(450)		(435)	(442)								
	0.70	424	(419)	(413)	408	(445)		(432)	(439)								
	0.85	426	(421)	(415)	410	(449)		(434)	(441)								
	0.95	425	(420)	(414)	409	(447)		(433)	(440)								
	1.00					(448)											
	1.05	423	(418)	(412)	407	(446)		(431)	(438)								
	1.10					(444)											

○ FLEXSTAB solution available

Note: On the data tapes and in the tables of appendix A, the above run numbers have been incremented by 1 000 to give the FLEXSTAB results unique identification.

Figure B-2 shows a typical paneling scheme used for the TEA-230 representation of the arrow-wing body model. The source panels are placed on the configuration surface; consequently, new paneling was required for each configuration. The linearly varying internal and trailing vortex panel networks are not shown but extend 228.6 m (9000 in.) behind the model. Table B-3 summarizes the configurations and Mach numbers for which solutions were obtained.

#### **NASA CONTRACT NAS1-14141**

This contract was again divided into experimental and theoretical tasks with the same objectives as the previous contract, but for supersonic Mach numbers up to 2.5.

#### **EXPERIMENTAL TASK**

The model used in this contract is the same as used in NASA contract NAS1-12875.

The 9- by 7-ft supersonic leg of the NASA Ames Unitary Wind Tunnel is a continuous-flow, closed-return, variable-density facility with an operating range of Mach number from 1.54 to 2.50. A schematic is shown in figure B-3. The tunnel is equipped with an asymmetric, sliding-block nozzle and a flexible upper plate; variation of the test section Mach number is achieved by translating, in the streamwise direction, the fixed contour block that forms the floor of the nozzle. For this test, the Reynolds number was selected as  $8.65 \times 10^6$  based on the mean aerodynamic chord ( $\bar{c}$ ) of this model. The test section is 2.74 by 2.13 by 5.49 m (9 by 7 by 18 ft).

The data acquisition system is comprised of a Beckman 210 analog-digital recorder and a minicomputer. Output from the Beckman 210 is converted to an acceptable format and transmitted by the minicomputer to an IBM 360 computer located in the Ames Research Center central computer facility for processing and preparation of final data. This flow is illustrated in figure B-4.

Table B-4 lists the 13 configurations that were tested. Photographs of two of these are shown in figures B-5 and B-6; a diagram of the model installation in the test section is shown in figure B-7. Pressure and total force data were obtained at Mach numbers of 1.70, 2.10, and 2.50 for all configurations. Table B-4 shows the run numbers for each Mach number and configuration for which these data were obtained. Test angles of attack were from  $-8^\circ$  to  $+14^\circ$  in  $2^\circ$  increments and  $+15^\circ$ .

#### **THEORETICAL TASK**

The only theoretical method used in this contract was FLEXSTAB. It was determined that the interference paneling used for subsonic Mach numbers is also adequate at these supersonic Mach numbers (see fig. 40(a)). The combinations of Mach number and configuration for which predictions were made are shown in Table B-5.



**Table B-3.—Summary of TEA-230 Conditions by Run Number  
(NASA Contract NAS1-12875)**

Leading-edge deflection, deg	Mach number	Trailing-edge deflection, deg																
		Full span									Outboard (inboard = 0.0)				Inboard (outboard = 0.0)			
		30.2	17.7	8.3	4.1	0.0	-4.1	-8.3	-17.7	-30.2	17.7	8.3	-8.3	-17.7	17.7	8.3	-8.3	-17.7
Flat wing, rounded leading edge																		
Full span= 0.0	0.40	(37)	(32)	(46)	48	21,269	(55)	(78)	66	75	280	275			252	259		
	0.85	36	(31)	45	52	25,267	59	82	65,69	74	279	274			250	258		
Full span = 5.1	0.40		177	149	138	(183)		189	132									
	0.85		175	148	142	(182)		188	136									
Full Span = 12.8	0.40		118	115	109	(98)		85	126									
	0.85		123	114	108	102		89	130									
Flat wing, sharp leading edge																		
Full span= 0.0	0.40					(368)												
	0.85					(372)												
Twisted wing, rounded leading edge																		
Full span= 0.0	0.40	427	422	416	411	(450)		435	442									
	0.85	426	421	415	410	(449)		434	441									

○ = TEA-230 solution available

Note: On the data tapes and in the tables of Appendix A, the above run numbers have been incremented by 2000 to give the TEA-230 results unique identification.

**Table B-4.—Summary of Test Conditions by Run Number. (NASA Contract NAS1-14141)**  
**Reynolds Number =  $8.65 \times 10^6$**

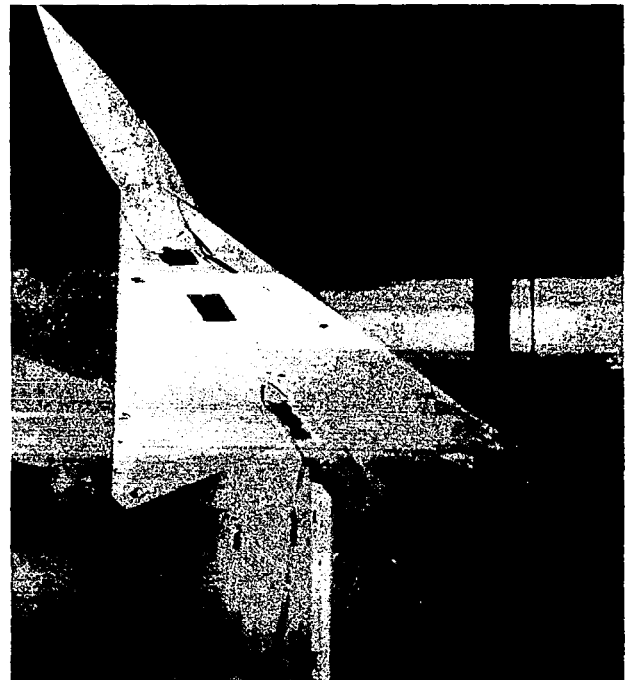
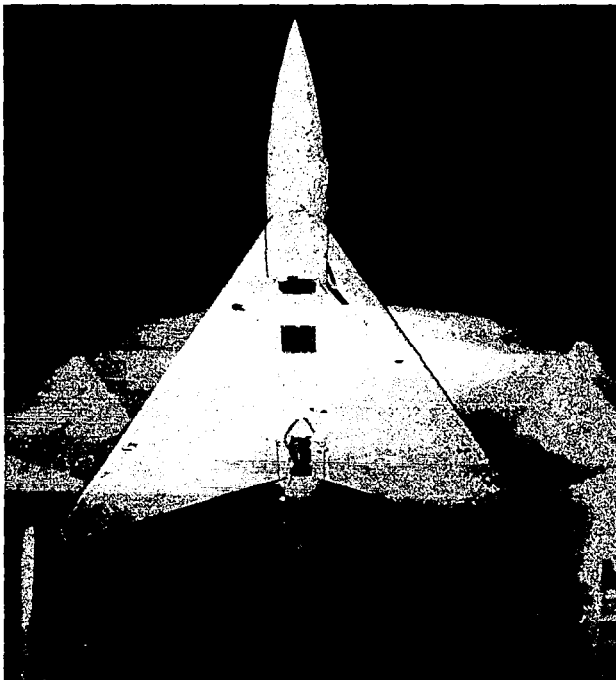
Leading-edge deflection, deg	Mach number	Trailing-edge deflection, deg							
		Full span				Outboard (inboard = 0.0)		Inboard (outboard = 0.0)	
		8.3	4.1	0.0	-4.1	8.3	4.1	8.3	4.1
Flat wing, rounded L.E.									
Full span = 0.0	1.543			19					
	1.70	26	37	20	44	23	40	30	34
	2.10	27	38	21	45	24	41	31	35
	2.50	28	39	22	46	25	42	32	36
Full span = 5.1	1.70			16					
	2.10			17					
	2.50			18					
Flat wing, sharp L.E.									
Full span = 0.0	1.70			51					
	2.10			52					
	2.50			53					
Full span = 5.1	1.70			48					
	2.10			49					
	2.50			50					
Twisted wing, rounded L.E.									
Full span = 0.0	1.60			1					
	1.70	11		3					
	1.90			4, 6					
	2.10	12		9					
	2.50	13		10					

**Table B-5.—Summary of FLEXSTAB Conditions by Run Number  
(NASA Contract NAS1-14141)**

Leading-edge deflection, deg	Mach number	Trailing-edge deflection, deg							
		Full span				Outboard (inboard = 0.0)		Inboard (outboard = 0.0)	
		8.3	4.1	0.0	-4.1	8.3	4.1	8.3	4.1
Flat wing, rounded L.E.									
Full span = 0.0	1.543			19					
	1.70	(26)	(37)	(20)	(44)	(23)	(40)	(30)	(34)
	2.10	(27)	(38)	(21)	(45)	(24)	(41)	(31)	(35)
	2.50	(28)	(39)	(22)	(46)	(25)	(42)	(32)	(36)
Full span = 5.1	1.70			(16)					
	2.10			(17)					
	2.50			(18)					
Flat wing, sharp L.E.									
Full span = 0.0	1.70			51					
	2.10			52					
	2.50			53					
Full span = 5.1	1.70			48					
	2.10			49					
	2.50			50					
Twisted wing, rounded L.E.									
Full span = 0.0	2.60			1					
	1.70	(11)		(3)					
	1.90			4, 6					
	2.10	(12)		(9)					
	2.50	(13)		(10)					

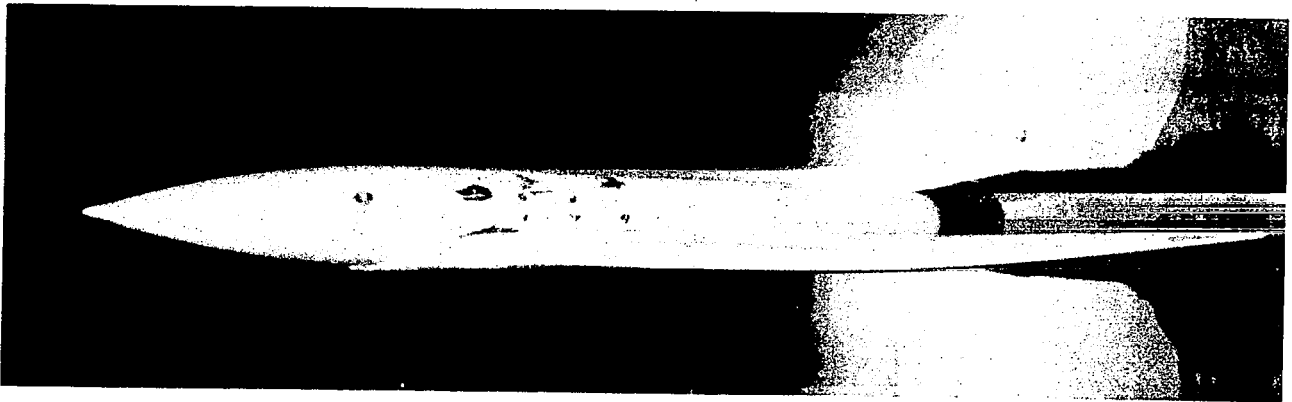
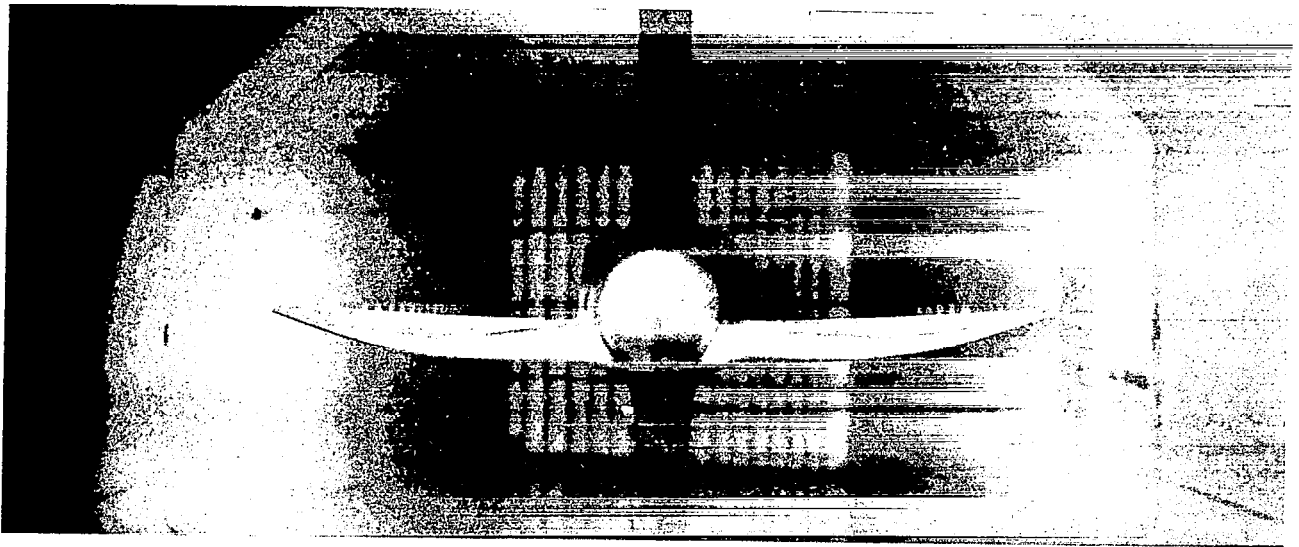
○ FLEXSTAB solution available

Note: On the data tapes and in the tables of appendix A, the above run numbers have been incremented by 1 000 to give the FLEXSTAB results unique identification.



(a) Flat Wing, Rounded L.E.; L.E. Deflection, Full Span =  $0.0^\circ$ ; T.E. Deflection, Full Span =  $0.0^\circ$

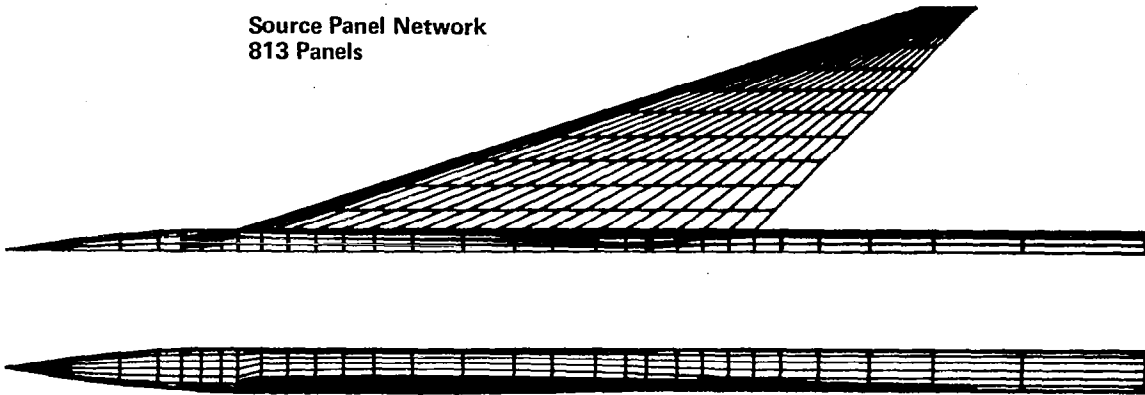
*Figure B-1.—Model in Boeing Transonic Wind Tunnel  
(NASA Contract NAS1-12875)*



(b) Twisted Wing, Rounded L.E.; L.E. Deflection, Full Span =  $0.0^\circ$ ; T.E. Deflection, Full Span =  $4.1^\circ$

*Figure B-1.—(Concluded)*

Source Panel Network  
813 Panels



Vortex Network  
293 Panels

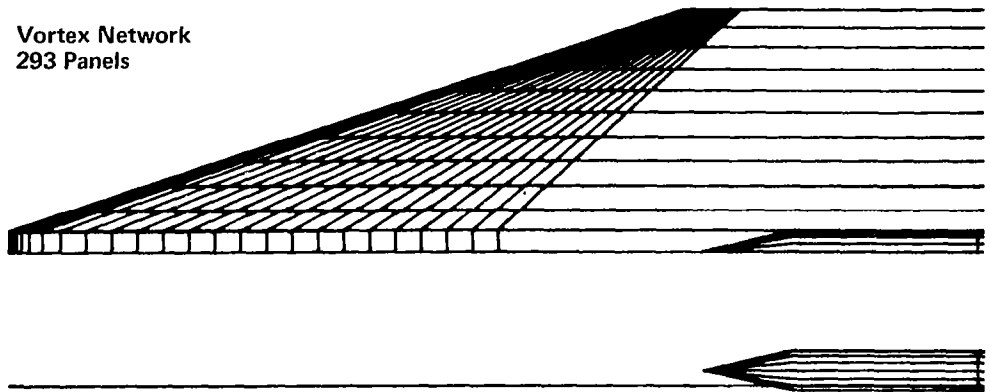


*Figure B-2.—Paneling for TEA-230 Computer Program—Flat Wing,  
Rounded Leading Edge, 1106 Singularities*

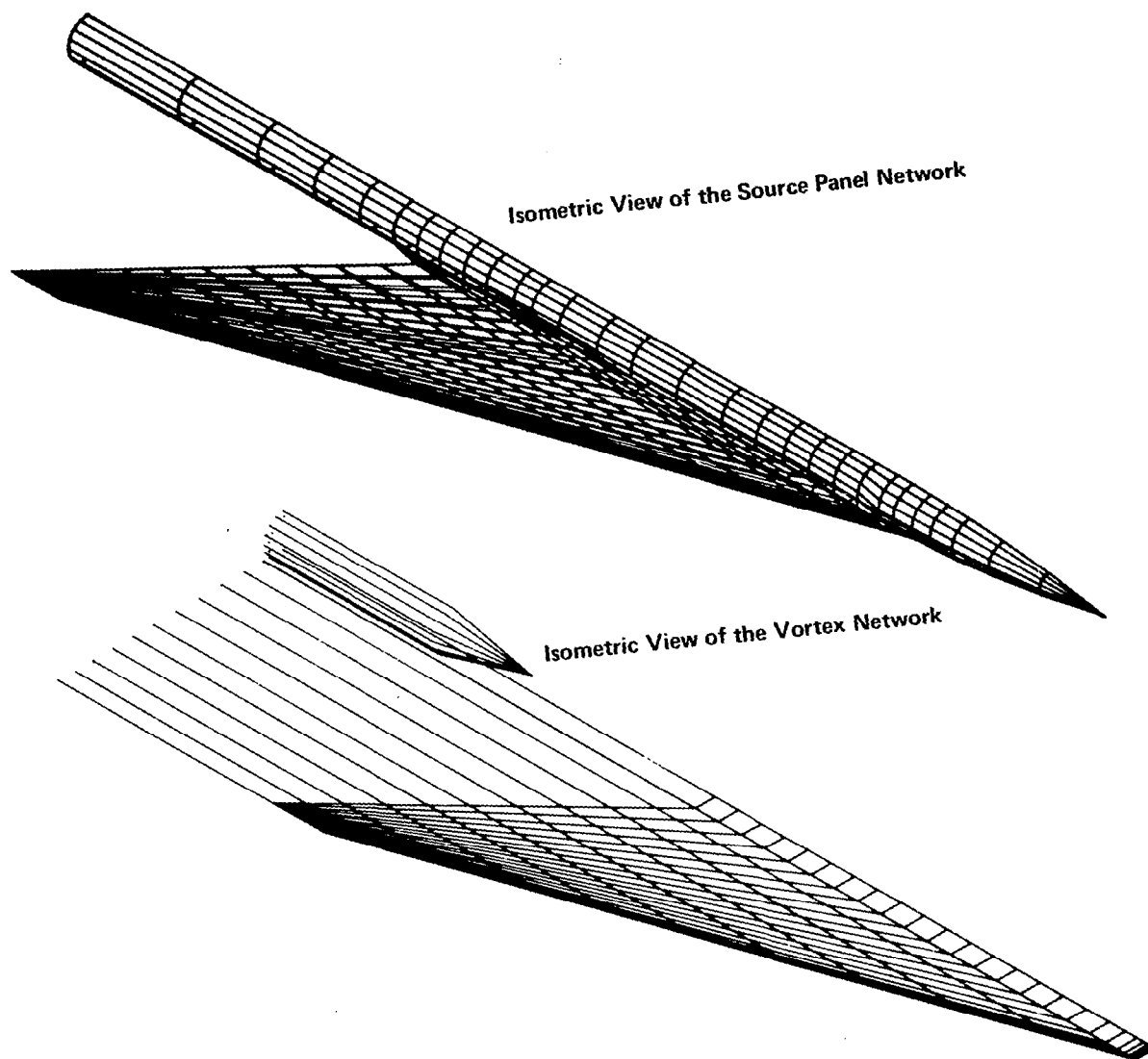


*Figure B-2.—(Concluded)*

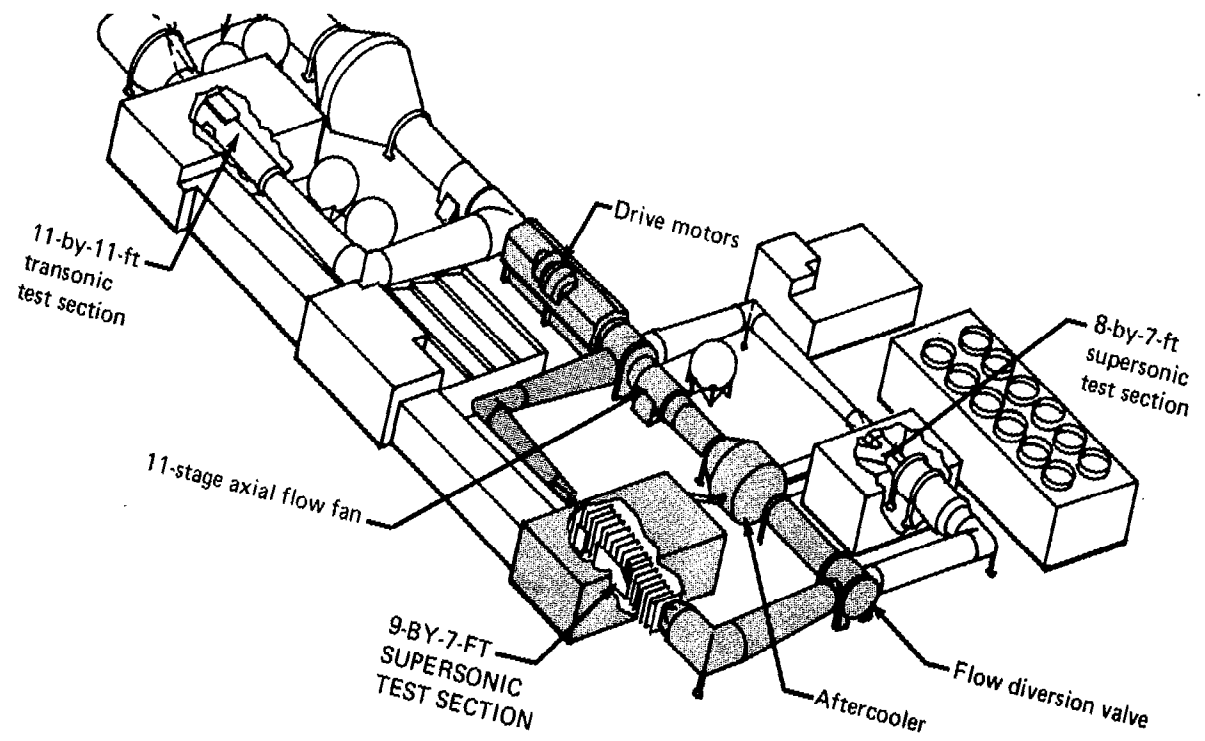
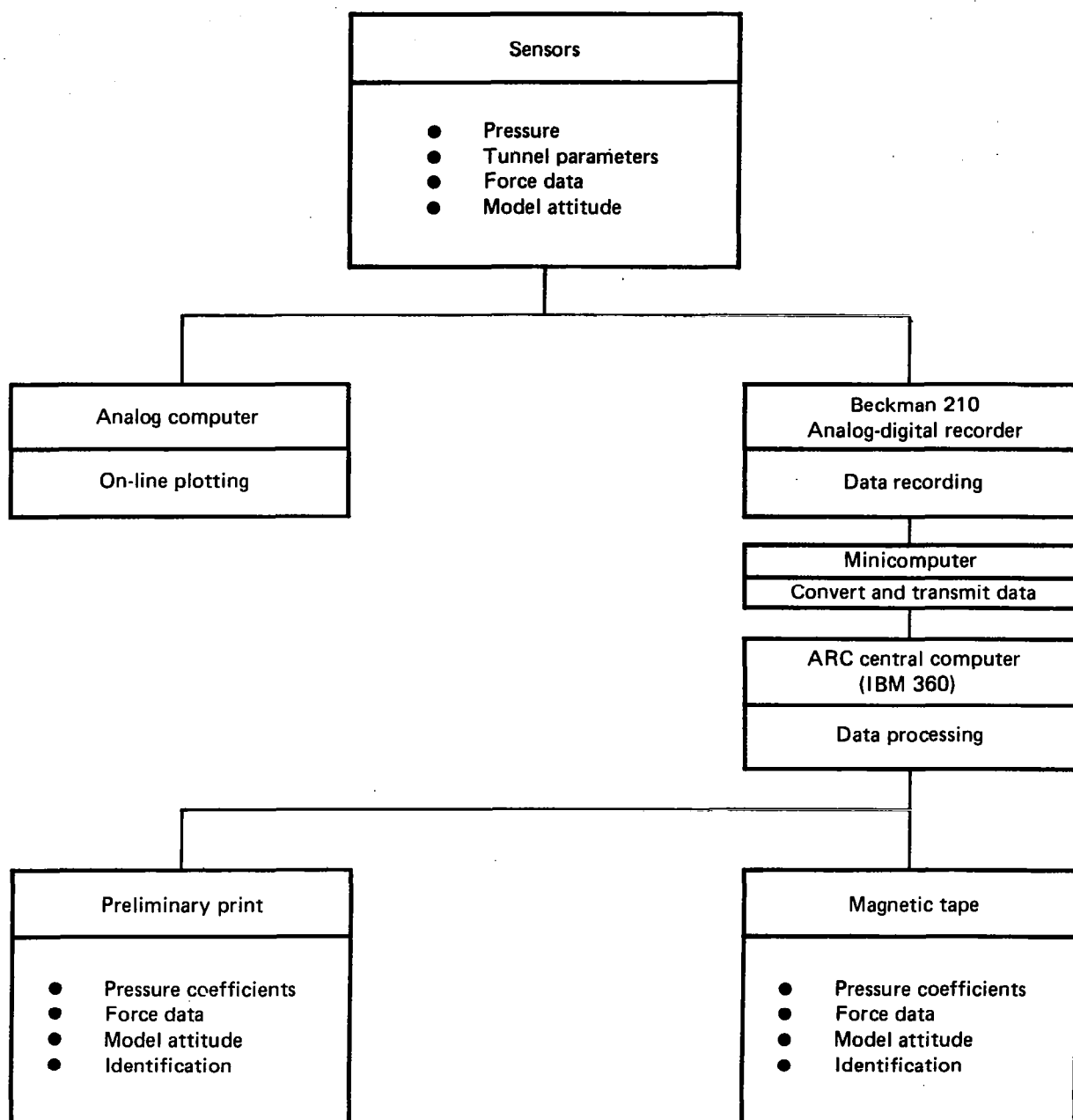
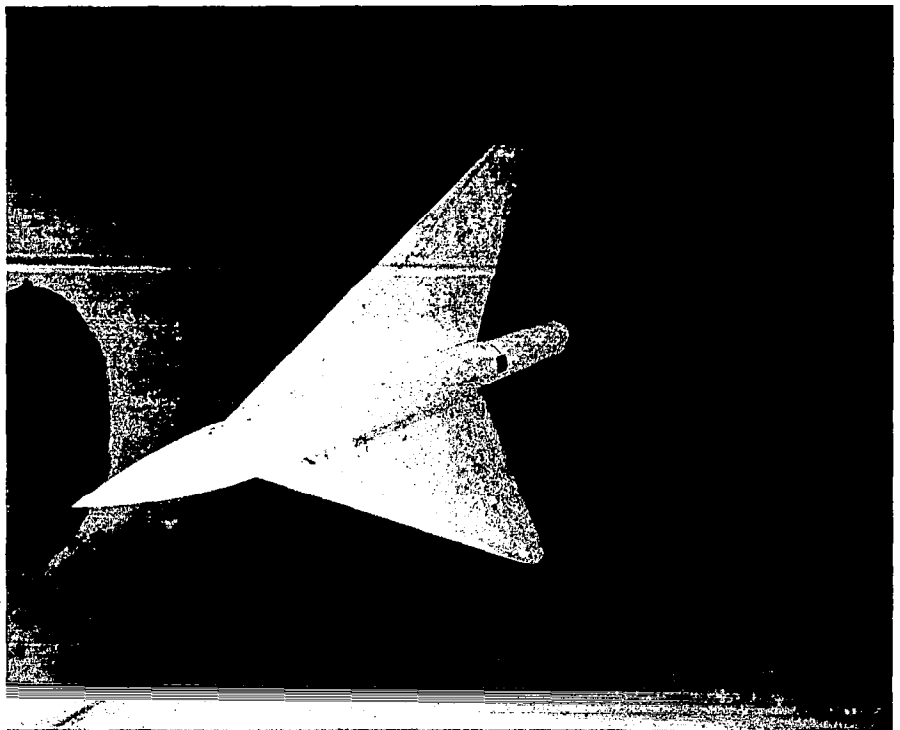
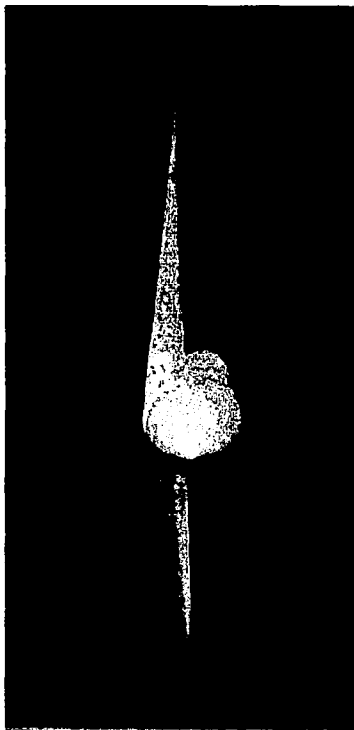


Figure B-3.—Schematic of 9-by-7-ft Leg of NASA Ames Unitary Wind Tunnel





*Figure B-4.—Data Acquisition and Reduction System—9-by-7-ft Leg of NASA Ames Unitary Wind Tunnel*



*Figure B-5.—Wind Tunnel Model—Flat Wing, Rounded L.E. (NASA Contract NAS1-14141)*

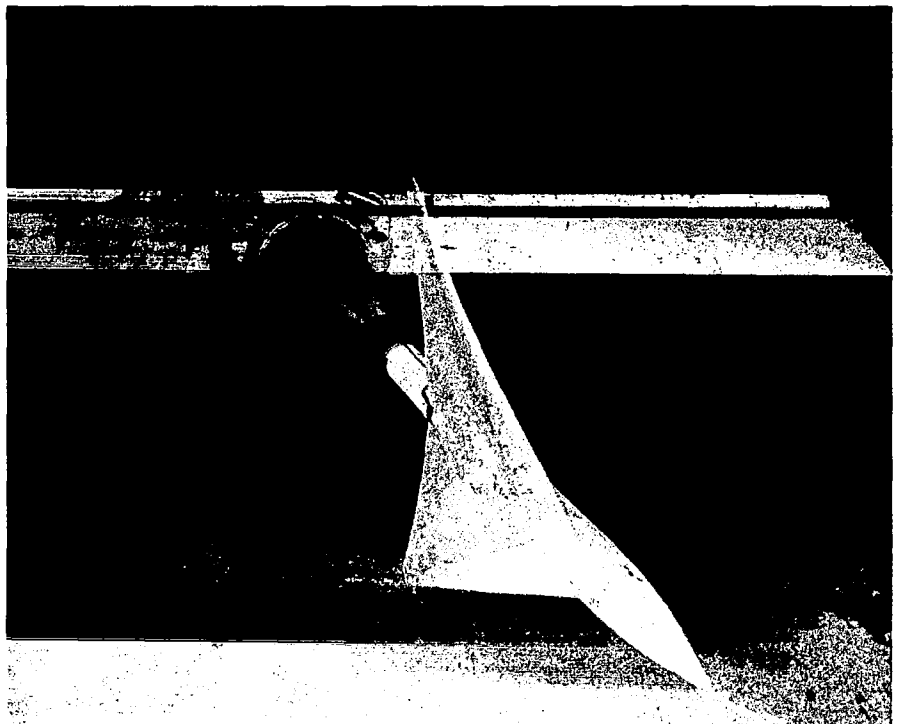
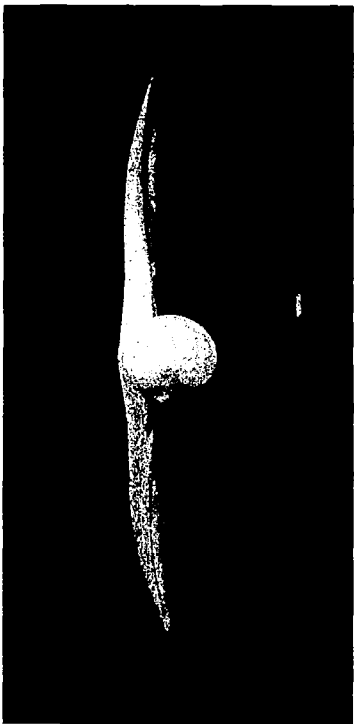


*Figure B-6.—Wind Tunnel Model—Twisted Wing (NASA Contract NAS1-14141)*

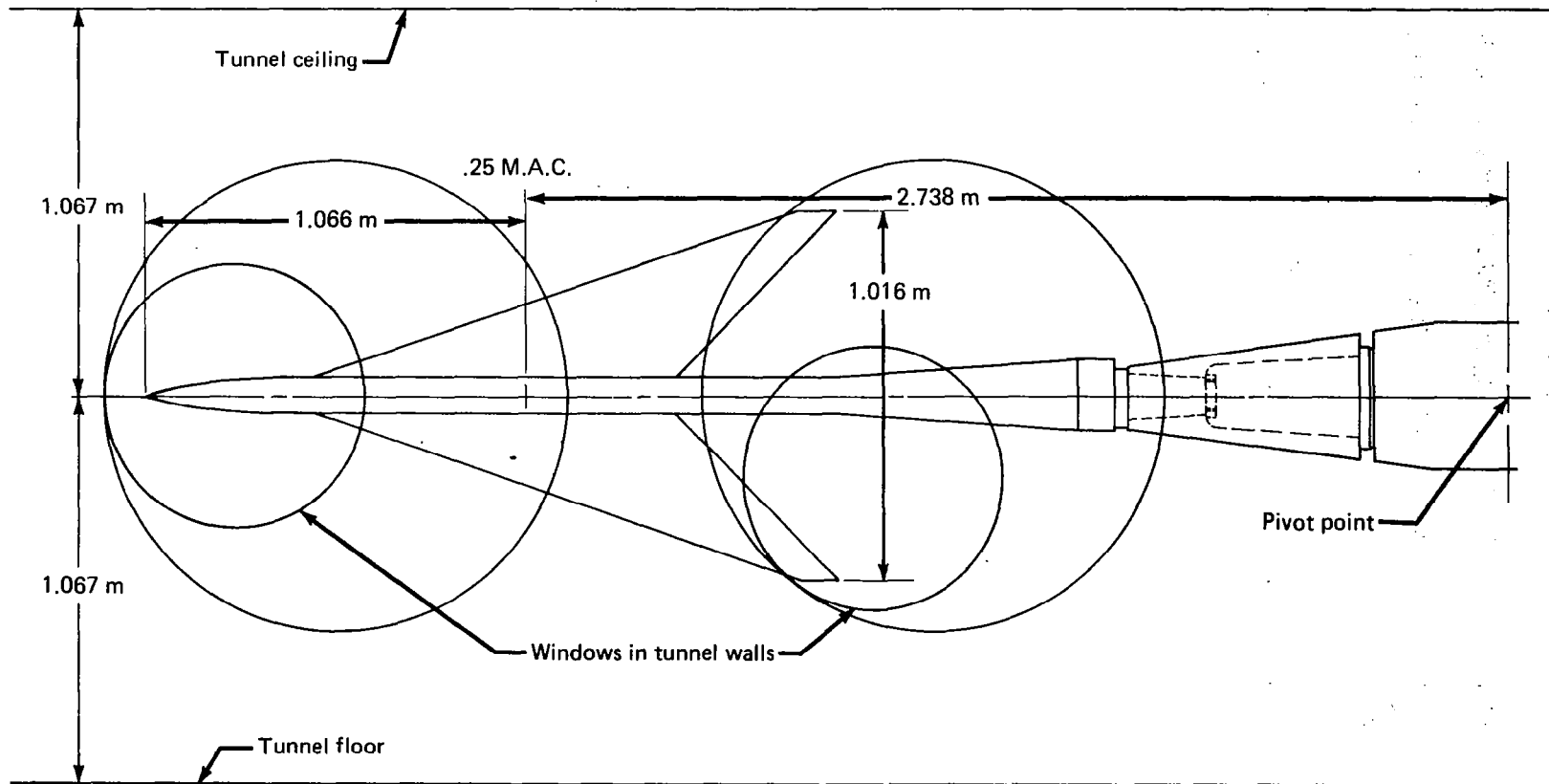


*Figure B-7.—Model Installation in 9-by-7-ft Leg of NASA Ames Unitary Wind Tunnel*

## **APPENDIX C**

### **DATA REDUCTION AND PRESENTATION**

#### **DATA EDITING AND INTEGRATION PROCEDURE**

##### **DATA EDITING**

Some cases were encountered with these data where the methods of data editing available within the integration programs were not adequate. Because the plotting program assumes that geometry for all configurations is the same and the chordwise location of orifices on the various model parts was not absolutely identical, points were added as required. Therefore, some interpolations or extrapolations using selected orifices were done before the integration program was used. The row of orifices on the body at the wing-body intersection was extended in front of the wing and aft of the wing by interpolating between the orifices located at  $90^\circ$  and  $135^\circ$ .

Damage to one of the quick disconnects for the wing caused the loss of measurements at a series of orifices ( $x/c$  from 0.125 through 0.600) on the lower surface at 0.80  $b/2$ . Replacement values were obtained by a linear spanwise interpolation between the adjacent sections.

Several methods were introduced into the integration program to replace or add data points to account for:

- Plugged or leaking orifices or bad data points
- Extrapolating the data to leading and trailing edges
- Hingeline discontinuities in the pressure data

These procedures were selected by code for each point. The codes are described in the following list and are illustrated in figure C-1. An additional use of these codes is to ensure that only measured pressure data ( $CODE_i = 0$ ) are identified with symbols on the plots.

IF  $CODE_i = 0$ , use pressure as entered on tape (measured pressure)

= 20, use as entered on tape (previously replaced value)

= 1, interpolate from adjacent points

= 2, extrapolate from two preceding points

= 3, extrapolate from two following points

= 4, set equal to preceding point

= 5, set equal to following point

= 6, interpolate using points  $(i-2)$  and  $(i+1)$

= 7, interpolate using points  $(i-1)$  and  $(i+2)$

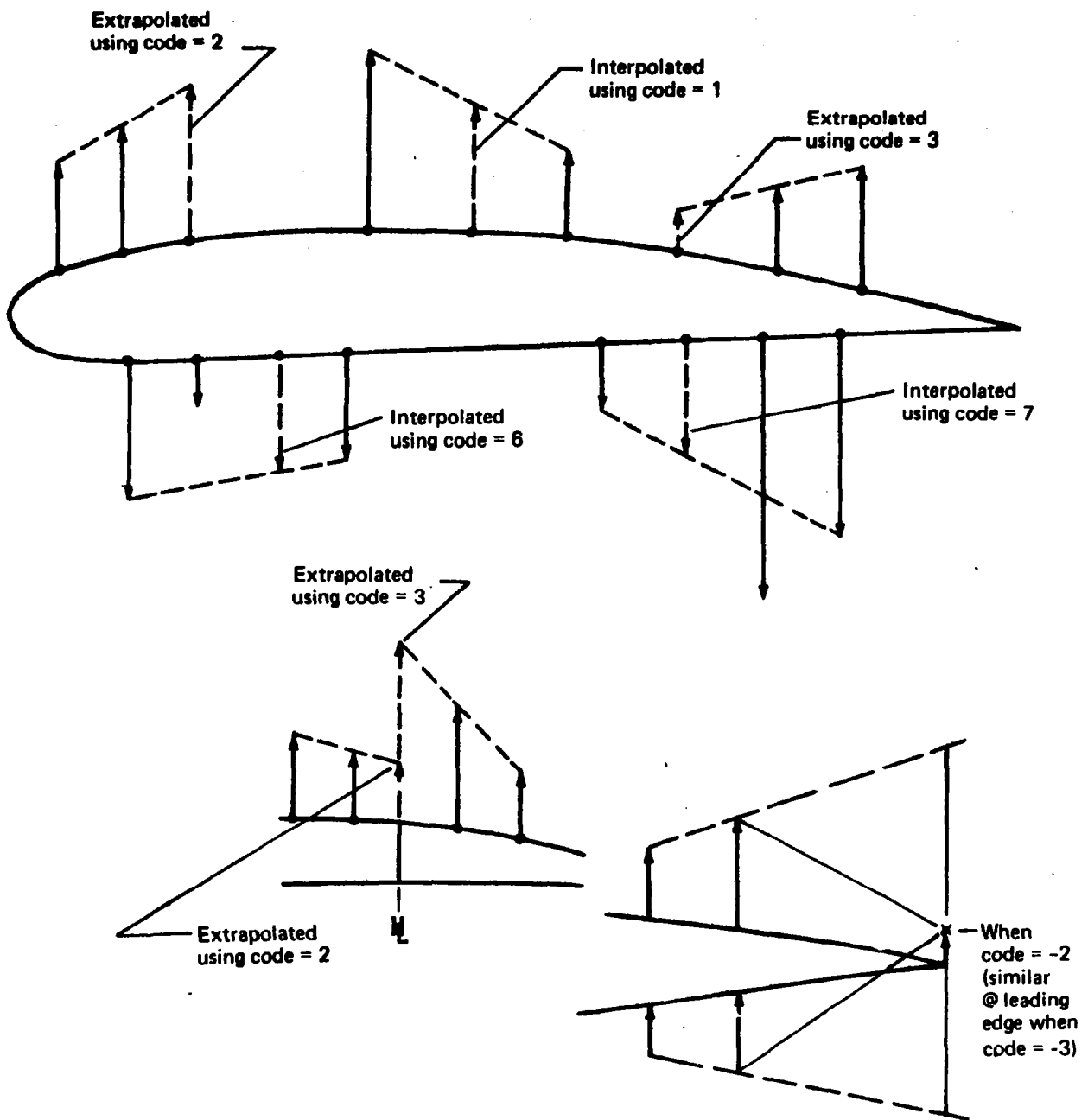


Figure C-1. - Codes Used to Interpolate and Extrapolate

IF CODE<sub>i</sub> = negative of above, evaluate as above but average with corresponding point on opposite surface - used for leading and trailing edges of section only

where

i identifies the position of the point from the leading edge of the upper or lower surface section.

Editing of the pressure data is done in the following order:

1. Each section is done separately.
2. Each surface (upper or lower) per section is done in the following sequence:
  - a. Starting at leading edge, points with codes of 1, 2, and 4
  - b. Starting at trailing edge, points with codes of 3, 5, 6, and 7.
3. Leading- and trailing-edge points with negative codes are evaluated. Upper and lower surface codes need not both be negative and need not be the same negative code.

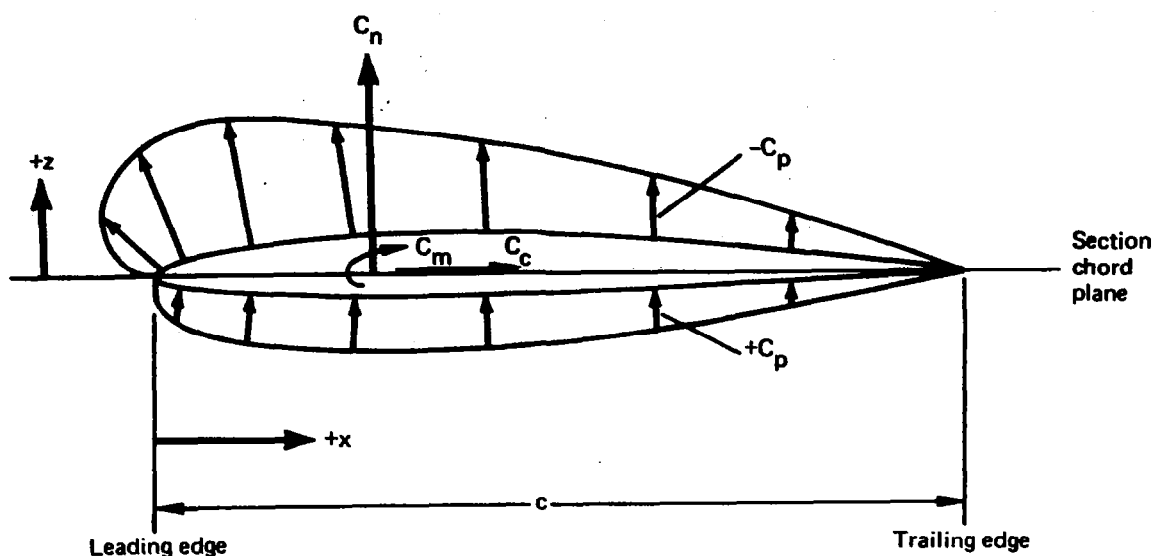
### **CALCULATION OF NET PRESSURE COEFFICIENTS**

The net lift distribution on the section is calculated by:

$$C_{p,net} = C_{p,lower} - C_{p,upper} \quad (C-1)$$

### **INTEGRATION OF PRESSURE DATA**

To account for the effects on integrated coefficients of the deflected control surfaces, each streamwise section (of which there are NSECT) is divided into segments (of which there are NSEG). These segments are the leading-edge control surface, wing box, and trailing-edge control surface. The upper and lower surfaces of each are integrated separately over the number of points available ((number of orifices + 2) = NP1) and are based on the segment chord length  $c$ . Sign conventions are shown in the following sketch. The equations, which use a rectangular integration process, follow.



### Segment Coefficients

Integration of the pressures for each segment per surface per section is the first step.

- Normal force coefficient  $C_{n,s}$

$$C_{n,s} = 0.5 \sum_{i=2}^{NP1} \left[ (C_p)_i + (C_p)_{i-1} \right] \left[ \left( \frac{x}{c} \right)_i - \left( \frac{x}{c} \right)_{i-1} \right] \quad (C-2)$$

$$C_{n,s,net} = C_{n,s,lower} - C_{n,s,upper} \quad (C-3)$$

- Chord force coefficient  $C_{c,s}$

$$C_{c,s} = 0.5 \sum_{i=2}^{NP1} \left[ (C_p)_i + (C_p)_{i-1} \right] \left[ \left( \frac{z}{c} \right)_i - \left( \frac{z}{c} \right)_{i-1} \right] \quad (C-4)$$

$$C_{c,s,net} = C_{c,s,upper} - C_{c,s,lower} \quad (C-5)$$

- Pitching moment coefficient about segment leading edge  $C_{m,s}$

$$C_{m,s} = 0.5 \sum_{i=2}^{NP1} \left[ (C_p)_i + (C_p)_{i-1} \right] \left[ \left( \frac{x}{c} \right)_{i-1} + \frac{\left( \frac{x}{c} \right)_i - \left( \frac{x}{c} \right)_{i-1}}{2.0} \right] \left[ \left( \frac{x}{c} \right)_i - \left( \frac{x}{c} \right)_{i-1} \right]$$

$$= 0.25 \sum_{i=2}^{NP1} \left[ (C_p)_i + (C_p)_{i-1} \right] \left[ \left( \frac{x}{c} \right)_i^2 - \left( \frac{x}{c} \right)_{i-1}^2 \right] \quad (C-6)$$

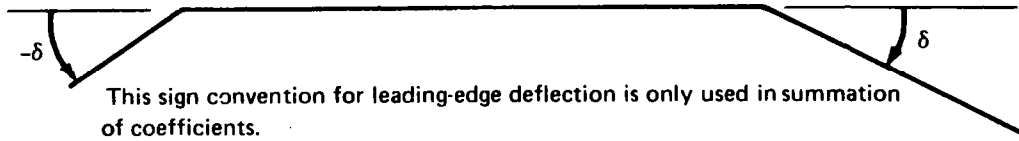
$$C_{m,s,net} = C_{m,s,upper} - C_{m,s,lower} \quad (C-7)$$

- Pitching moment coefficient about 0.25 c of segment  $C_{m,25c,s}$

$$C_{m,25c,s} = C_{m,s} + 0.25 C_{n,s} \quad (C-8)$$

### Section Coefficients

Total section coefficients are obtained by summing the segment coefficients, taking into account segment deflections as defined in the following sketch and segment chord lengths. These coefficients are based on the section chord length  $c_T$ .



- Normal force coefficient  $C_n$

$$C_n = \sum_{j=1}^{NSEG} (C_{n,s})_j \left( \frac{c_s}{c} \right)_j \cos \delta_j - \sum_{j=1}^{NSEG} (C_{c,s})_j \left( \frac{c_s}{c} \right)_j \sin \delta_j \quad (C-9)$$

- Pitching moment coefficient about section leading edge  $C_m$

$$C_m = \sum_{j=1}^{NSEG} (C_{m,s})_j \left( \frac{c_s}{c} \right)_j^2 + \left[ (C_{n,s})_1 (1.0 - \cos \delta_1) + (C_{c,s})_1 \sin \delta_1 \right] \left( \frac{c_s}{c} \right)_1^2$$

$$- \sum_{j=2}^{NSEG} \left[ (C_{n,s})_j \cos \delta_j - (C_{c,s})_j \sin \delta_j \right] \left( \frac{c_s}{c} \right)_j \left[ \frac{x_{L.E.,s} - x_{L.E.}}{c} \right] \quad (C-10)$$



where

$c_s$  is segment chord, cm

$c$  is section chord, cm

$\delta$  is deflection of segment relative to section chord plane, leading edge up, degrees

$x_{L.E.,s}$  is leading edge of segment, cm

$x_{L.E.}$  is leading edge of section, cm

- Pitching moment coefficient about 0.25 c of section  $C_{m.25c}$

$$C_{m.25c} = C_m + 0.25 C_n \quad (C-11)$$

### Total Surface Coefficients

To obtain total surface coefficients, the assumption is made that the section coefficients apply for a finite distance on both sides of each row of orifices. The equations for total surface coefficients are as follows:

- Normal force coefficient  $C_N$

$$C_N = \frac{1}{S} \sum_{k=1}^{N_{SECT}} (C_n)_k (S_h)_k \quad (C-12)$$

- Bending moment coefficient  $C_B$

$$C_B = \frac{1}{S(b/2)} \sum_{k=1}^{N_{SECT}} (C_n)_k (S_h y)_k \quad (C-13)$$

- Pitching moment coefficient about 0.25 M.A.C.  $C_M$

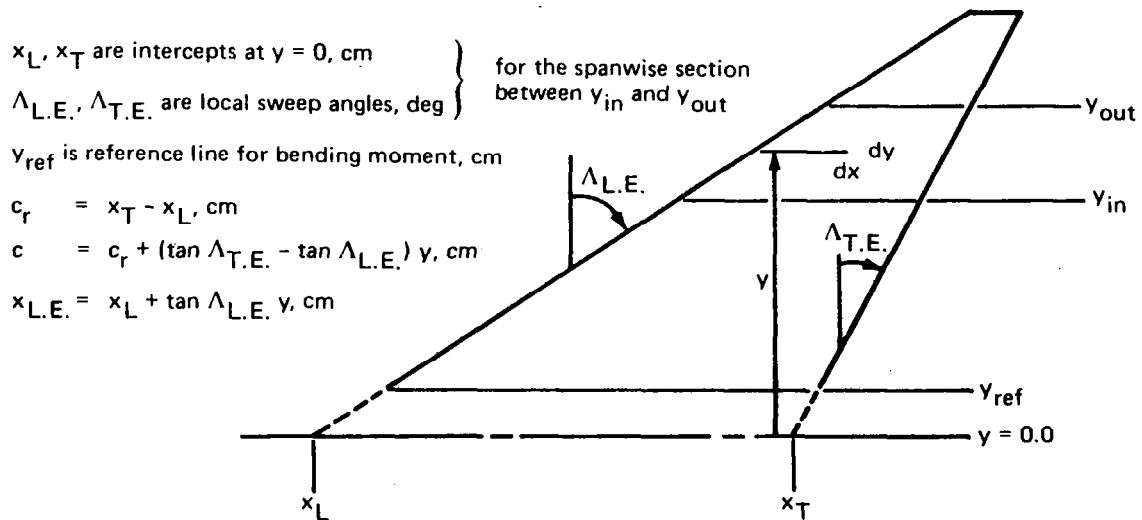
$$C_M = \frac{1}{S\bar{c}} \sum_{k=1}^{N_{SECT}} \left\{ (C_m)_k (S_h c)_k + (C_n)_k (S_h)_k [x_{ref} - (x_{L.E.})_k] \right\} \quad (C-14)$$

where

- $\bar{c}$  is reference chord for pitching moment, cm
- $x_{ref}$  is reference station for pitching moment, cm (0.25 M.A.C.)
- $x_{L.E.}$  is leading edge of section chord, cm
- $b/2$  is reference length for bending moment, cm

### Determination of Geometric Constants Required for Integration

To obtain total surface coefficients, the assumption is made that the section coefficients apply for a finite distance on both sides of each row of orifices. The input geometry required to calculate the areas, and products of area and length required for the summation of total surface coefficients, are shown in the following sketch.



#### • Section area:

$$\begin{aligned}
 S_h &= \int_{y_{in}}^{y_{out}} \int_{x_L + \tan \Lambda_{L.E.} y}^{x_T + \tan \Lambda_{T.E.} y} dy dx \\
 &= c_r (y_{out} - y_{in}) + 0.5 (\tan \Lambda_{T.E.} - \tan \Lambda_{L.E.}) (y_{out}^2 - y_{in}^2) \quad (C-15)
 \end{aligned}$$

- **Product of section area and mean chord:**

$$\begin{aligned}
 S_{hc} &= \int_{y_{in}}^{y_{out}} \int_{x_L + \tan \Lambda_{L.E.} y}^{x_T + \tan \Lambda_{T.E.} y} c \, dy \, dx \\
 &= c_r^2 (y_{out} - y_{in}) + c_r (\tan \Lambda_{T.E.} - \tan \Lambda_{L.E.}) (y_{out}^2 - y_{in}^2) \\
 &\quad + \frac{(\tan \Lambda_{T.E.} - \tan \Lambda_{L.E.})^2}{3.0} (y_{out}^3 - y_{in}^3) \quad (C-16)
 \end{aligned}$$

- **Product of section area and moment arm:**

$$\begin{aligned}
 S_{hy} &= \int_{y_{in}}^{y_{out}} \int_{x_L + \tan \Lambda_{L.E.} y}^{x_T + \tan \Lambda_{T.E.} y} (y - y_{ref}) \, dy \, dx \\
 &= \frac{c_r - (\tan \Lambda_{T.E.} - \tan \Lambda_{L.E.}) y_{ref}}{2.0} (y_{out}^2 - y_{in}^2) \\
 &\quad + \frac{(\tan \Lambda_{T.E.} - \tan \Lambda_{L.E.})}{3.0} (y_{out}^3 - y_{in}^3) - c_r y_{ref} (y_{out} - y_{in}) \quad (C-17)
 \end{aligned}$$

- **Product of section area and leading edge coordinate:**

$$\begin{aligned}
 S_{hx} &= \int_{y_{in}}^{y_{out}} \int_{x_L + \tan \Lambda_{L.E.} y}^{x_T + \tan \Lambda_{T.E.} y} x_{L.E.} \, dy \, dx \\
 &= x_L c_r (y_{out} - y_{in}) + \frac{\tan \Lambda_{L.E.} c_r + x_L (\tan \Lambda_{T.E.} - \tan \Lambda_{L.E.})}{2.0} (y_{out}^2 - y_{in}^2) \\
 &\quad + \tan \Lambda_{L.E.} \frac{(\tan \Lambda_{T.E.} - \tan \Lambda_{L.E.})}{3.0} (y_{out}^3 - y_{in}^3) \quad (C-18)
 \end{aligned}$$

- **Total surface reference area:**

$$S = \sum_{k=1}^{NSECT} (S_h)_k \quad (C-19)$$

- M.A.C. and X coordinate of M.A.C. leading edge:

$$\bar{c} = \frac{1}{S} \sum_{k=1}^{NSECT} (S_{hc})_k \quad (C-20)$$

$$x_{L.E.,M.A.C.} = \frac{1}{S} \sum_{k=1}^{NSECT} (S_{hx})_k \quad (C-21)$$

The required integration constants for the wing and body are shown in table C-1.

## DATA PRESENTATION

Computer programs were used to generate plots in order to minimize the amount of manual labor. The following sections describe the forms of data presentation used in this report.

### PRESSURE COEFFICIENTS

Chordwise distributions of upper surface, lower surface, and net (lower-upper) pressure coefficients are plotted as a function of local  $x/c$ . Any interpolated or extrapolated values are used in fairing the lines, but only actual measured values are plotted as symbols. In cases where the measurement at a particular orifice was not valid for a particular test point, the symbol is not shown on the plot either for local surface or net distributions. Longitudinal pressure distributions of surface pressures are presented for the body.

The variation of net pressure coefficients with angle of attack at specific orifice locations is compared with theoretical predictions.

Isobar plots are drawn on the surface planform after interpolating the pressure coefficients from the input locations (for this model all interpolated and extrapolated data from the integration program were used) to a more dense rectangular grid of streamwise lines (orifice stations are retained) and constant percent chord lines. This is a linear interpolation and extrapolation process which ignores the presence of all discontinuities such as deflected control surfaces. The final isobars in the regions near such discontinuities will therefore be inaccurate.

Each set of four adjacent points in the rectangular grid is treated in turn and a fifth point is added to form four triangles as shown in the following sketch. The pressure coefficient at the center point is calculated by averaging the outer four.

The values of pressure coefficient which will be mapped are determined by marking off a series of specified increments above and below zero, up to the maximum and minimum pressure coefficients which exist in the rectangular grid. The upper and lower surfaces are treated separately and can have different increments between isobars.

Table C-1. - Integration Constants

Reference area = 3128.45 cm<sup>2</sup>

M.A.C. = 75.311 cm

Half span = 50.80 cm

Pitching moment referenced to 0.25 M.A.C.

Bending moment referenced to  $0.086 \frac{b}{2}$  ( $y_{ref} = 4.374$  cm)

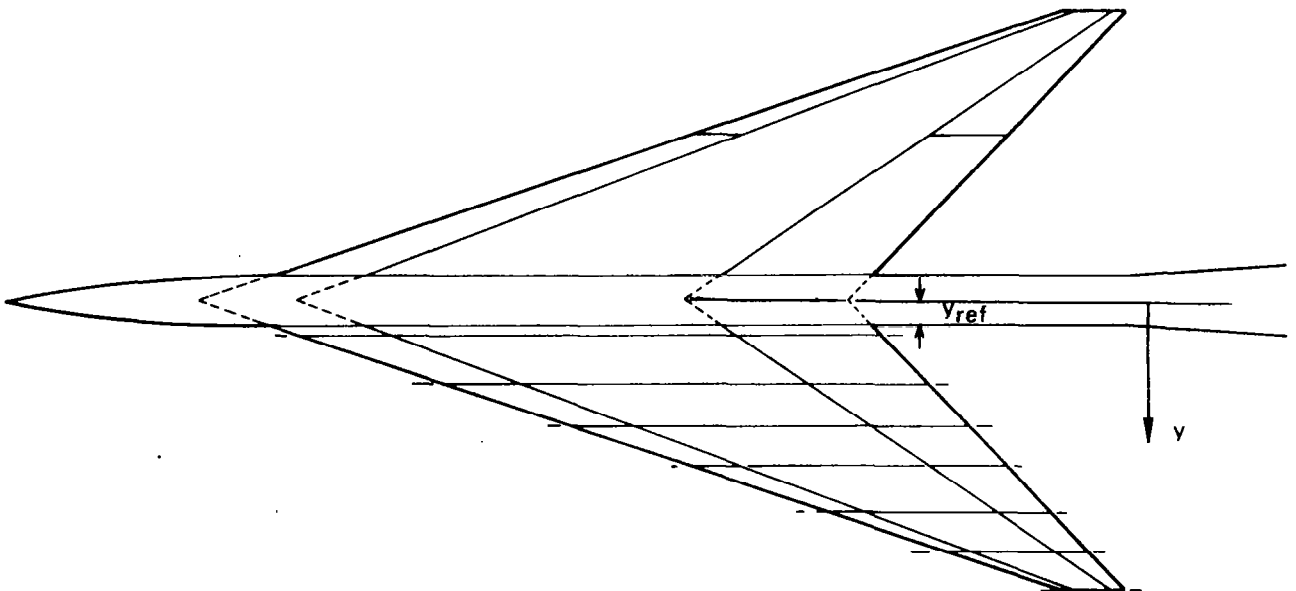
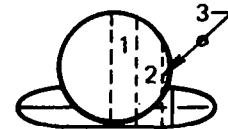
L.E. of M.A.C. @ B.S. 87.760 cm

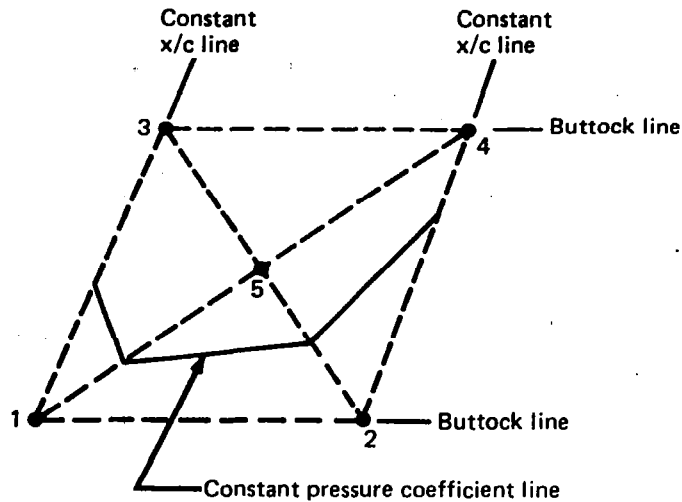
Wing

$2y/b$	$\frac{\Delta y}{(b/2)}$	Area cm <sup>2</sup>	Area • chord cm <sup>3</sup>	Area • ( $y - y_{ref}$ ) cm <sup>3</sup>
0.09	0.0425	219.69	22 357.	167.
0.20	0.1575	733.51	67 415.	4 206.
0.35	0.1500	580.54	44 374.	7 857.
0.50	0.1400	437.93	27 084.	9 148.
0.65	0.1600	377.64	17 722.	10 729.
0.80	0.1300	210.35	6 794.	7 528.
0.93	0.1400	129.79	2 487.	5 505.

Body

Longitudinal section	Area cm <sup>2</sup>	Area • L cm <sup>3</sup>
1	356.61	81 258.
2	504.32	114 916.
3	70.94	16 164.





The isobars are drawn by checking each triangle to determine if the pressure coefficients at the ends of any triangle side are above and below the desired value, in which case the isobar must cross that triangle side. The location of the crossing is found by linear interpolation between the end points, and when two adjacent triangle sides are found to contain the desired pressure coefficient a small segment of the isobar is drawn. As each set of four points is processed, the whole isobar will be constructed from many of these small segments. A letter symbol identifying the pressure coefficient value is generated wherever an isobar crosses one of the rows of orifices.

## SECTION AND SPANWISE LOADING CHARACTERISTICS

Section aerodynamic coefficients  $C_n$  and  $C_m$  are presented as a function of angle of attack.

The spanwise loading is illustrated by plots of the loading parameters  $C_{nc}/\bar{c}$  and  $C_{m.25c} c^2/\bar{c}^2$  along the span of the surfaces.

## TOTAL SURFACE CHARACTERISTICS

The total surface coefficients  $C_N$ ,  $C_M$ , and  $C_B$  are shown as a function of angle of attack.

## REFERENCES

1. Manro, Marjorie E.; Manning, Kenneth J. R.; Hallstaff, Thomas H.; and Rogers, John T.: Transonic Pressure Measurements and Comparison of Theory to Experiment for an Arrow-Wing Configuration - Summary Report. NASA CR-2610, 1976.
2. Manro, Marjorie E.; Manning, Kenneth J. R.; Hallstaff, Thomas H.; and Rogers, John T.: Transonic Pressure Measurements and Comparison of Theory to Experiment for an Arrow-Wing Configuration, Volume I: Experimental Data Report - Base Configuration and Effects of Wing Twist and Leading-Edge Configuration. NASA CR-132727, 1975.
3. Manro, Marjorie E.; Manning, Kenneth J. R.; Hallstaff, Thomas H.; and Rogers, John T.: Transonic Pressure Measurements and Comparison of Theory to Experiment for an Arrow-Wing Configuration, Volume II: Experimental Data Report - Effects of Control Surface Deflection. NASA CR-132728, 1975.
4. Manro, Marjorie E.; Manning, Kenneth J. R.; Hallstaff, Thomas H.; and Rogers, John T.: Transonic Pressure Measurements and Comparison of Theory to Experiment for an Arrow-Wing Configuration, Volume III: Data Report - Comparison of Attached Flow Theories to Experiment. NASA CR-132729, 1975.
5. Manro, M. E.: Supersonic Pressure Measurements and Comparison of Theory to Experiment for an Arrow-Wing Configuration. NASA CR-145046, 1976.
6. Manro, Marjorie E.; Tinoco, Edward N.; Bobbitt, Percy J.; and Rogers, John T.: Comparisons of Theoretical and Experimental Pressure Distributions on an Arrow-Wing Configuration at Transonic Speeds. Aerodynamic Analyses Requiring Advanced Computers - Part II, NASA SP-347, 1975, pp. 1141-1188.
7. Manro, M. E.; Bobbitt, P. J.; and Rogers, J. T.: Comparisons of Theoretical and Experimental Pressure Distributions on an Arrow-Wing Configuration at Subsonic, Transonic, and Supersonic Speeds. Prediction of Aerodynamic Loading, AGARD-CP-204, Feb. 1977, pp. 11-1 - 11-14.
8. Bobbitt, Percy J.; and Manro, Marjorie E.: Theoretical and Experimental Pressure Distributions for a  $71.2^\circ$  Swept Arrow-Wing Configuration at Subsonic, Transonic, and Supersonic Speeds. Proceedings of the SCAR Conference - Part I, NASA CP-001, (1977), pp. 85-122.
9. Tinoco, E. N.; and Mercer, J. E.: FLEXSTAB - A Summary of the Functions and Capabilities of the NASA Flexible Airplane Analysis Computer System. NASA CR-2564, 1975.
10. Woodward, F. A.; Tinoco, E. N.; and Larsen, J. W.: Analysis and Design of Supersonic Wing-Body Combinations, Including Flow Properties in the Near Field, Part 1 - Theory and Application. NASA CR-73106, 1967.
11. Woodward, F. A.: Analysis and Design of Wing-Body Combinations at Subsonic and Supersonic Speeds. J. of Airc., Vol. 5, No. 6, Nov.- Dec. 1968, pp. 528-534.

12. Dusto, A. R., et al.: A Method for Predicting the Stability Characteristics of an Elastic Airplane. Volume 1 - FLEXSTAB Theoretical Description. NASA CR-114712, 1974.
13. Ehlers, F. E.; Epton, M. A.; Johnson, F. T.; Magnus, A. E.; and Rubbert, P. E.: An Improved Higher Order Panel Method for Linearized Supersonic Flow. AIAA Paper No. 78-15, January 1978.
14. Moran, Jack; and Tinoco, E. N.: User's Manuals - Subsonic/Supersonic Advanced Panel Pilot Code. NASA CR-152047, 1978.
15. Ehlers, F. Edward; Epton, Michael A.; Johnson, Forrester T.; Magnus, Alfred E.; and Rubbert, Paul E.: A Higher Order Panel Method for Linearized Supersonic Flow. NASA CR-3062, 1979.
16. Johnson, Forrester T.; and Rubbert, Paul E.: Advanced Panel-Type Influence Coefficient Methods Applied to Subsonic Flows. AIAA Paper No. 75-50, January 1975.
17. Tinoco, E. N.; Johnson, F. T.; and Freeman, L. M.: The Application of a Higher Order Panel Method to Realistic Supersonic Configurations. AIAA Paper No. 79-274, January 1979.
18. Rubbert, P. E.; Saaris, G. R.; Scholey, M. B.; Standen, N. M.; and Wallace, R. E.: A General Method for Determining the Aerodynamic Characteristics of Fan-In-Wing Configurations. Volume I - Theory and Application. USAAVLABS Technical Report 67-61A, U.S. Army, December 1967. (Available from DTIC as AD-667980.)
19. Rubbert, P. E.; and Saaris, G. R.: A General Three-Dimensional Potential-Flow Method Applied to V/STOL Aerodynamics. SAE J., Vol. 77, September 1969.
20. Rubbert, P. E.; and Saaris, G. R.: Review and Evaluation of a Three-Dimensional Lifting Potential Flow Analysis Method for Arbitrary Configurations. AIAA Paper No. 72-188, 1972.



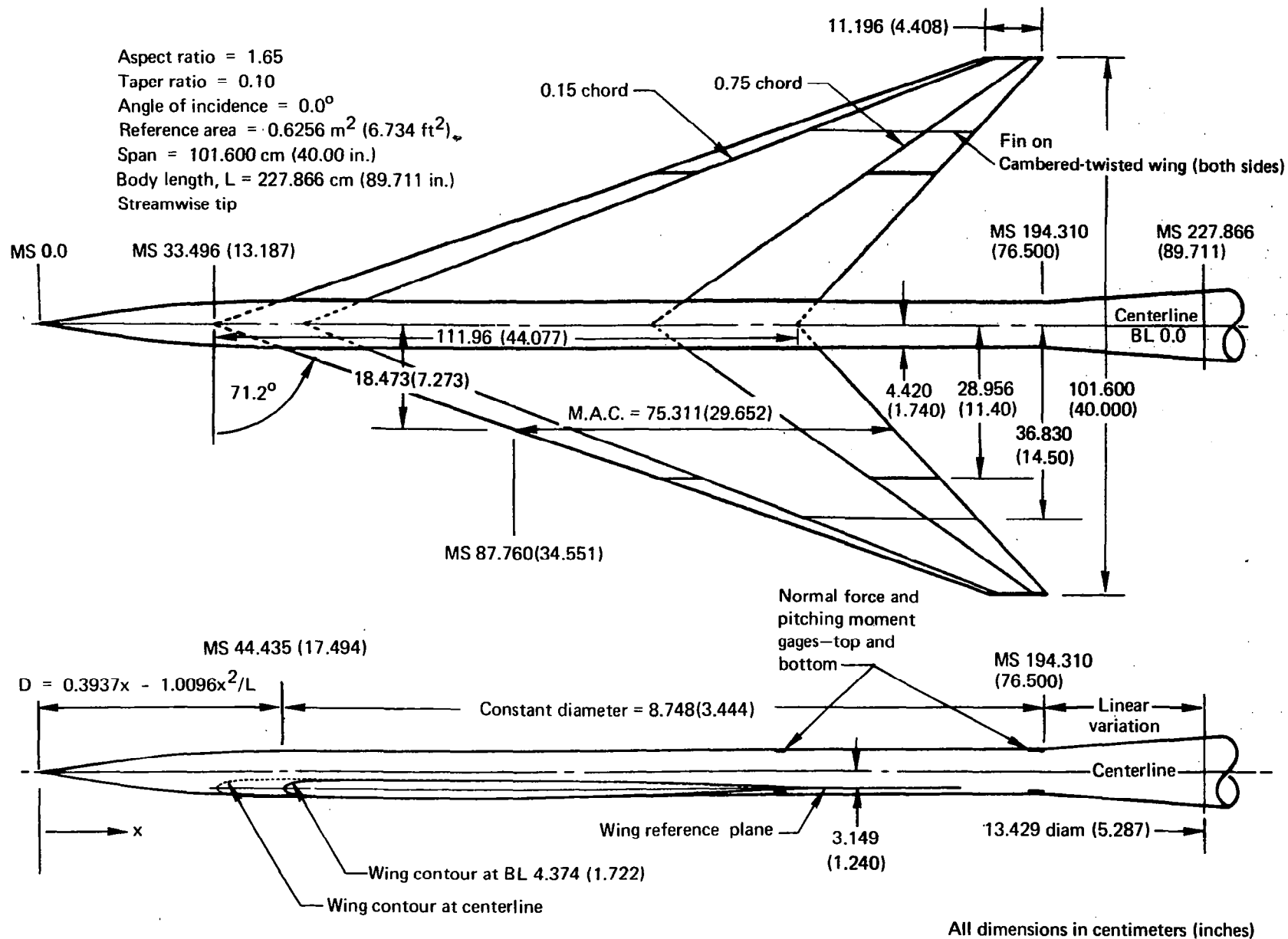


Figure 1.—General Arrangement and Characteristics

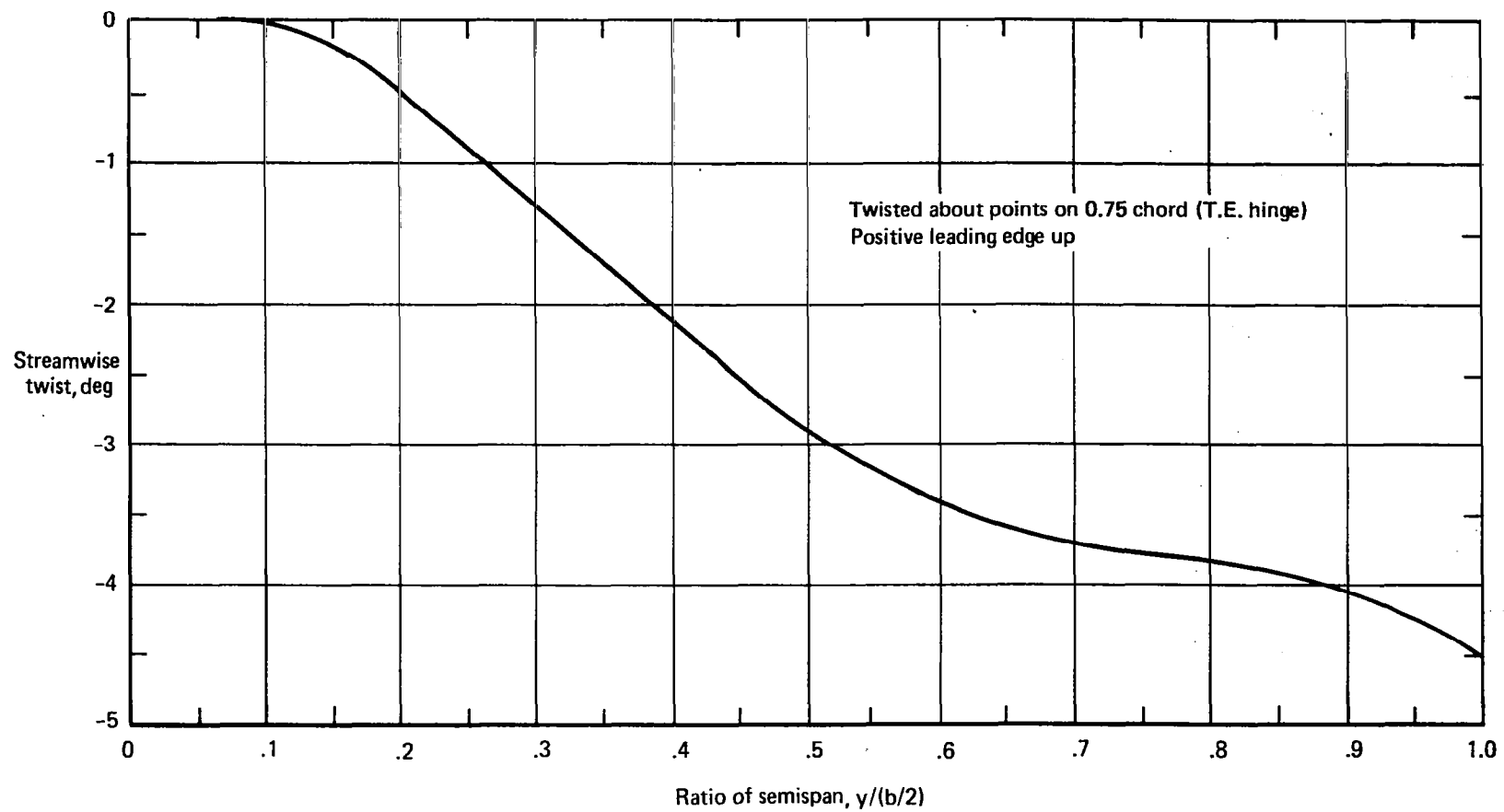
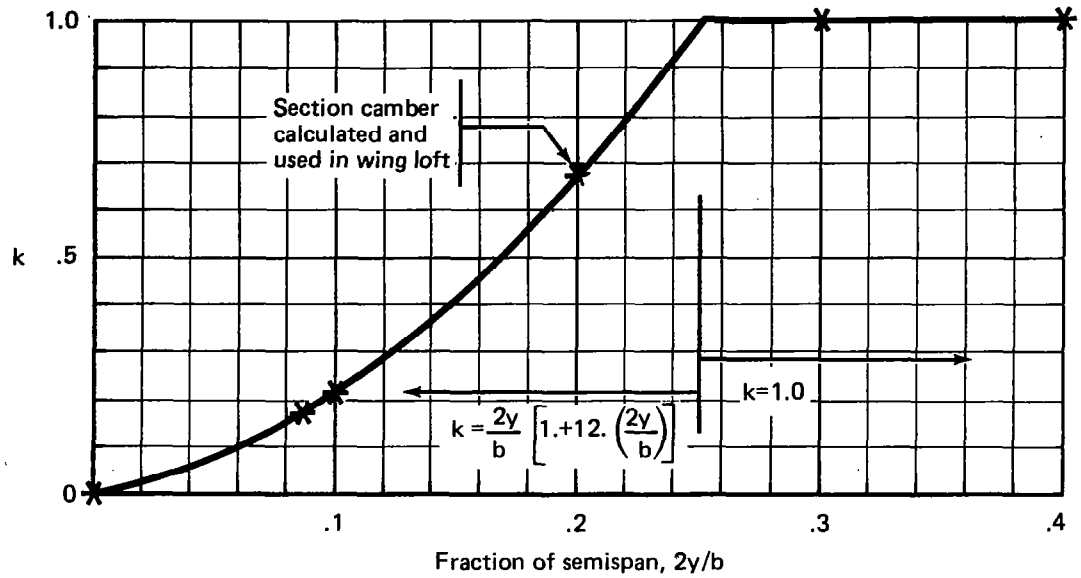
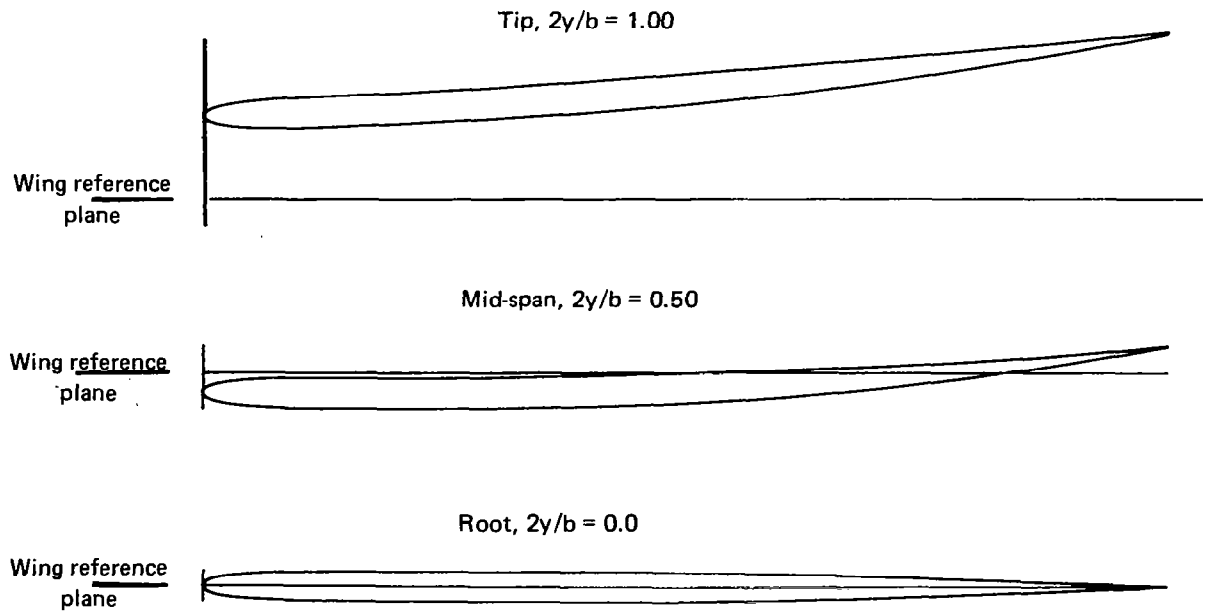


Figure 2.—Spanwise Twist Distribution for the Model Wing

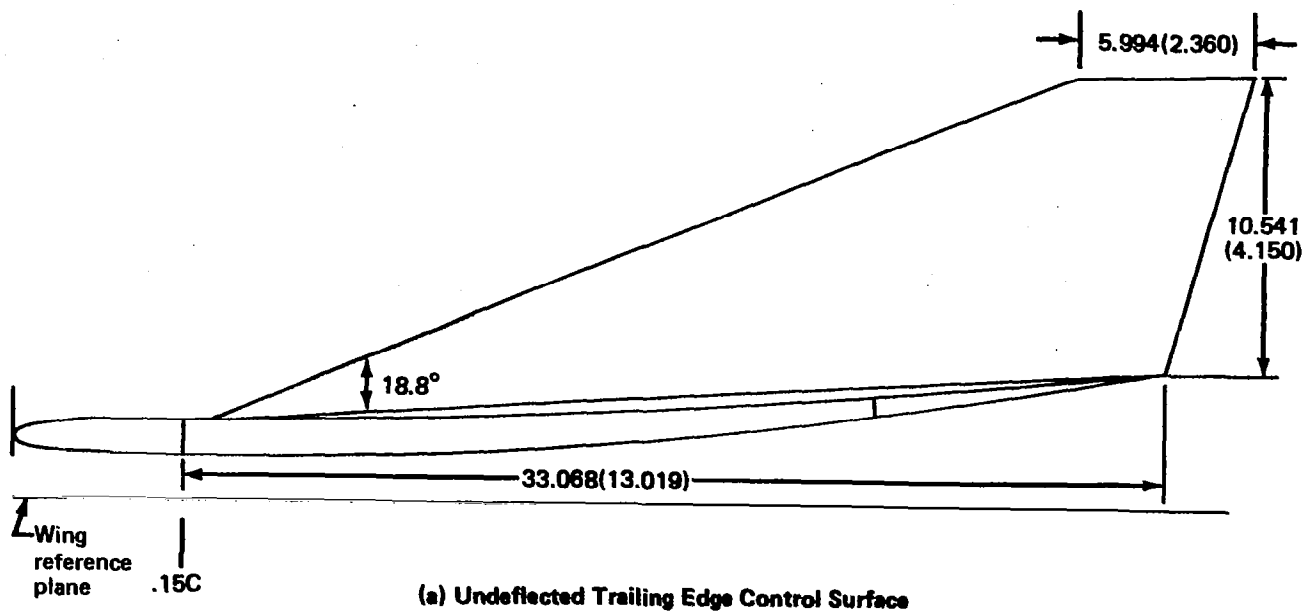


(a) Definition of  $k$ , Factor on Basic Camber



(b) Typical Sections

Figure 3.—Cambered-Twisted Wing Section Geometry



All dimensions in centimeters (inches)

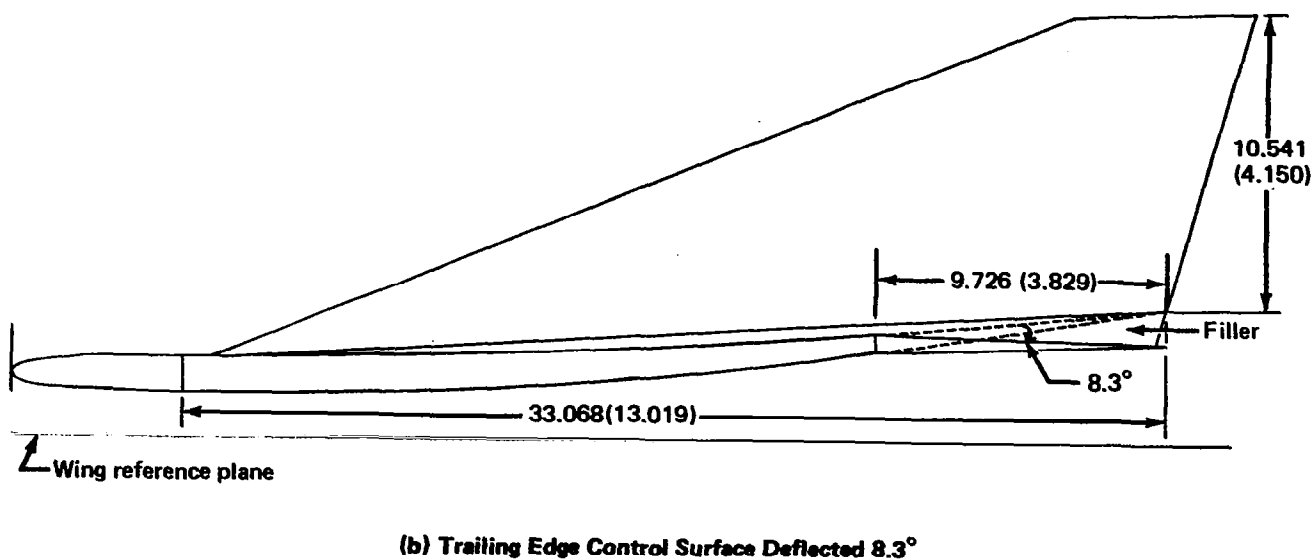


Figure 4.—Fin Geometry, Section at 0.725 Semispan

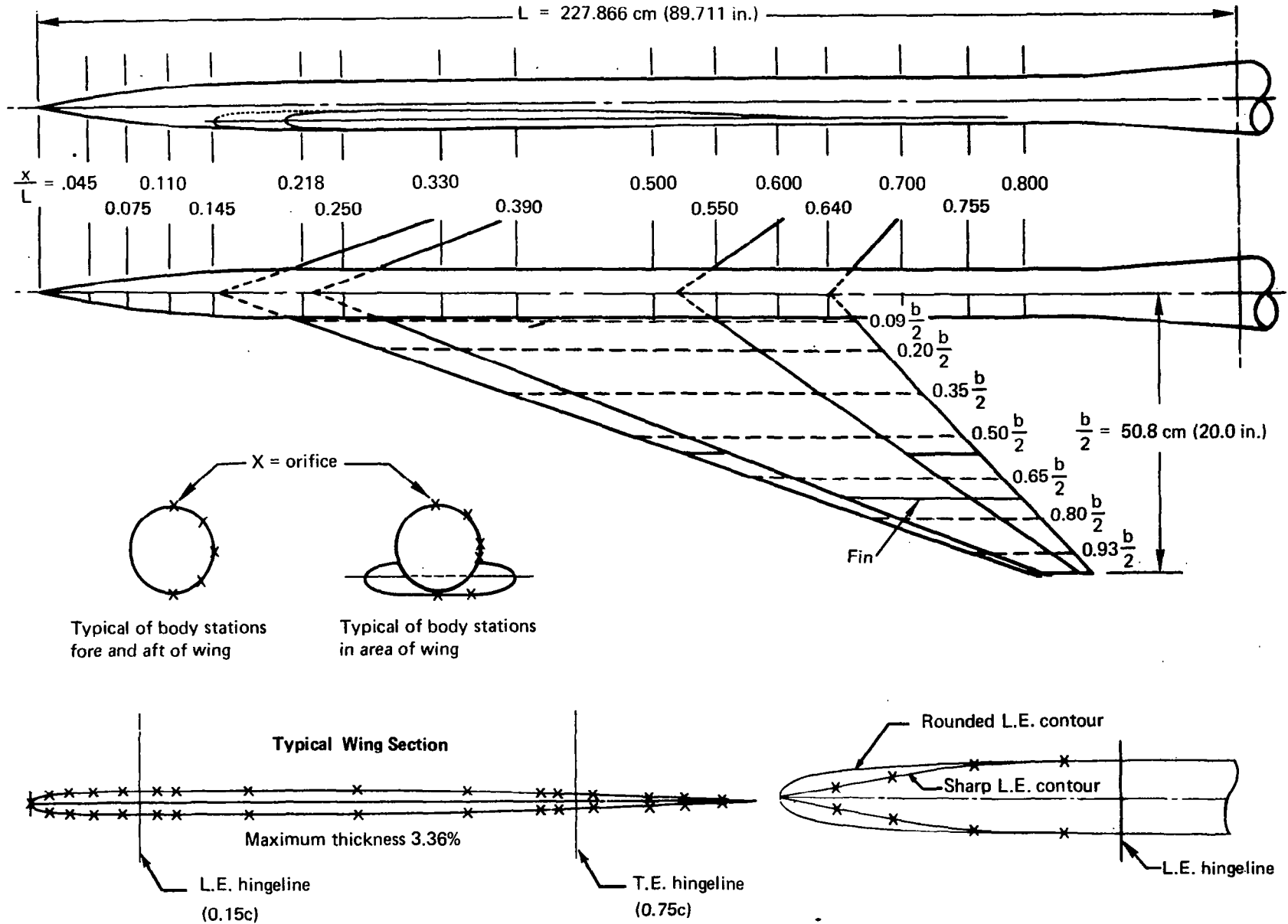


Figure 5.—Pressure Orifice Locations

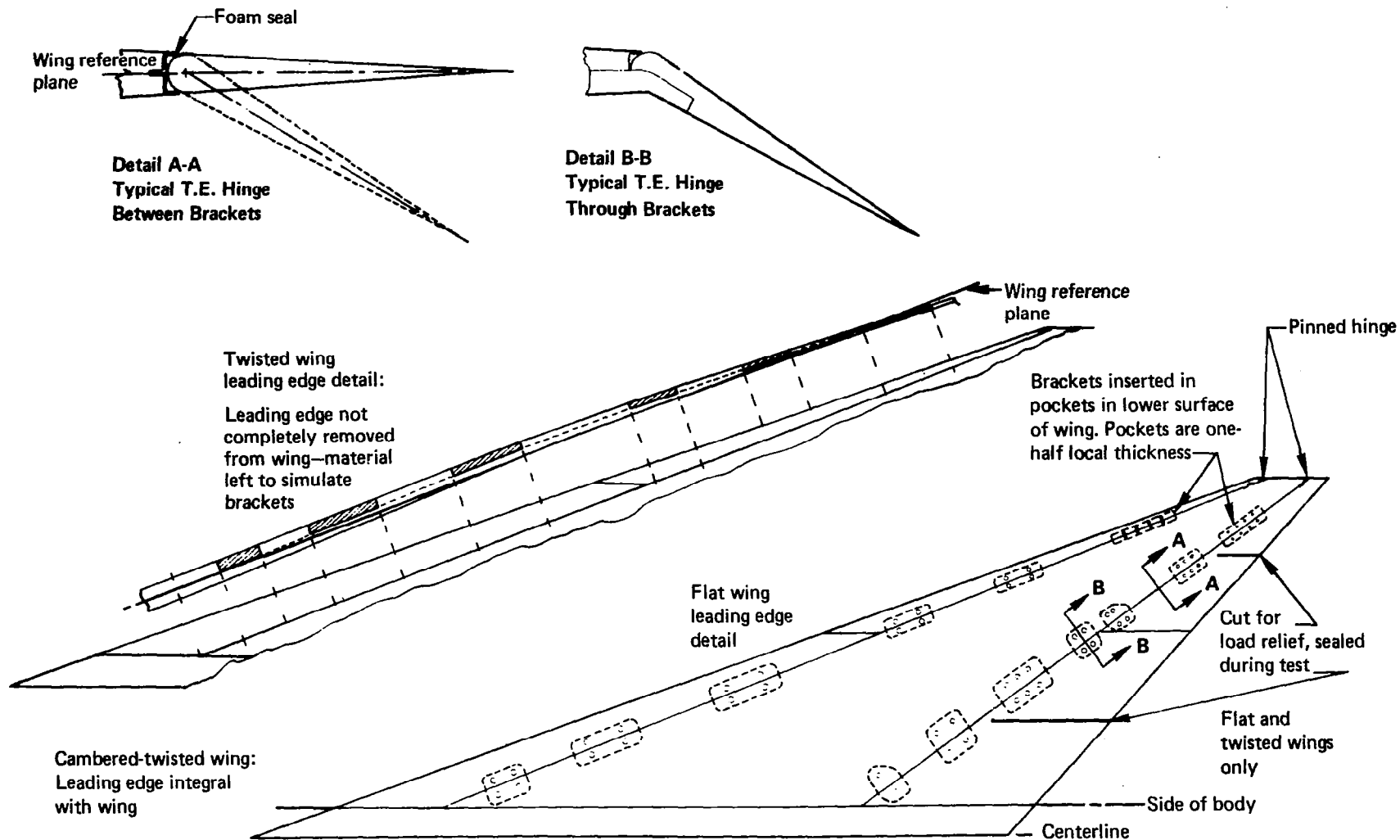
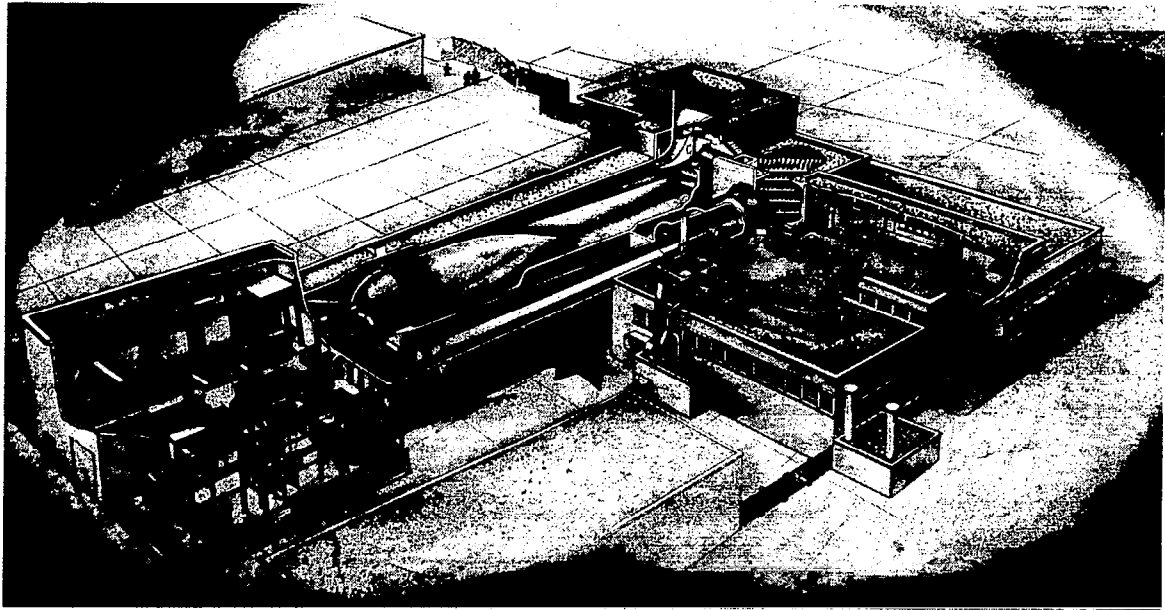
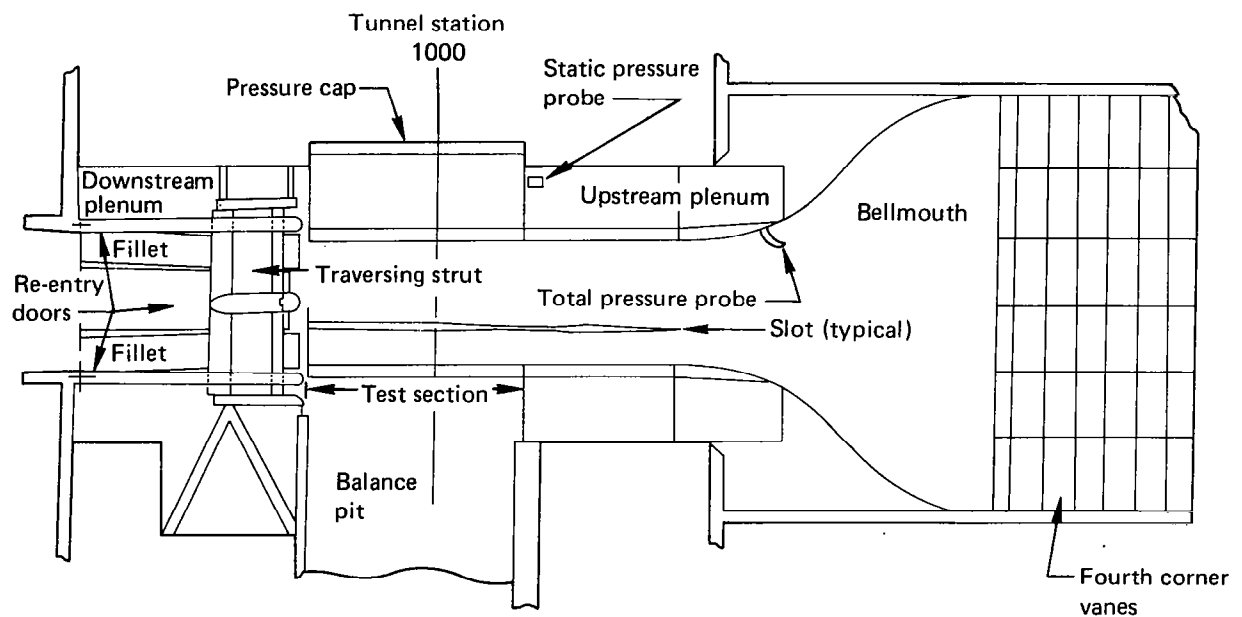


Figure 6.—Control Surface Bracket Details



(a) Schematic



(b) Test Section

*Figure 7.—Boeing Transonic Wind Tunnel*

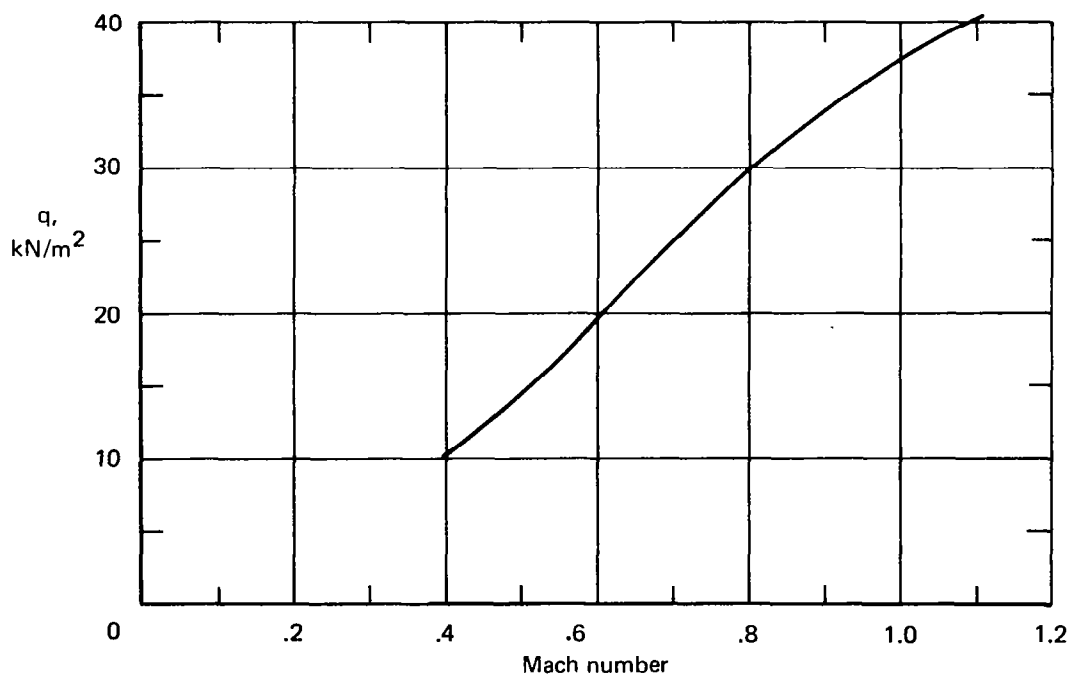
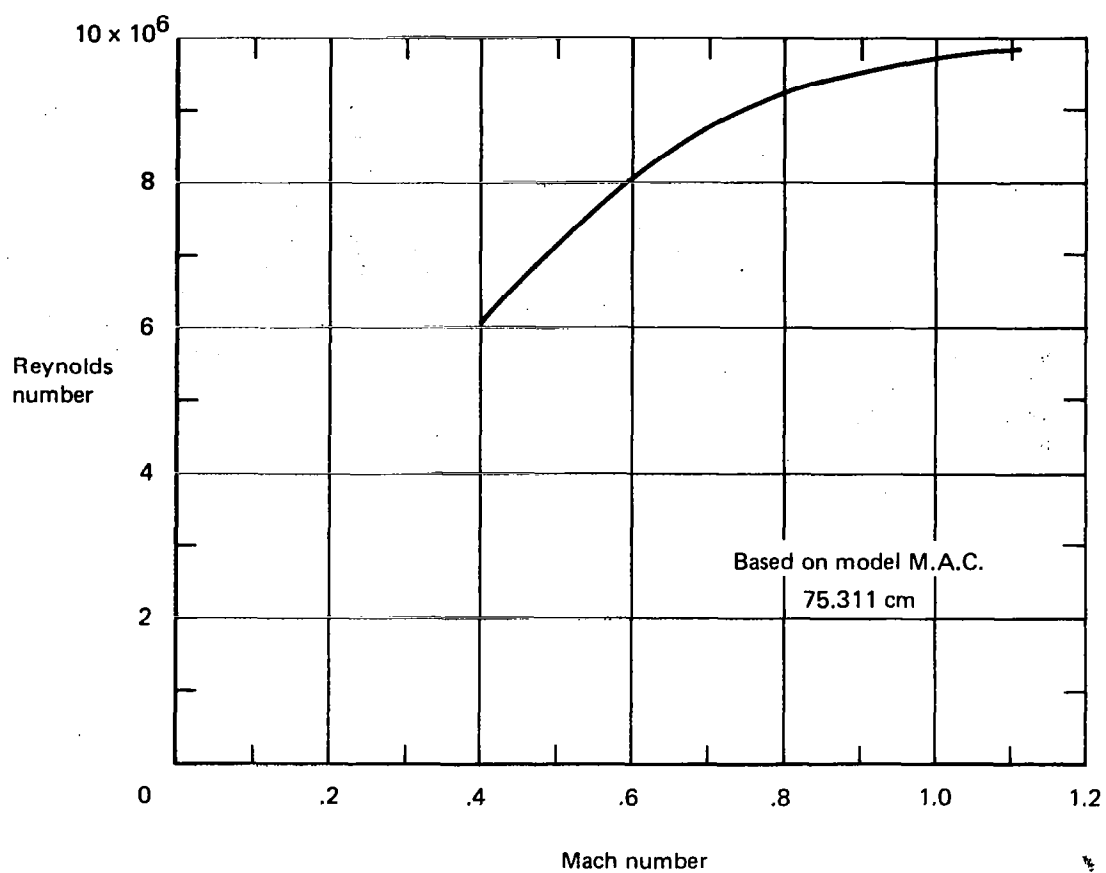


**Figure 8.—Variation of Reynolds Number and Dynamic Pressure With Mach Number**



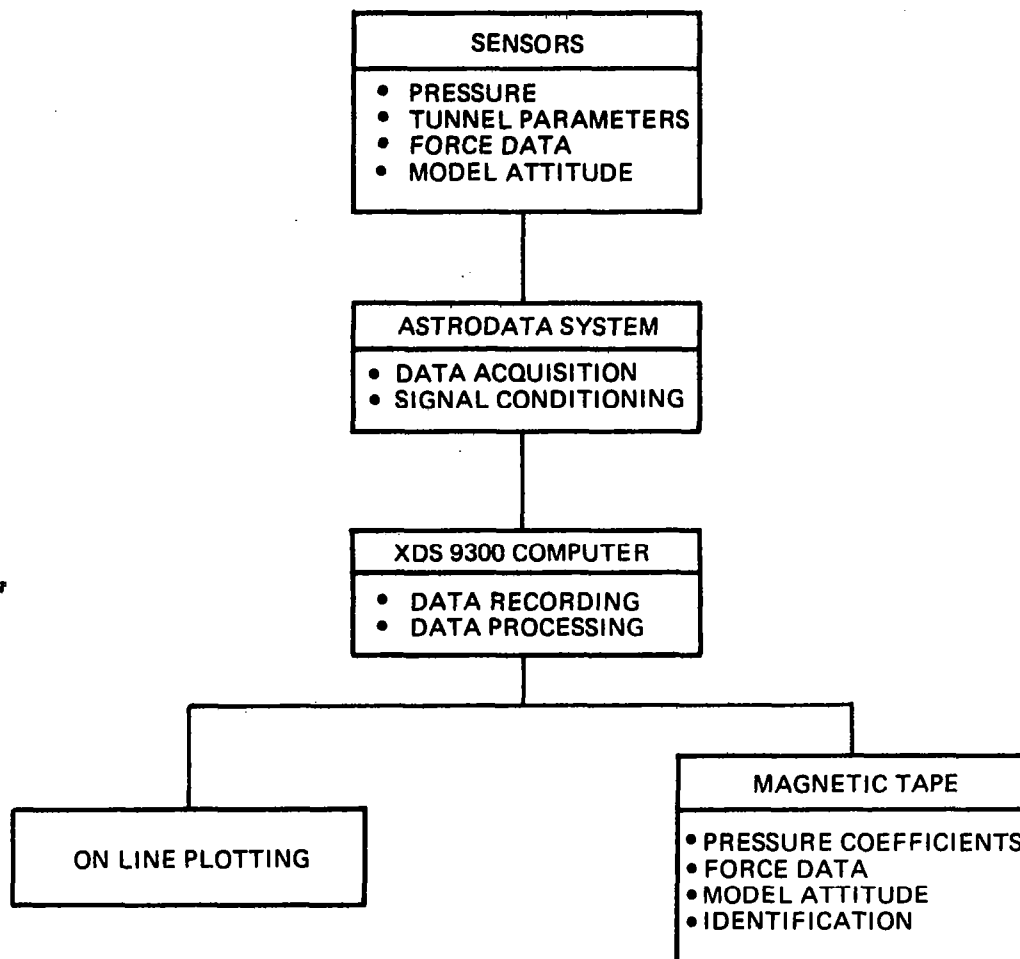


*Figure 9.—Data Acquisition and Reduction System—Boeing Transonic Wind Tunnel*

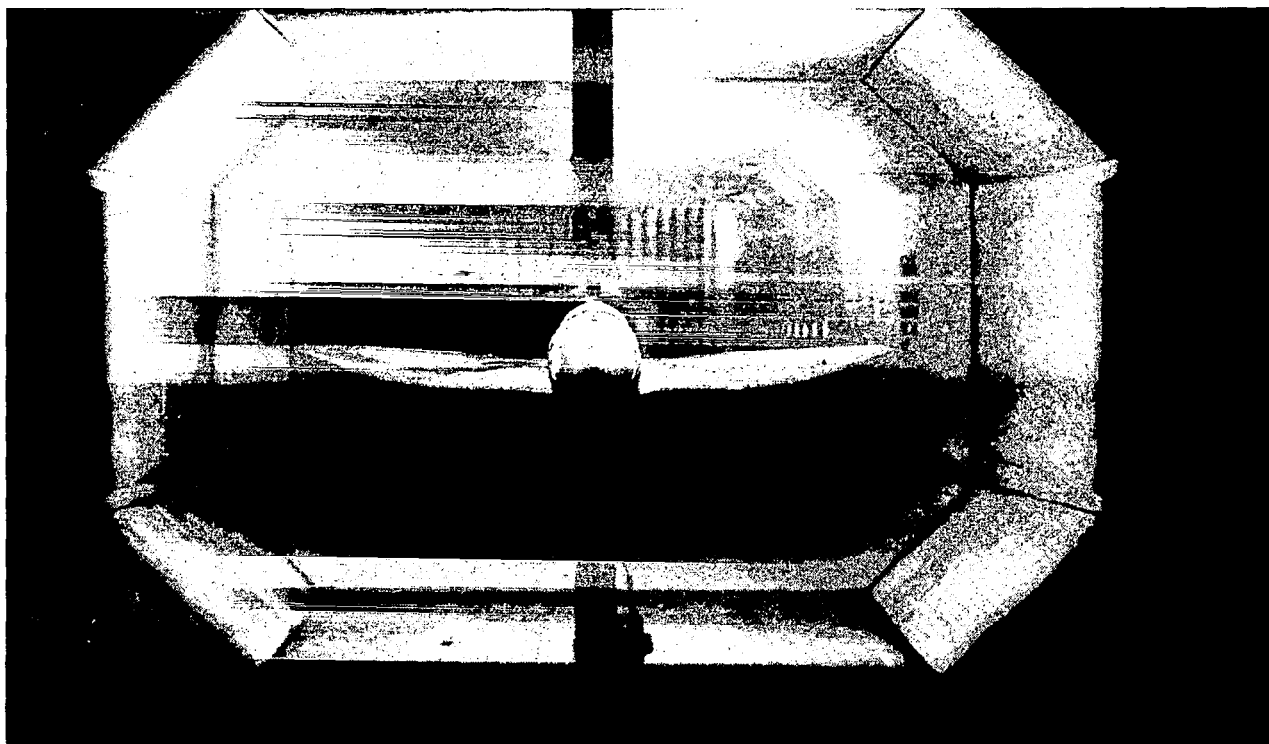


*Figure 10.—Wind Tunnel Photographs - Twisted Wing; T.E. Deflection, Full Span =  $0.0^\circ$*

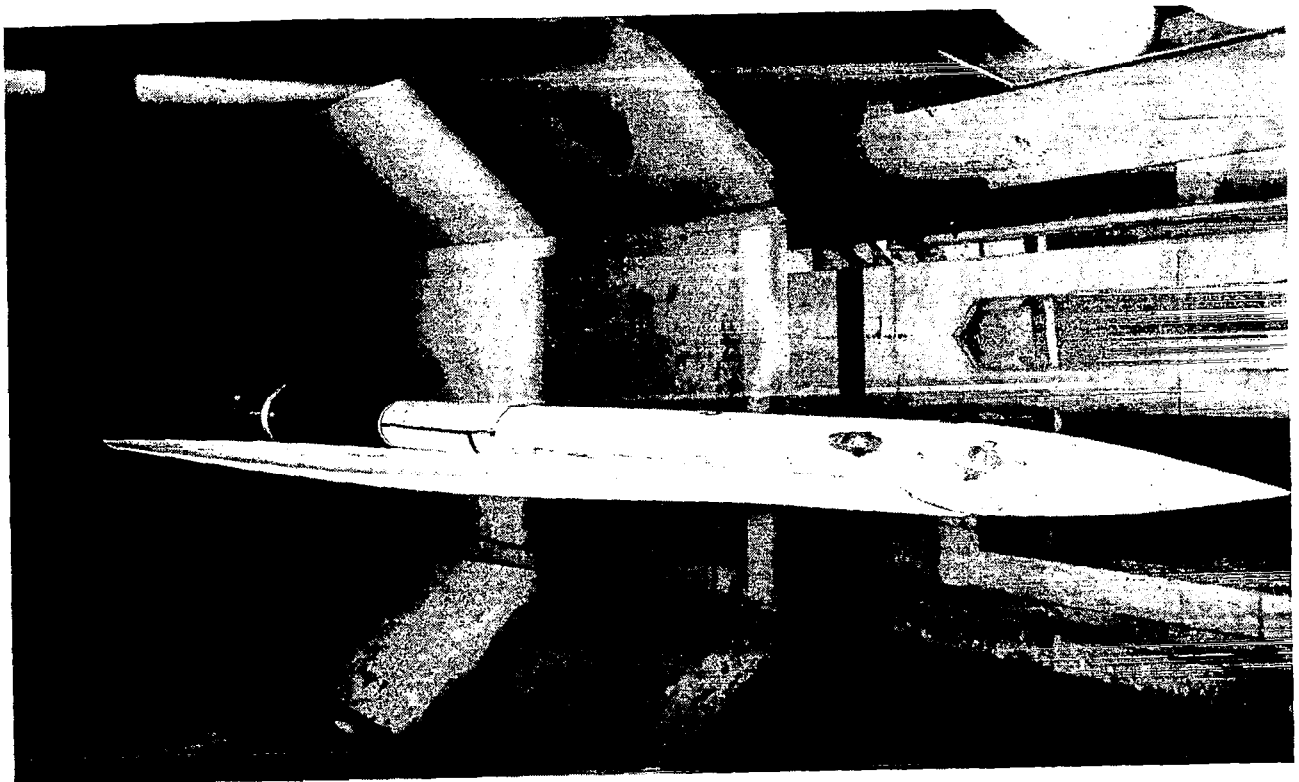
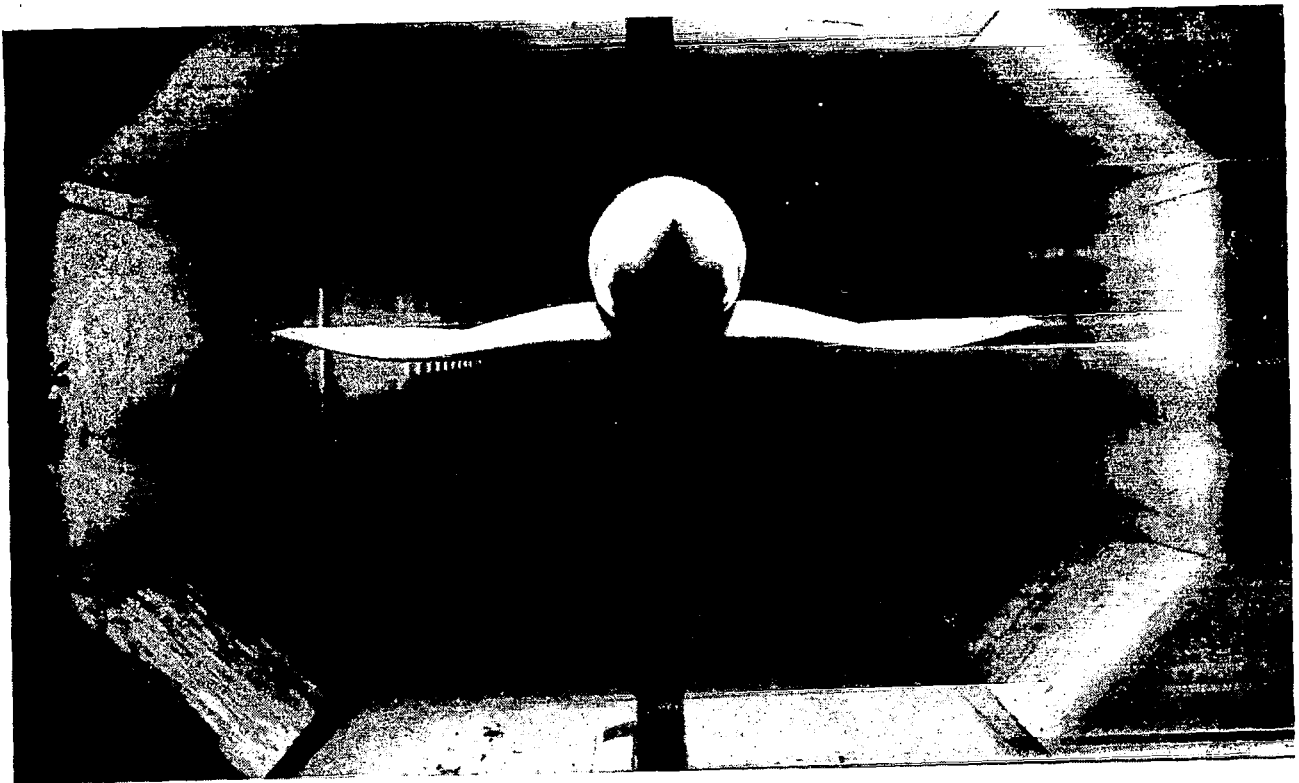


*Figure 11.—Wind Tunnel Photographs - Cambered-Twisted Wing, Fin Off; T.E. Deflection,  
Full Span =  $0.0^\circ$*

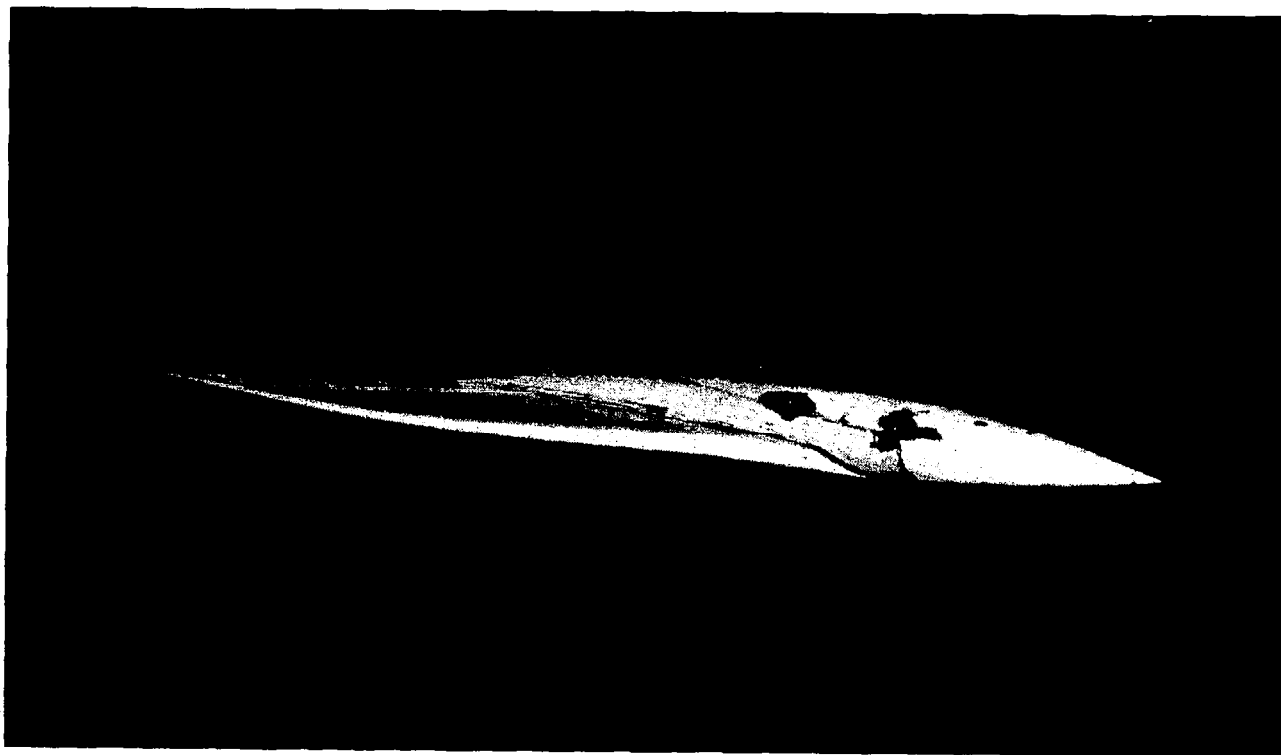
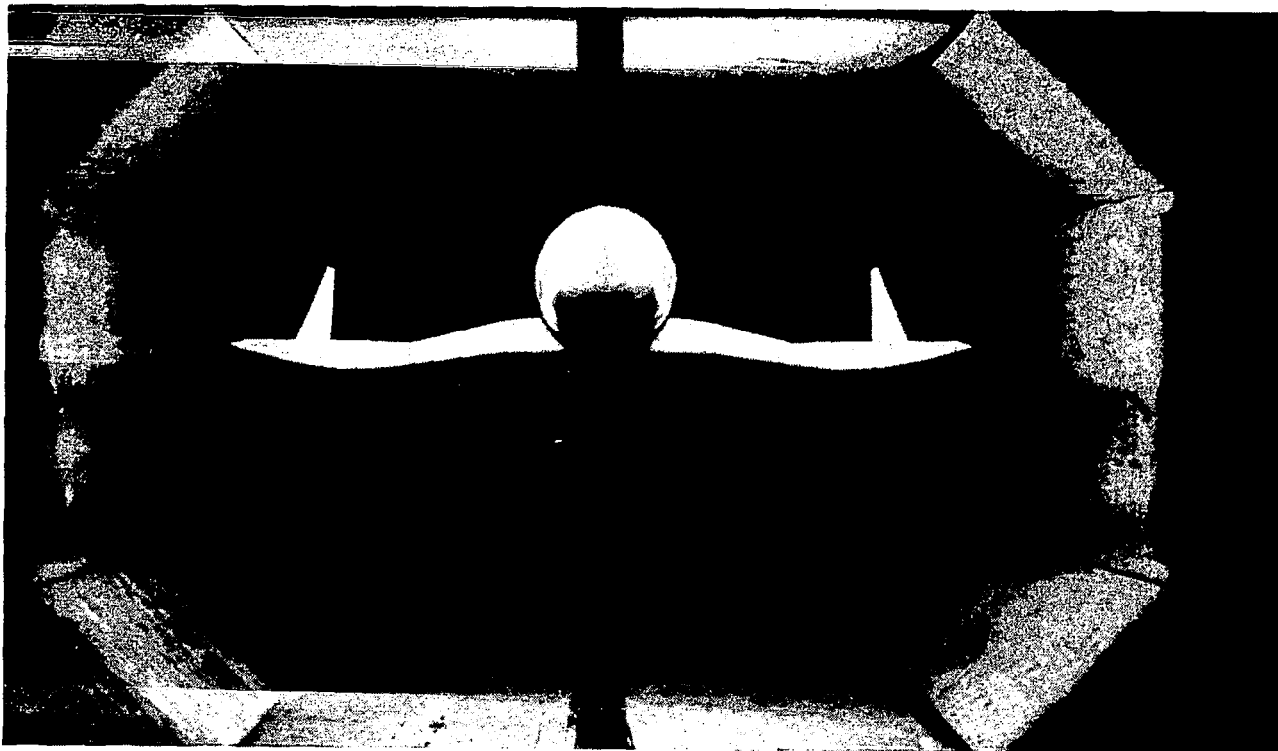


*Figure 12.—Wind Tunnel Photographs - Cambered-Twisted Wing, Fin On; T.E. Deflection,  
Full Span = 0.0°*

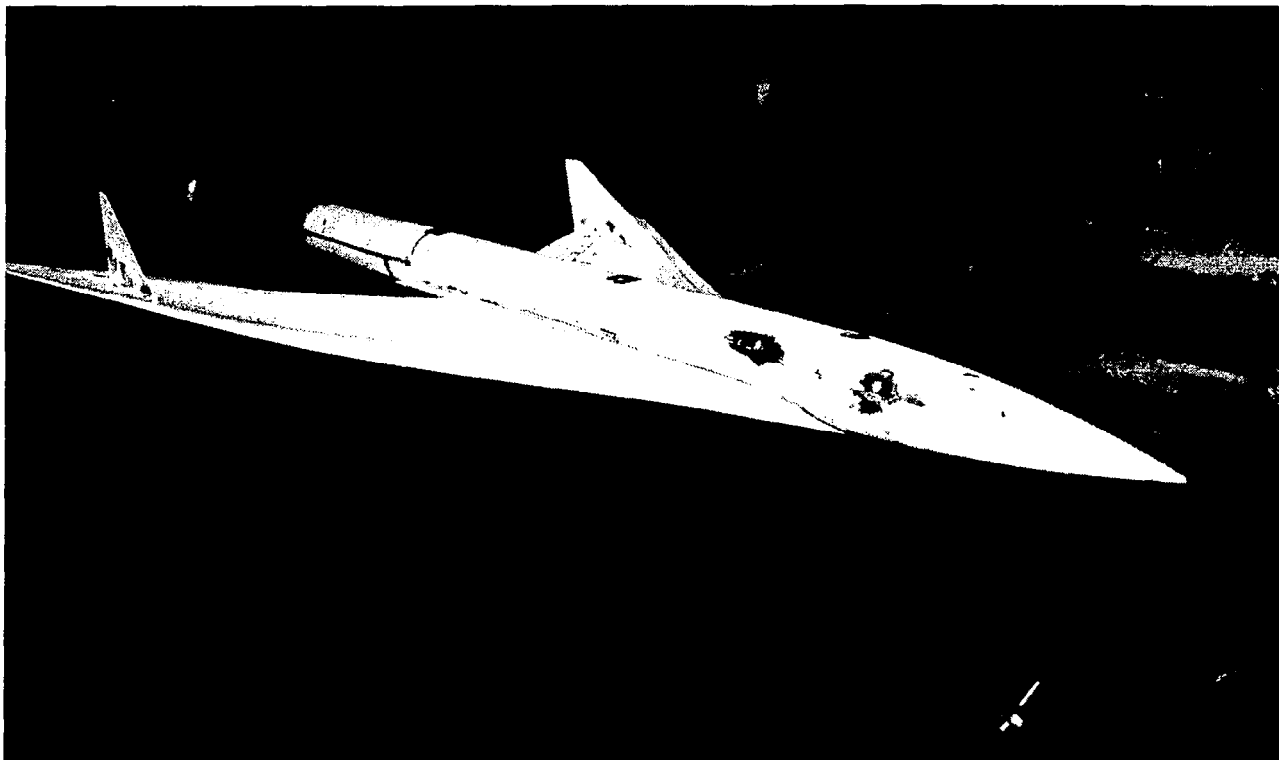


*Figure 13.—Wind Tunnel Photograph - Cambered-Twisted Wing, Fin On; T.E. Deflection, Full Span  
Full Span =  $8.3^{\circ}$*

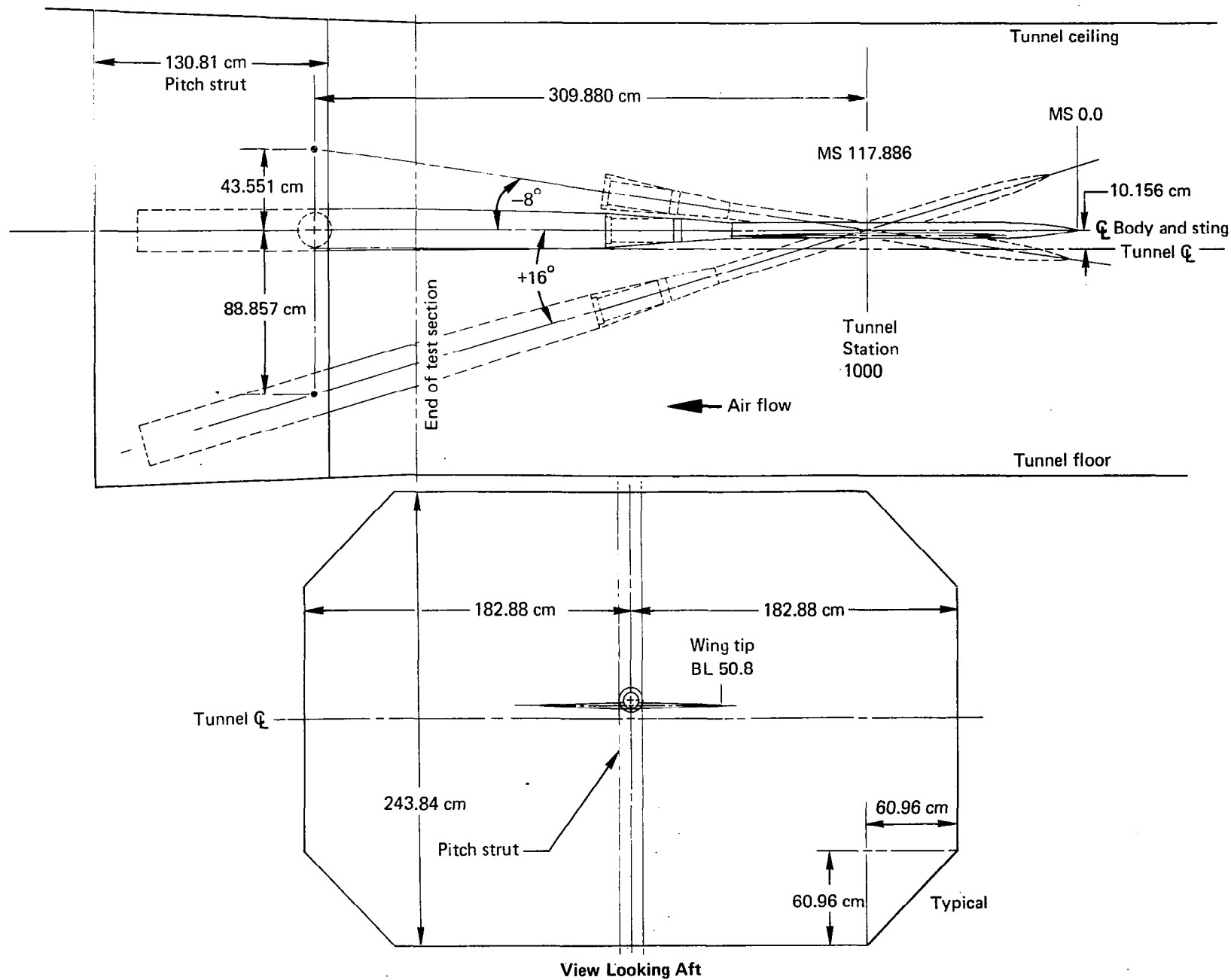
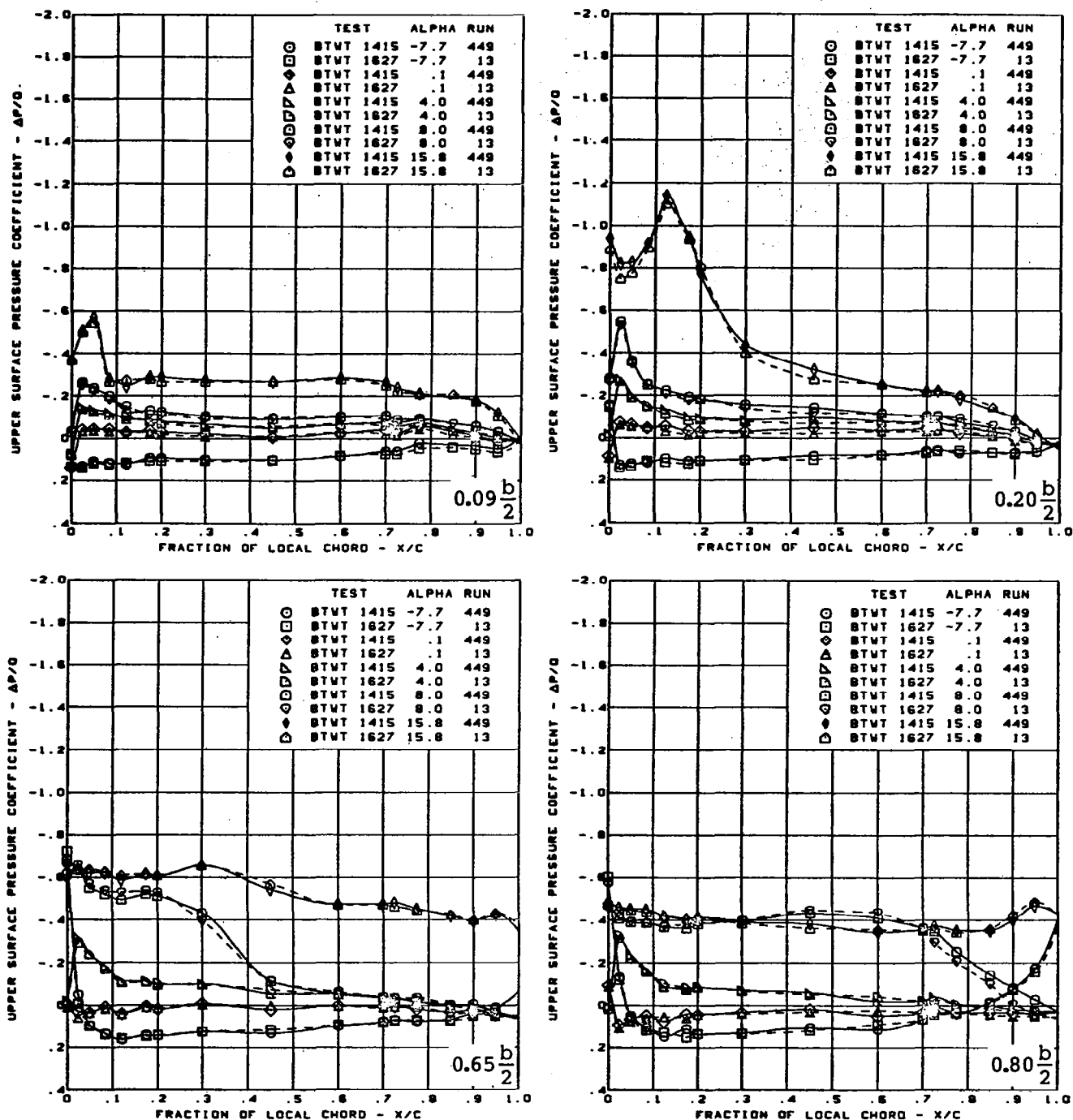
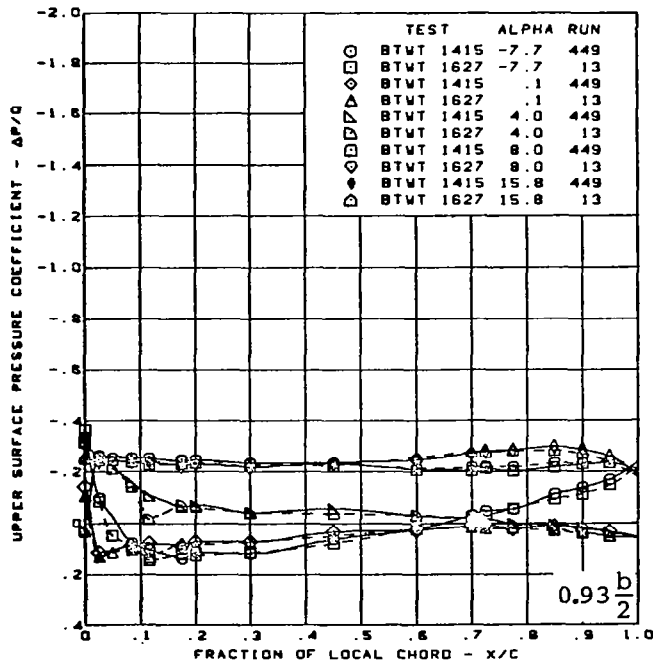
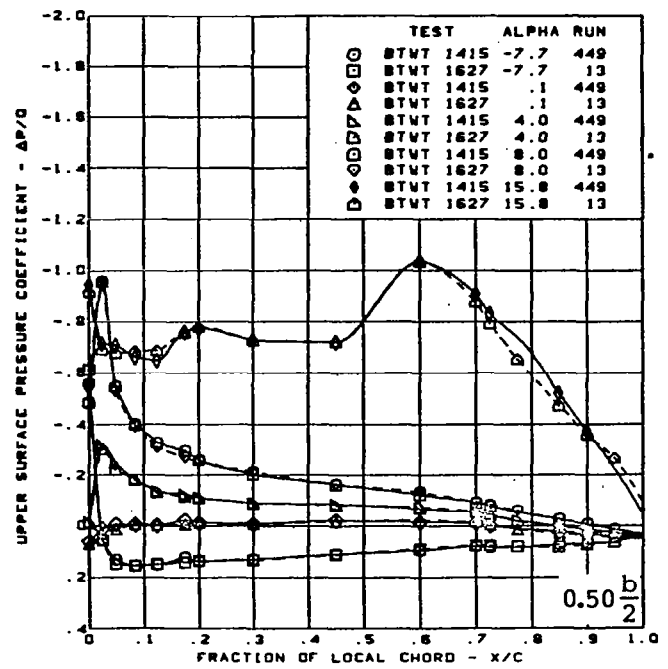
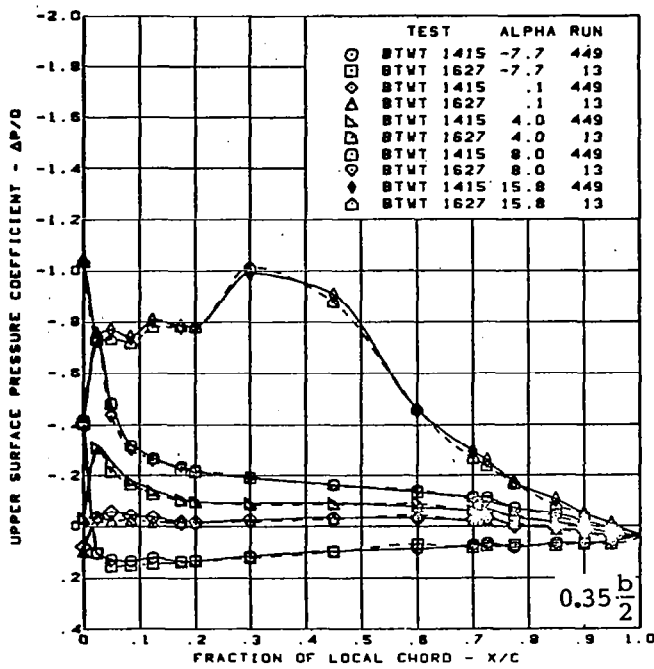


Figure 14.—Model Installation Diagram



(a) Upper Surface Chordwise Pressure Distributions

Figure 15. — Wing Experimental Data—Comparison of Data From Two Wind Tunnel Tests; Twisted Wing; T.E. Deflection, Full Span =  $0.0^\circ$ ;  $M = 0.85$



$M = 0.85$

Twisted wing, rounded L.E.

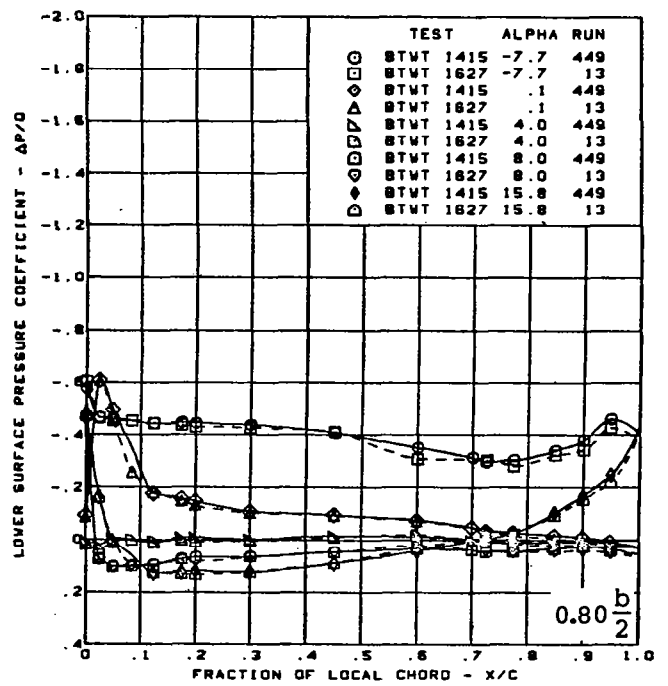
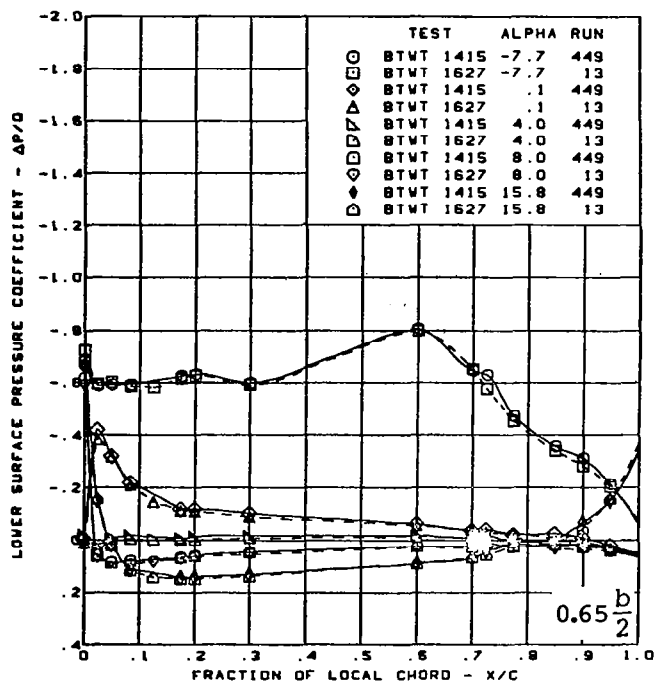
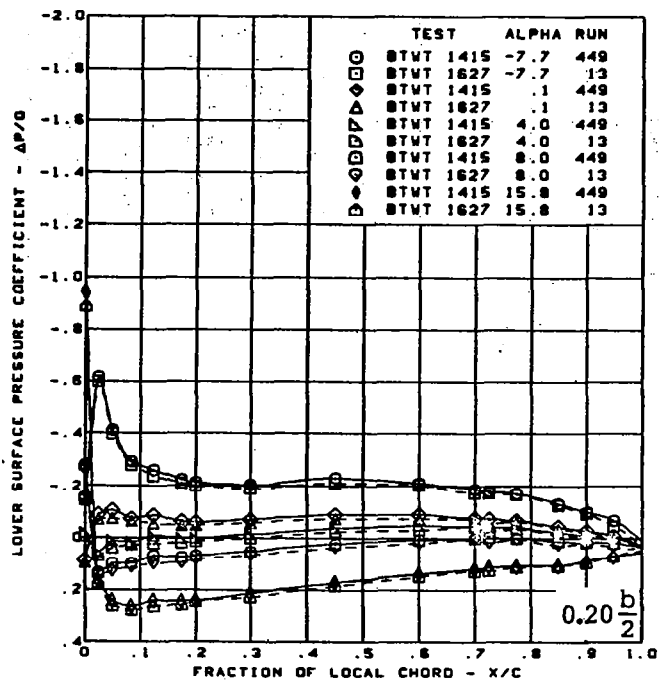
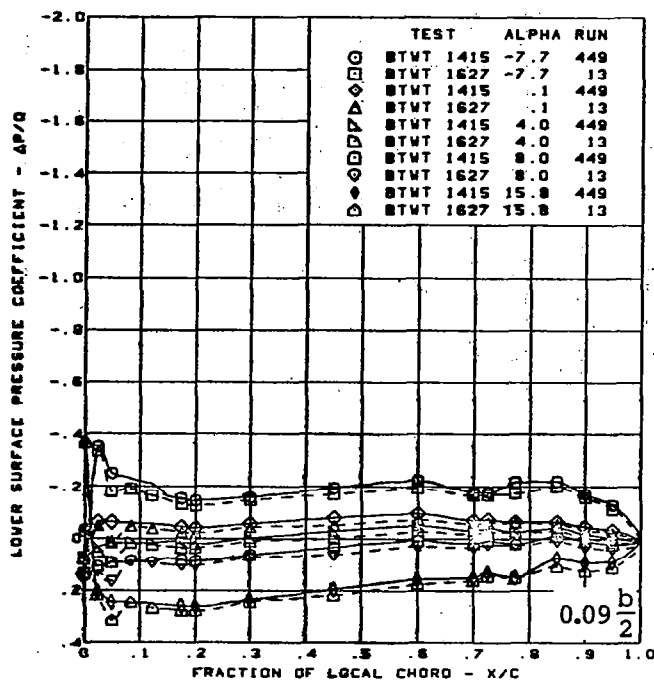
L.E. deflection, full span =  $0.0^\circ$

T.E. deflection, full span =  $0.0^\circ$

(a) (Concluded)

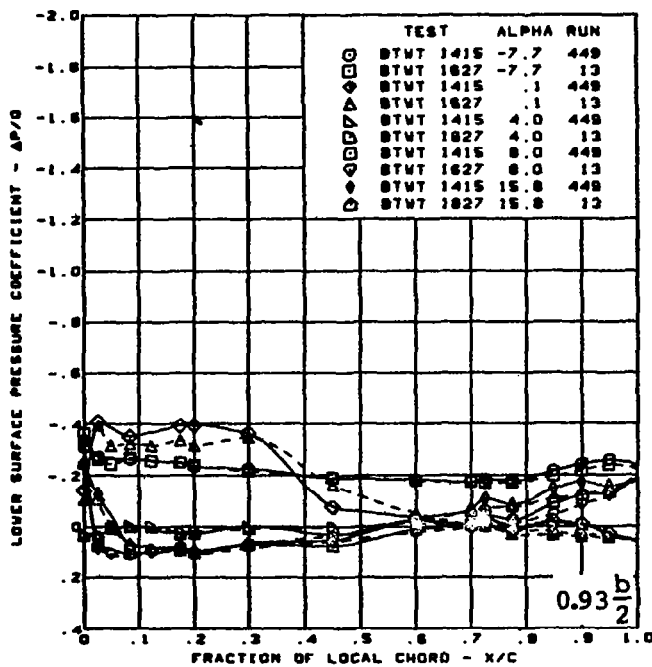
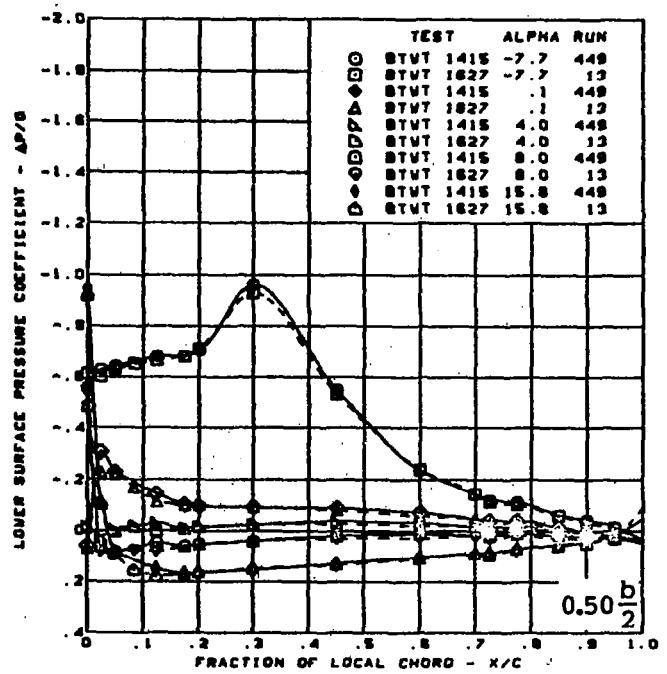
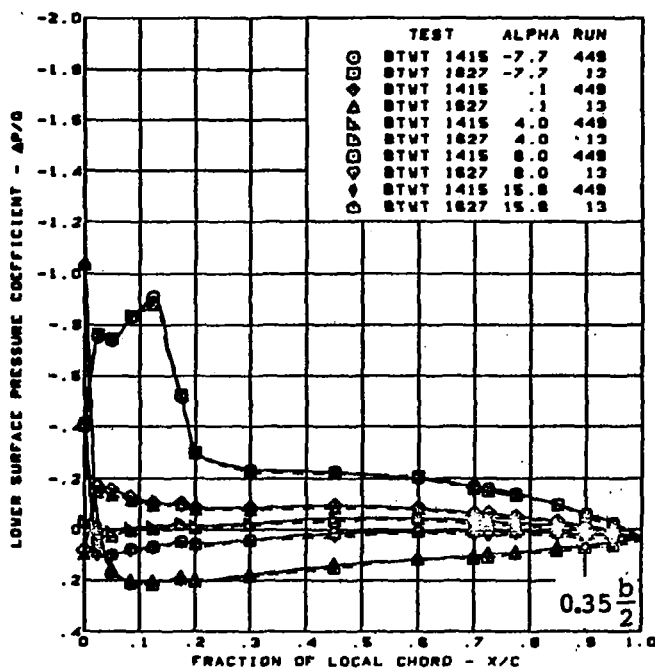
Figure 15. — (Continued)





(b) Lower Surface Chordwise Pressure Distributions

Figure 15. - (Continued)



$M = 0.85$

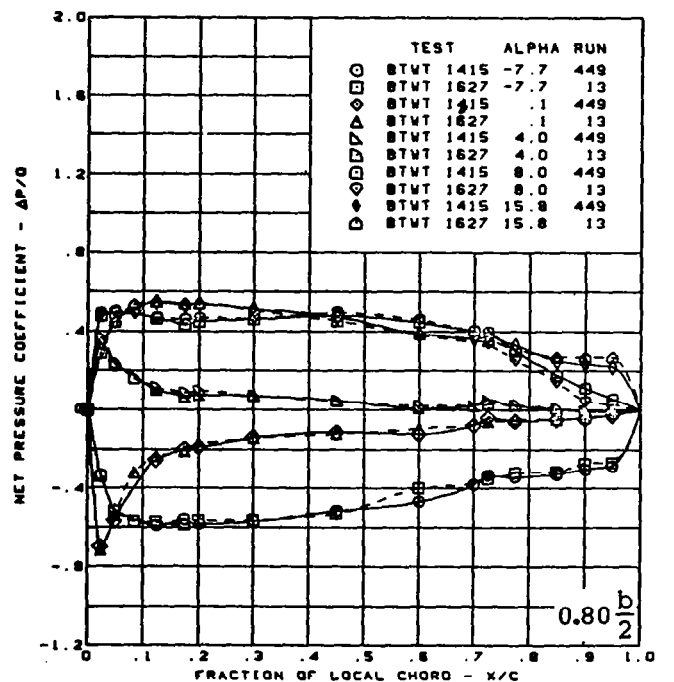
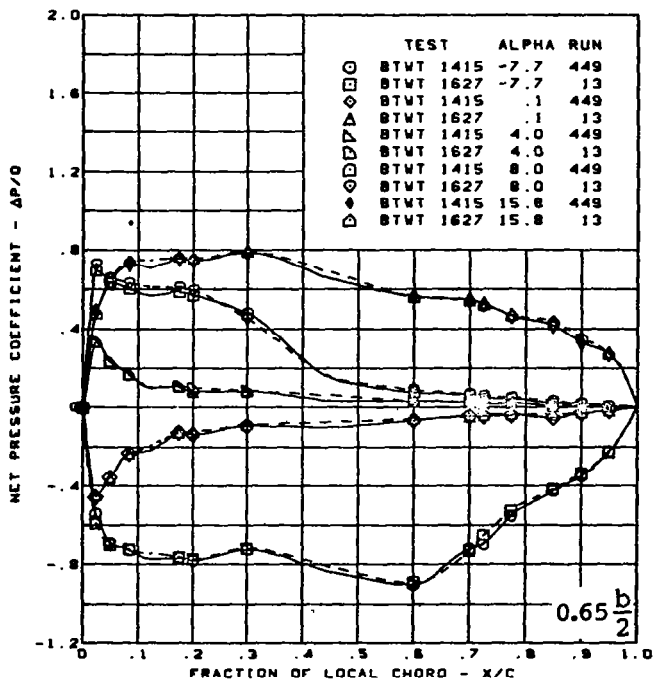
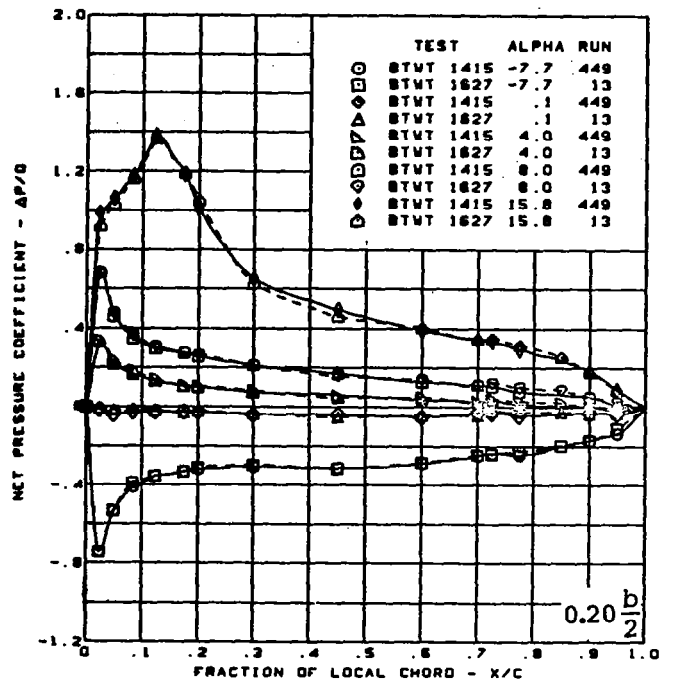
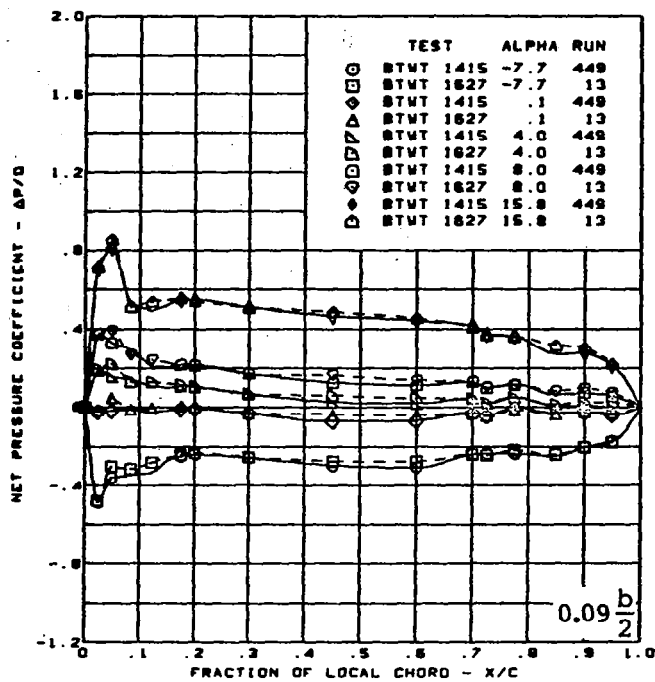
Twisted wing, rounded L.E.

L.E. deflection, full span =  $0.0^\circ$

T.E. deflection, full span =  $0.0^\circ$

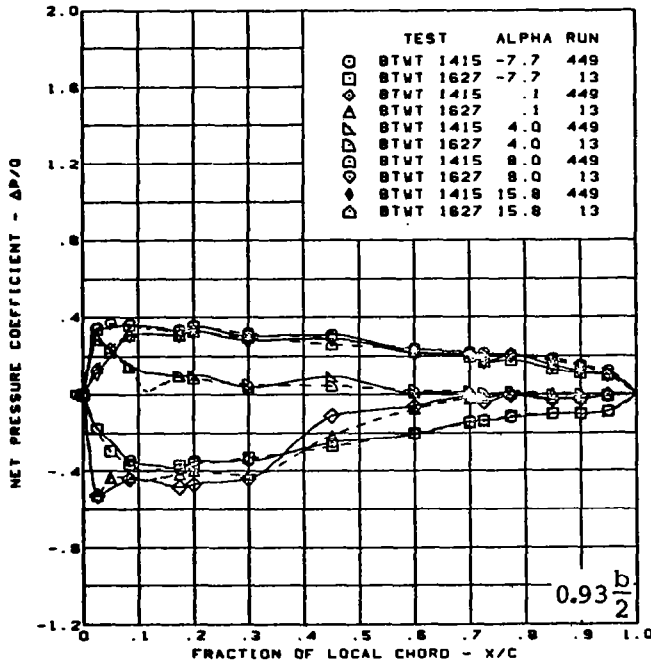
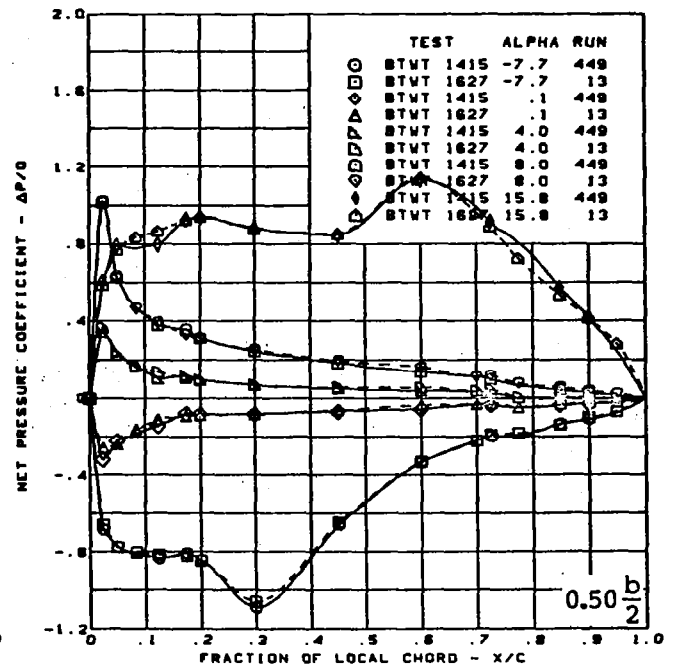
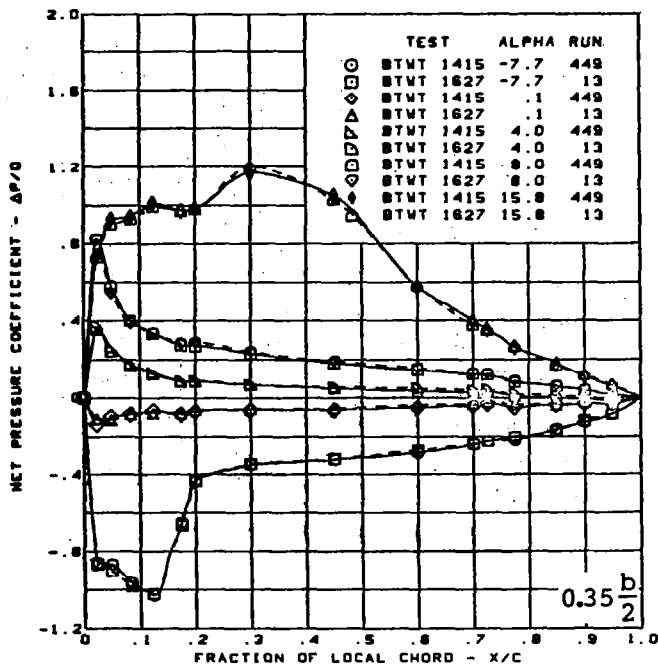
(b) (Concluded)

Figure 15. — (Continued)



(c) Net Chordwise Pressure Distributions

Figure 15. - (Continued)



$M = 0.85$

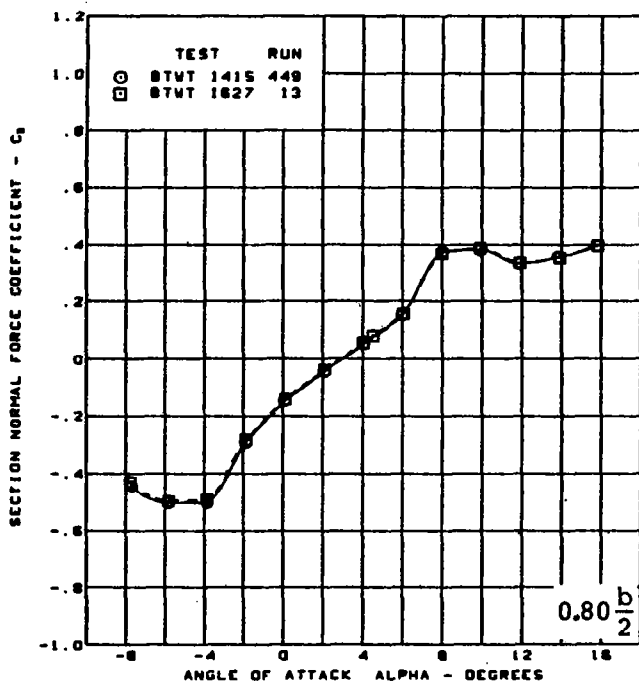
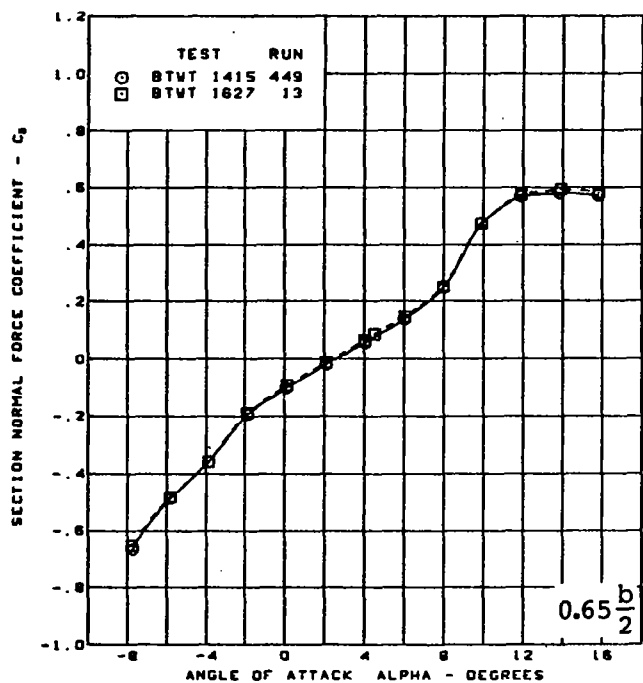
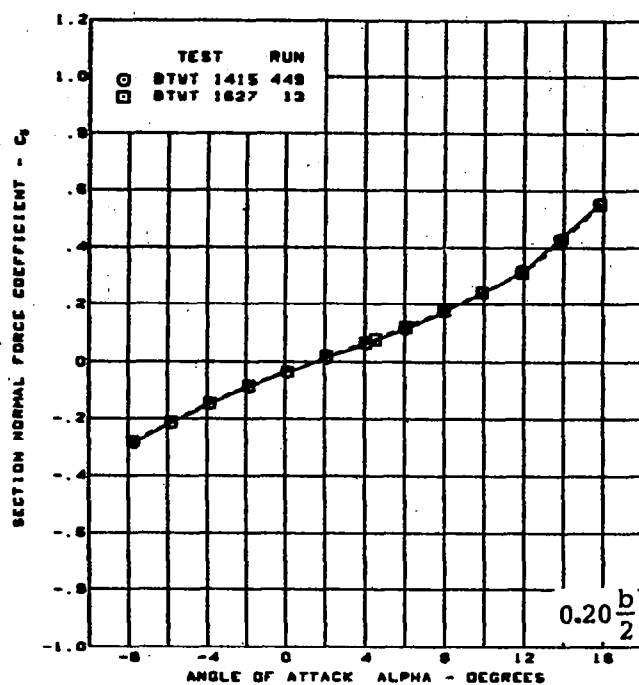
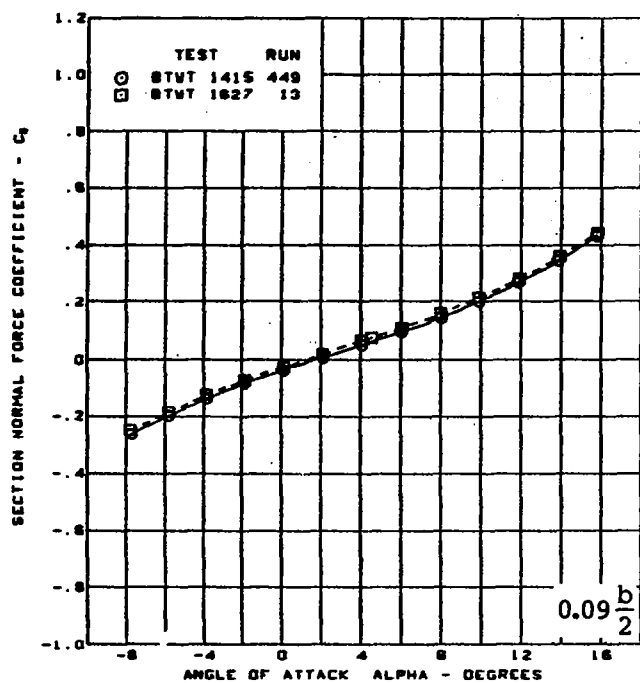
Twisted wing, rounded L.E.

L.E. deflection, full span =  $0.0^\circ$

T.E. deflection, full span =  $0.0^\circ$

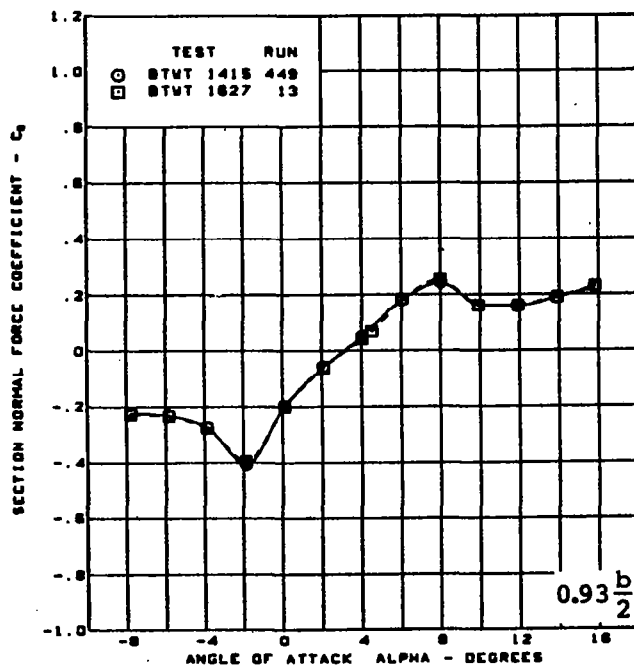
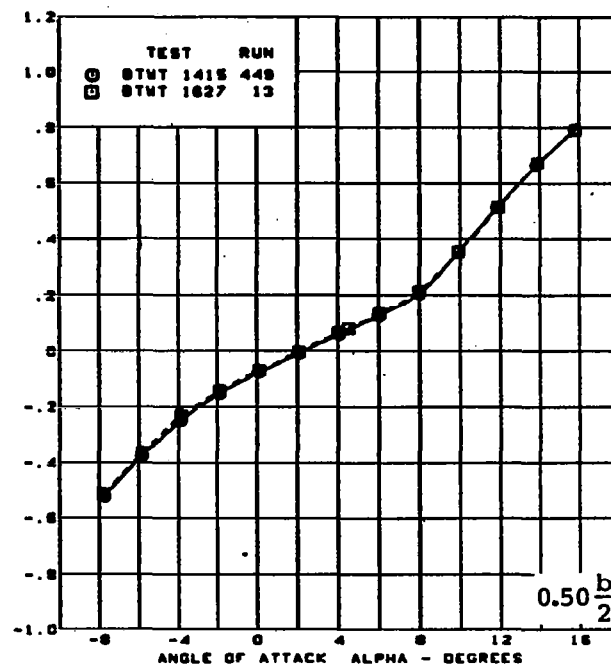
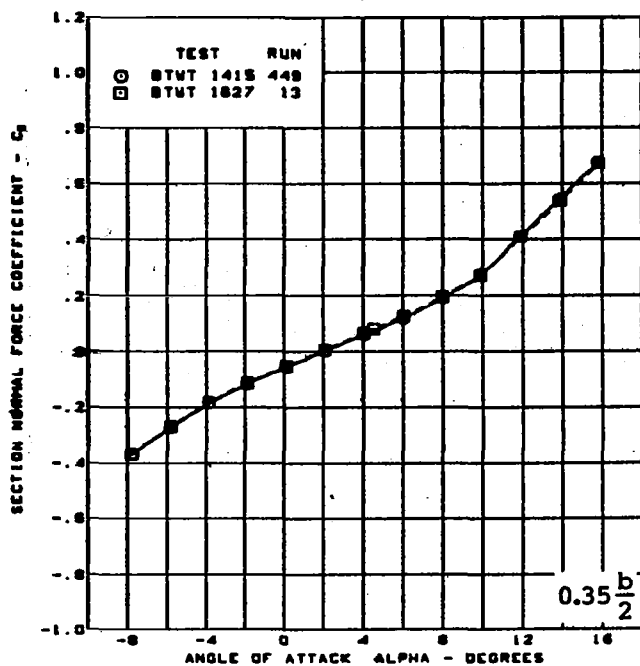
(c) (Concluded)

Figure 15. - (Continued)



(d) Section Aerodynamic Coefficients - Normal Force

Figure 15. - (Continued)



$M = 0.85$

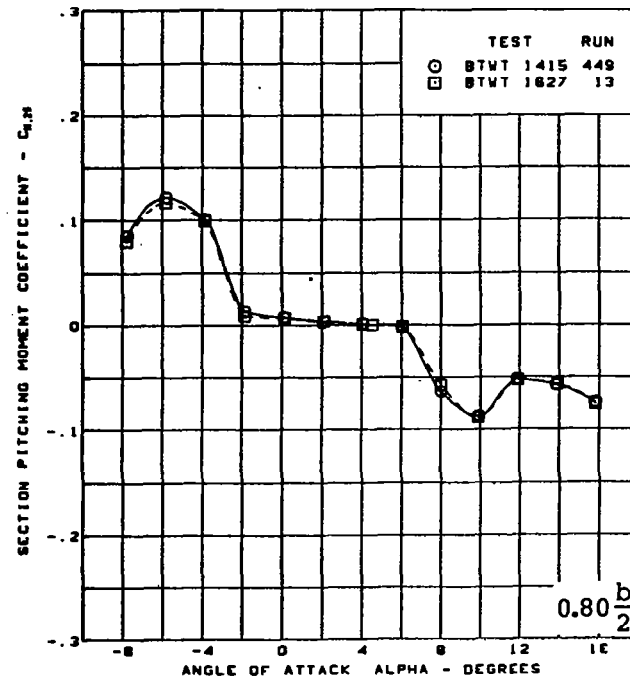
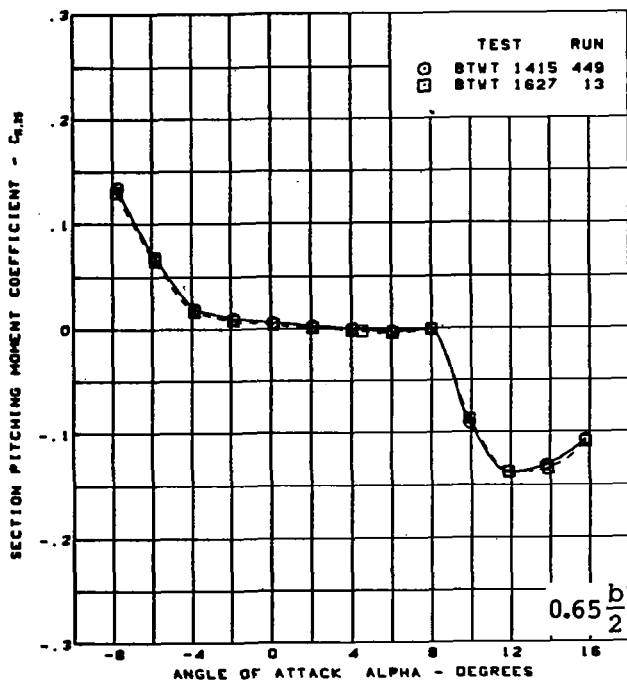
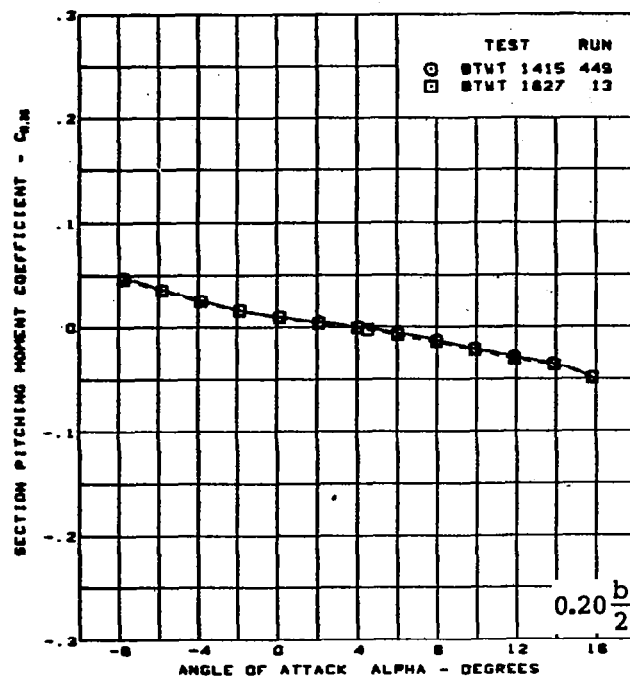
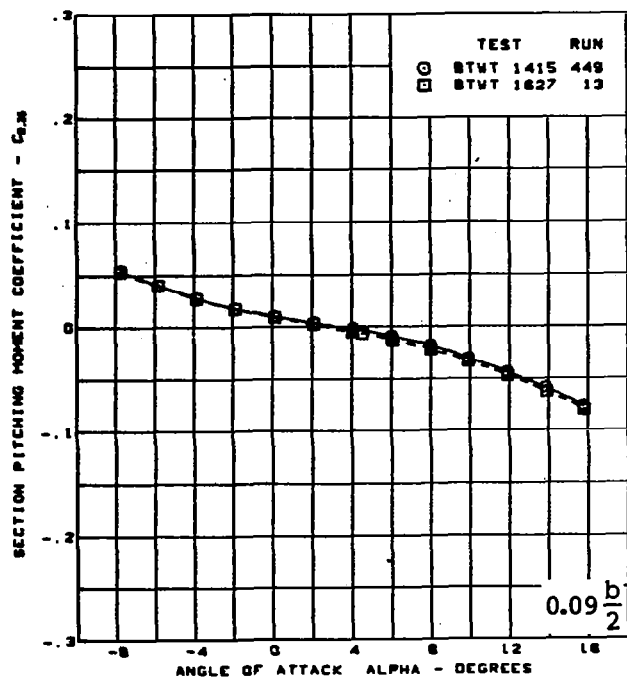
Twisted wing, rounded L.E.

L.E. deflection, full span =  $0.0^\circ$

T.E. deflection, full span =  $0.0^\circ$

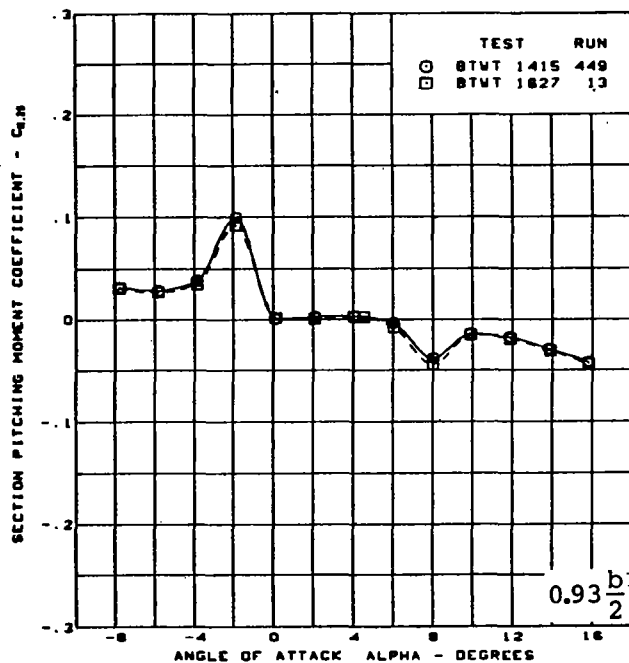
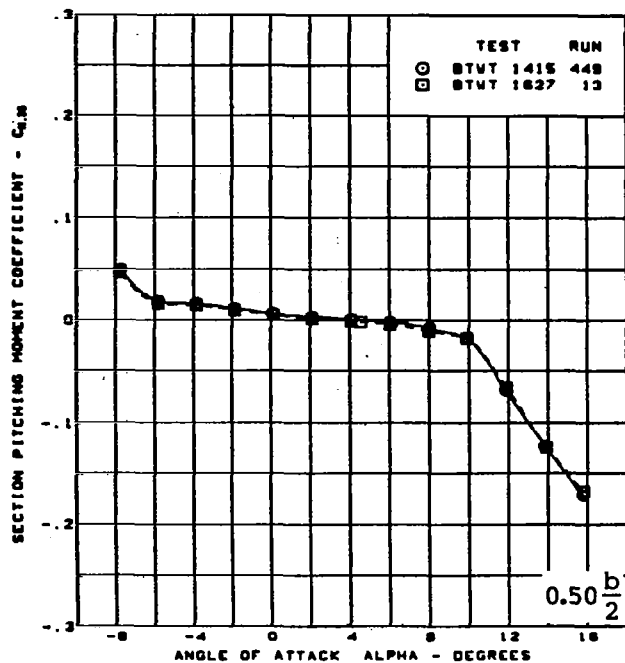
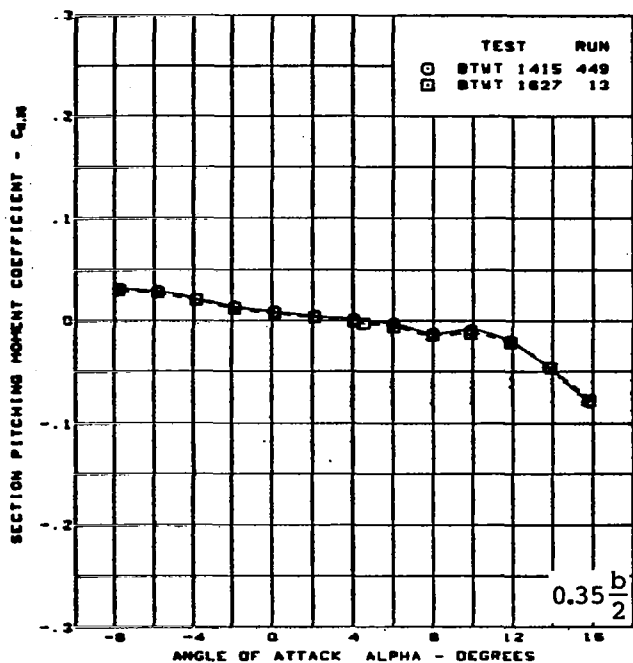
(d) (Concluded)

Figure 15. — (Continued)



(e) Section Aerodynamic Coefficients - Pitching Moment

Figure 15. - (Continued)

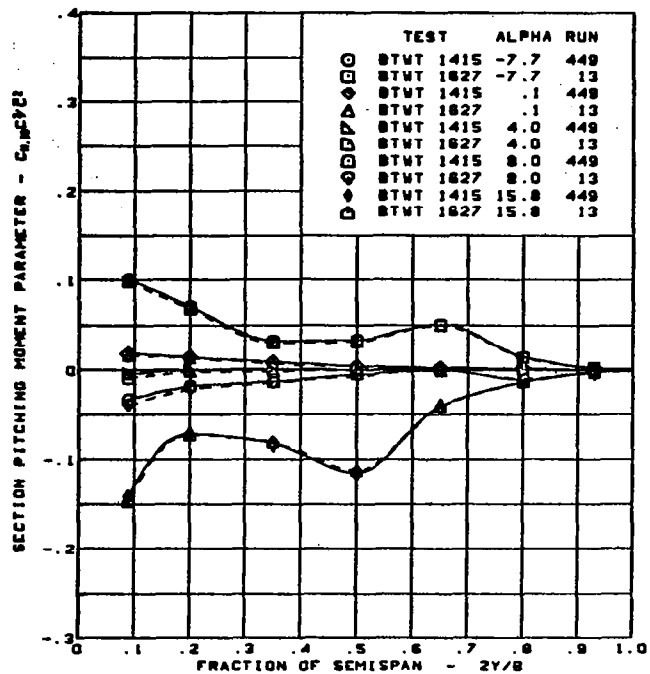
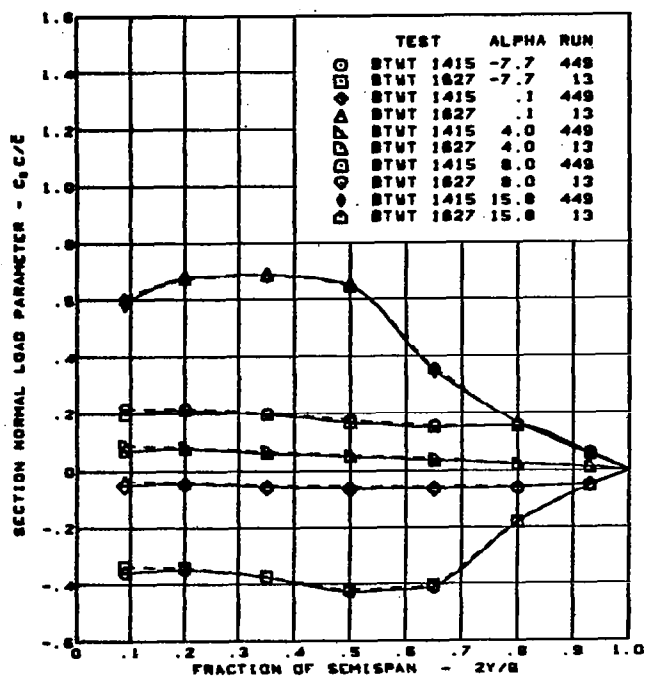


$M = 0.85$   
 Twisted wing, rounded L.E.  
 L.E. deflection, full span =  $0.0^\circ$   
 T.E. deflection, full span =  $0.0^\circ$

(e) (Concluded)

Figure 15. — (Continued)





$M = 0.85$

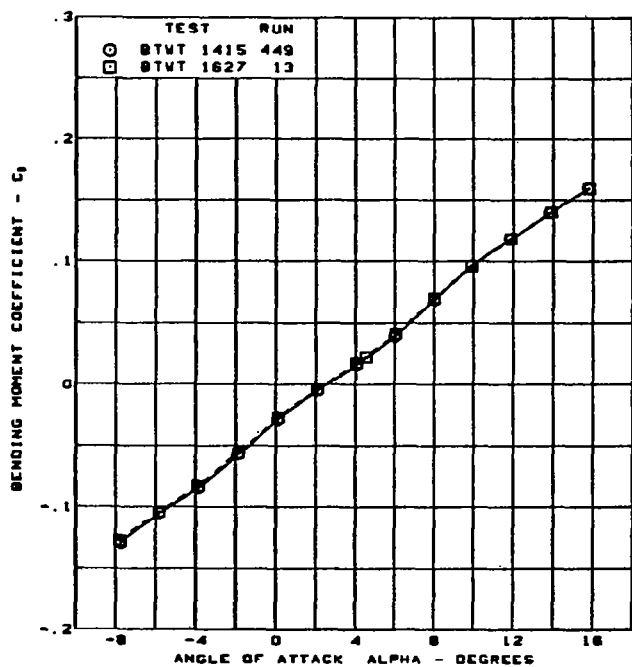
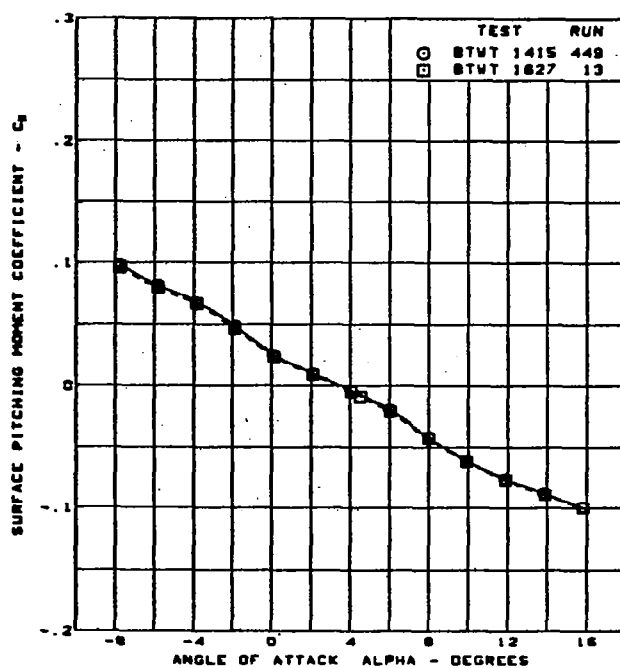
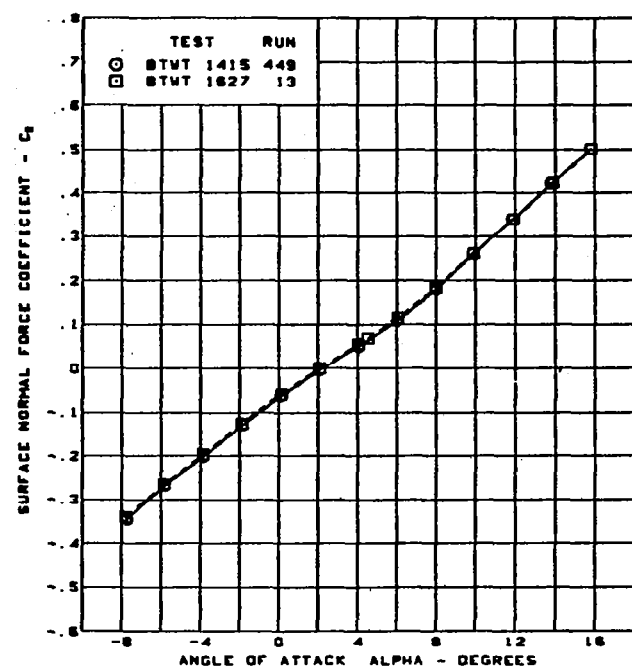
Twisted wing, rounded L.E.

L.E. deflection, full span =  $0.0^\circ$

T.E. deflection, full span =  $0.0^\circ$

(f) Spanload Distributions

Figure 15. — (Continued)



$M = 0.85$

Twisted wing, rounded L.E.

L.E. deflection, full span =  $0.0^\circ$

T.E. deflection, full span =  $0.0^\circ$

(g) Wing Aerodynamic Coefficients

Figure 15. - (Concluded)

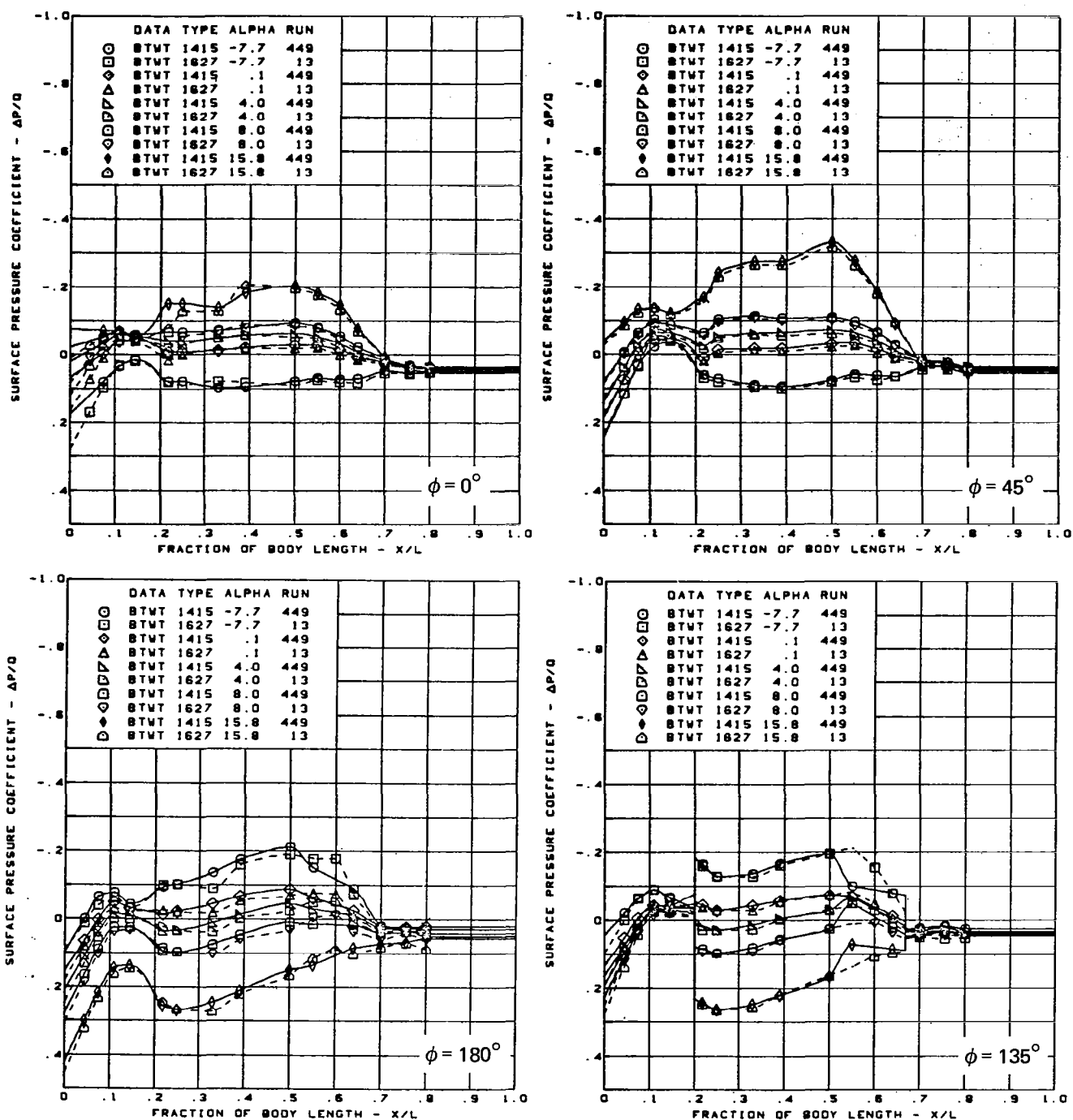
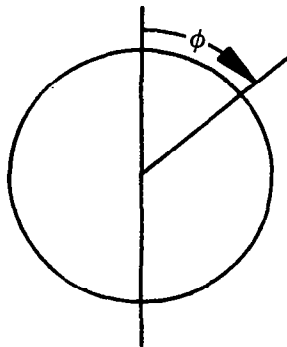
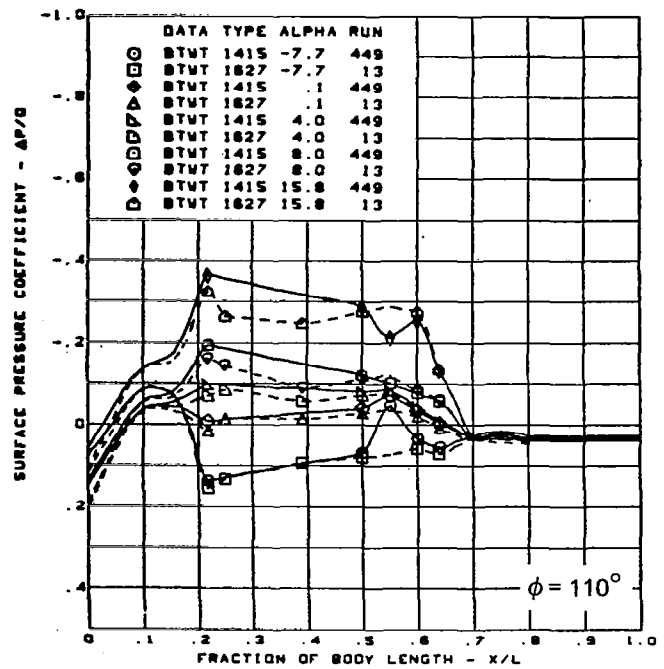
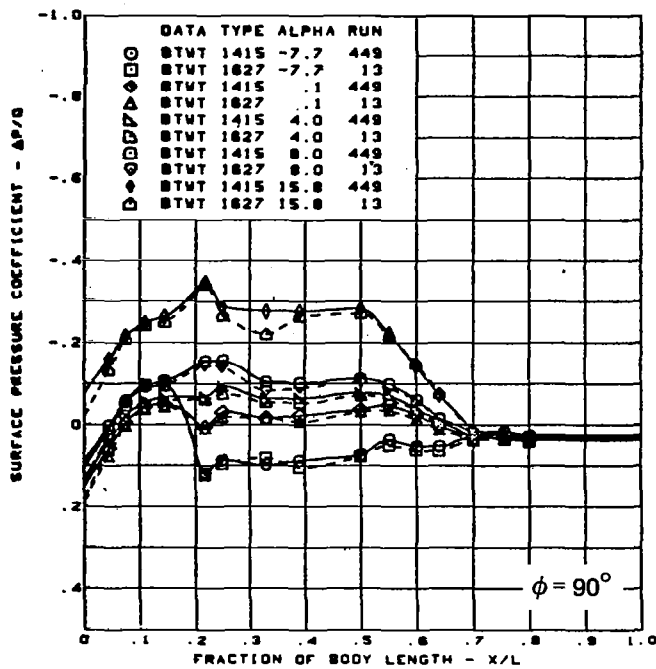
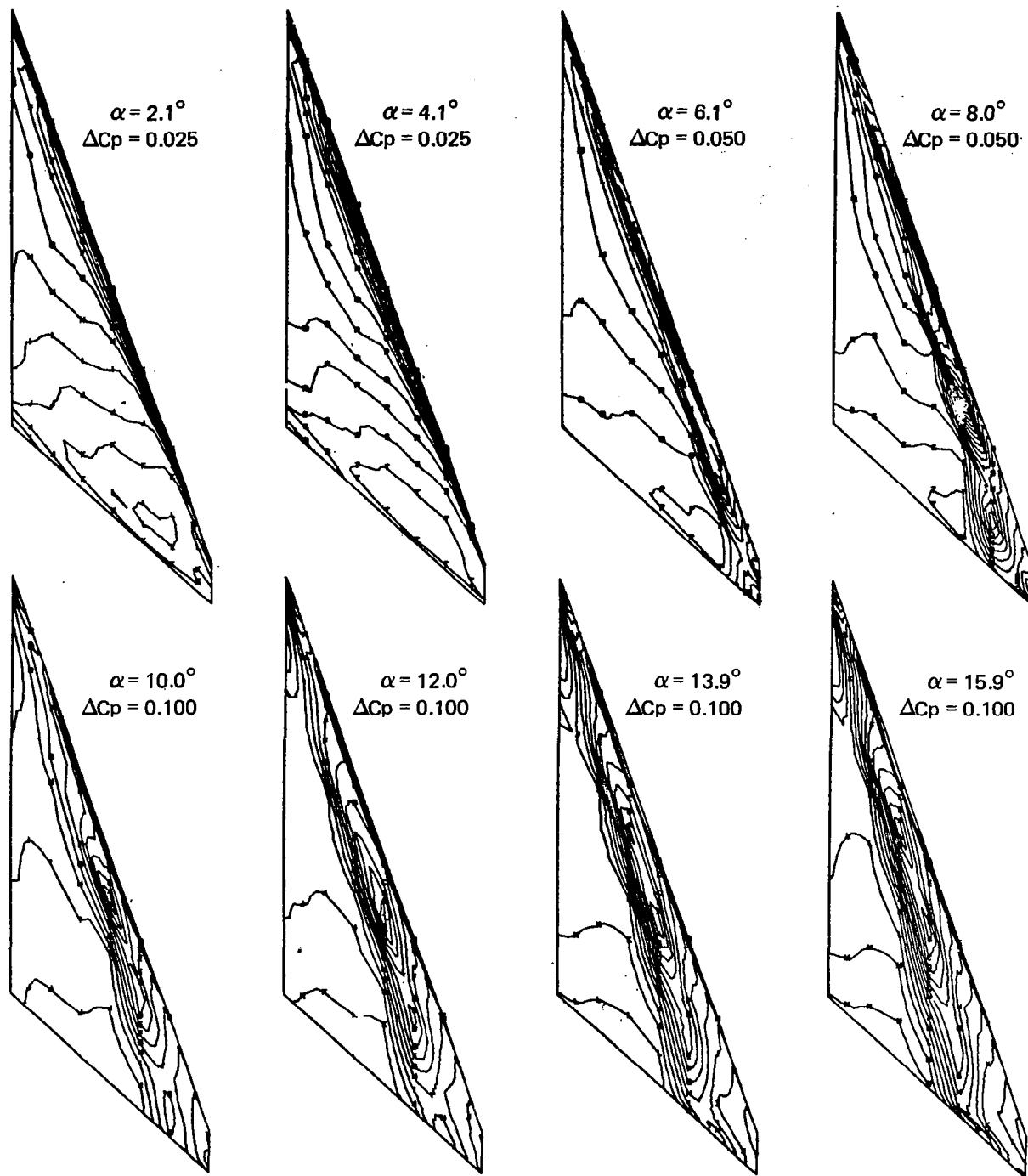


Figure 16. — Body Experimental Surface Longitudinal Pressure Distributions—Comparison of Data From Two Wind Tunnel Tests; Twisted Wing, T.E. Deflection, Full Span =  $0.0^\circ$ ;  $M = 0.85$



$M = 0.85$   
 Twisted wing, rounded L.E.  
 L.E. deflection, full span =  $0.0^\circ$   
 T.E. deflection, full span =  $0.0^\circ$

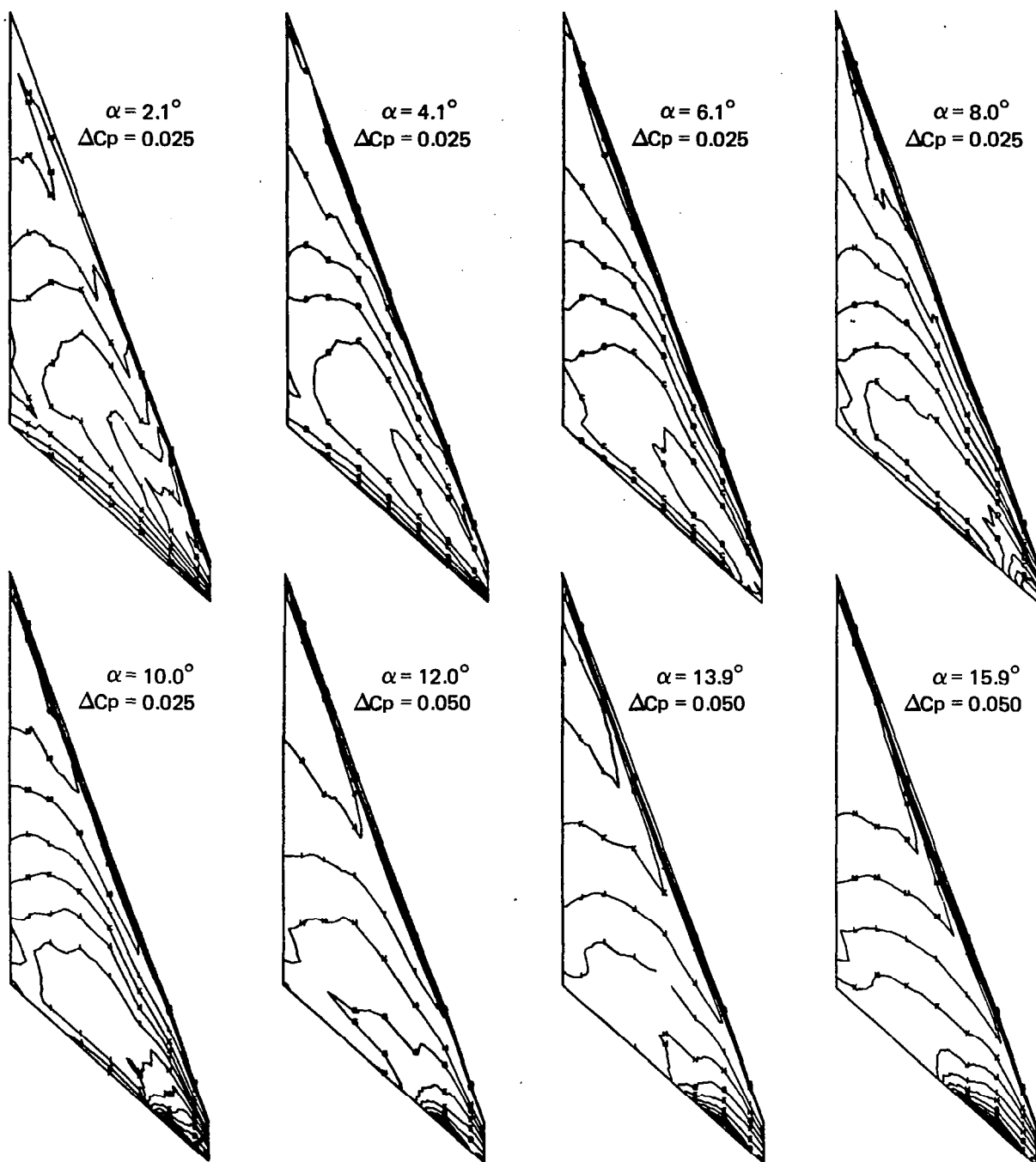
Figure 16. — (Concluded)



Note:  $\Delta C_p$  = increment between adjacent isobars

(a) Upper Surface Isobars

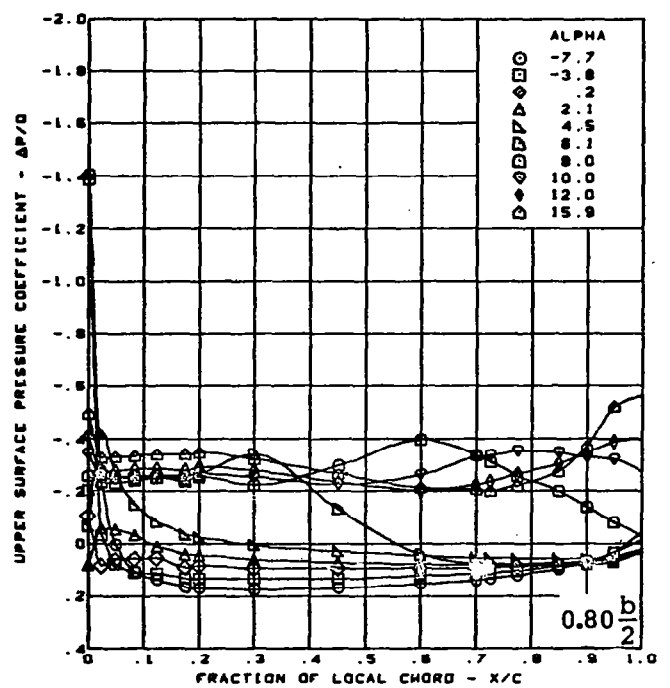
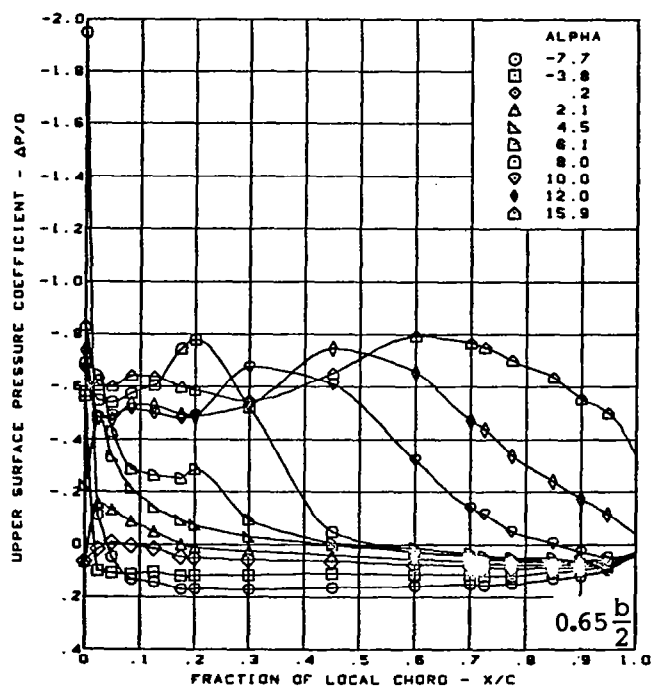
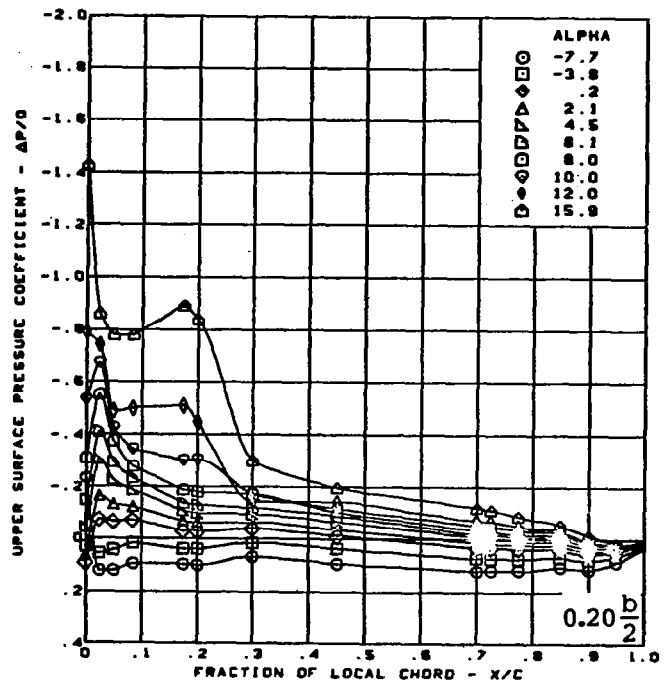
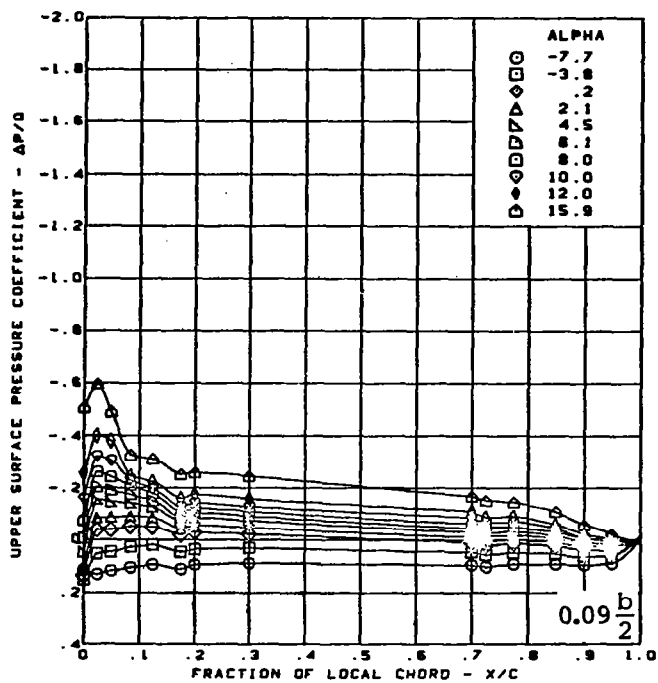
Figure 17. — Wing Experimental Data—Effect of Angle of Attack; Cambered-Twisted Wing; Fin Off; T.E. Deflection, Full Span =  $0.0^\circ$ ;  $M = 0.40$



Note:  $\Delta C_p$  = increment between adjacent isobars

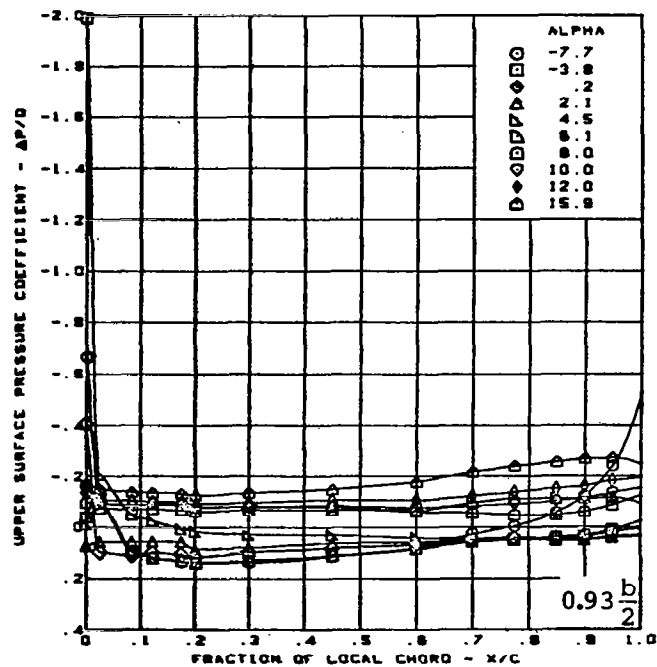
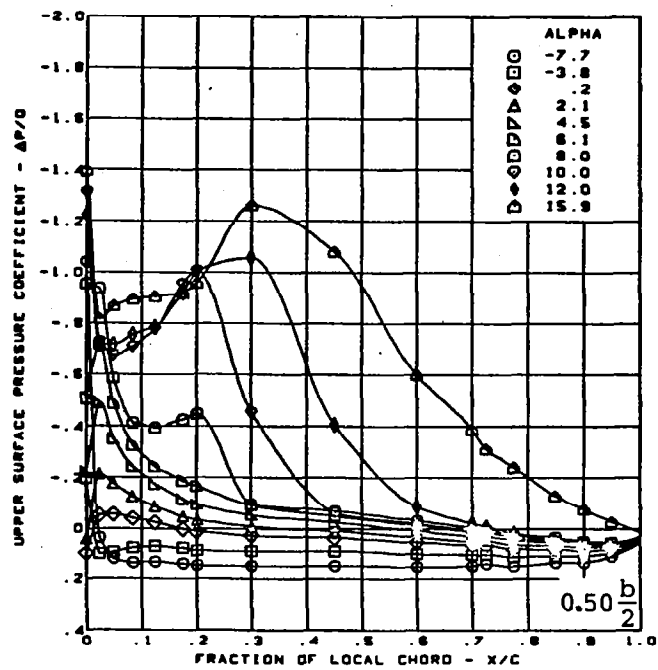
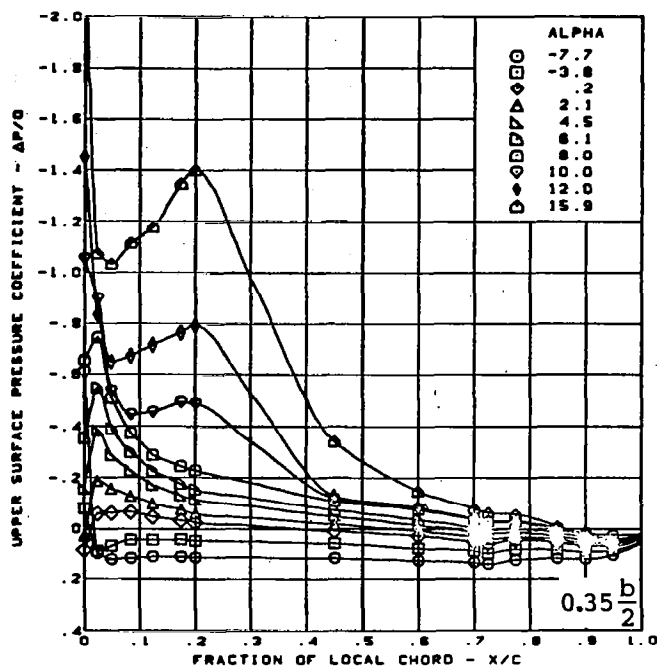
(b) Lower Surface Isobars

Figure 17. — (Continued)



(c) Upper Surface Chordwise Pressure Distributions

Figure 17. - (Continued)

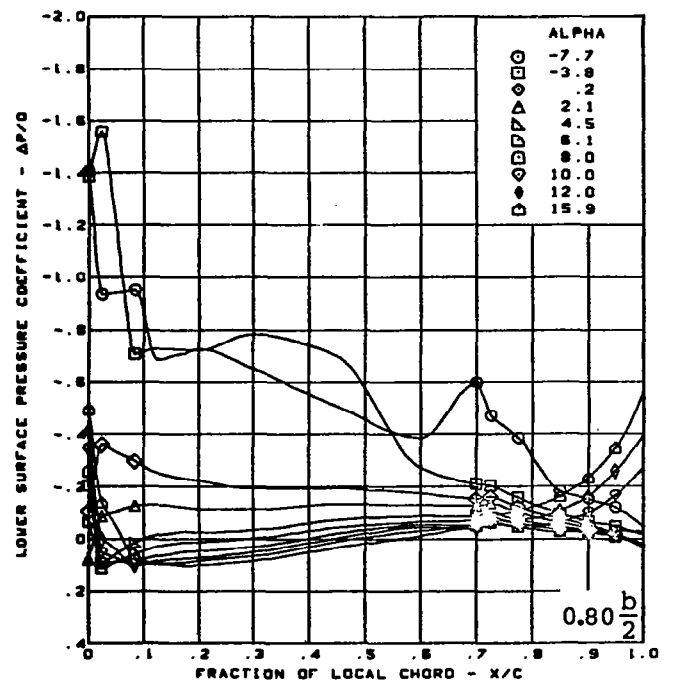
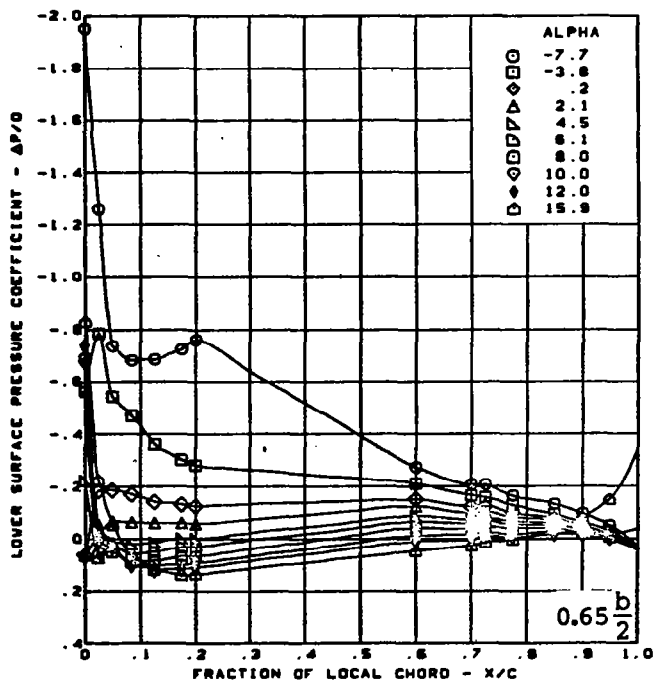
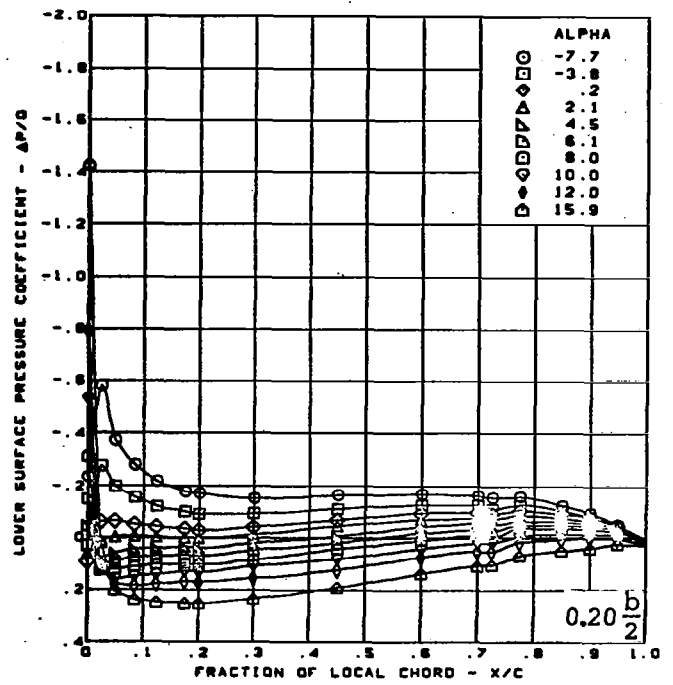
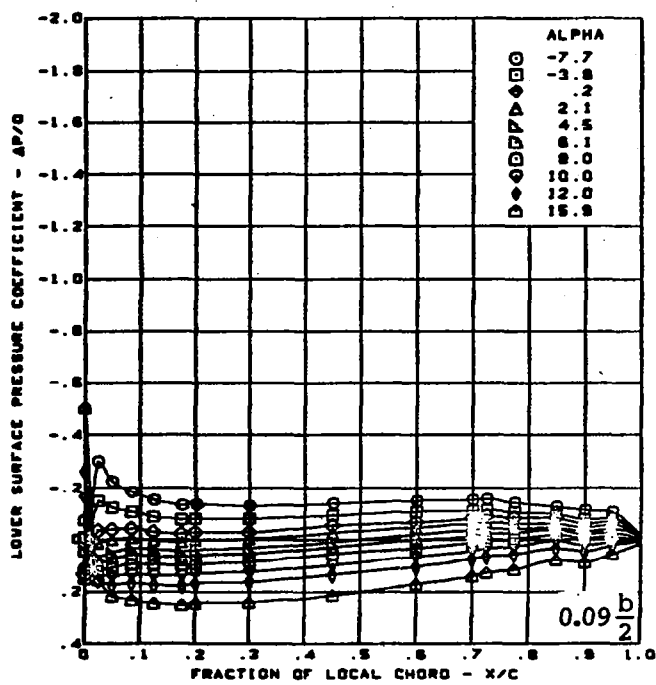


$M = 0.40$  (run 43)  
 Cambered-twisted wing, rounded L.E.  
 Fin off  
 L.E. deflection, full span =  $0.0^\circ$   
 T.E. deflection, full span =  $0.0^\circ$

(c) (Concluded)

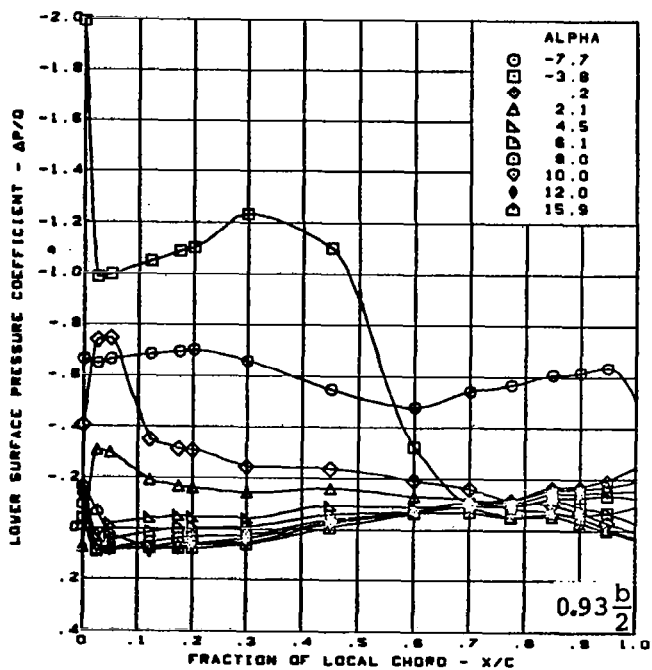
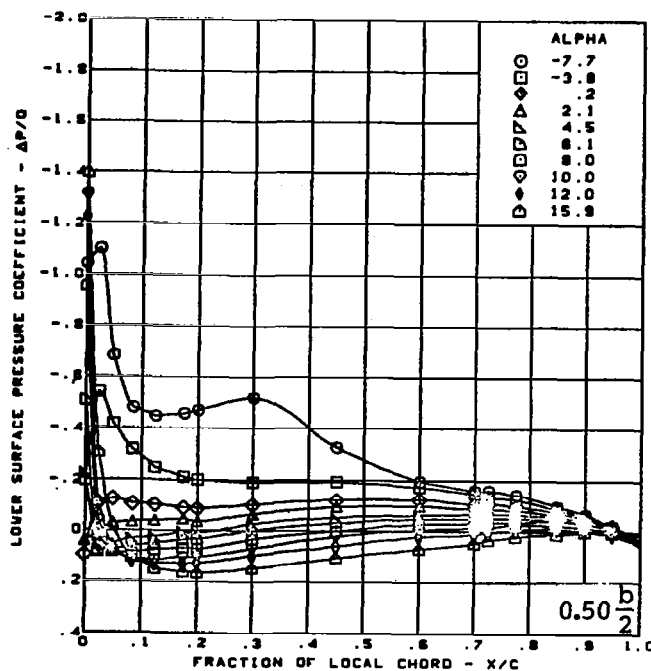
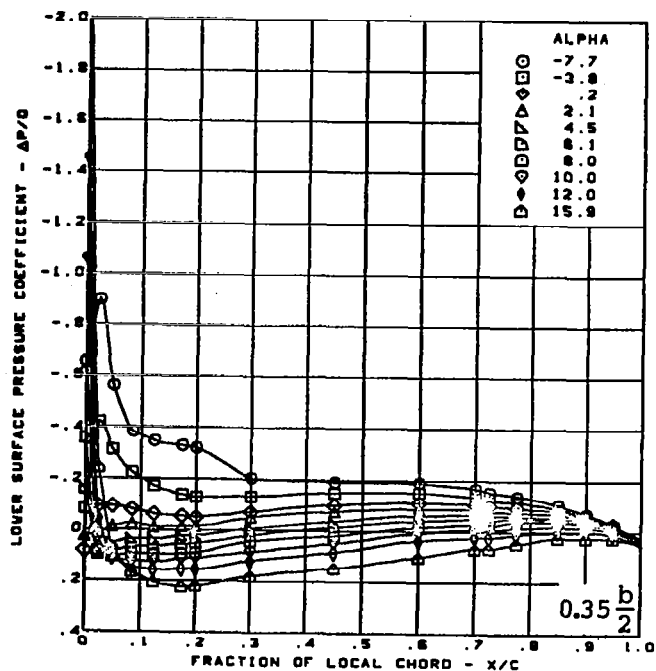
Figure 17. — (Continued)





(d) Lower Surface Chordwise Pressure Distributions

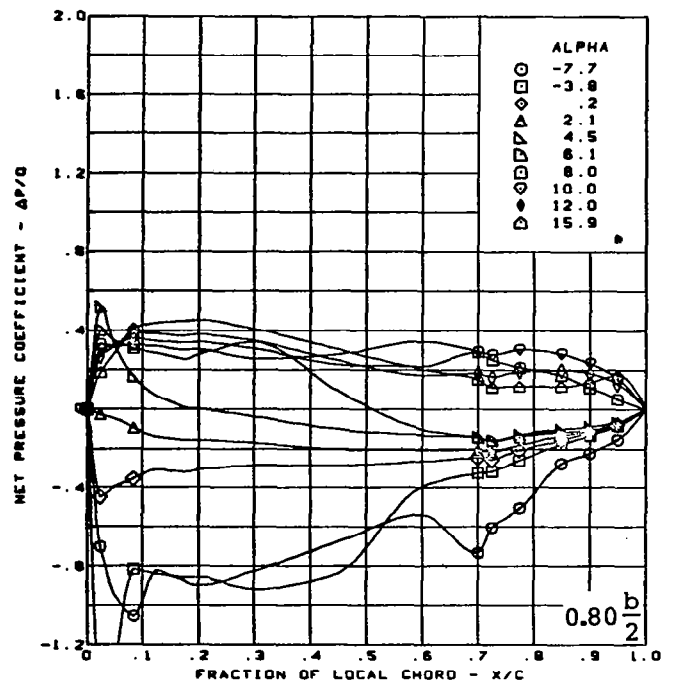
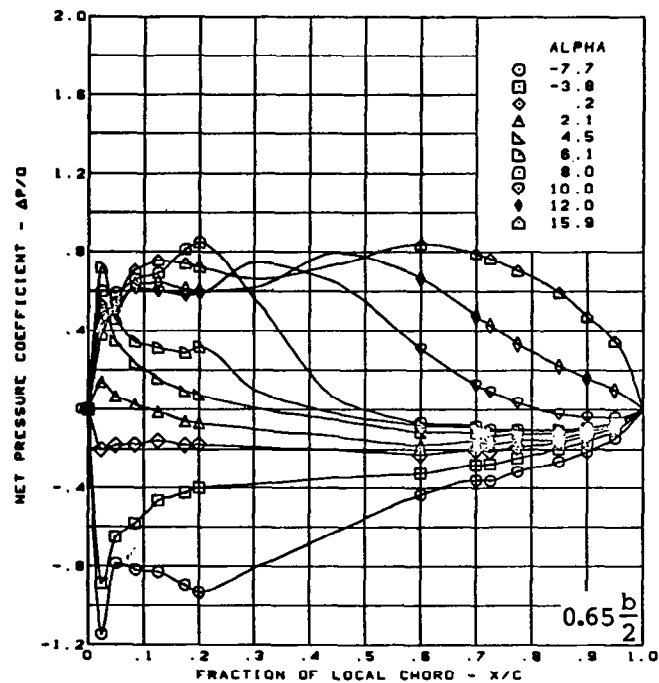
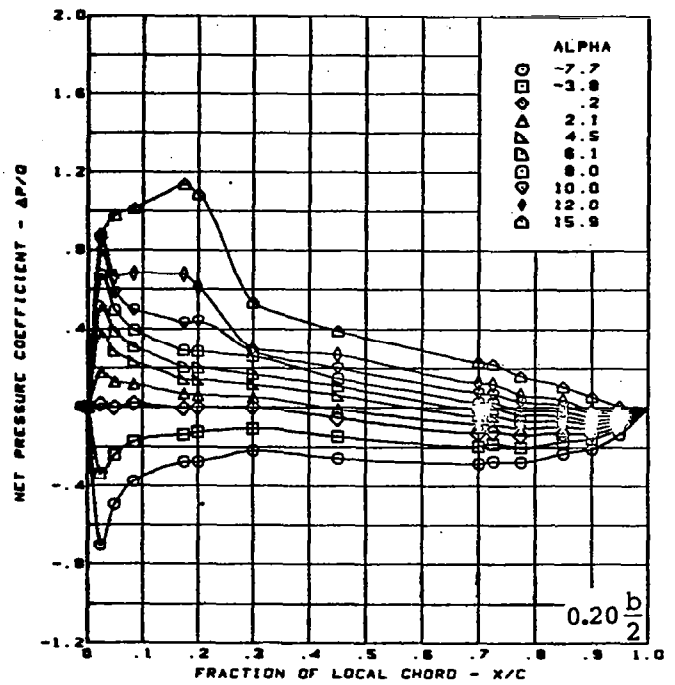
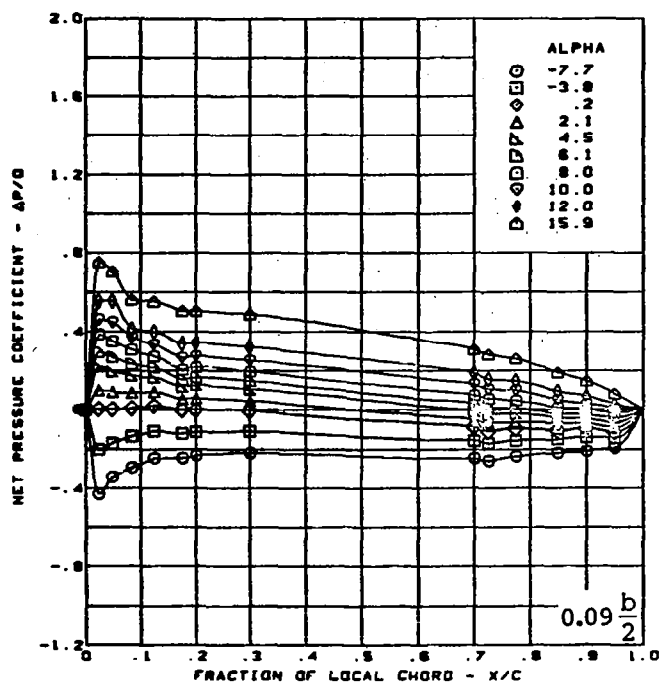
Figure 17. — (Continued)



$M = 0.40$  (run 43)  
 Cambered-twisted wing, rounded L.E.  
 Fin off  
 L.E. deflection, full span =  $0.0^\circ$   
 T.E. deflection, full span =  $0.0^\circ$

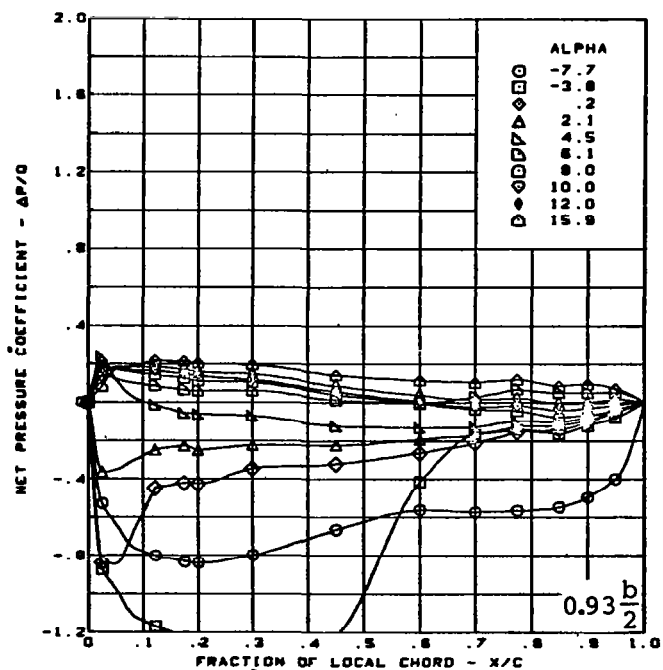
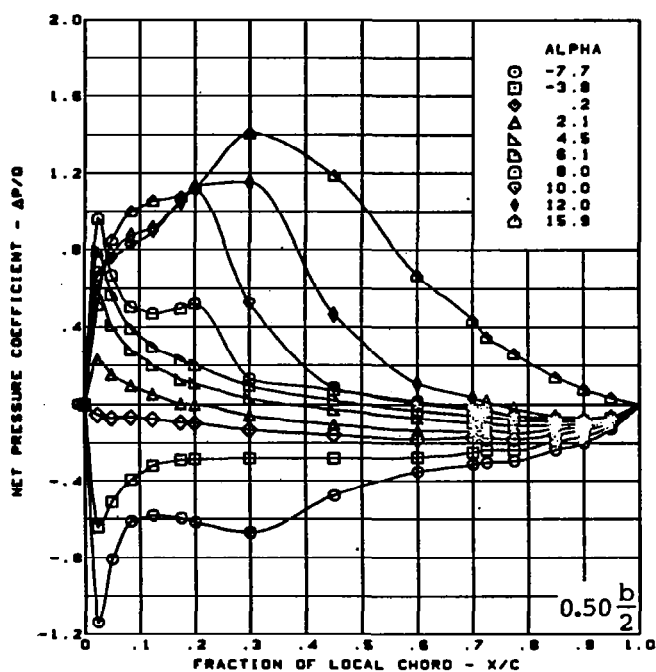
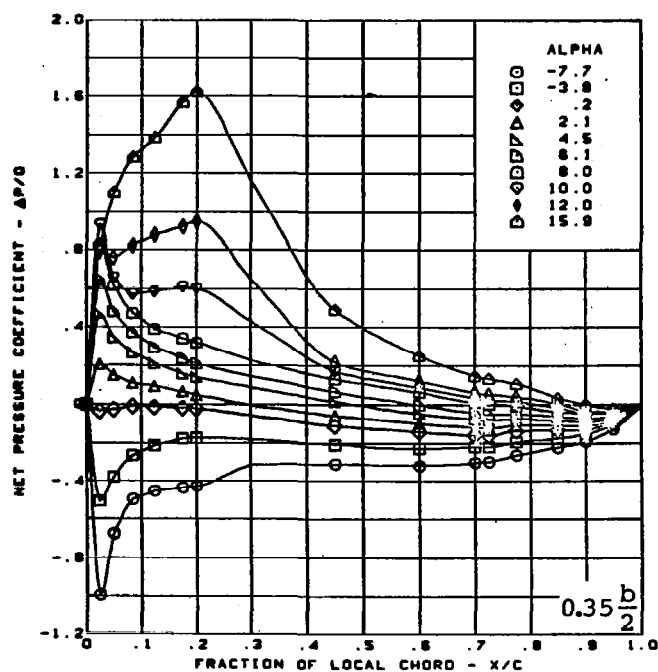
(d) (Concluded)

Figure 17. — (Continued)



(e) Net Chordwise Pressure Distributions

Figure 17. - (Continued)

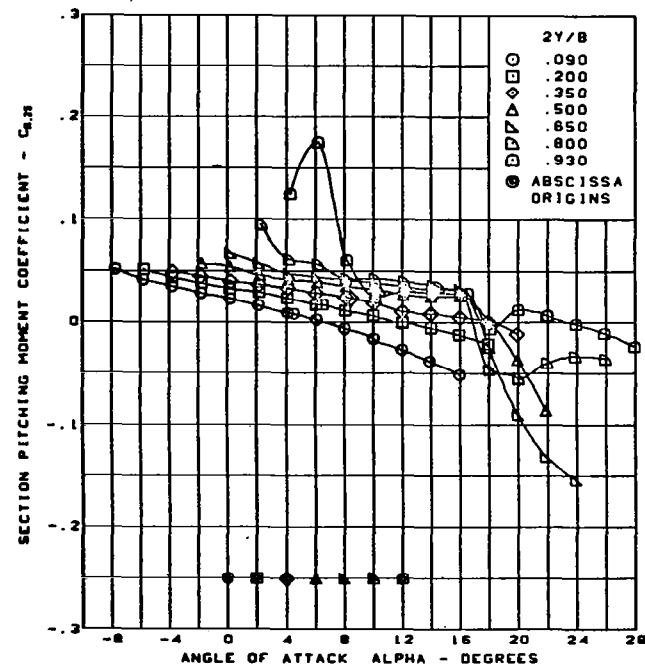
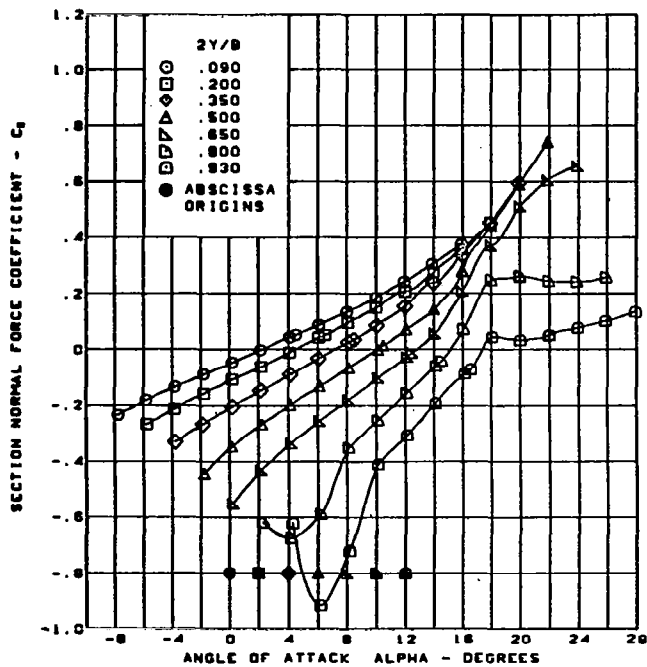
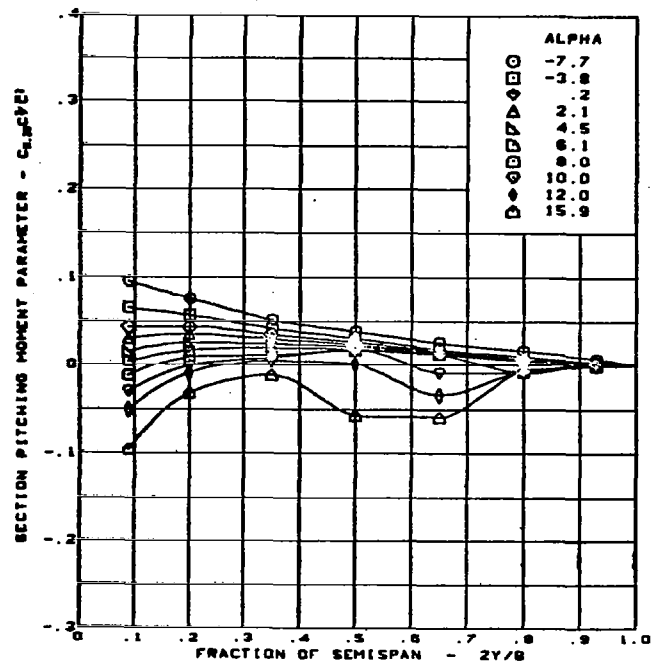
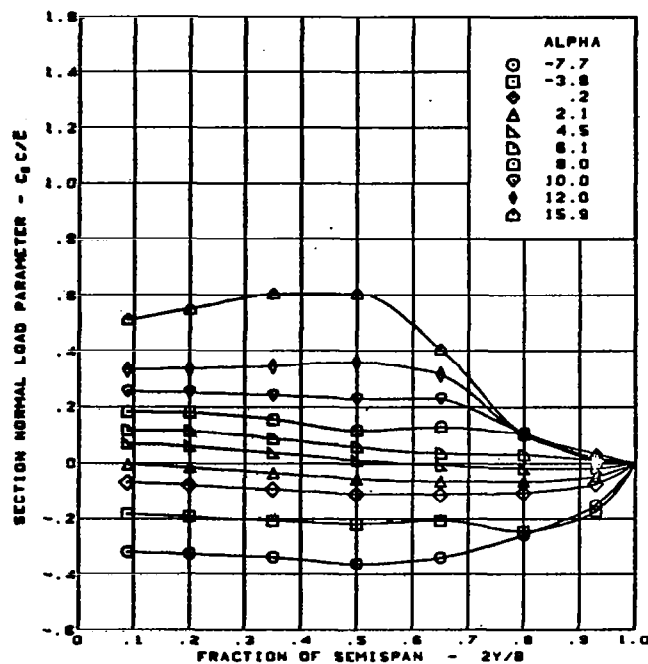


$M = 0.40$  (run 43)  
 Cambered-twisted wing, rounded L.E.  
 Fin off  
 L.E. deflection, full span =  $0.0^\circ$   
 T.E. deflection, full span =  $0.0^\circ$

(e) (Concluded)

Figure 17. — (Continued)



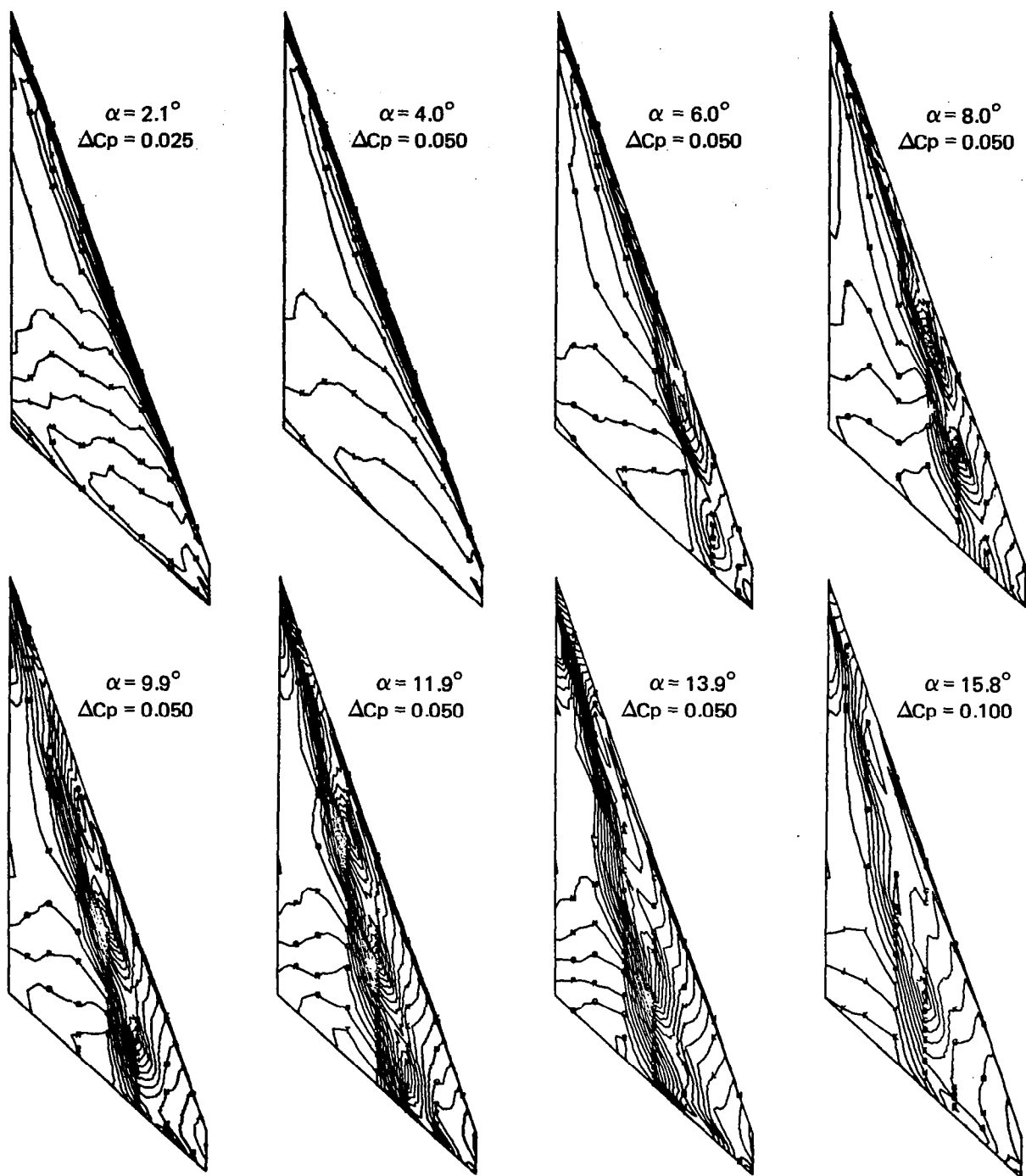


$M = 0.40$  (run 43)  
 Cambered-twisted wing, rounded L.E.  
 Fin off

L.E. deflection, full span =  $0.0^\circ$   
 T.E. deflection, full span =  $0.0^\circ$

(f) Spanload Distributions and Section Aerodynamic Coefficients

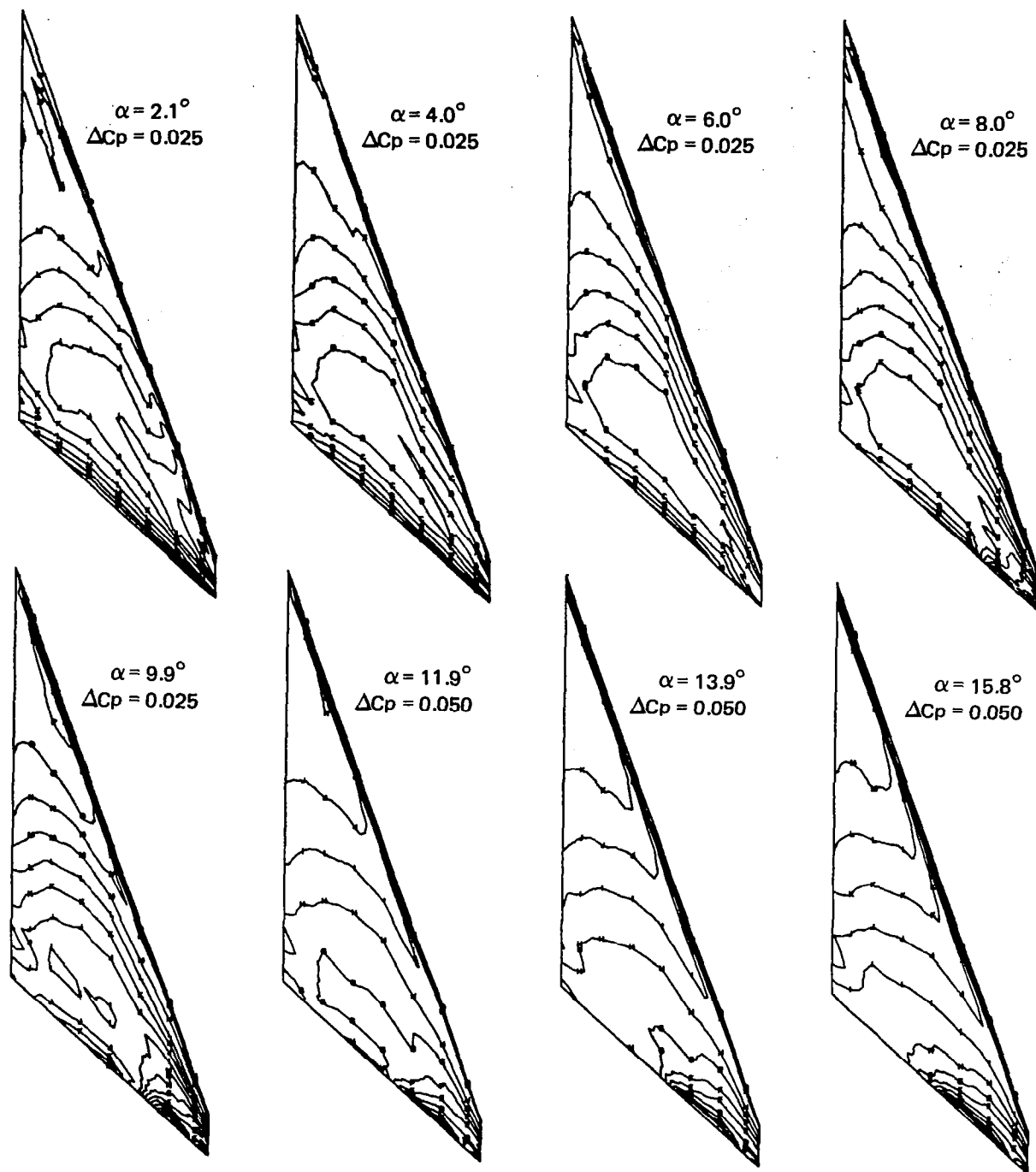
Figure 17. — (Concluded)



Note:  $\Delta C_p$  = increment between adjacent isobars

(a) Upper Surface Isobars

Figure 18. — Wing Experimental Data—Effect of Angle of Attack; Cambered-Twisted Wing; Fin Off; T.E. Deflection, Full Span =  $0.0^\circ$ ;  $M = 0.85$

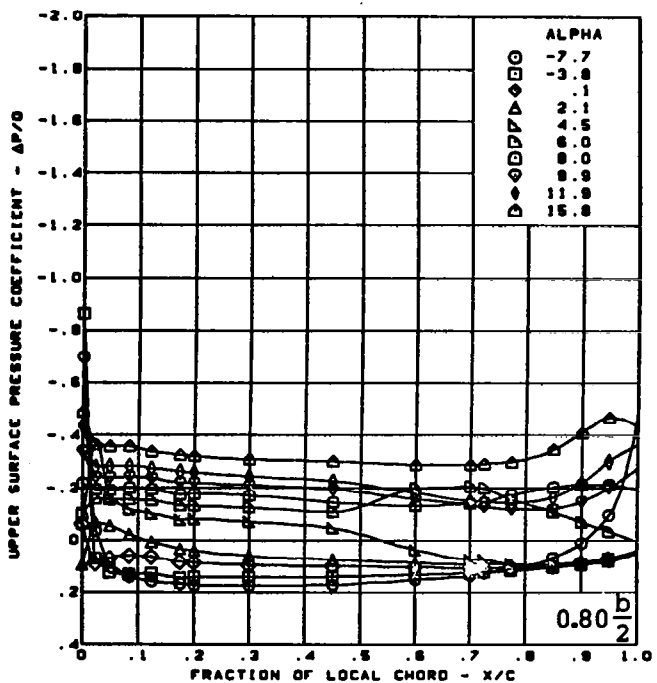
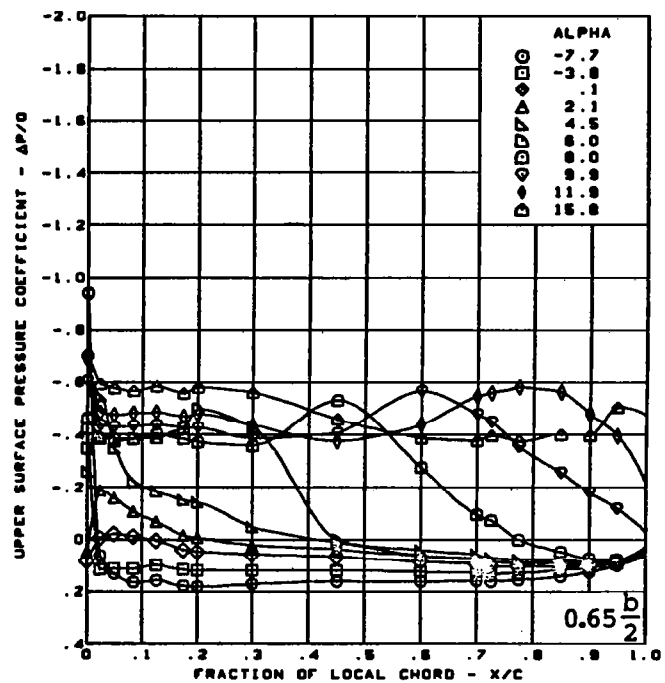
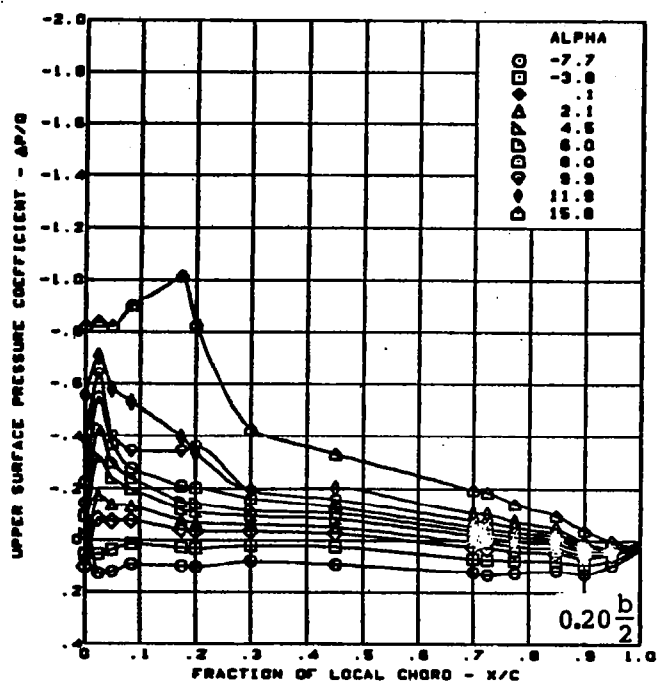
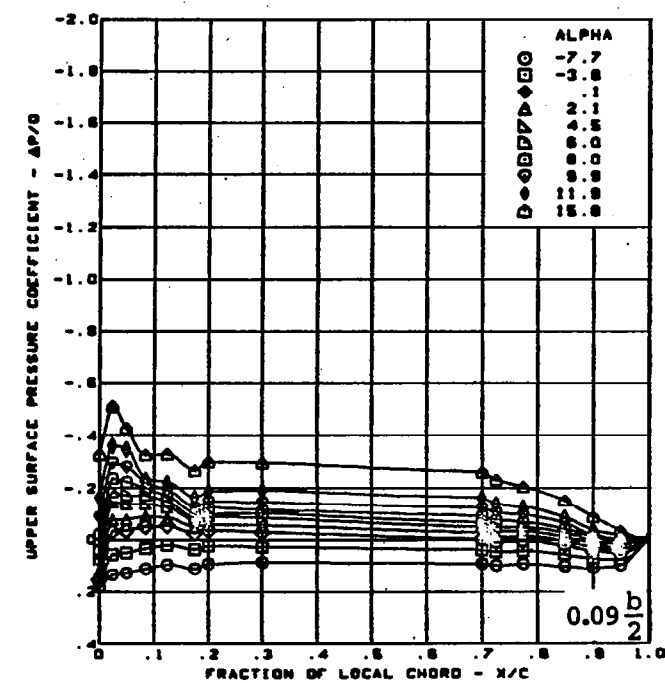


Note:  $\Delta C_p$  = increment between adjacent isobars

(b) Lower Surface Isobars

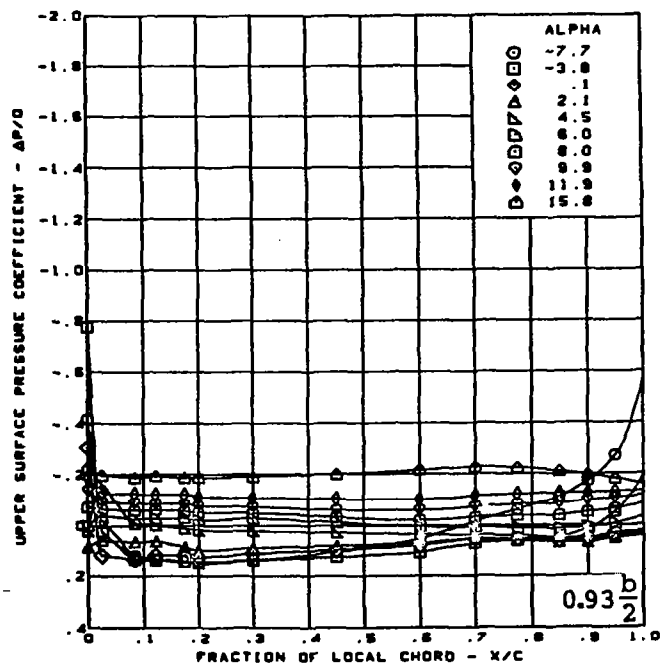
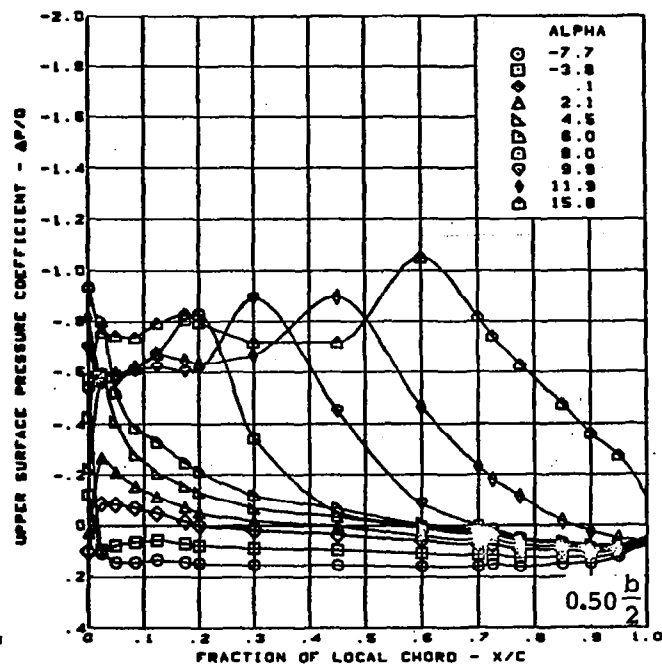
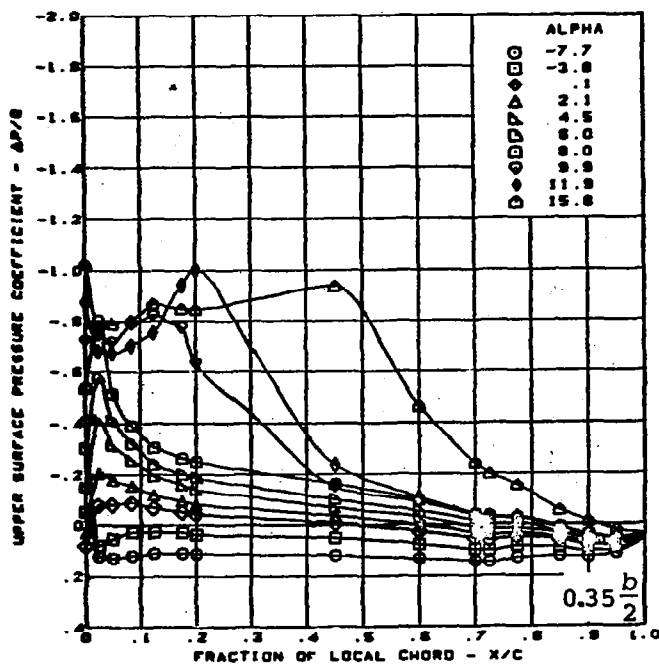
Figure 18. — (Continued)





(c) Upper Surface Chordwise Pressure Distributions

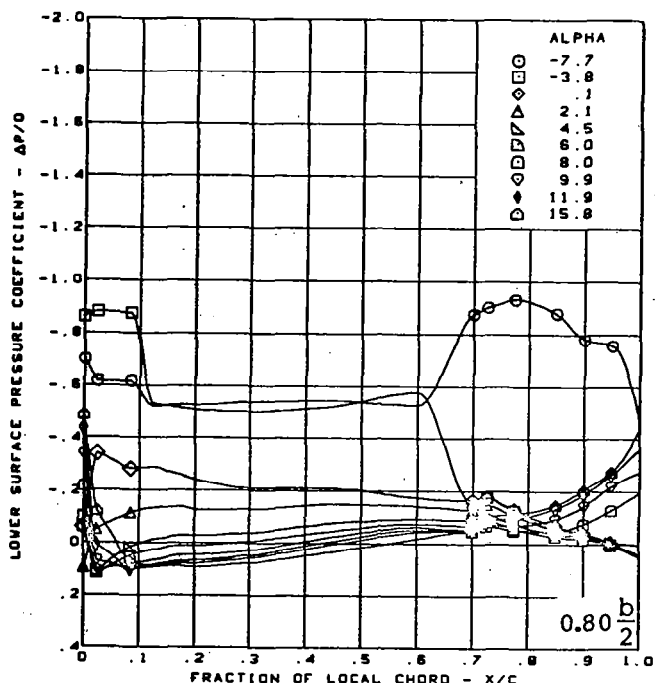
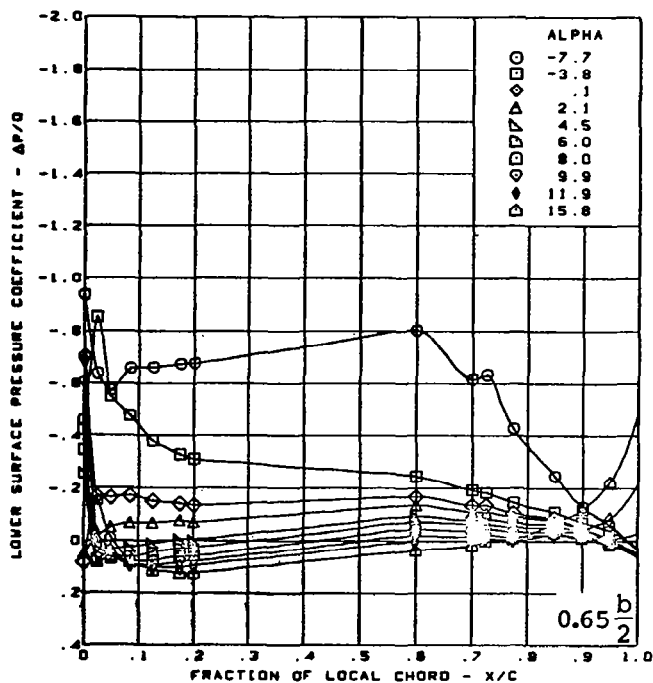
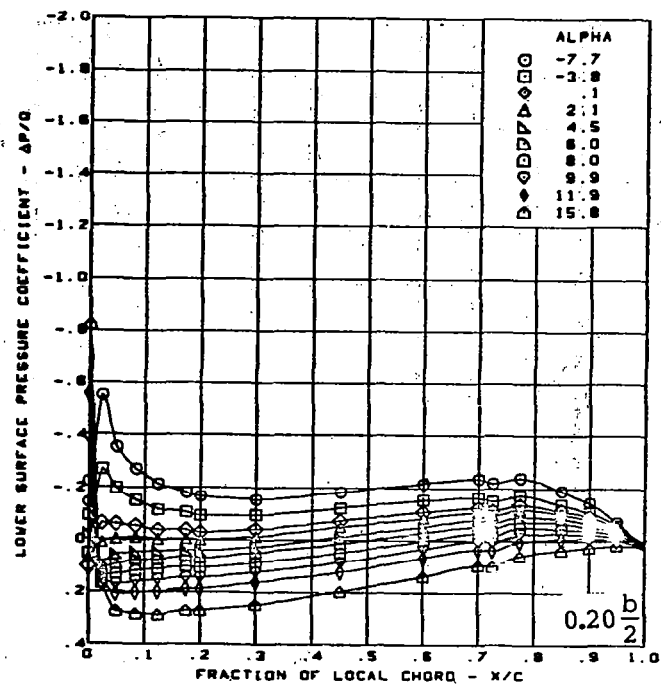
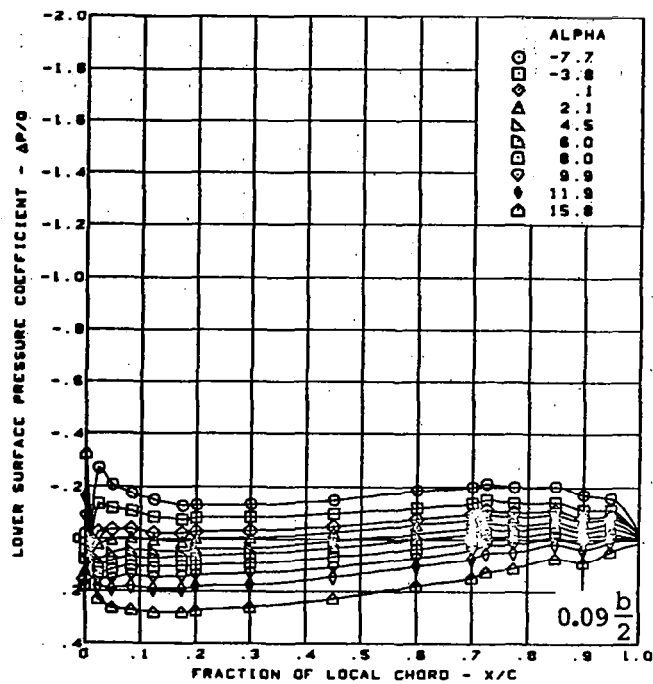
Figure 18. — (Continued)



$M = 0.85$  (run 40)  
 Cambered-twisted wing, rounded L.E.  
 Fin off  
 L.E. deflection, full span =  $0.0^\circ$   
 T.E. deflection, full span =  $0.0^\circ$

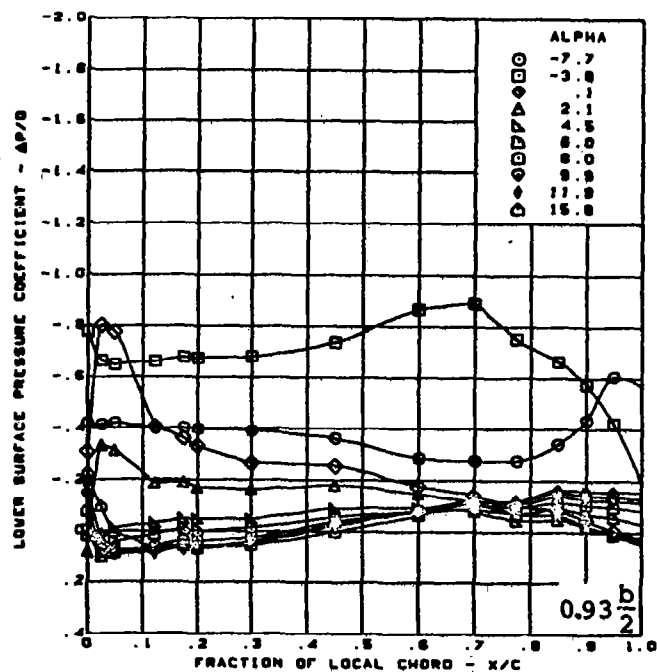
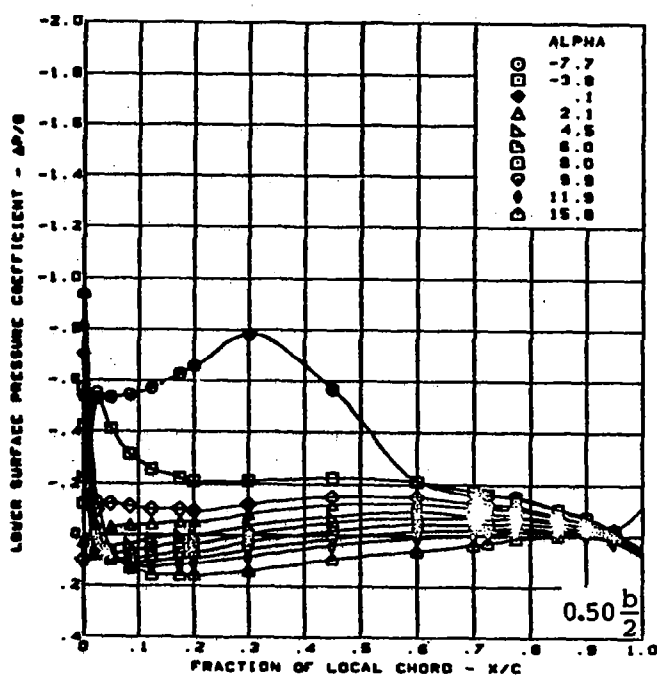
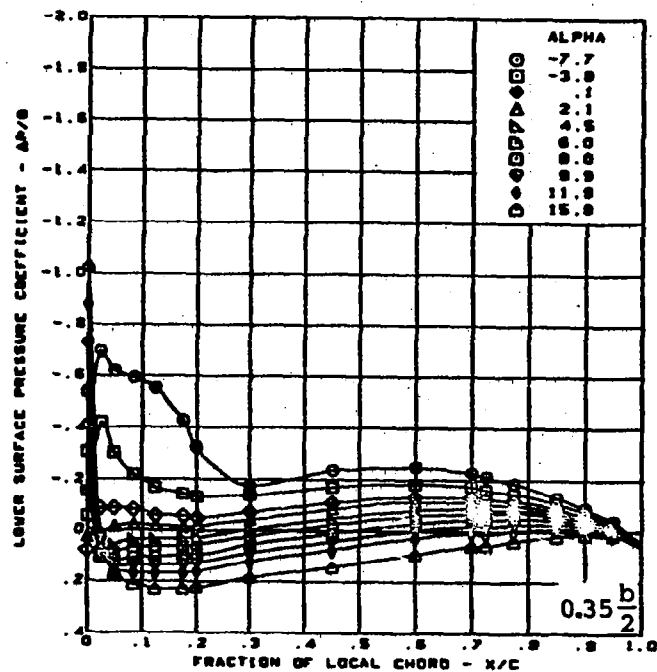
(c) (Concluded)

Figure 18. — (Continued)



(d) Lower Surface Chordwise Pressure Distributions

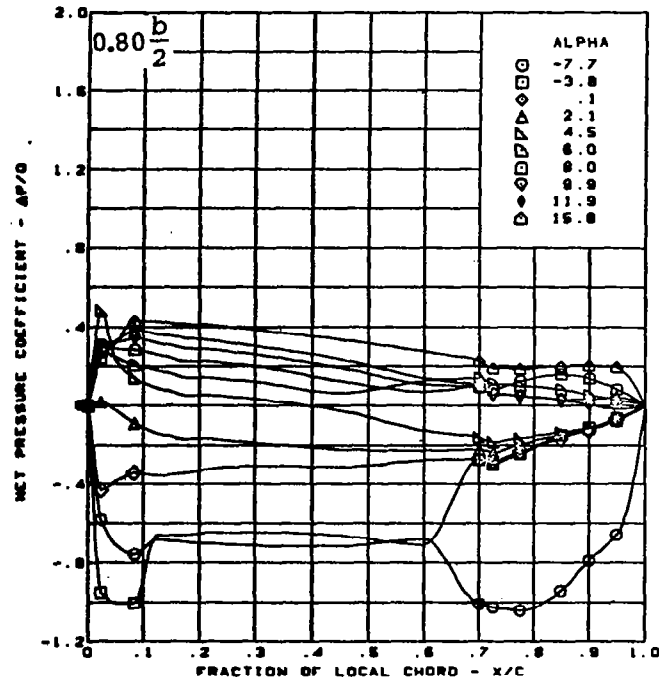
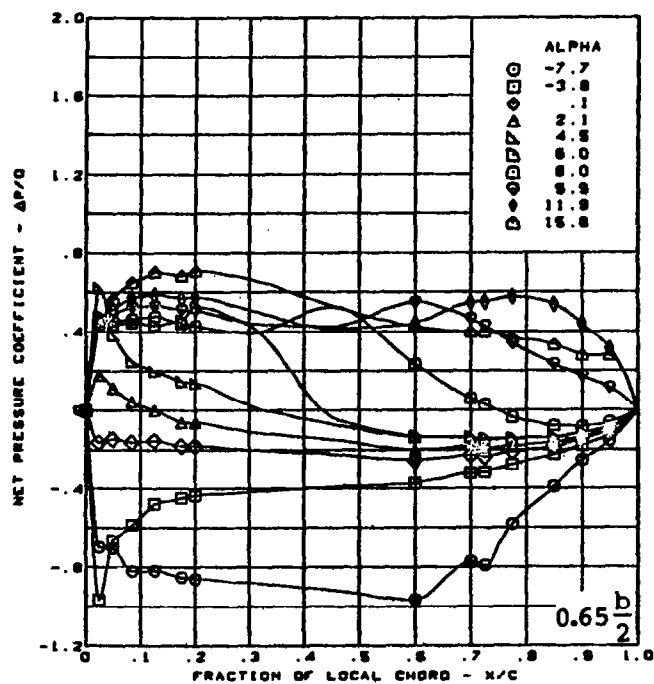
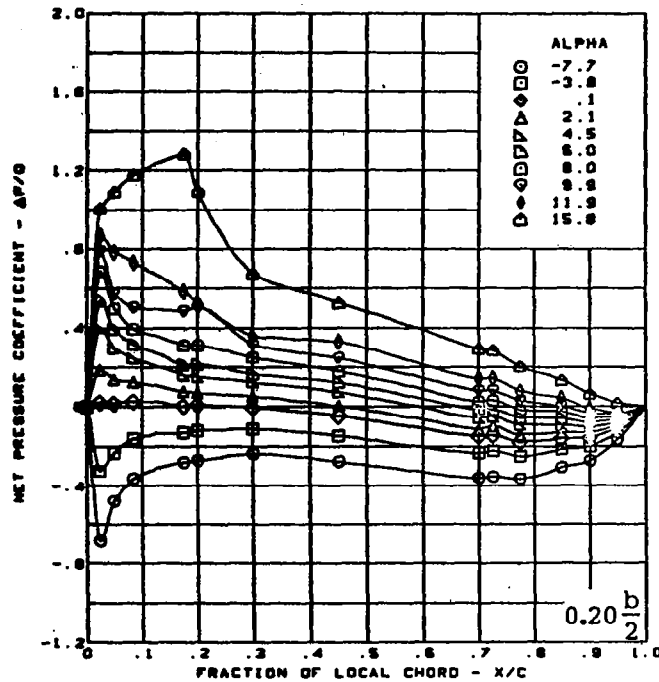
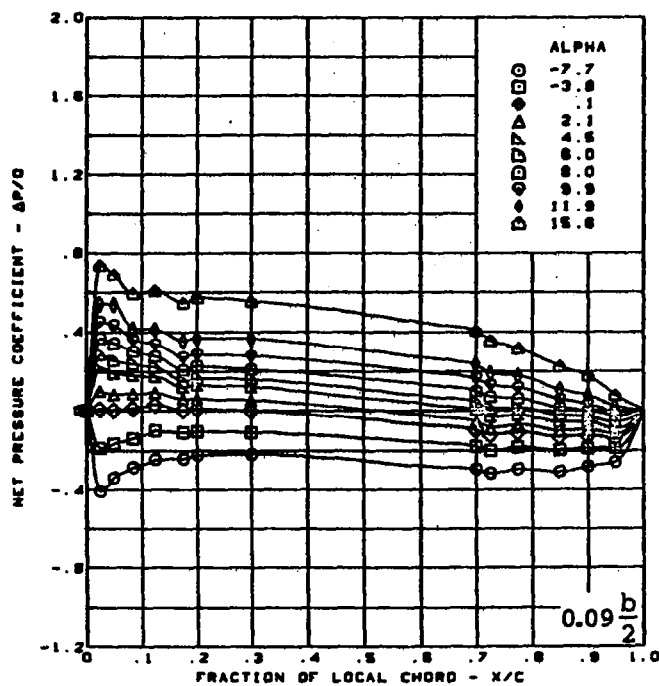
Figure 18. - (Continued)



$M = 0.85$  (run 40)  
 Cambered-twisted wing, rounded L.E.  
 Fin off  
 L.E. deflection, full span =  $0.0^\circ$   
 T.E. deflection, full span =  $0.0^\circ$

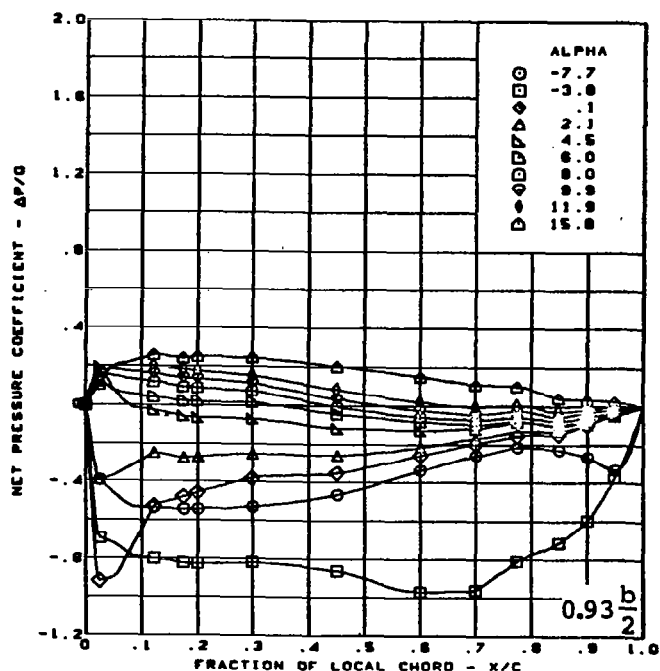
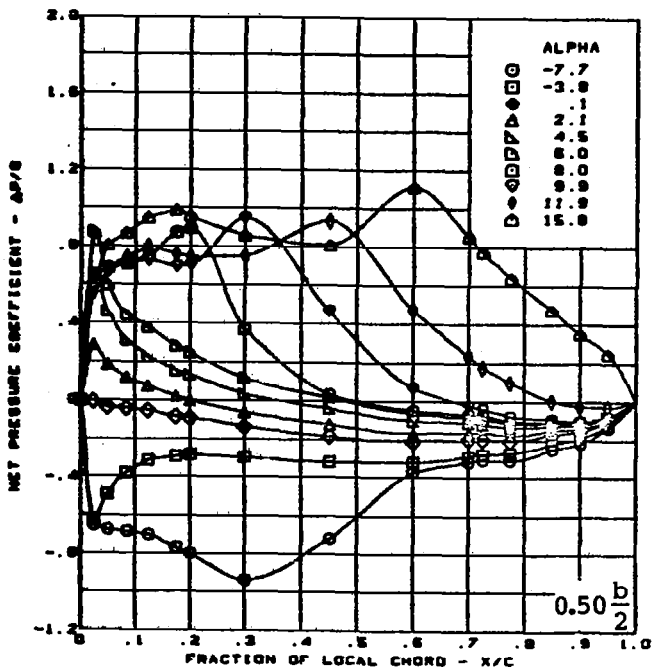
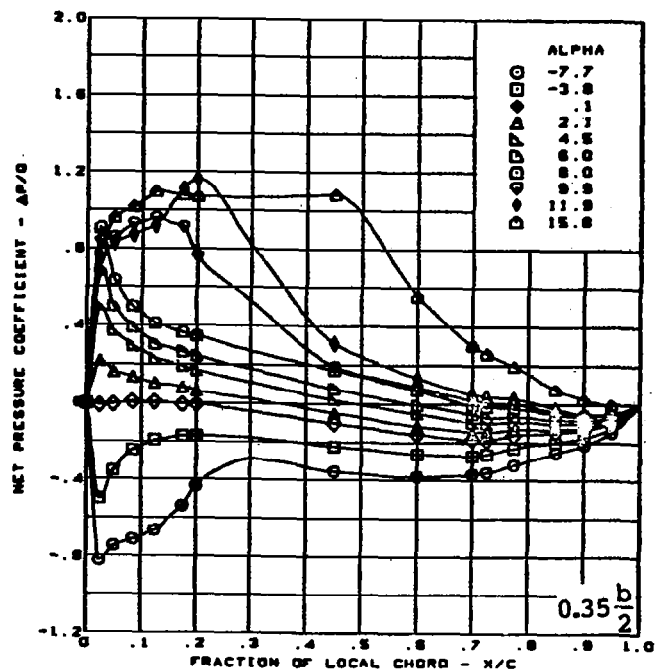
(d) (Concluded)

Figure 18. -- (Continued)



(e) Net Chordwise Pressure Distributions

Figure 18. - (Continued)

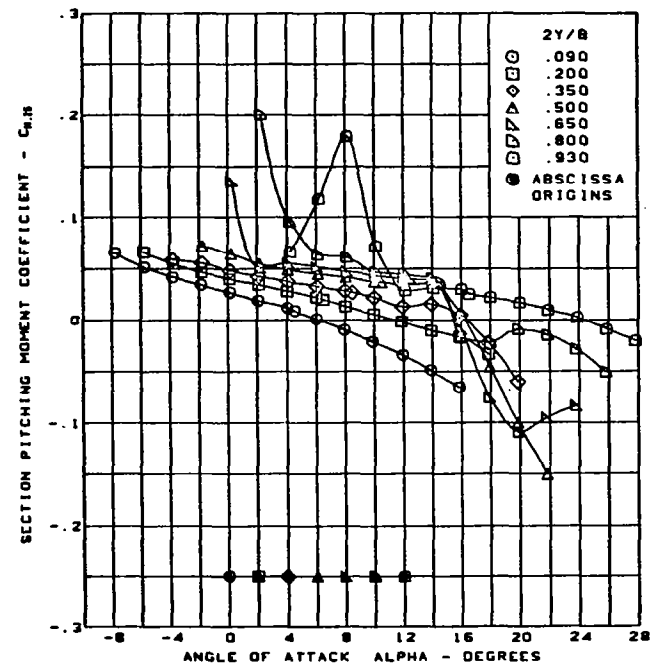
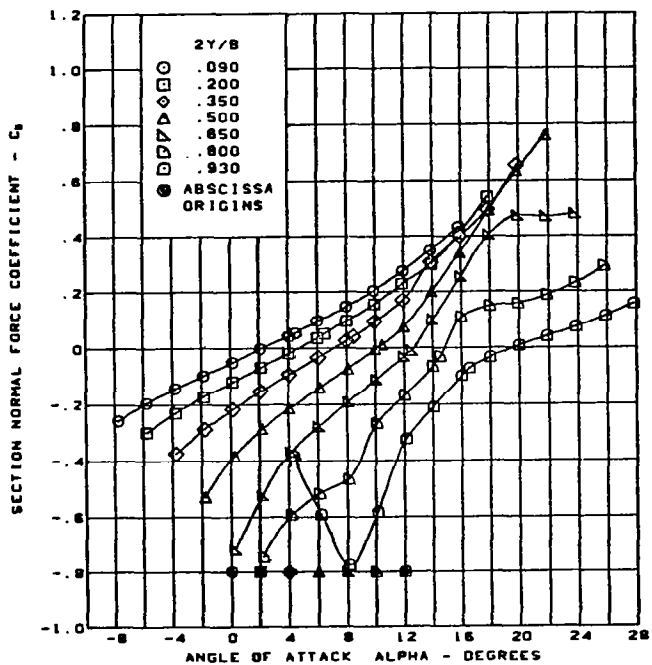
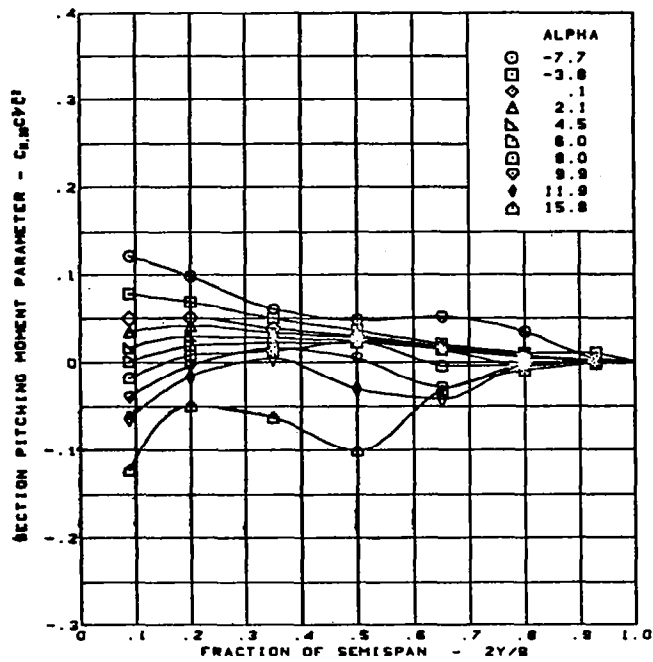
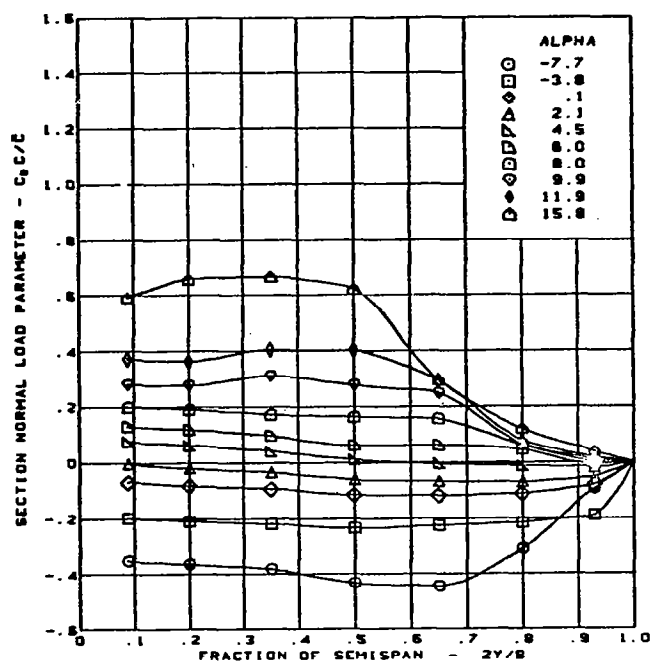


$M = 0.85$  (run 40)  
 Cambered-twisted wing, rounded L.E.  
 Fin off  
 L.E. deflection, full span =  $0.0^\circ$   
 T.E. deflection, full span =  $0.0^\circ$

(e) (Concluded)

Figure 18. - (Continued)





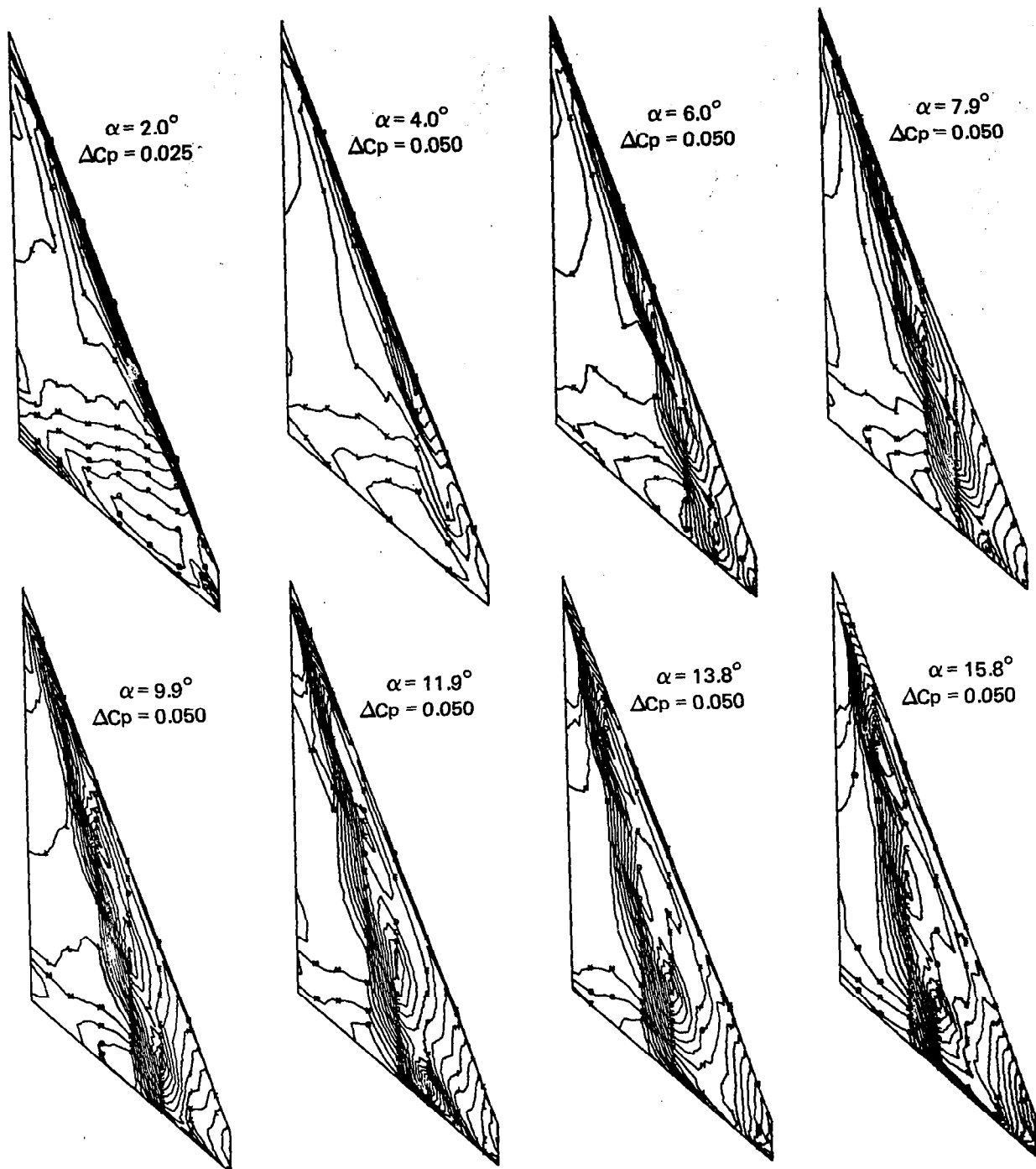
M = 0.85 (run 40)  
 Cambered-twisted wing, rounded L.E.  
 Fin off

L.E. deflection, full span =  $0.0^\circ$   
 T.E. deflection, full span =  $0.0^\circ$

(f) Spanload Distributions and Section Aerodynamic Coefficients

Figure 18. - (Concluded)

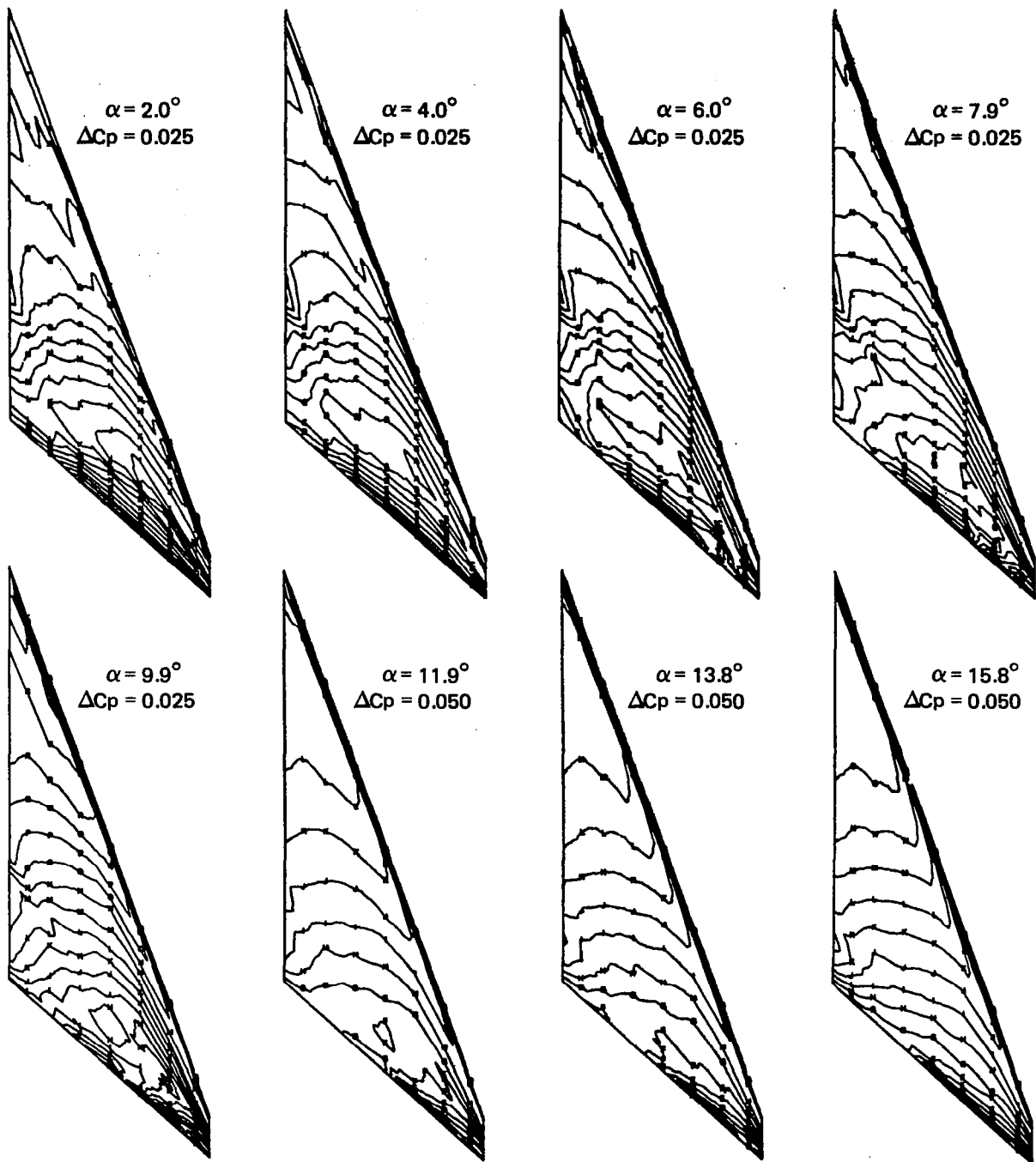




Note:  $\Delta C_p$  = increment between adjacent isobars

(a) Upper Surface Isobars

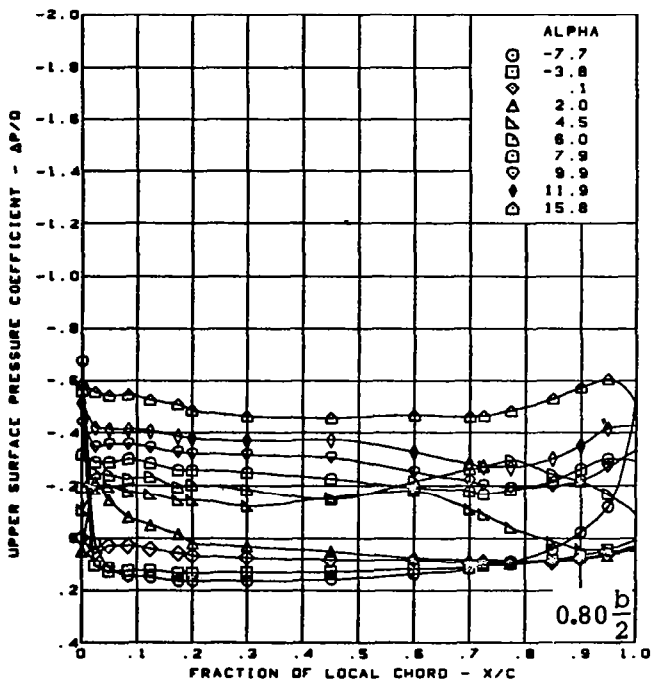
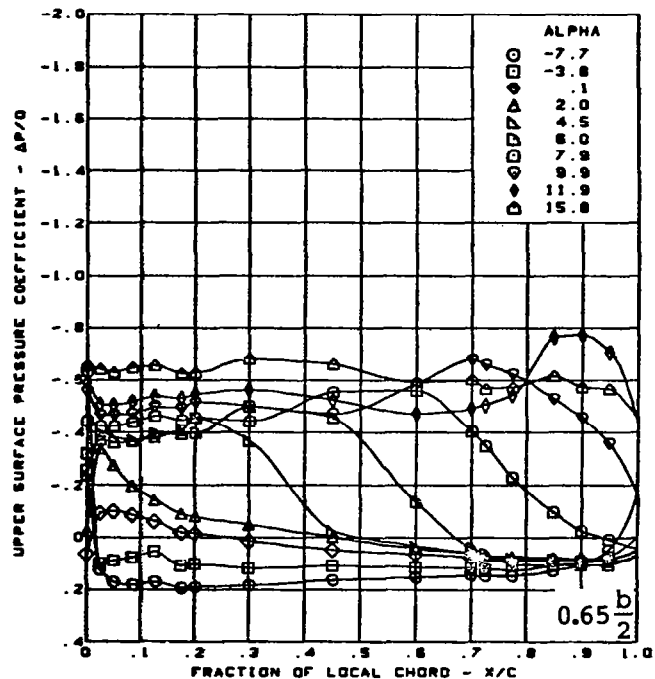
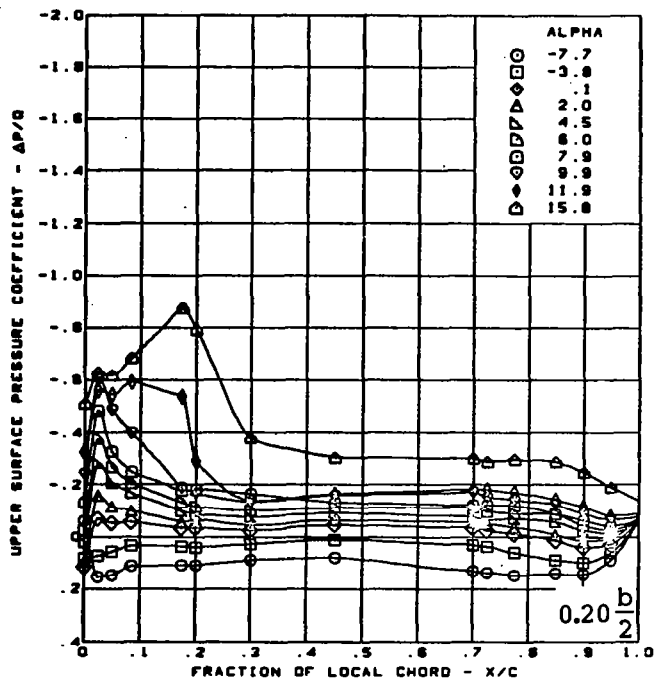
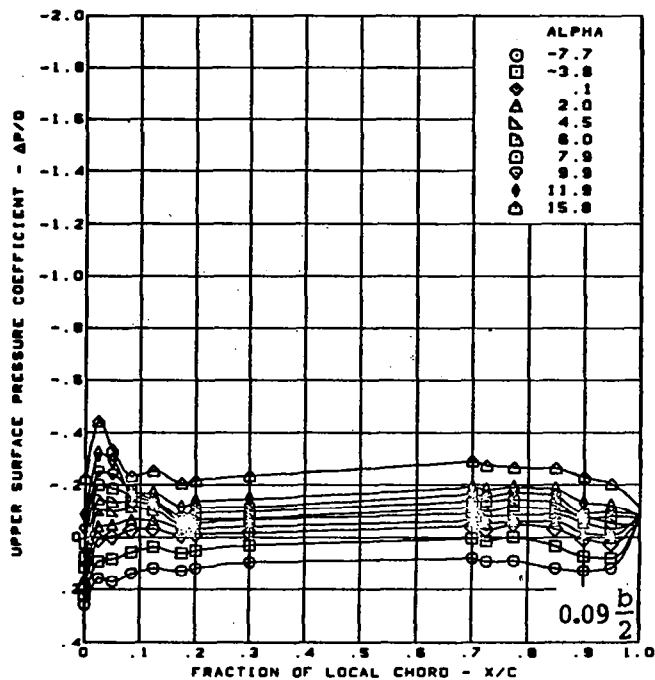
Figure 19. — Wing Experimental Data—Effect of Angle of Attack; Cambered-Twisted Wing;  
 Fin Off; T.E. Deflection, Full Span =  $0.0^\circ$ ;  $M = 1.05$



Note:  $\Delta C_p$  = increment between adjacent isobars

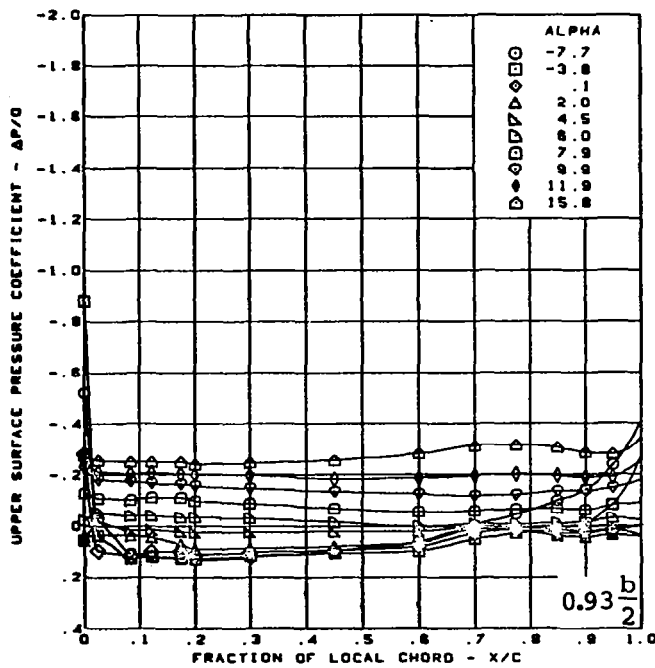
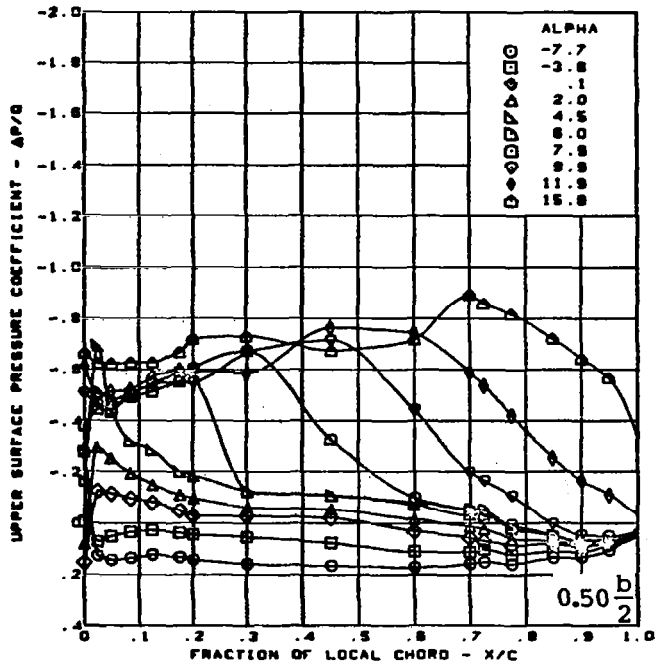
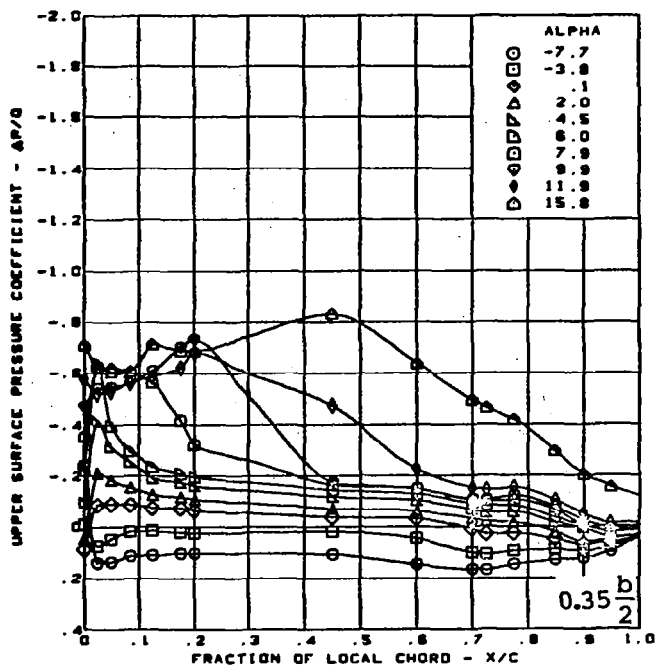
(b) Lower Surface Isobars

Figure 19. — (Continued)



(c) Upper Surface Chordwise Pressure Distributions

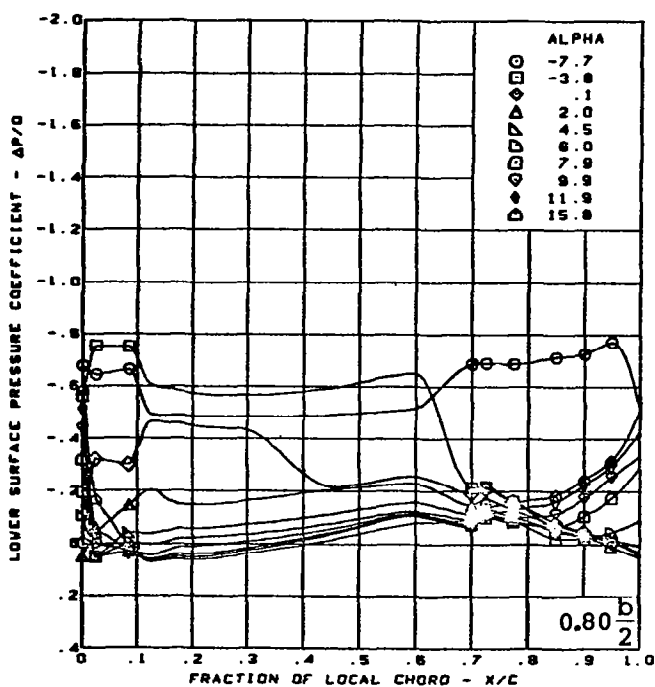
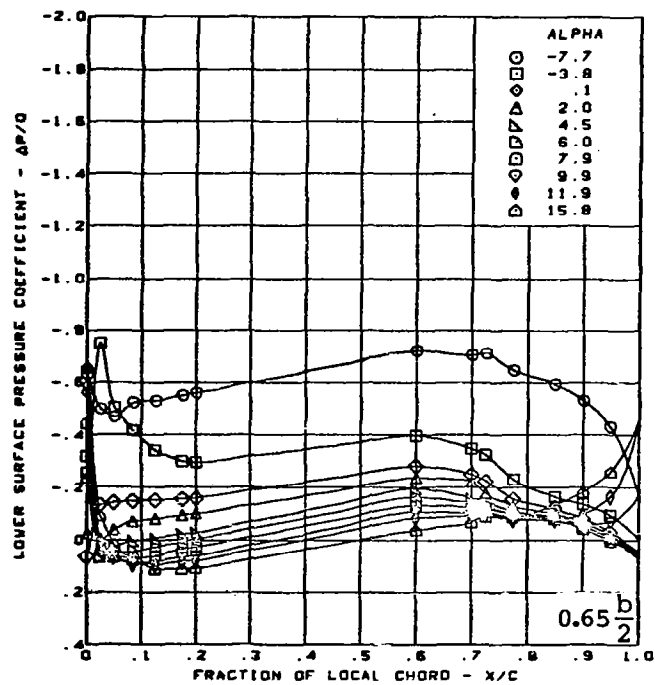
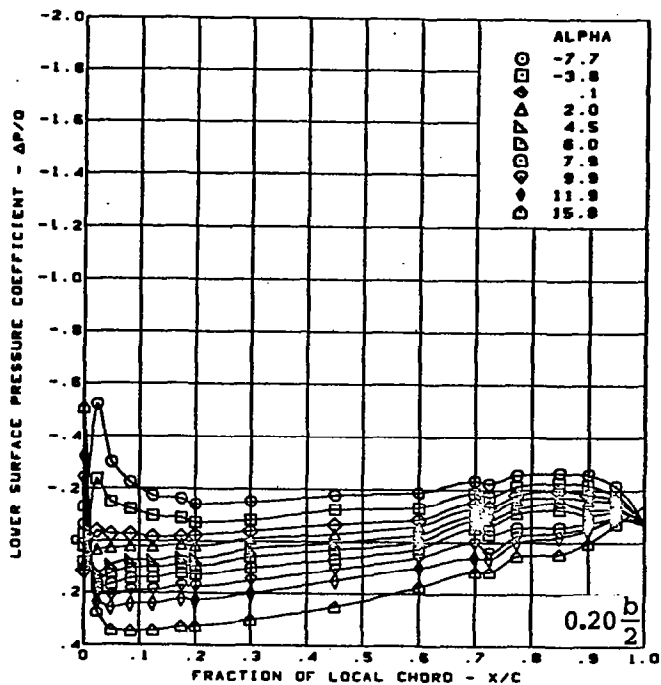
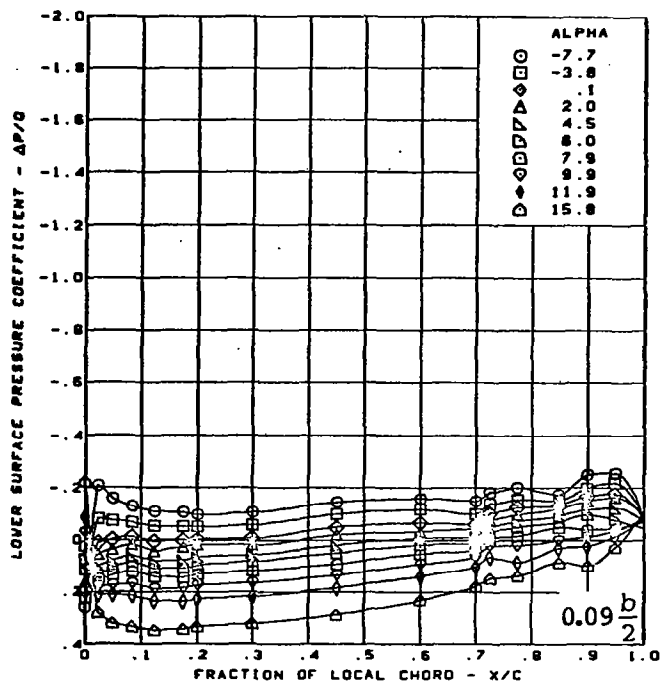
Figure 19. — (Continued)



$M = 1.05$  (run 37)  
 Cambered-twisted wing, rounded L.E.  
 Fin off  
 L.E. deflection, full span =  $0.0^\circ$   
 T.E. deflection, full span =  $0.0^\circ$

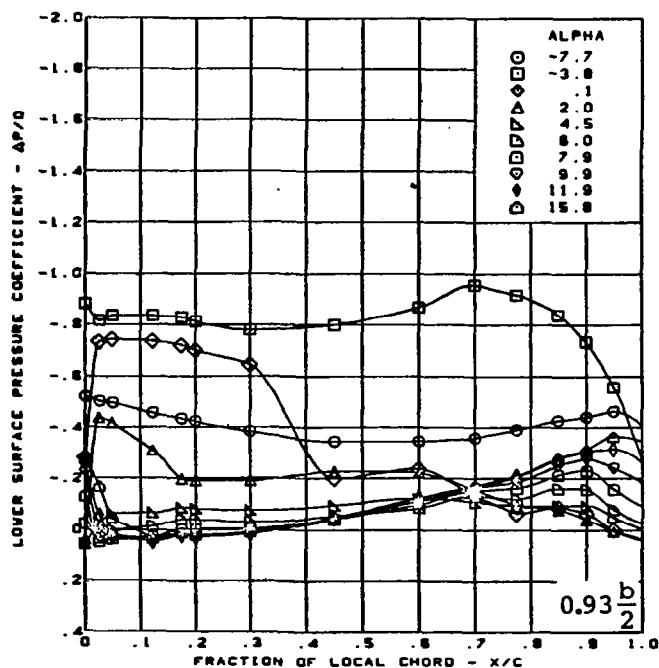
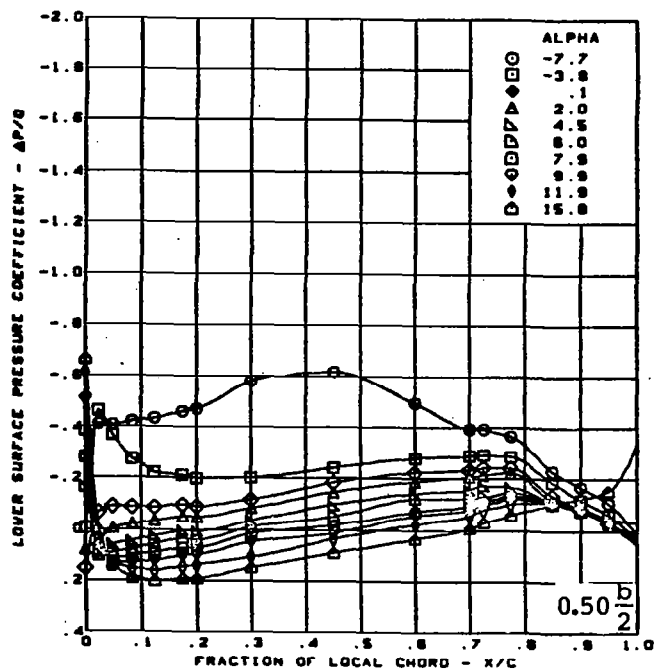
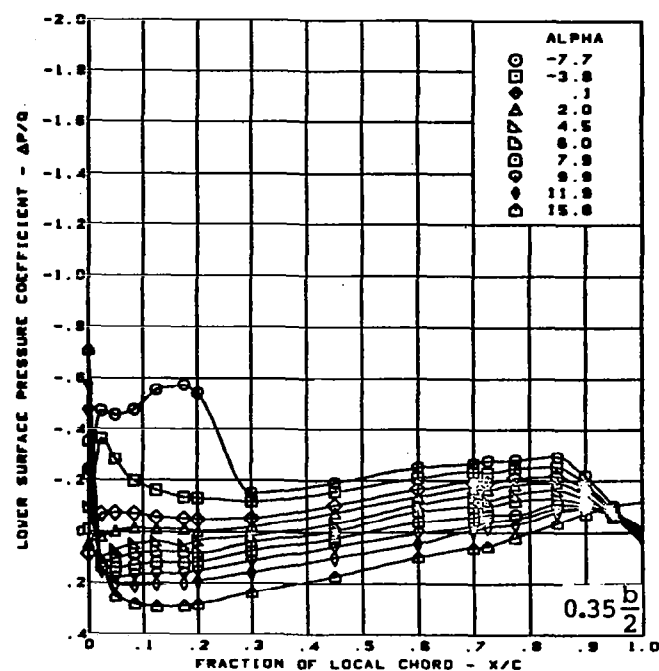
(c) (Concluded)

Figure 19. — (Continued)



(d) Lower Surface Chordwise Pressure Distributions

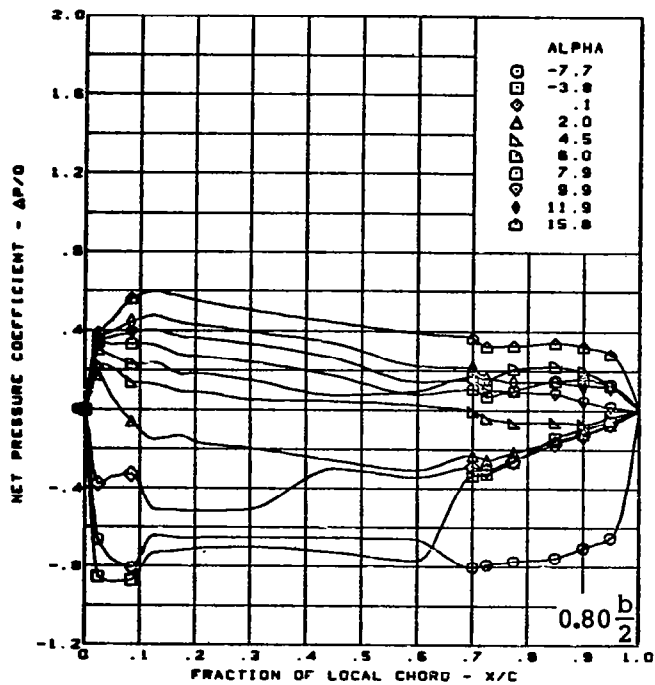
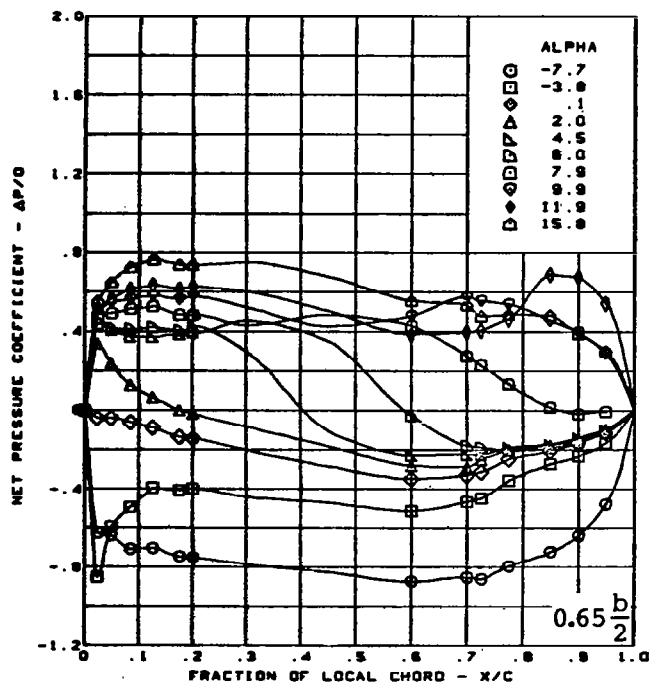
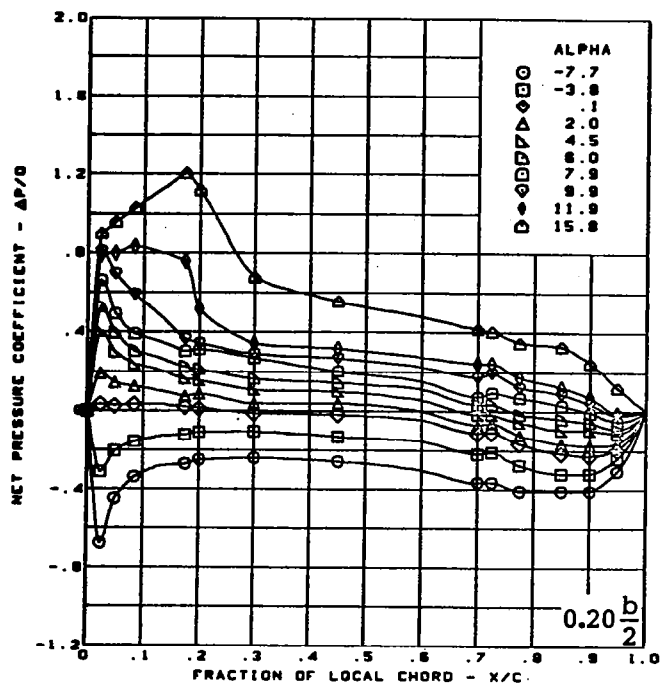
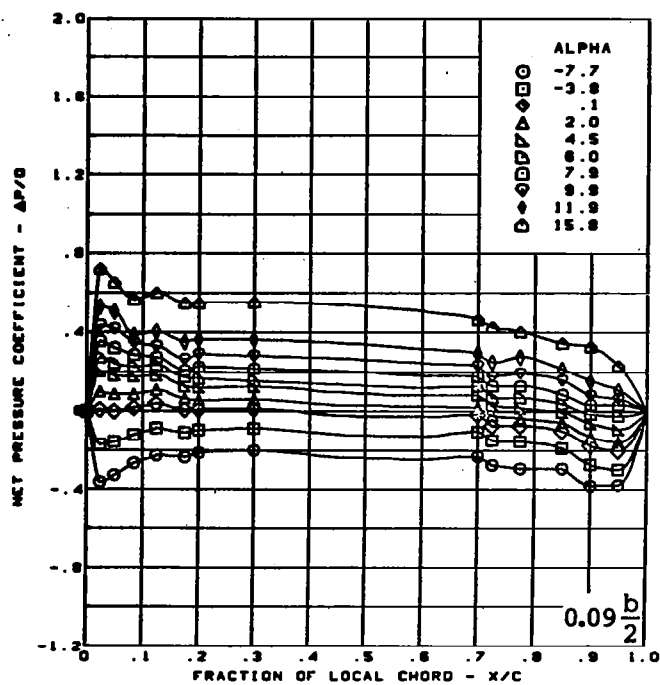
Figure 19. — (Continued)



$M = 1.05$  (run 37)  
 Cambered-twisted wing, rounded L.E.  
 Fin off  
 L.E. deflection, full span =  $0.0^\circ$   
 T.E. deflection, full span =  $0.0^\circ$

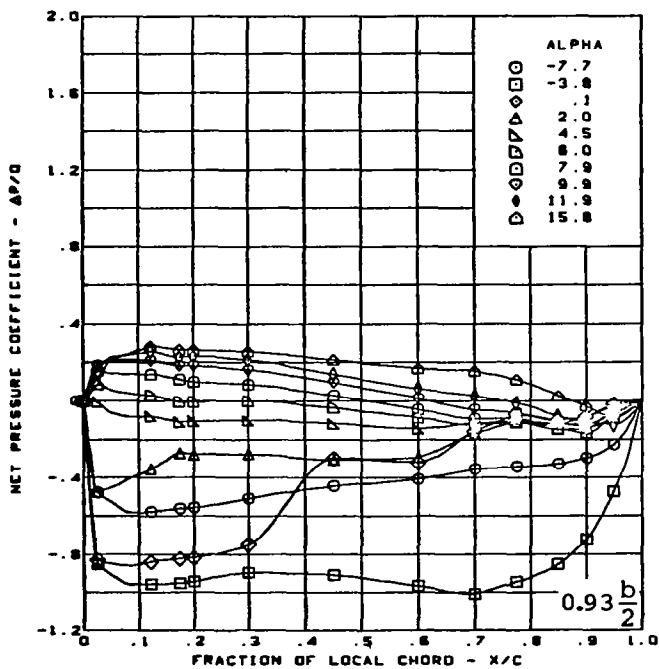
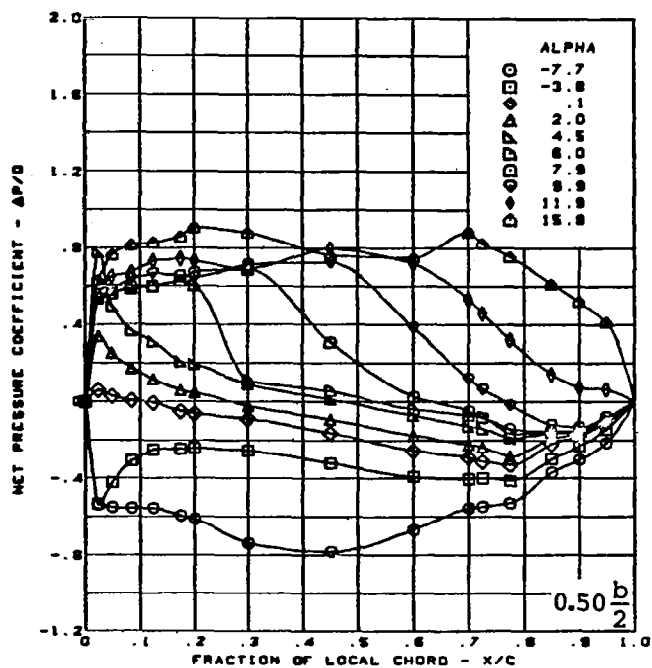
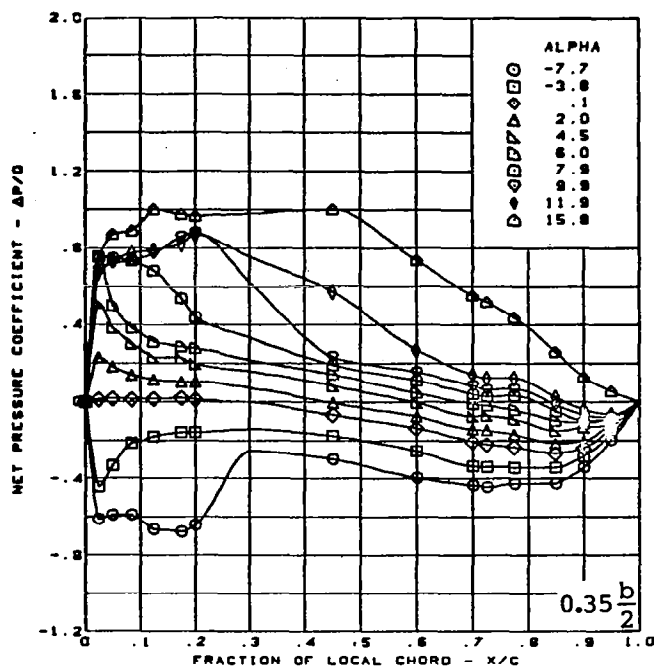
(d) (Concluded)

Figure 19. — (Continued)



(e) Net Chordwise Pressure Distributions

Figure 19. - (Continued)



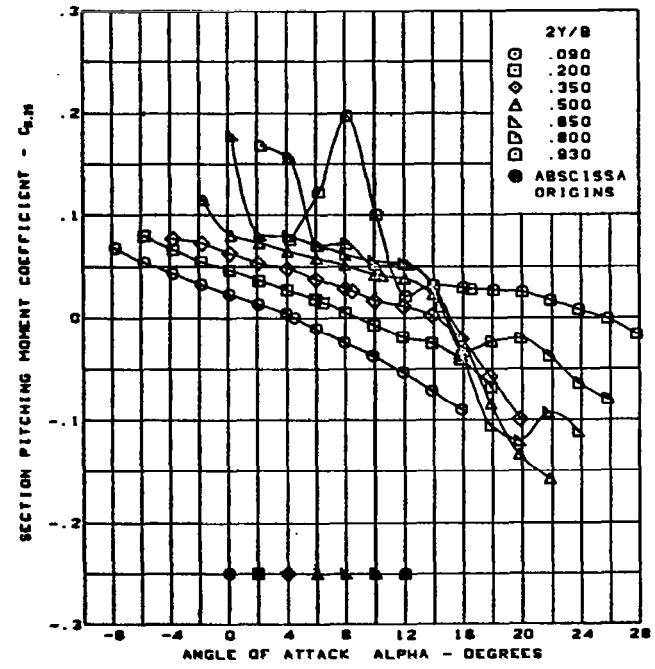
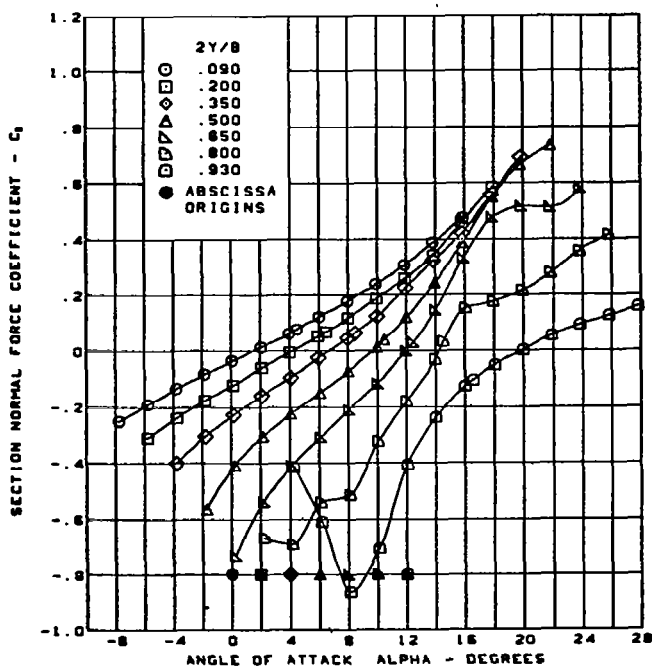
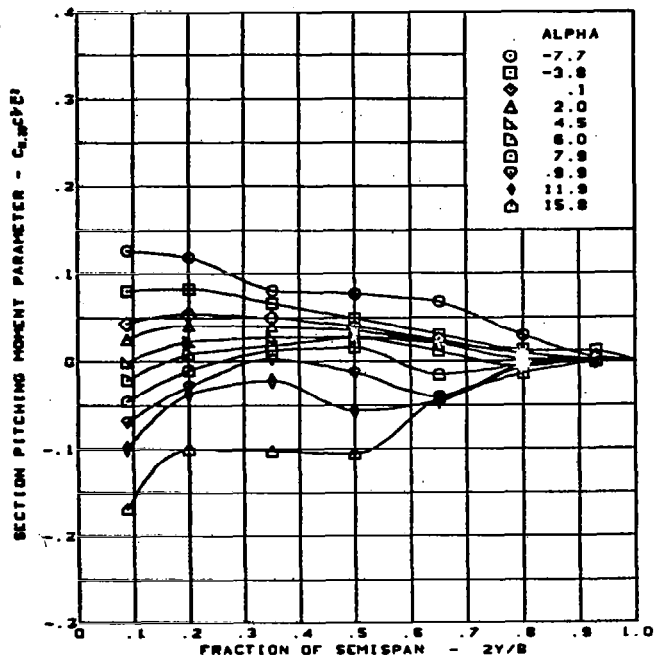
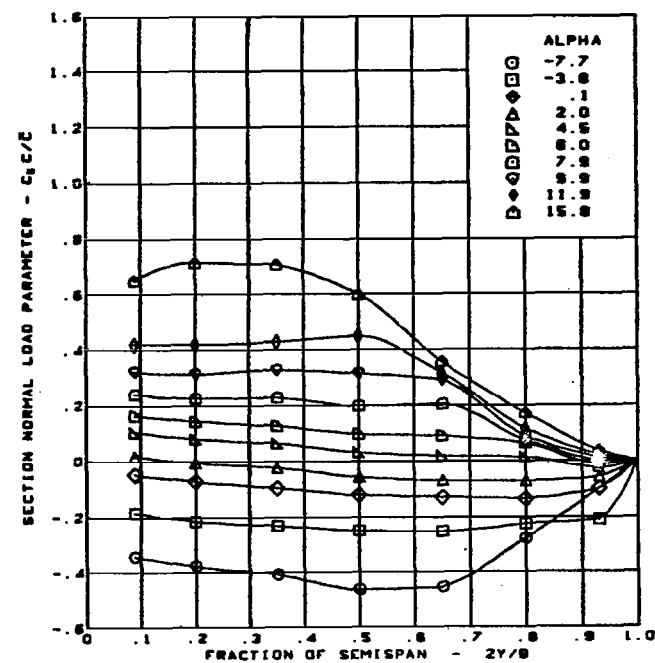
$M = 1.05$  (run 37)  
 Cambered-twisted wing, rounded L.E.  
 Fin off  
 L.E. deflection, full span =  $0.0^\circ$   
 T.E. deflection, full span =  $0.0^\circ$

(e) (Concluded)

Figure 19. - (Continued)





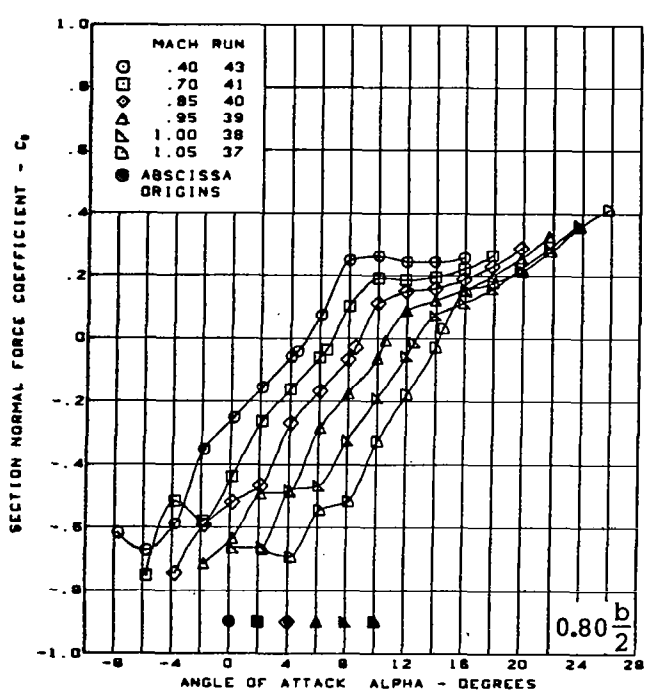
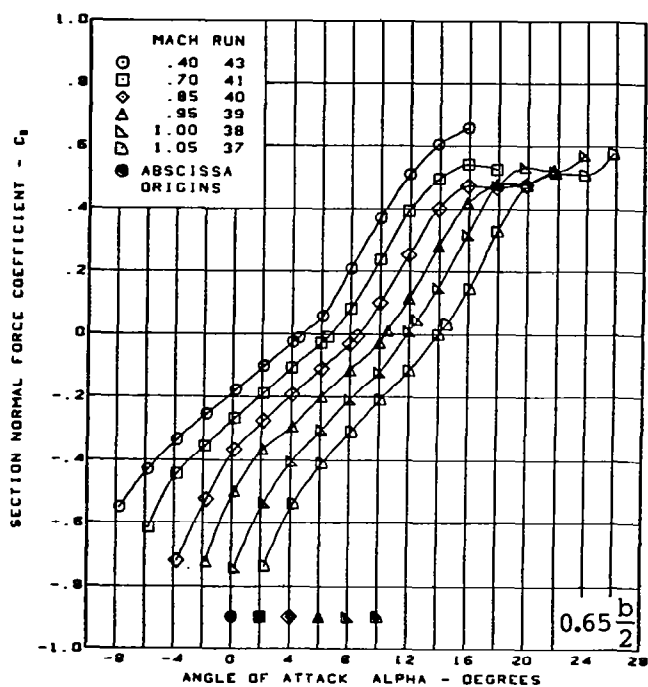
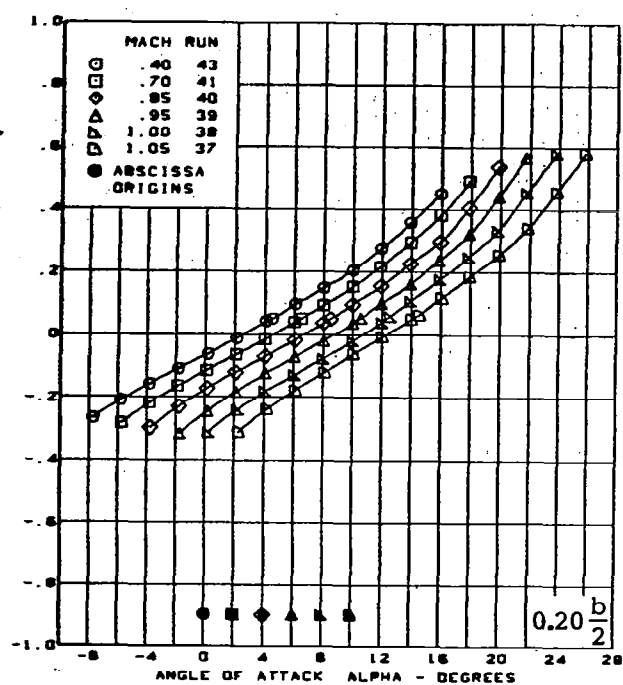
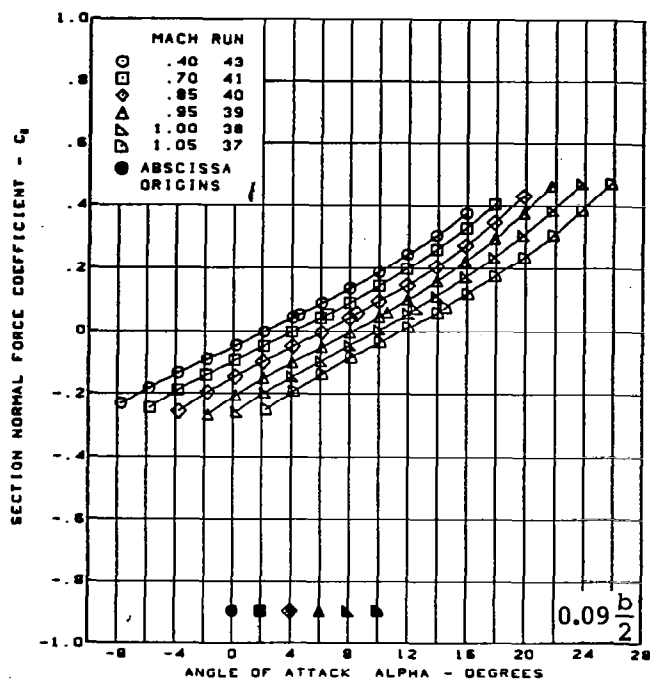


$M = 1.05$  (run 37)  
 Cambered-twisted wing, rounded L.E.  
 Fin off

L.E. deflection, full span =  $0.0^\circ$   
 T.E. deflection, full span =  $0.0^\circ$

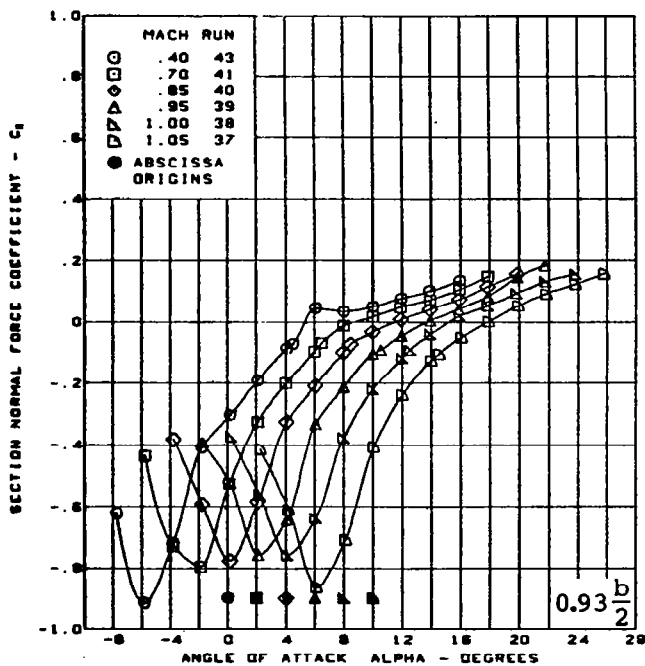
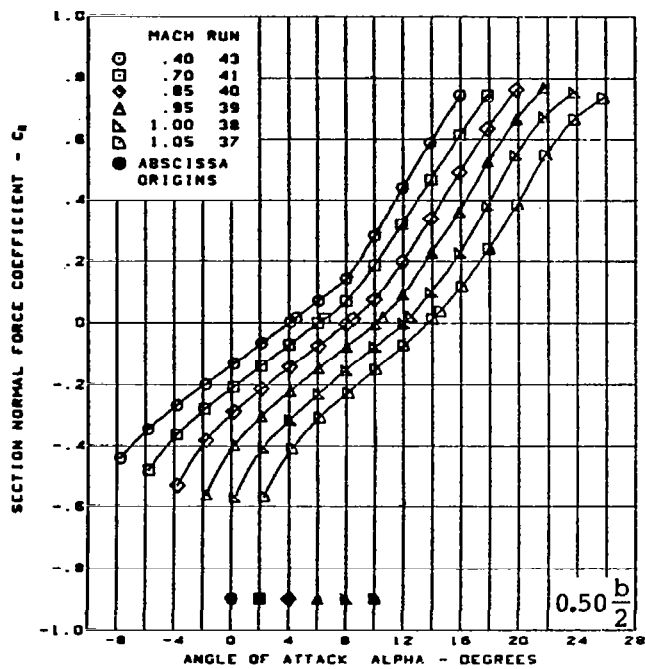
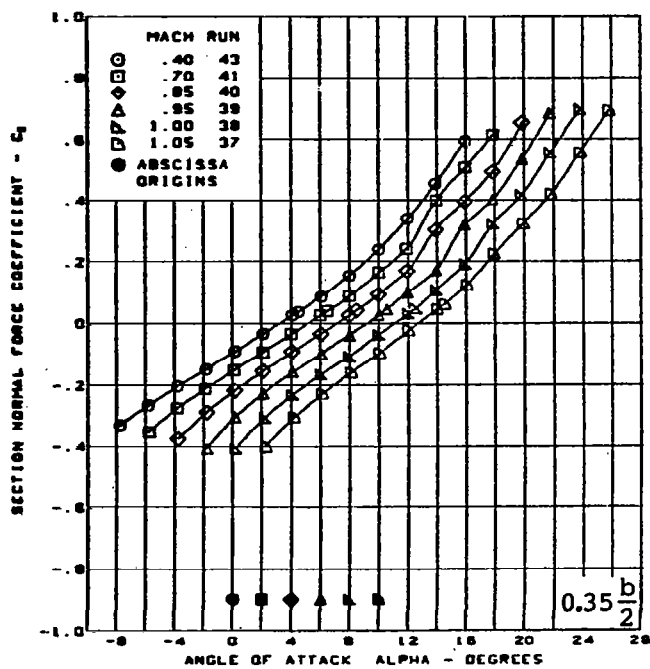
(f) Spanload Distributions and Section Aerodynamic Coefficients

Figure 19. - (Concluded)



(a) Section Aerodynamic Coefficients - Normal Force

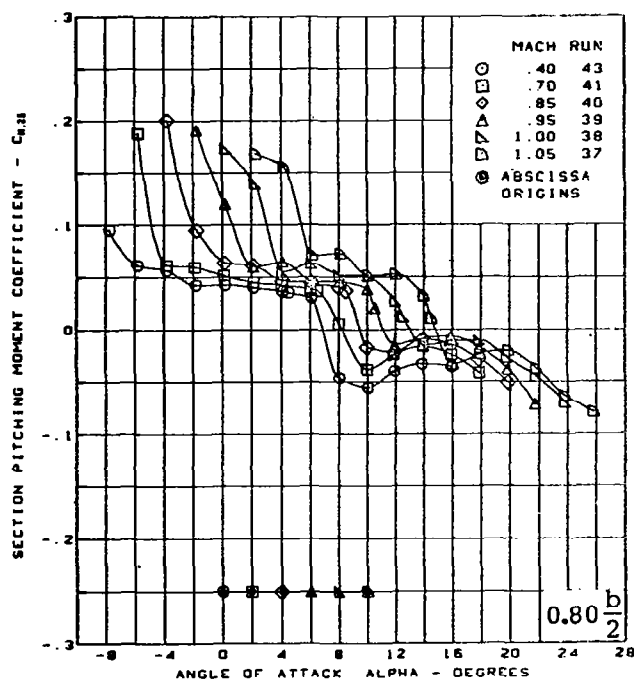
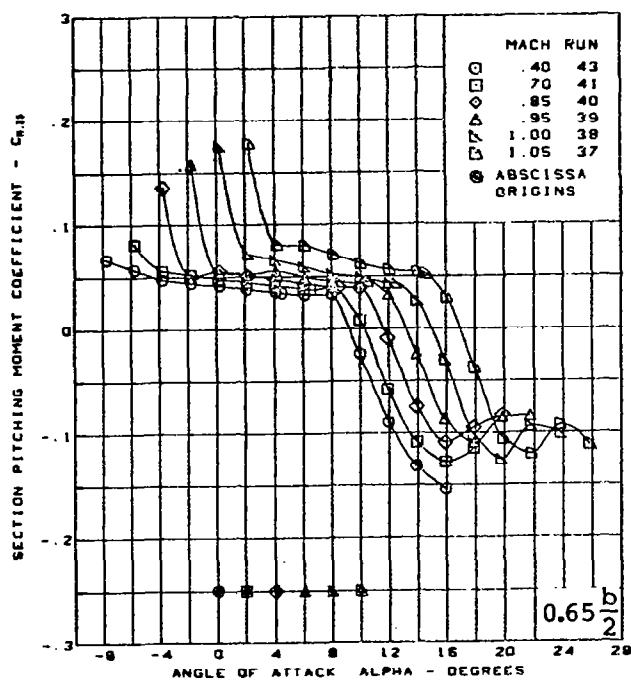
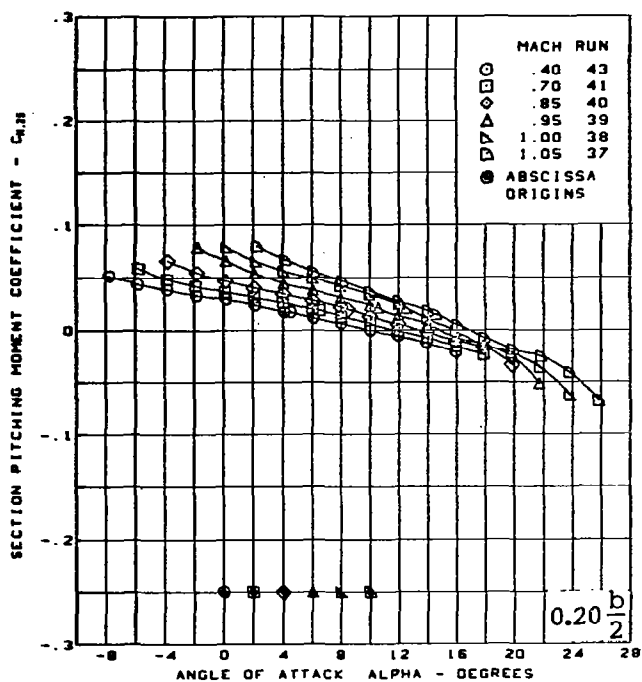
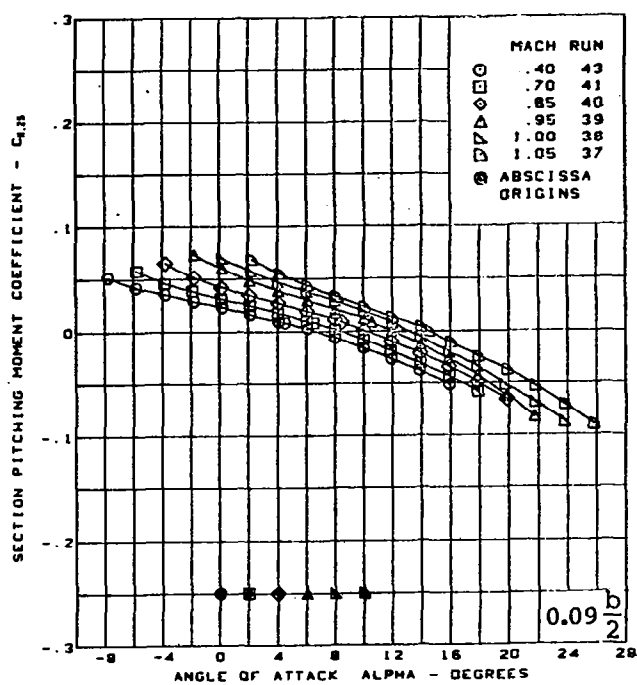
Figure 20. — Wing Experimental Data—Effect of Angle of Attack and Mach Number;  
Cambered-Twisted Wing; Fin Off; T.E. Deflection, Full Span =  $0.0^\circ$



Cambered-twisted wing, rounded L.E.  
 Fin off  
 L.E. deflection, full span =  $0.0^\circ$   
 T.E. deflection, full span =  $0.0^\circ$

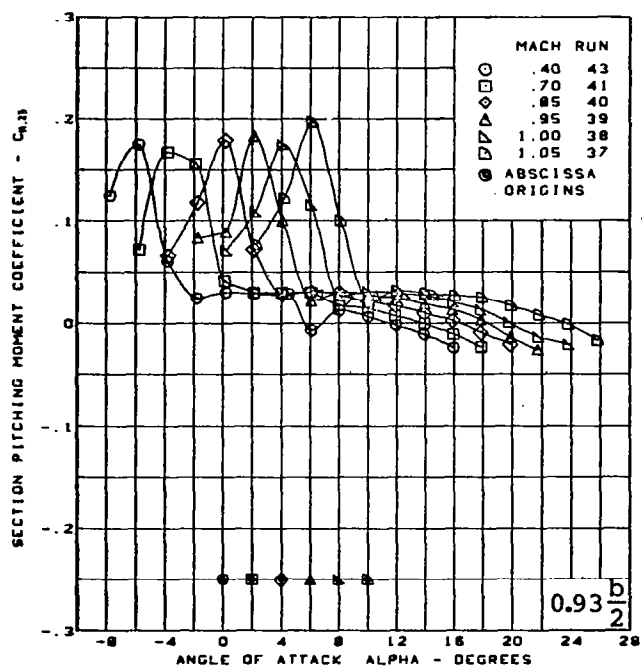
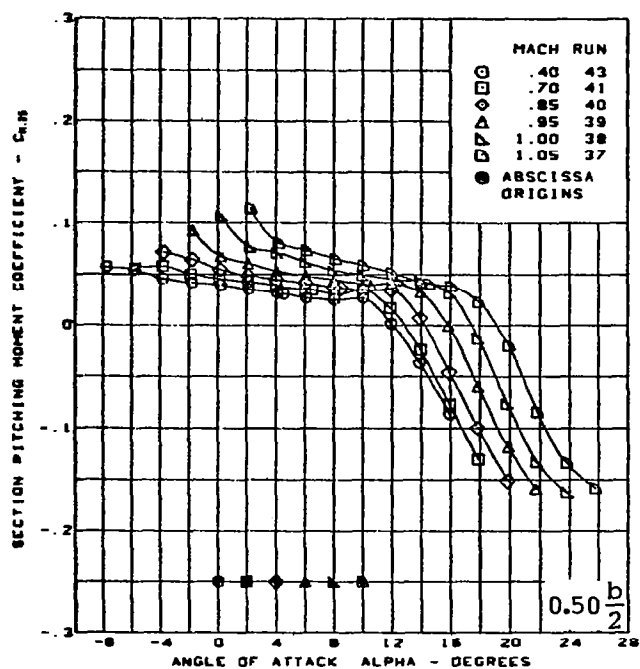
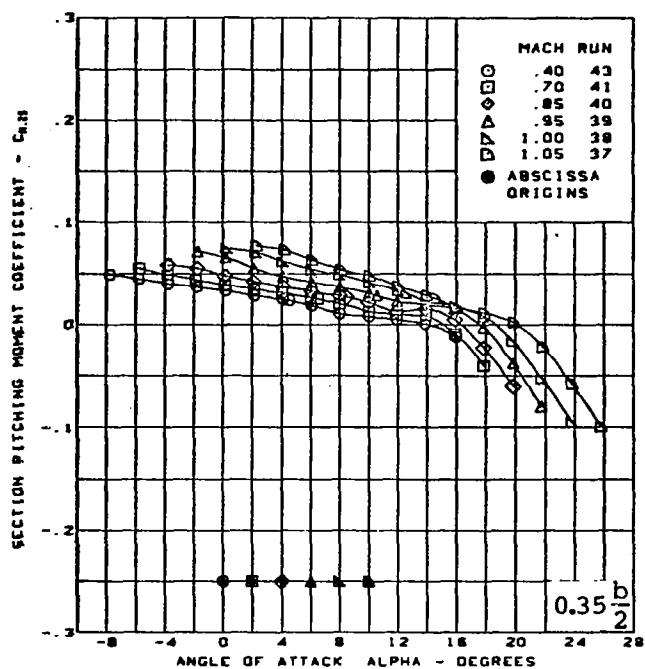
(a) (Concluded)

Figure 20. - (Continued)



(b) Section Aerodynamic Coefficients - Pitching Moment

Figure 20. - (Continued)

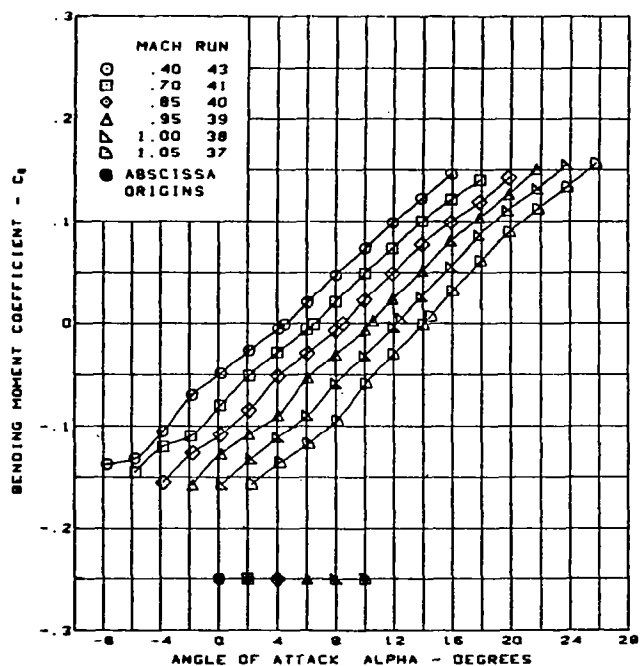
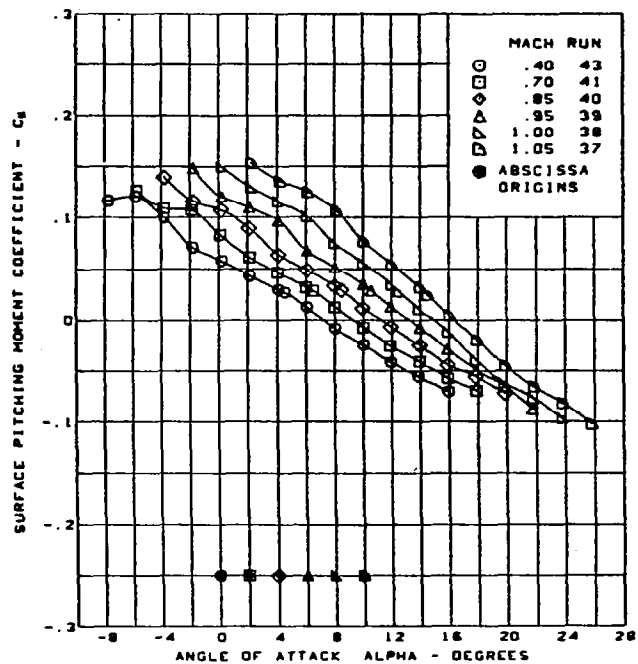
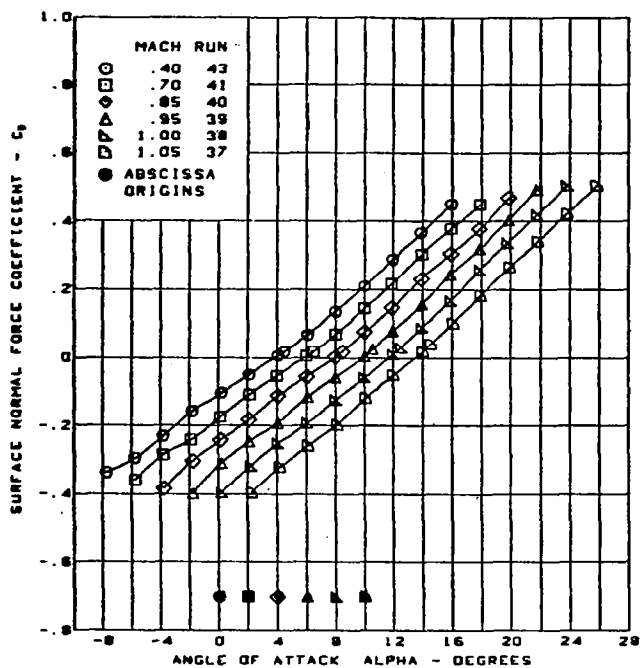


Cambered-twisted wing, rounded L.E.  
 Fin off  
 L.E. deflection, full span =  $0.0^\circ$   
 T.E. deflection, full span =  $0.0^\circ$

(b) (Concluded)

Figure 20. — (Continued)





Cambered-twisted wing, rounded L.E.  
 Fin off  
 L.E. deflection, full span =  $0.0^\circ$   
 T.E. deflection, full span =  $0.0^\circ$

(c) Wing Aerodynamic Coefficients

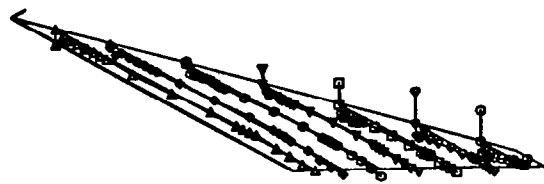
Figure 20. — (Concluded)



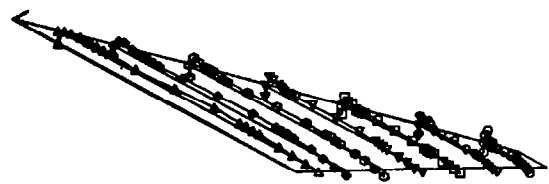


$\alpha = -3.9^\circ$

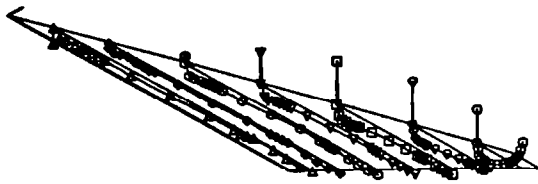
$\alpha = 0.1^\circ$



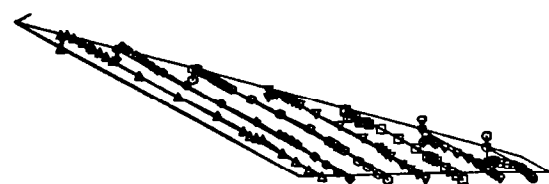
Flat wing



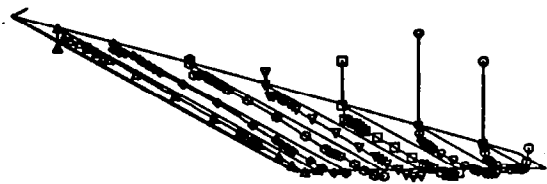
Flat wing



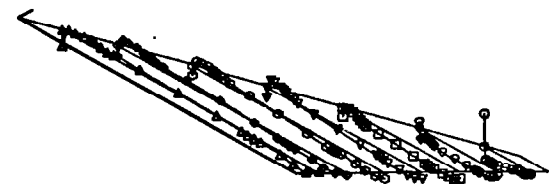
Twisted wing



Twisted wing



Cambered-twisted wing



Cambered-twisted wing

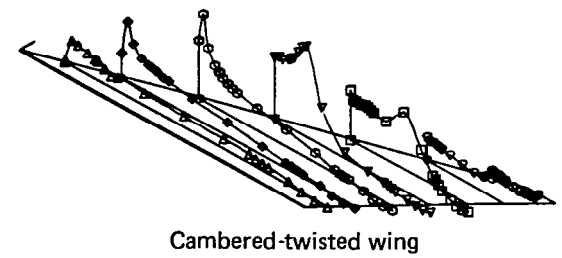
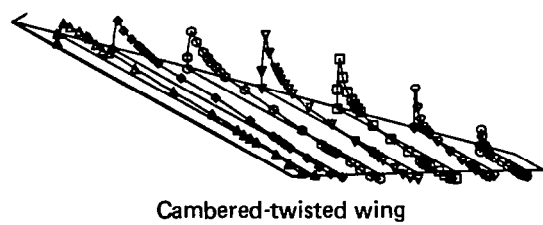
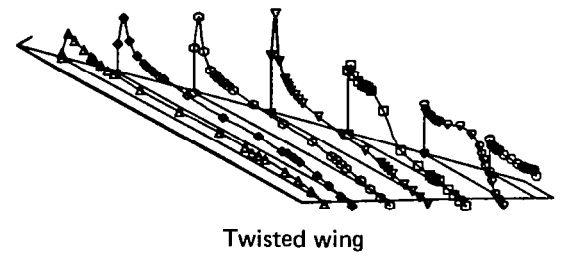
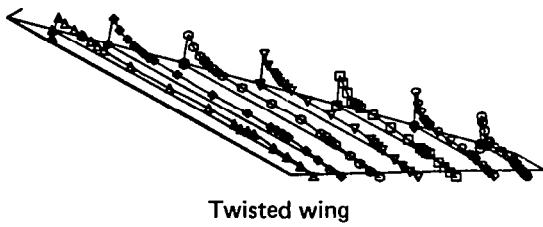
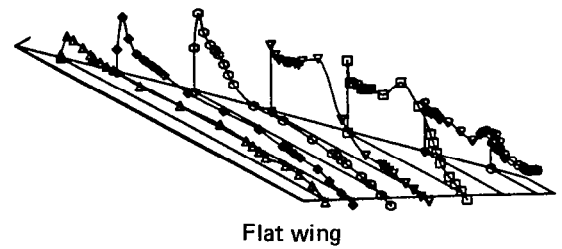
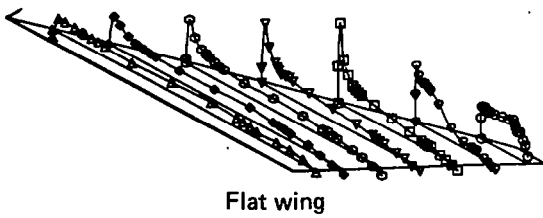
$M = 0.85$   
 Rounded L.E.  
 L.E. deflection, full span =  $0.0^\circ$   
 T.E. deflection, full span =  $0.0^\circ$

(a) Upper Surface Pressure Distribution

Figure 21. — Wing Experimental Data—Effect of Wing Shape; T.E. Deflection, Full Span =  $0.0^\circ$ ;  $M = 0.85$

$\alpha = 4.0^\circ$

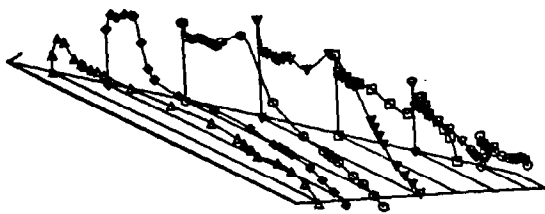
$\alpha = 8.0^\circ$



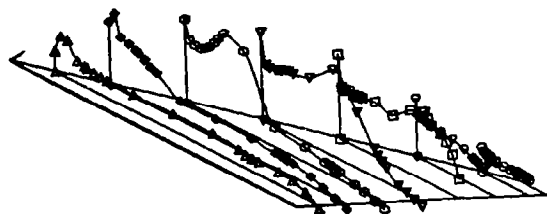
(a) (Continued)

Figure 21. — (Continued)

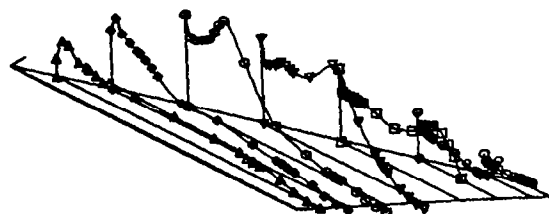
$\alpha = 11.9^\circ$



Flat wing

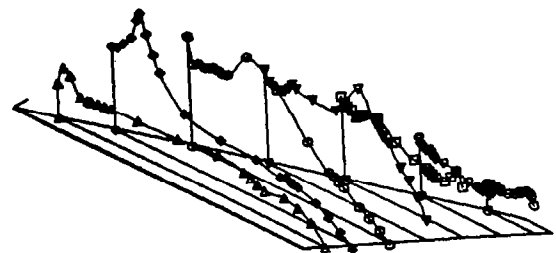


Twisted wing

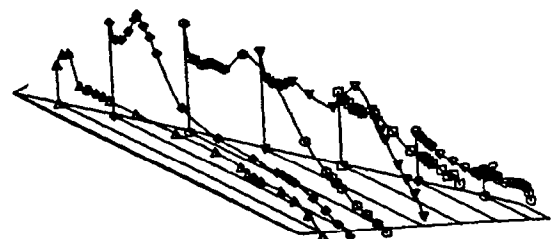


Cambered-twisted wing

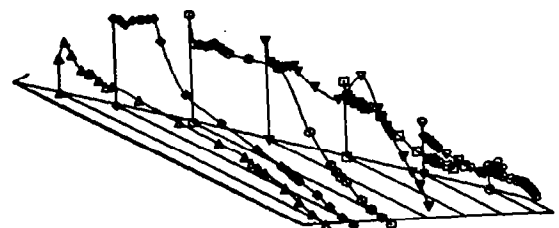
$\alpha = 15.8^\circ$



Flat wing



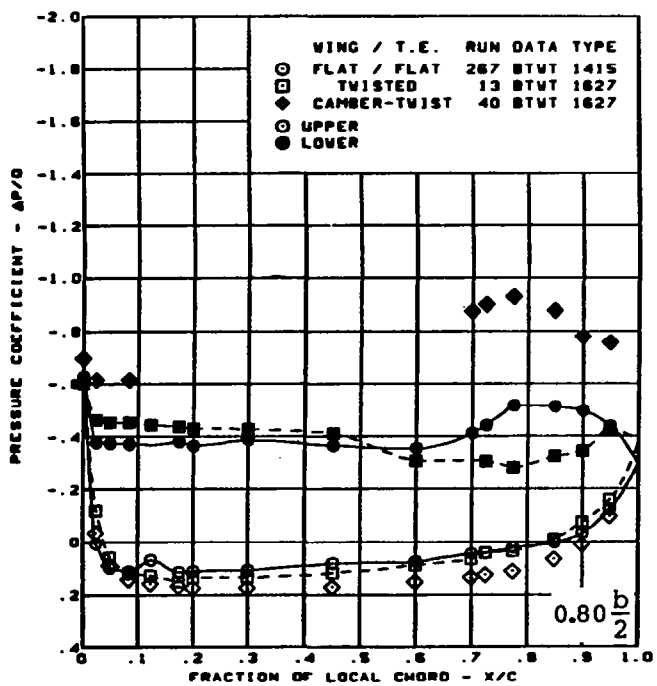
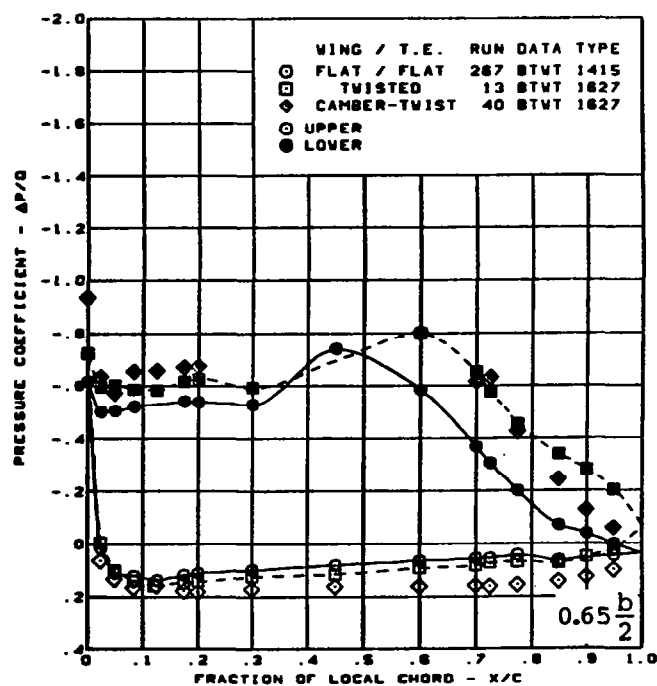
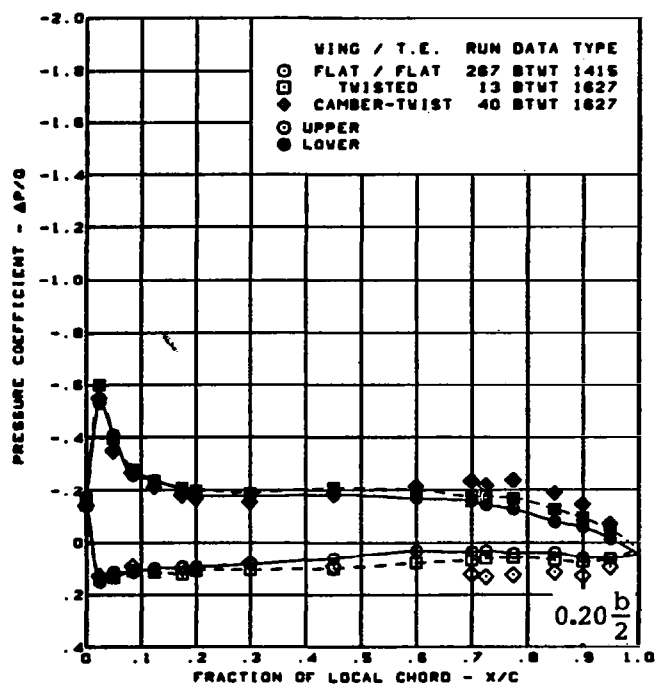
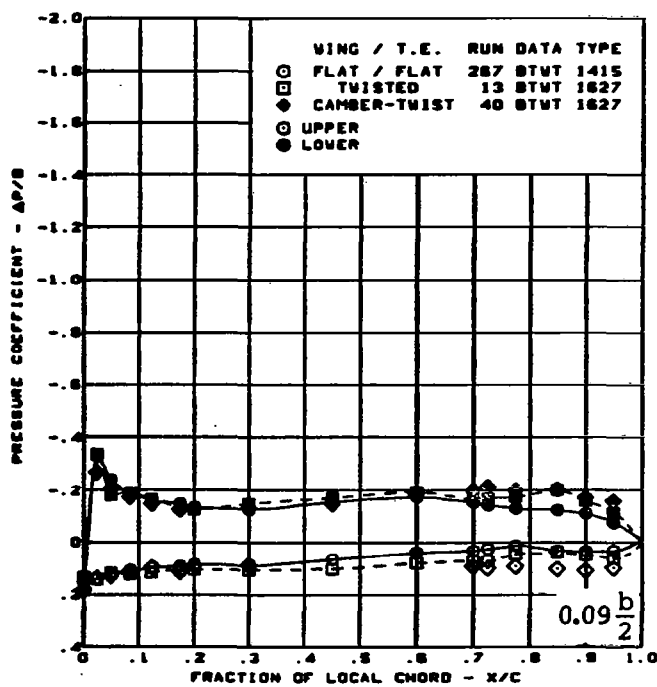
Twisted wing



Cambered-twisted wing

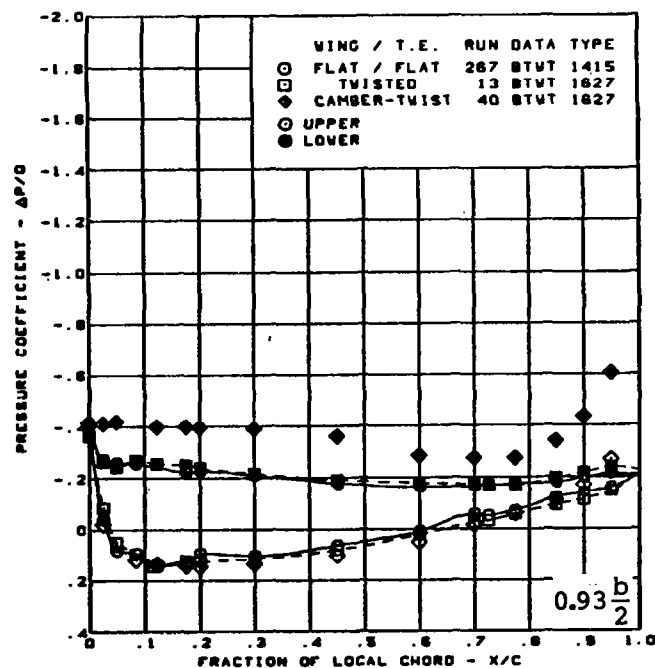
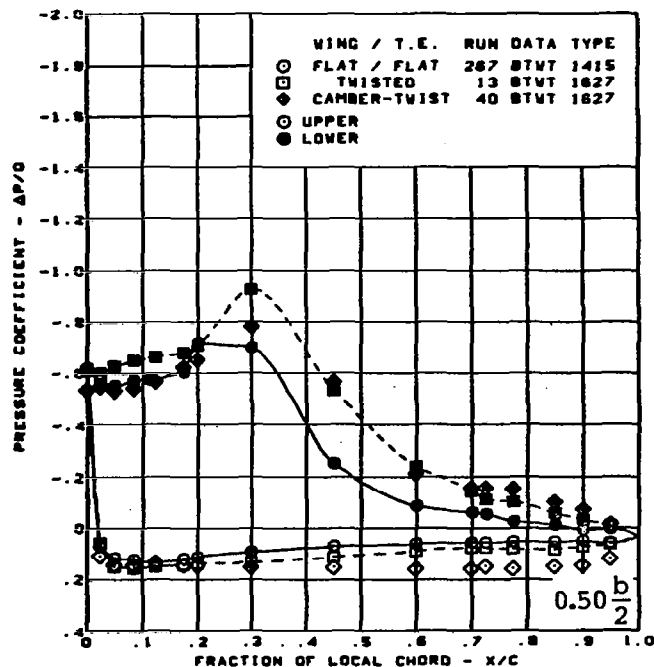
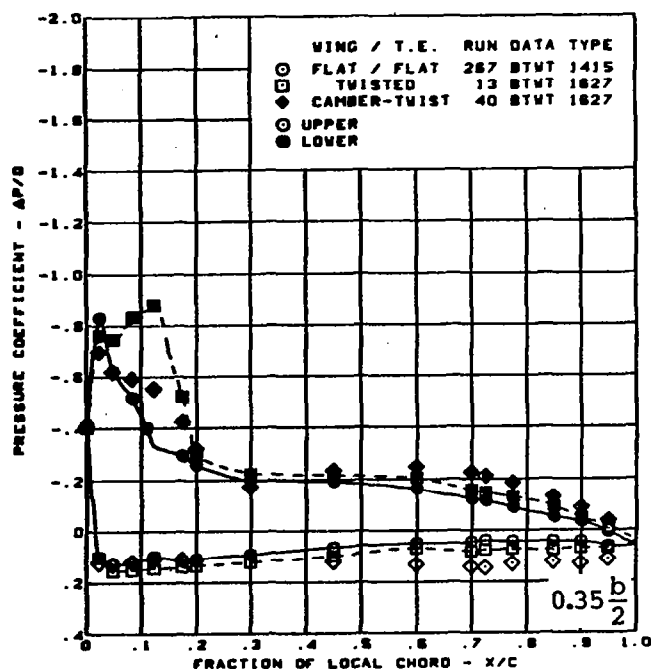
(a) (Concluded)

Figure 21. — (Continued)



(b) Surface Chordwise Pressure Distributions -  $\alpha = -8^\circ$

Figure 21. - (Continued)



$M = 0.85$

$\alpha = -8^\circ$

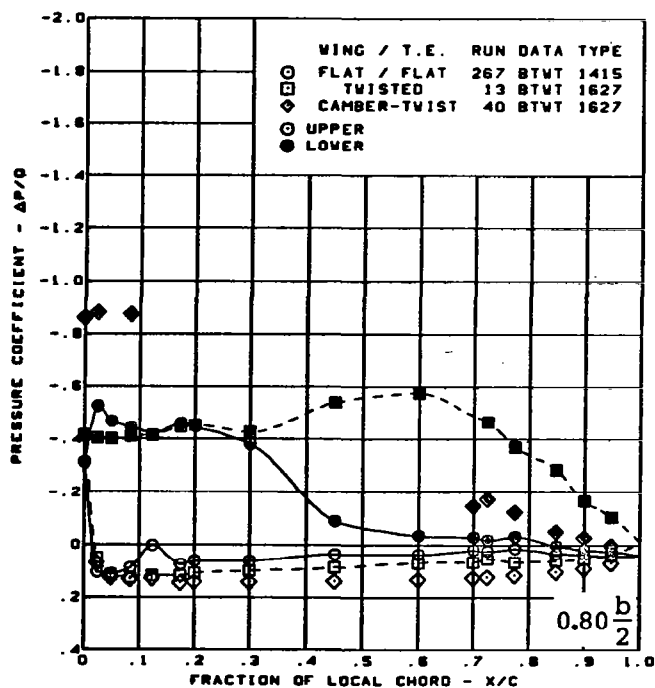
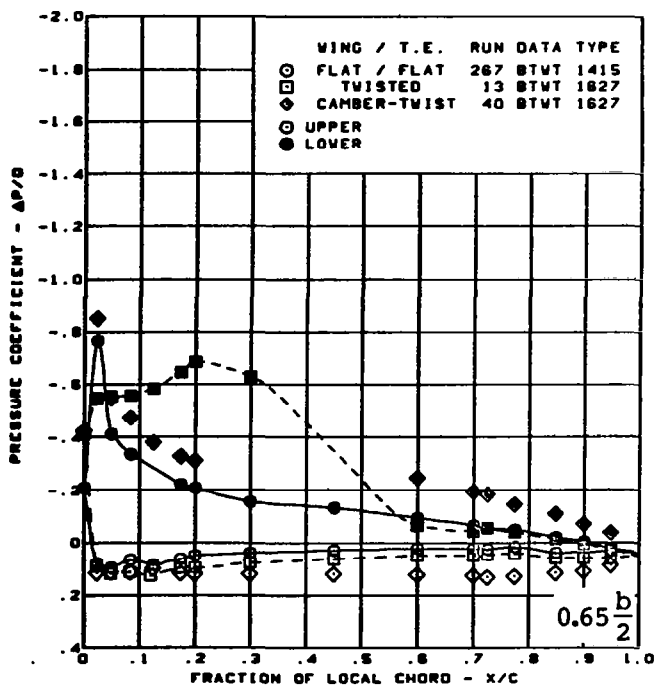
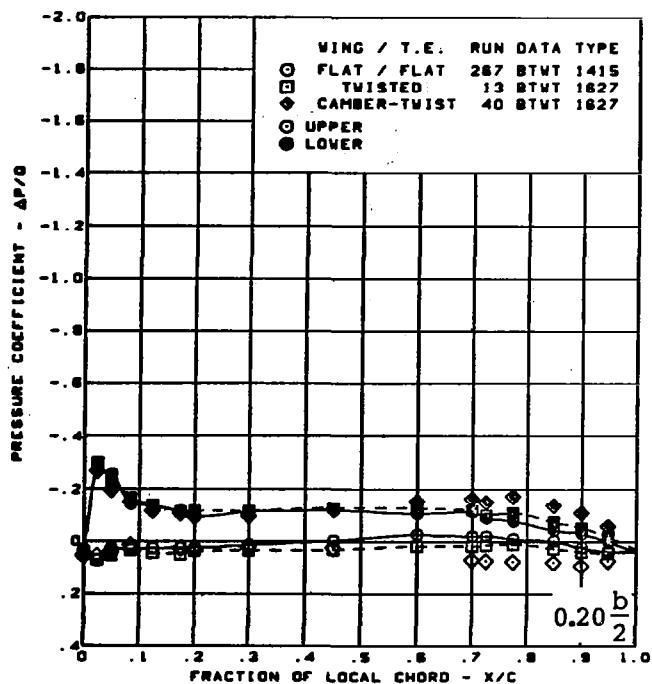
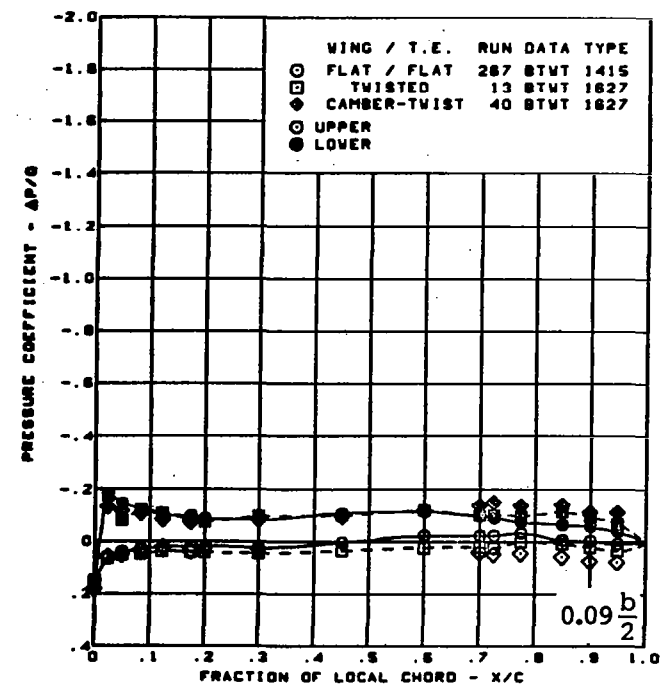
Rounded L.E.

L.E. deflection, full span =  $0.0^\circ$

T.E. deflection, full span =  $0.0^\circ$

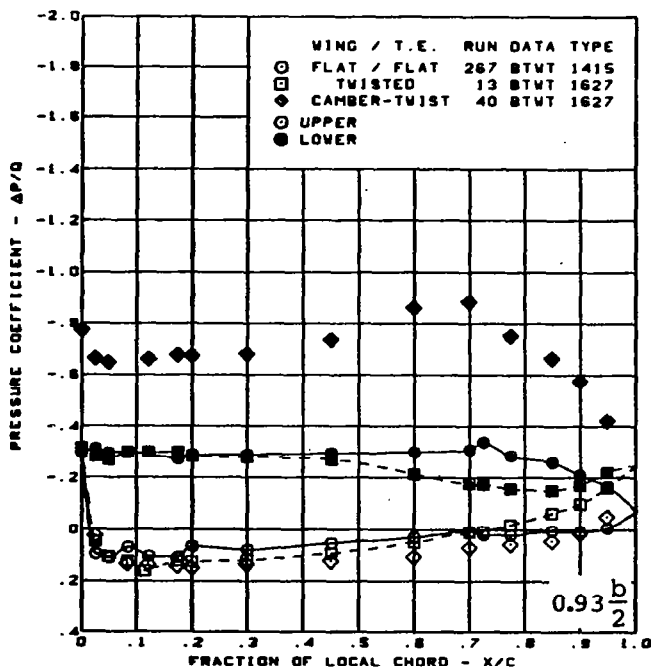
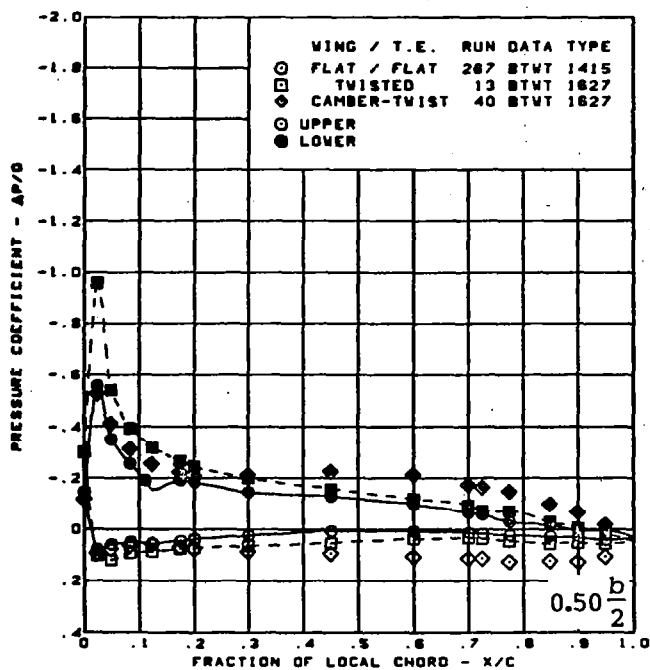
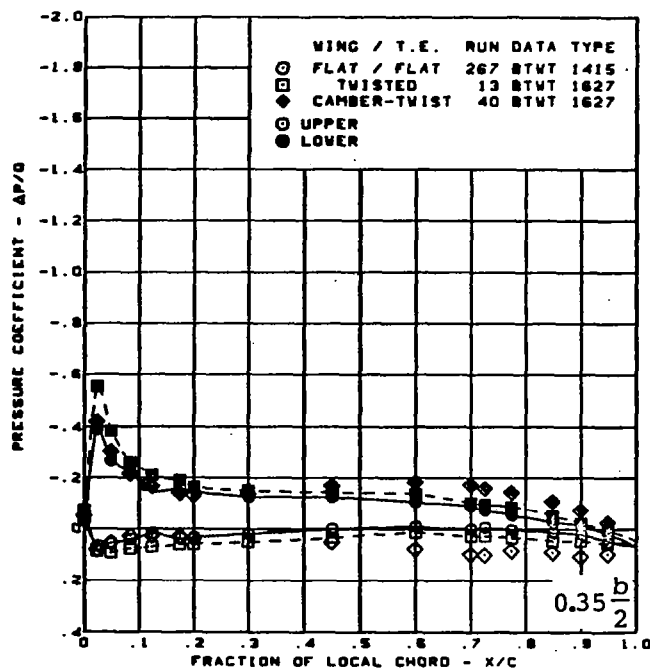
(b) (Concluded)

Figure 21. - (Continued)



(c) Surface Chordwise Pressure Distributions -  $\alpha = -4$

Figure 21. - (Continued)



$M = 0.85$

$\alpha = -4^\circ$

Rounded L.E.

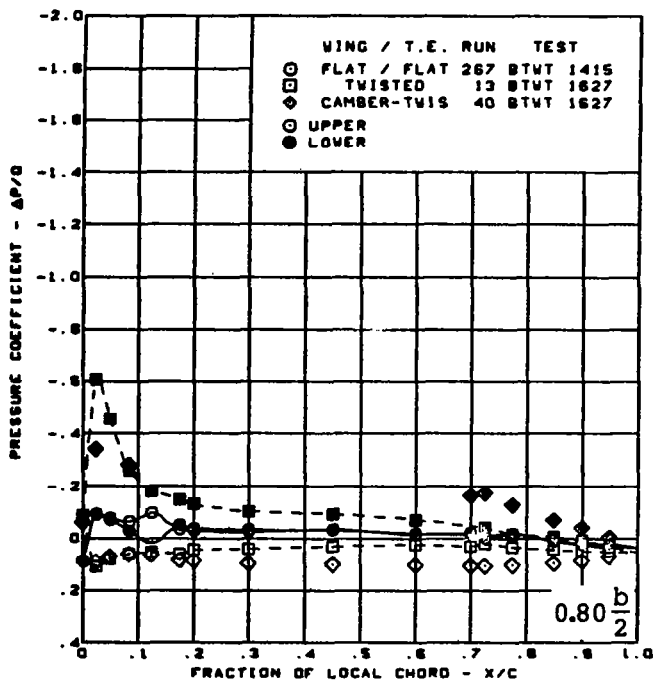
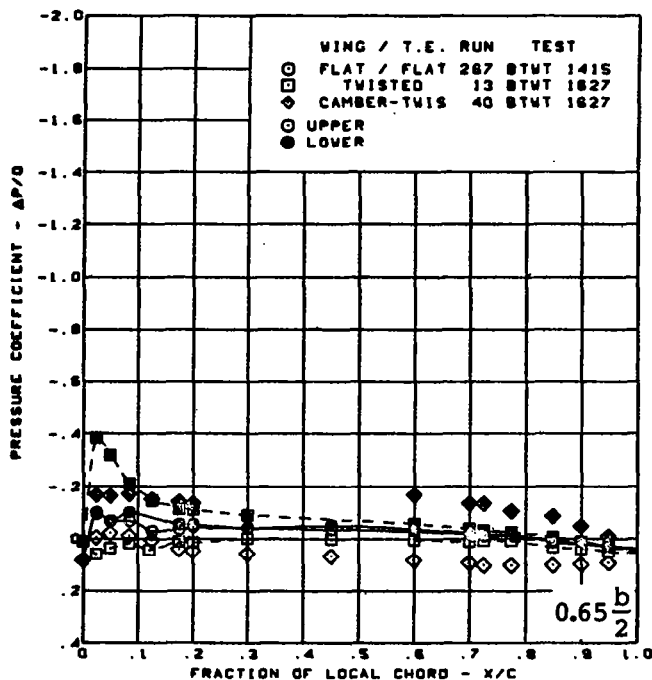
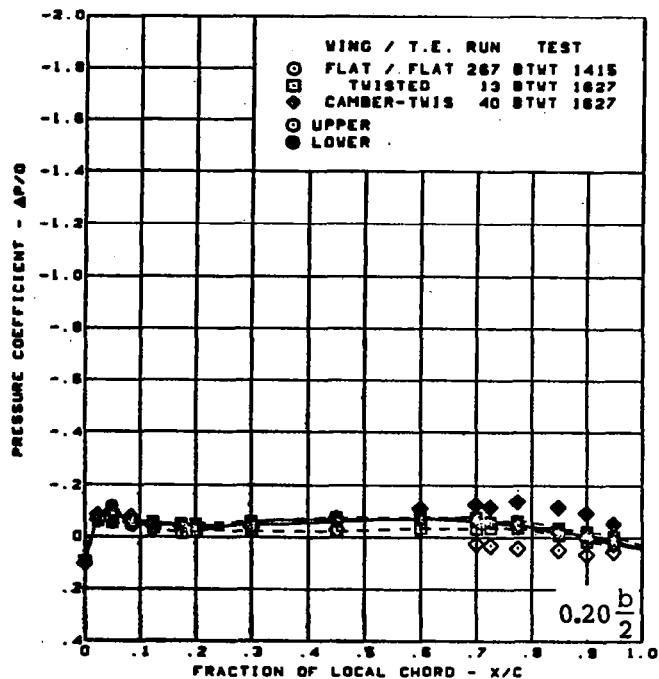
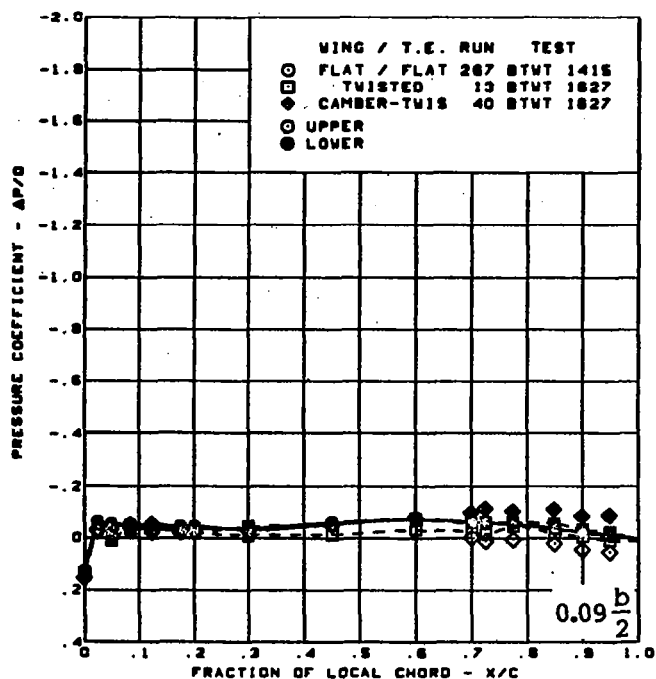
L.E. deflection, full span =  $0.0^\circ$

T.E. deflection, full span =  $0.0^\circ$

(c) (Concluded)

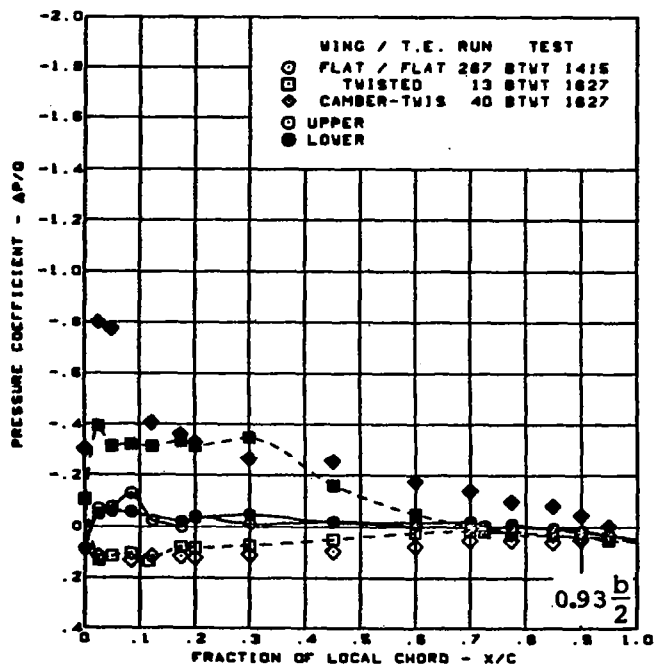
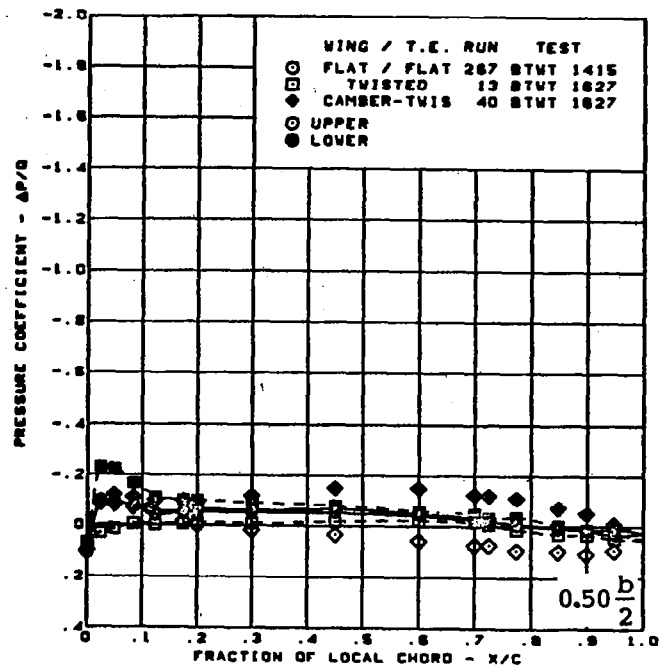
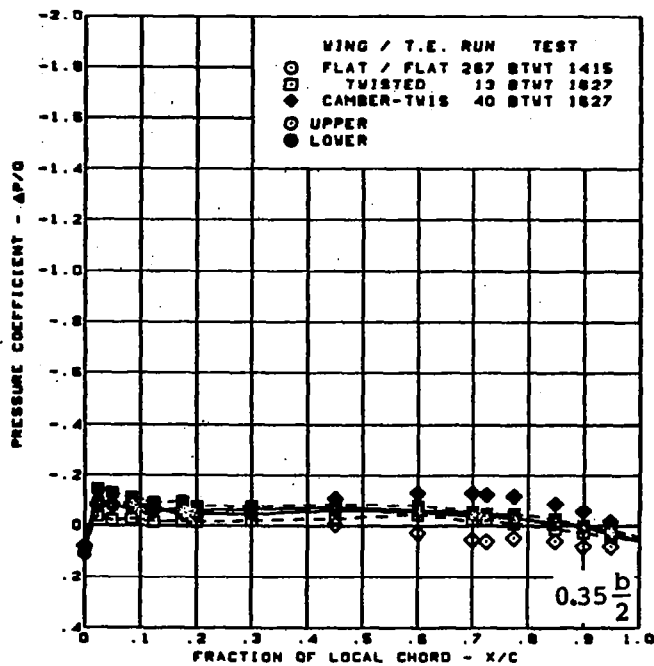
Figure 21. - (Continued)





(d) Surface Chordwise Pressure Distributions -  $\alpha = 0^\circ$

Figure 21. - (Continued)



$M = 0.85$

$\alpha = 0^\circ$

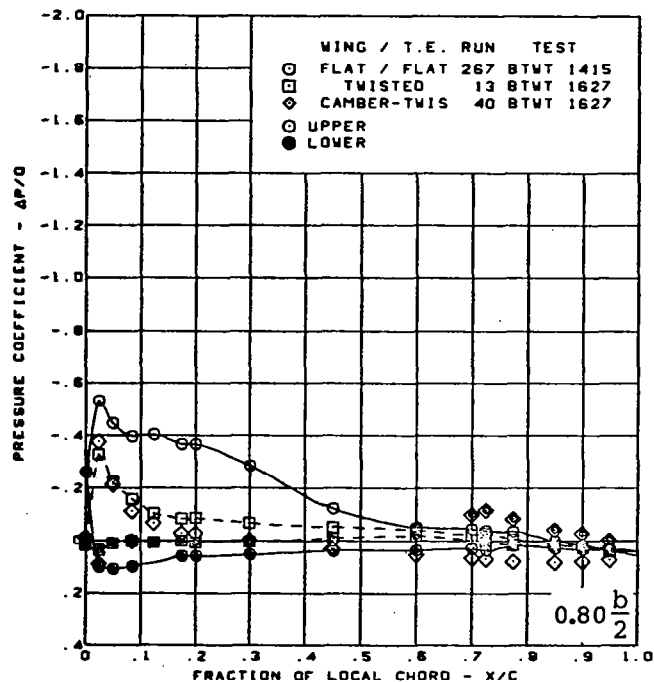
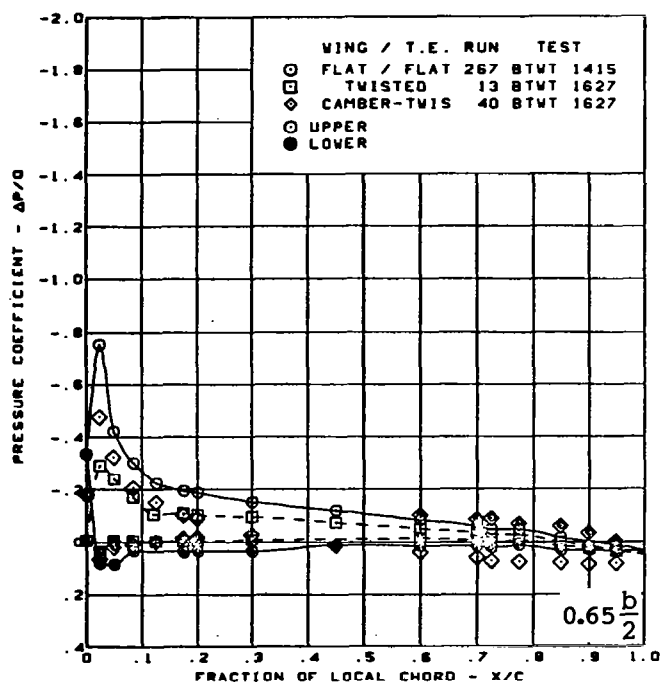
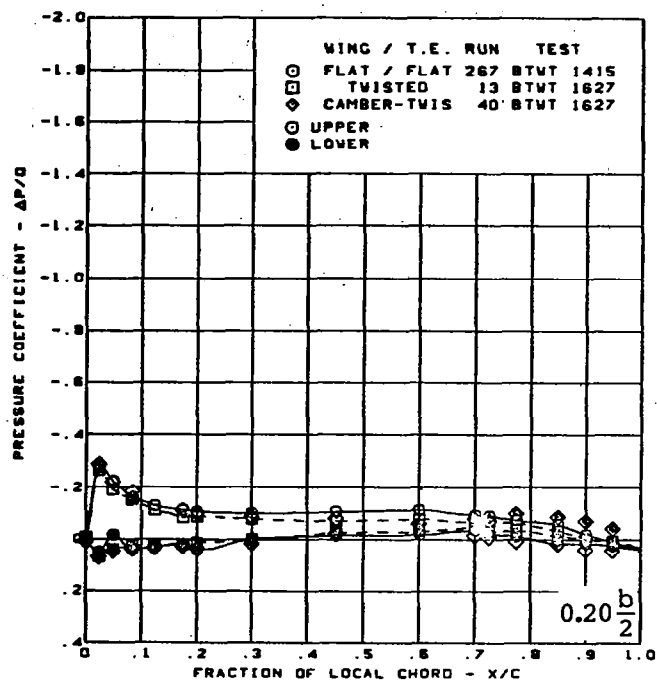
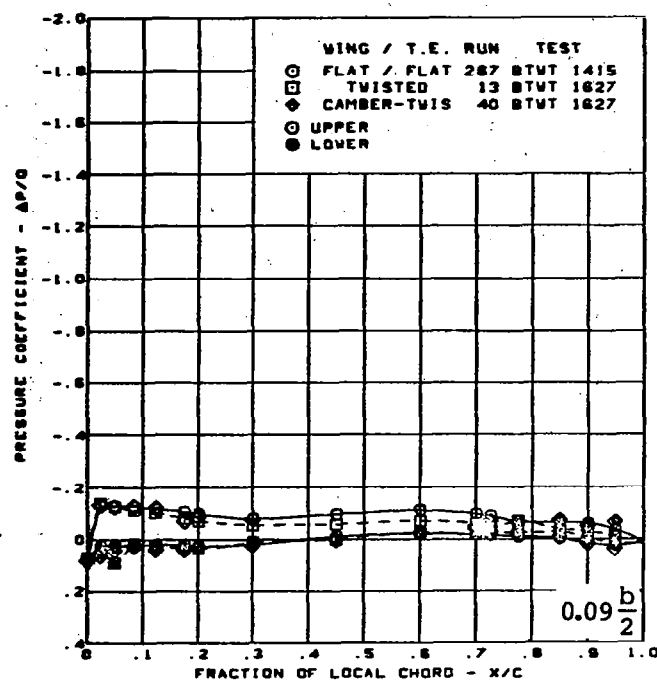
Rounded L.E.

L.E. deflection, full span =  $0.0^\circ$

T.E. deflection, full span =  $0.0^\circ$

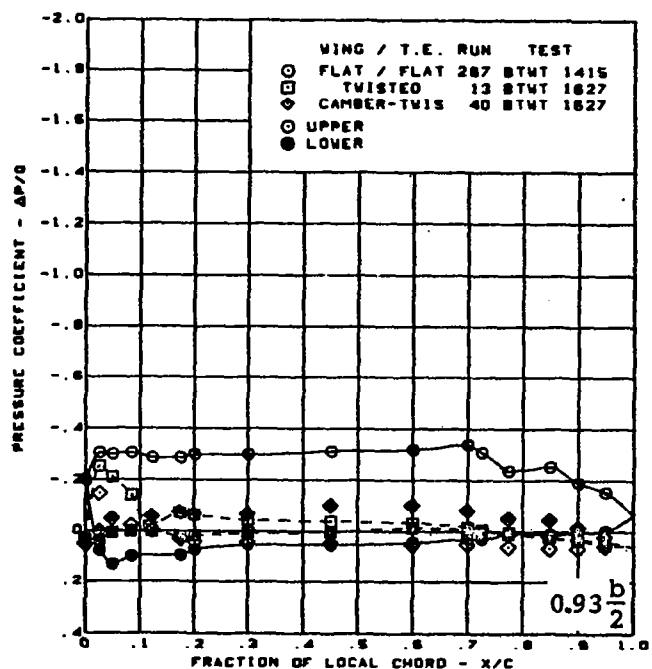
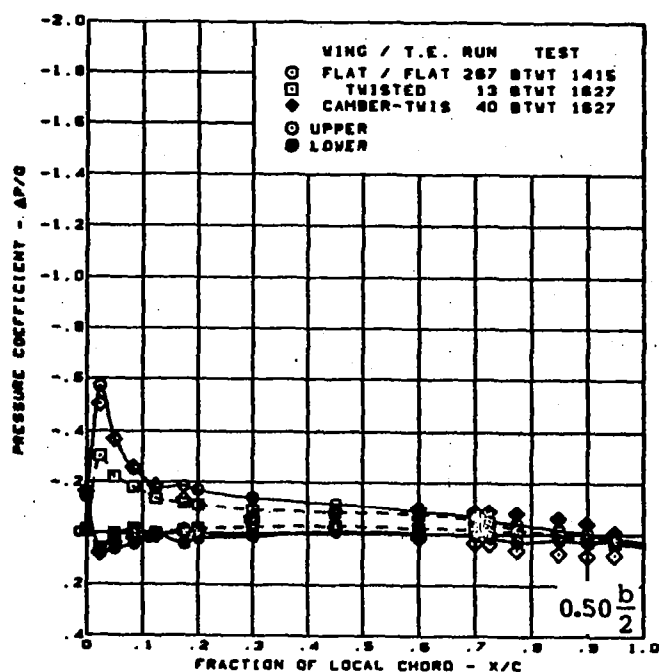
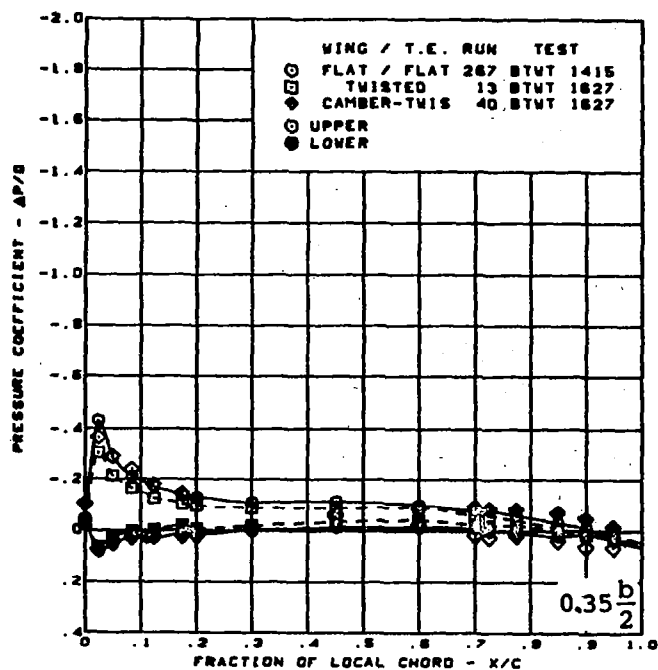
(d) (Concluded)

Figure 21. - (Continued)



(e) Surface Chordwise Pressure Distributions -  $\alpha = 4^\circ$

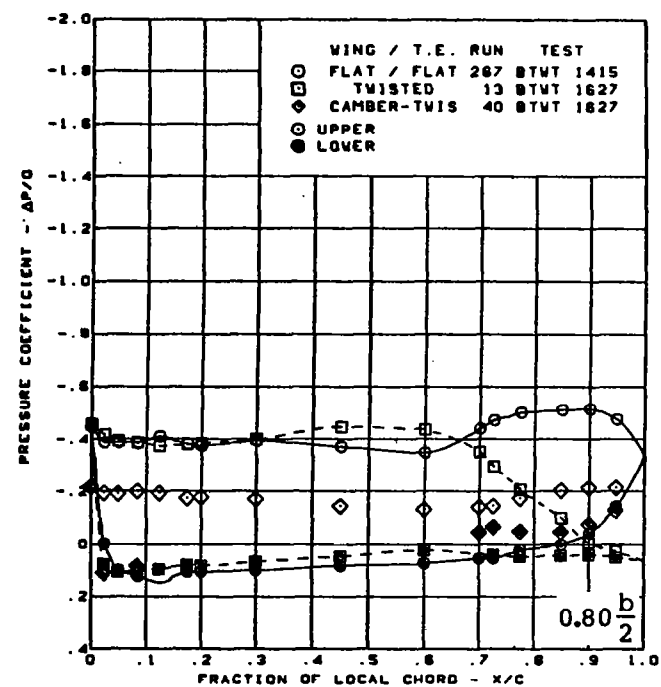
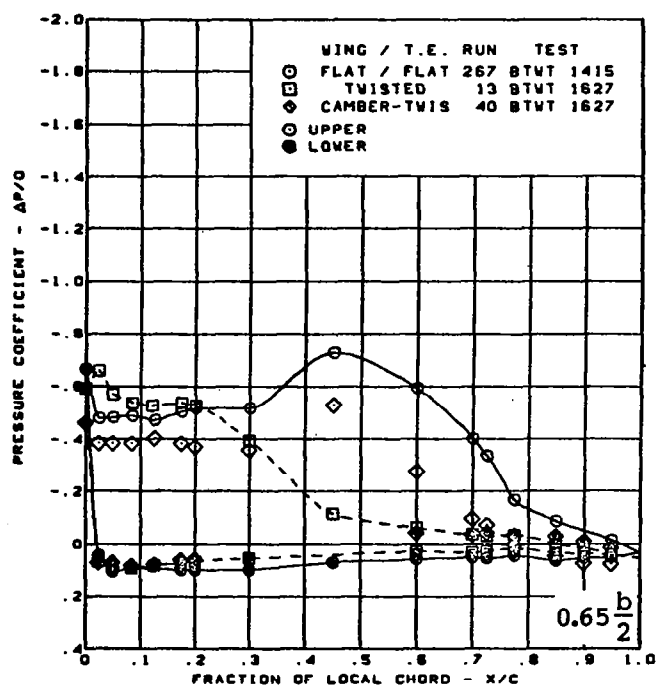
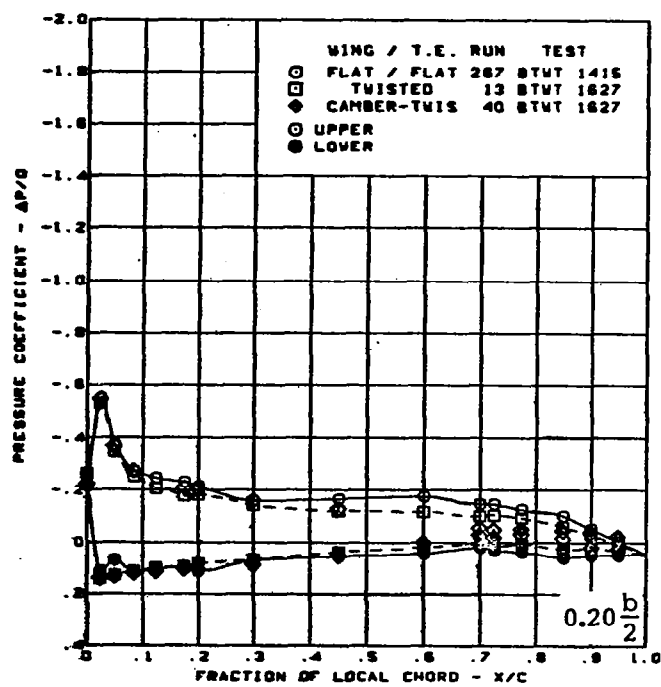
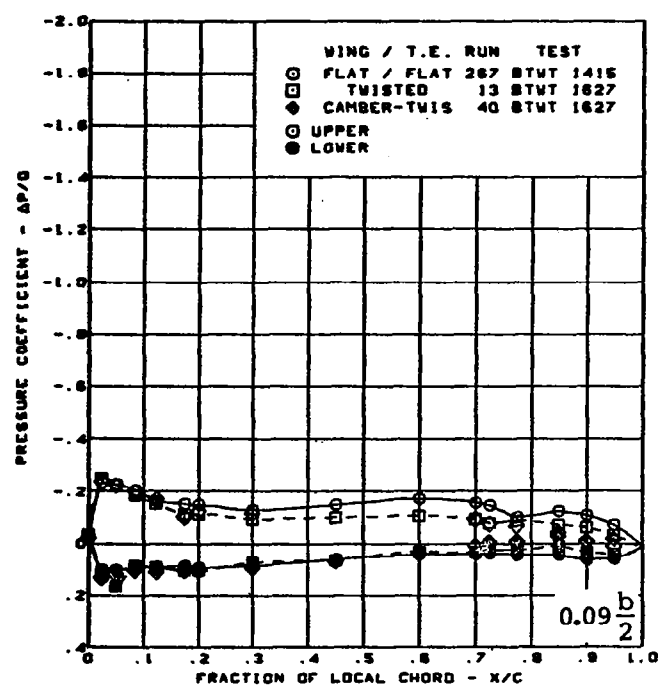
Figure 21. - (Continued)



$M = 0.85$   
 $\alpha = 4^\circ$   
 Rounded L.E.  
 L.E. deflection, full span  $\approx 0.0^\circ$   
 T.E. deflection, full span  $\approx 0.0^\circ$

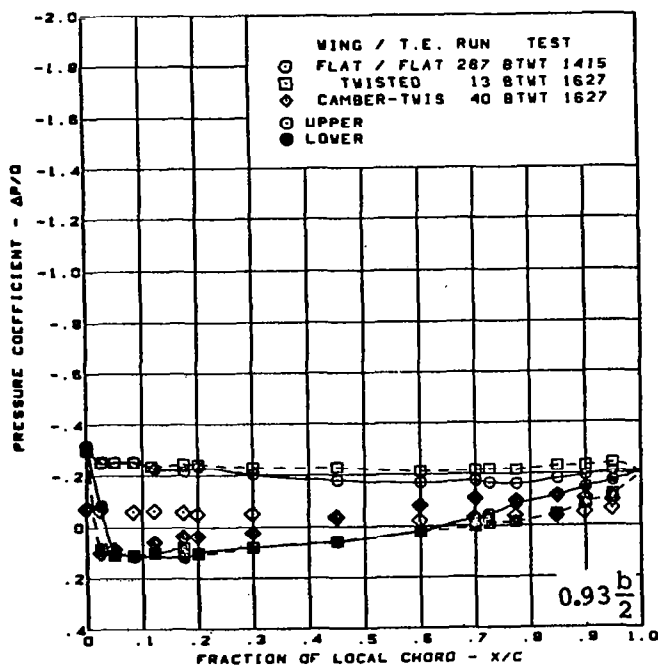
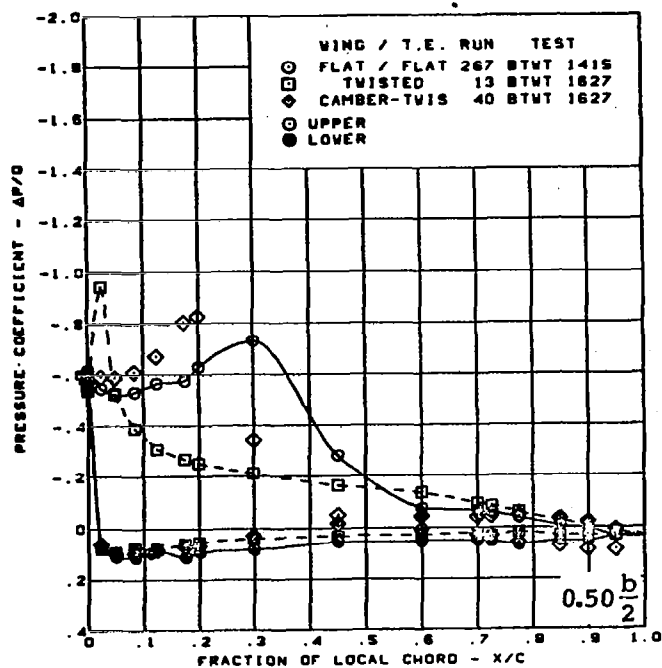
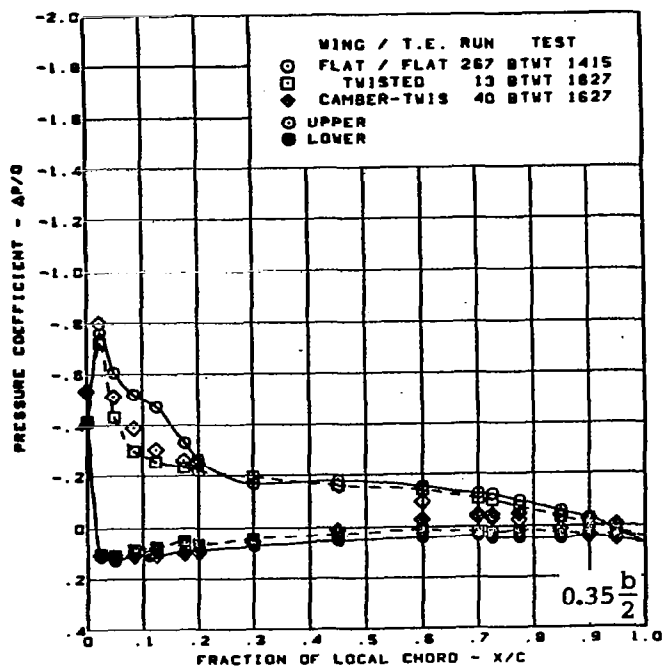
(e) (Concluded)

Figure 21. — (Continued)



(f) Surface Chordwise Pressure Distributions -  $\alpha = 8^\circ$

Figure 21. - (Continued)



$M = 0.85$

$\alpha = 8^\circ$

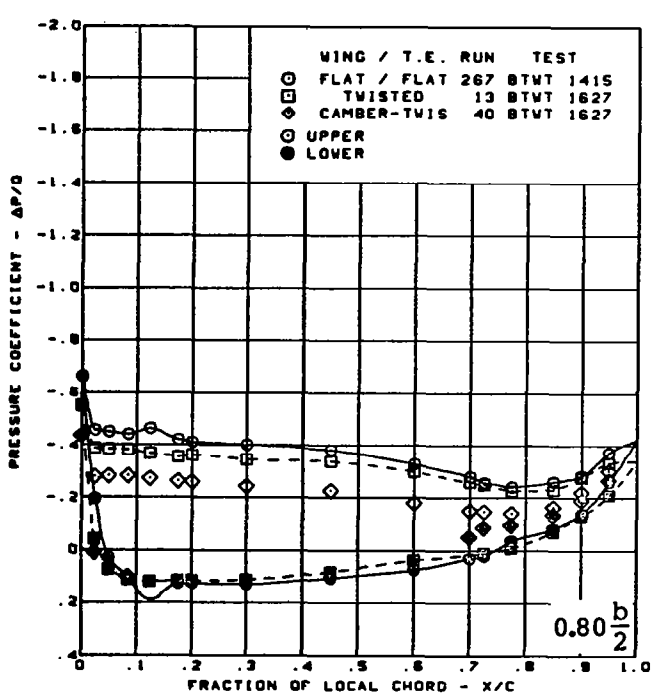
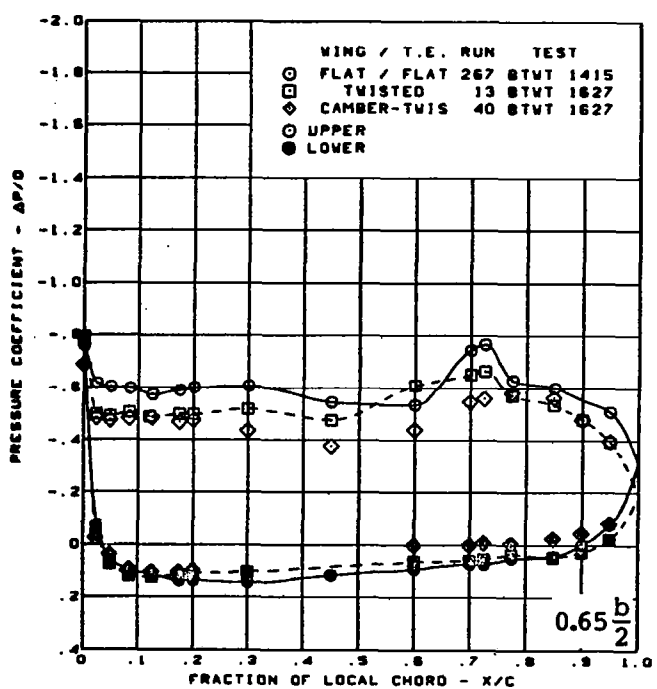
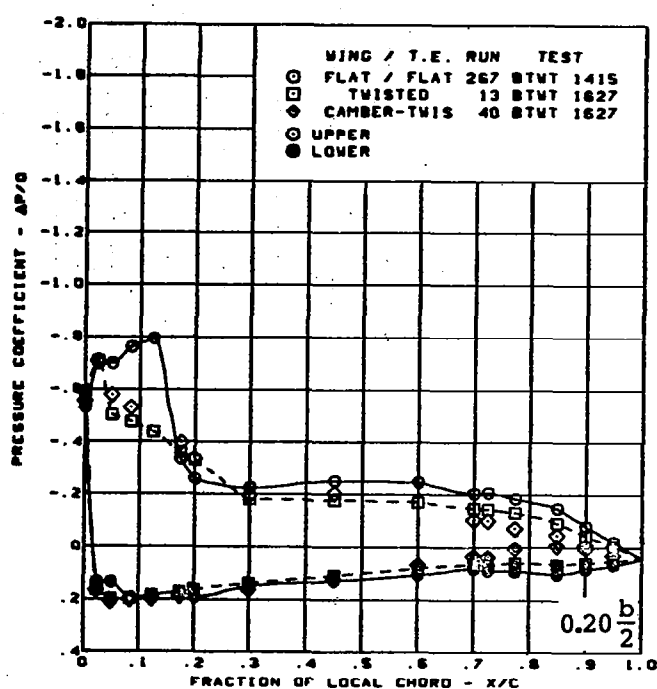
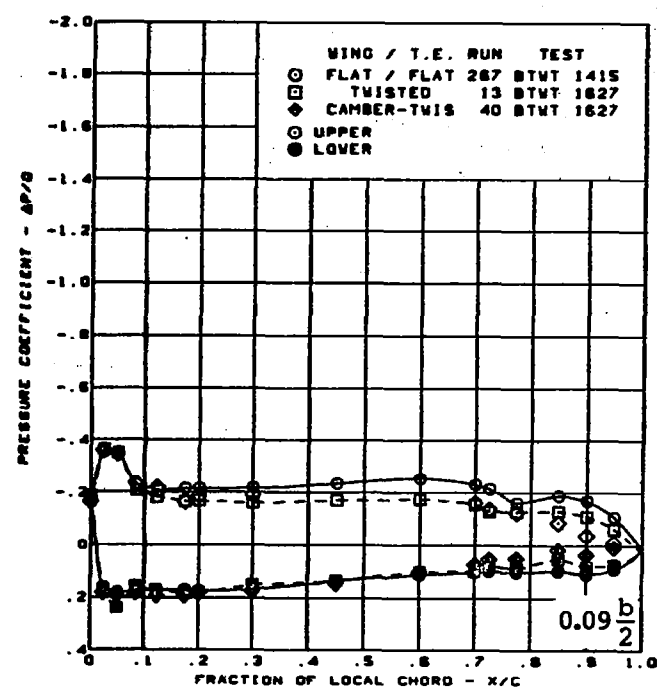
Rounded L.E.

L.E. deflection, full span =  $0.0^\circ$

T.E. deflection, full span =  $0.0^\circ$

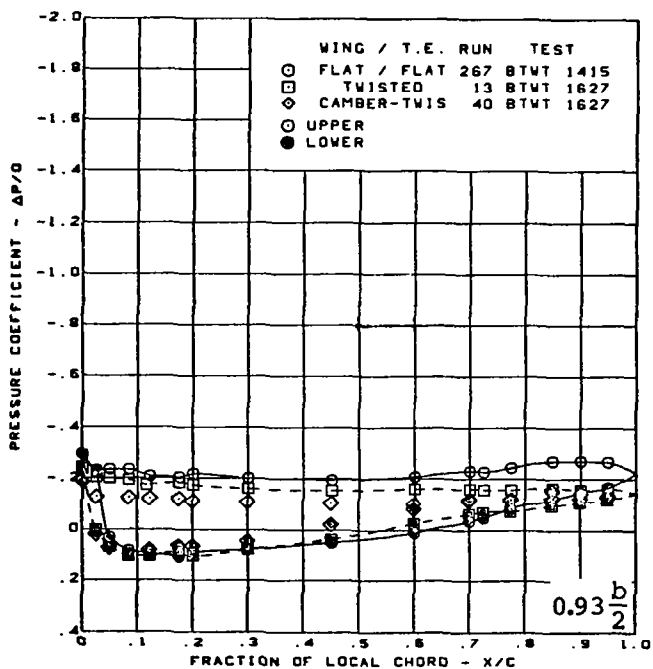
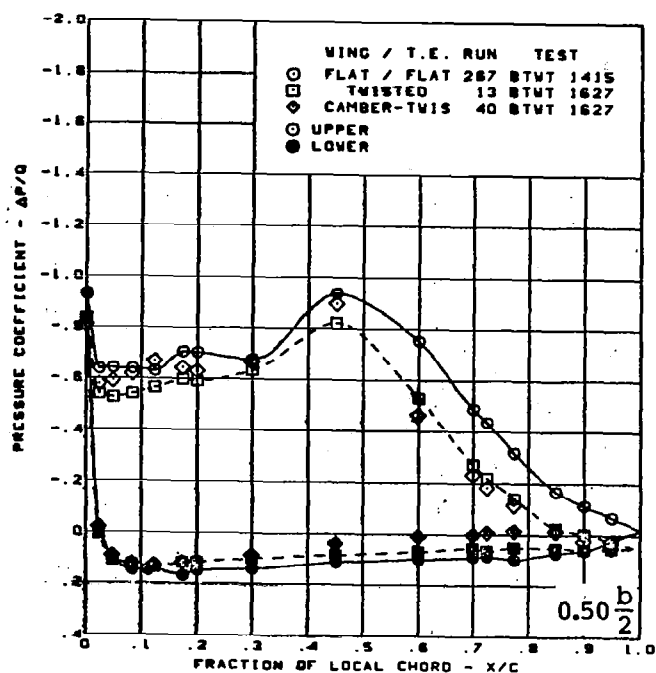
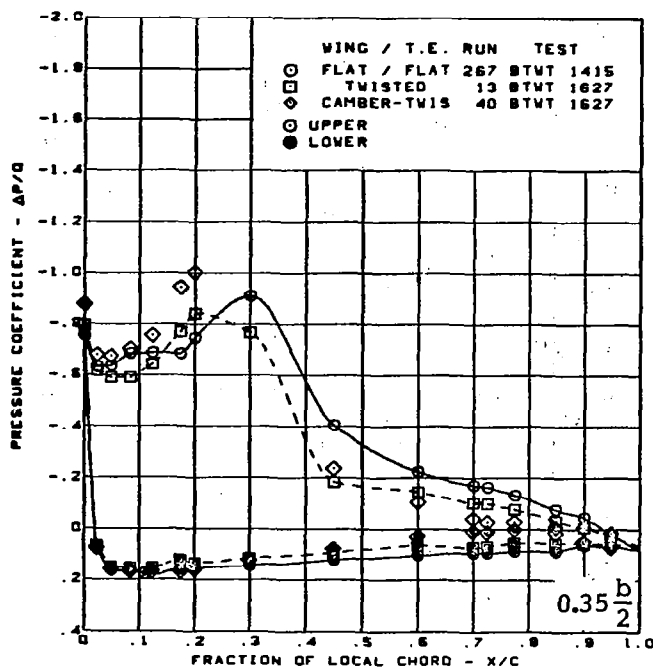
(f) (Concluded)

Figure 21. - (Continued)



(g) Surface Chordwise Pressure Distributions -  $\alpha = 12^\circ$

Figure 21. - (Continued)



$M = 0.85$

$\alpha = 12^\circ$

Rounded L.E.

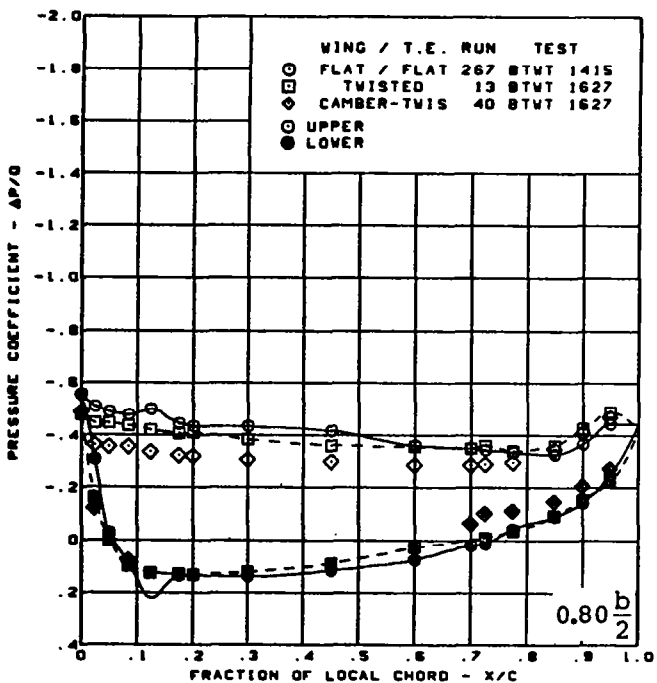
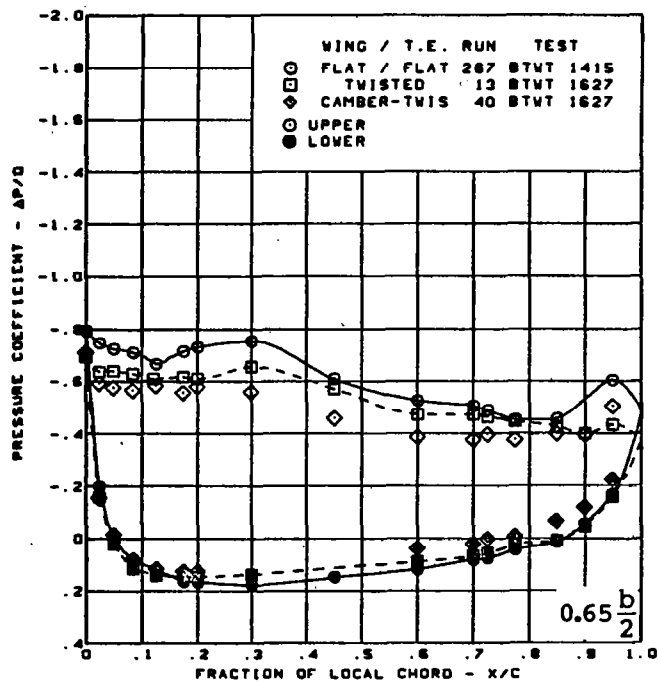
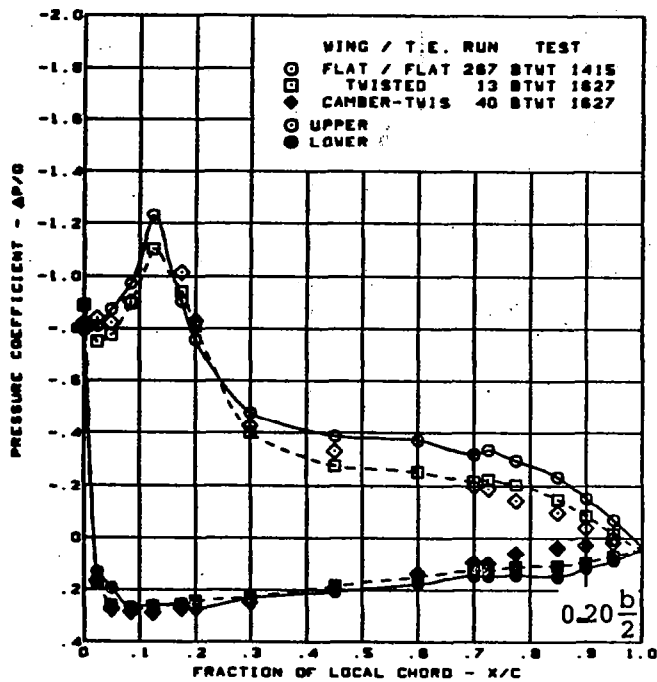
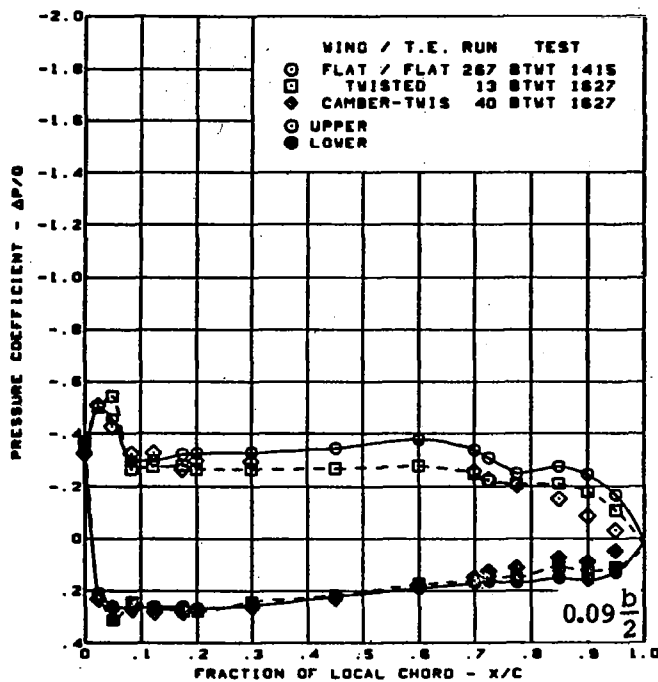
L.E. deflection, full span =  $0.0^\circ$

T.E. deflection, full span =  $0.0^\circ$

(g) (Concluded)

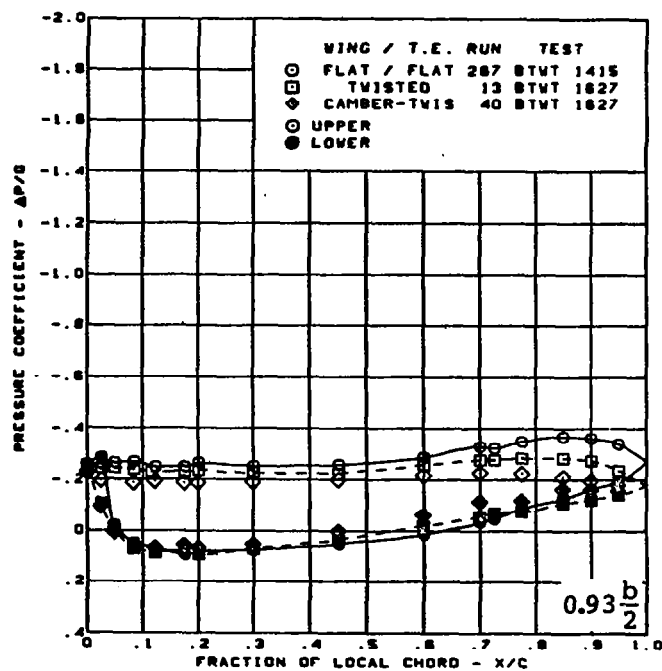
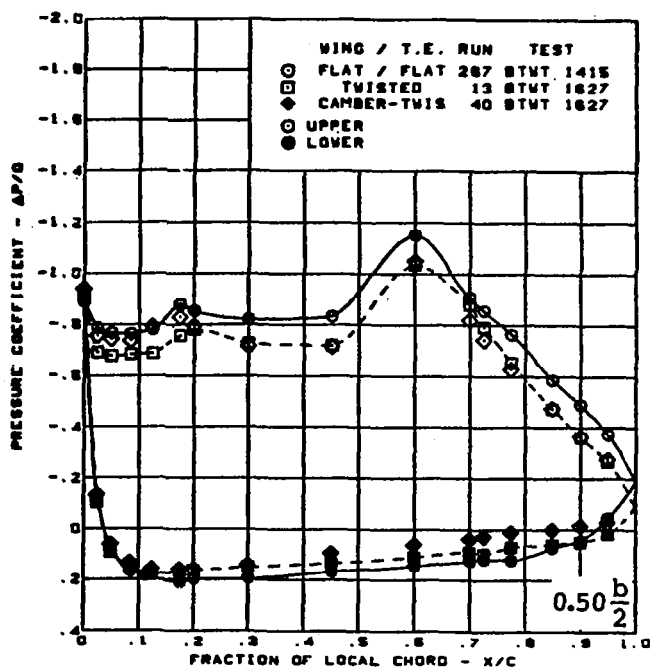
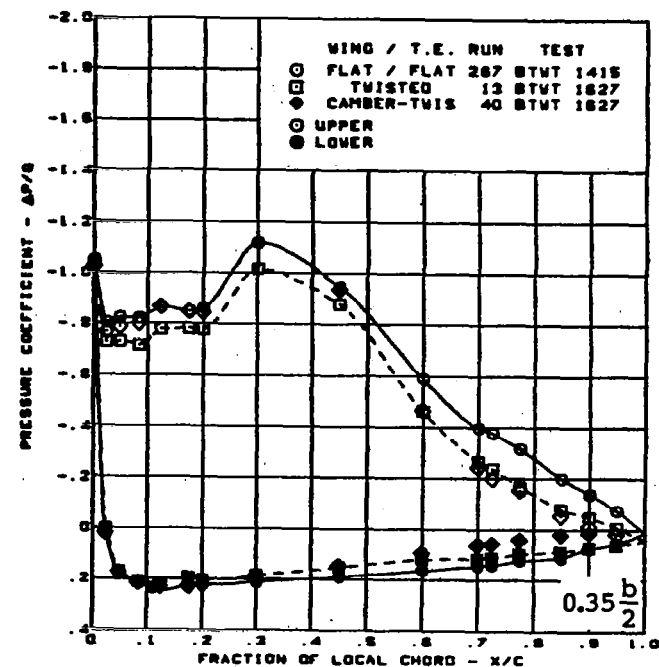
Figure 21. — (Continued)





(h) Surface Chordwise Pressure Distributions -  $\alpha = 16^\circ$

Figure 21. - (Continued)



$M = 0.85$

$\alpha = 16^\circ$

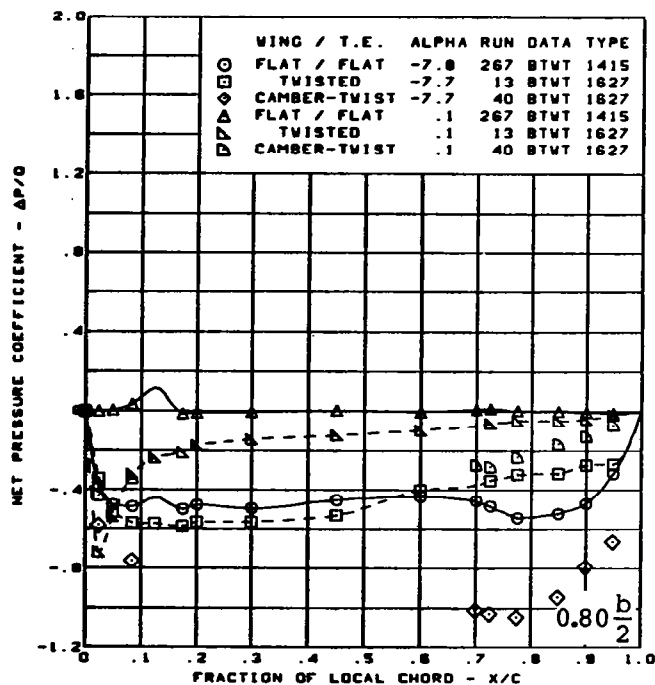
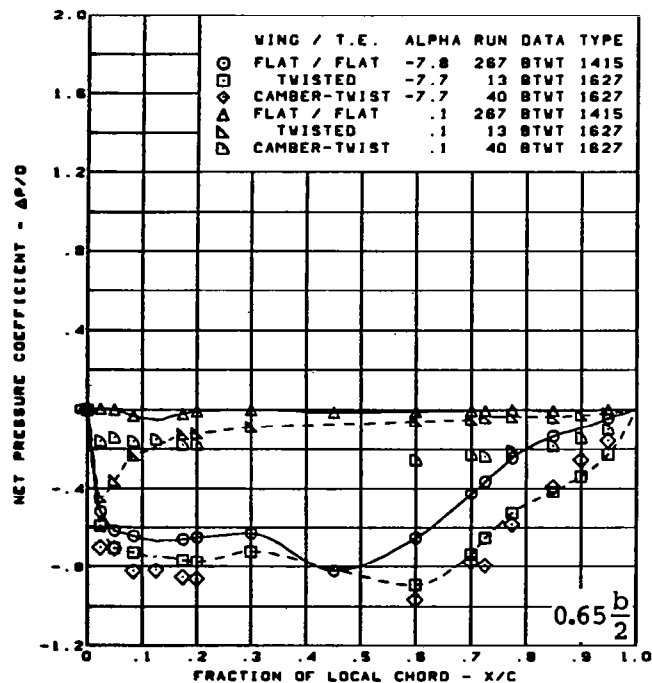
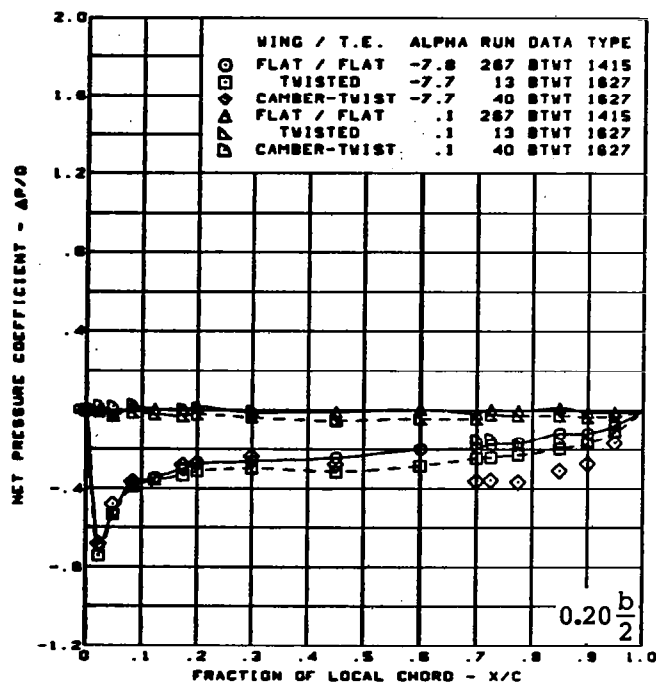
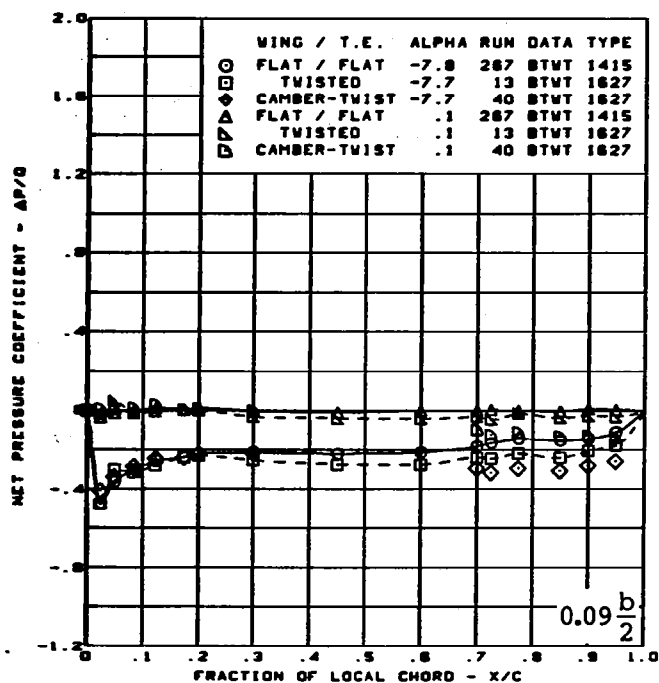
Rounded L.E.

L.E. deflection, full span =  $0.0^\circ$

T.E. deflection, full span =  $0.0^\circ$

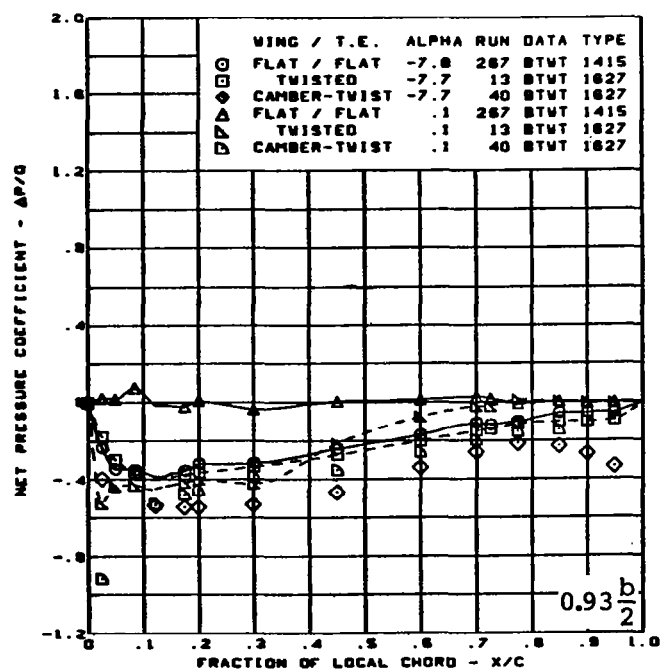
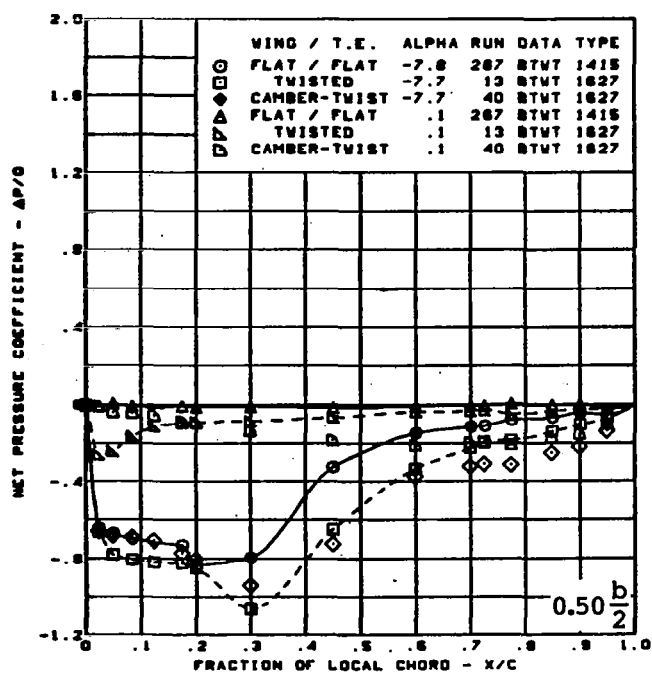
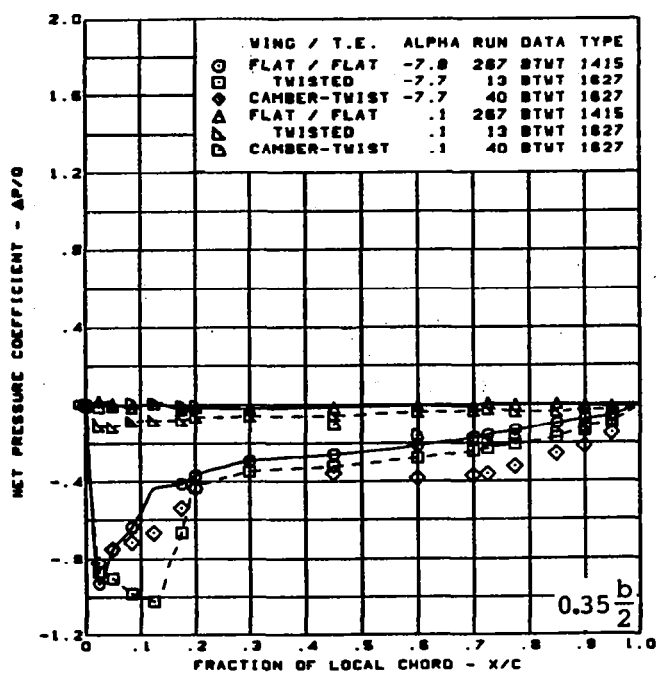
(h) (Concluded)

Figure 21. — (Continued)



(i) Net Chordwise Pressure Distributions -  $\alpha = -8^\circ$  and  $0^\circ$

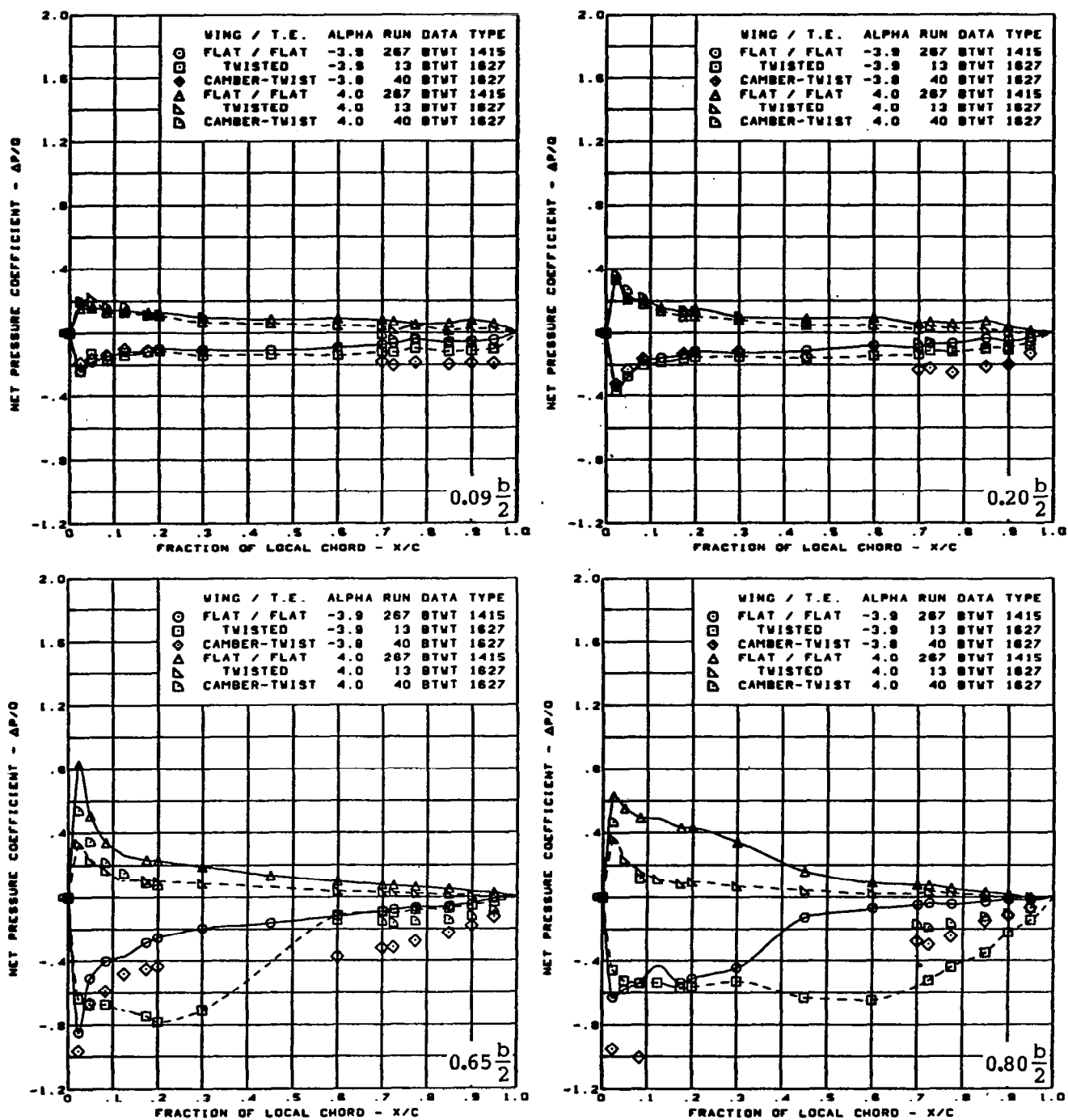
Figure 21. - (Continued)



$M = 0.85$   
 $\alpha = -8^\circ$  and  $0^\circ$   
 Rounded L.E.  
 L.E. deflection, full span =  $0.0^\circ$   
 T.E. deflection, full span =  $0.0^\circ$

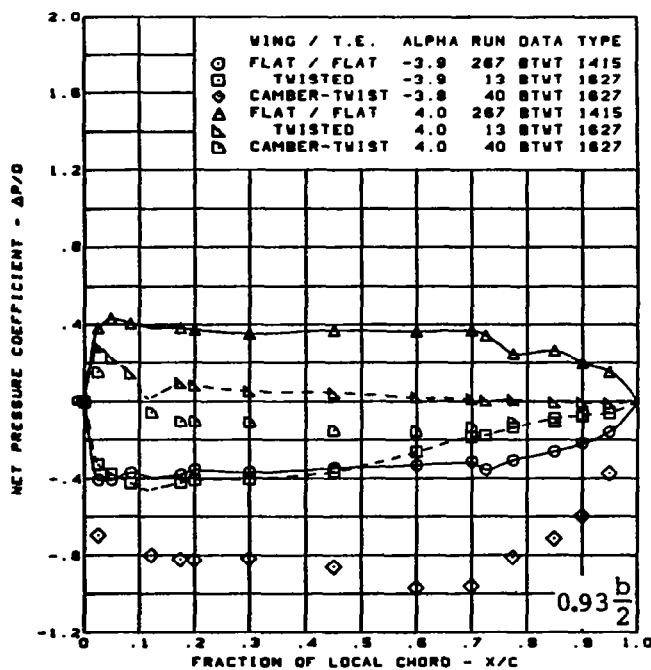
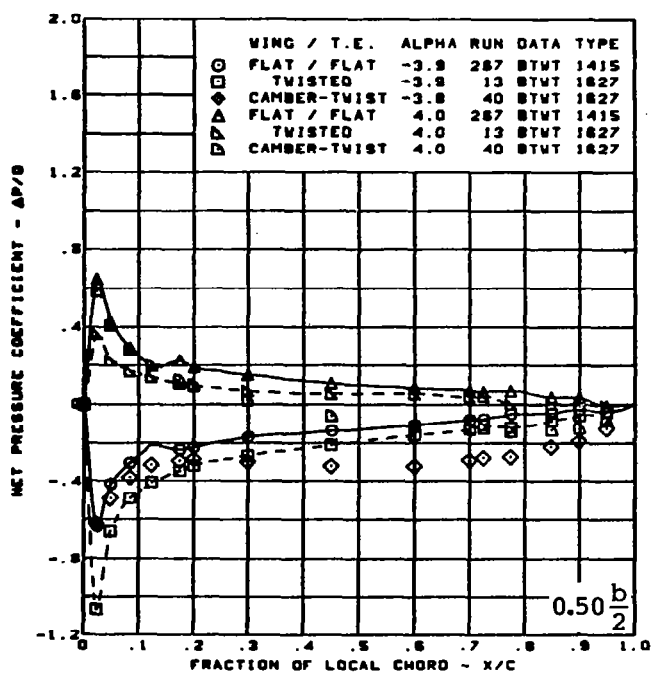
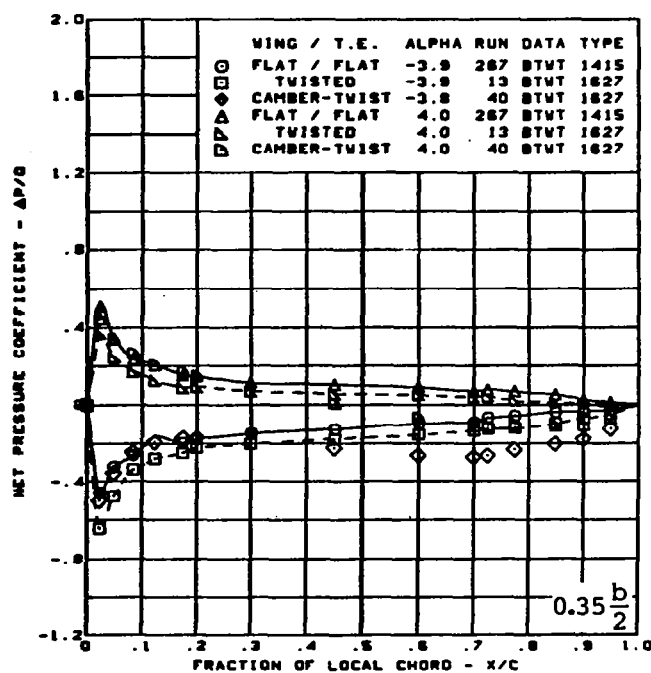
(i) (Concluded)

Figure 21. — (Continued)



(j) Net Chordwise Pressure Distributions -  $\alpha = -4^\circ$  and  $4^\circ$

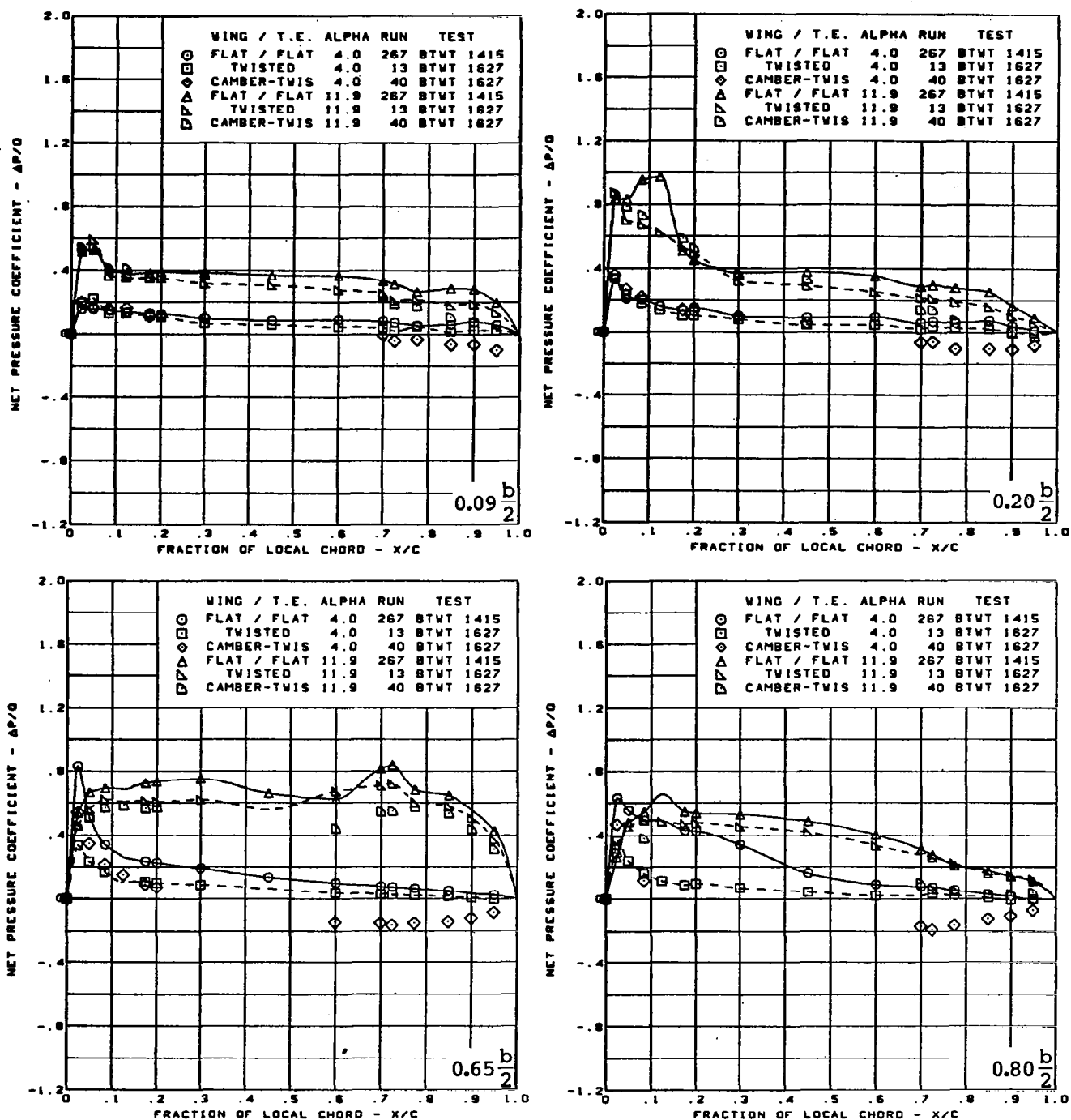
Figure 21. - (Continued)



$M = 0.85$   
 $\alpha = -4^\circ$  and  $4^\circ$   
 Rounded L.E.  
 L.E. deflection, full span =  $0.0^\circ$   
 T.E. deflection, full span =  $0.0^\circ$

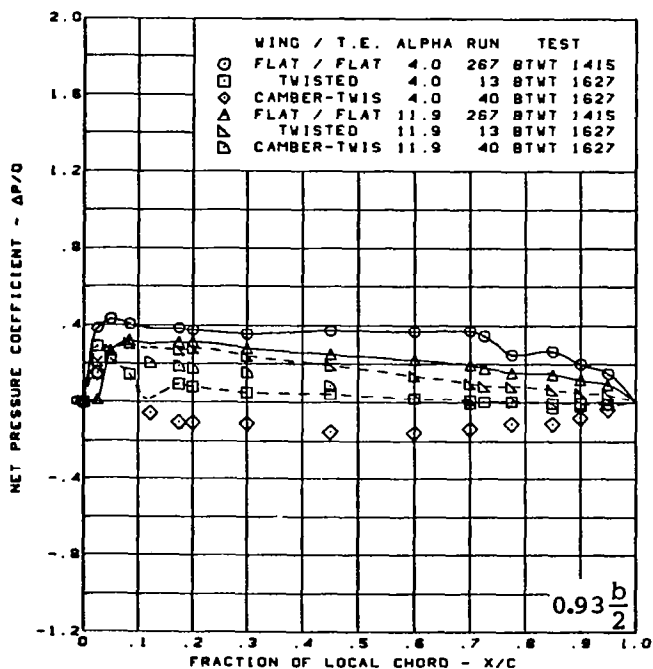
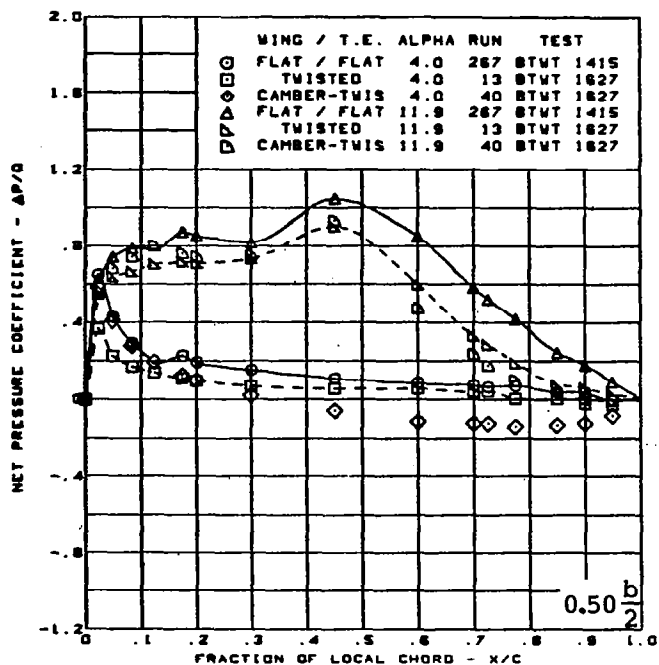
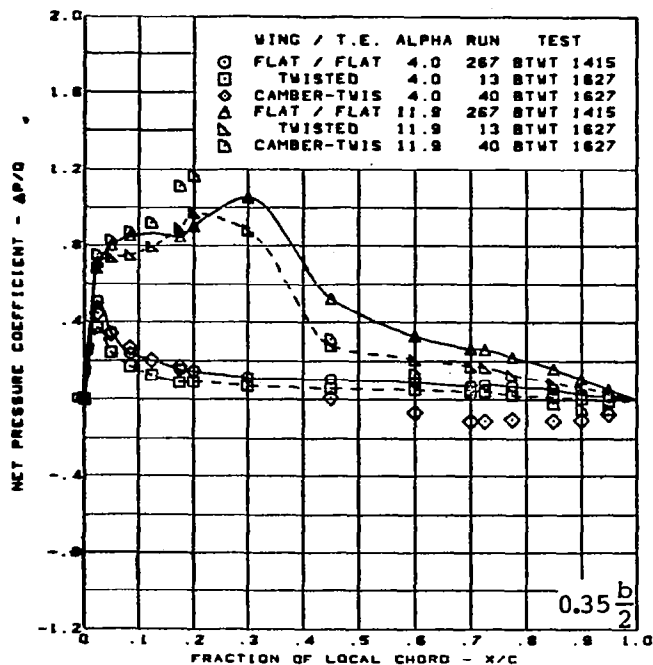
(j) (Concluded)

Figure 21. - (Continued)



(k) Net Chordwise Pressure Distributions -  $\alpha = 4^\circ$  and  $12^\circ$

Figure 21. - (Continued)

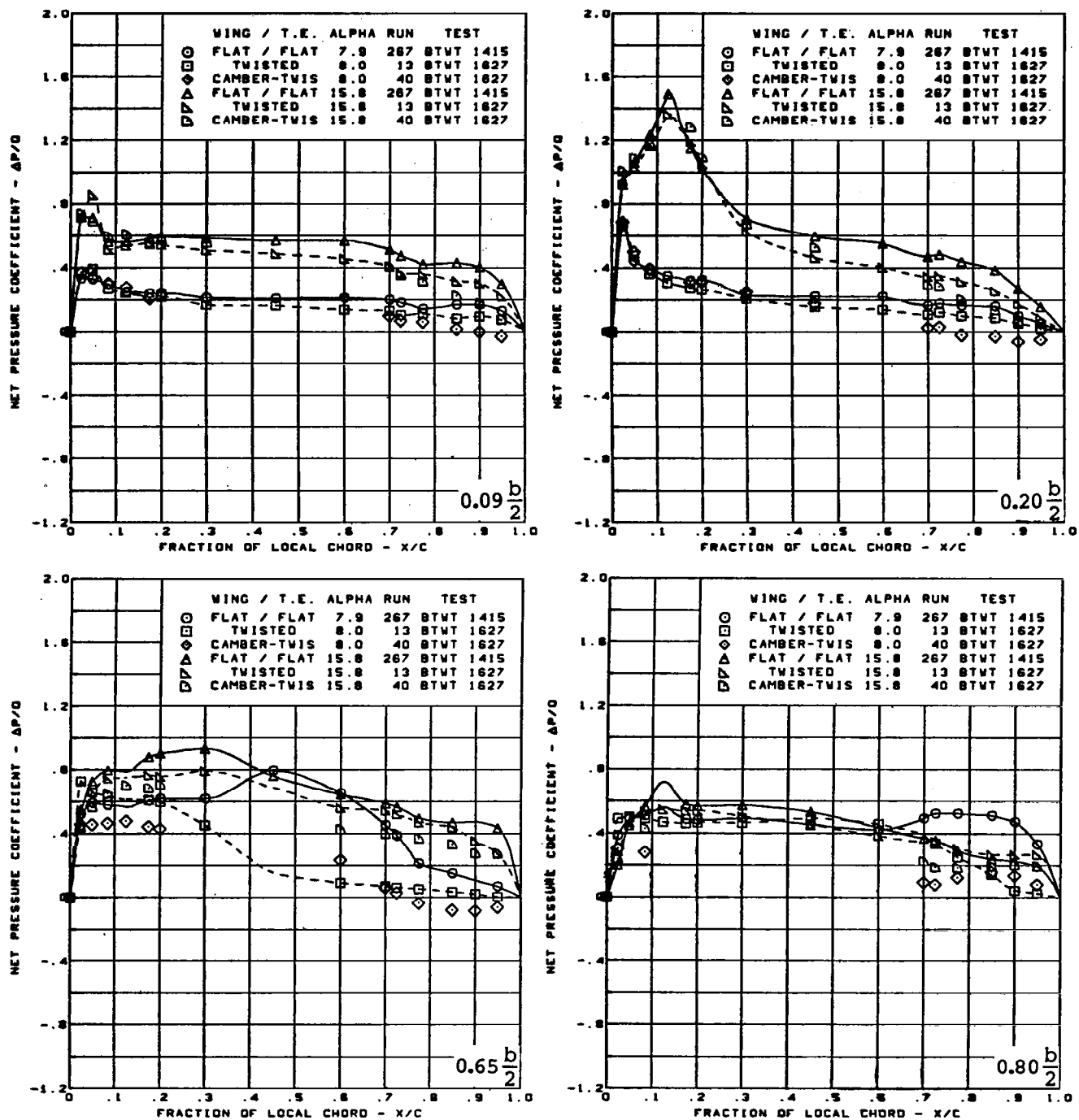


$M = 0.85$   
 $\alpha = 4^\circ \text{ and } 12^\circ$   
 Rounded L.E.  
 L.E. deflection, full span =  $0.0^\circ$   
 T.E. deflection, full span =  $0.0^\circ$

(k) (Concluded)

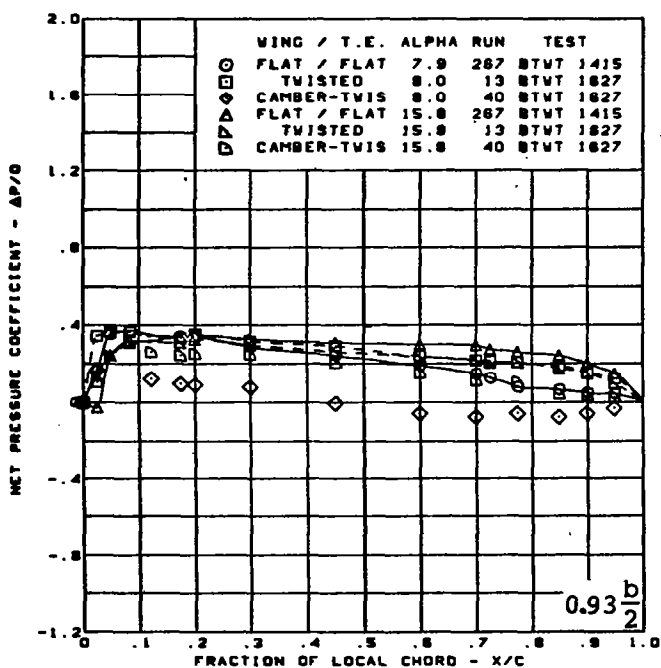
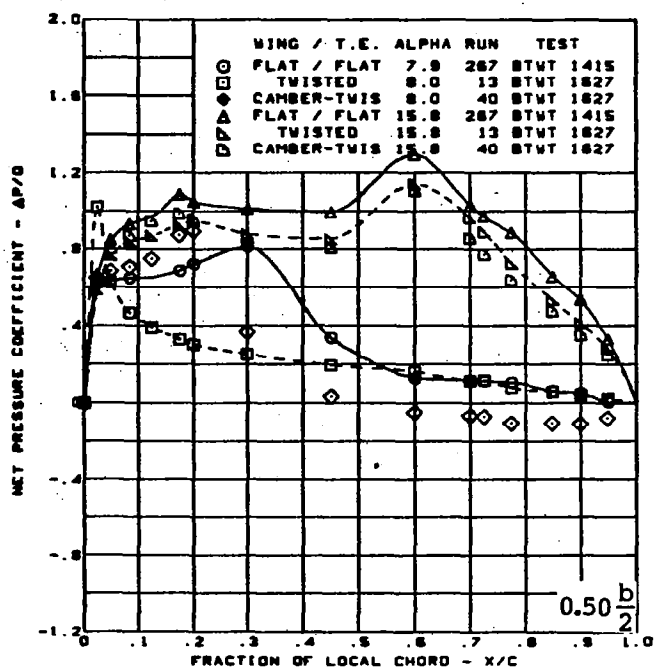
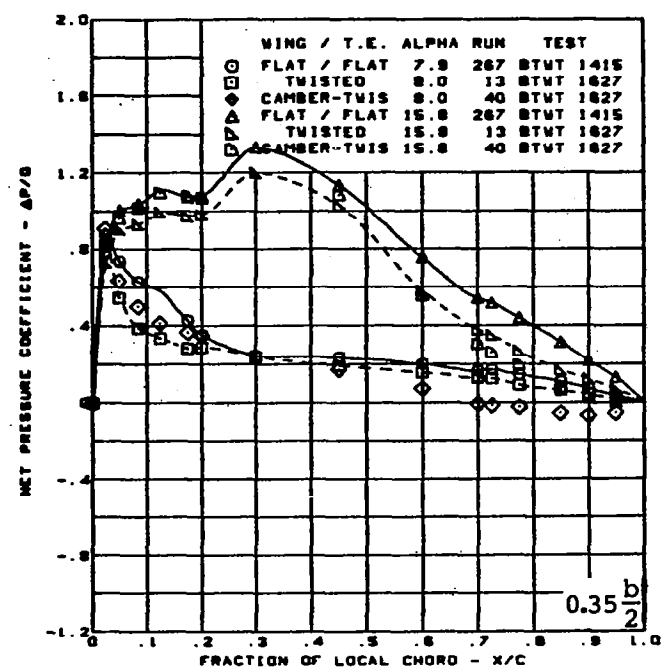
Figure 21. — (Continued)





(I) Net Chordwise Pressure Distributions -  $\alpha = 8^\circ$  and  $16^\circ$

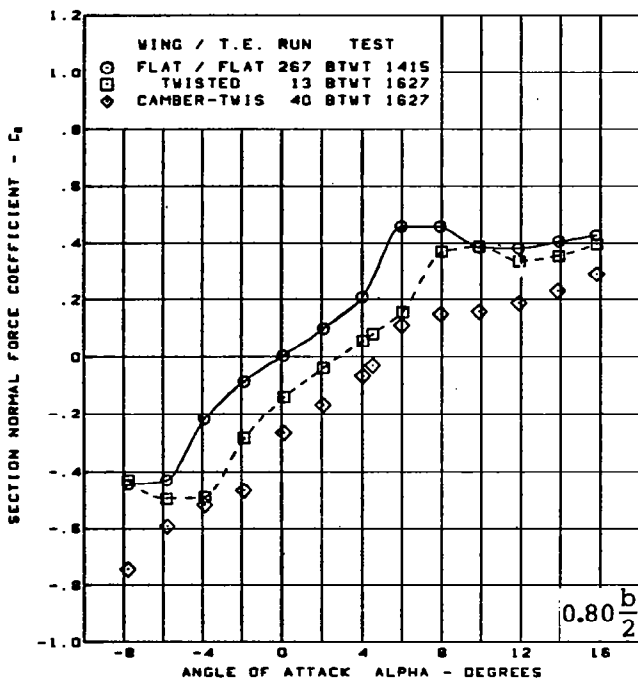
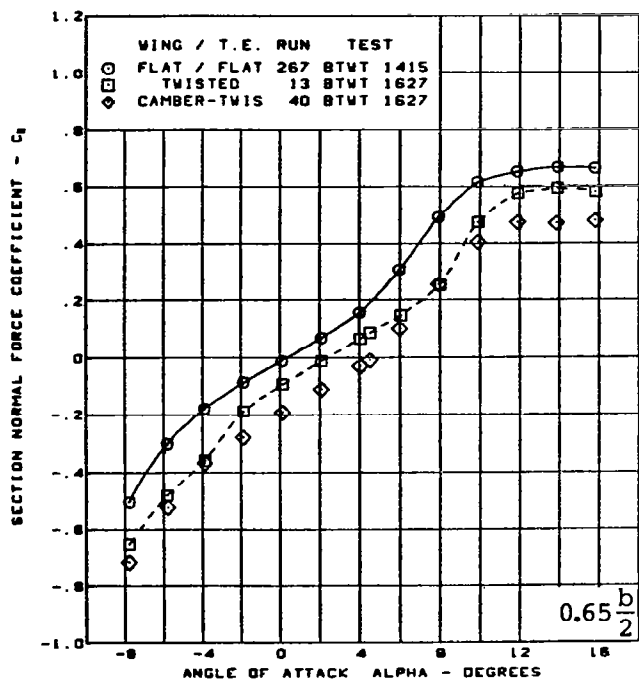
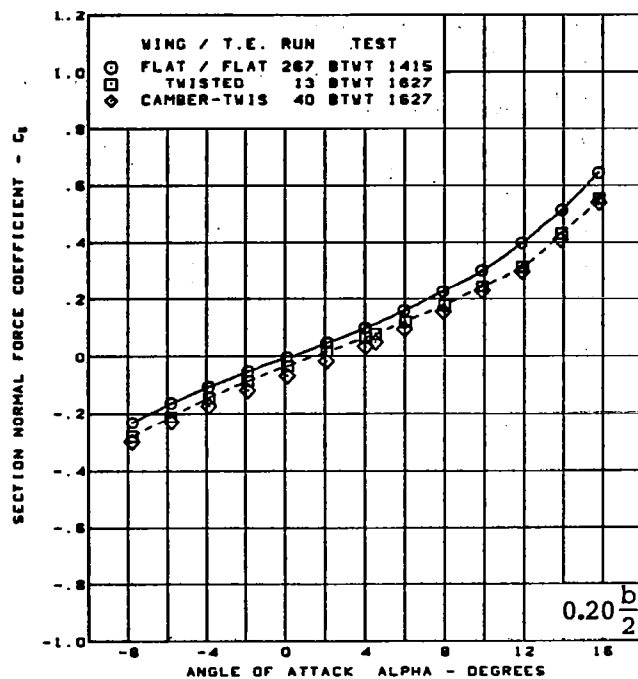
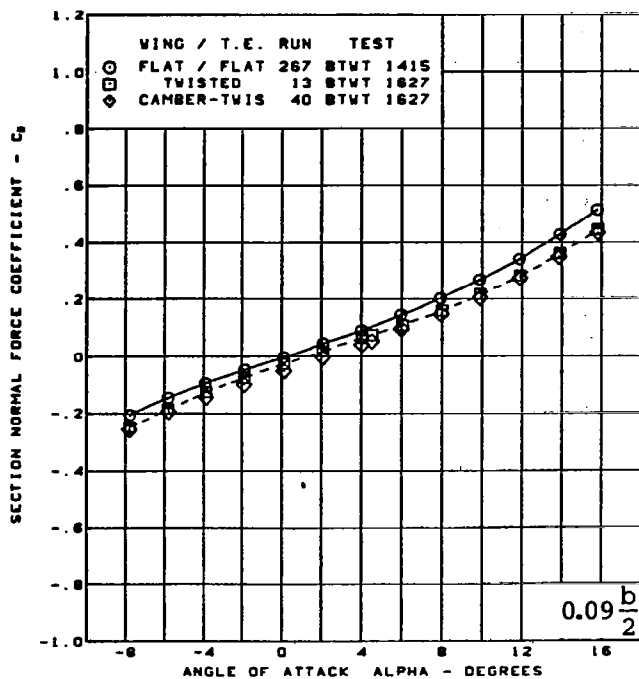
Figure 21. - (Continued)



$M = 0.85$   
 $\alpha = 8^\circ$  and  $16^\circ$   
 Rounded L.E.  
 L.E. deflection, full span =  $0.0^\circ$   
 T.E. deflection, full span =  $0.0^\circ$

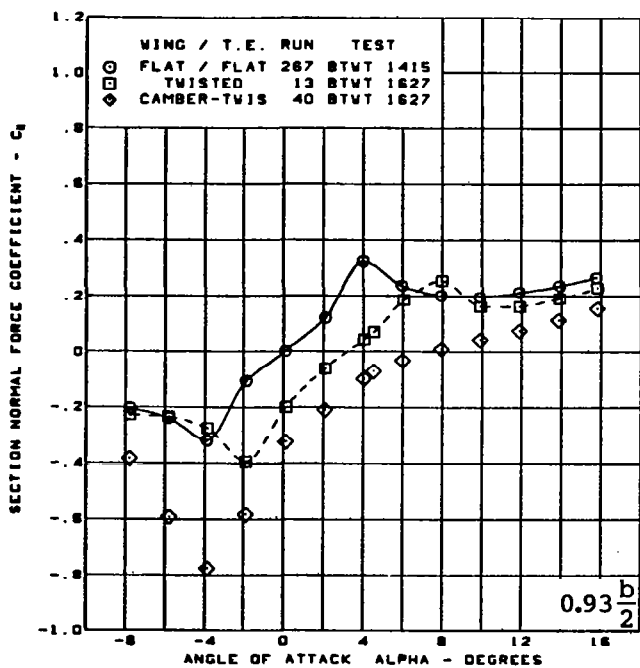
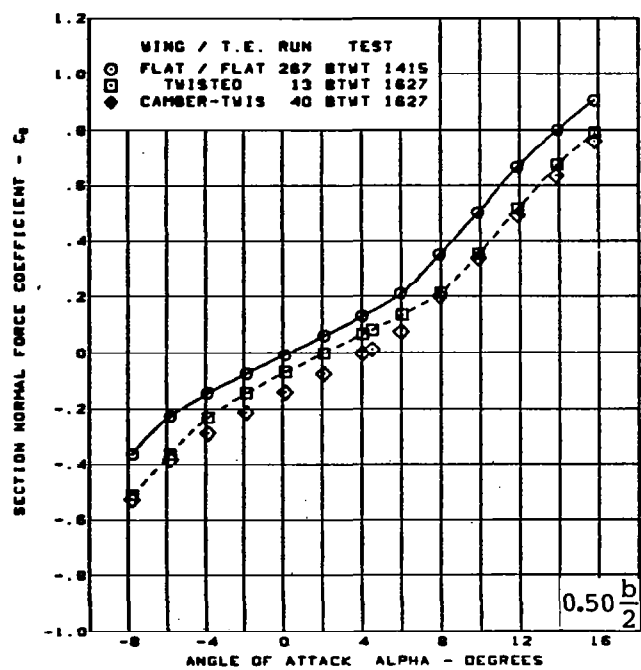
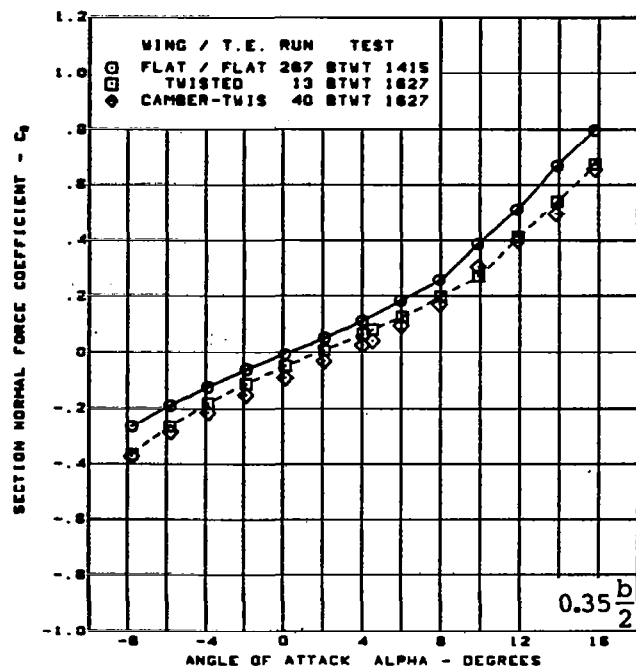
(II) (Concluded)

Figure 21. — (Continued)



(m) Section Aerodynamic Coefficients - Normal Force

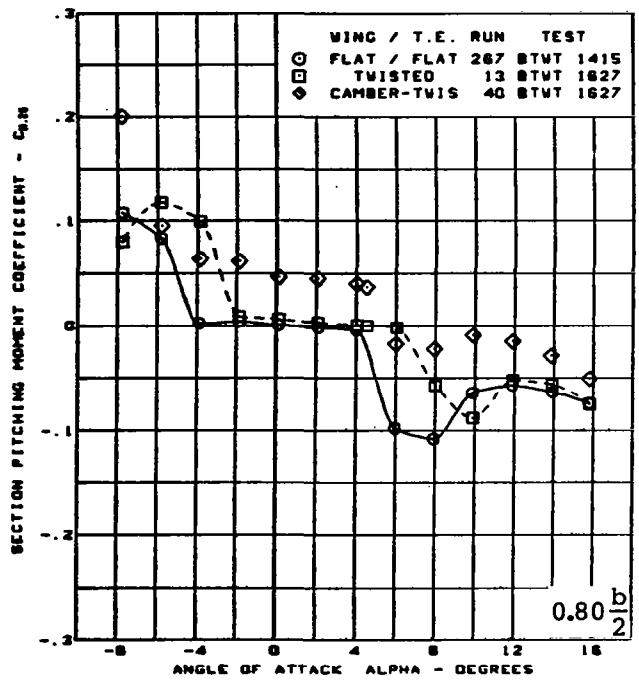
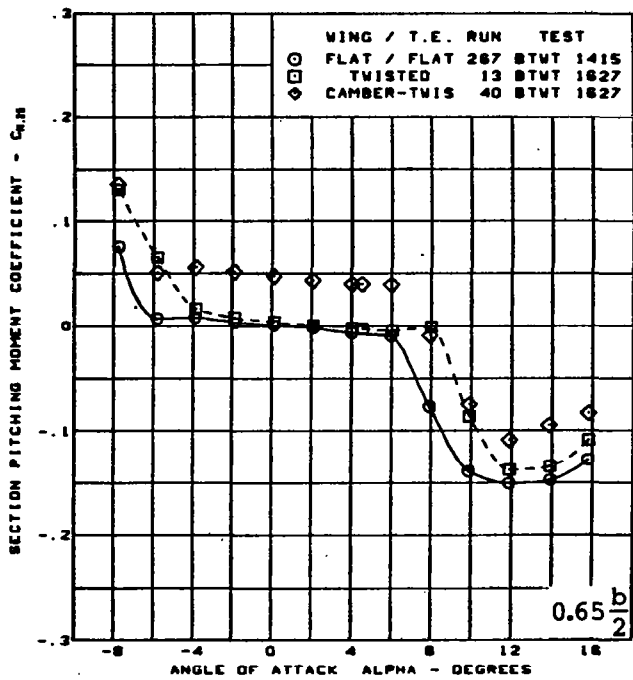
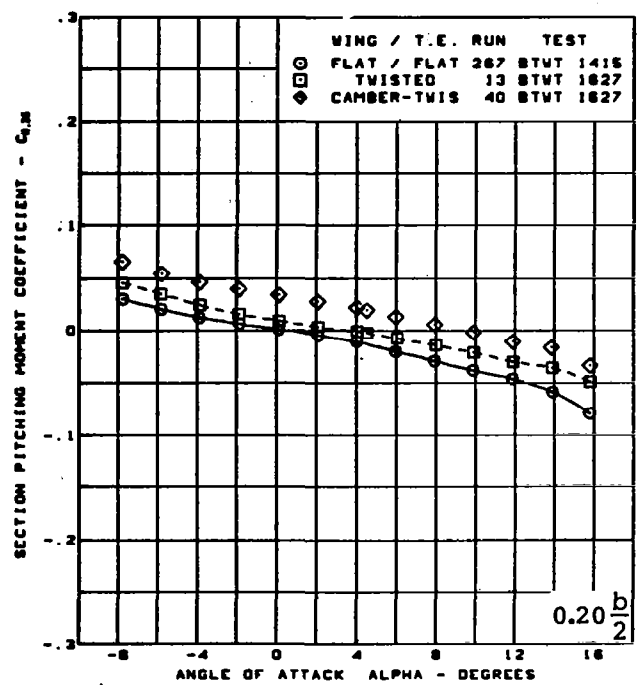
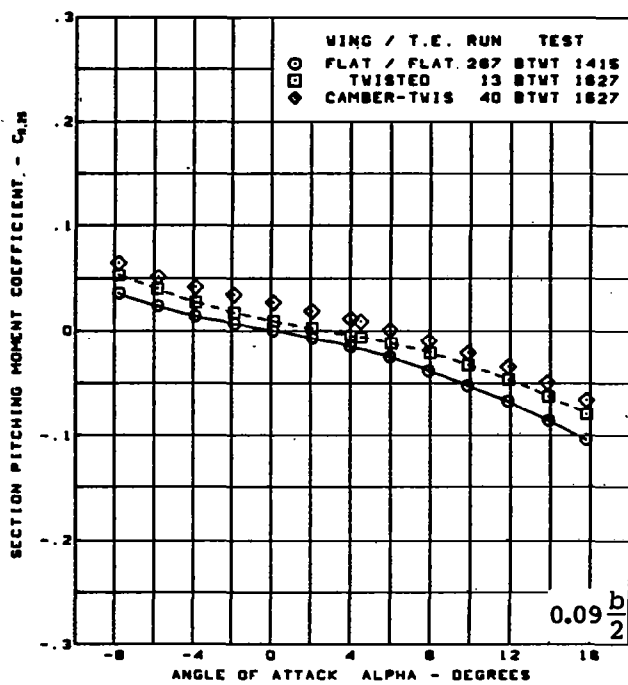
Figure 21. - (Continued)



$M = 0.85$   
 Rounded L.E.  
 L.E. deflection, full span =  $0.0^\circ$   
 T.E. deflection, full span =  $0.0^\circ$

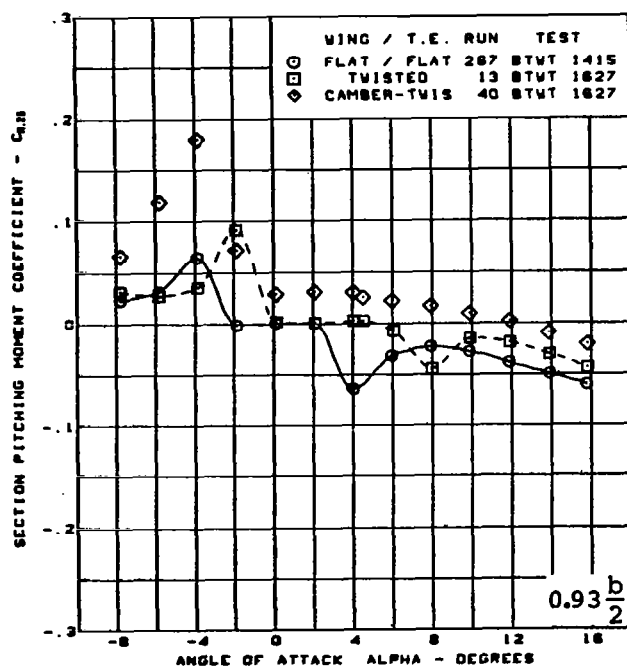
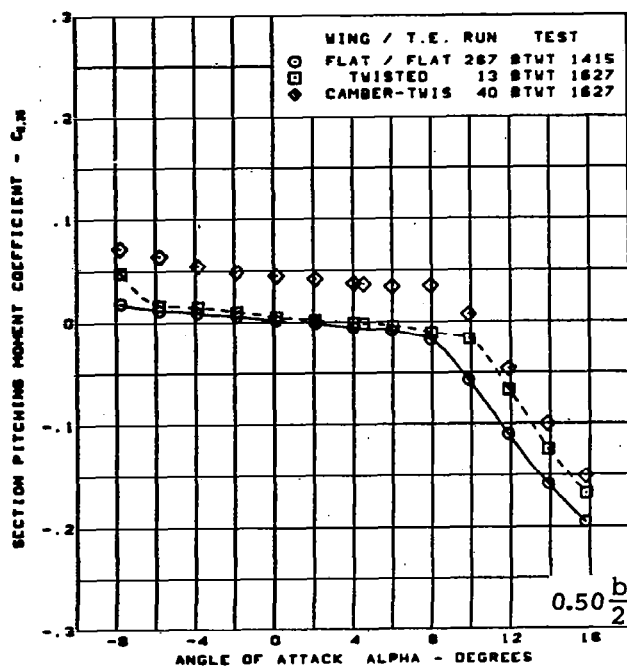
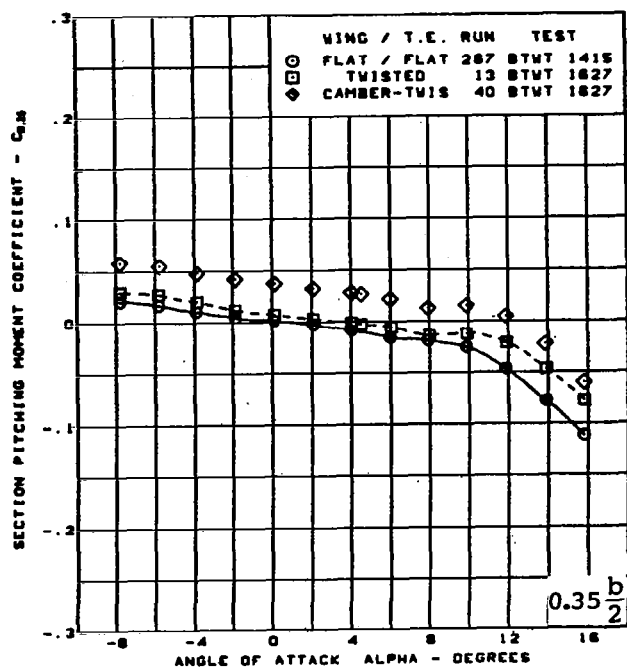
(m) (Concluded)

Figure 21. — (Continued)



(n) Section Aerodynamic Coefficients - Pitching Moment

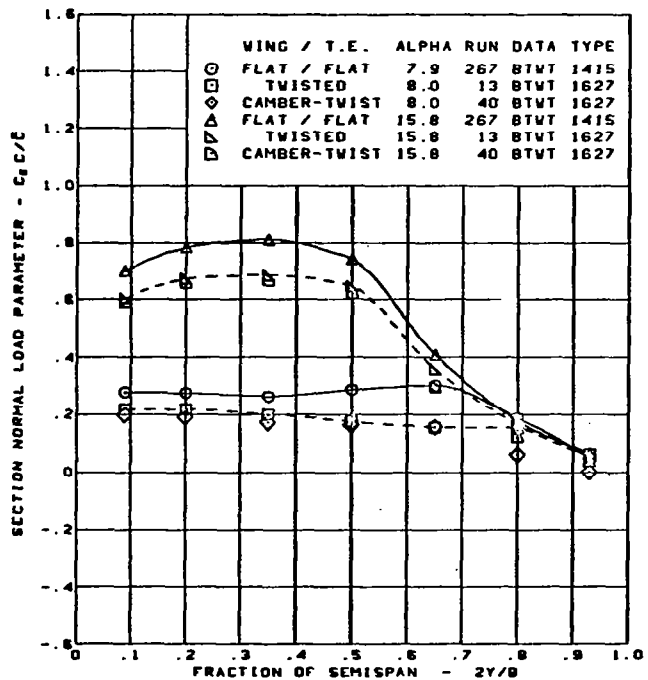
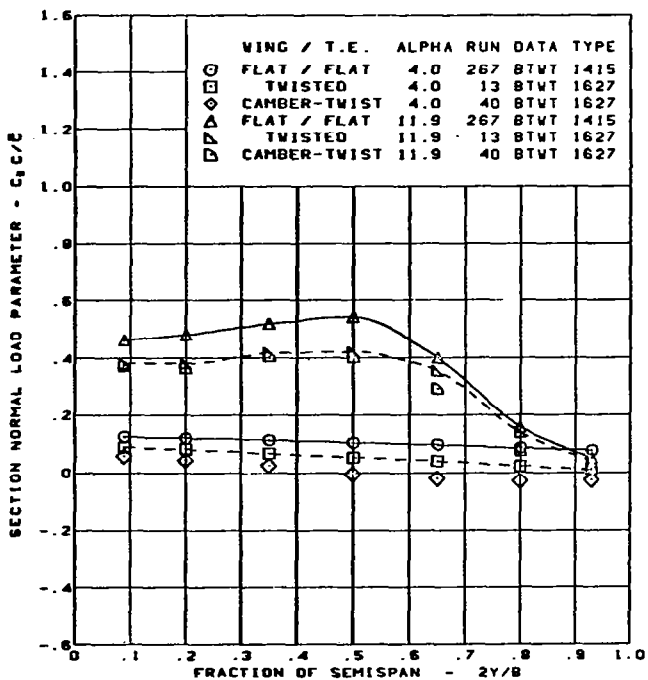
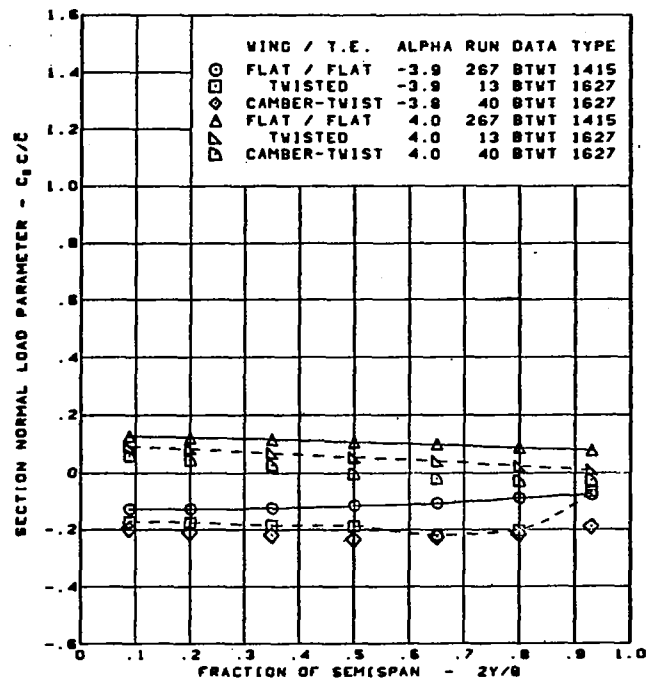
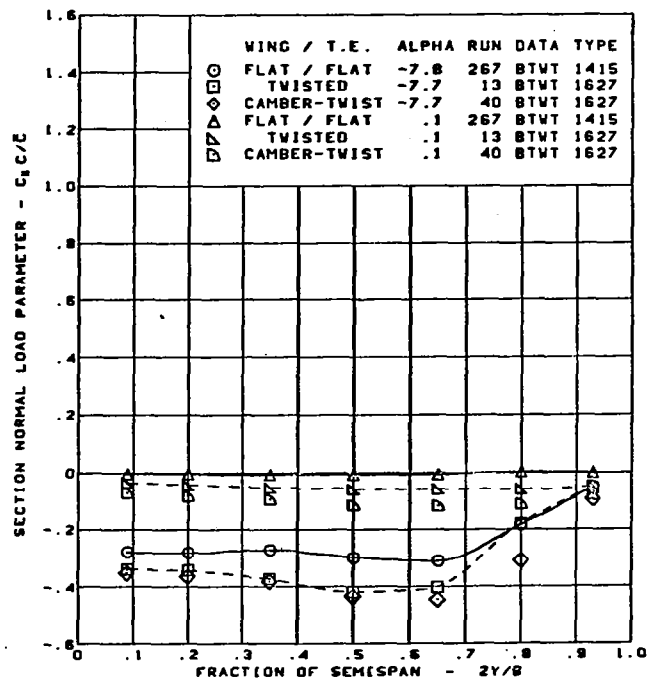
Figure 21. — (Continued)



M = 0.85  
 Rounded L.E.  
 L.E. deflection, full span =  $0.0^\circ$   
 T.E. deflection, full span =  $0.0^\circ$

(n) (Concluded)

Figure 21.—(Continued)

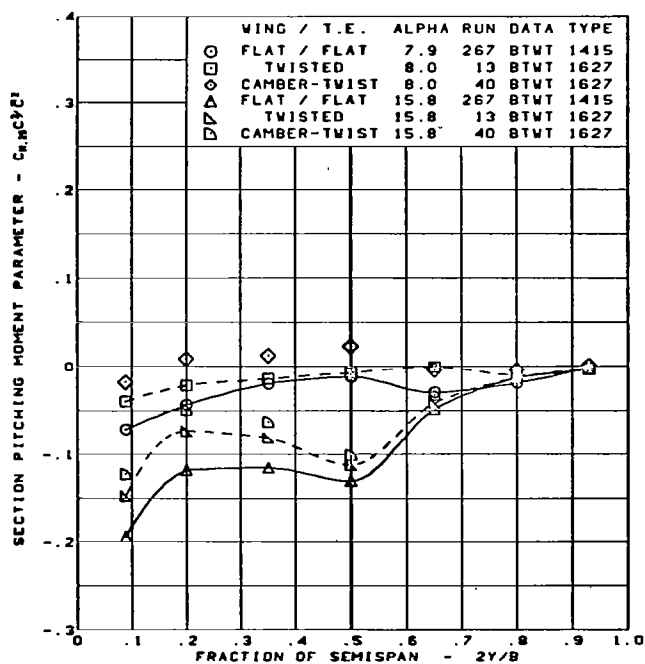
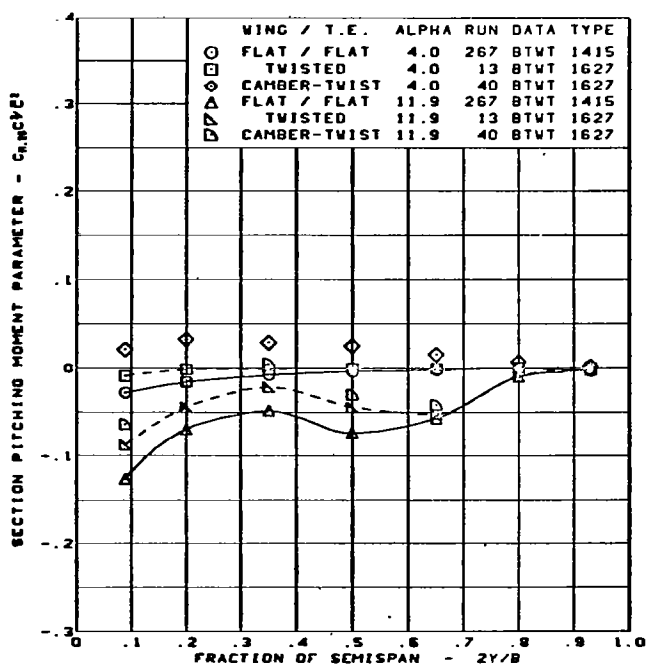
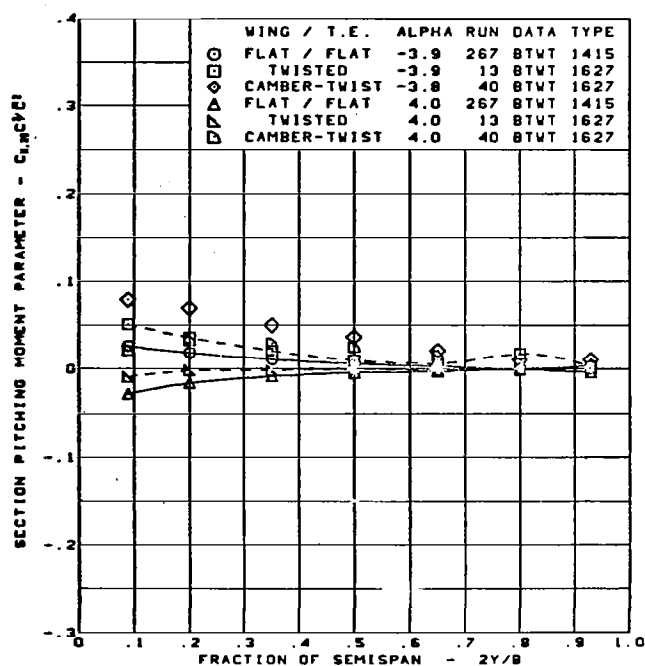
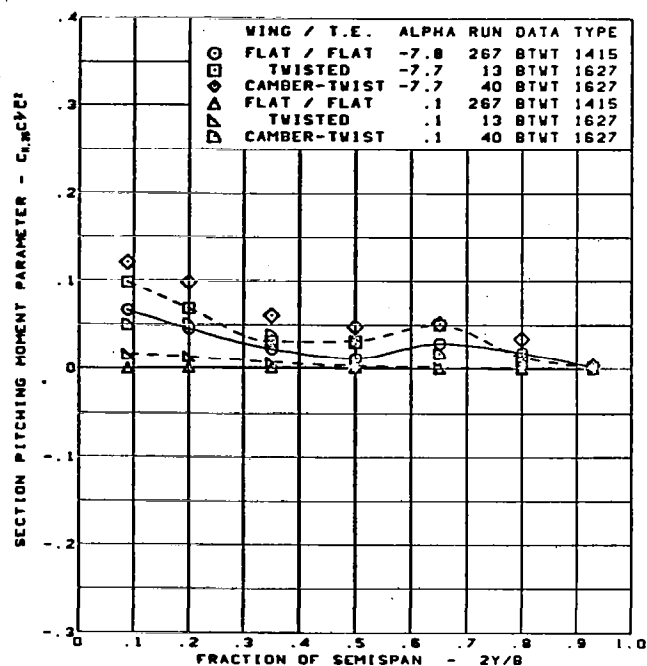


M = 0.85  
Rounded L.E.

L.E. deflection, full span = 0.0°  
T.E. deflection, full span = 0.0°

(o) Spanload Distributions - Normal Force

Figure 21. - (Continued)



M = 0.85  
Rounded L.E.

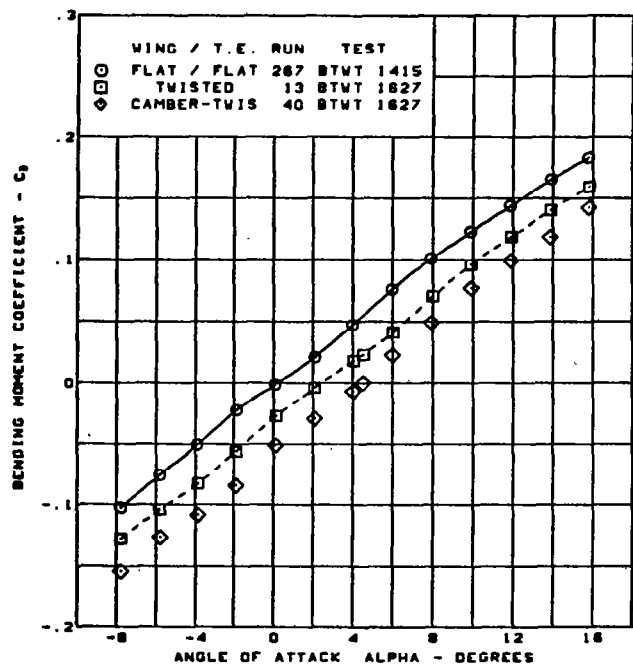
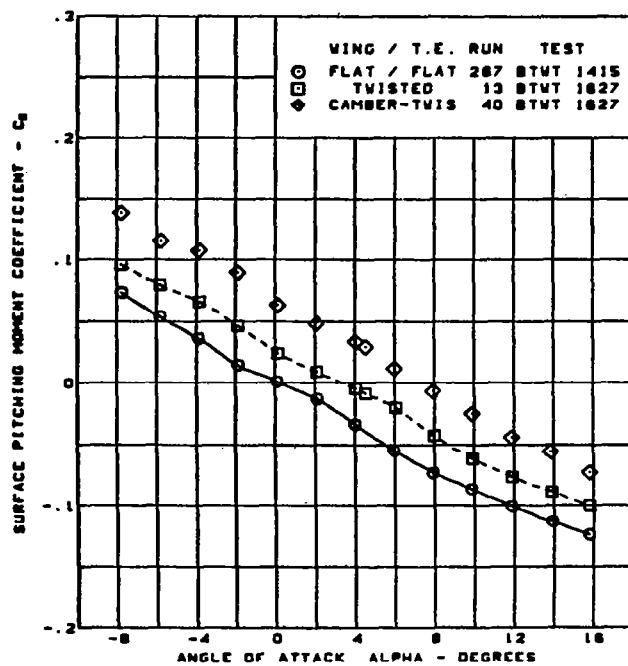
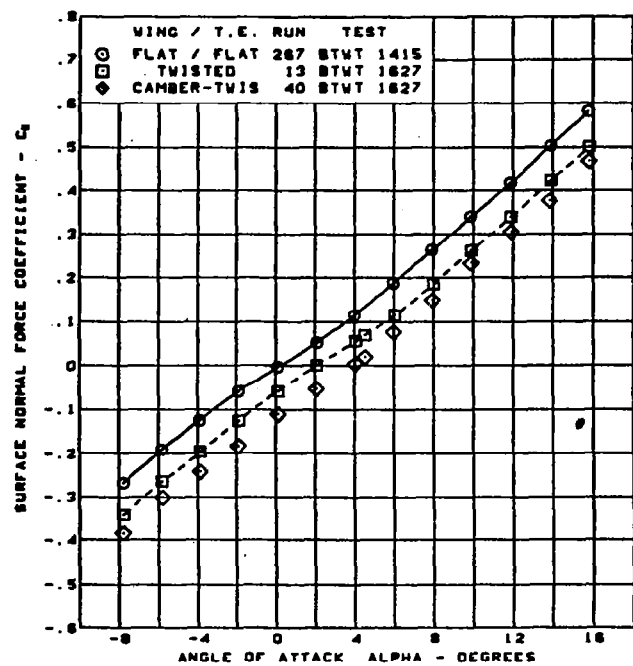
L.E. deflection, full span =  $0.0^\circ$   
T.E. deflection, full span =  $0.0^\circ$

(p) Spanload Distributions - Pitching Moment

Figure 21. — (Continued)



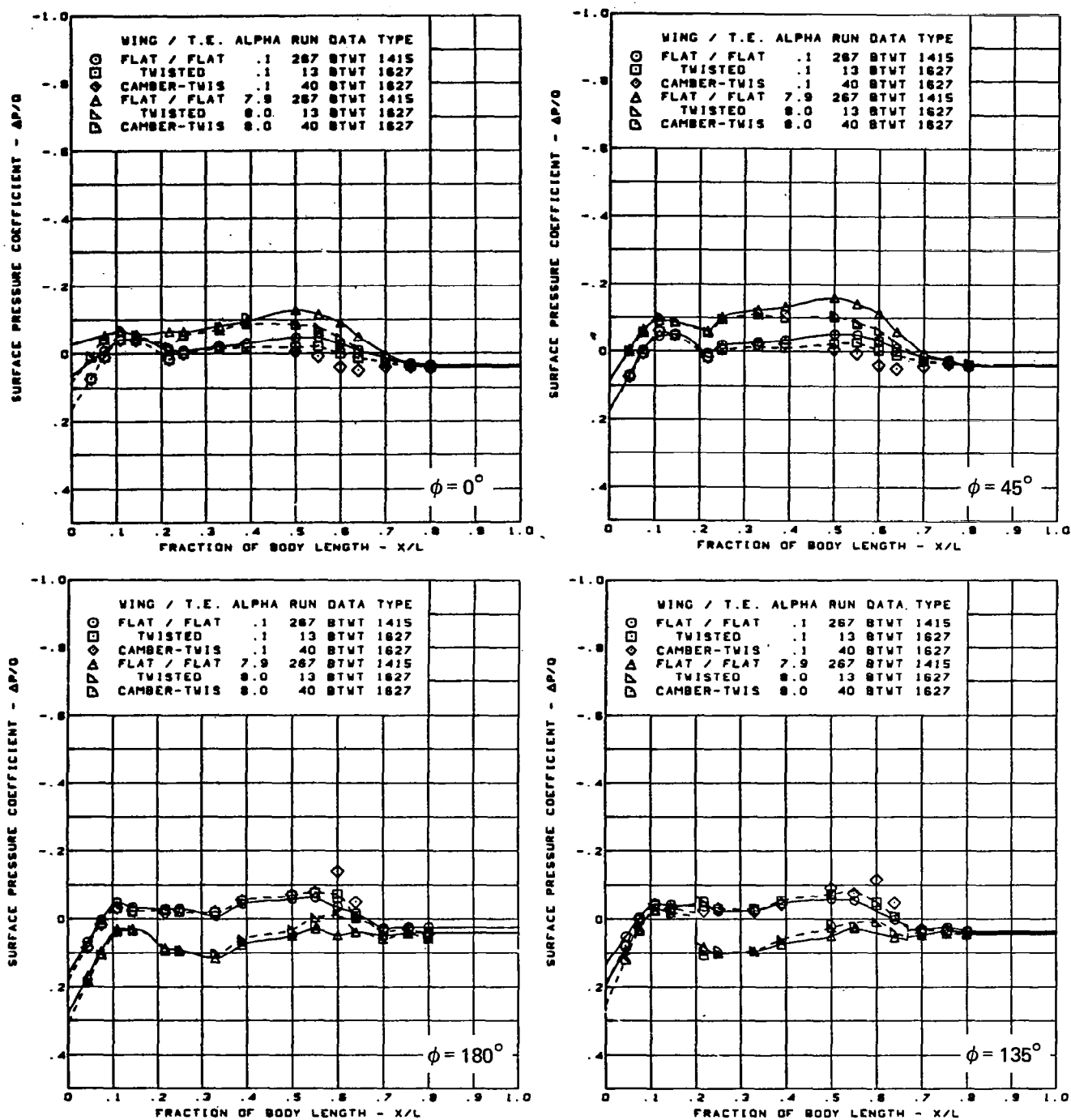




$M = 0.85$   
 Rounded L.E.  
 L.E. deflection, full span =  $0.0^\circ$   
 T.E. deflection, full span =  $0.0^\circ$

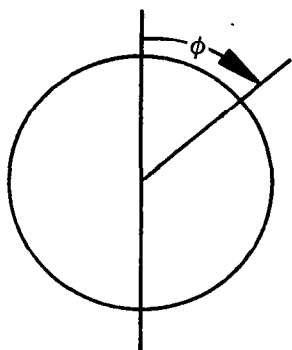
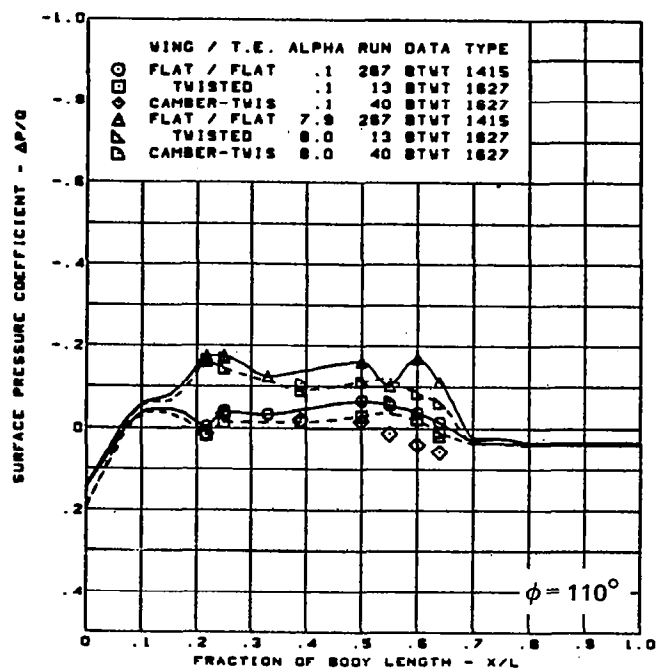
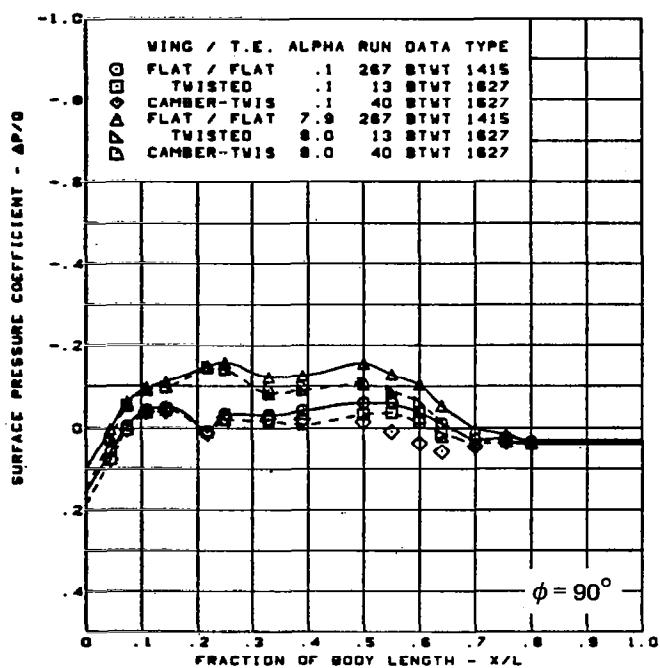
(q) Wing Aerodynamic Coefficients

Figure 21. - (Concluded)



(a) Surface Longitudinal Pressure Distributions,  $\alpha = 0^\circ$  and  $8^\circ$

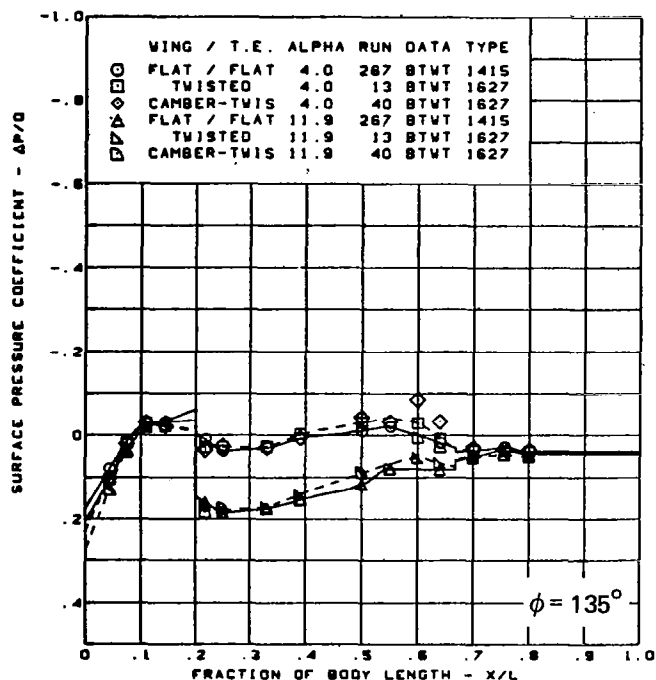
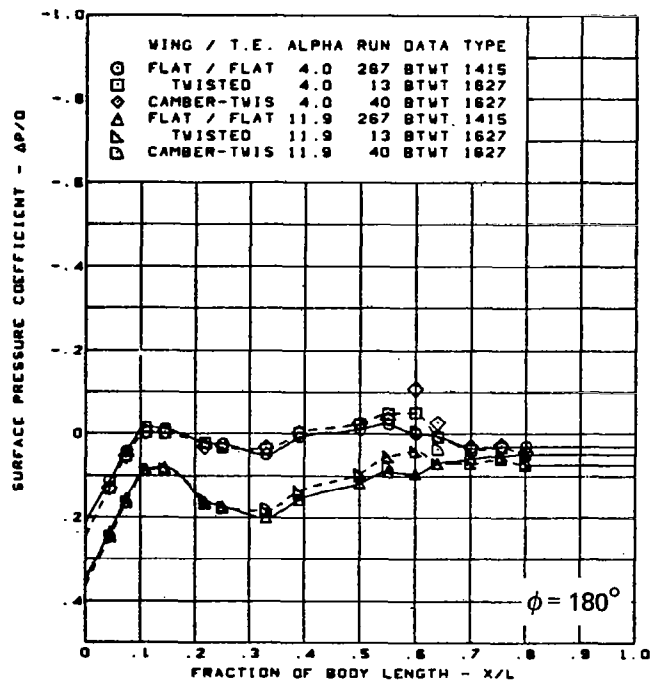
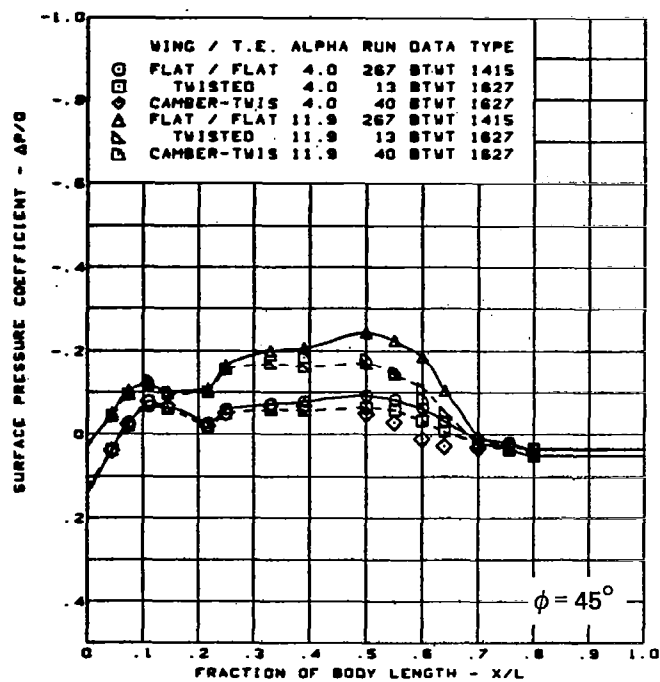
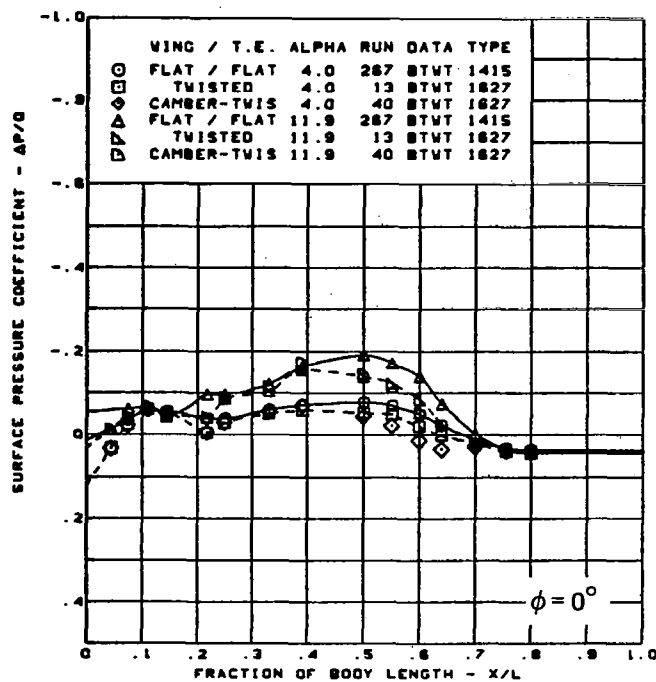
Figure 22. — Body Experimental Data—Effect of Wing Shape; T.E. Deflection, Full Span =  $0.0^\circ$ ;  $M = 0.85$



$M = 0.85$   
 $\alpha = 0^\circ$  and  $8^\circ$   
 Rounded L.E.  
 L.E. deflection, full span =  $0.0^\circ$   
 T.E. deflection, full span =  $0.0^\circ$

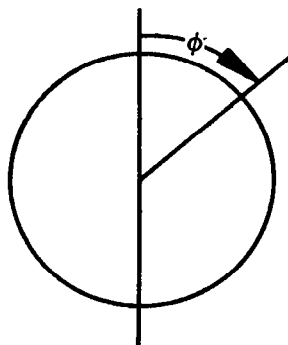
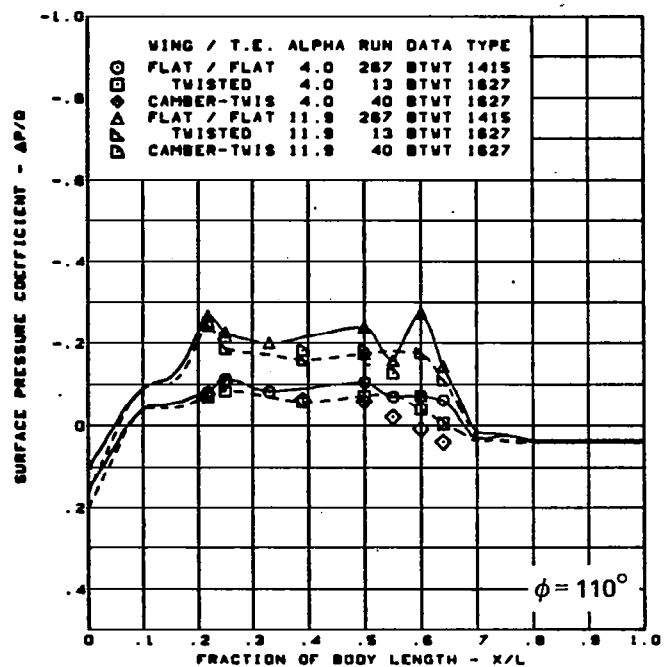
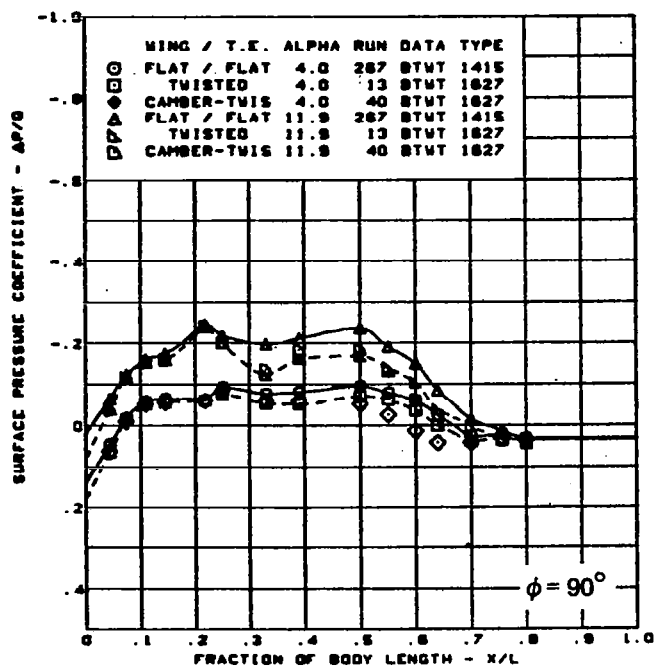
(a) (Concluded)

Figure 22. — (Continued)



(b) Surface Longitudinal Pressure Distributions,  $\phi = 4^\circ$  and  $12^\circ$

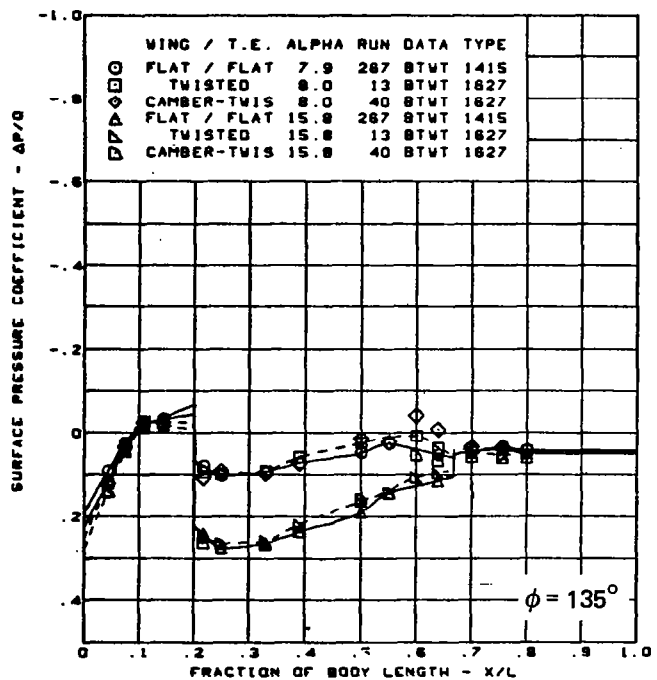
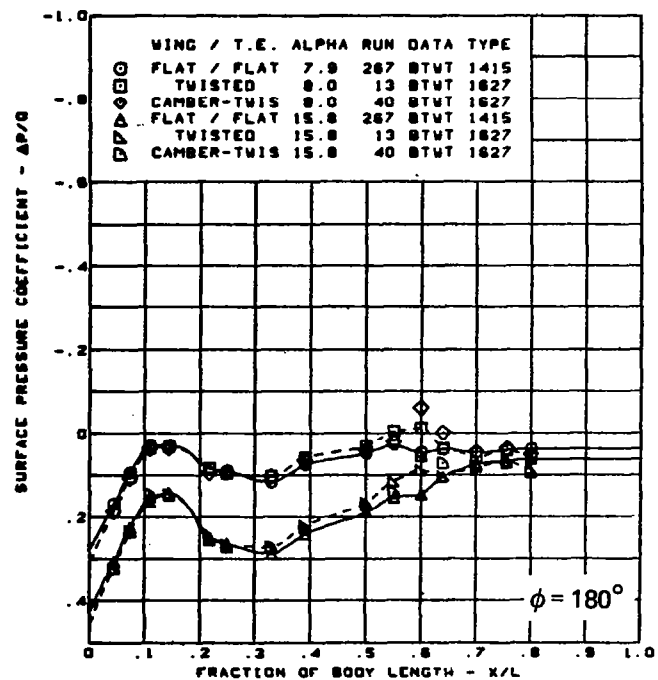
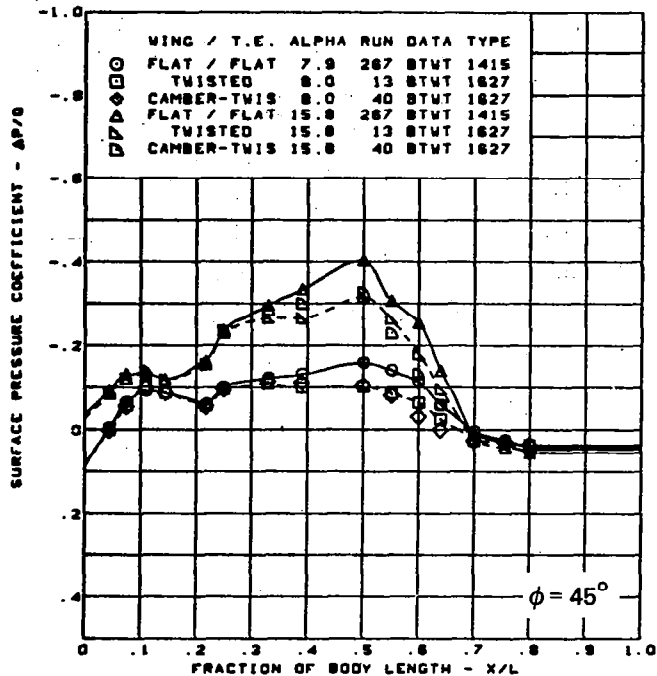
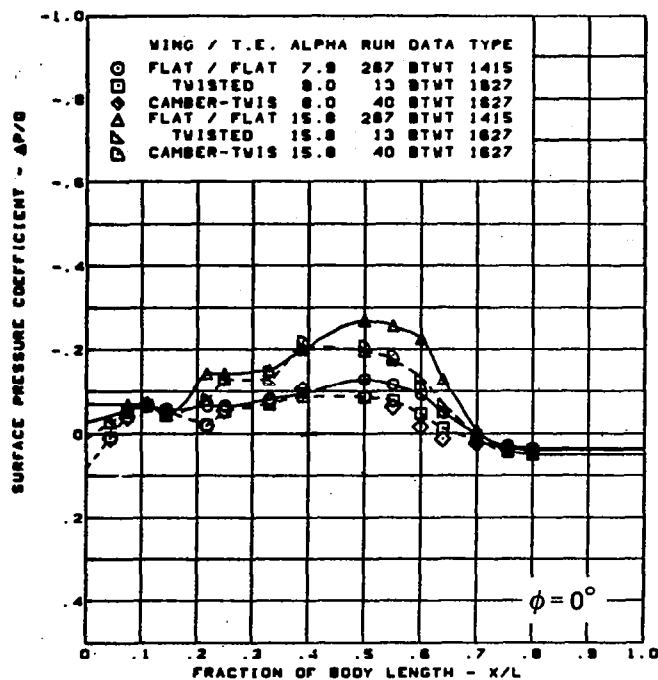
Figure 22. - (Continued)



$M = 0.85$   
 $\alpha = 4^\circ$  and  $12^\circ$   
 Rounded L.E.  
 L.E. deflection, full span =  $0.0^\circ$   
 T.E. deflection, full span =  $0.0^\circ$

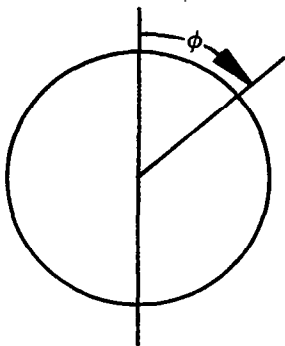
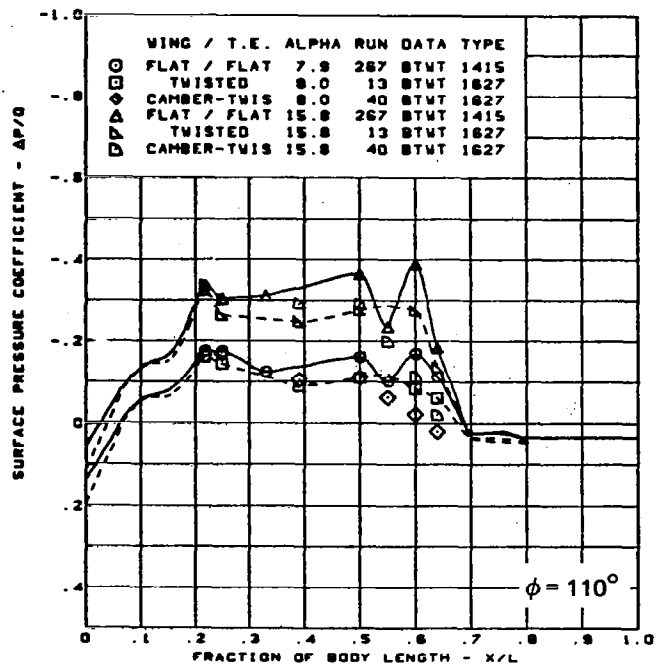
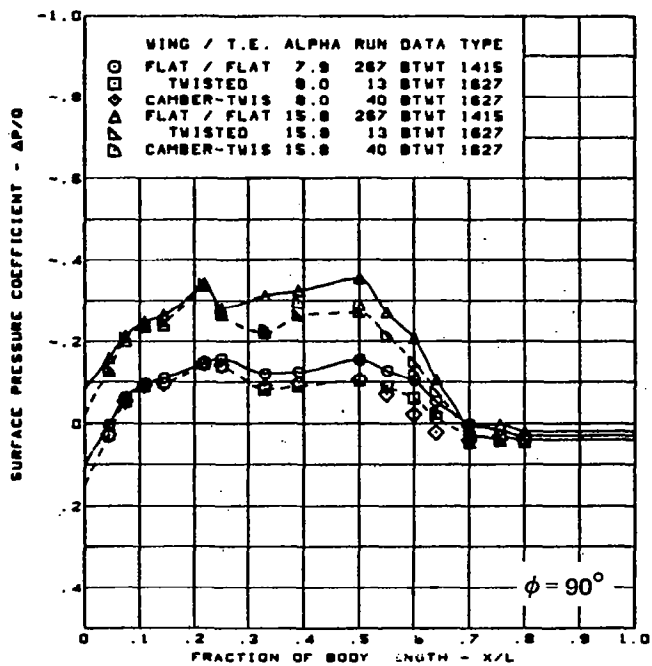
(b) (Concluded)

Figure 22. — (Continued)



(c) Surface Longitudinal Pressure Distributions,  $\alpha = 8^\circ$  and  $16^\circ$

Figure 22. — (Continued)

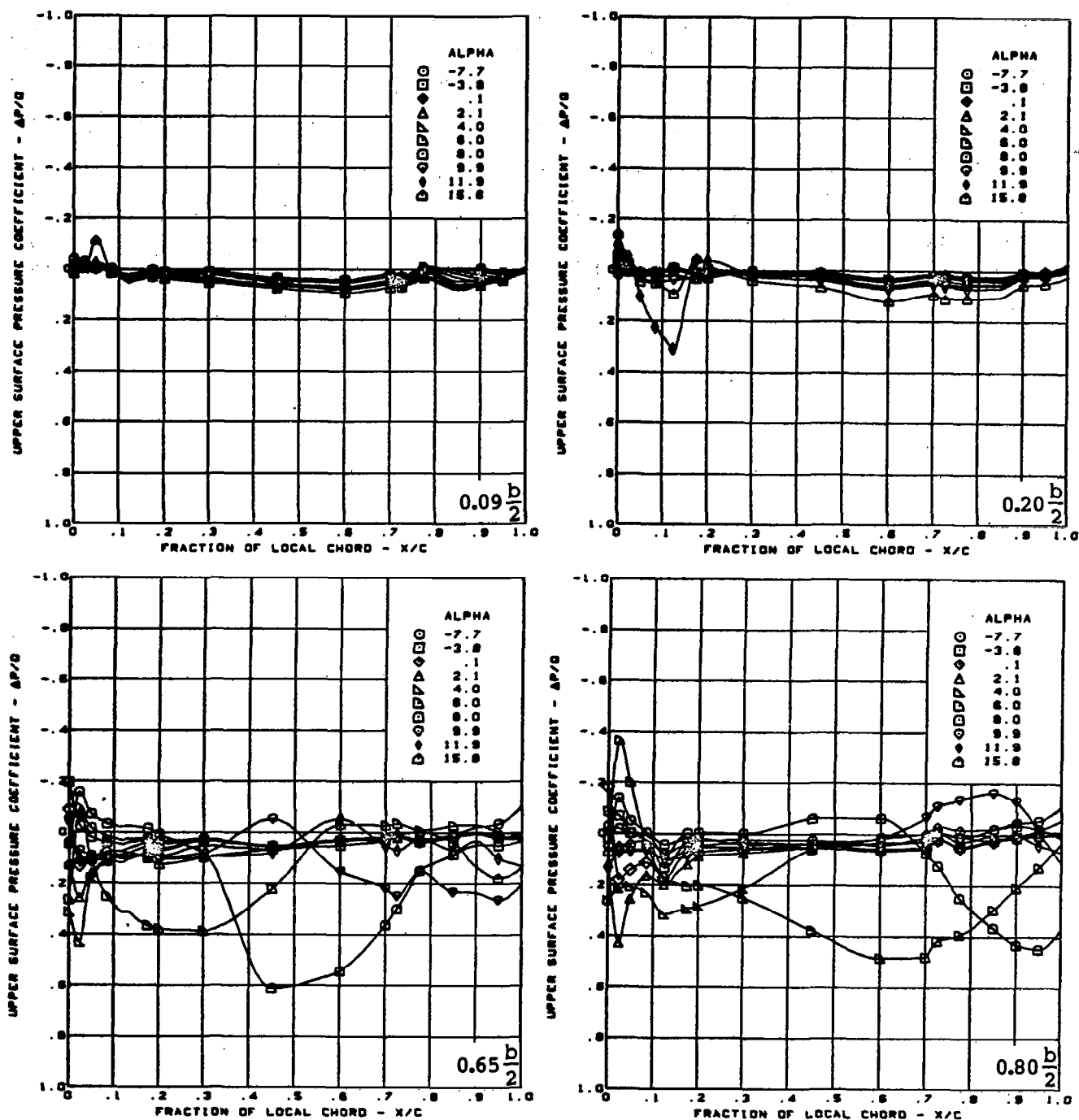


$M = 0.85$   
 $\alpha = 8^\circ$  and  $16^\circ$   
 Rounded L.E.  
 L.E. deflection, full span =  $0.0^\circ$   
 T.E. deflection, full span =  $0.0^\circ$

(c) (Concluded)

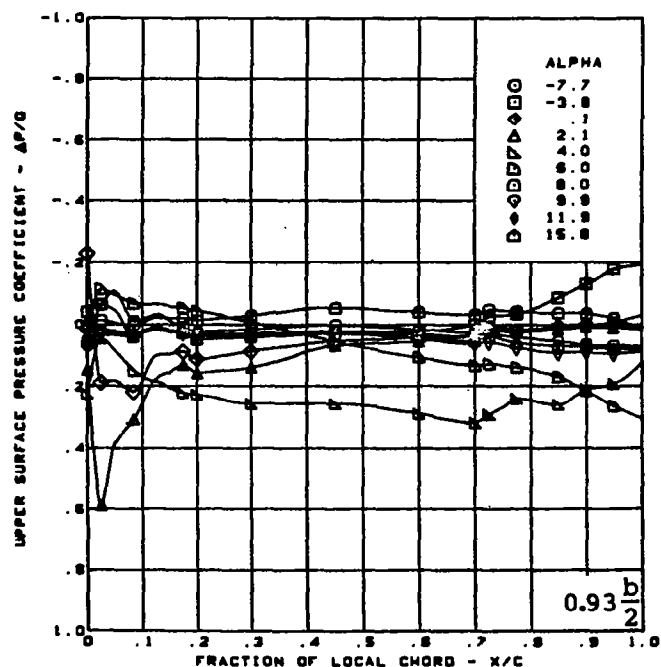
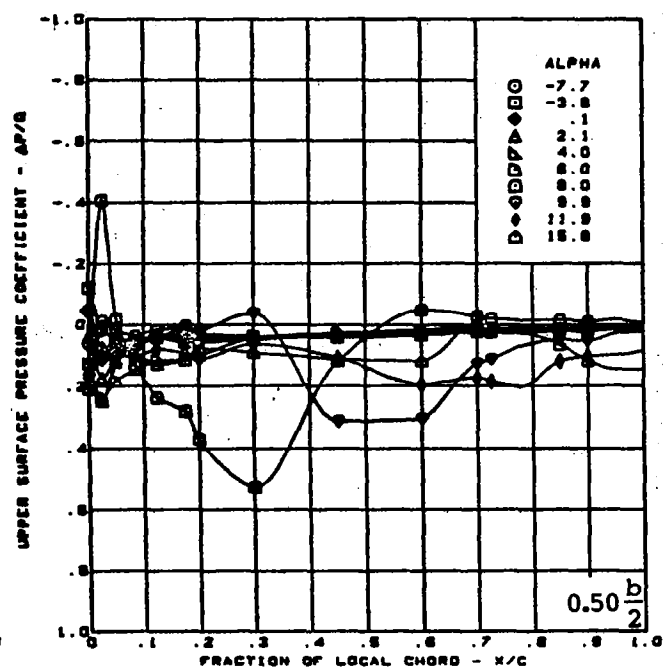
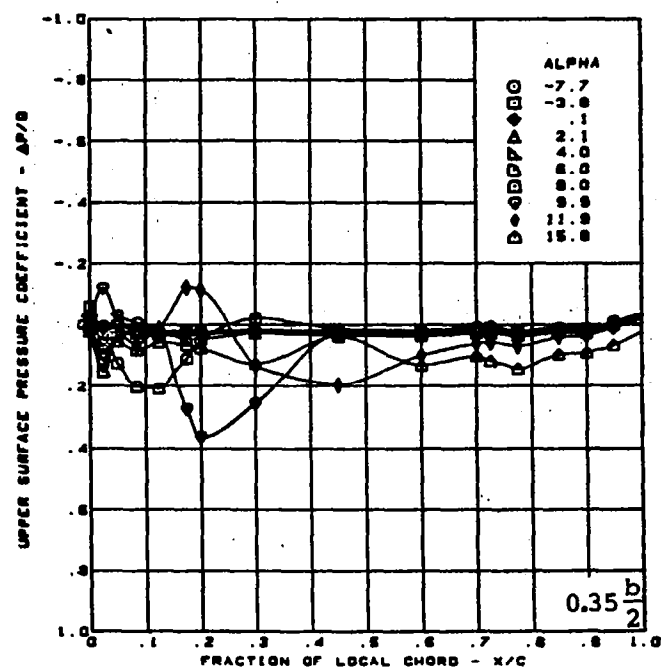
Figure 22. - (Concluded)





(a) Upper Surface Chordwise Pressure Distributions

Figure 23. — Wing Experimental Data—Effect of Incremental Twist;  
T.E. Deflection, Full Span =  $0.0^\circ$ ;  $M = 0.85$



$M = 0.85$

Twisted wing data minus flat wing data

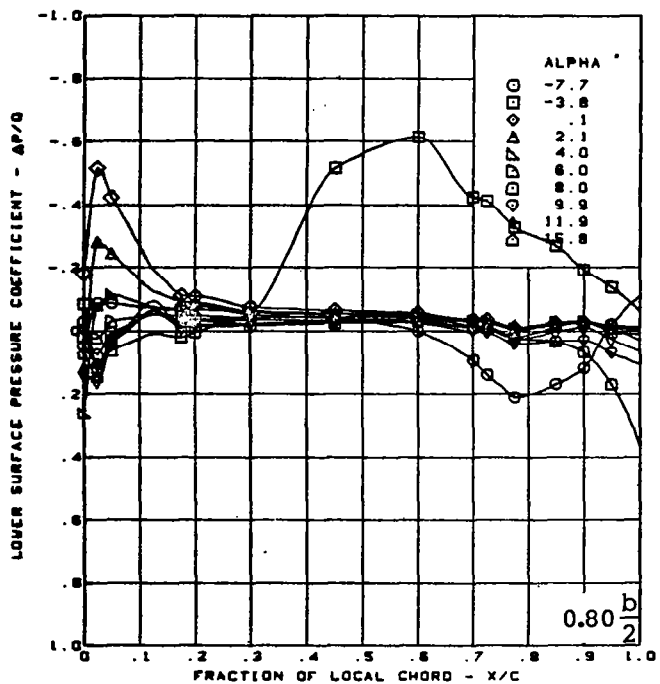
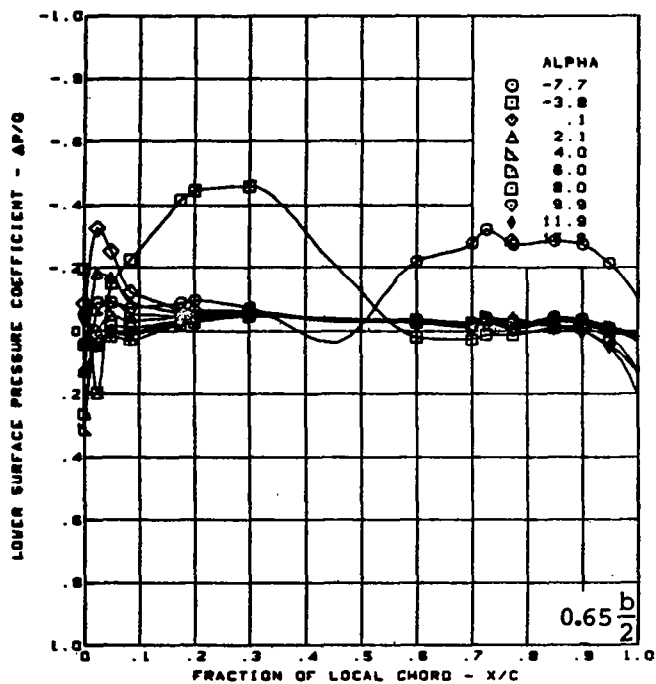
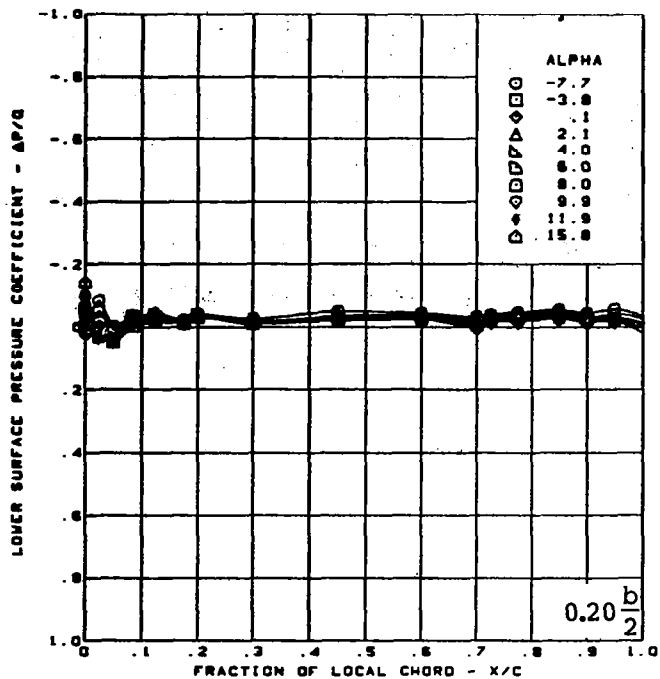
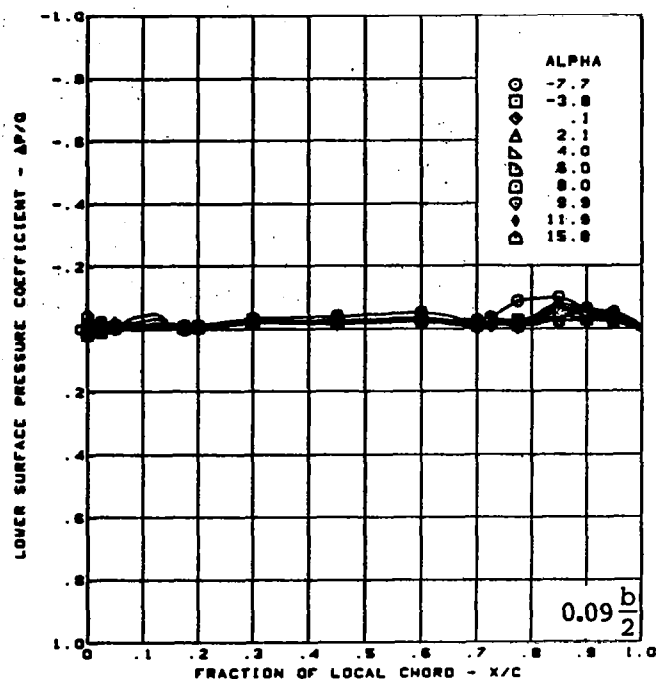
Rounded L.E.

L.E. deflection, full span =  $0.0^\circ$

T.E. deflection, full span =  $0.0^\circ$

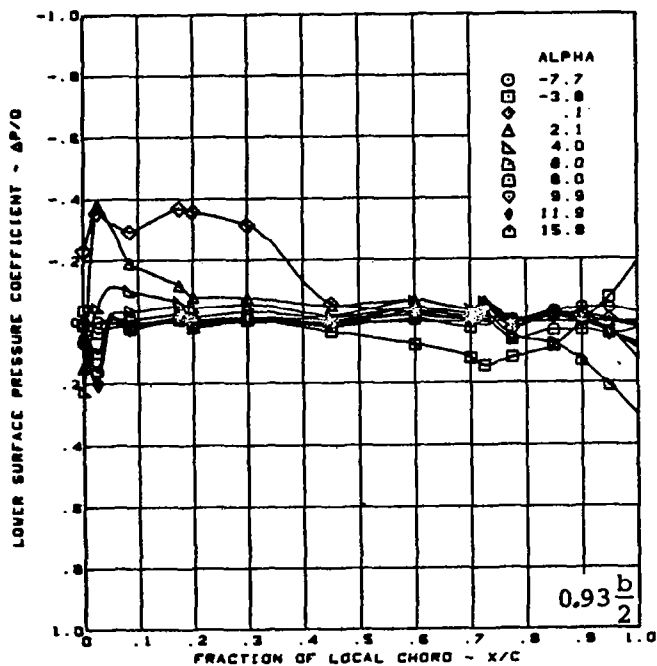
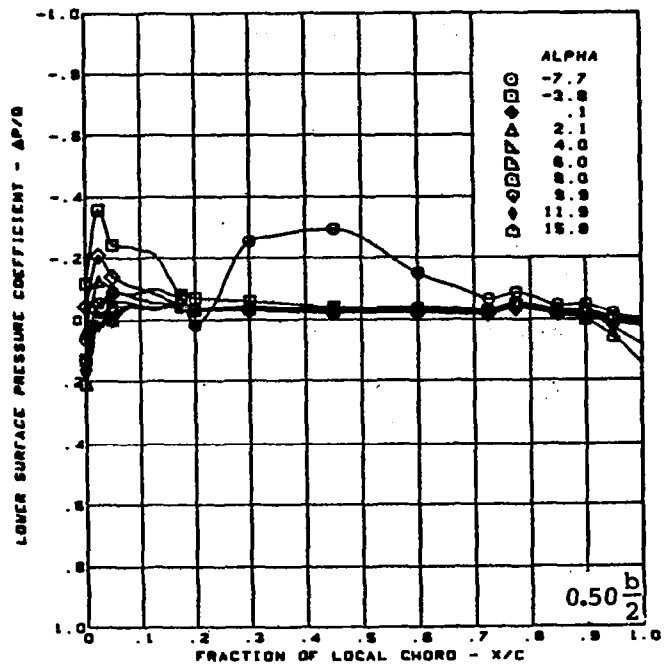
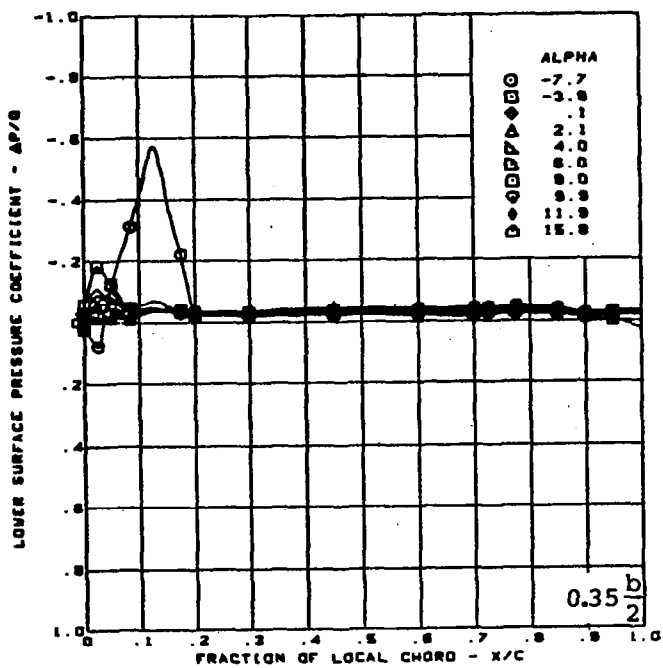
(a) (Concluded)

Figure 23. — (Continued)



(b) Lower Surface Chordwise Pressure Distributions

Figure 23. - (Continued)



$M = 0.85$

Twisted wing data minus flat wing data

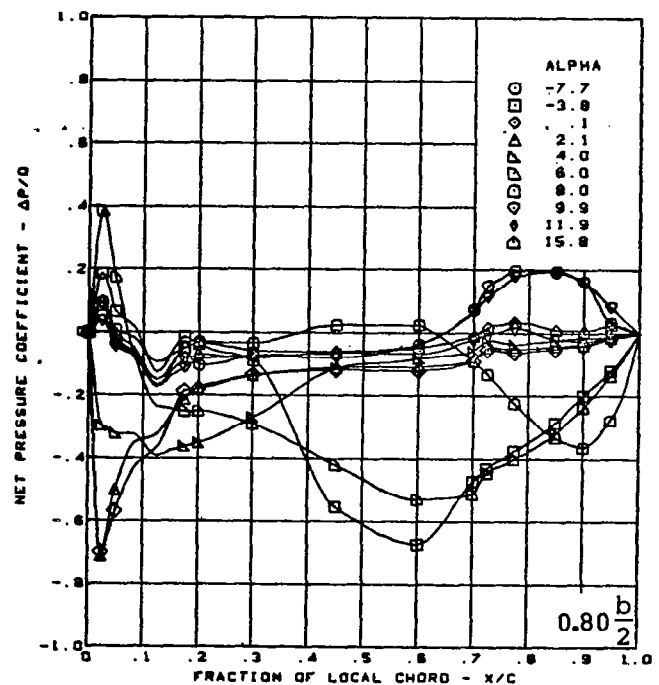
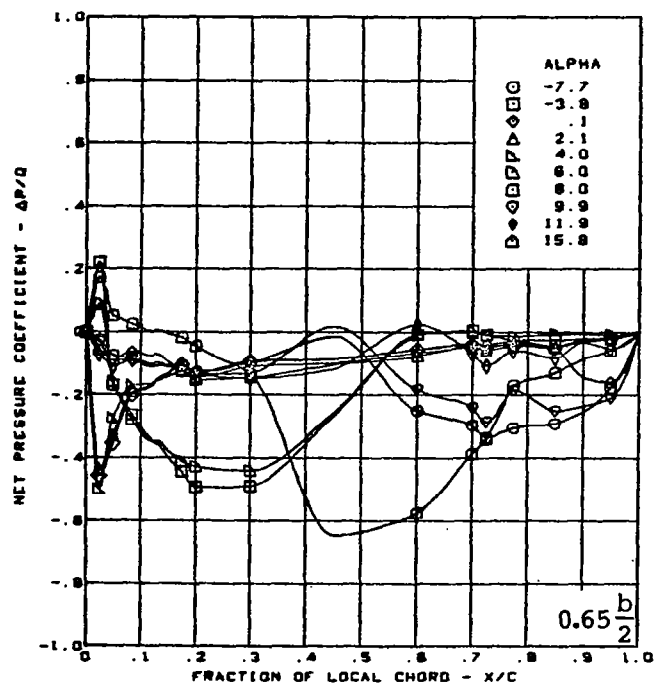
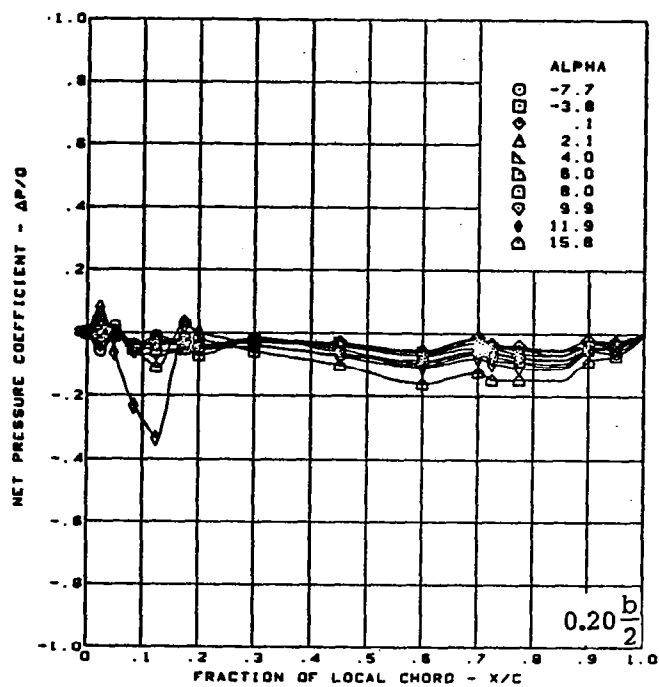
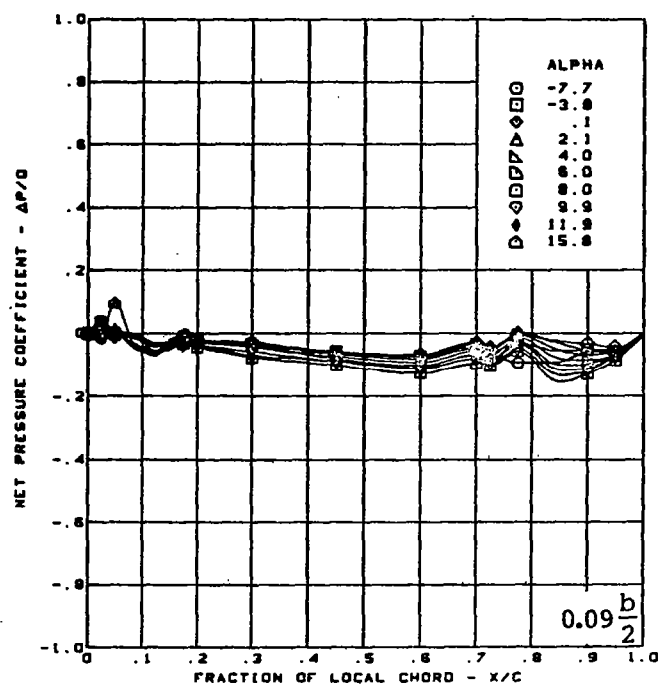
Rounded L.E.

L.E. deflection, full span =  $0.0^\circ$

T.E. deflection, full span =  $0.0^\circ$

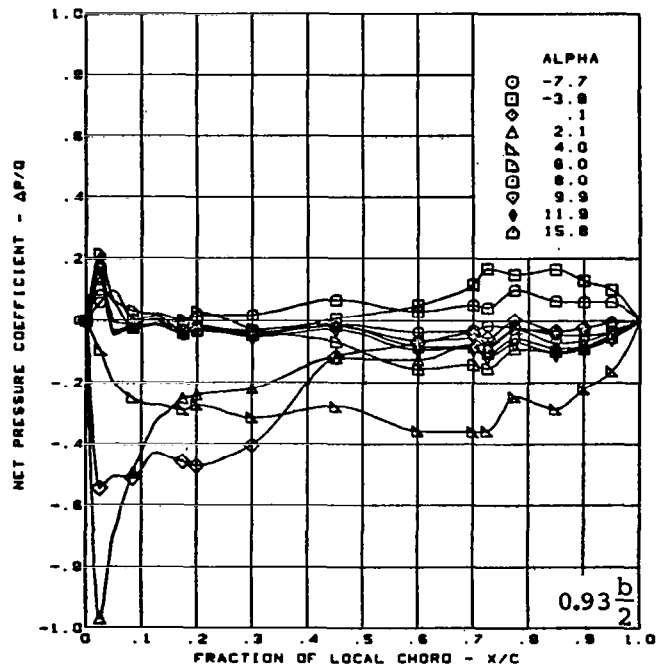
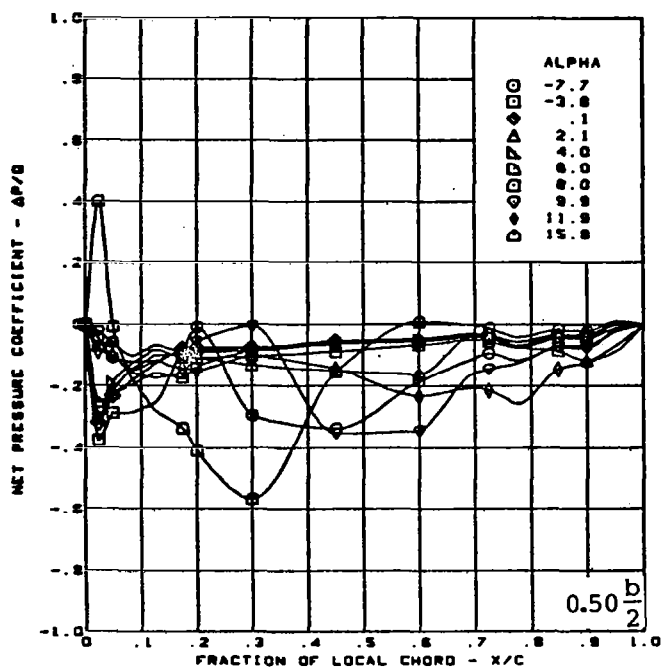
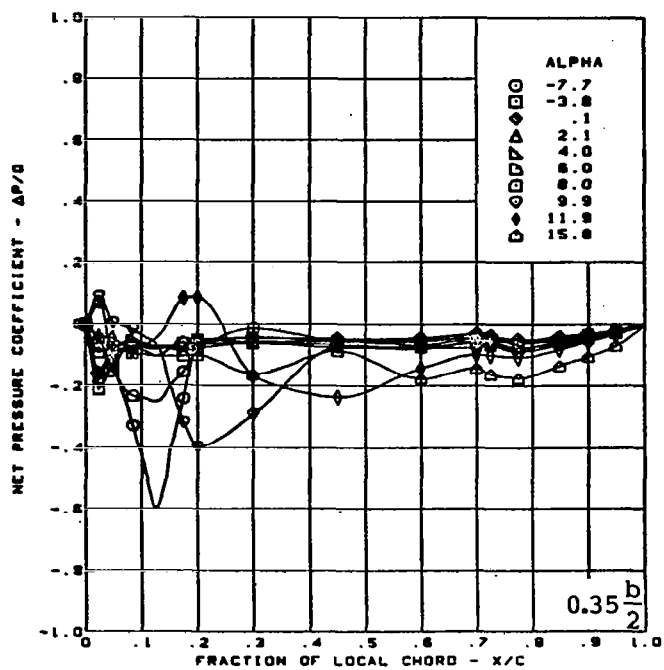
(b) (Concluded)

Figure 23. - (Continued)



(c) Net Chordwise Pressure Distributions

Figure 23. — (Continued)

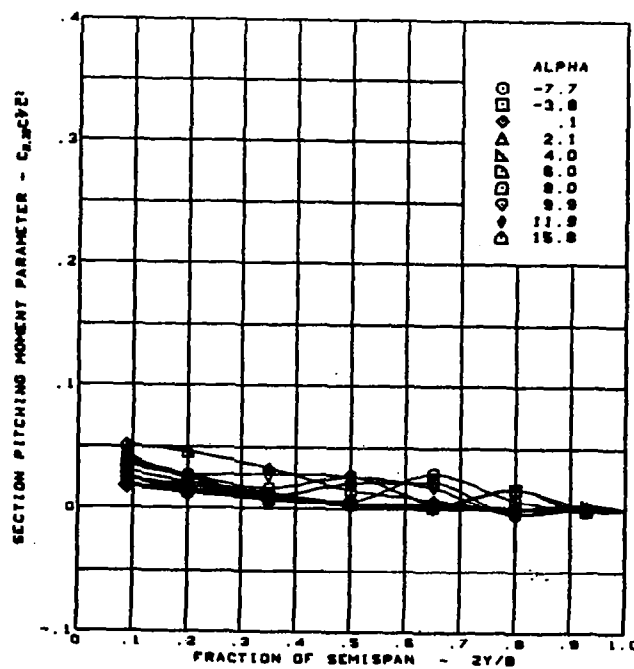
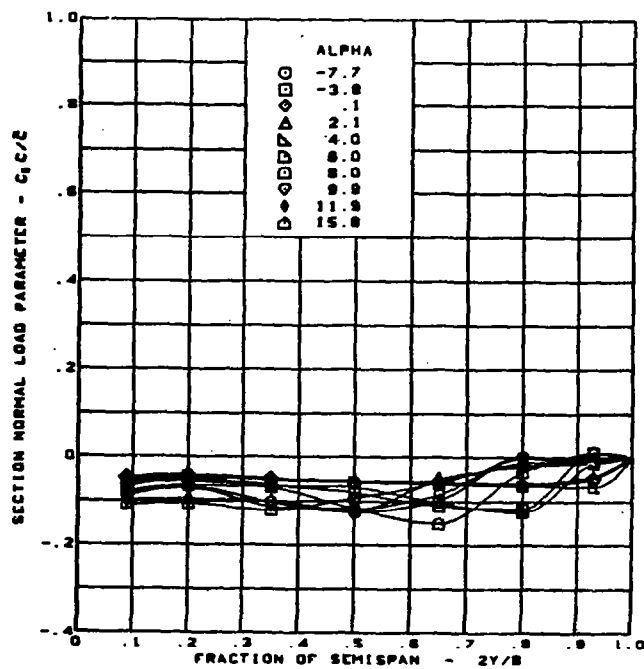


$M = 0.85$   
 Twisted wing data minus flat wing data  
 Rounded L.E.  
 L.E. deflection, full span =  $0.0^\circ$

(c) (Concluded)

Figure 23. — (Continued)



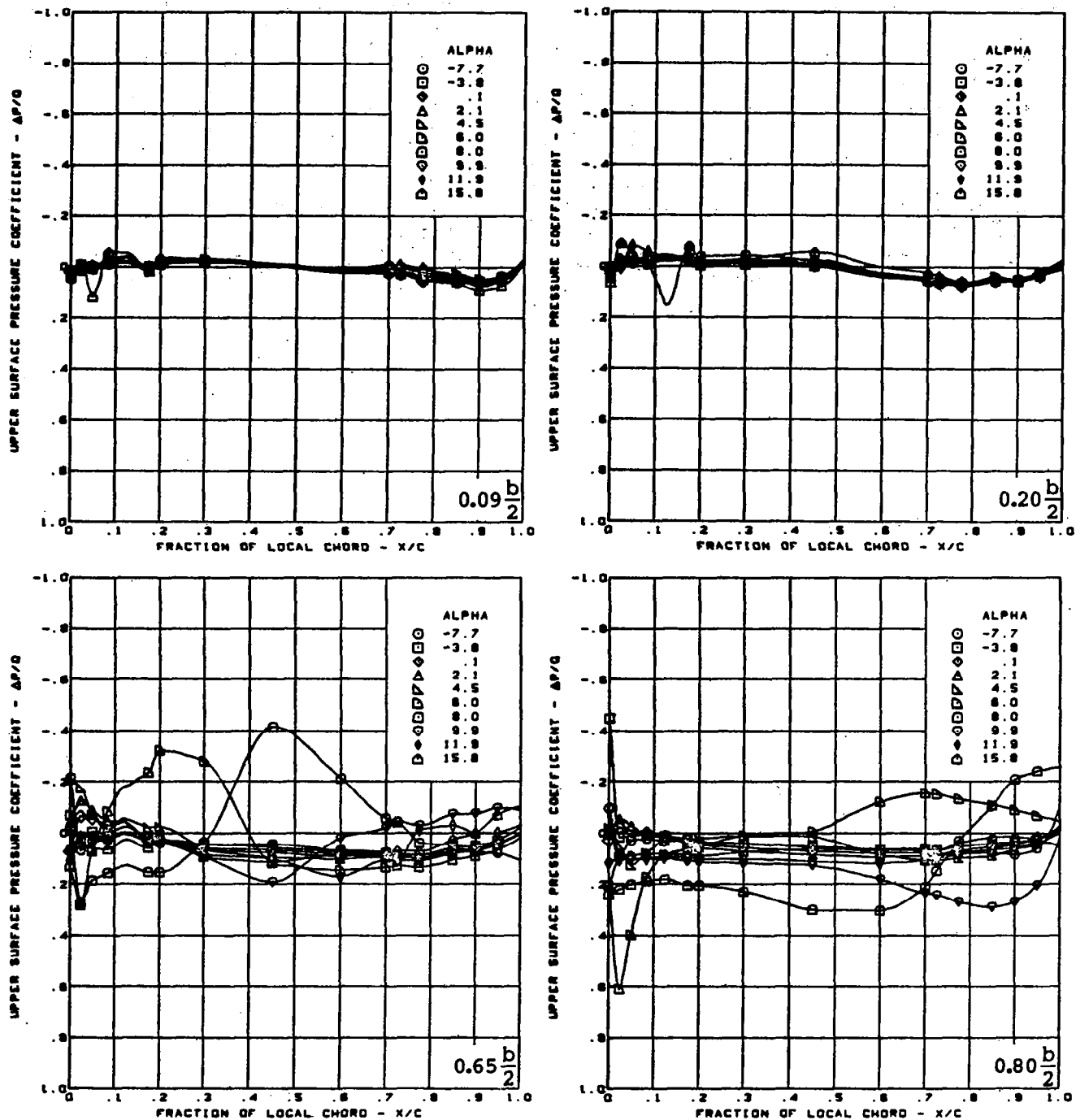


$M = 0.85$   
 Twisted wing data minus flat wing data  
 Rounded L.E.  
 L.E. deflection, full span =  $0.0^\circ$   
 T.E. deflection, full span =  $0.0^\circ$

(d) Spanload Distributions

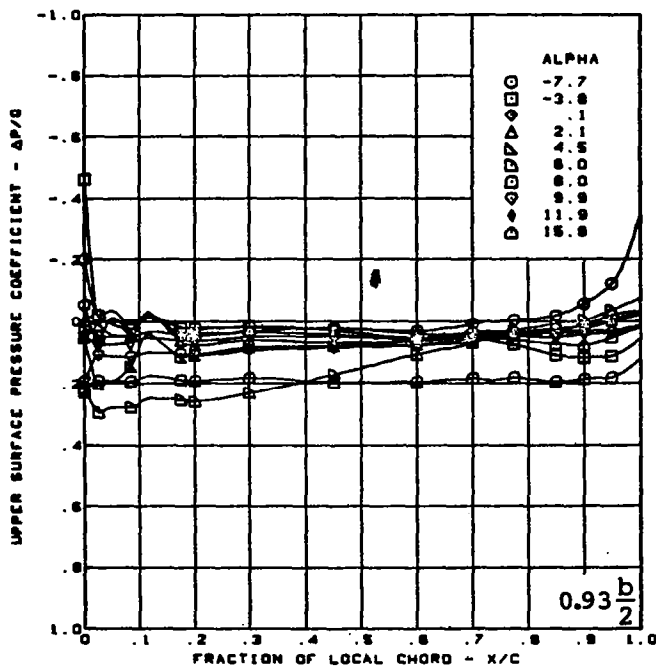
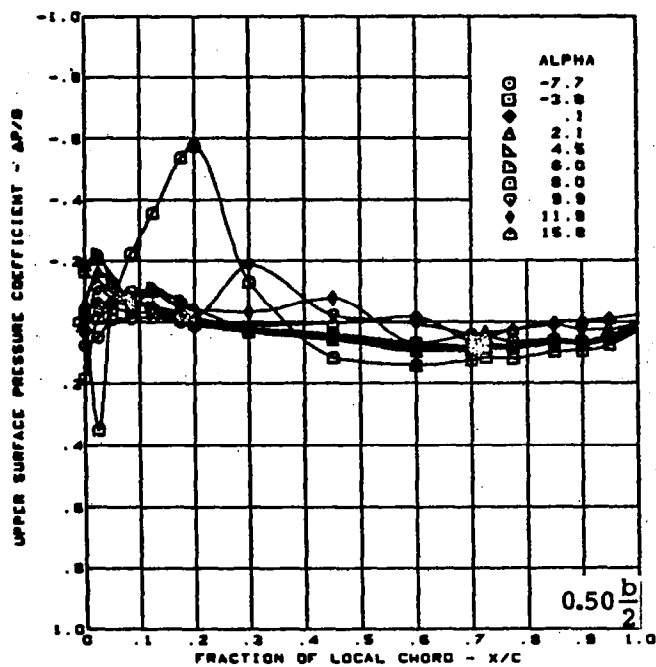
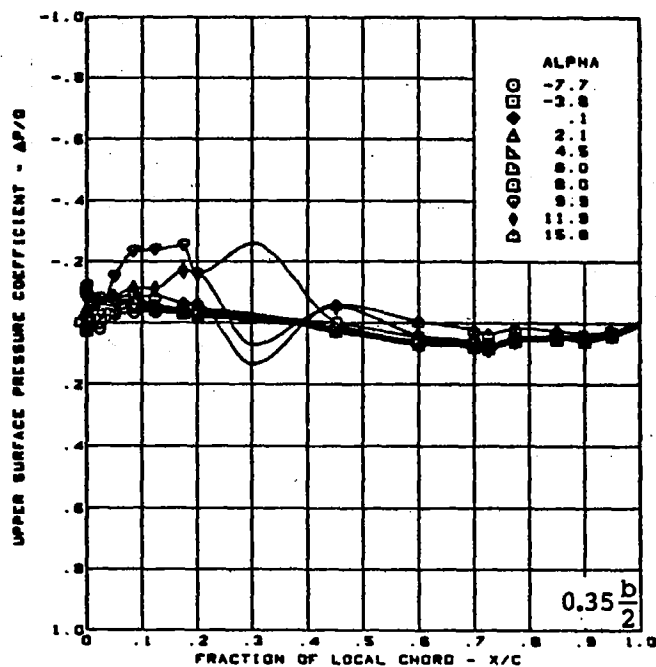
Figure 23. — (Concluded)





(a) Upper Surface Chordwise Pressure Distributions

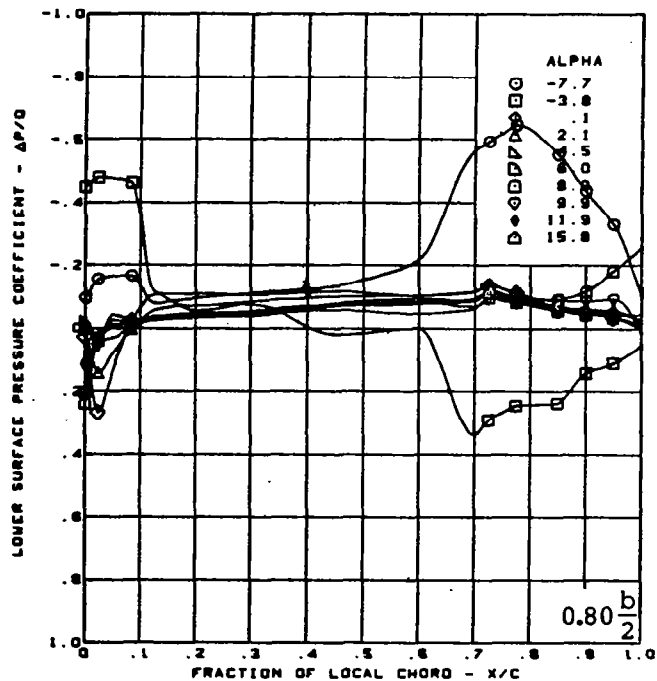
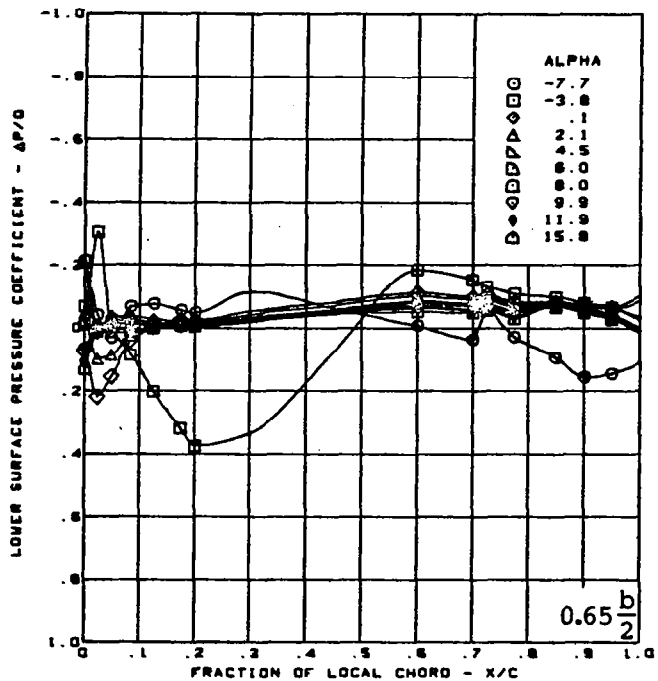
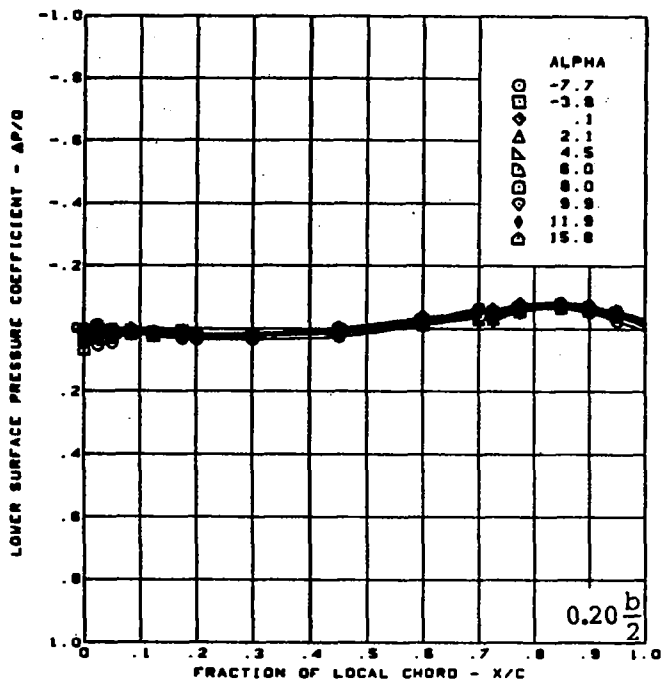
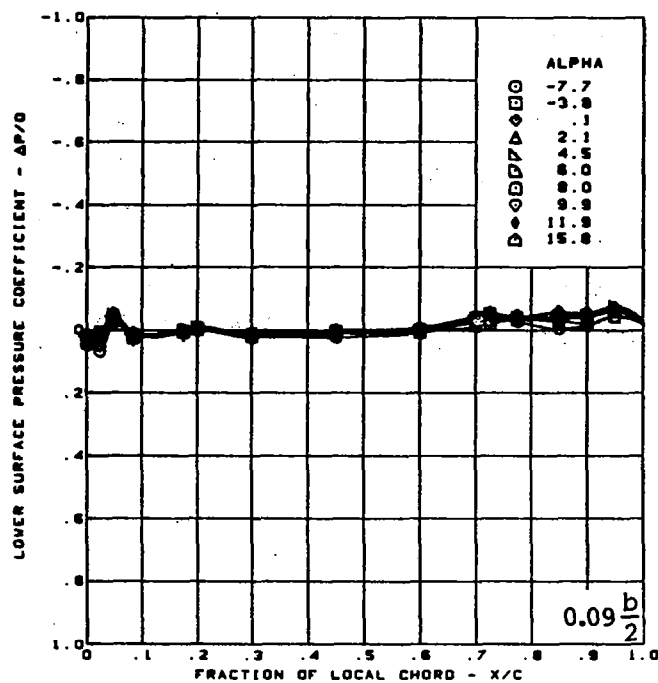
Figure 24. — Wing Experimental Data—Effect of Incremental Camber;  
T.E. Deflection, Full Span =  $0.0^\circ$ ;  $M = 0.85$



$M = 0.85$   
 Cambered-twisted wing data  
 minus twisted wing data  
 Rounded L.E.  
 Fin off  
 L.E. deflection, full span =  $0.0^\circ$   
 T.E. deflection, full span =  $0.0^\circ$

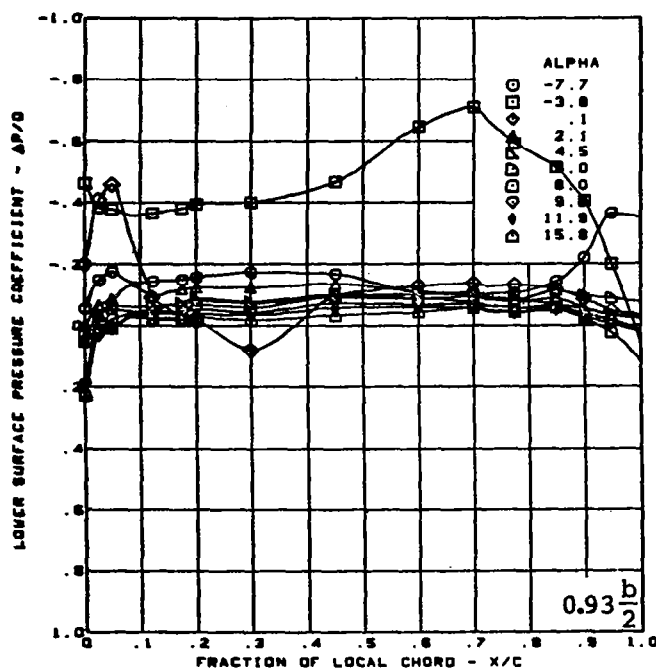
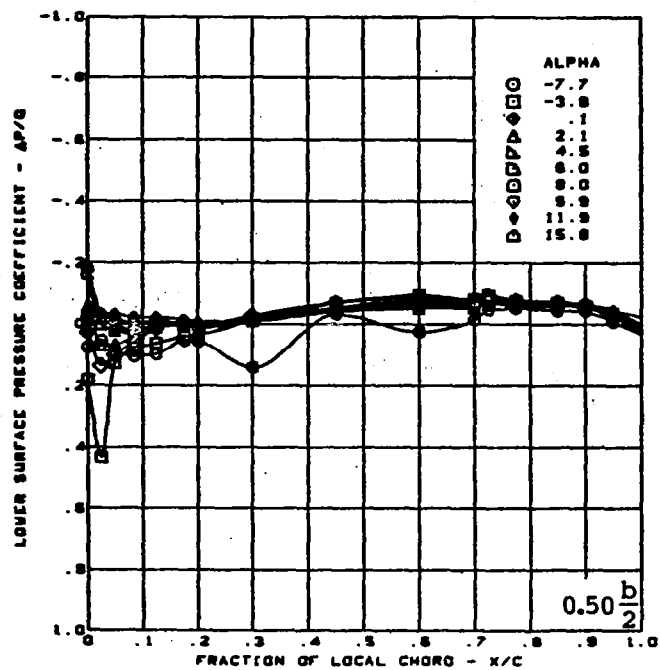
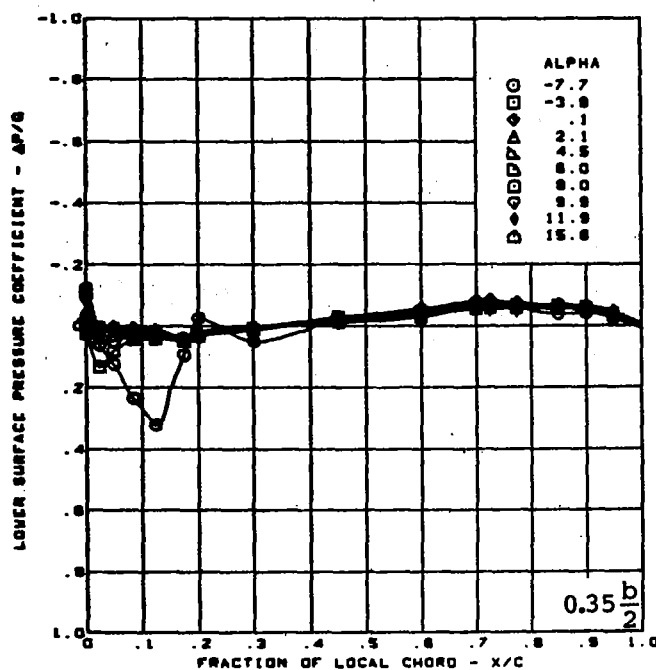
(a) (Concluded)

Figure 24. — (Continued)



(b) Lower Surface Chordwise Pressure Distributions

Figure 24. — (Continued)



$M = 0.85$

Cambered-twisted wing data  
minus twisted wing data

Rounded L.E.

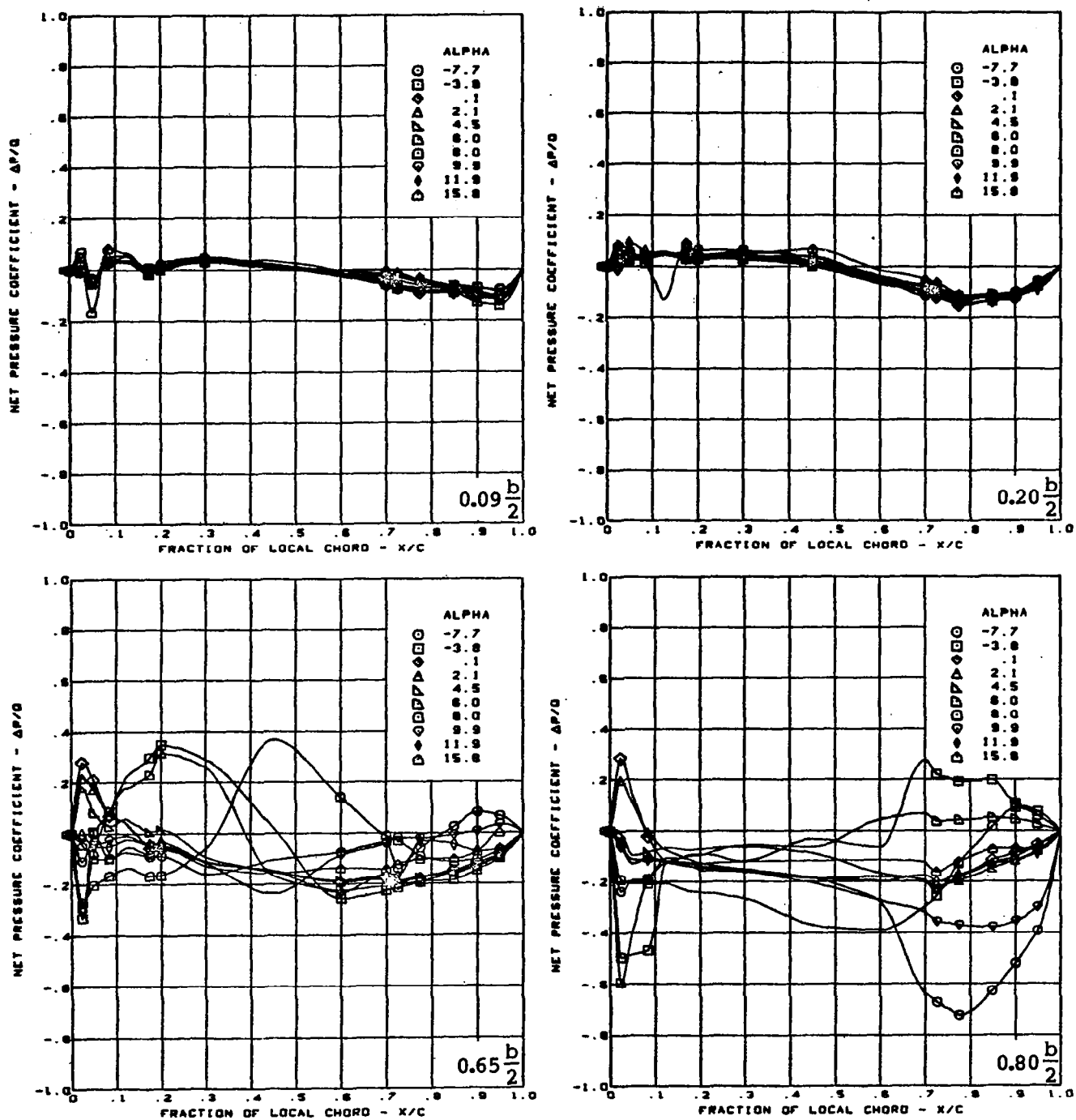
Fin off

L.E. deflection, full span =  $0.0^\circ$

T.E. deflection, full span =  $0.0^\circ$

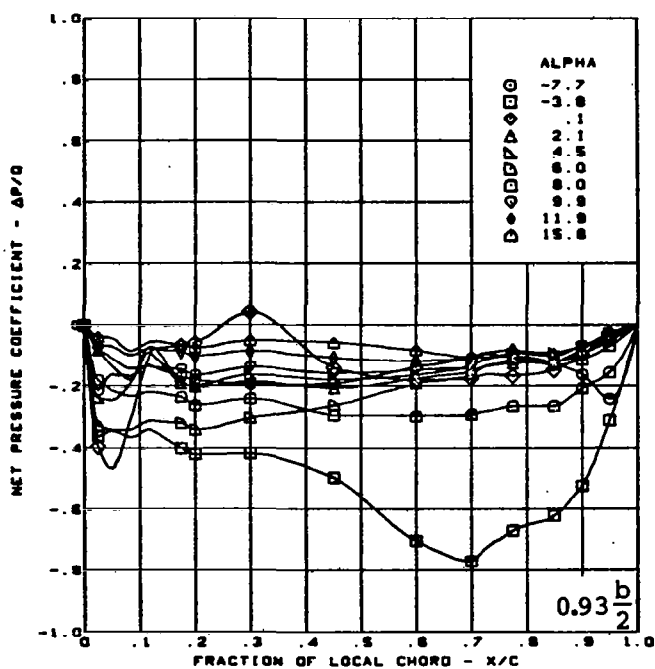
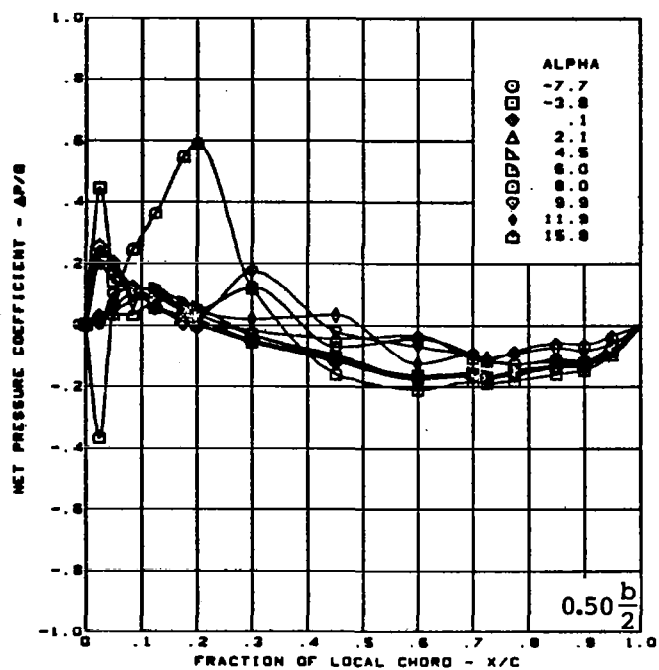
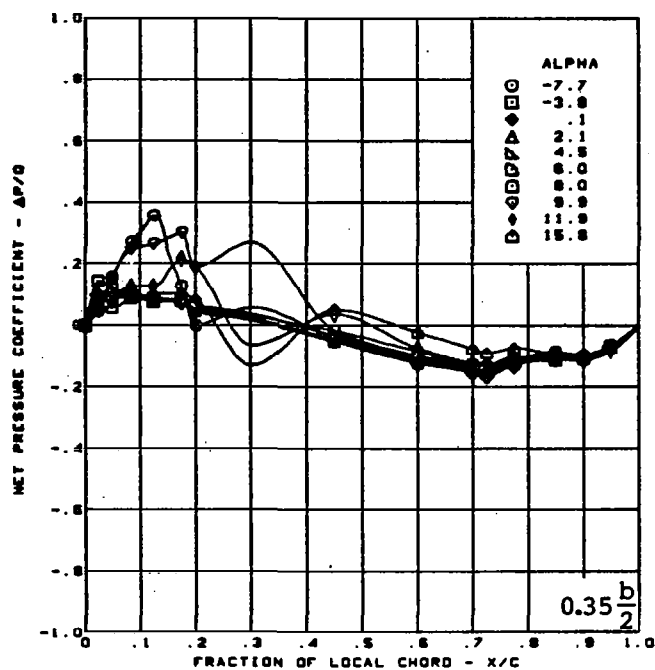
(b) (Concluded)

Figure 24. — (Continued)



(c) Net Chordwise Pressure Distributions

Figure 24. — (Continued)

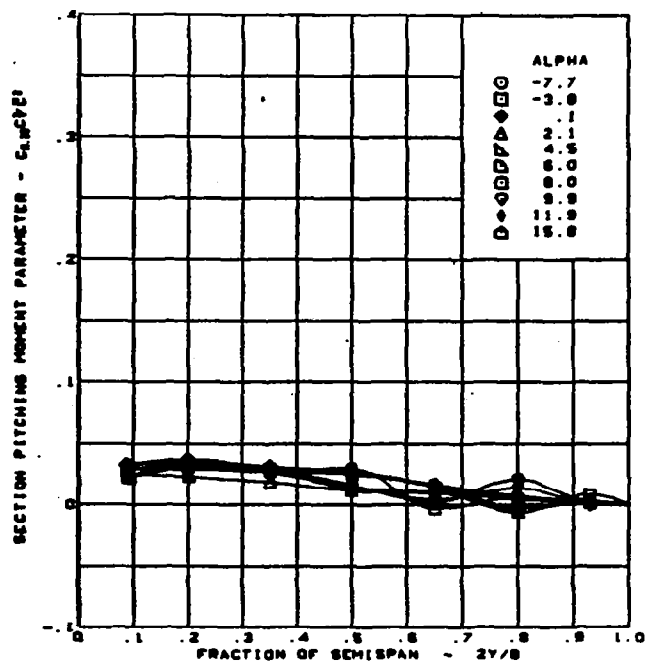
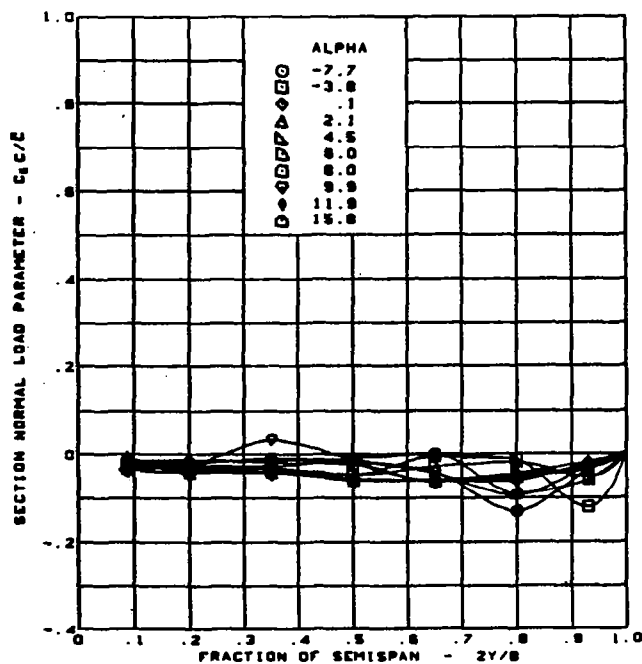


$M = 0.85$   
 Cambered-twisted wing data  
 minus twisted wing data  
 Rounded L.E.  
 Fin off  
 L.E. deflection, full span =  $0.0^\circ$   
 T.E. deflection, full span =  $0.0^\circ$

(c) (Concluded)

Figure 24. — (Continued)



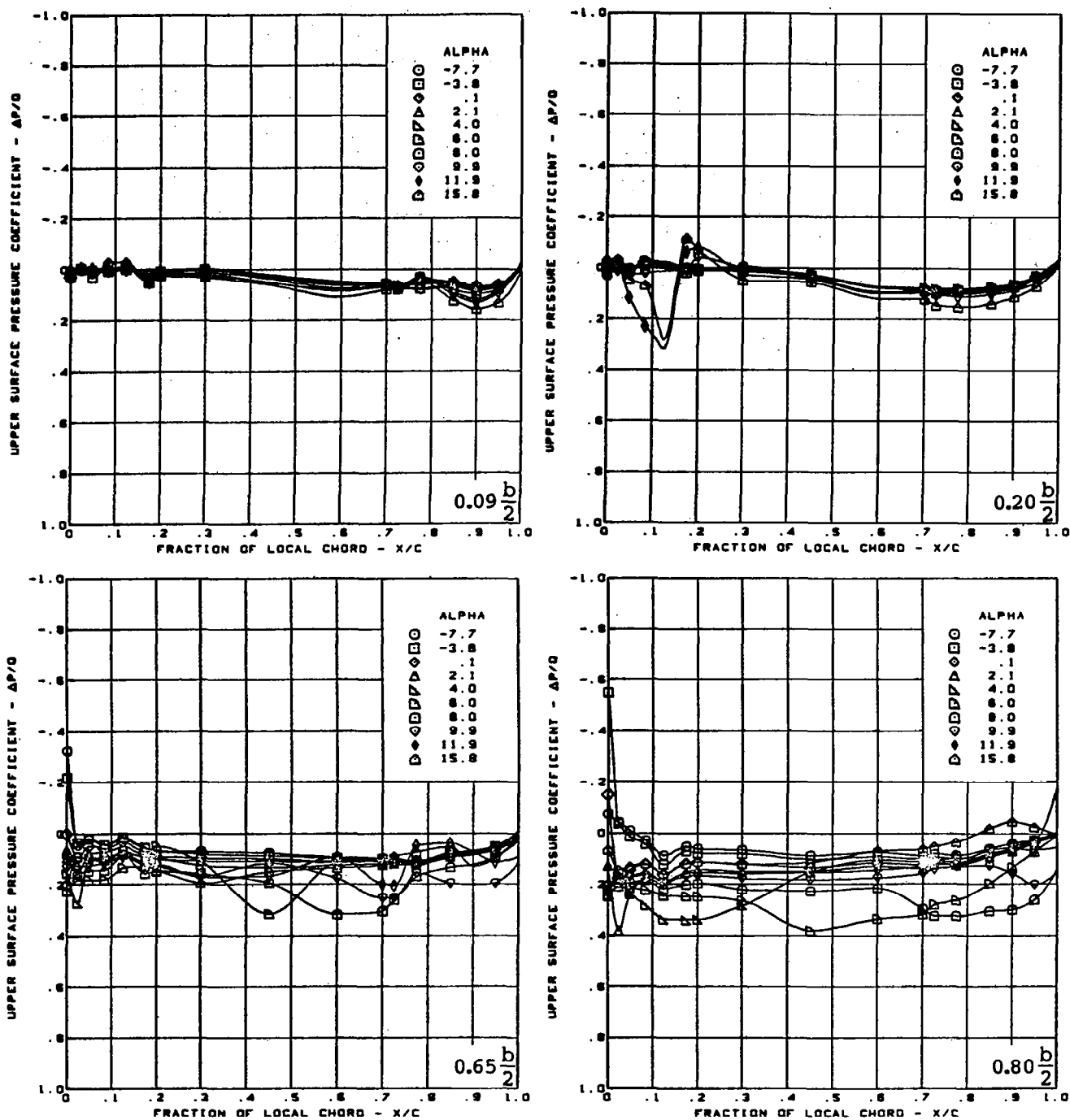


M = 0.85  
 Cambered-twisted wing data  
 minus twisted wing data  
 Rounded L.E.  
 Fin off  
 L.E. deflection, full span =  $0.0^\circ$   
 T.E. deflection, full span =  $0.0^\circ$

(d) Spanload Distributions

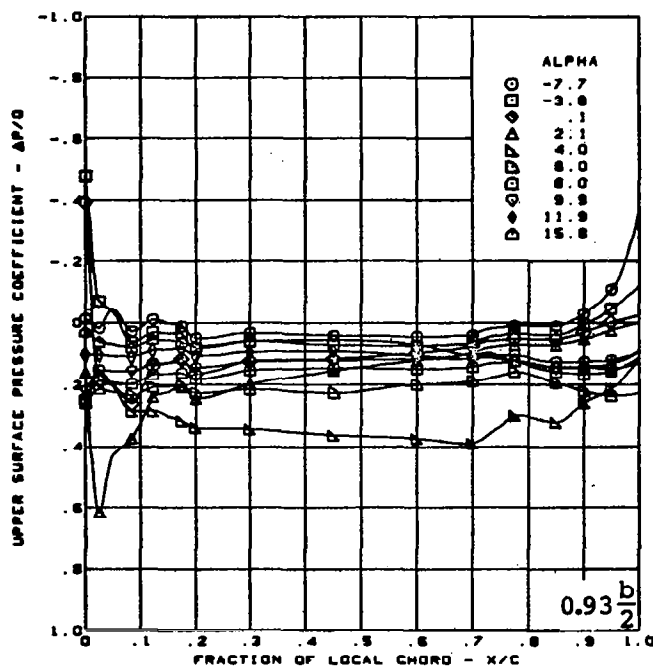
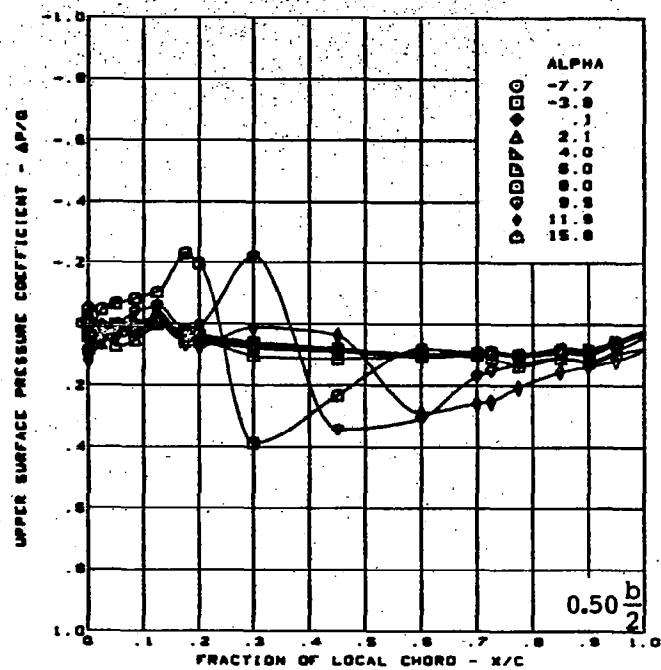
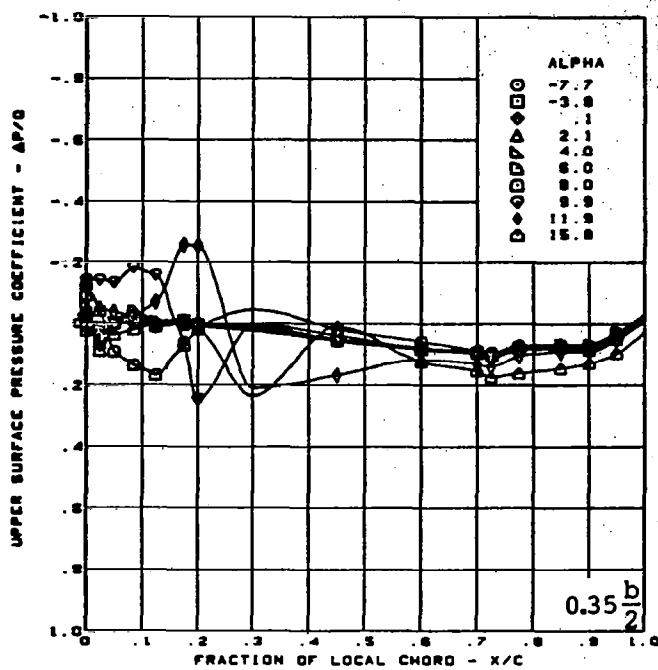
Figure 24. - (Concluded)





(a) Upper Surface Chordwise Pressure Distributions

Figure 25. — Wing Experimental Data—Effect of Incremental Camber and Twist;  
T.E. Deflection, Full Span =  $0.0^\circ$ ;  $M = 0.85$



$M = 0.85$

Cambered-twisted wing data minus flat wing data  
Rounded L.E.

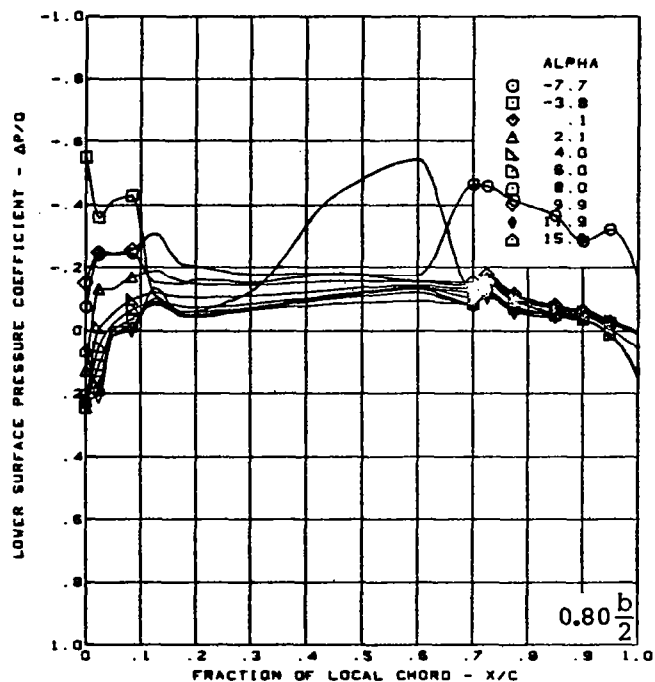
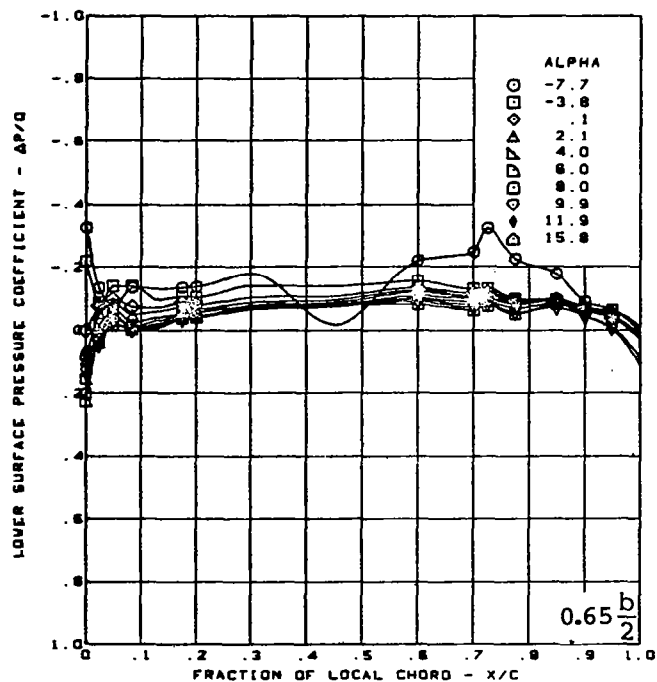
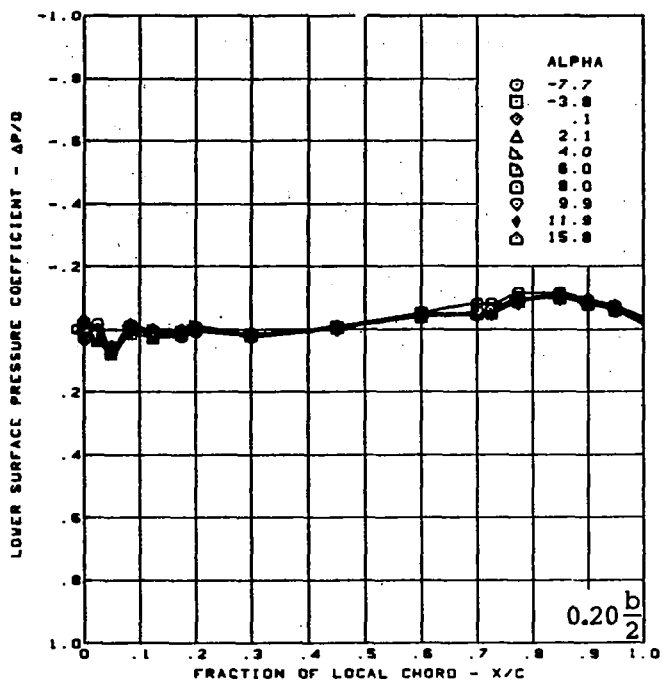
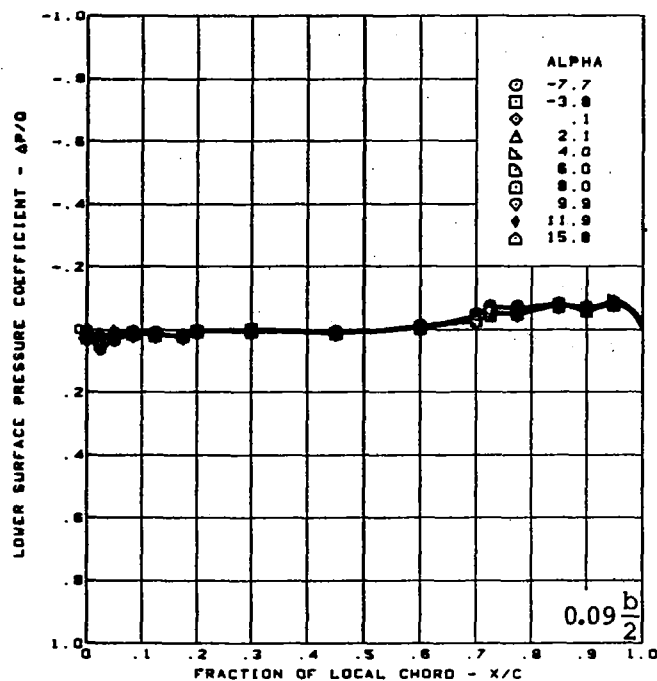
Fin off

L.E. deflection, full span =  $0.0^\circ$

T.E. deflection, full span =  $0.0^\circ$

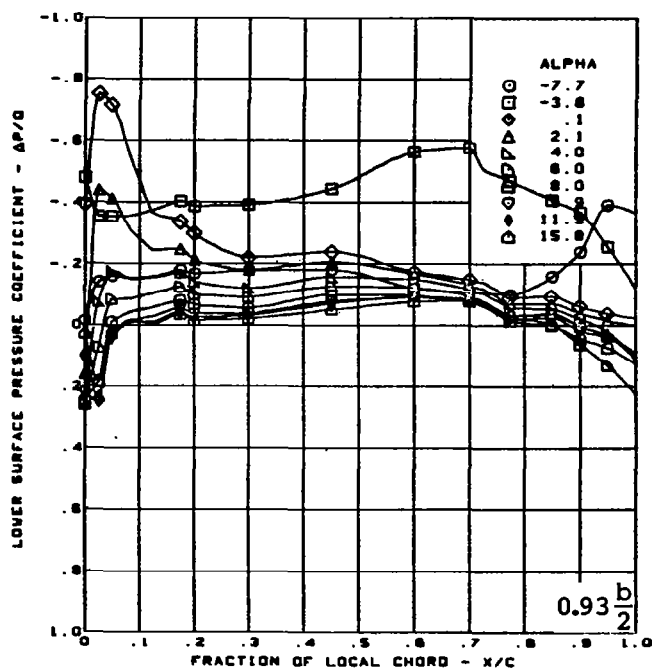
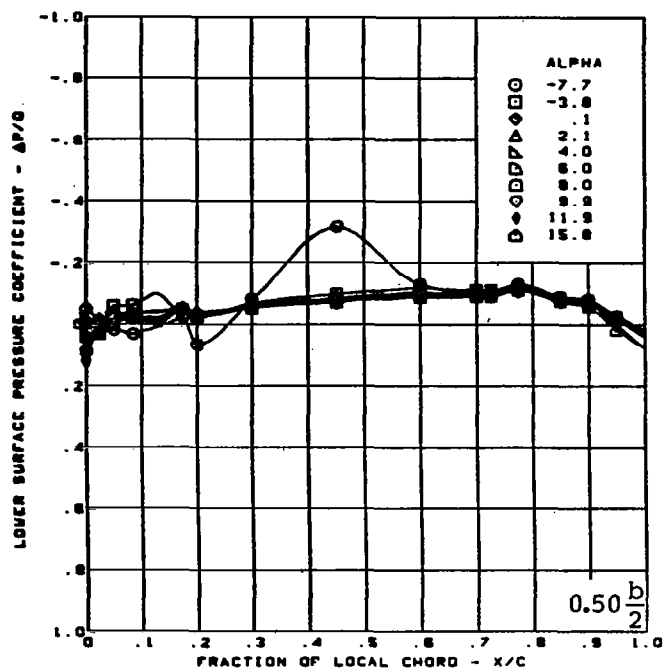
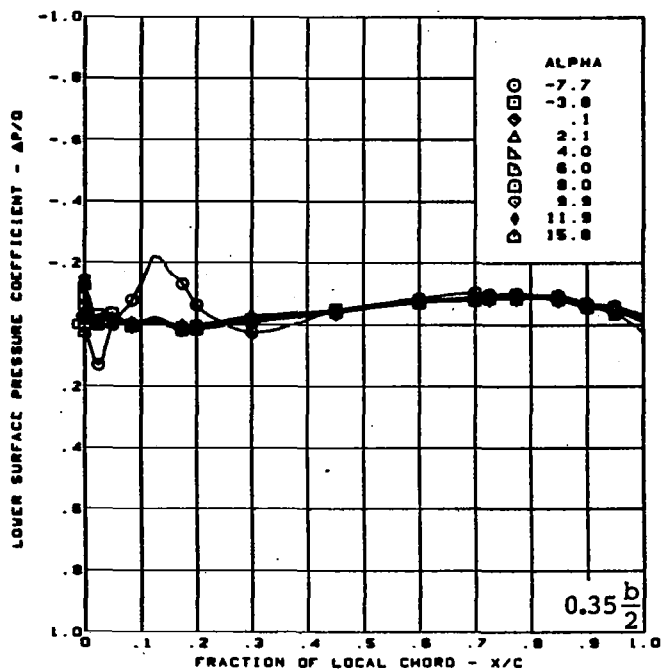
(a) (Concluded)

Figure 25. — (Continued)



(b) Lower Surface Chordwise Pressure Distributions

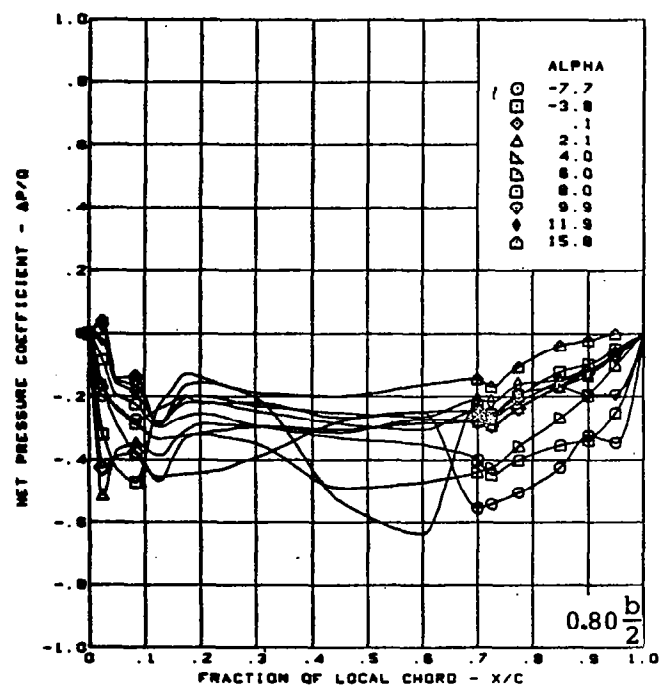
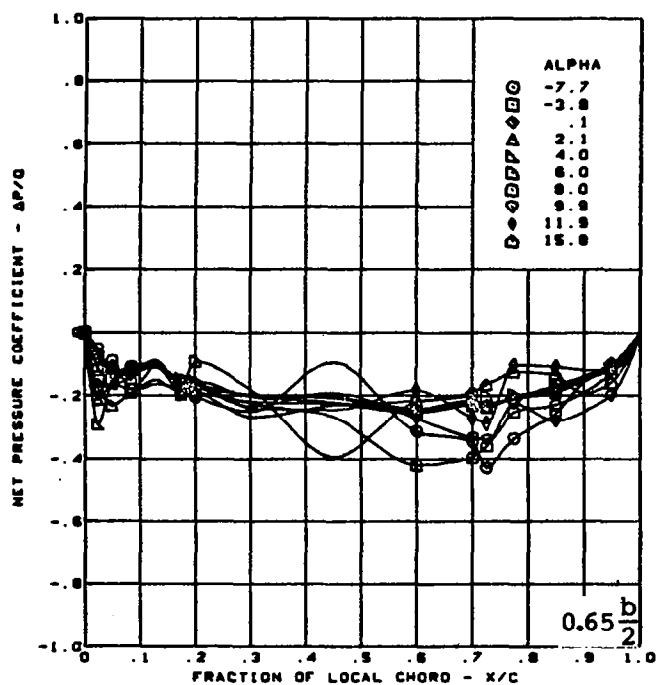
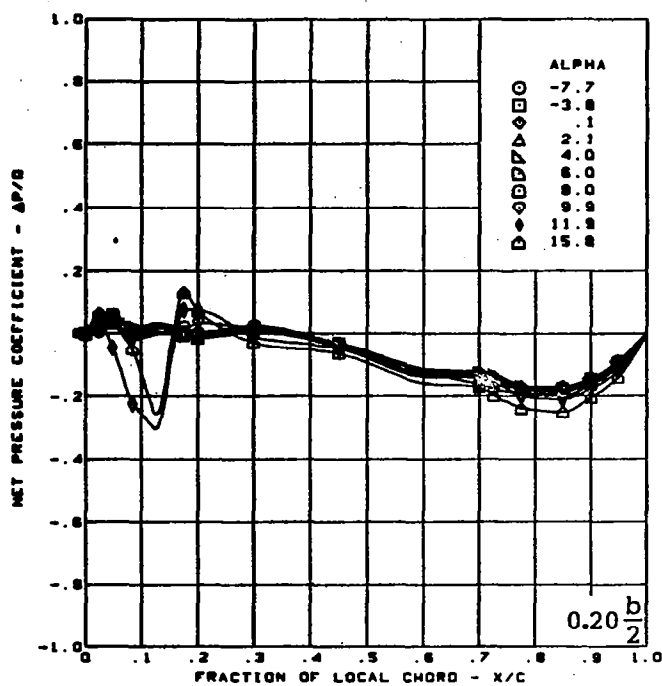
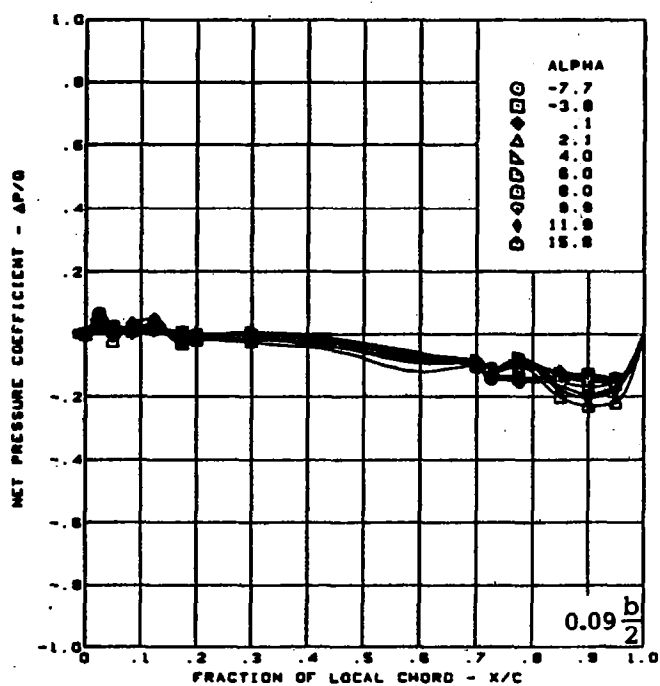
Figure 25. — (Continued)



$M = 0.85$   
 Cambered-twisted wing data minus flat wing data  
 Rounded L.E.  
 Fin off  
 L.E. deflection, full span =  $0.0^\circ$   
 T.E. deflection, full span =  $0.0^\circ$

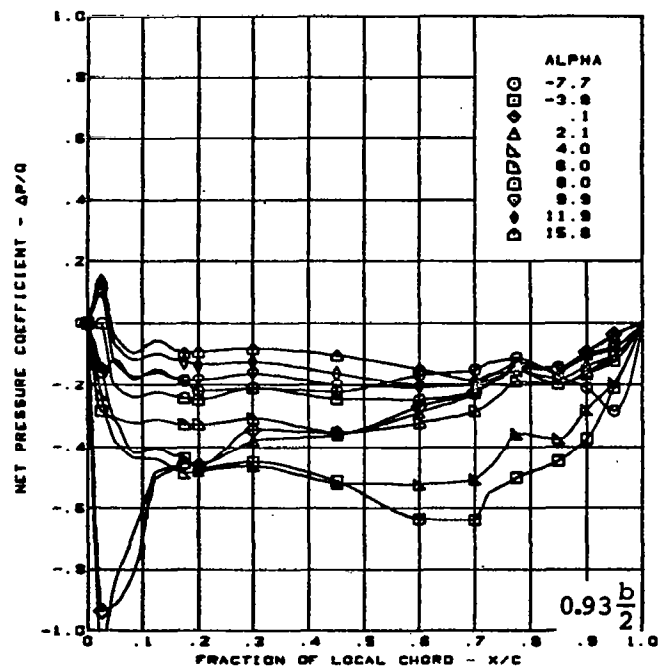
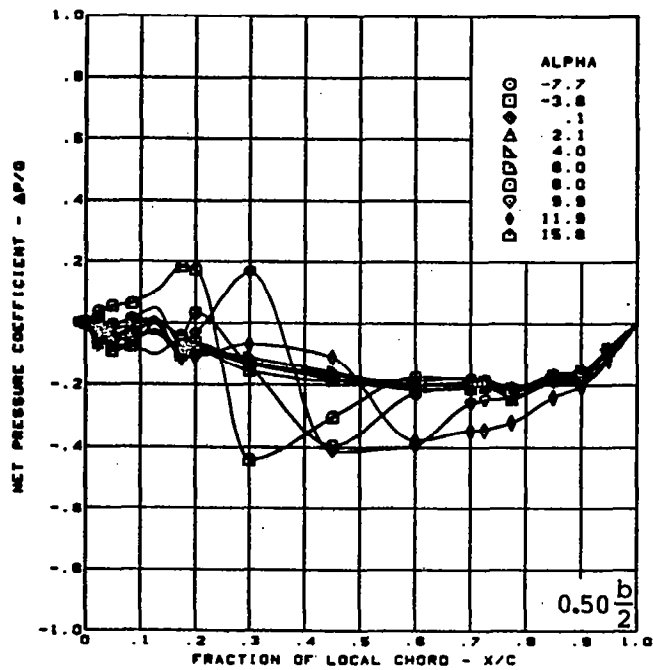
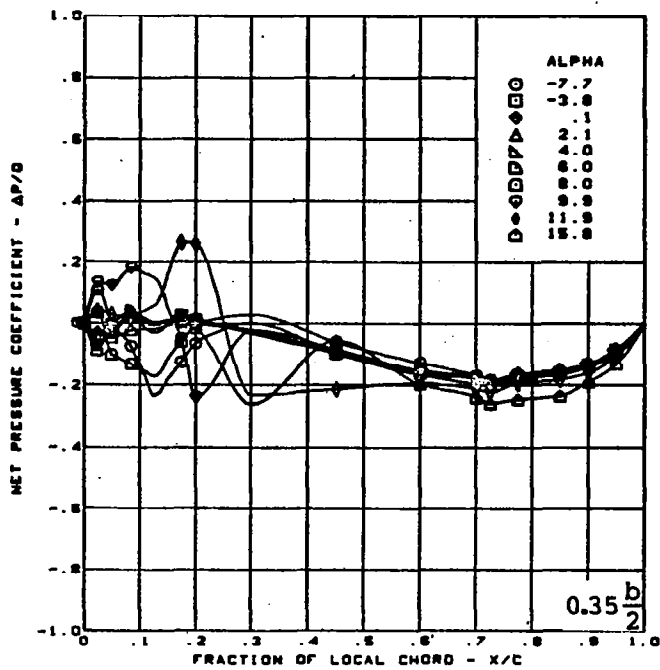
(b) (Concluded)

Figure 25. -- (Continued)



(c) Net Chordwise Pressure Distributions

Figure 25. - (Continued)



$M = 0.85$

Cambered-twisted wing data minus flat wing data

Rounded L.E.

Fin off

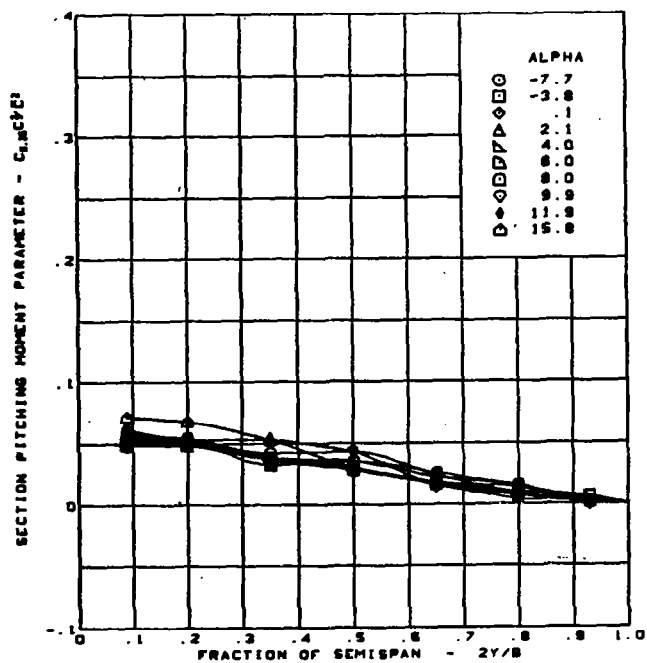
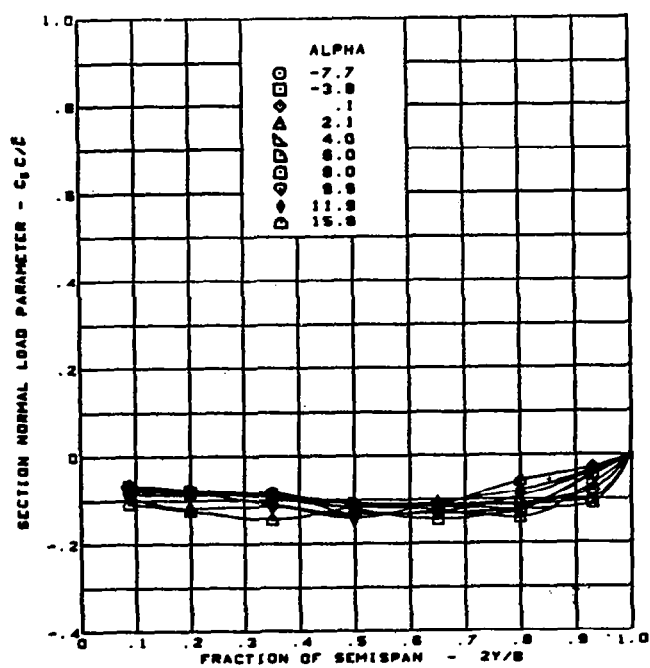
L.E. deflection, full span =  $0.0^\circ$

T.E. deflection, full span =  $0.0^\circ$

(c) (Concluded)

Figure 25. - (Continued)





$M = 0.85$

Cambered-twisted wing data minus flat wing data  
Rounded L.E.

Fin off

L.E. deflection, full span =  $0.0^\circ$

T.E. deflection, full span =  $0.0^\circ$

(d) Spanload Distributions

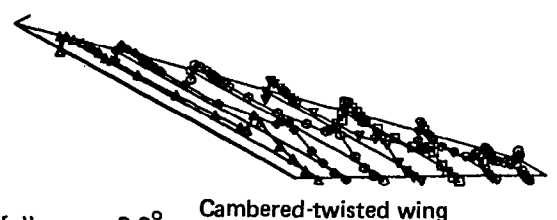
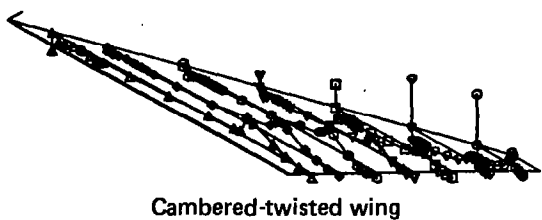
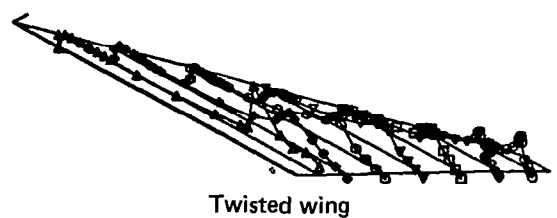
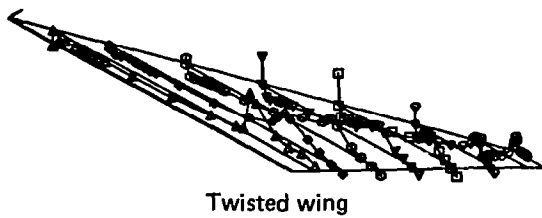
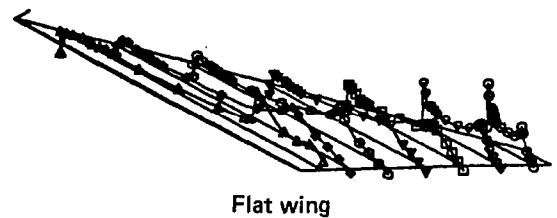
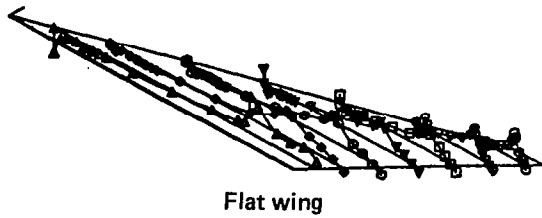
Figure 25. - (Concluded)





$\alpha = -3.9^\circ$

$\alpha = 0.0^\circ$

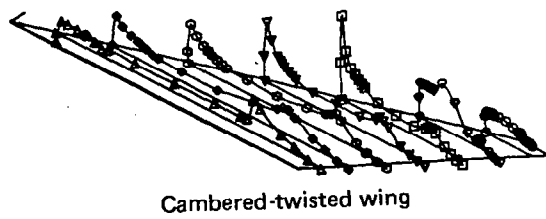
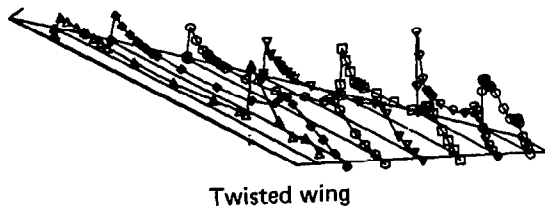
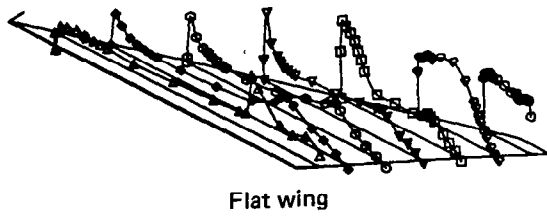


$M = 0.85$   
 Rounded L.E.  
 L.E. deflection, full span =  $0.0^\circ$   
 T.E. deflection, full span =  $8.3^\circ$

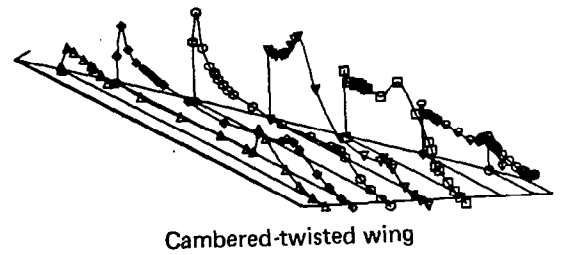
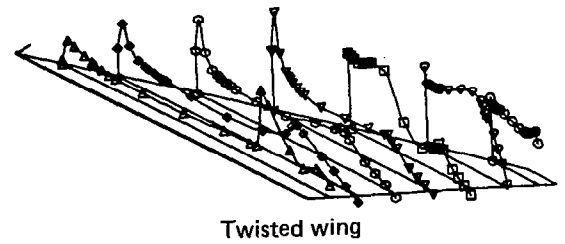
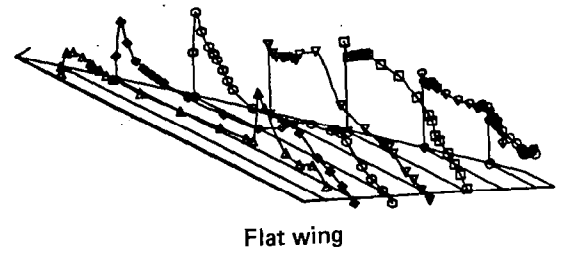
(a) Upper Surface Pressure Distribution

Figure 26. — Wing Experimental Data—Effect of Wing Shape; T.E. Deflection, Full Span =  $8.3^\circ$ ;  $M = 0.85$

$\alpha = 4.0^\circ$



$\alpha = 8.0^\circ$

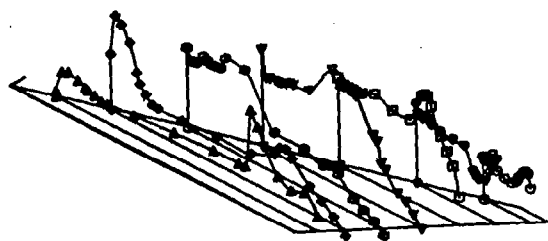


(a) (Continued)

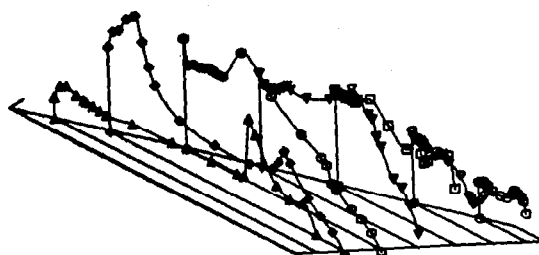
Figure 26. — (Continued)

$\alpha = 11.9^\circ$

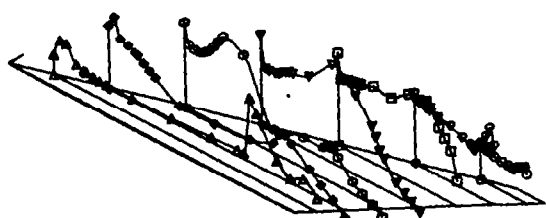
$\alpha = 15.8^\circ$



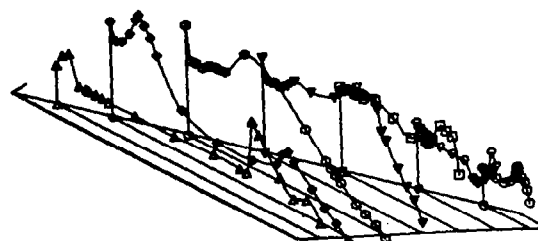
Flat wing



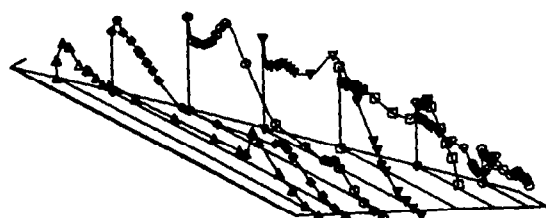
Flat wing



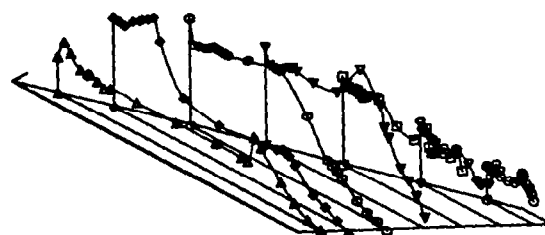
Twisted wing



Twisted wing



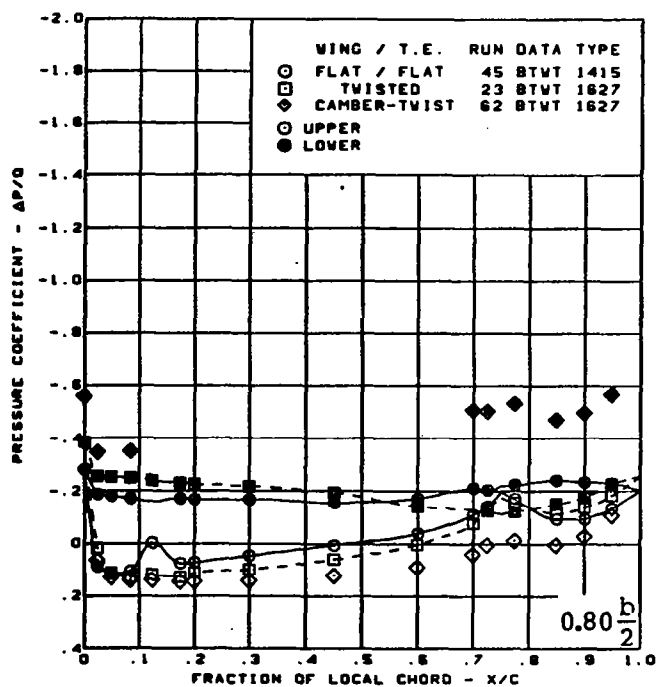
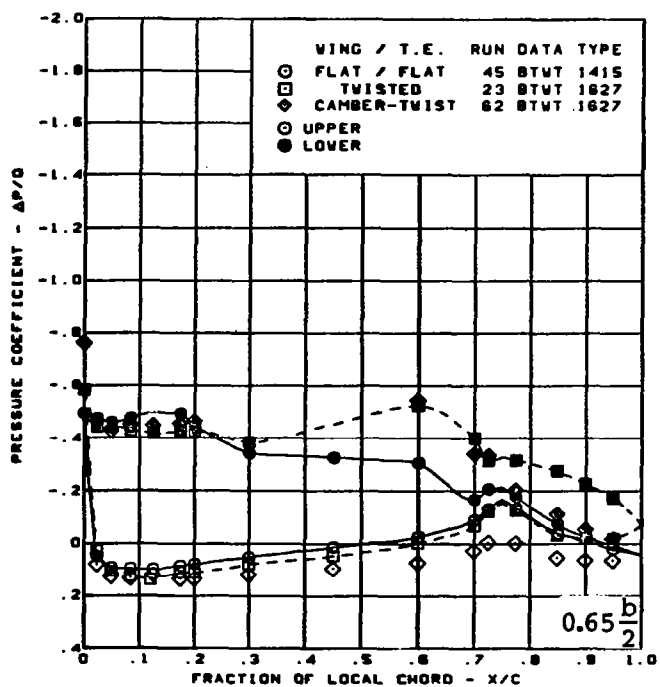
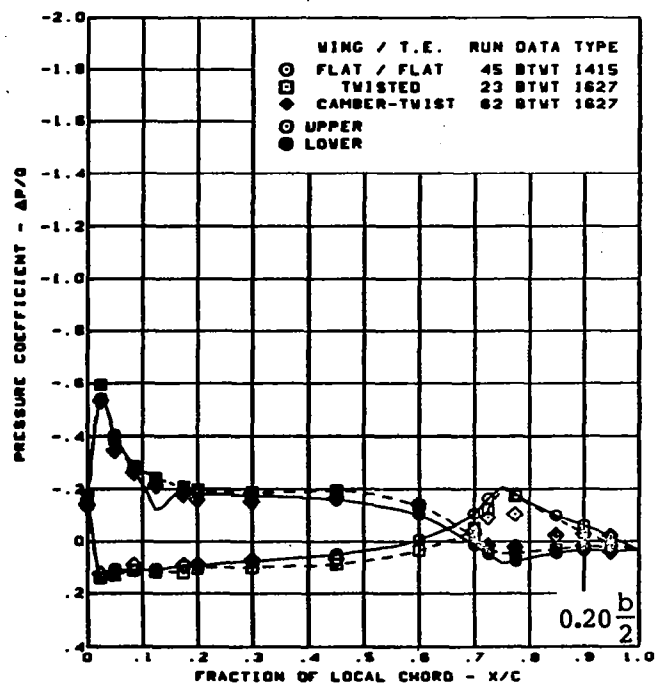
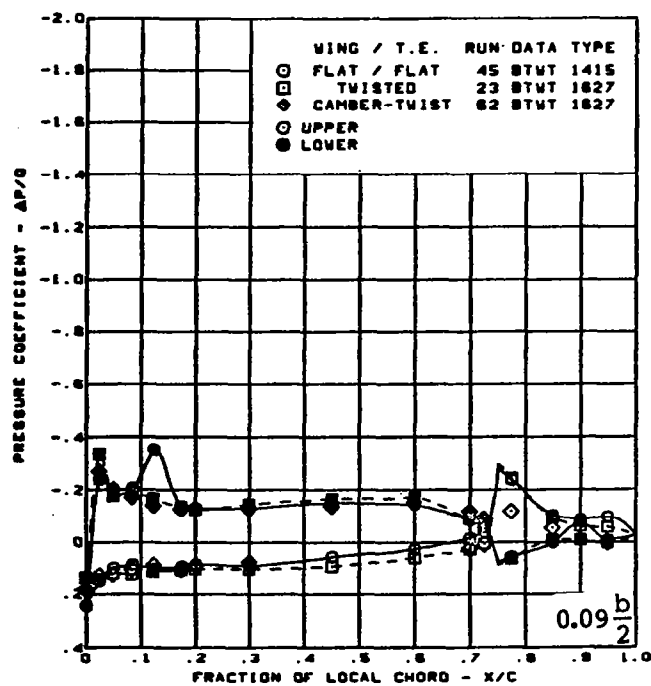
Cambered-twisted wing



Cambered-twisted wing

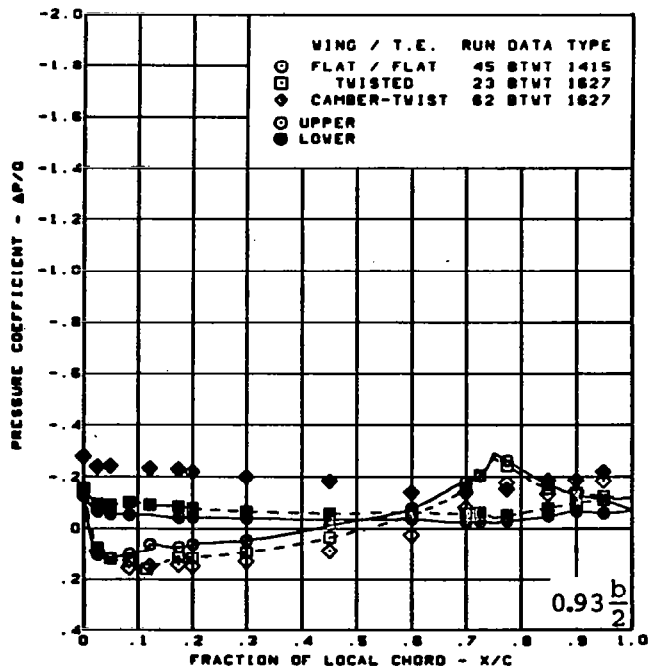
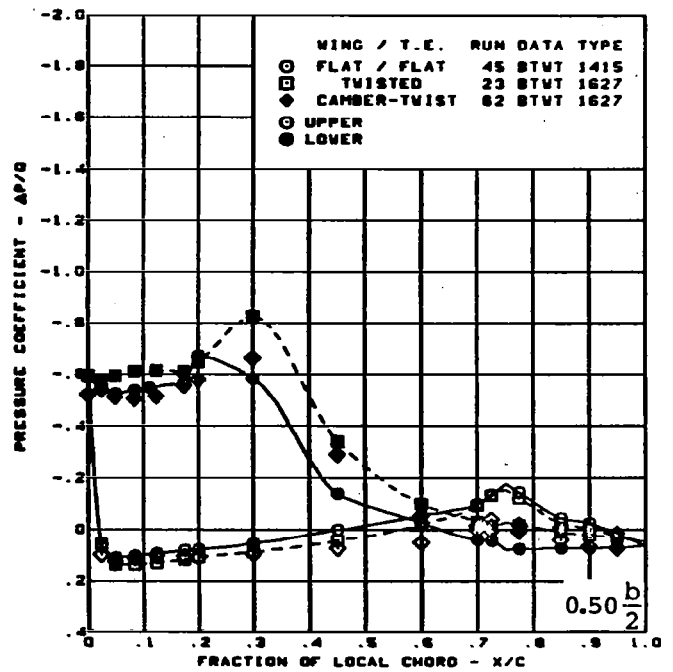
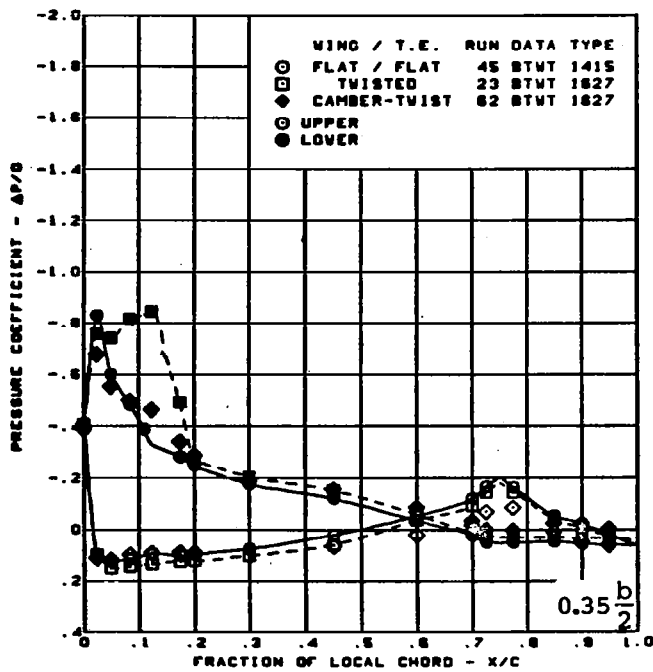
(a) (Concluded)

Figure 26. — (Continued)



(b) Surface Chordwise Pressure Distributions -  $\alpha = -8^\circ$

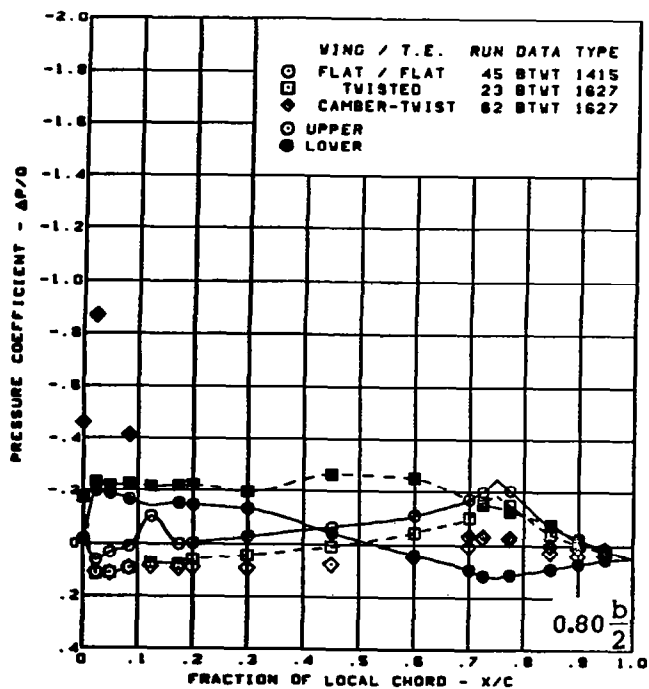
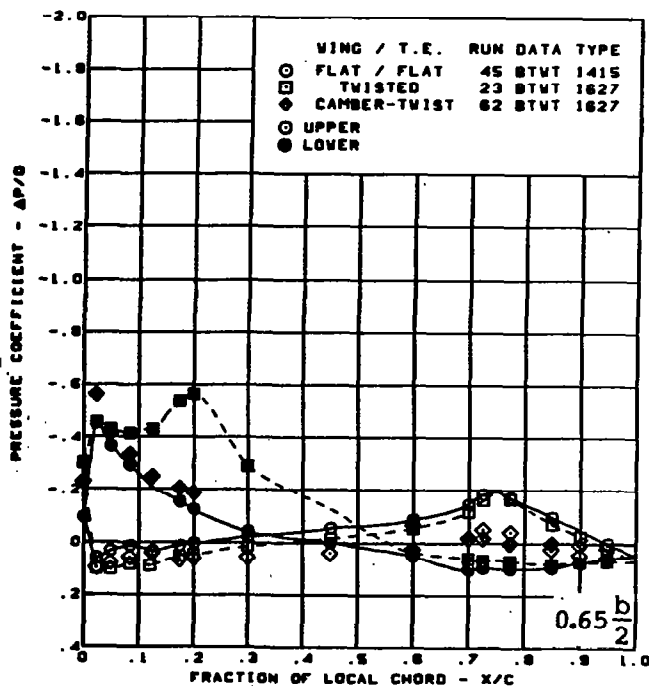
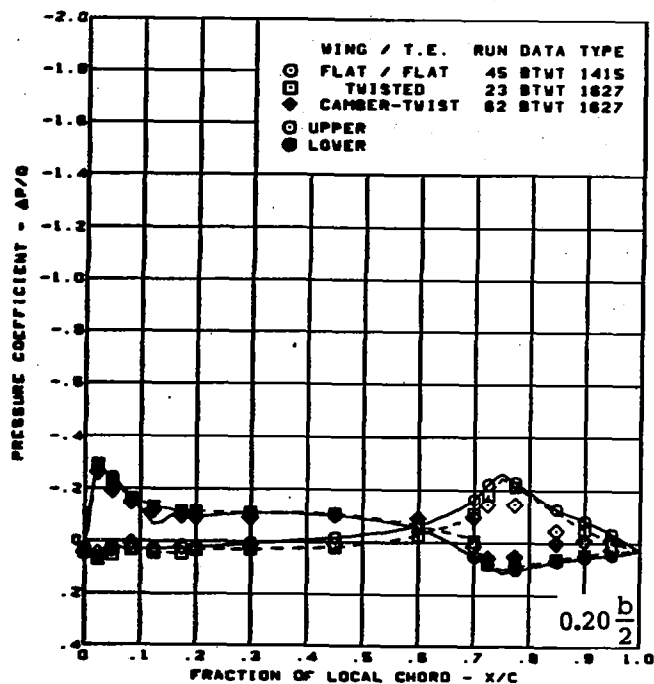
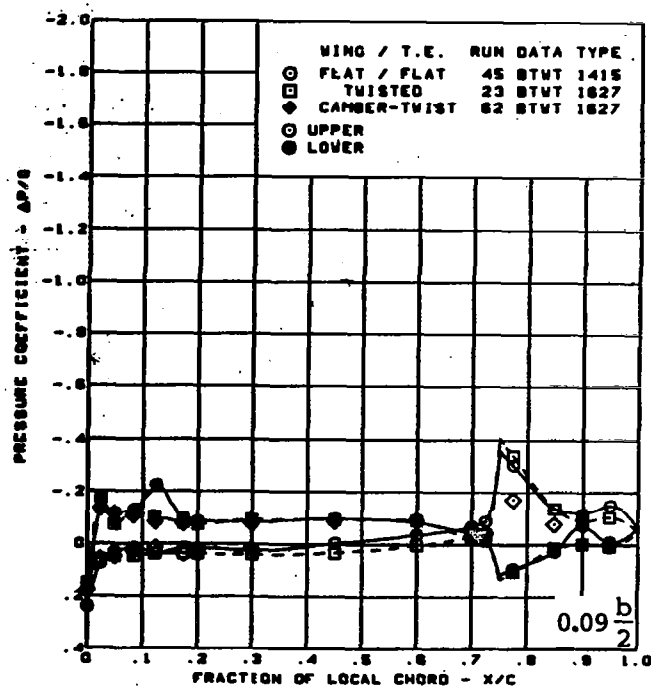
Figure 26. — (Continued)



$M = 0.85$   
 $\alpha = -8^\circ$   
 Rounded L.E.  
 L.E. deflection, full span =  $0.0^\circ$   
 T.E. deflection, full span =  $8.3^\circ$

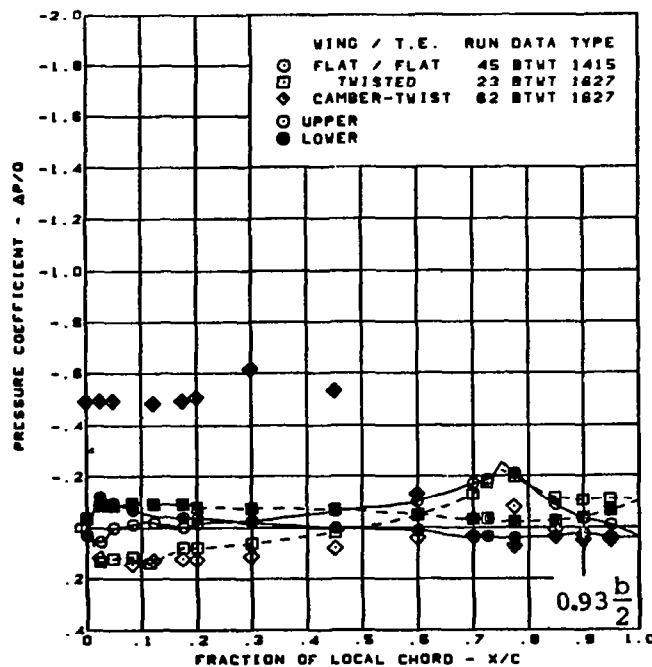
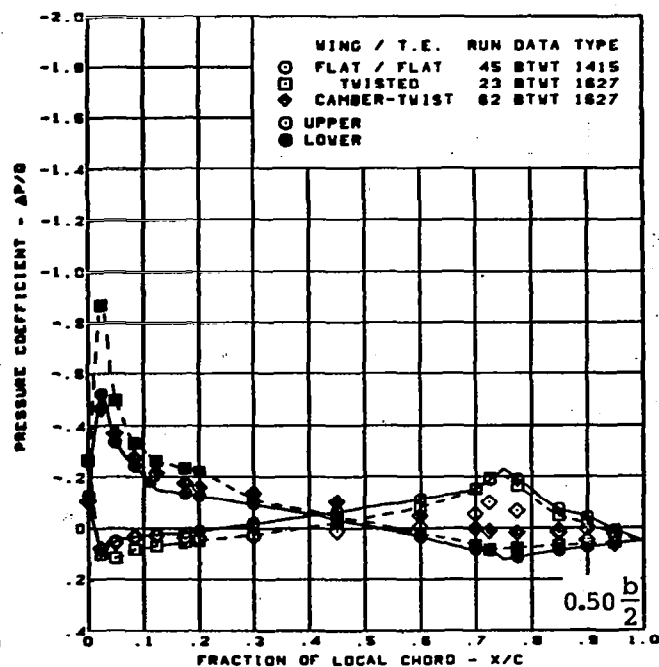
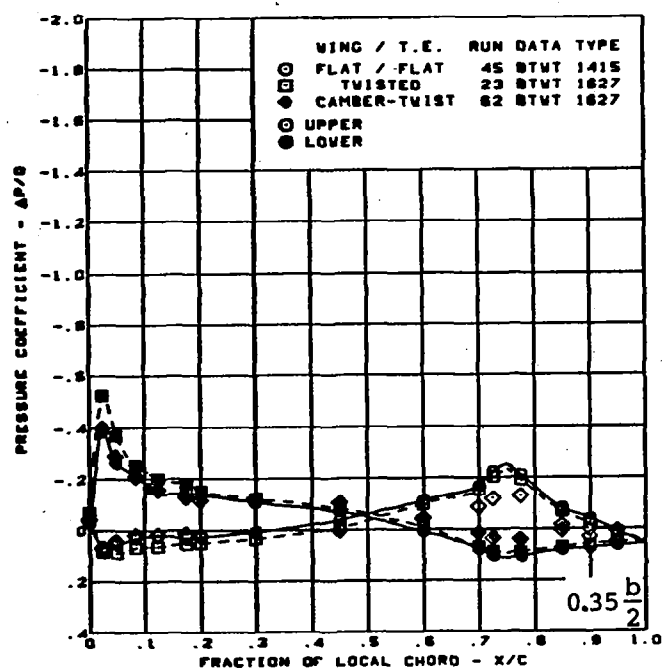
(b) (Concluded)

Figure 26. - (Continued)



(c) Surface Chordwise Pressure Distributions -  $\alpha = -4^\circ$

Figure 26. — (Continued)



$M = 0.85$

$\alpha = -4^\circ$

Rounded L.E.

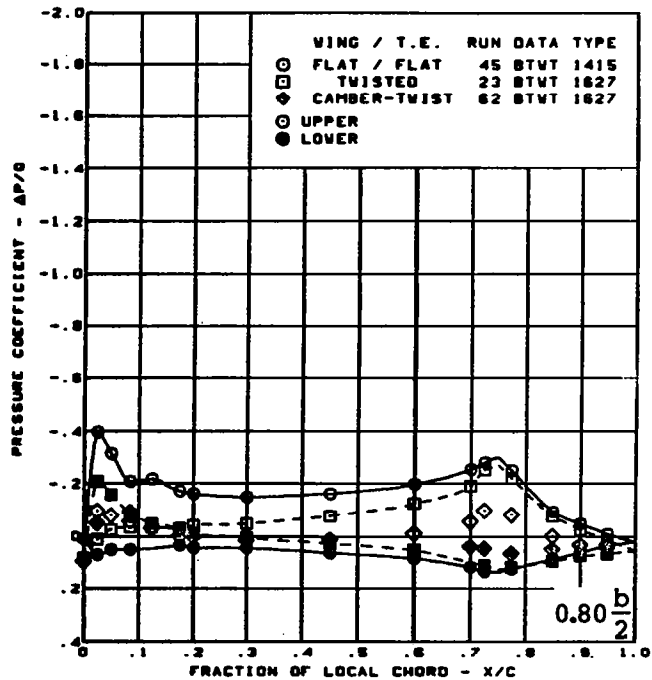
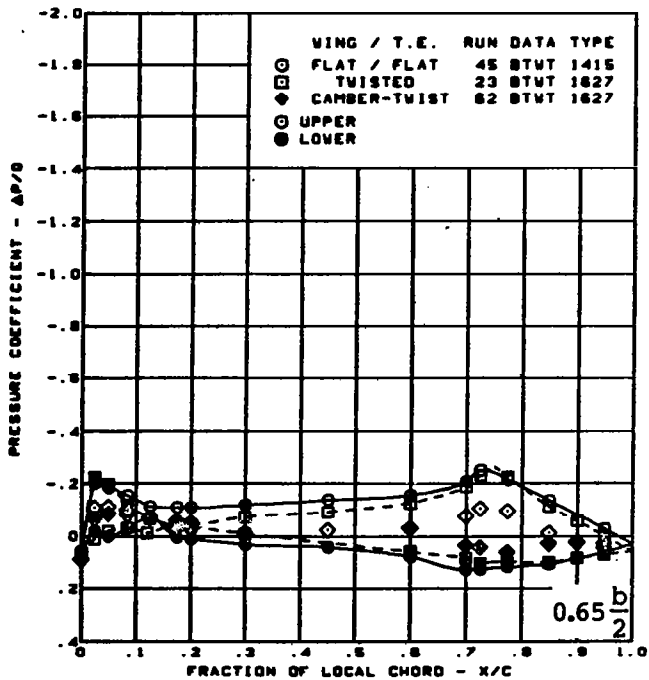
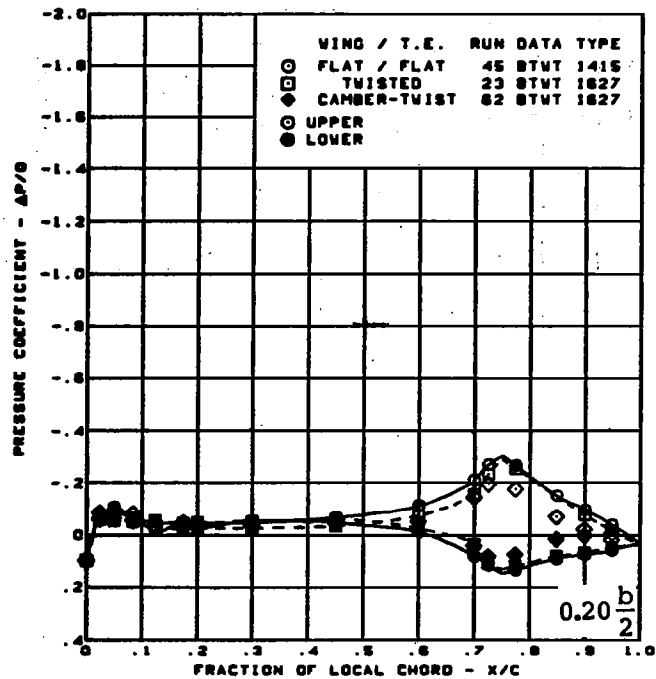
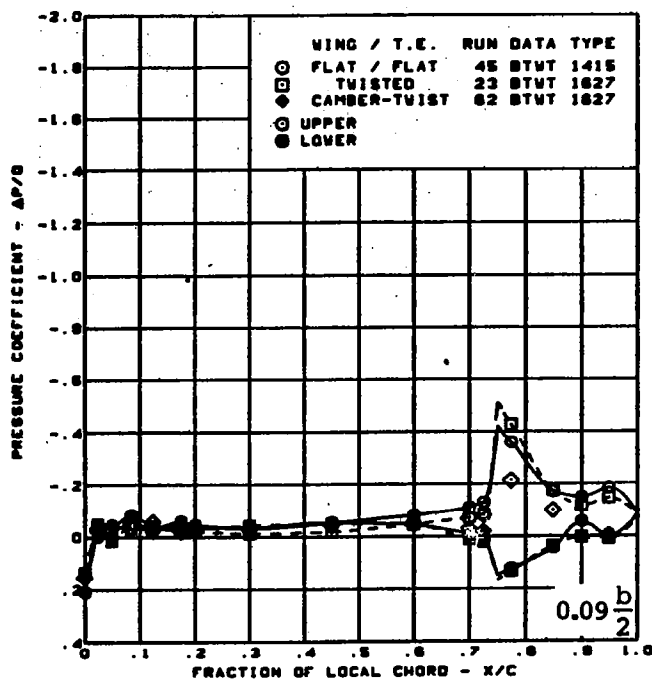
L.E. deflection, full span =  $0.0^\circ$

T.E. deflection, full span =  $8.3^\circ$

(c) (Concluded)

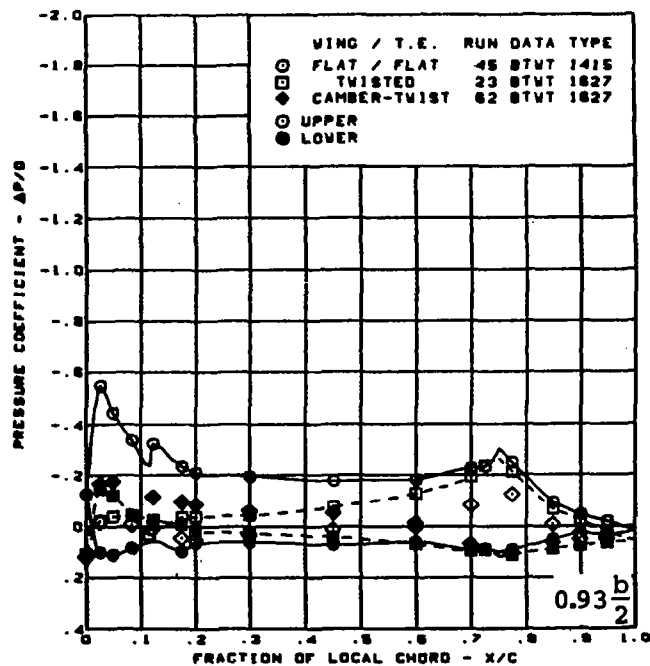
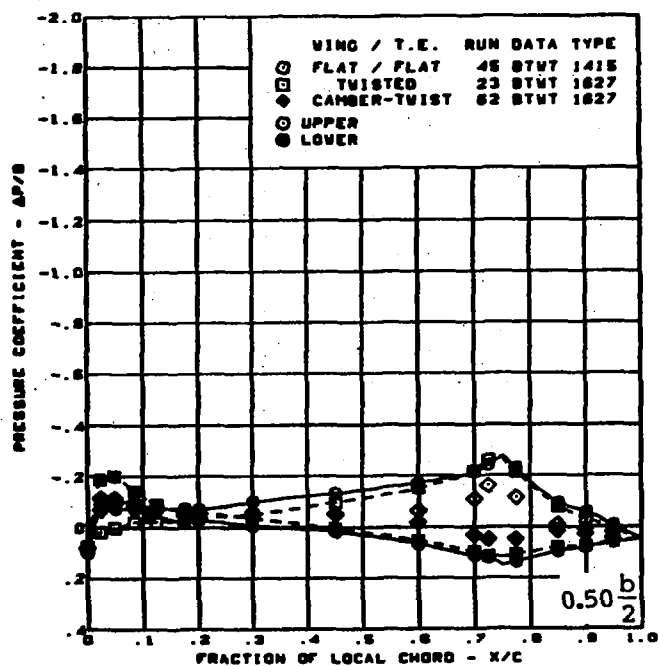
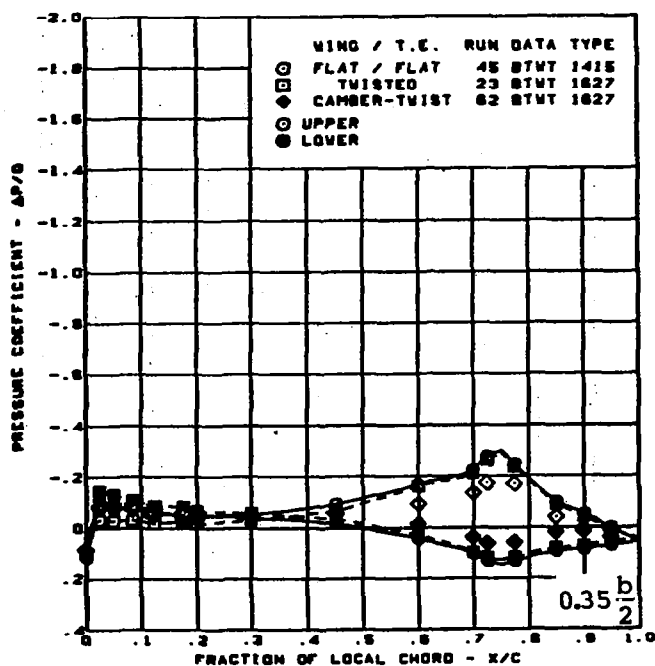
Figure 26. — (Continued)





(d) Surface Chordwise Pressure Distributions -  $\alpha = 0^\circ$

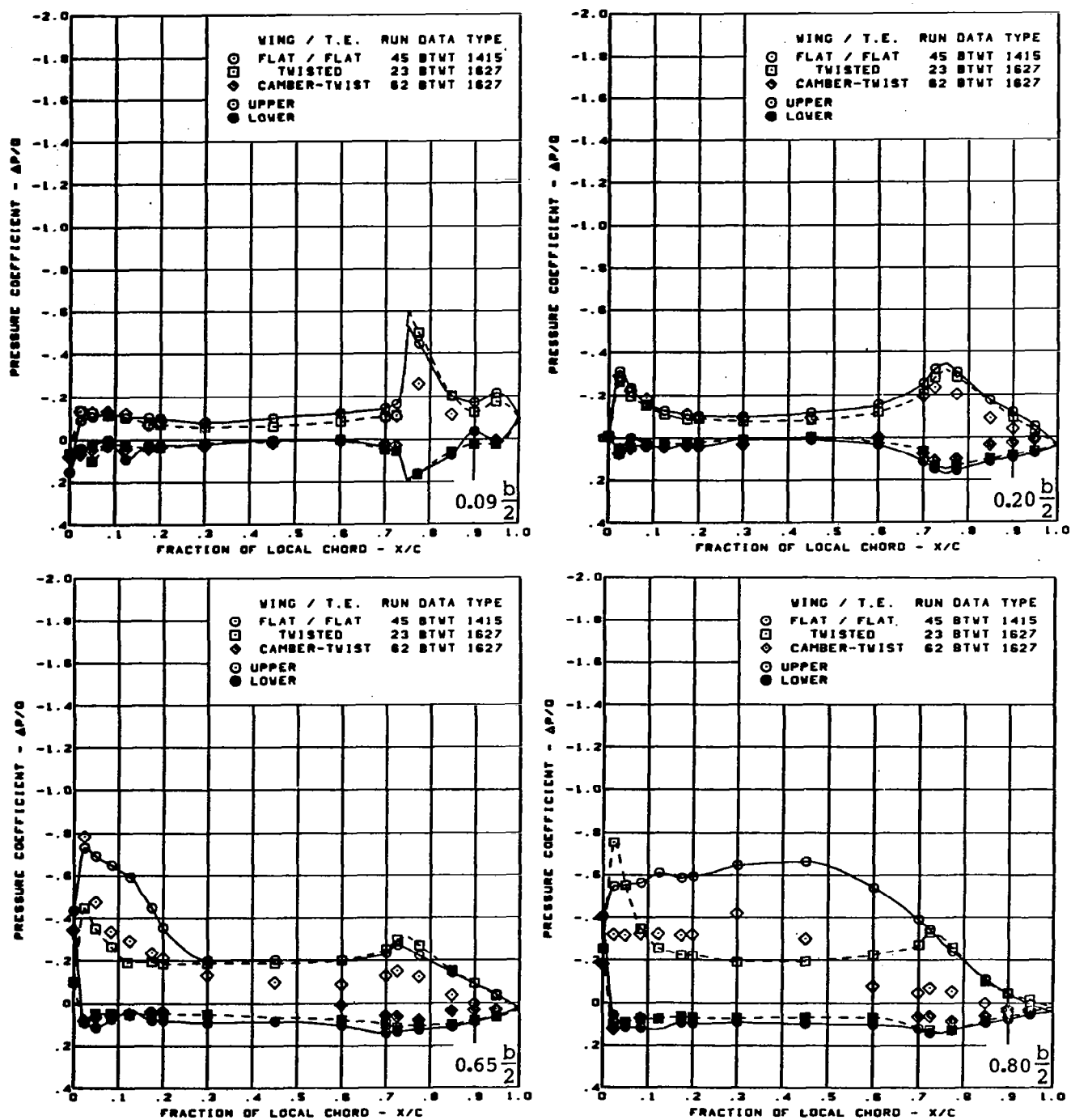
Figure 26. - (Continued)



$M = 0.85$   
 $\alpha = 0^\circ$   
 Rounded L.E.  
 L.E. deflection, full span =  $0.0^\circ$   
 T.E. deflection, full span =  $8.3^\circ$

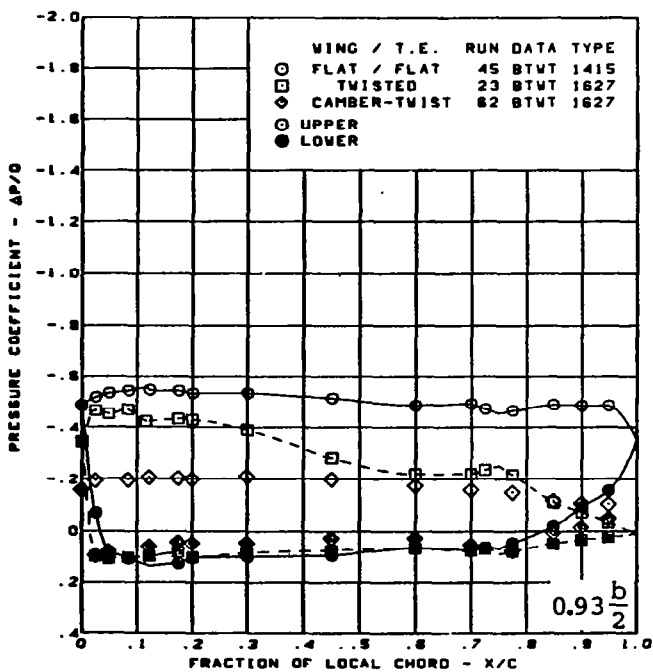
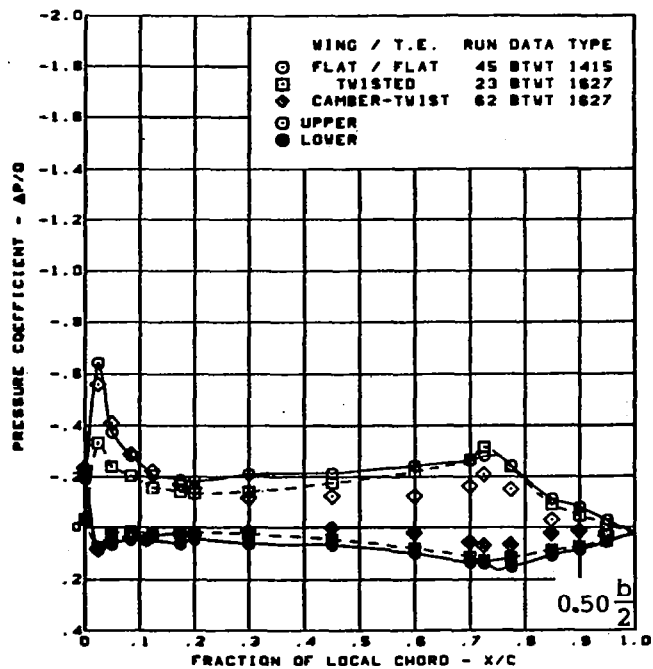
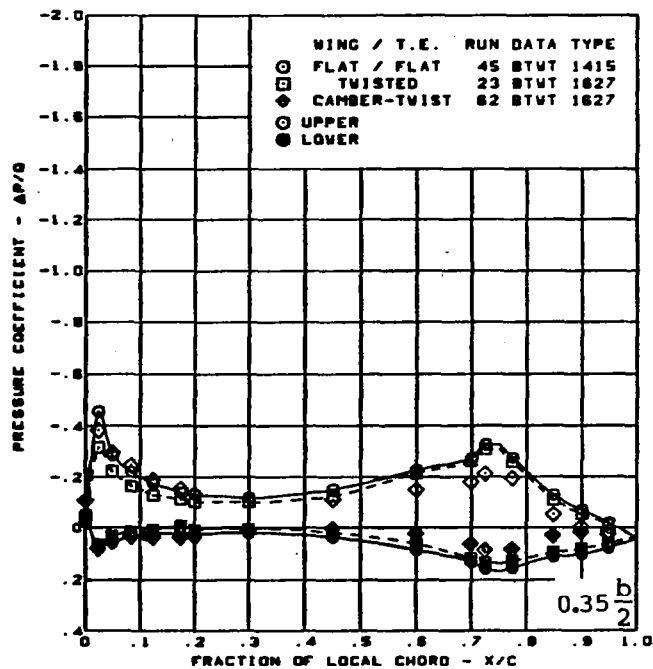
(d) (Concluded)

Figure 26. — (Continued)



(e) Surface Chordwise Pressure Distributions -  $\alpha = 4^\circ$

Figure 26. — (Continued)



$M = 0.85$

$\alpha = 4^\circ$

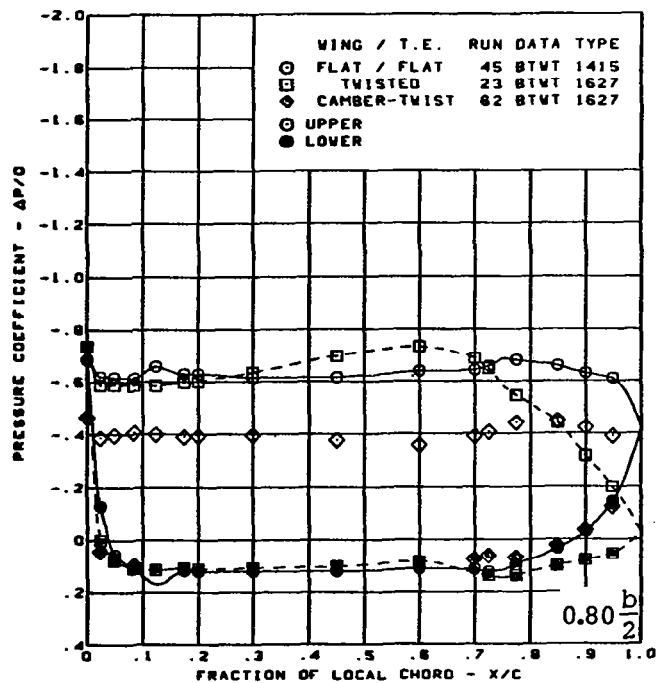
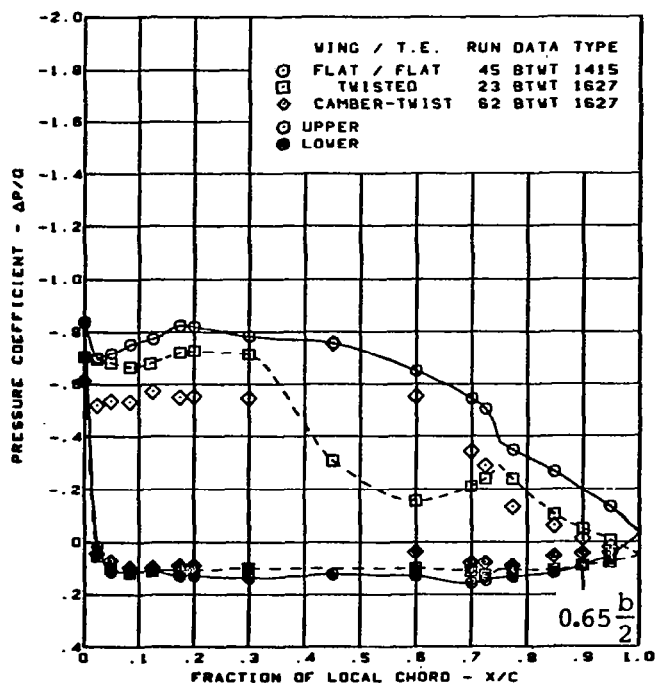
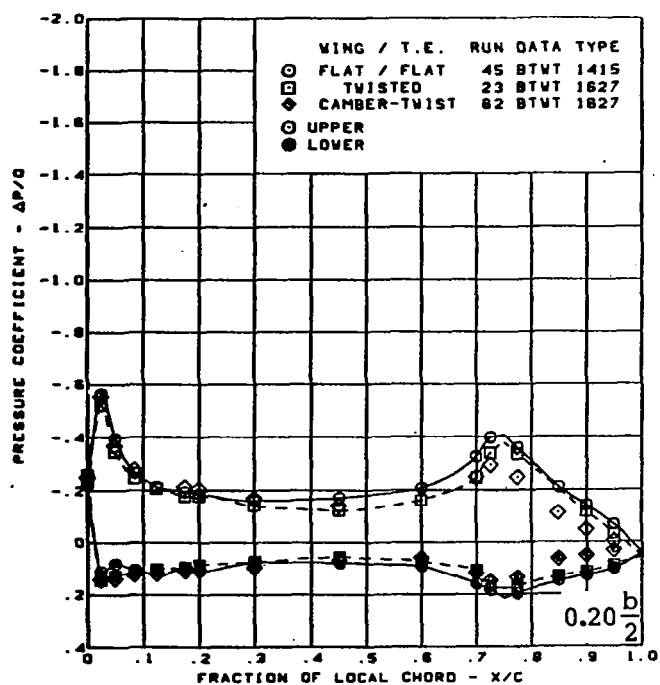
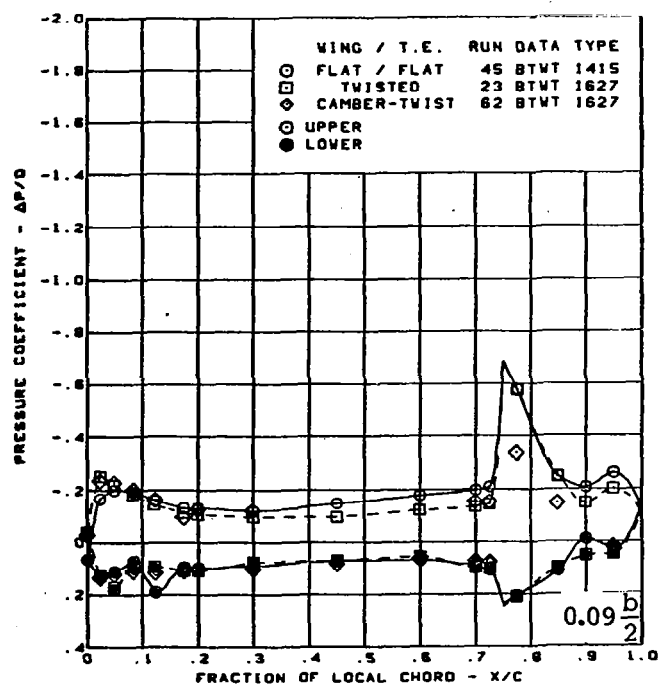
Rounded L.E.

L.E. deflection, full span =  $0.0^\circ$

T.E. deflection, full span =  $8.3^\circ$

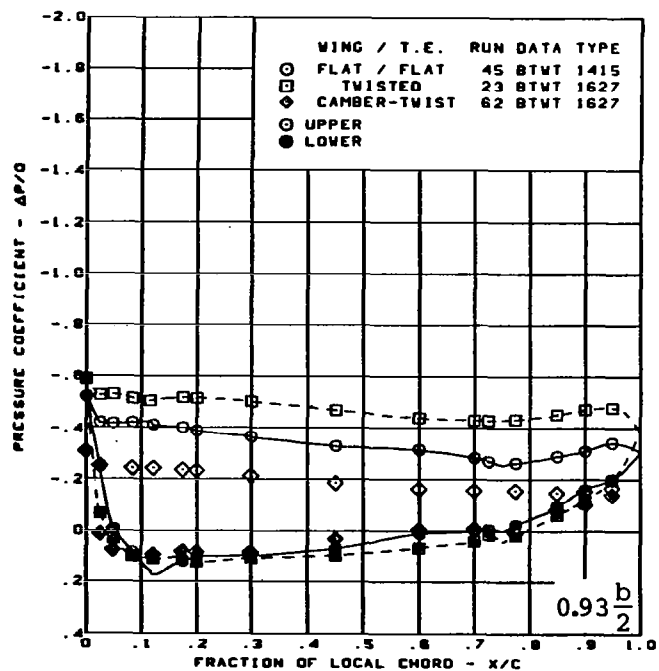
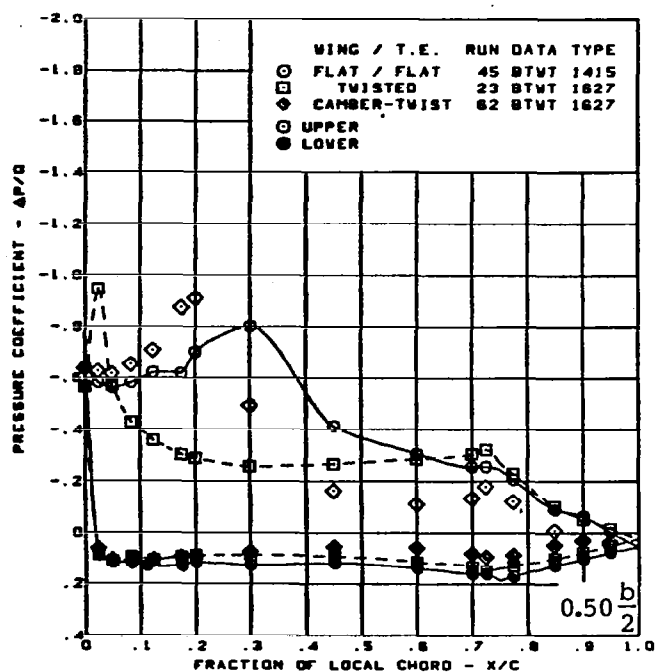
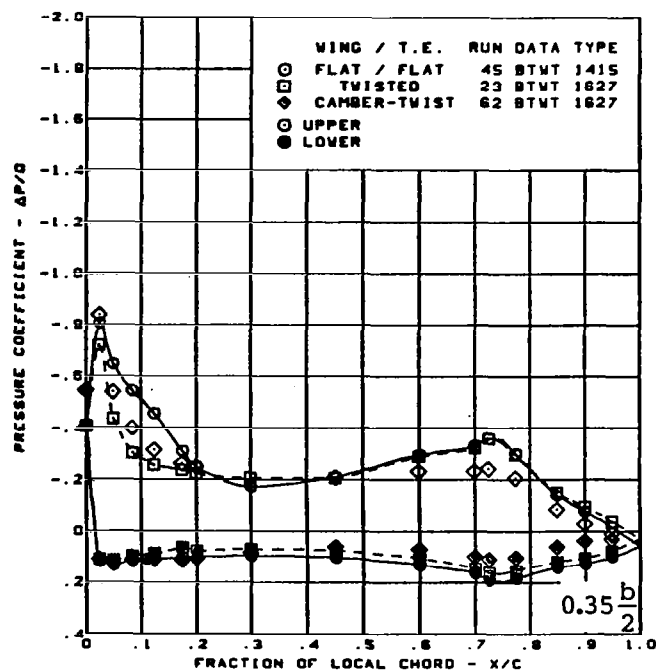
(e) (Concluded)

Figure 26. - (Continued)



(f) Surface Chordwise Pressure Distributions -  $\alpha = 8^\circ$

Figure 26. - (Continued)



$M = 0.85$

$\alpha = 8^\circ$

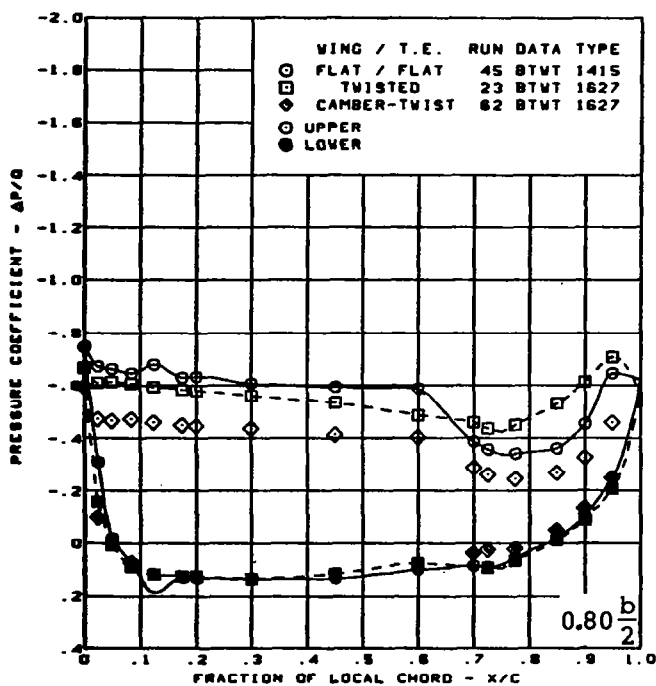
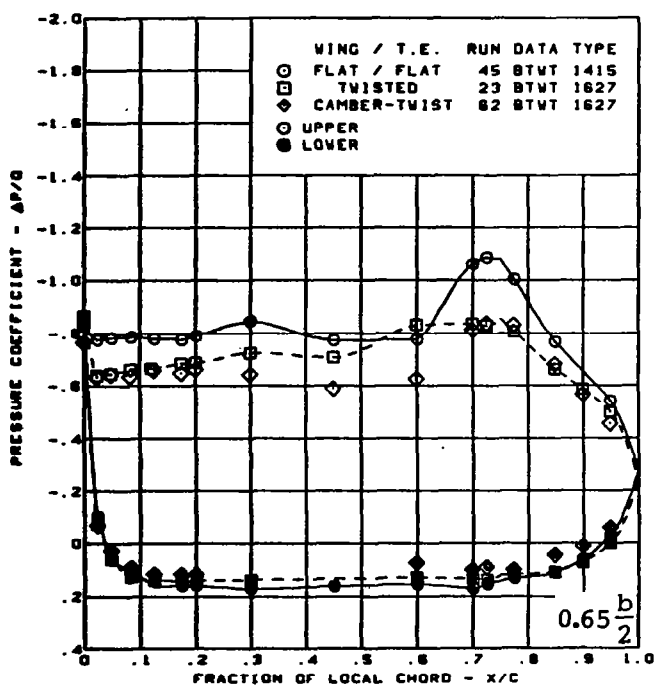
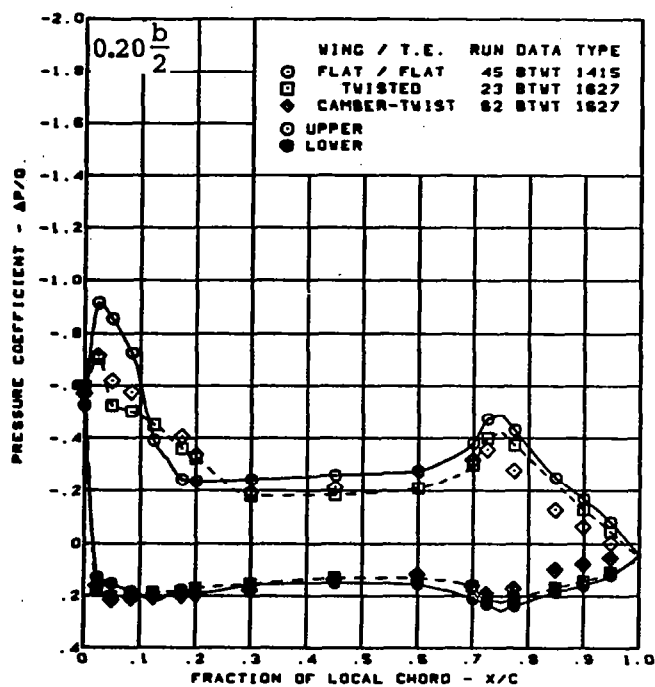
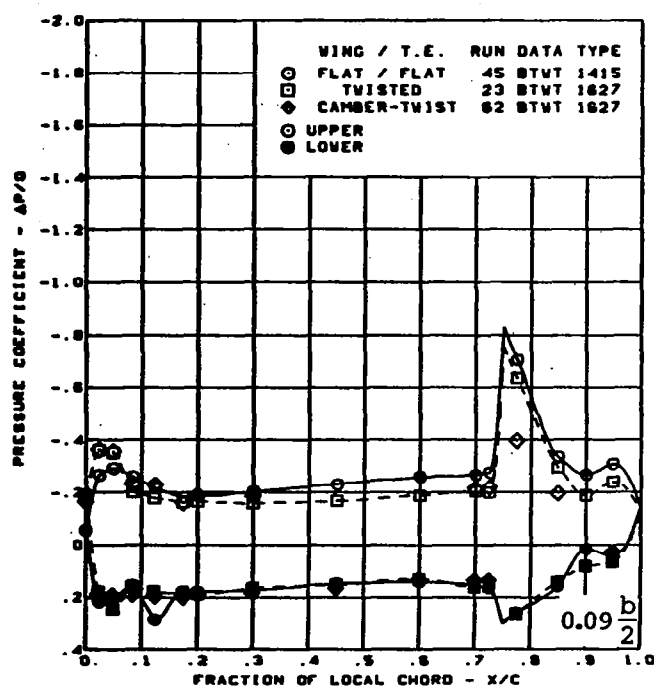
Rounded L.E.

L.E. deflection, full span =  $0.0^\circ$

T.E. deflection, full span =  $8.3^\circ$

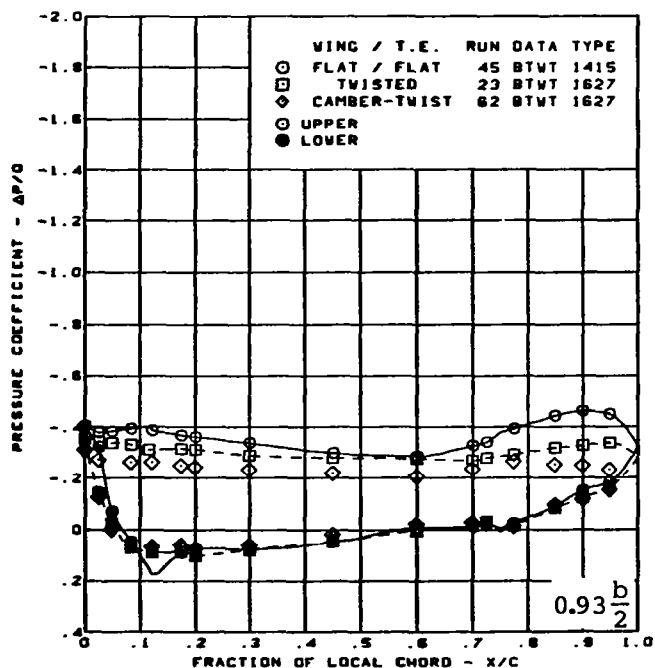
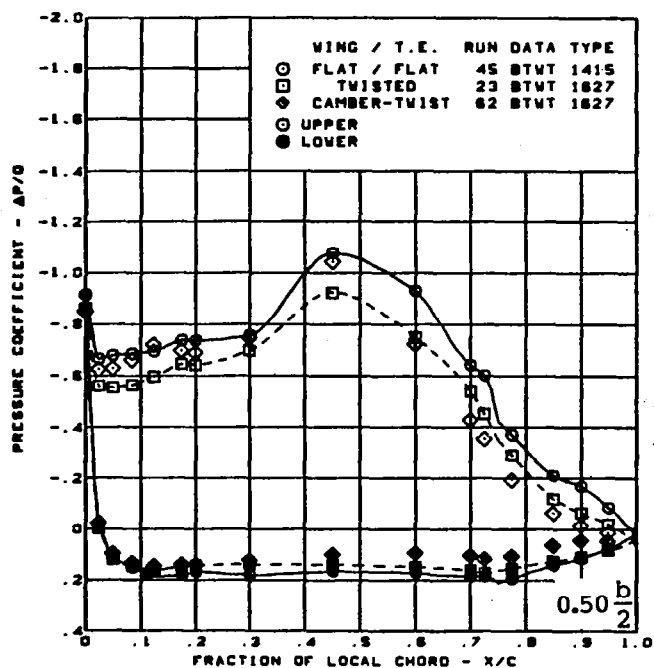
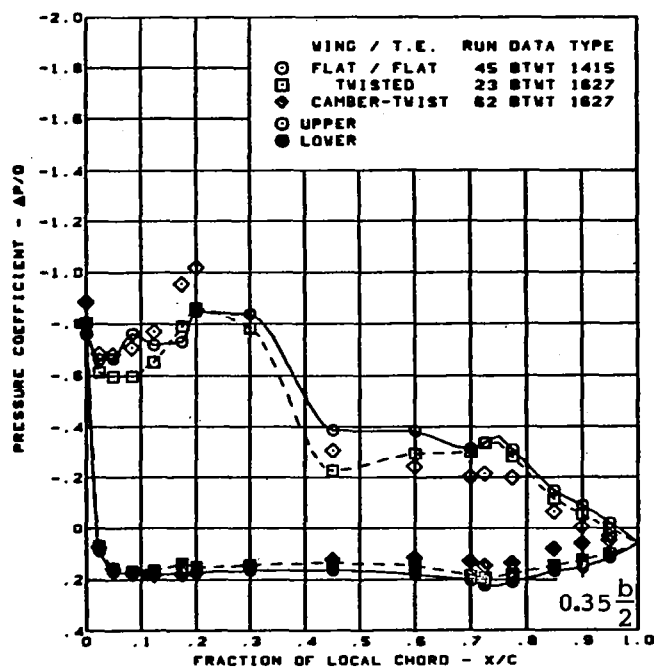
(f) (Concluded)

Figure 26. — (Continued)



(g) Surface Chordwise Pressure Distributions -  $\alpha = 12^\circ$

Figure 26. - (Continued)

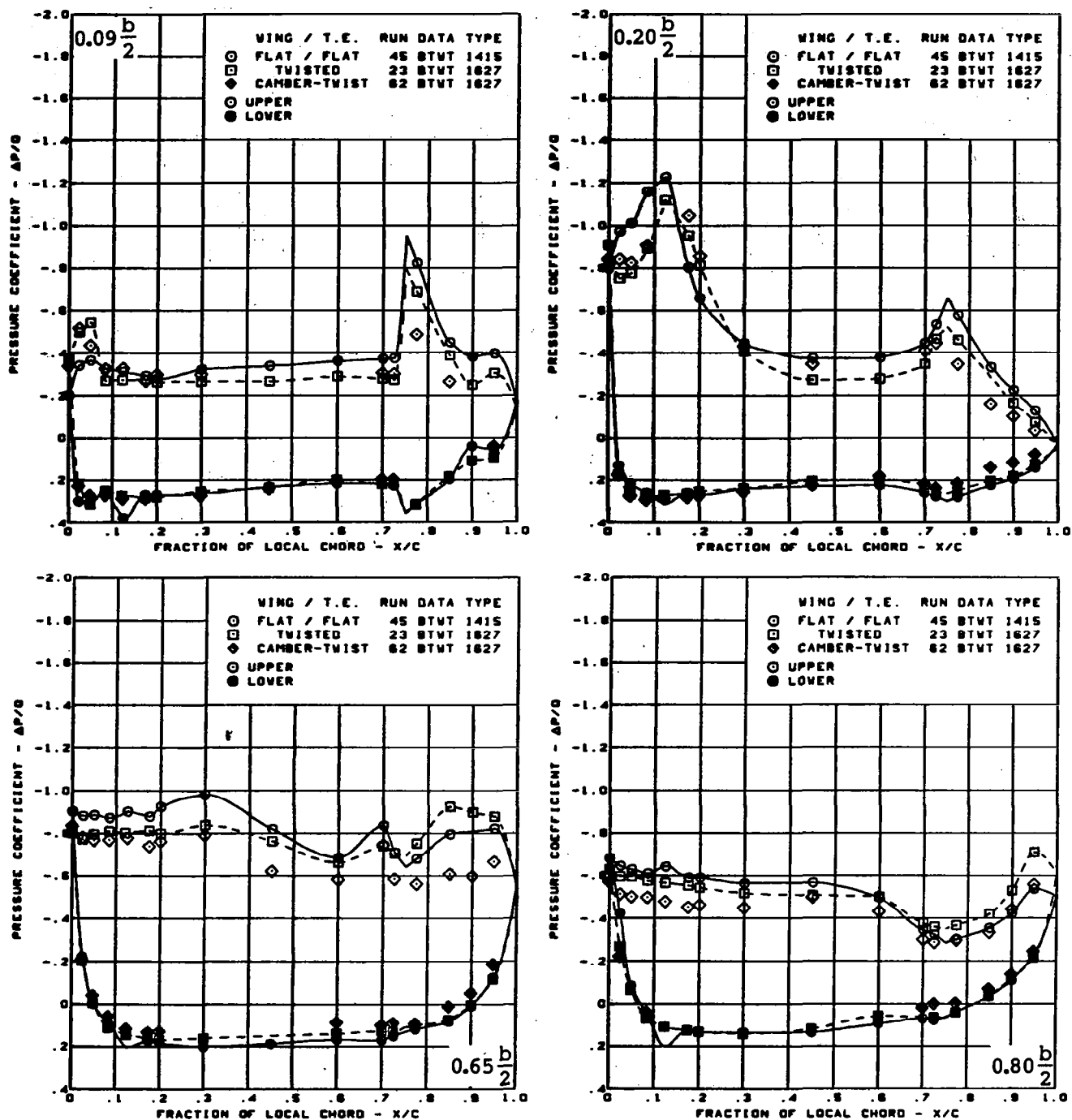


$M = 0.85$   
 $\alpha = 12^\circ$   
 Rounded L.E.  
 L.E. deflection, full span =  $0.0^\circ$   
 T.E. deflection, full span =  $8.3^\circ$

(g) (Concluded)

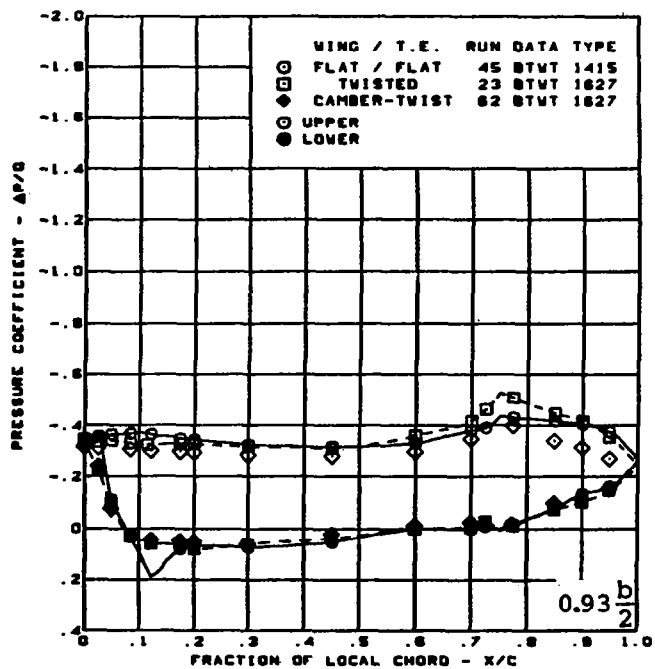
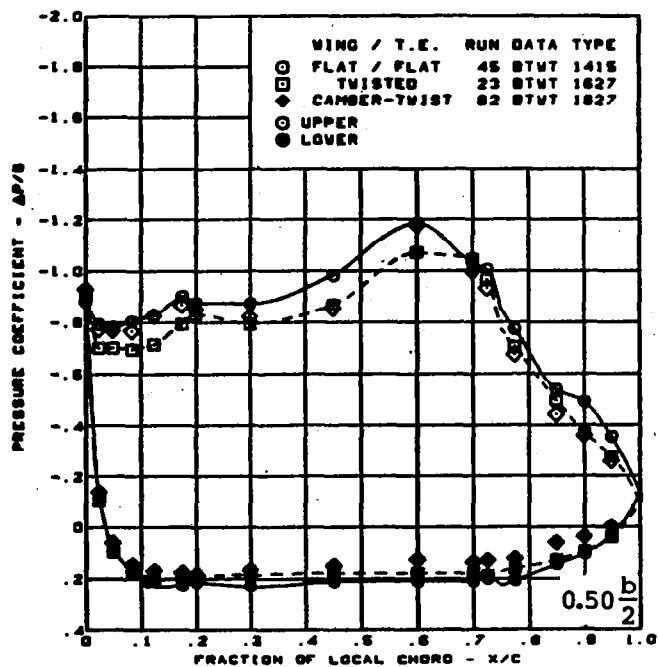
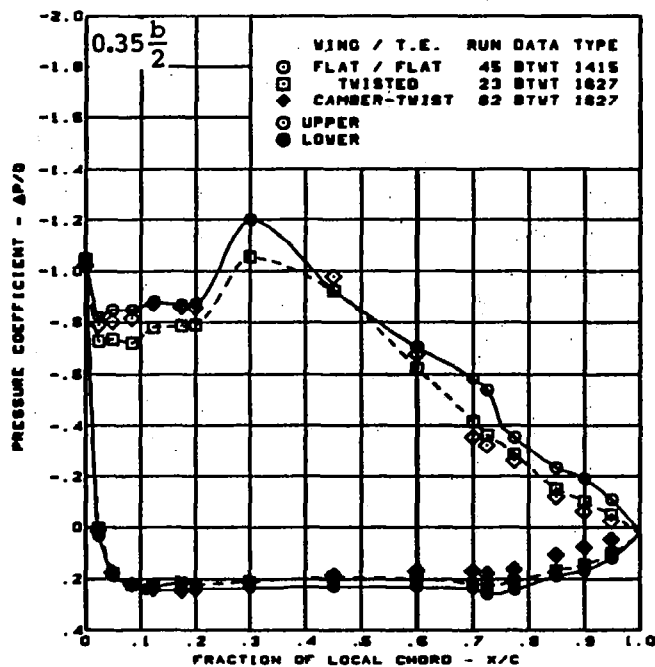
Figure 26. - (Continued)





(h) Surface Chordwise Pressure Distributions -  $\alpha = 16^\circ$

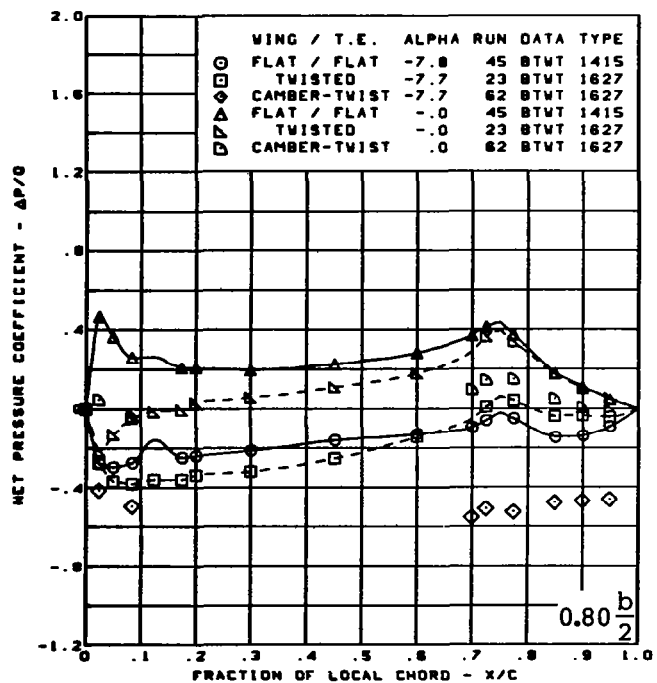
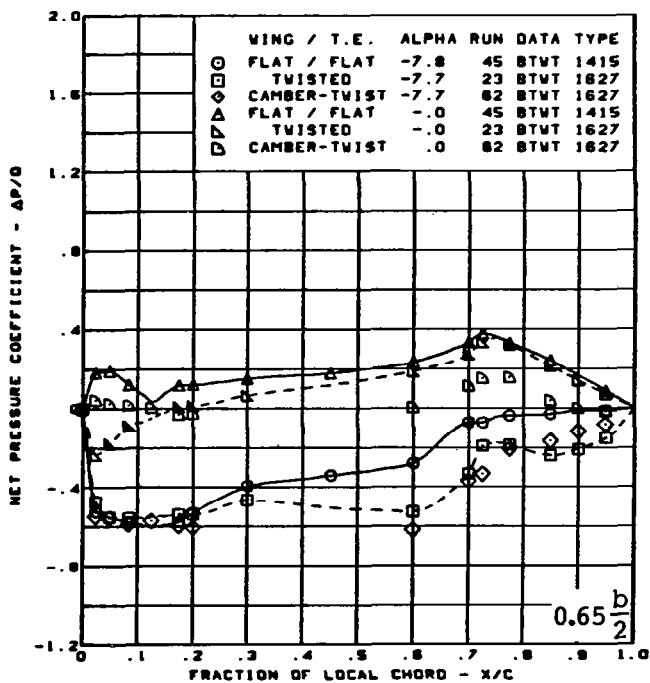
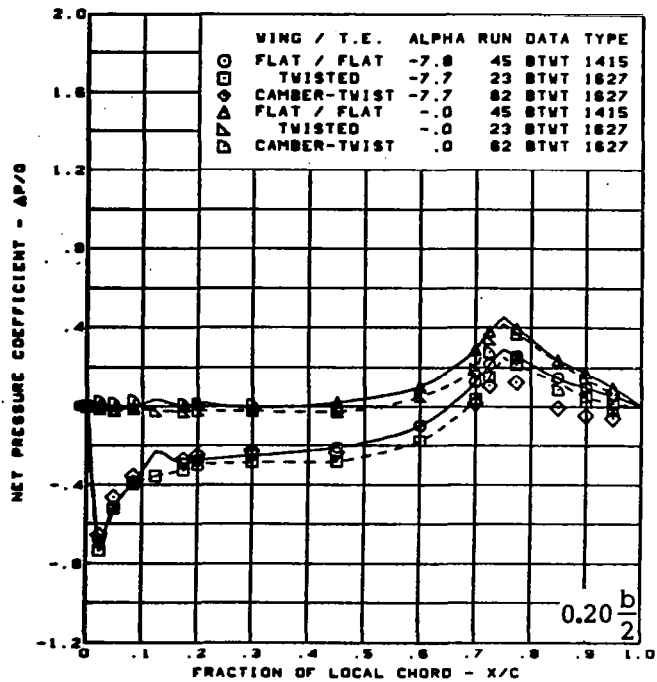
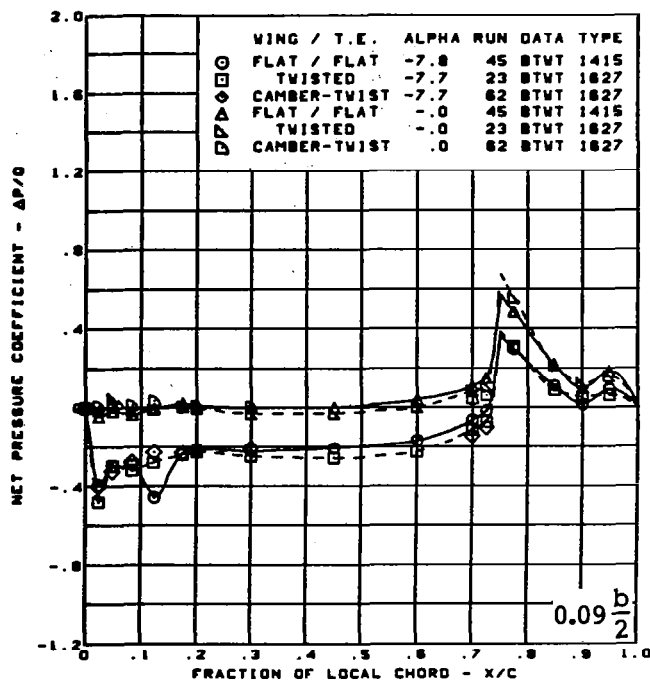
Figure 26. - (Continued)



$M = 0.85$   
 $\alpha = 16^\circ$   
 Rounded L.E.  
 L.E. deflection, full span =  $0.0^\circ$   
 T.E. deflection, full span =  $8.3^\circ$

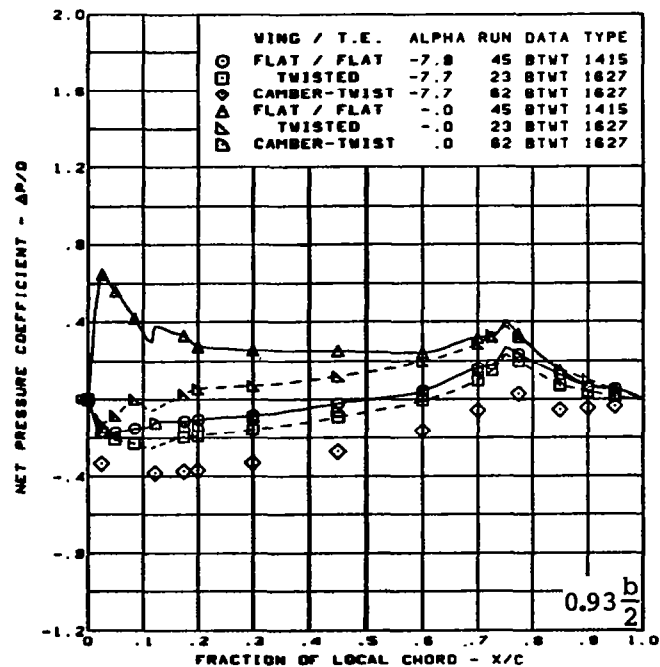
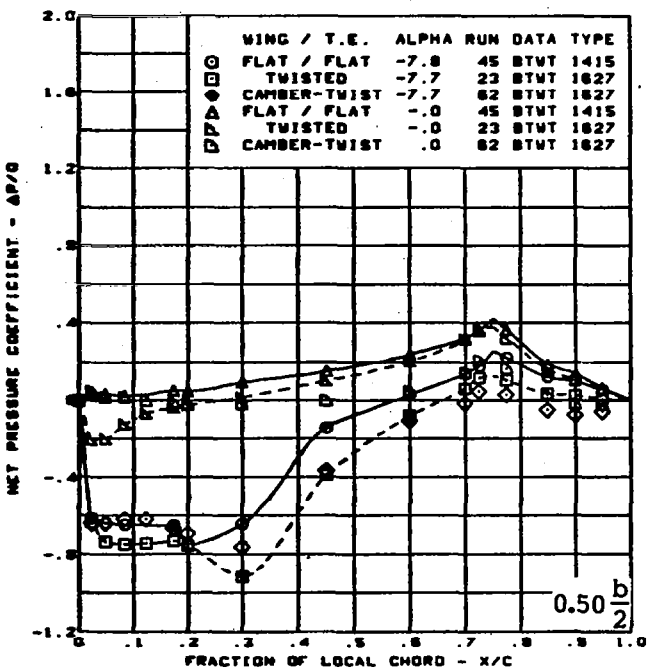
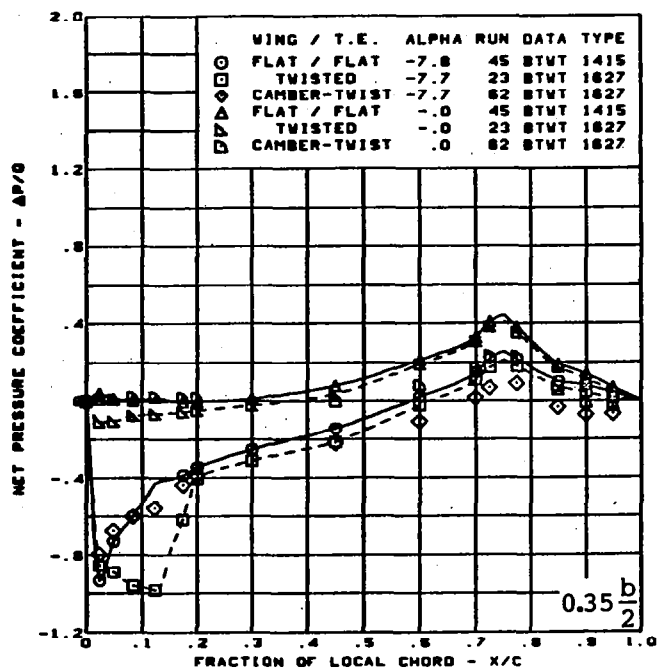
(h) (Concluded)

Figure 26. - (Continued)



(i) Net Chordwise Pressure Distributions -  $\alpha = -8^\circ$  and  $0^\circ$

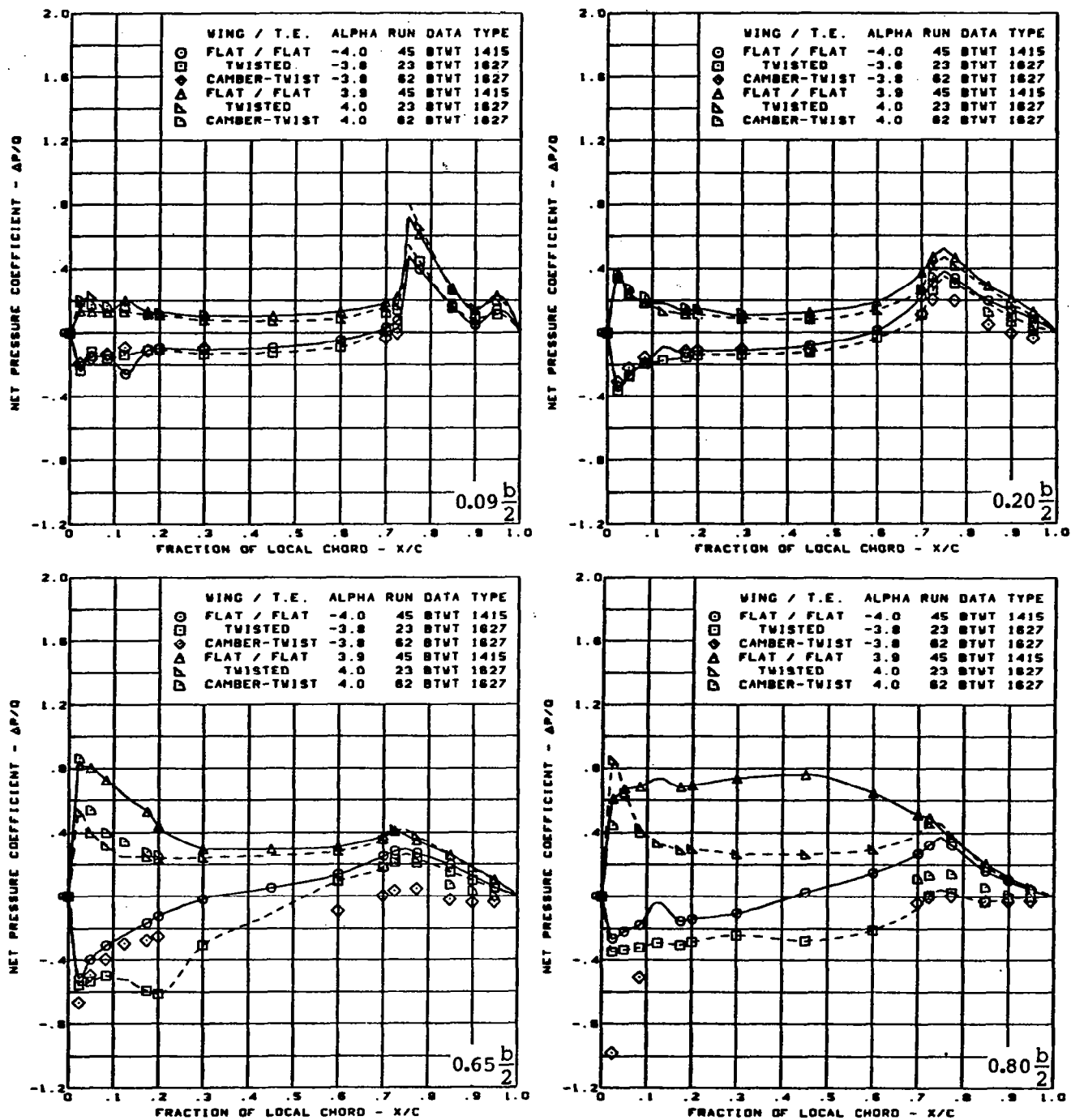
Figure 26. - (Continued)



$M = 0.85$   
 $\alpha = -8^\circ$  and  $0^\circ$   
 Rounded L.E.  
 L.E. deflection, full span =  $0.0^\circ$   
 T.E. deflection, full span =  $8.3^\circ$

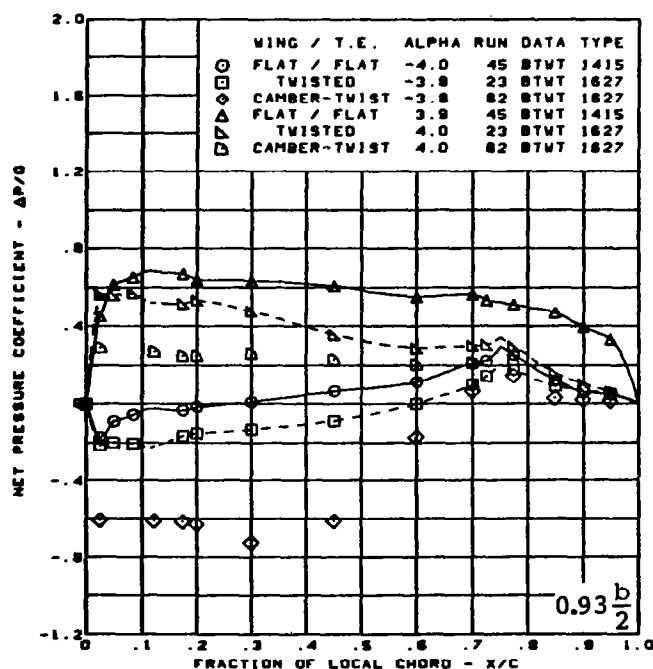
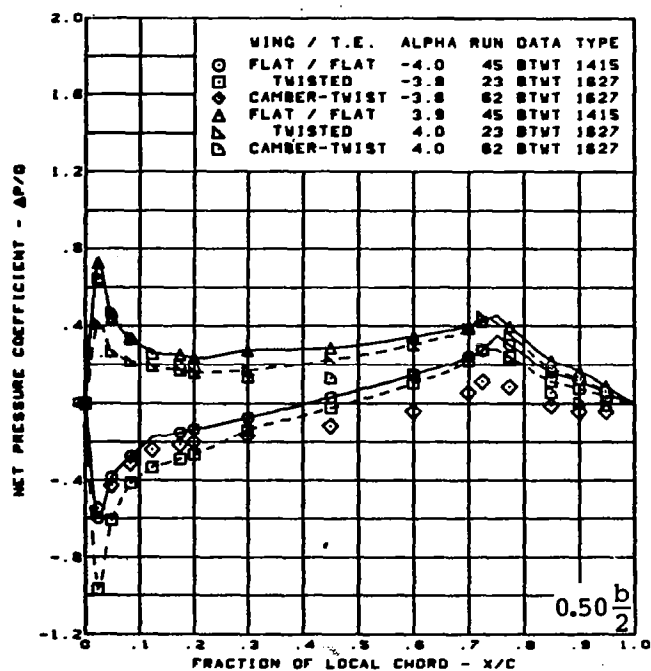
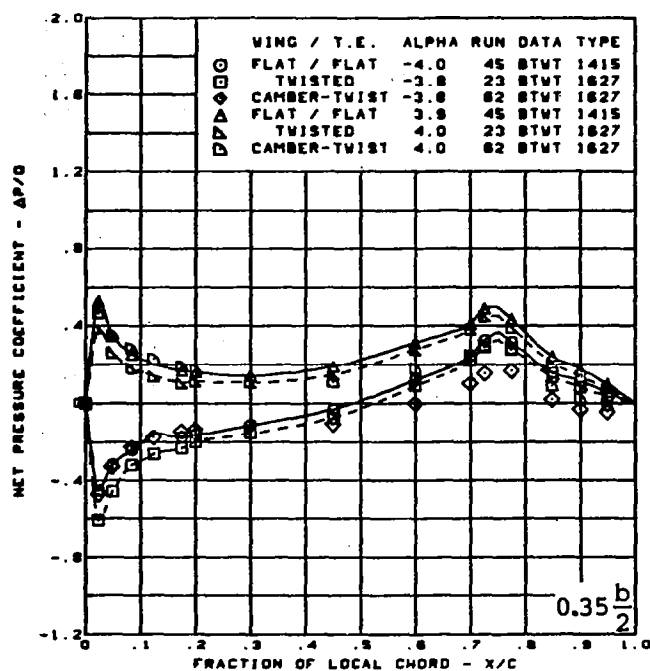
(i) (Concluded)

Figure 26. — (Continued)



(j) Net Chordwise Pressure Distributions -  $\alpha = -4^\circ$  and  $4^\circ$

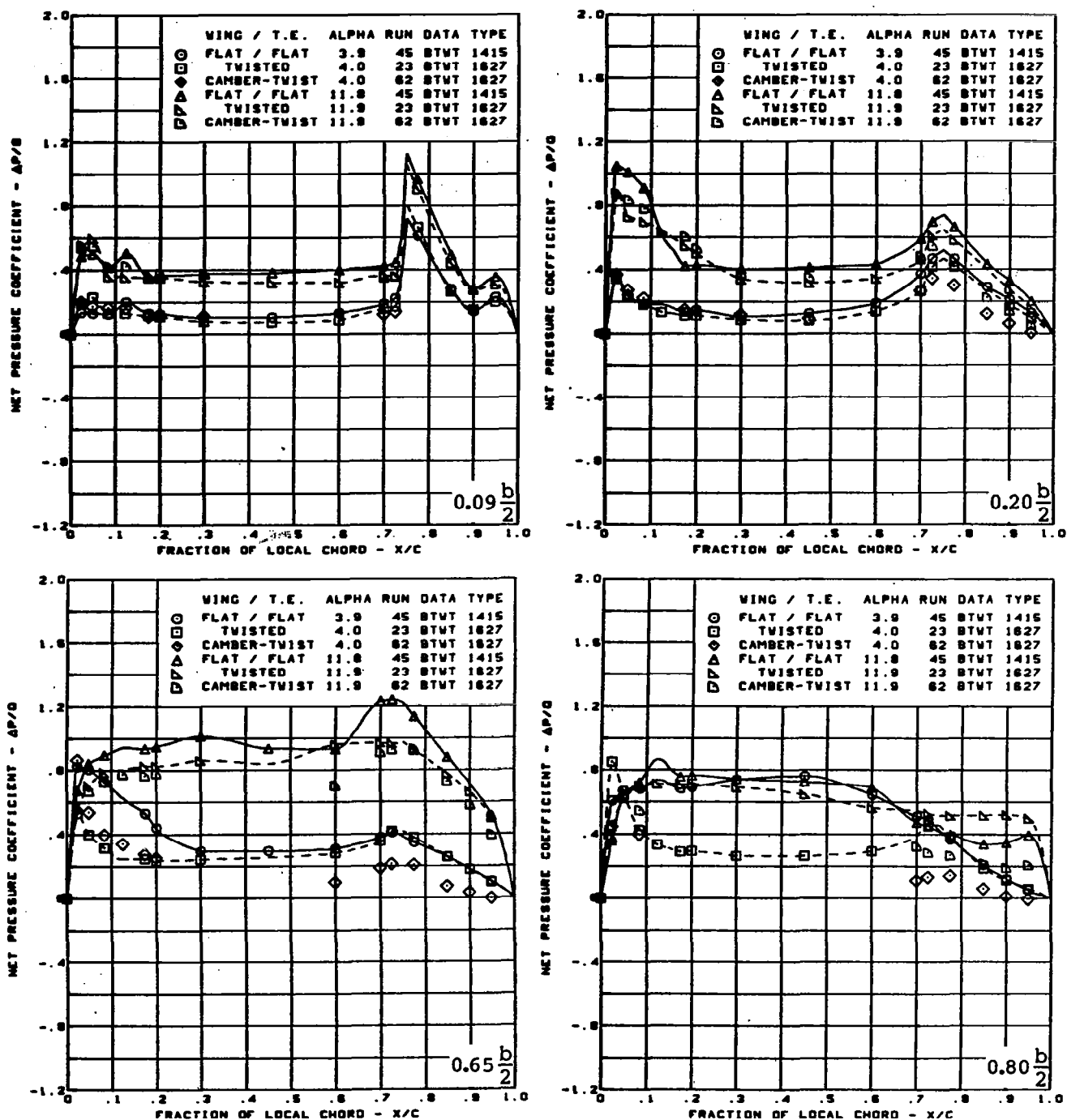
Figure 26. — (Continued)



$M = 0.85$   
 $\alpha = -4^\circ$  and  $4^\circ$   
 Rounded L.E.  
 L.E. deflection, full span =  $0.0^\circ$   
 T.E. deflection, full span =  $8.3^\circ$

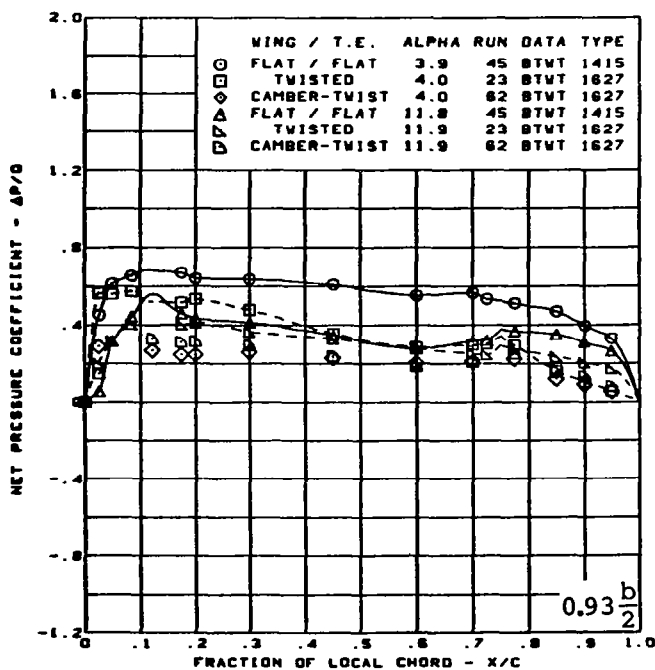
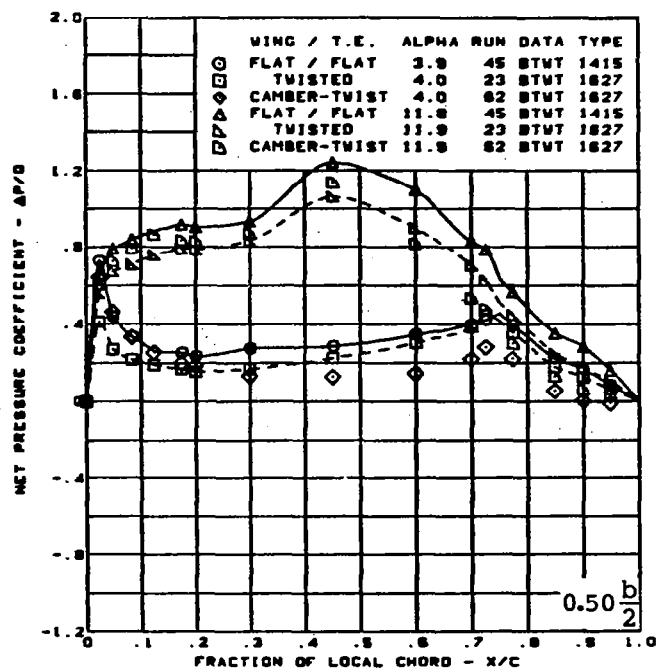
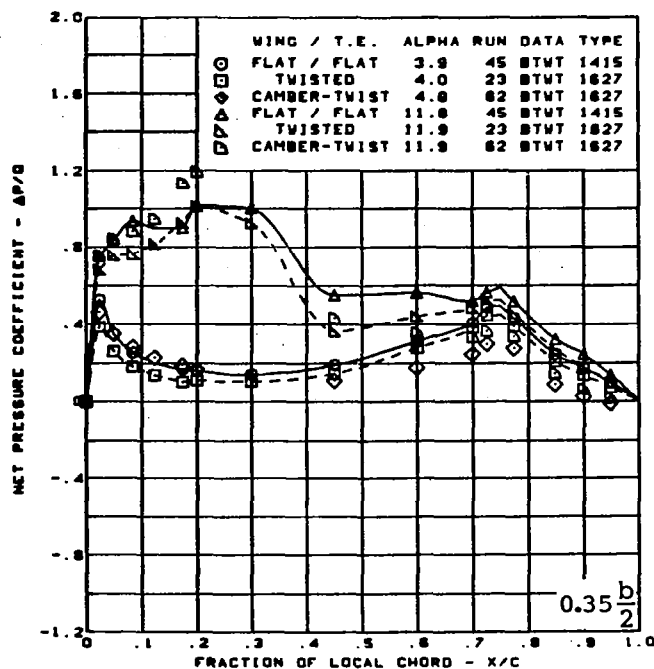
(j) (Concluded)

Figure 26. - (Continued)



(k) Net Chordwise Pressure Distributions -  $\alpha = 4^\circ$  and  $12^\circ$

Figure 26. — (Continued)

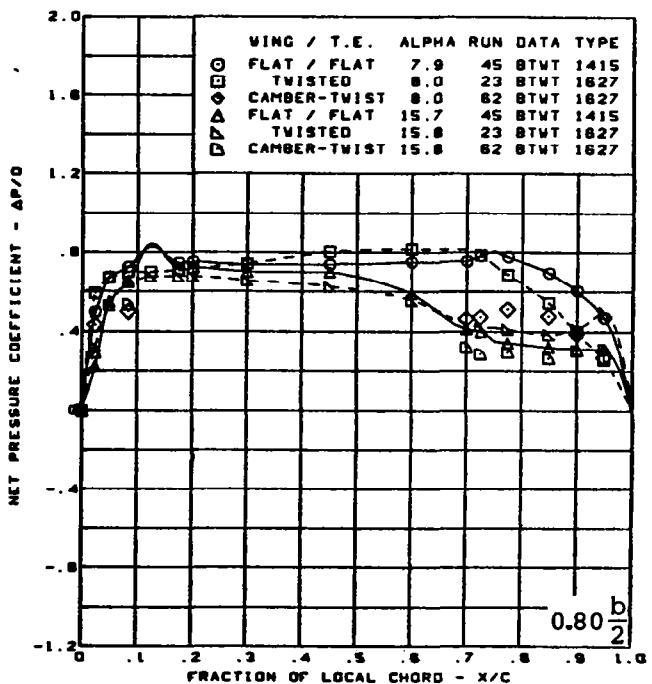
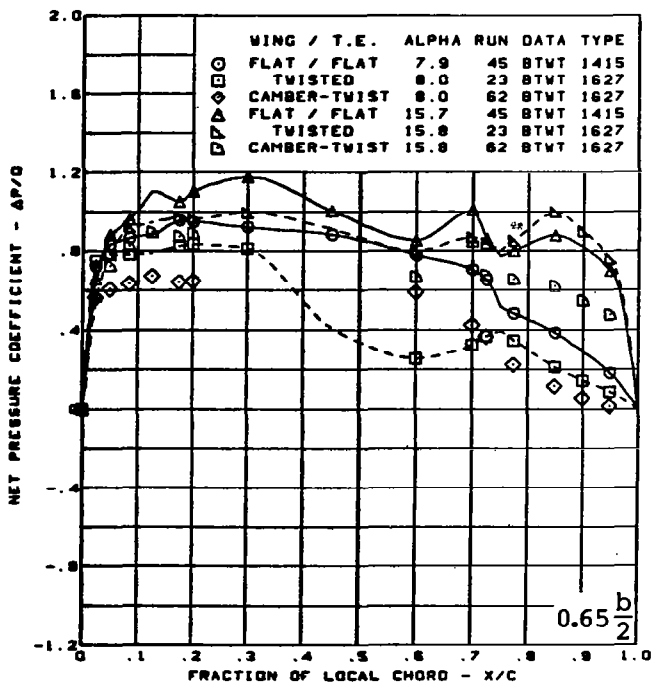
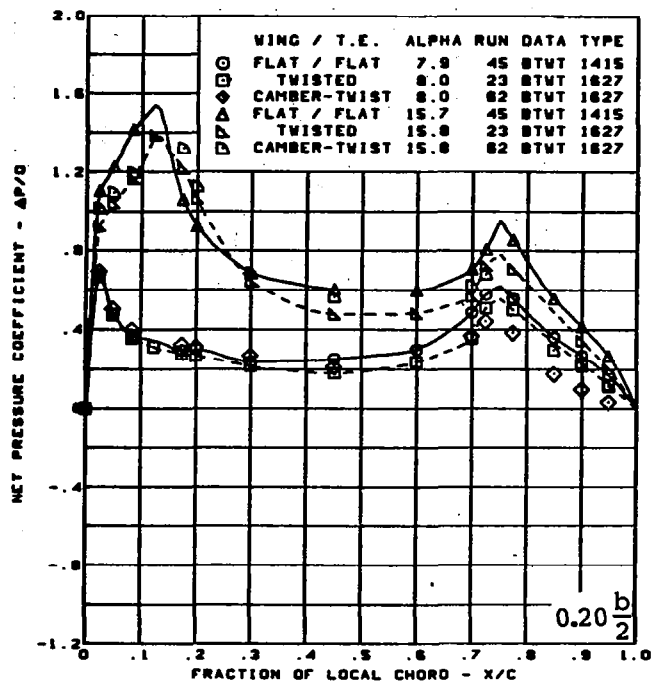
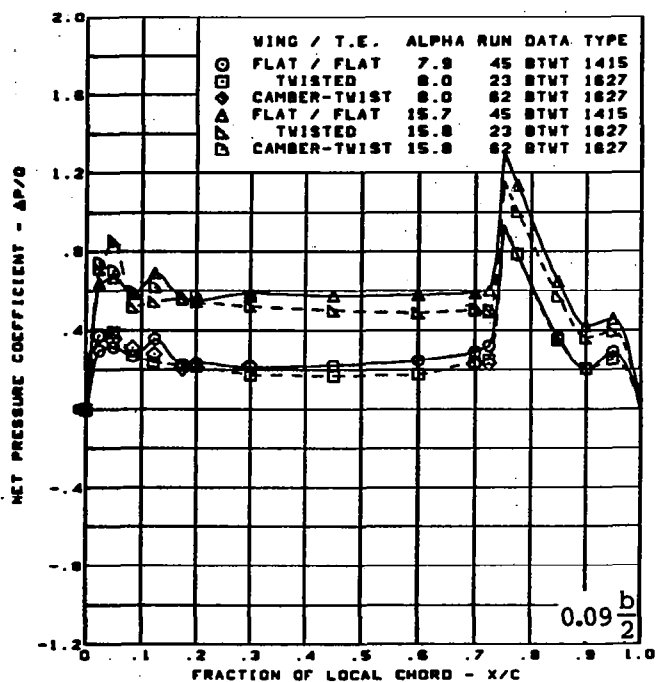


$M = 0.85$   
 $\alpha = 4^\circ$  and  $12^\circ$   
 Rounded L.E.  
 L.E. deflection, full span =  $0.0^\circ$   
 T.E. deflection, full span =  $8.3^\circ$

(k) (Concluded)

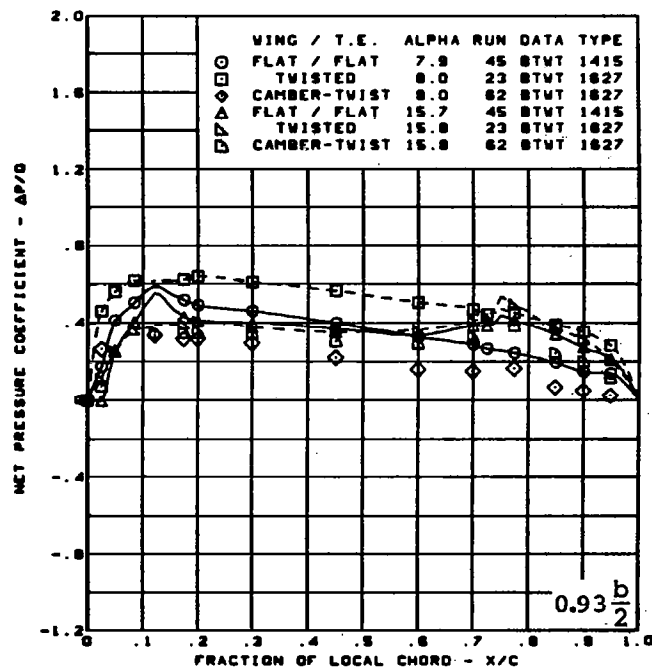
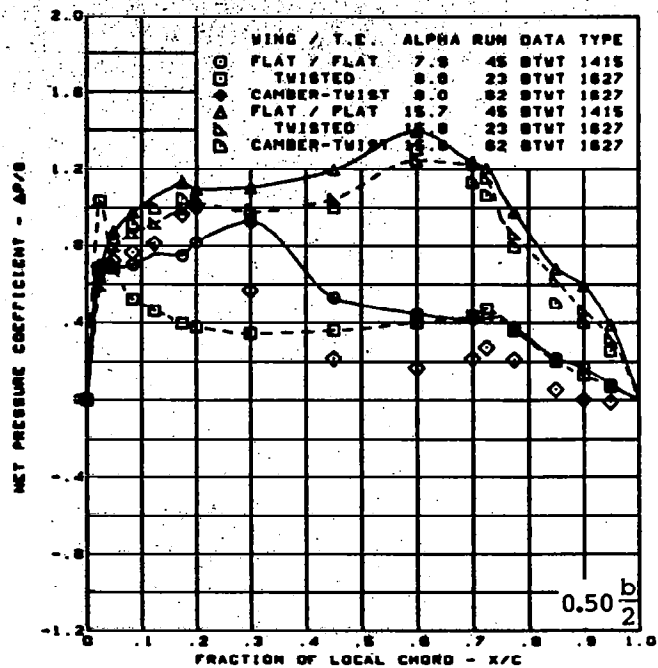
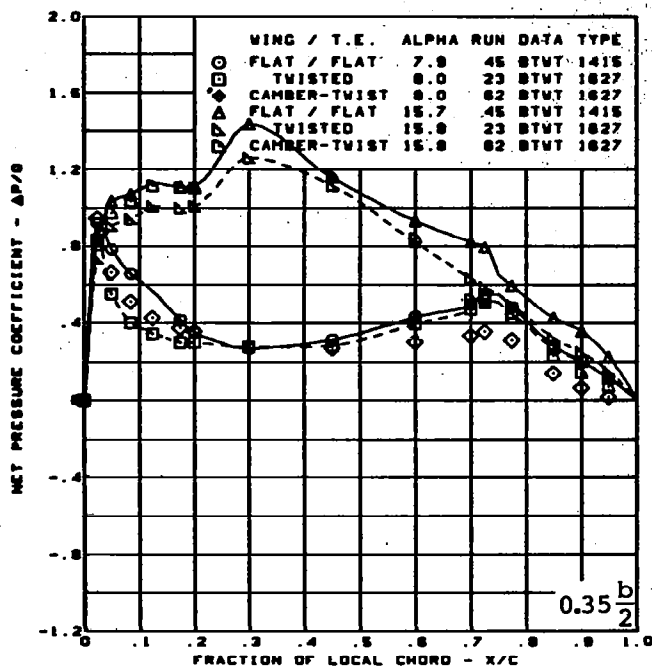
Figure 26. — (Continued)





(I) Net Chordwise Pressure Distributions -  $\alpha = 8^\circ$  and  $16^\circ$

Figure 26. - (Continued)



$M = 0.85$

$\alpha = 8^\circ$  and  $16^\circ$

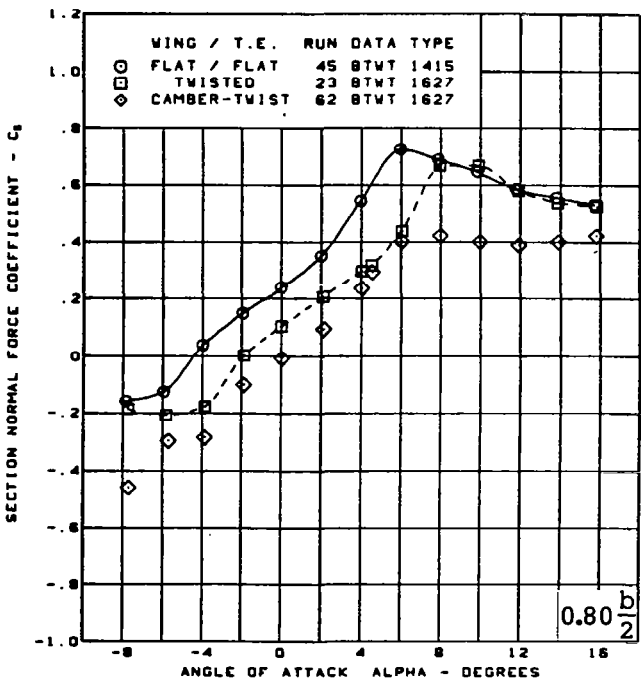
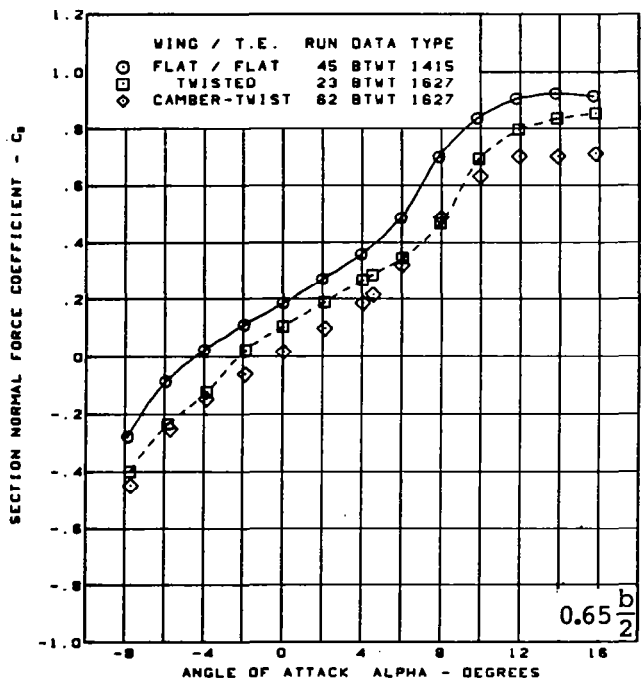
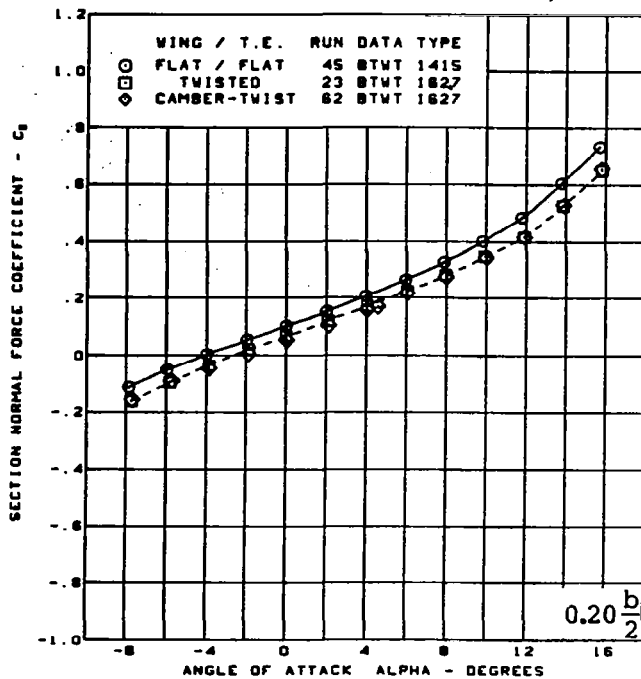
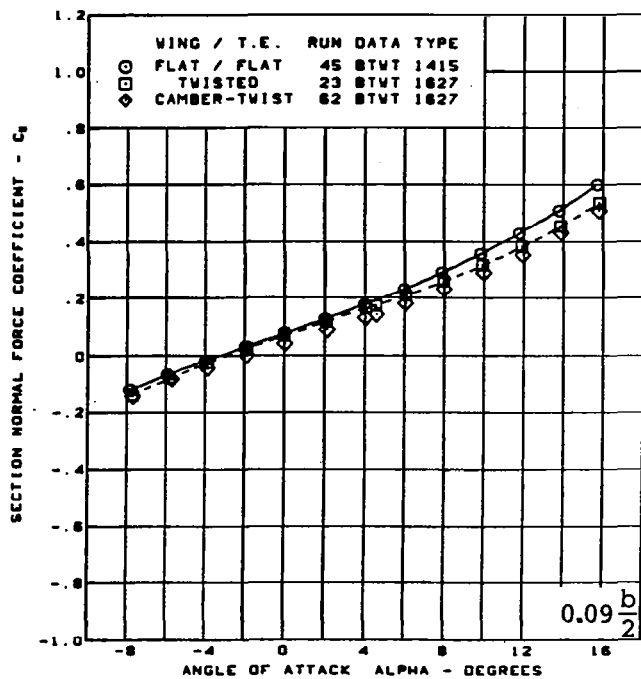
Rounded L.E.

L.E. deflection, full span =  $0.0^\circ$

T.E. deflection, full span =  $8.3^\circ$

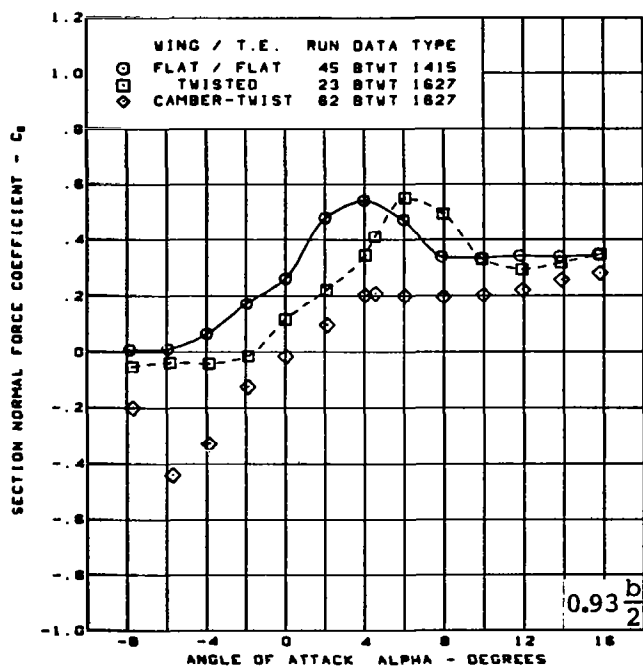
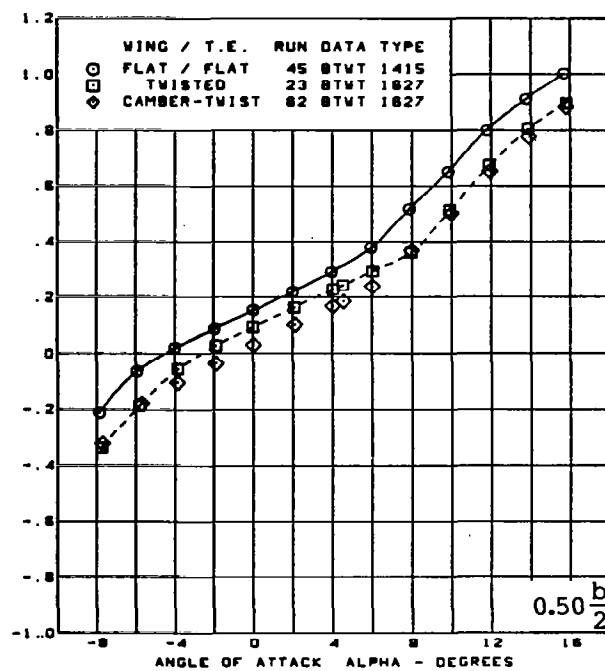
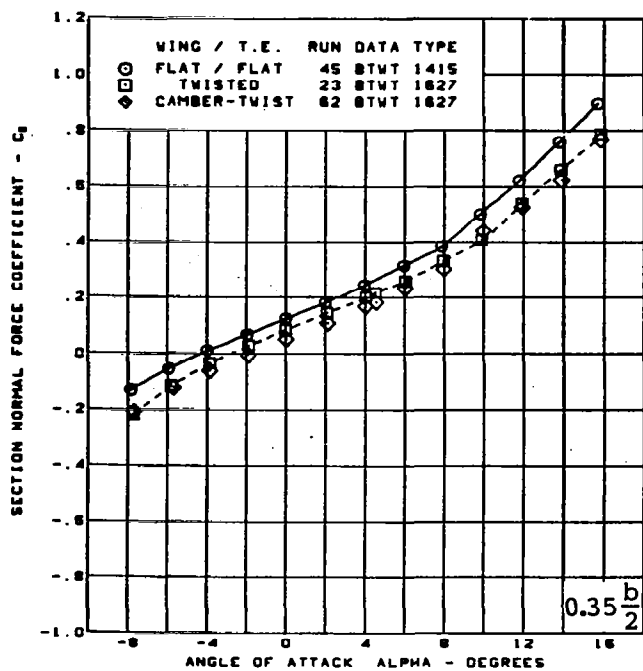
(I) (Concluded)

Figure 26. - (Continued)



(m) Section Aerodynamic Coefficients - Normal Force

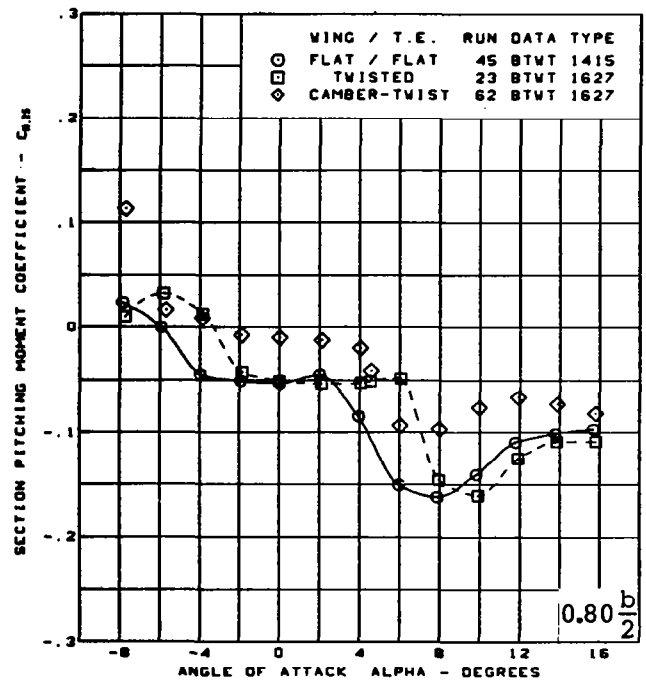
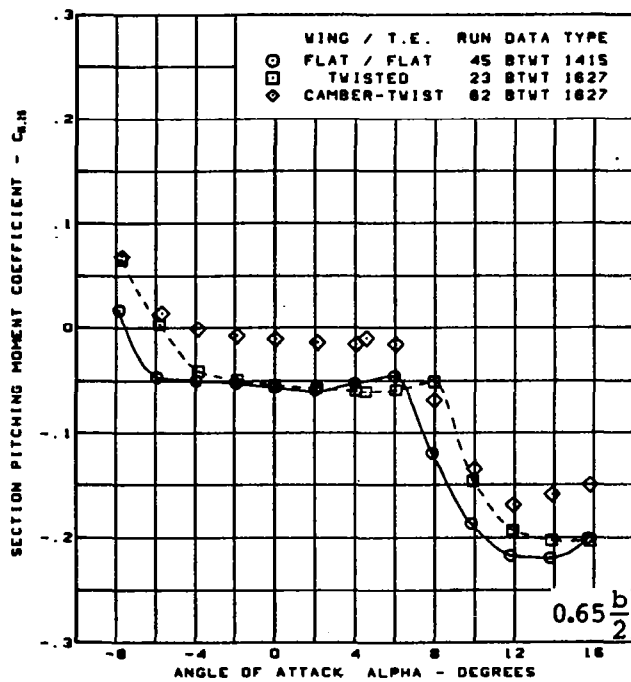
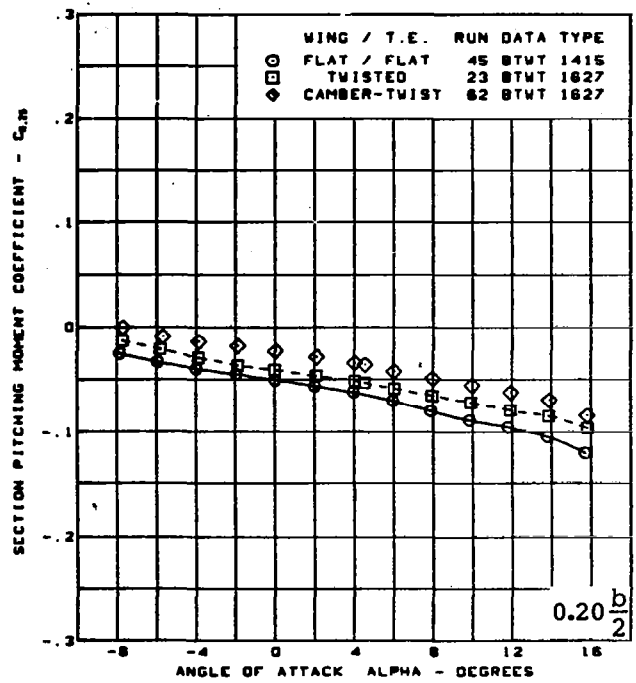
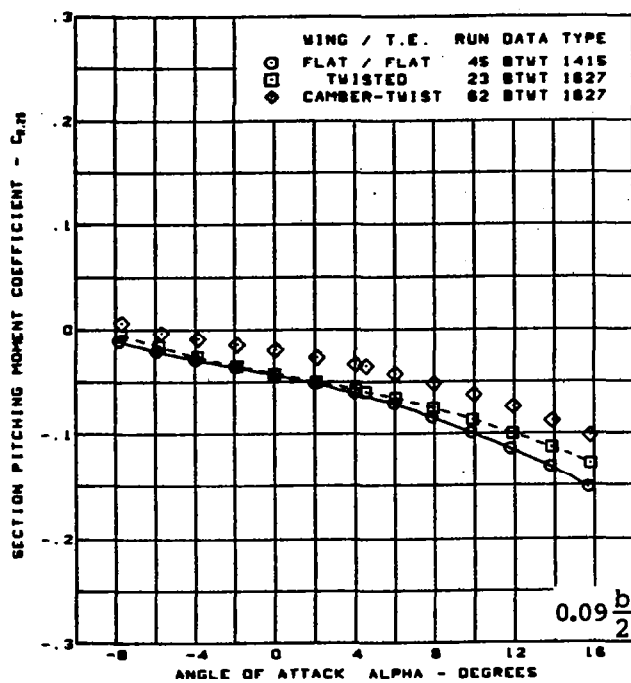
Figure 26. - (Continued)



$M = 0.85$   
 Rounded L.E.  
 L.E. deflection, full span =  $0.0^\circ$   
 T.E. deflection, full span =  $8.3^\circ$

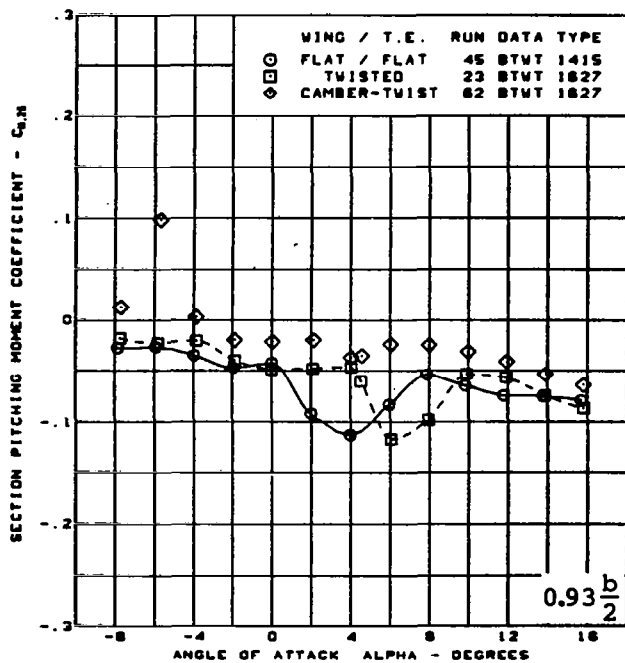
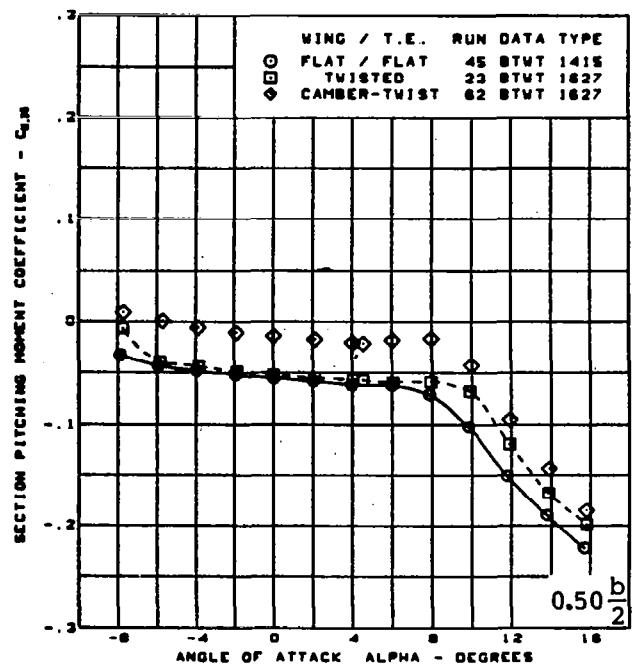
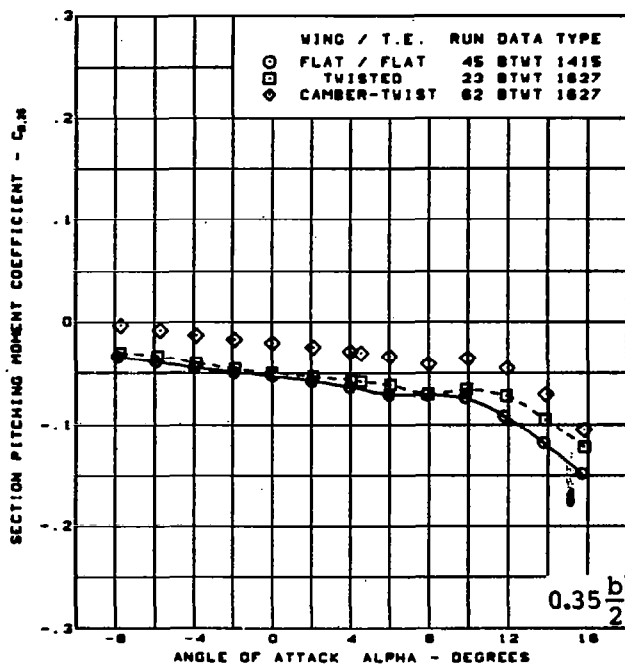
(m) (Concluded)

Figure 26. - (Continued)



(n) Section Aerodynamic Coefficients - Pitching Moment

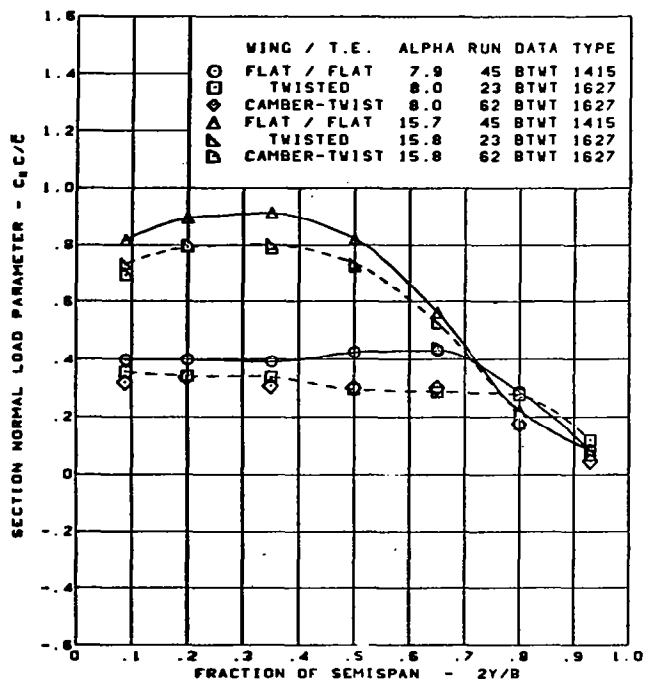
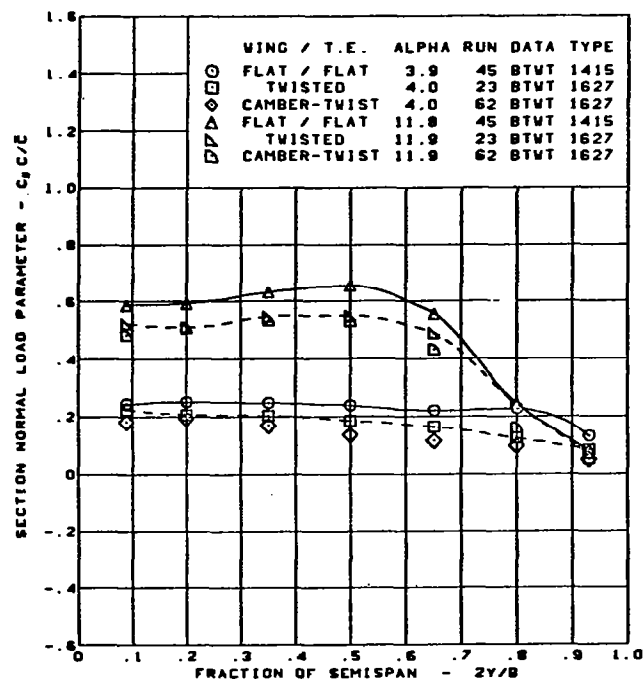
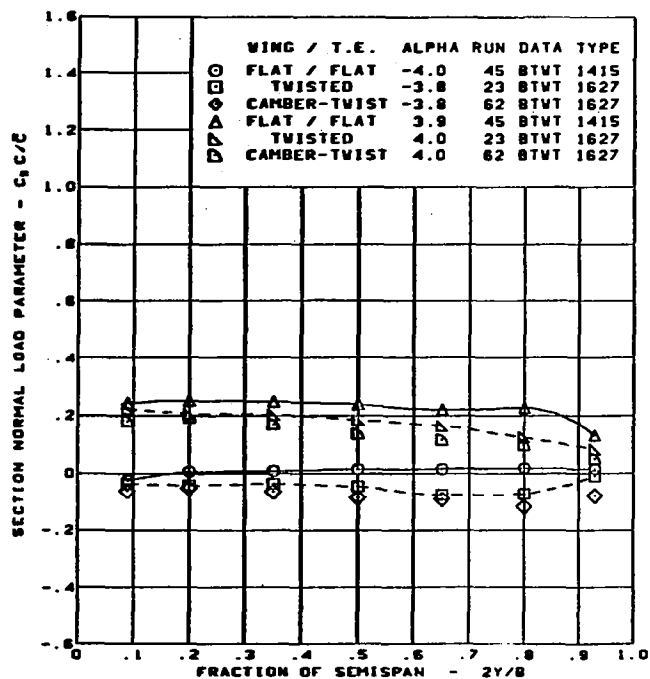
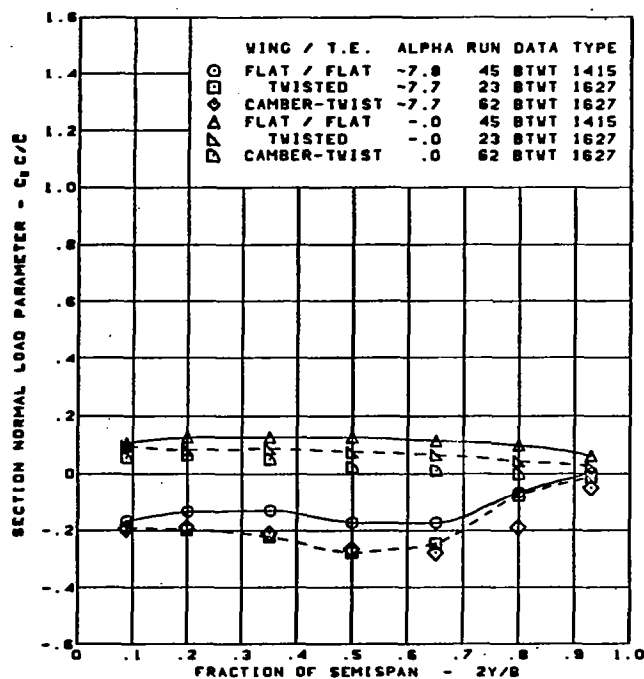
Figure 26. - (Continued)



M = 0.85  
 Rounded L.E.  
 L.E. deflection, full span =  $0.0^\circ$   
 T.E. deflection, full span =  $8.3^\circ$

(n) (Concluded)

Figure 26. -(Continued)

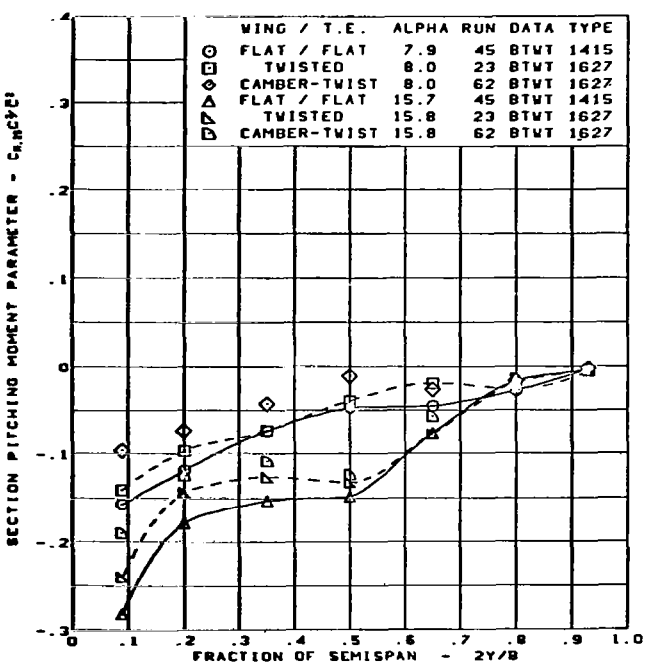
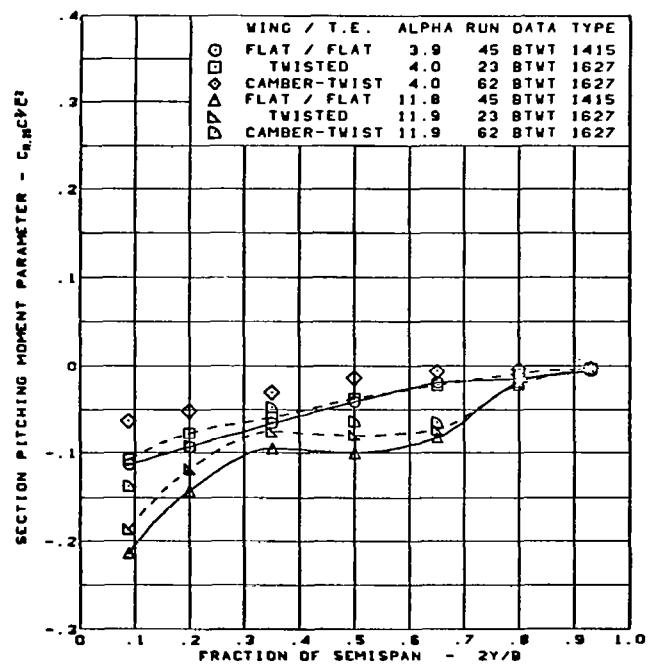
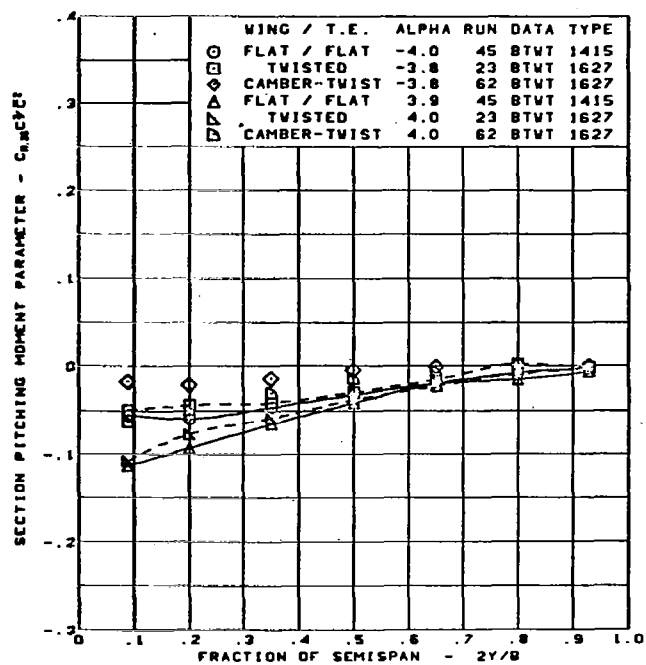
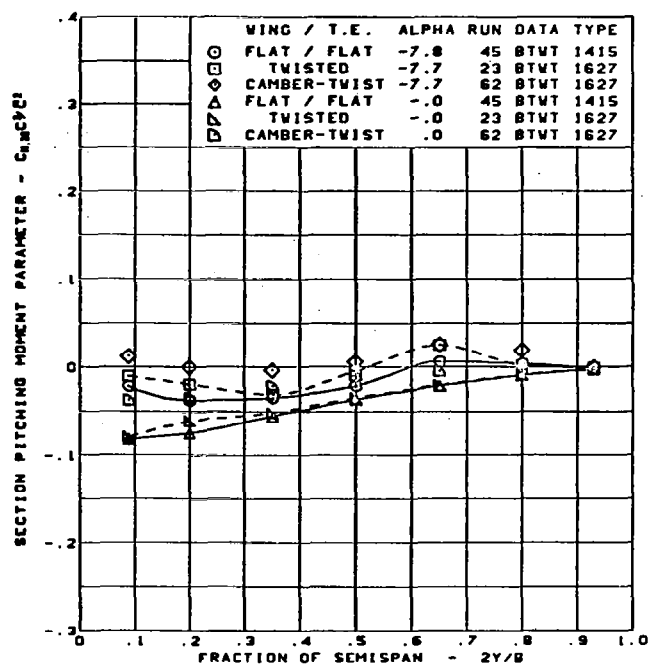


M = 0.85  
Rounded L.E.

L.E. deflection, full span =  $0.0^\circ$   
T.E. deflection, full span =  $8.3^\circ$

(a) Spanload Distributions - Normal Force

Figure 26. — (Continued)



M = 0.85  
Rounded L.E.

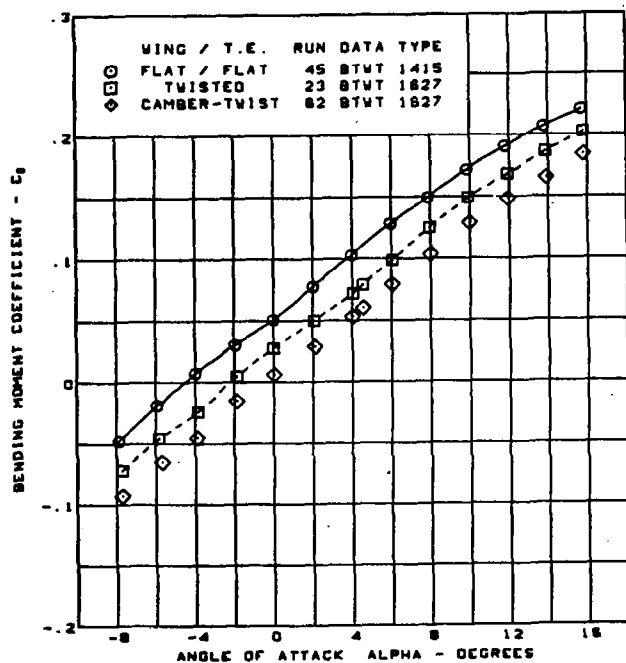
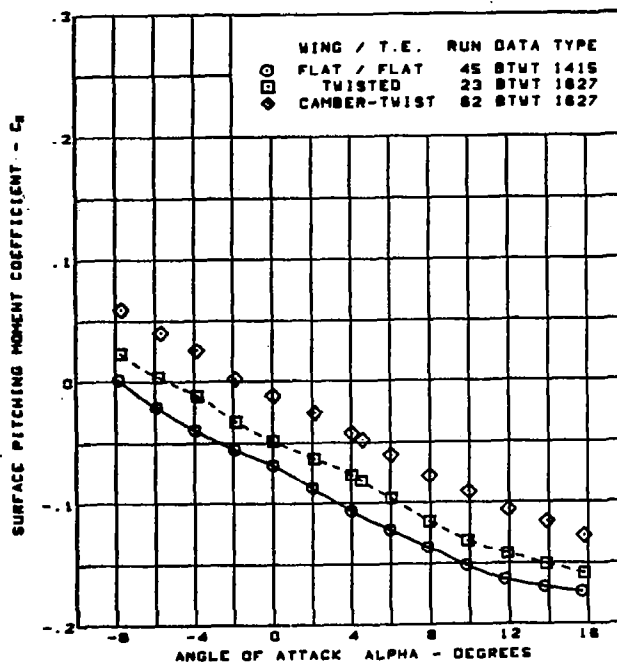
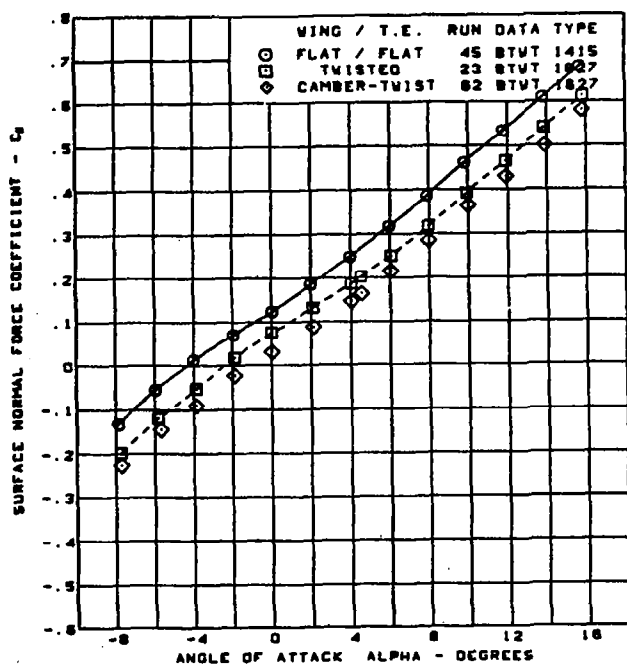
L.E. deflection, full span =  $0.0^\circ$   
T.E. deflection, full span =  $8.3^\circ$

(p) Spanload Distributions - Pitching Moment

Figure 26. - (Continued)







$M = 0.85$

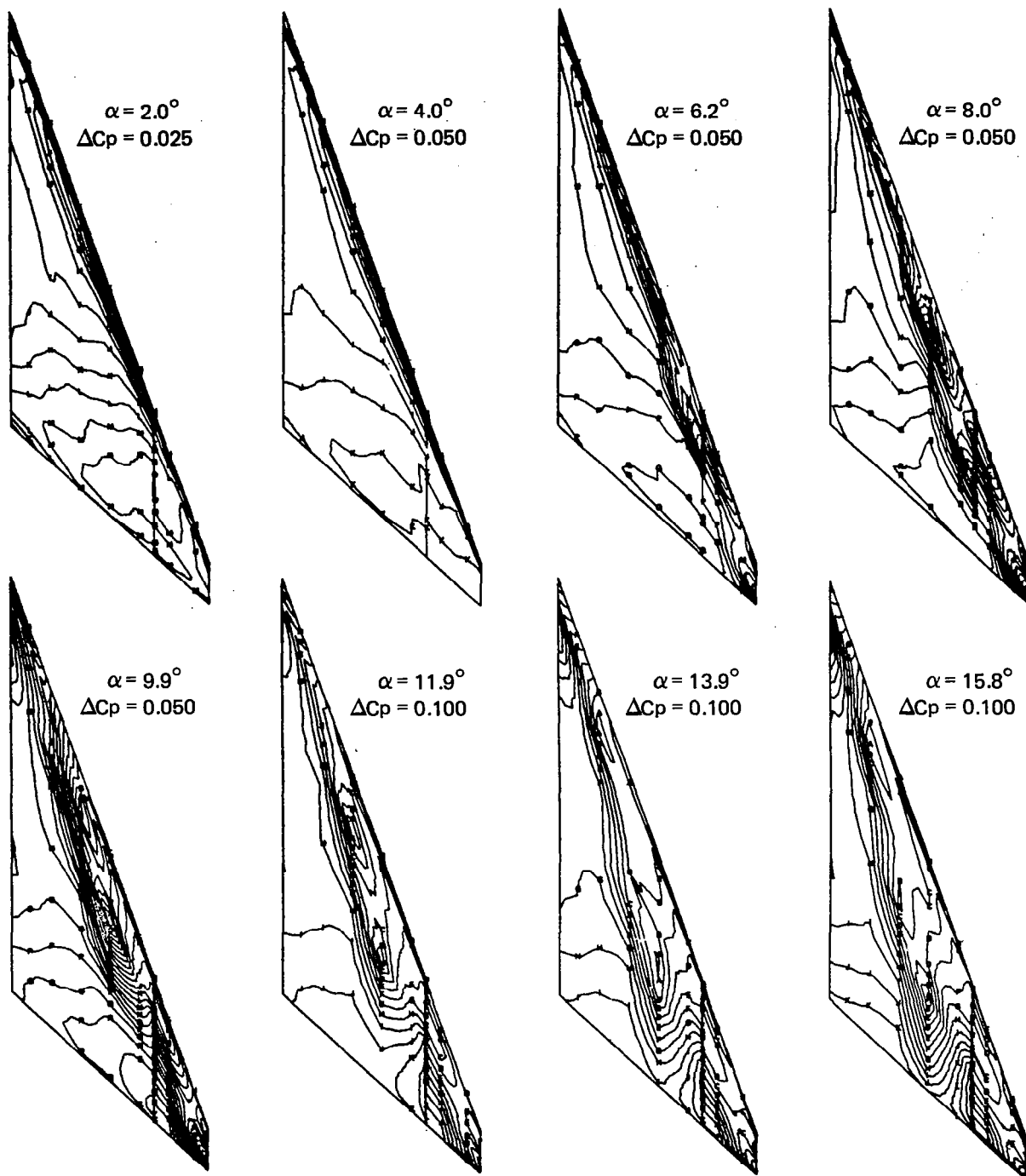
Rounded L.E.

L.E. deflection, full span =  $0.0^\circ$

T.E. deflection, full span =  $8.3^\circ$

(q) Wing Aerodynamic Coefficients

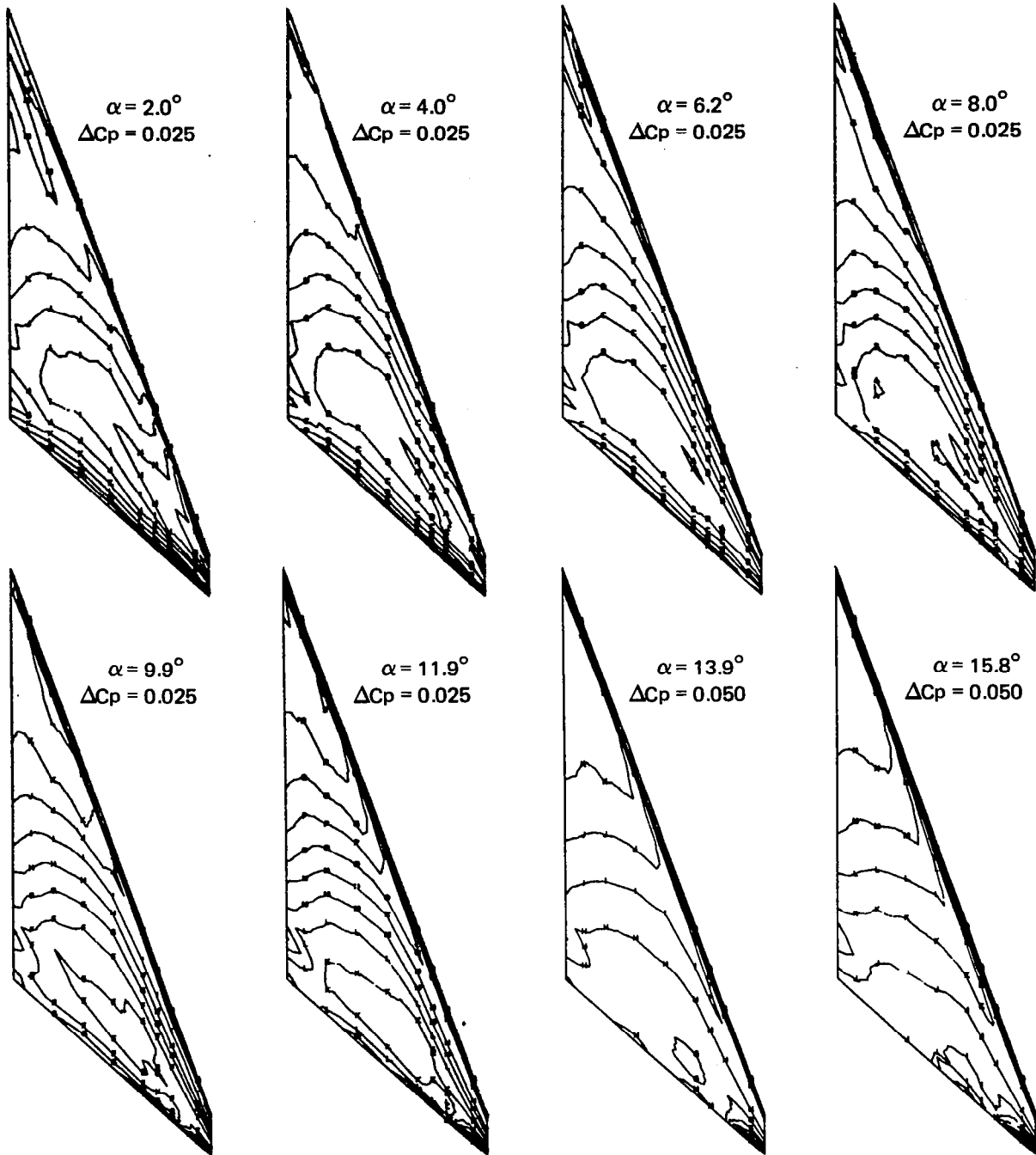
Figure 26. - (Concluded)



Note:  $\Delta C_p$  = increment between adjacent isobars

(a) Upper Surface Isobars

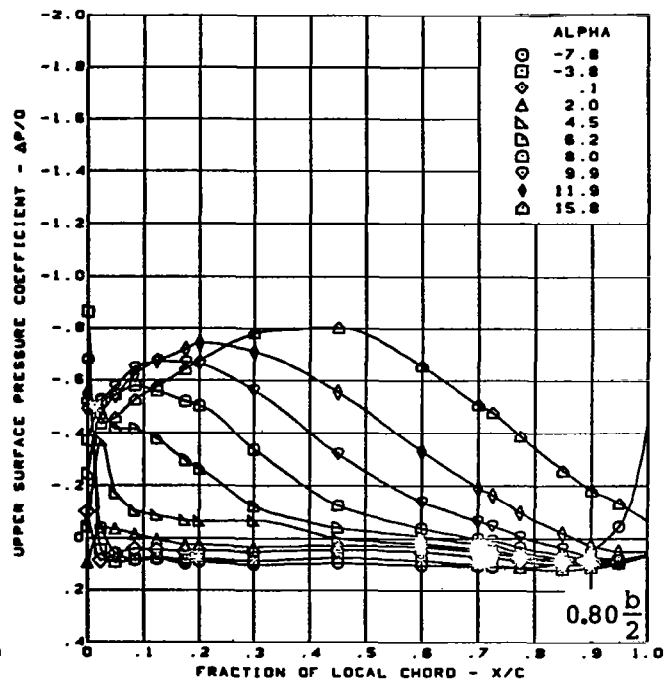
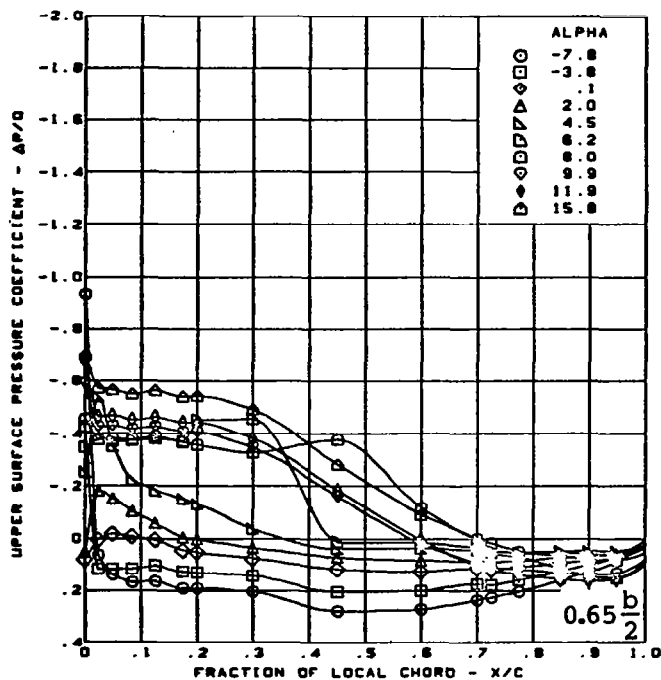
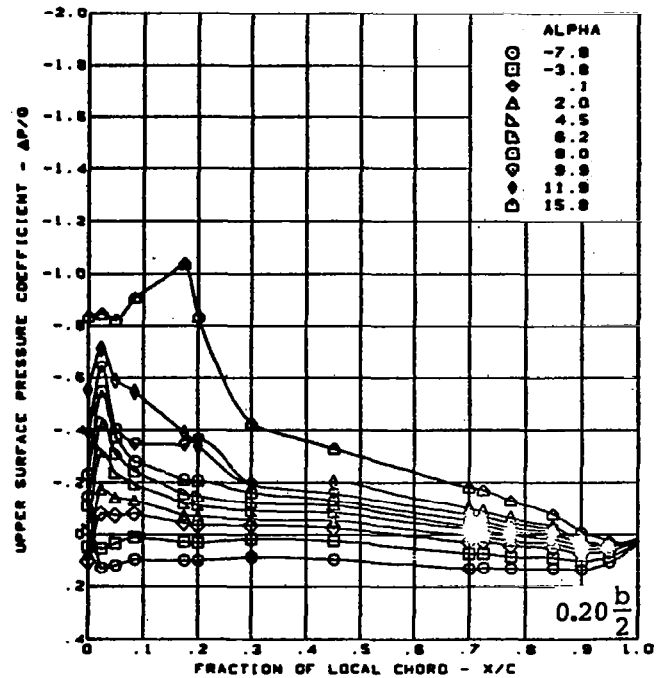
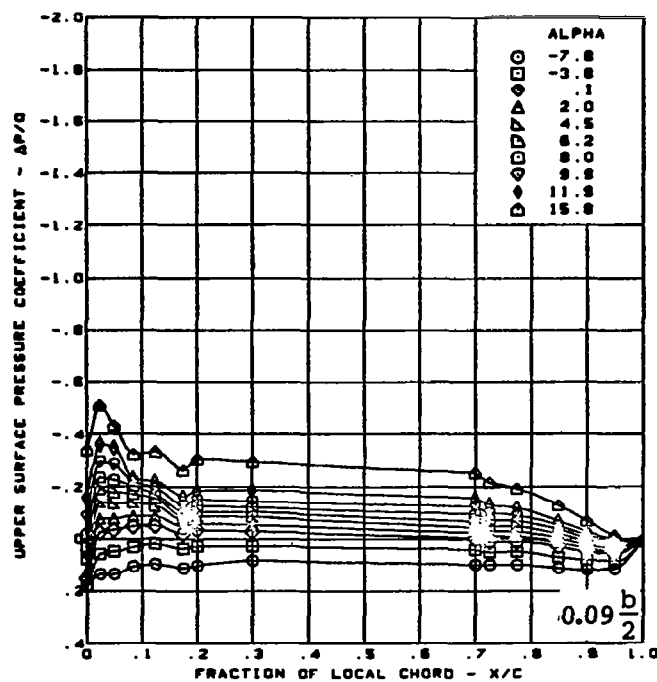
Figure 27. — Wing Experimental Data—Effect of Angle of Attack; Cambered-Twisted Wing; Fin On; T.E. Deflection, Full Span =  $0.0^\circ$ ;  $M = 0.85$



Note:  $\Delta C_p$  = increment between adjacent isobars

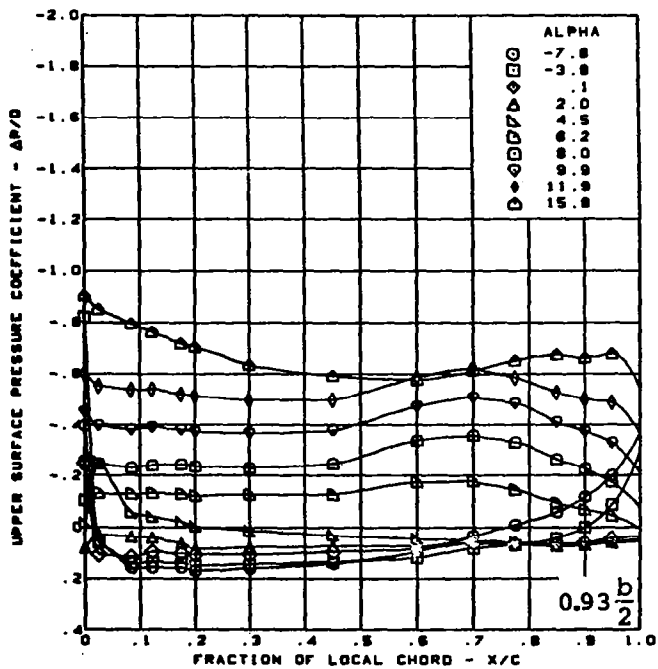
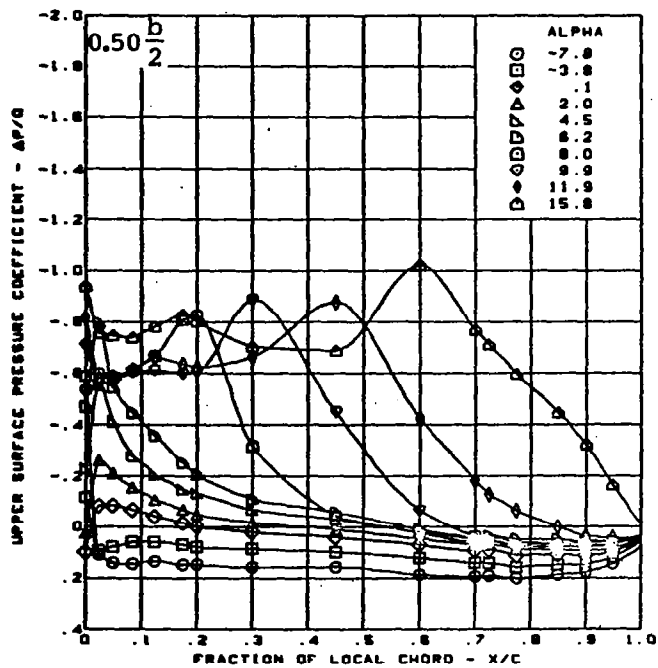
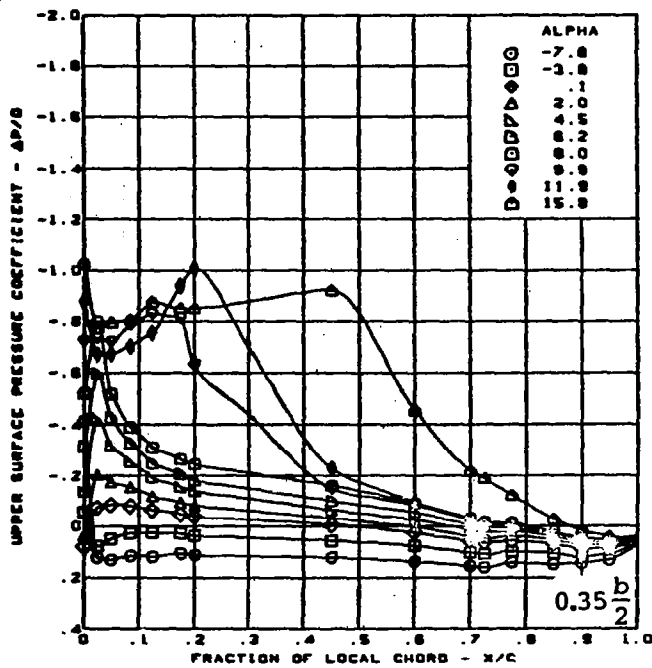
(b) Lower Surface Isobars

Figure 27. — (Continued)



(c) Upper Surface Chordwise Pressure Distributions

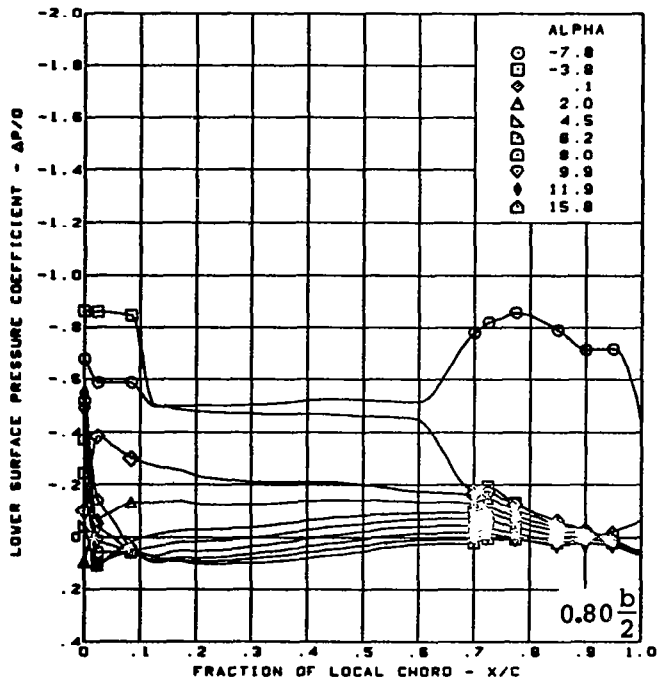
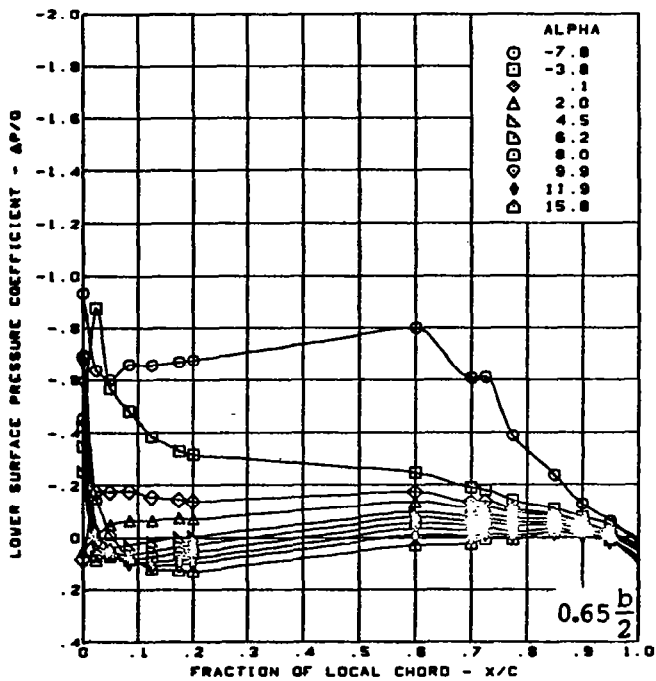
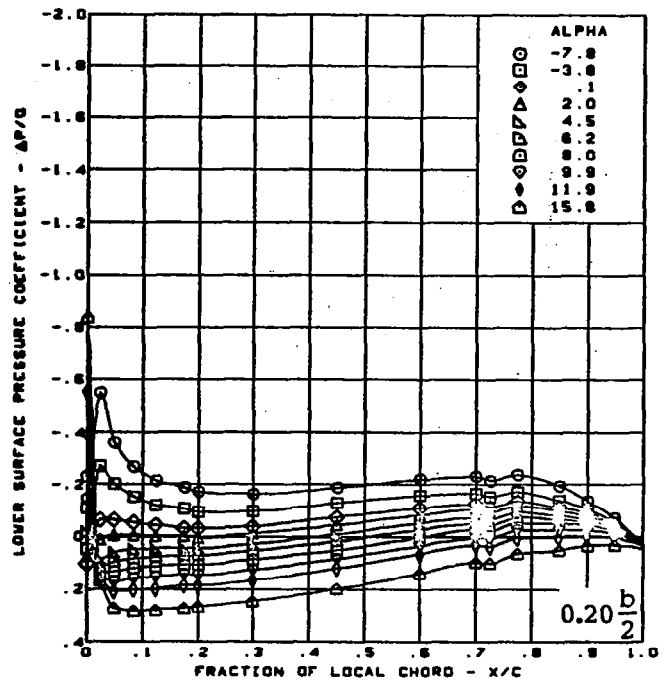
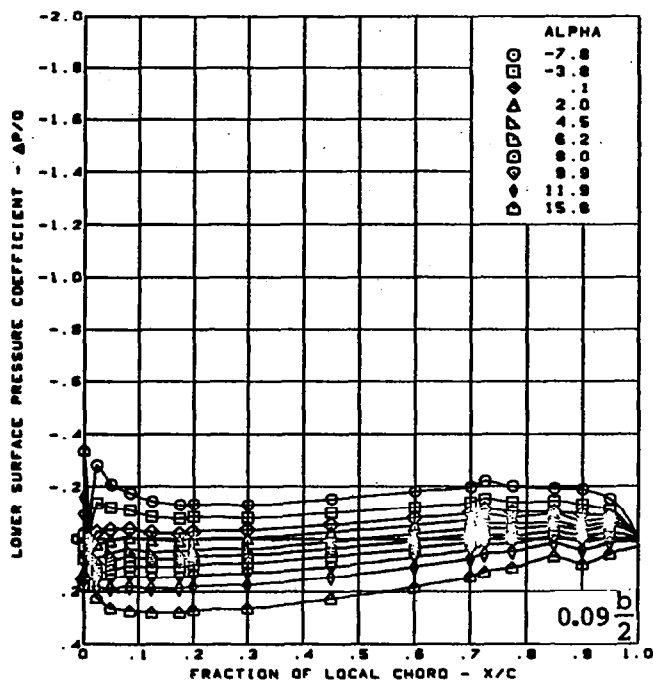
Figure 27. — (Continued)



$M = 0.85$  (run 48)  
 Cambered-twisted wing, rounded L.E.  
 Fin on  
 L.E. deflection, full span =  $0.0^\circ$   
 T.E. deflection, full span =  $0.0^\circ$

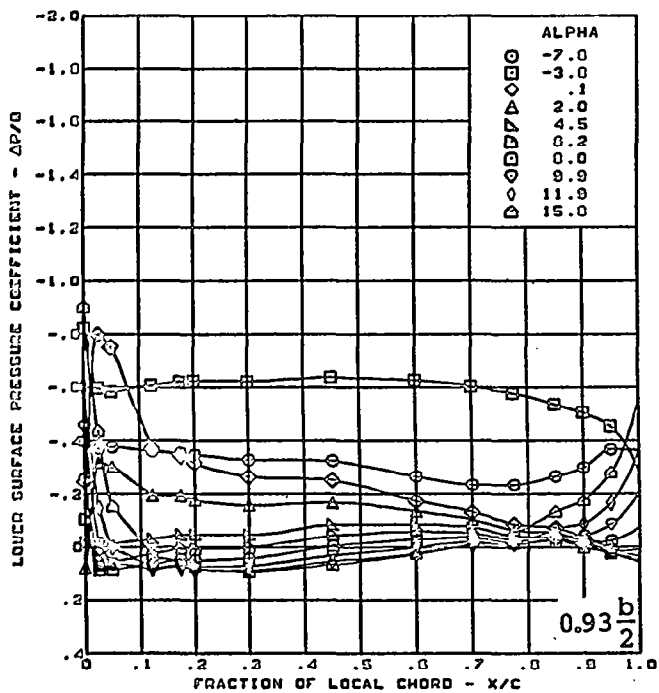
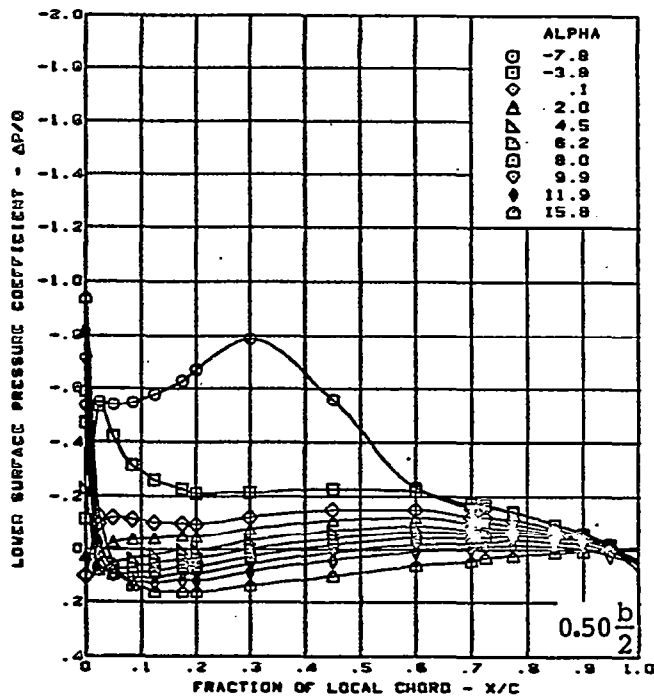
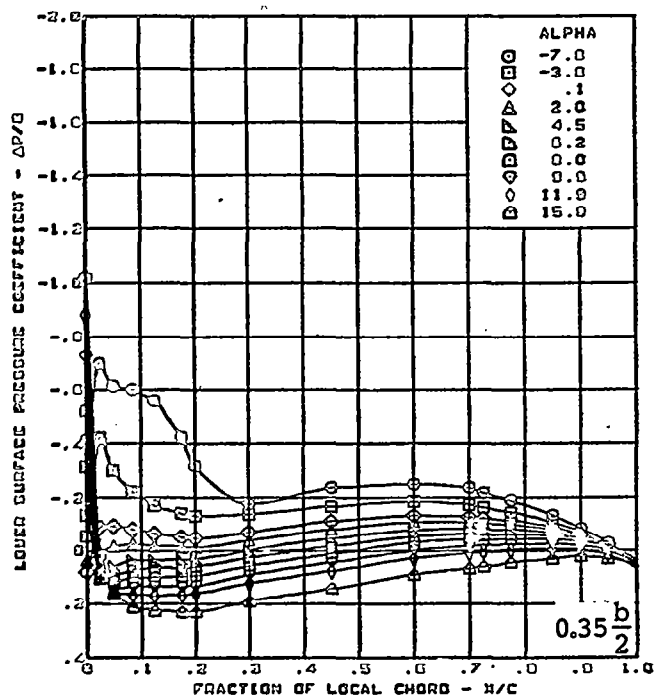
(c) (Concluded)

Figure 27. — (Continued)



(d) Lower Surface Chordwise Pressure Distributions

Figure 27. - (Continued)

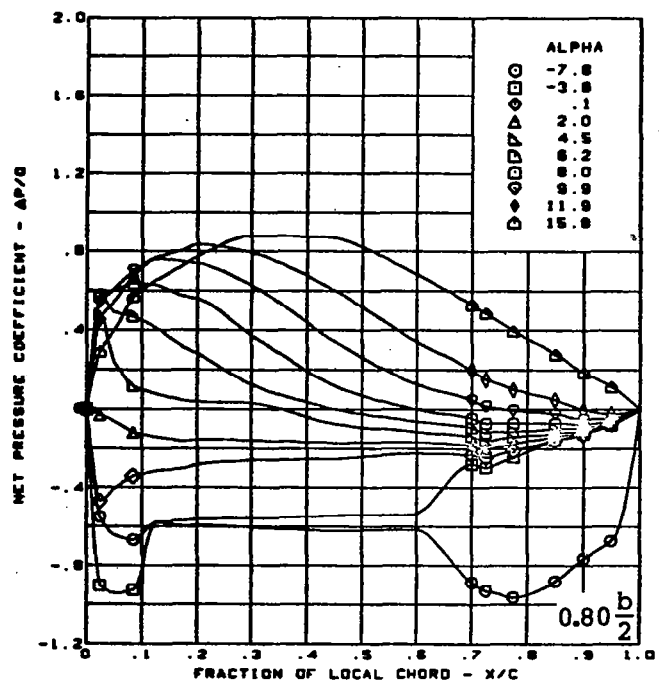
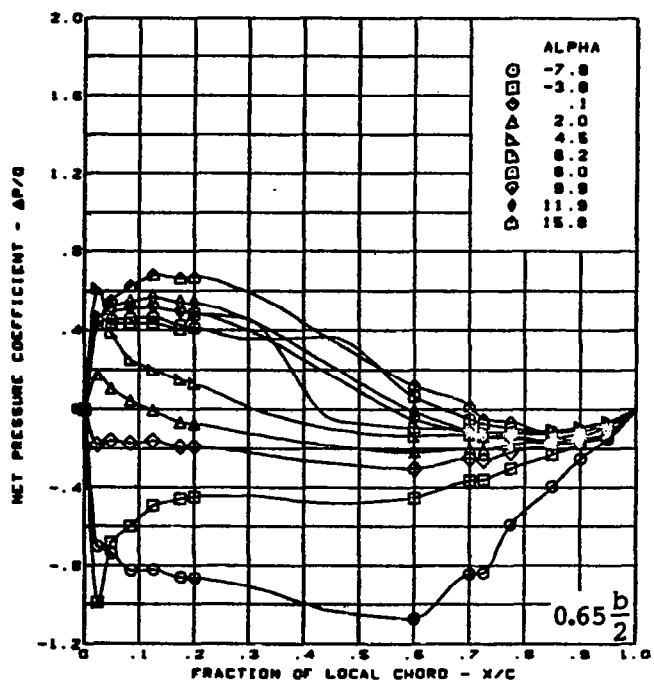
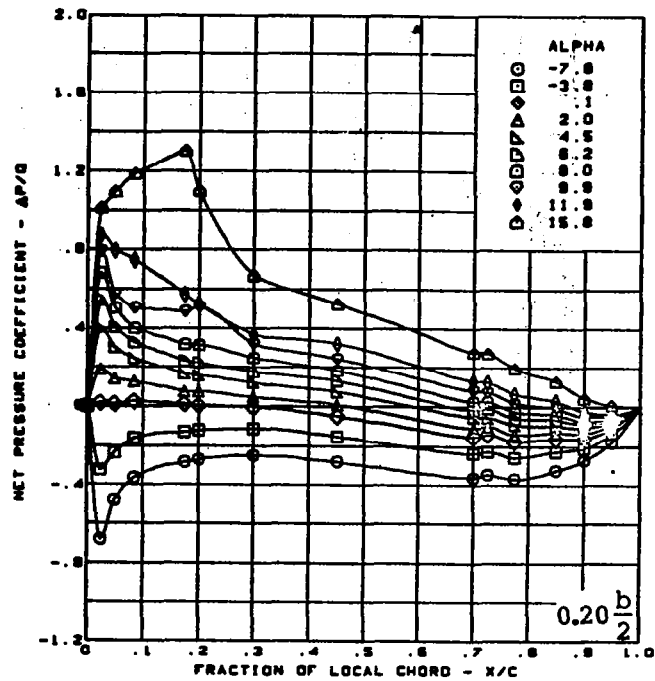
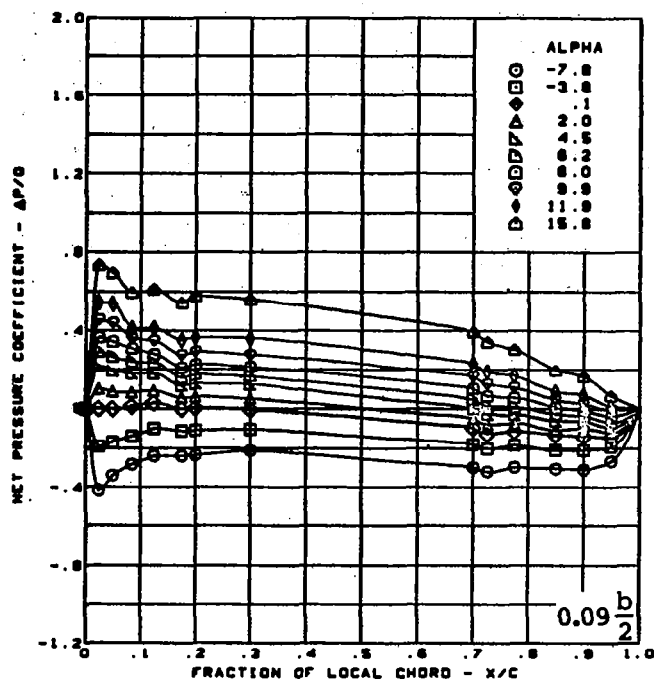


$M = 0.85$  (run 48)  
 Cambered-twisted wing, rounded L.E.  
 Fin on  
 L.E. deflection, full span =  $0.0^\circ$   
 T.E. deflection, full span =  $0.0^\circ$

(d) (Concluded)

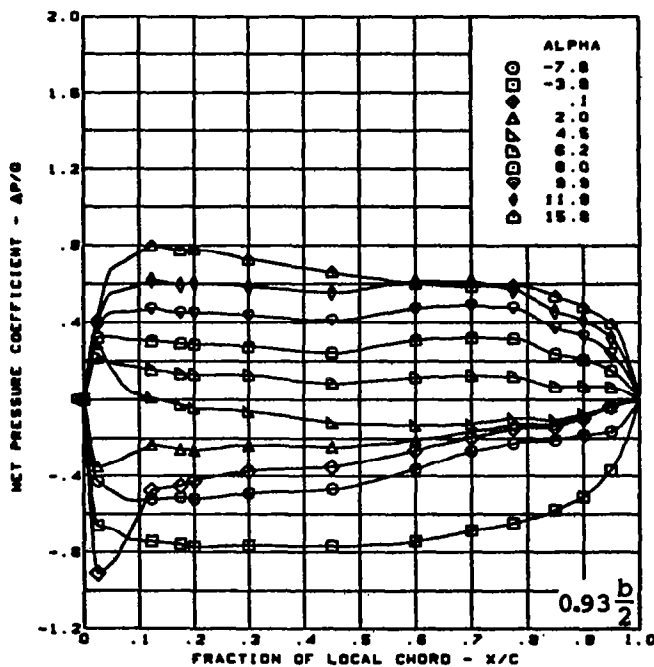
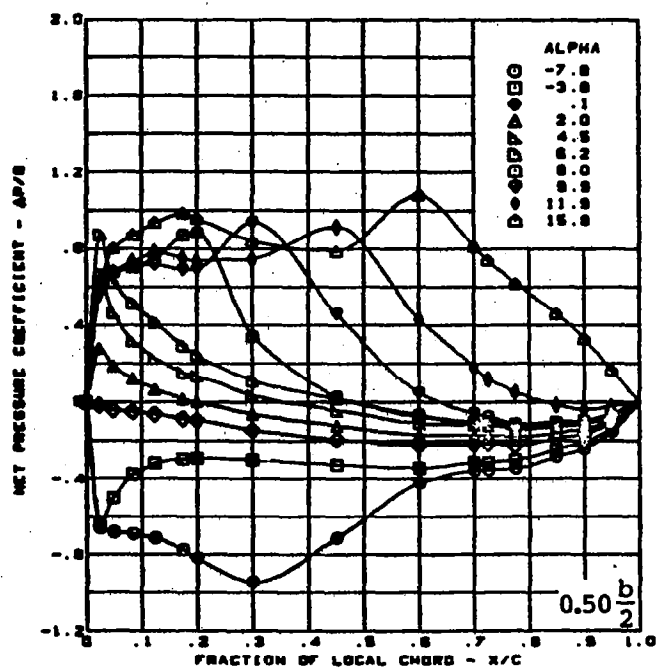
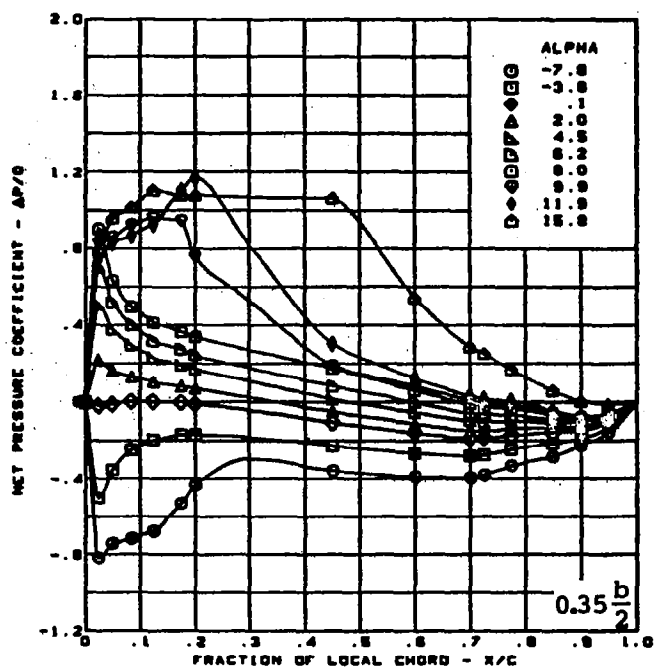
Figure 27. — (Continued)





(e) Net Chordwise Pressure Distributions

Figure 27. — (Continued)

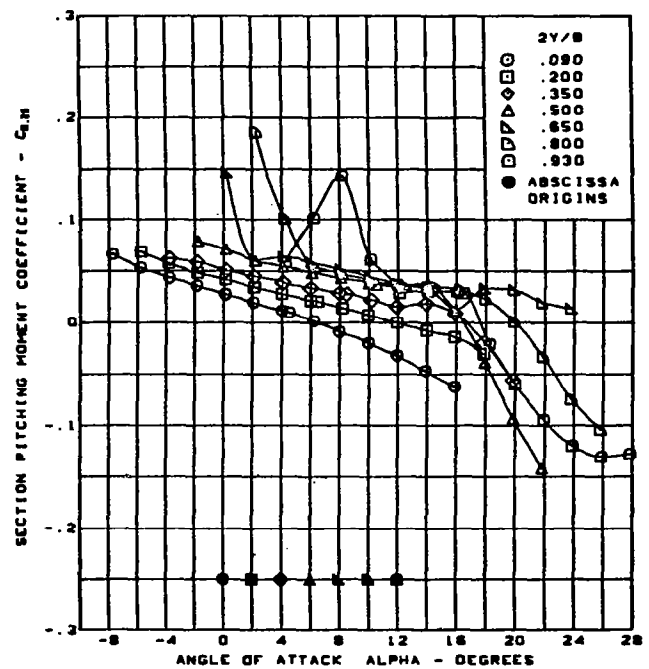
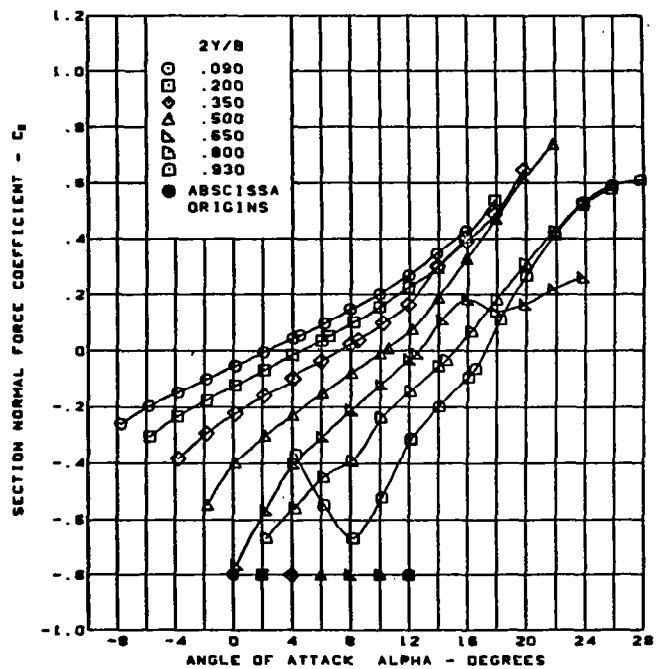
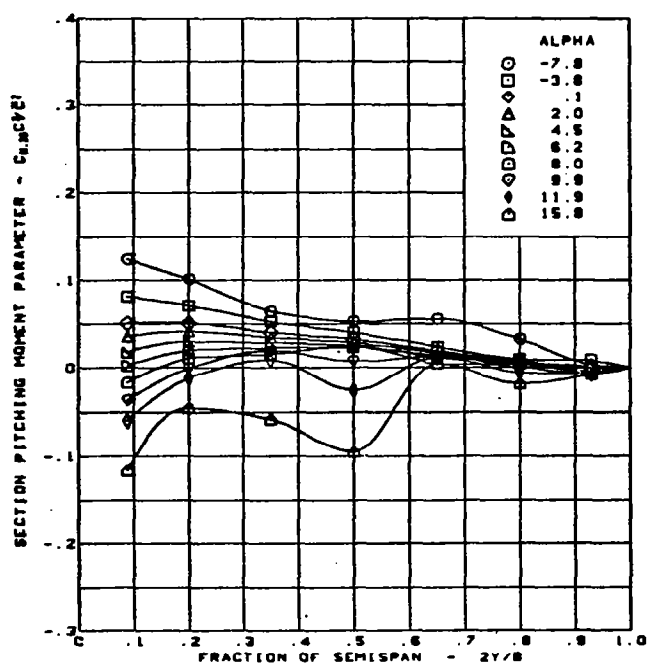
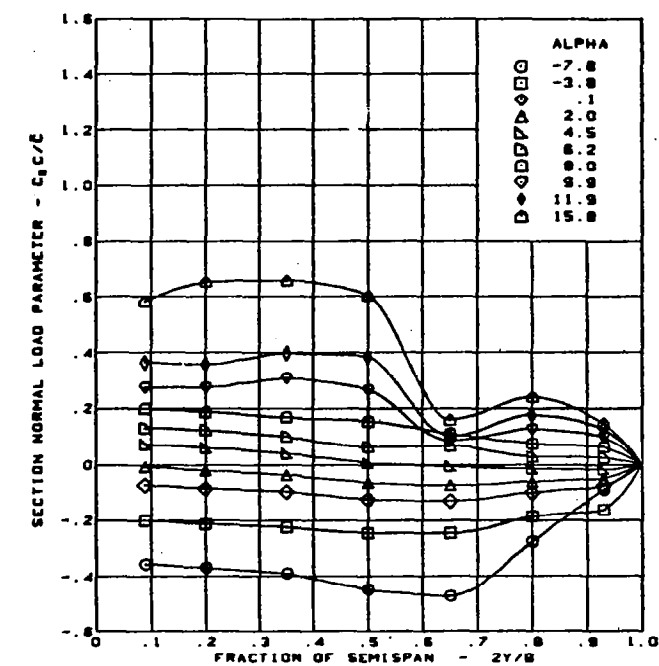


$M = 0.85$  (run 48)  
 Cambered-twisted wing, rounded L.E.  
 Fin on  
 L.E. deflection, full span =  $0.0^\circ$   
 T.E. deflection, full span =  $0.0^\circ$

(e) (Concluded)

Figure 27. - (Continued)



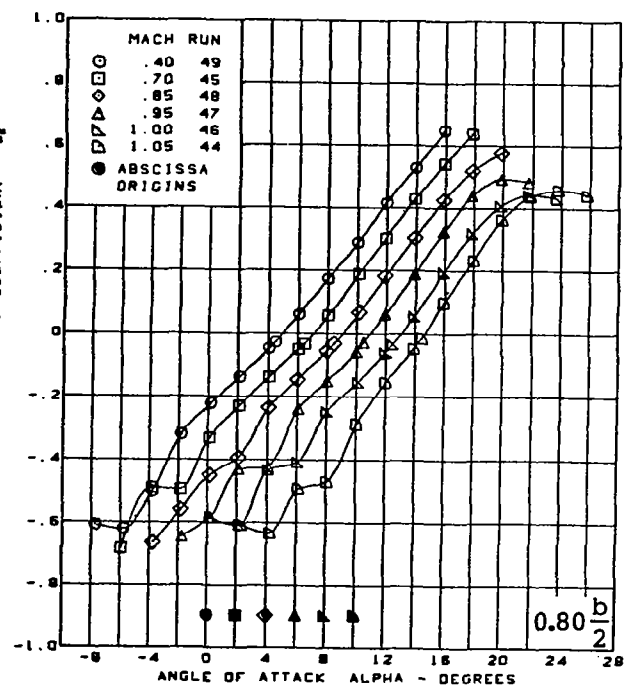
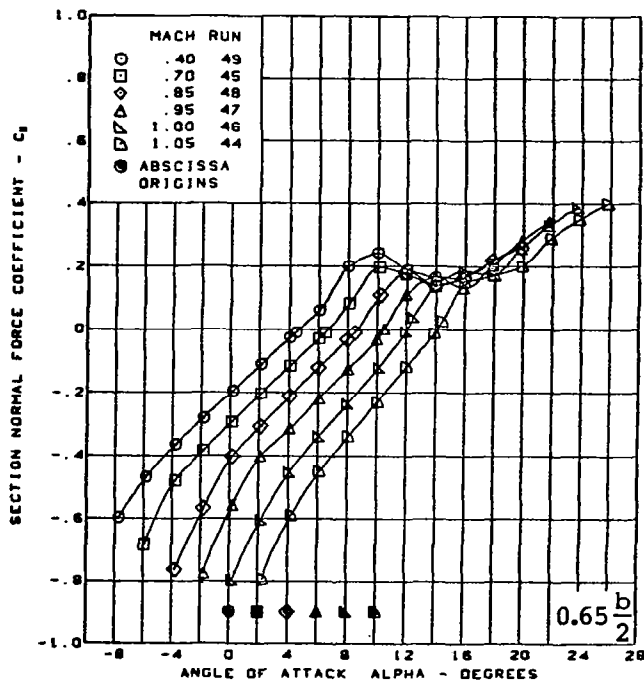
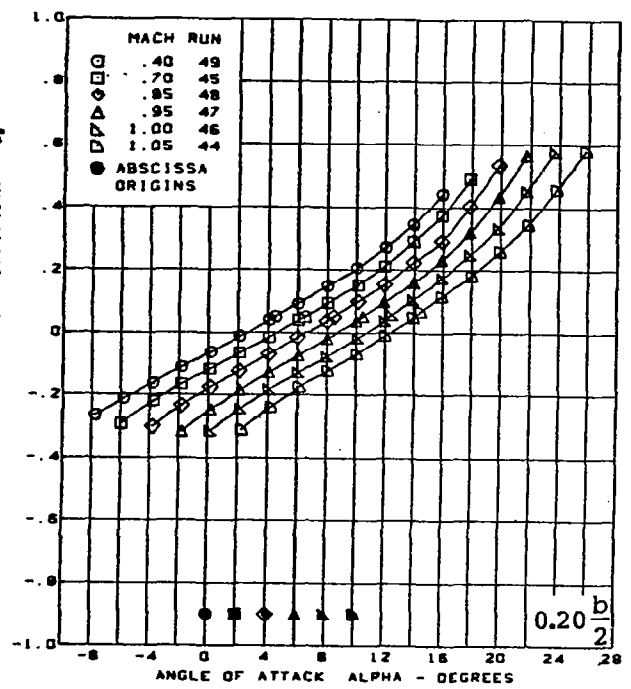
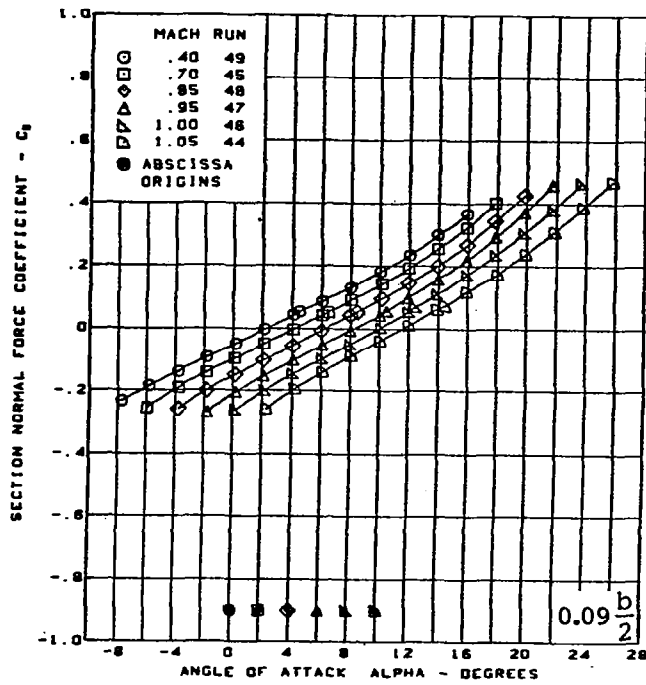


M = 0.85 (run 48)  
 Cambered-twisted wing, rounded L.E.  
 Fin on

L.E. deflection, full span  $\approx 0.0^\circ$   
 T.E. deflection, full span  $\approx 0.0^\circ$

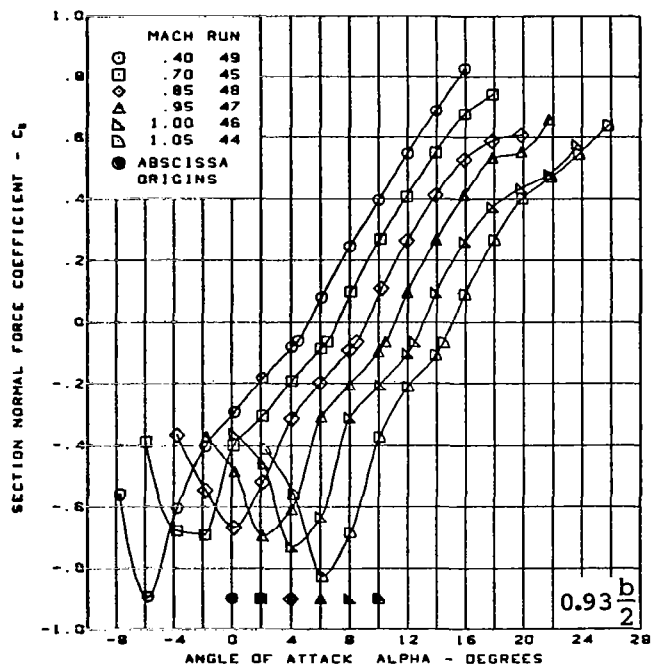
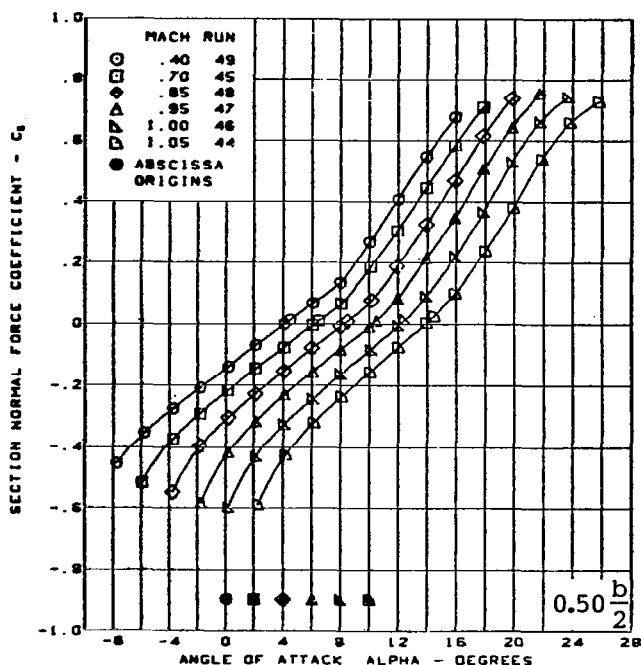
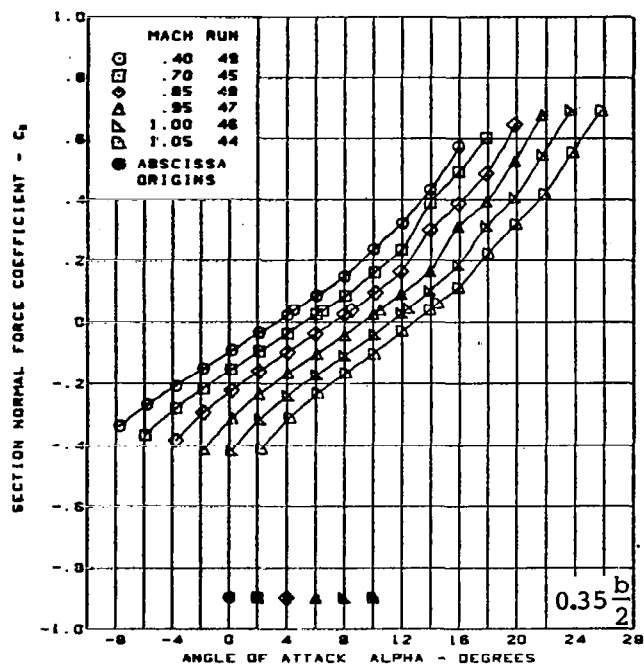
(f) Spanload Distributions and Section Aerodynamic Coefficients

Figure 27. — (Concluded)



(a) Section Aerodynamic Coefficients - Normal Force

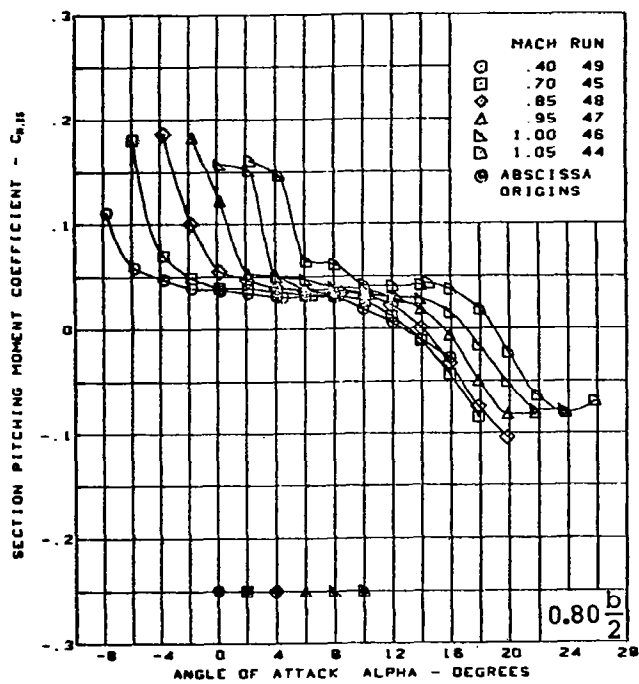
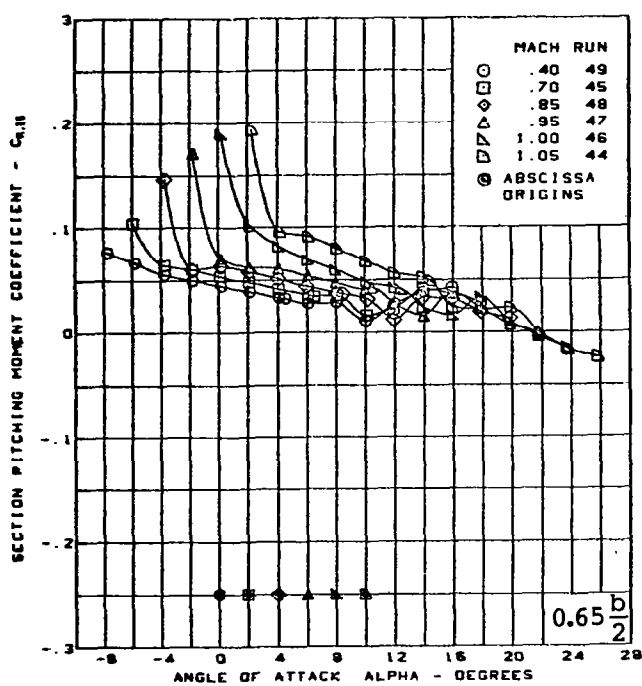
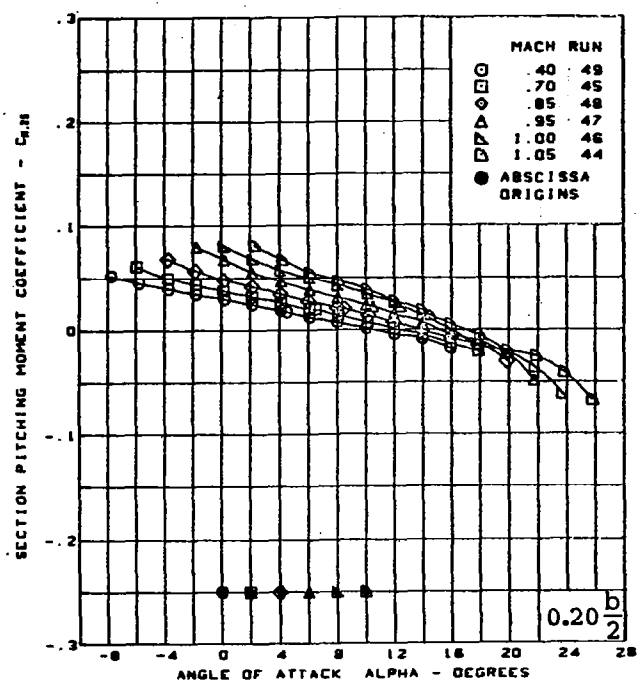
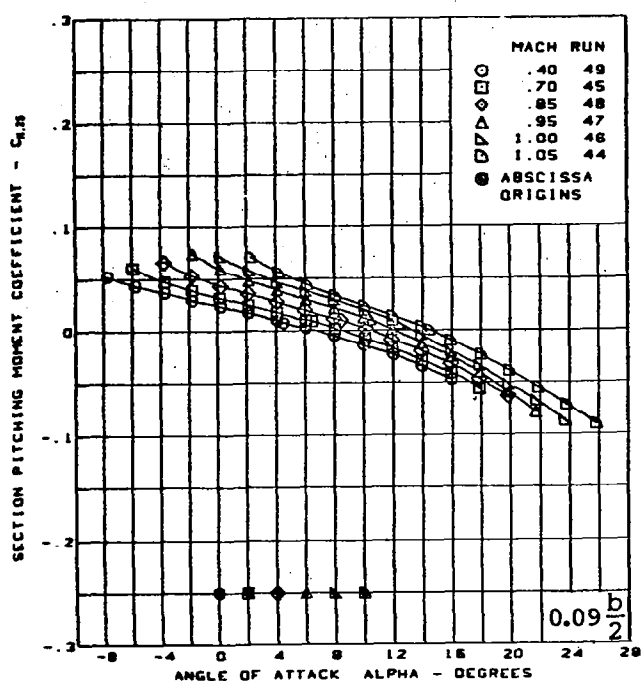
Figure 28. — Wing Experimental Data—Effect of Angle of Attack and Mach Number;  
Cambered-Twisted Wing; Fin On; T.E. Deflection, Full Span =  $0.0^\circ$



Cambered-twisted wing, rounded L.E.  
 Fin on  
 L.E. deflection, full span =  $0.0^\circ$   
 T.E. deflection, full span =  $0.0^\circ$

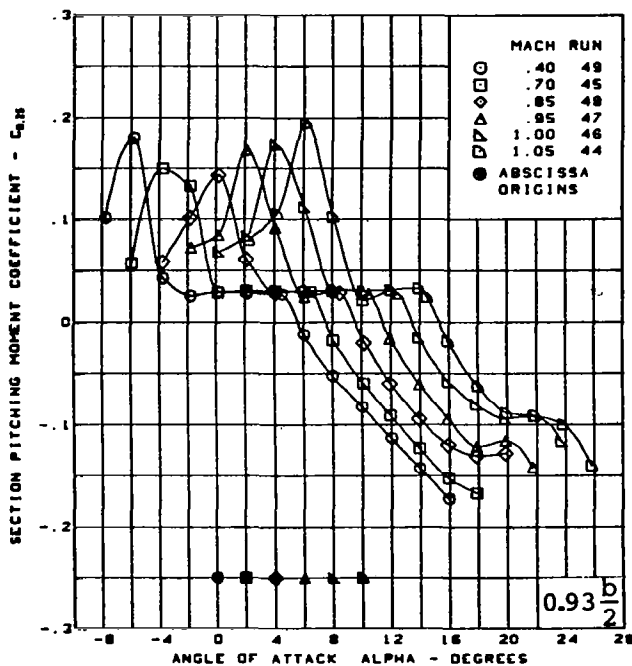
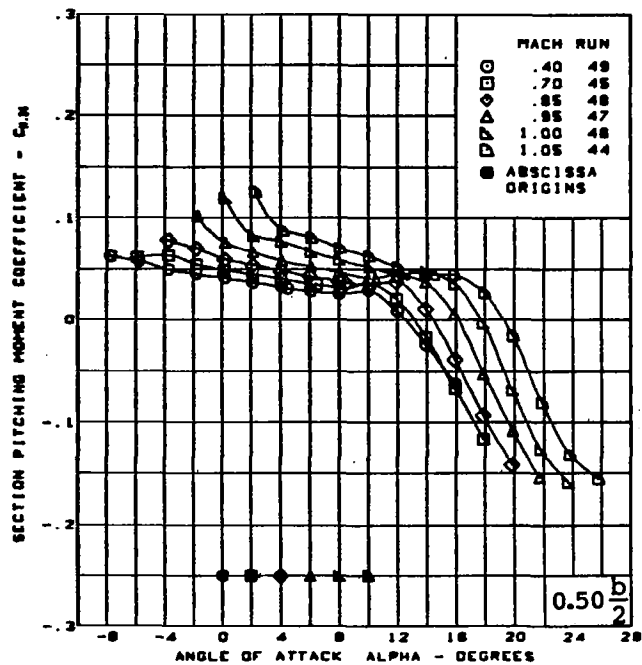
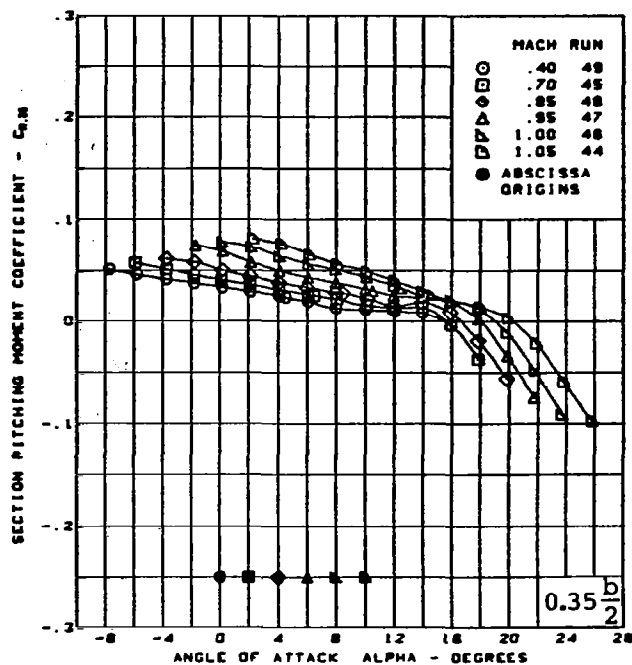
(a) (Concluded)

Figure 28. — (Continued)



(b) Section Aerodynamic Coefficients - Pitching Moment

Figure 28. — (Continued)



Cambered-twisted wing, rounded L.E.

Fin on

L.E. deflection, full span =  $0.0^\circ$

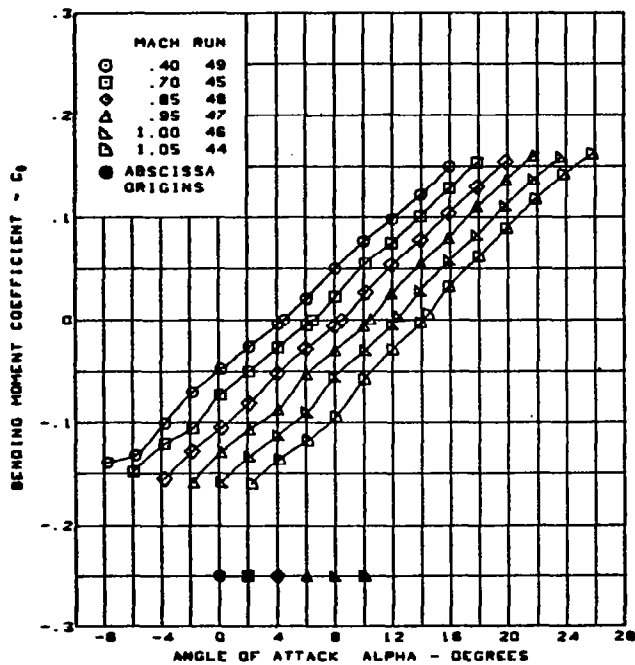
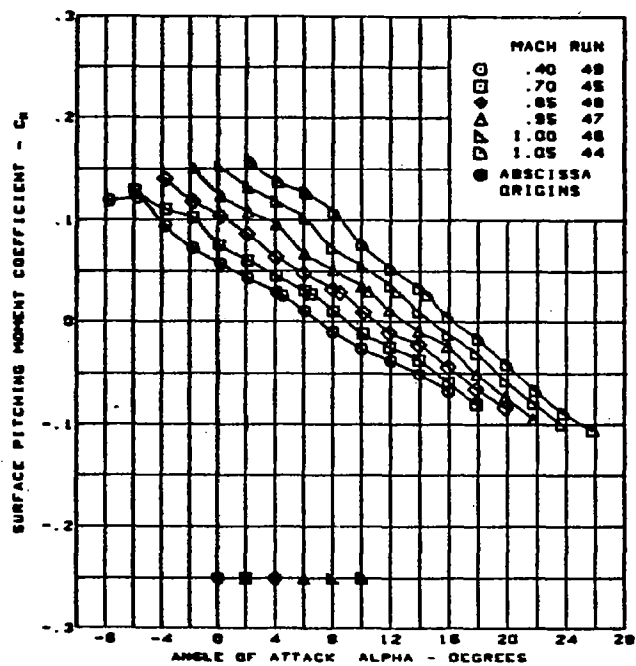
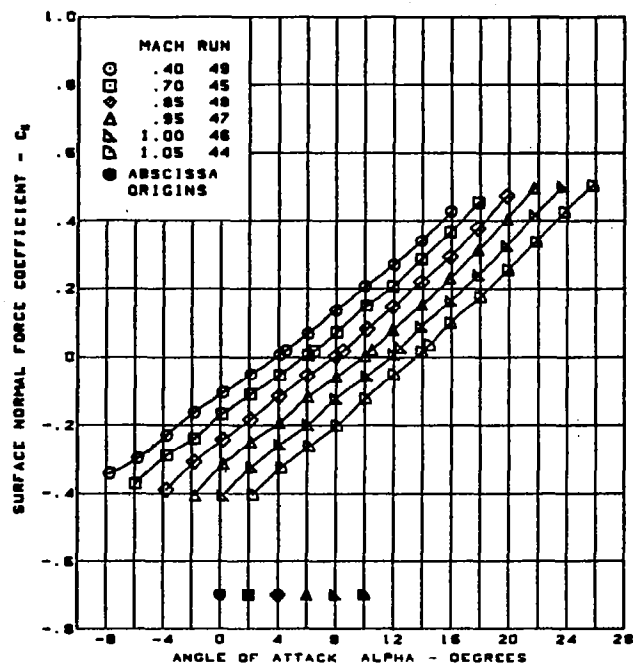
T.E. deflection, full span =  $0.0^\circ$

(b) (Concluded)

Figure 28. — (Continued)







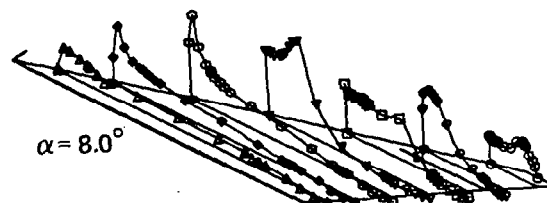
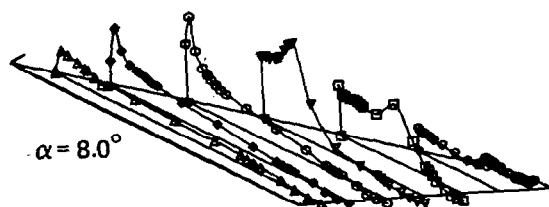
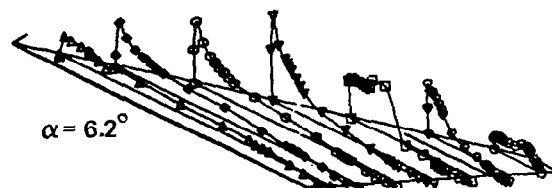
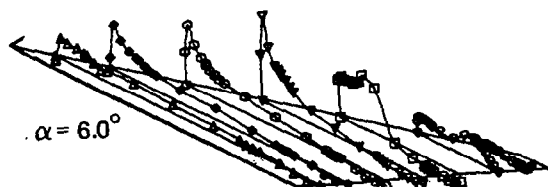
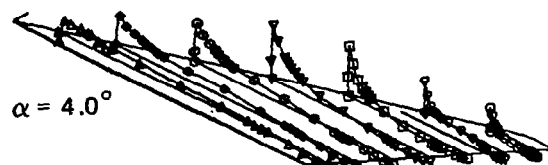
Cambered-twisted wing, rounded L.E.  
 Fin on  
 L.E. deflection, full span =  $0.0^\circ$   
 T.E. deflection, full span =  $0.0^\circ$

(c) Wing Aerodynamic Coefficients

Figure 28. — (Concluded)

Fin off  
(run 40)

Fin on  
(run 48)

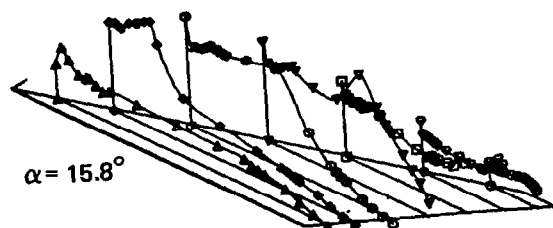
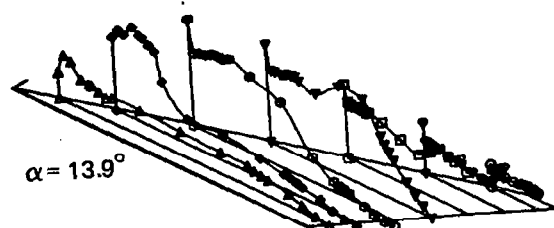
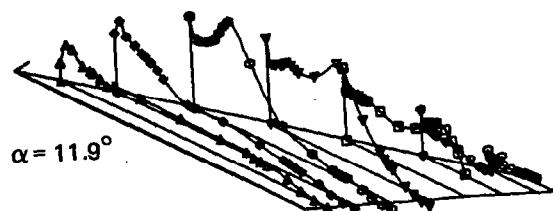
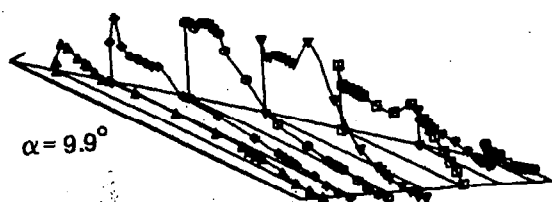


$M = 0.85$   
Cambered-twisted wing, rounded L.E.  
L.E. deflection, full span =  $0.0^\circ$   
T.E. deflection, full span =  $0.0^\circ$

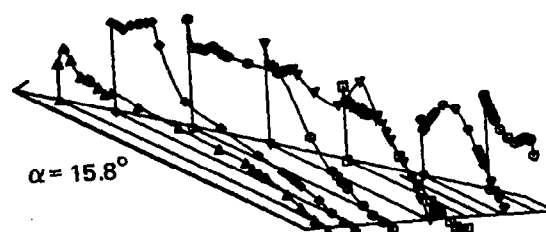
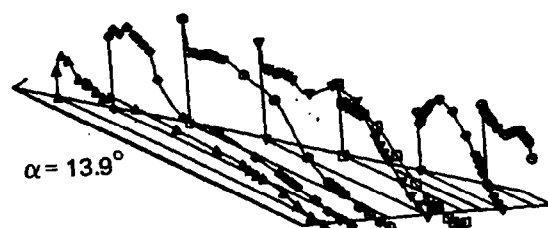
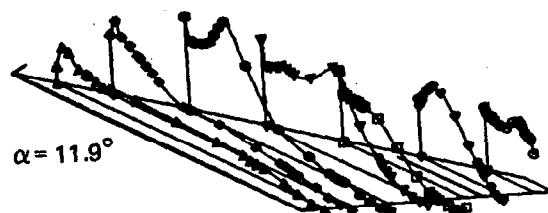
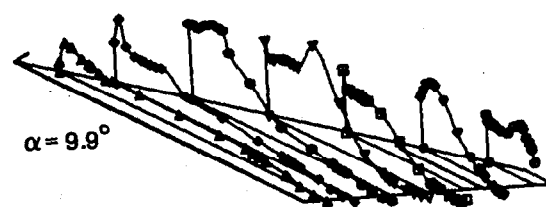
(a) Upper Surface Pressure Distribution

Figure 29. — Wing Experimental Data—Effect of a Wing Fin and Angle of Attack;  
Cambered-Twisted Wing; T.E. Deflection, Full Span =  $0.0^\circ$ ;  $M = 0.85$

Fin off  
(run 40)

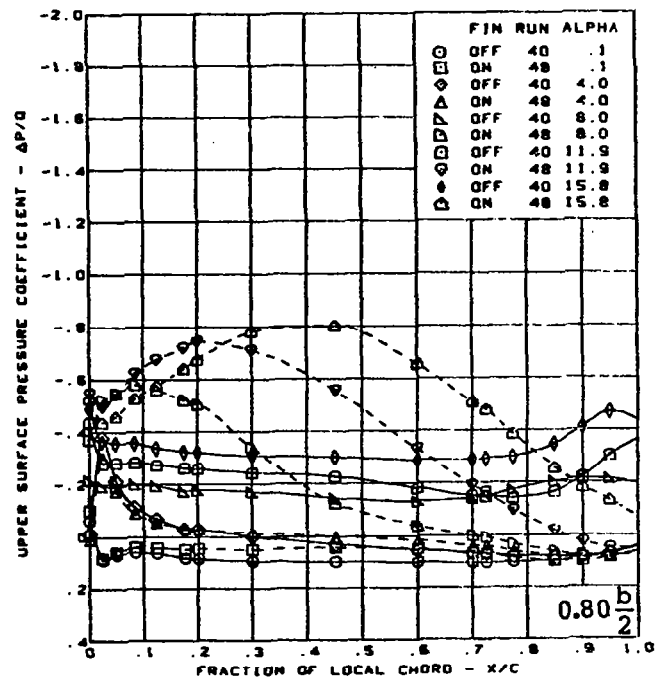
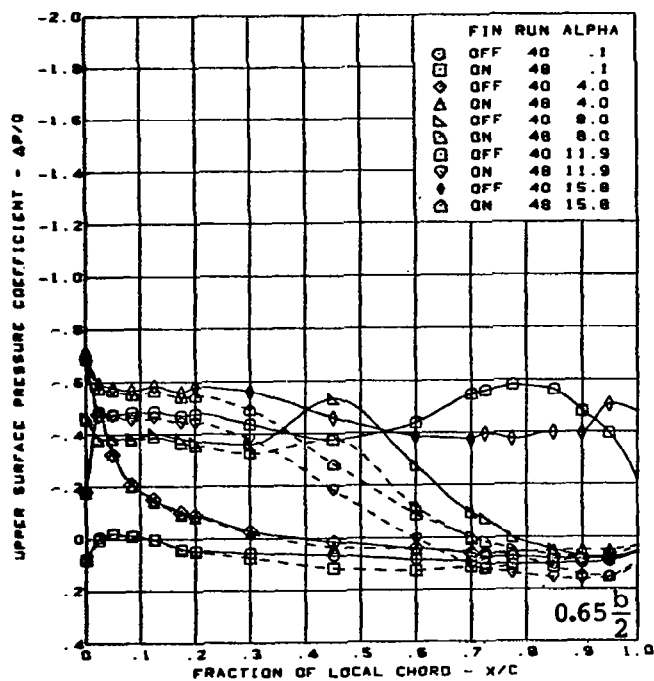
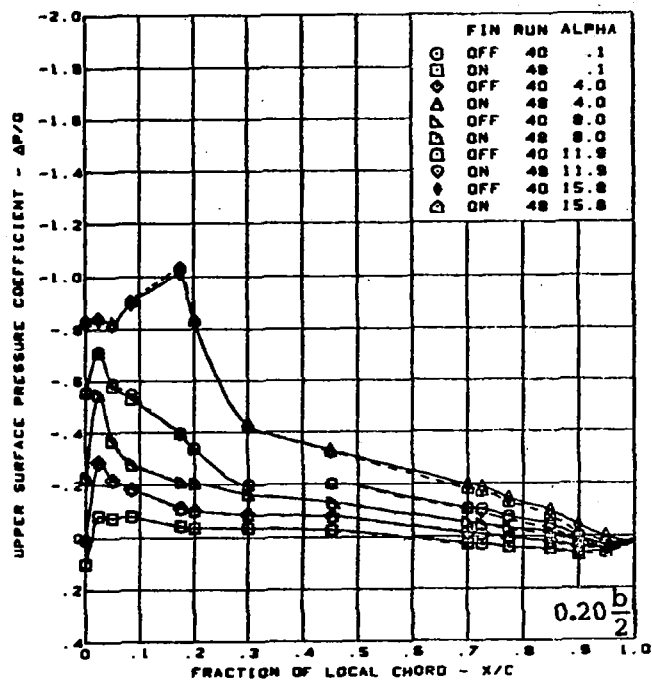
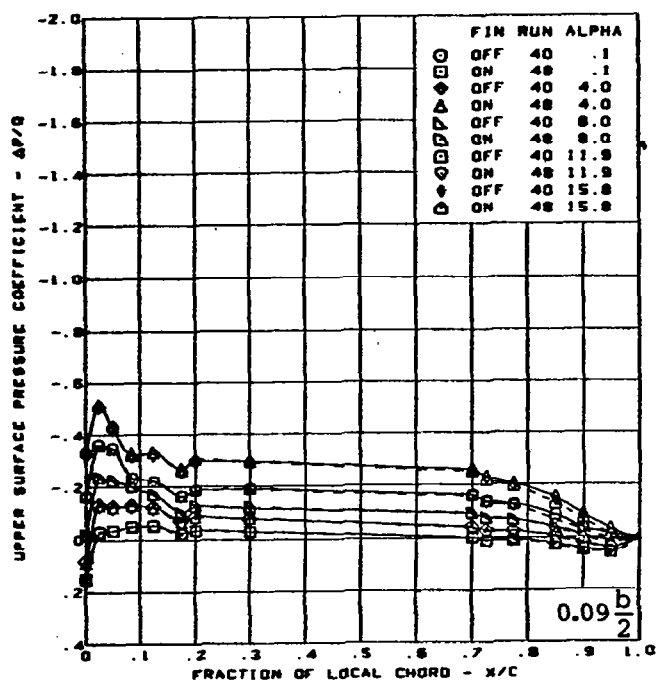


Fin on  
(run 48)



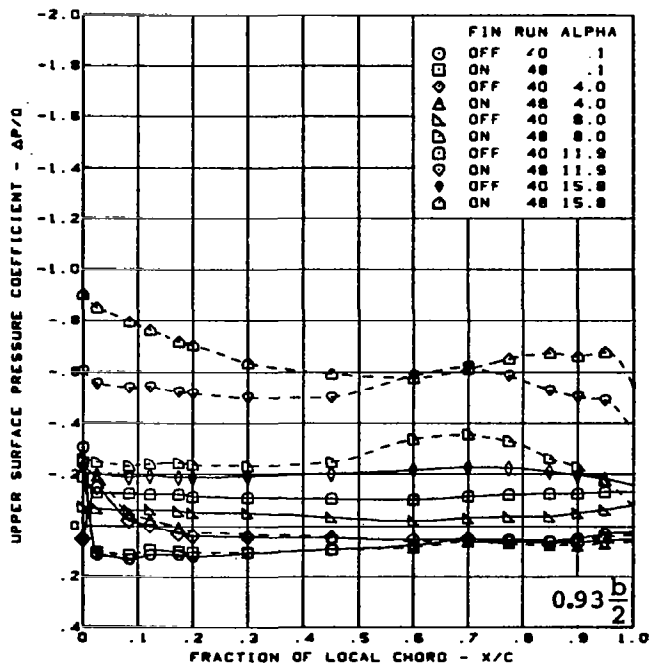
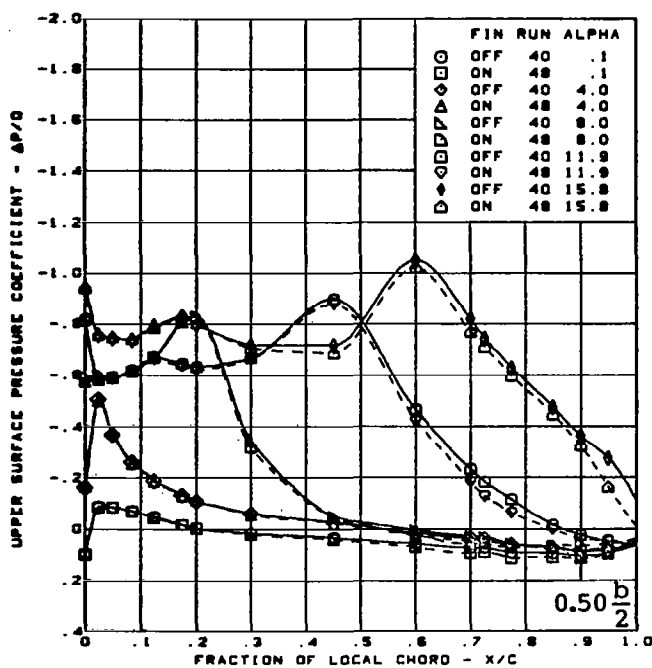
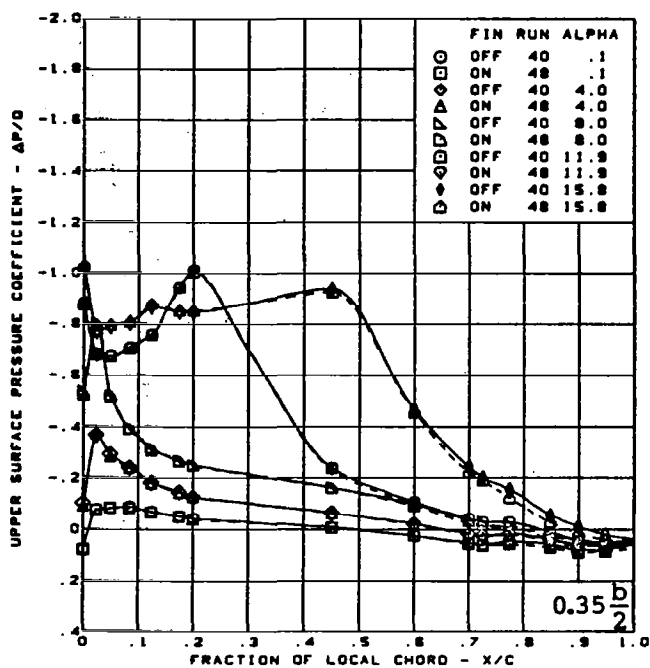
(a) (Concluded)

Figure 29. — (Continued)



(b) Upper Surface Chordwise Pressure Distributions

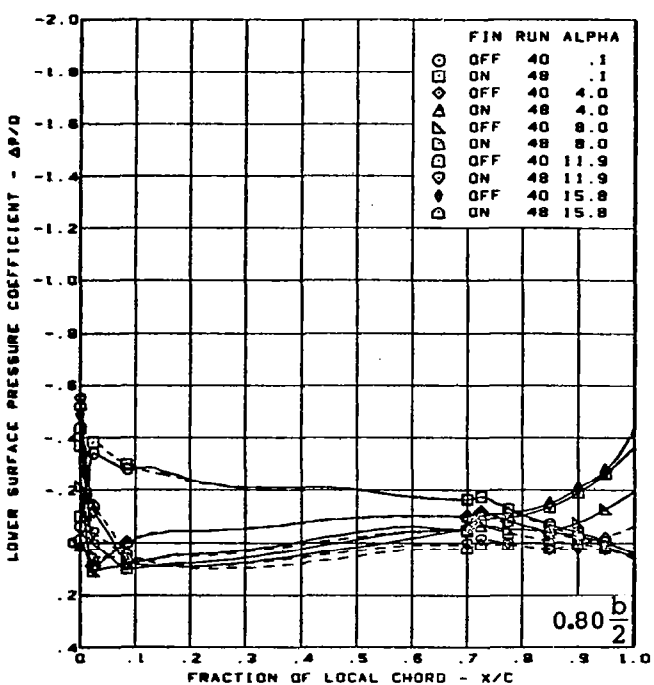
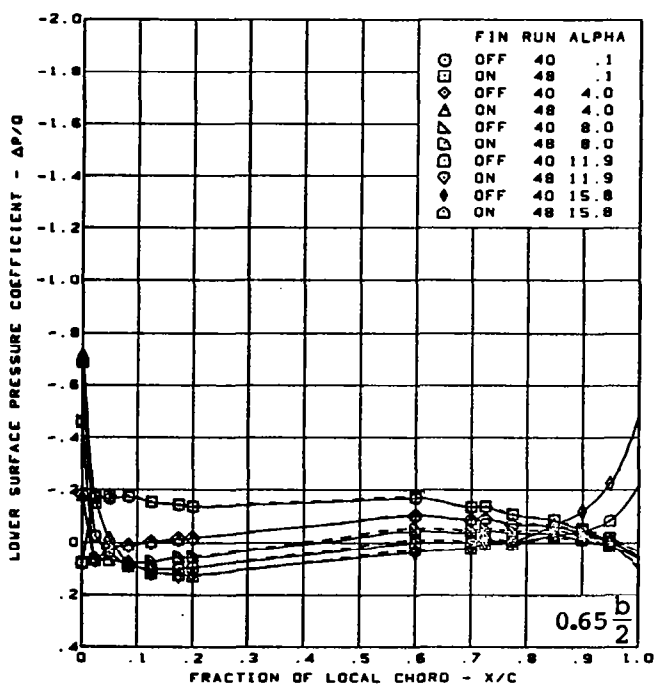
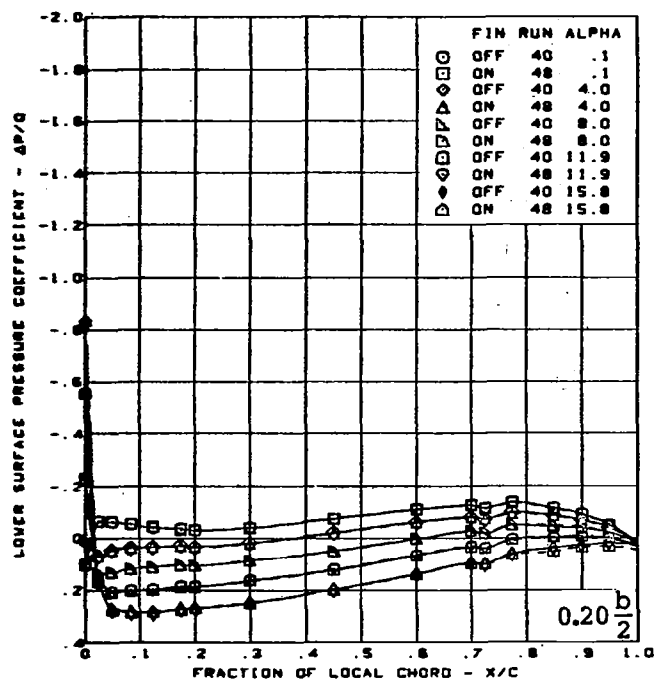
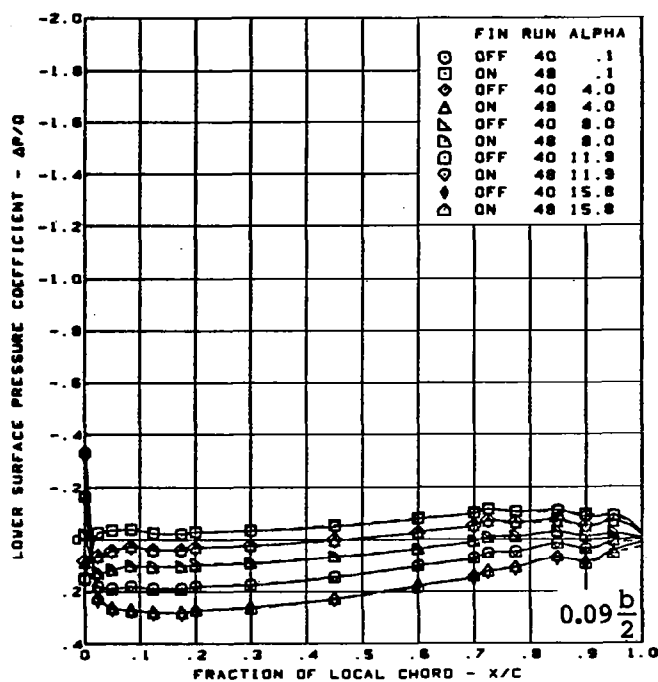
Figure 29. — (Continued)



$M = 0.85$   
 Cambered-twisted wing, rounded L.E.  
 L.E. deflection, full span =  $0.0^\circ$   
 T.E. deflection, full span =  $0.0^\circ$

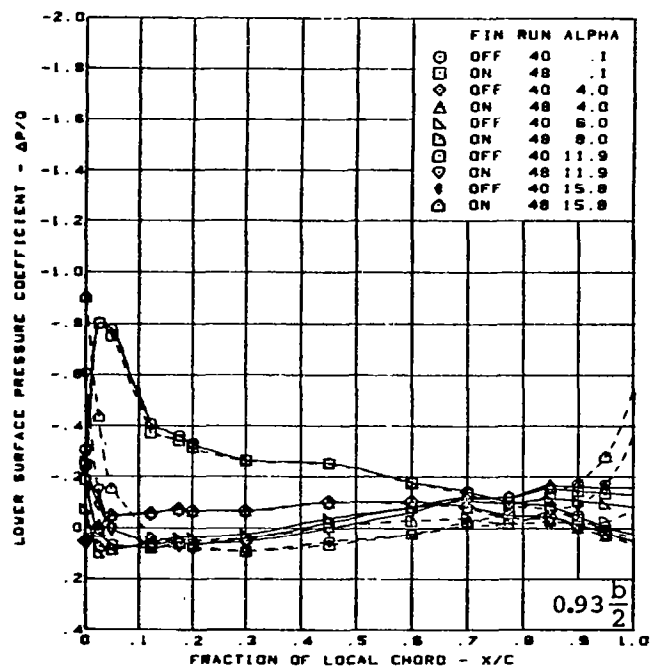
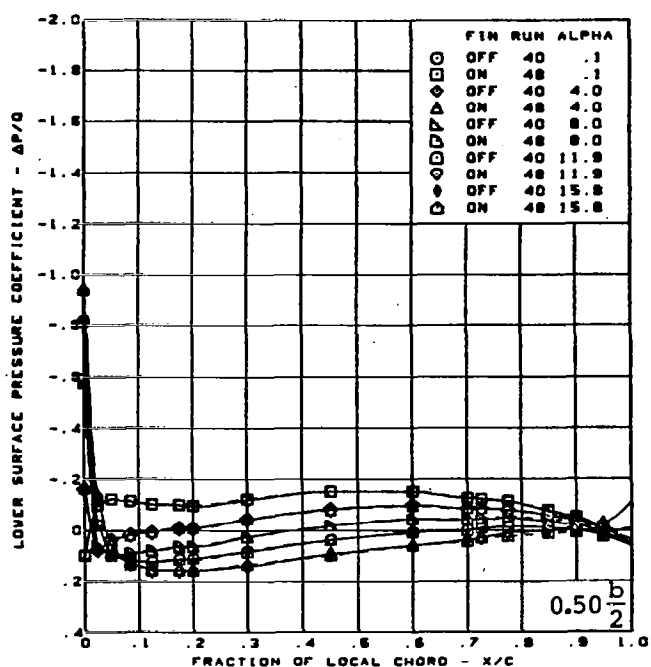
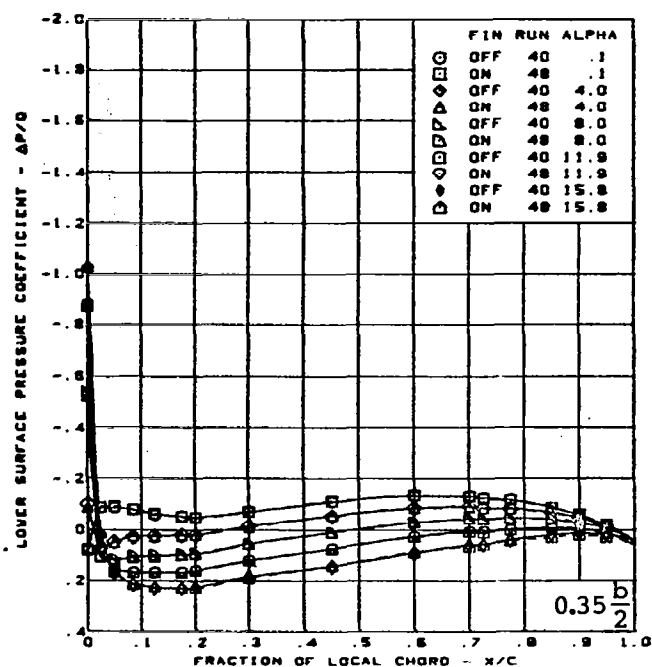
(b) (Concluded)

Figure 29. — (Continued)



(c) Lower Surface Chordwise Pressure Distributions

Figure 29. — (Continued)

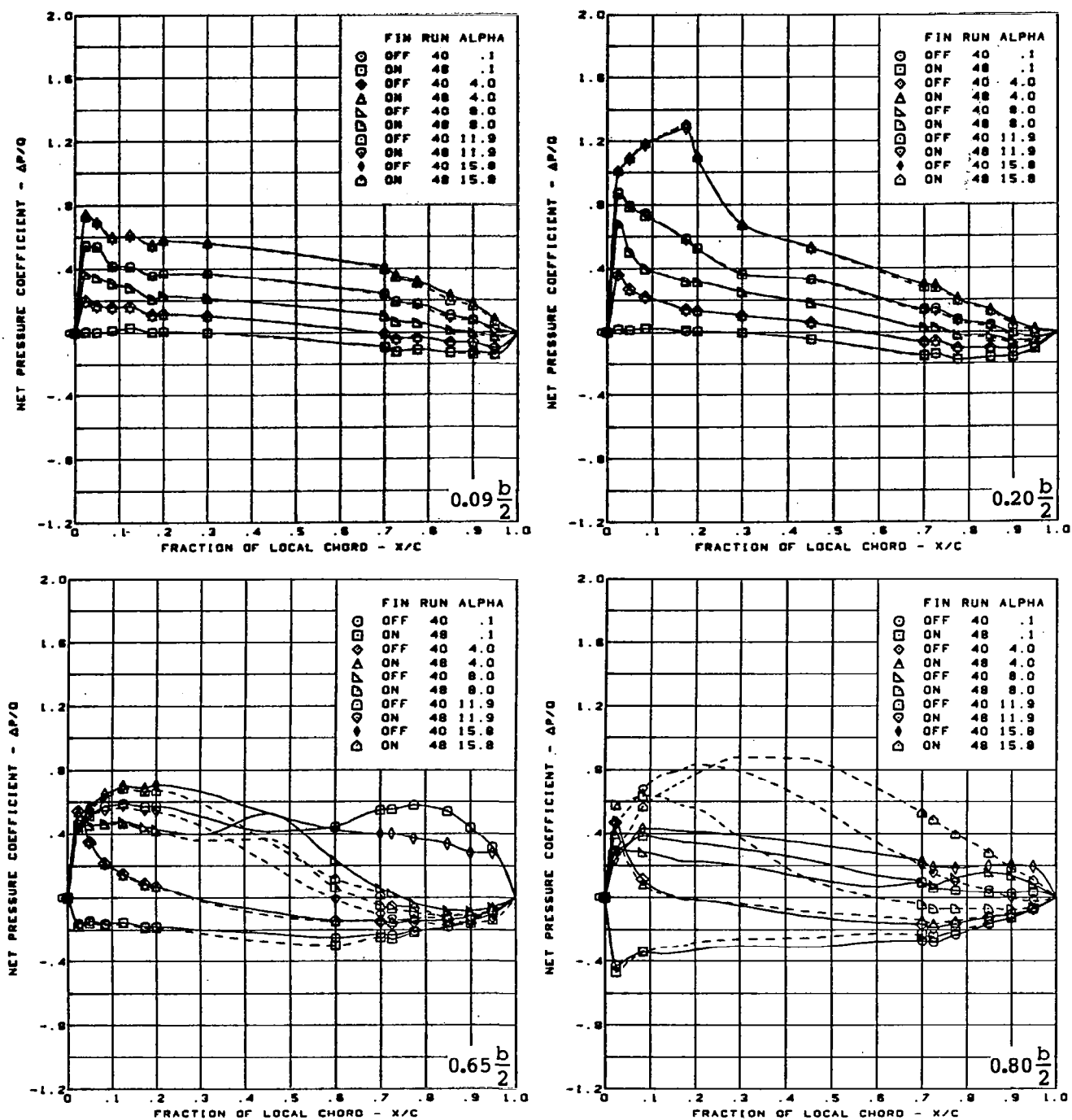


$M = 0.85$   
 Cambered-twisted wing, rounded L.E.  
 L.E. deflection, full span =  $0.0^\circ$   
 T.E. deflection, full span =  $0.0^\circ$

(c) (Concluded)

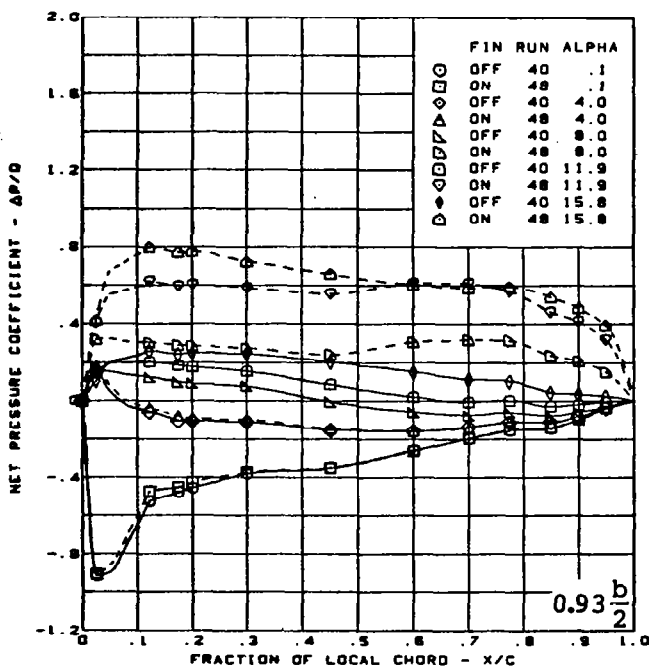
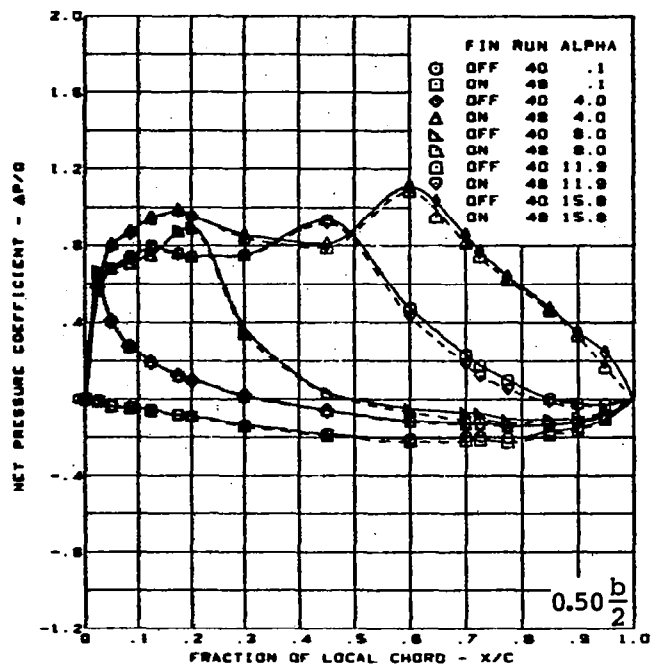
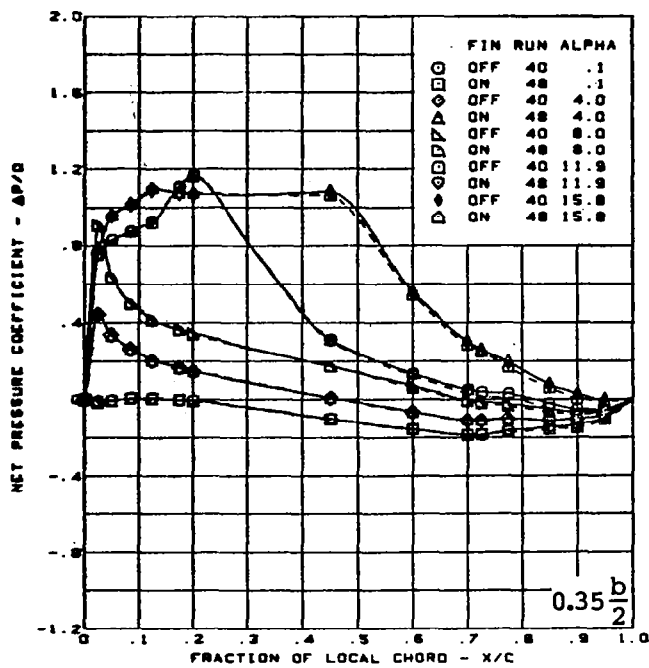
Figure 29. - (Continued)





(d) Net Chordwise Pressure Distributions

Figure 29. — (Continued)



$M = 0.85$

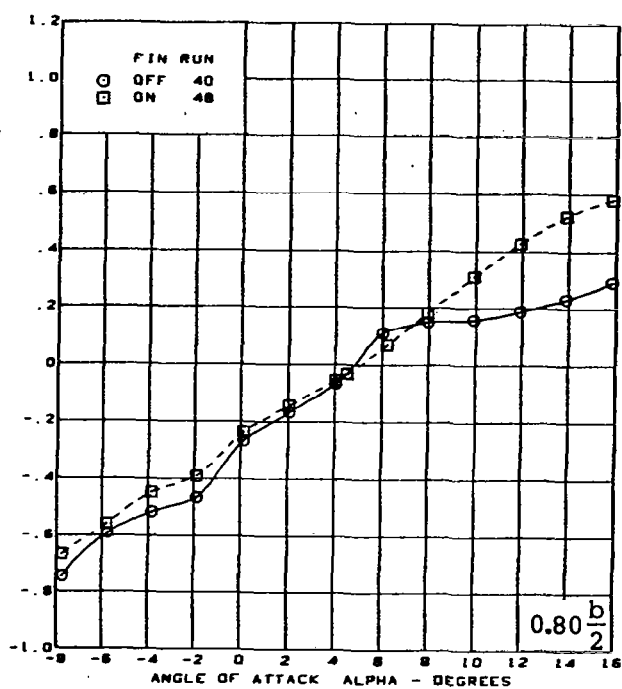
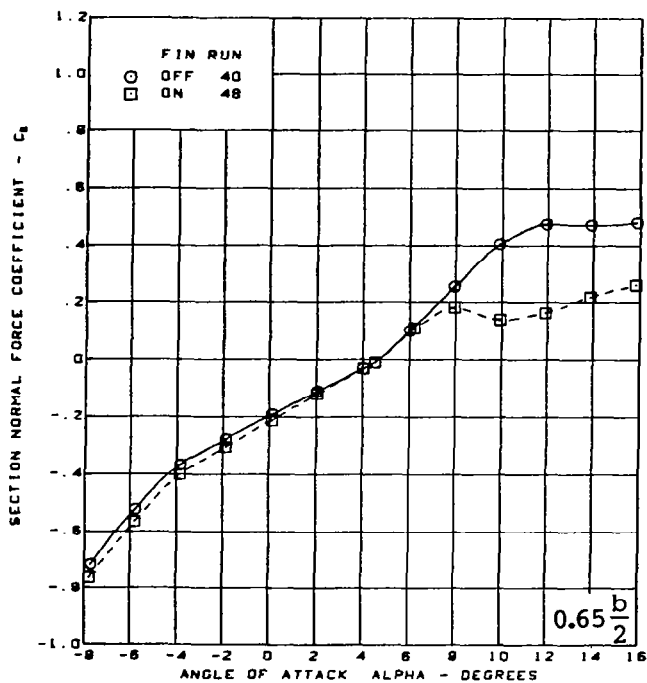
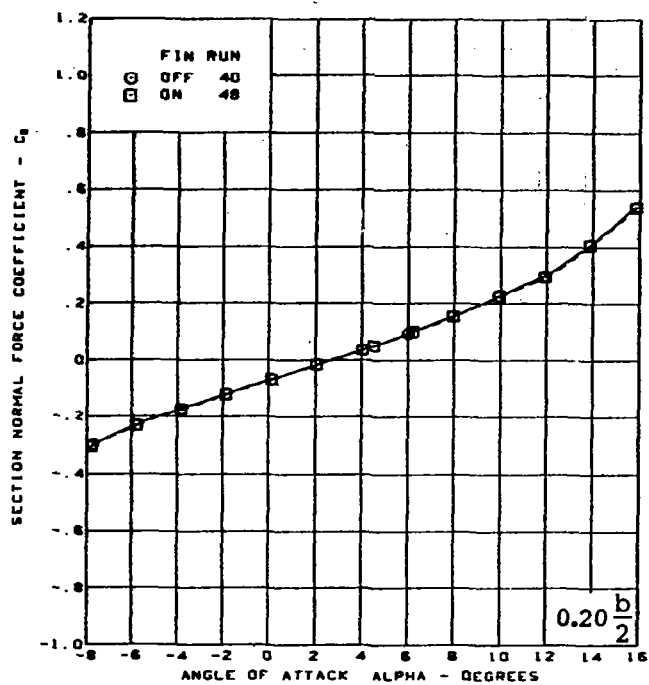
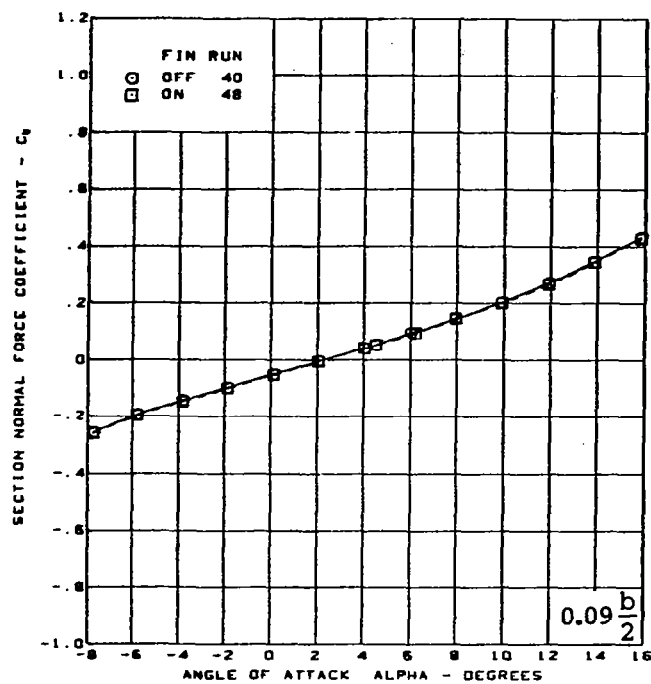
Cambered-twisted wing, rounded L.E.

L.E. deflection, full span =  $0.0^\circ$

T.E. deflection, full span =  $0.0^\circ$

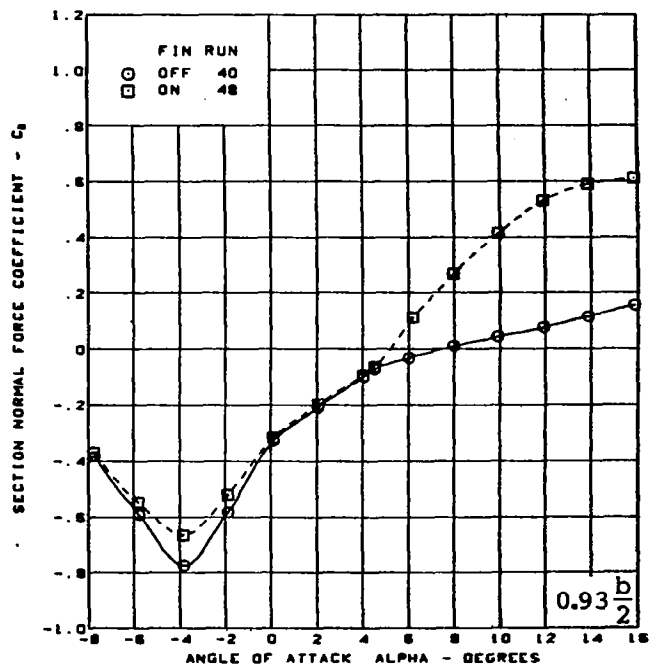
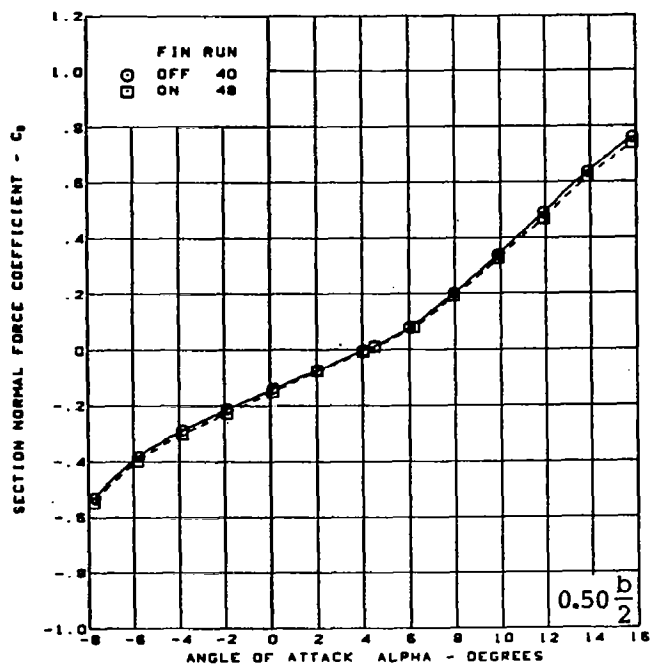
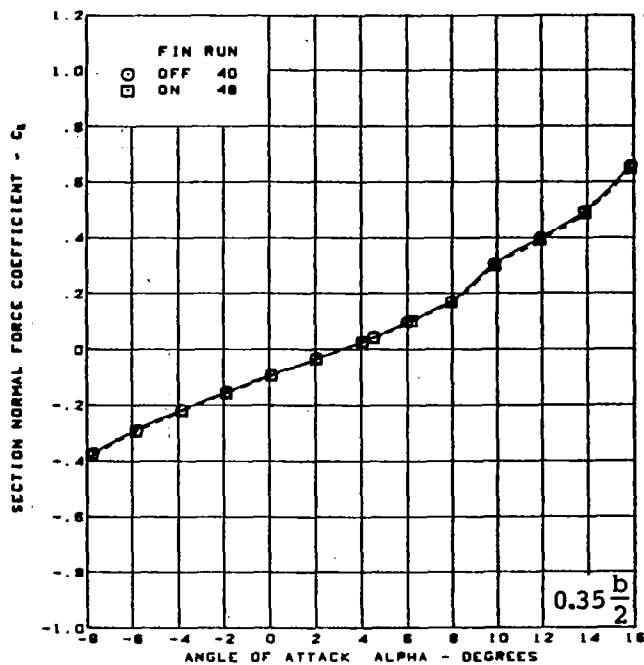
(d) (Concluded)

Figure 29. — (Continued)



(e) Section Aerodynamic Coefficients - Normal Force

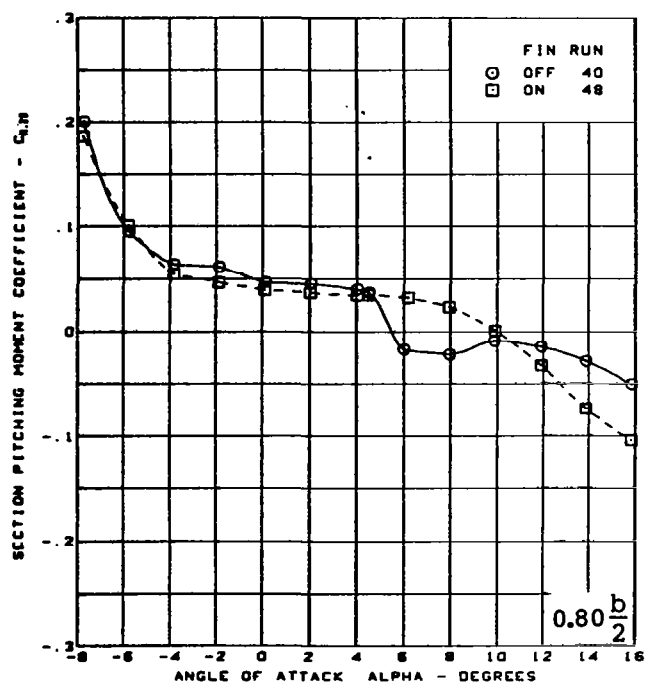
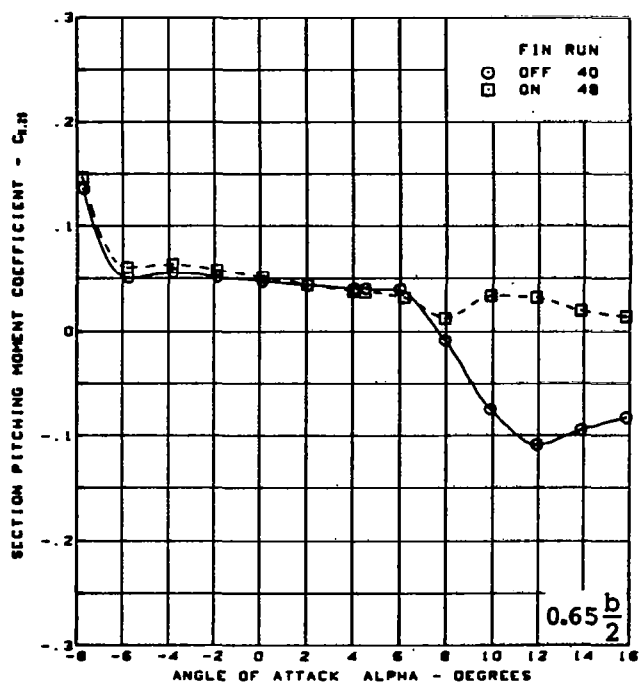
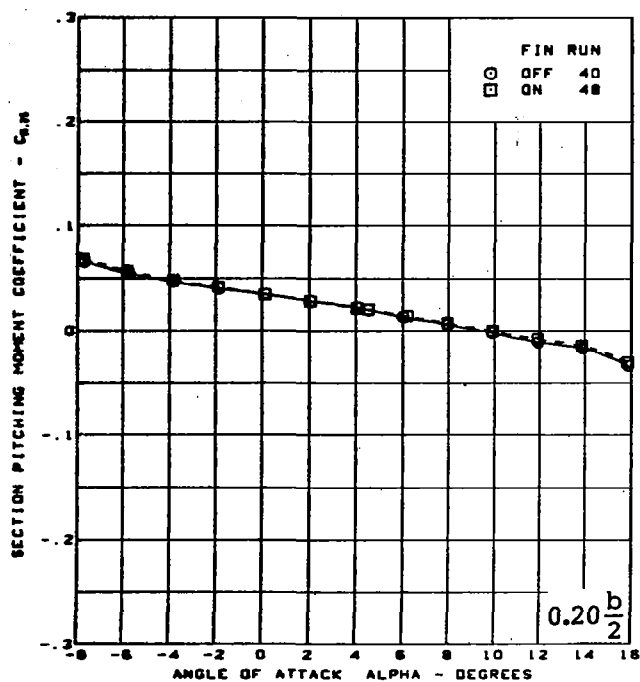
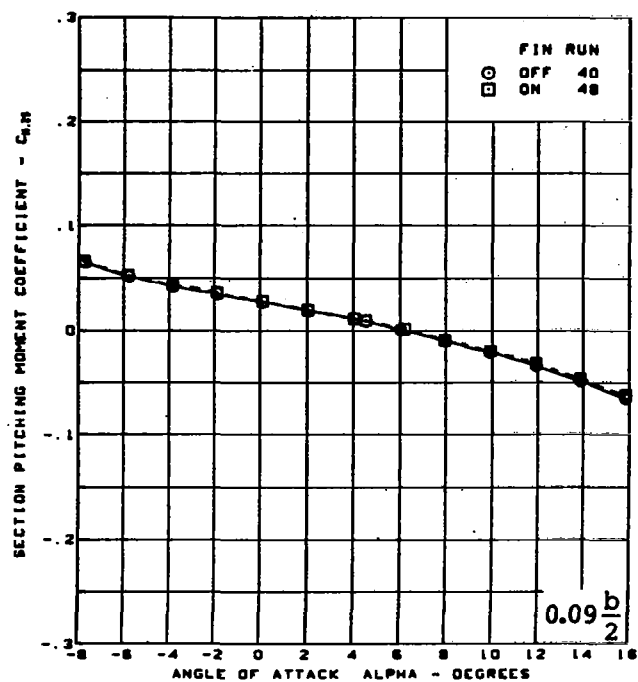
Figure 29. - (Continued)



$M = 0.85$   
 Cambered-twisted wing, rounded L.E.  
 L.E. deflection, full span =  $0.0^\circ$   
 T.E. deflection, full span =  $0.0^\circ$

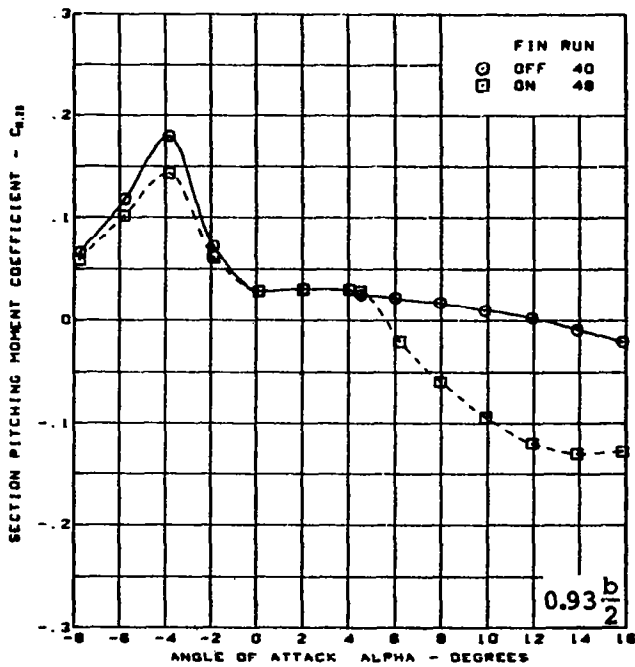
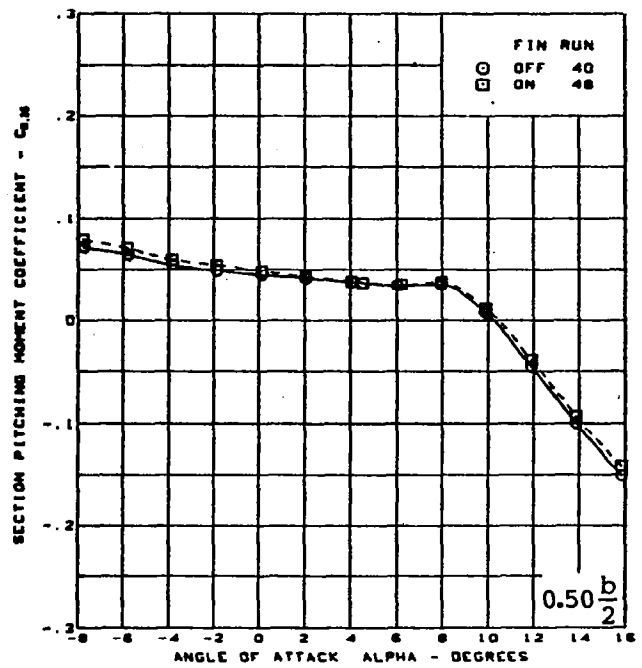
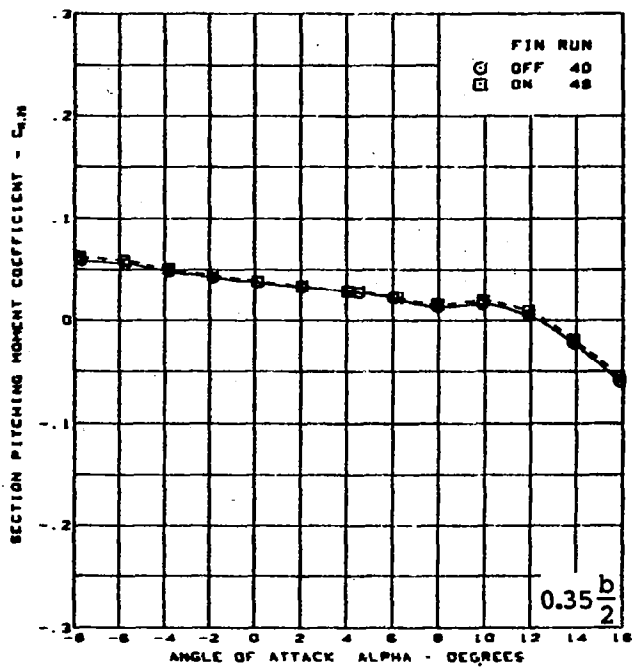
(e) (Concluded)

Figure 29. - (Continued)



(f) Section Aerodynamic Coefficients - Pitching Moment

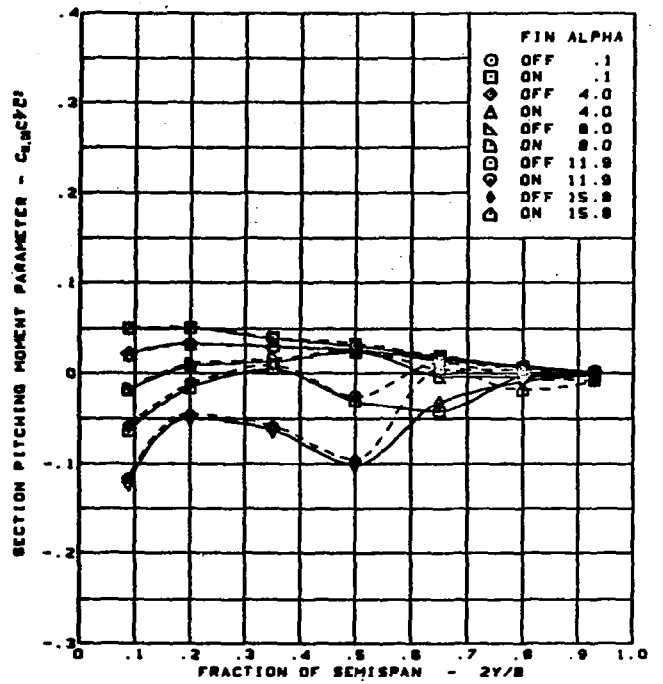
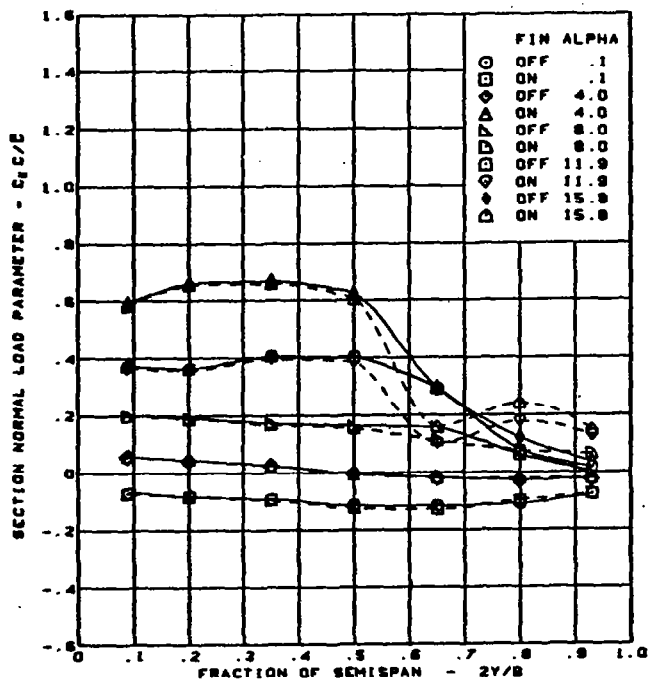
Figure 29. - (Continued)



$M = 0.85$   
 Cambered-twisted wing, rounded L.E.  
 L.E. deflection, full span =  $0.0^\circ$   
 T.E. deflection, full span =  $0.0^\circ$

(f) (Concluded)

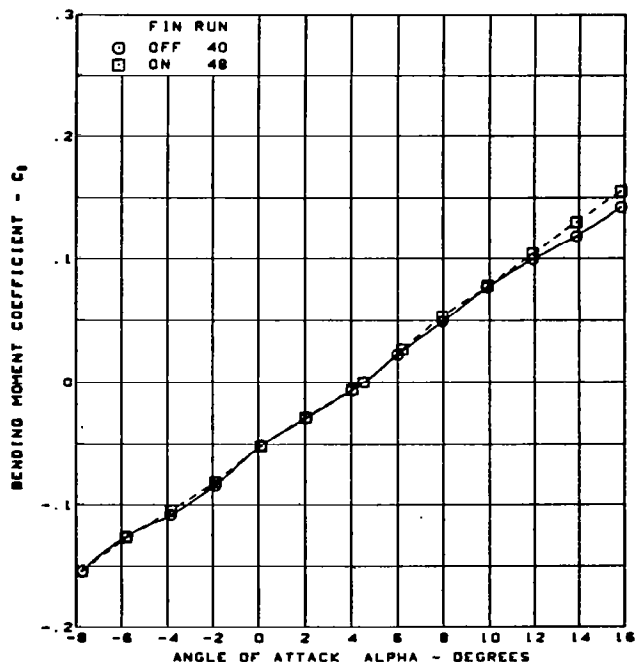
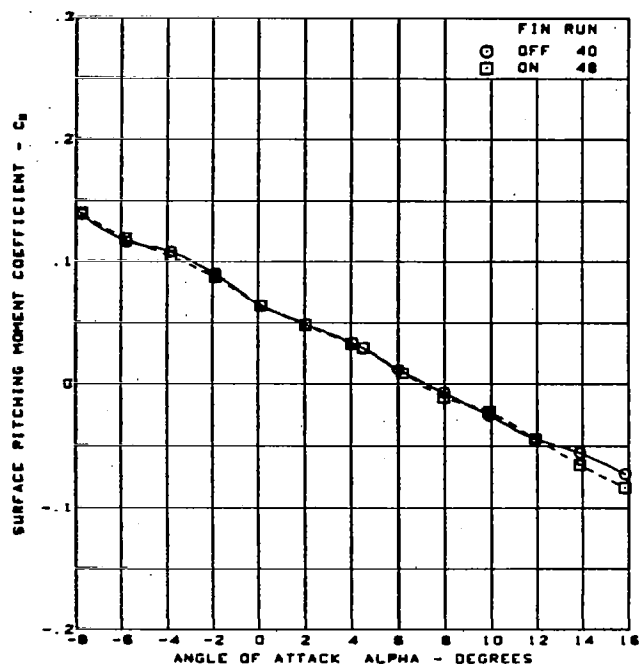
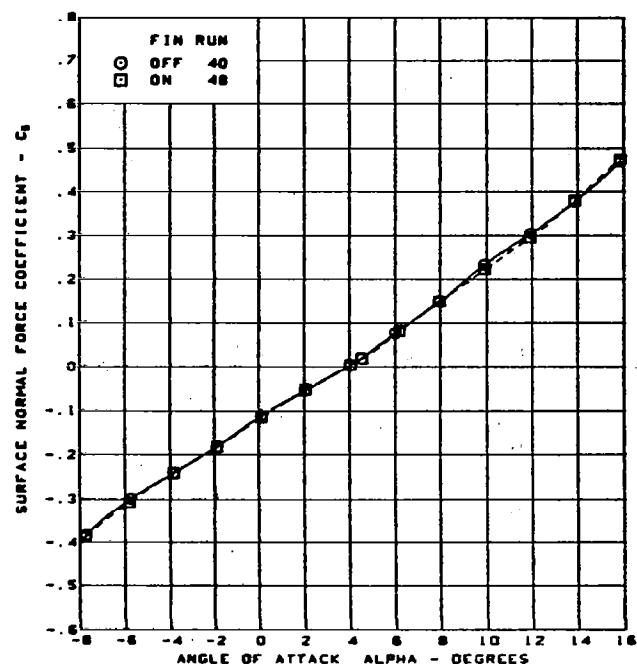
Figure 29. — (Continued)



$M = 0.85$   
 Cambered-twisted wing, rounded L.E.  
 L.E. deflection, full span =  $0.0^\circ$   
 T.E. deflection, full span =  $0.0^\circ$

(g) Spanload Distributions

Figure 29. - (Continued)

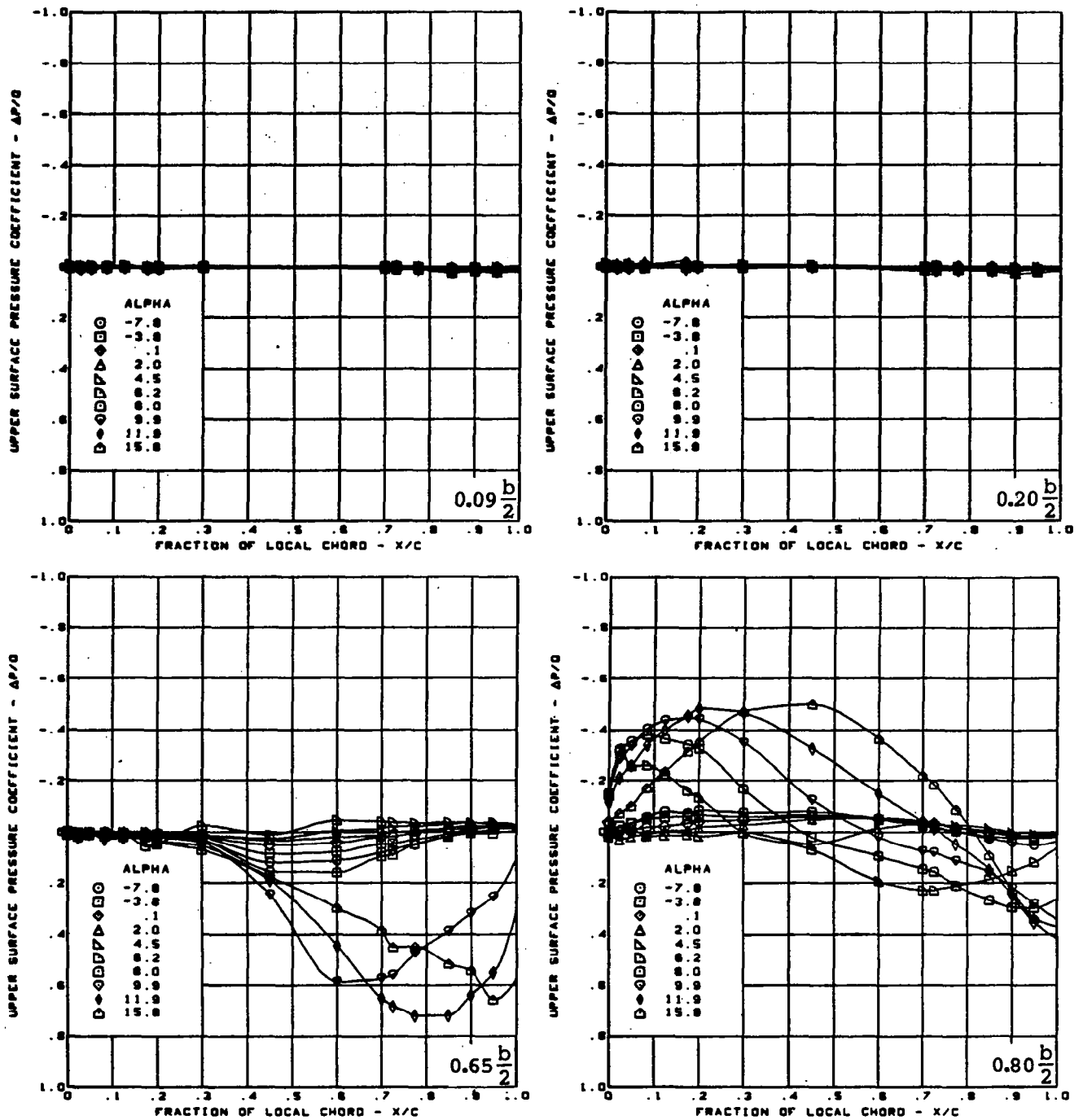


$M = 0.85$   
 Cambered-twisted wing, rounded L.E.  
 L.E. deflection, full span =  $0.0^\circ$   
 T.E. deflection, full span =  $0.0^\circ$

#### (h) Wing Aerodynamic Coefficients

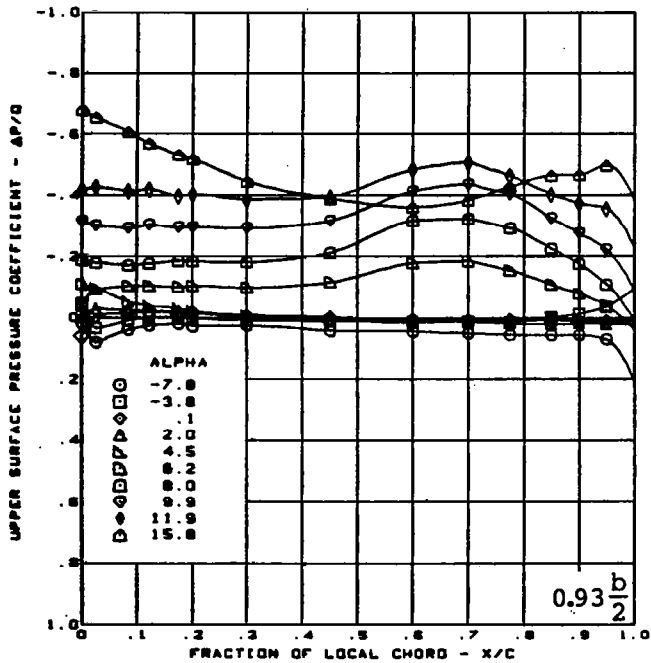
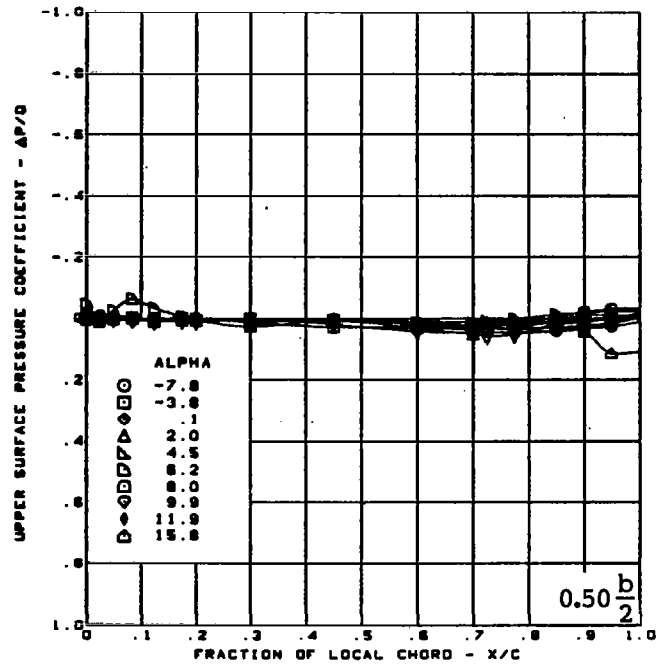
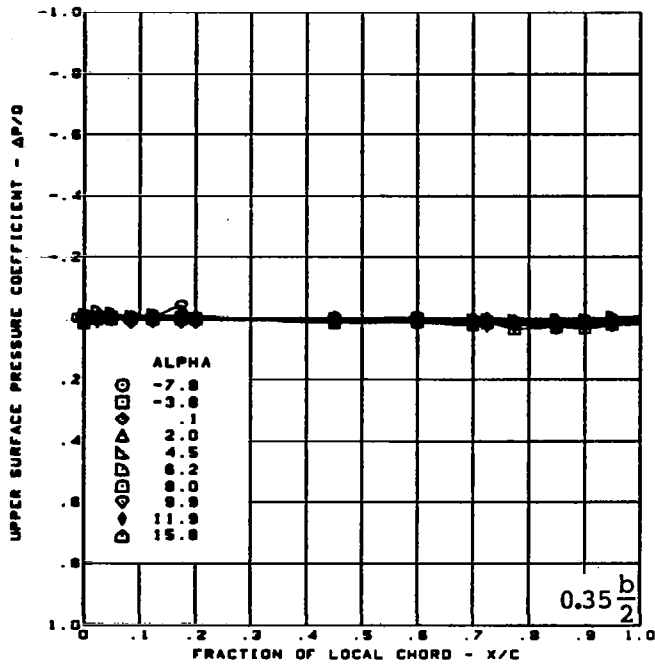
Figure 29. — (Concluded)





(a) Upper Surface Chordwise Pressure Distributions

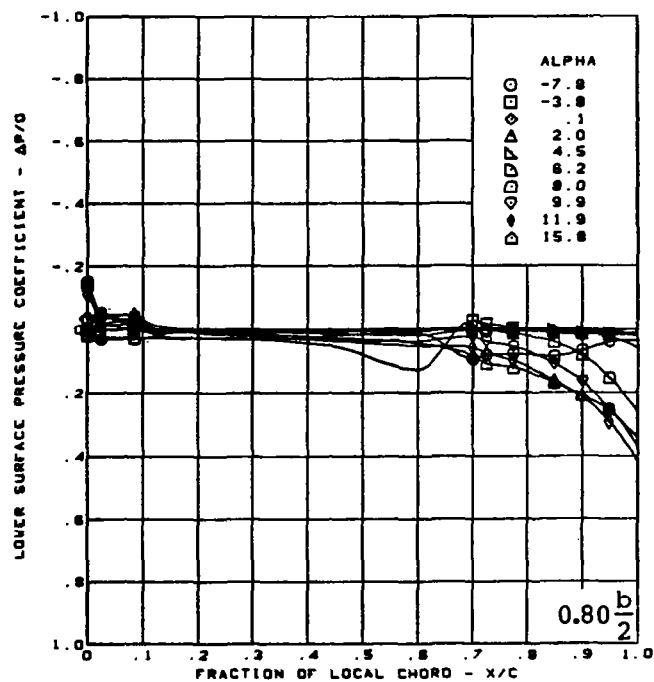
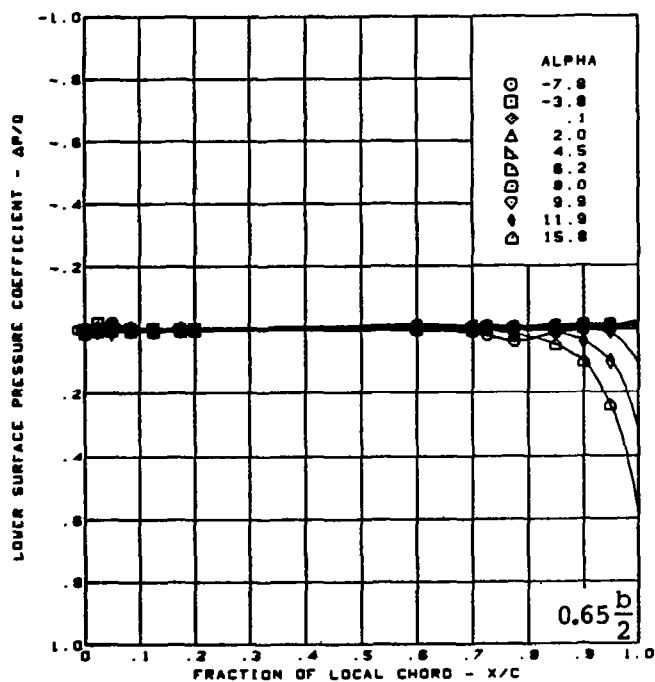
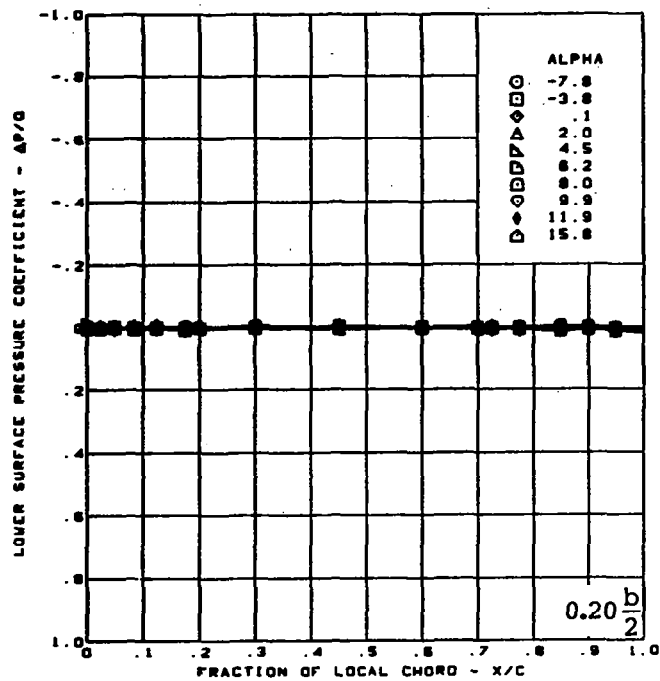
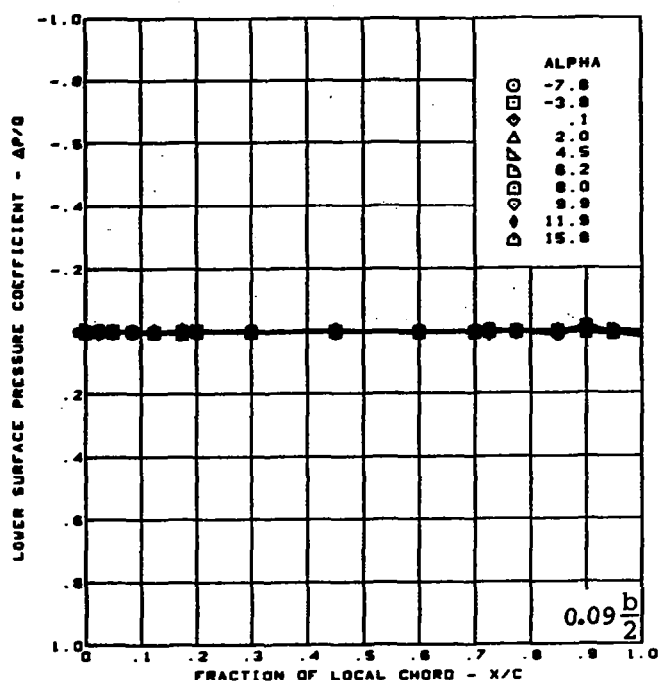
Figure 30. — Wing Experimental Data—Incremental Effect of a Wing Fin; Cambered-Twisted Wing; T.E. Deflection, Full Span =  $0.0^\circ$ ;  $M = 0.85$



$M = 0.85$   
 Camber-twisted wing, rounded L.E.  
 Fin on data minus fin off data  
 L.E. deflection, full span =  $0.0^\circ$   
 T.E. deflection, full span =  $0.0^\circ$

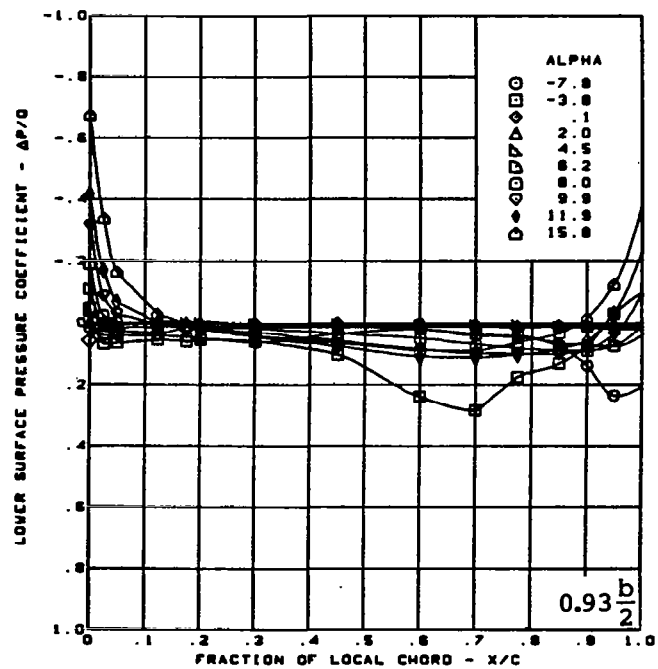
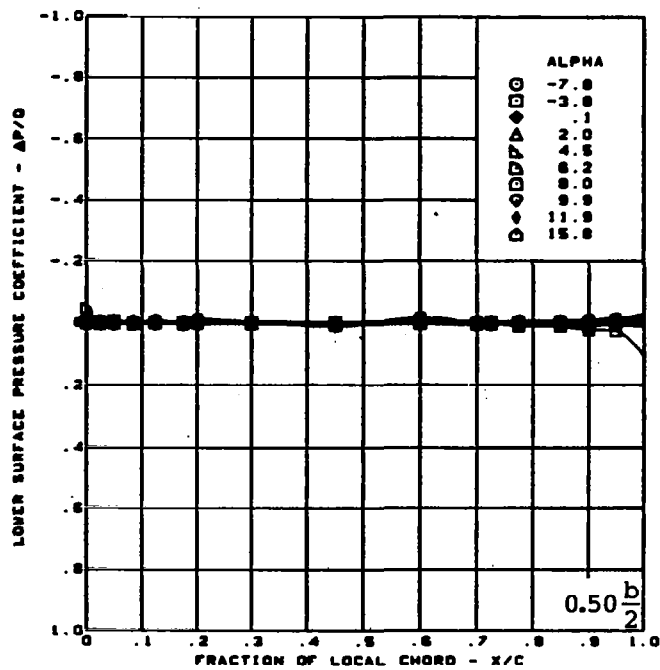
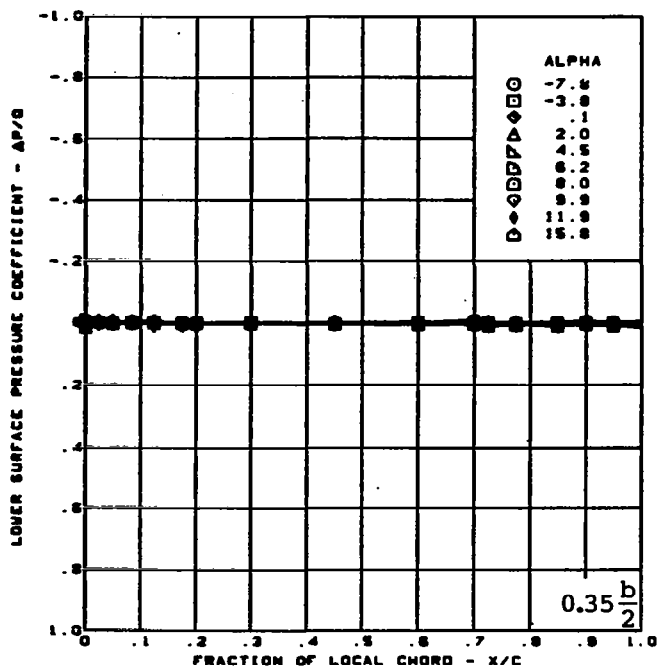
(a) (Concluded)

Figure 30. — (Continued)



(b) Lower Surface Chordwise Pressure Distributions

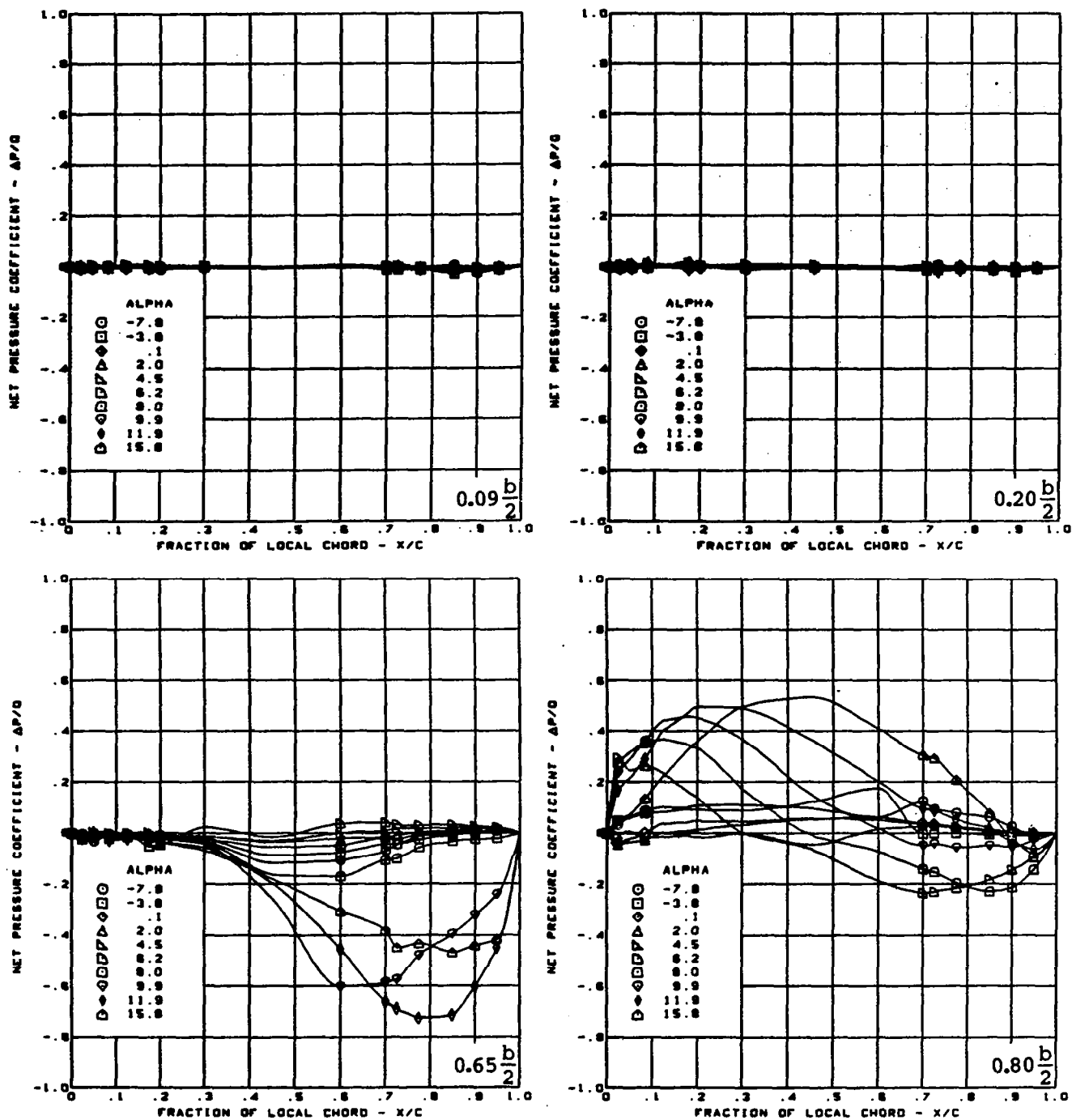
Figure 30. — (Continued)



$M = 0.85$   
 Camber-twisted wing, rounded L.E.  
 Fin on data minus fin off data  
 L.E. deflection, full span =  $0.0^\circ$   
 T.E. deflection, full span =  $0.0^\circ$

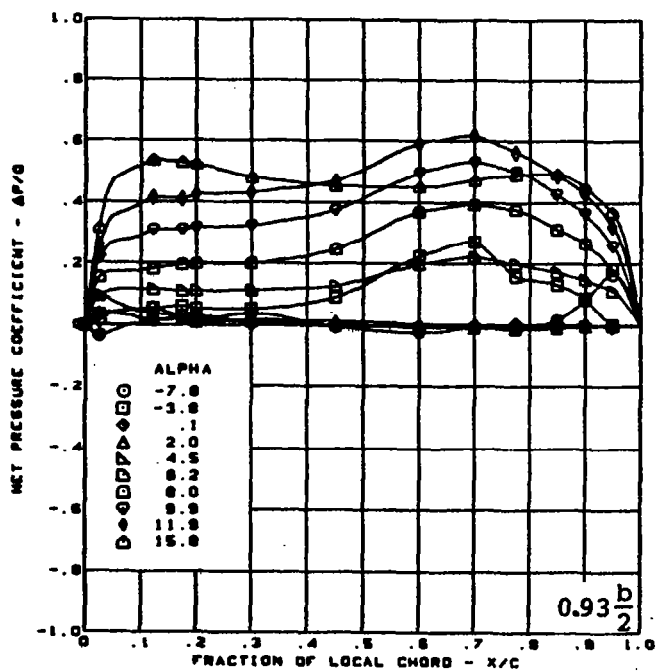
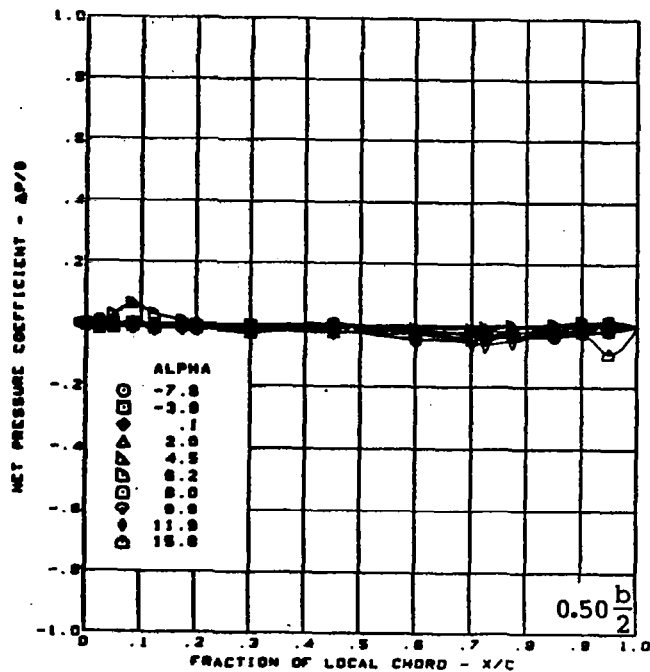
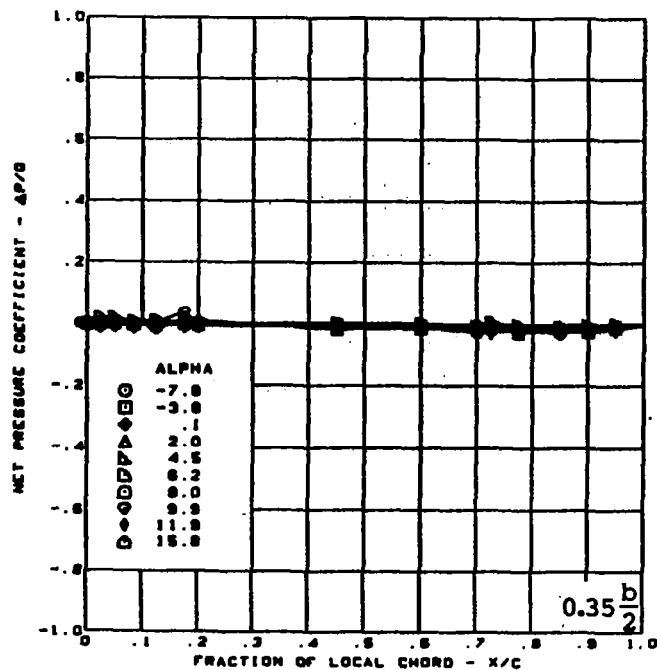
(b) (Concluded)

Figure 30. — (Continued)



(c) Net Chordwise Pressure Distributions

Figure 30. - (Continued)

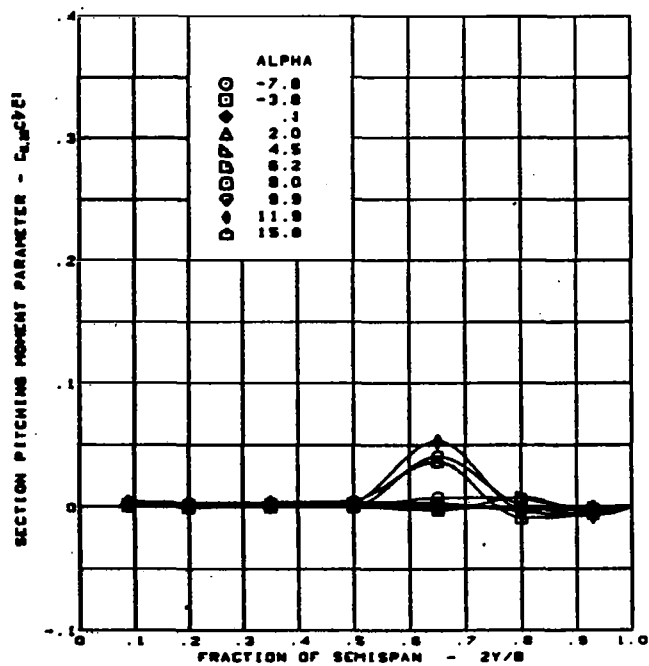
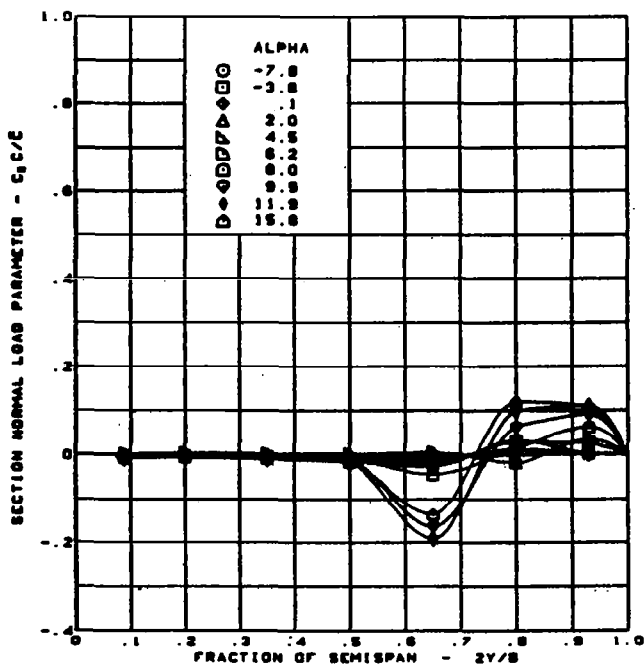


$M = 0.85$   
 Camber-twisted wing, rounded L.E.  
 Fin on data minus fin off data  
 L.E. deflection, full span =  $0.0^\circ$   
 T.E. deflection, full span =  $0.0^\circ$

(c) (Concluded)

Figure 30. — (Continued)



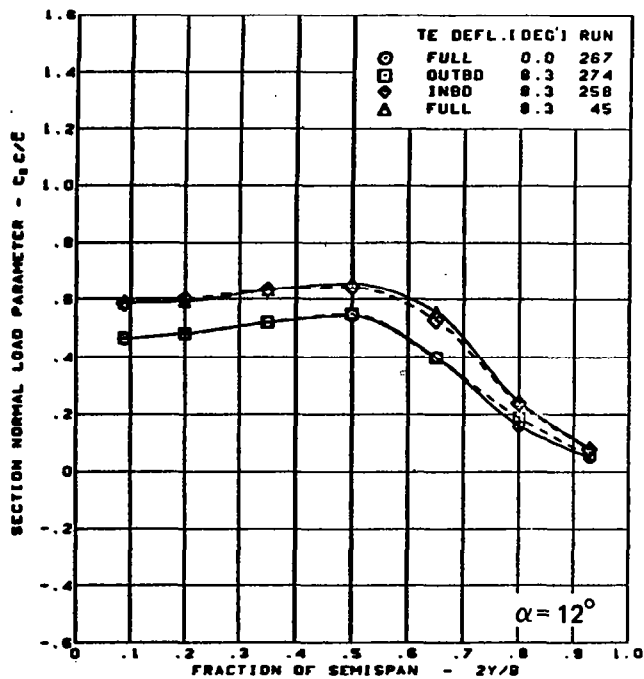
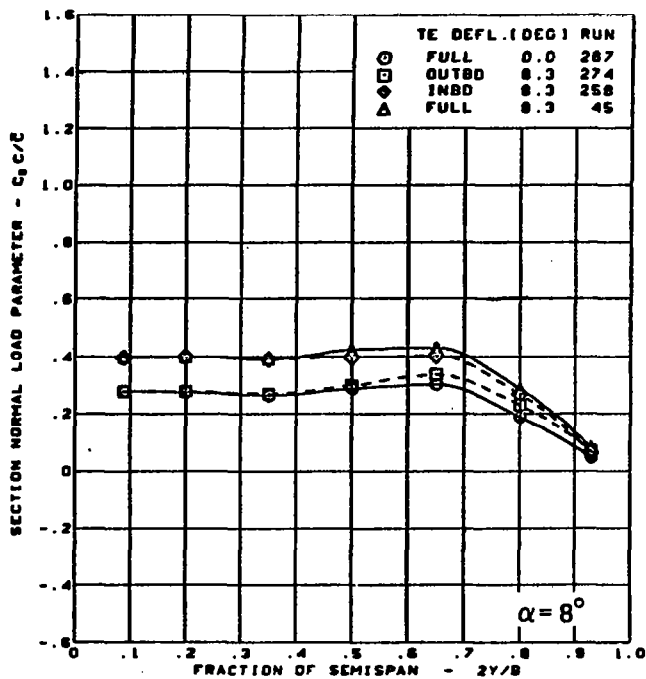
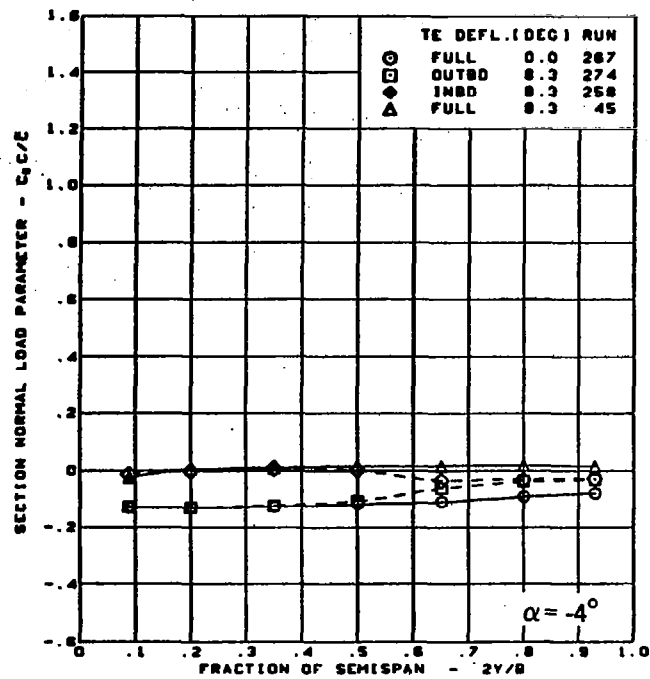
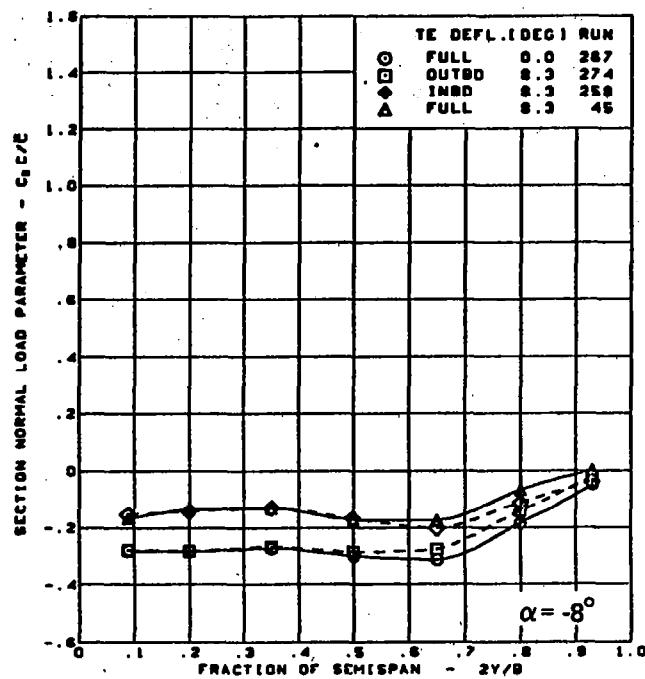


M = 0.85  
 Cambered-twisted wing, rounded L.E.  
 Fin on data minus fin off data  
 L.E. deflection, full span =  $0.0^\circ$   
 T.E. deflection, full span =  $0.0^\circ$

(d) Spanload Distributions

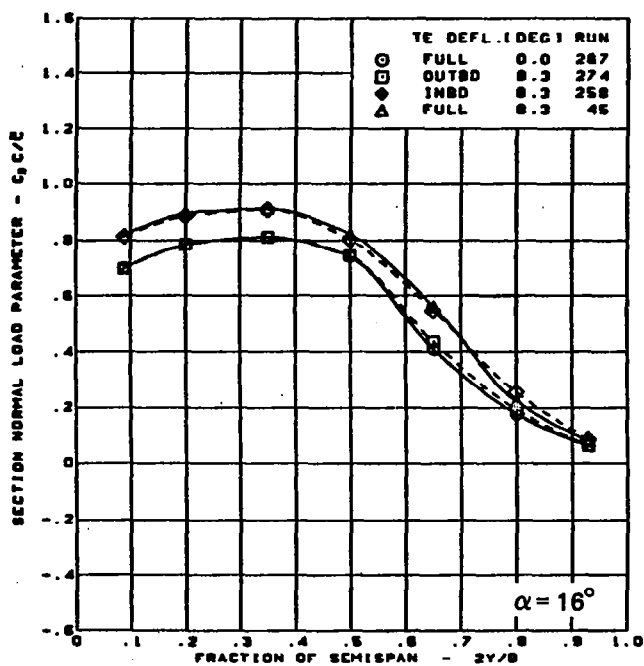
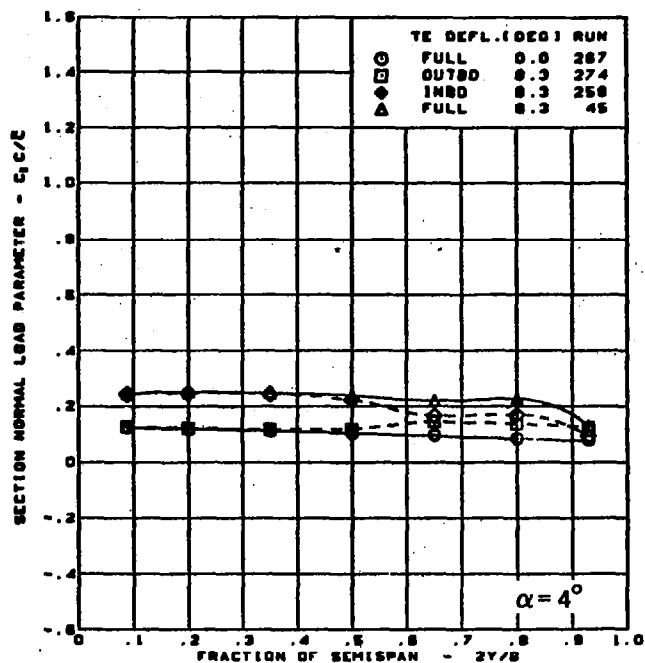
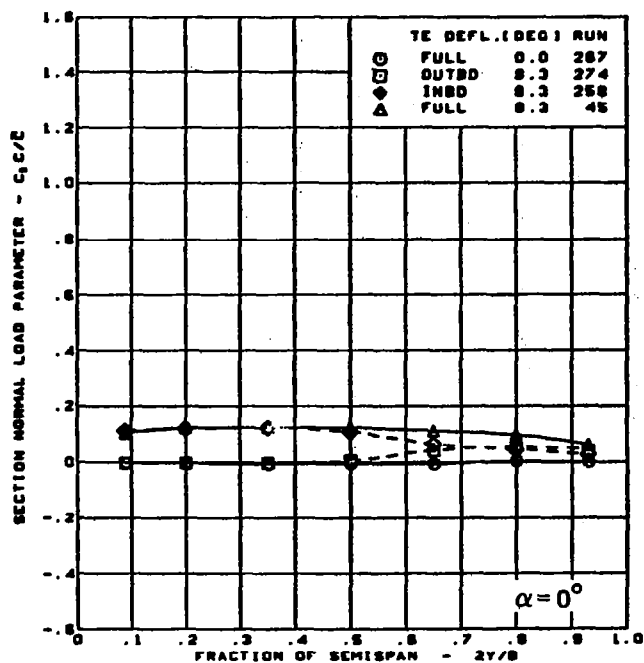
Figure 30. ~ (Concluded)





(a) Spanload Distribution - Normal Force Variation With T.E. Control Surface Configuration

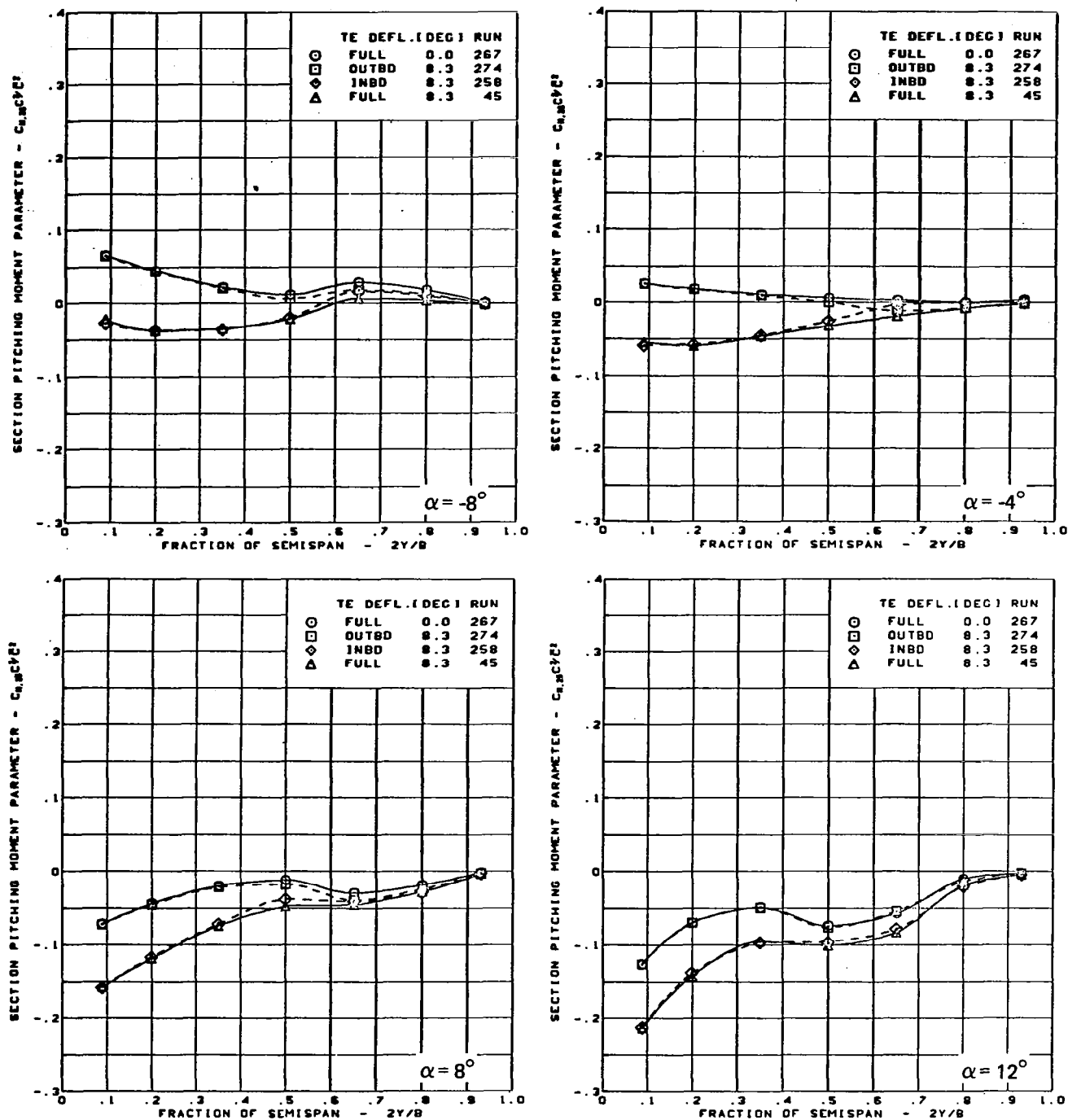
Figure 31. — Wing Experimental Data—Effect of Full- and Partial-Span Trailing Edge Control Surface Deflection; Flat Wing;  $M = 0.85$



M = 0.85  
 Flat wing, rounded L.E.  
 L.E. deflection, full span =  $0.0^\circ$

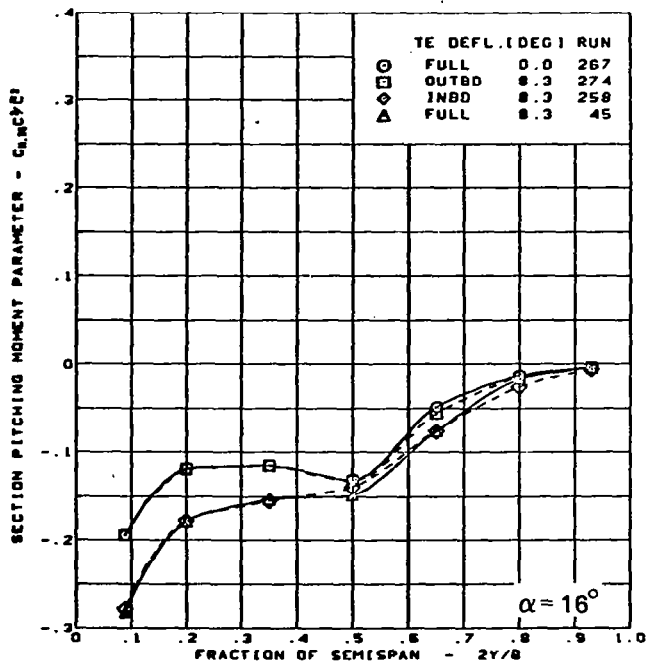
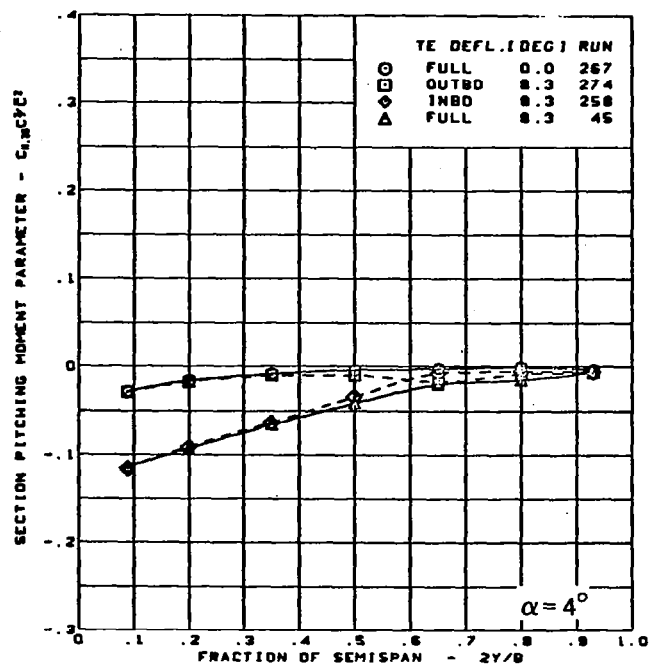
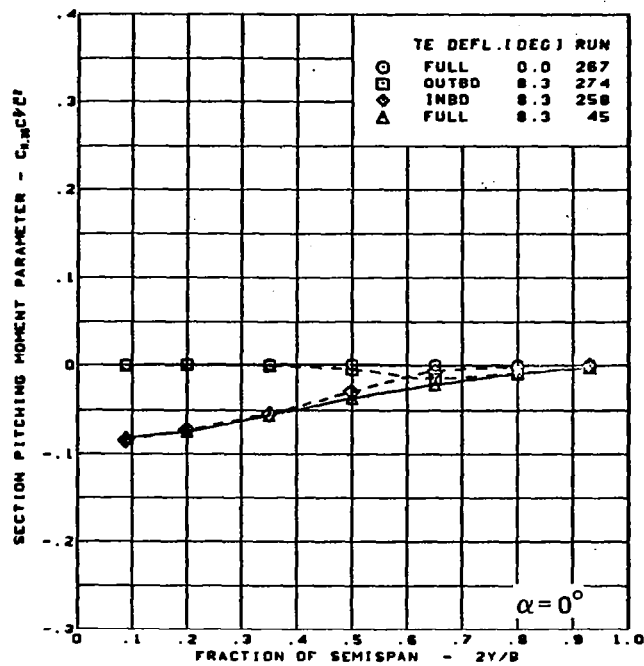
(a) (Concluded)

Figure 31. — (Continued)



(b) Spanload Distribution - Pitching Moment Variation With T.E. Control Surface Configuration

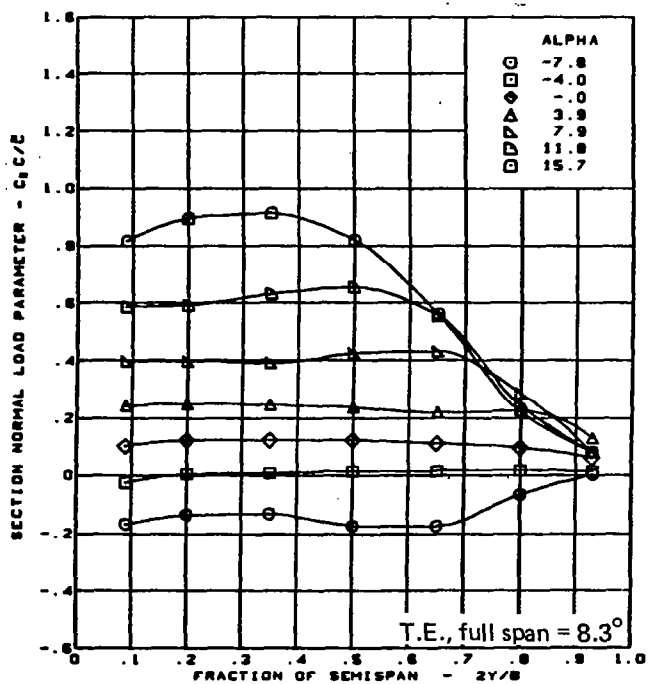
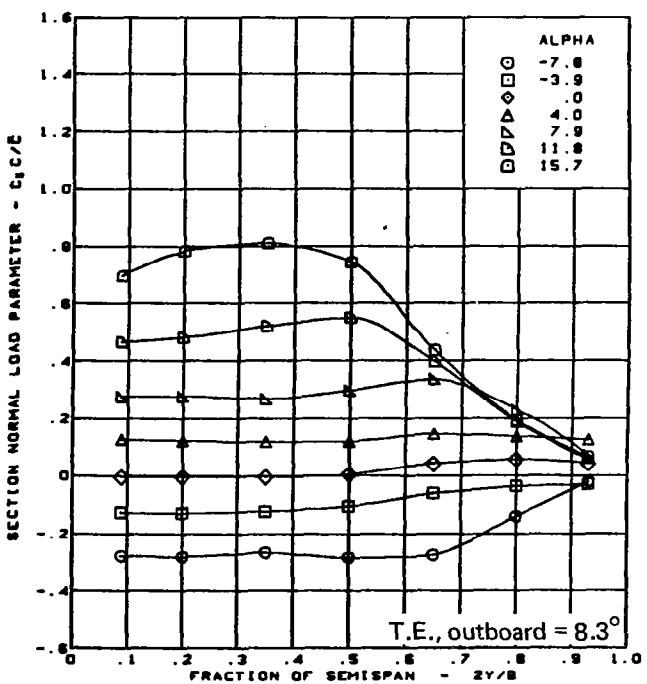
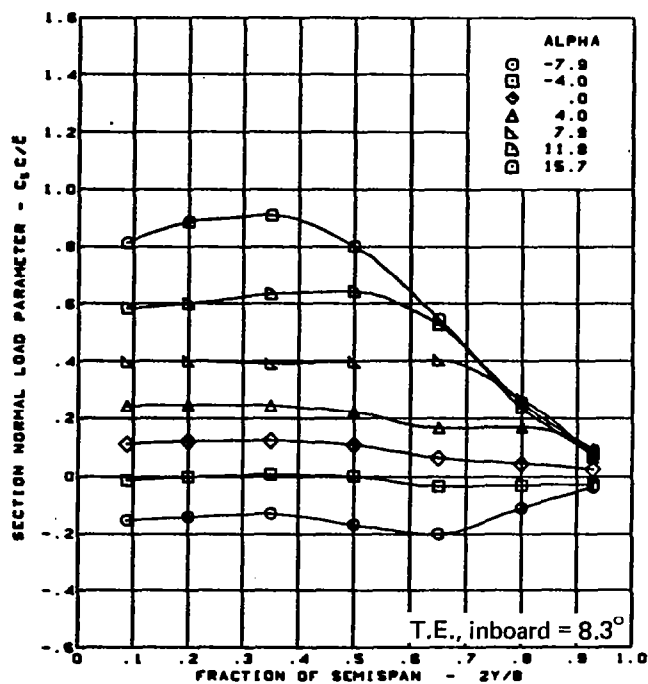
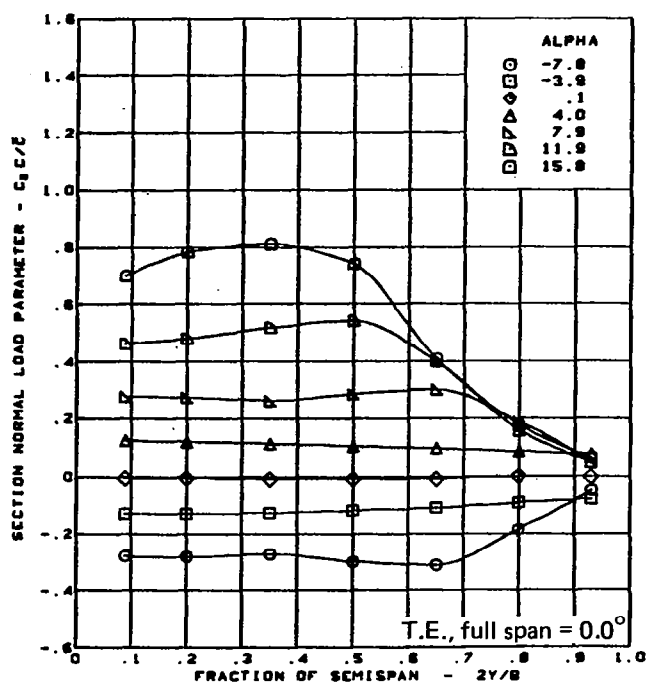
Figure 31. - (Continued)



$M = 0.85$   
 Flat wing, rounded L.E.  
 L.E. deflection, full span =  $0.0^\circ$

(b) (Concluded)

Figure 31. - (Continued)



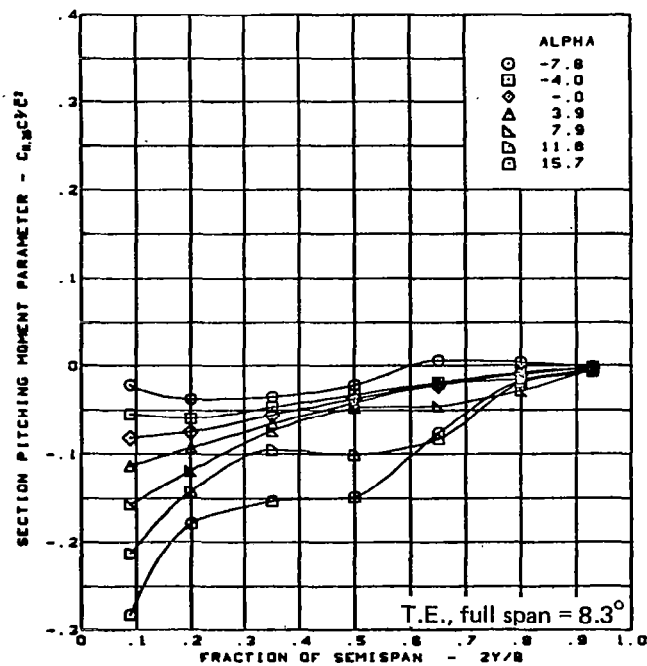
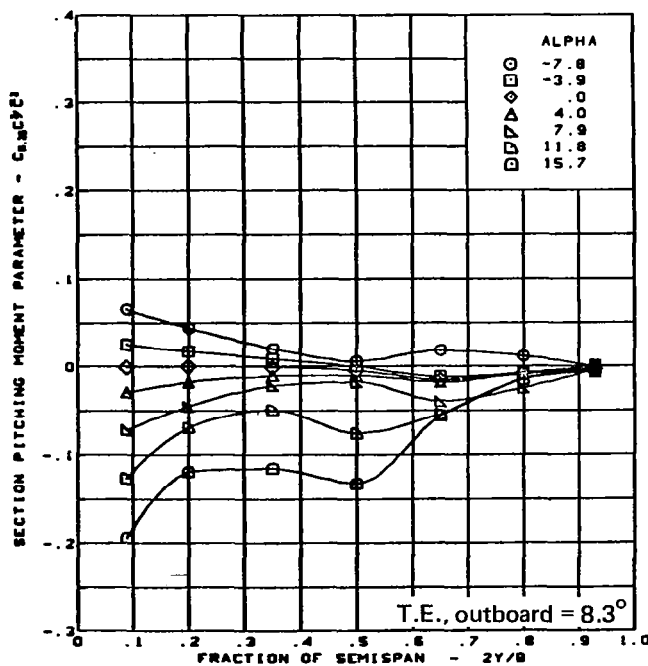
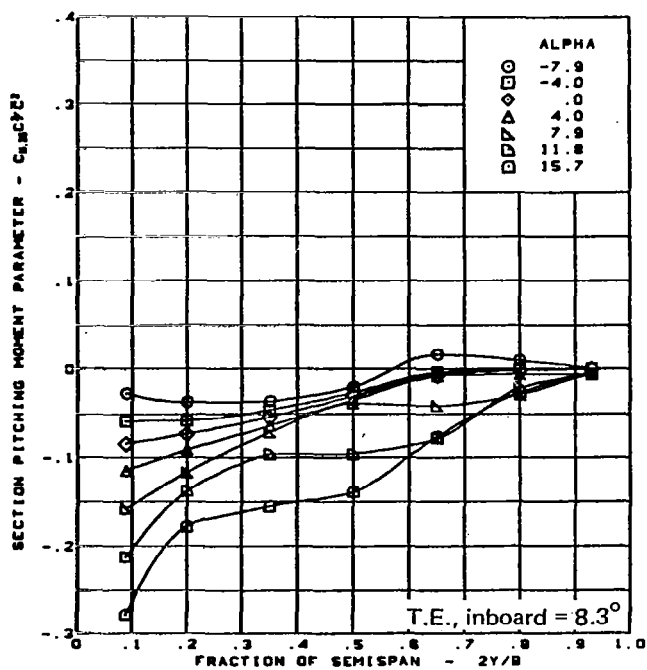
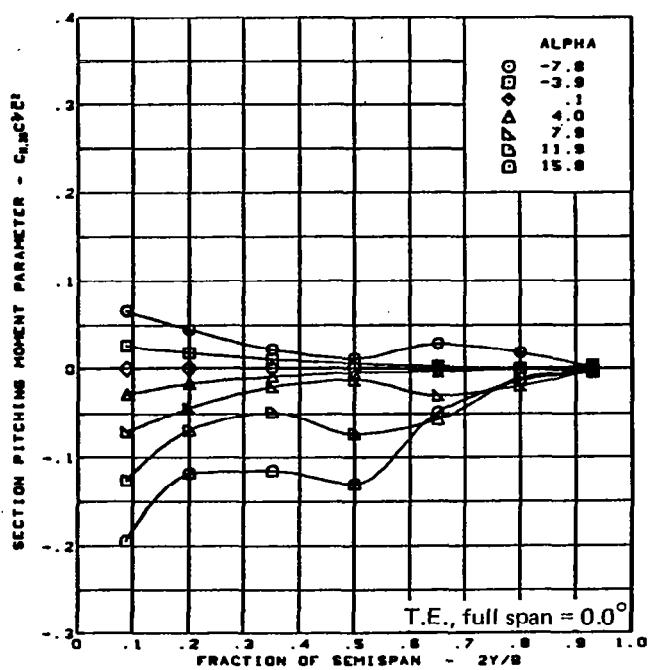
$M = 0.85$

Flat wing, rounded L.E.

L.E. deflection, full span  $= 0.0^\circ$

(c) Spanload Distribution - Normal Force Variation With Angle of Attack

Figure 31. — (Continued)



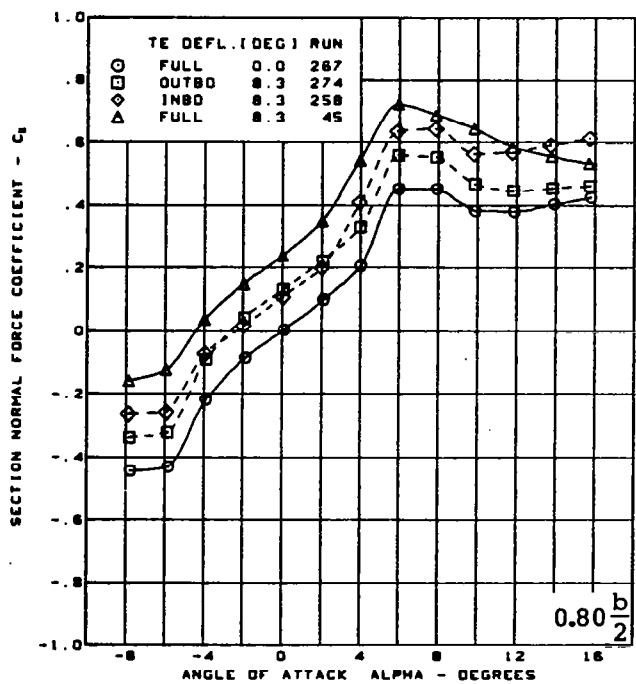
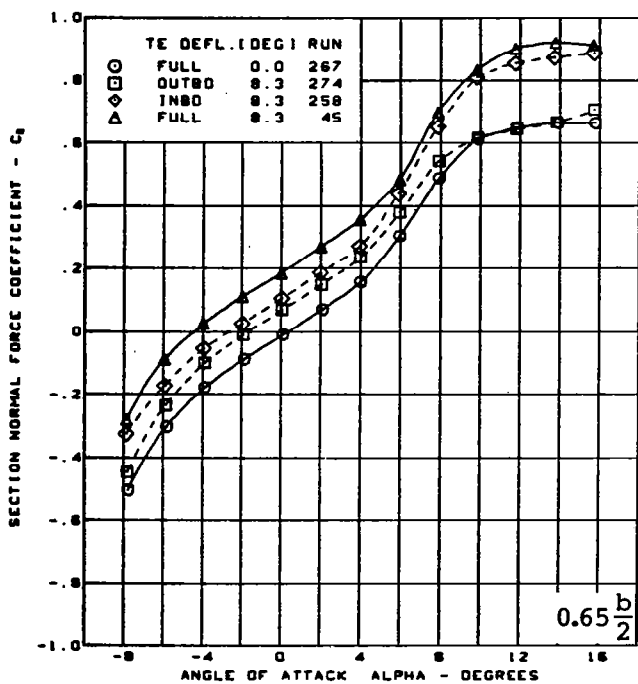
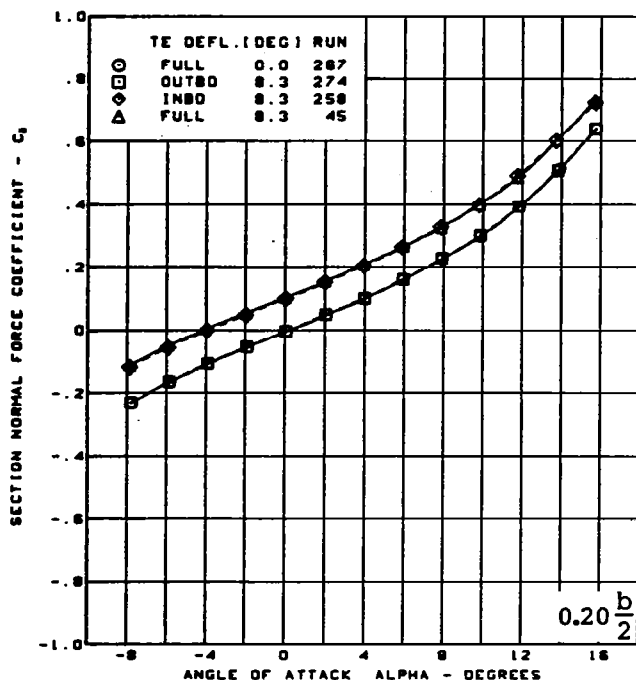
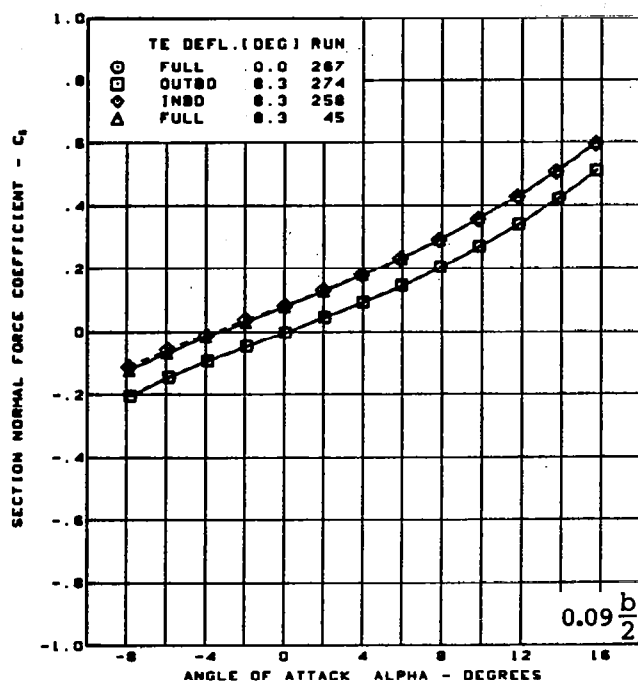
$M = 0.85$

Flat wing, rounded L.E.

L.E. deflection, full span =  $0.0^\circ$

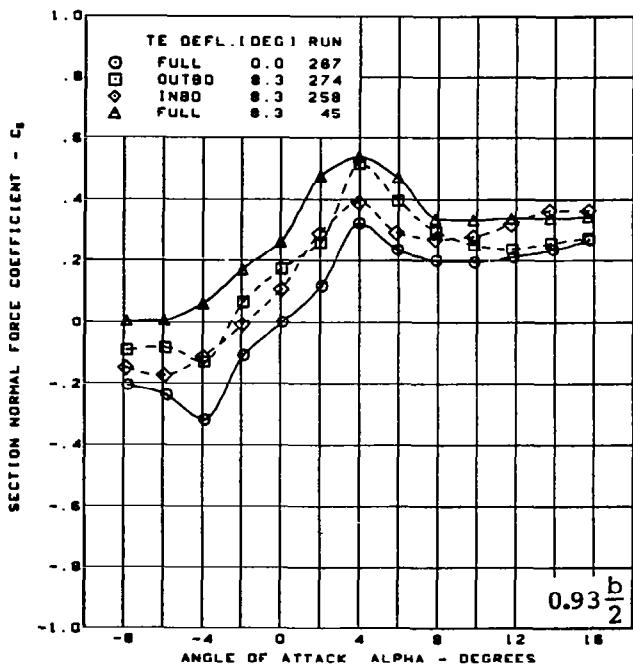
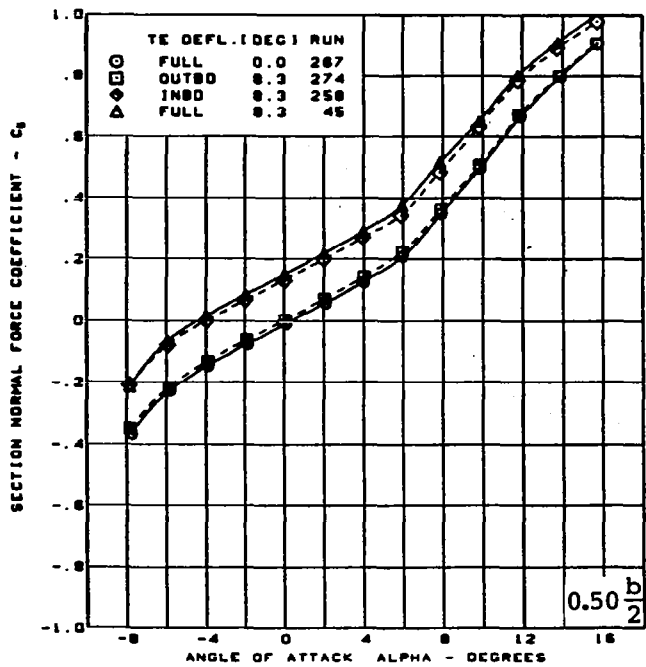
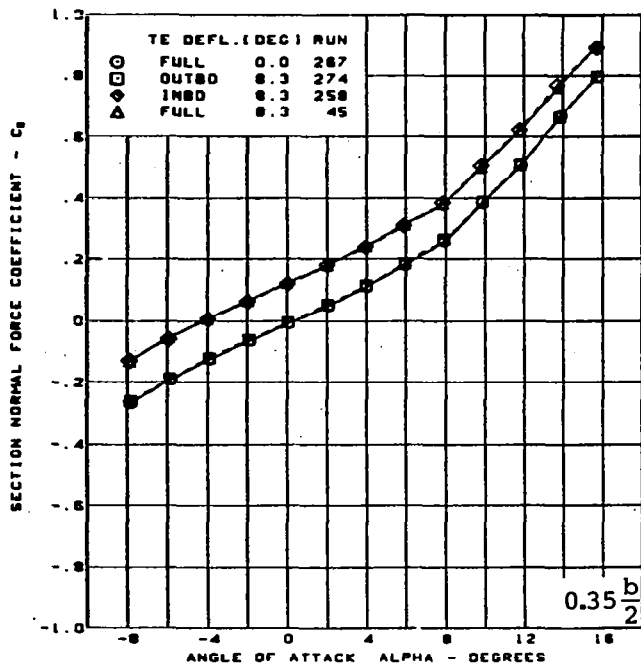
(d) Spanload Distribution - Pitching Moment Variation With Angle of Attack

Figure 31. — (Continued)



(e) Section Aerodynamic Coefficients - Normal Force

Figure 31. - (Continued)

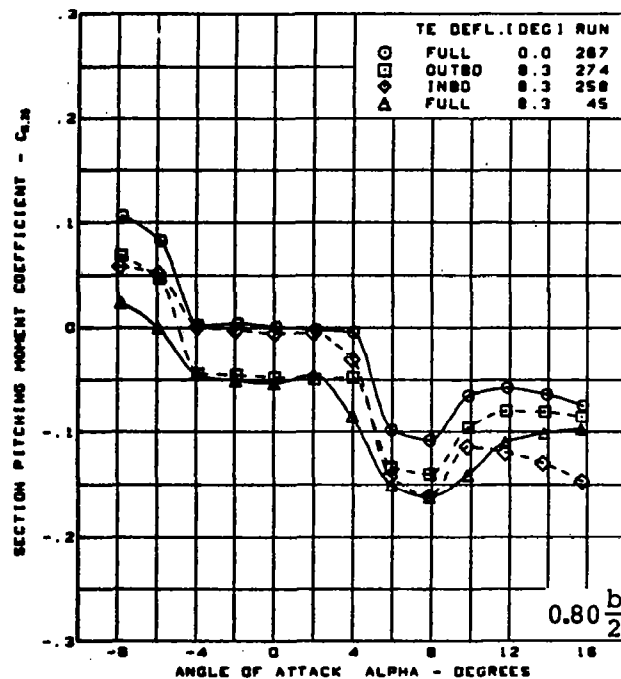
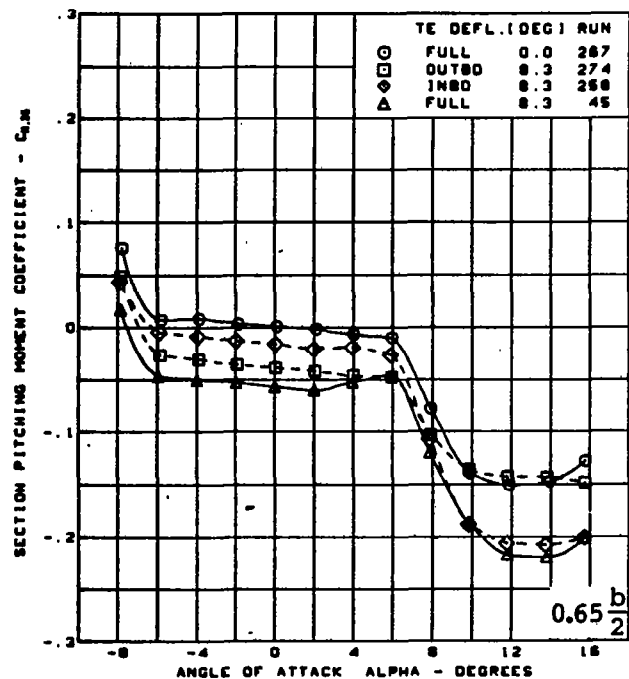
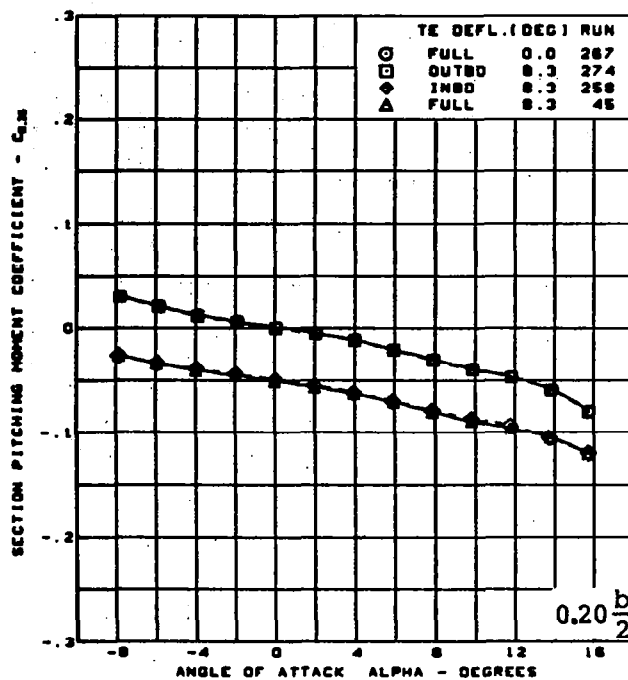
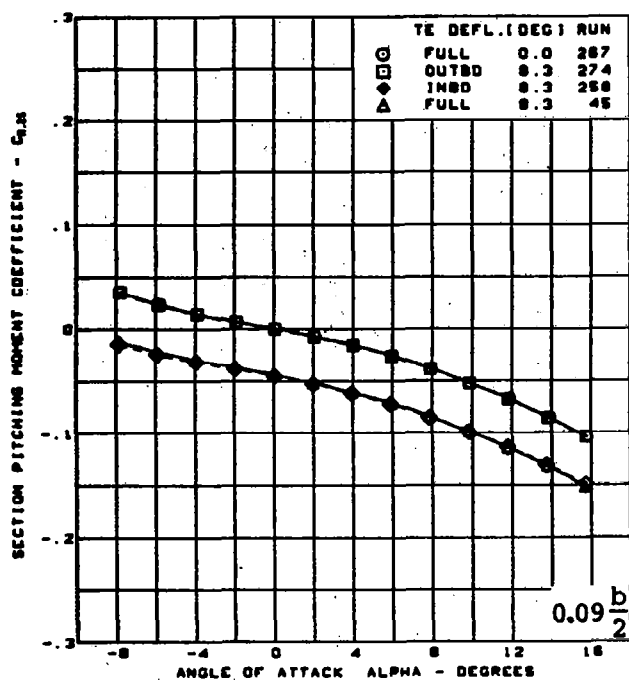


$M = 0.85$   
 Flat wing, rounded L.E.  
 L.E. deflection, full span =  $0.0^\circ$

(e) (Concluded)

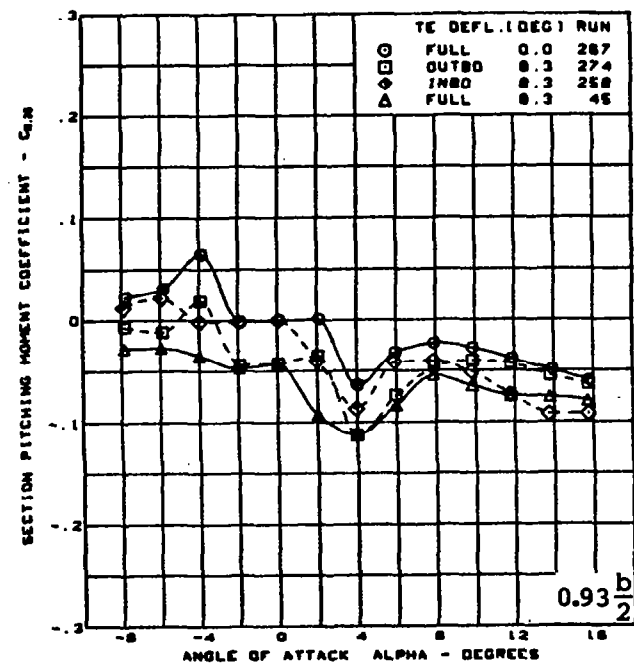
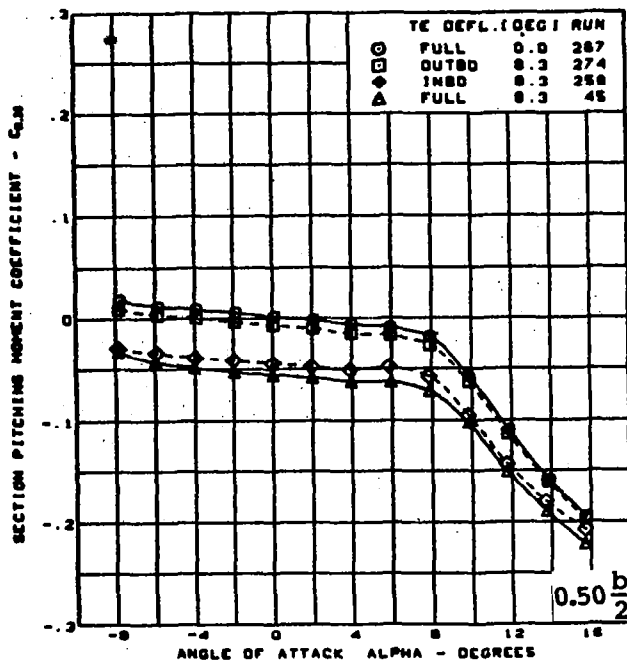
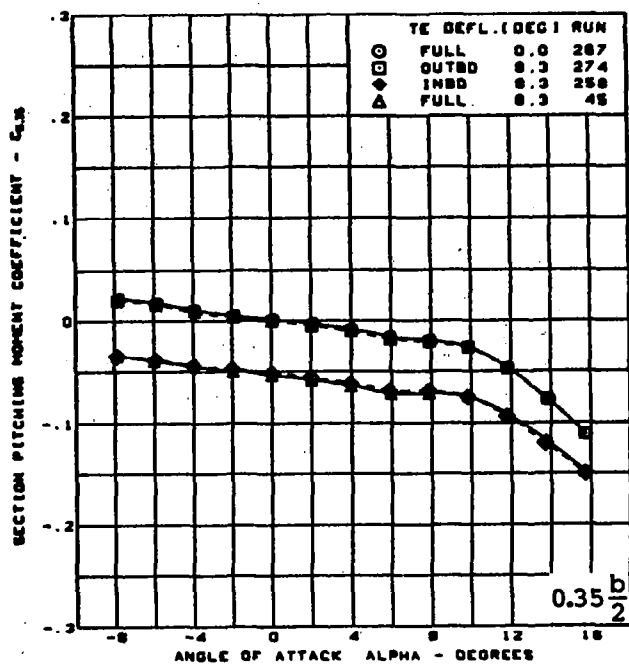
Figure 31. - (Continued)





(f) Section Aerodynamic Coefficients - Pitching Moment

Figure 31. - (Continued)

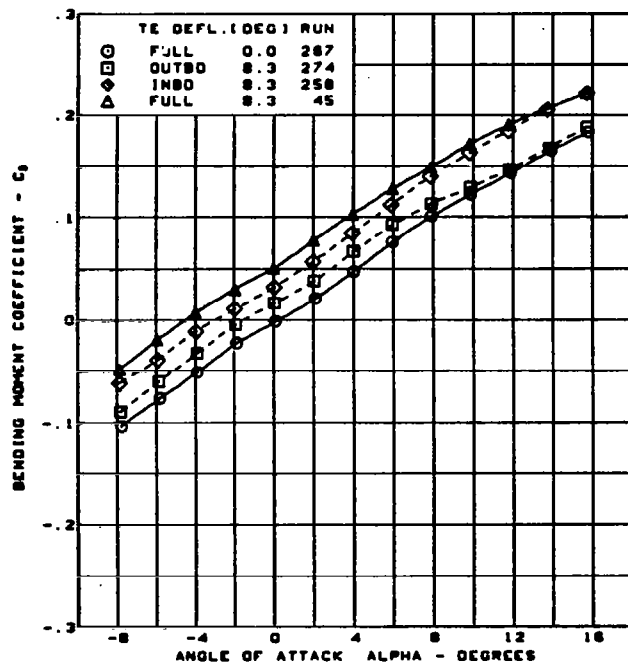
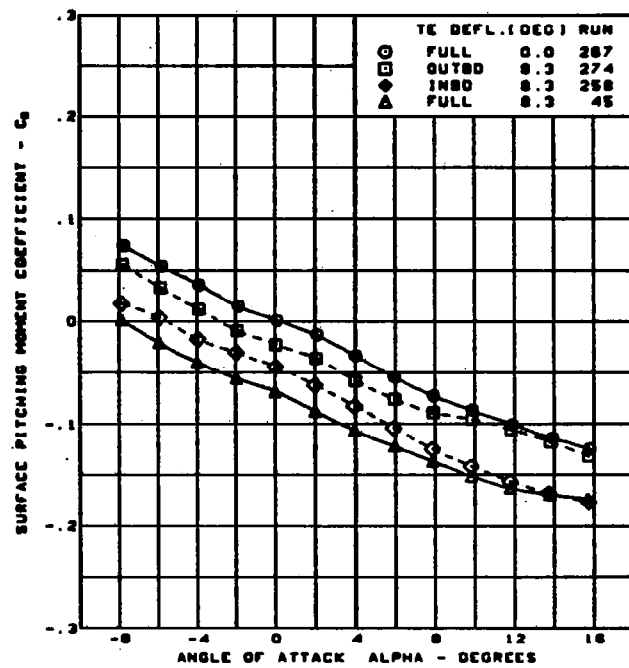
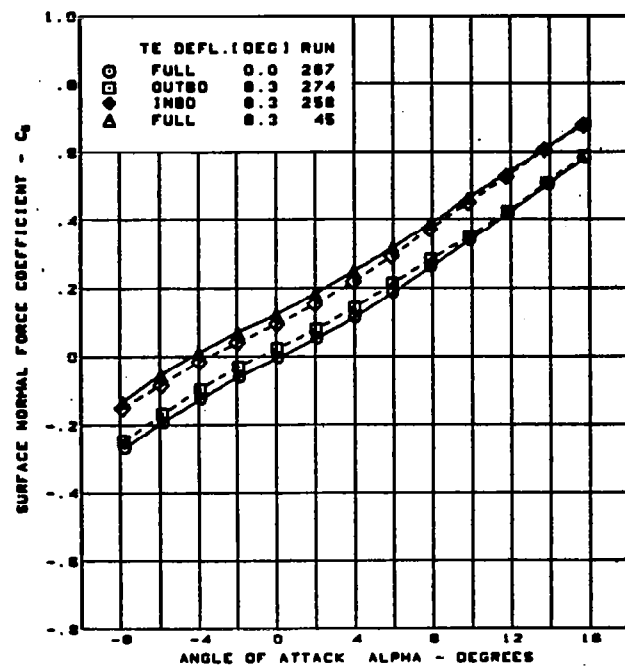


$M = 0.85$   
 Flat wing, rounded L.E.  
 L.E. deflection, full span =  $0.0^\circ$

(f) (Concluded)

Figure 31. - (Continued)



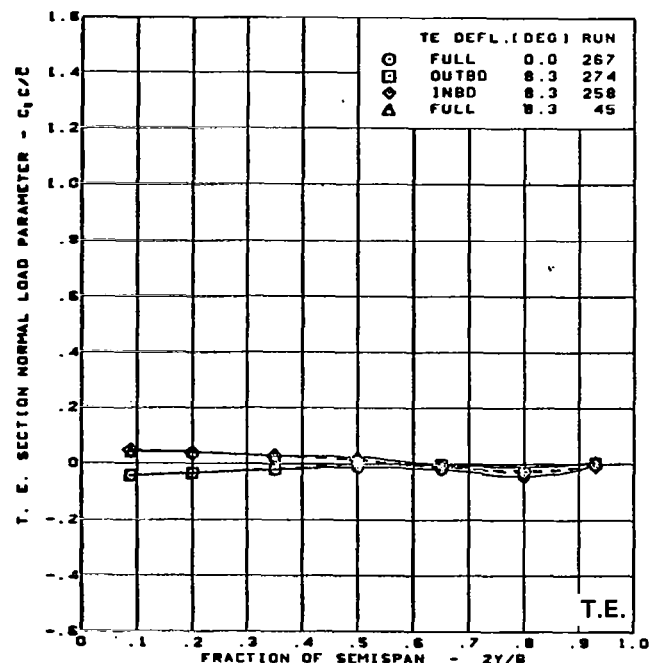
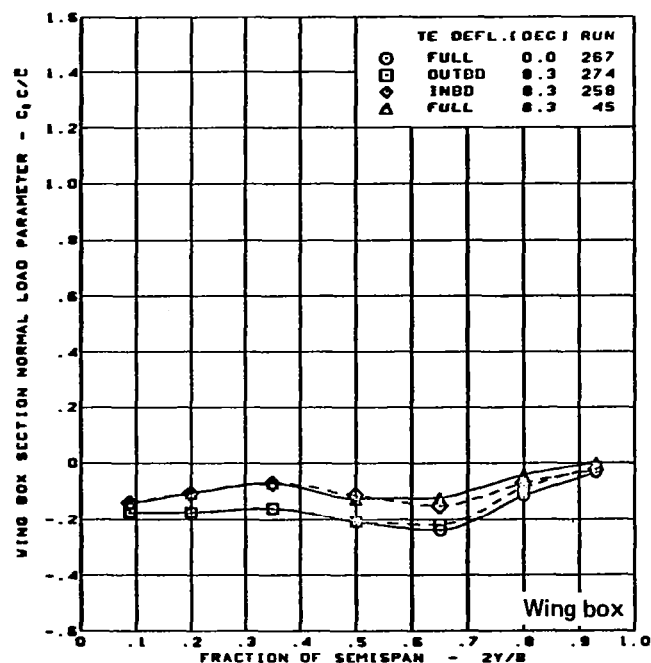
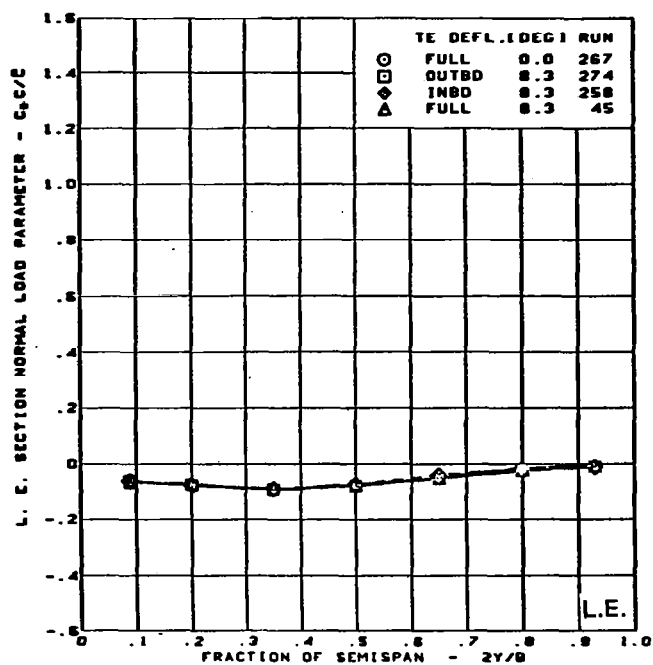
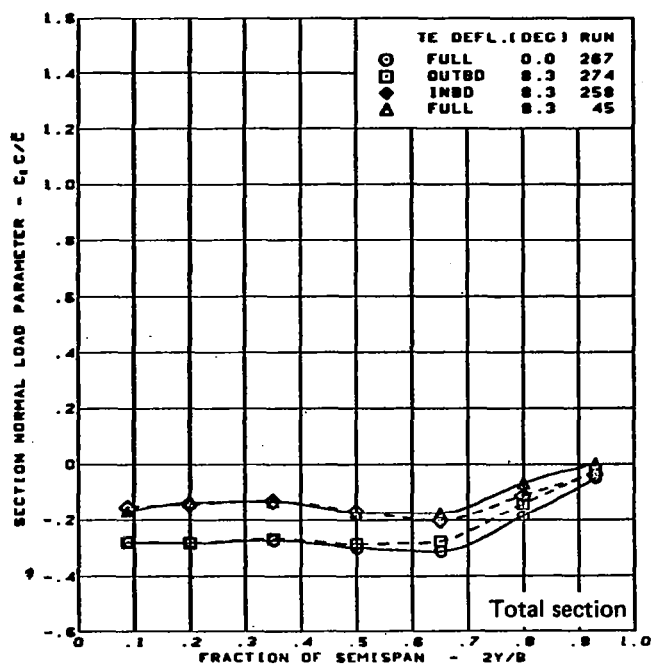


$M = 0.85$   
 Flat wing, rounded L.E.  
 L.E. deflection, full span =  $0.0^\circ$

(g) Wing Aerodynamic Coefficients

Figure 31. — (Concluded)



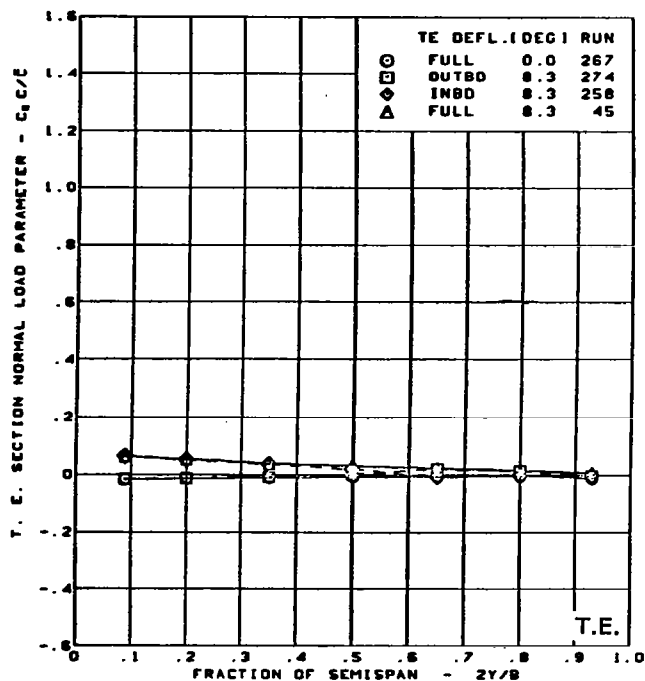
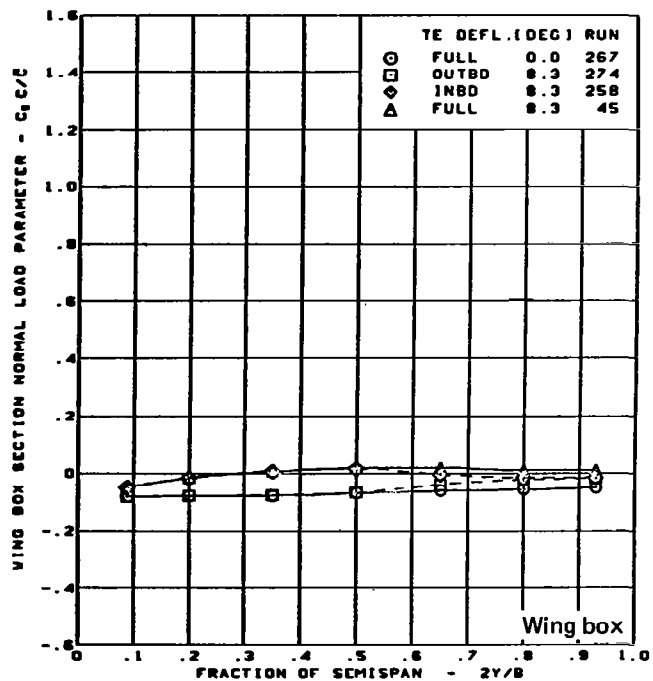
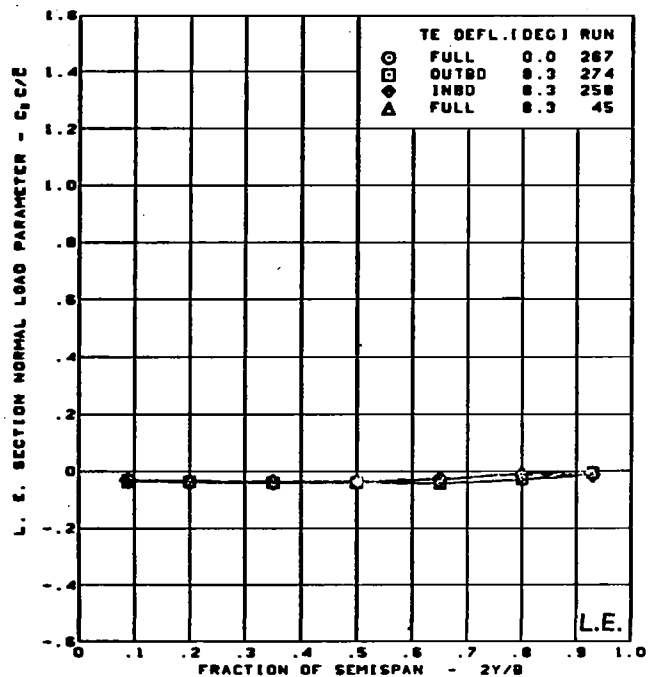
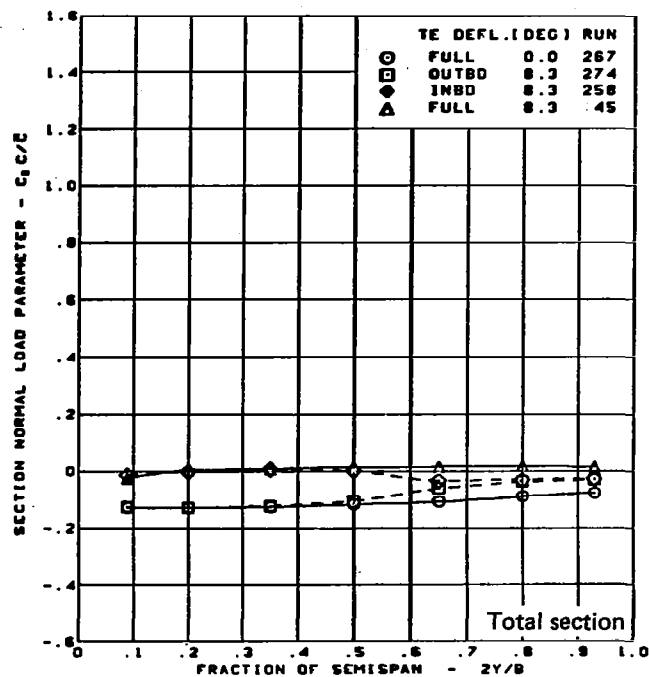


$M = 0.85$   
 $\alpha = -8^\circ$

Flat wing, rounded L.E.  
 L.E. deflection, full span =  $0.0^\circ$

(a) Spanload Distributions - Normal Force,  $\alpha = -8^\circ$

Figure 32. — Wing Experimental Data—Effect of Full- and Partial-Span Trailing Edge Control Surface Deflection on Chordwise Segments; Flat Wing;  $M = 0.85$

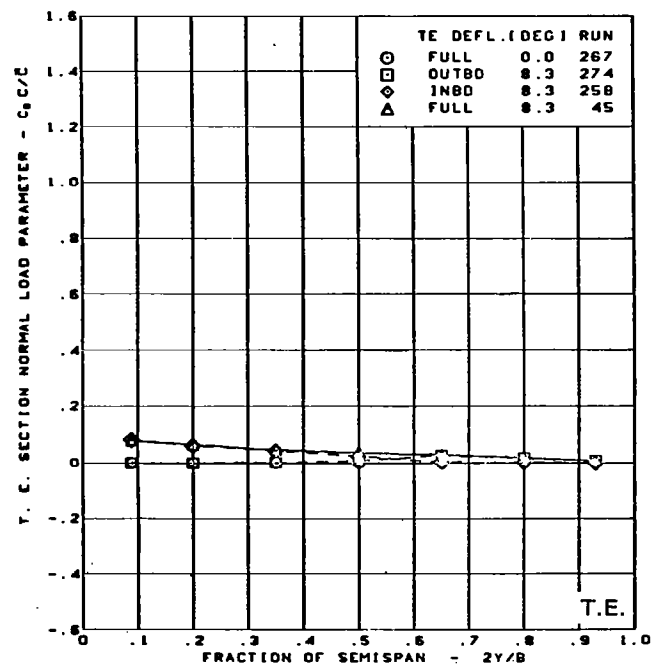
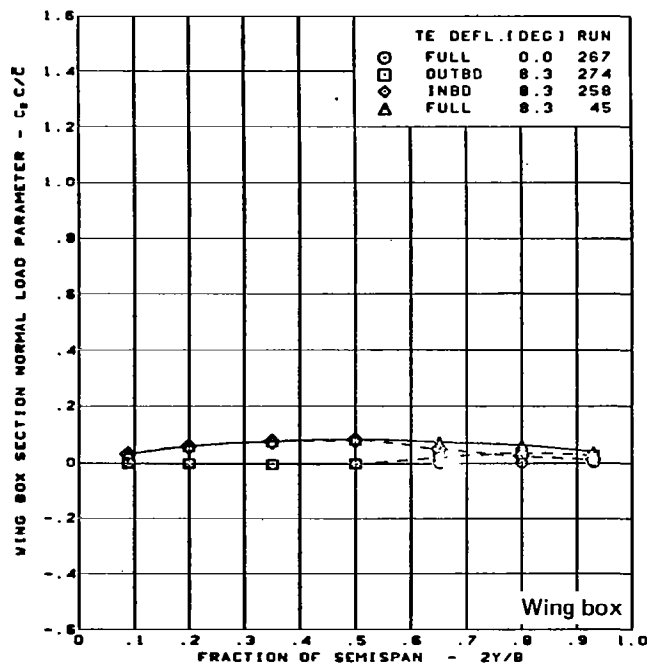
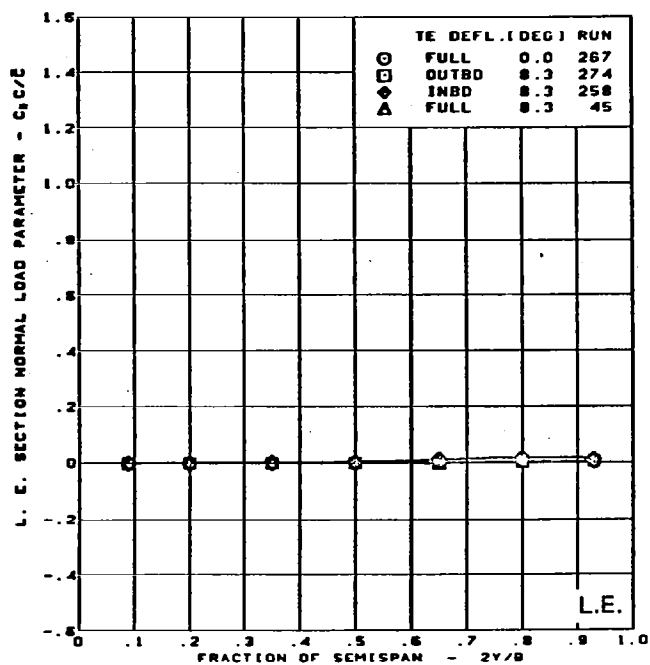
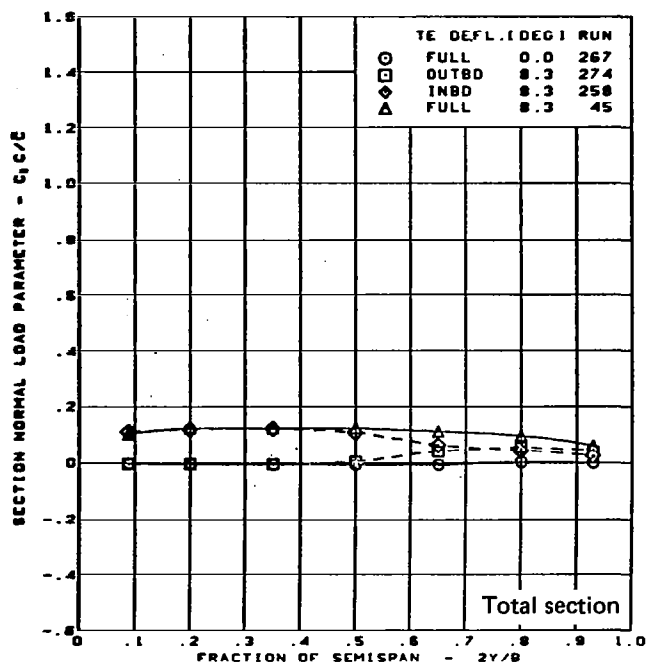


$M = 0.85$   
 $\alpha = -4^\circ$

Flat wing, rounded L.E.  
 L.E. deflection, full span =  $0.0^\circ$

(b) Spanload Distributions - Normal Force,  $\alpha = -4^\circ$

Figure 32. -- (Continued)



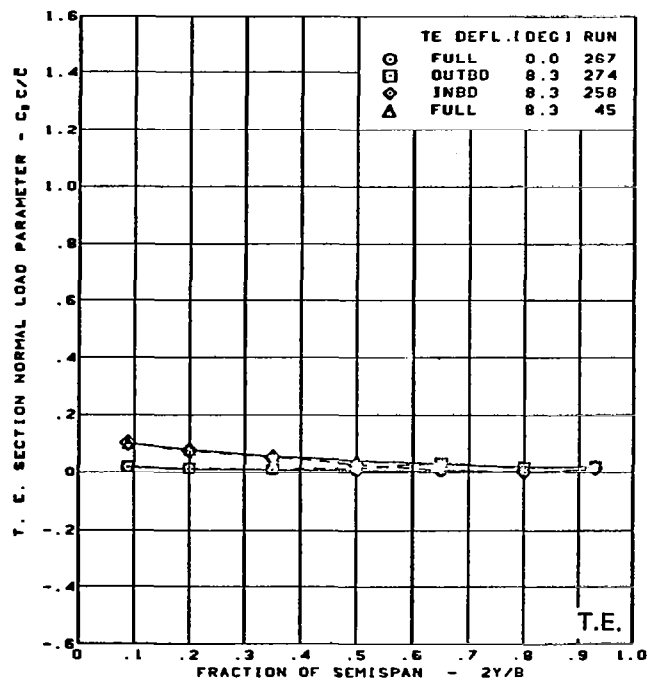
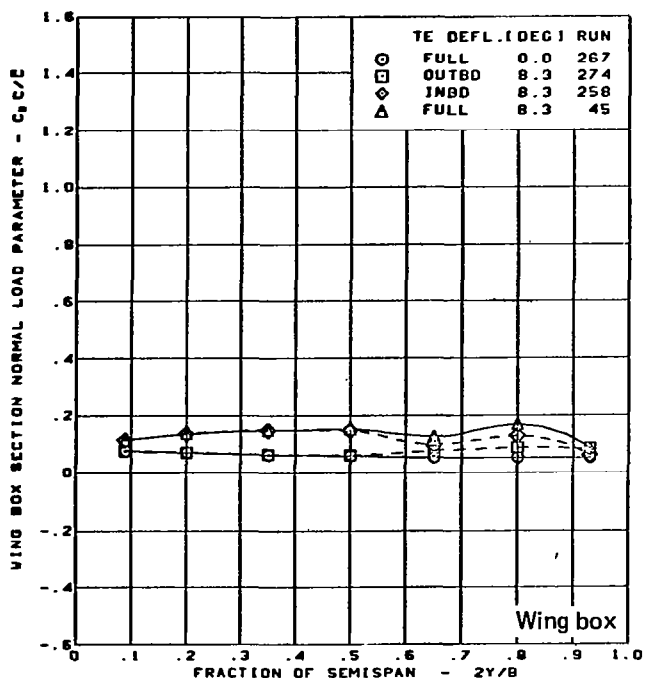
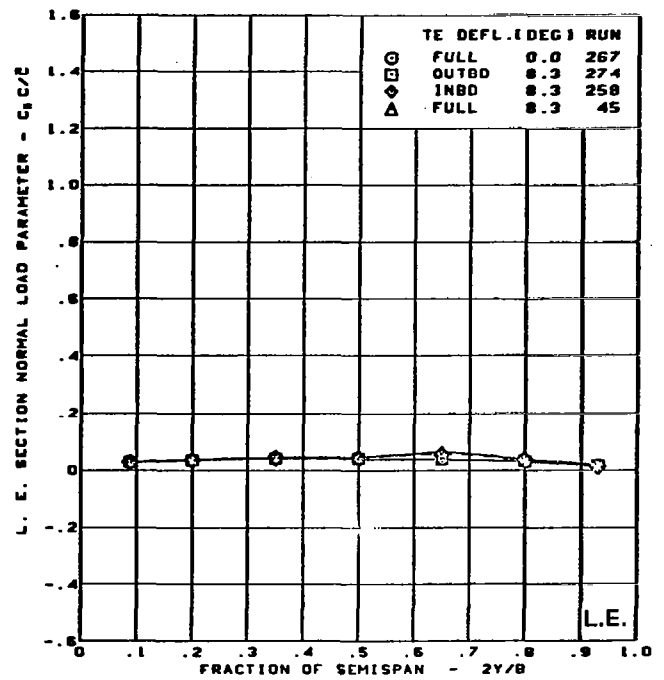
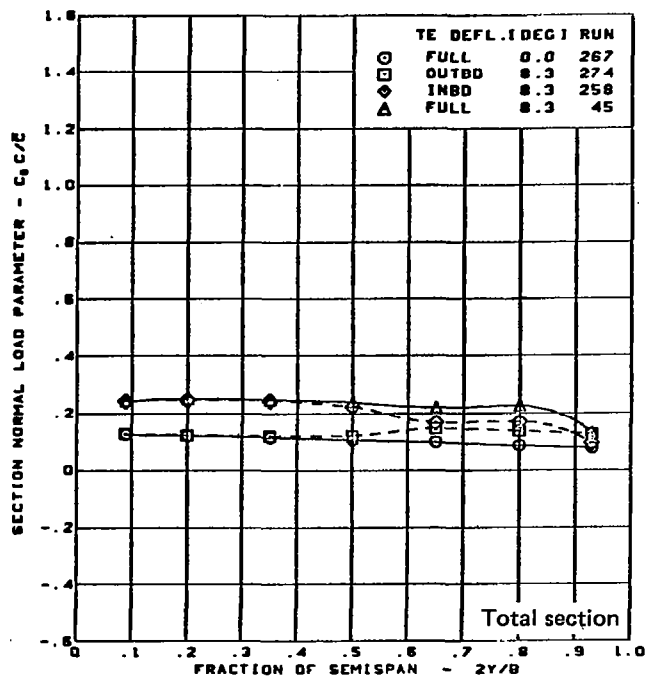
$M = 0.85$   
 $\alpha = 0^\circ$

Flat wing, rounded L.E.  
 L.E. deflection, full span =  $0.0^\circ$

(c) Spanload Distributions - Normal Force,  $\alpha = 0^\circ$

Figure 32. - (Continued)



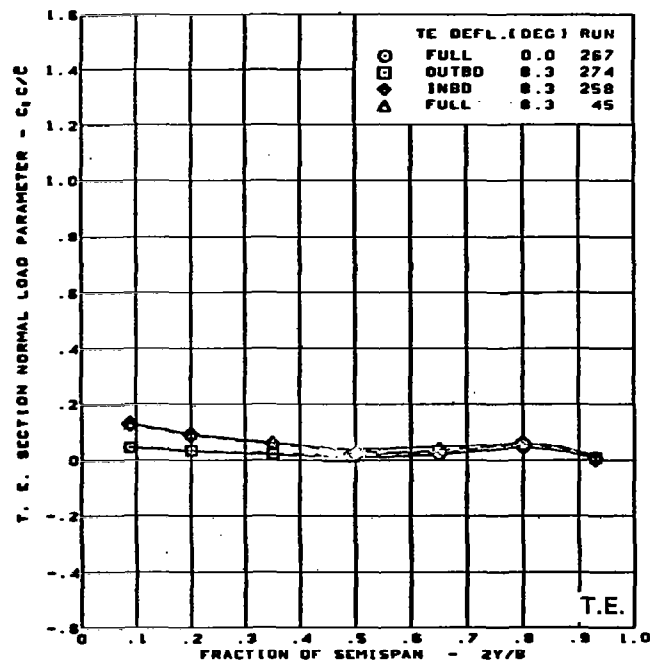
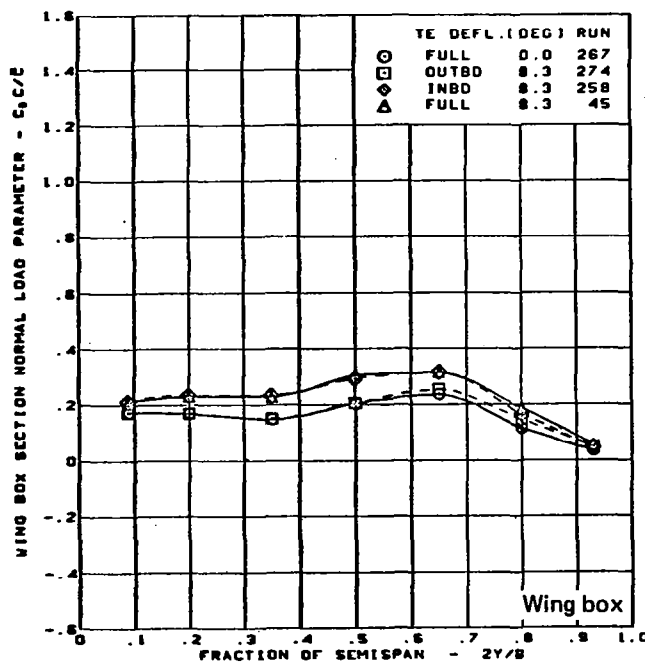
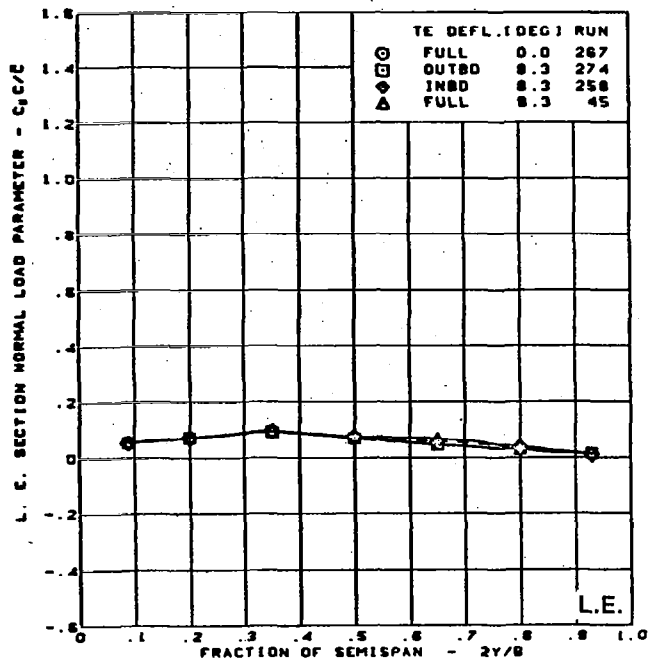
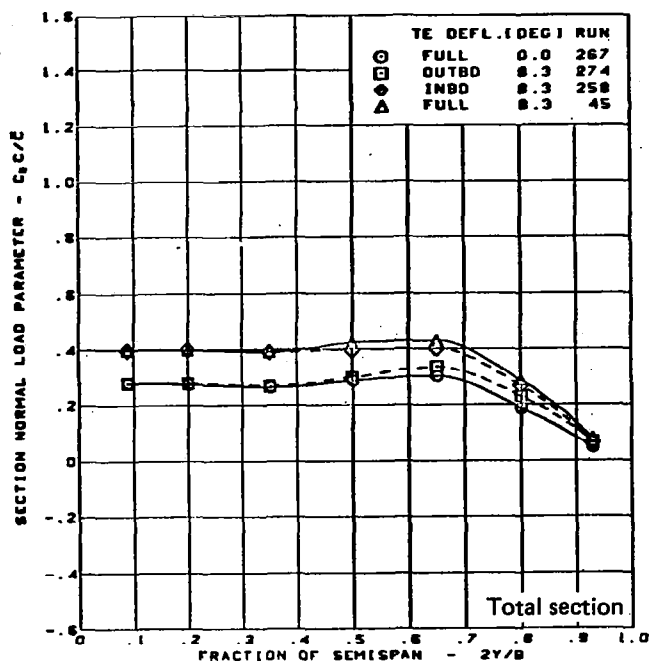


$M = 0.85$   
 $\alpha = 4^\circ$

Flat wing, rounded L.E.  
 L.E. deflection, full span =  $0.0^\circ$

(d) Spanload Distributions - Normal Force,  $\alpha = 4^\circ$

Figure 32. - (Continued)

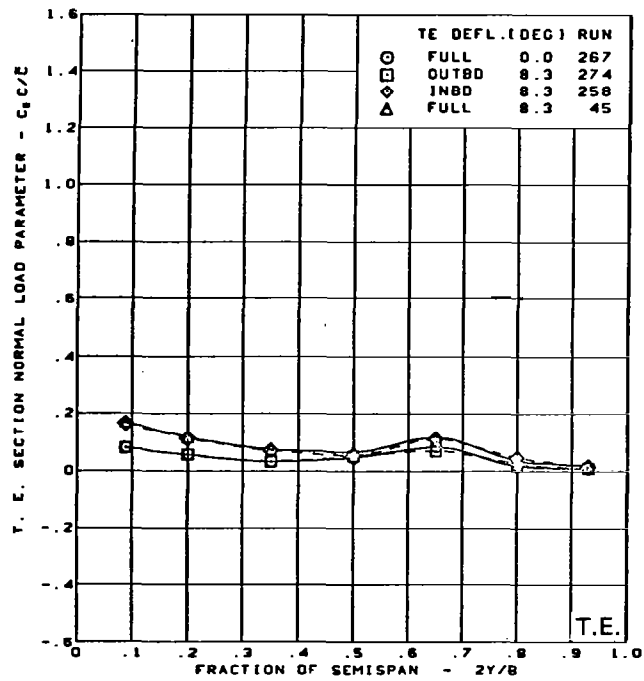
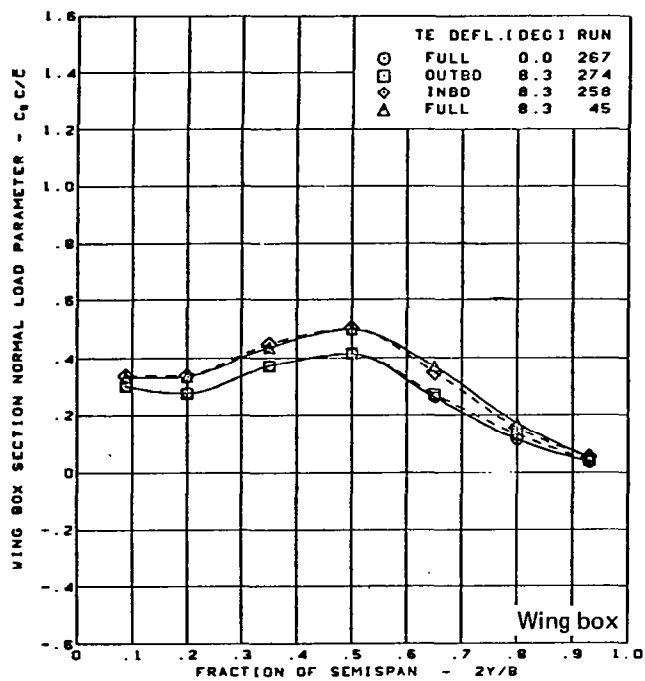
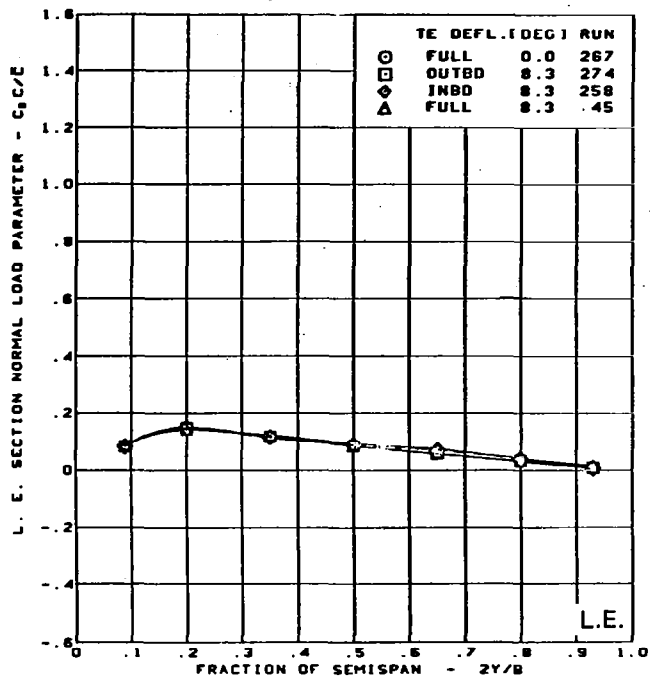
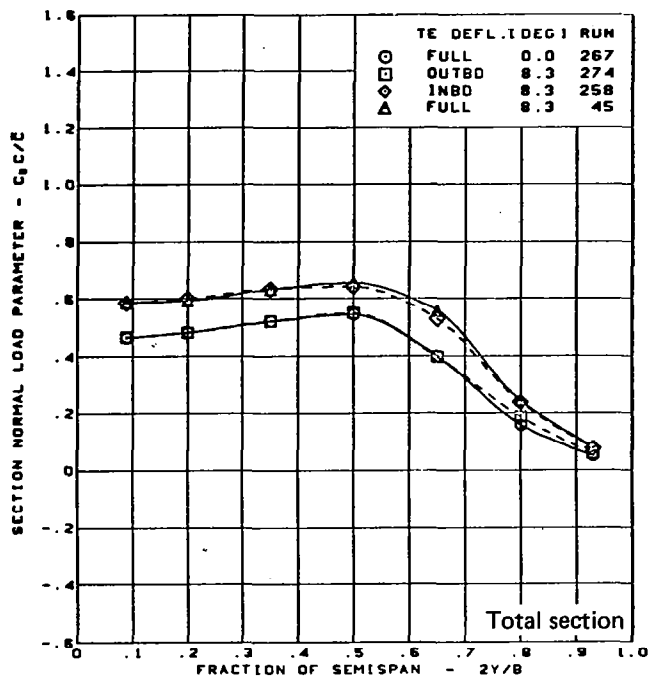


$M = 0.85$   
 $\alpha = 8^\circ$

Flat wing, rounded L.E.  
 L.E. deflection, full span =  $0.0^\circ$

(e) Spanload Distributions - Normal Force,  $\alpha = 8^\circ$

Figure 32. - (Continued)

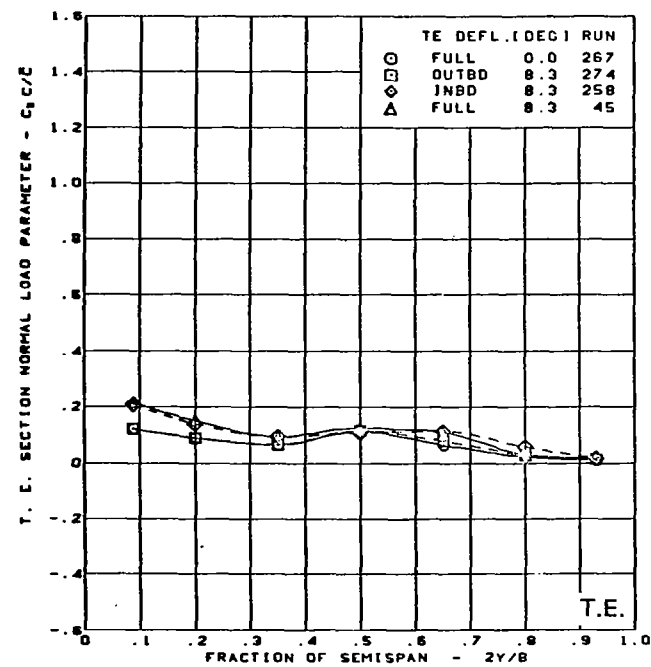
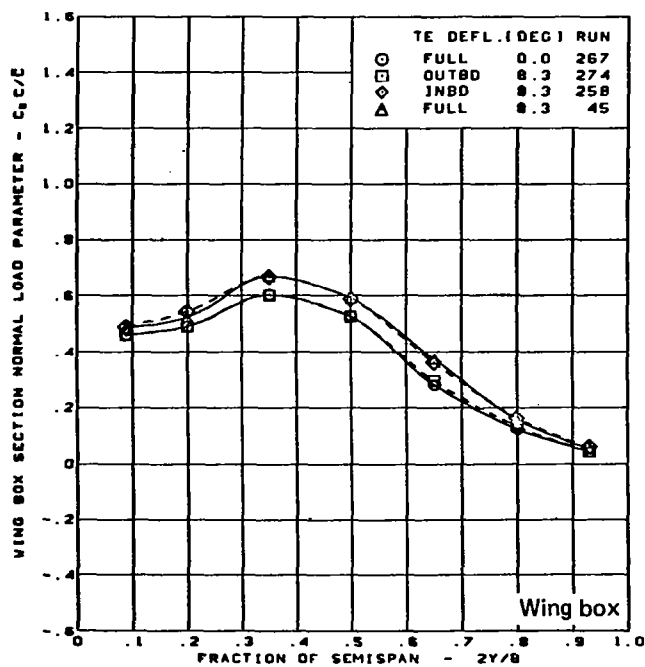
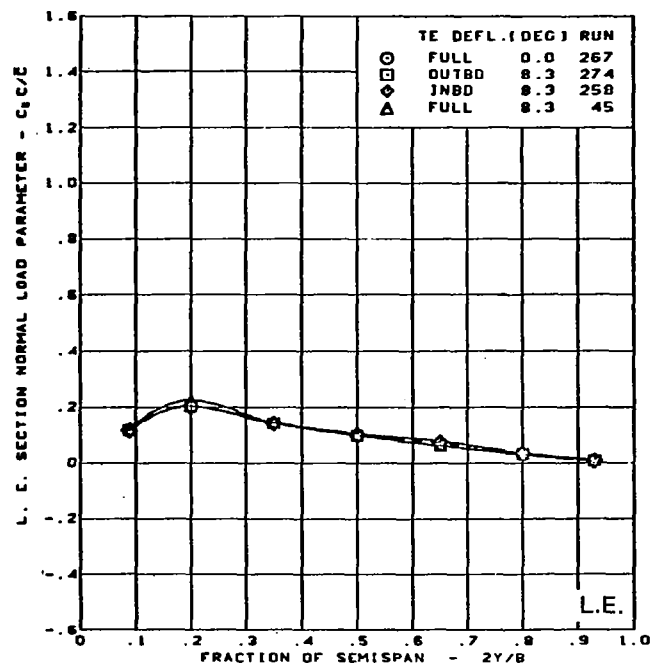
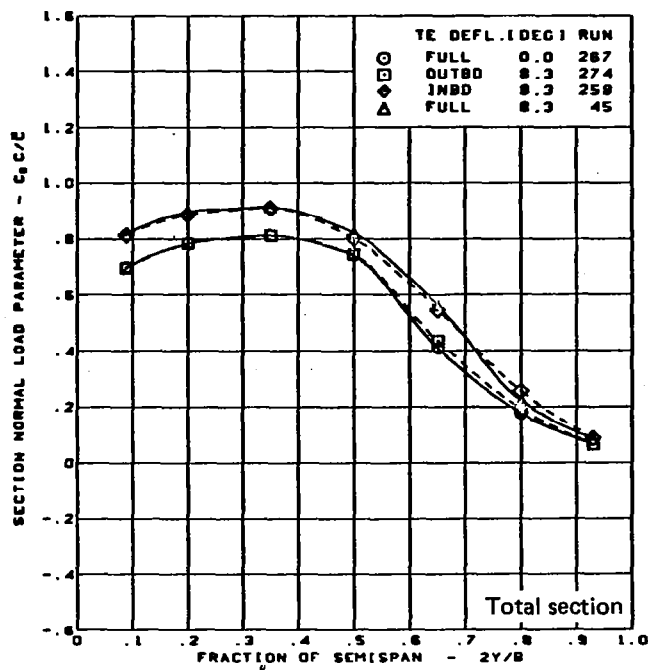


$M = 0.85$   
 $\alpha = 12^\circ$

Flat wing, rounded L.E.  
 L.E. deflection, full span =  $0.0^\circ$

(f) Spanload Distributions - Normal Force,  $\alpha = 12^\circ$

Figure 32. - (Continued)

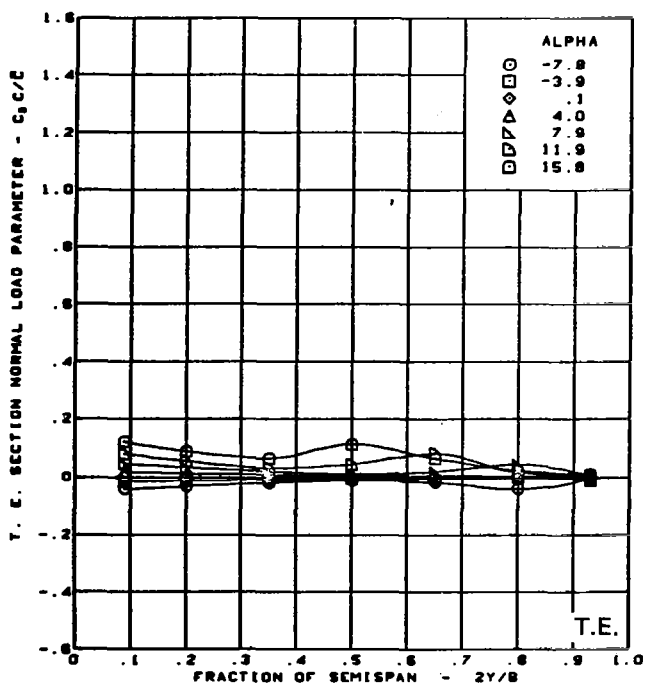
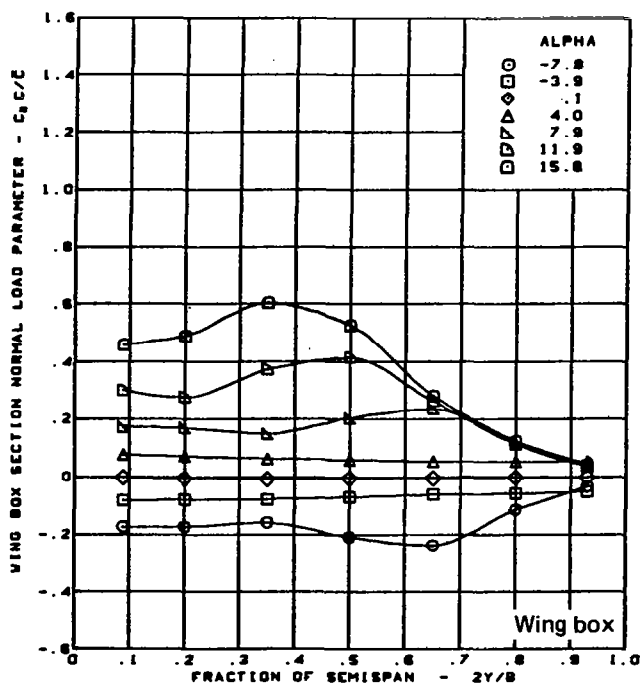
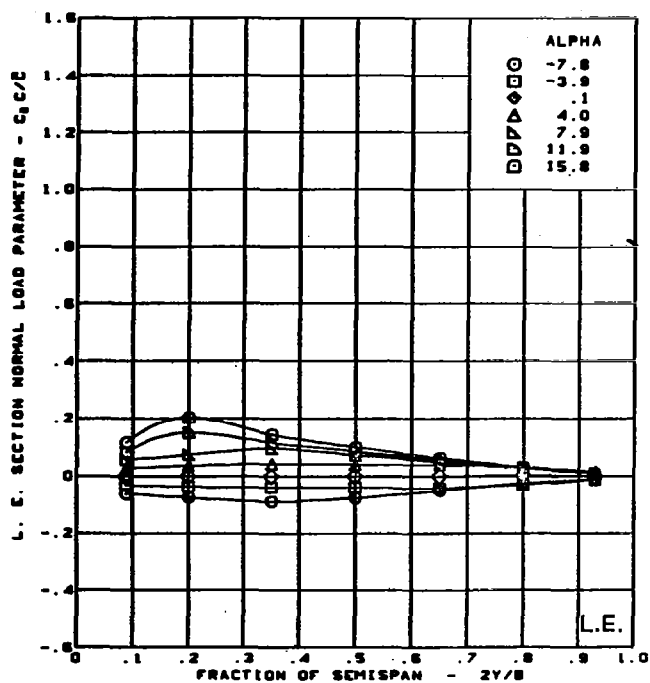
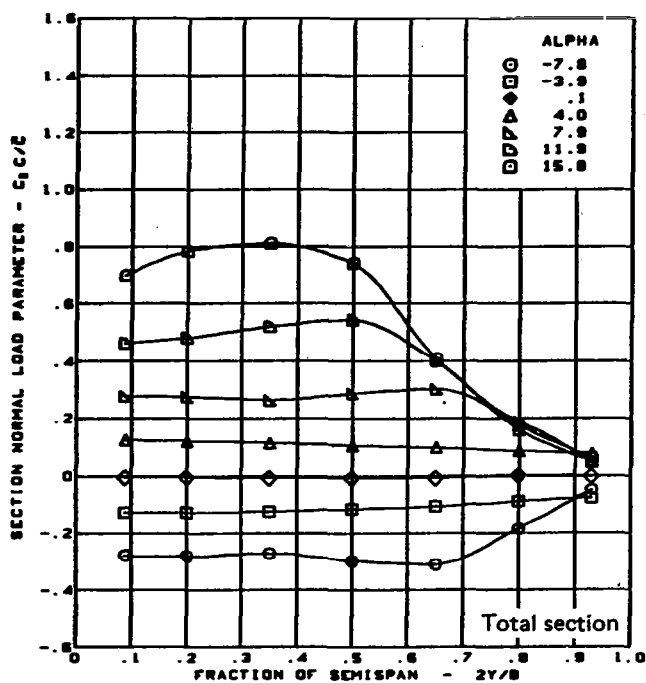


$M = 0.85$   
 $\alpha = 16^\circ$

Flat wing, rounded L.E.  
 L.E. deflection, full span =  $0.0^\circ$

(g) Spanload Distributions - Normal Force,  $\alpha = 16^\circ$

Figure 32. - (Continued)

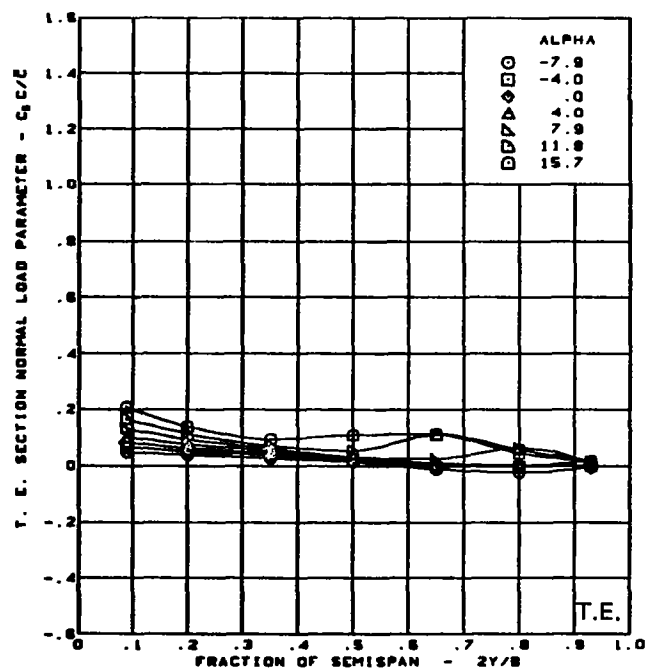
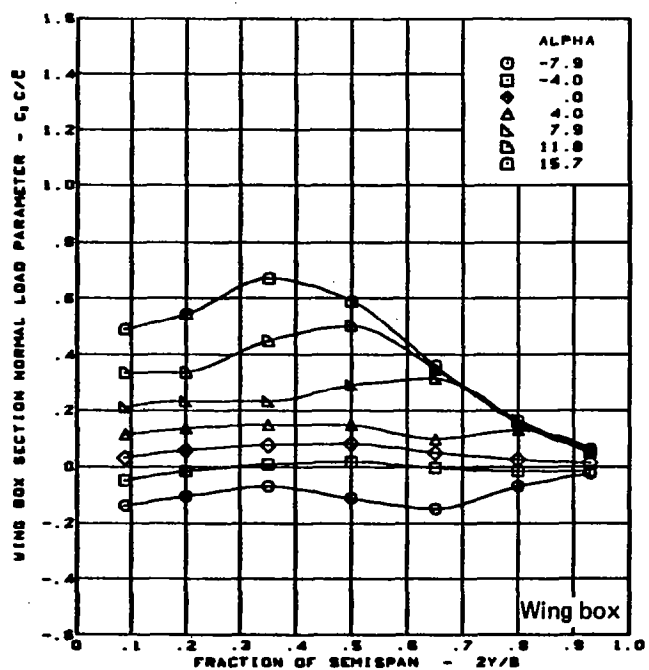
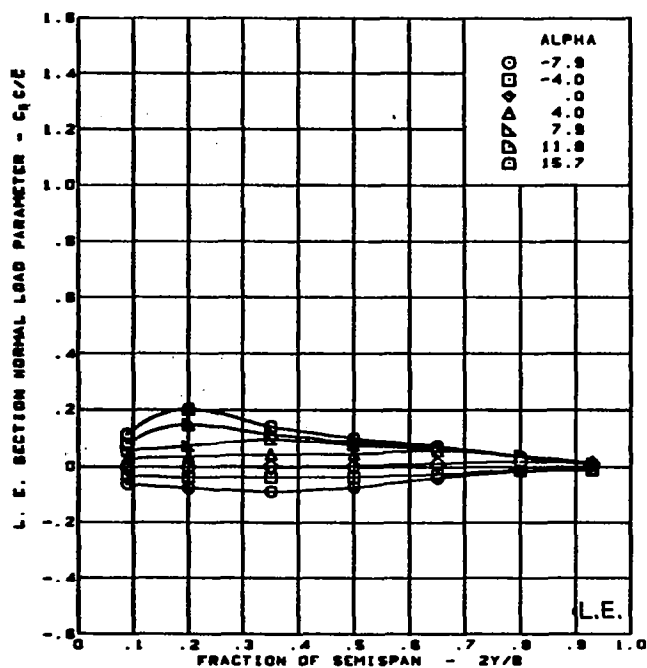
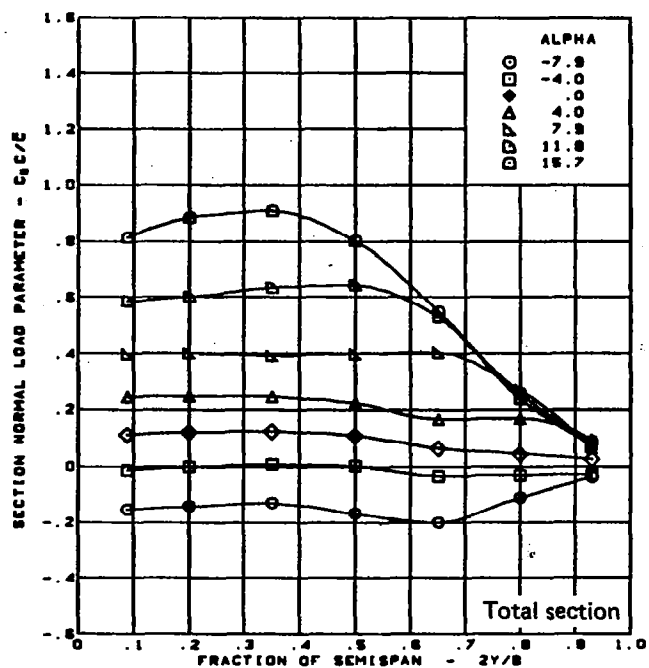


$M = 0.85$   
Flat wing, rounded L.E.

L.E. deflection, full span =  $0.0^\circ$   
T.E. deflection, full span =  $0.0^\circ$

(h) Spanload Distributions - Normal Force, T.E. Deflection, Full Span =  $0.0^\circ$

Figure 32. — (Continued)

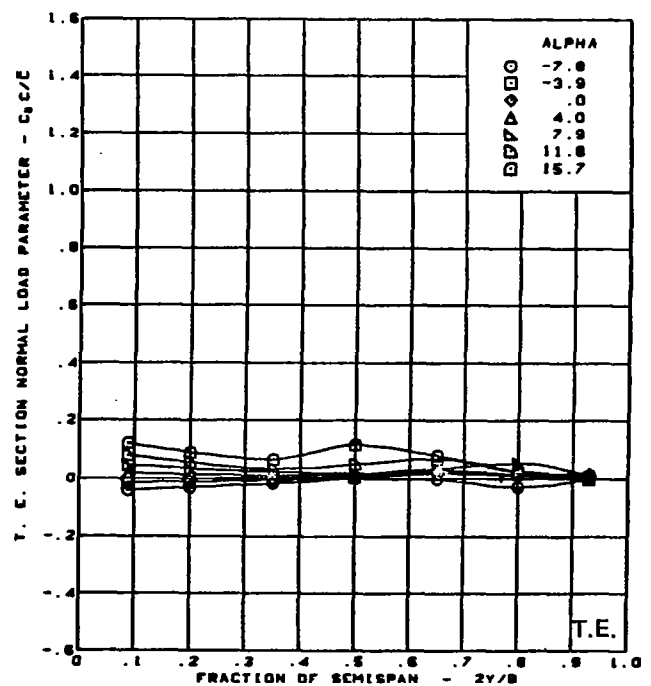
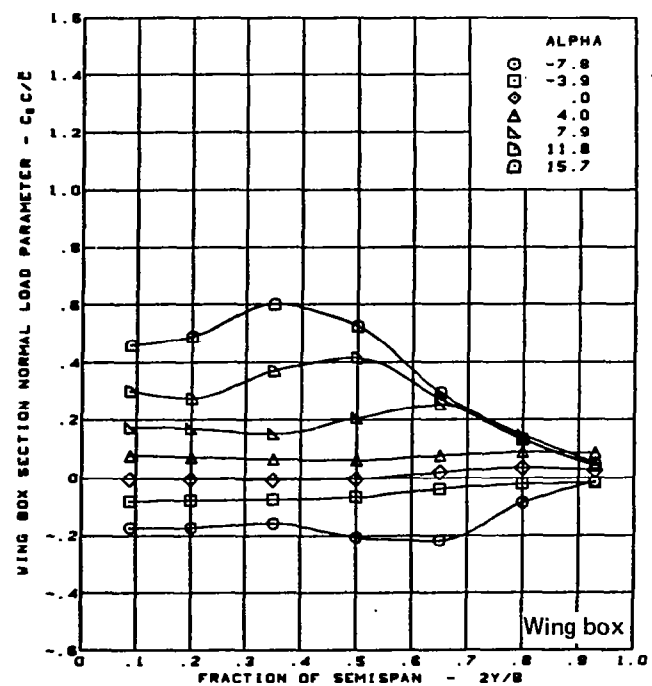
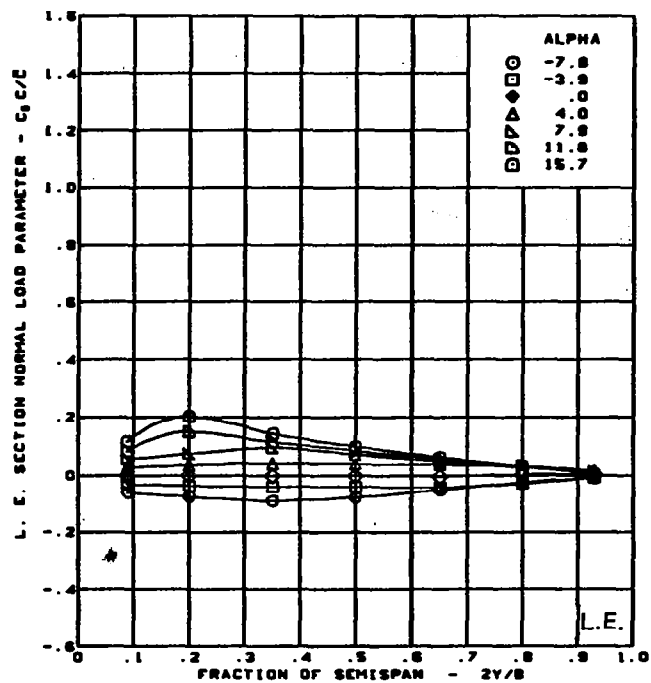
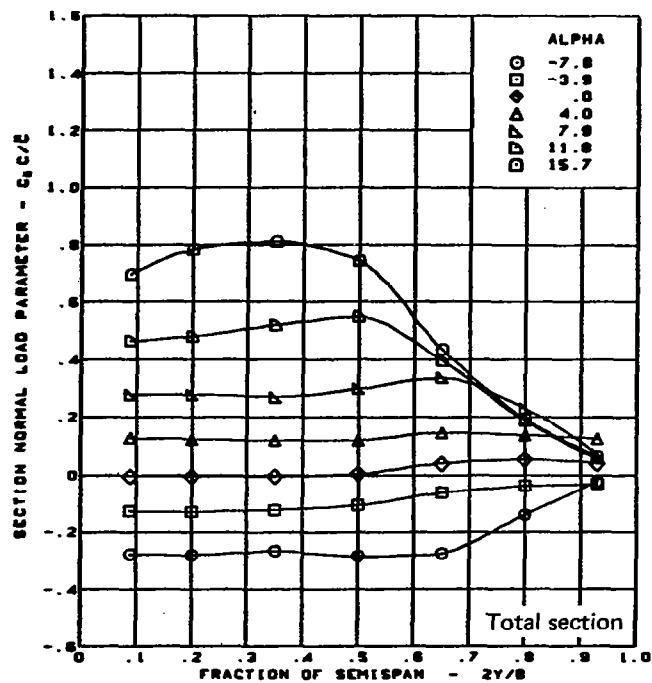


$M = 0.85$   
Flat wing, rounded L.E.

L.E. deflection, full span =  $0.0^\circ$   
T.E. deflection, inboard =  $8.3^\circ$ , outboard =  $0.0^\circ$

(i) Spanload Distributions - Normal Force, T.E. Deflection, Inboard =  $8.3^\circ$ , Outboard =  $0.0^\circ$

Figure 32. - (Continued)

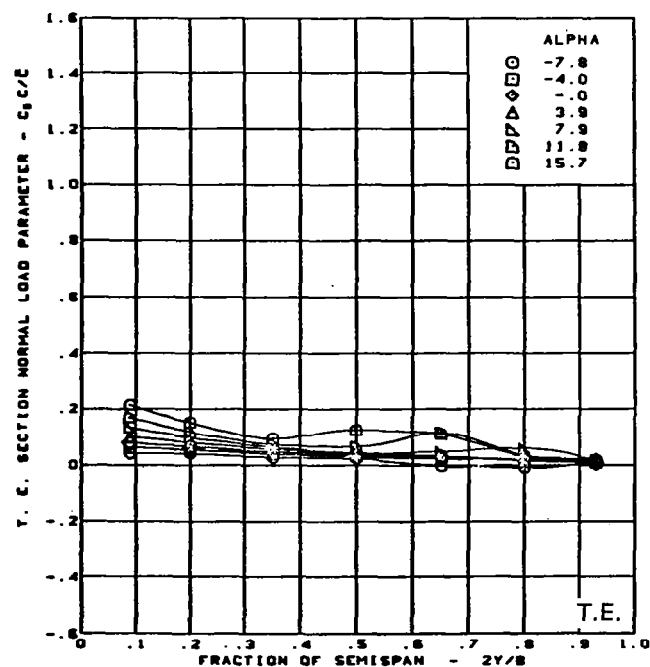
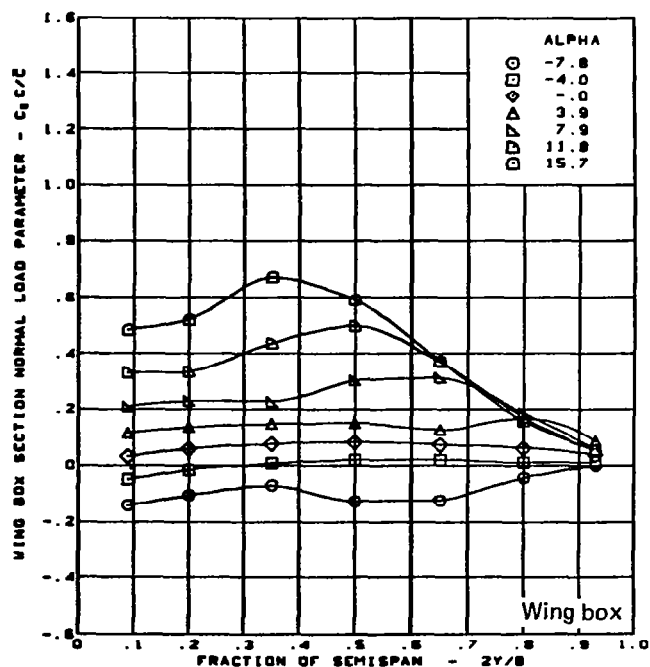
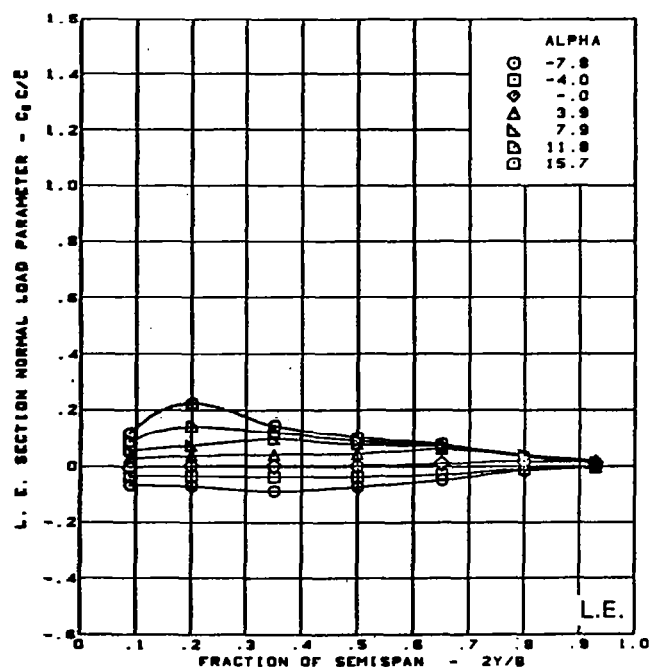
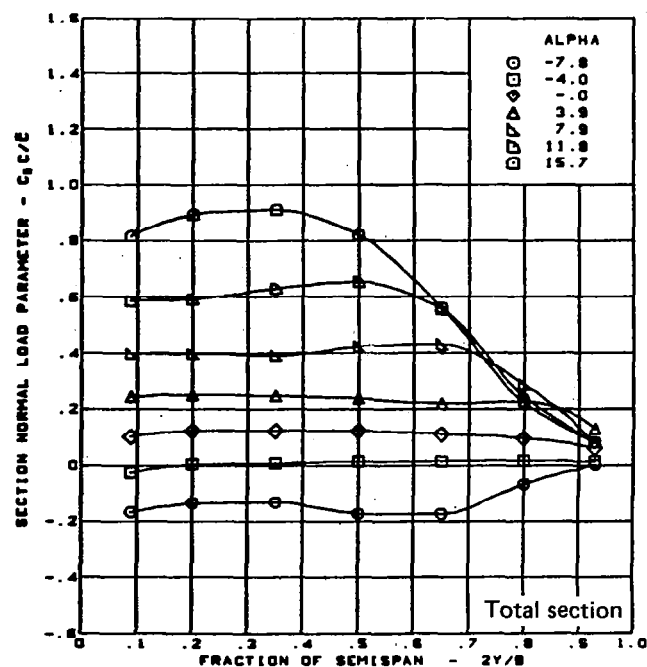


$M = 0.85$   
Flat wing, rounded L.E.

L.E. deflection, full span =  $0.0^\circ$   
T.E. deflection, inboard =  $0.0^\circ$ , outboard =  $8.3^\circ$

(i) Spanload Distributions - Normal Force, T.E. Deflection, Inboard =  $0.0^\circ$ , Outboard =  $8.3^\circ$

Figure 32. - (Continued)



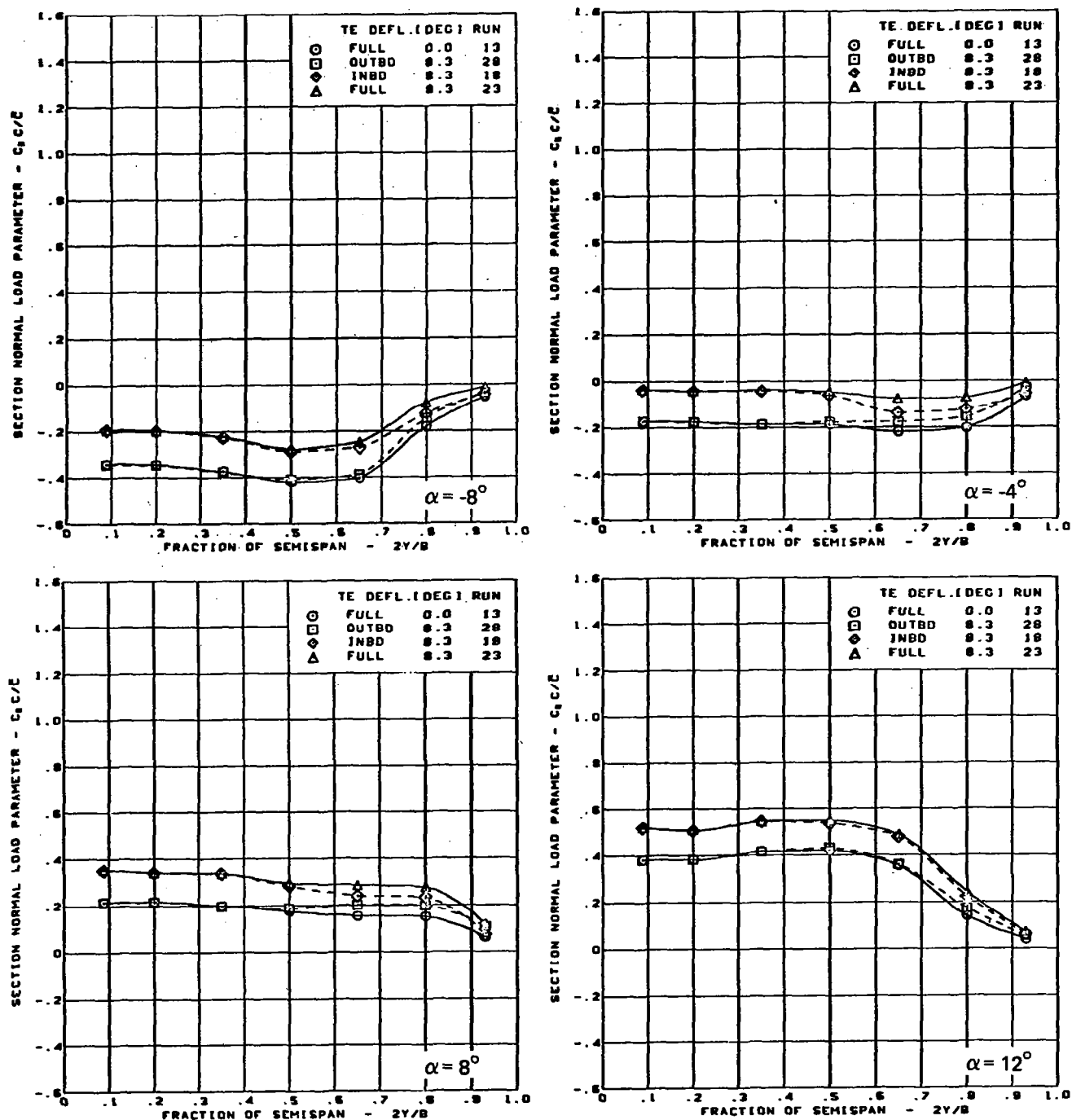
$M = 0.85$   
Flat wing, rounded L.E.

L.E. deflection, full span =  $0.0^\circ$   
T.E. deflection, full span =  $8.3^\circ$

(k) Spanload Distributions - Normal Force, T.E. Deflection, Full Span =  $8.3^\circ$

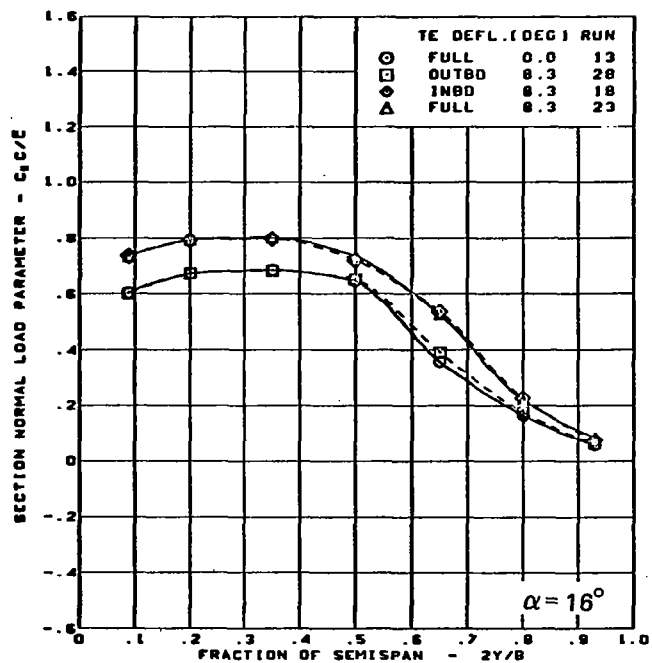
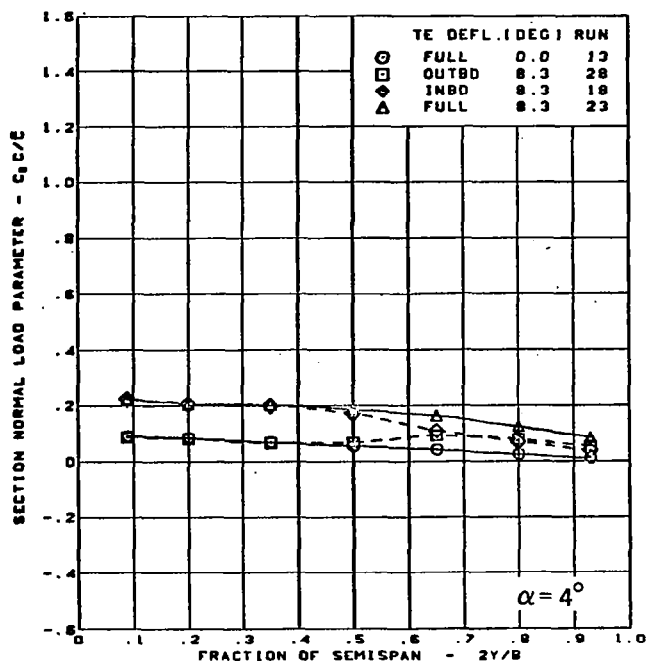
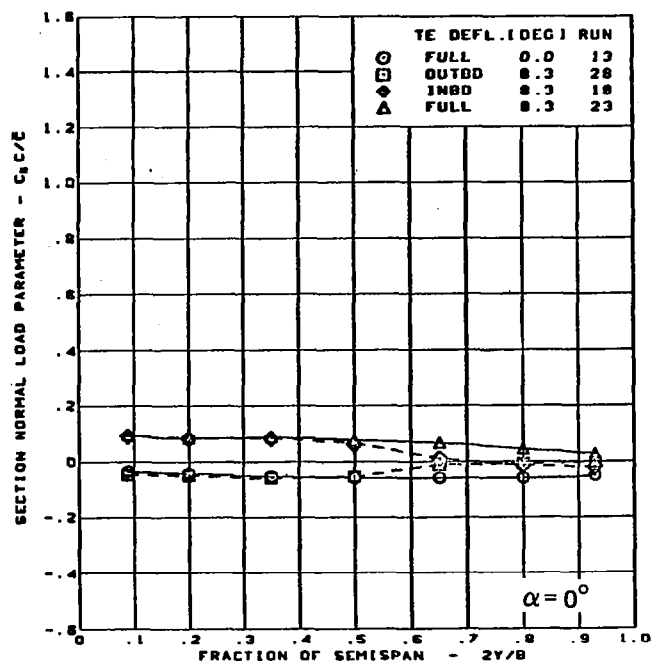
Figure 32. — (Concluded)





(a) Spanload Distribution - Normal Force Variation With T.E. Control Surface Configuration

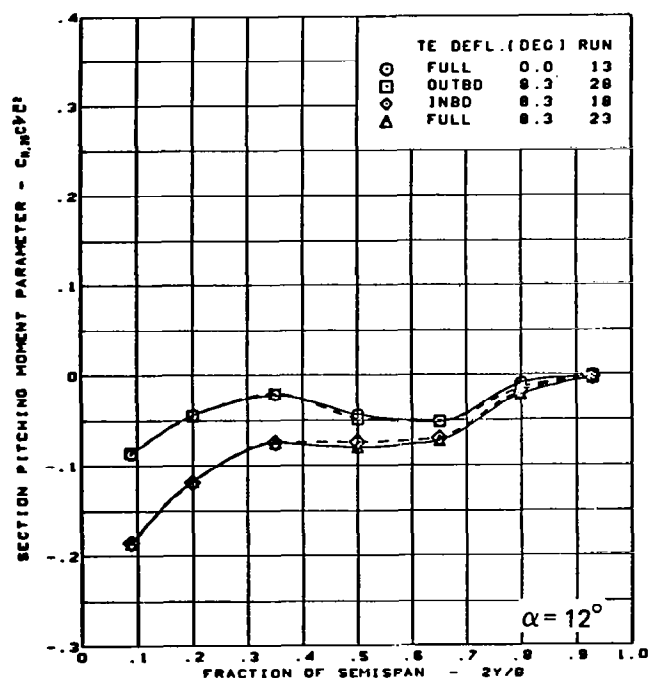
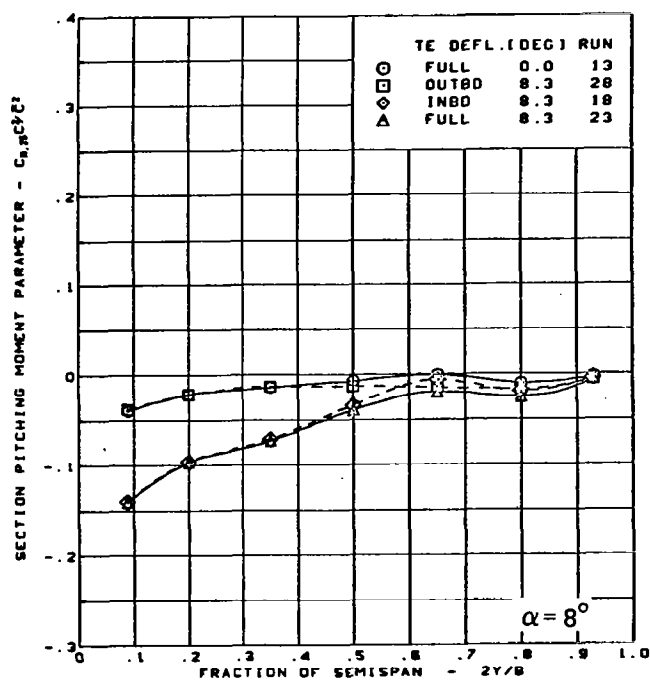
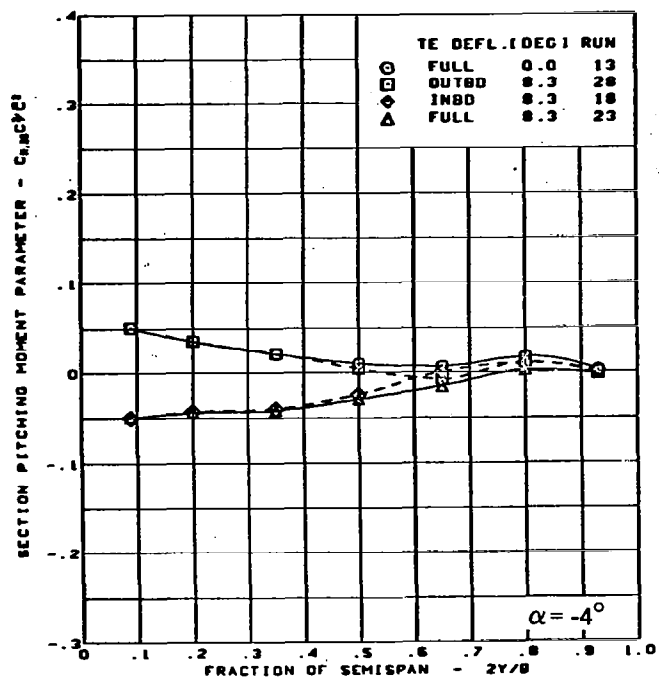
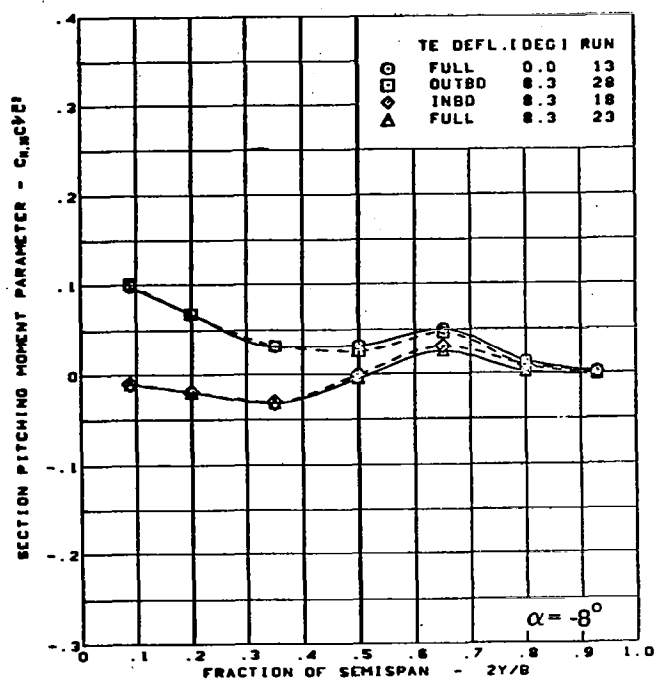
Figure 33. — Wing Experimental Data—Effect of Full- and Partial-Span Trailing Edge Control Surface Deflection; Twisted Wing;  $M = 0.85$



$M = 0.85$   
 Twisted wing, rounded L.E.  
 L.E. deflection, full span =  $0.0^\circ$

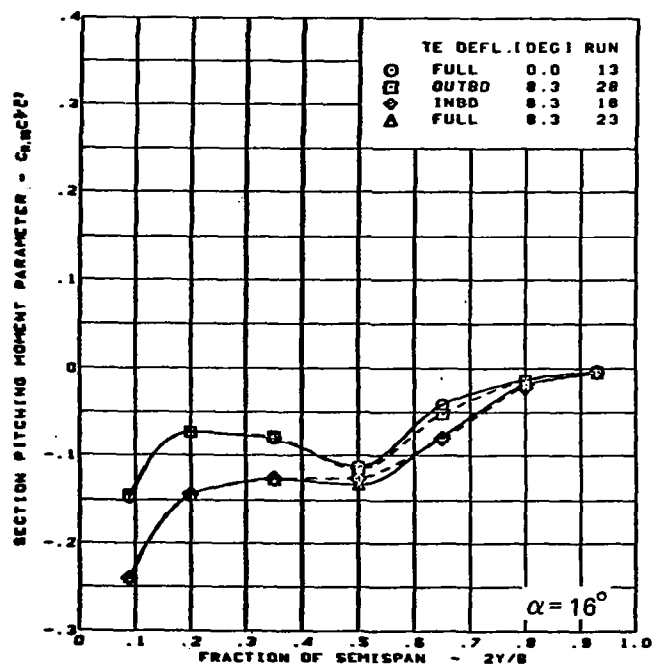
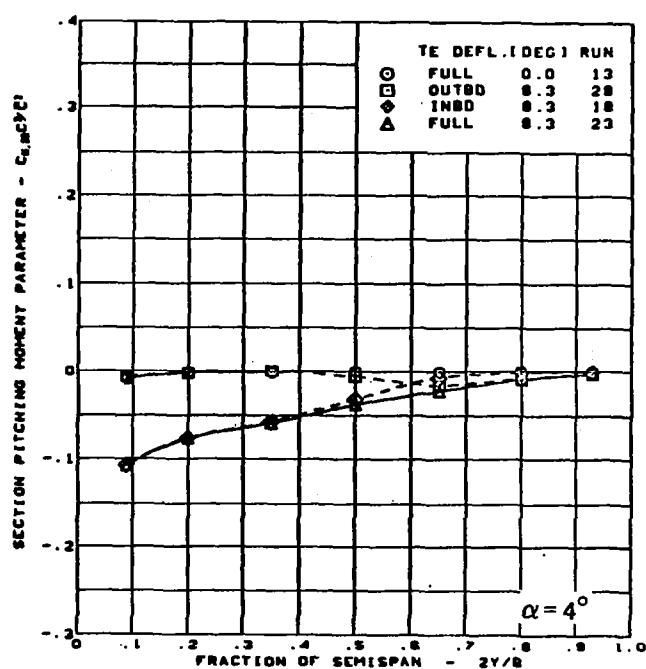
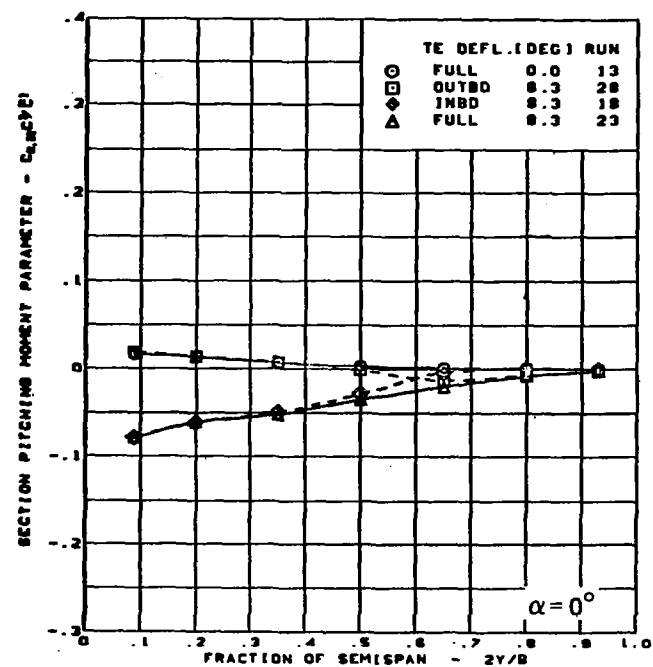
(a) (Concluded)

Figure 33. - (Continued)



(b) Spanload Distribution - Pitching Moment Variation With T.E. Control Surface Configuration

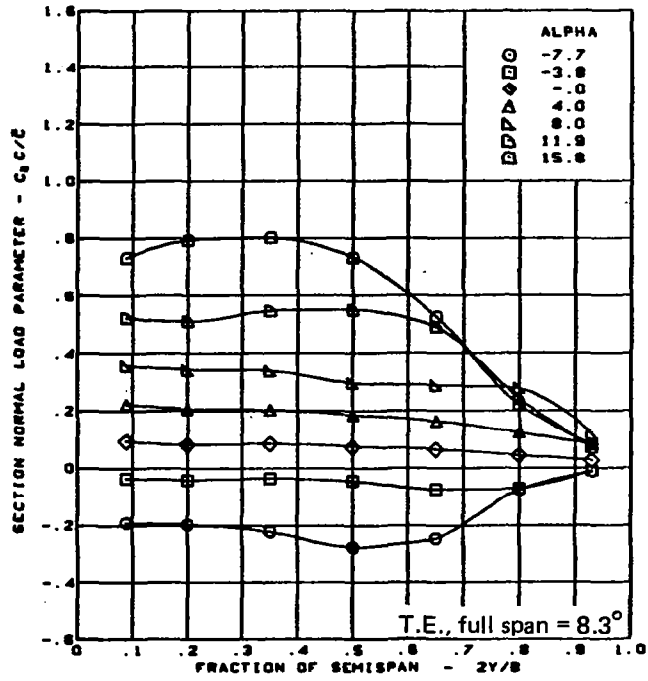
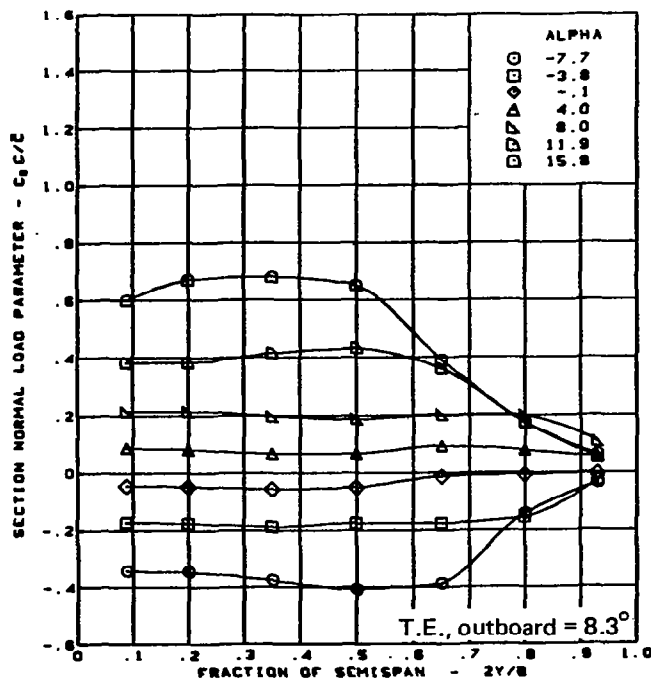
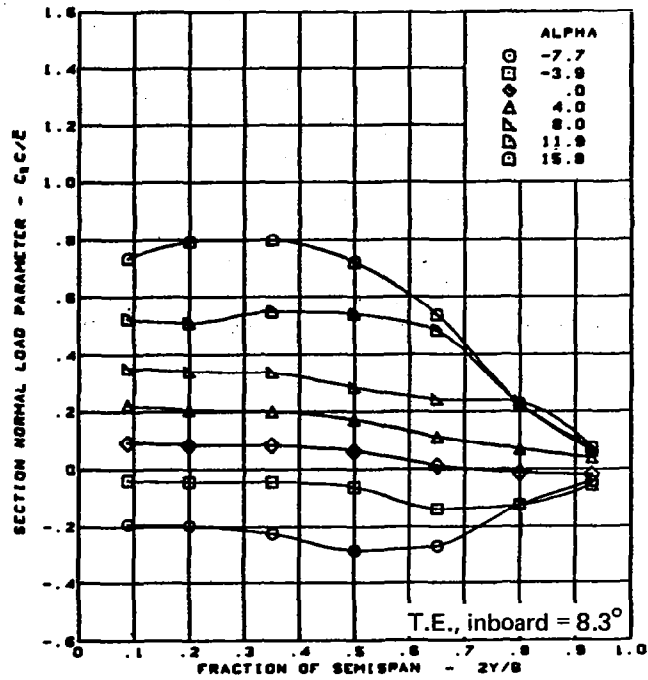
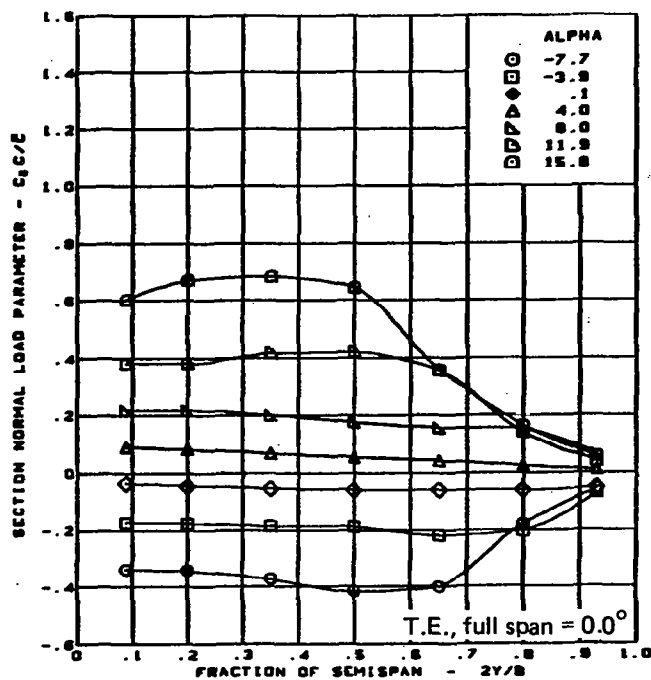
Figure 33. - (Continued)



$M = 0.85$   
 Twisted wing, rounded L.E.  
 L.E. deflection, full span =  $0.0^\circ$

(b) (Concluded)

Figure 33. - (Continued)



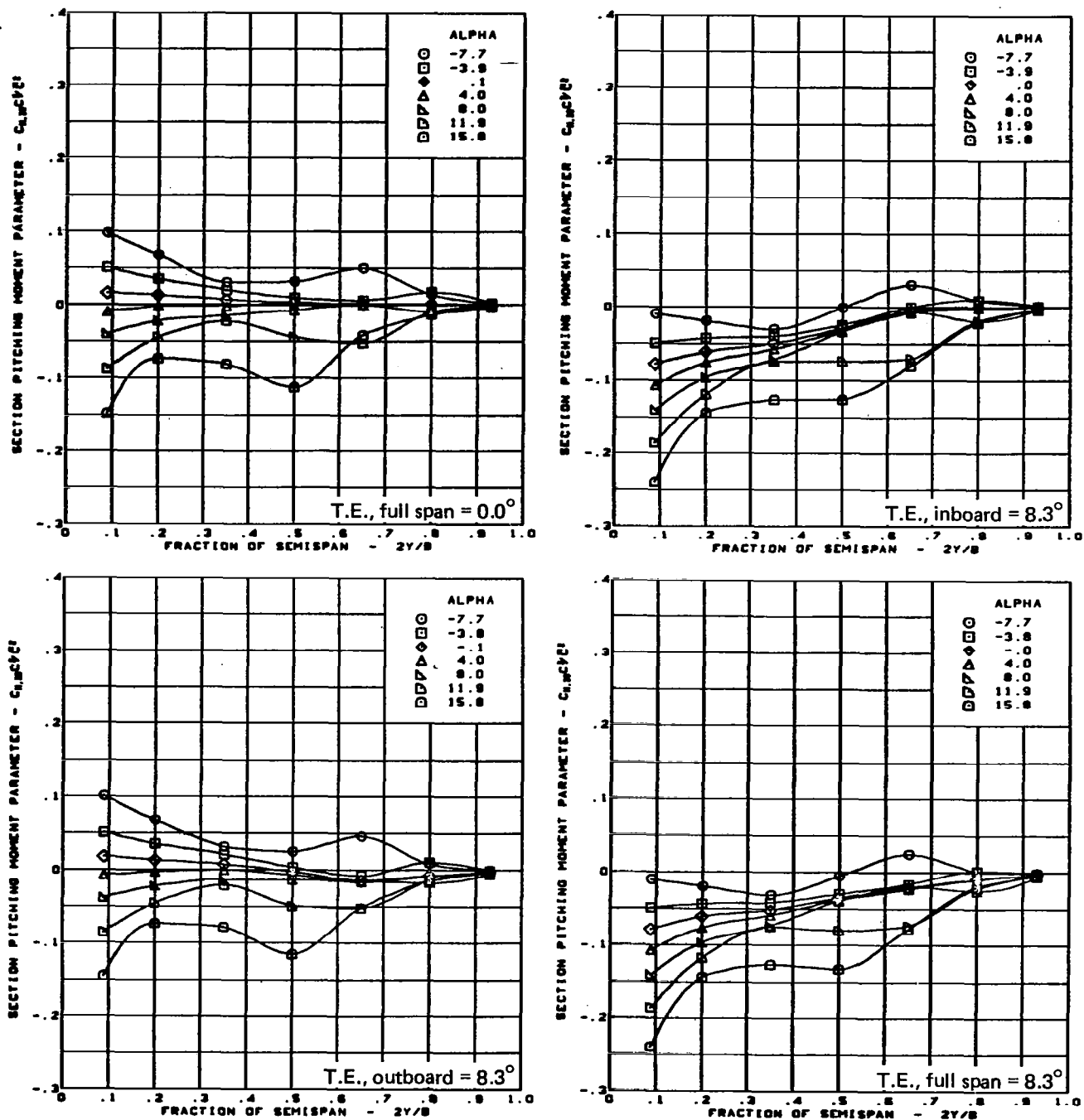
$M = 0.85$

Twisted wing, rounded L.E.

L.E. deflection, full span =  $0.0^\circ$

(c) Spanload Distribution - Normal Force Variation With Angle of Attack

Figure 33. - (Continued)



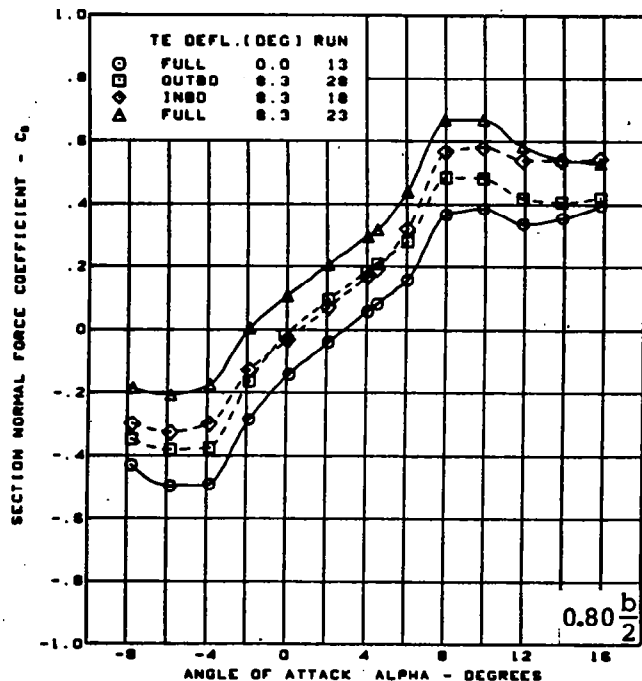
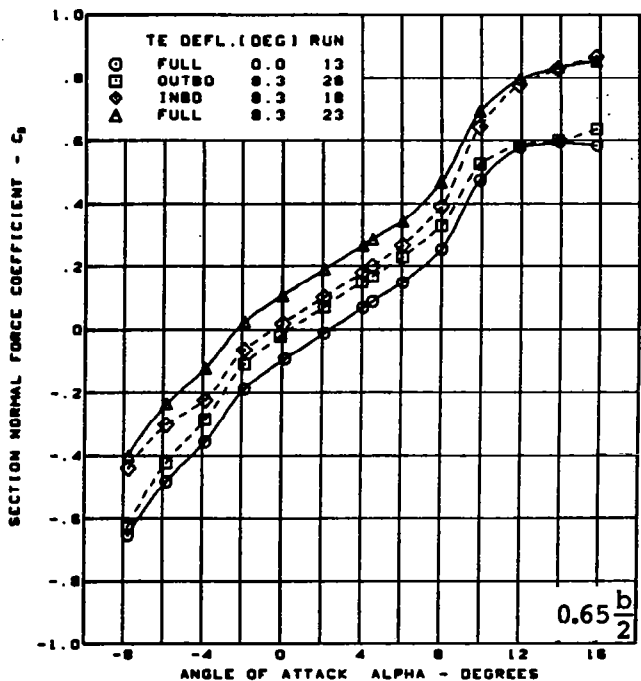
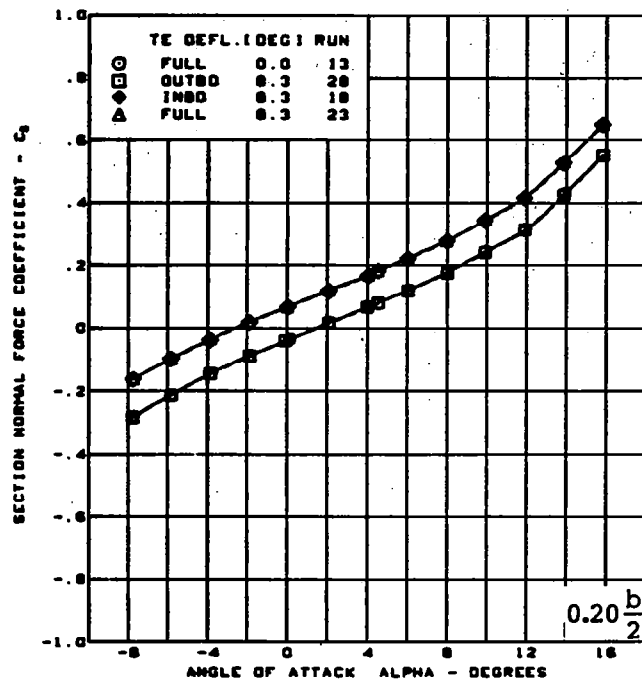
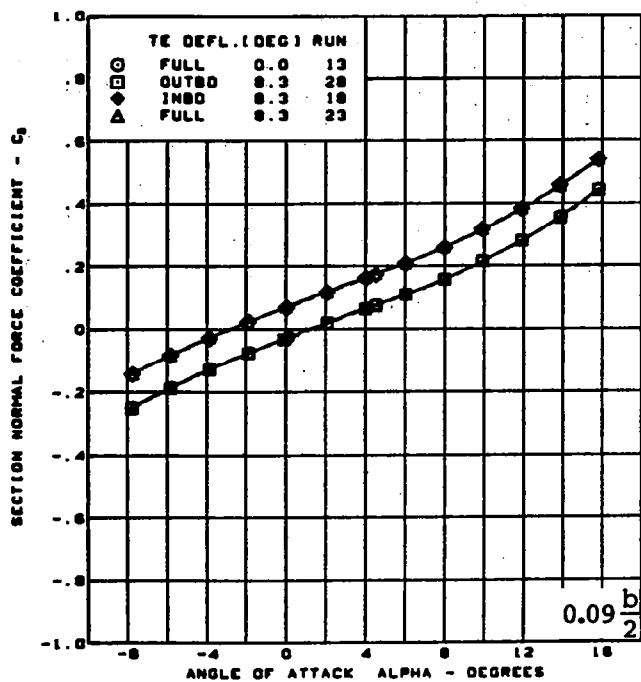
$M = 0.85$

Twisted wing, rounded L.E.

L.E. deflection, full span =  $0.0^\circ$

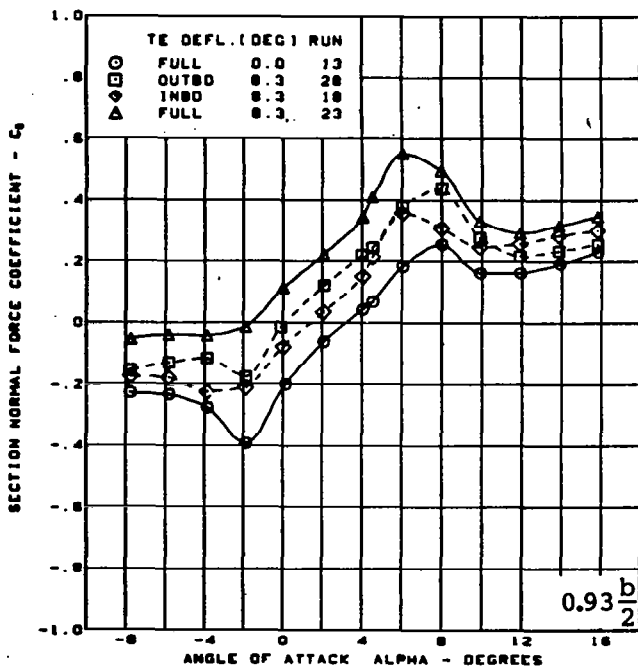
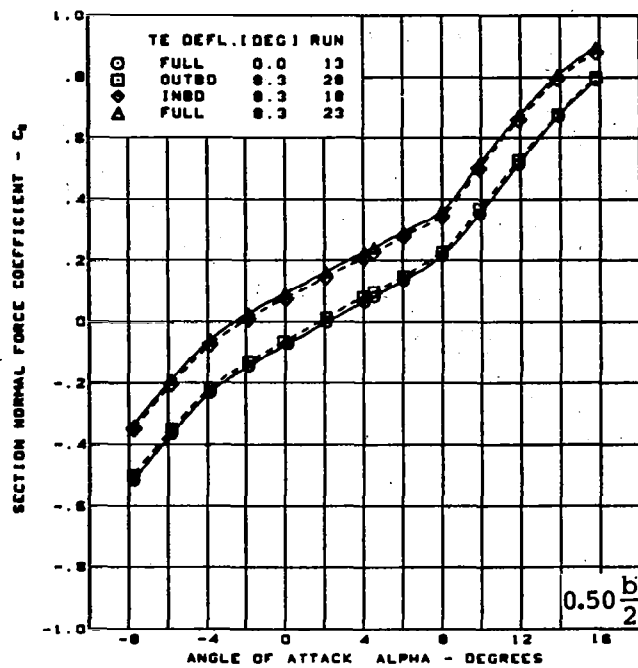
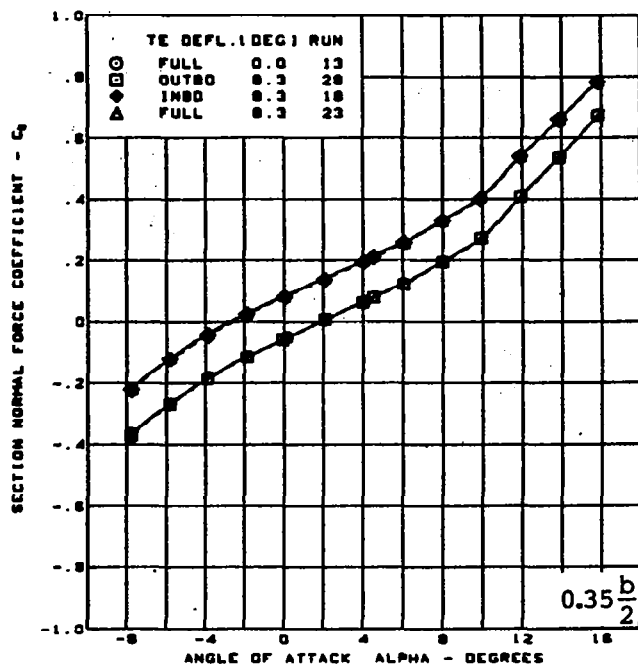
(d) Spanload Distribution - Pitching Moment Variation With Angle of Attack

Figure 33. — (Continued)



(a) Section Aerodynamic Coefficients - Normal Force

Figure 33. - (Continued)

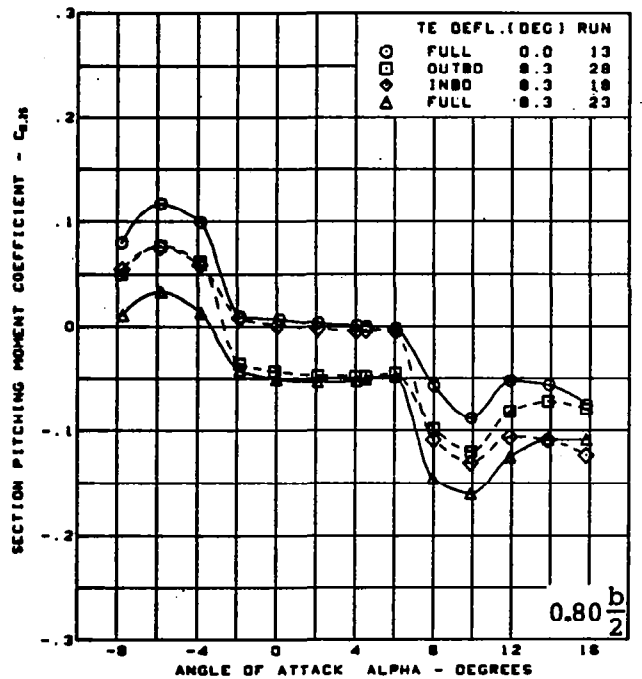
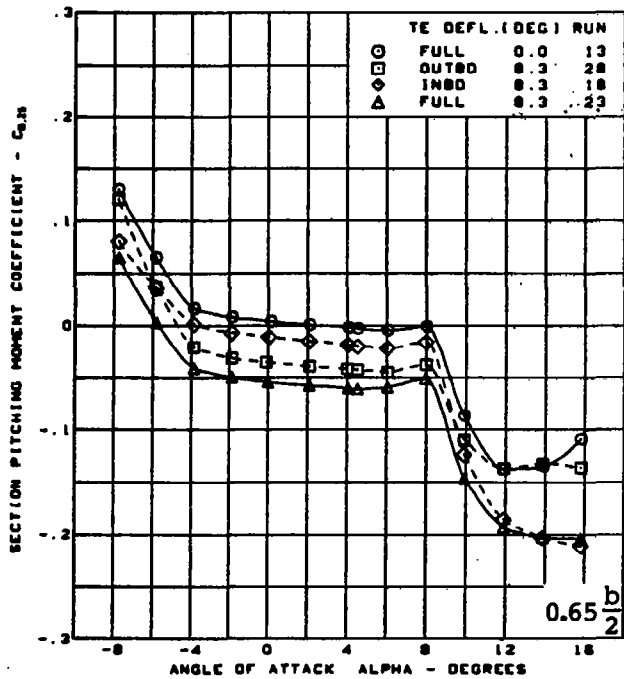
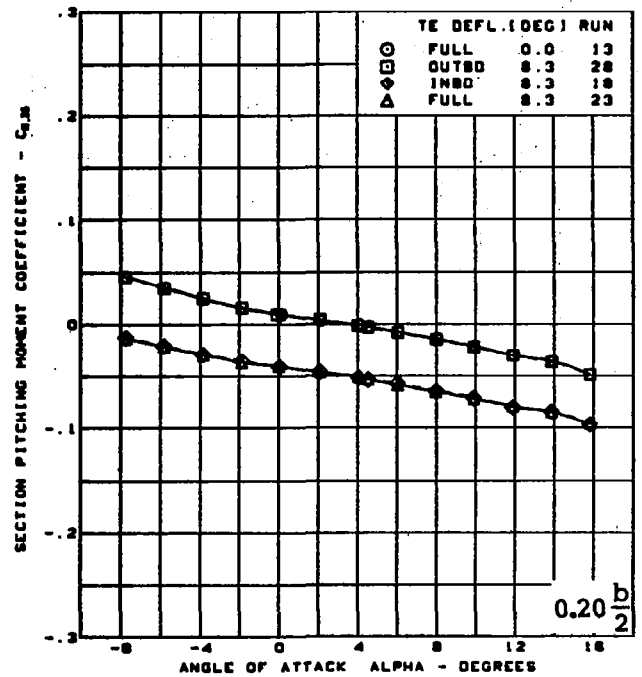
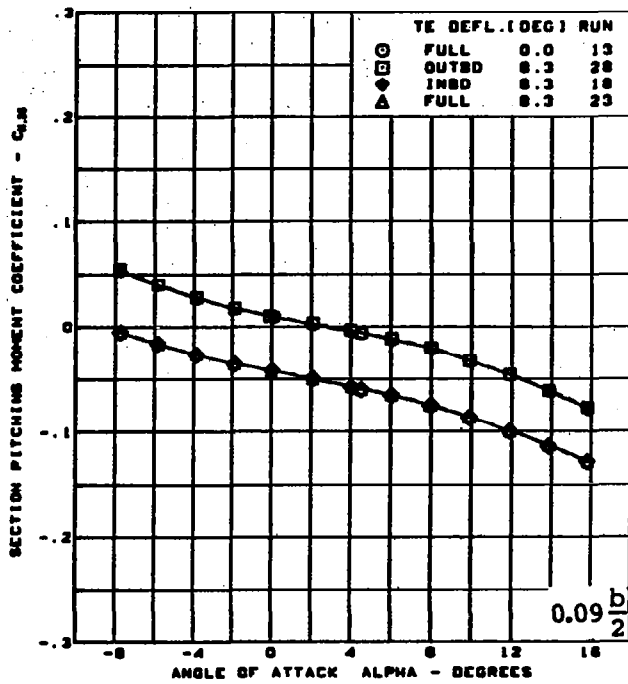


M = 0.85  
Twisted wing, rounded L.E.  
L.E. deflection, full span = 0.0°

(e) (Concluded)

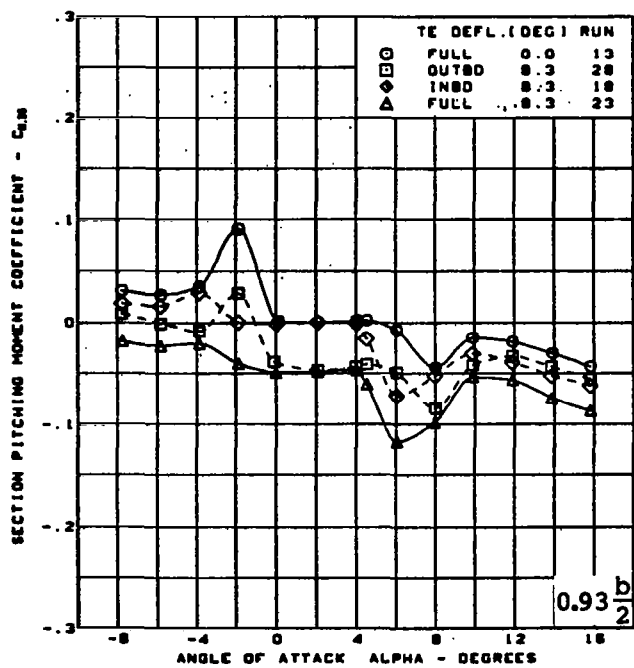
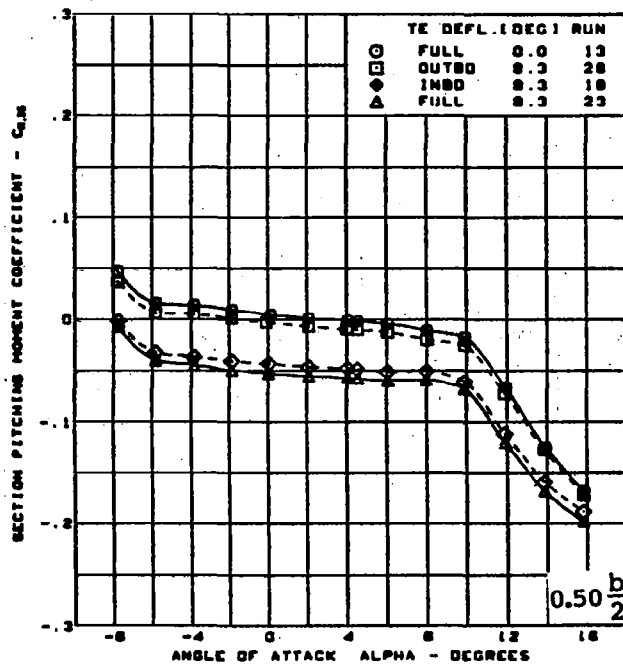
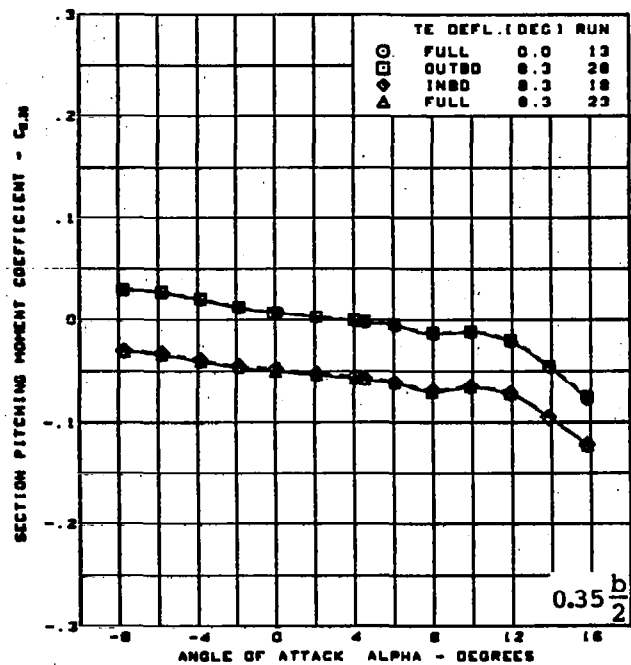
Figure 33. - (Continued)





(f) Section Aerodynamic Coefficients - Pitching Moment

Figure 33. - (Continued)

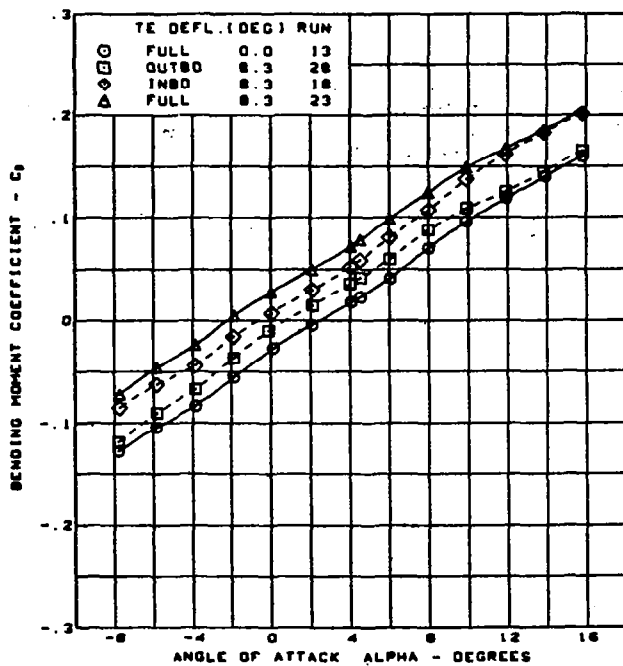
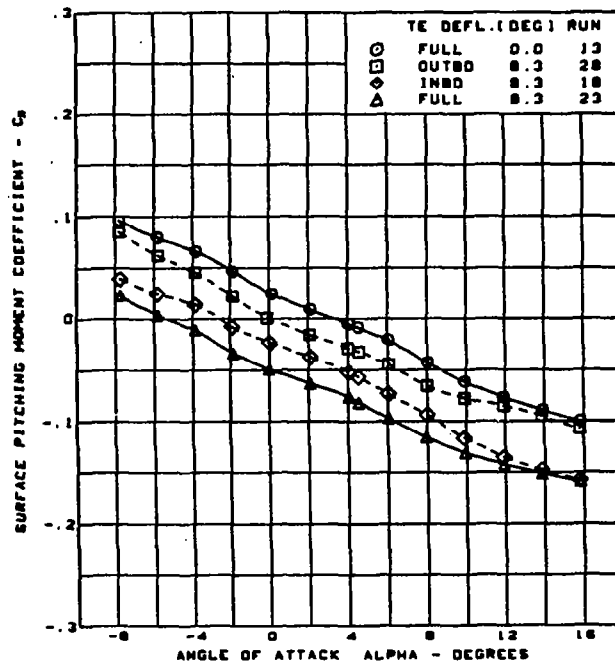
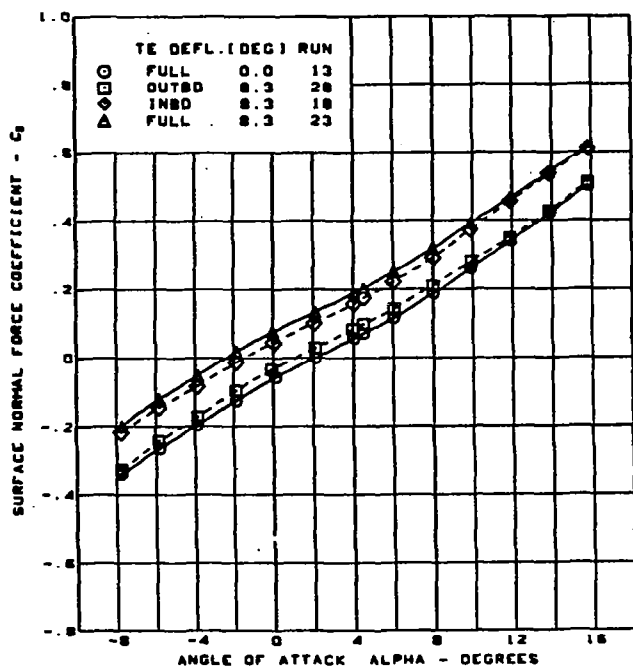


M = 0.85  
 Twisted wing, rounded L.E.  
 L.E. deflection, full span = 0.0°

(f) (Concluded)

Figure 33. - (Continued)



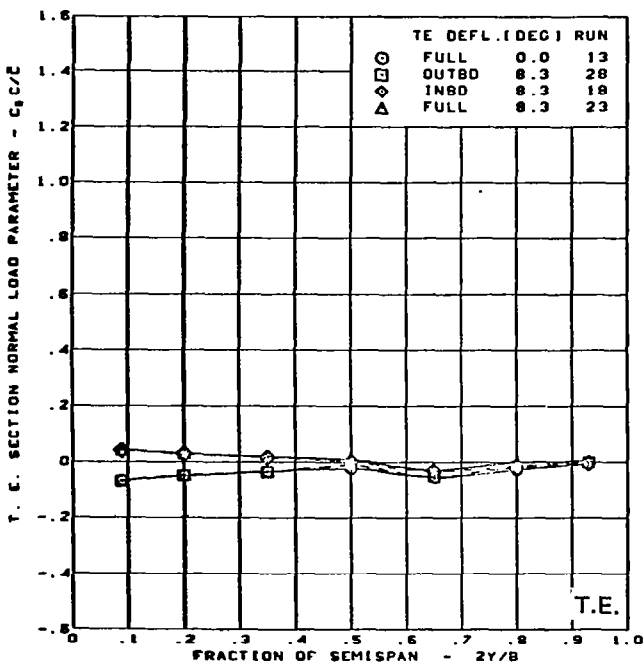
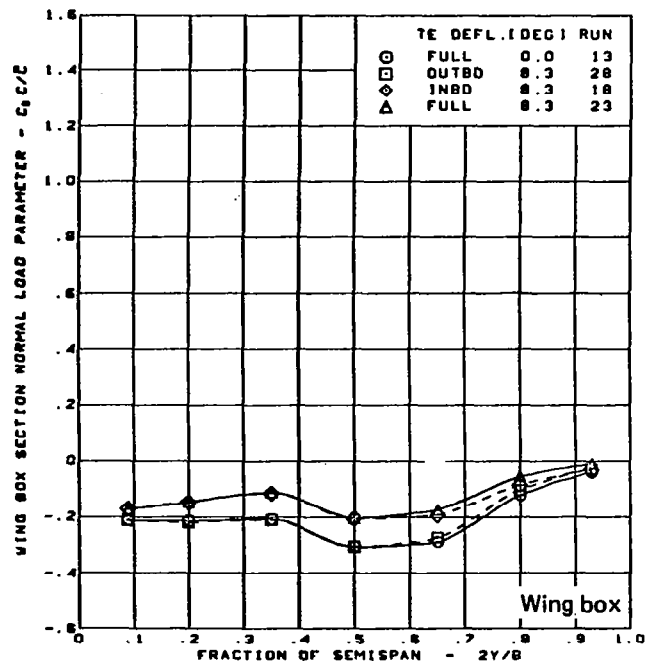
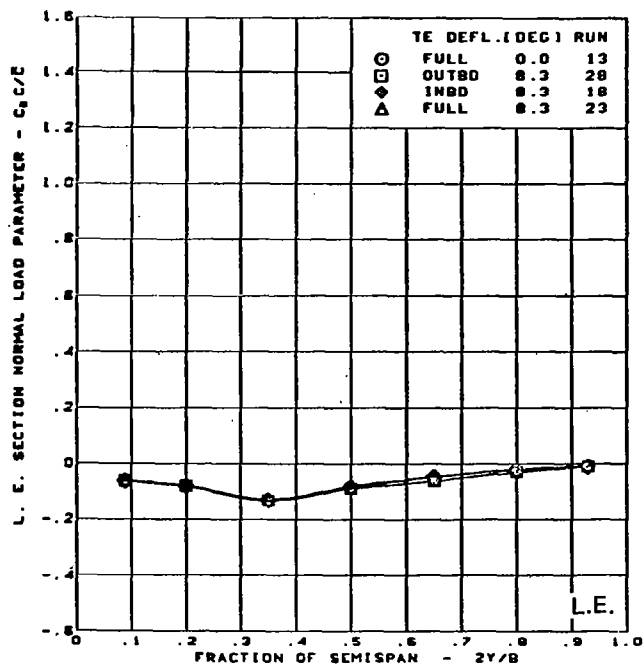
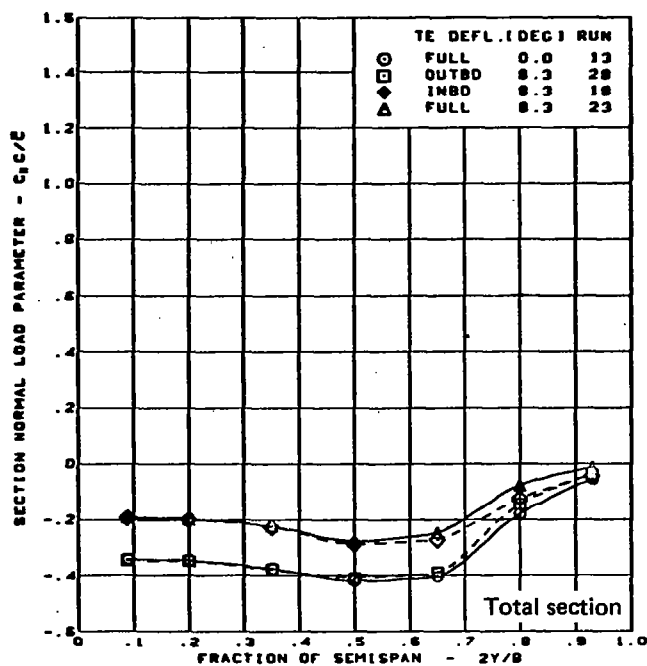


$M = 0.85$   
 Twisted wing, rounded L.E.  
 L.E. deflection, full span =  $0.0^\circ$

(g) Wing Aerodynamic Coefficients

Figure 33. — (Concluded)



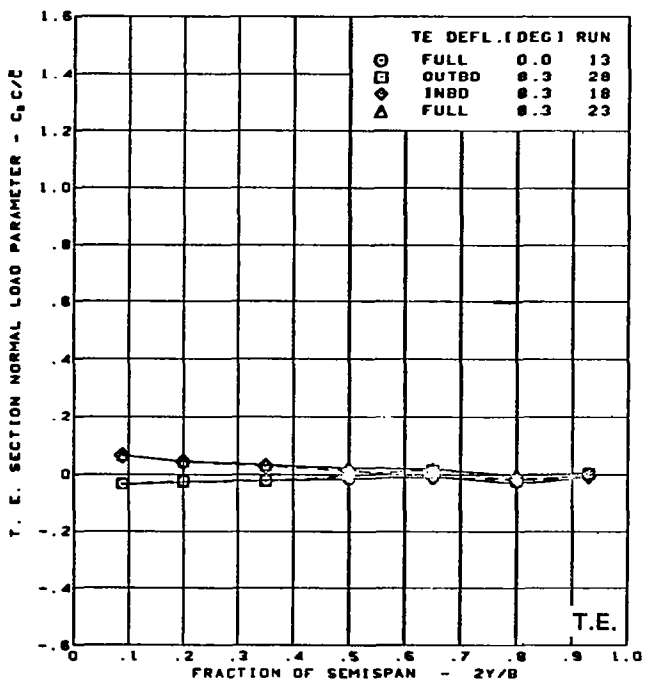
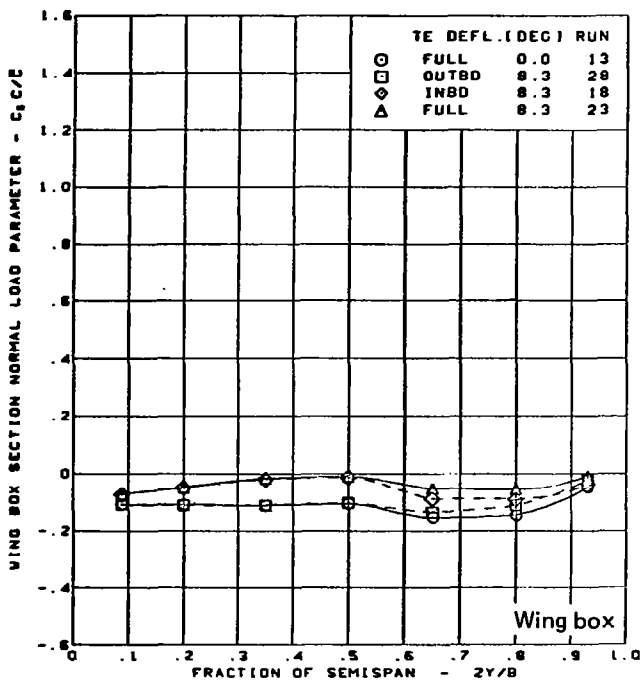
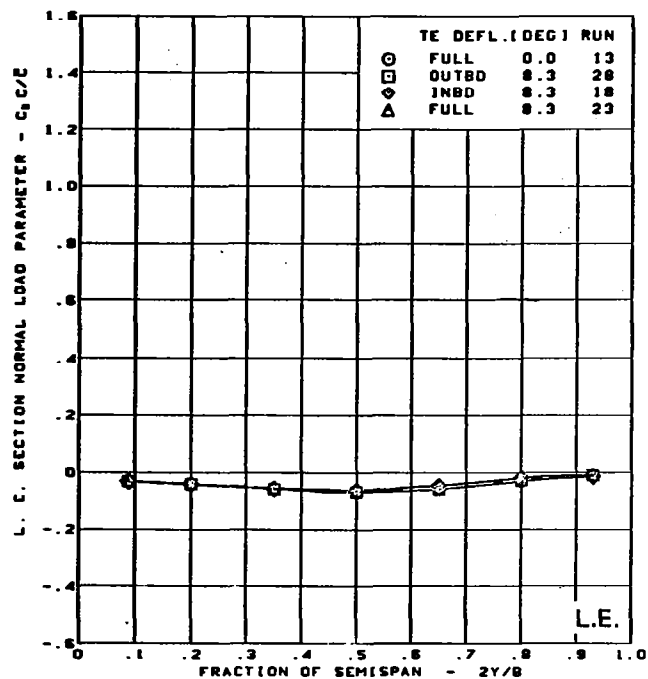
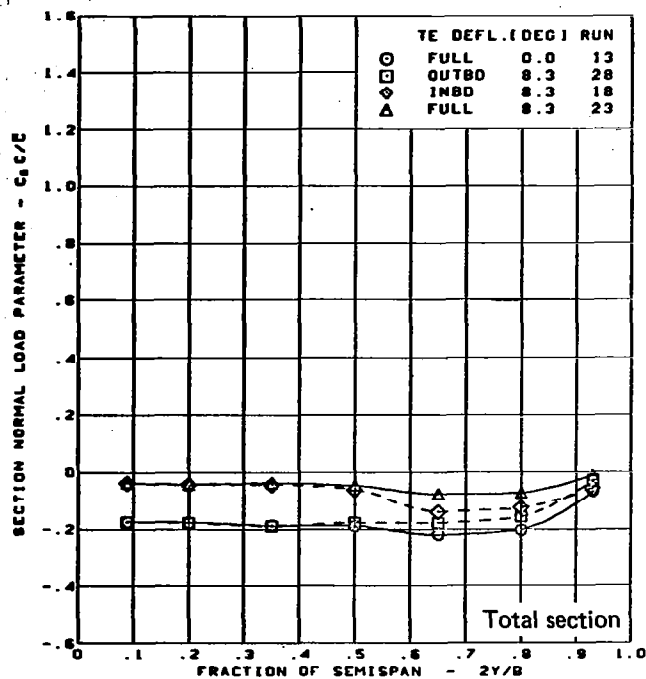


$M = 0.85$   
 $\alpha = -8^\circ$

Twisted wing, rounded L.E.  
 L.E. deflection, full span =  $0.0^\circ$

(a) Spanload Distributions - Normal Force,  $\alpha = -8^\circ$

Figure 34. — Wing Experimental Data—Effect of Full- and Partial-Span Trailing Edge Control Surface Deflection on Chordwise Segments; Twisted Wing;  $M = 0.85$

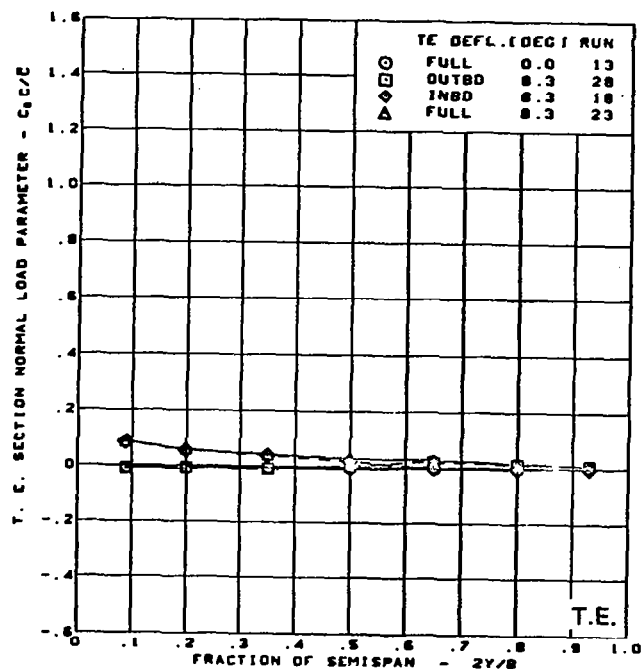
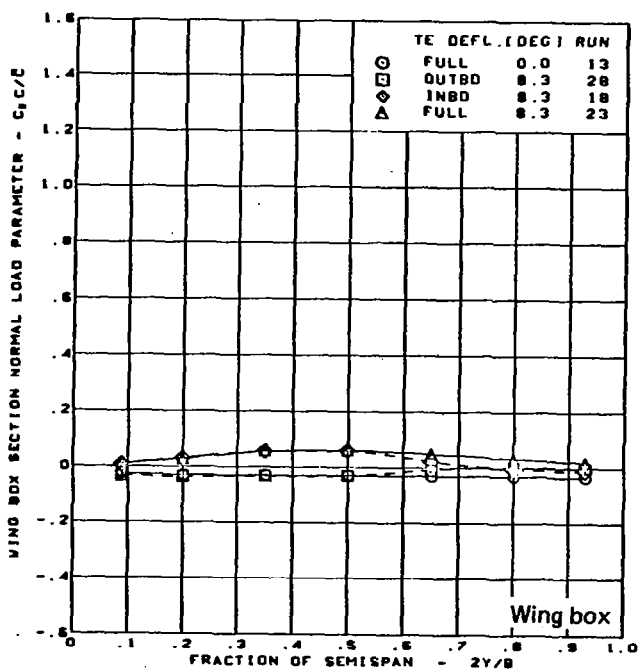
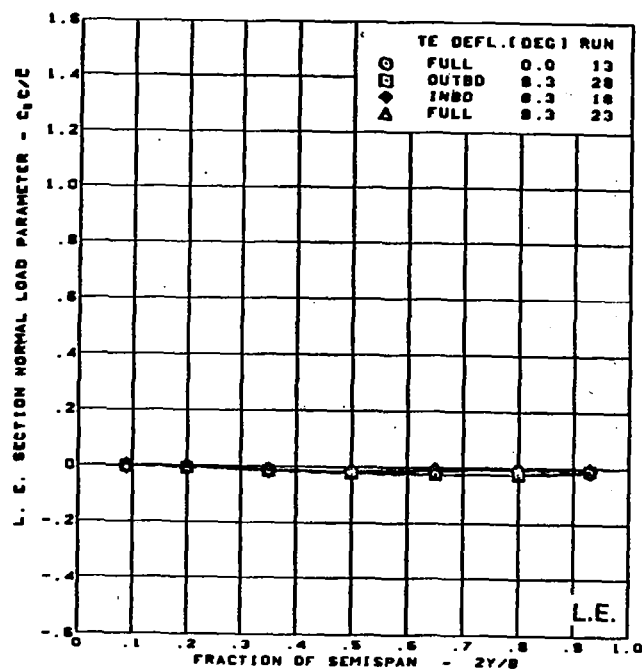
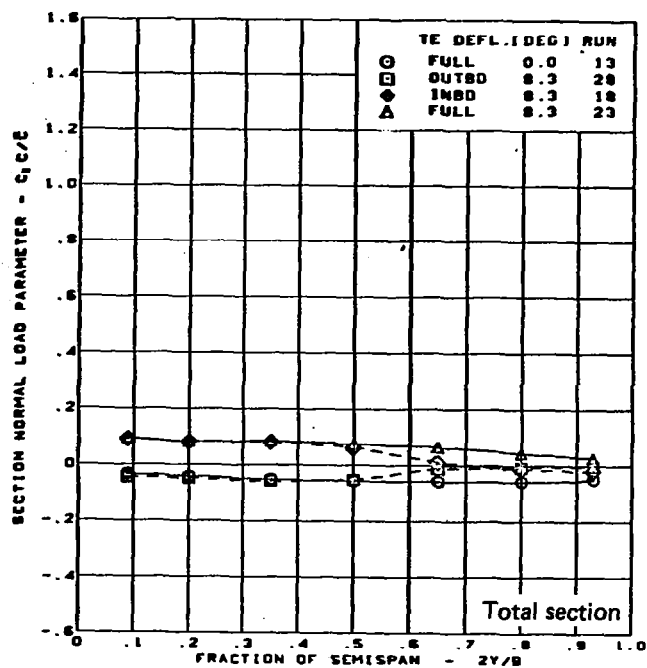


$M = 0.85$   
 $\alpha = -4^\circ$

Twisted wing, rounded L.E.  
 L.E. deflection, full span =  $0.0^\circ$

(b) Spanload Distributions - Normal Force,  $\alpha = -4^\circ$

Figure 34. - (Continued)



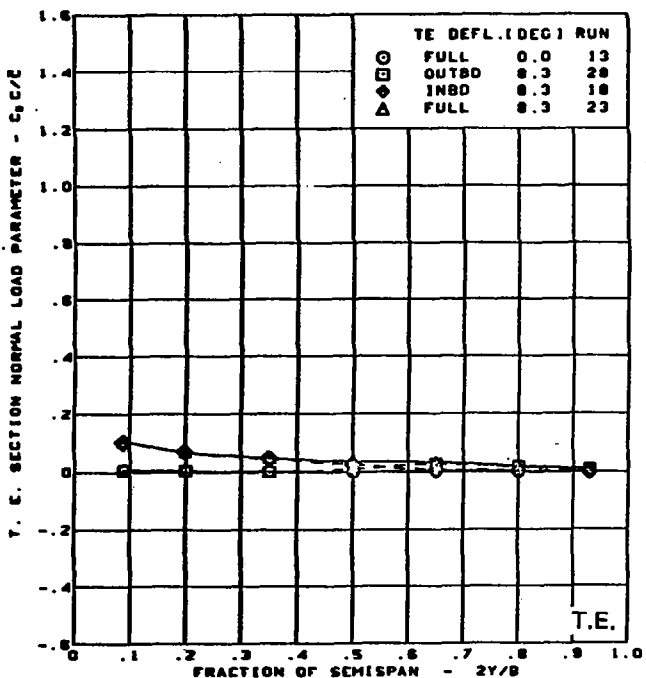
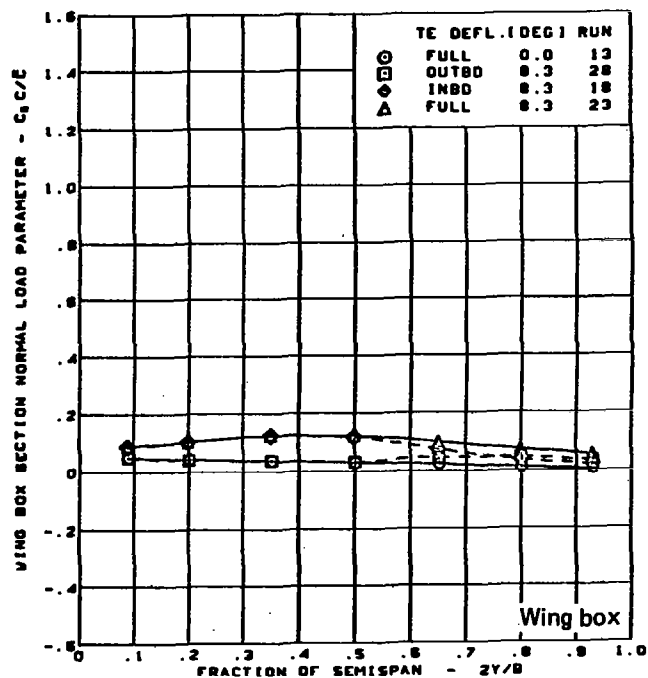
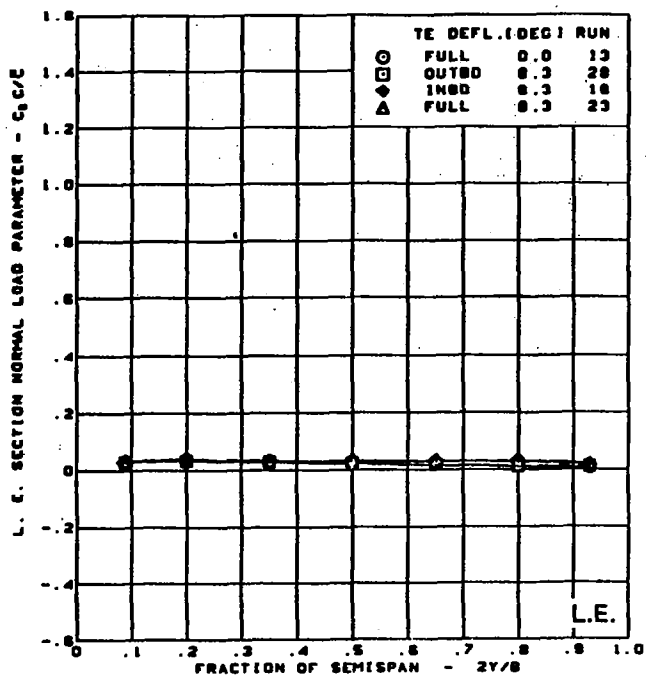
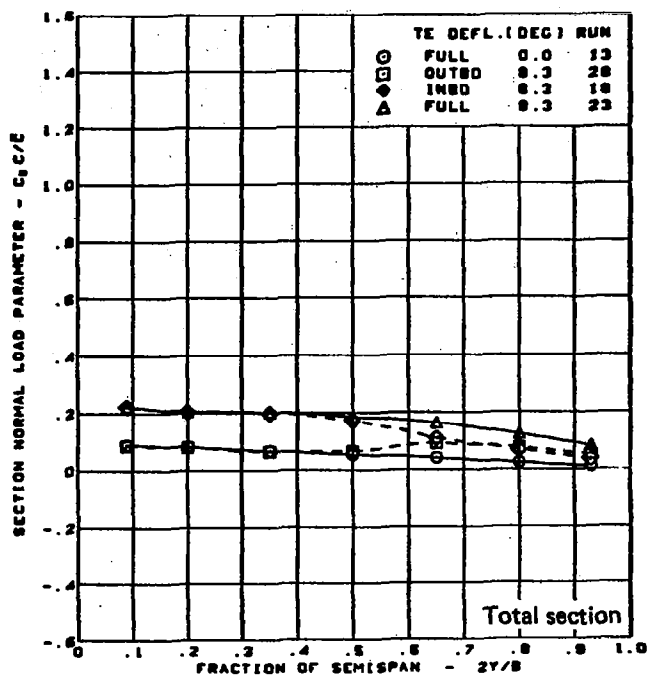
$M = 0.85$   
 $\alpha = 0^\circ$

Twisted wing, rounded L.E.  
 L.E. deflection, full span =  $0.0^\circ$

(c) Spanload Distributions - Normal Force,  $\alpha = 0^\circ$

Figure 34. - (Continued)



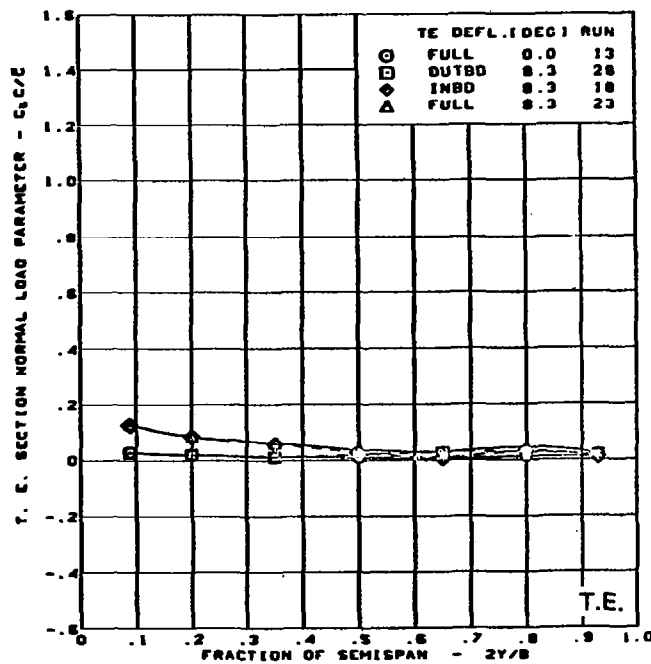
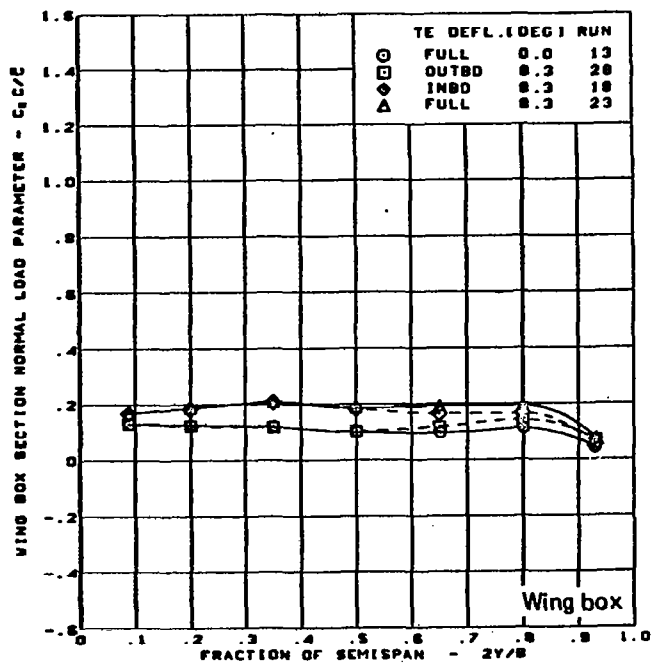
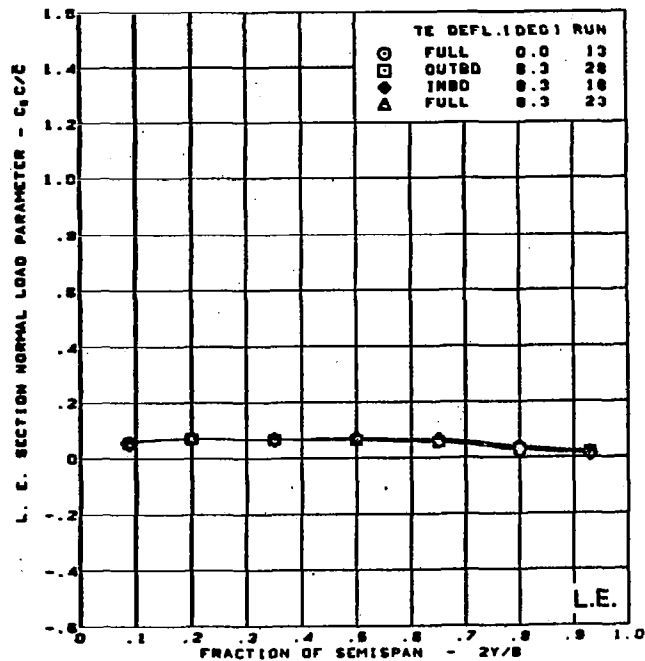
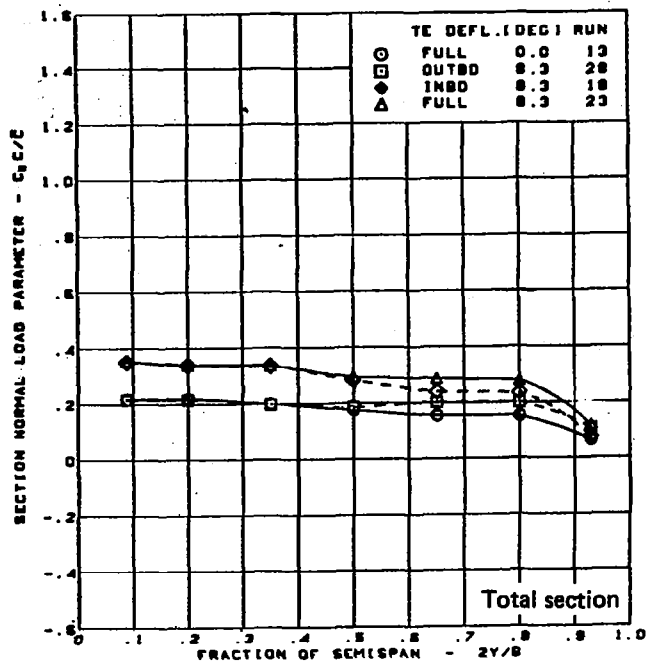


$M = 0.85$   
 $\alpha = 4^\circ$

Twisted wing, rounded L.E.  
 L.E. deflection, full span =  $0.0^\circ$

(d) Spanload Distributions - Normal Force,  $\alpha = 4^\circ$

Figure 34. - (Continued)

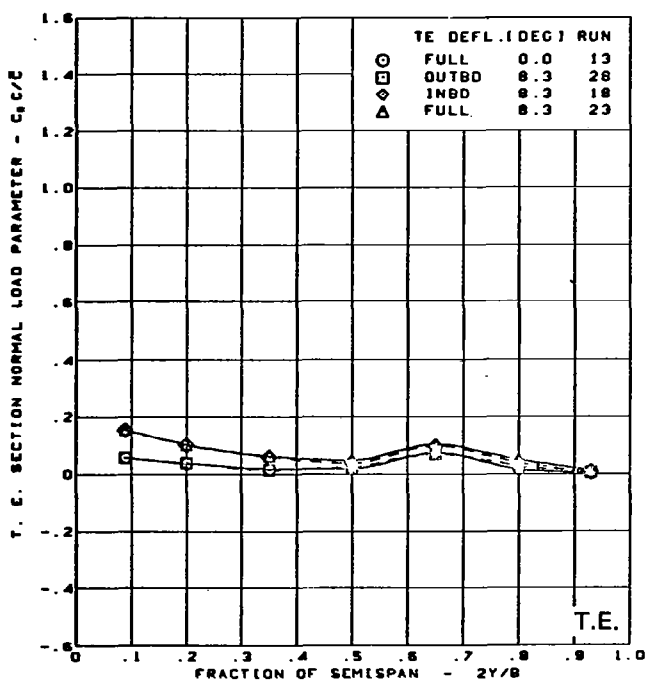
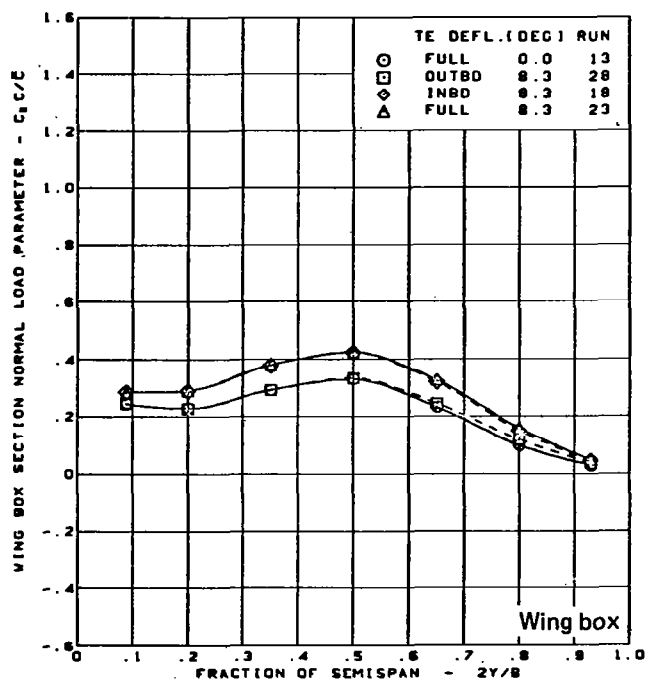
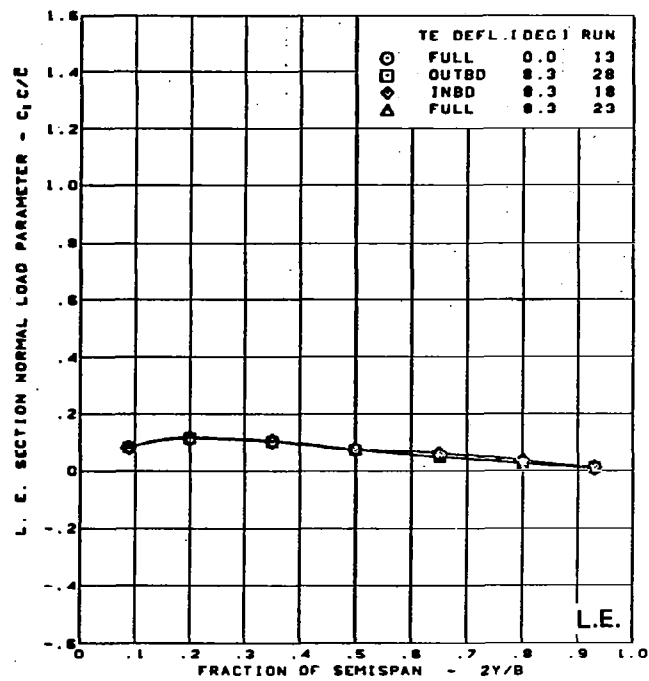
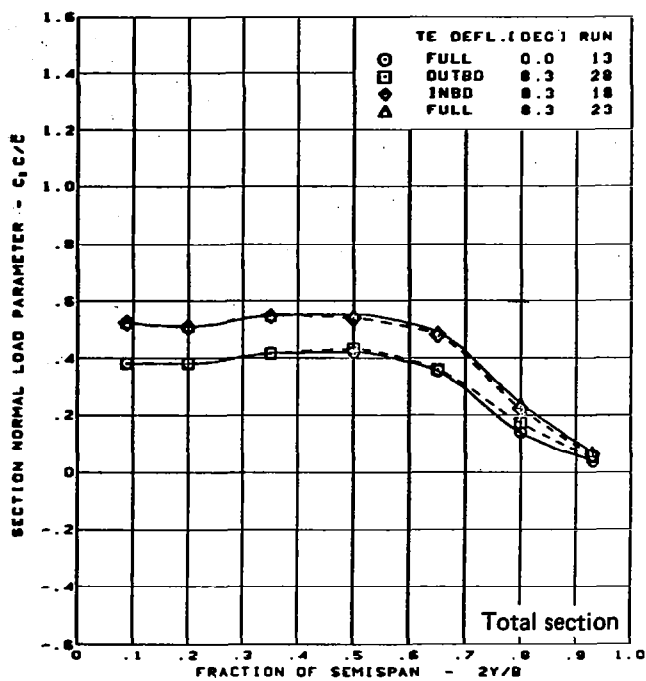


$M = 0.85$   
 $\alpha = 8^\circ$

Twisted wing, rounded L.E.  
 L.E. deflection, full span =  $0.0^\circ$

(e) Spanload Distributions - Normal Force,  $\alpha = 8^\circ$

Figure 34. — (Continued)

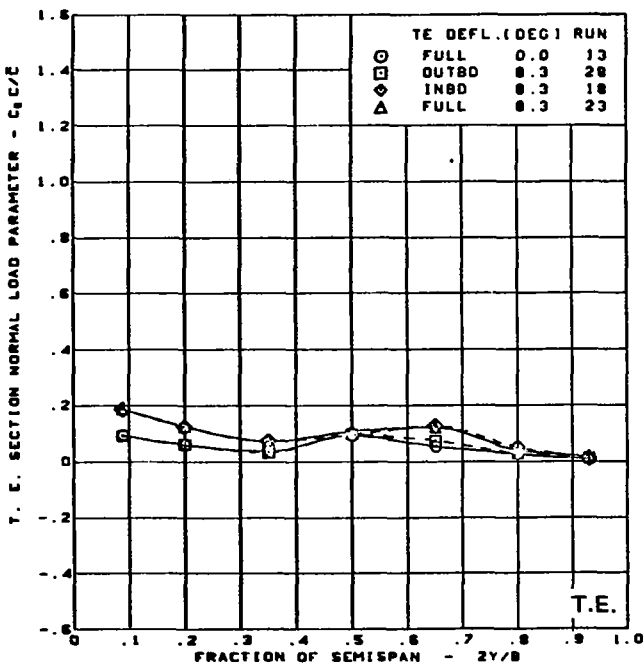
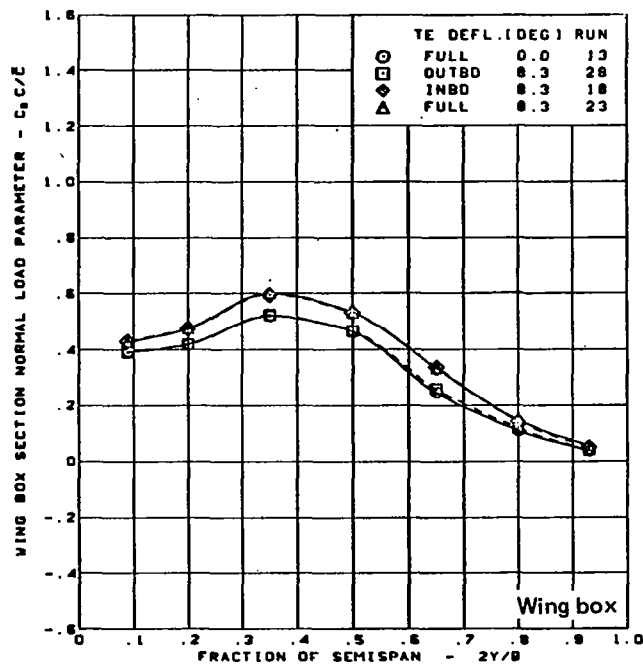
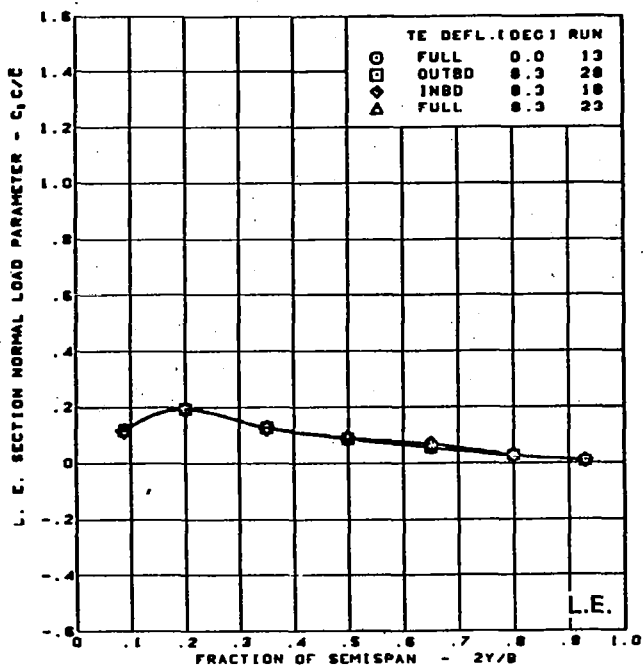
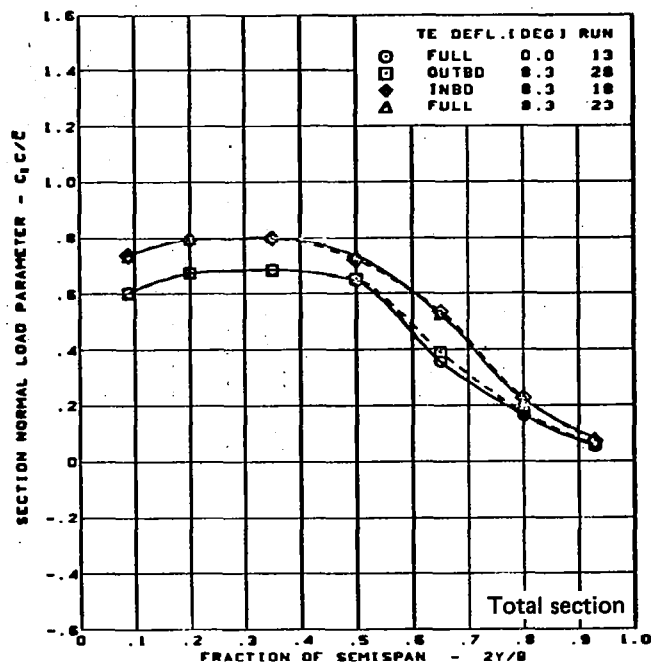


$M = 0.85$   
 $\alpha = 12^\circ$

Twisted wing, rounded L.E.  
 L.E. deflection, full span =  $0.0^\circ$

(f) Spanload Distributions - Normal Force,  $\alpha = 12^\circ$

Figure 34. - (Continued)

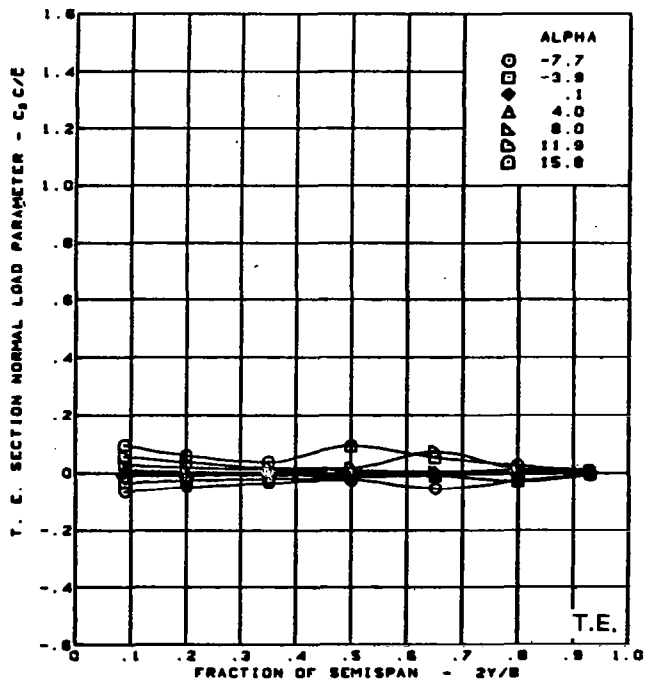
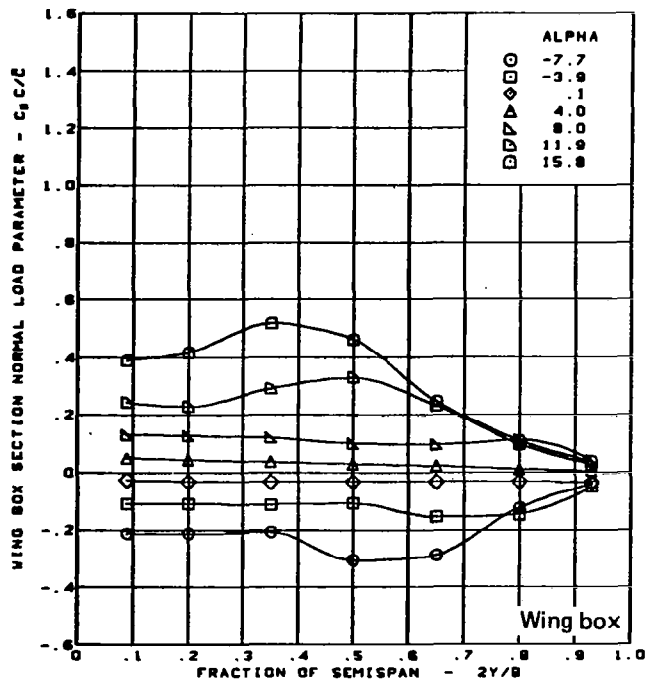
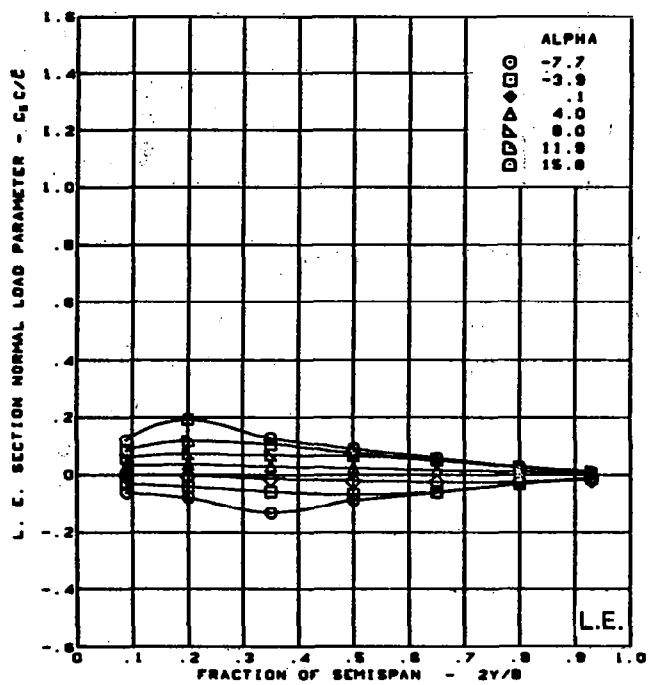
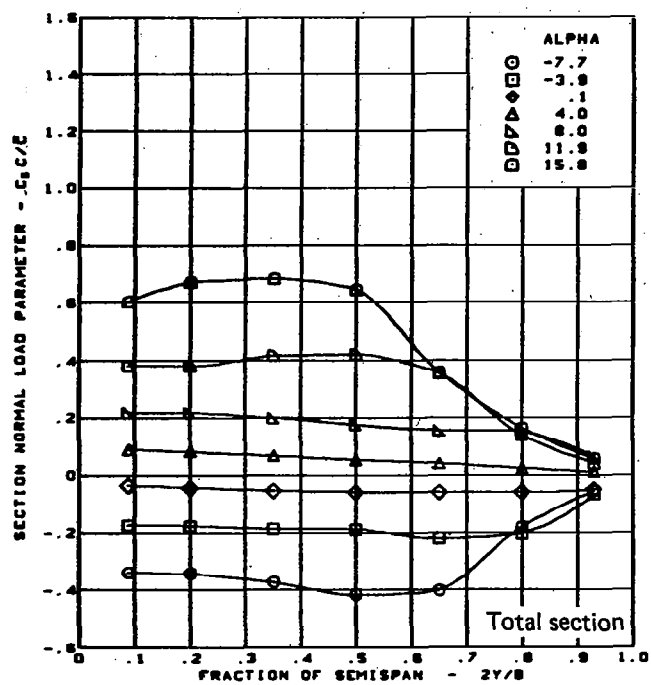


$M = 0.85$   
 $\alpha = 16^\circ$

Twisted wing, rounded L.E.  
 L.E. deflection, full span =  $0.0^\circ$

(g) Spanload Distributions - Normal Force,  $\alpha = 16^\circ$

Figure 34. - (Continued)



$M = 0.85$

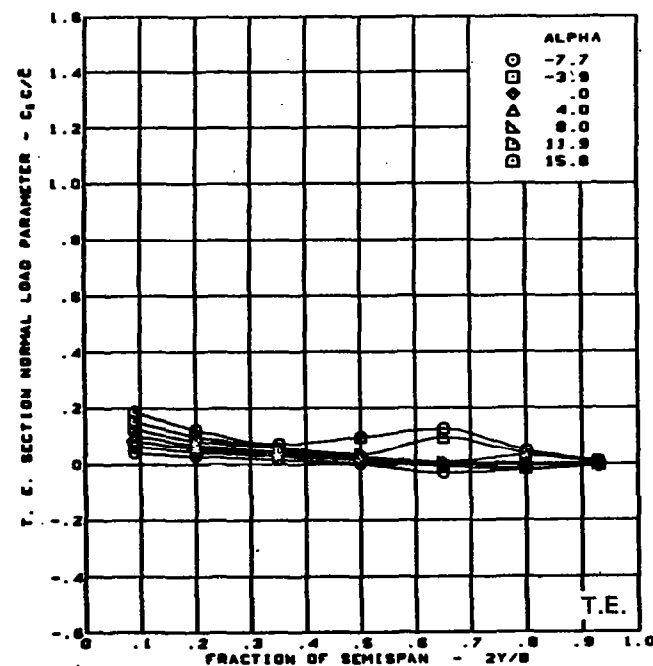
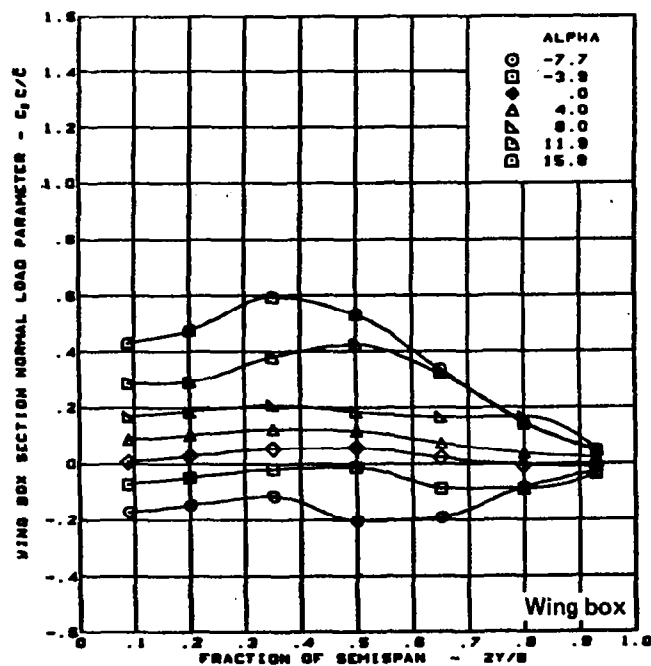
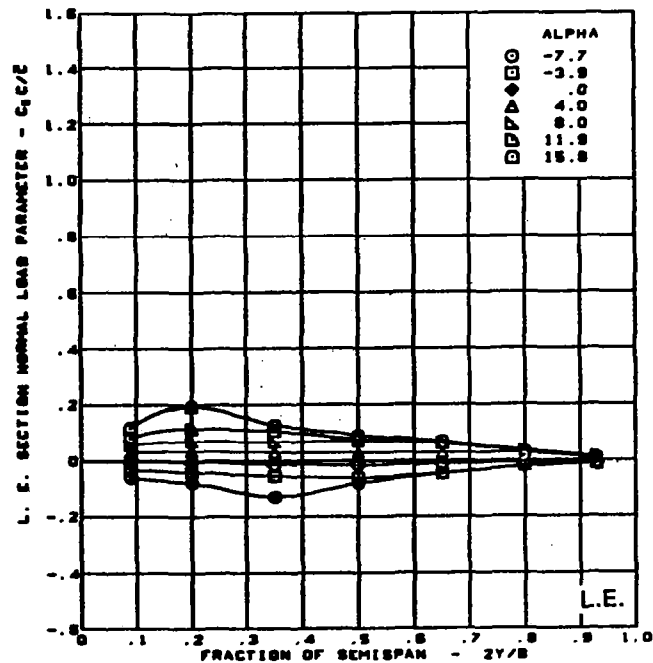
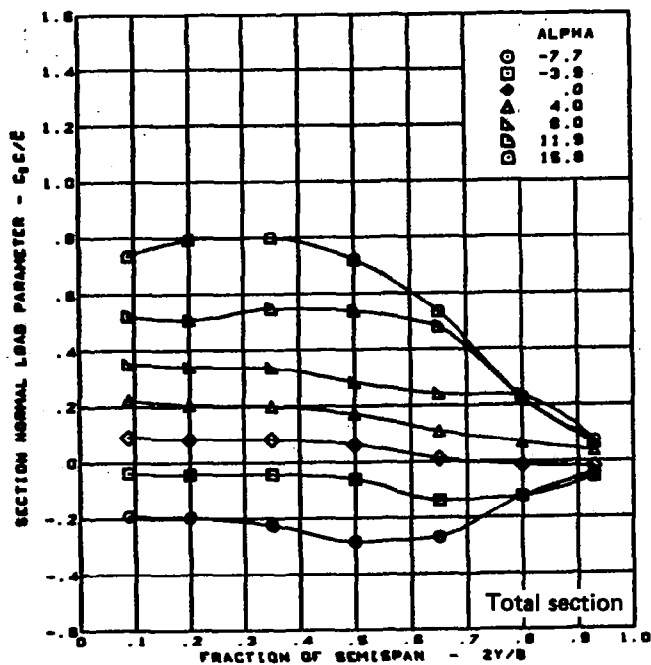
Twisted wing, rounded L.E.

L.E. deflection, full span  $= 0.0^\circ$

T.E. deflection, full span  $= 0.0^\circ$

(h) Spanload Distributions - Normal Force, T.E. Deflection, Full Span  $= 0.0^\circ$

Figure 34. — (Continued)

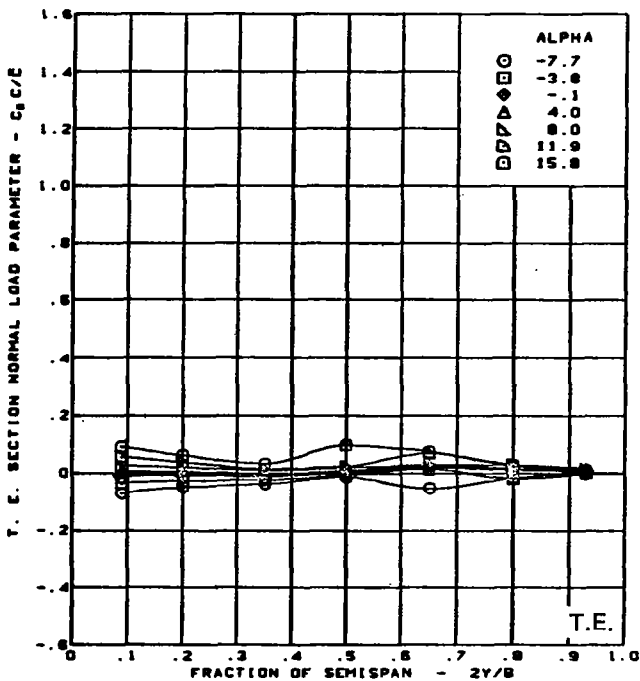
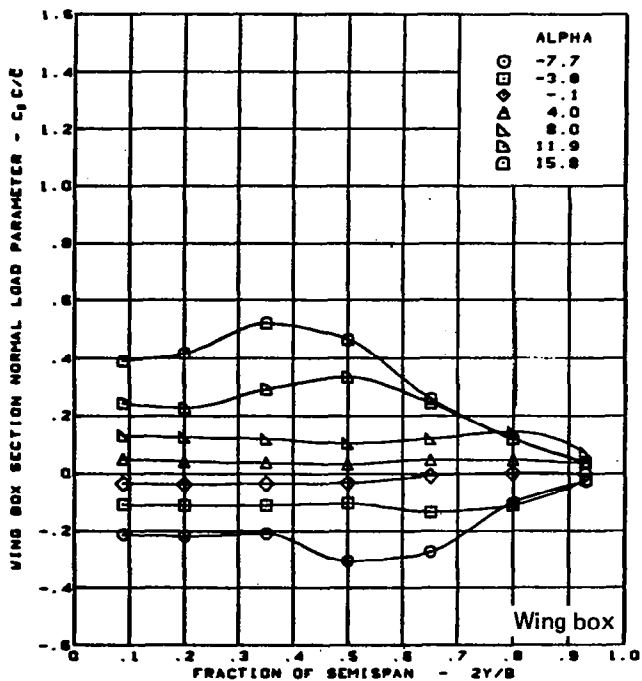
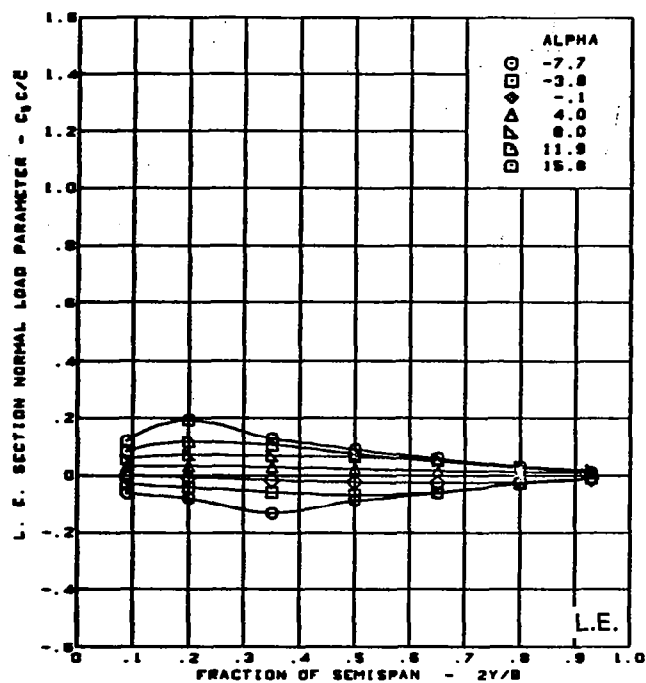
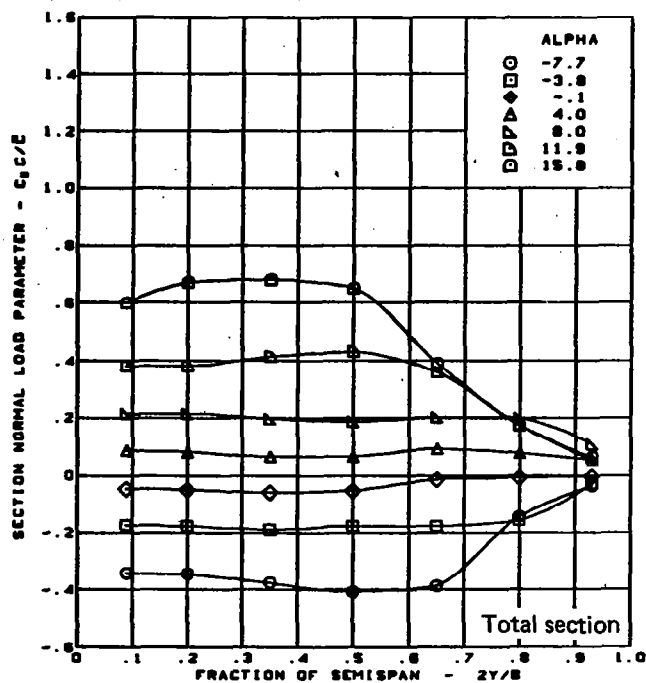


$M = 0.85$   
Twisted wing, rounded L.E.

L.E. deflection, full span =  $0.0^\circ$   
T.E. deflection, inboard =  $8.3^\circ$ , outboard =  $0.0^\circ$

(i) Spanload Distributions - Normal Force, T.E. Deflection, Inboard =  $8.3^\circ$ , Outboard =  $0.0^\circ$

Figure 34. - (Continued)

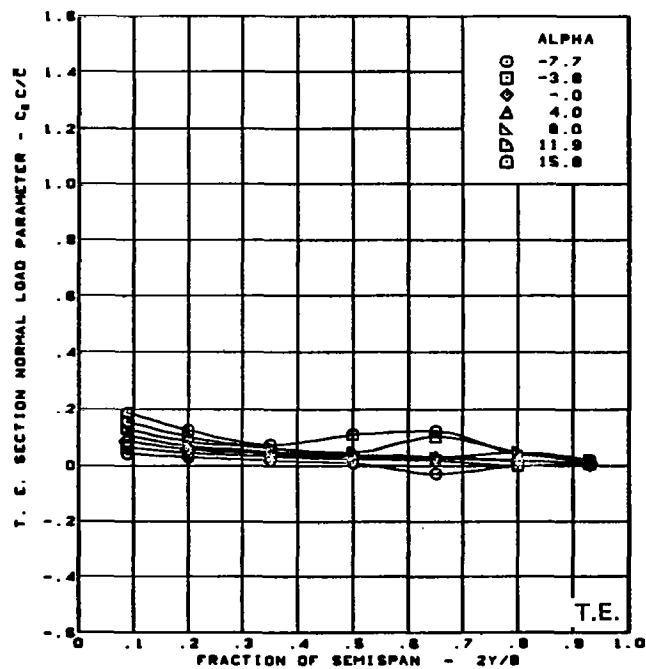
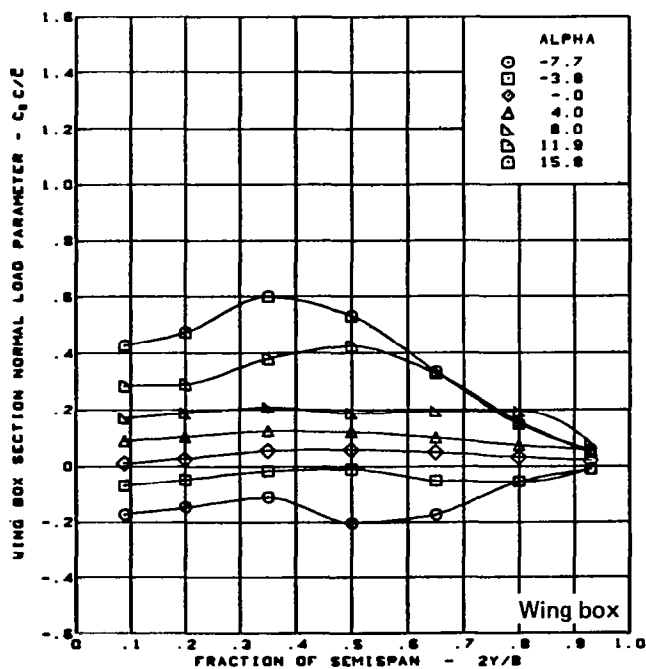
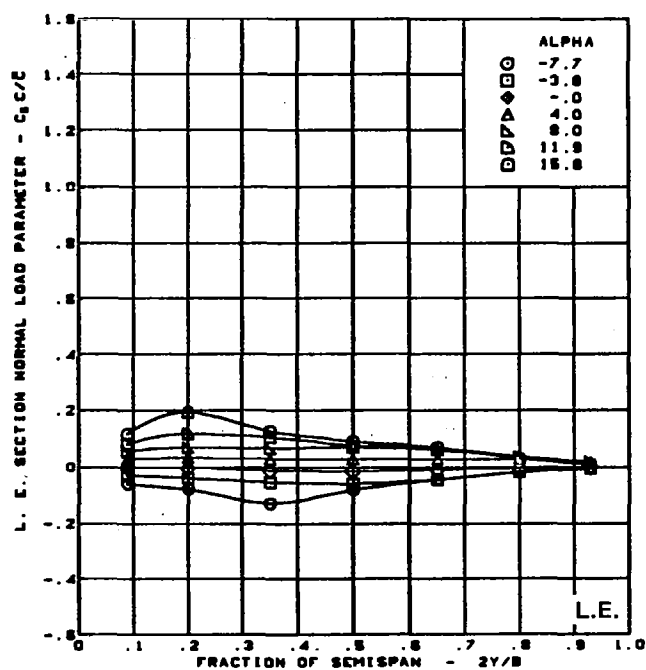
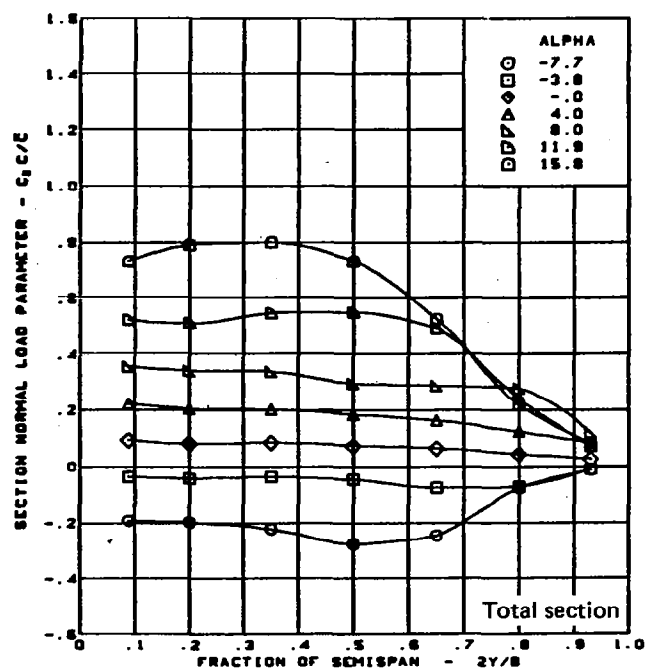


$M = 0.85$   
Twisted wing, rounded L.E.

L.E. deflection, full span =  $0.0^\circ$   
T.E. deflection, inboard =  $0.0^\circ$ , outboard =  $8.3^\circ$

(j) Spanload Distributions - Normal Force, T.E. Deflection, Inboard =  $0.0^\circ$ , Outboard =  $8.3^\circ$

Figure 34. - (Continued)



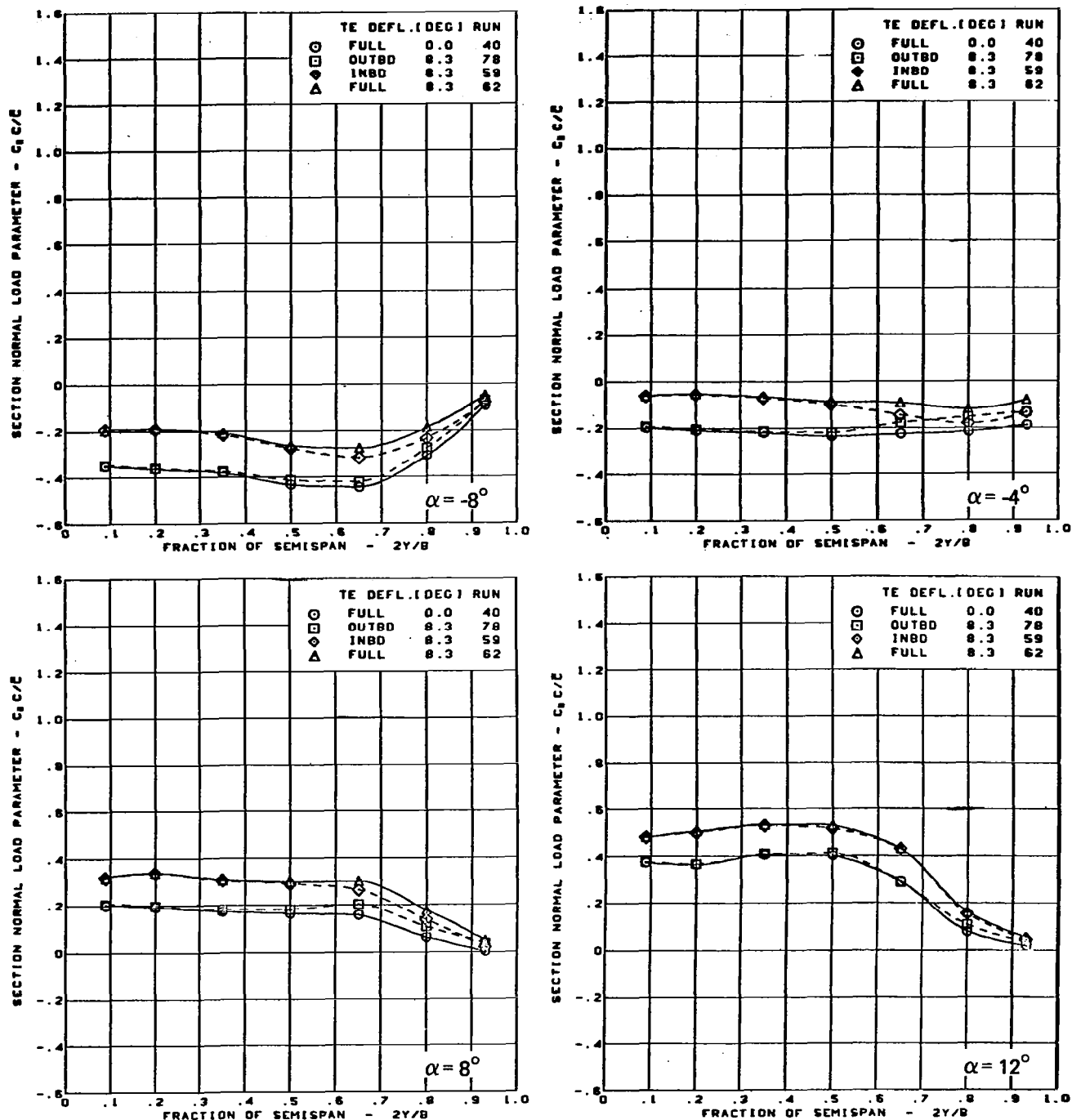
$M = 0.85$   
Twisted wing, rounded L.E.

L.E. deflection, full span =  $0.0^\circ$   
T.E. deflection, full span =  $8.3^\circ$

(k) Spanload Distributions - Normal Force, T.E. Deflection, Full Span =  $8.3^\circ$

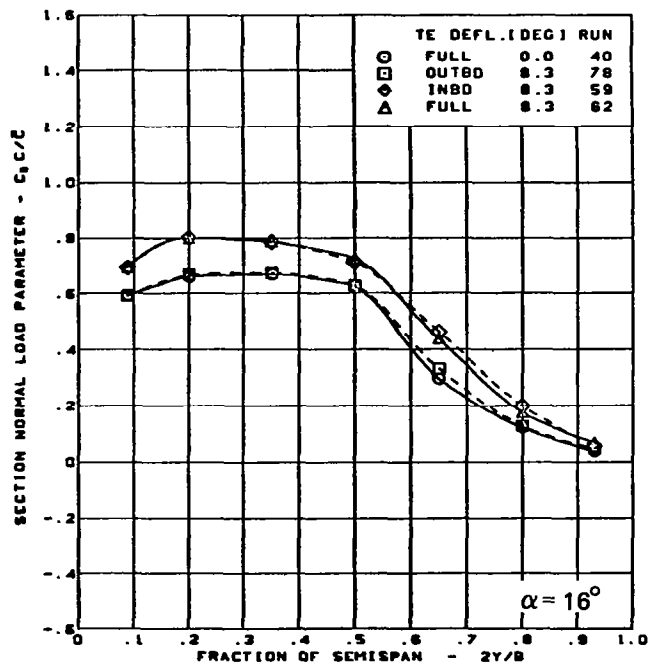
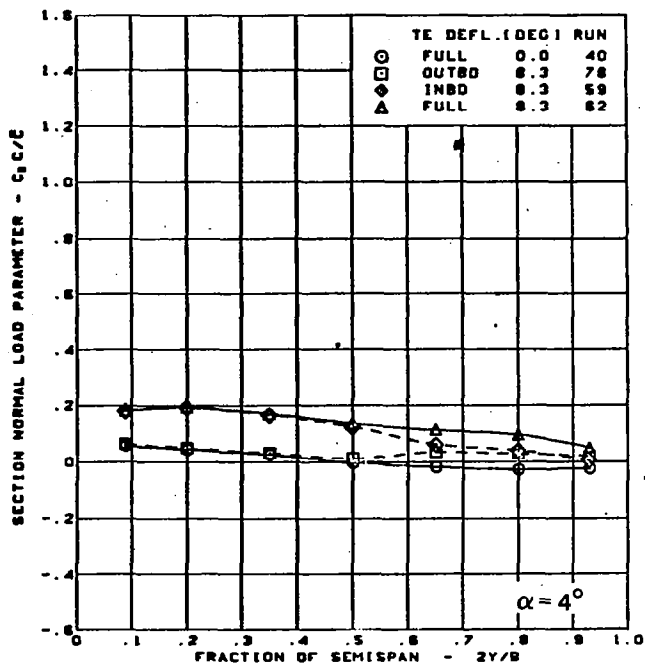
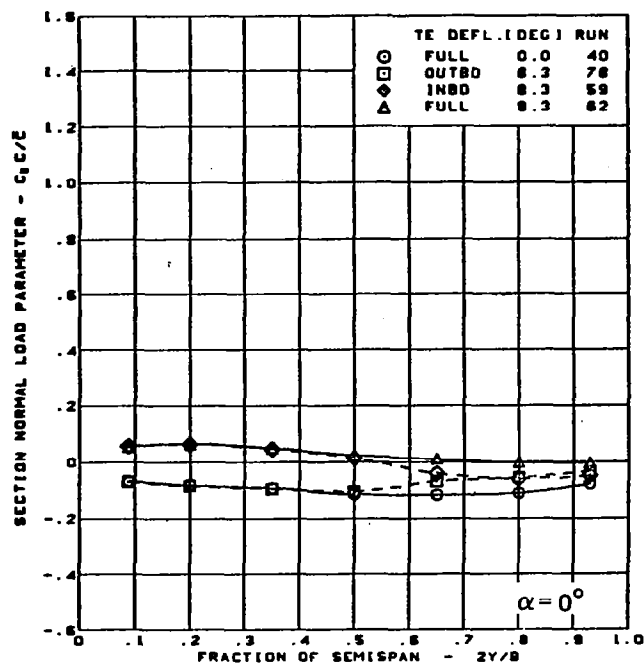
Figure 34. - (Concluded)





(a) Spanload Distribution - Normal Force Variation With T.E. Control Surface Configuration

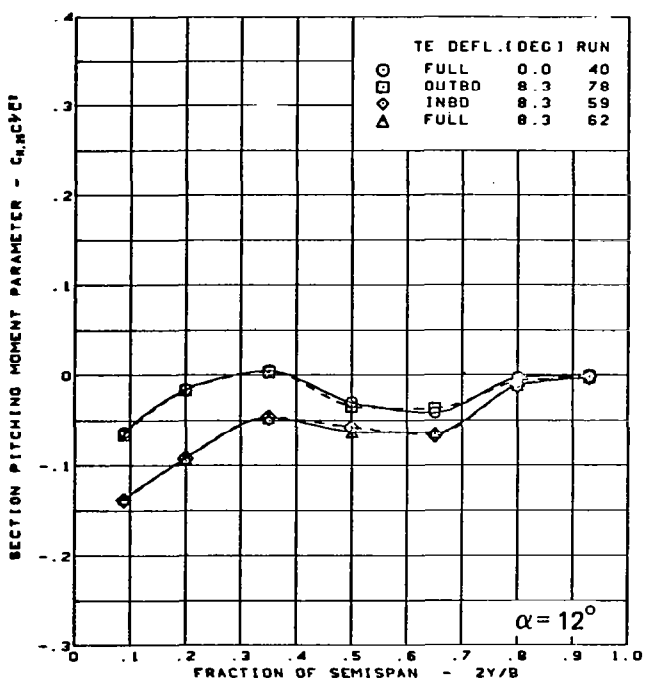
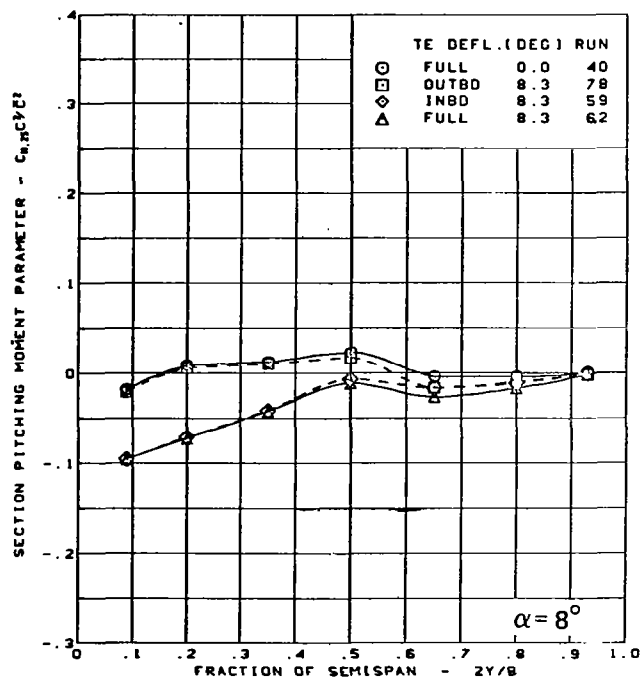
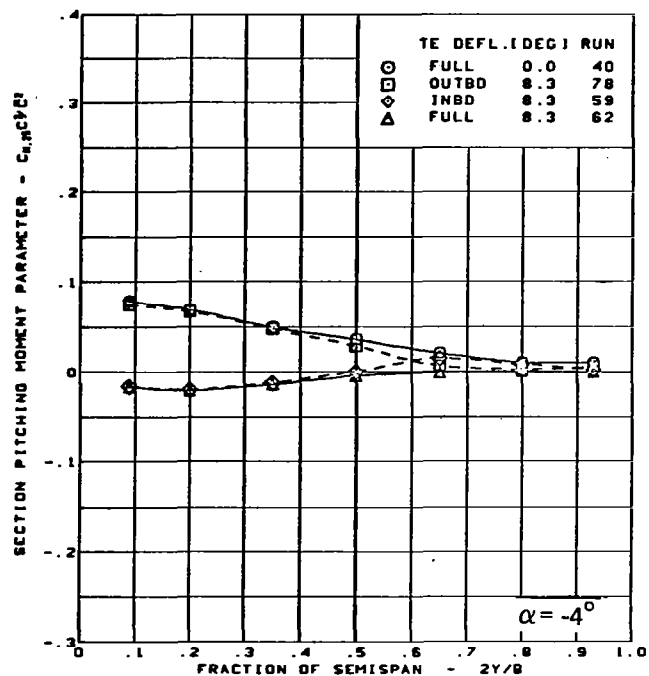
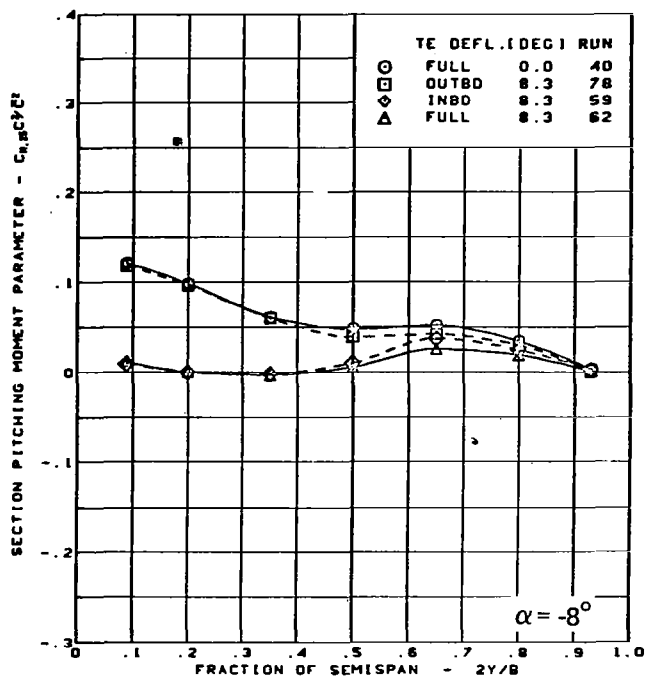
Figure 35. — Wing Experimental Data—Effect of Full- and Partial-Span Trailing Edge Control Surface Deflection; Cambered-Twisted Wing; Fin Off;  $M = 0.85$



$M = 0.85$   
 Cambered-twisted wing, rounded L.E.  
 Fin off  
 L.E. deflection, full span =  $0.0^\circ$

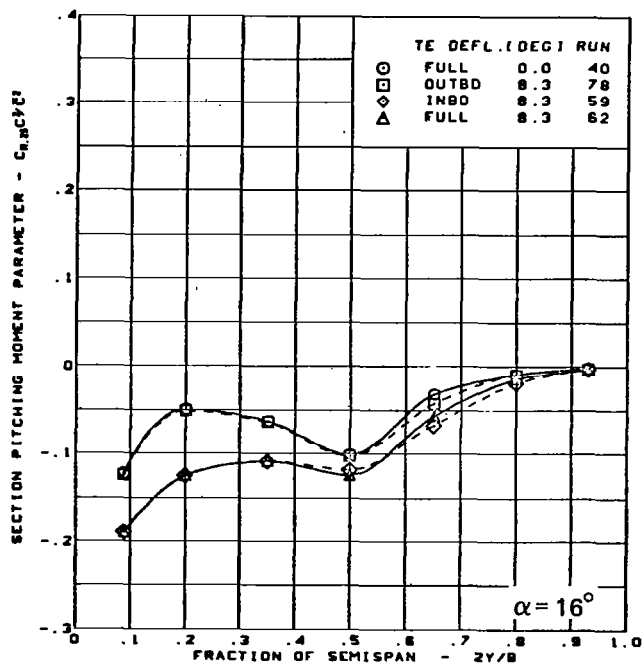
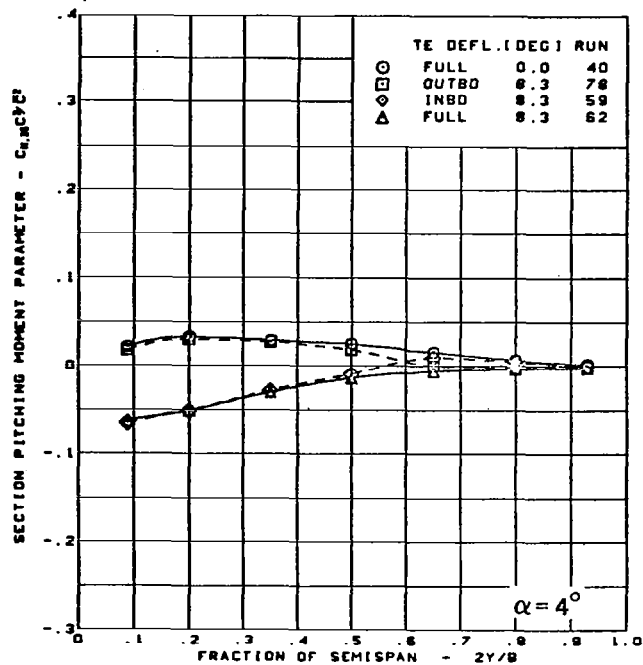
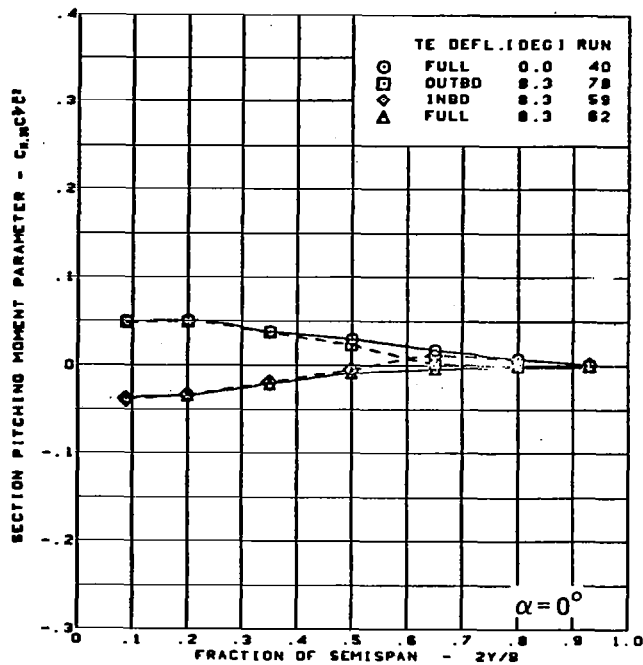
(a) (Concluded)

Figure 35. — (Continued)



(b) Spanload Distribution - Pitching Moment Variation With T.E. Control Surface Configuration

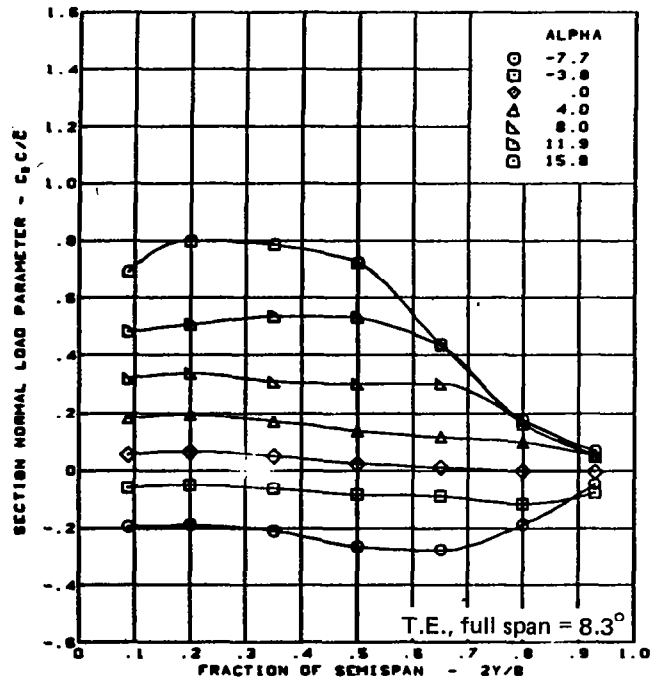
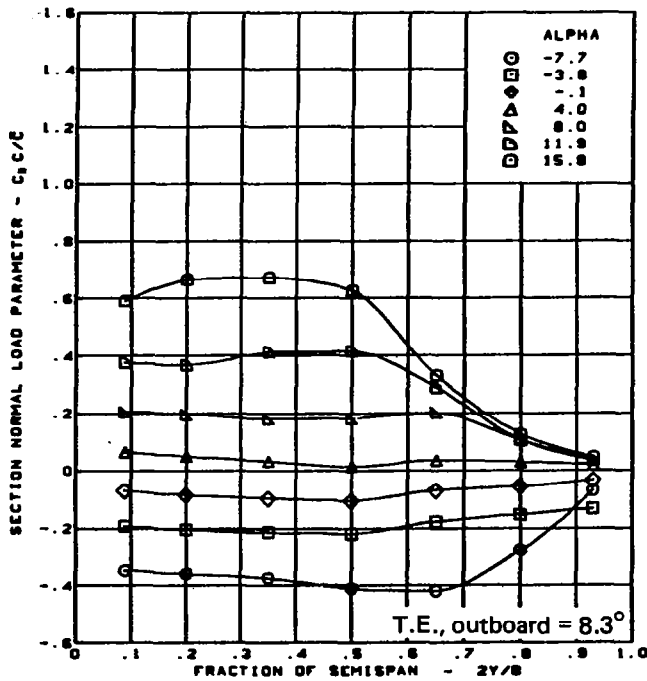
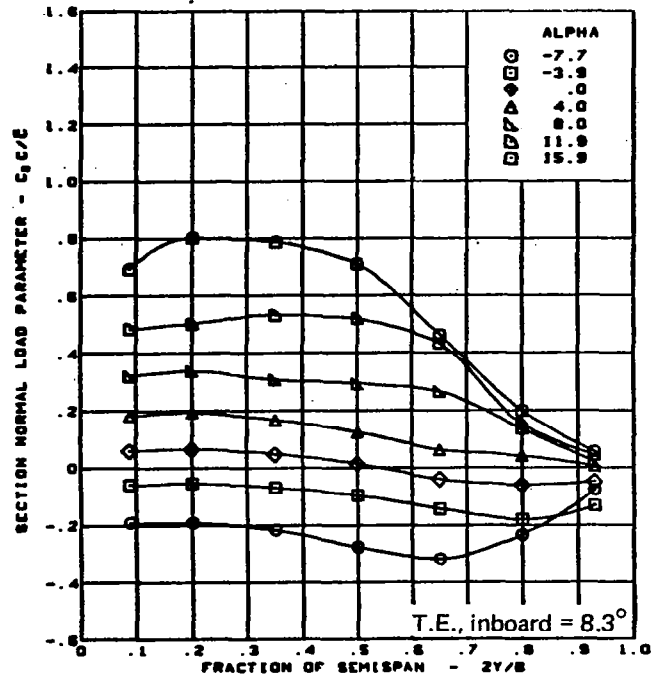
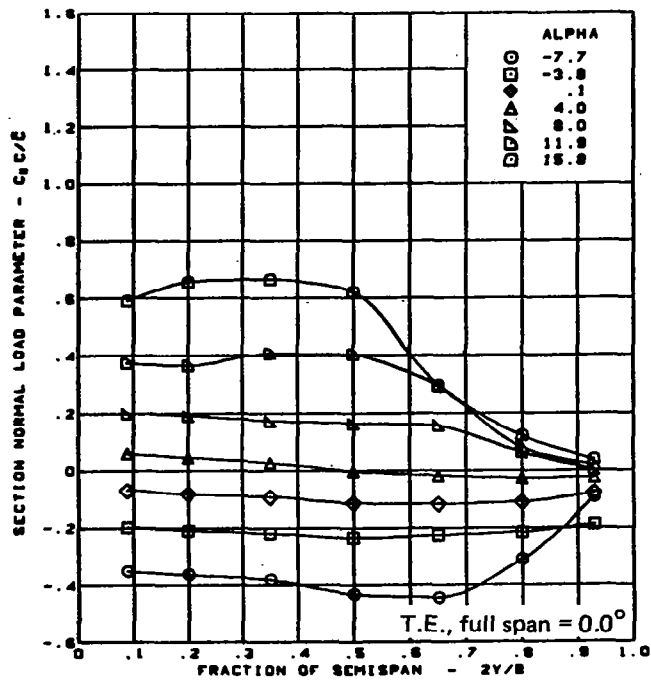
Figure 35. - (Continued)



$M = 0.85$   
 Cambered-twisted wing, rounded L.E.  
 Fin off  
 L.E. deflection, full span =  $0.0^\circ$

(b) (Concluded)

Figure 35. — (Continued)

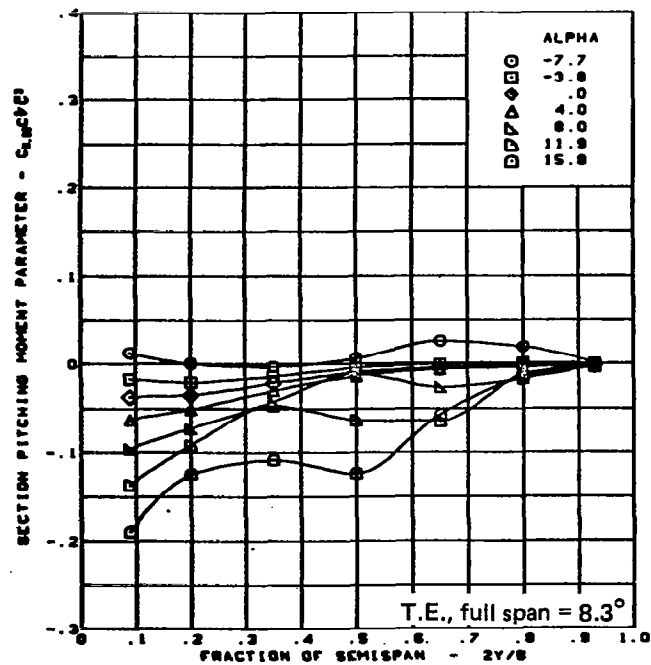
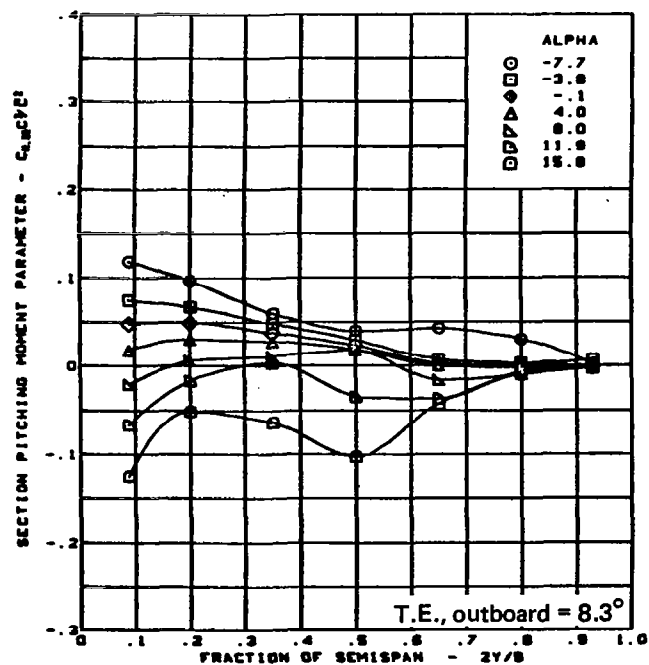
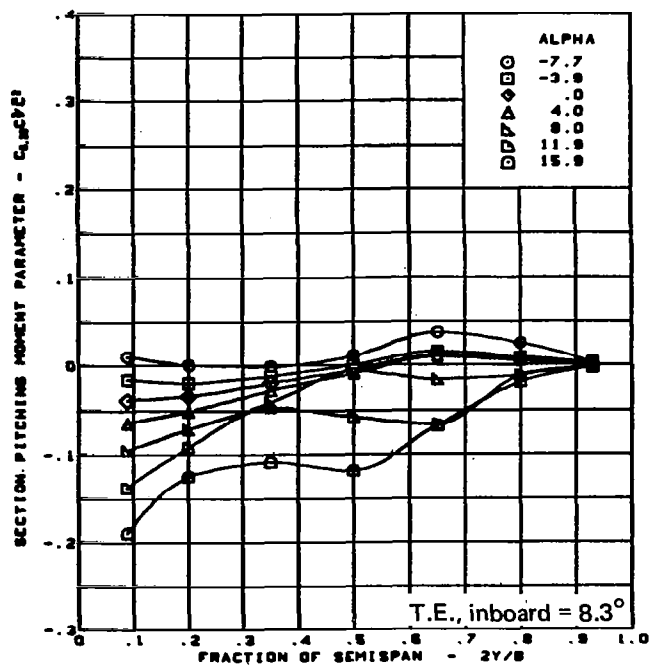
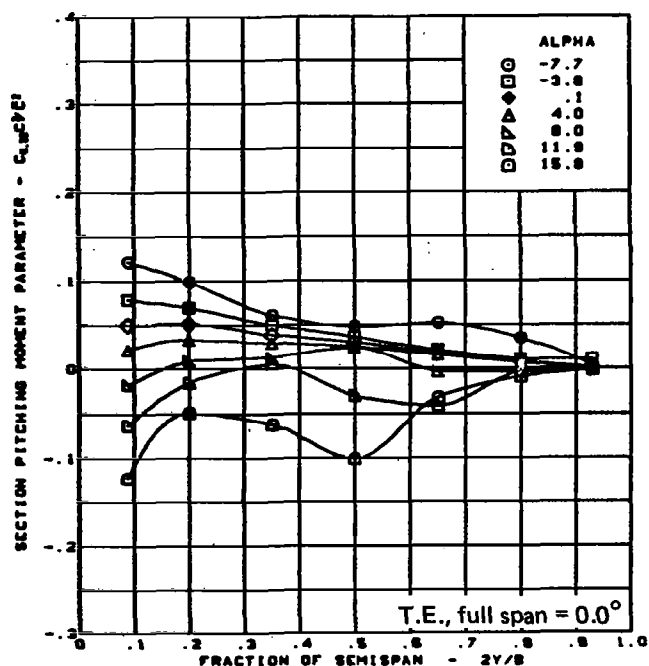


$M = 0.85$   
Cambered-twisted wing, rounded L.E.

Fin off  
L.E. deflection, full span =  $0.0^\circ$

(c) Spanload Distribution - Normal Force Variation With Angle of Attack

Figure 35. — (Continued)

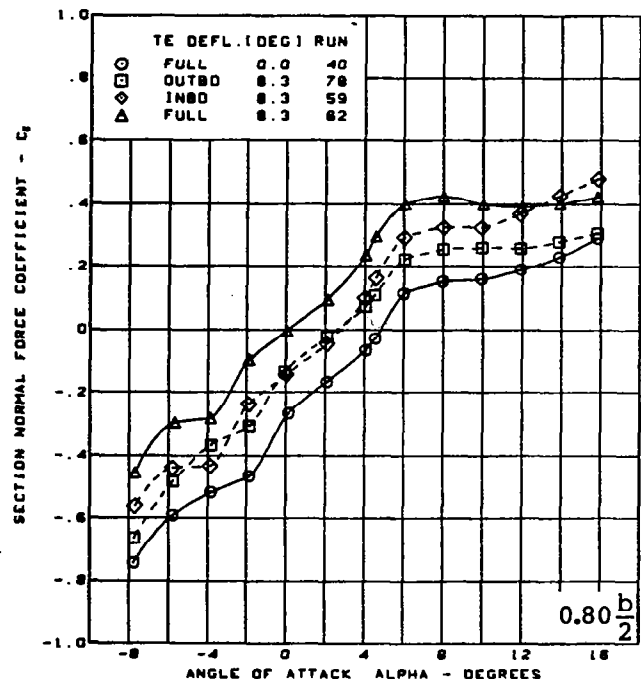
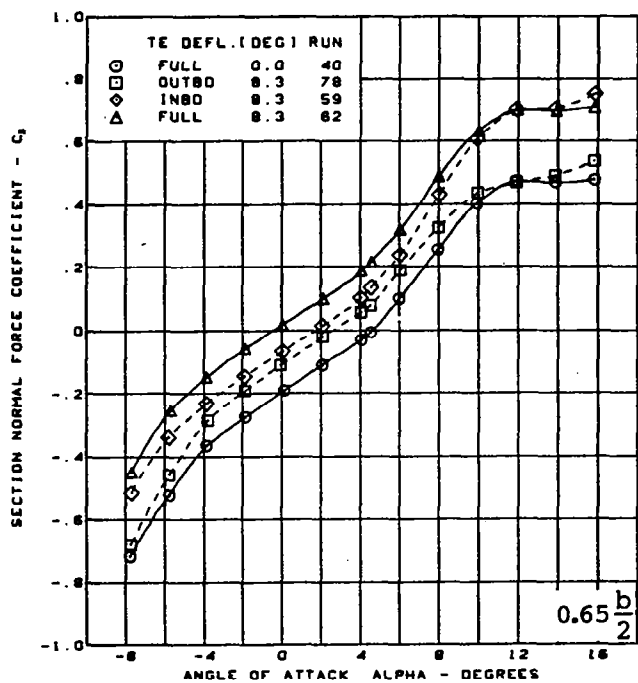
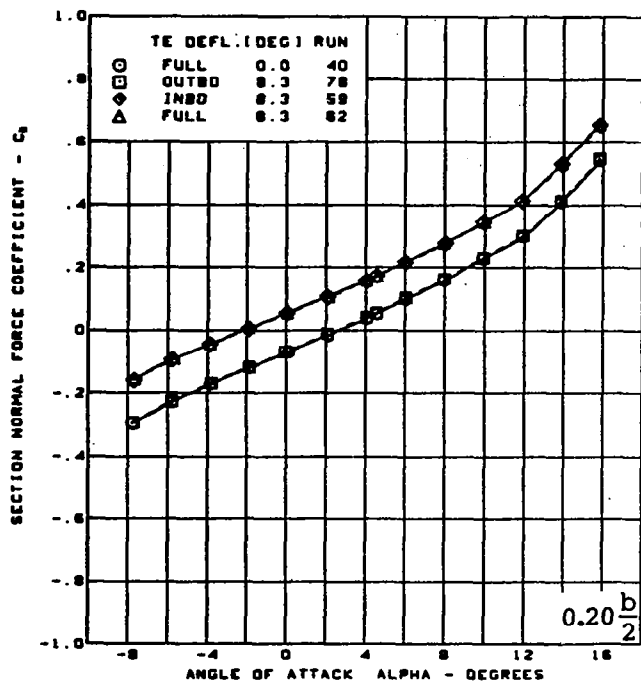
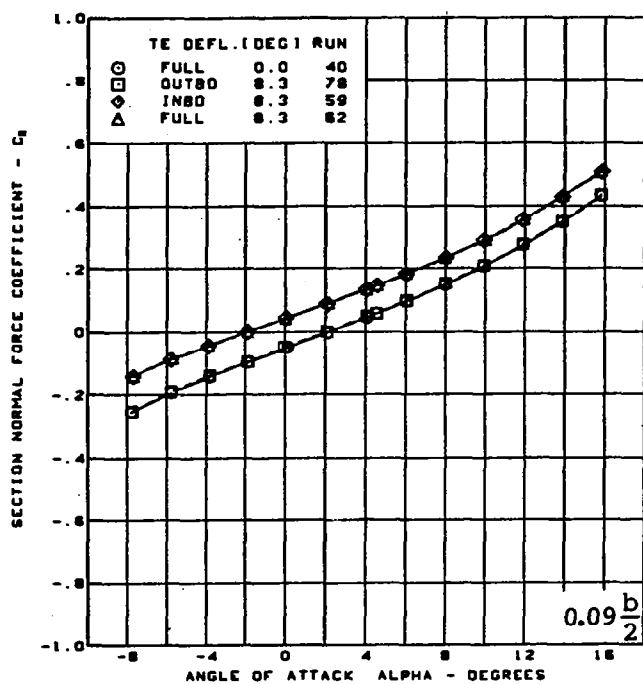


$M = 0.85$   
Cambered-twisted wing, rounded L.E.

Fin off  
L.E. deflection, full span =  $0.0^\circ$

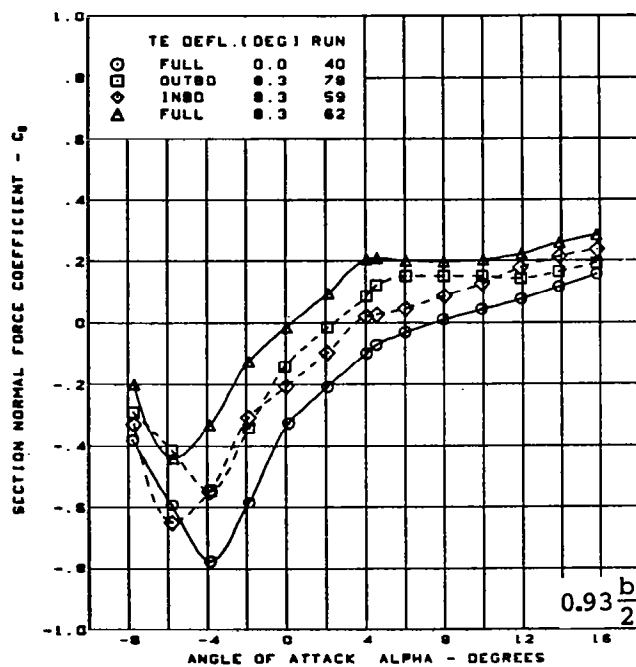
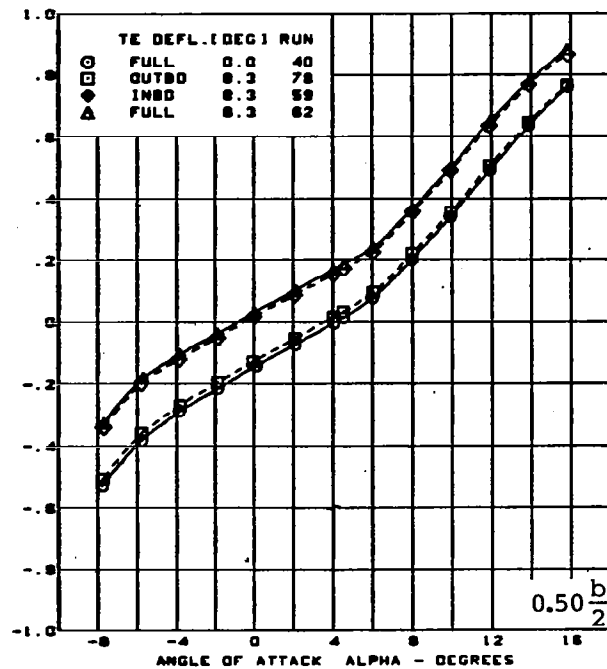
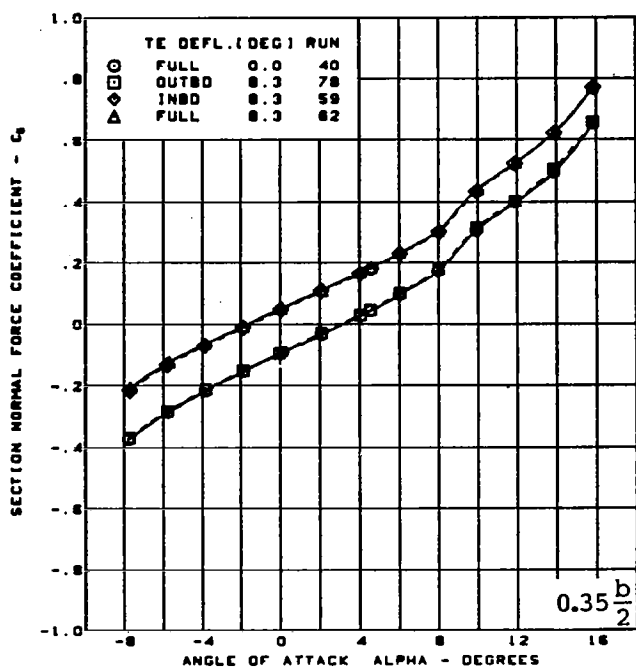
(d) Spanload Distribution - Pitching Moment Variation With Angle of Attack

Figure 35. - (Continued)



(e) Section Aerodynamic Coefficients - Normal Force

Figure 35. - (Continued)

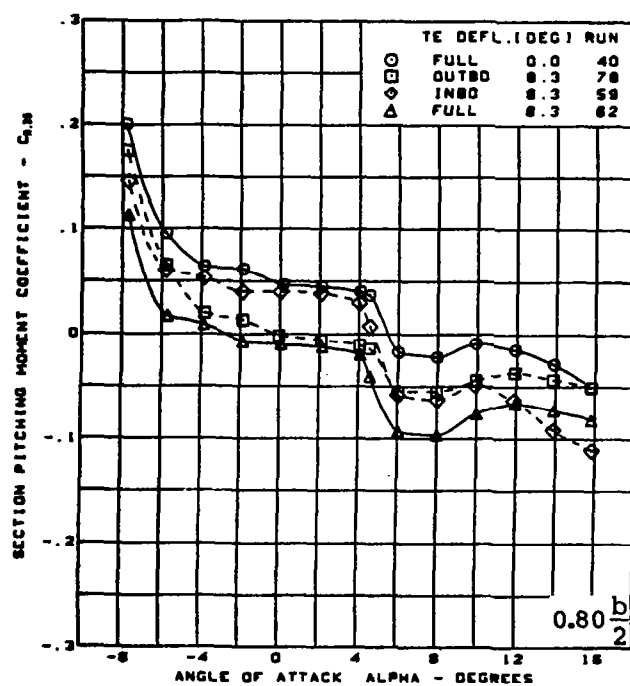
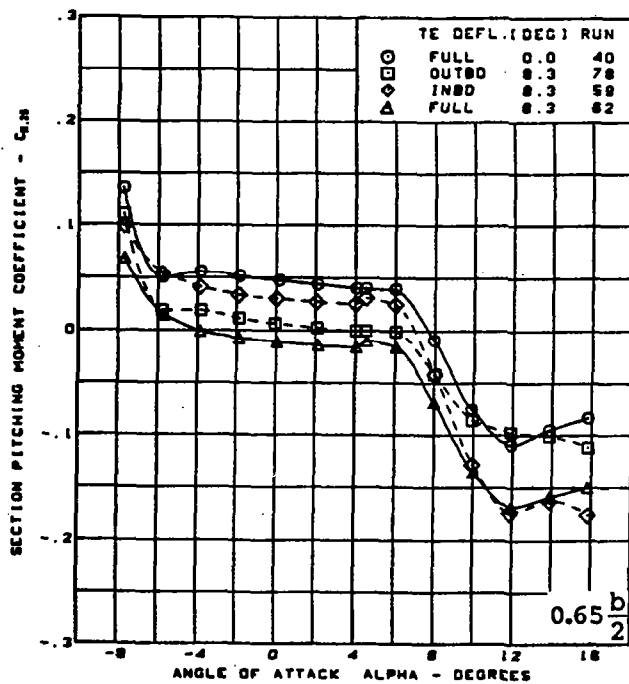
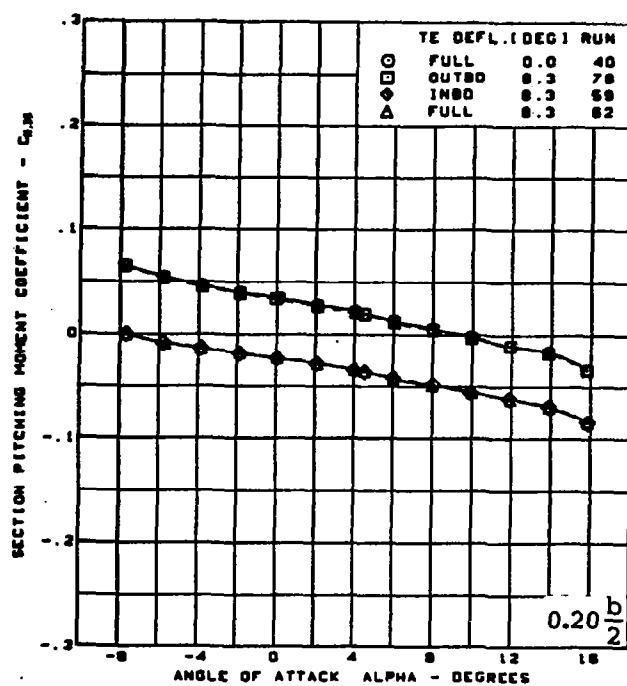
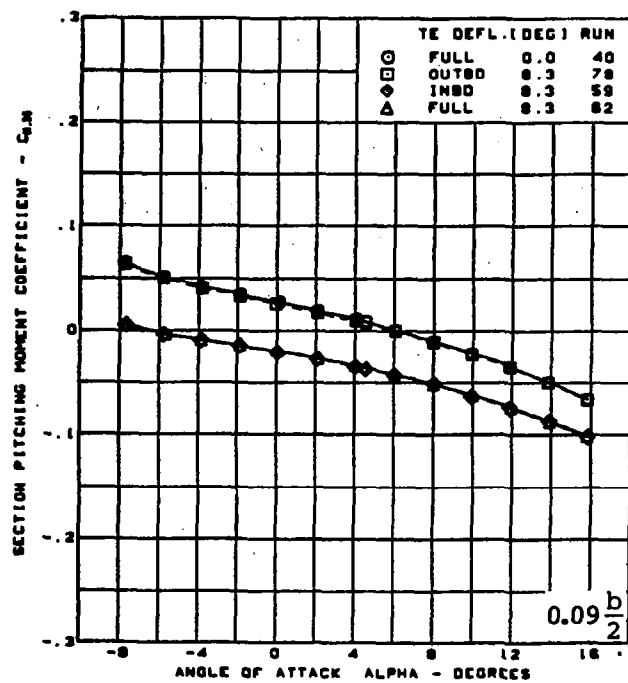


M = 0.85  
 Cambered-twisted wing, rounded L.E.  
 Fin off  
 L.E. deflection, full span =  $0.0^\circ$

(e) (Concluded)

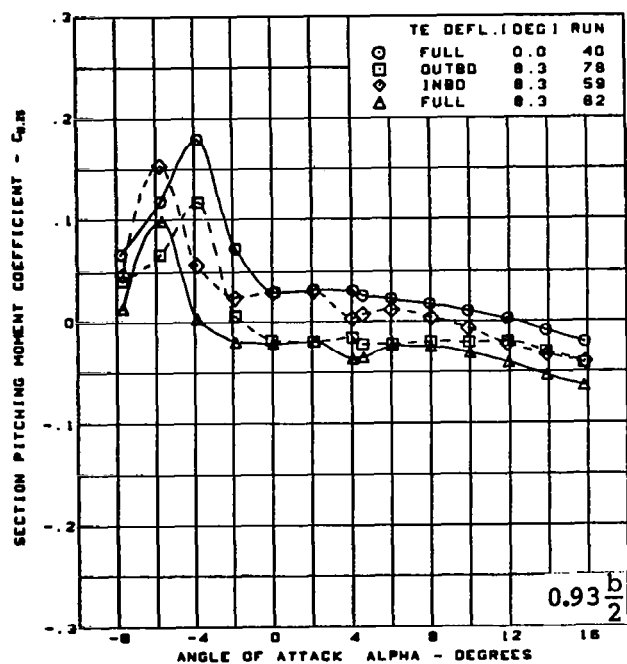
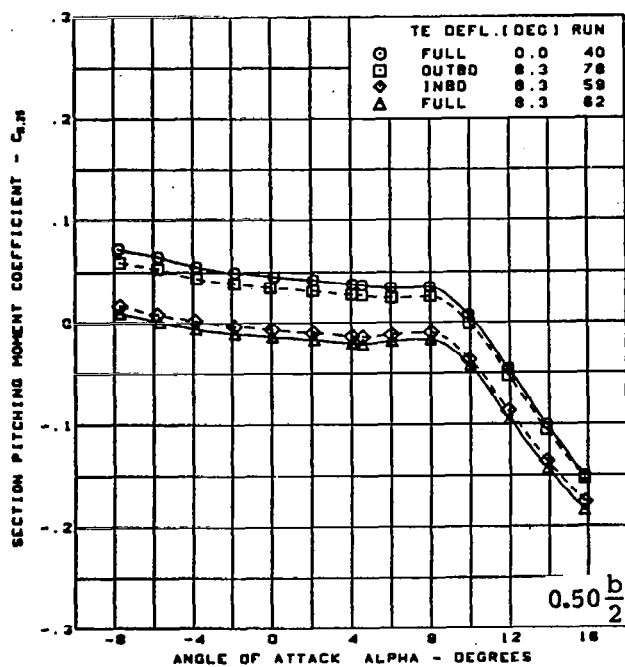
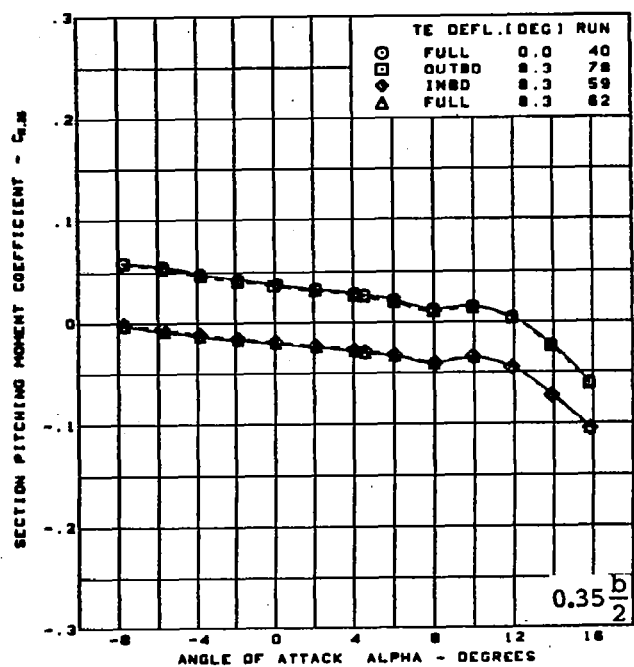
Figure 35. - (Continued)





(f) Section Aerodynamic Coefficients - Pitching Moment

Figure 35. - (Continued)

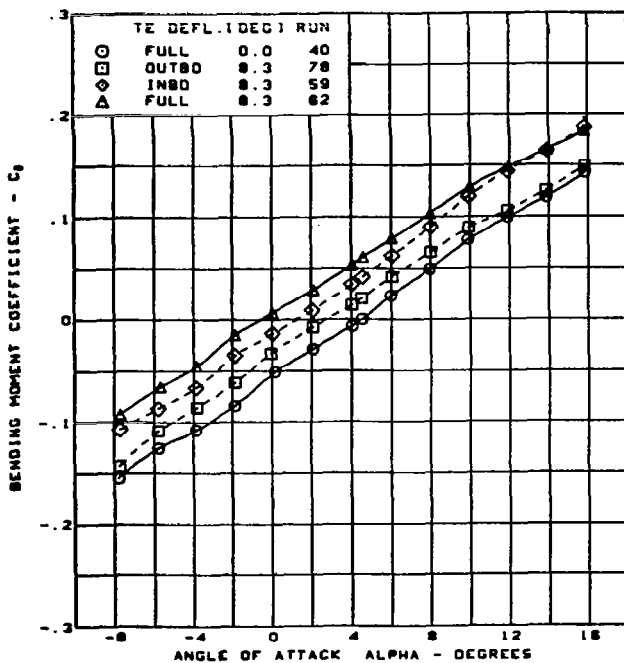
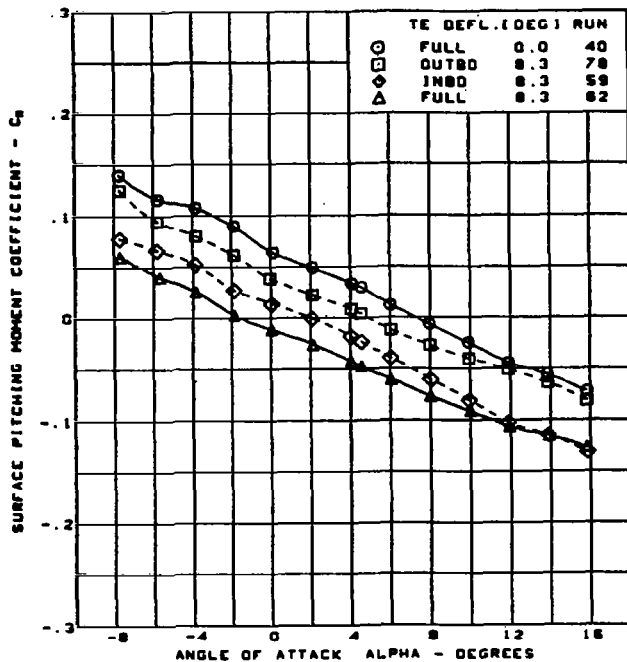
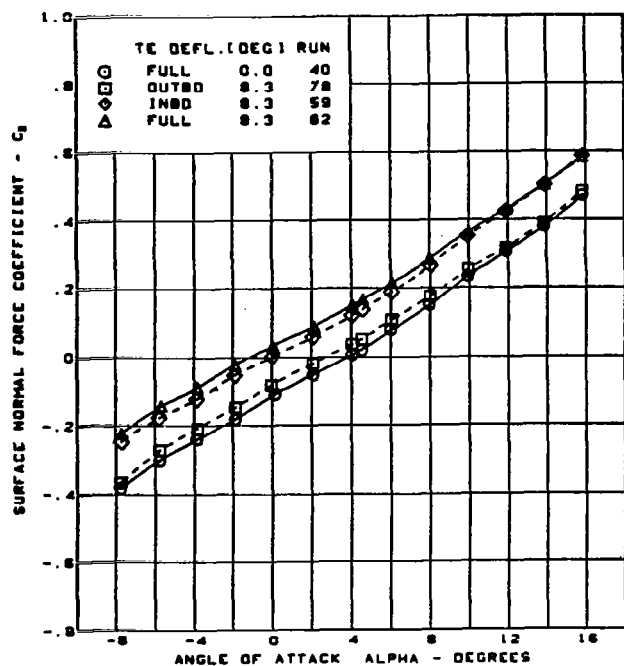


M = 0.85  
 Cambered-twisted wing, rounded L.E.  
 Fin off  
 L.E. deflection, full span = 0.0°

(f) (Concluded)

Figure 35. — (Continued)



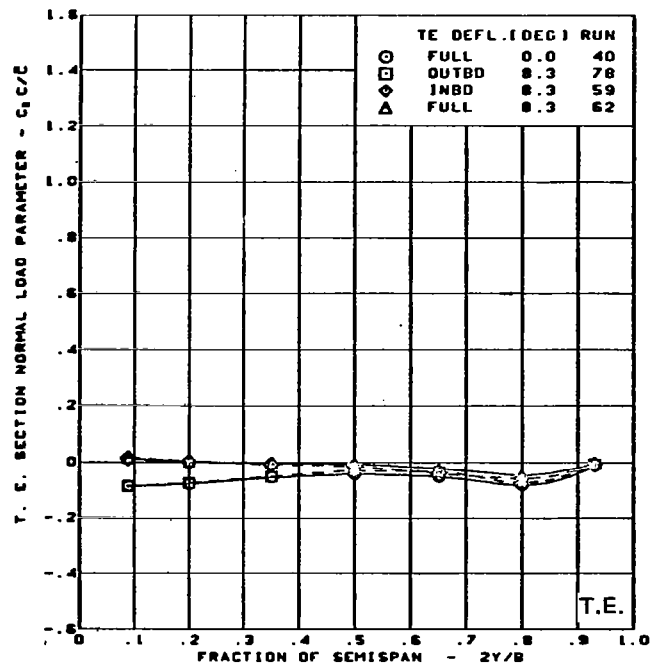
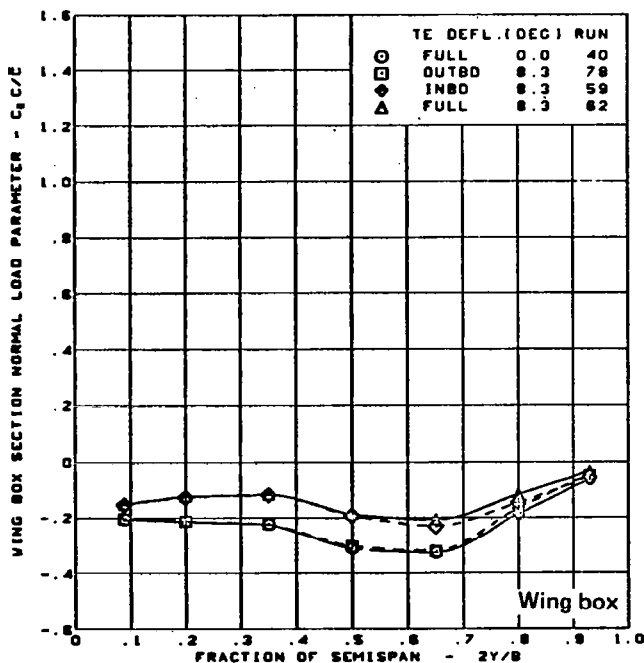
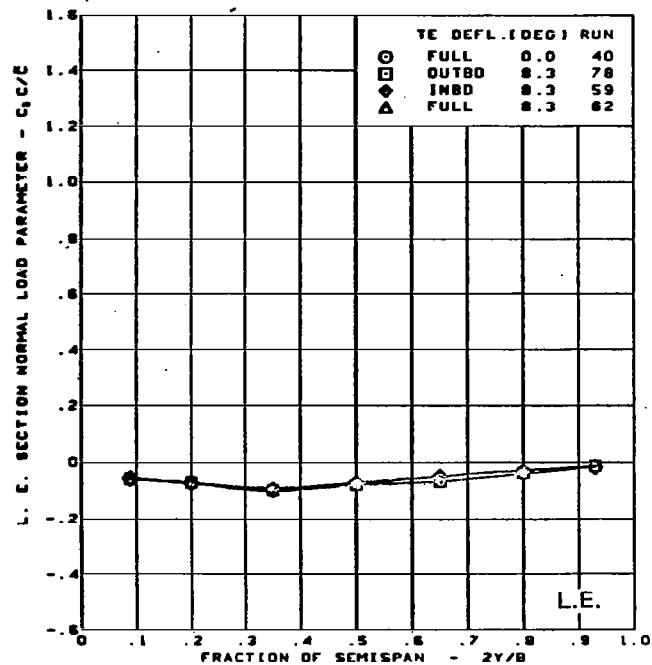
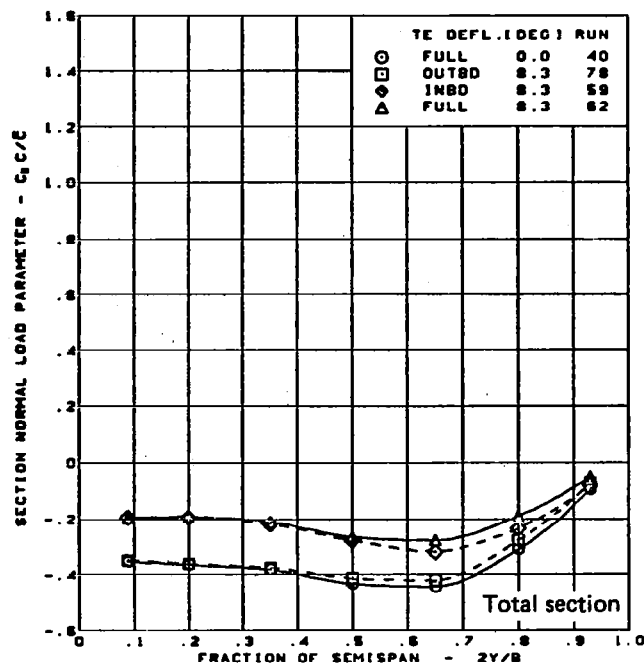


$M = 0.85$   
 Cambered-twisted wing, rounded L.E.  
 Fin off  
 L.E. deflection, full span =  $0.0^\circ$

(g) Wing Aerodynamic Coefficients

Figure 35. — (Concluded)





$M = 0.85$

$\alpha = -8^\circ$

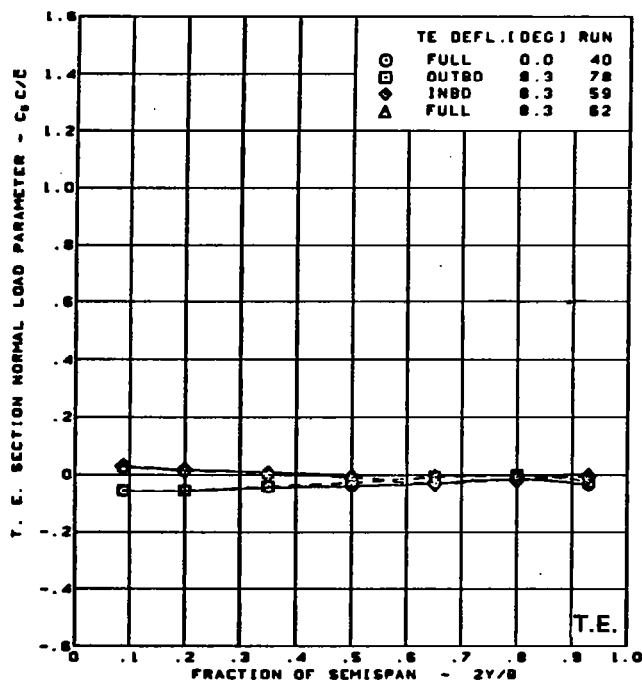
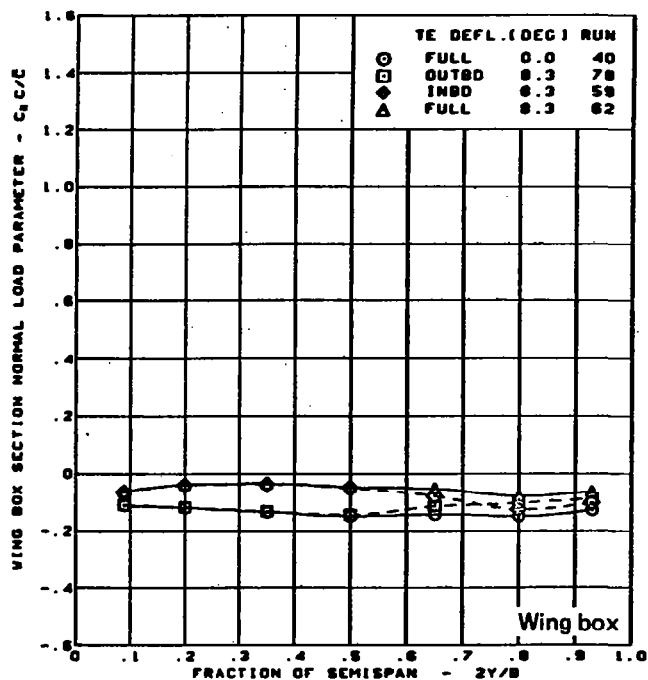
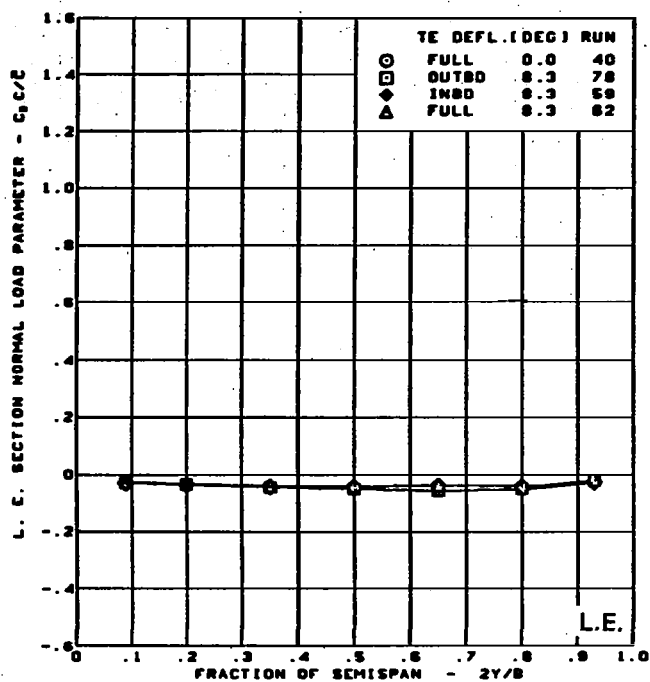
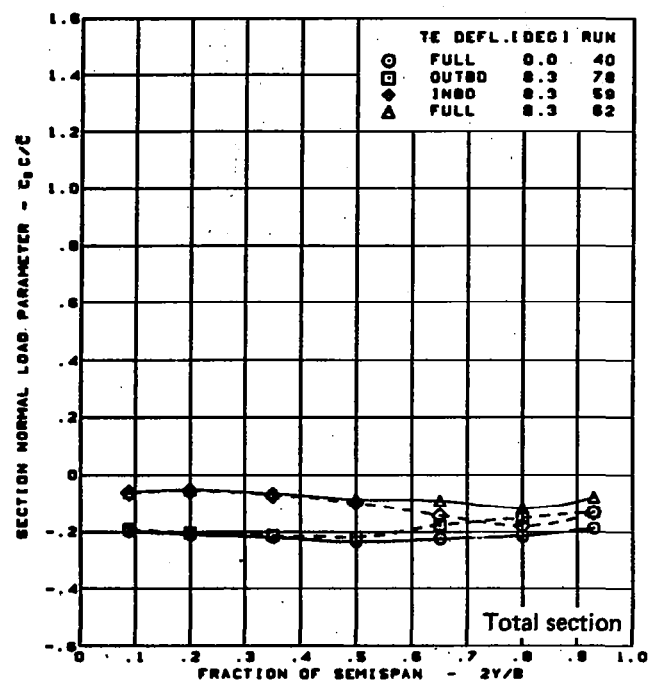
Cambered-twisted wing, rounded L.E.

Fin off

L.E. deflection, full span =  $0.0^\circ$

(a) Spanload Distributions - Normal Force,  $\alpha = -8^\circ$

Figure 36. — Wing Experimental Data—Effect of Full- and Partial Span Trailing Edge Control Surface Deflection on Chordwise Segments; Cambered-Twisted Wing; Fin Off;  $M = 0.85$



$M = 0.85$

$\alpha = -4^\circ$

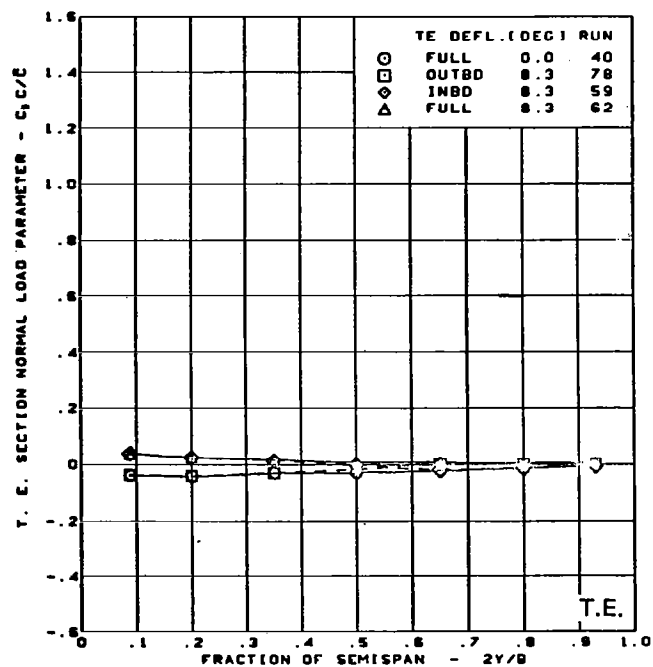
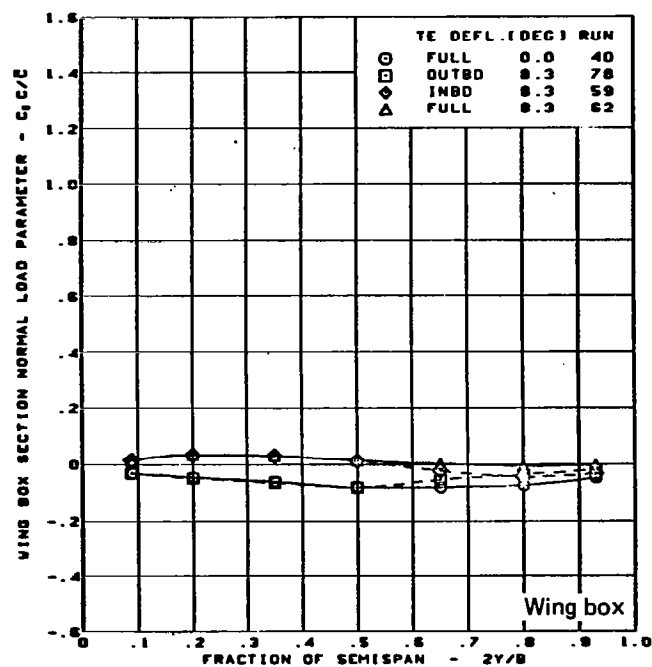
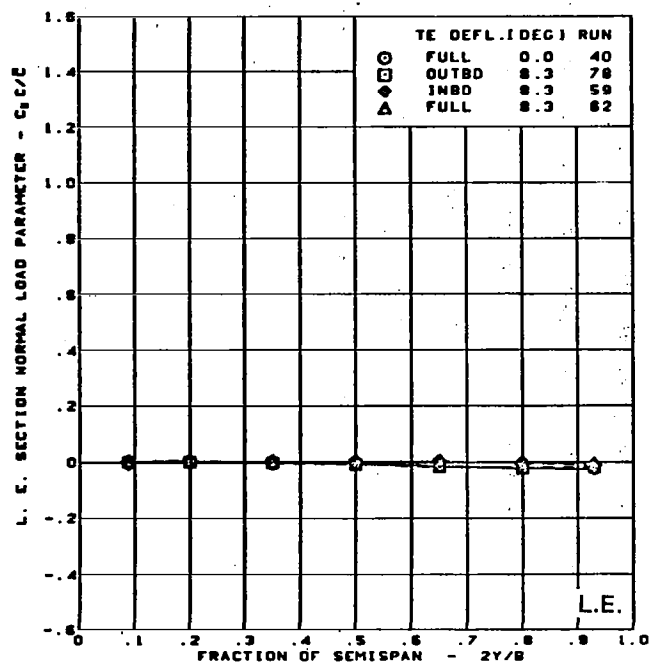
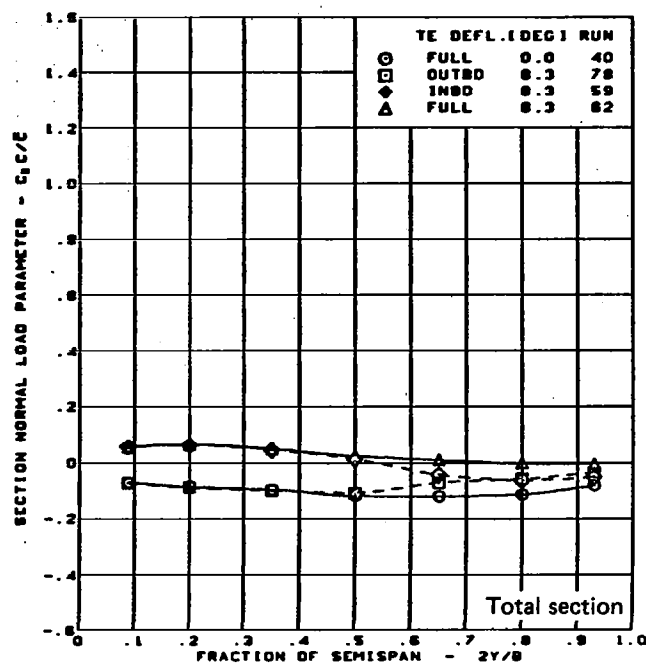
Cambered-twisted wing, rounded L.E.

Fin off

L.E. deflection, full span =  $0.0^\circ$

(b) Spanload Distributions - Normal Force,  $\alpha = -4^\circ$

Figure 36. - (Continued)



$M = 0.85$

$\alpha = 0^\circ$

Cambered-twisted wing, rounded L.E.

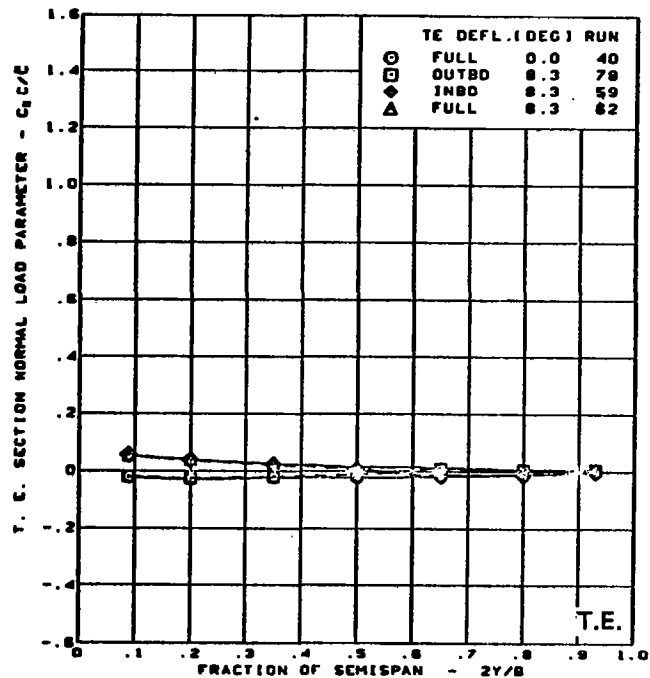
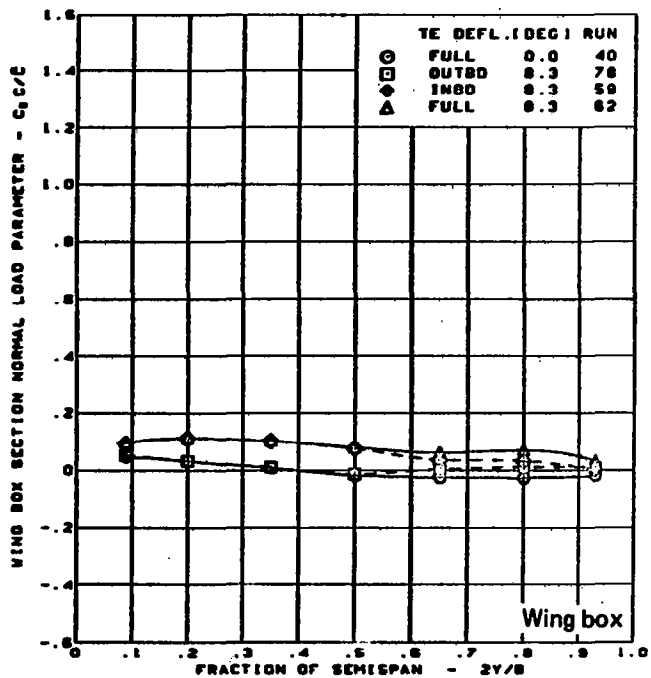
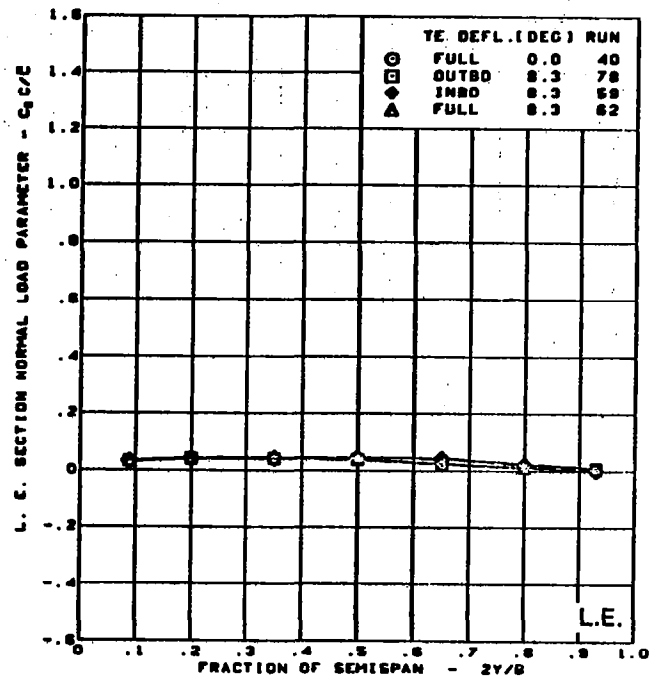
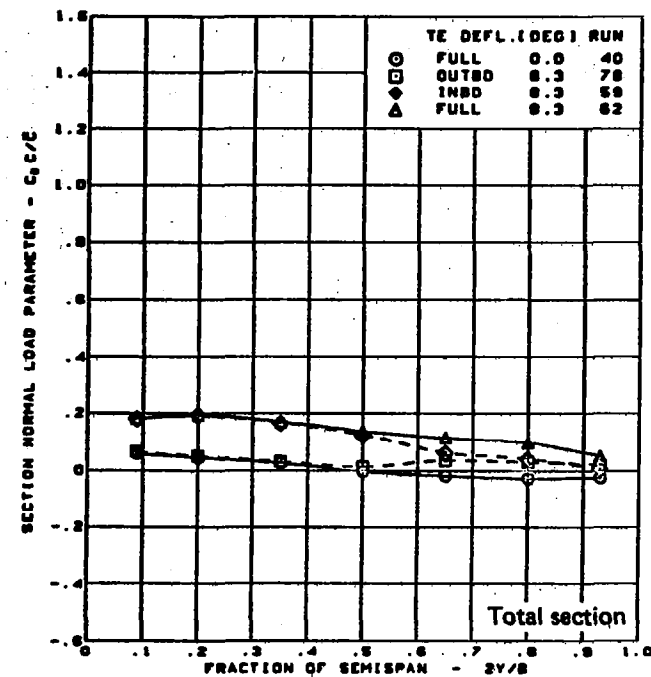
Fin off

L.E. deflection, full span =  $0.0^\circ$

(c) Spanload Distributions - Normal Force,  $\alpha = 0^\circ$

Figure 36. — (Continued)





$M = 0.85$

$\alpha = 4^\circ$

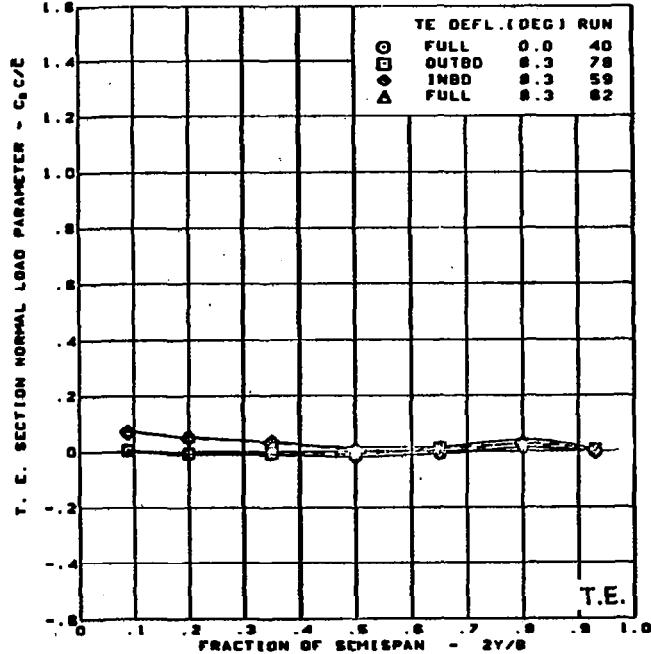
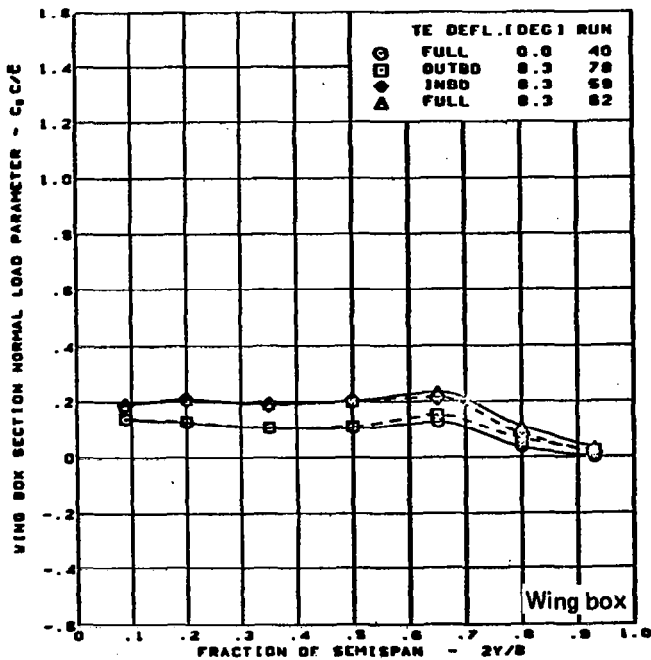
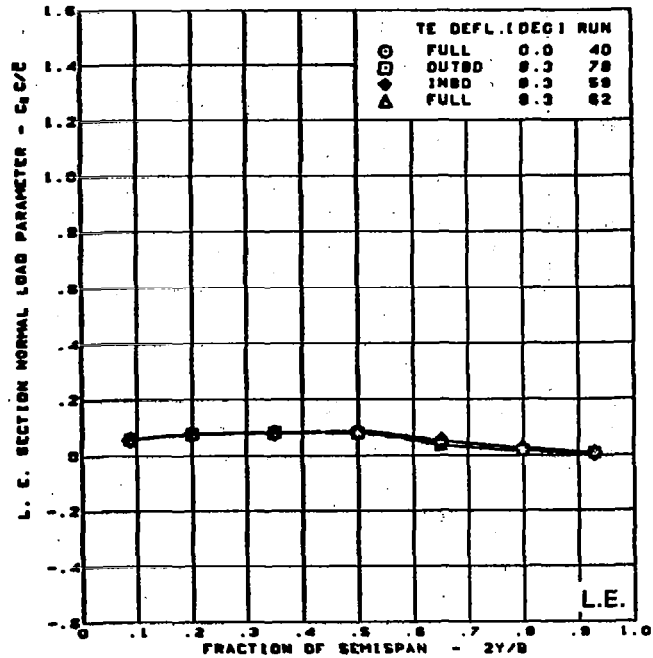
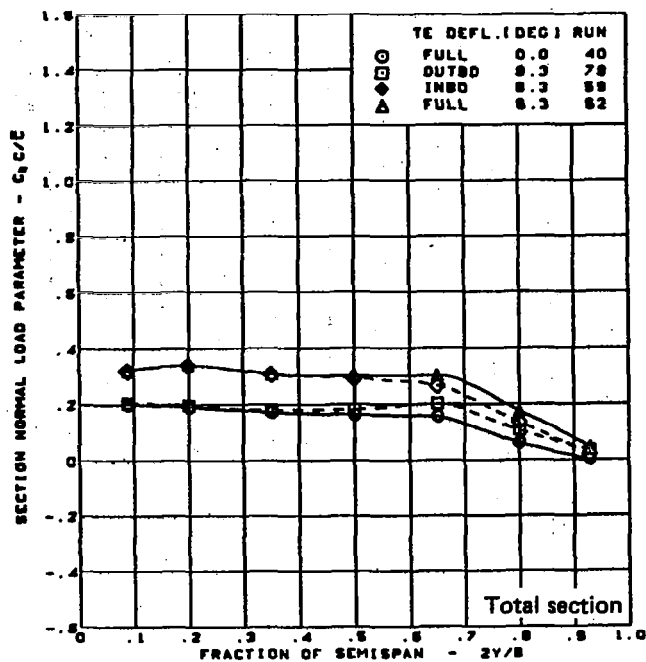
Cambered-twisted wing, rounded L.E.

Fin off

L.E. deflection, full span =  $0.0^\circ$

(d) Spanload Distributions - Normal Force,  $\alpha = 4^\circ$

Figure 36. - (Continued)



$M = 0.85$

$\alpha = 8^\circ$

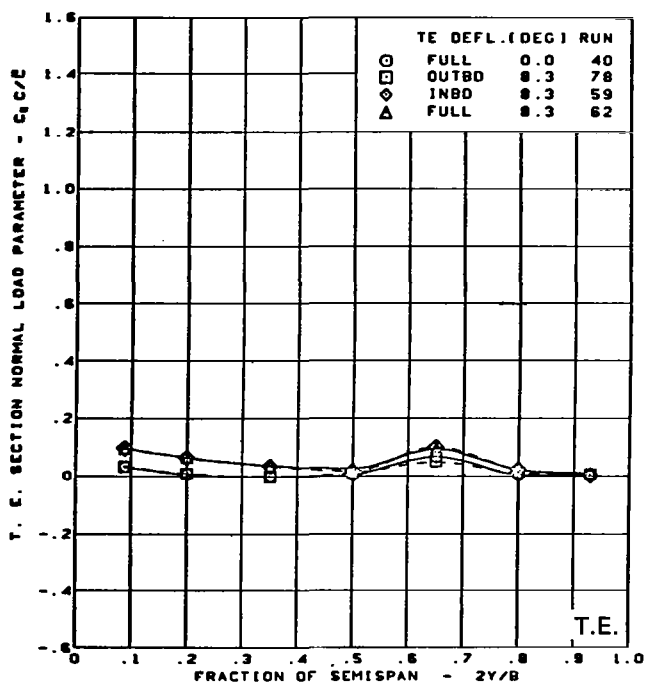
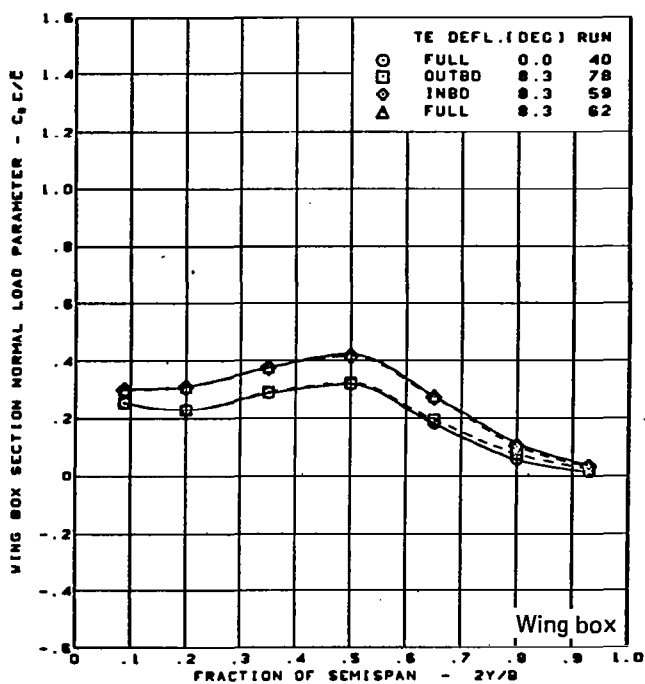
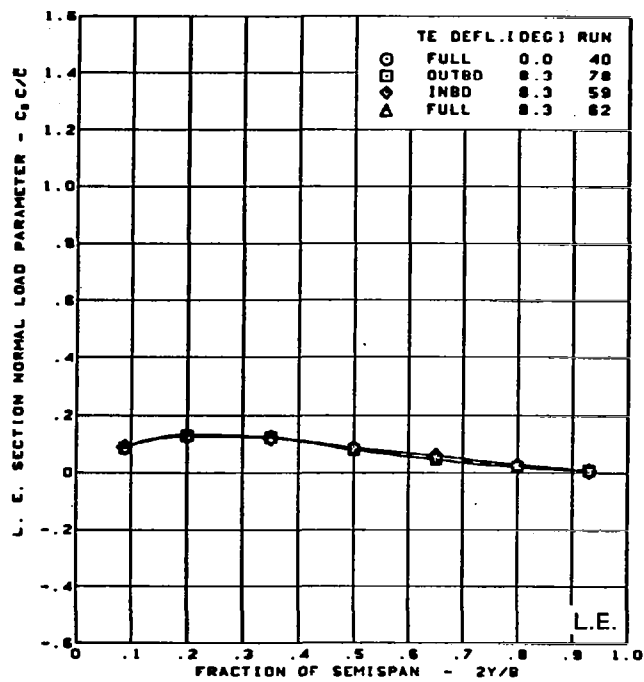
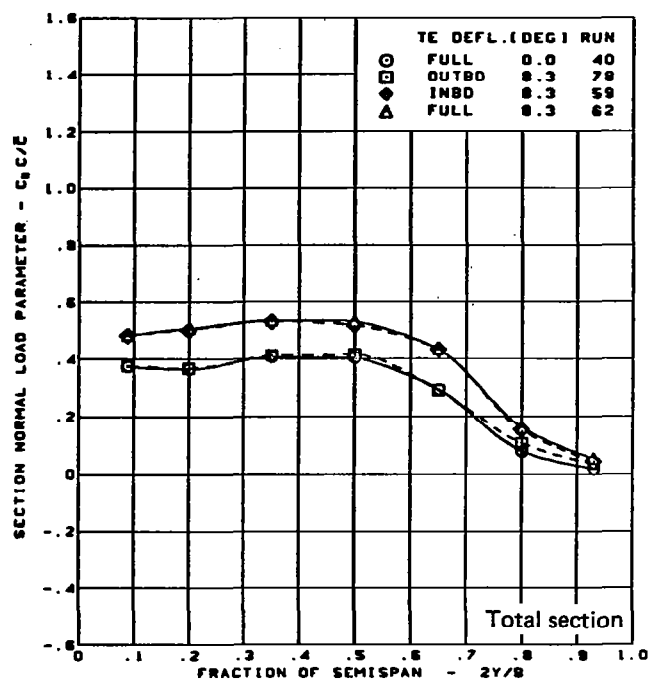
Cambered-twisted wing, rounded L.E.

Fin off

L.E. deflection, full span =  $0.0^\circ$

(e) Spanload Distributions - Normal Force,  $\alpha = 8^\circ$

Figure 36. - (Continued)



$M = 0.85$

$\alpha = 12^\circ$

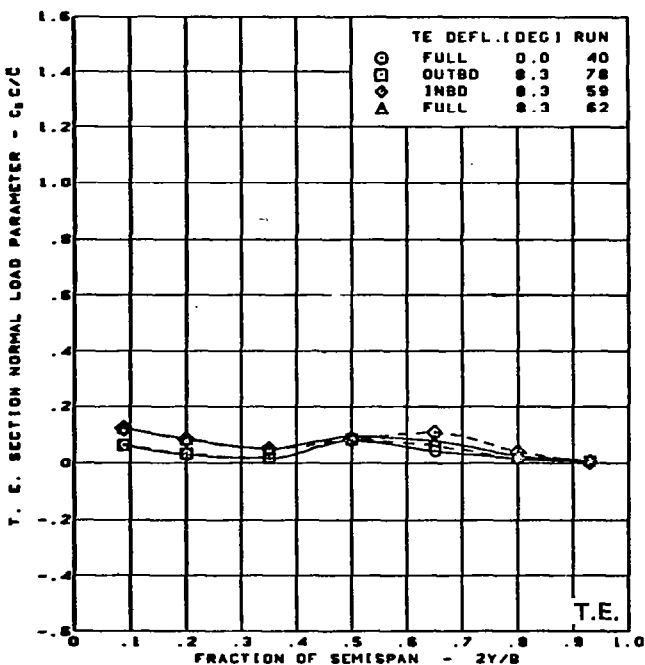
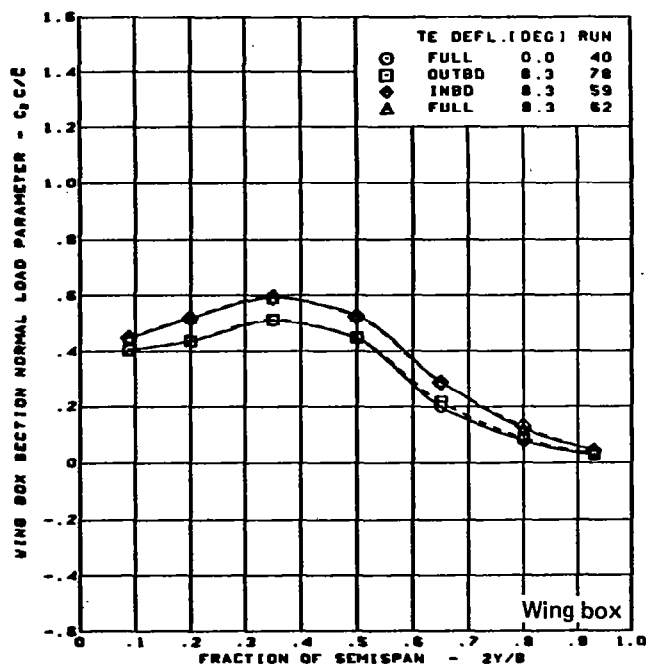
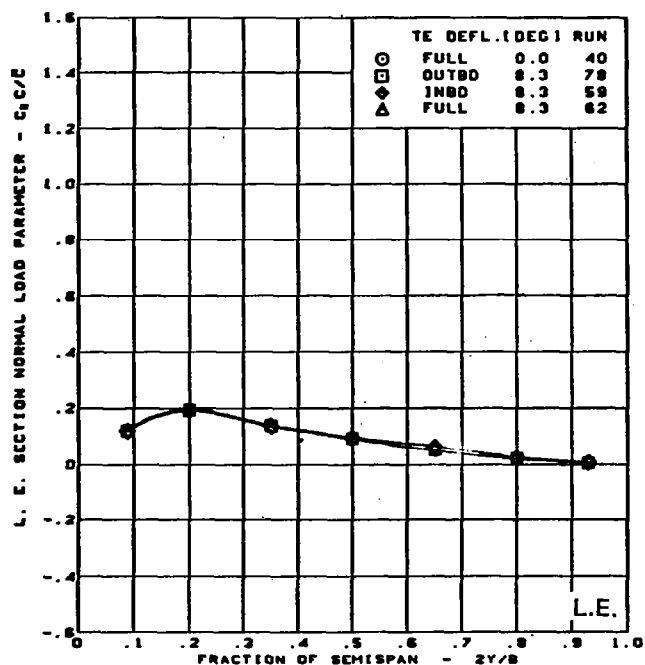
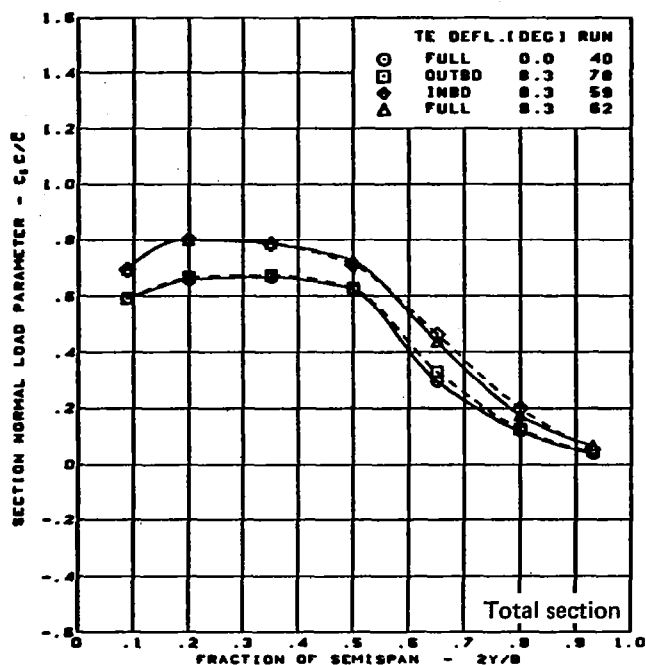
Cambered-twisted wing, rounded L.E.

Fin off

L.E. deflection, full span =  $0.0^\circ$

(f) Spanload Distributions - Normal Force,  $\alpha = 12^\circ$

Figure 36. - (Continued)



$M = 0.85$

$\alpha = 16^\circ$

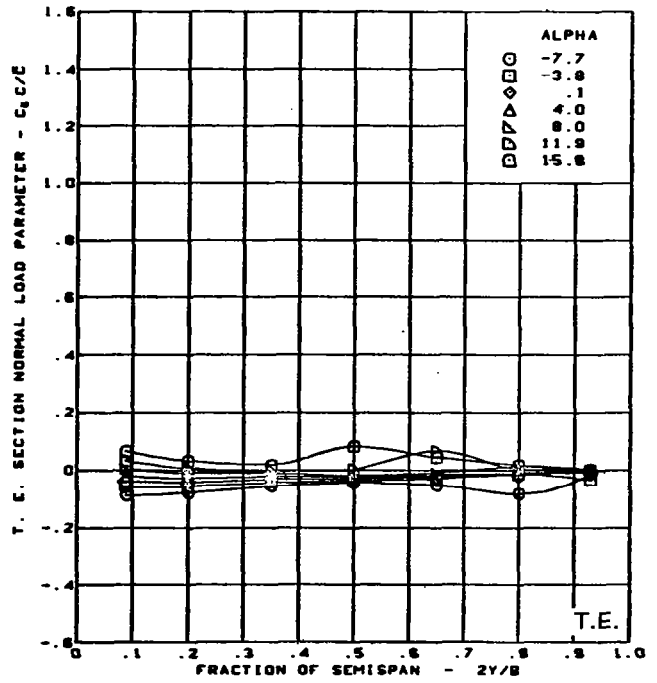
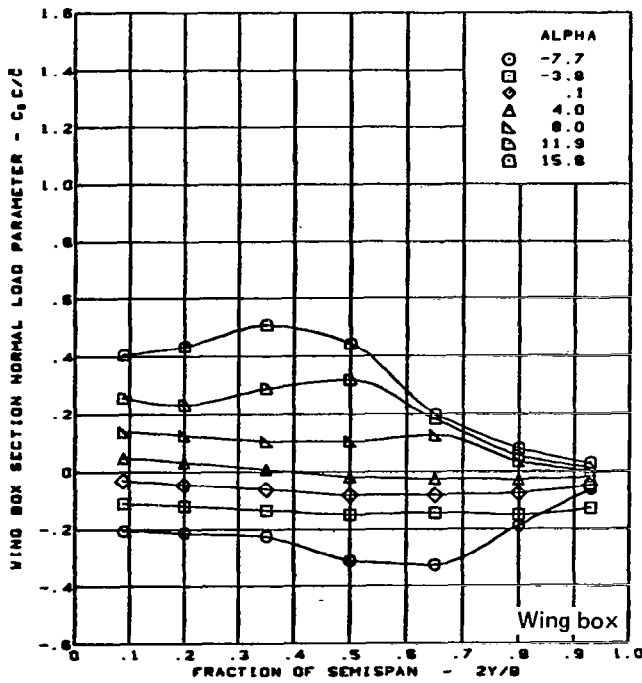
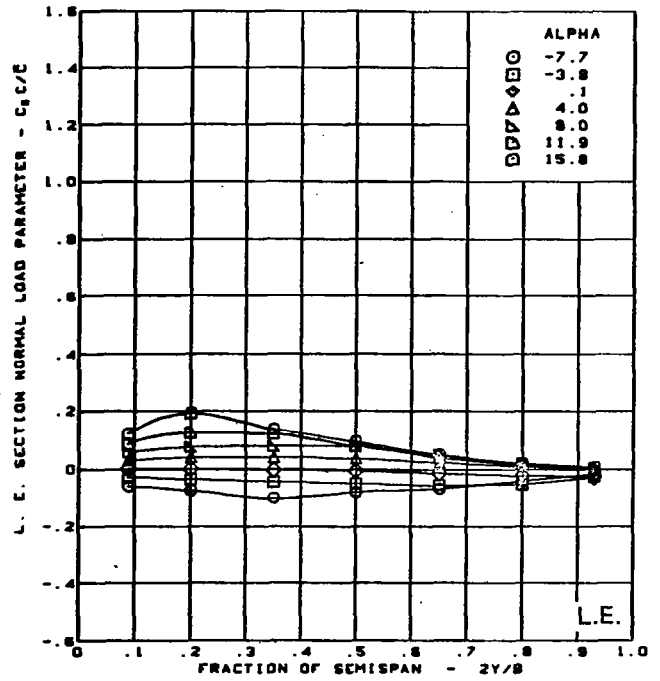
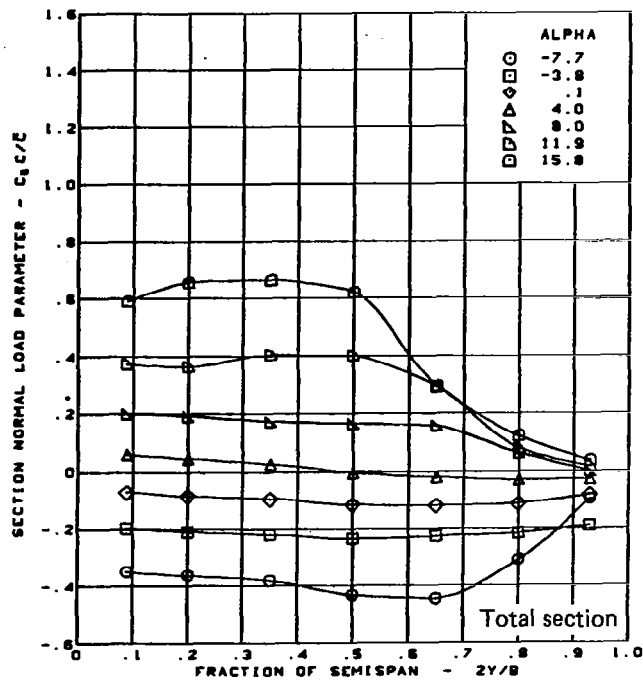
Cambered-twisted wing, rounded L.E.

Fin off

L.E. deflection, full span =  $0.0^\circ$

(g) Spanload Distributions - Normal Force,  $\alpha = 16^\circ$

Figure 36. - (Continued)

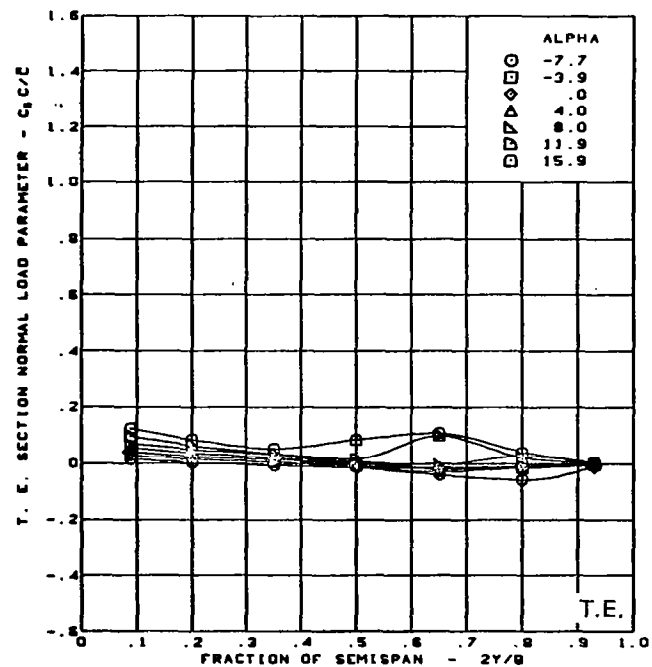
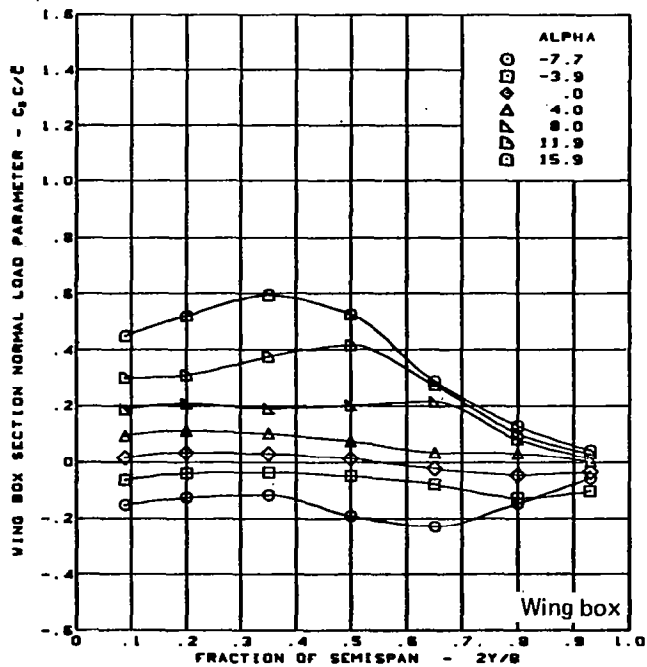
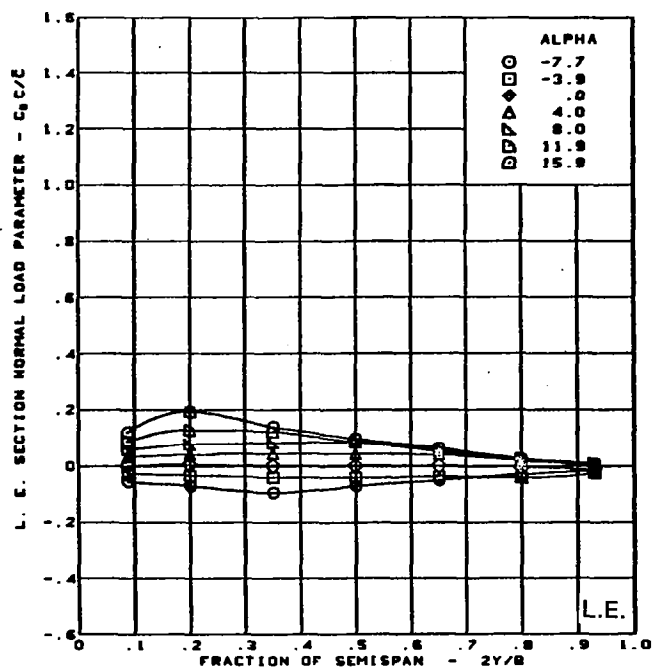
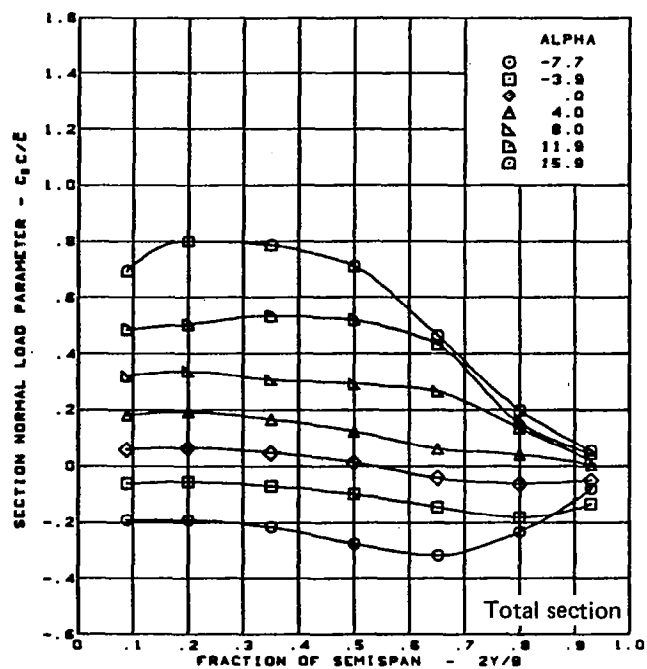


M = 0.85  
Cambered-twisted wing, rounded L.E.  
Fin off

L.E. deflection, full span =  $0.0^\circ$   
T.E. deflection, full span =  $0.0^\circ$

(h) Spanload Distributions - Normal Force, T.E. Deflection, Full Span =  $0.0^\circ$

Figure 36. - (Continued)



$M = 0.85$

Cambered-twisted wing, rounded L.E.

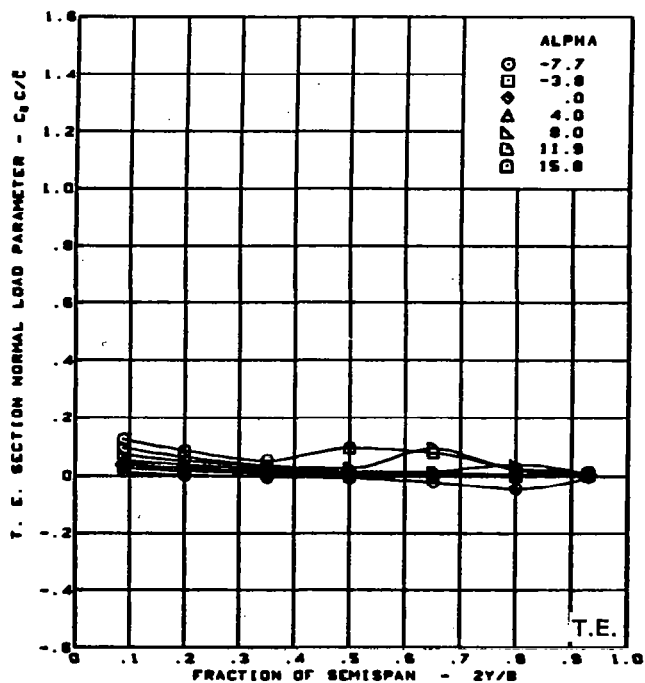
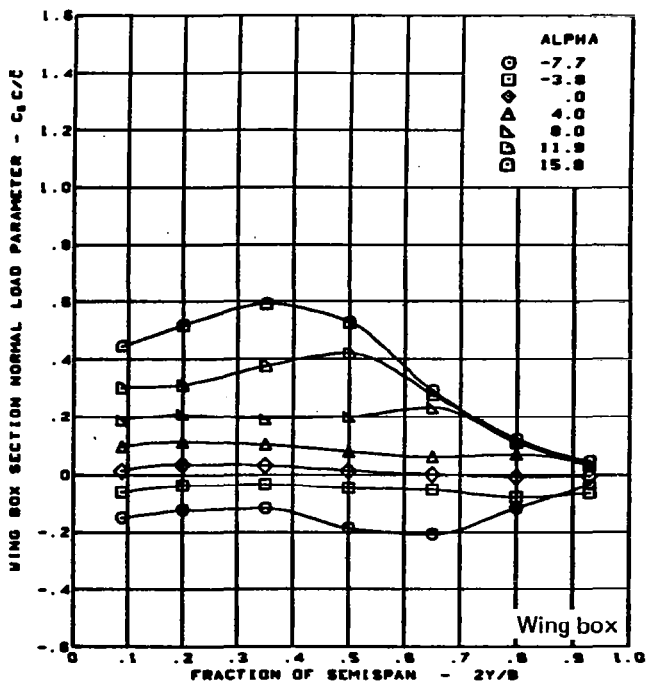
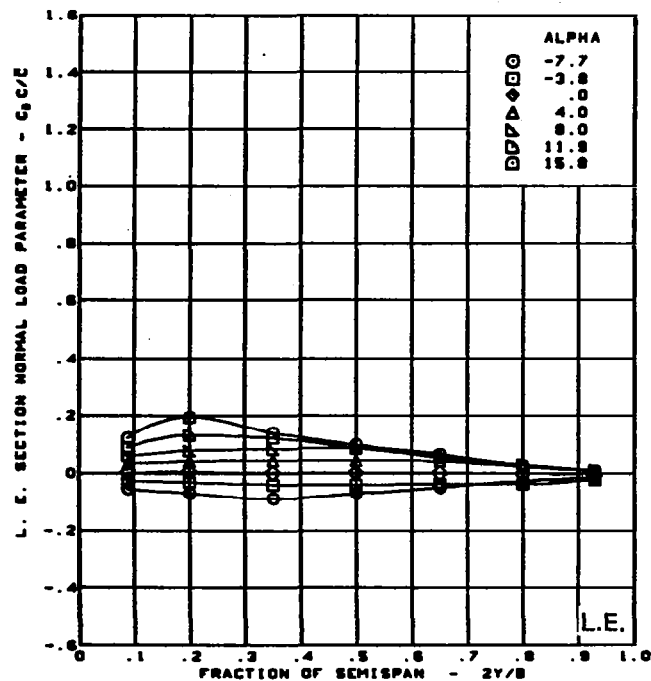
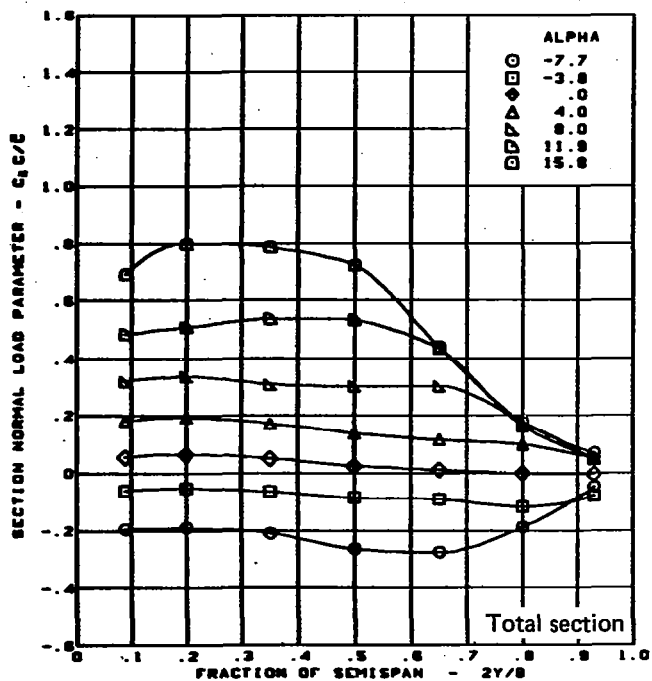
Fin off

(i) Spanload Distributions - Normal Force, T.E. Deflection, Inboard =  $8.3^\circ$ , Outboard =  $0.0^\circ$

L.E. deflection, full span =  $0.0^\circ$

T.E. deflection, inboard =  $8.3^\circ$ , outboard =  $0.0^\circ$

Figure 36. - (Continued)



$M = 0.85$

Cambered-twisted wing, rounded L.E.

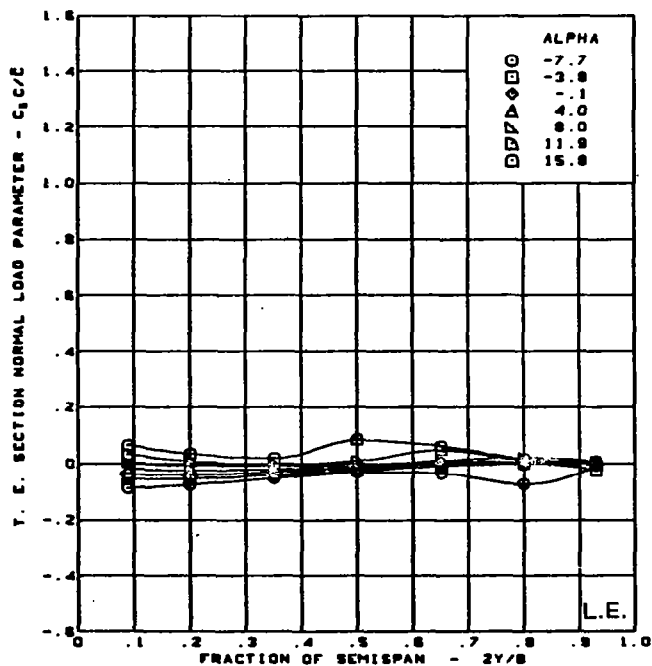
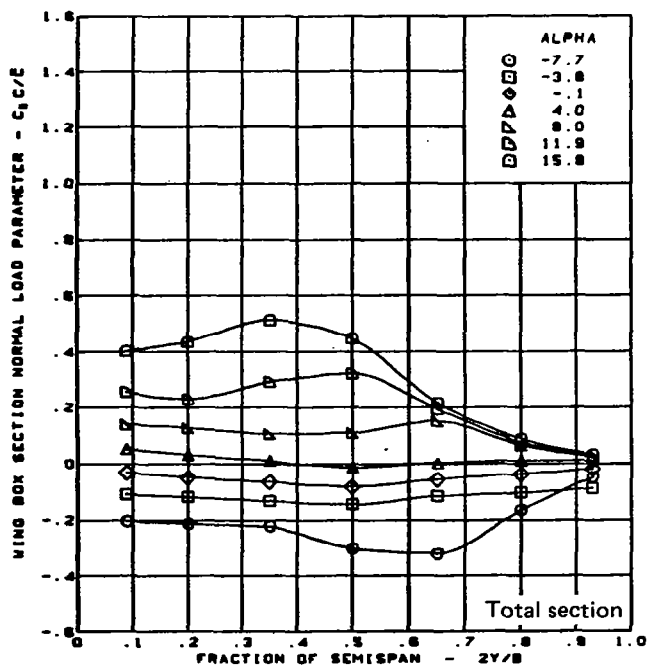
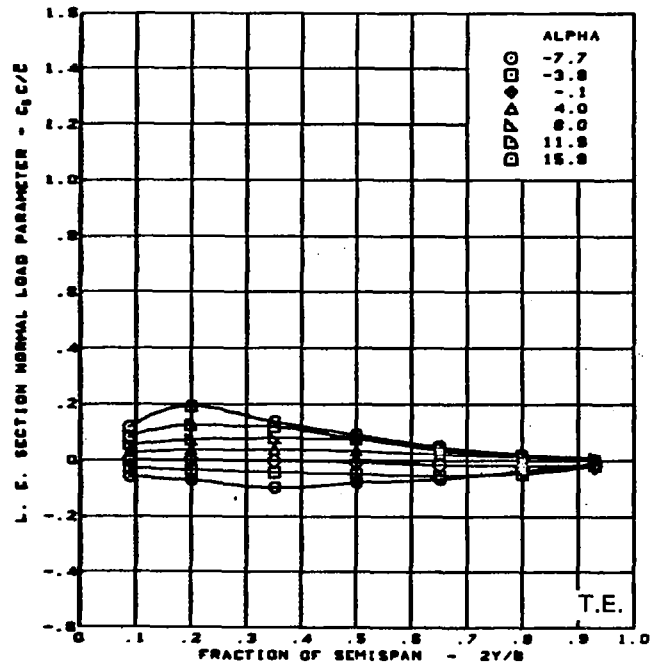
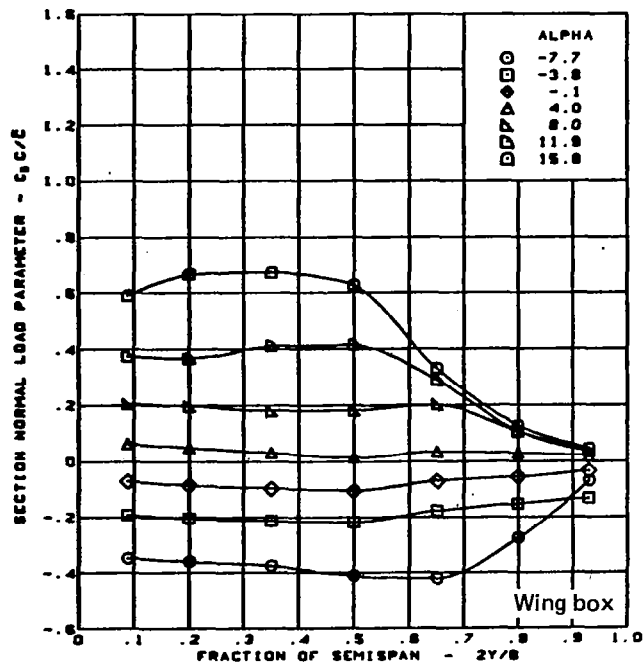
Fin off

(j) Spanload Distributions - Normal Force, T.E. Deflection, Inboard =  $0.0^\circ$ , Outboard =  $8.3^\circ$

L.E. deflection, full span =  $0.0^\circ$

T.E. deflection, inboard =  $0.0^\circ$ , outboard =  $8.3^\circ$

Figure 36. - (Continued)



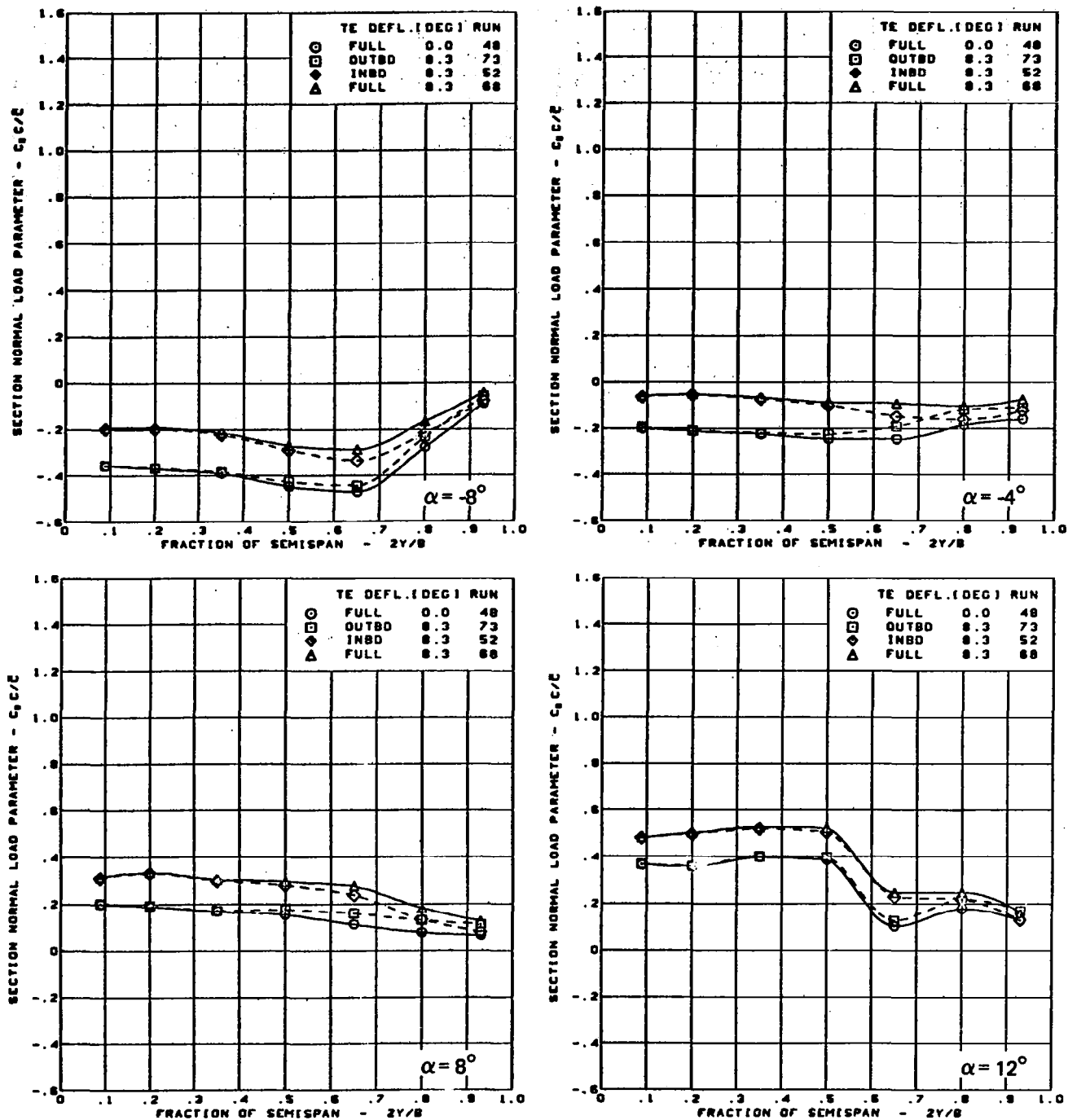
$M = 0.85$   
Cambered-twisted wing, rounded L.E.  
Fin off

L.E. deflection, full span  $= 0.0^\circ$   
T.E. deflection, full span  $= 8.3^\circ$

(k) Spanload Distributions - Normal Force, T.E. Deflection, Full Span  $= 8.3^\circ$

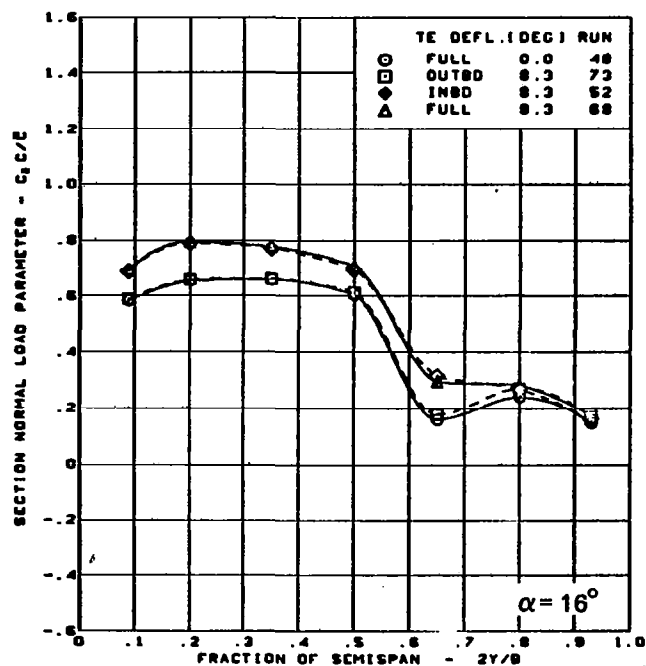
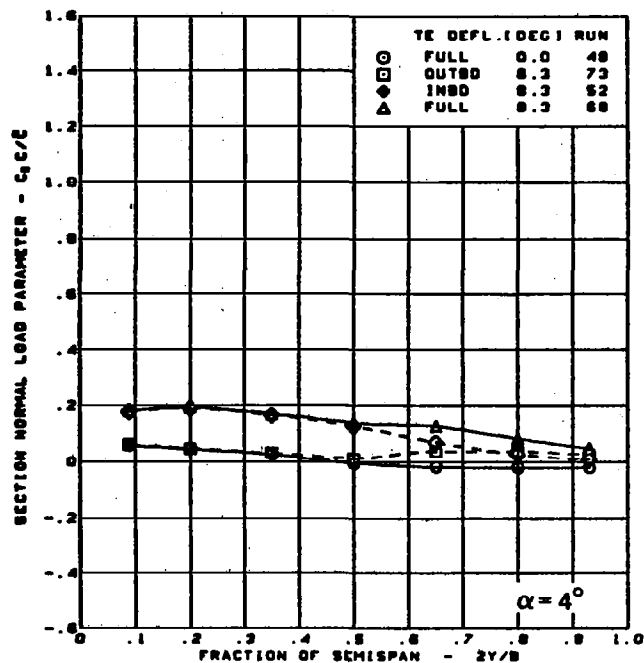
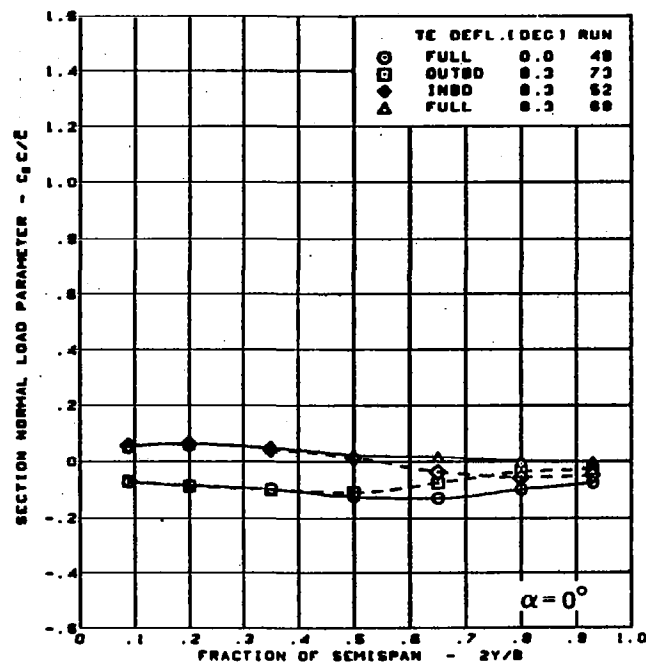
Figure 36. -- (Concluded)





(a) Spanload Distribution - Normal Force Variation With T.E. Control Surface Configuration

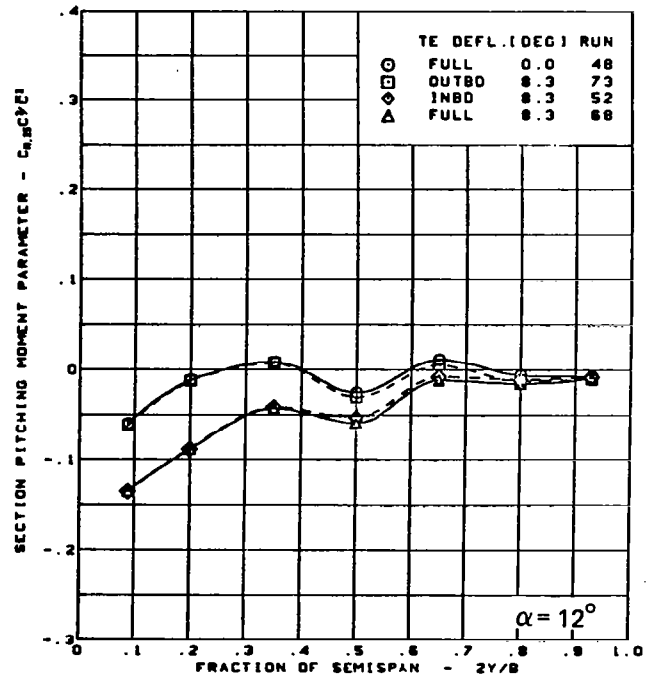
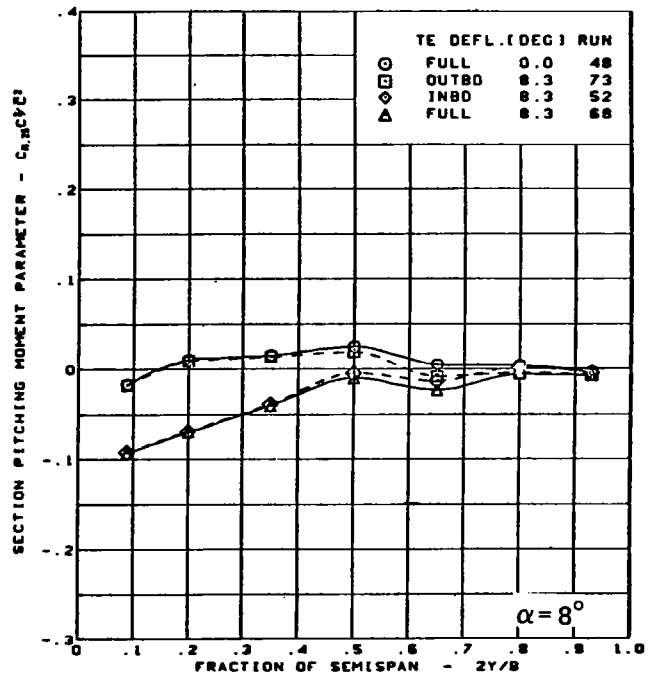
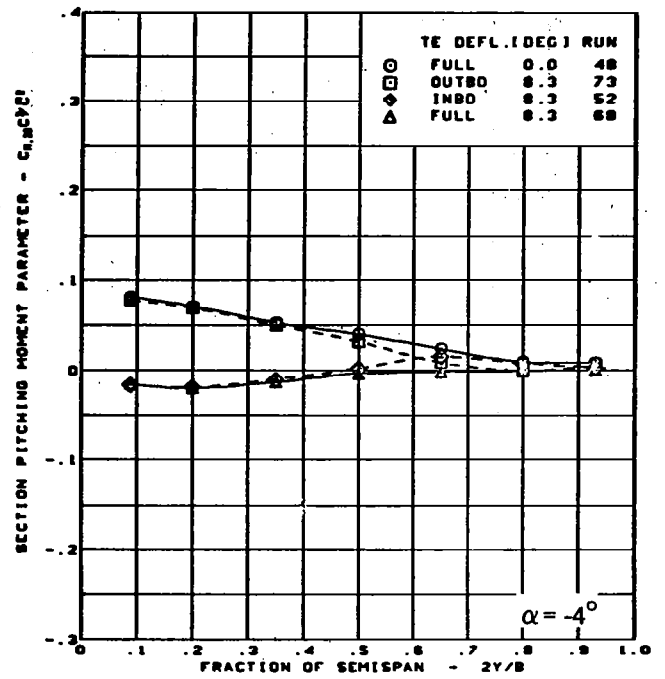
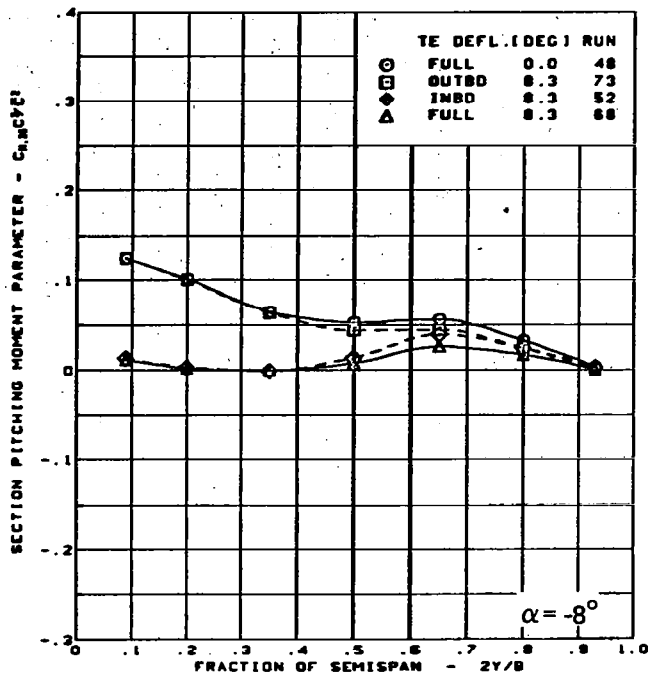
Figure 37. — Wing Experimental Data—Effect of Full- and Partial-Span Trailing Edge Control Surface Deflection; Cambered-Twisted Wing; Fin On;  $M = 0.85$



M = 0.85  
 Cambered-twisted wing, rounded L.E.  
 Fin on  
 L.E. deflection, full span =  $0.0^\circ$

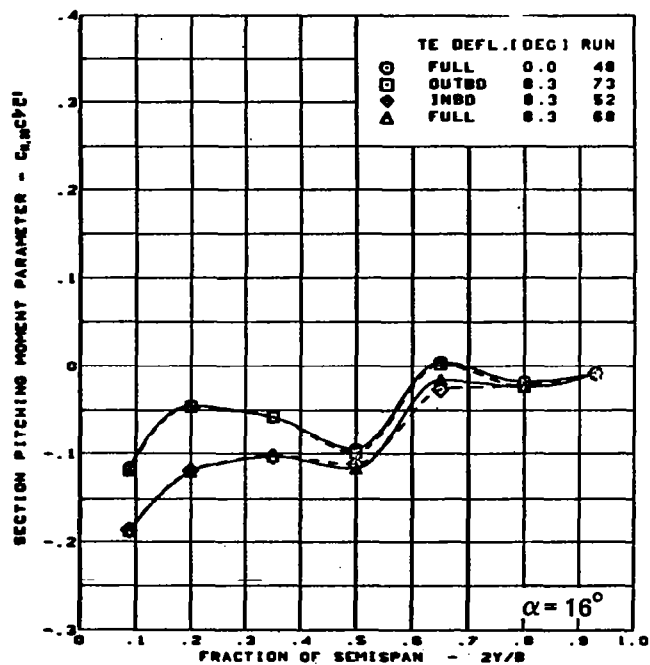
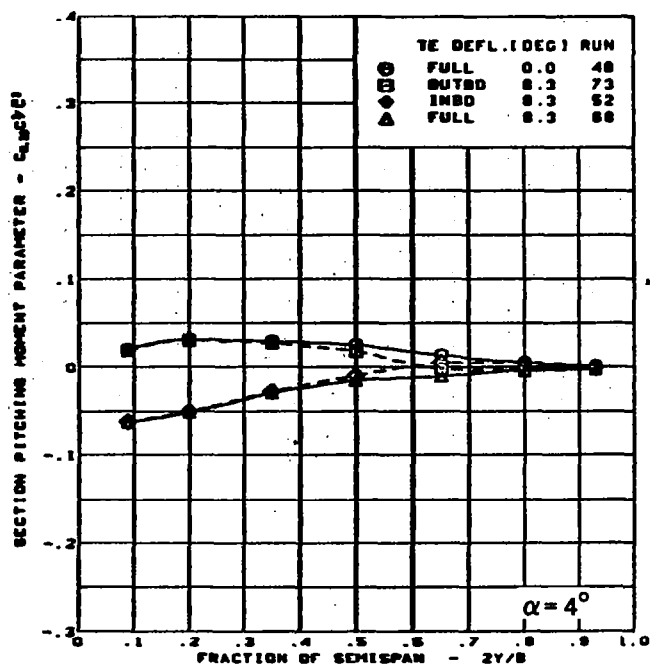
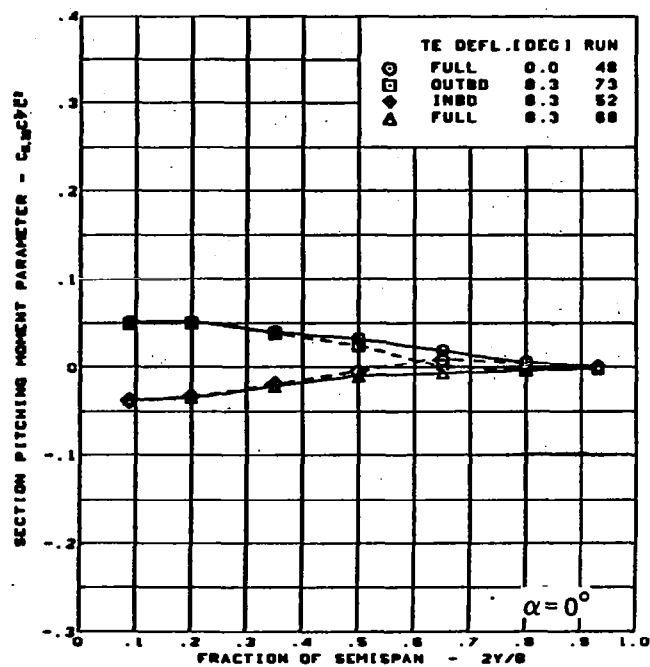
(a) (Concluded)

Figure 37. - (Continued)



(b) Spanload Distribution - Pitching Moment Variation With T.E. Control Surface Configuration

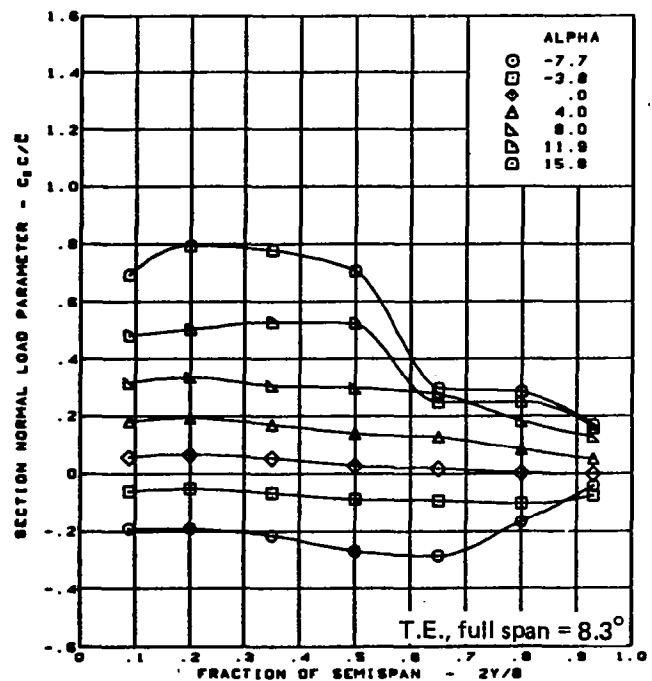
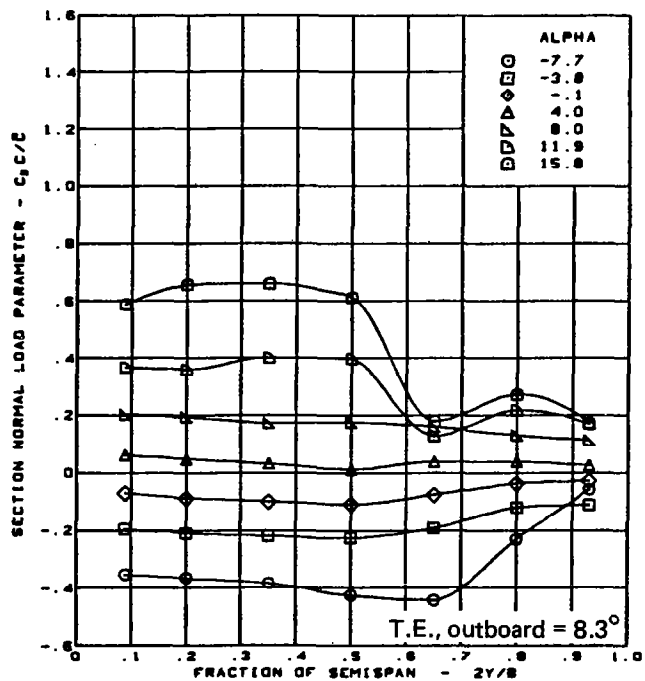
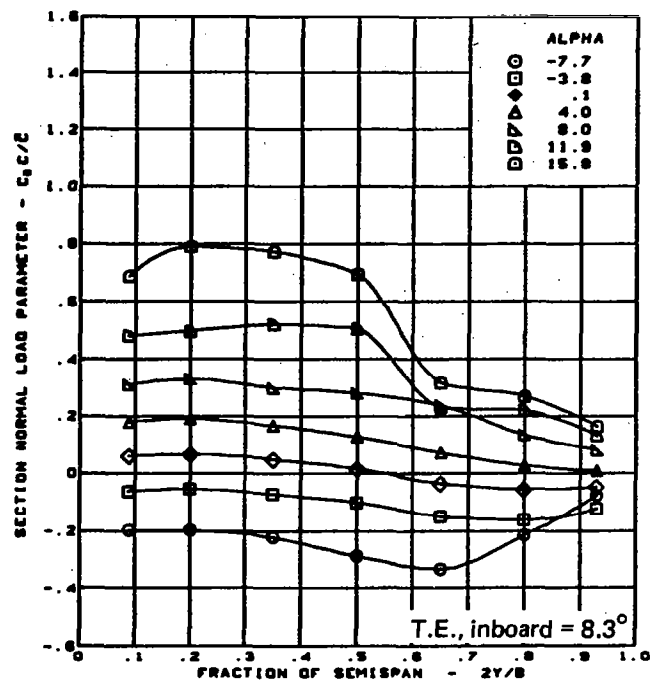
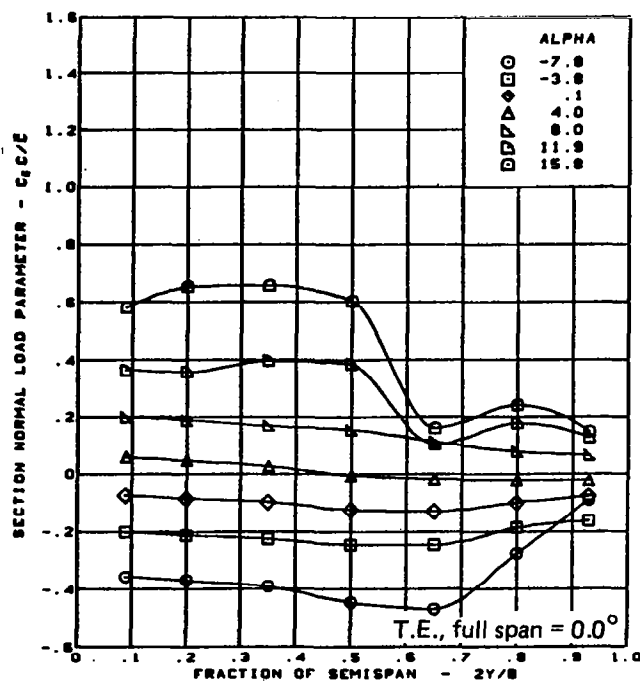
Figure 37. - (Continued)



$M = 0.85$   
 Cambered-twisted wing, rounded L.E.  
 Fin on  
 L.E. deflection, full span =  $0.0^\circ$

(b) (Concluded)

Figure 37. - (Continued)

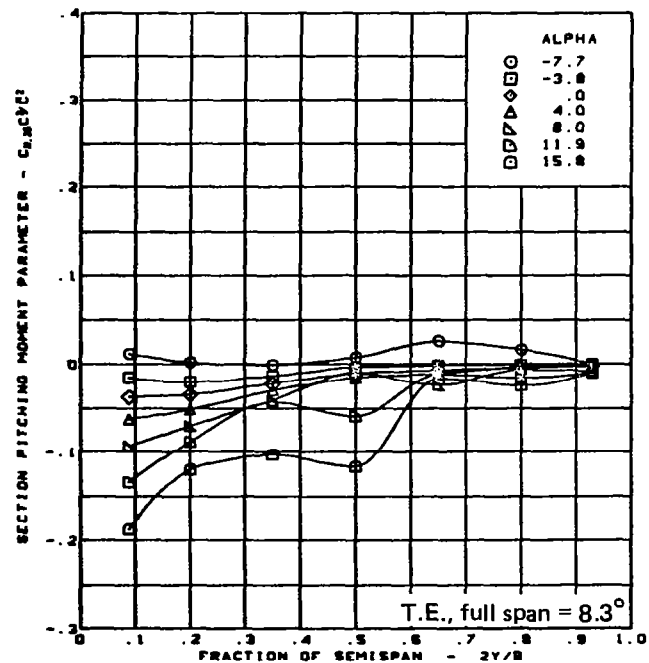
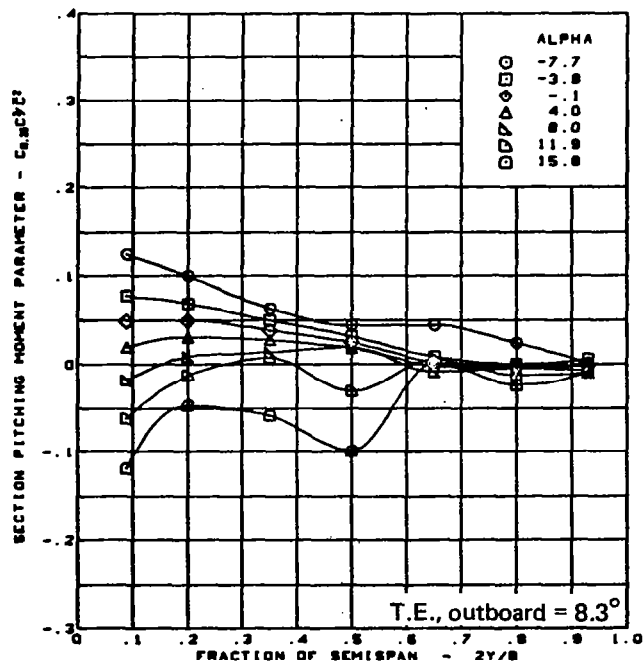
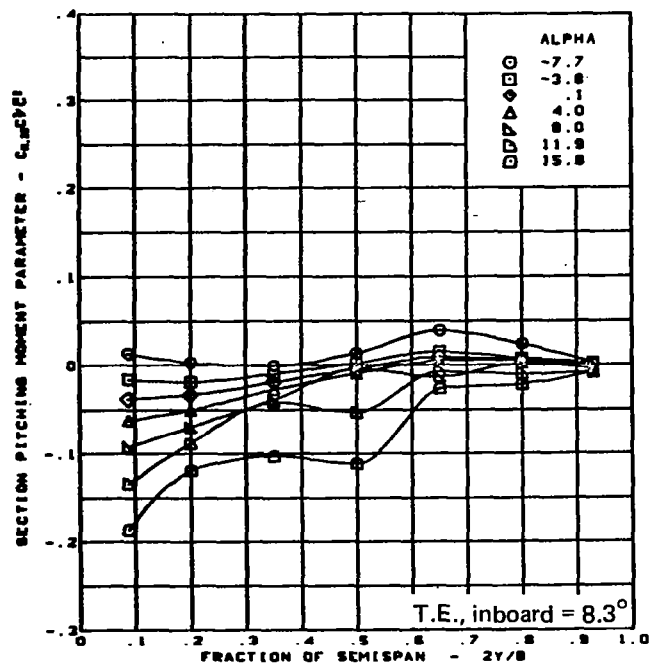
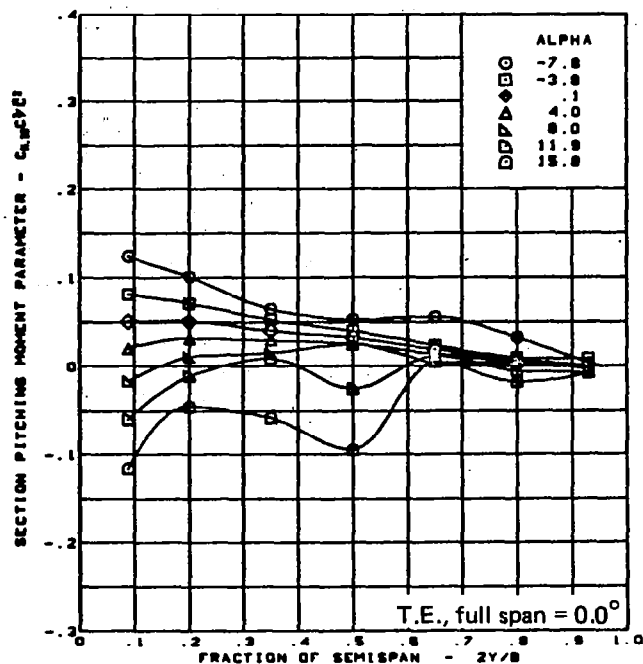


$M = 0.85$   
Cambered-twisted wing, rounded L.E.

Fin on  
L.E. deflection, full span =  $0.0^\circ$

(c) Spanload Distribution - Normal Force Variation With Angle of Attack

Figure 37. — (Continued)

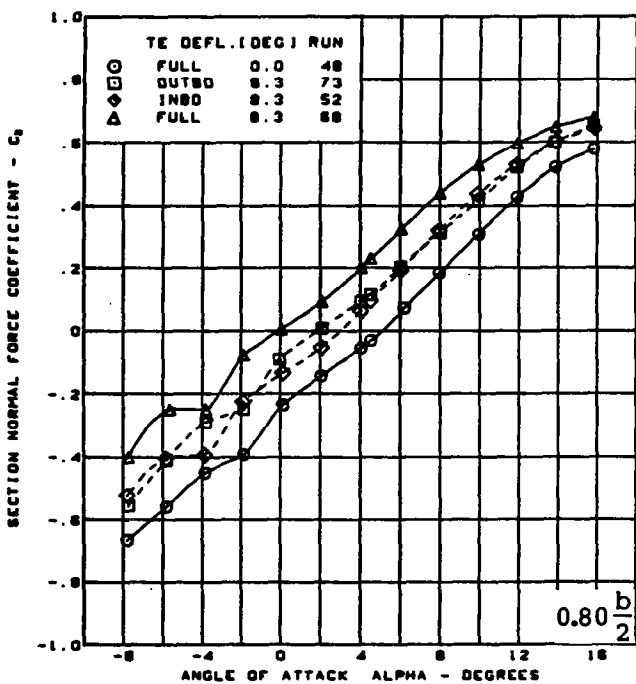
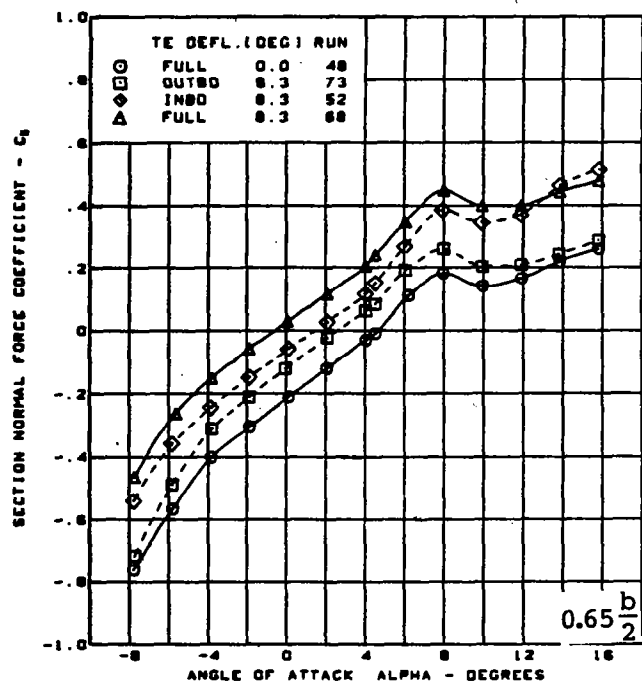
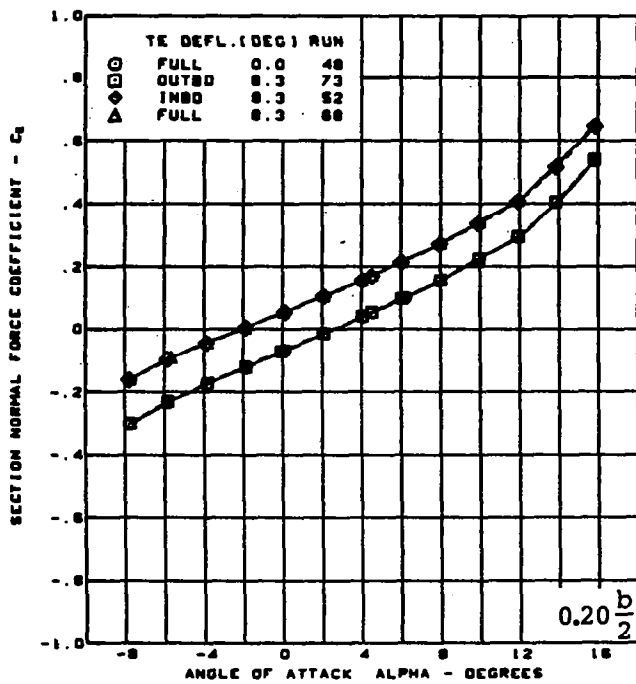
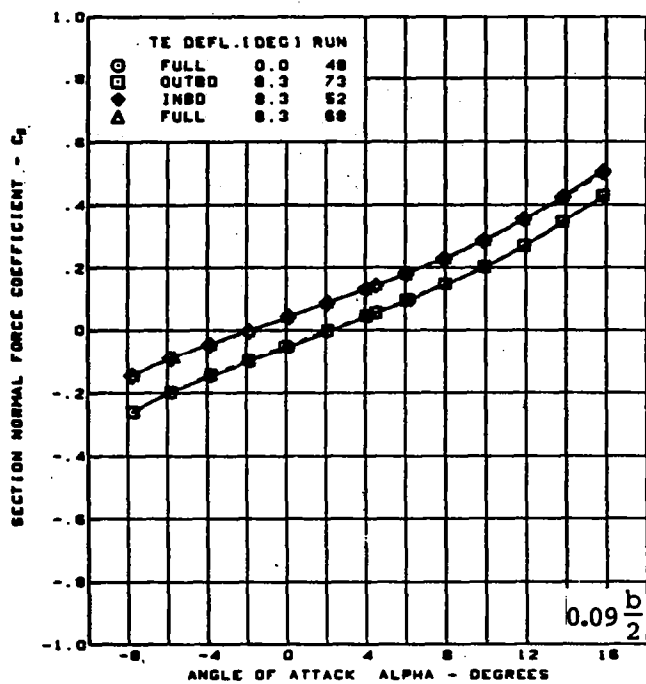


M = 0.85  
Cambered-twisted wing, rounded L.E.

Fin on  
L.E. deflection, full span =  $0.0^\circ$

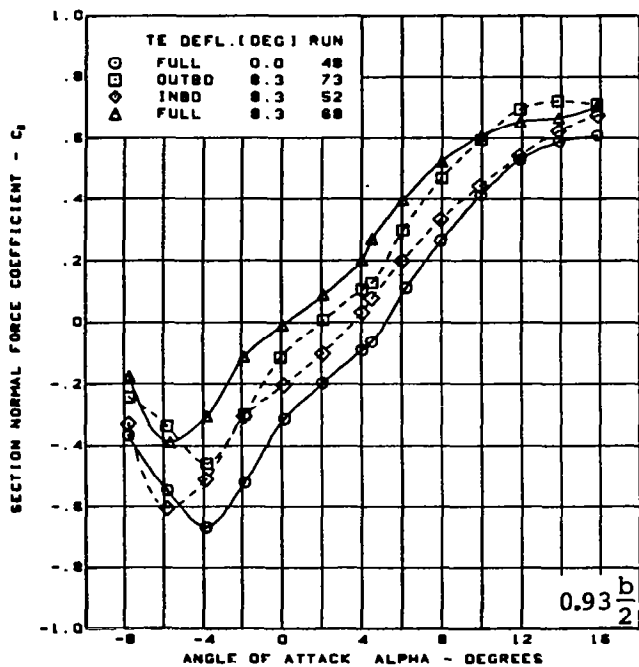
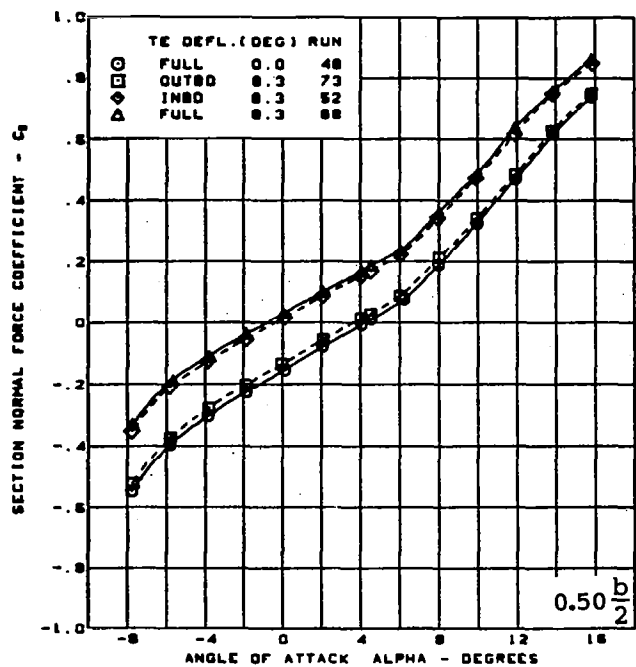
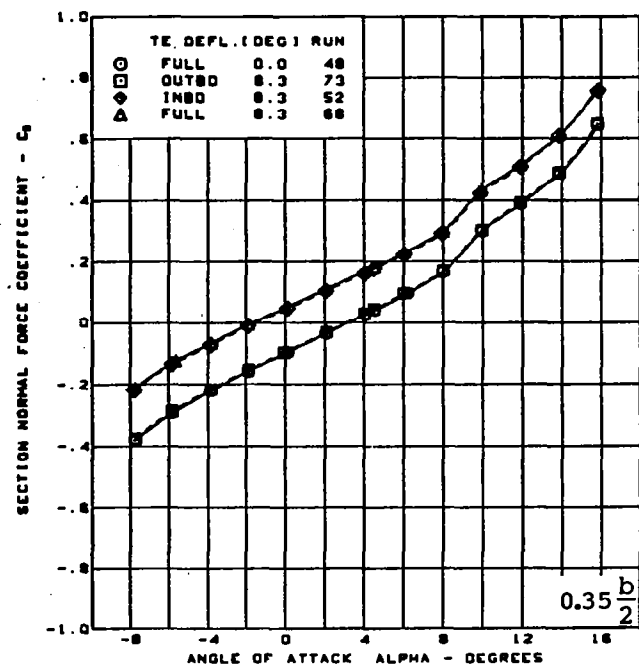
(d) Spanload Distribution - Pitching Moment Variation With Angle of Attack

Figure 37. - (Continued)



(e) Section Aerodynamic Coefficients - Normal Force

Figure 37. - (Continued)

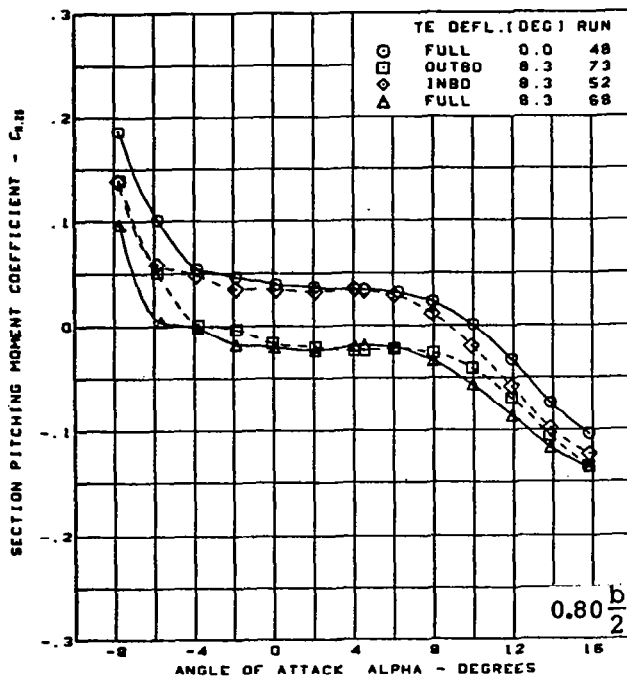
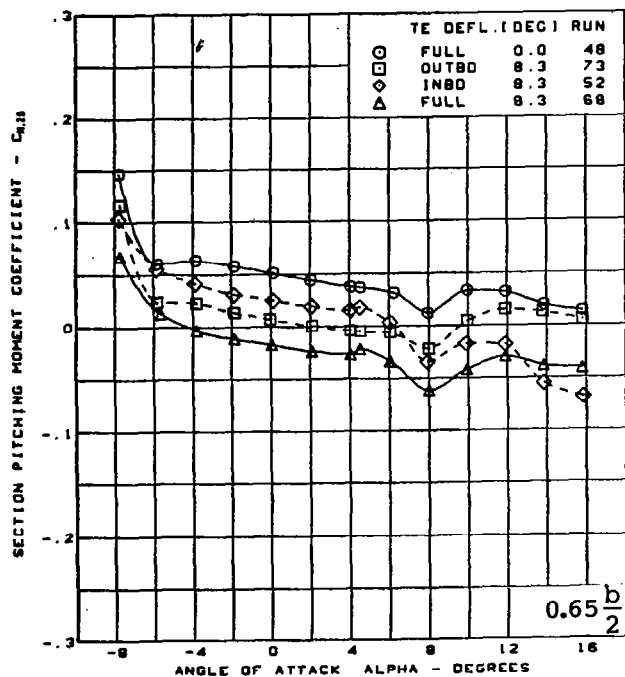
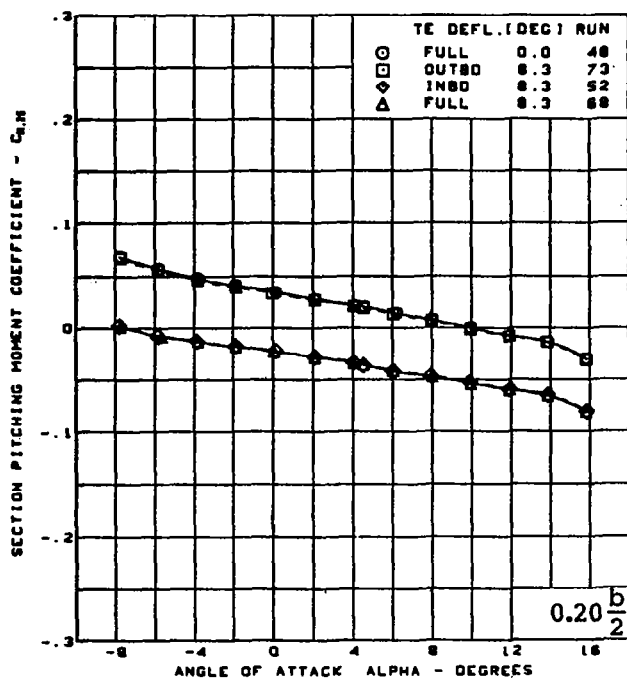
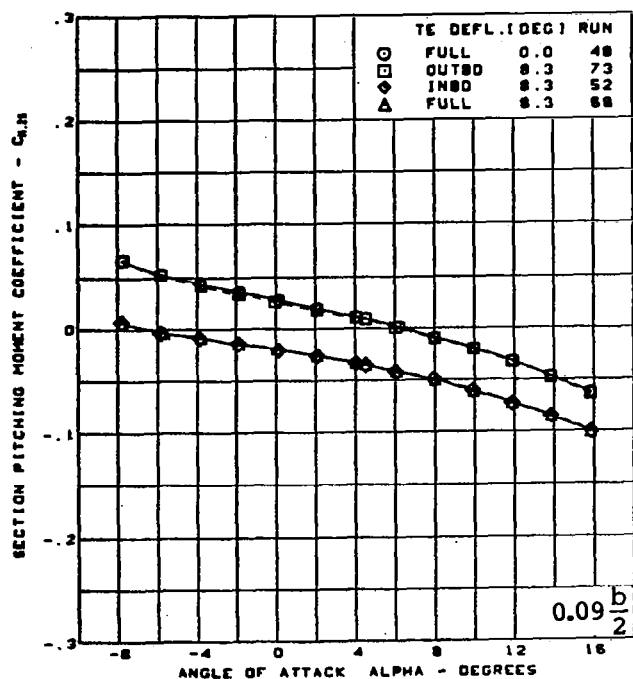


$M = 0.85$   
 Cambered-twisted wing, rounded L.E.  
 Fin on  
 L.E. deflection, full span =  $0.0^\circ$

(e) (Concluded)

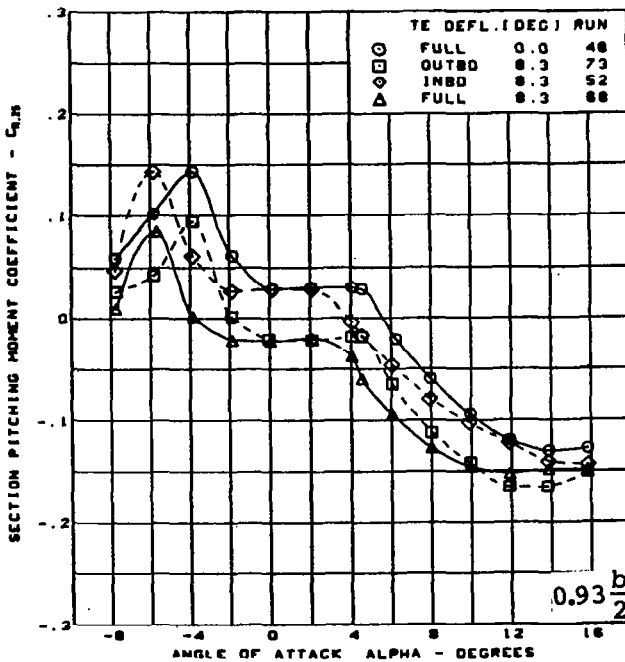
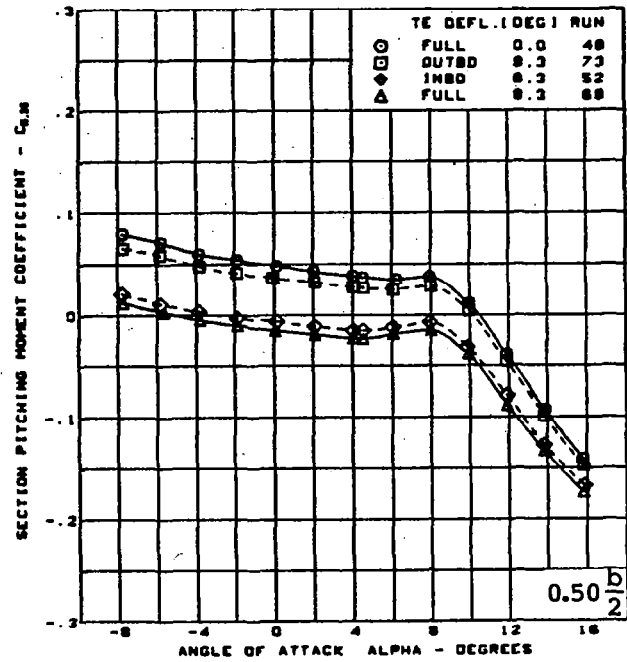
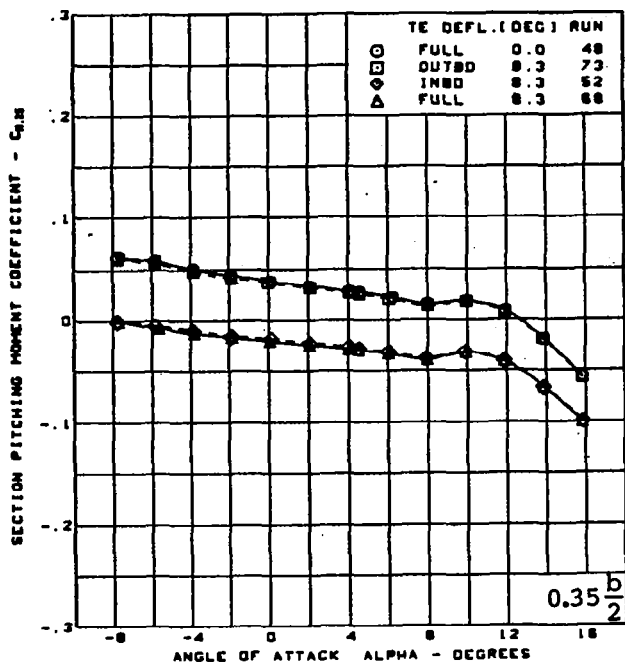
Figure 37. — (Continued)





(f) Section Aerodynamic Coefficients - Pitching Moment

Figure 37. - (Continued)

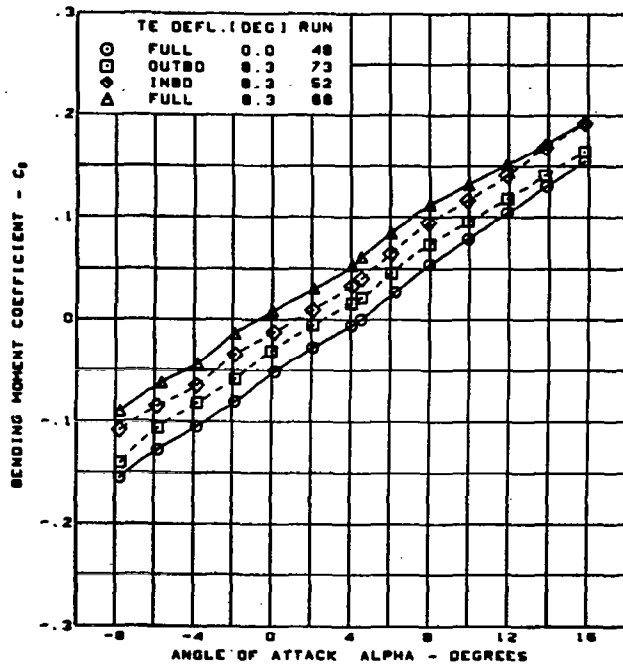
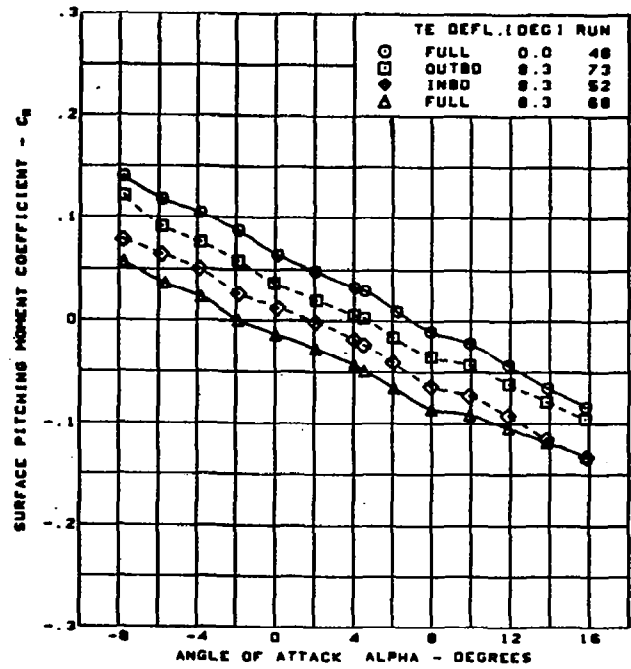
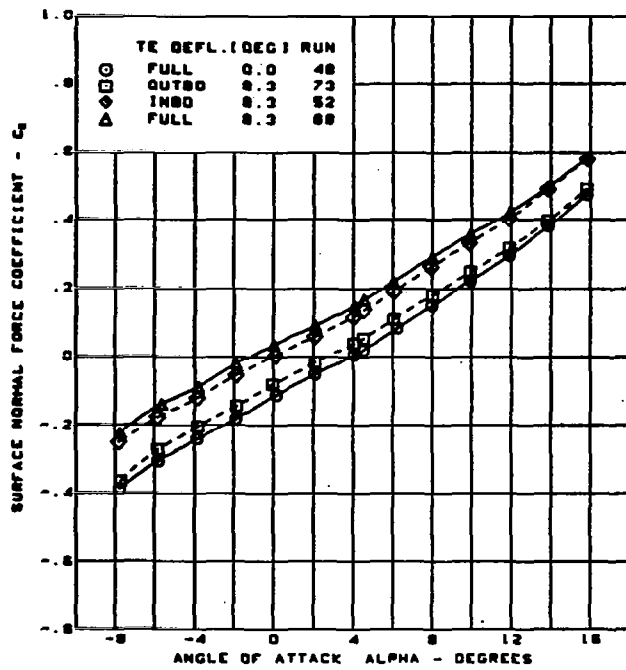


$M = 0.85$   
 Cambered-twisted wing, rounded L.E.  
 Fin on  
 L.E. deflection, full span =  $0.0^\circ$

(f) (Concluded)

Figure 37. - (Continued)



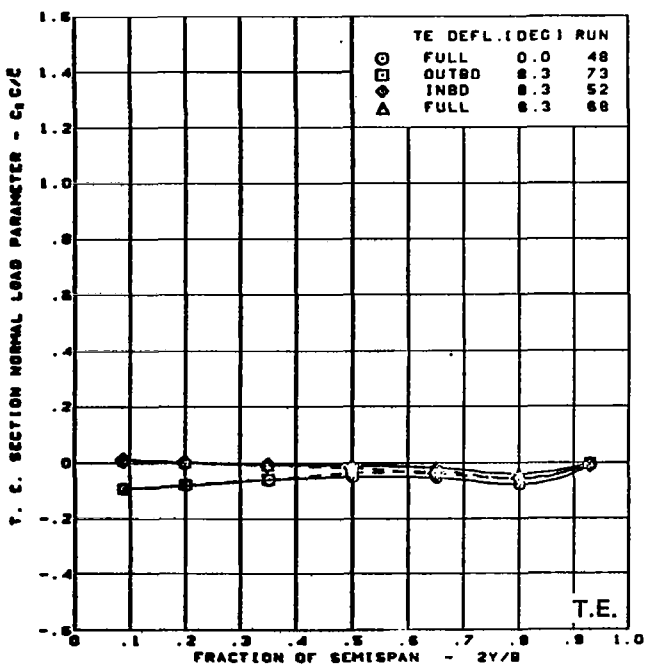
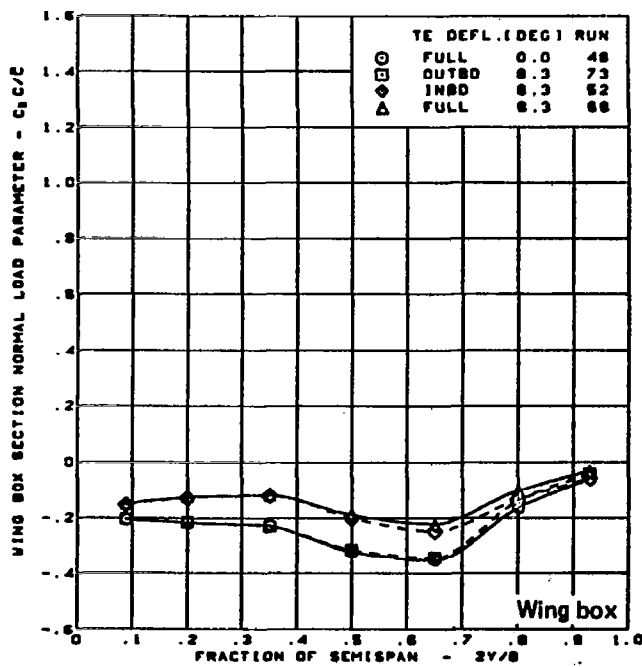
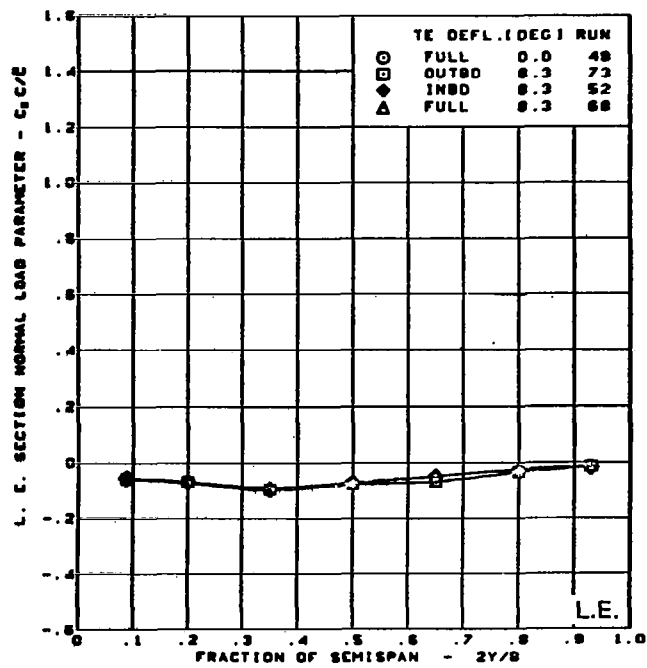
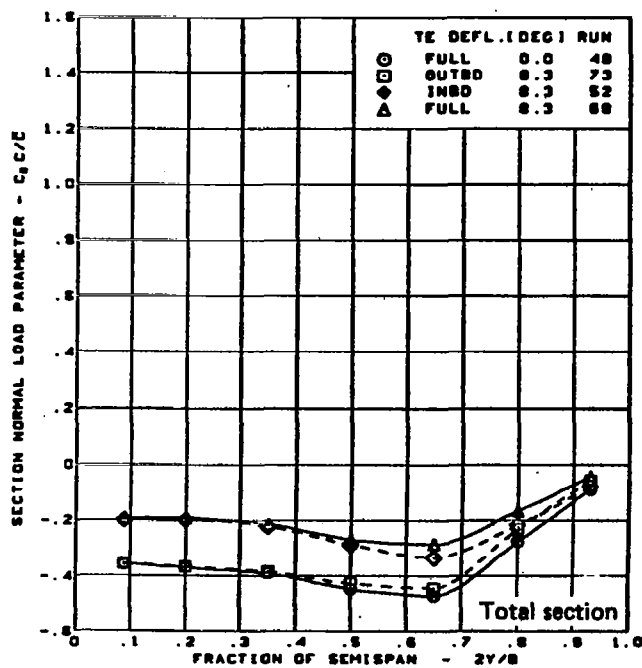


$M = 0.85$   
 Cambered-twisted wing, rounded L.E.  
 Fin on  
 L.E. deflection, full span  $\approx 0.0^\circ$

(g) Wing Aerodynamic Coefficients

Figure 37. — (Concluded)





$M = 0.85$

$\alpha = -8^\circ$

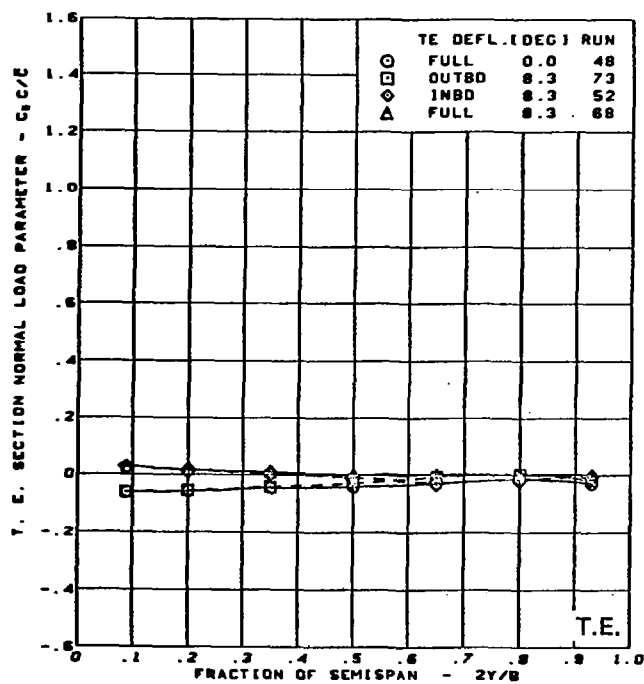
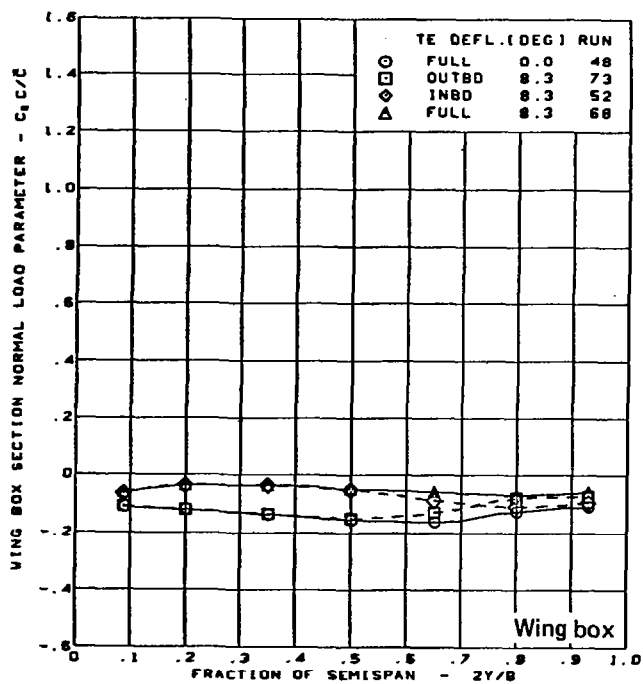
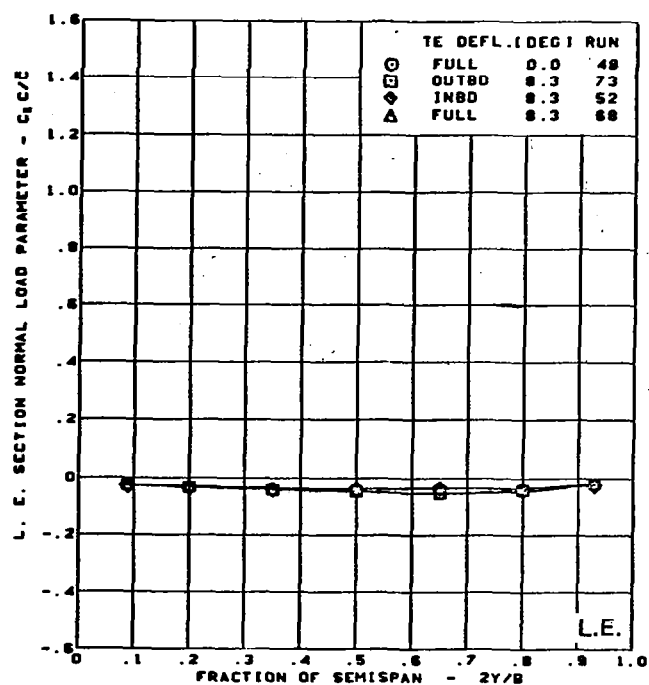
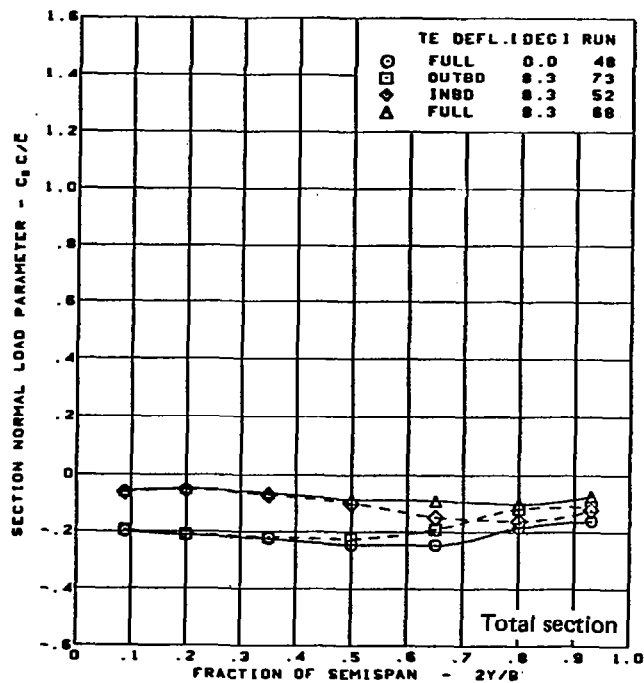
Cambered-twisted wing, rounded L.E.

Fin on

L.E. deflection, full span =  $0.0^\circ$

(a) Spanload Distributions - Normal Force,  $\alpha = -8^\circ$

Figure 38. — Wing Experimental Data—Effect of Full- and Partial-Span Trailing Edge Control Surface Deflection on Chordwise Segments; Cambered-Twisted Wing; Fin On;  $M = 0.85$



$M = 0.85$

$\alpha = -4^\circ$

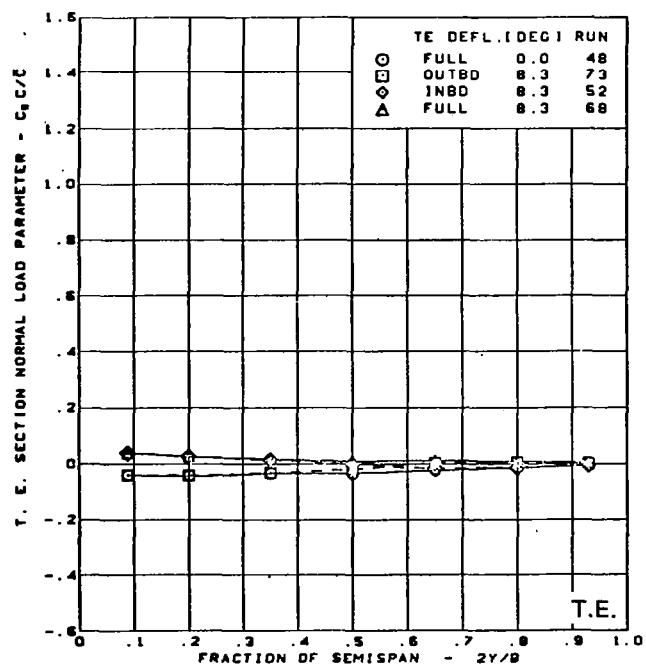
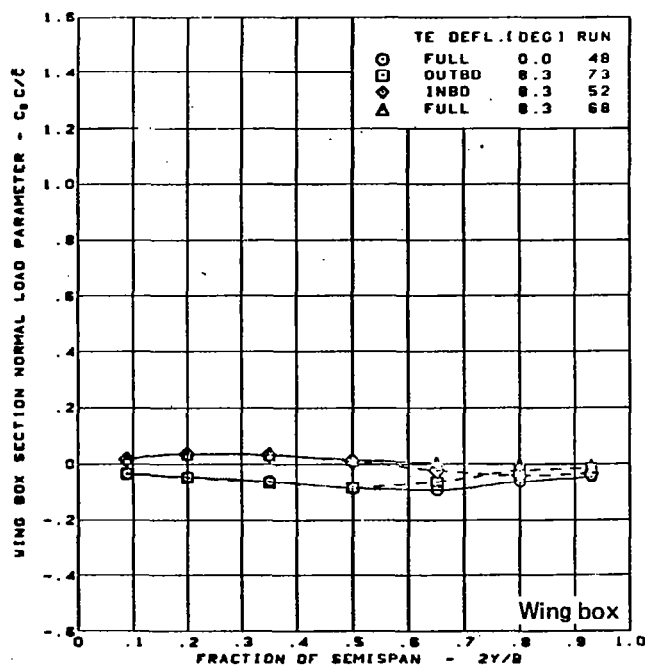
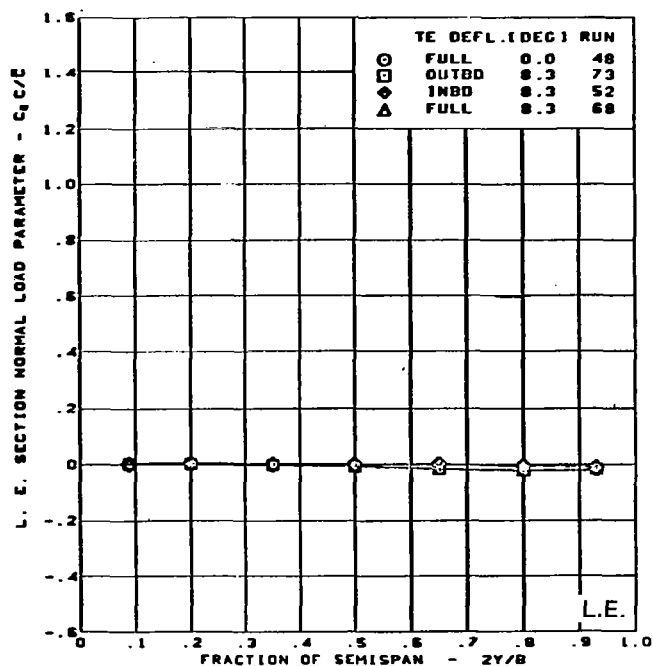
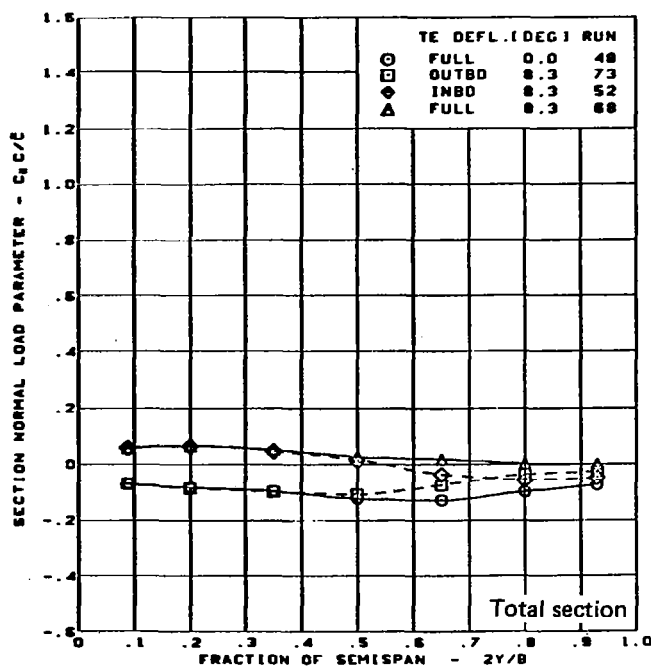
Cambered-twisted wing, rounded L.E.

Fin on

L.E. deflection, full span =  $0.0^\circ$

(b) Spanload Distributions - Normal Force,  $\alpha = -4^\circ$

Figure 38. - (Continued)



$M = 0.85$

$\alpha = 0^\circ$

Cambered-twisted wing, rounded L.E.

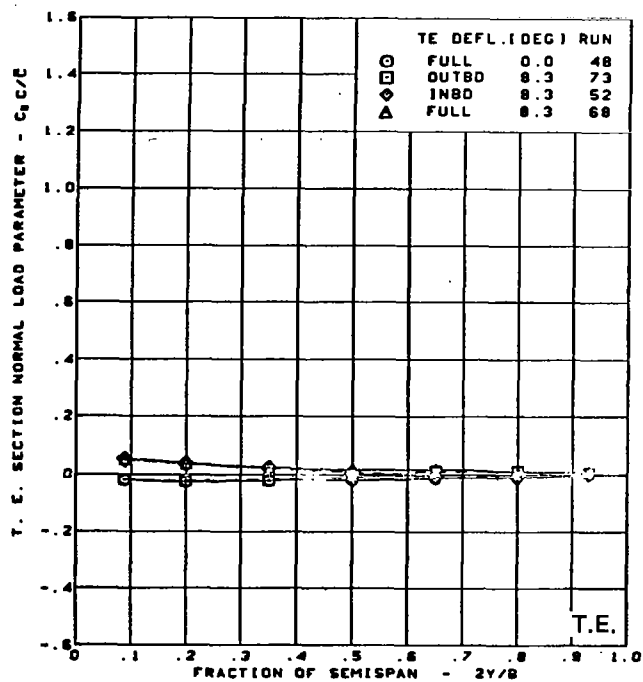
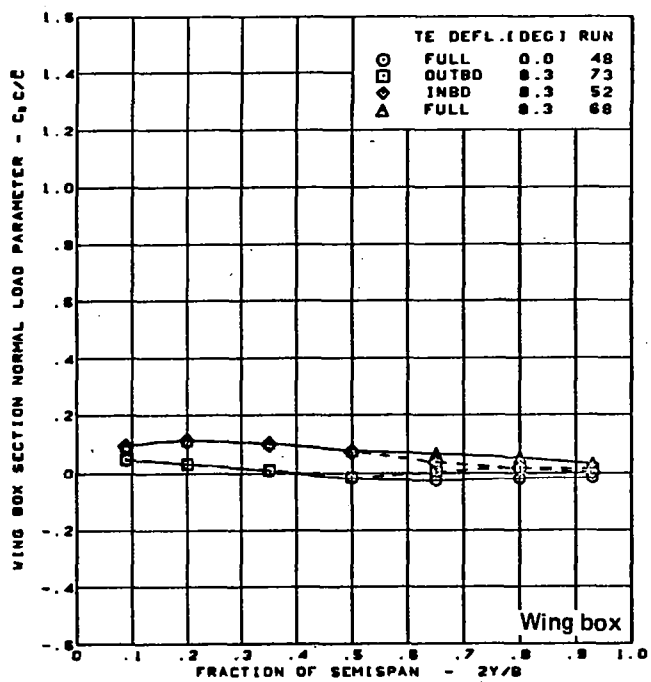
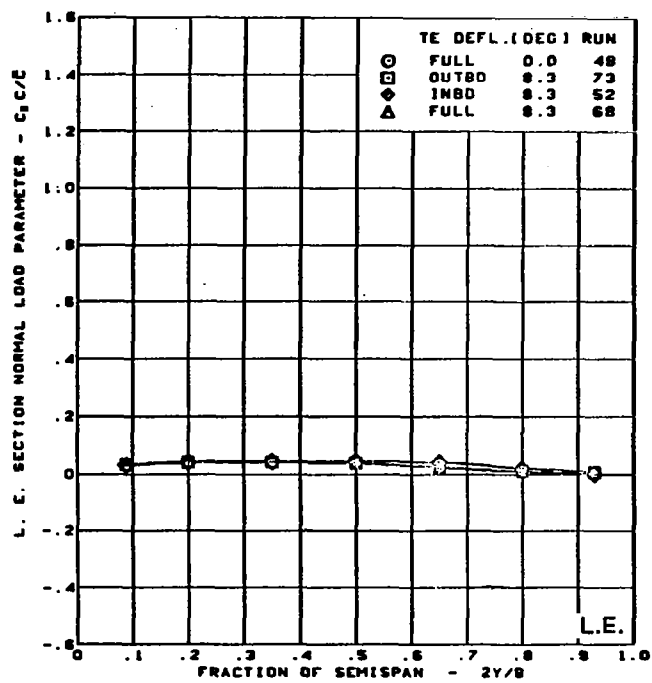
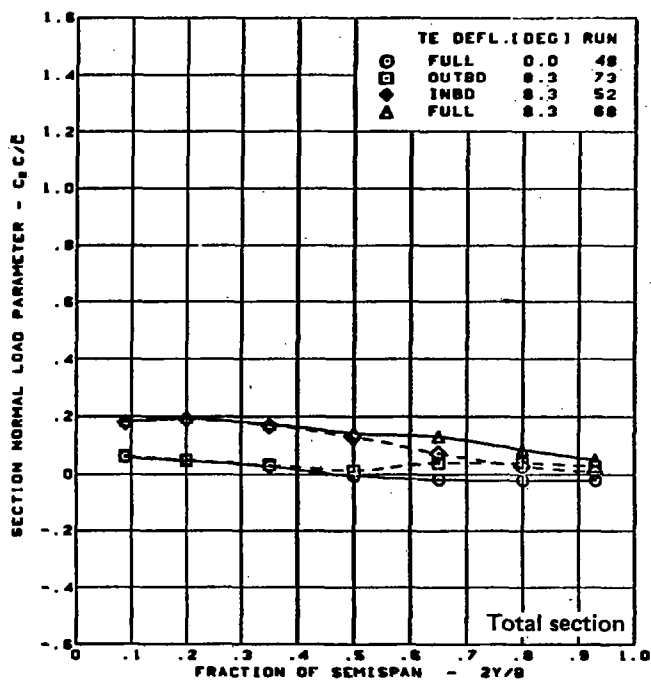
Fin on

L.E. deflection, full span  $= 0.0^\circ$

(c) Spanload Distributions - Normal Force,  $\alpha = 0^\circ$

Figure 38. - (Continued)





$M = 0.85$

$\alpha = 4^\circ$

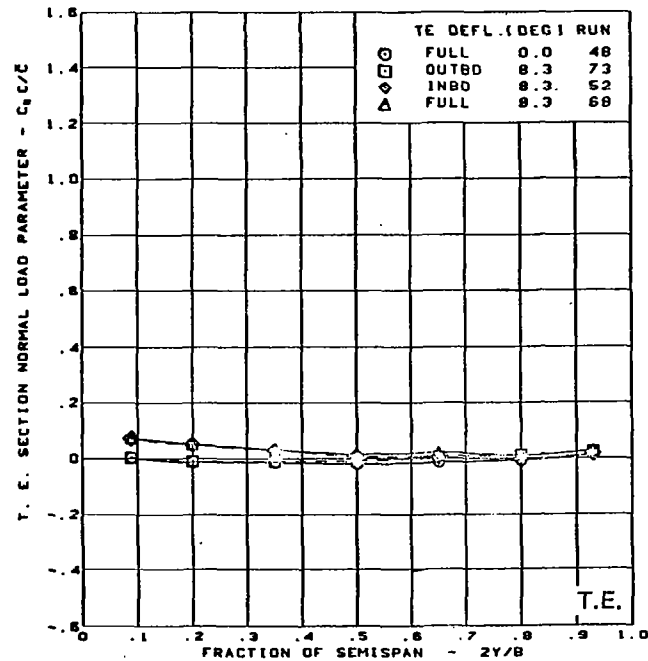
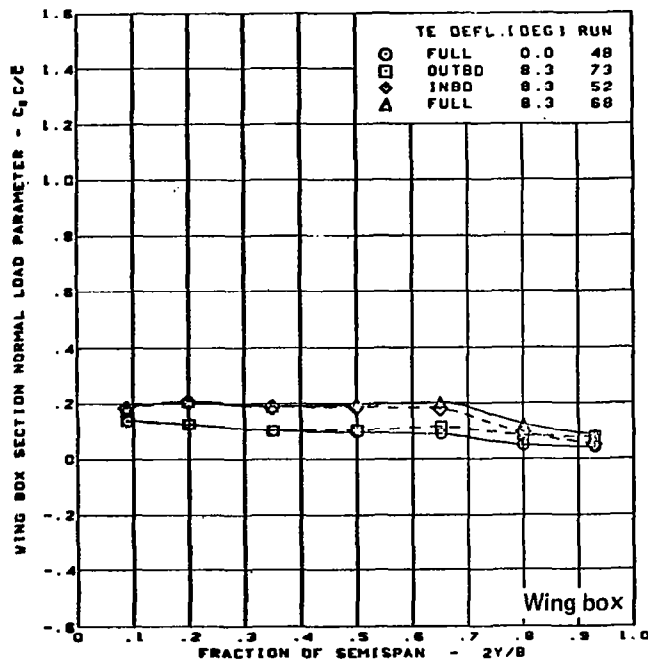
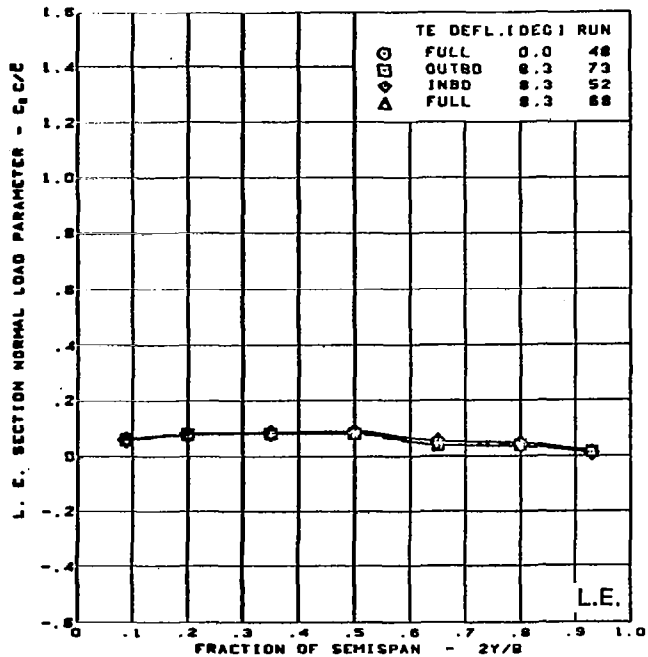
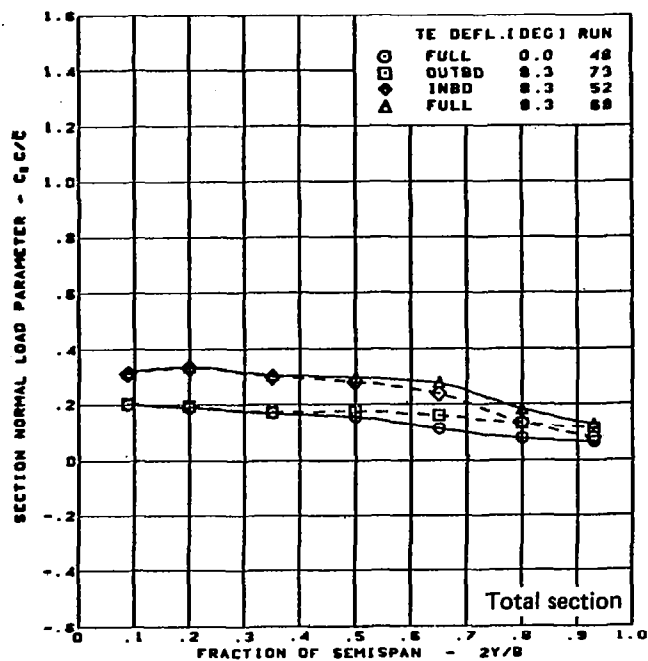
Cambered-twisted wing, rounded L.E.

Fin on

L.E. deflection, full span =  $0.0^\circ$

(d) Spanload Distributions - Normal Force,  $\alpha = 4^\circ$

Figure 38. - (Continued)



$M = 0.85$

$\alpha = 8^\circ$

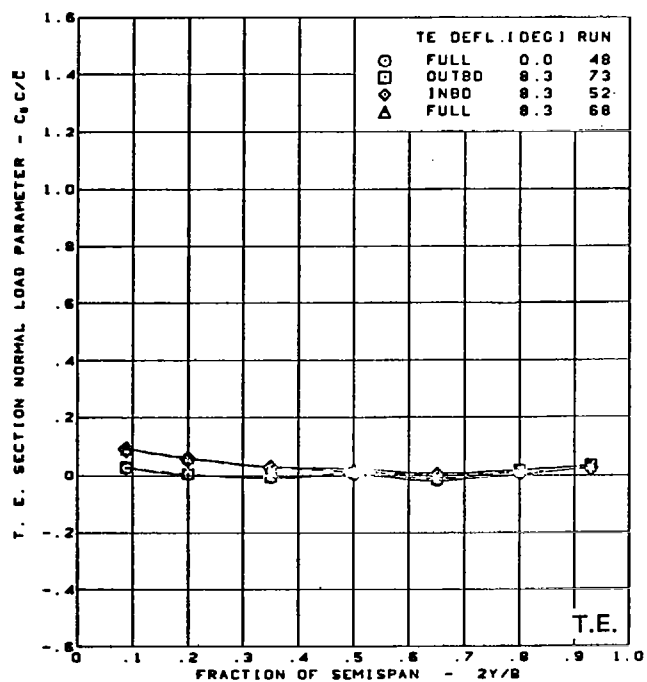
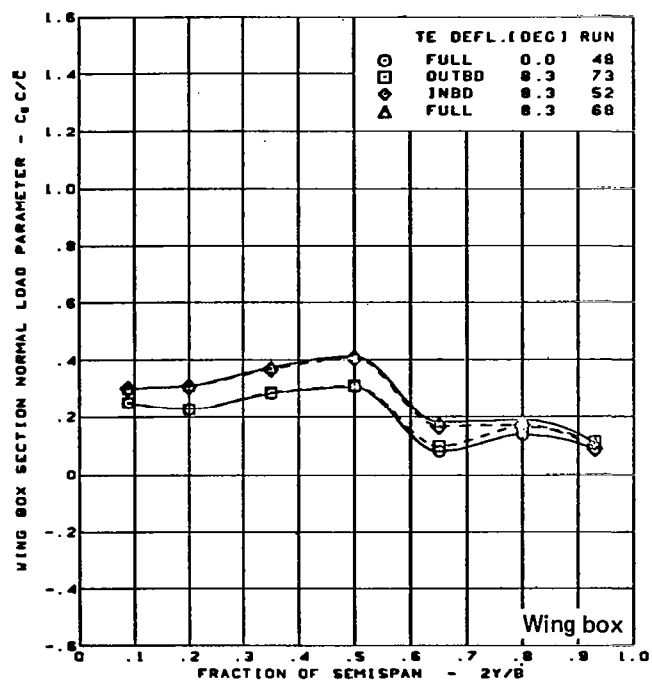
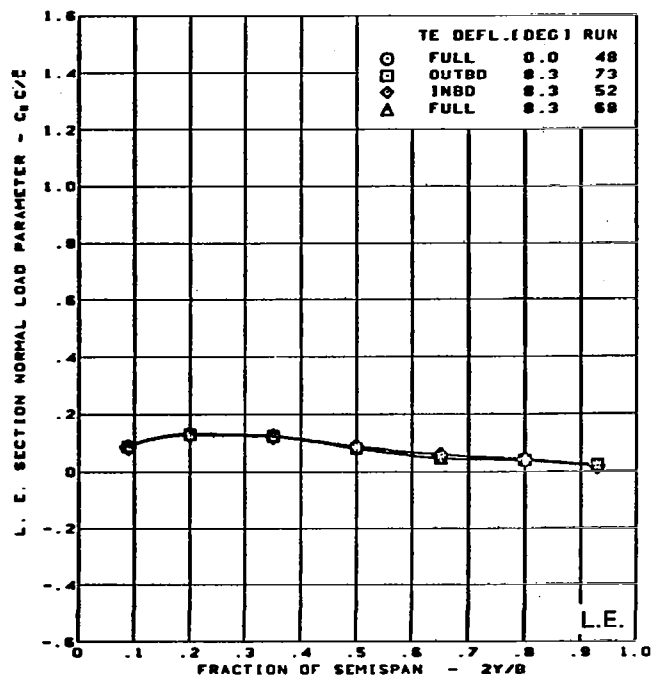
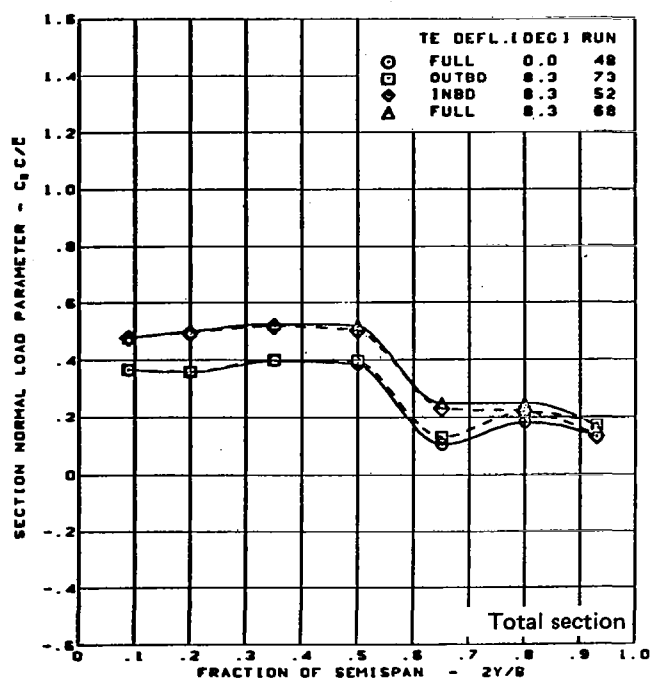
Cambered-twisted wing, rounded L.E.

Fin on

L.E. deflection, full span =  $0.0^\circ$

(e) Spanload Distributions - Normal Force,  $\alpha = 8^\circ$

Figure 38. - (Continued)



$M = 0.85$

$\alpha = 12^\circ$

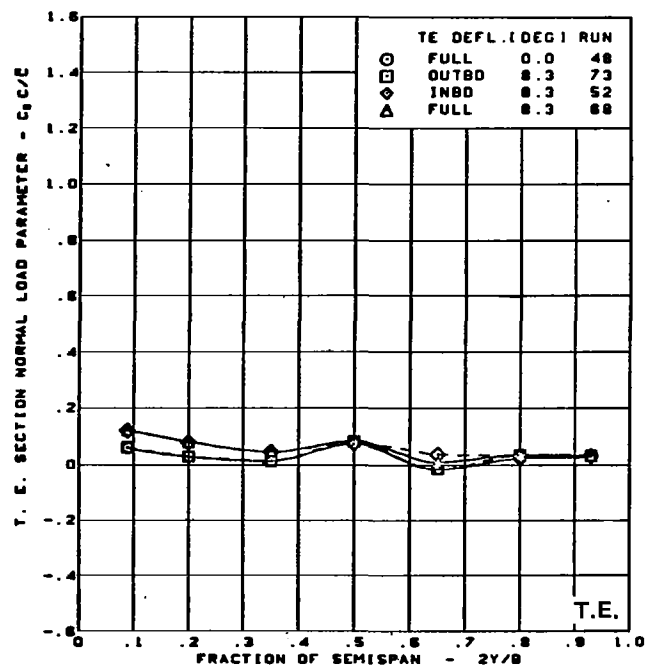
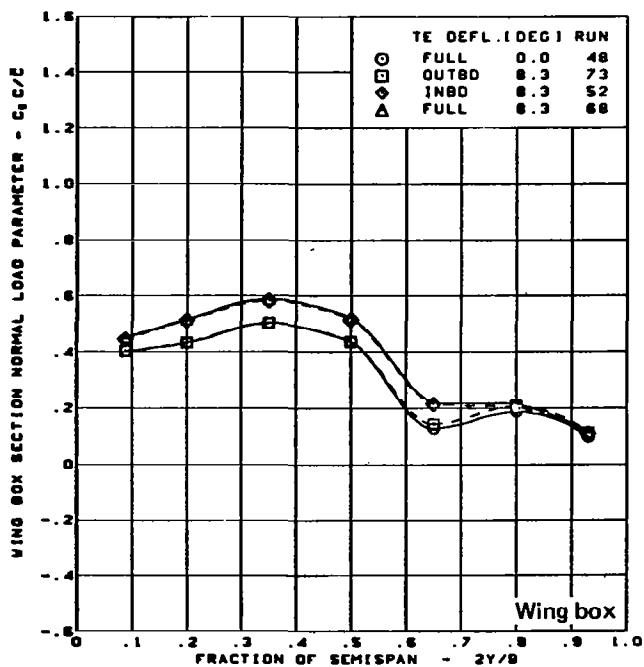
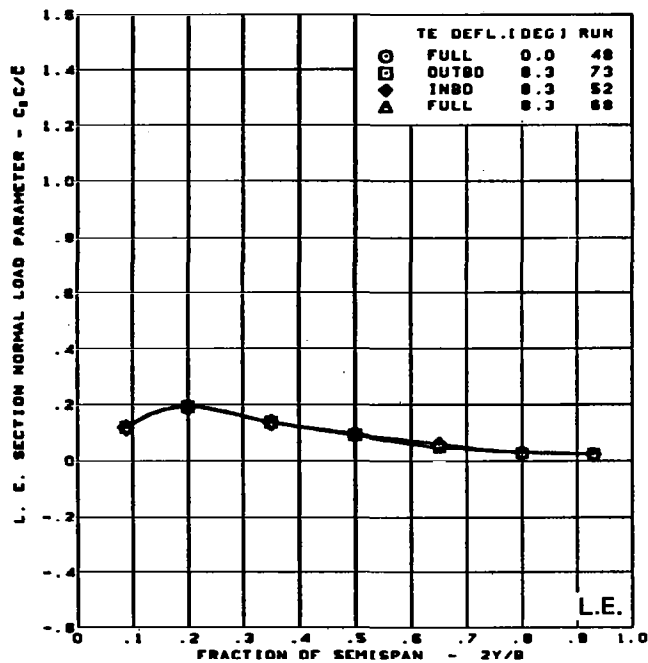
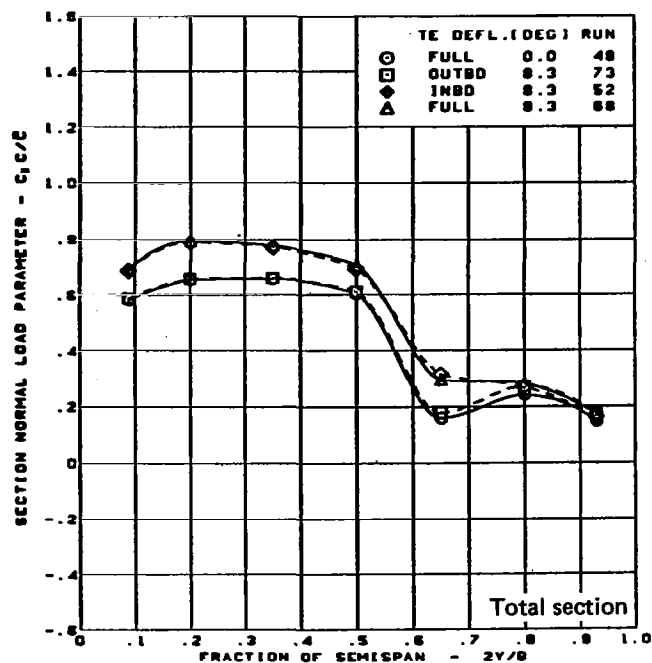
Cambered-twisted wing, rounded L.E.

Fin on

L.E. deflection, full span =  $0.0^\circ$

(f) Spanload Distributions - Normal Force,  $\alpha = 12^\circ$

Figure 38. - (Continued)



$M = 0.85$

$\alpha = 16^\circ$

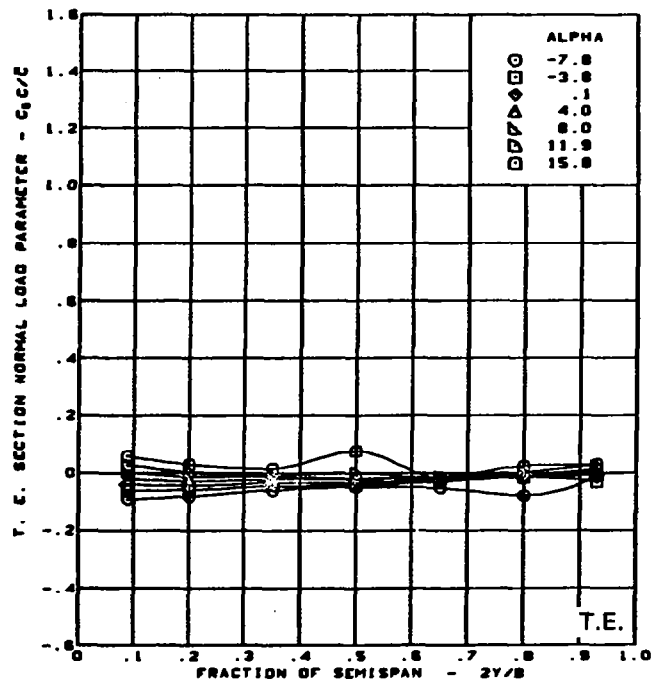
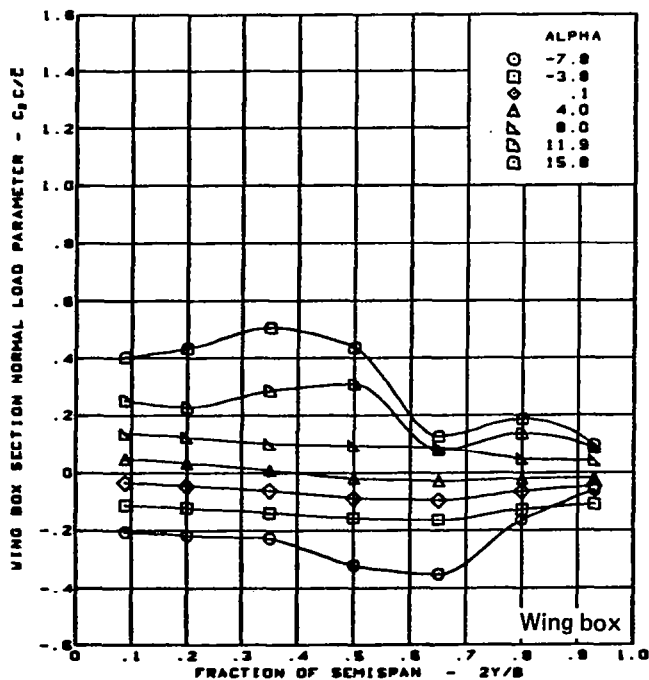
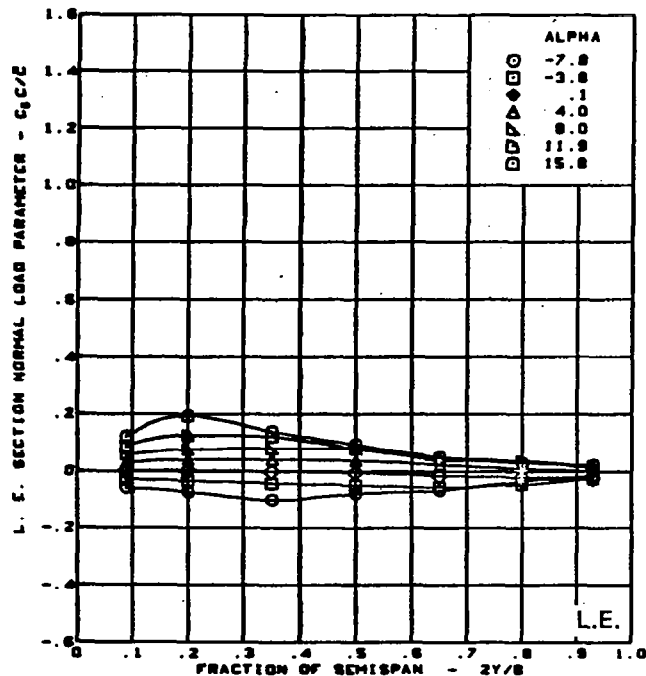
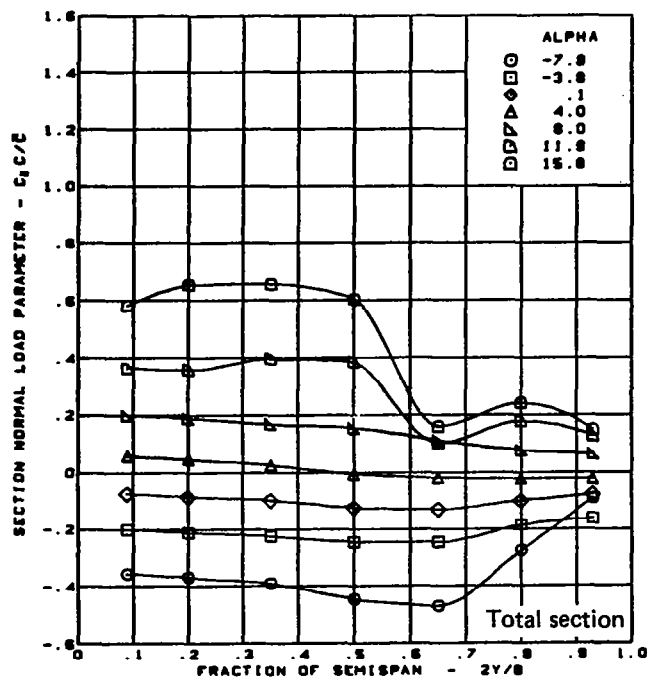
Cambered-twisted wing, rounded L.E.

Fin on

L.E. deflection, full span =  $0.0^\circ$

(g) Spanload Distributions - Normal Force,  $\alpha = 16^\circ$

Figure 38. - (Continued)

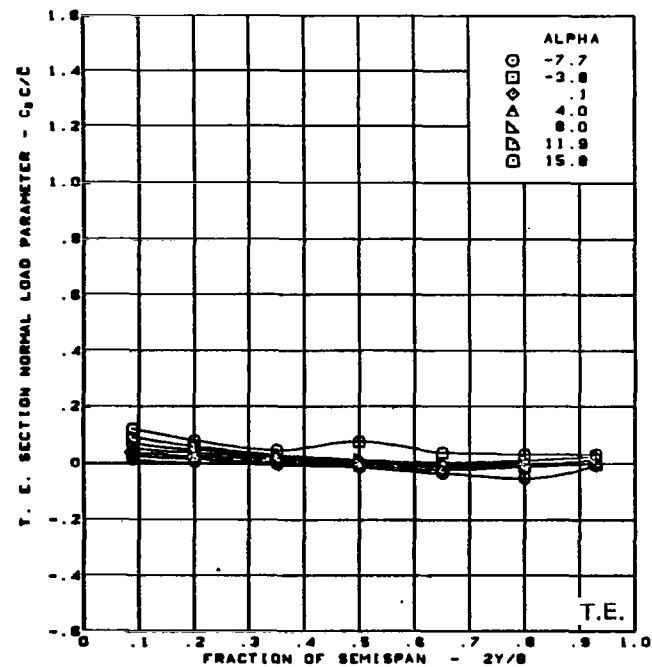
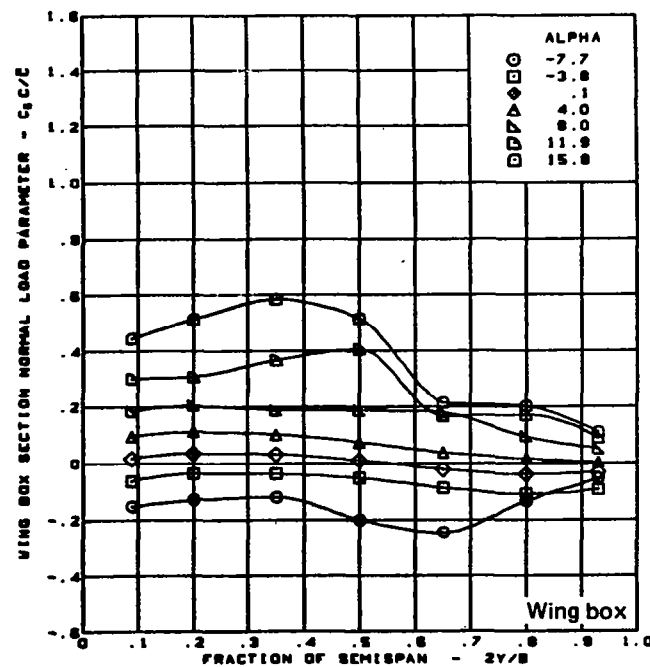
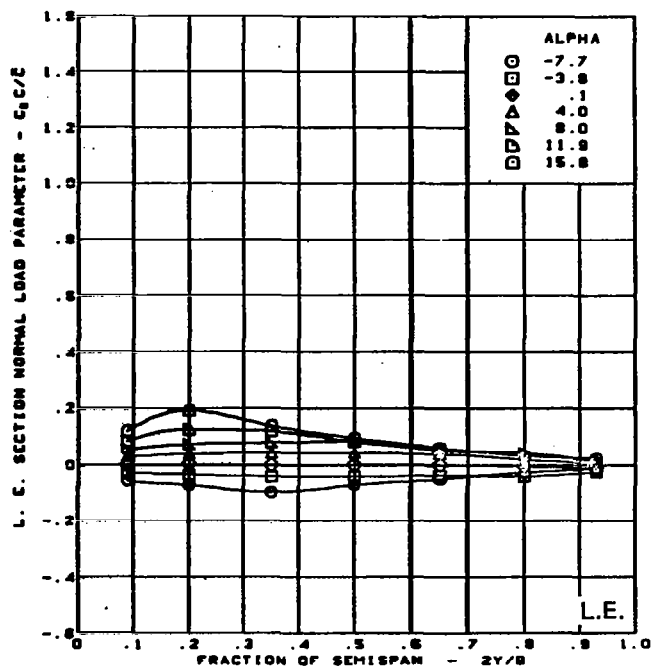
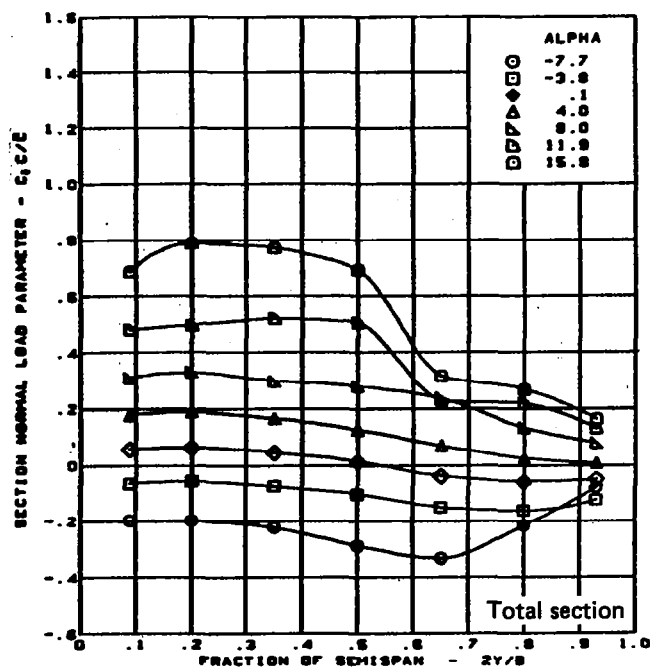


$M = 0.85$   
 Cambered-twisted wing, rounded L.E.  
 Fin on

L.E. deflection, full span =  $0.0^\circ$   
 T.E. deflection, full span =  $0.0^\circ$

(h) Spanload Distributions - Normal Force, T.E. Deflection, Full Span =  $0.0^\circ$

Figure 38. — (Continued)



$M \approx 0.85$

Cambered-twisted wing, rounded L.E.

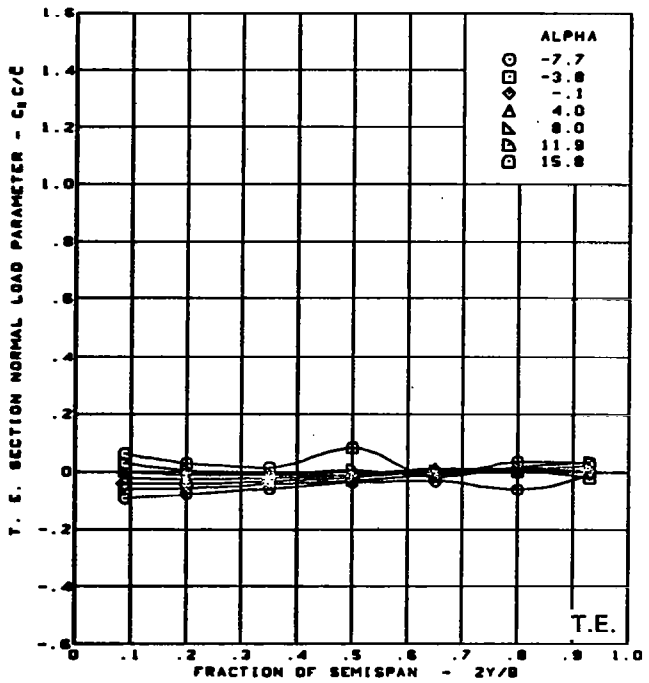
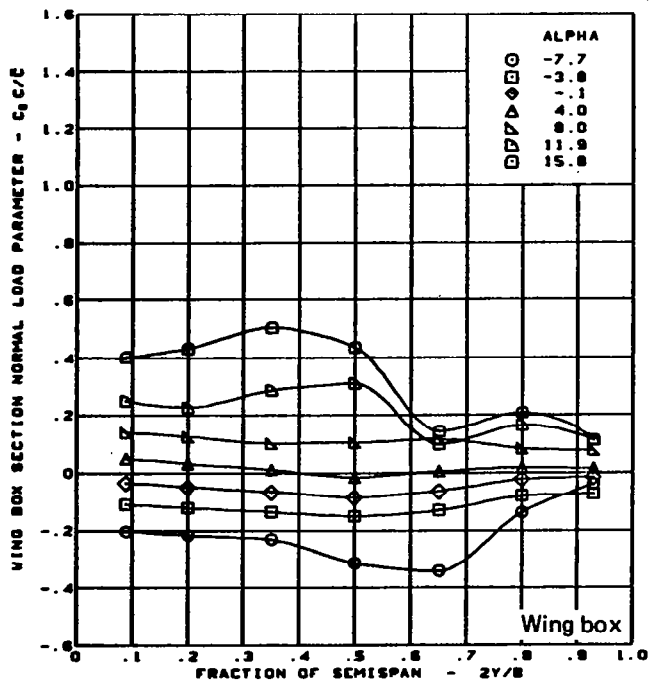
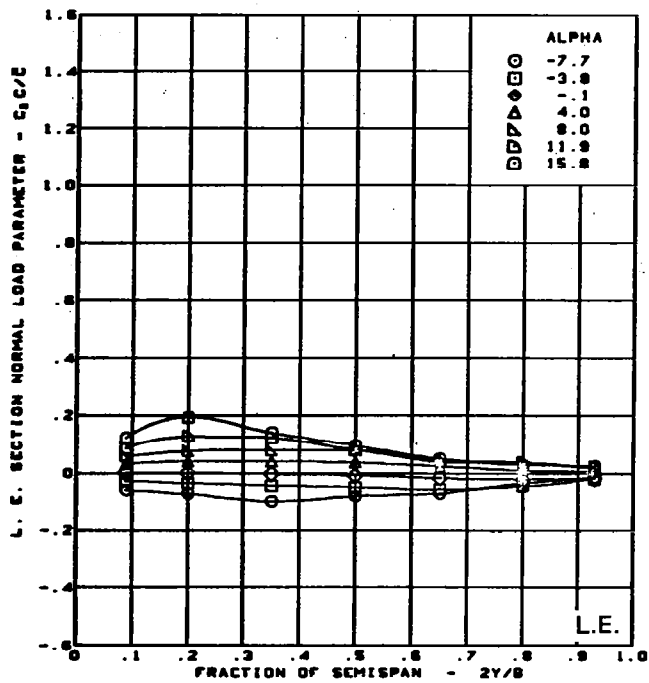
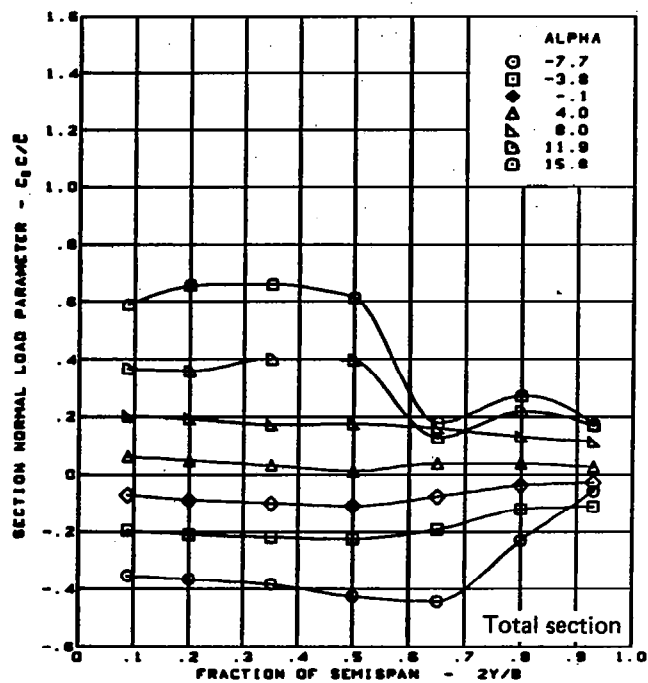
Fin on

(i) Spanload Distributions - Normal Force, T.E. Deflection, Inboard =  $8.3^\circ$ , Outboard =  $0.0^\circ$

L.E. deflection, full span =  $0.0^\circ$

T.E. deflection, inboard =  $8.3^\circ$ , outboard =  $0.0^\circ$

Figure 38. — (Continued)

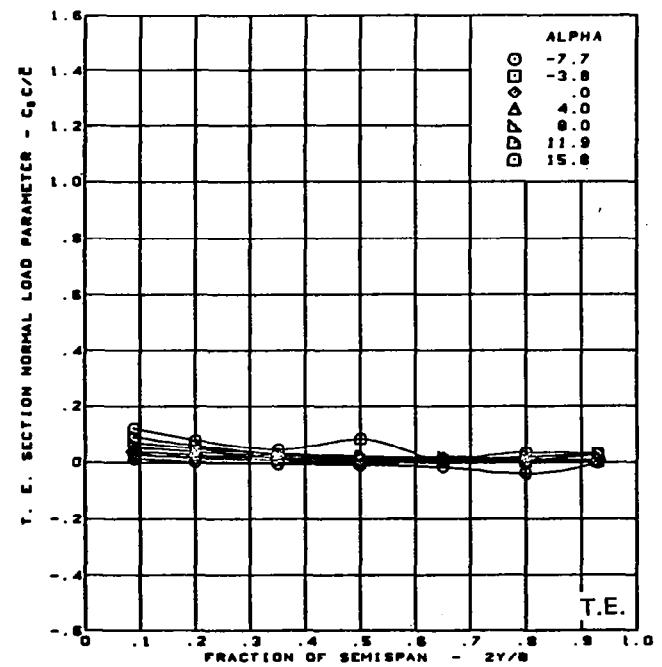
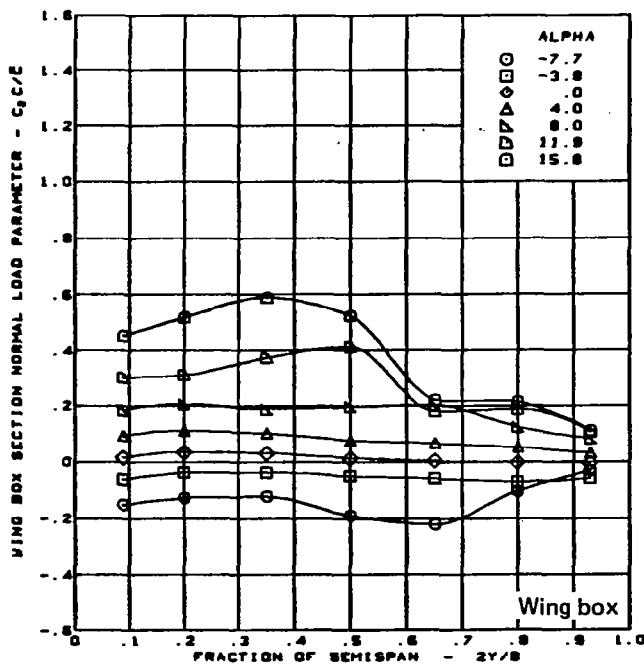
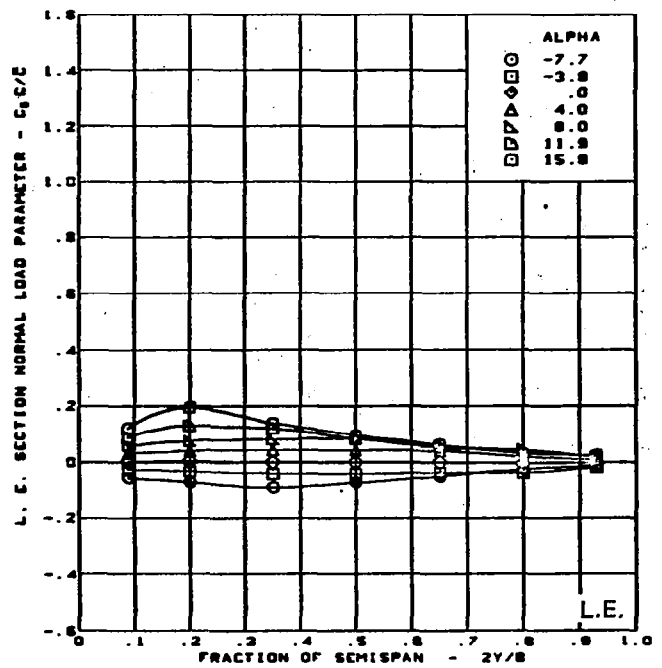
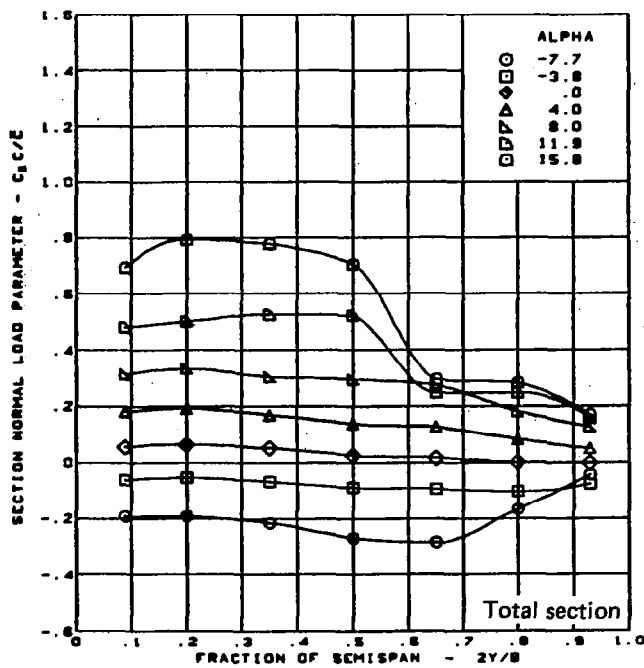


$M = 0.85$   
 Cambered-twisted wing, rounded L.E.  
 Fin on

L.E. deflection, full span =  $0.0^\circ$   
 T.E. deflection, inboard =  $0.0^\circ$ , outboard =  $8.3^\circ$

(j) Spanload Distributions - Normal Force, T.E. Deflection, Inboard =  $0.0^\circ$ , Outboard =  $8.3^\circ$

Figure 38. - (Continued)



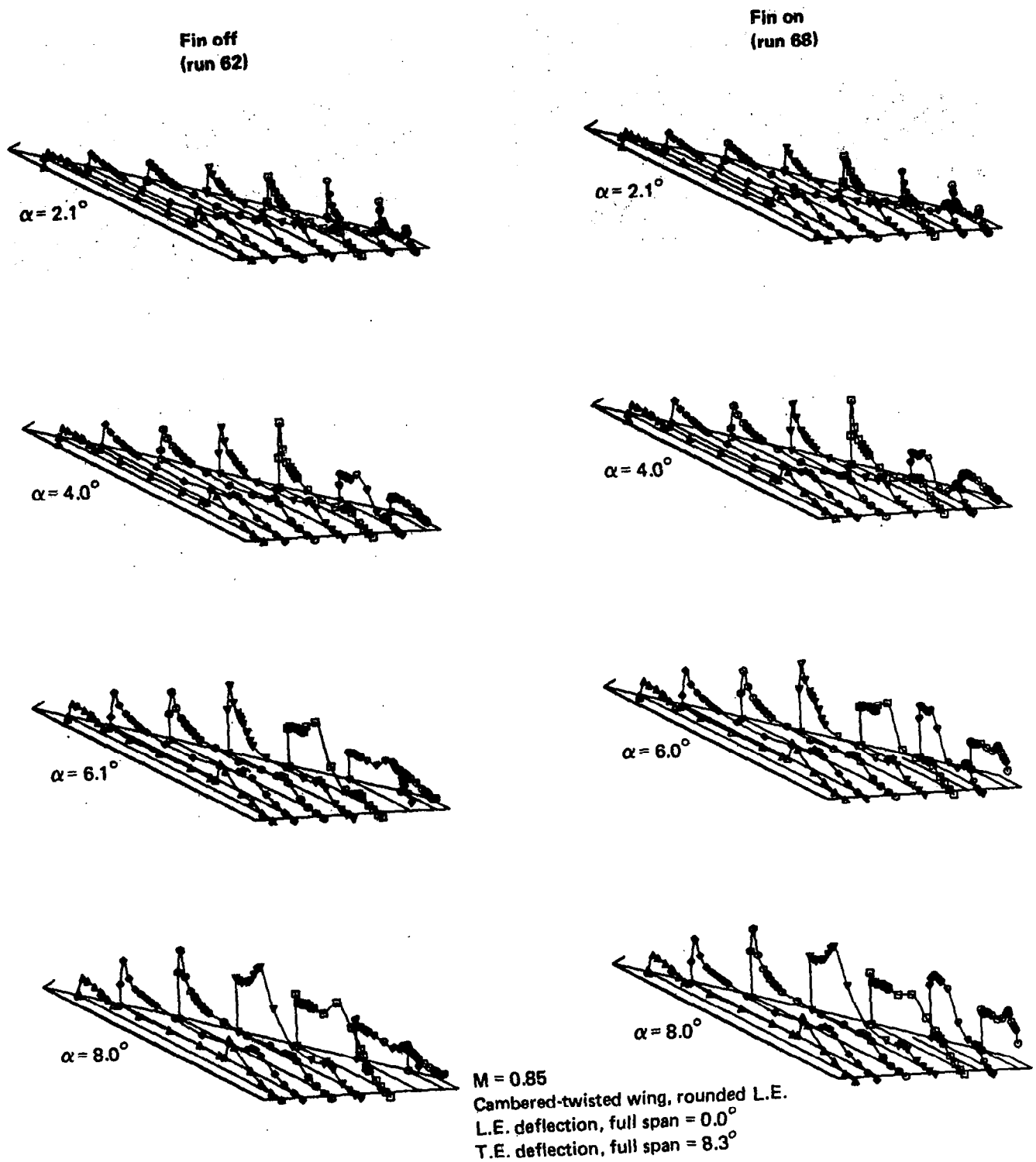
$M = 0.85$   
 Cambered-twisted wing, rounded L.E.  
 Fin on

L.E. deflection, full span =  $0.0^\circ$   
 T.E. deflection, full span =  $8.3^\circ$

(k) Spanload Distributions - Normal Force, T.E. Deflection, Full Span =  $8.3^\circ$

Figure 38. - (Concluded)

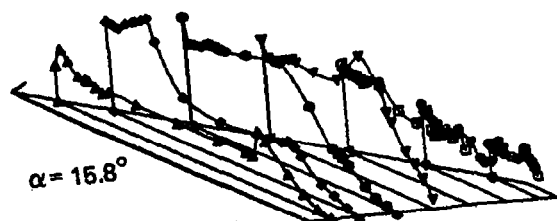
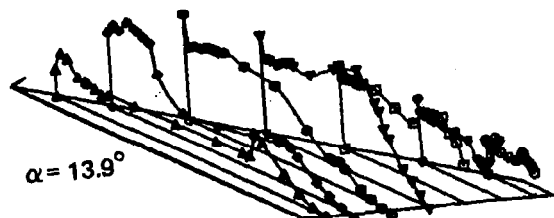
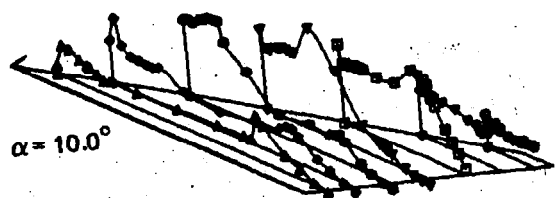




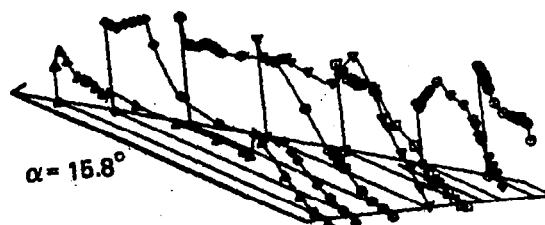
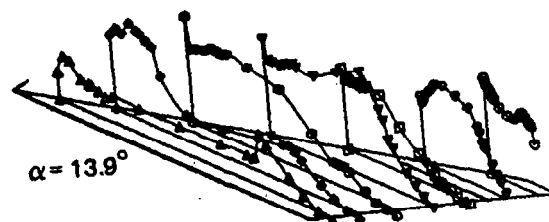
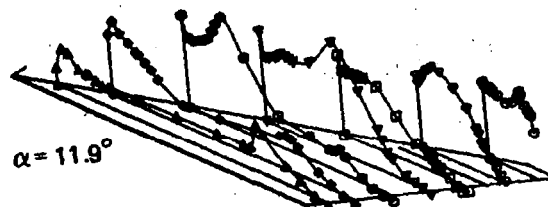
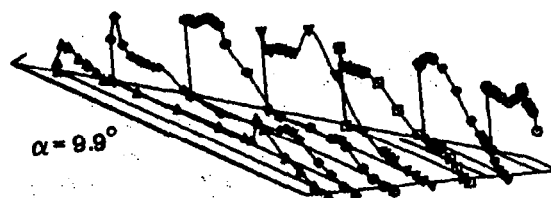
(a) Upper Surface Pressure Distribution

Figure 39. — Wing Experimental Data—Effect of a Wing Fin and Angle of Attack;  
 Cambered-Twisted Wing; T.E. Deflection, Full Span =  $8.3^\circ$ ;  $M = 0.85$

Fin off  
(run 62)

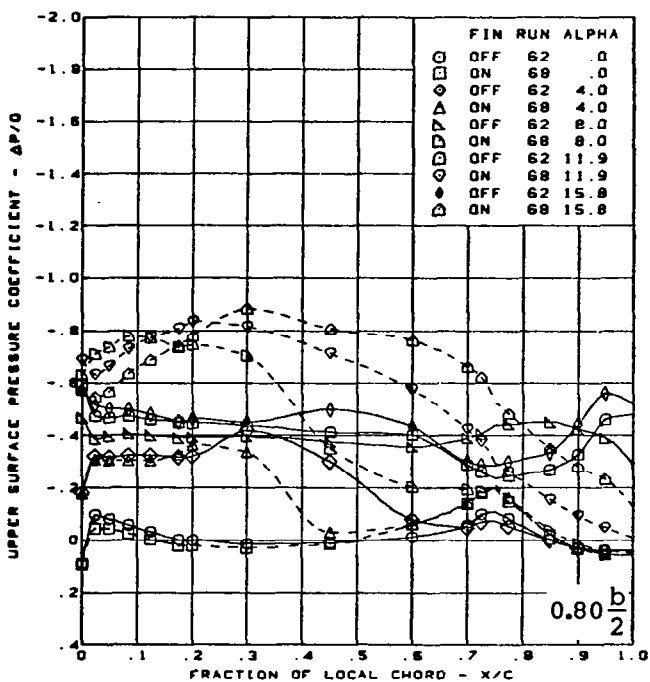
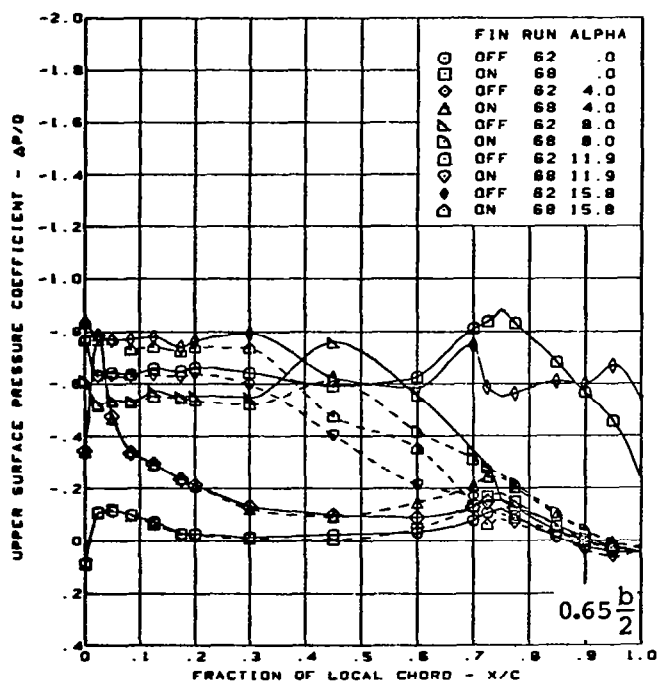
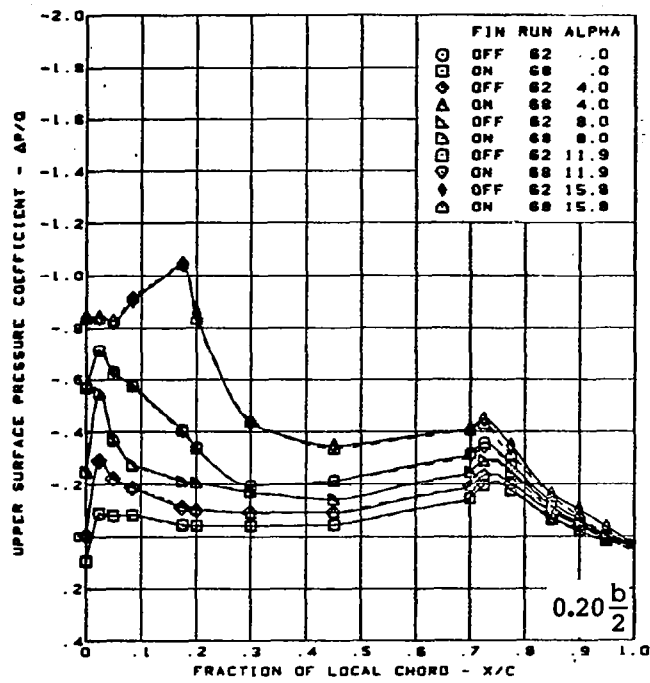
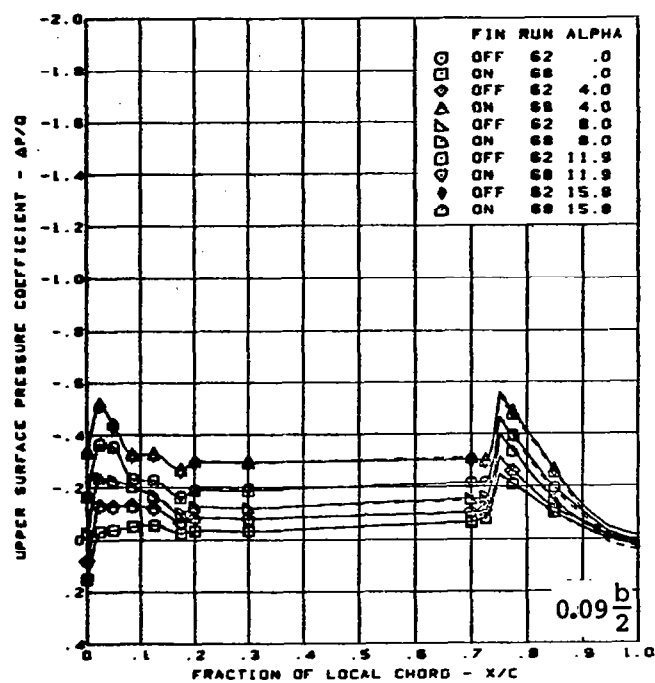


Fin on  
(run 68)



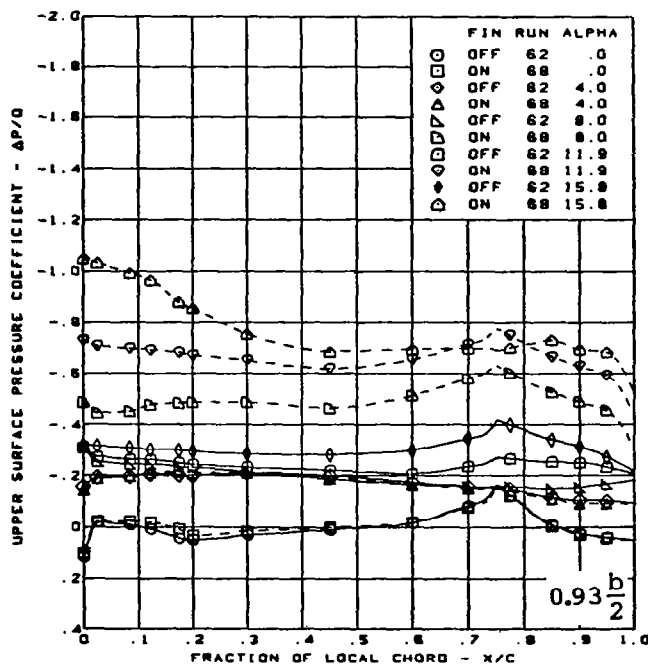
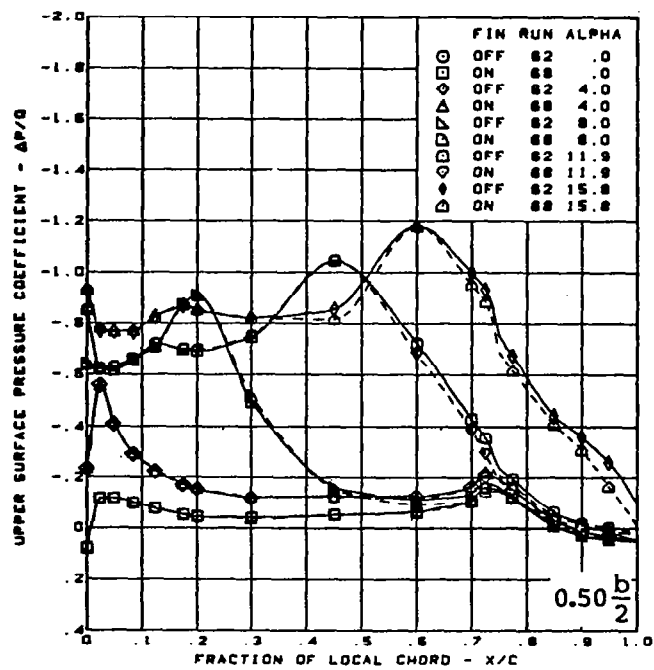
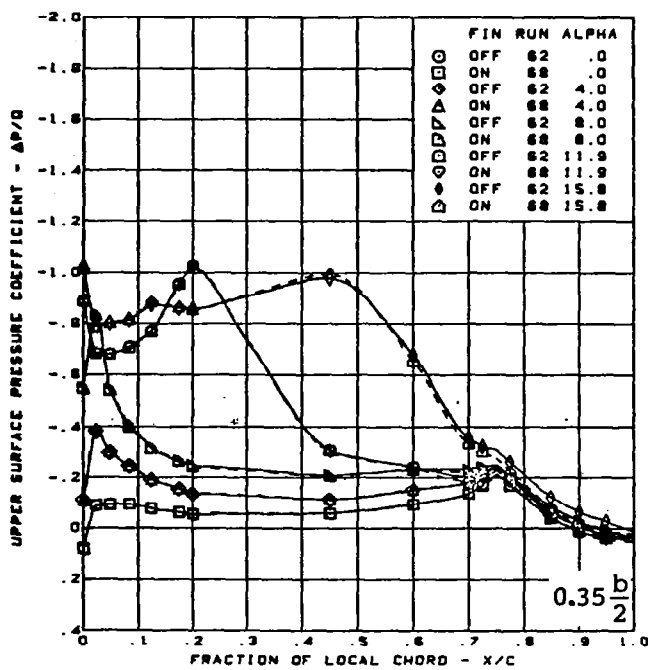
(a) (Concluded)

Figure 39. — (Continued)



(b) Upper Surface Chordwise Pressure Distributions

Figure 39. - (Continued)



$M = 0.85$

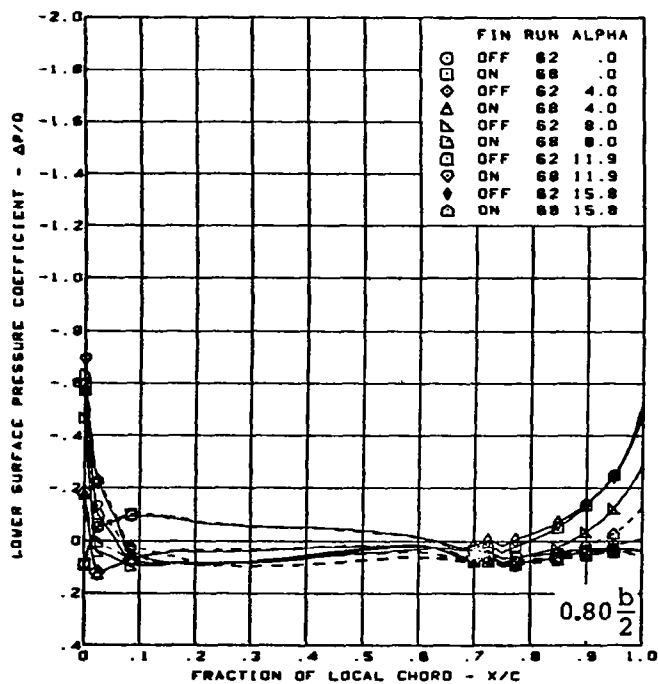
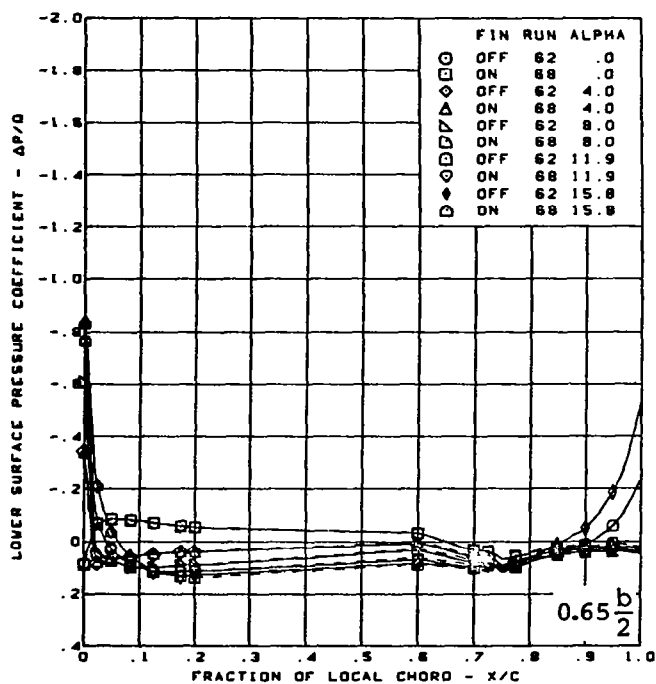
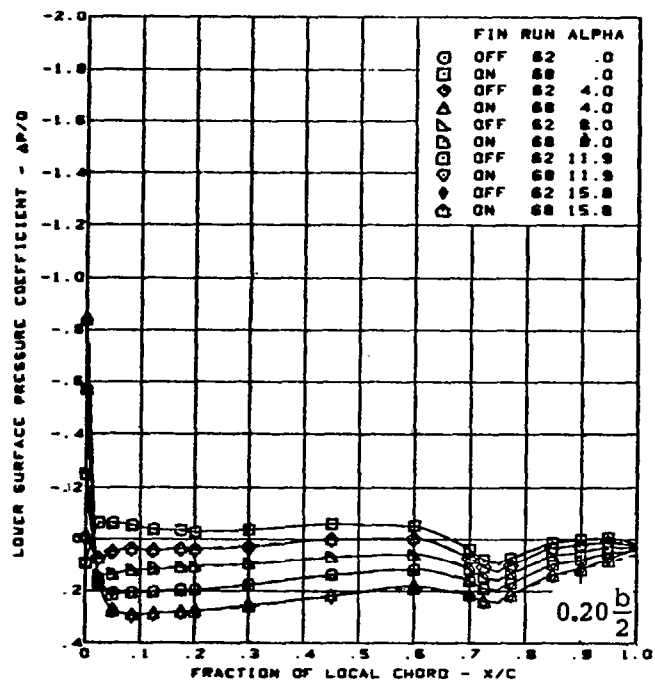
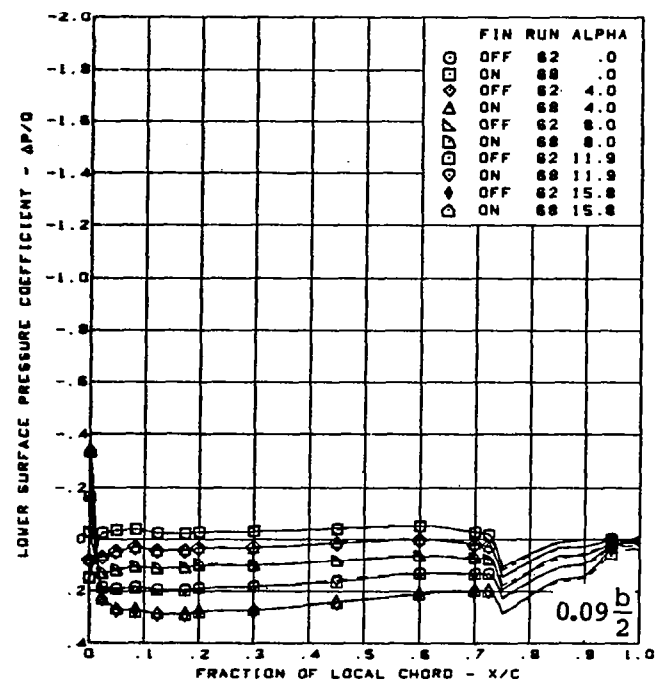
Cambered-twisted wing, rounded L.E.

L.E. deflection, full span =  $0.0^\circ$

T.E. deflection, full span =  $8.3^\circ$

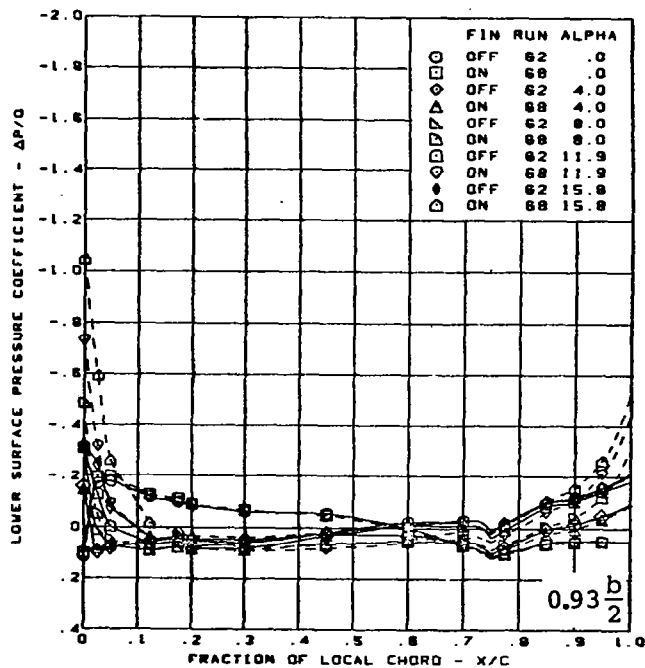
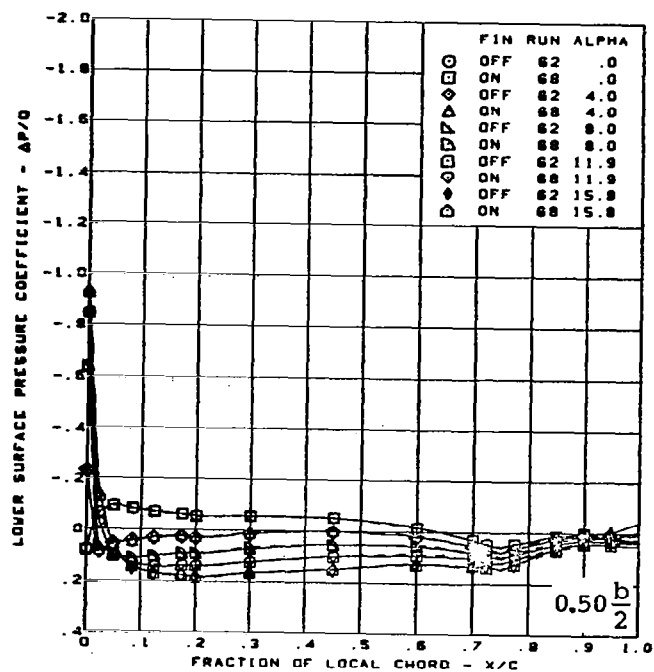
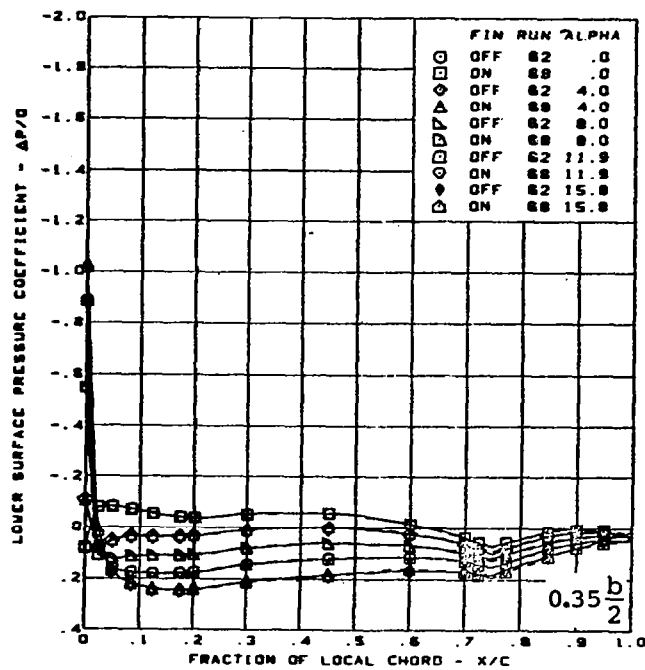
(b) (Concluded)

Figure 39. - (Continued)



(c) Lower Surface Chordwise Pressure Distributions

Figure 39. — (Continued)



$M = 0.85$

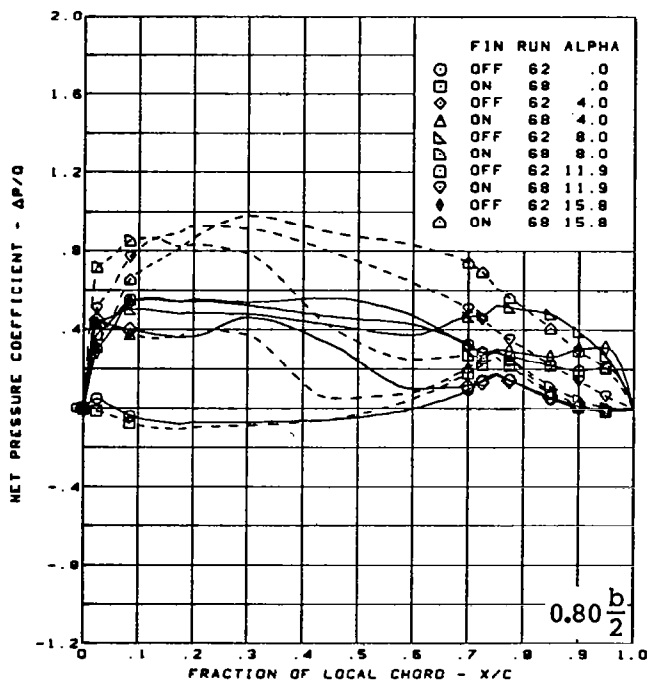
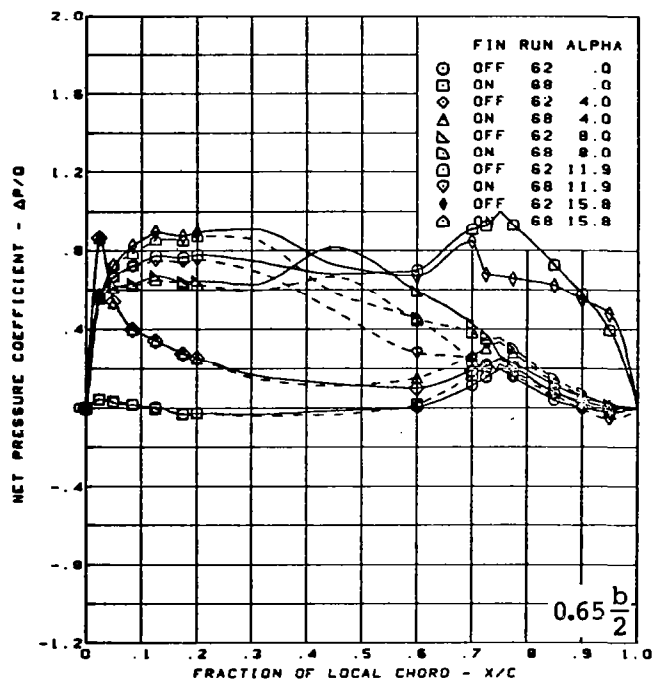
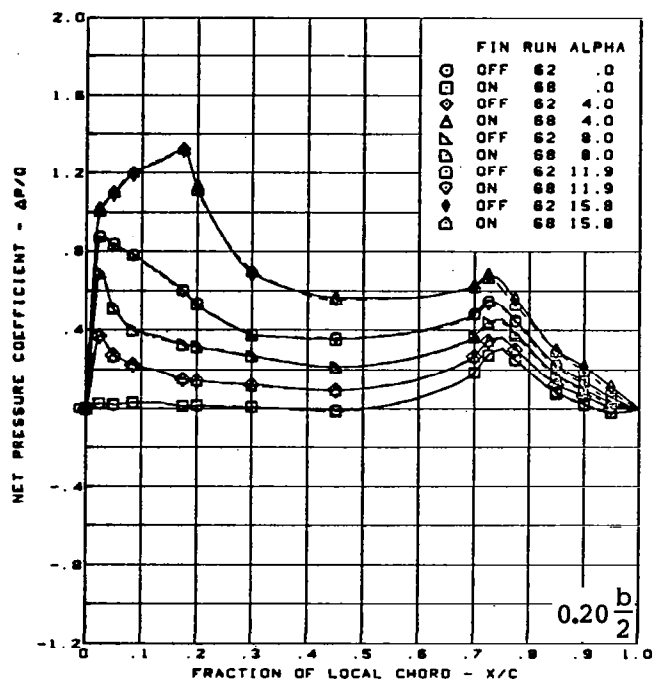
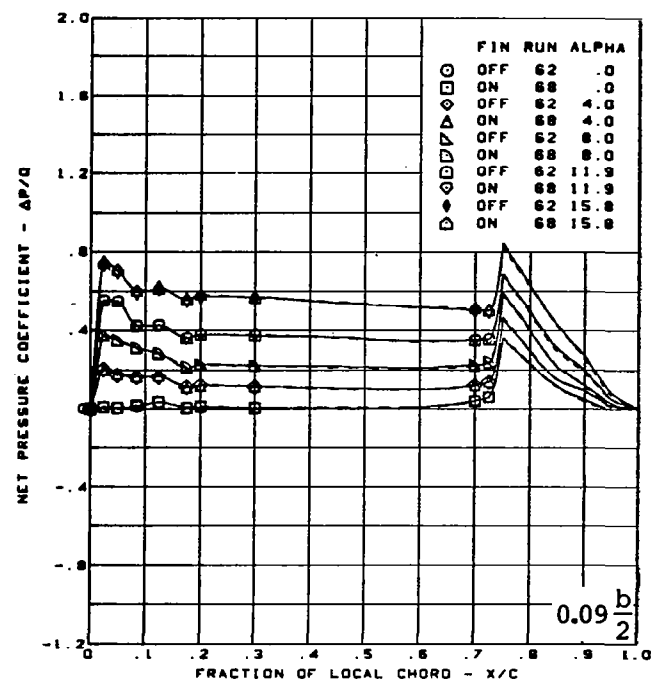
Cambered-twisted wing, rounded L.E.

L.E. deflection, full span =  $0.0^\circ$

T.E. deflection, full span =  $8.3^\circ$

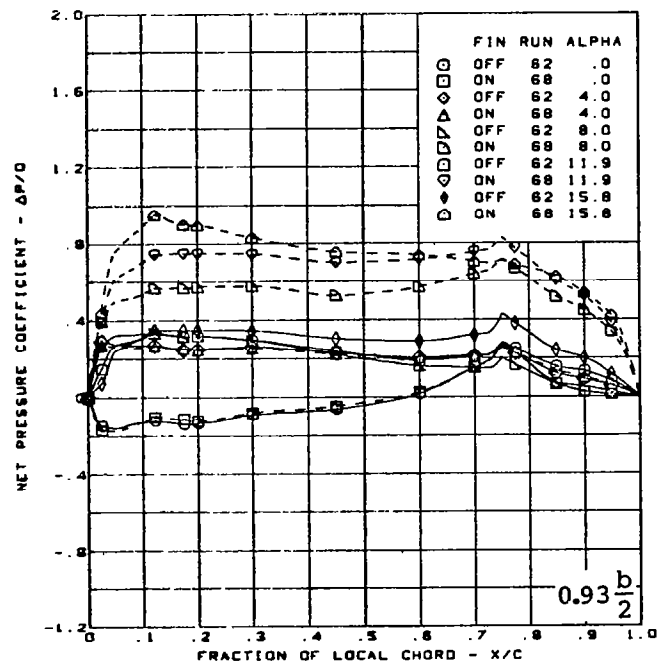
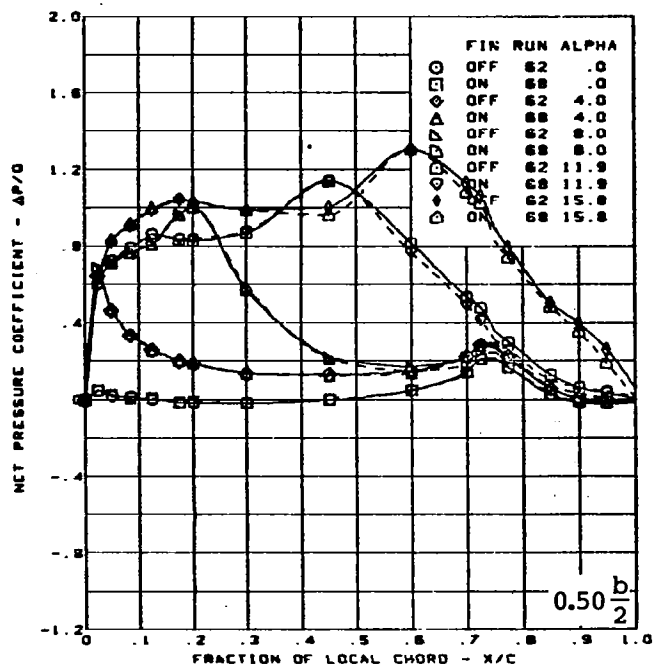
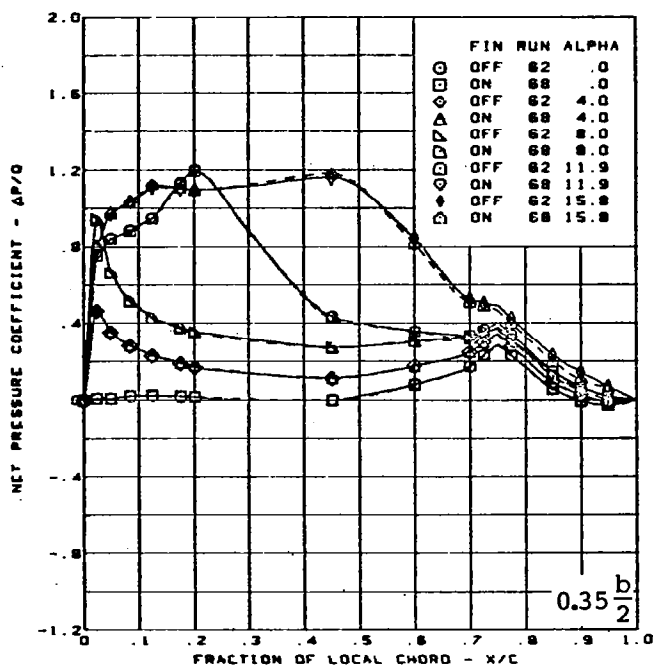
(c) (Concluded)

Figure 39. — (Continued)



(d) Net Chordwise Pressure Distributions

Figure 39. - (Continued)

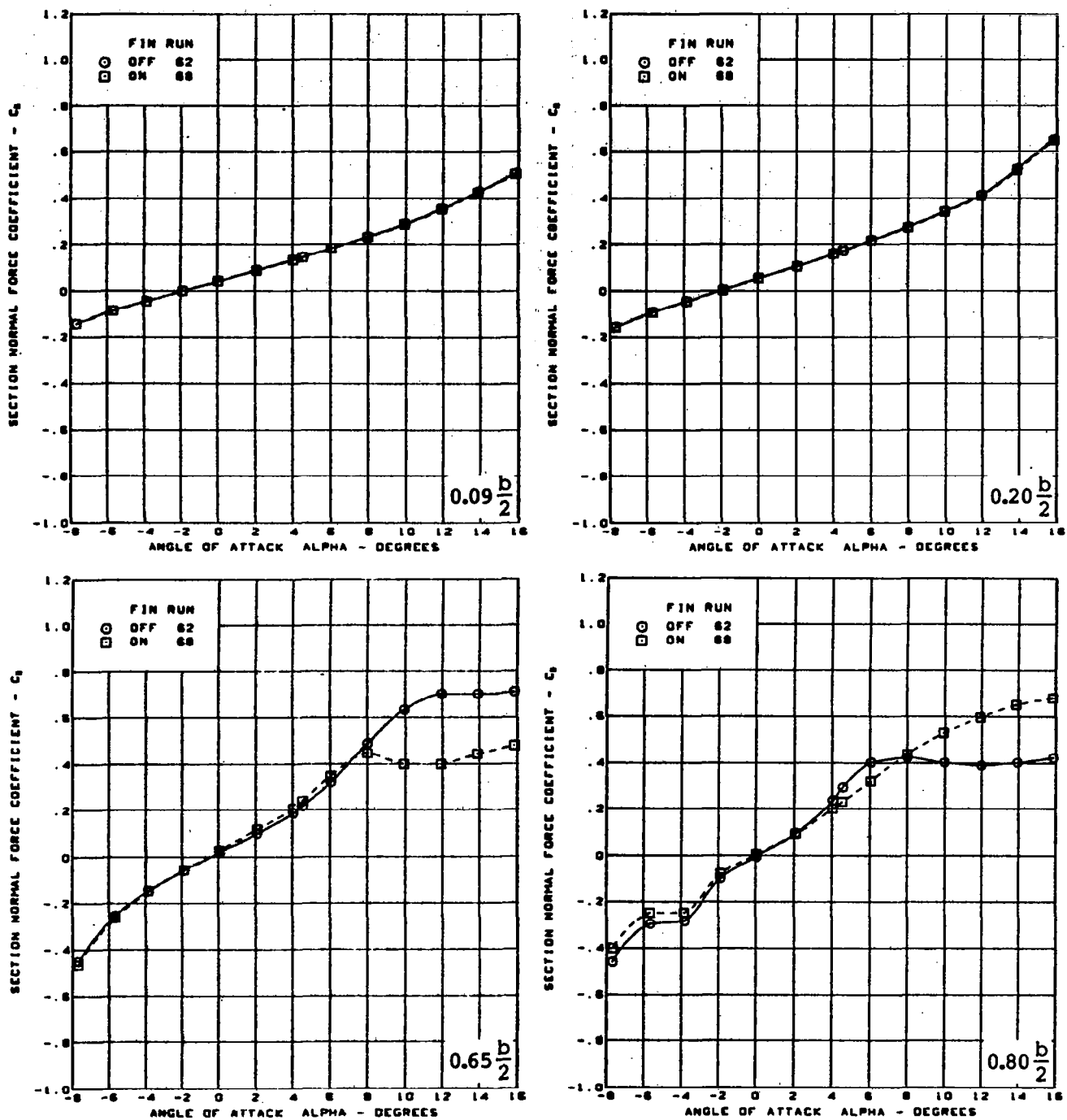


$M = 0.85$   
 Cambered-twisted wing, rounded L.E.  
 L.E. deflection, full span =  $0.0^\circ$   
 T.E. deflection, full span =  $8.3^\circ$

(d) (Concluded)

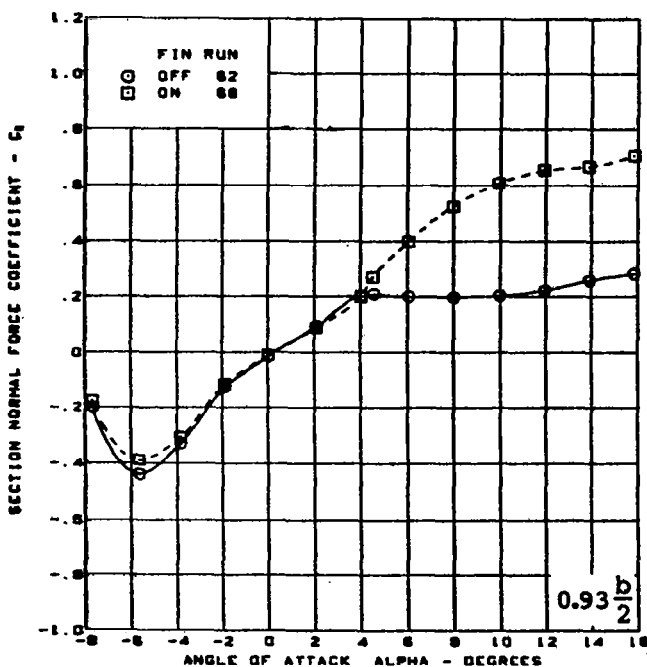
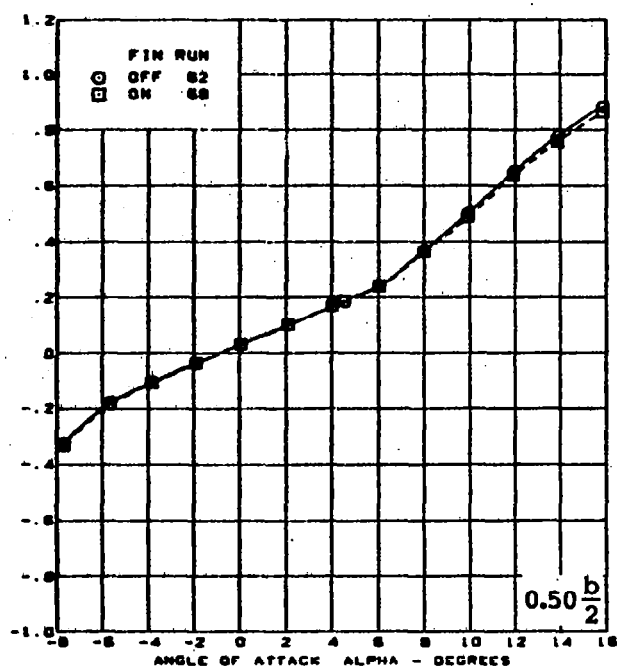
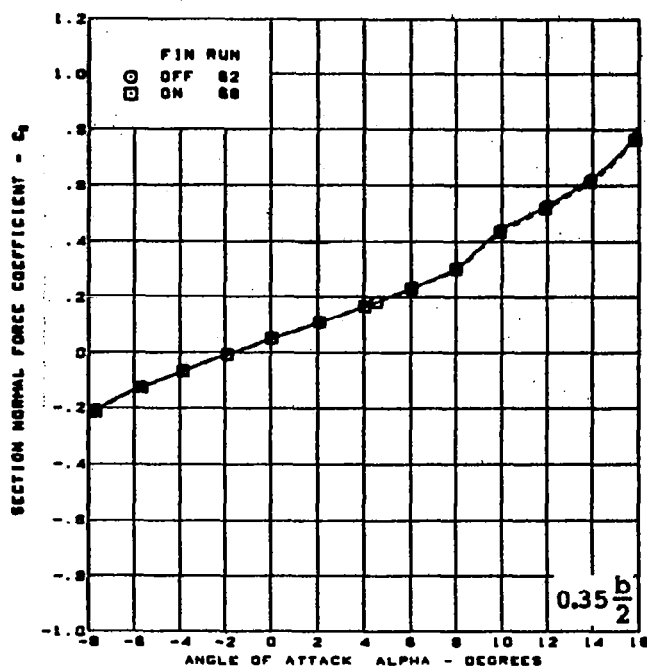
Figure 39. - (Continued)





(e) Section Aerodynamic Coefficients - Normal Force

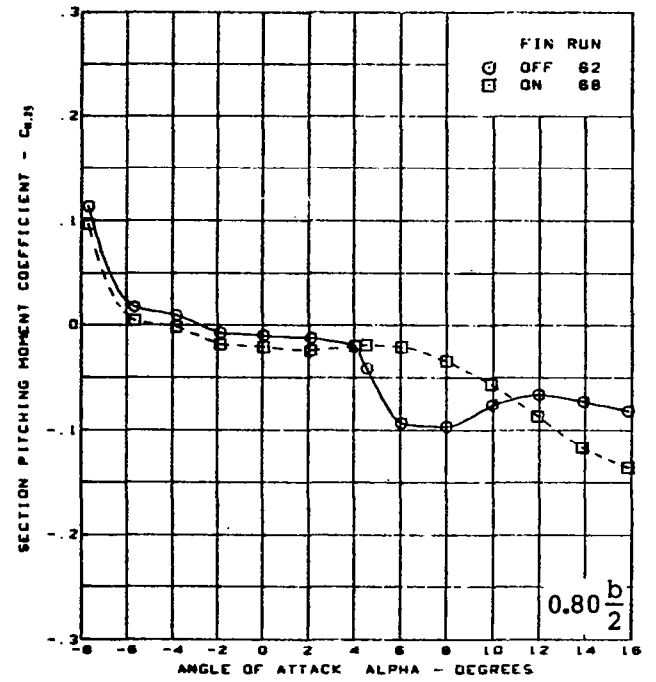
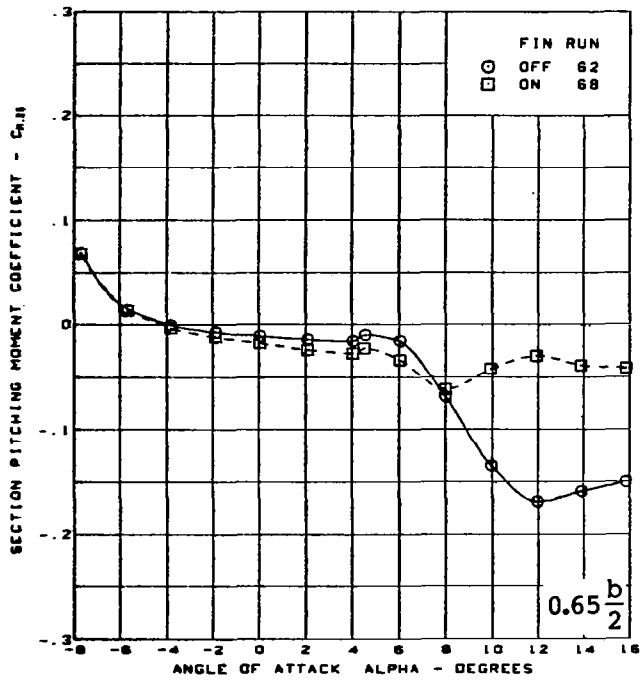
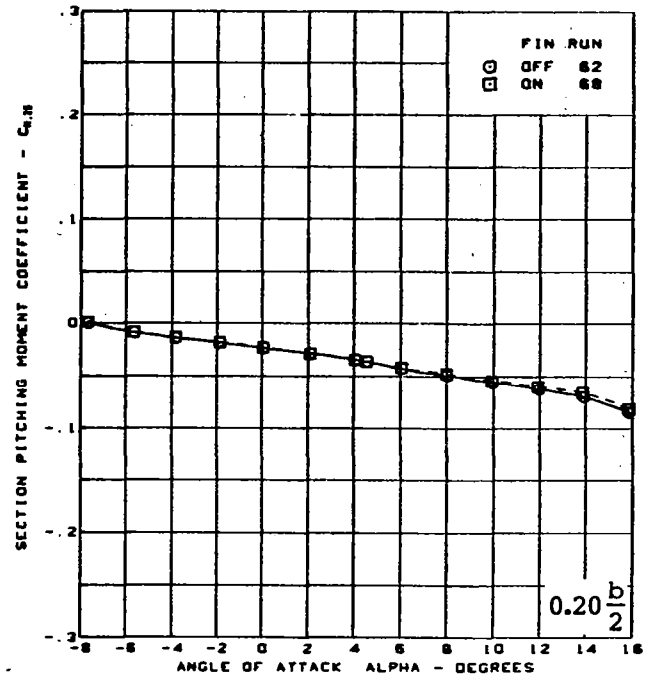
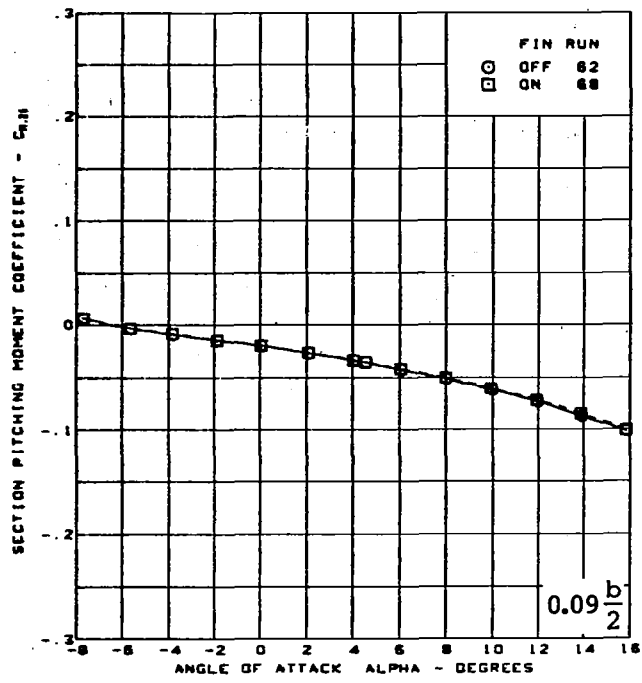
Figure 39. - (Continued)



$M = 0.85$   
 Cambered-twisted wing, rounded L.E.  
 L.E. deflection, full span =  $0.0^\circ$   
 T.E. deflection, full span =  $8.3^\circ$

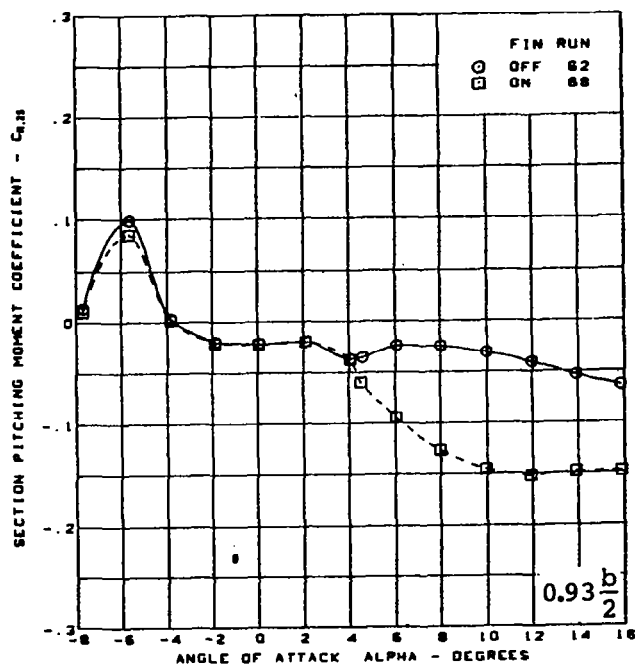
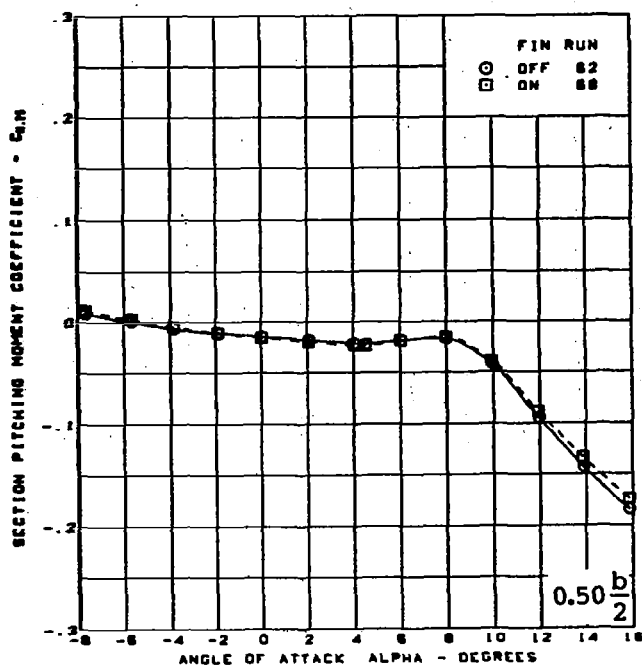
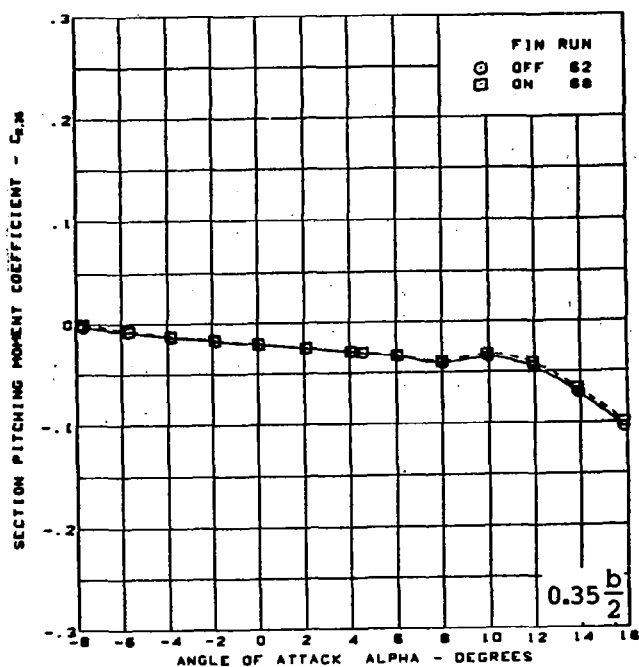
(e) (Concluded)

Figure 39. -- (Continued)



(f) Section Aerodynamic Coefficients - Pitching Moment

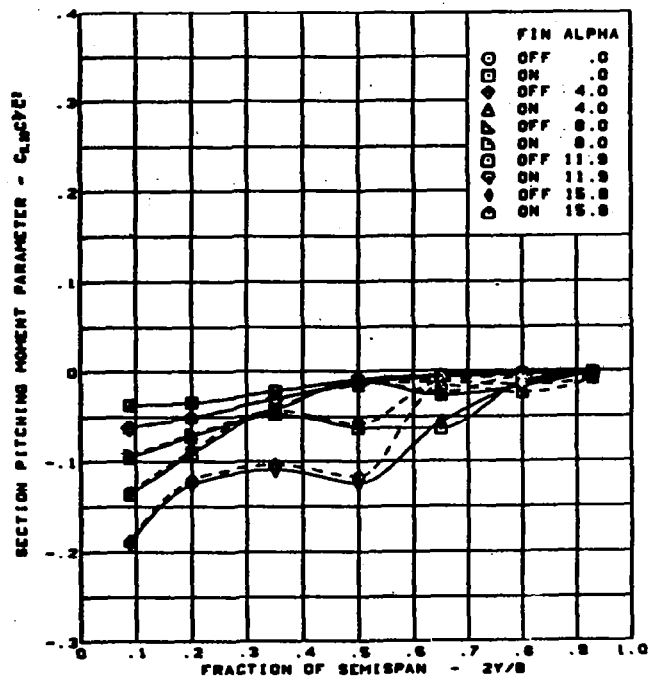
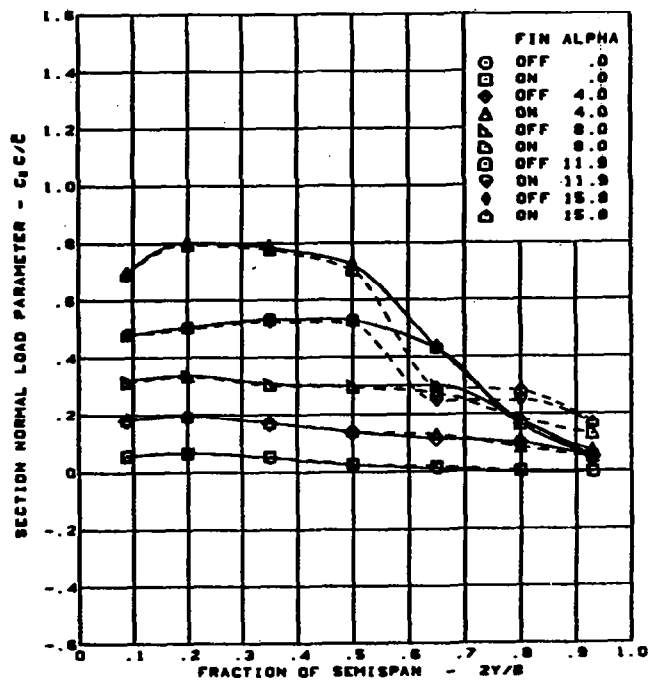
Figure 39. - (Continued)



$M = 0.85$   
 Cambered-twisted wing, rounded L.E.  
 L.E. deflection, full span =  $0.0^\circ$   
 T.E. deflection, full span =  $8.3^\circ$

(f) (Concluded)

Figure 39. — (Continued)



$M = 0.85$

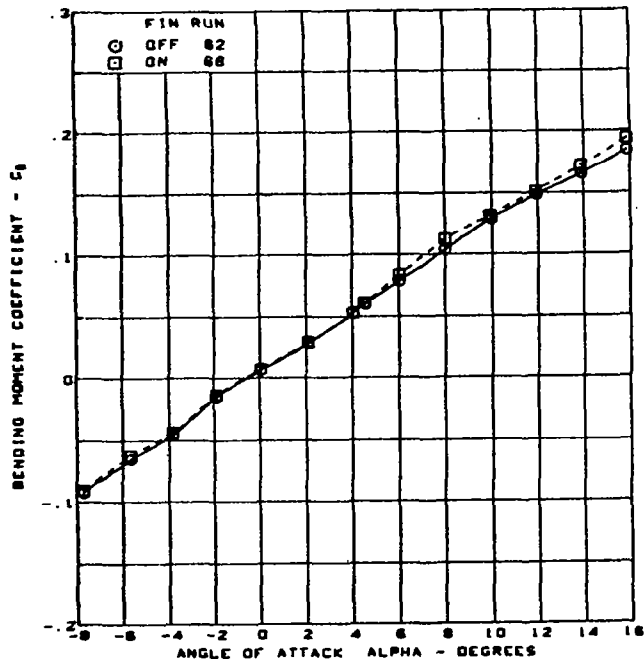
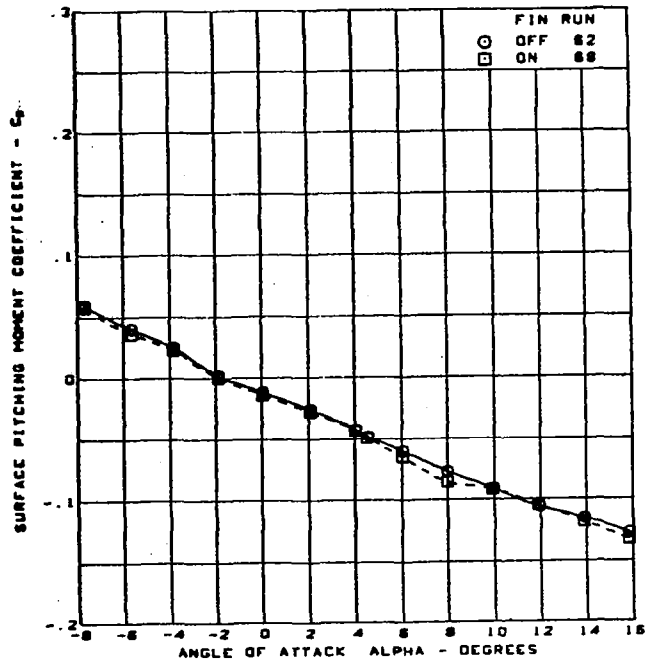
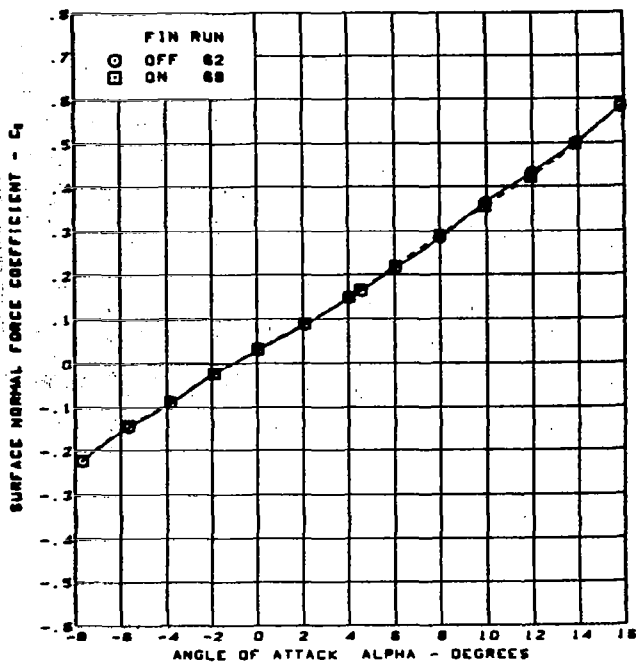
Cambered-twisted wing, rounded L.E.

L.E. deflection, full span =  $0.0^\circ$

T.E. deflection, full span =  $8.3^\circ$

(g) Spanload Distributions

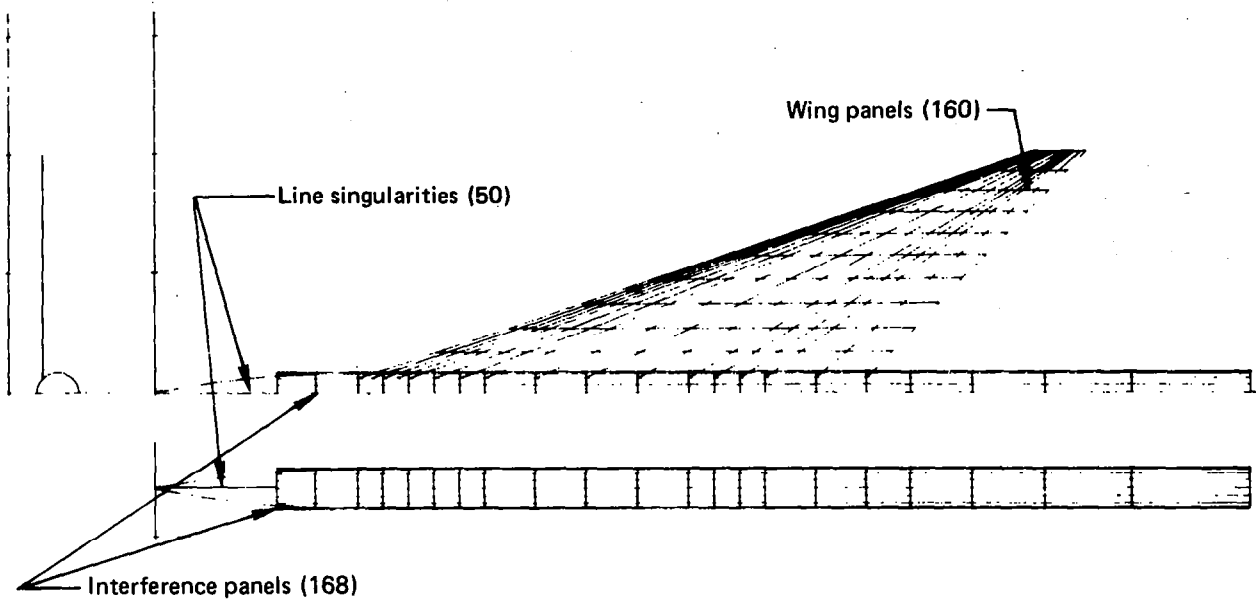
Figure 39. — (Continued)



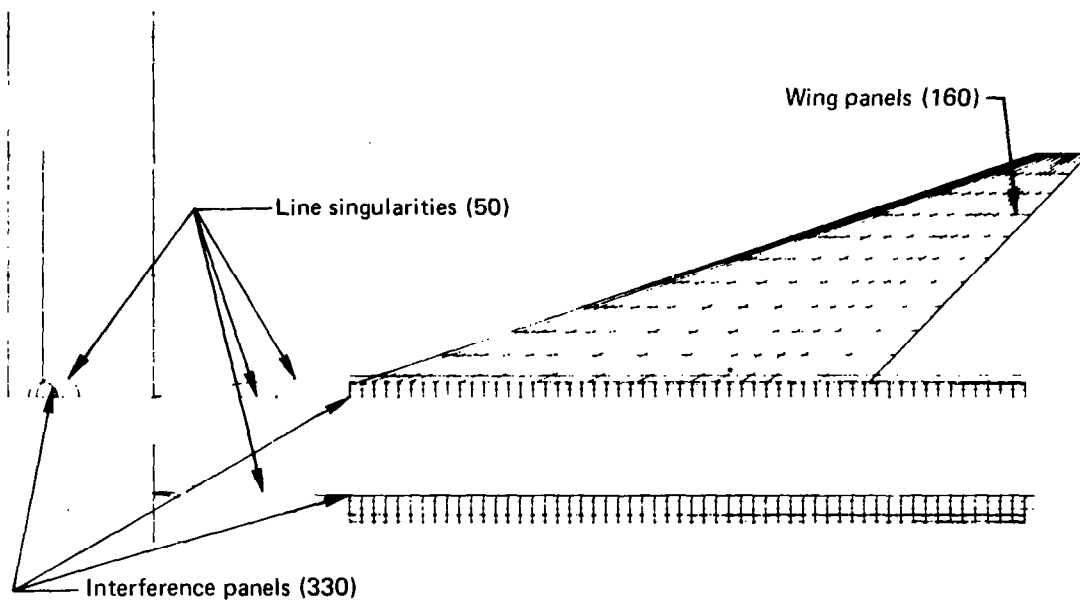
$M = 0.85$   
 Cambered-twisted wing, rounded L.E.  
 L.E. deflection, full span =  $0.0^\circ$   
 T.E. deflection, full span =  $8.3^\circ$

(h) Wing Aerodynamic Coefficients

Figure 39. - (Concluded)

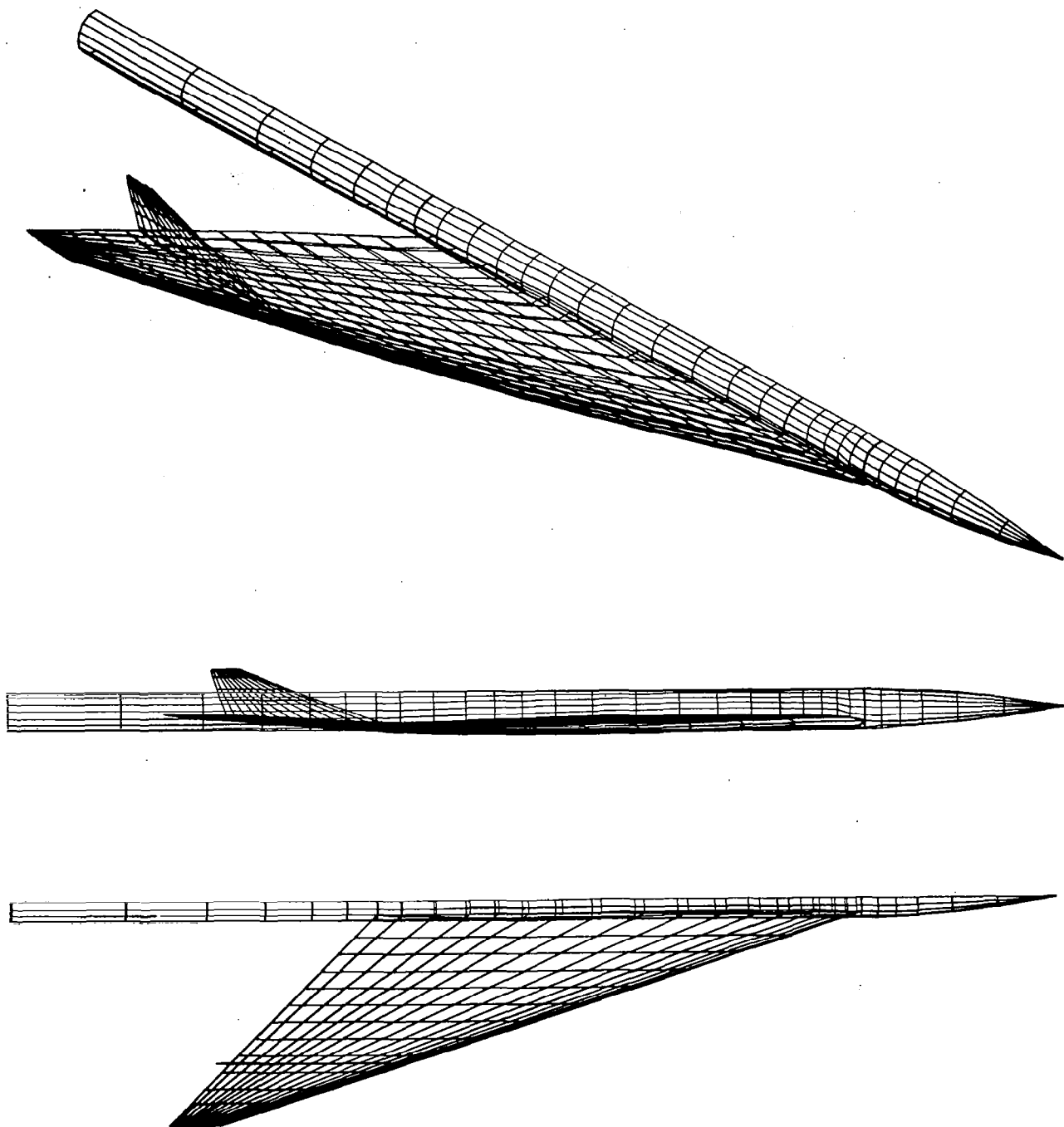


(a) Arrangement of Panels Used for Subsonic Mach Numbers



(b) Arrangement of Panels Used for Supersonic Mach Numbers

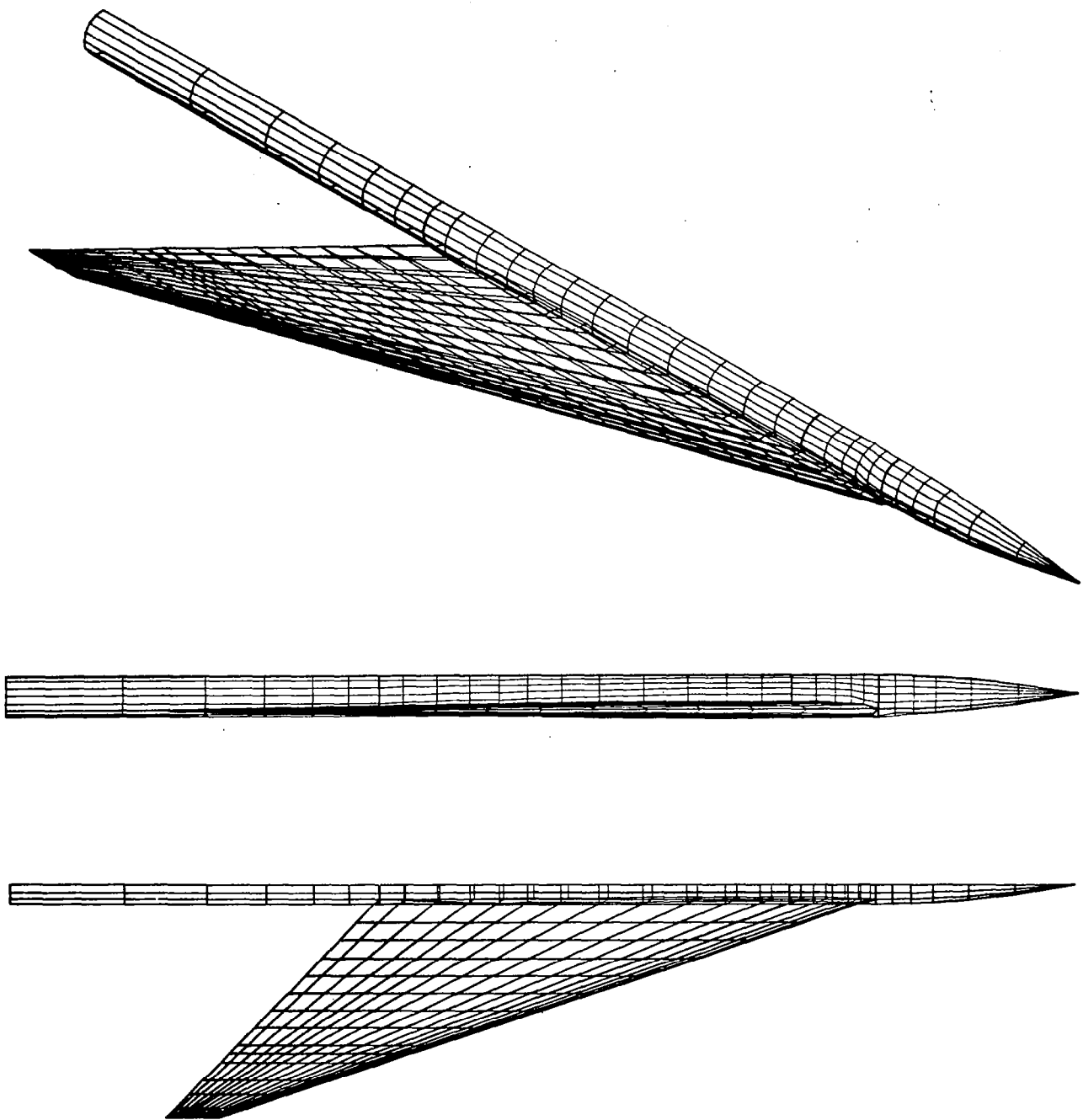
Figure 40. —Paneling for FLEXSTAB Computer Program



(a) Cambered-twisted Wing, Fin On

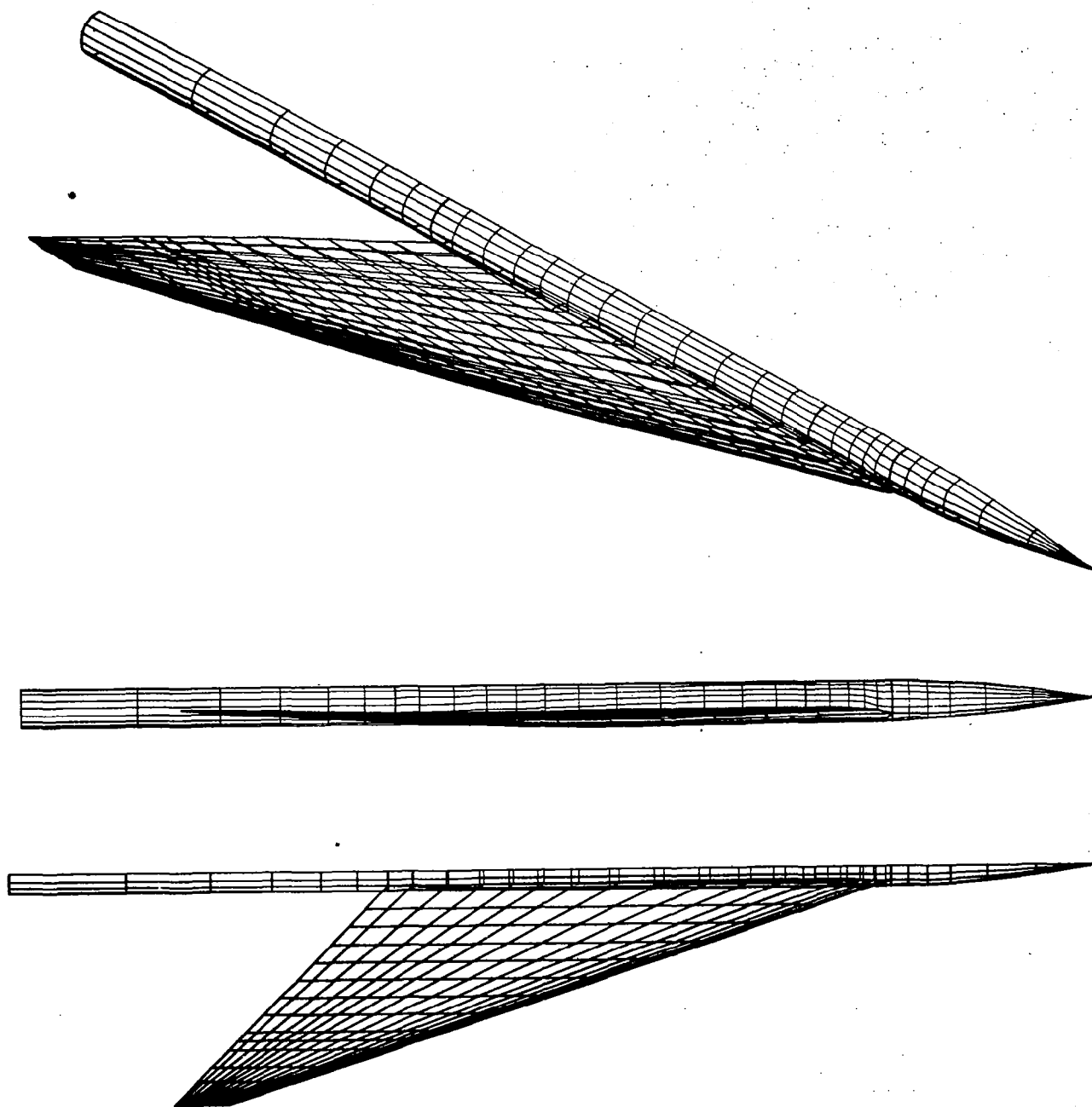
*Figure 41.—Paneling for PAN AIR Computer Program*





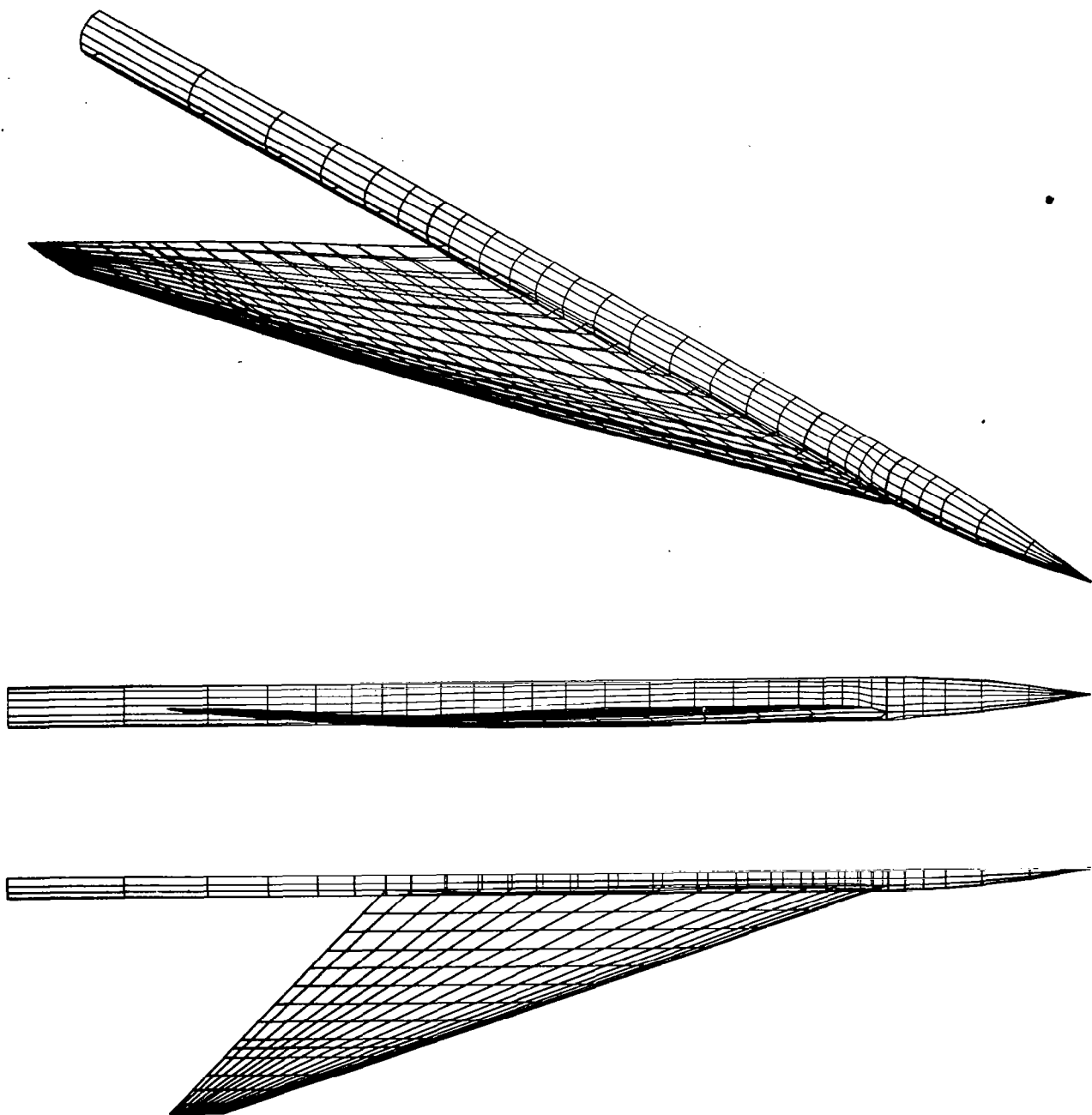
(b) Flat Wing

*Figure 41.—(Continued)*



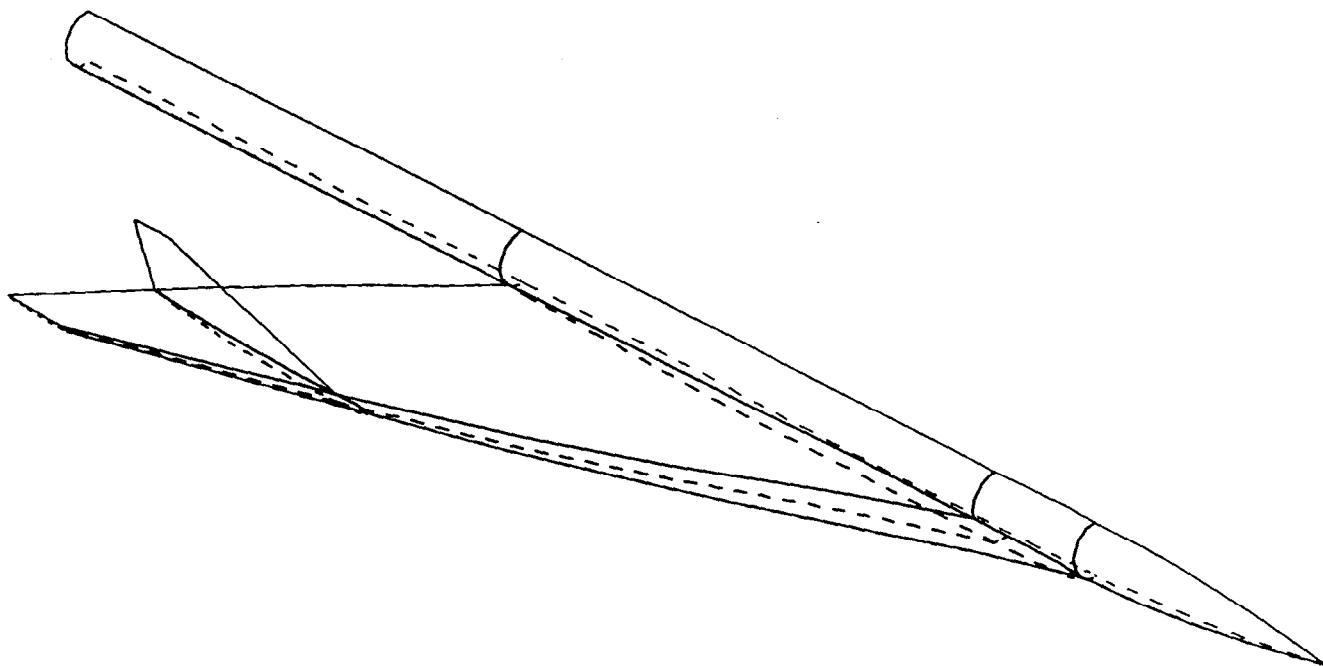
(c) Twisted Wing

Figure 41.—(Continued)



(d) Cambered-twisted Wing, Fin Off

*Figure 41.—(Concluded)*



*Figure 42.—Networks for PAN AIR Computer Program, Cambered-twisted Wing, Fin On*

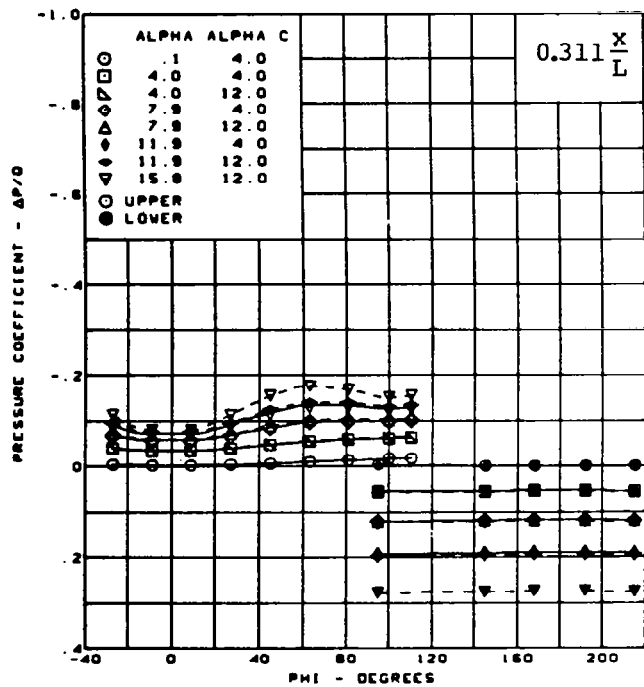
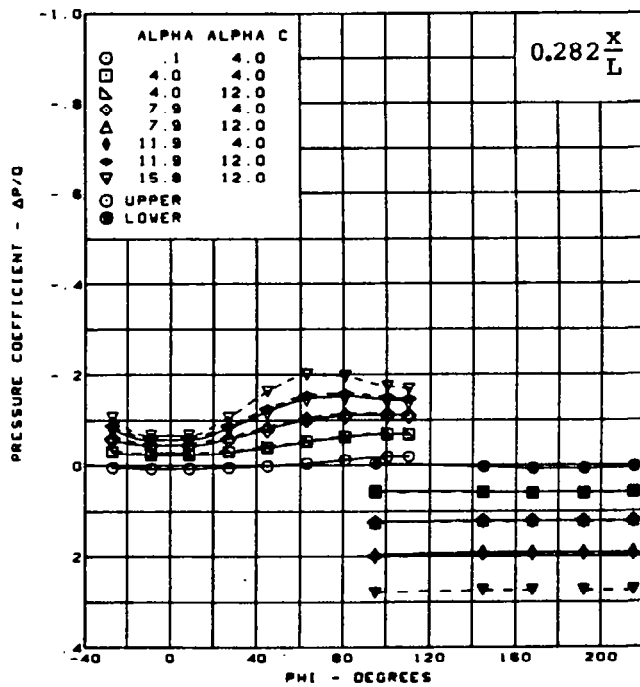
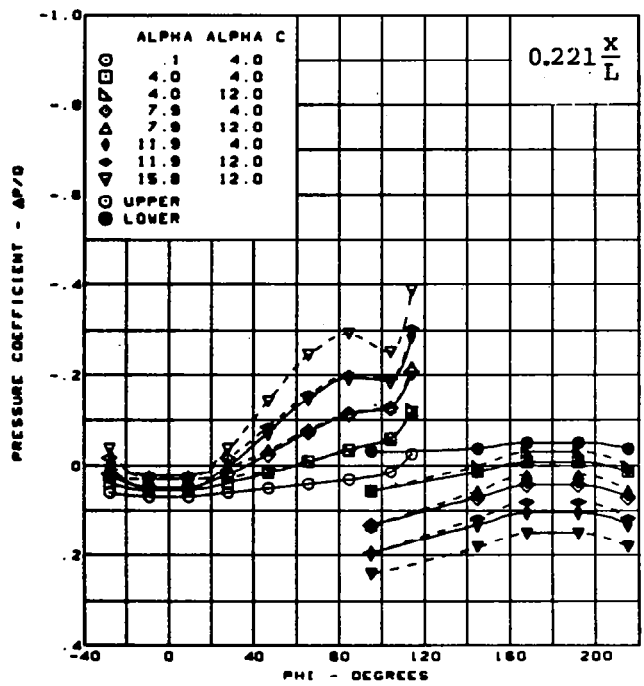
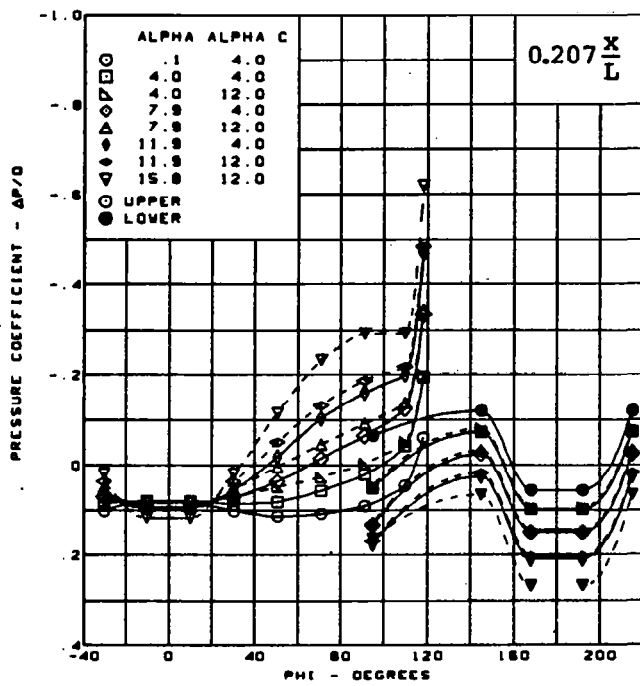
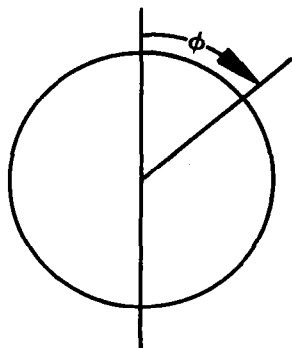
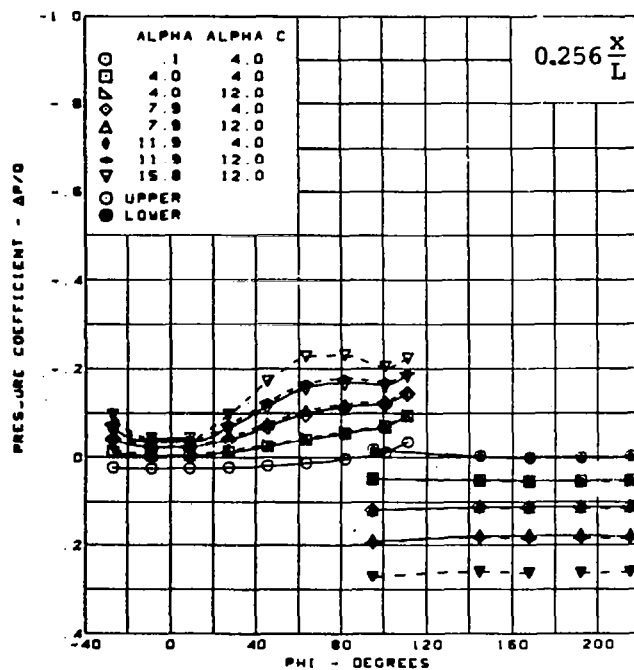
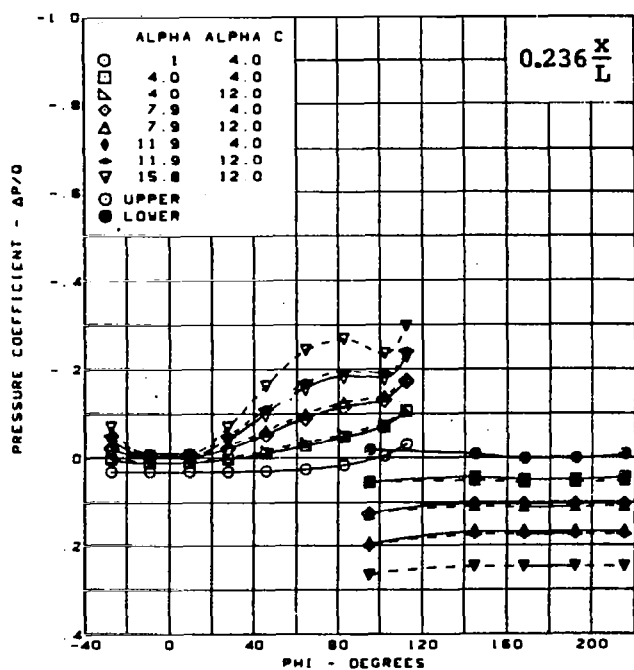
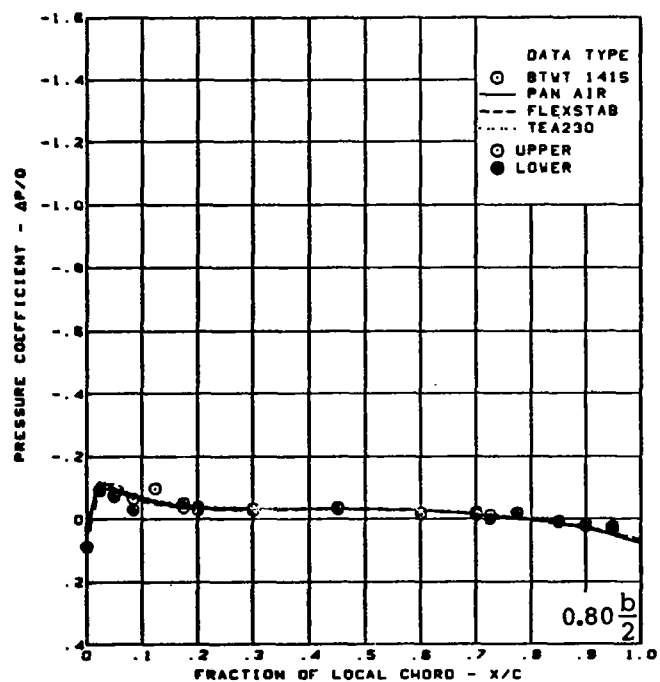
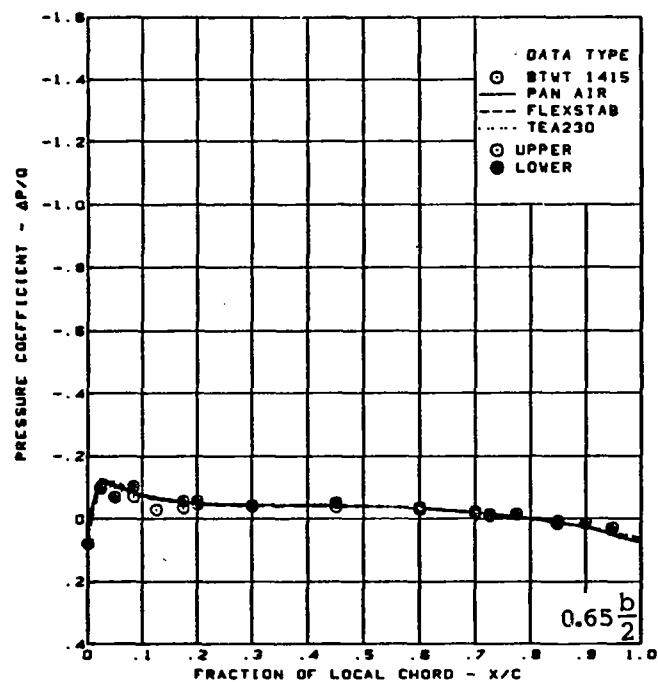
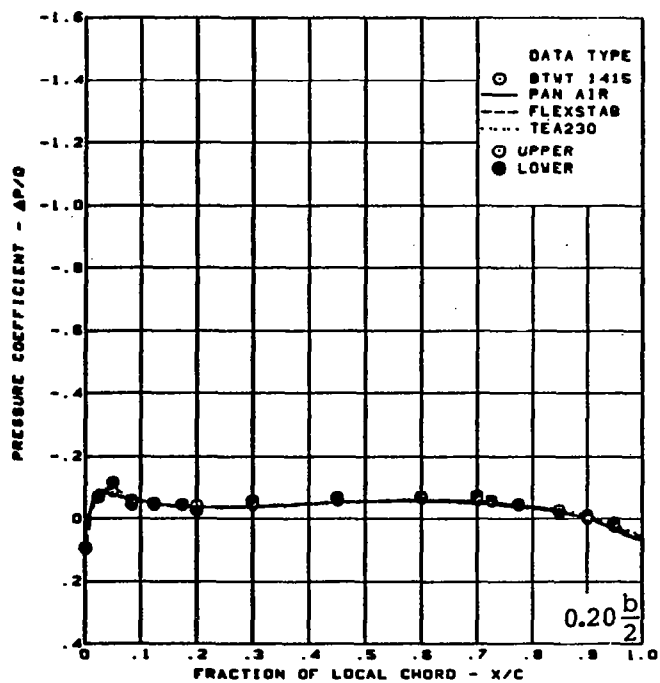
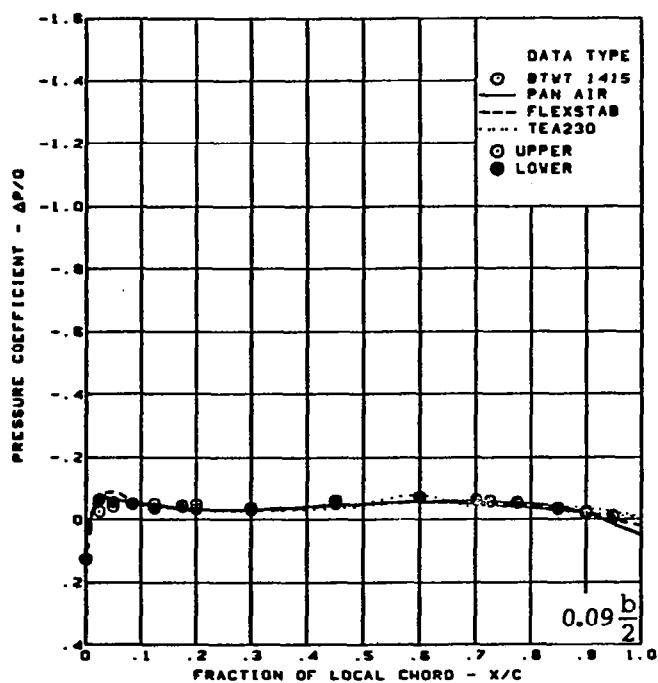


Figure 43.—Effect of Compressibility Axis on Body Pressures Predicted by PAN AIR



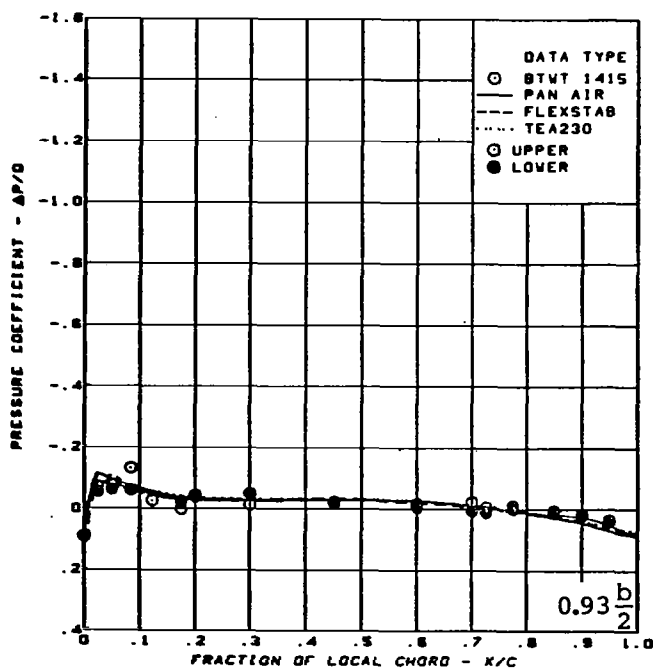
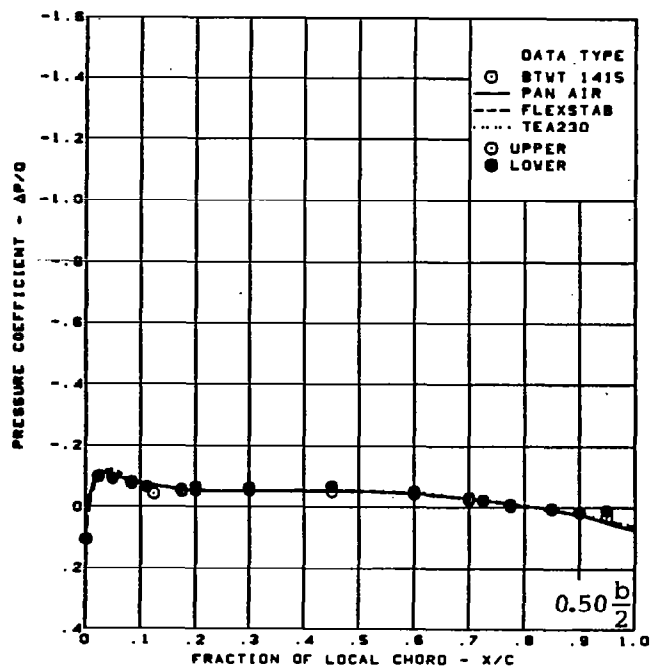
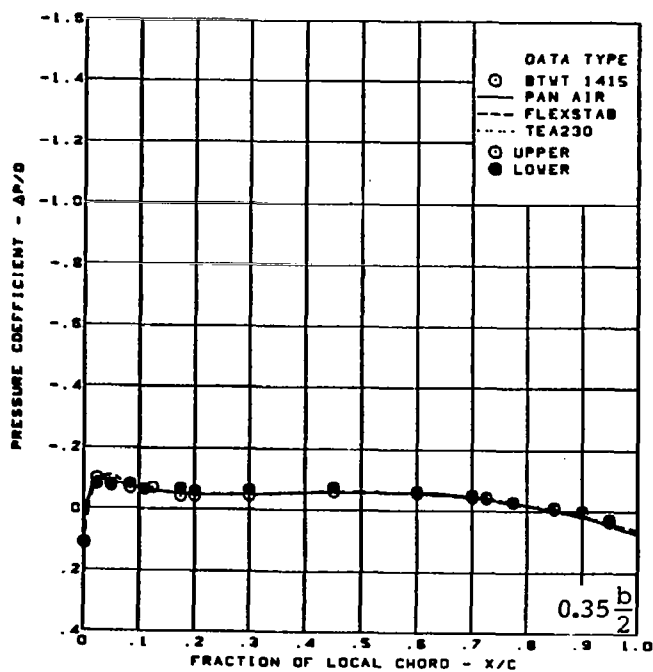
$M = 1.05$   
 Cambered - twisted wing, rounded L.E.  
 Fin off  
 L.E. deflection, full span =  $0.0^\circ$   
 T.E. deflection, full span =  $0.0^\circ$

Figure 43. -(Concluded)



(a) Surface Chordwise Pressure Distributions -  $\alpha = 0^\circ$

Figure 44. — Wing Theory-to-Experiment Comparison; Flat Wing; T.E. Deflection, Full Span =  $0.0^\circ$ ;  $M = 0.85$



$M = 0.85$  (run 267)

$\alpha = 0^\circ$

Flat wing, rounded L.E.

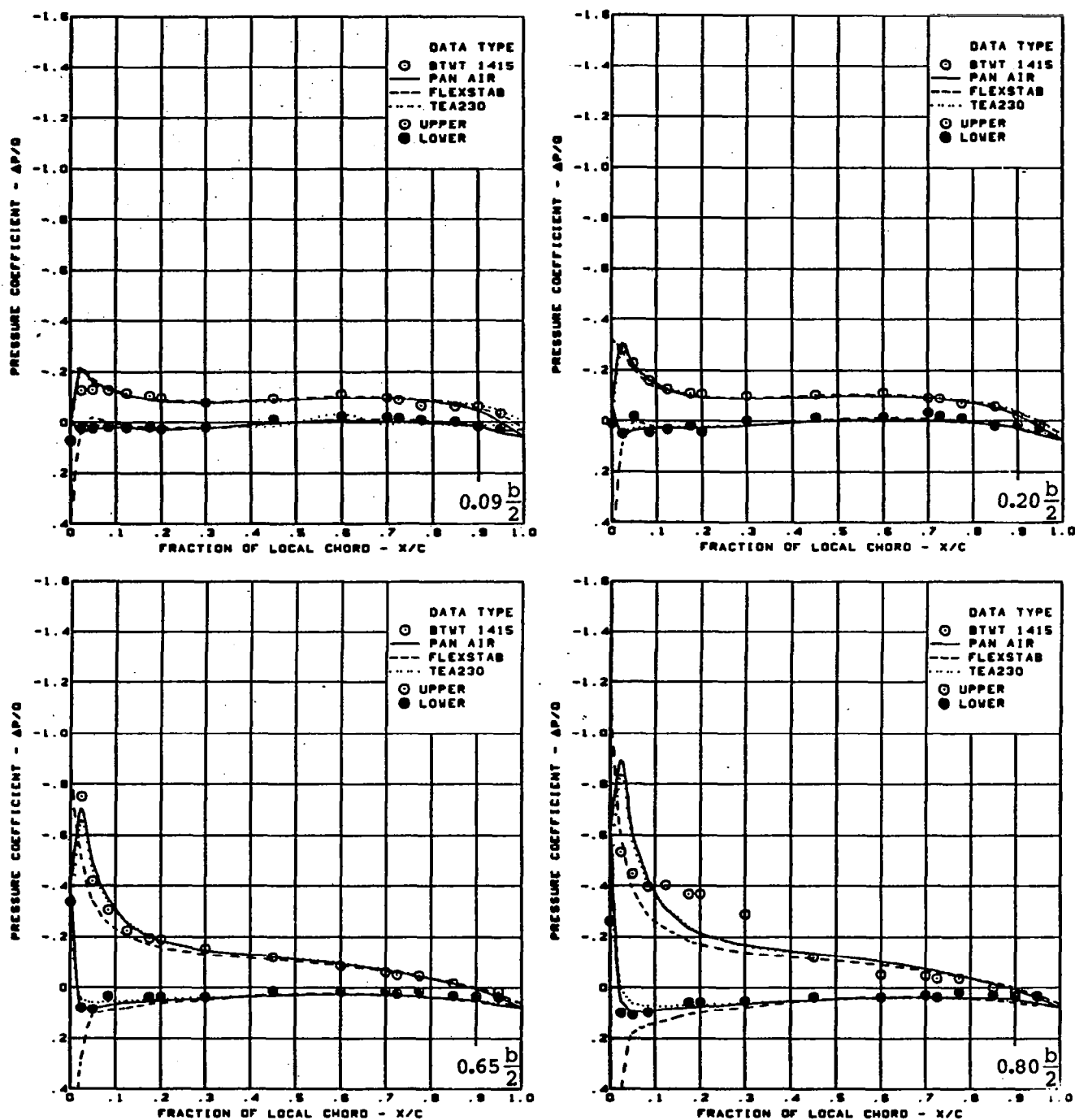
L.E. deflection, full span =  $0.0^\circ$

T.E. deflection, full span =  $0.0^\circ$

(a) (Concluded)

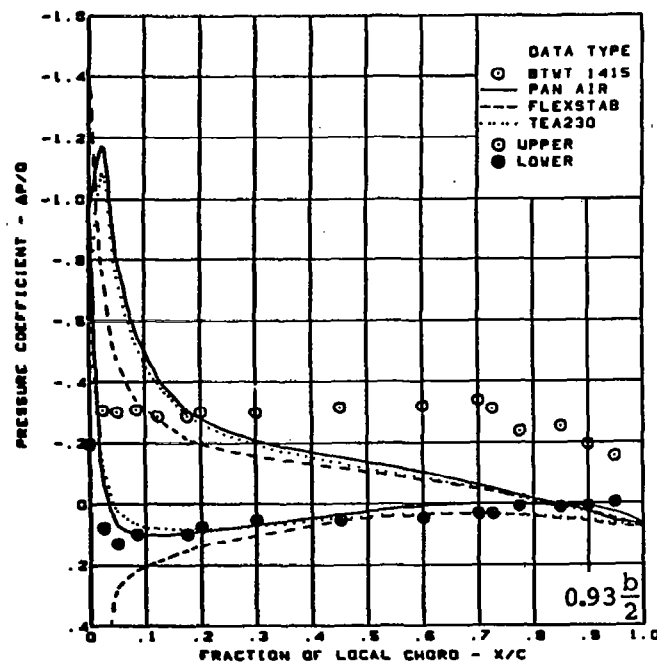
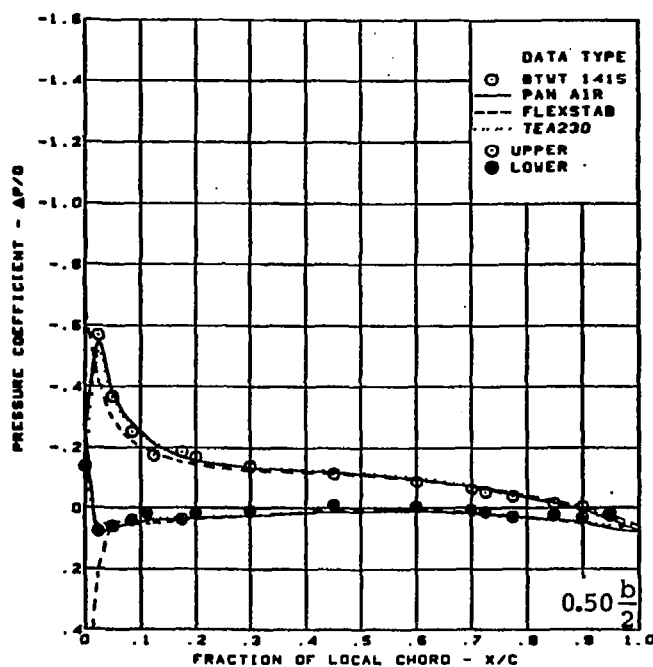
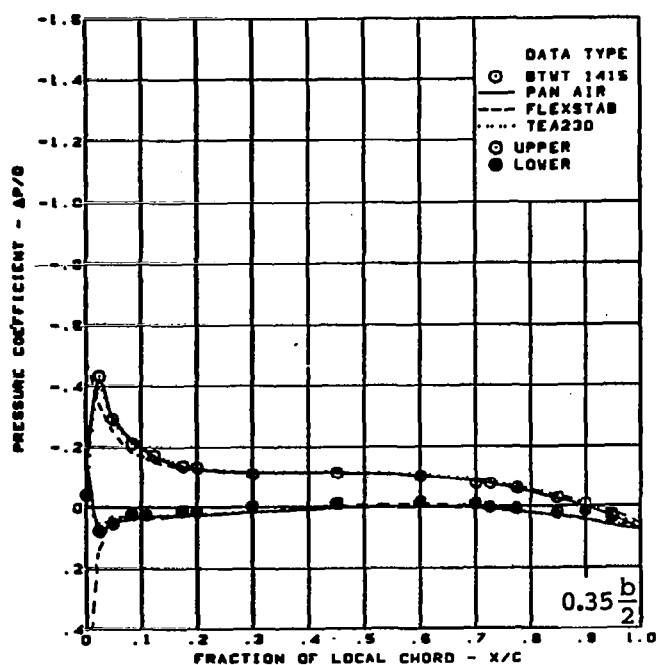
Figure 44. - (Continued)





(b) Surface Chordwise Pressure Distributions -  $\alpha = 4^\circ$

Figure 44. - (Continued)



$M = 0.85$  (run 267)

$\alpha = 4^\circ$

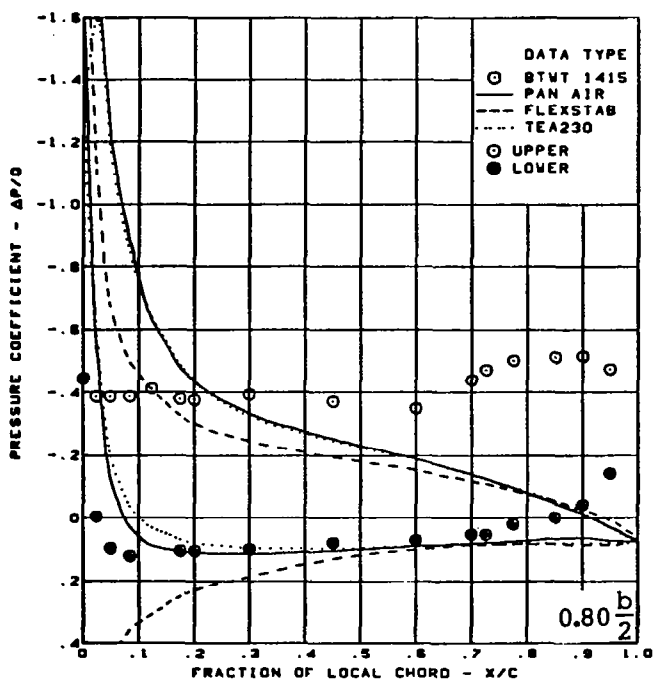
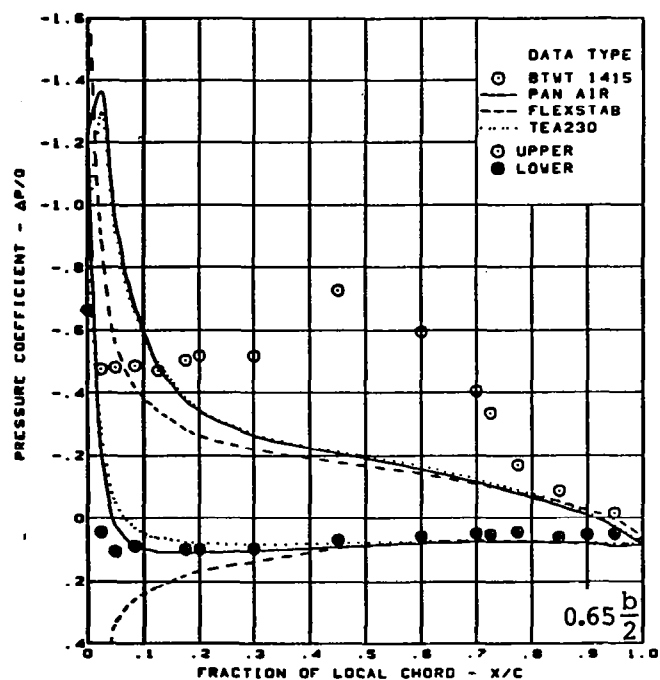
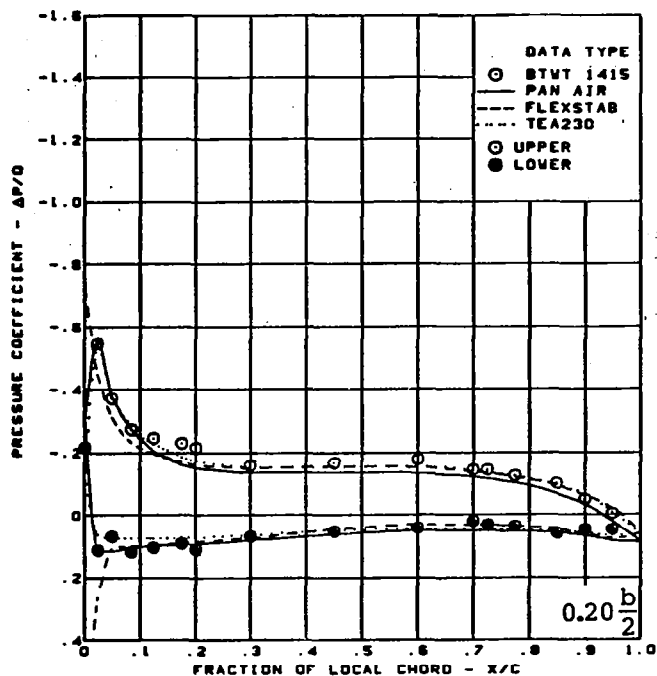
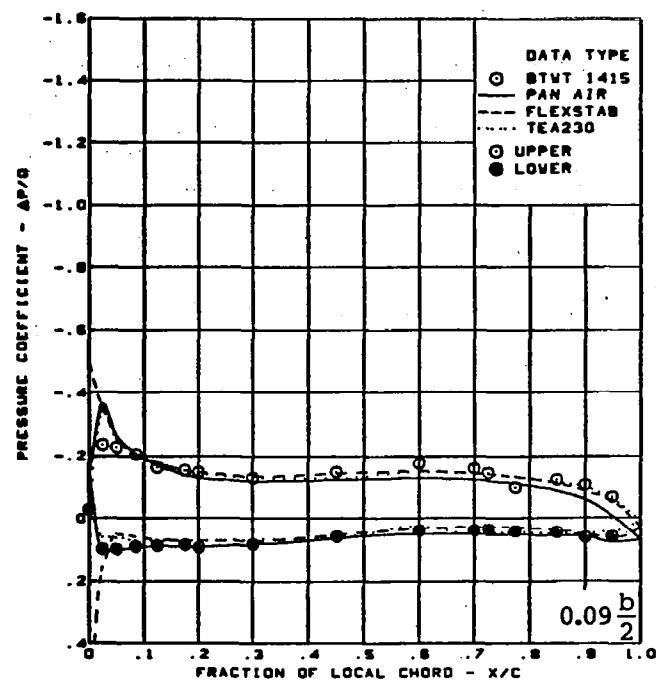
Flat wing, rounded L.E.

L.E. deflection, full span =  $0.0^\circ$

T.E. deflection, full span =  $0.0^\circ$

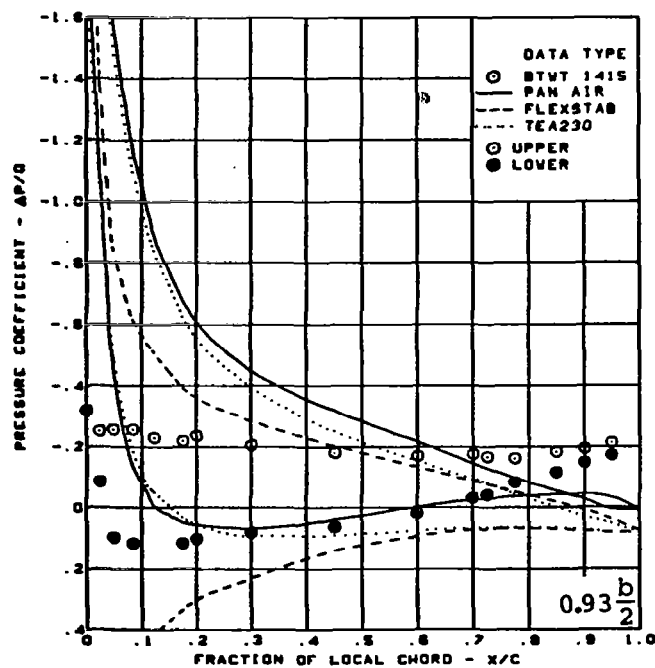
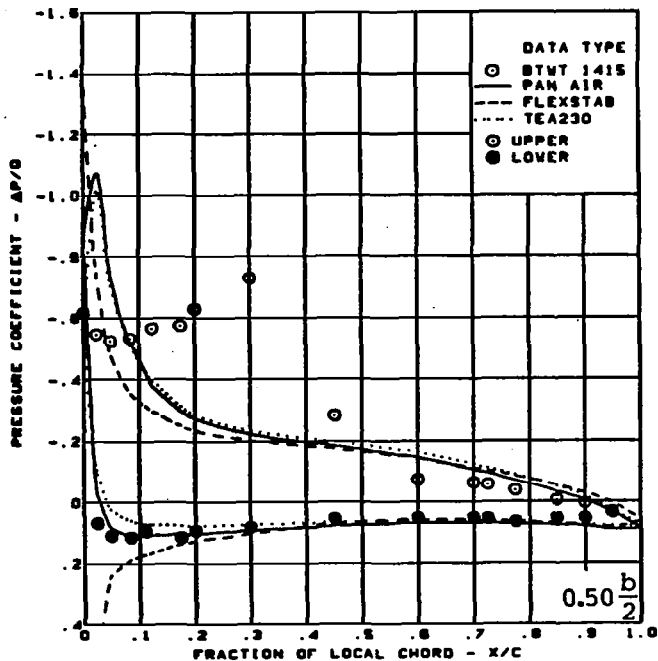
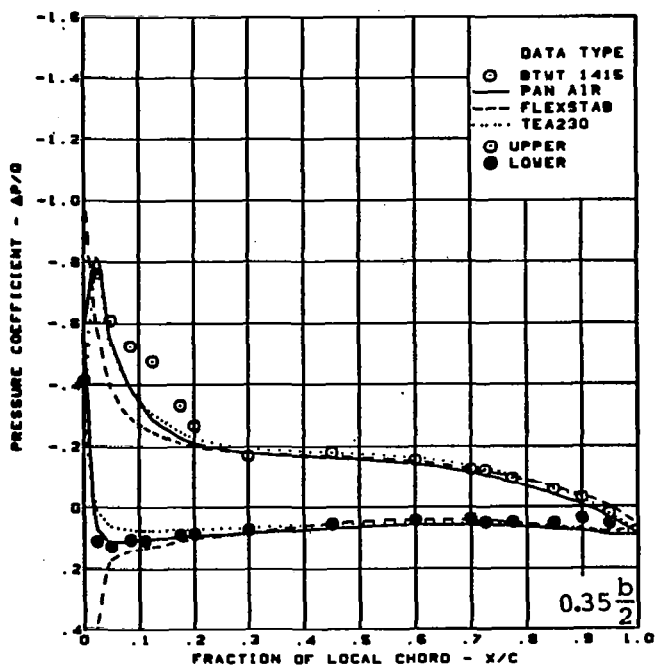
(b) (Concluded)

Figure 44. — (Continued)



(c) Surface Chordwise Pressure Distributions -  $\alpha = 8^\circ$

Figure 44. - (Continued)



$M = 0.85$  (run 267)

$\alpha = 8^\circ$

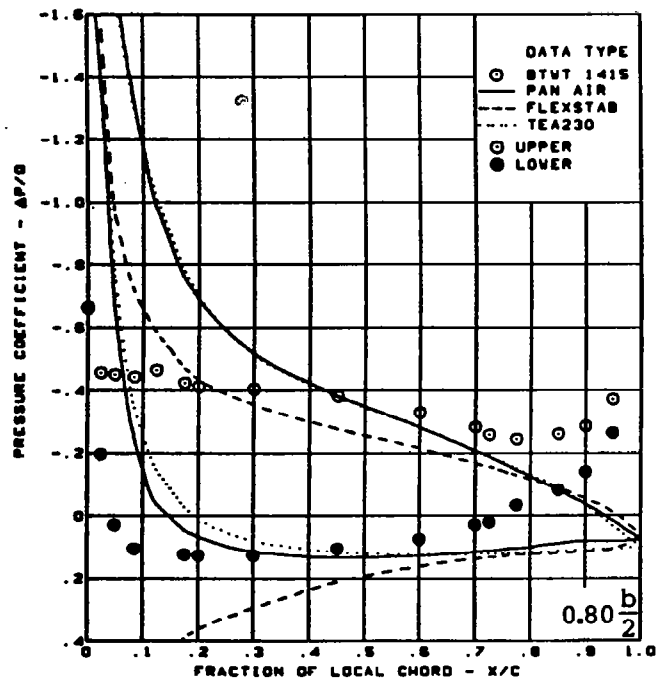
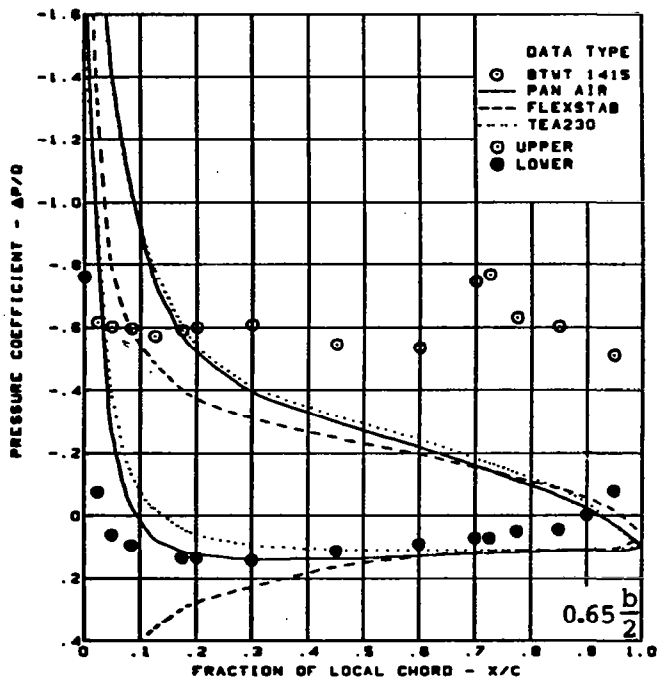
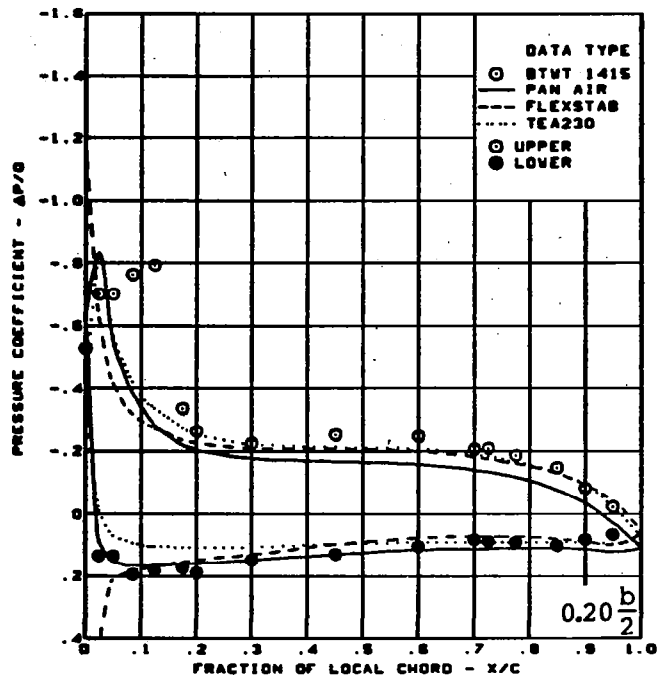
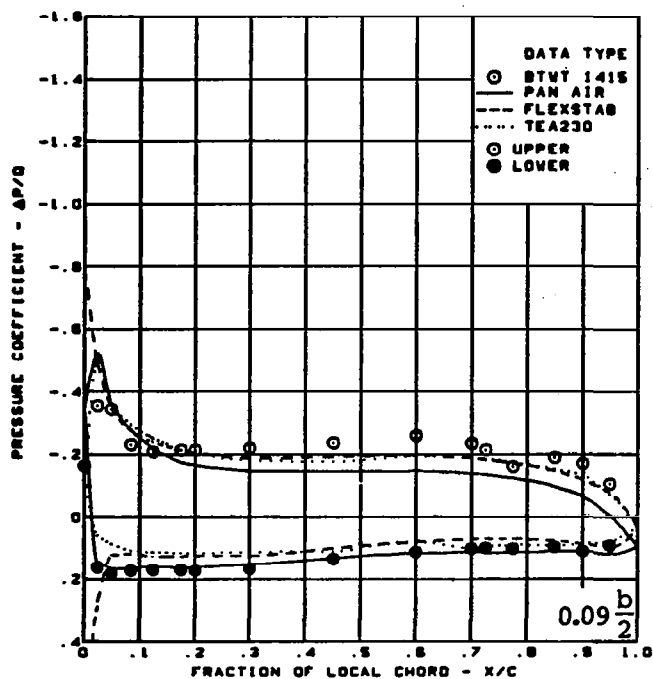
Flat wing, rounded L.E.

L.E. deflection, full span =  $0.0^\circ$

T.E. deflection, full span =  $0.0^\circ$

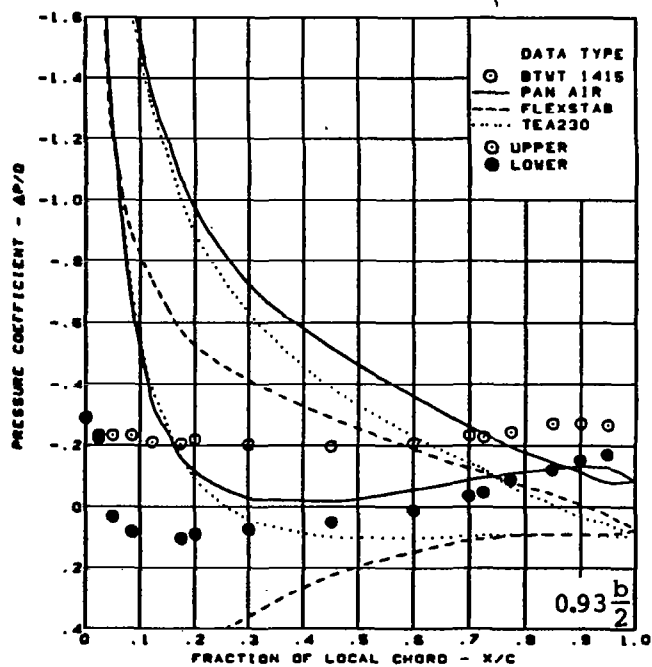
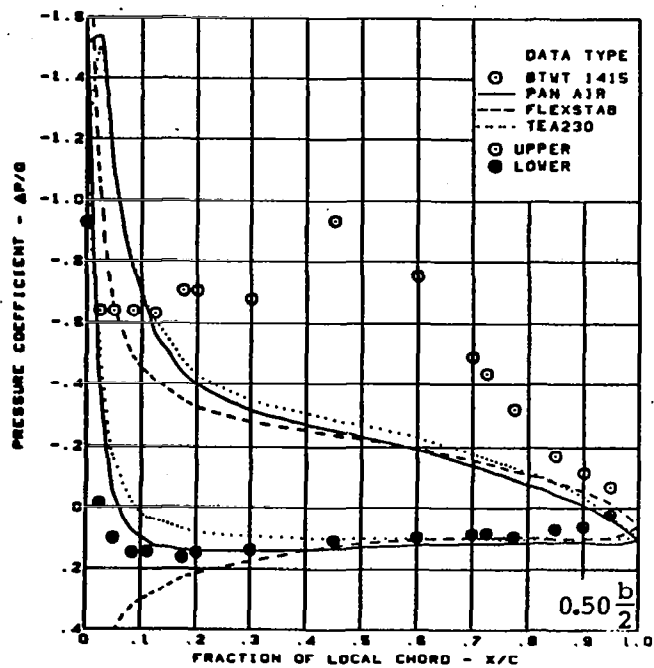
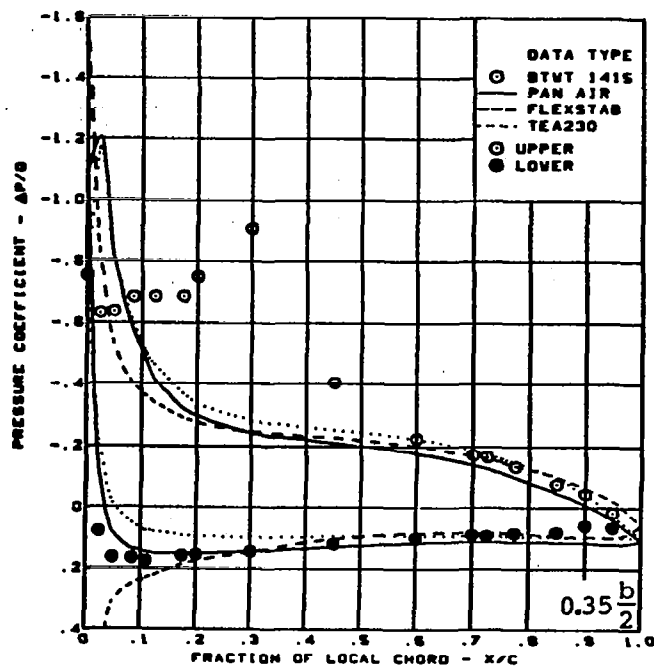
(c) (Concluded)

Figure 44. - (Continued)



(d) Surface Chordwise Pressure Distributions -  $\alpha = 12^\circ$

Figure 44. - (Continued)



$M = 0.85$  (run 267)

$\alpha = 12^\circ$

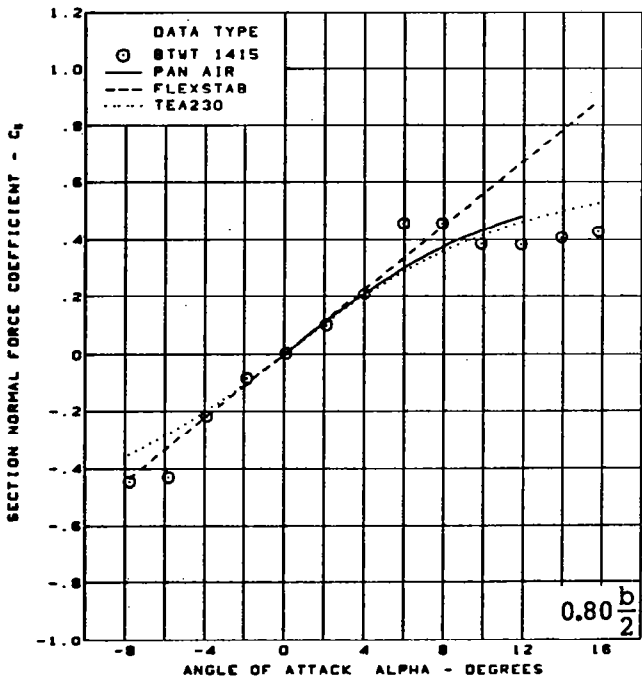
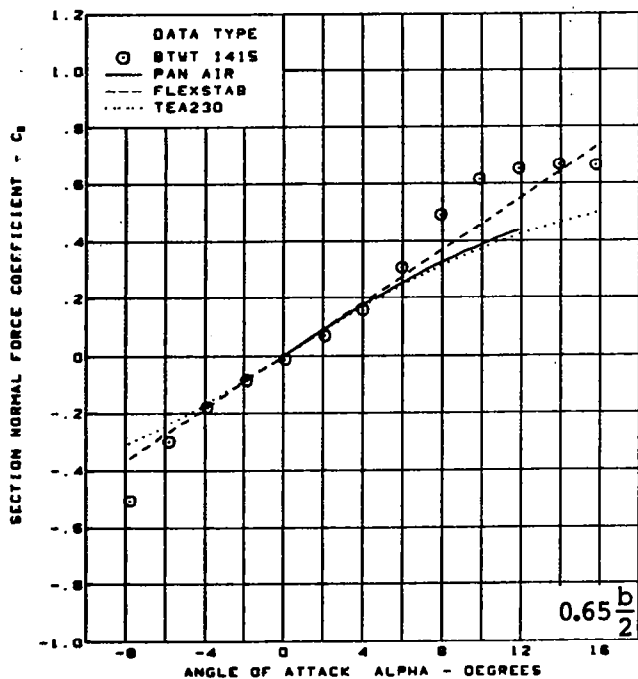
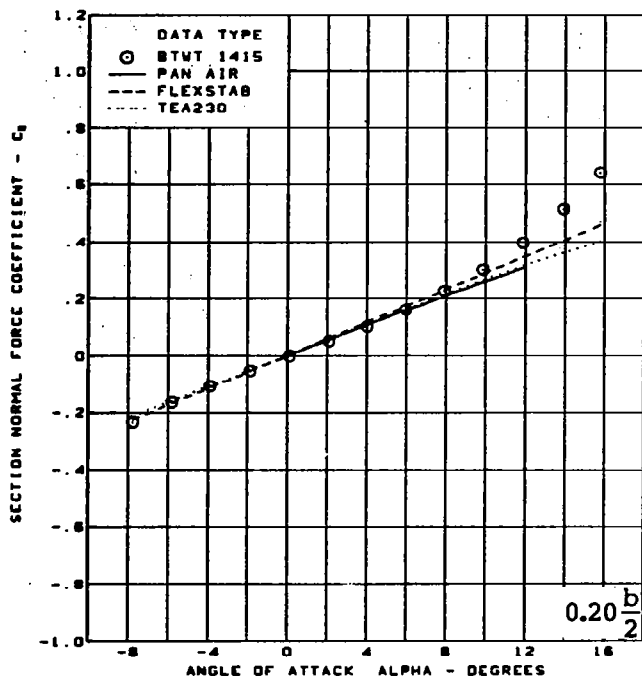
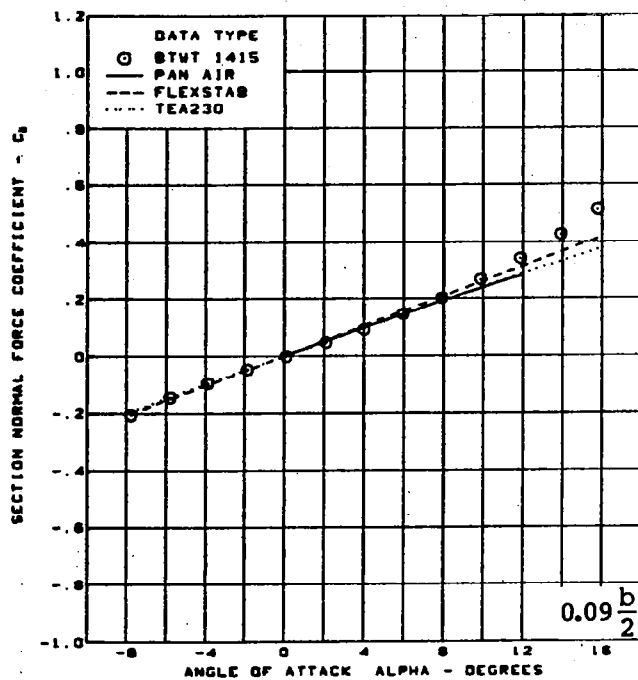
Flat wing, rounded L.E.

L.E. deflection, full span =  $0.0^\circ$

T.E. deflection, full span =  $0.0^\circ$

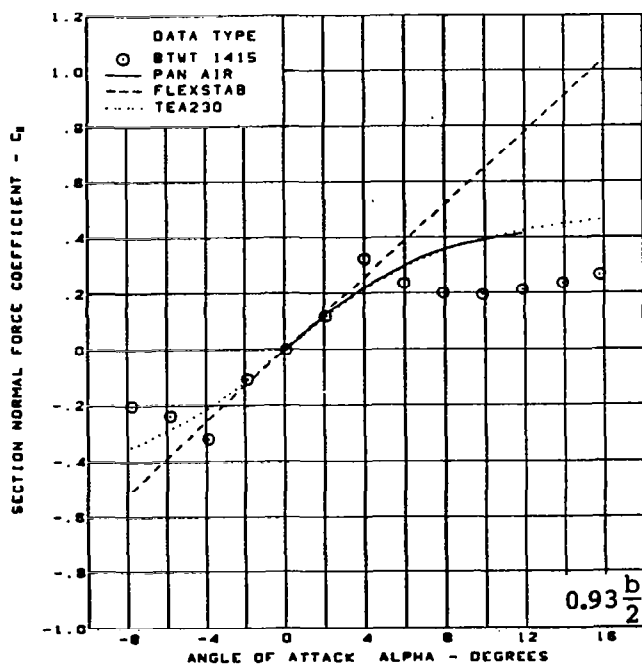
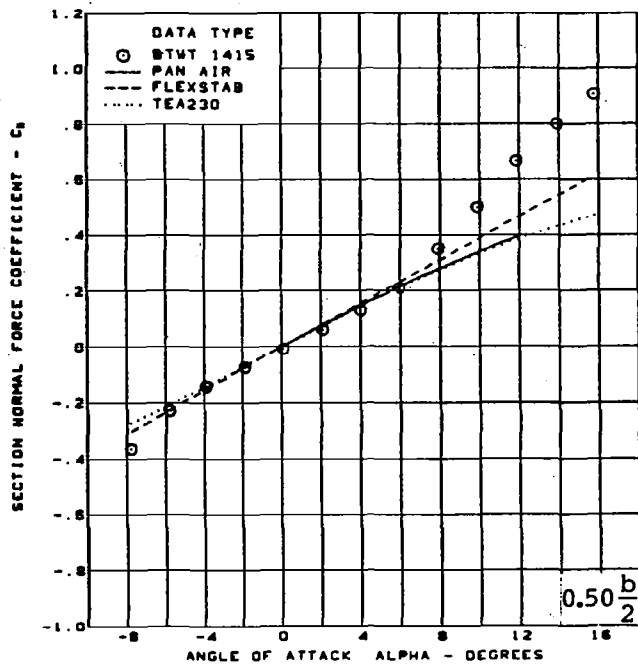
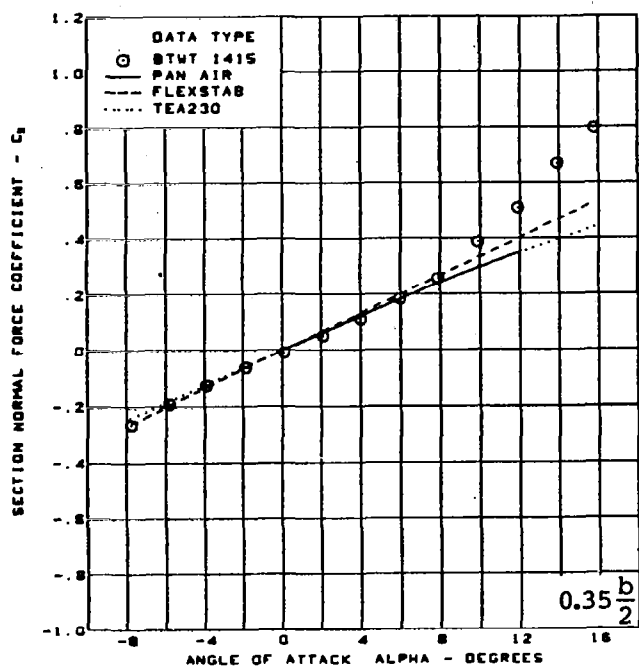
(d) (Concluded)

Figure 44. - (Continued)



(e) Section Aerodynamic Coefficients - Normal Force

Figure 44. - (Continued)

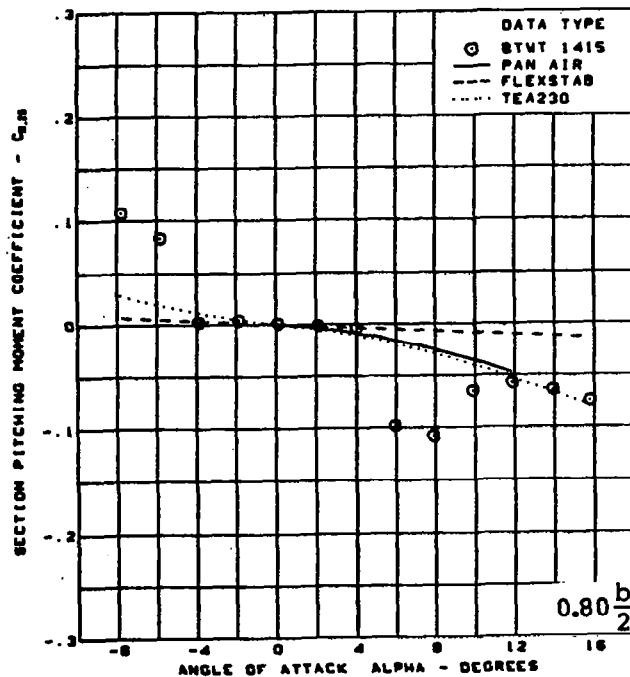
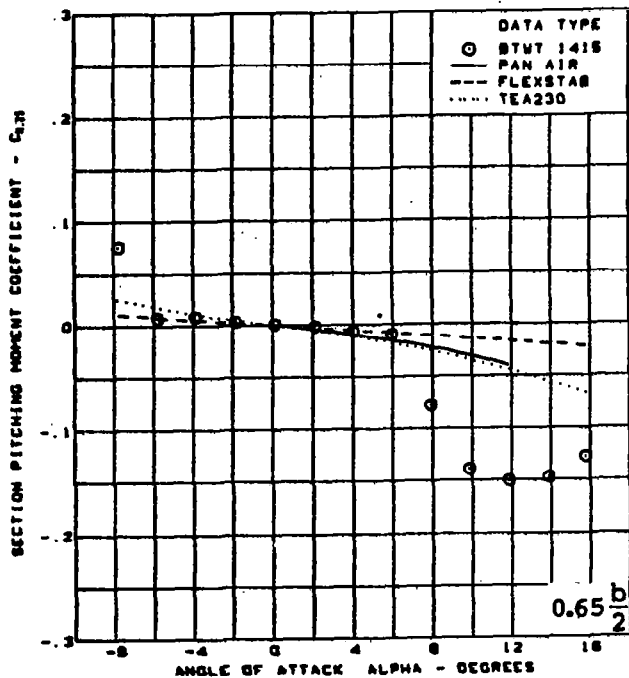
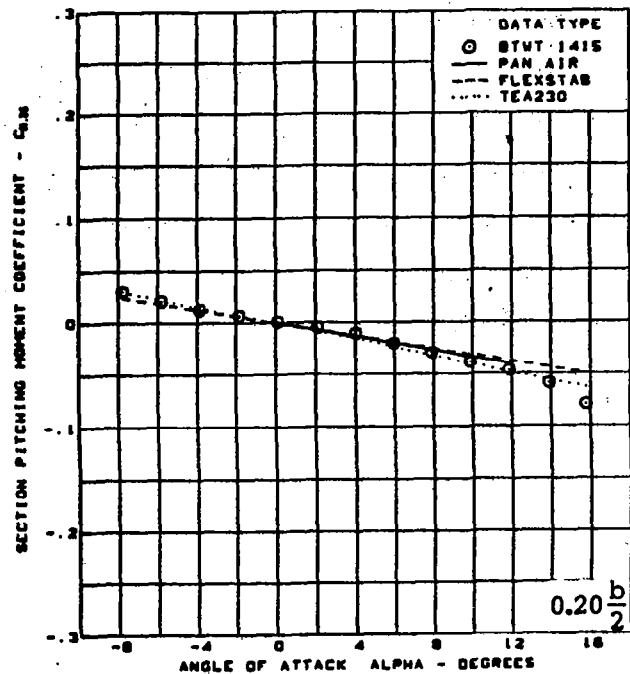
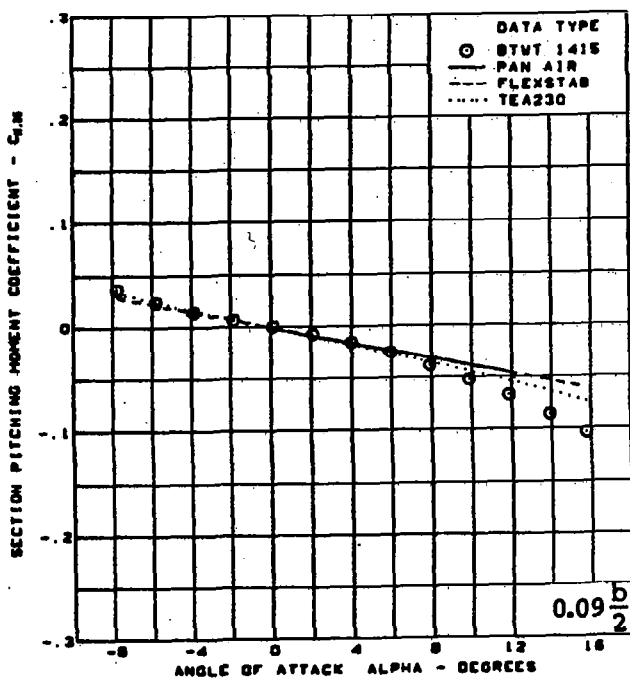


M = 0.85 (run 267)  
 Flat wing, rounded L.E.  
 L.E. deflection, full span =  $0.0^\circ$   
 T.E. deflection, full span =  $0.0^\circ$

(e) (Concluded)

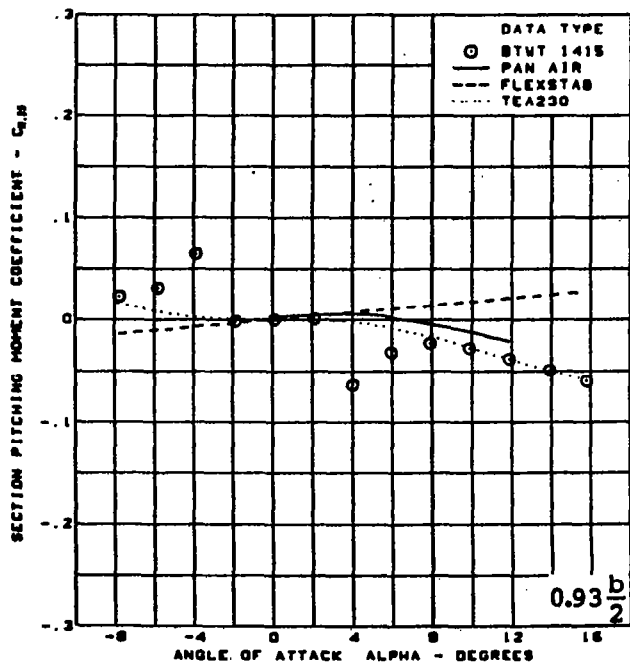
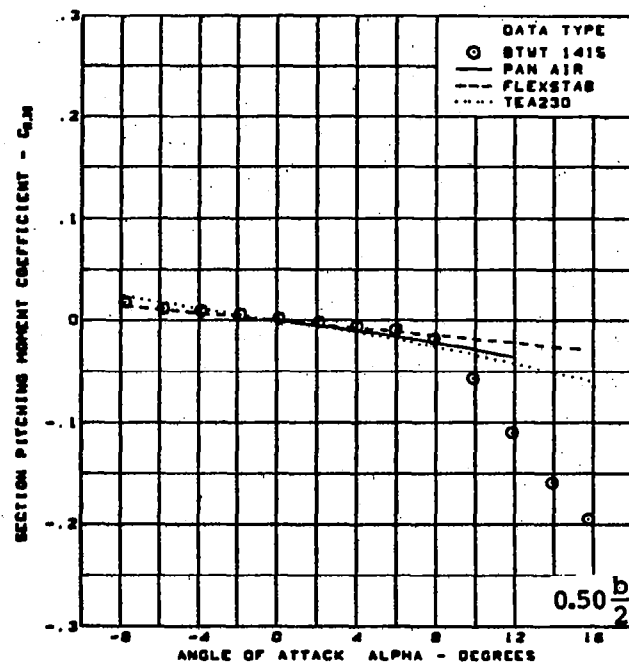
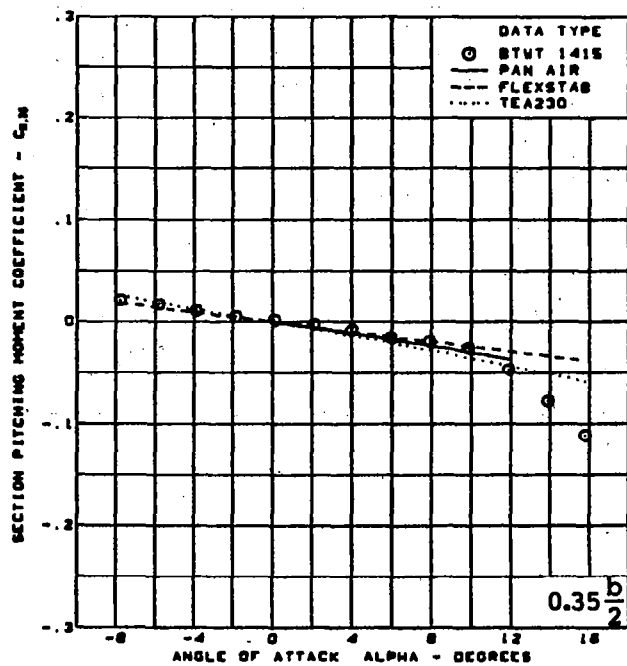
Figure 44. — (Continued)





(f) Section Aerodynamic Coefficients - Pitching Moment

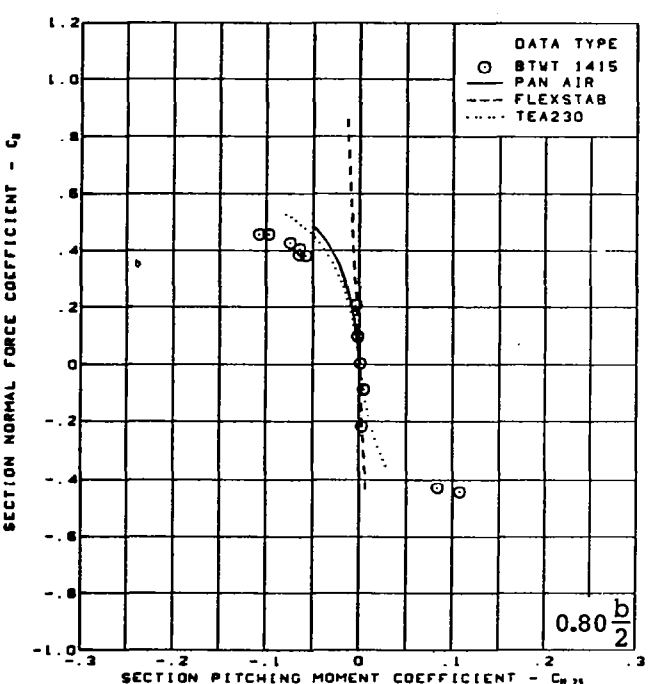
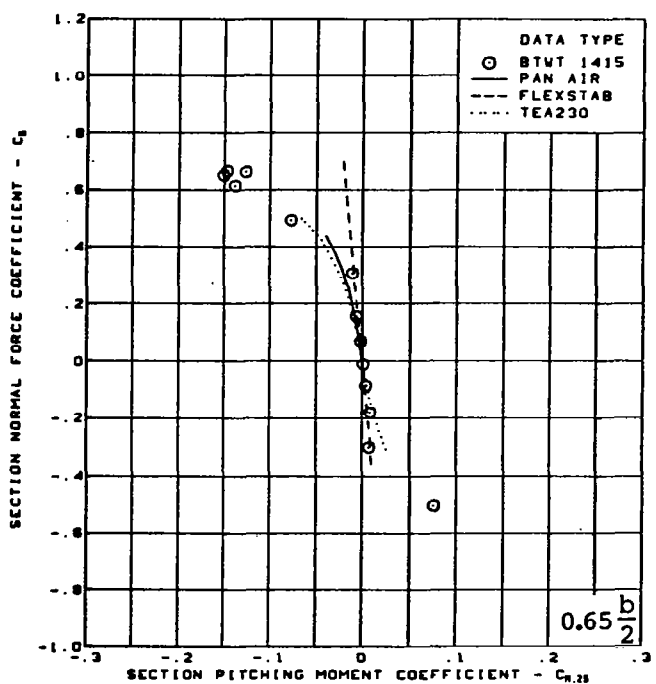
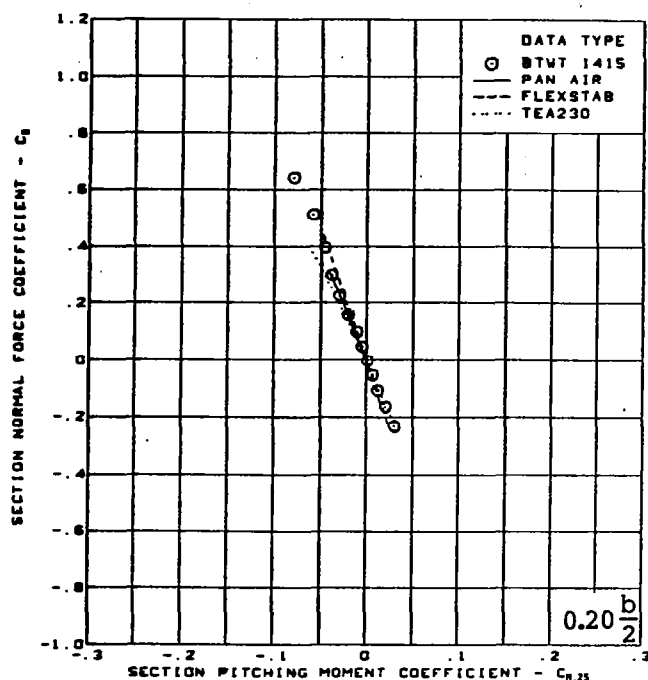
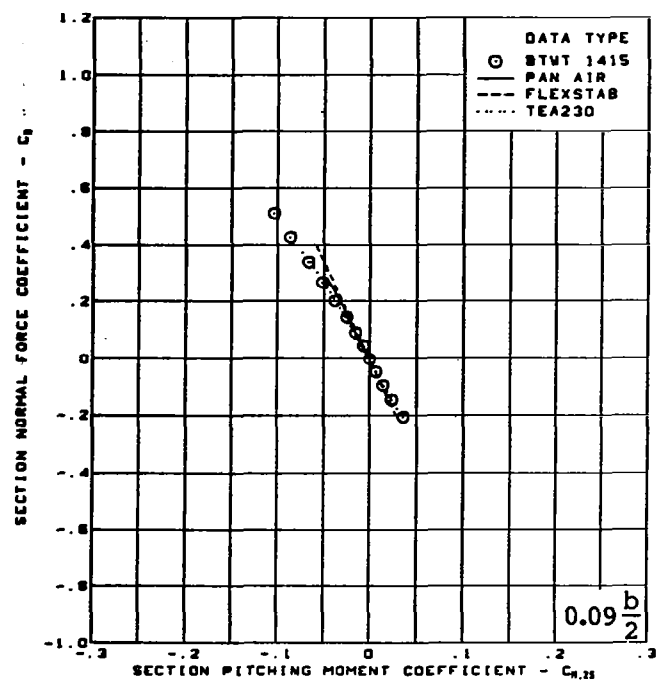
Figure 44. — (Continued)



$M = 0.85$  (run 267)  
 Flat wing, rounded L.E.  
 L.E. deflection, full span =  $0.0^\circ$   
 T.E. deflection, full span =  $0.0^\circ$

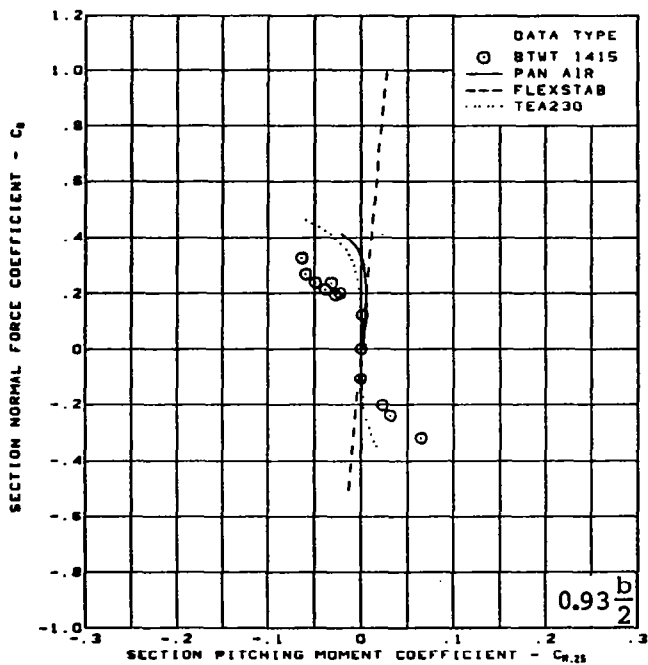
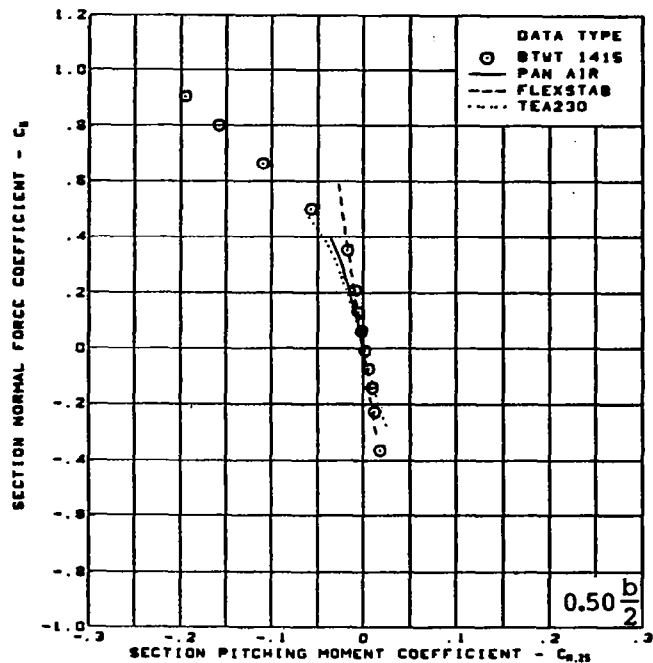
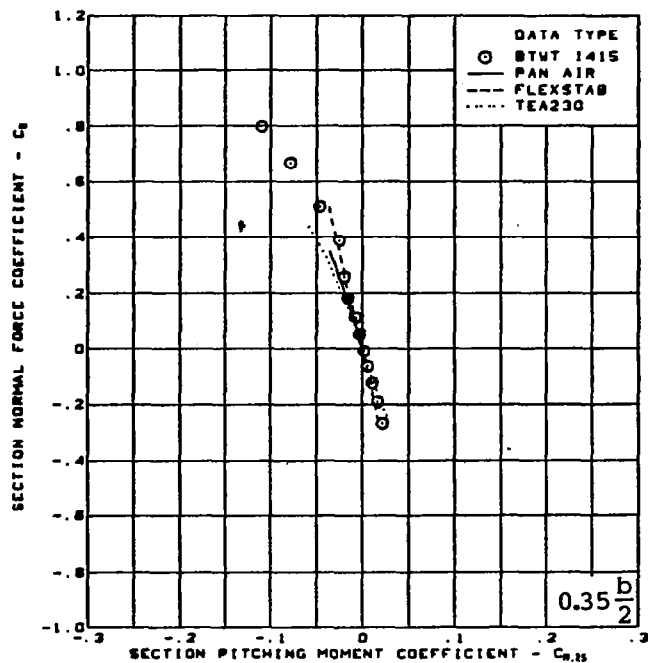
(f) (Concluded)

Figure 44. — (Continued)



(g) Section Aerodynamic Coefficients - Normal Force vs Pitching Moment

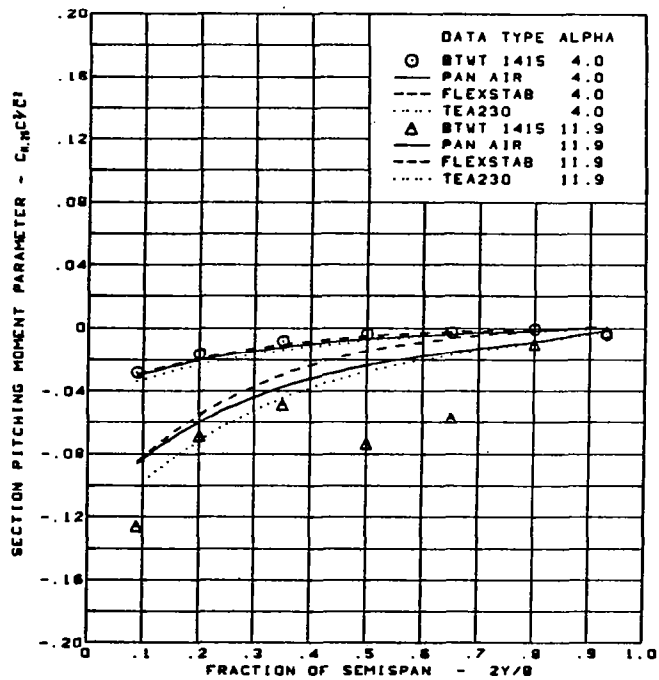
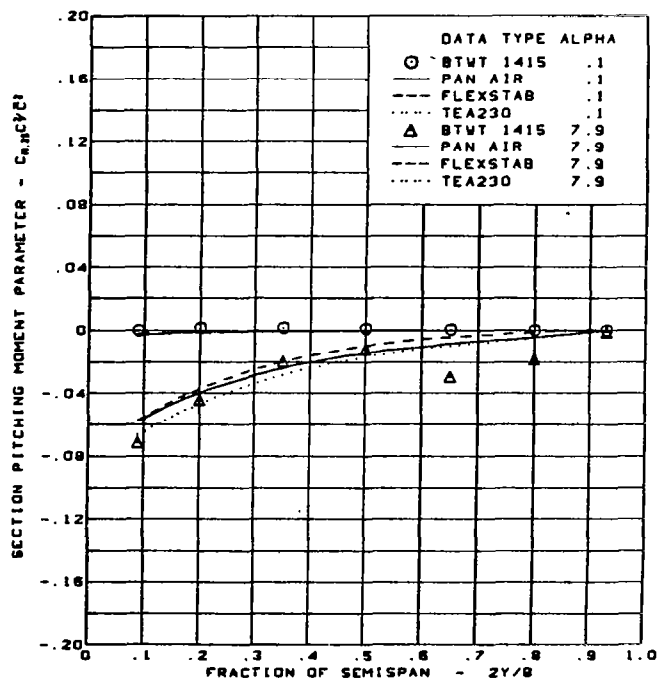
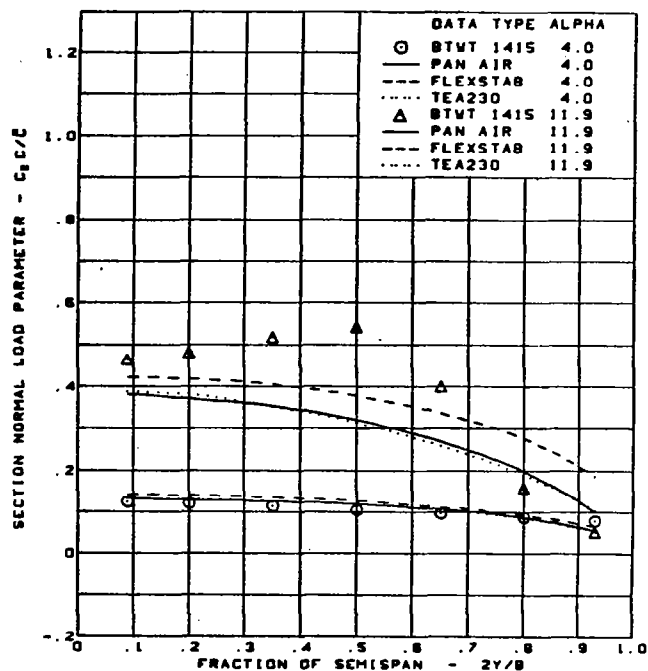
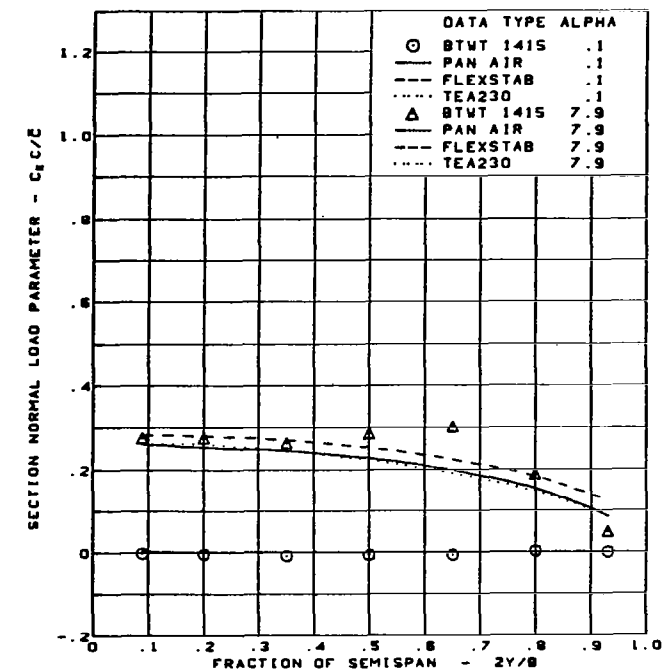
Figure 44. - (Continued)



$M = 0.85$  (run 267)  
 Flat wing, rounded L.E.  
 L.E. deflection, full span  $\approx 0.0^\circ$   
 T.E. deflection, full span  $\approx 0.0^\circ$

(g) (Concluded)

Figure 44. — (Continued)

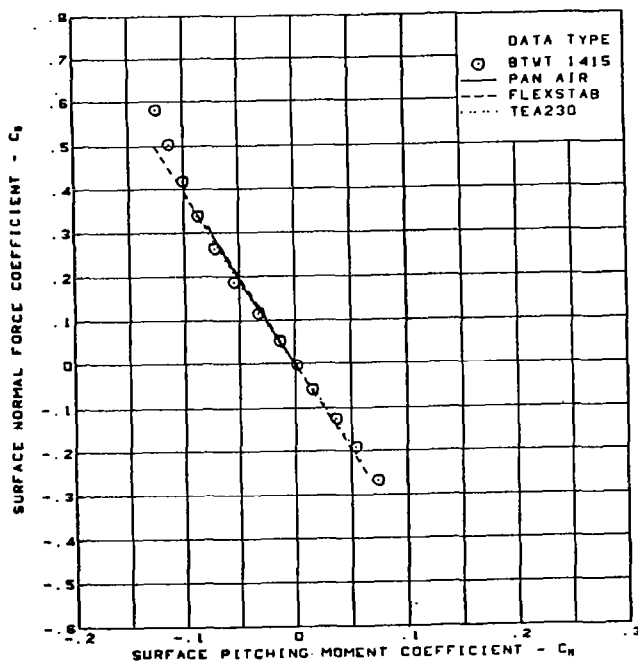
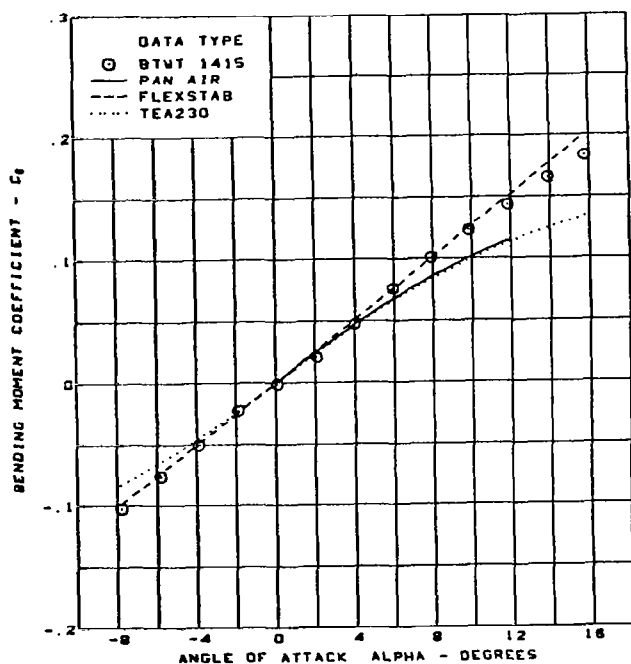
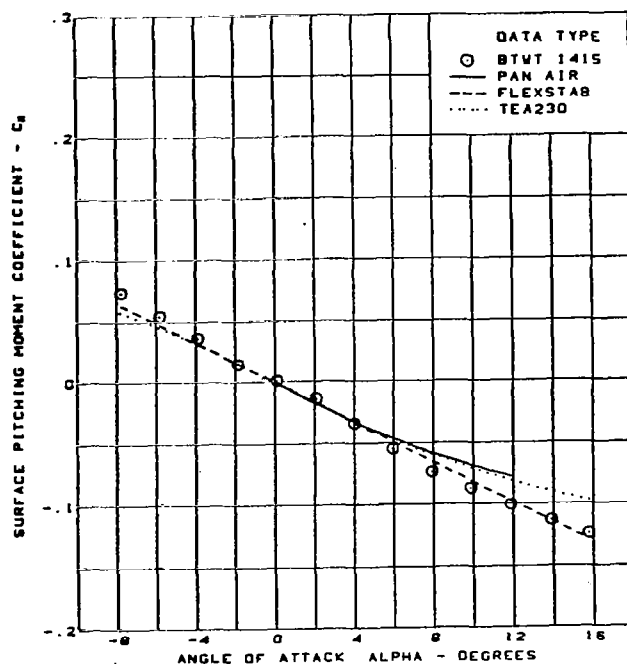
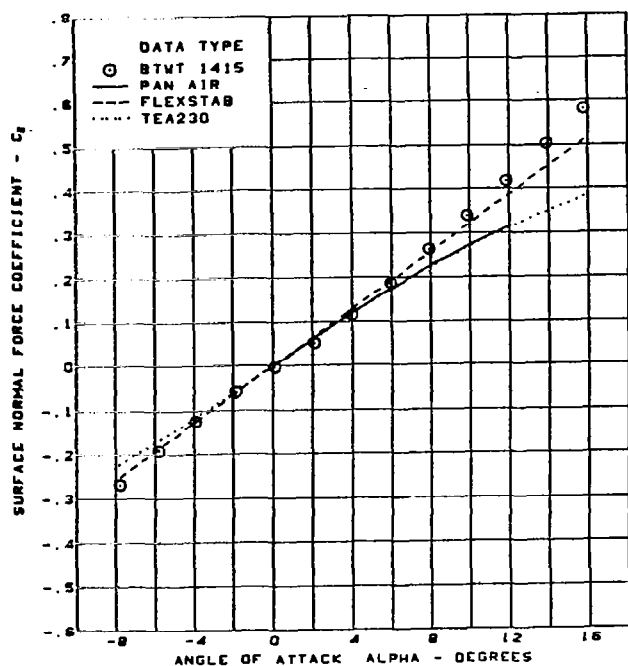


M = 0.85 (run 267)  
Flat wing, rounded L.E.

L.E. deflection, full span =  $0.0^\circ$   
T.E. deflection, full span =  $0.0^\circ$

(h) Spanload Distributions

Figure 44. — (Continued)

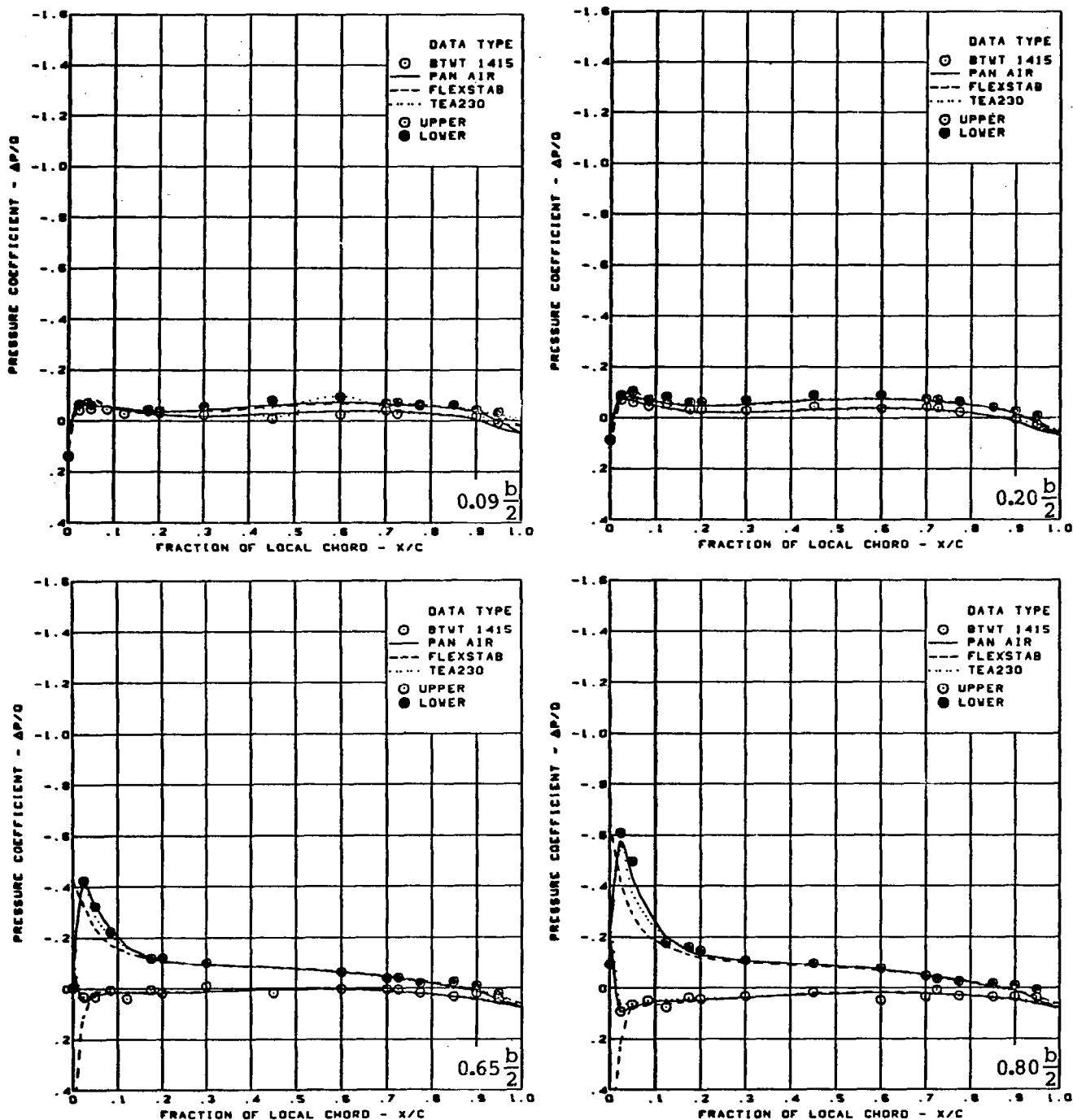


$M = 0.85$  (run 267)  
Flat wing, rounded L.E.

L.E. deflection, full span =  $0.0^\circ$   
T.E. deflection, full span =  $0.0^\circ$

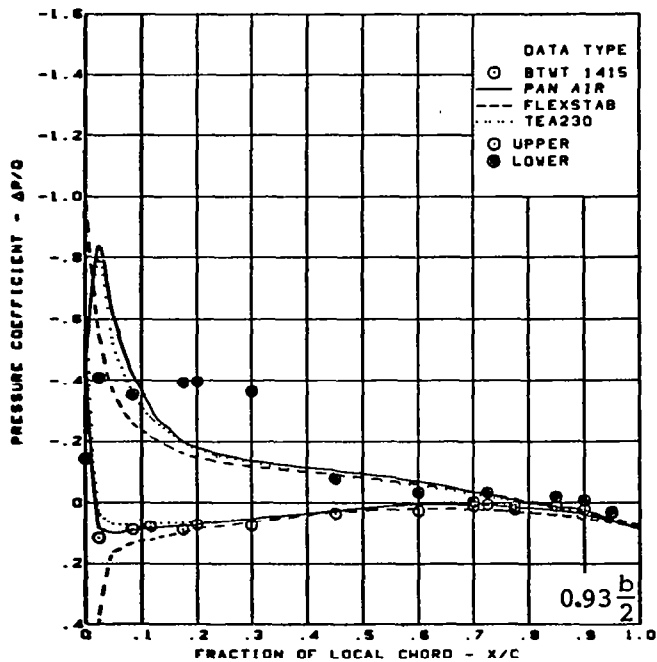
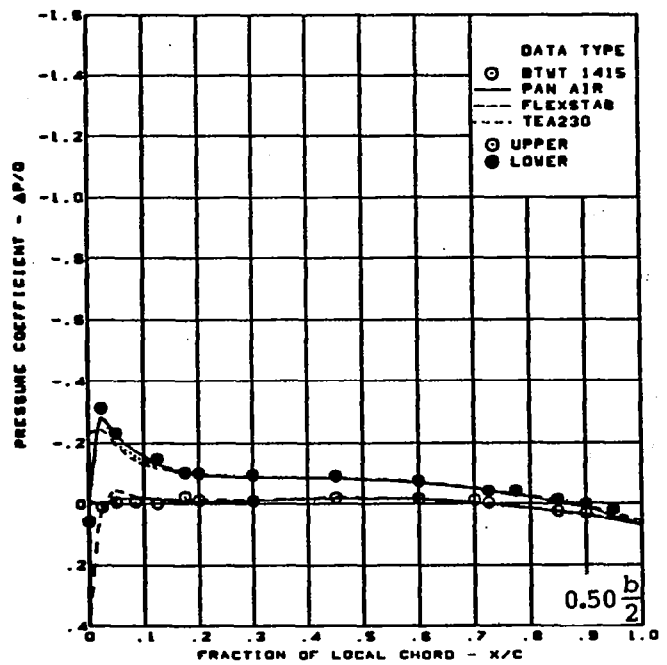
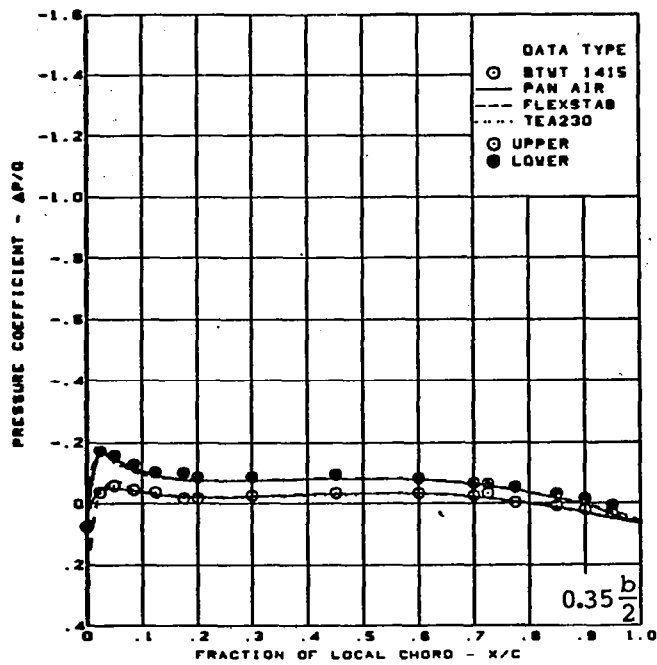
### (i) Wing Aerodynamic Coefficients

Figure 44. — (Concluded)



(a) Surface Chordwise Pressure Distributions -  $\alpha = 0^\circ$

Figure 45. — Wing Theory-to-Experiment Comparison; Twisted Wing; T.E. Deflection, Full Span =  $0.0^\circ$ ;  $M = 0.85$



$M = 0.85$  (run 449)

$\alpha = 0^\circ$

Twisted wing, rounded L.E.

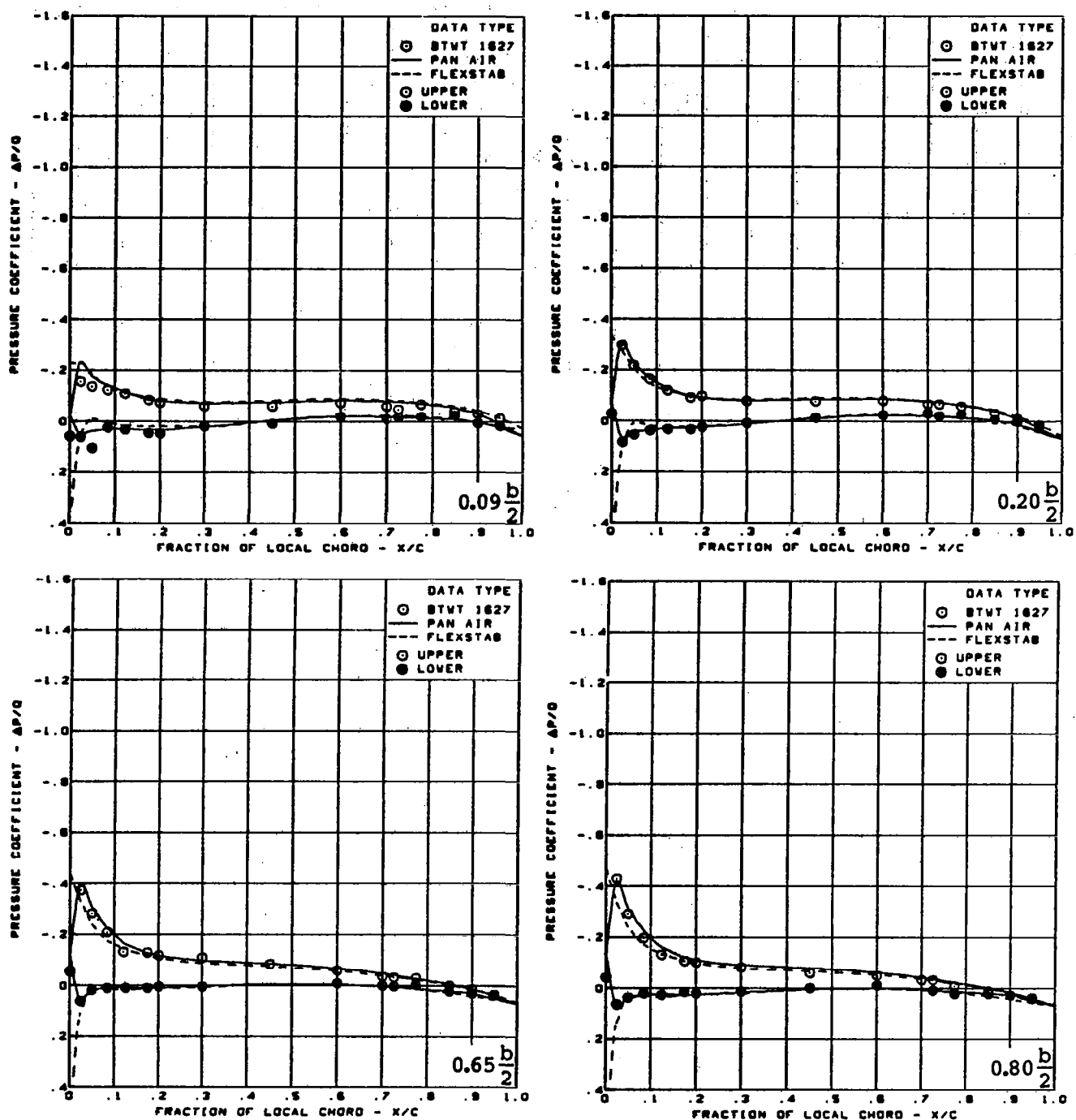
L.E. deflection, full span =  $0.0^\circ$

T.E. deflection, full span =  $0.0^\circ$

(a) (Concluded)

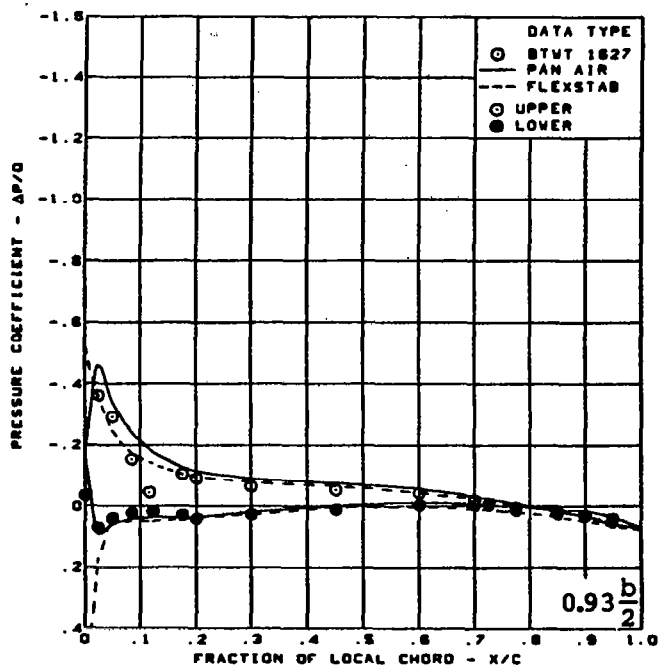
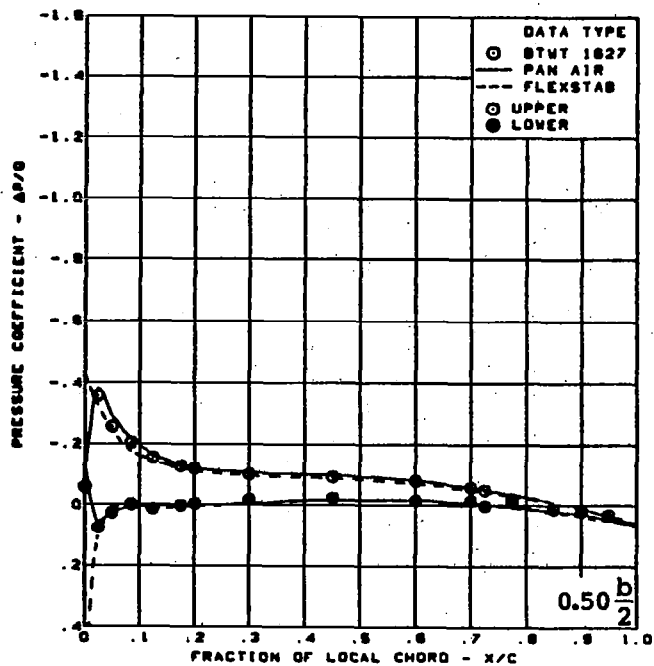
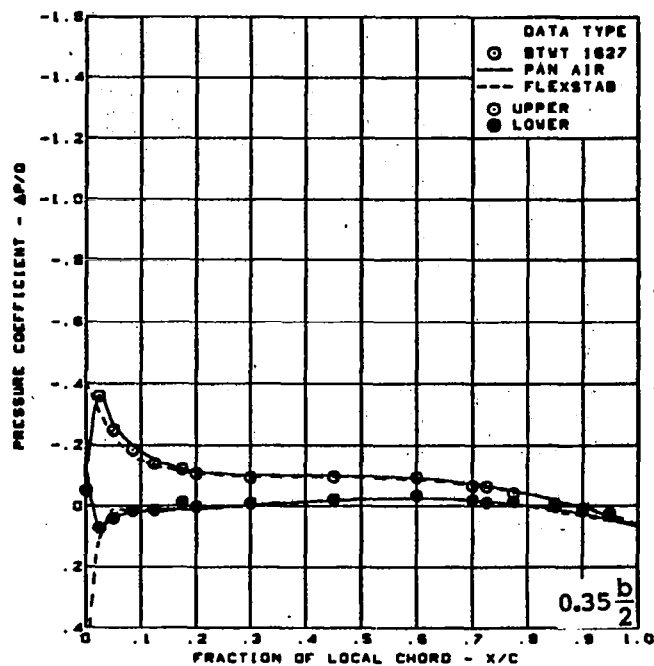
Figure 45. - (Continued)





(b) Surface Chordwise Pressure Distributions -  $\alpha = 4.5^\circ$

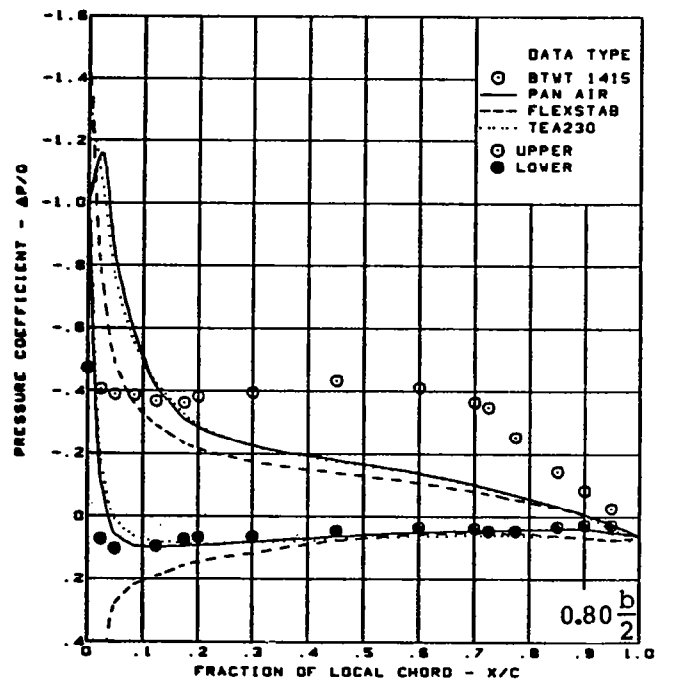
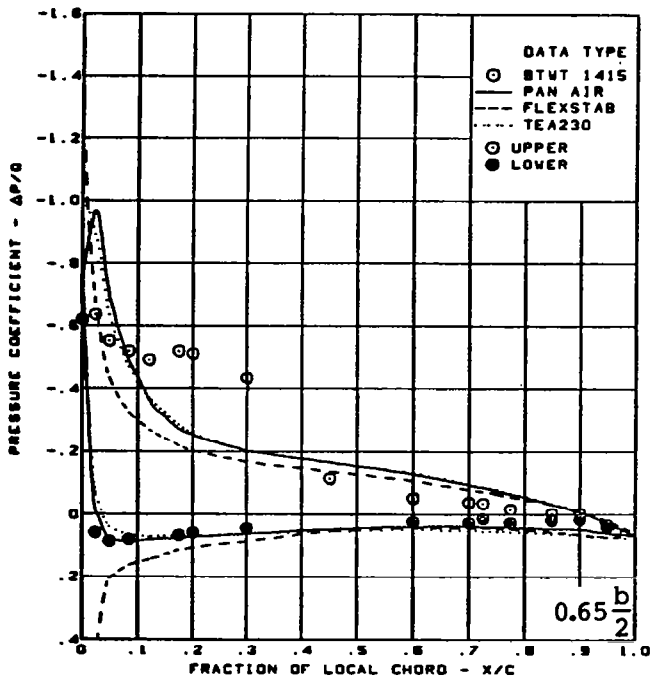
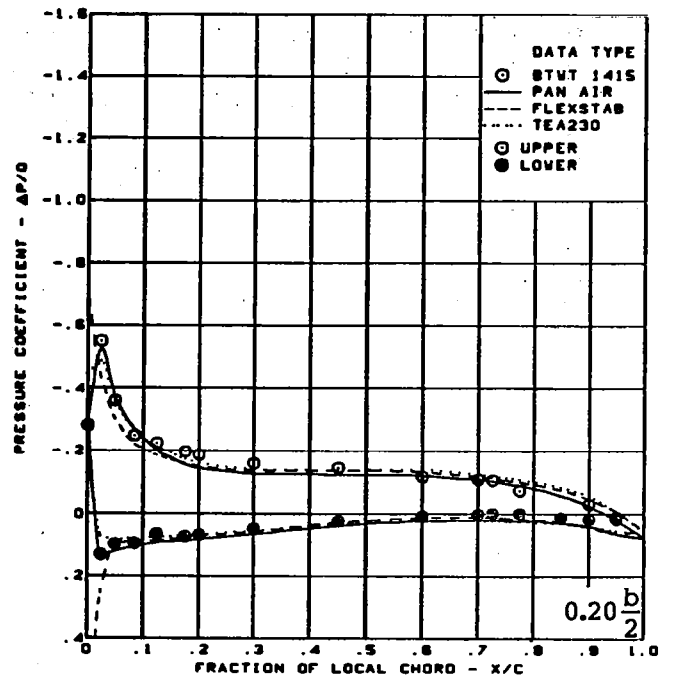
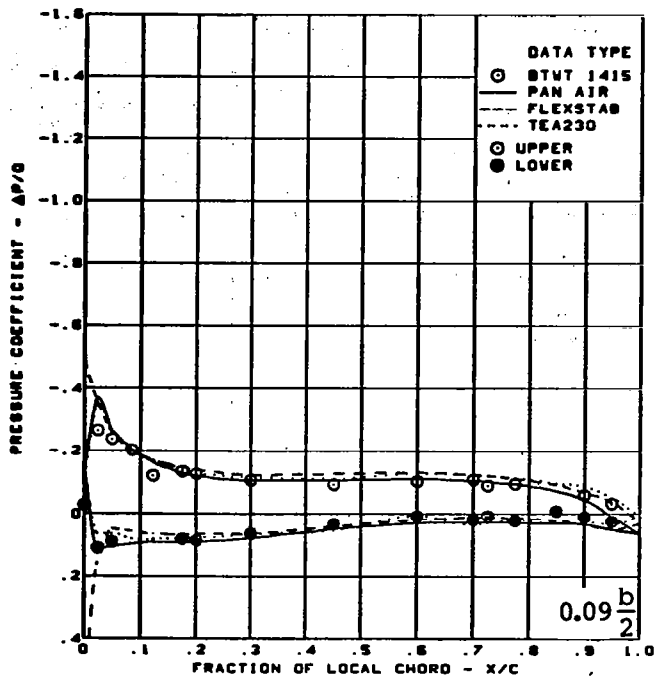
Figure 45. - (Continued)



$M = 0.85$  (run 449)  
 $\alpha = 4.5^\circ$   
 Twisted wing, rounded L.E.  
 L.E. deflection, full span =  $0.0^\circ$   
 T.E. deflection, full span =  $0.0^\circ$

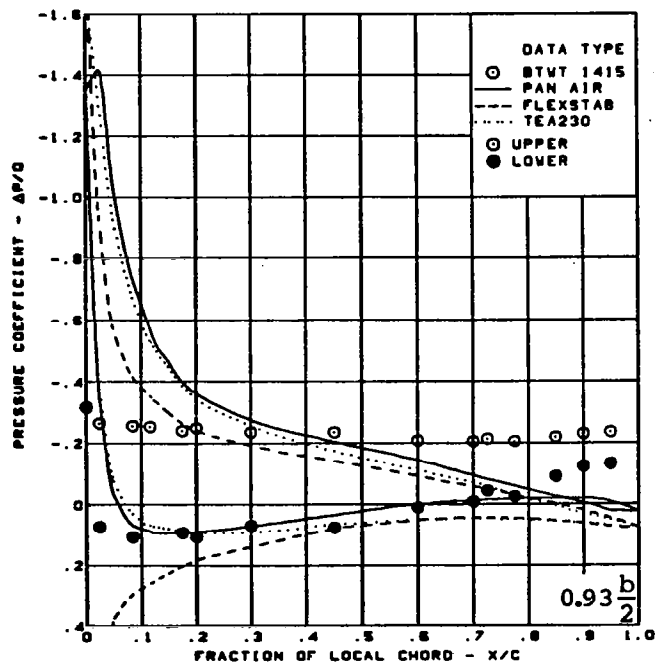
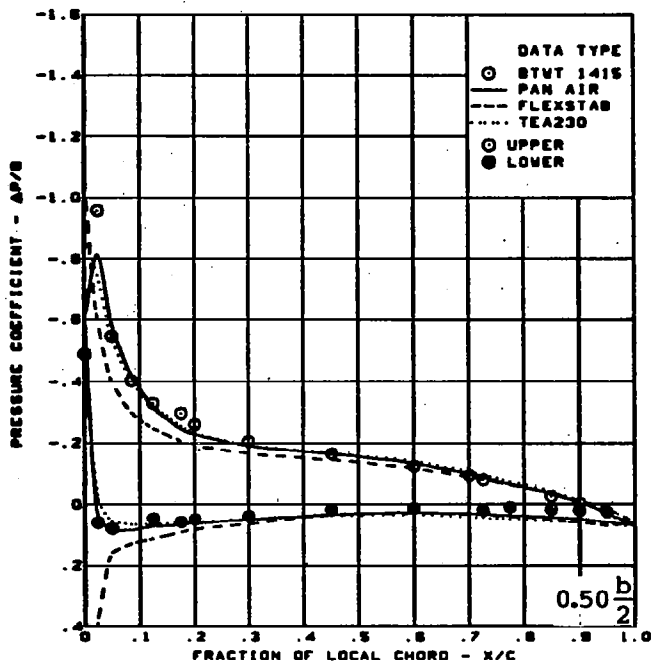
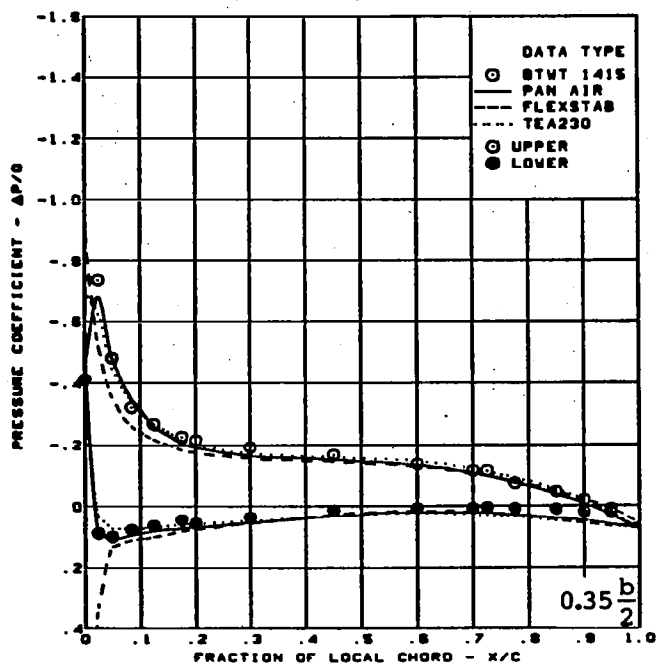
(b) (Concluded)

Figure 45. - (Continued)



(c) Surface Chordwise Pressure Distributions -  $\alpha = 8^\circ$

Figure 45. - (Continued)



$M = 0.85$  (run 449)

$\alpha = 8^\circ$

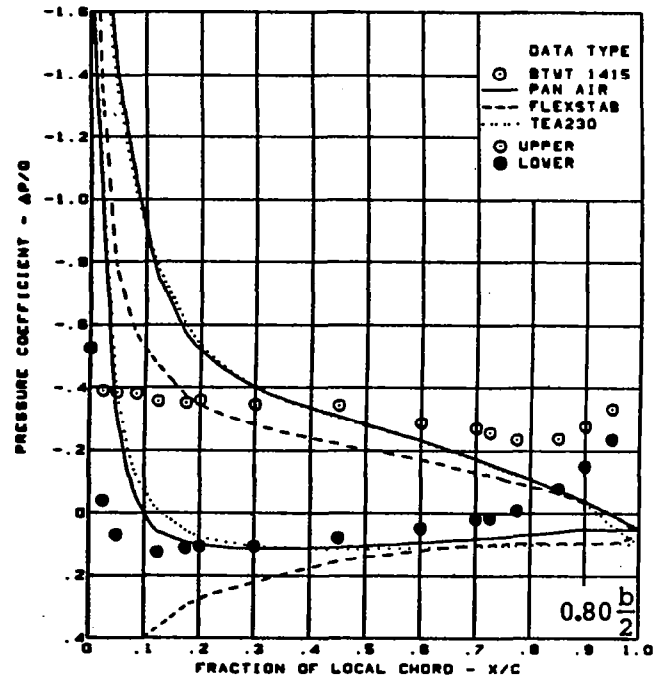
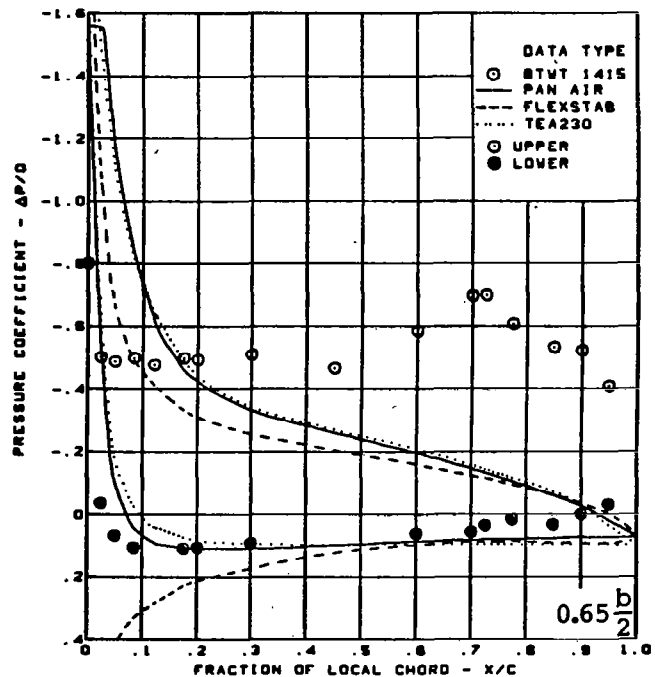
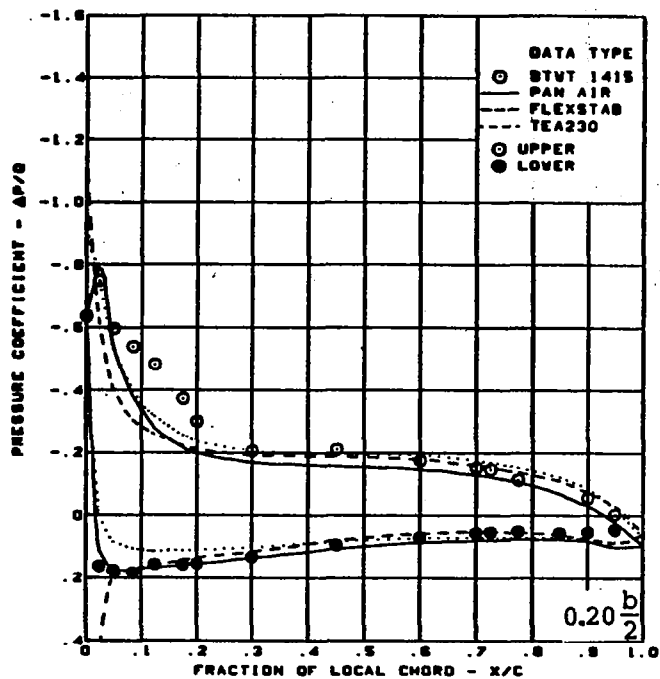
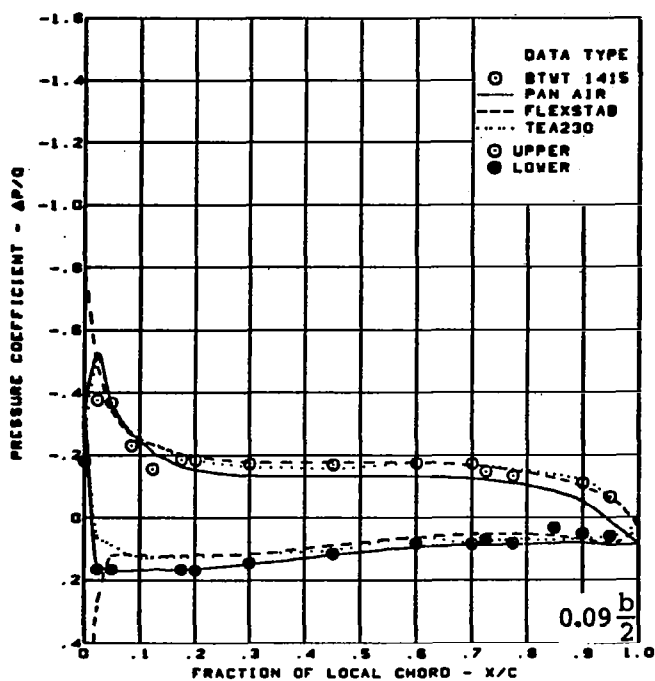
Twisted wing, rounded L.E.

L.E. deflection, full span =  $0.0^\circ$

T.E. deflection, full span =  $0.0^\circ$

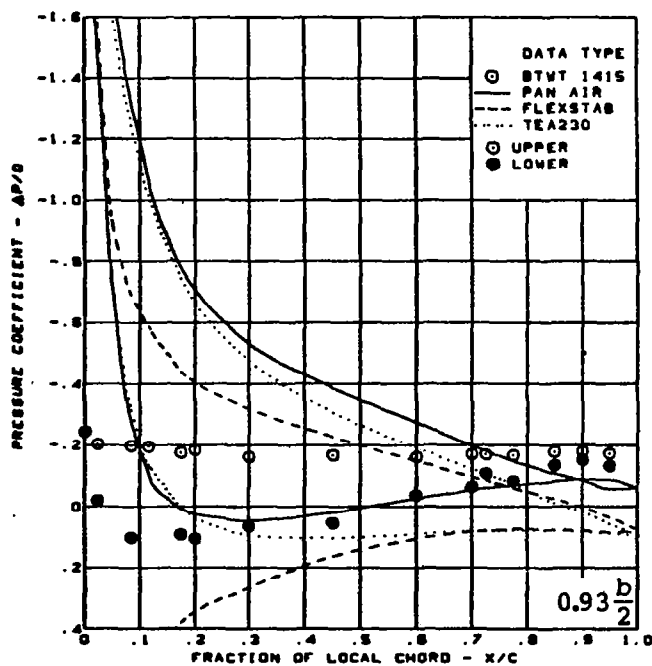
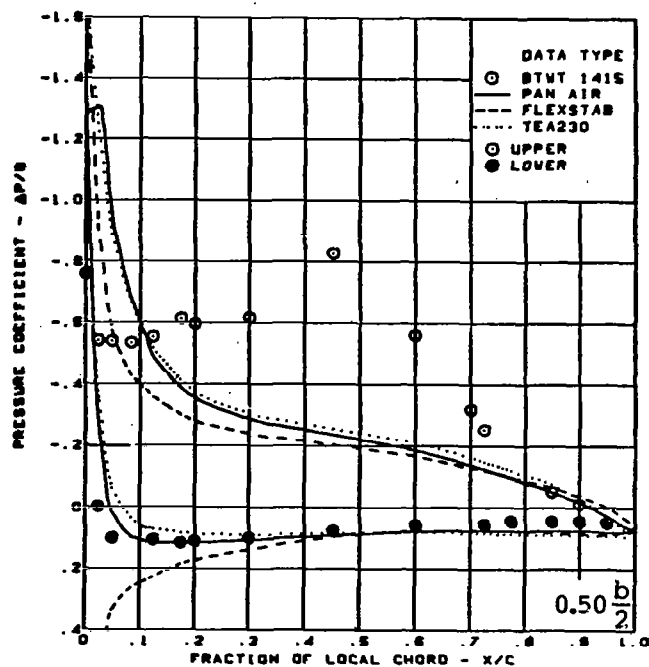
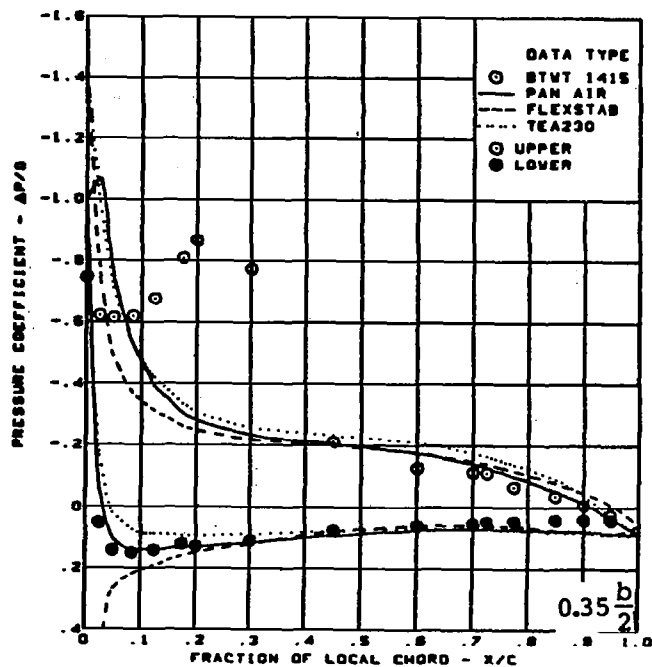
(c) (Concluded)

Figure 45. - (Continued)



(d) Surface Chordwise Pressure Distributions -  $\alpha = 12^\circ$

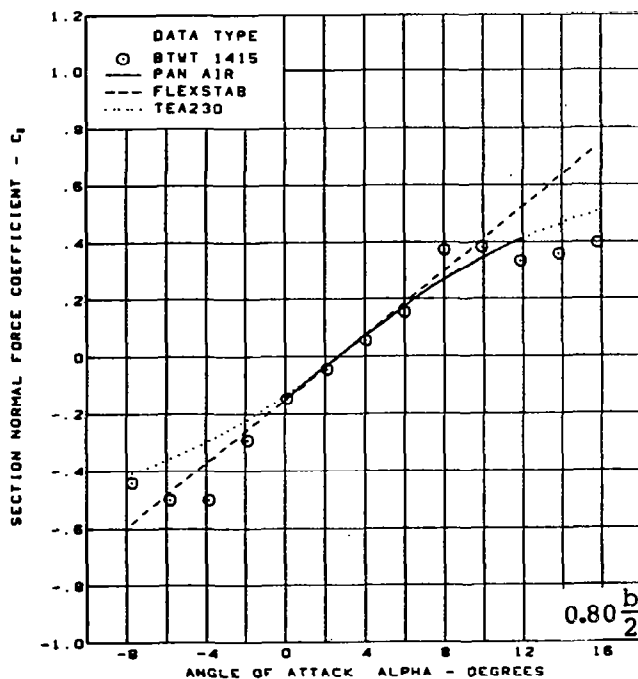
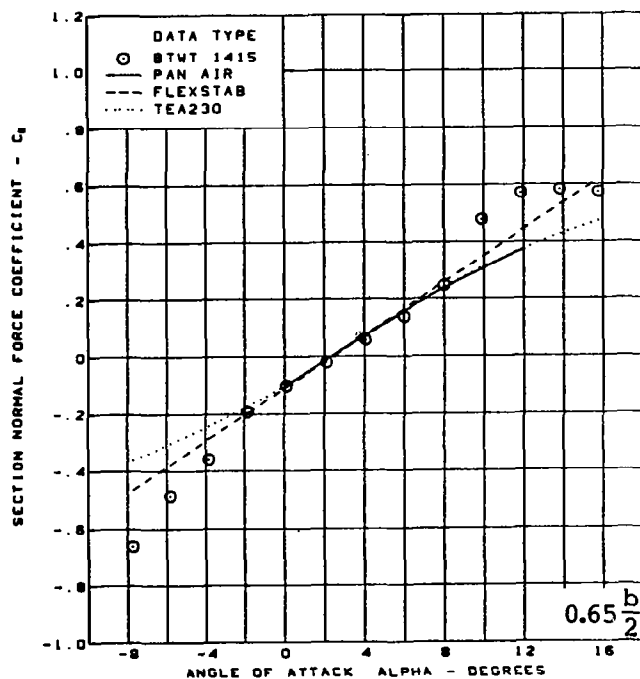
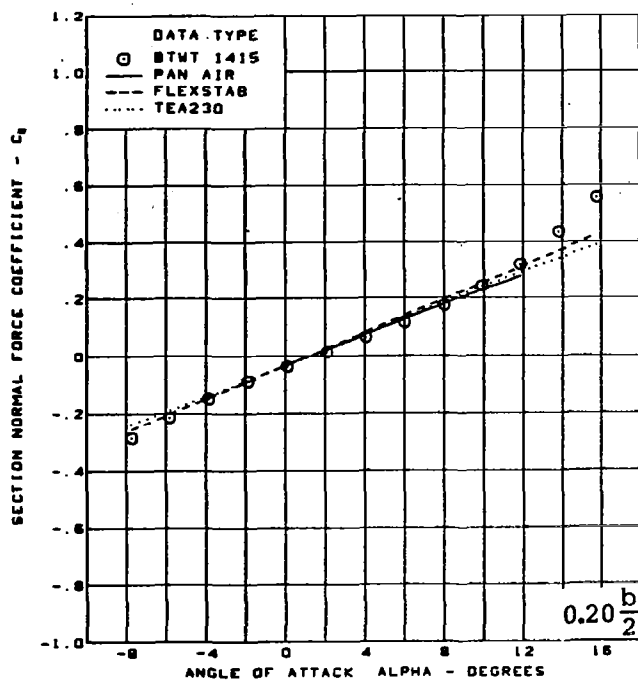
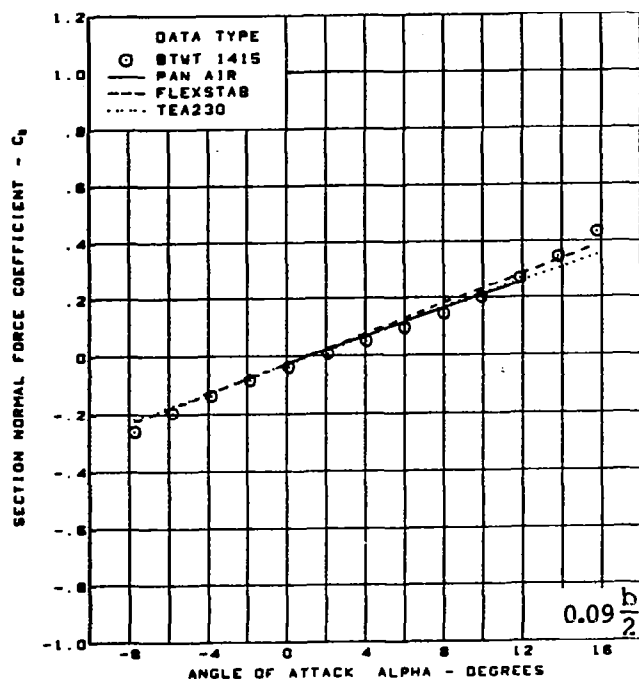
Figure 45. - (Continued)



$M = 0.85$  (run 449)  
 $\alpha = 12^\circ$   
 Twisted wing, rounded L.E.  
 L.E. deflection, full span =  $0.0^\circ$   
 T.E. deflection, full span =  $0.0^\circ$

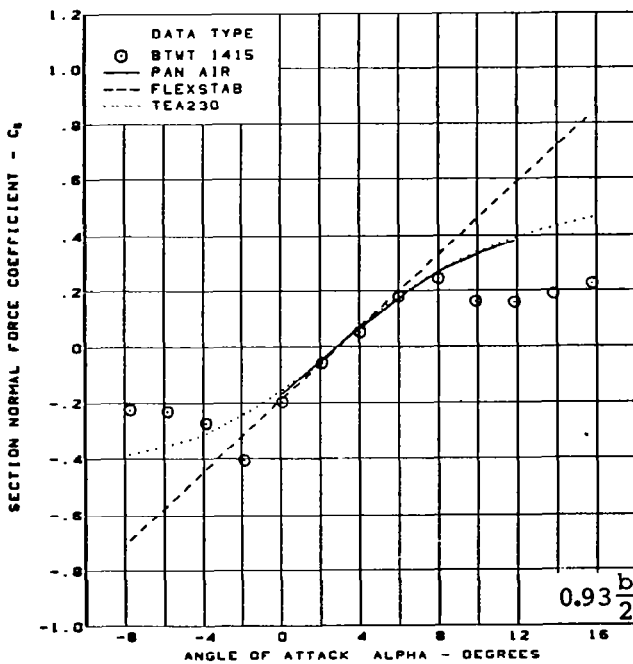
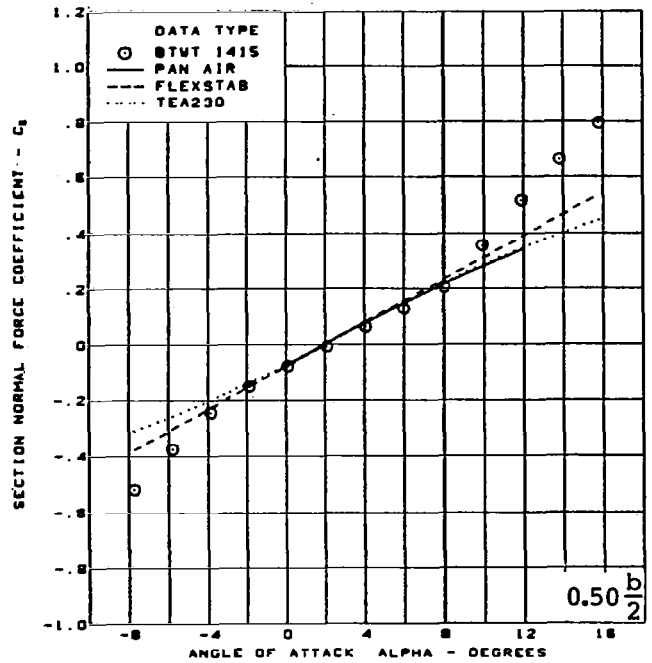
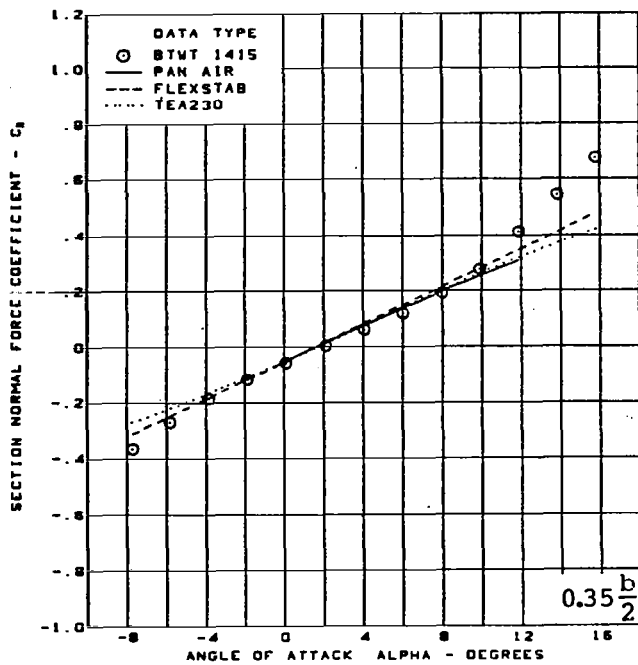
(d) (Concluded)

Figure 45. - (Continued)



(e) Section Aerodynamic Coefficients - Normal Force

Figure 45. — (Continued)

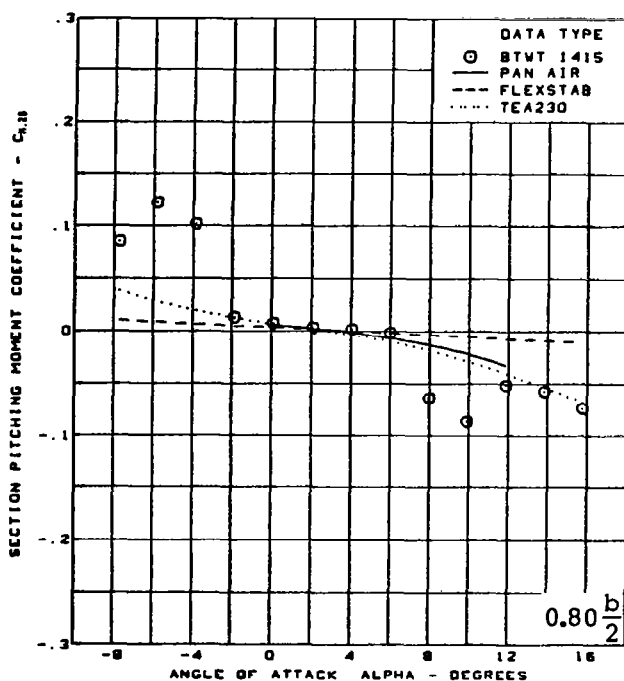
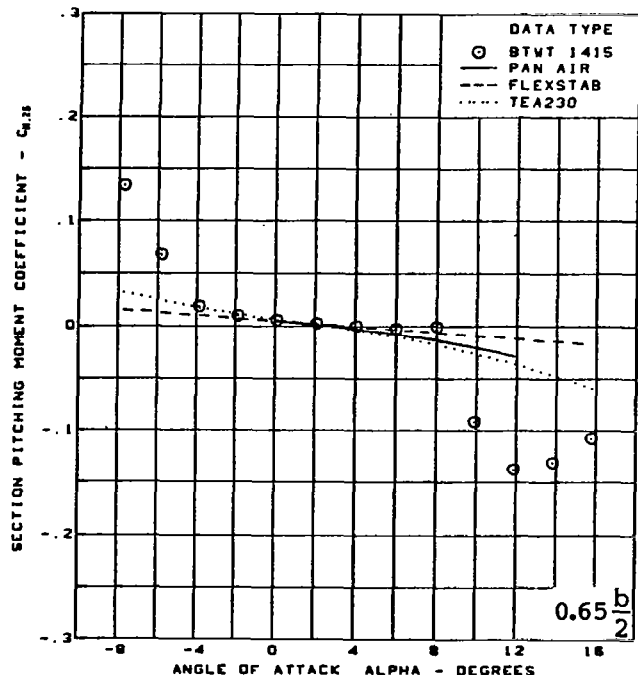
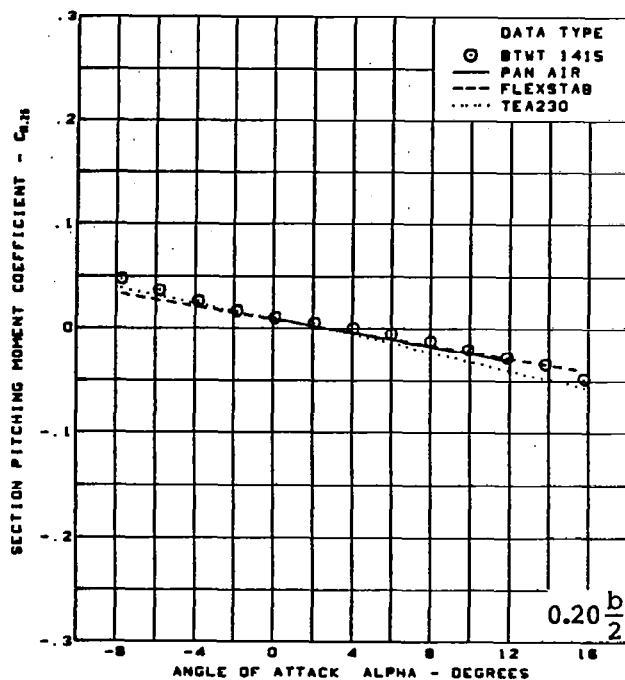
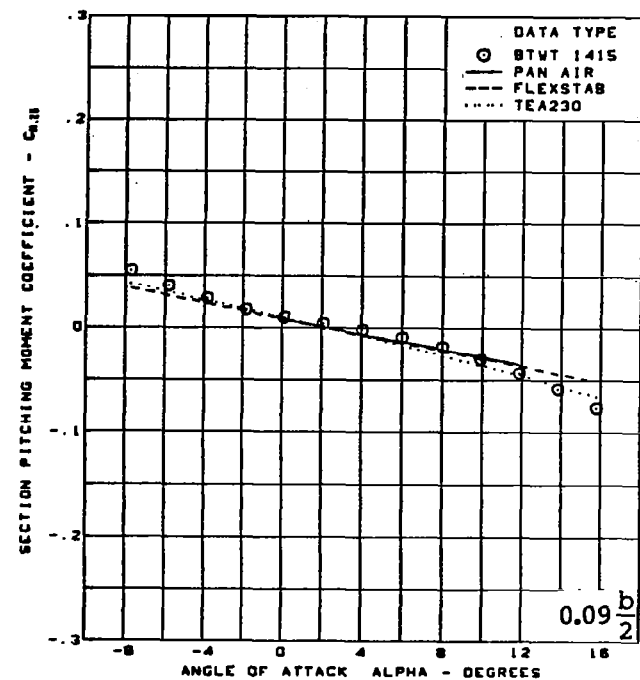


$M = 0.85$  (run 449)  
 Twisted wing, rounded L.E.  
 L.E. deflection, full span =  $0.0^\circ$   
 T.E. deflection, full span =  $0.0^\circ$

(e) (Concluded)

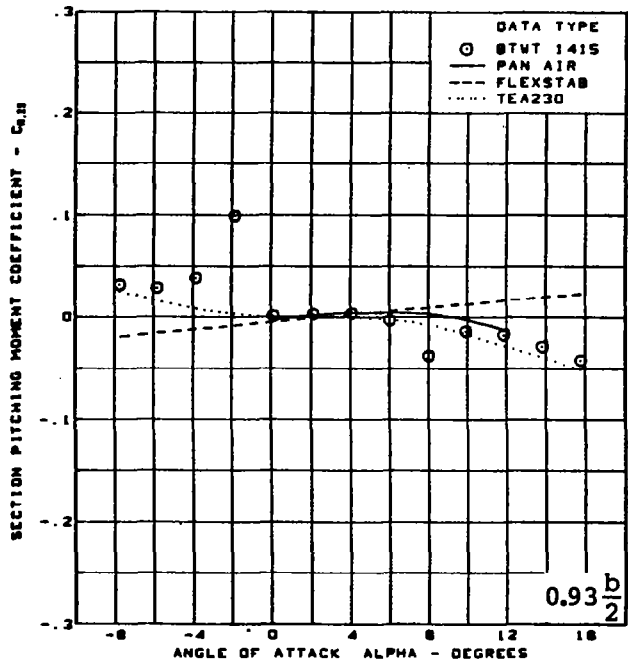
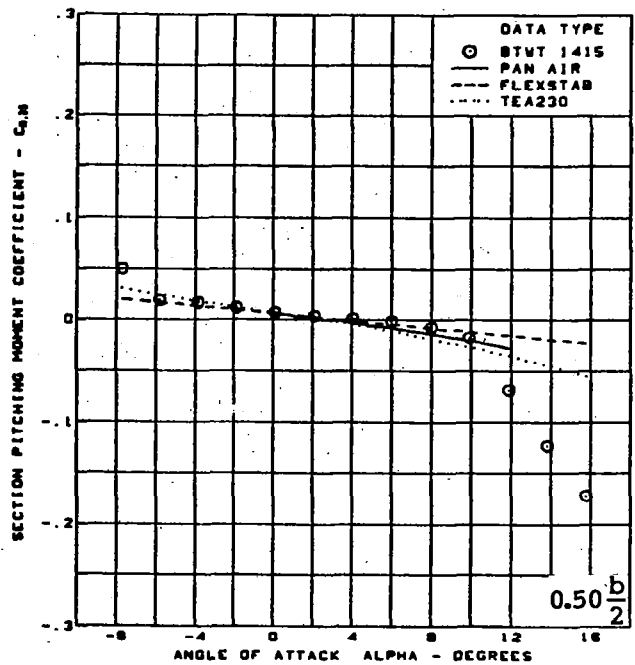
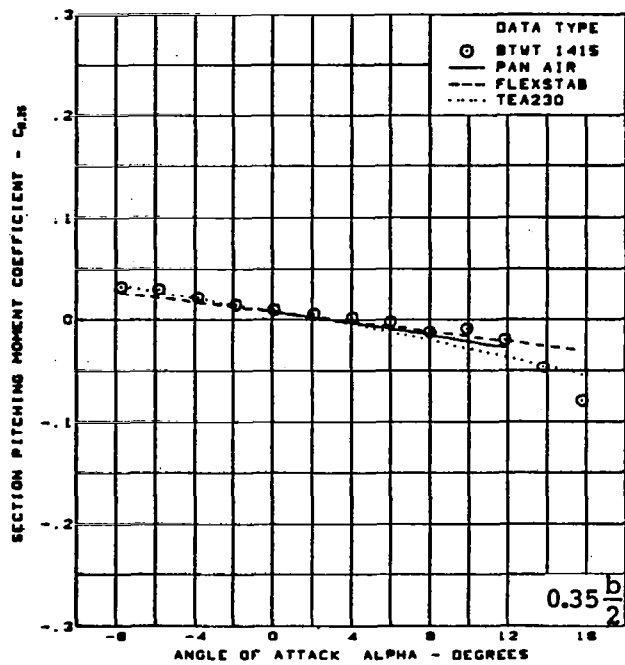
Figure 45. — (Continued)





(f) Section Aerodynamic Coefficients - Pitching Moment

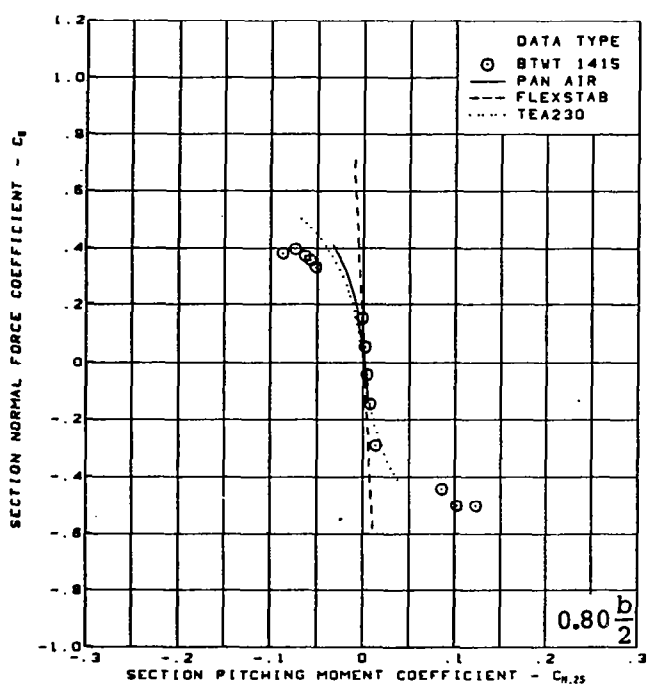
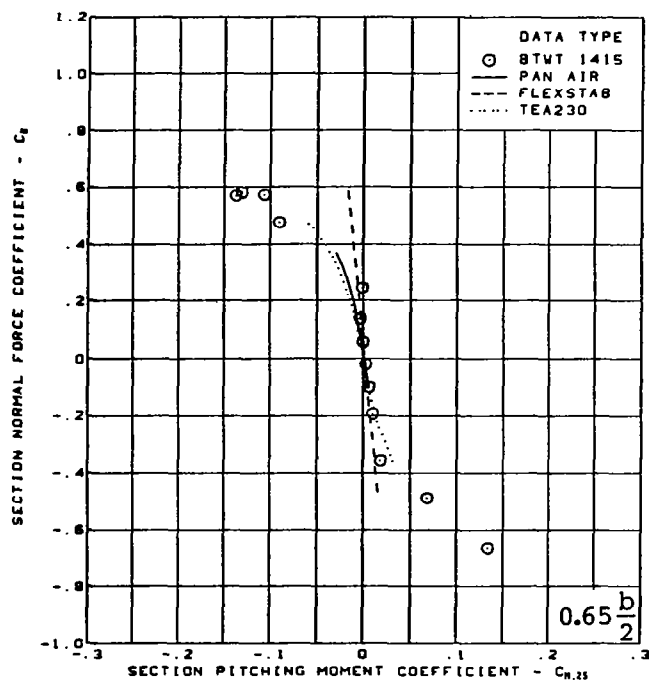
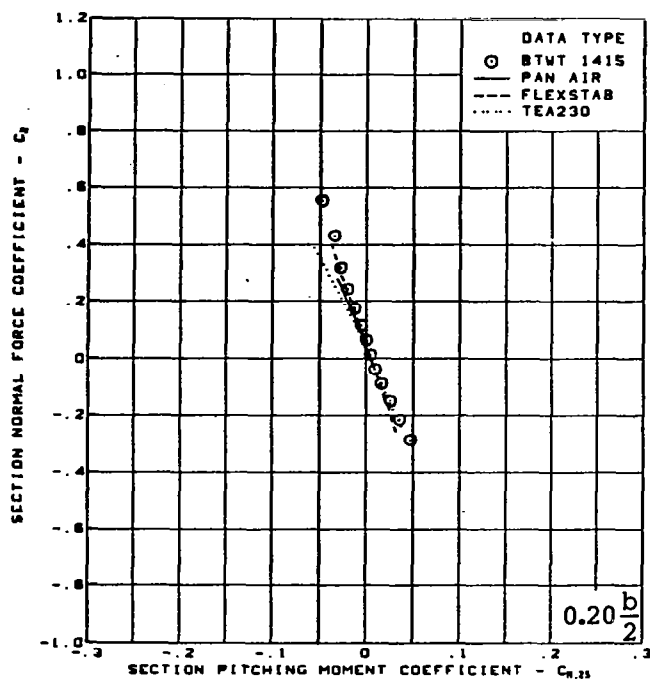
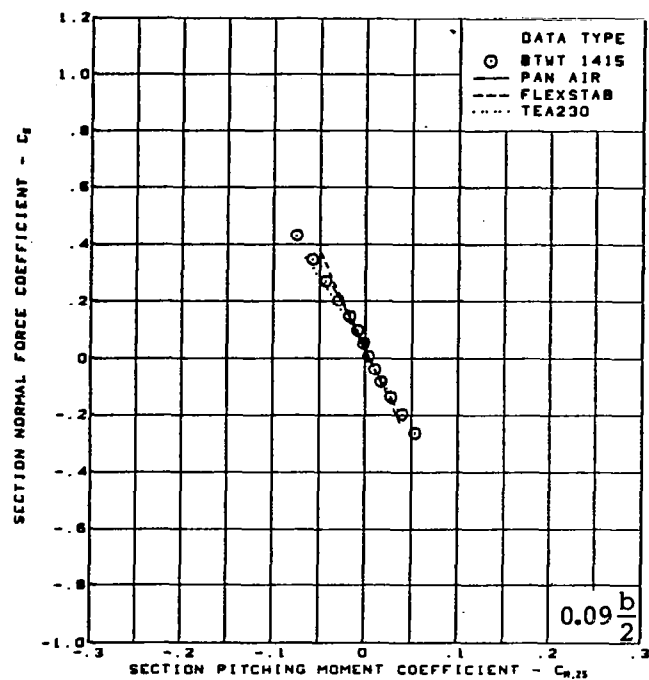
Figure 45. — (Continued)



$M = 0.85$  (run 449)  
 Twisted wing, rounded L.E.  
 L.E. deflection, full span =  $0.0^\circ$   
 T.E. deflection, full span =  $0.0^\circ$

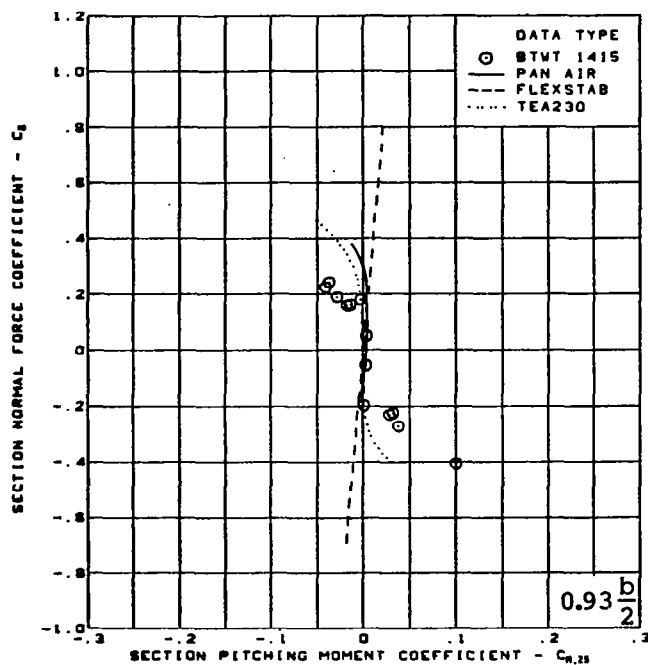
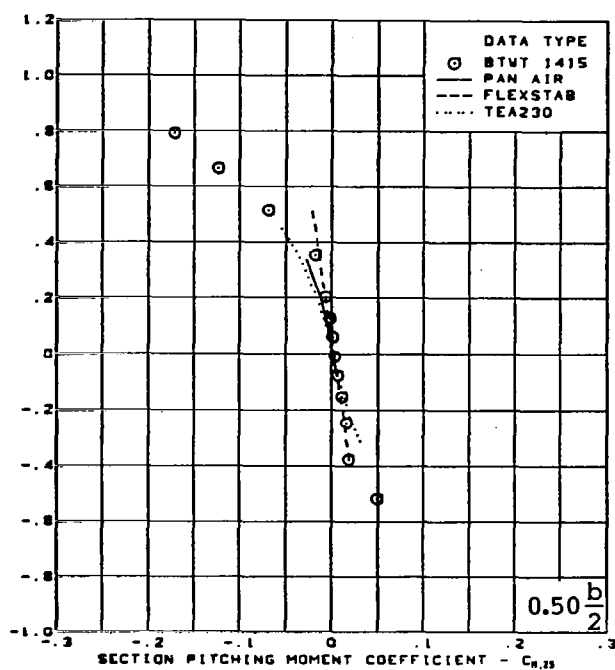
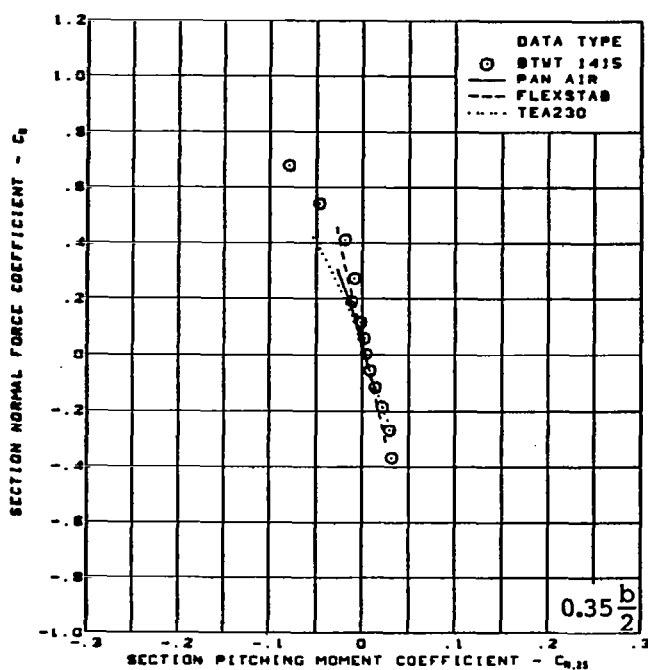
(f) (Concluded)

Figure 45. — (Continued)



(g) Section Aerodynamic Coefficients - Normal Force vs Pitching Moment

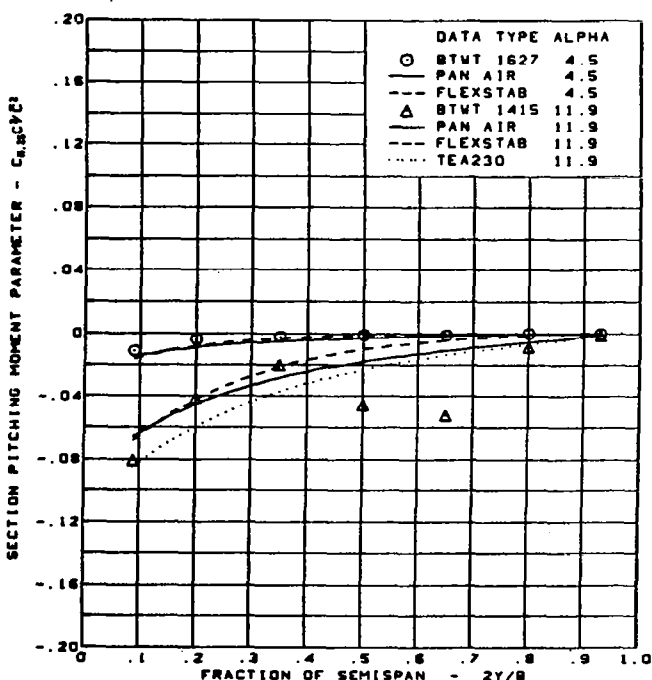
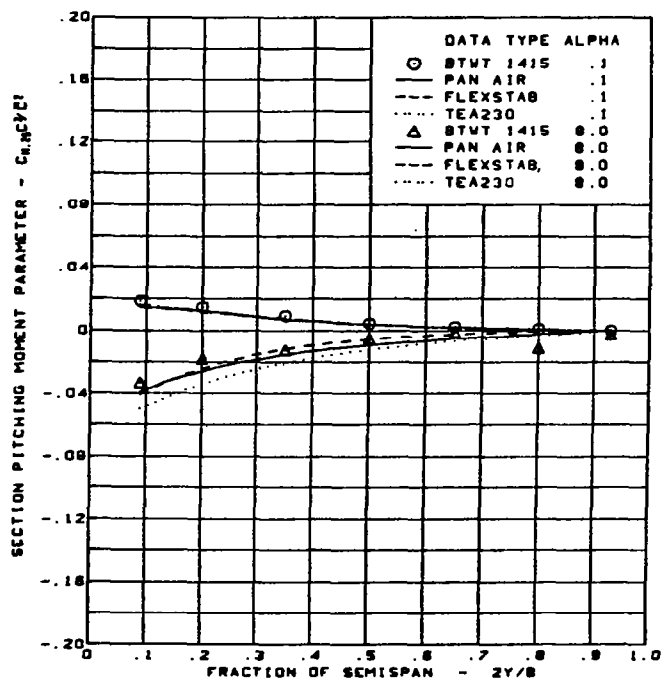
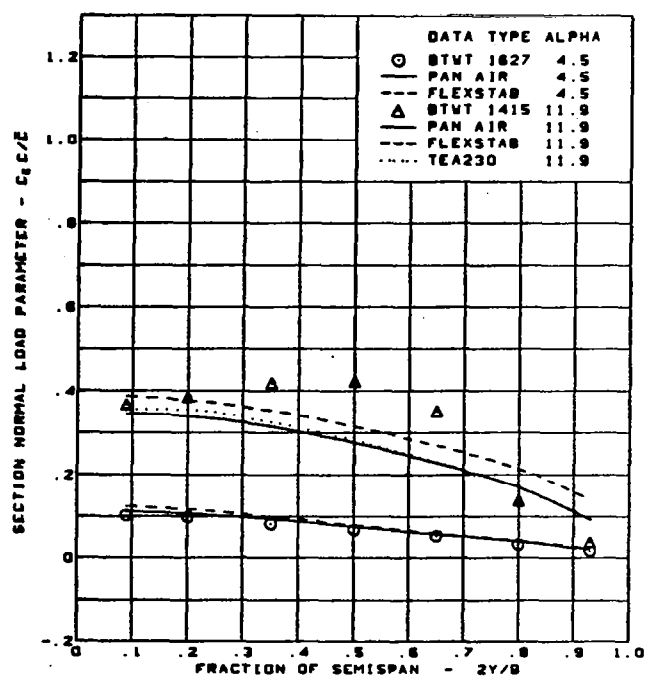
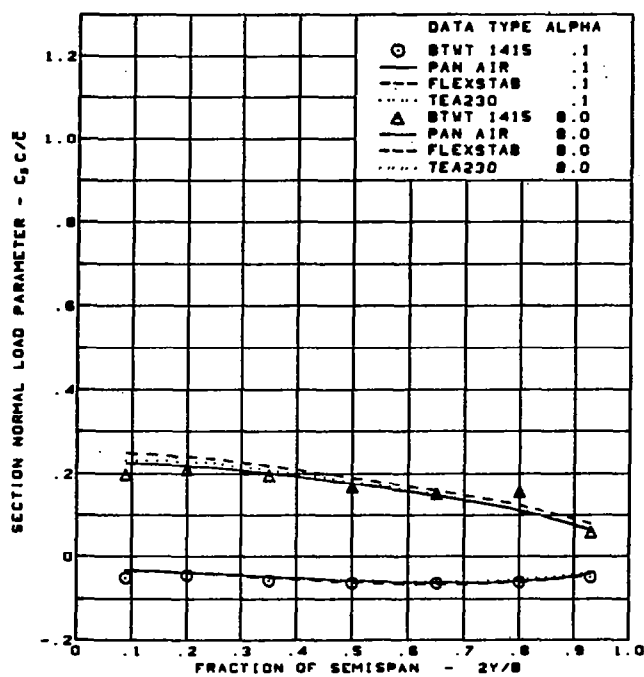
Figure 45. - (Continued)



M = 0.85 (run 449)  
 Twisted wing, rounded L.E.  
 L.E. deflection, full span =  $0.0^\circ$   
 T.E. deflection, full span =  $0.0^\circ$

(g) (Concluded)

Figure 45. — (Continued)

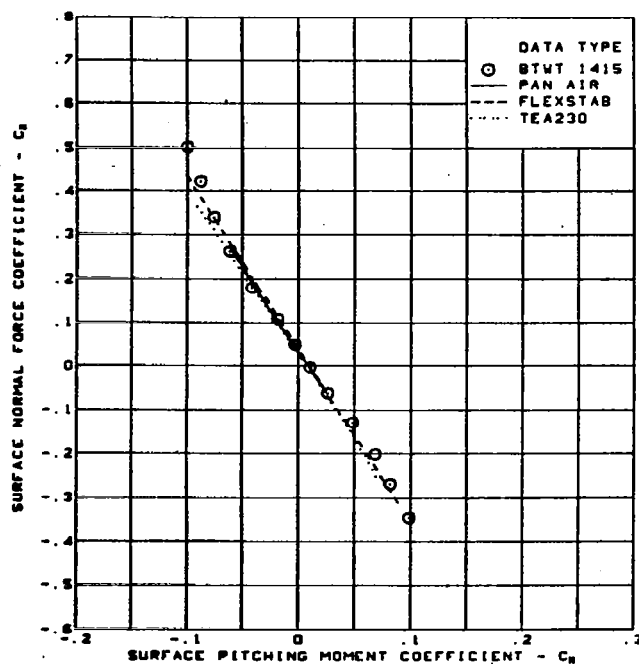
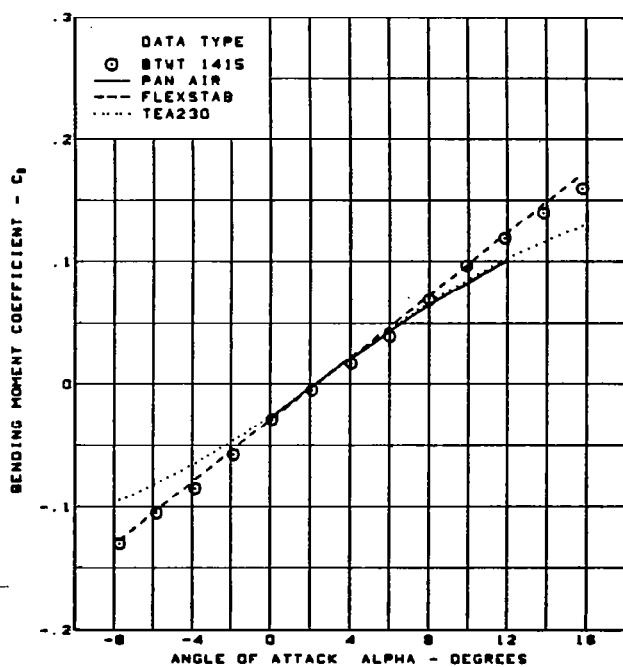
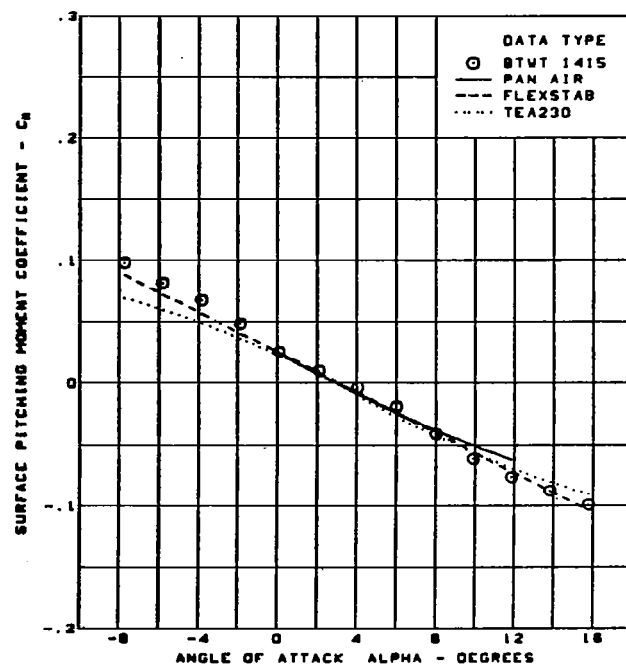
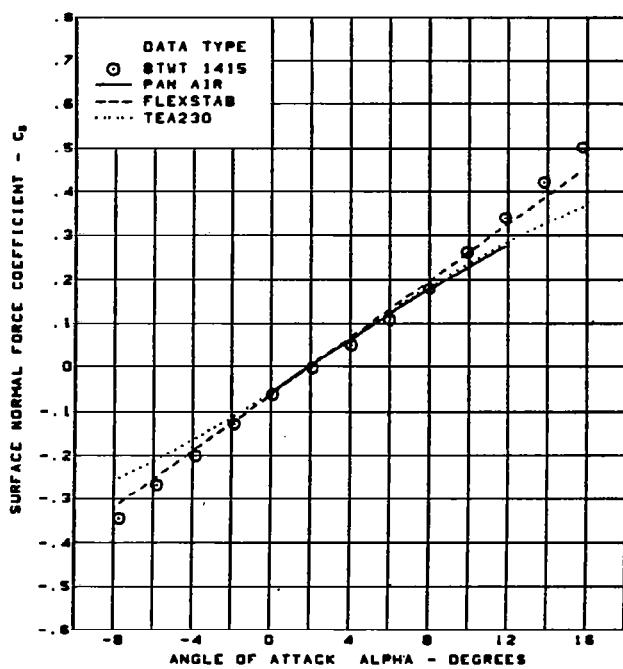


$M = 0.85$  (run 449)  
Twisted wing, rounded L.E.

L.E. deflection, full span =  $0.0^\circ$   
T.E. deflection, full span =  $0.0^\circ$

(h) Spanload Distributions

Figure 45. - (Continued)

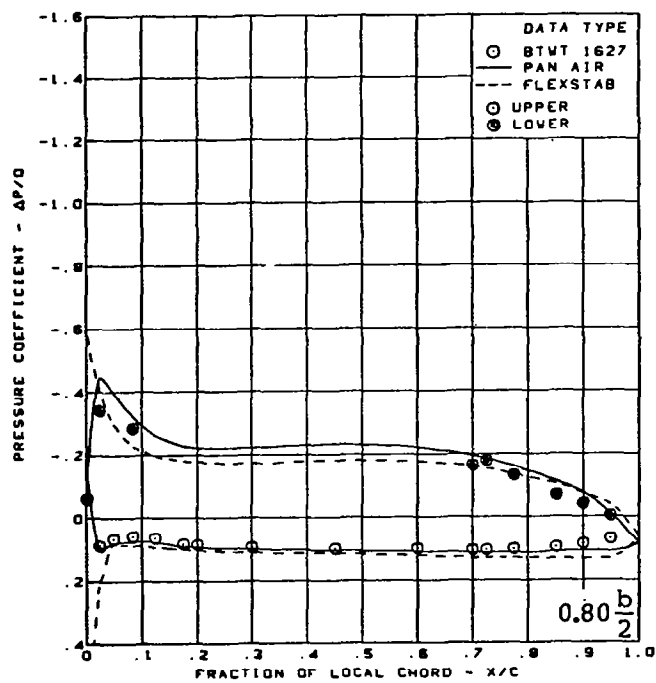
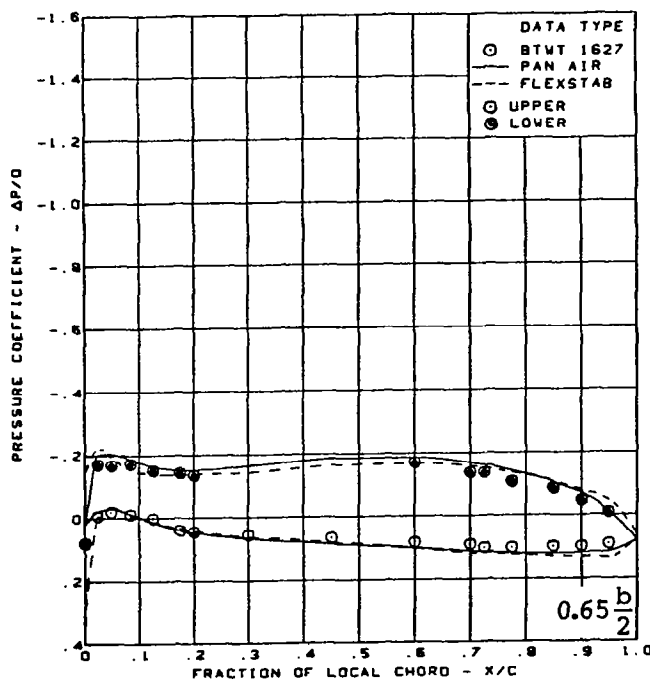
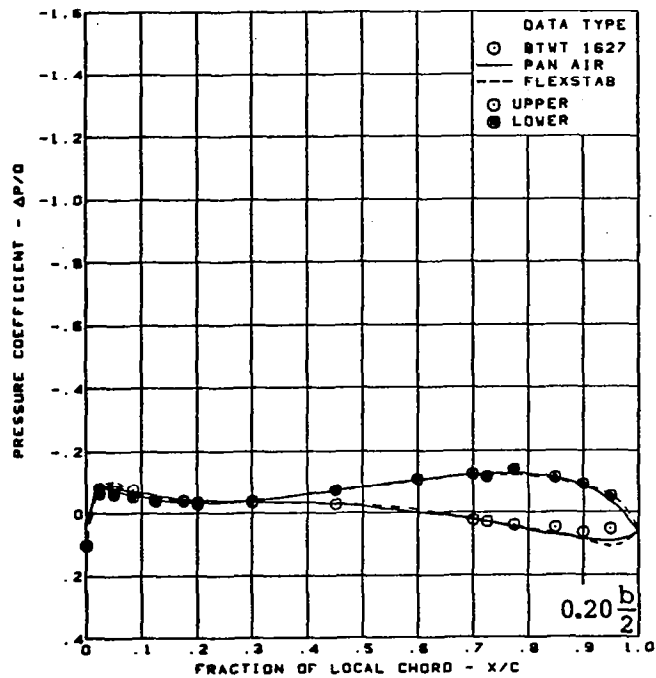
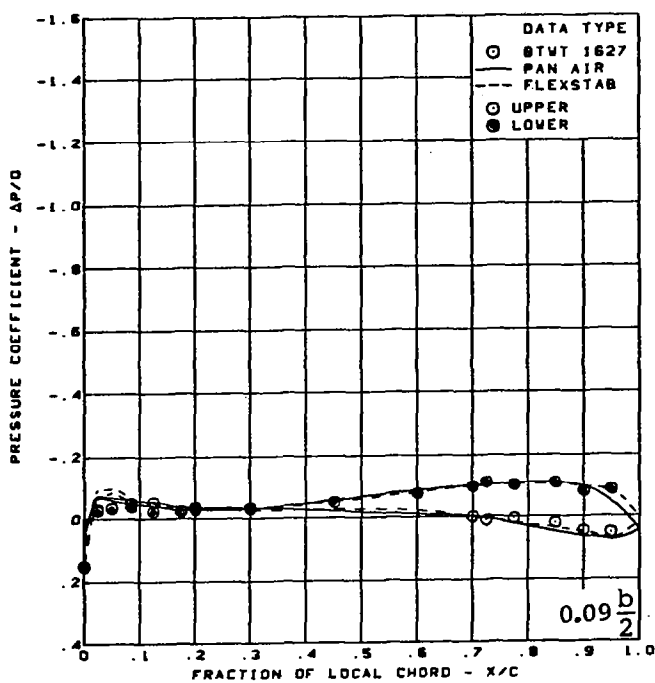


$M = 0.85$  (run 449)  
 Twisted wing, rounded L.E.

L.E. deflection, full span =  $0.0^\circ$   
 T.E. deflection, full span =  $0.0^\circ$

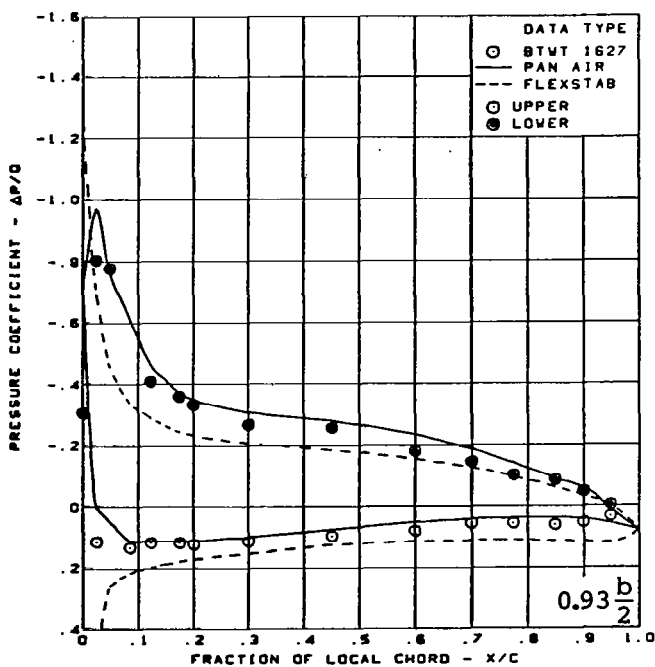
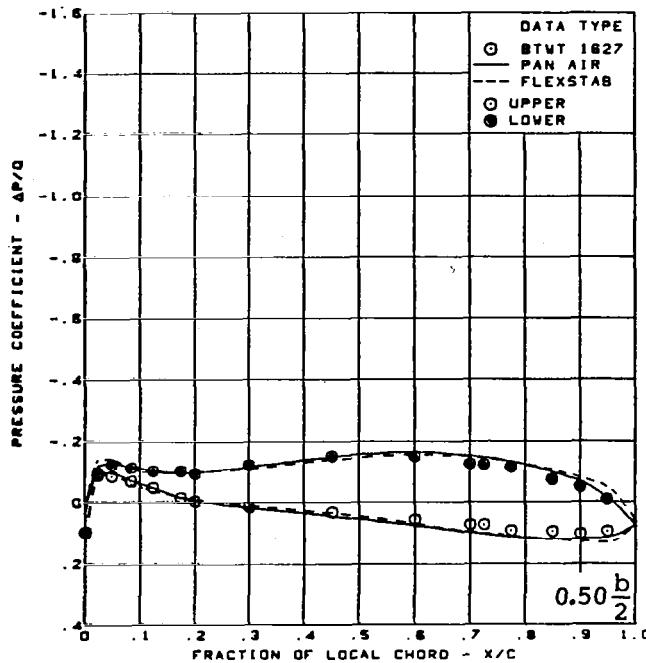
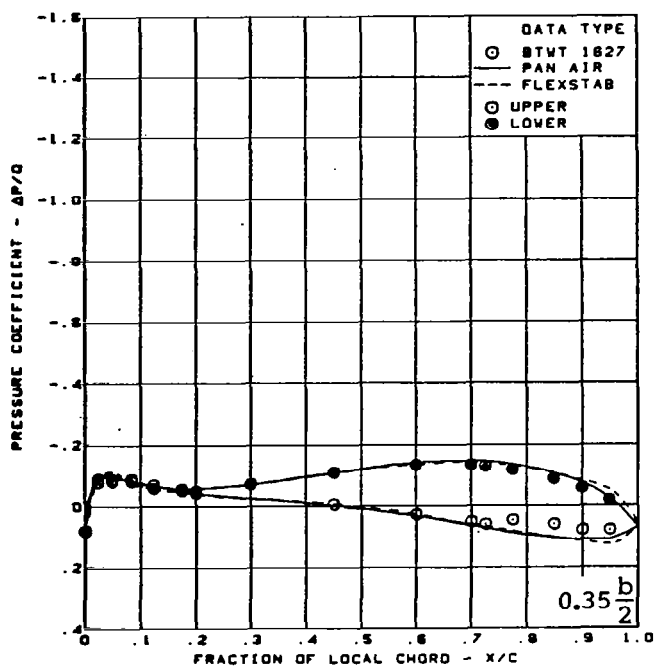
(i) Wing Aerodynamic Coefficients

Figure 45. — (Concluded)



(a) Surface Chordwise Pressure Distributions -  $\alpha = 0^\circ$

Figure 46. — Wing Theory-to-Experiment Comparison; Cambered-Twisted Wing; Fin Off; T.E. Deflection, Full Span =  $0.0^\circ$ ;  $M = 0.85$

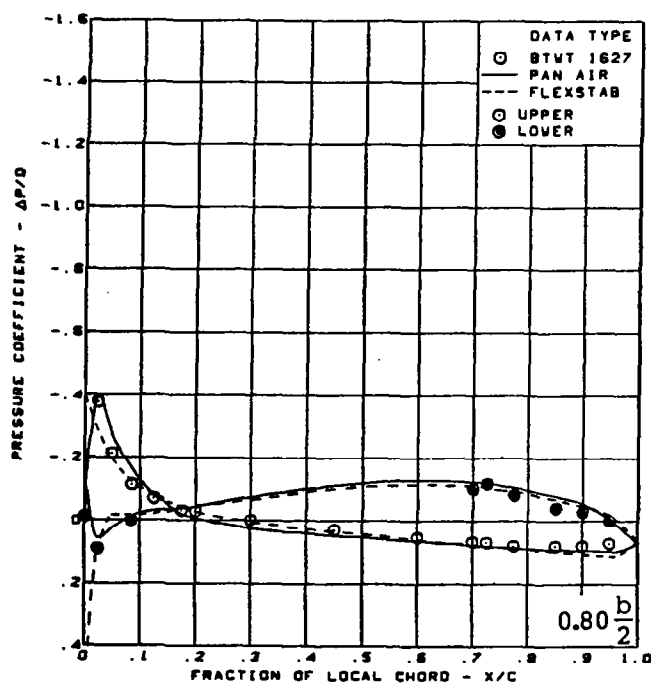
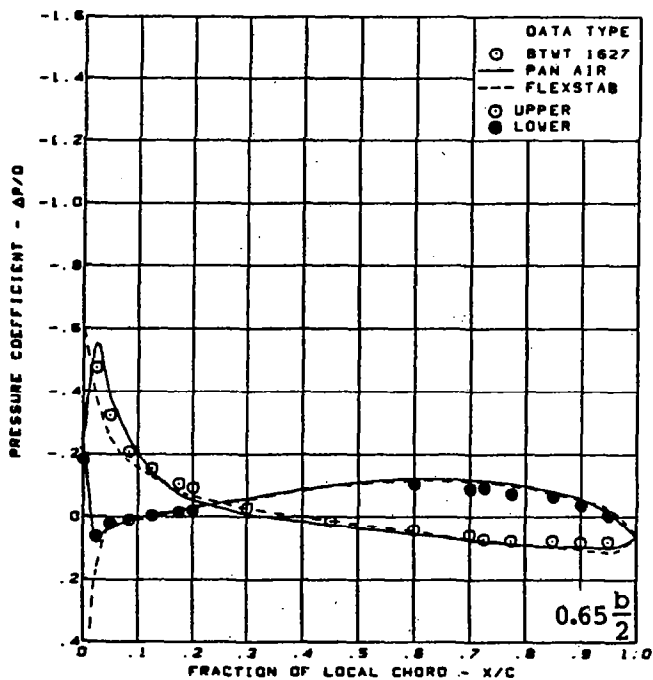
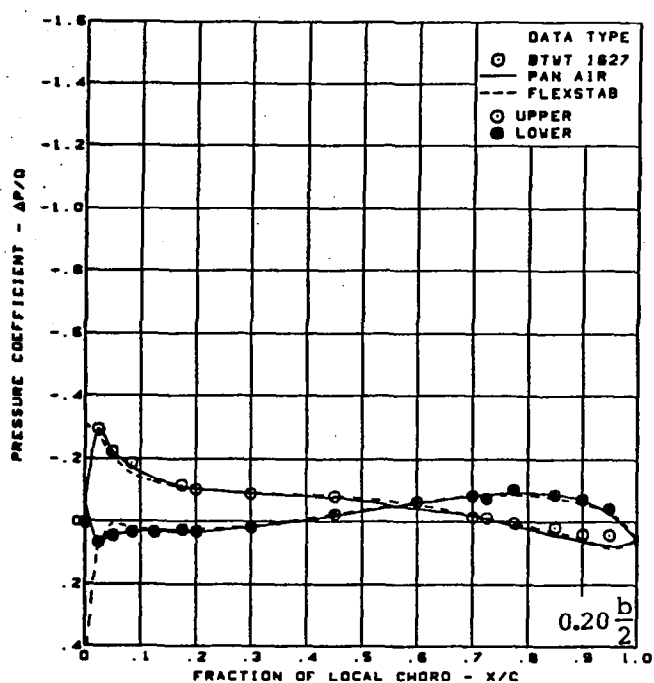
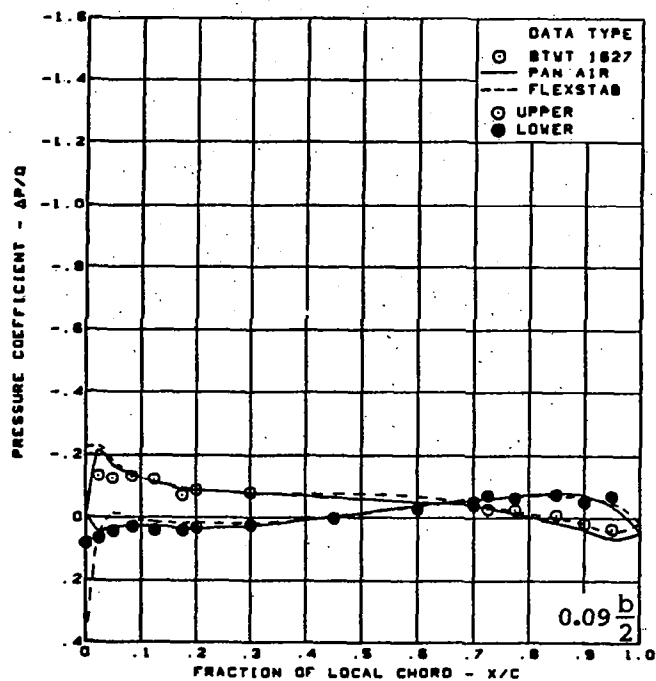


$M = 0.85$  (run 40)  
 $\alpha = 0^\circ$   
 Cambered-twisted wing, rounded L.E.  
 Fin off  
 L.E. deflection, full span =  $0.0^\circ$   
 T.E. deflection, full span =  $0.0^\circ$

(a) (Concluded)

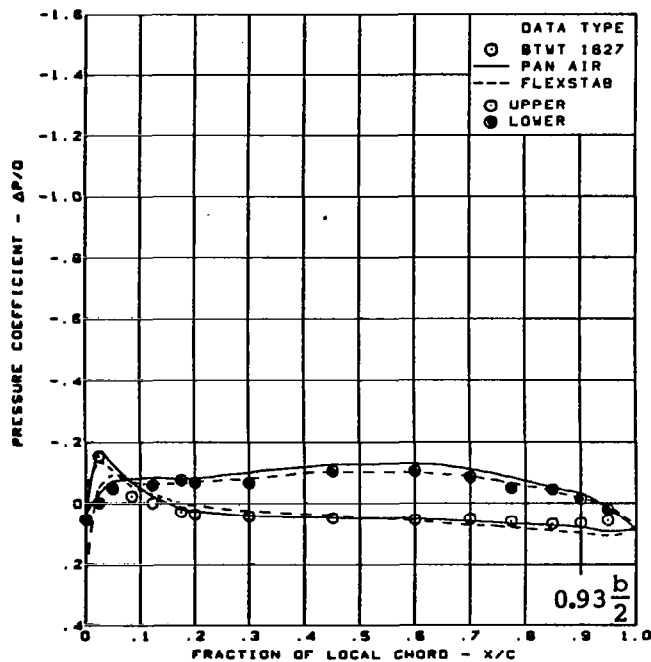
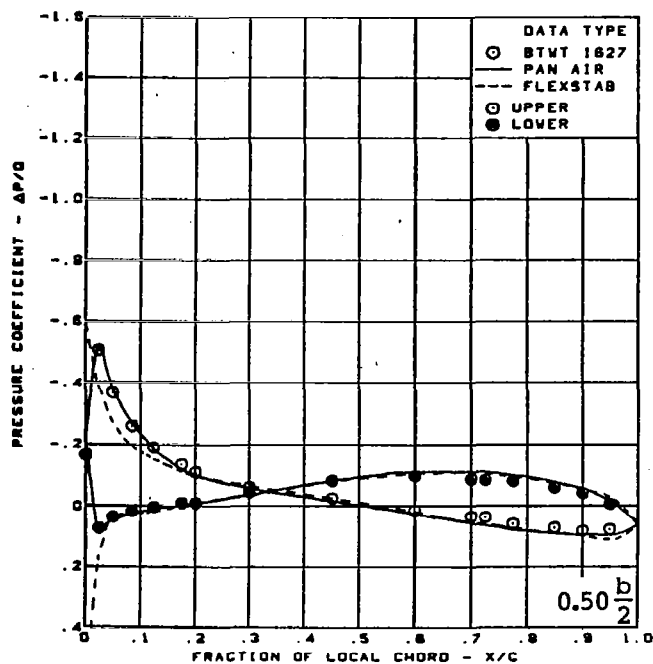
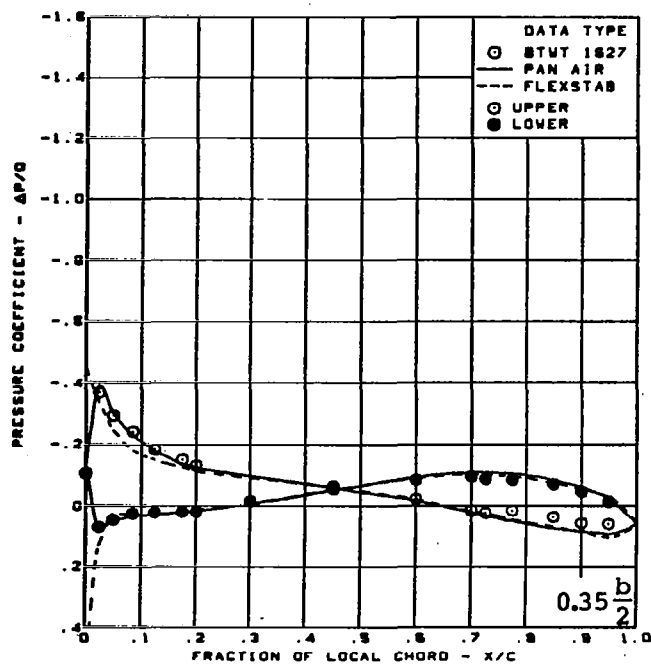
Figure 46. - (Continued)





(b) Surface Chordwise Pressure Distributions -  $\alpha = 4^\circ$

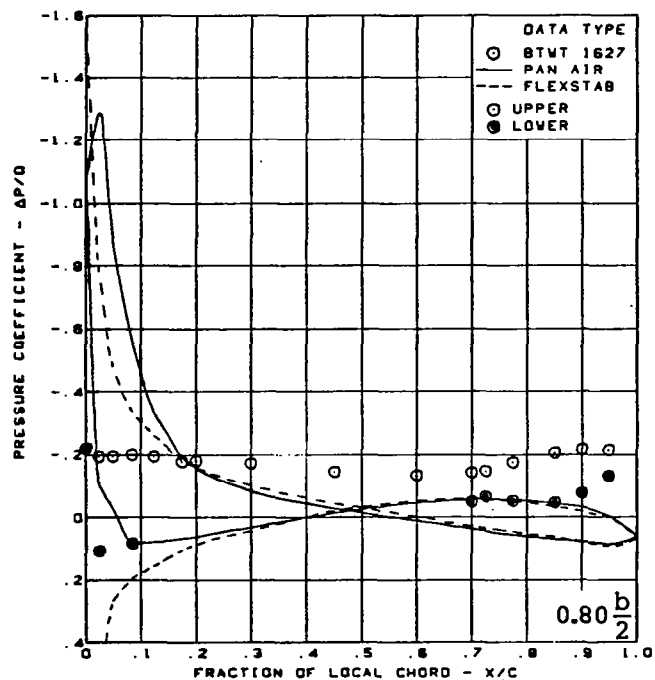
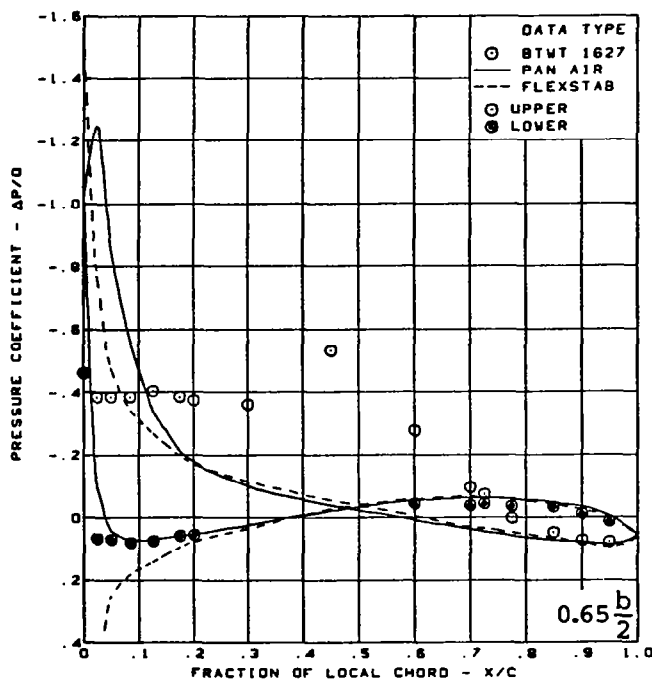
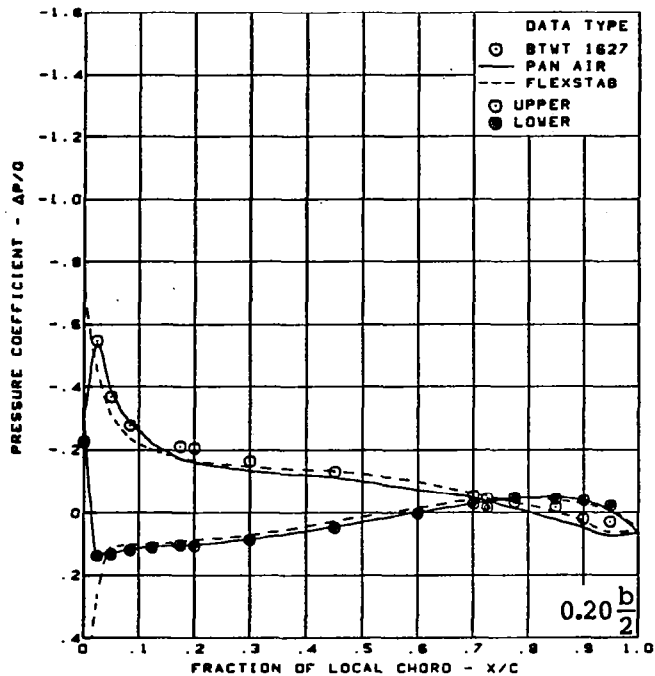
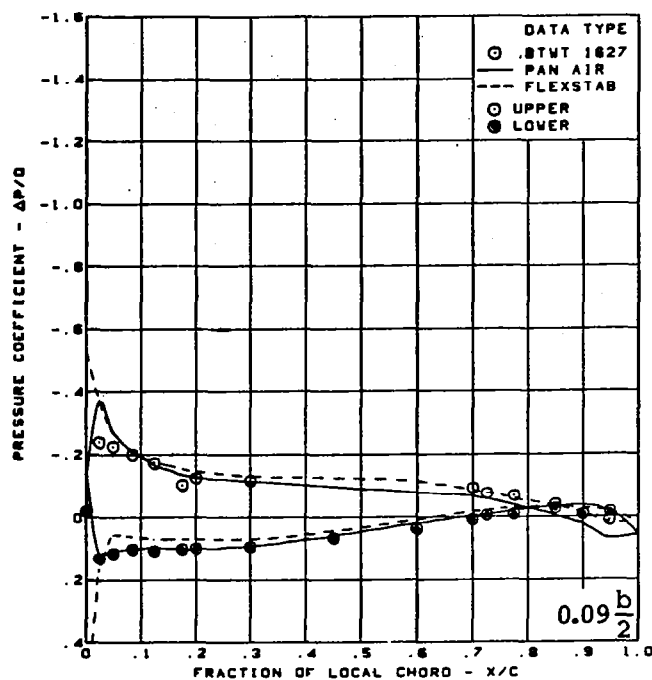
Figure 46. - (Continued)



$M = 0.85$  (run 40)  
 $\alpha = 4^\circ$   
 Cambered-twisted wing, rounded L.E.  
 Fin off  
 L.E. deflection, full span =  $0.0^\circ$   
 T.E. deflection, full span =  $0.0^\circ$

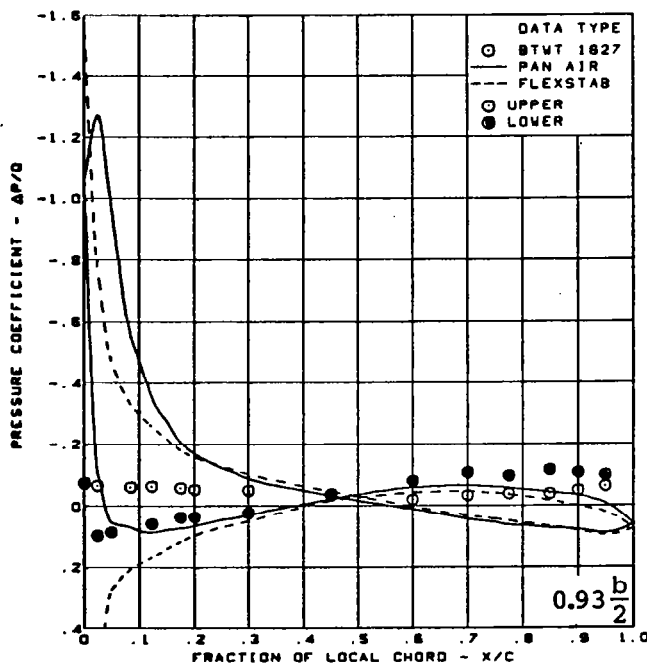
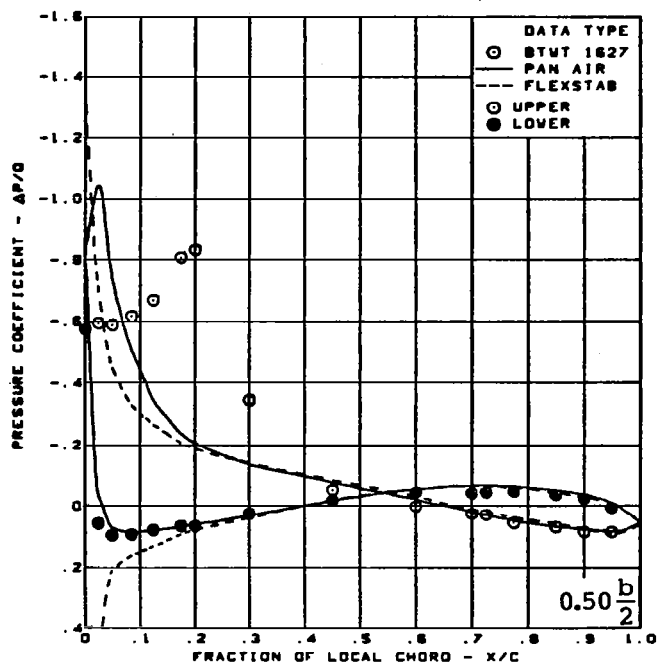
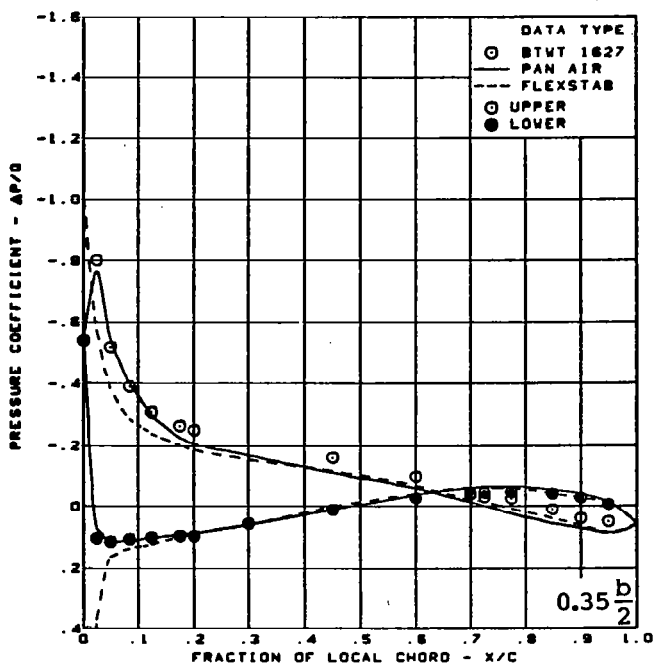
(b) (Concluded)

Figure 46. - (Continued)



(c) Surface Chordwise Pressure Distributions -  $\alpha = 8^\circ$

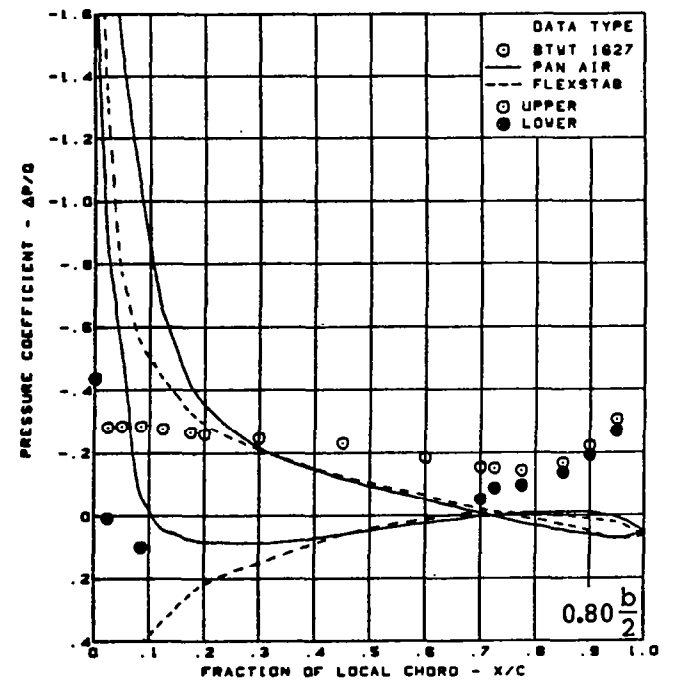
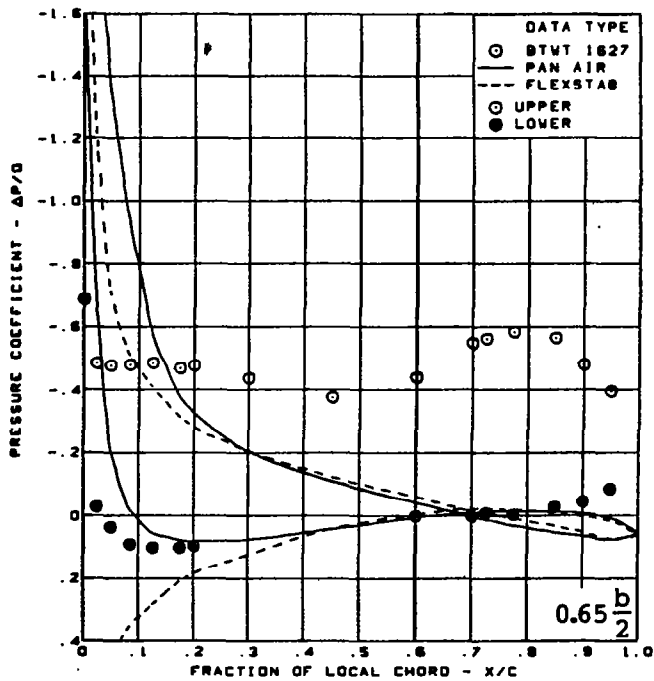
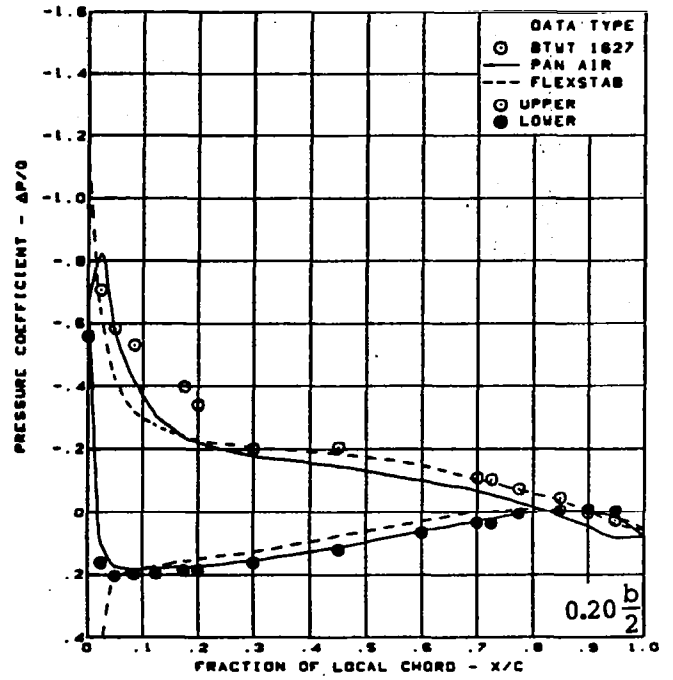
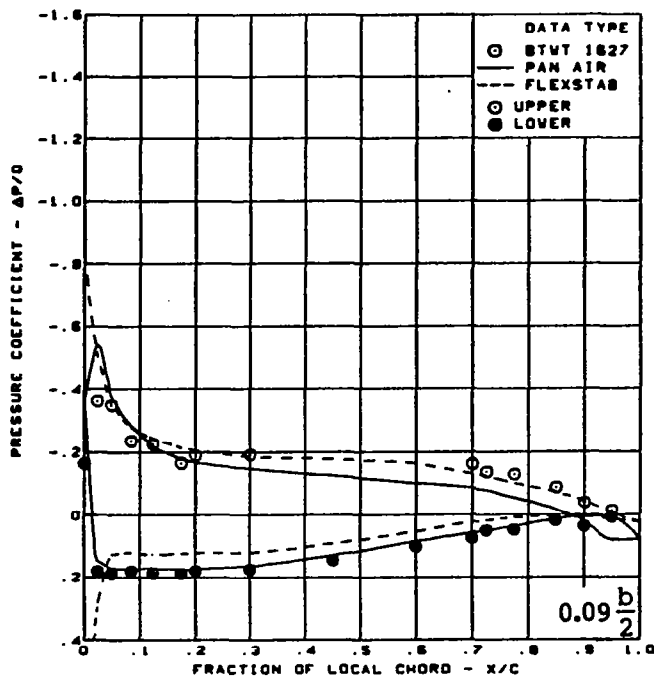
Figure 46. - (Continued)



$M = 0.85$  (run 40)  
 $\alpha = 8^\circ$   
 Cambered-twisted wing, rounded L.E.  
 Fin off  
 L.E. deflection, full span =  $0.0^\circ$   
 T.E. deflection, full span =  $0.0^\circ$

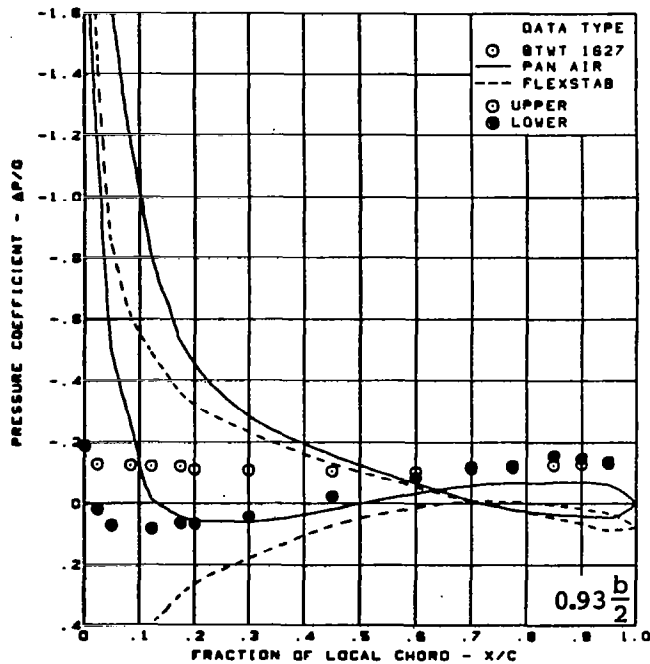
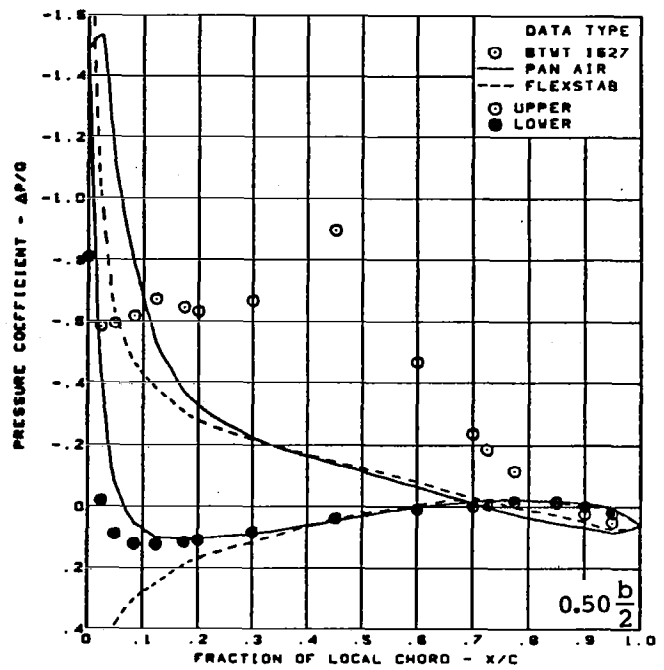
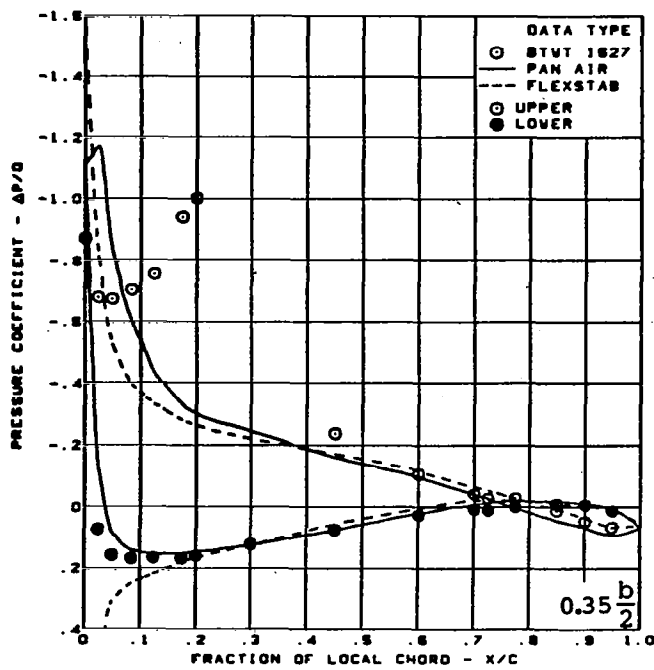
(c) (Concluded)

Figure 46. — (Continued)



(d) Surface Chordwise Pressure Distributions -  $\alpha = 12^\circ$

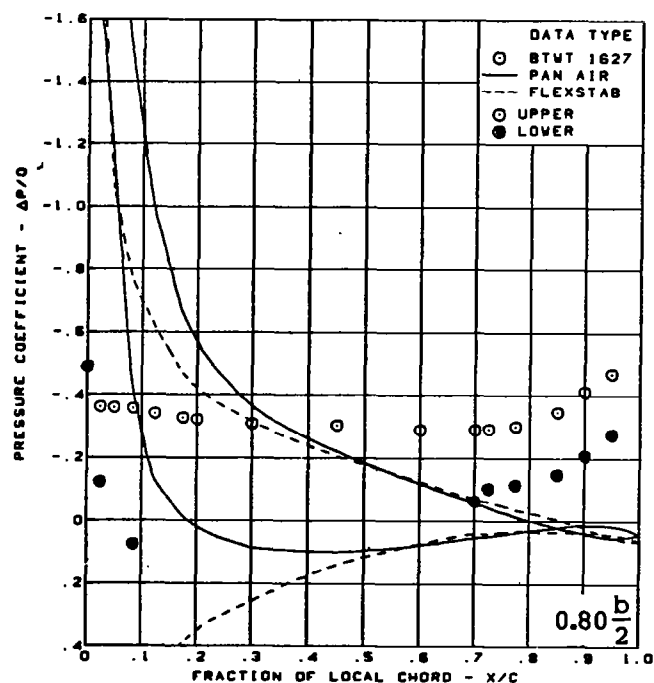
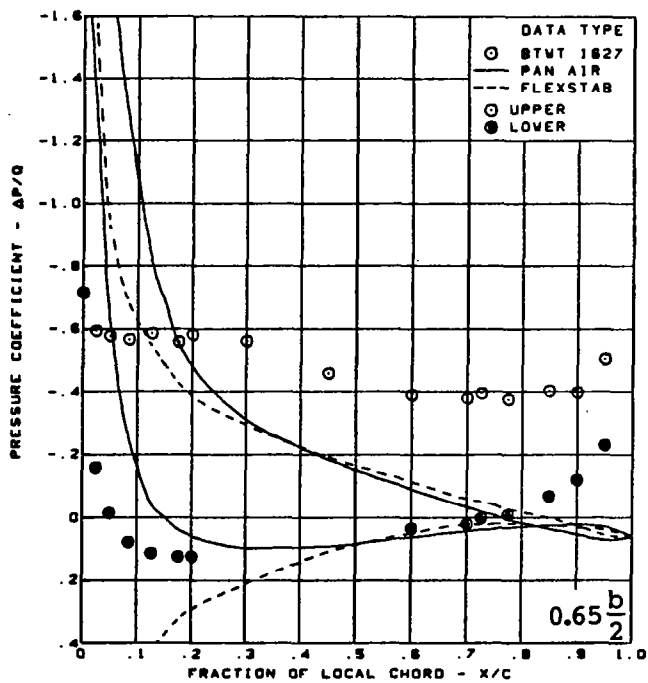
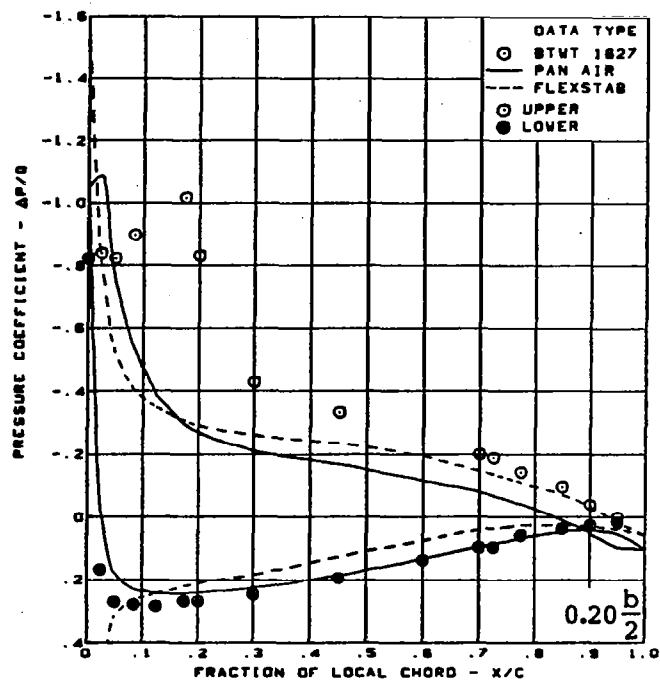
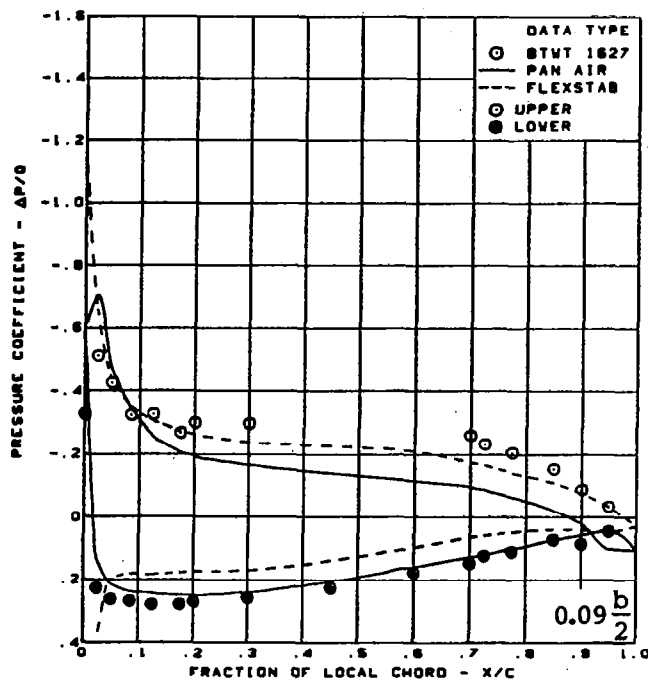
Figure 46. - (Continued)



$M = 0.85$  (run 40)  
 $\alpha = 12^\circ$   
 Cambered-twisted wing, rounded L.E.  
 Fin off  
 L.E. deflection, full span =  $0.0^\circ$   
 T.E. deflection, full span =  $0.0^\circ$

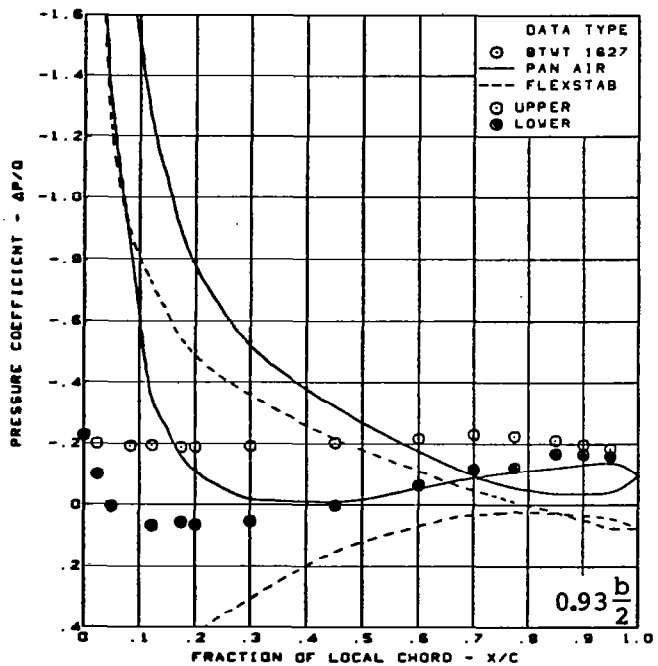
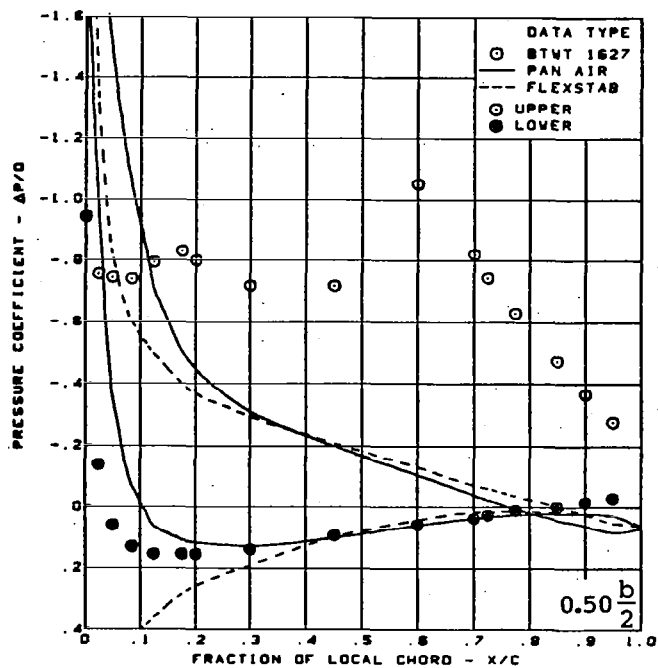
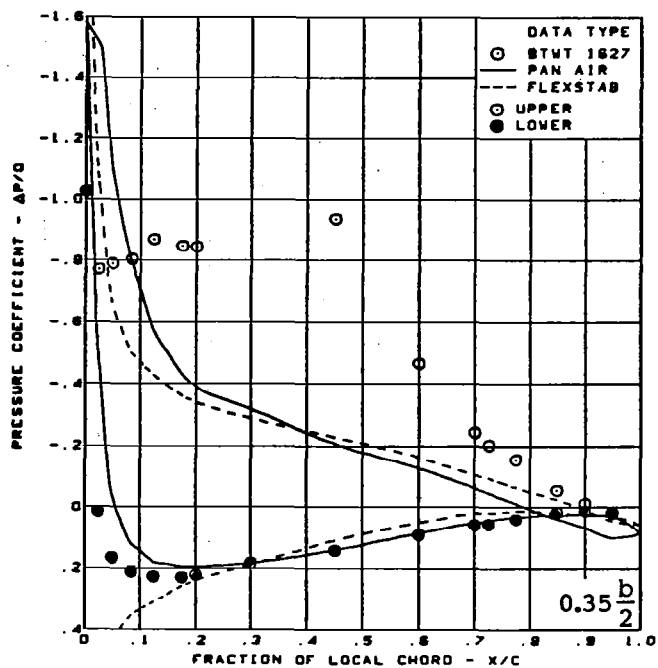
(d) (Concluded)

Figure 46. - (Continued)



(e) Surface Chordwise Pressure Distributions -  $\alpha = 16^\circ$

Figure 46. - (Continued)

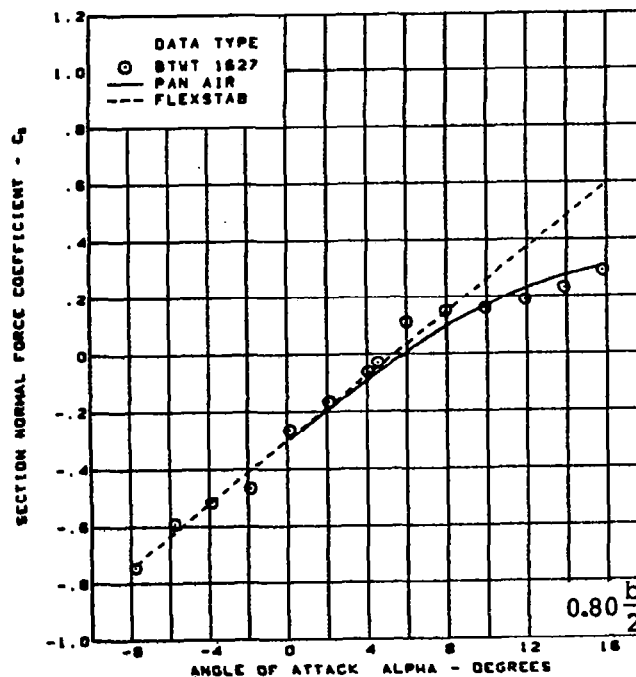
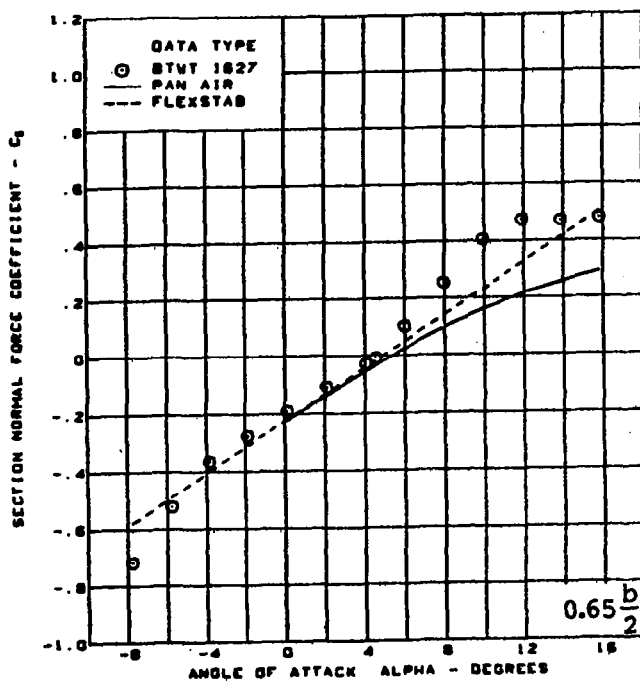
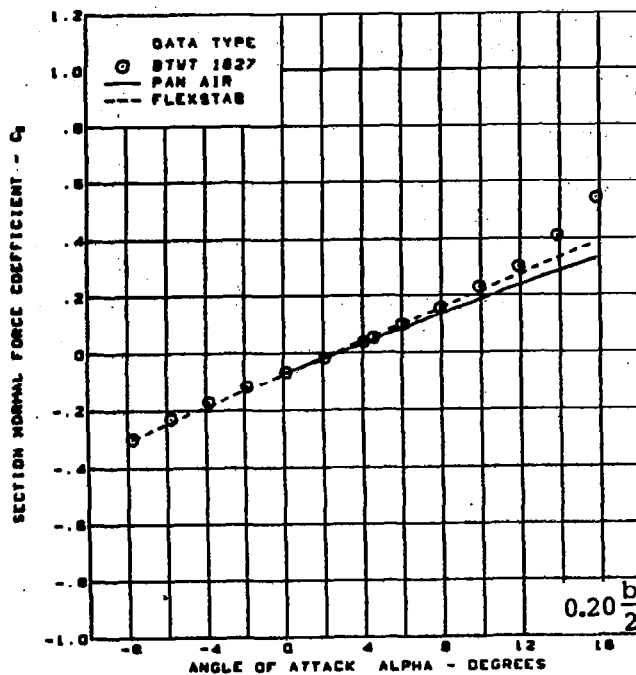
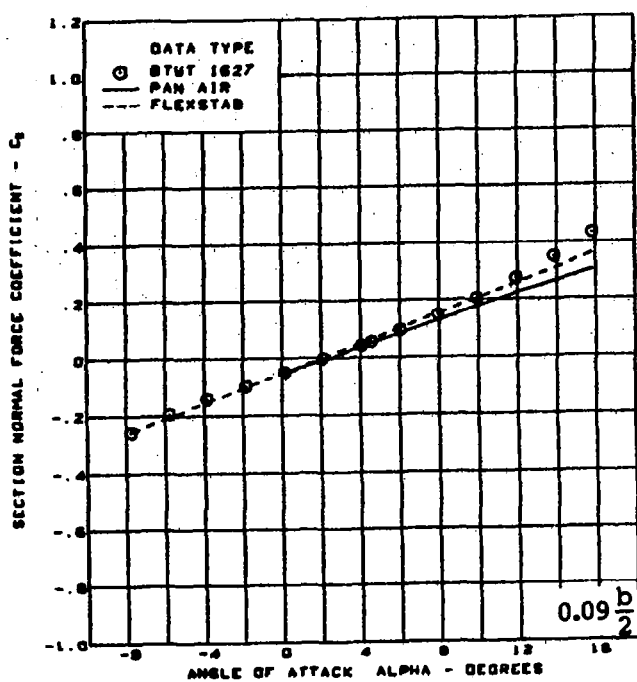


$M = 0.85$  (run 40)  
 $\alpha = 16^\circ$   
 Cambered-twisted wing, rounded L.E.  
 Fin off  
 L.E. deflection, full span =  $0.0^\circ$   
 T.E. deflection, full span =  $0.0^\circ$

(e) (Concluded)

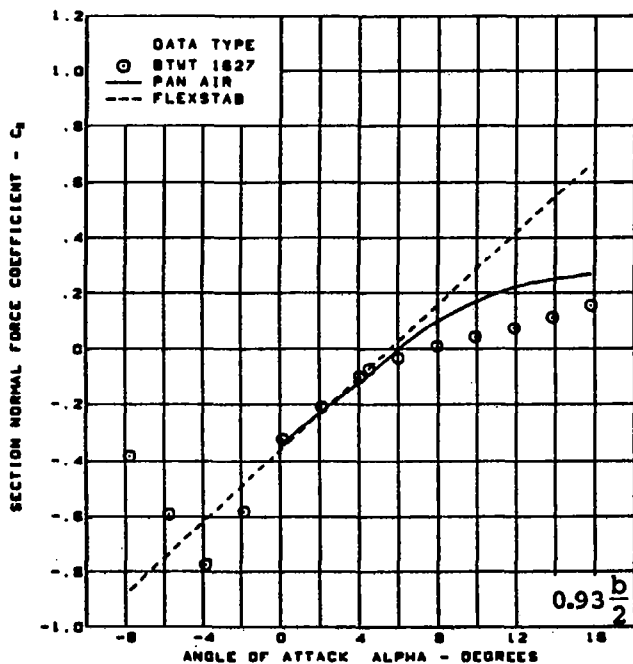
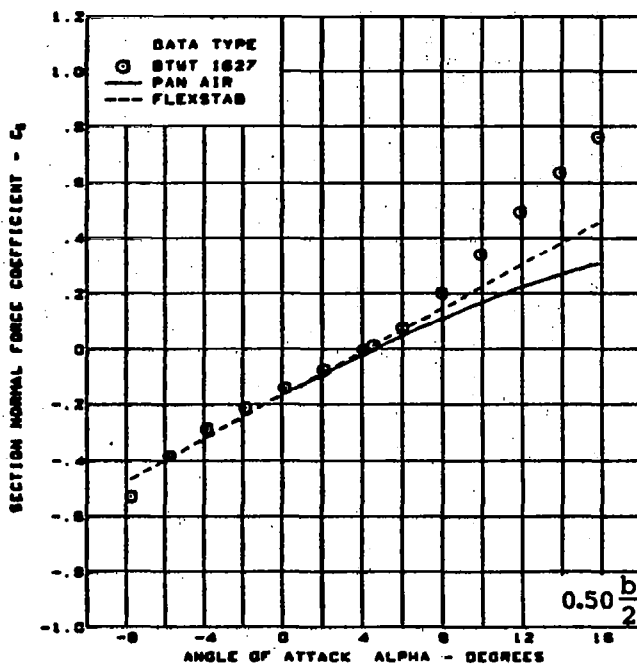
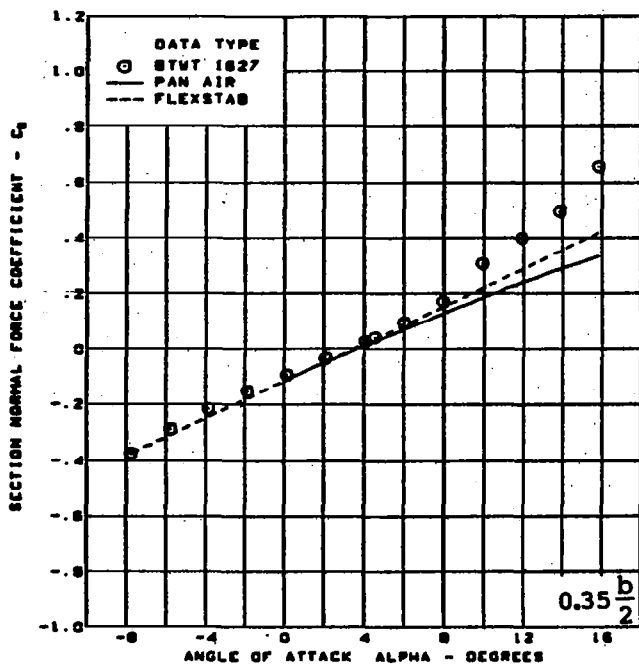
Figure 46. - (Continued)





(f) Section Aerodynamic Coefficients - Normal Force

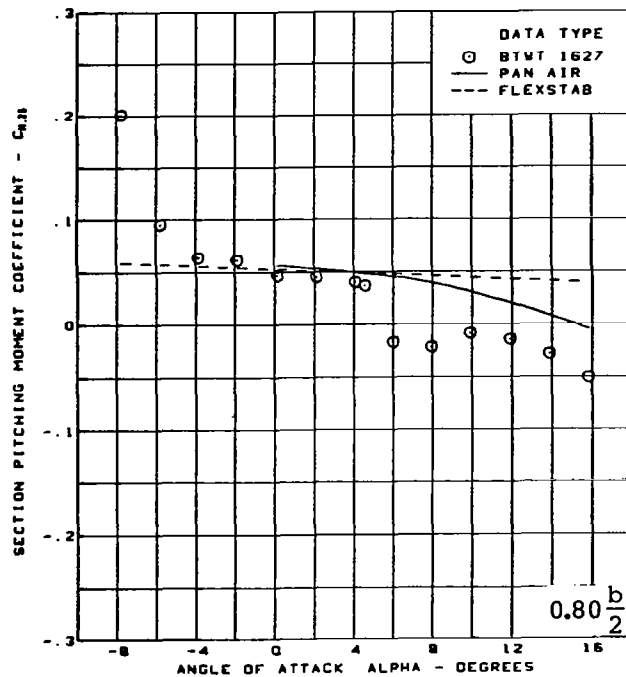
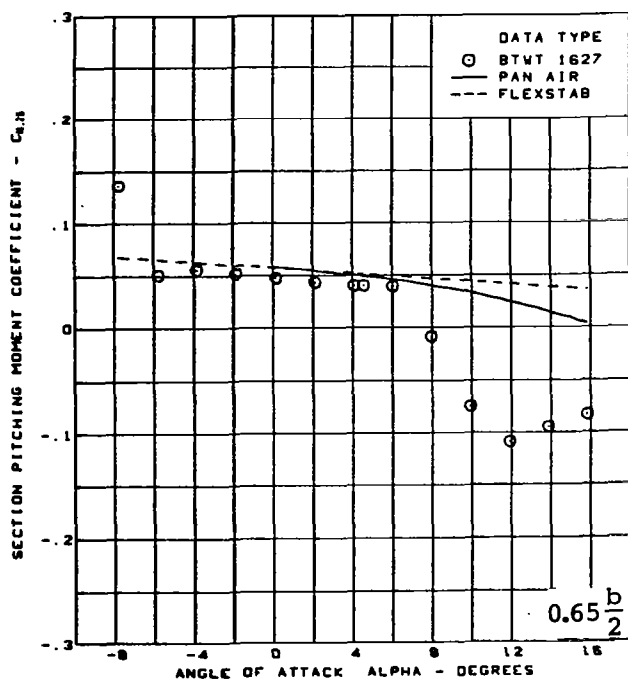
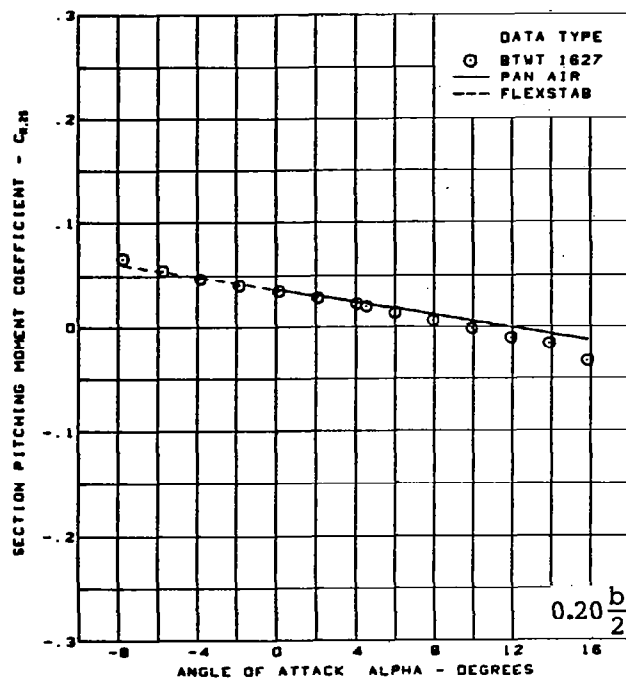
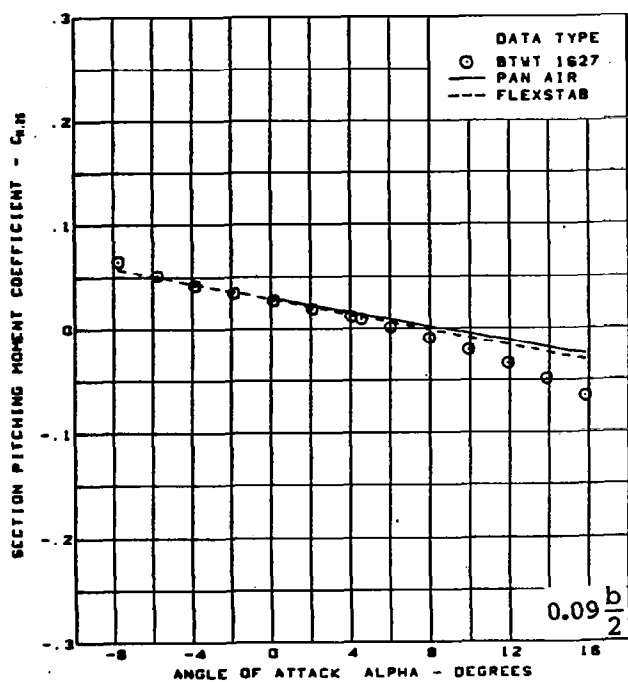
Figure 46. — (Continued)



$M = 0.85$  (run 40)  
 Cambered-twisted wing, rounded L.E.  
 Fin off  
 L.E. deflection, full span =  $0.0^\circ$   
 T.E. deflection, full span =  $0.0^\circ$

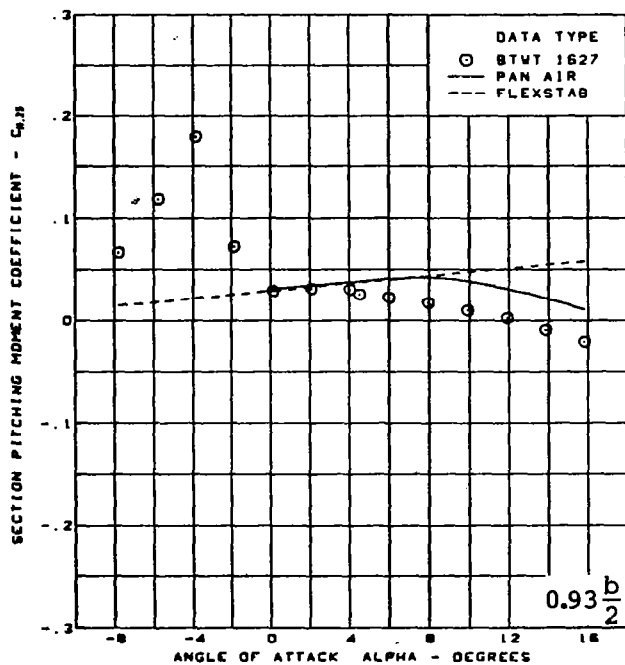
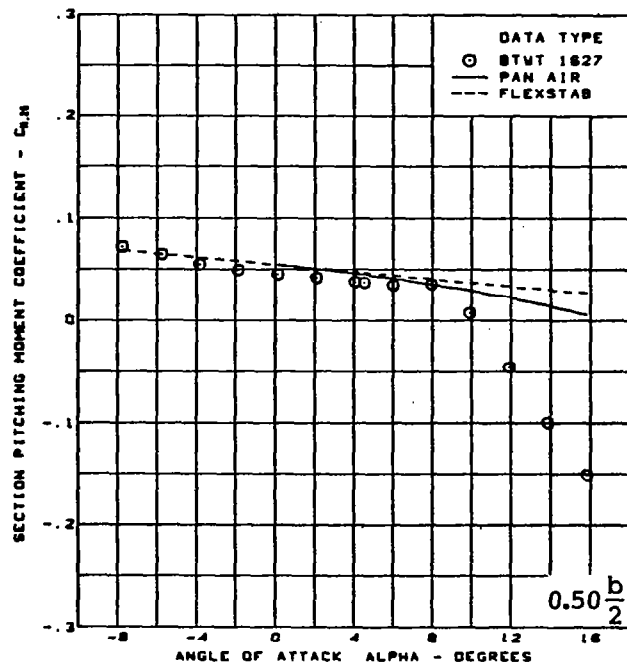
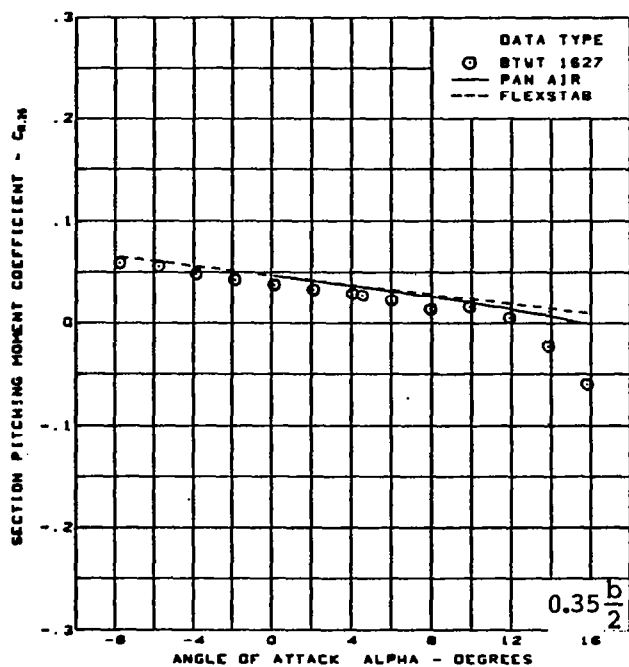
(f) (Concluded)

Figure 46. -- (Continued)



(g) Section Aerodynamic Coefficients - Pitching Moment

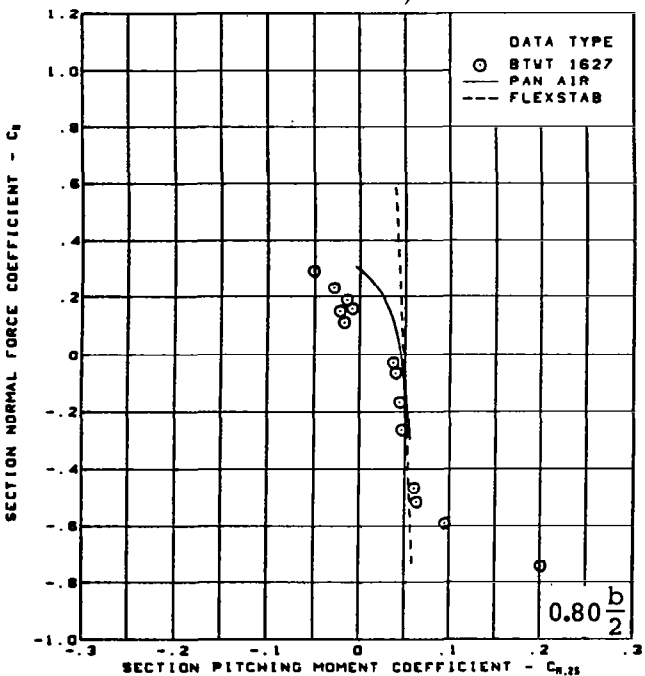
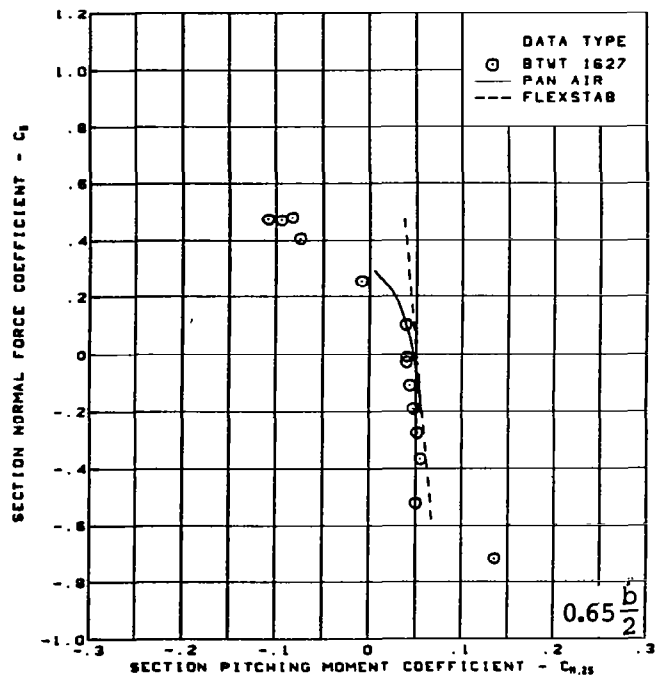
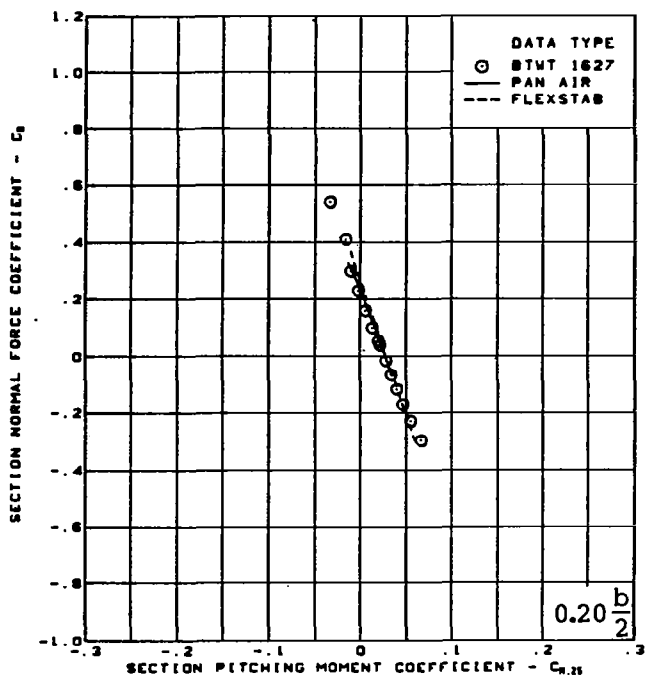
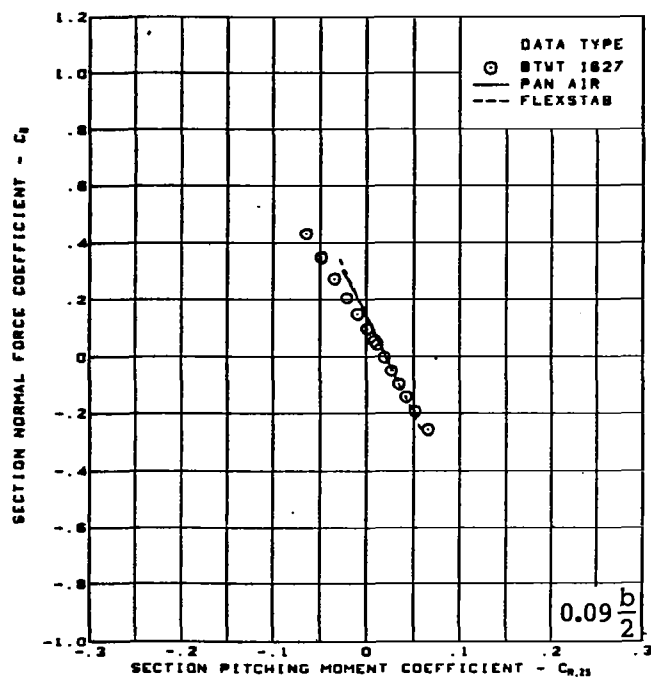
Figure 46. - (Continued)



M = 0.85 (run 40)  
 Cambered-twisted wing, rounded L.E.  
 Fin off  
 L.E. deflection, full span =  $0.0^\circ$   
 T.E. deflection, full span =  $0.0^\circ$

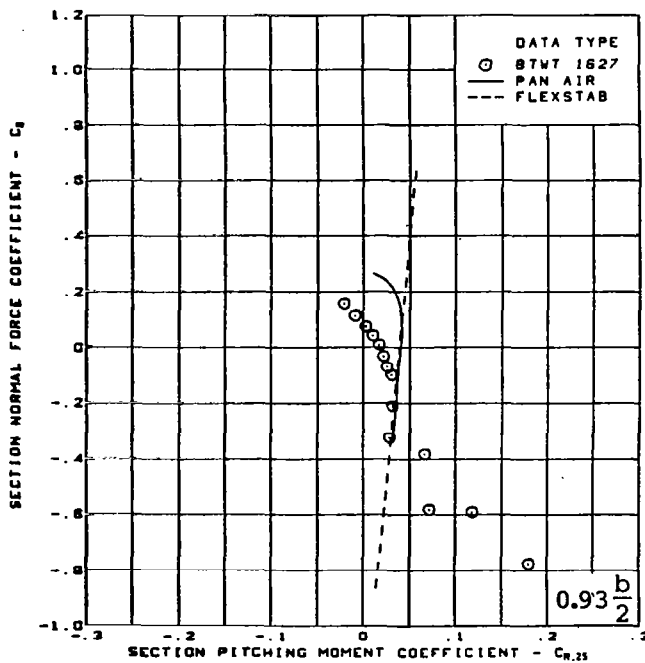
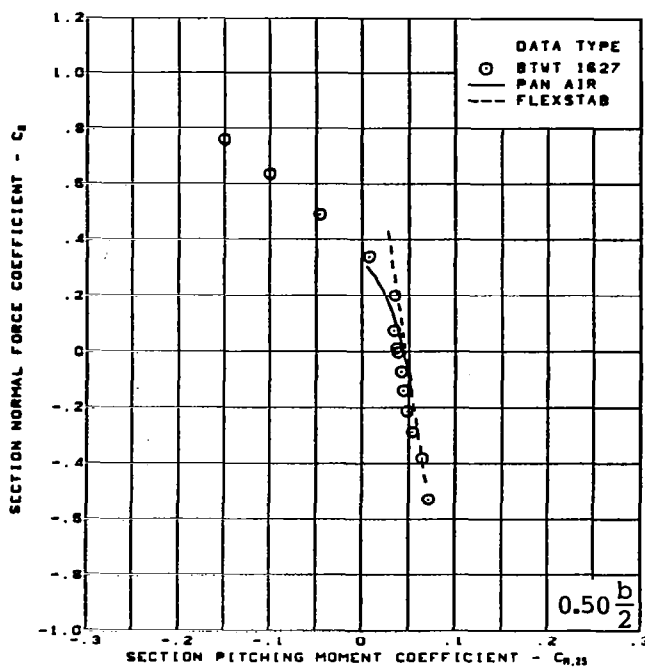
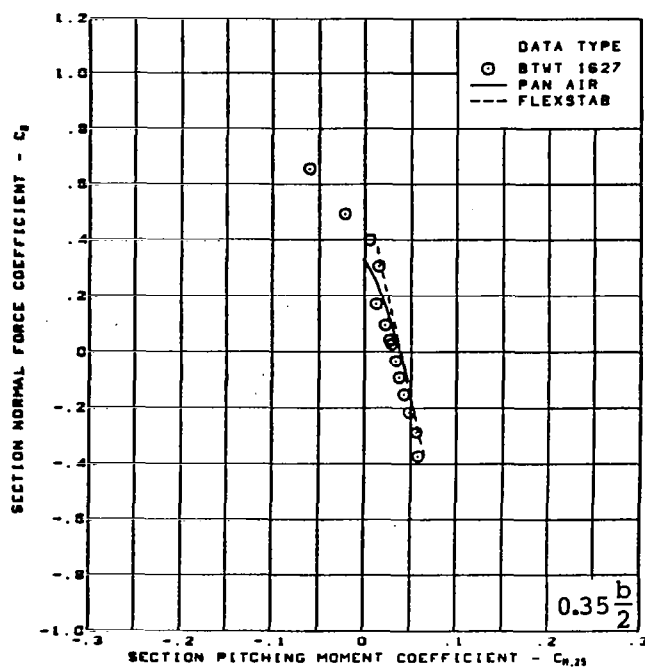
(g) (Concluded)

Figure 46. — (Continued)



(h) Section Aerodynamic Coefficients - Normal Force vs Pitching Moment

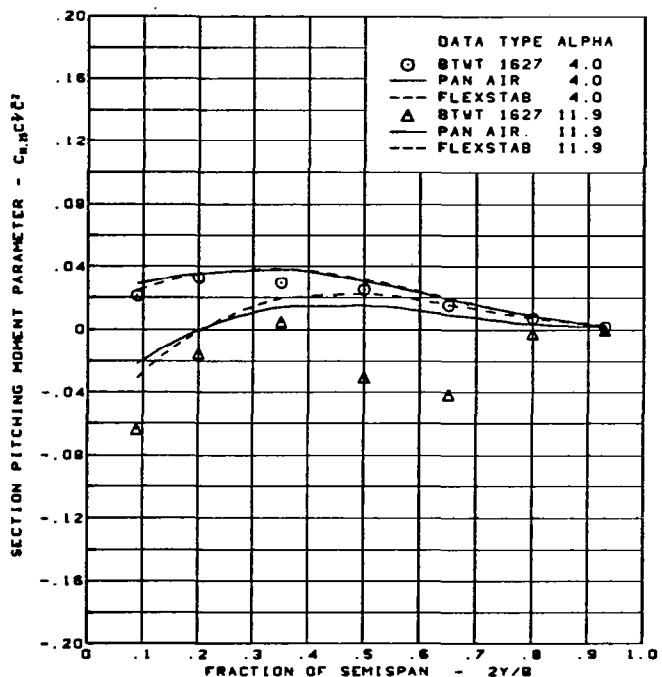
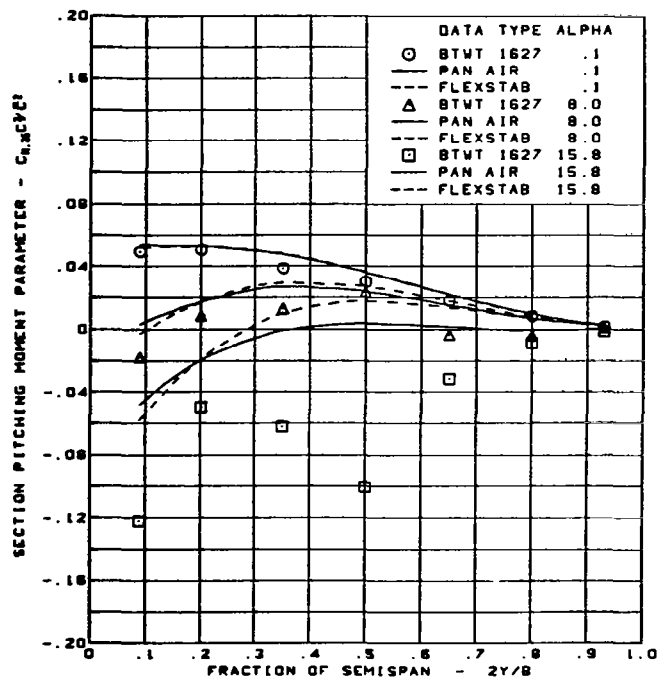
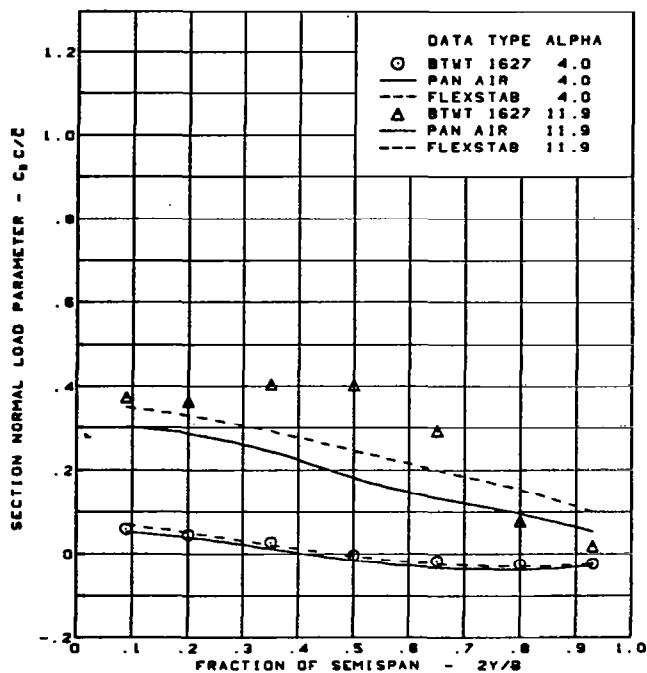
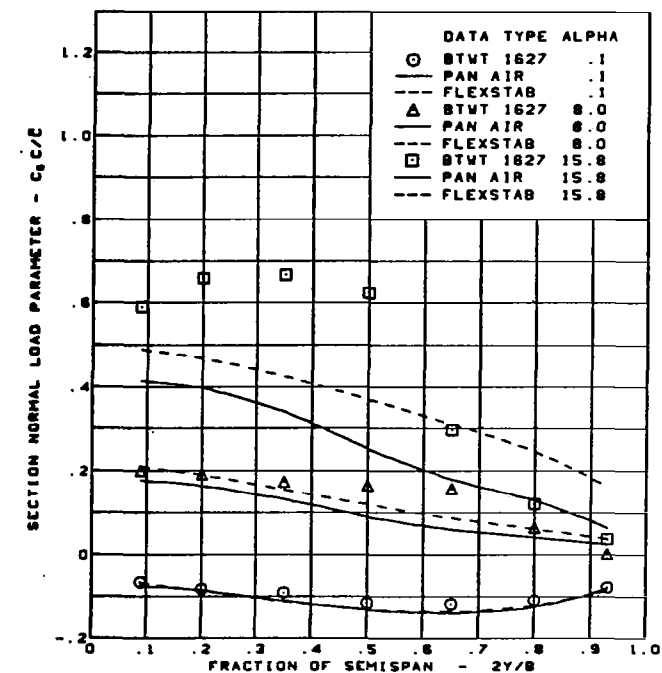
Figure 46. — (Continued)



M = 0.85 (run 40)  
 Cambered-twisted wing, rounded L.E.  
 Fin off  
 L.E. deflection, full span =  $0.0^\circ$   
 T.E. deflection, full span =  $0.0^\circ$

(h) (Concluded)

Figure 46. — (Continued)

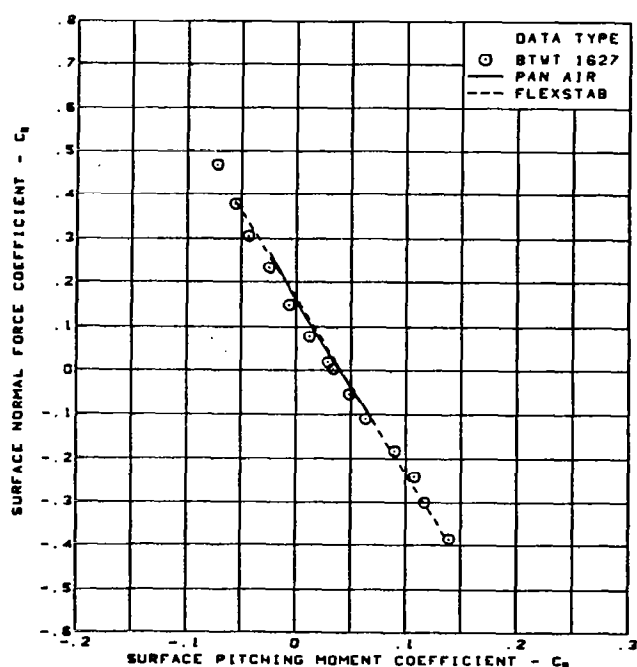
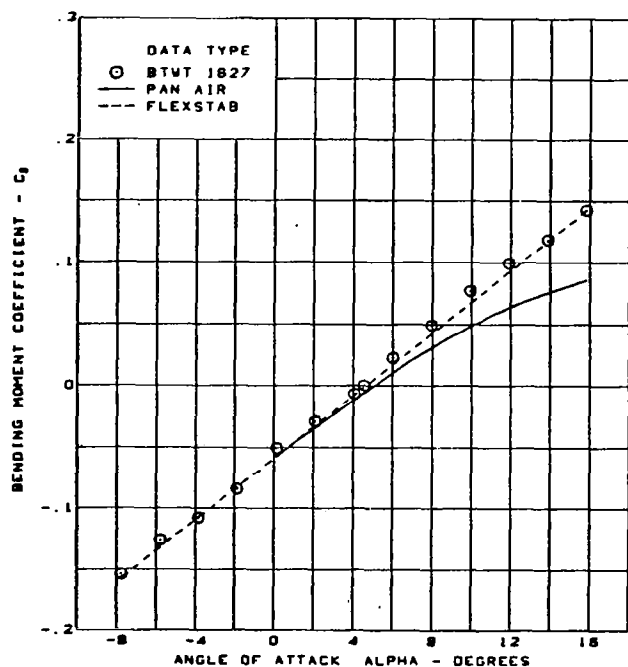
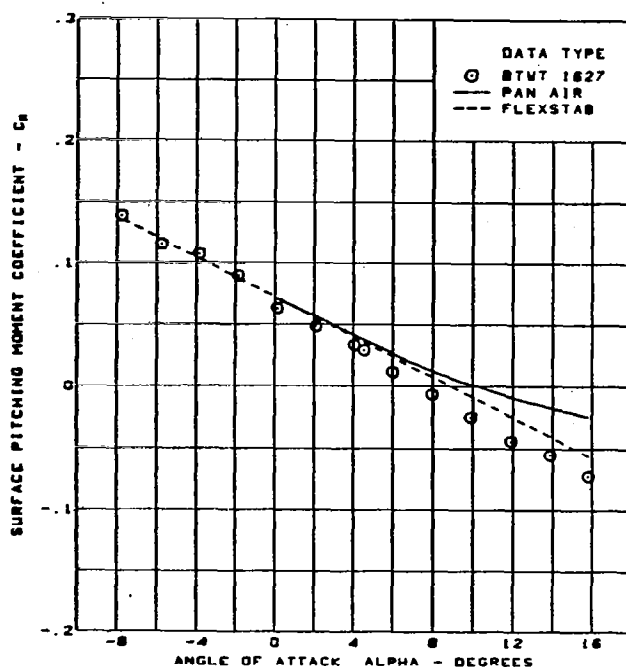
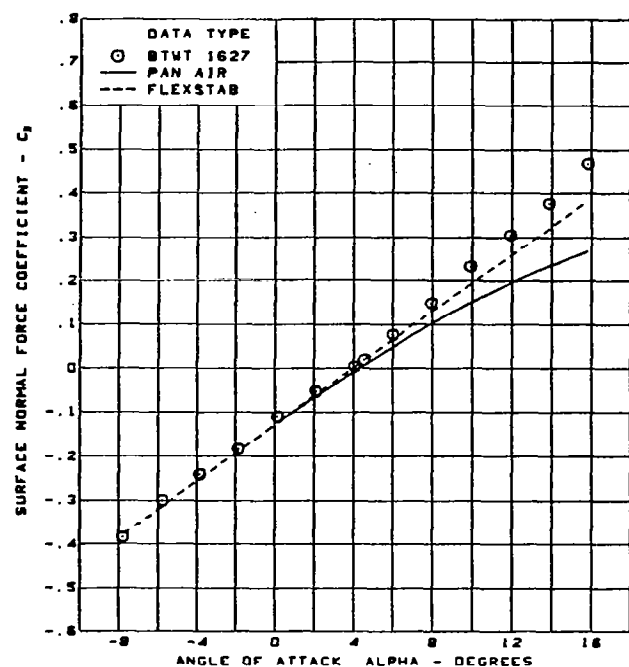


$M = 0.85$  (run 40)  
Cambered-twisted wing, rounded L.E.  
Fin off

L.E. deflection, full span =  $0.0^\circ$   
T.E. deflection, full span =  $0.0^\circ$

(i) Spanload Distributions

Figure 46. — (Continued)



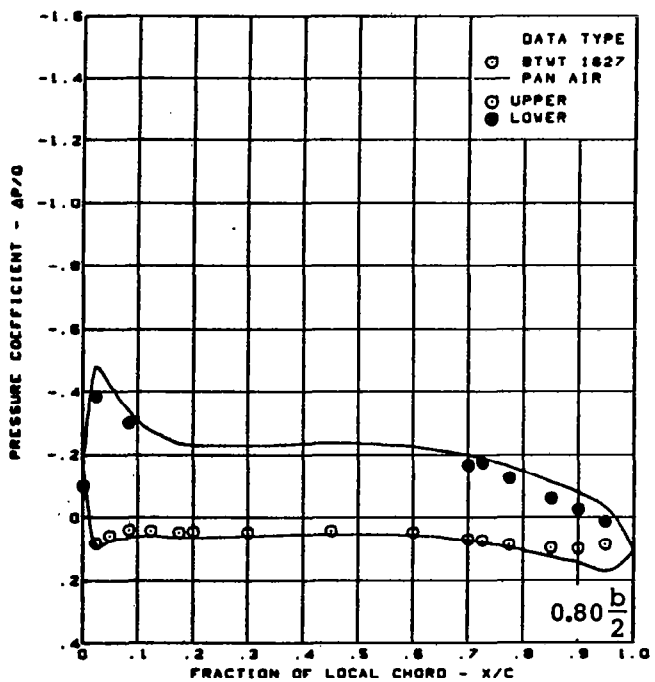
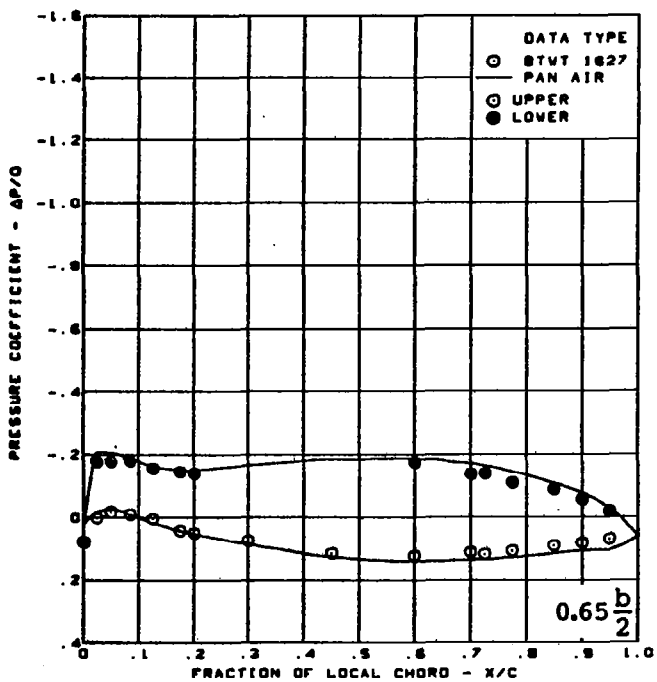
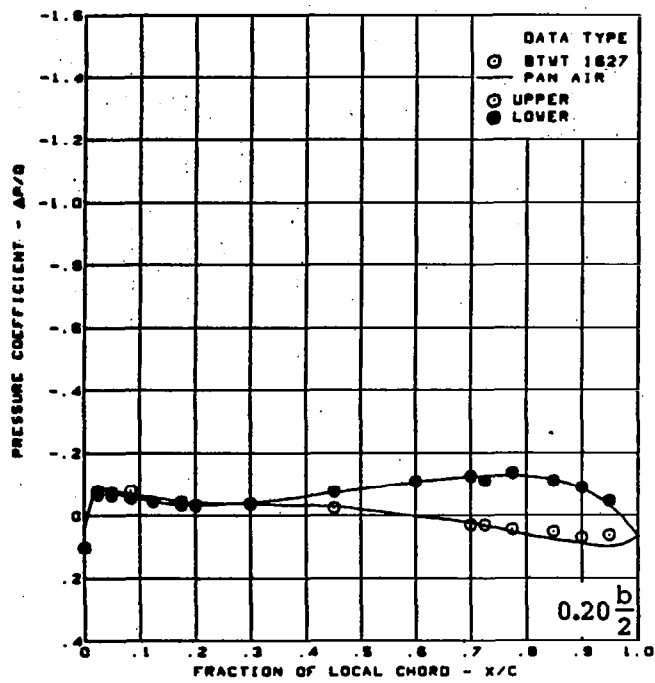
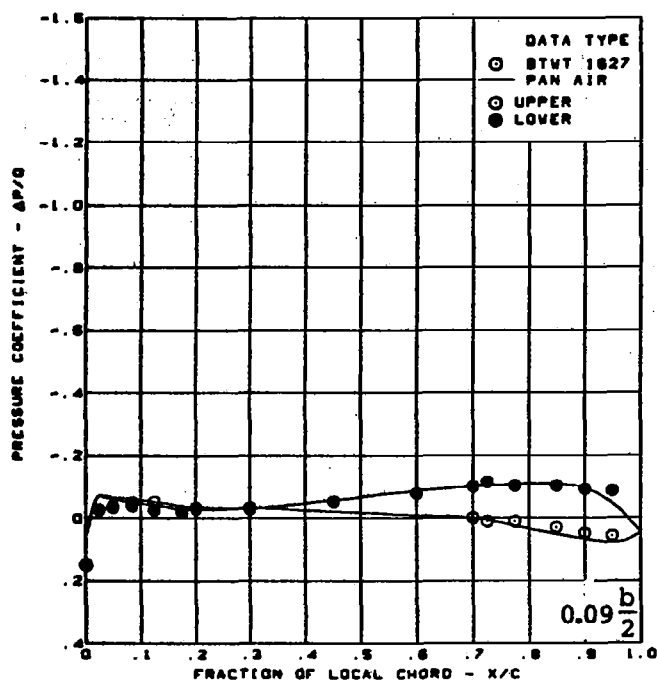
$M = 0.85$  (run 40)  
 Cambered-twisted wing, rounded L.E.  
 Fin off

L.E. deflection, full span =  $0.0^\circ$   
 T.E. deflection, full span =  $0.0^\circ$

#### (j) Wing Aerodynamic Coefficients

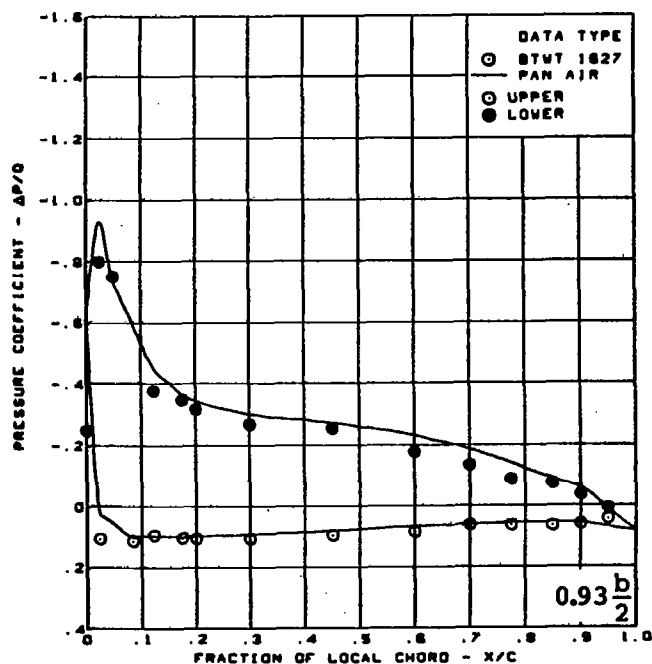
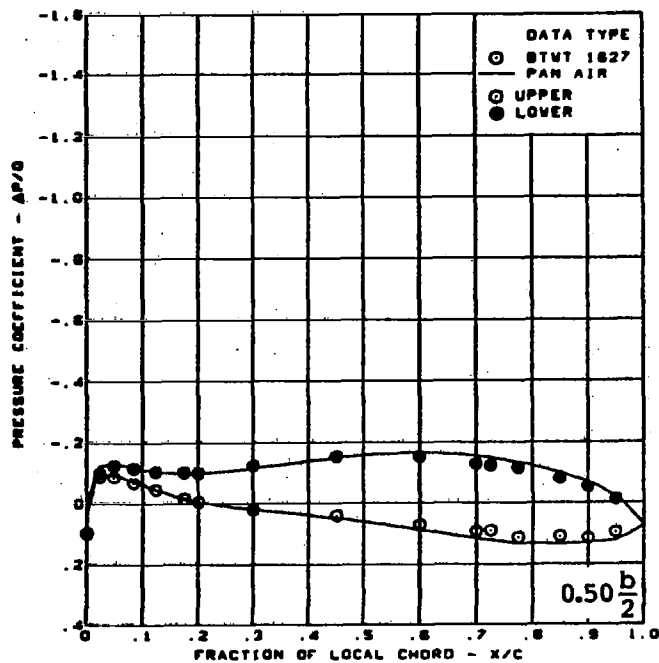
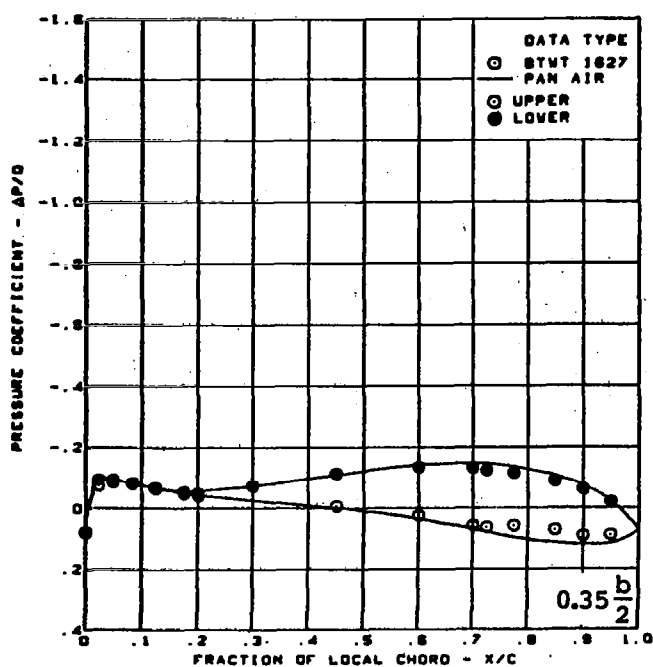
Figure 46. — (Concluded)





(a) Surface Chordwise Pressure Distributions -  $\alpha = 0^\circ$

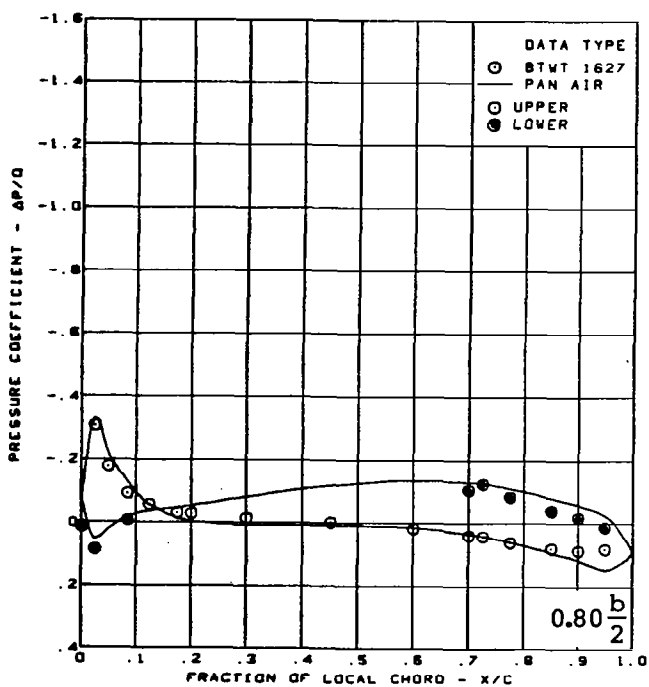
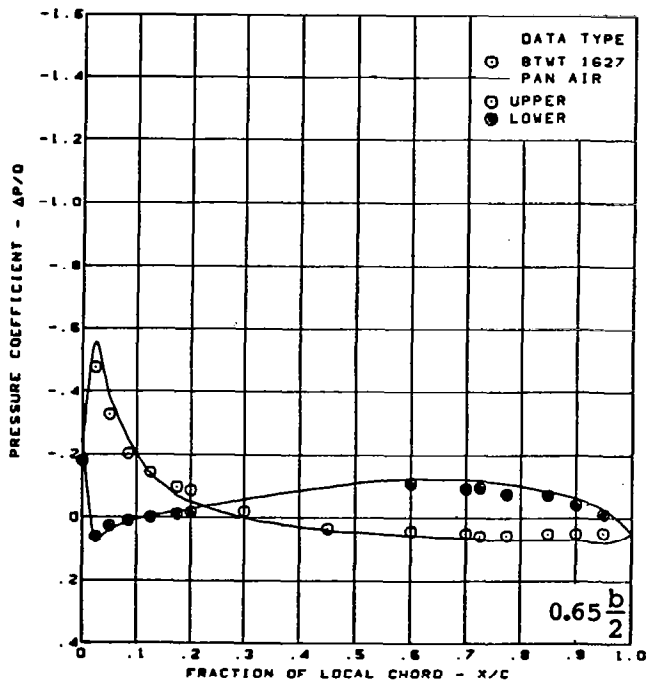
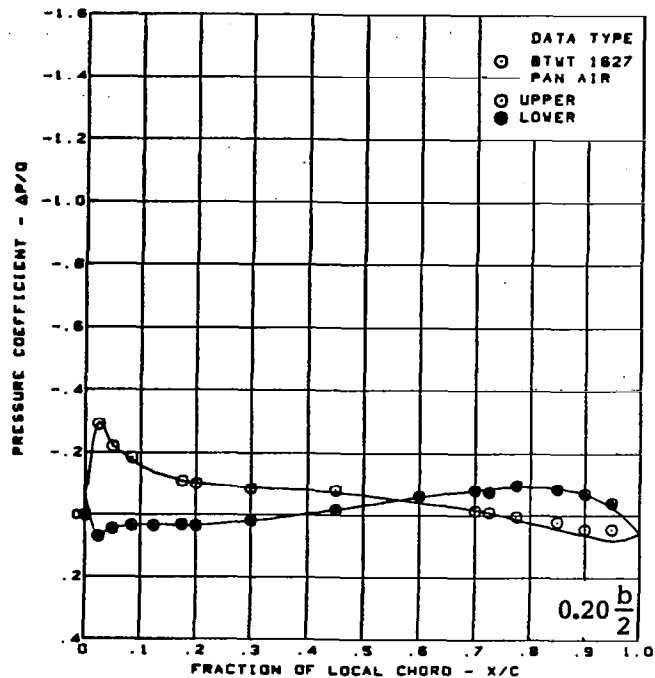
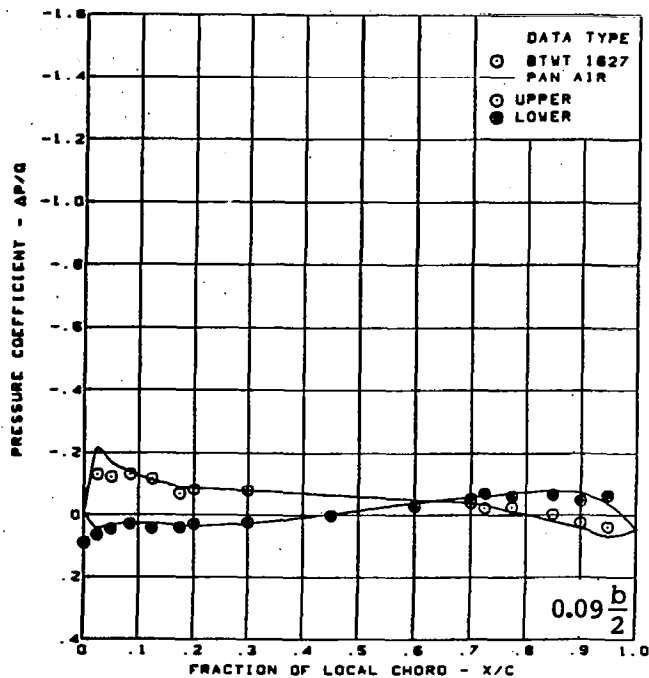
Figure 47. — Wing Theory-to-Experiment Comparison; Cambered-Twisted Wing; Fin On; T.E. Deflection, Full Span =  $0.0^\circ$ ;  $M = 0.85$



$M = 0.85$  (run 48)  
 $\alpha = 0^\circ$   
 Cambered-twisted wing, rounded L.E.  
 Fin on  
 L.E. deflection, full span =  $0.0^\circ$   
 T.E. deflection, full span =  $0.0^\circ$

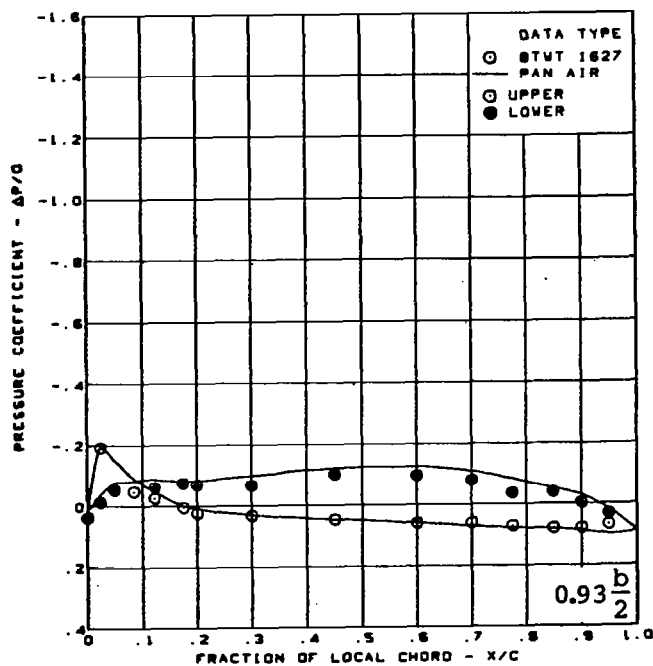
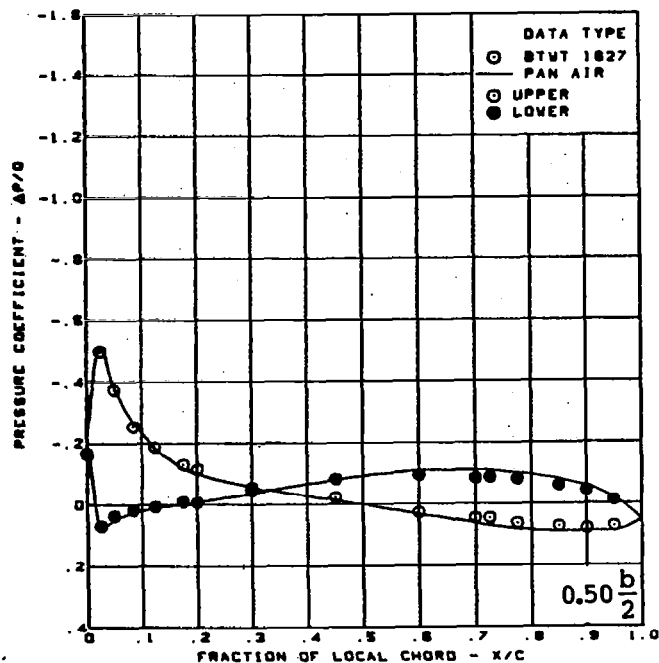
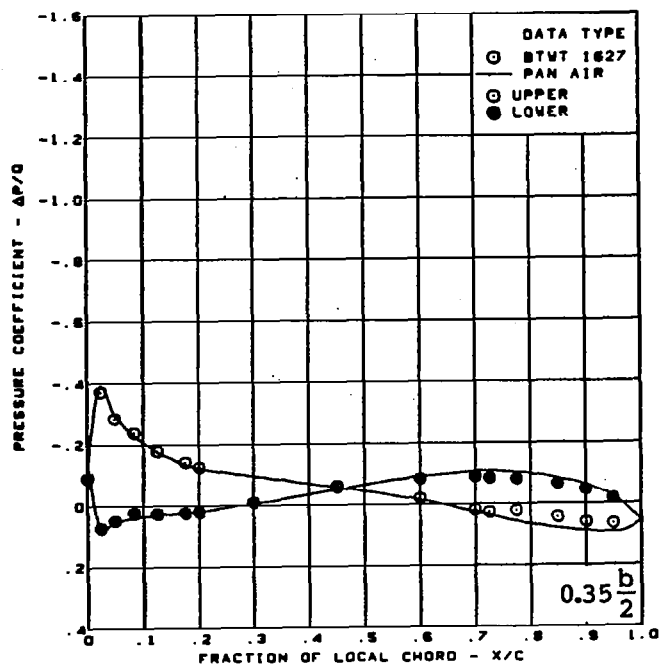
(a) (Concluded)

Figure 47. - (Continued)



(b) Surface Chordwise Pressure Distributions -  $\alpha = 4^\circ$

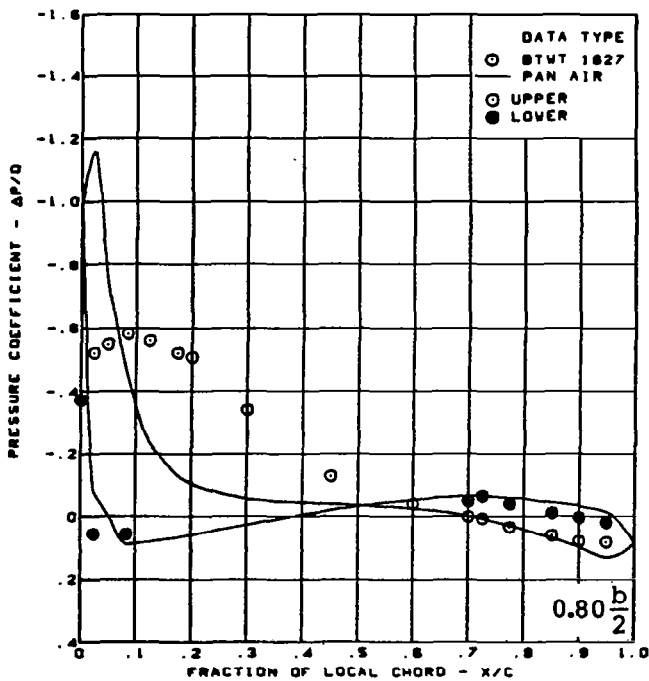
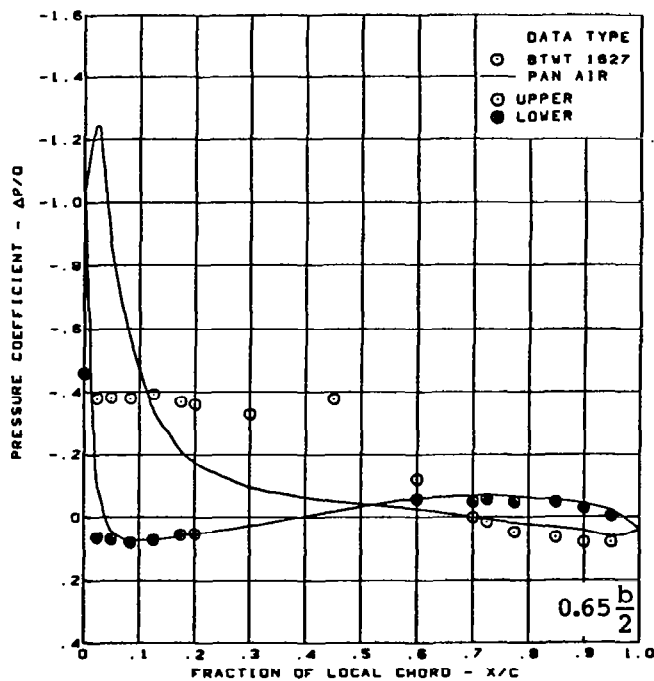
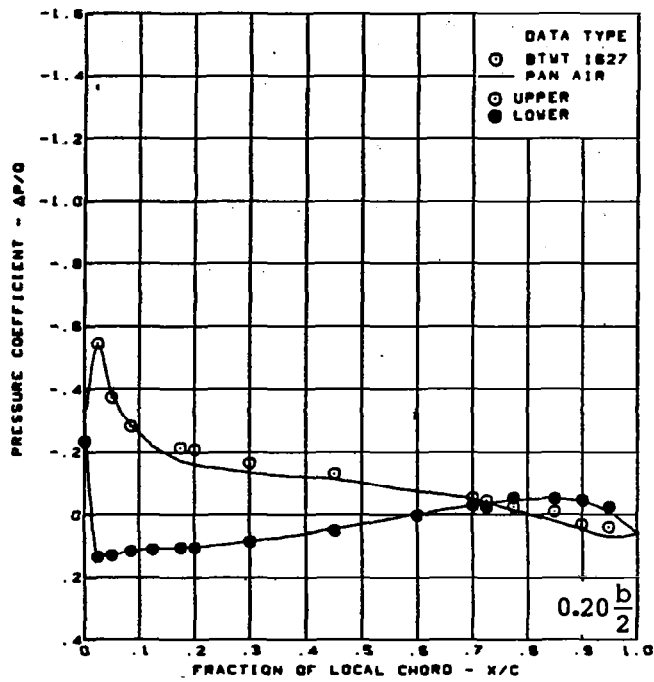
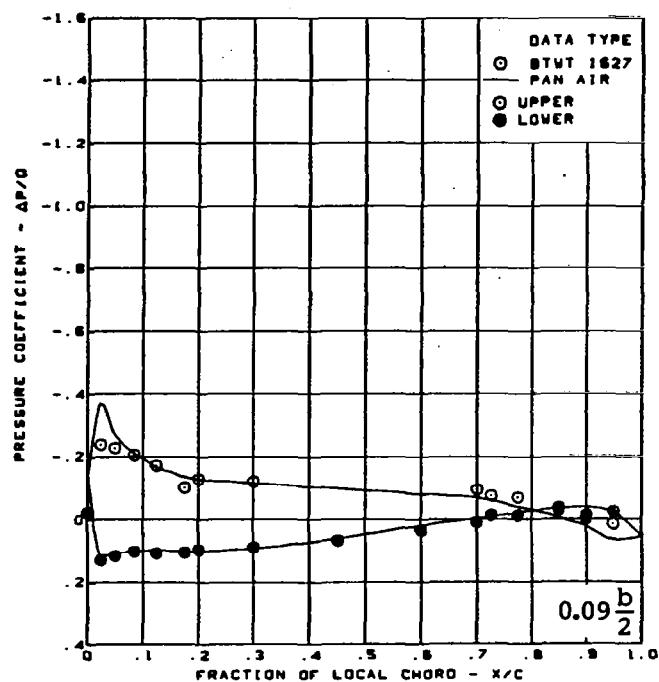
Figure 47. - (Continued)



$M = 0.85$  (run 48)  
 $\alpha = 4^\circ$   
 Cambered-twisted wing, rounded L.E.  
 Fin on  
 L.E. deflection, full span =  $0.0^\circ$   
 T.E. deflection, full span =  $0.0^\circ$

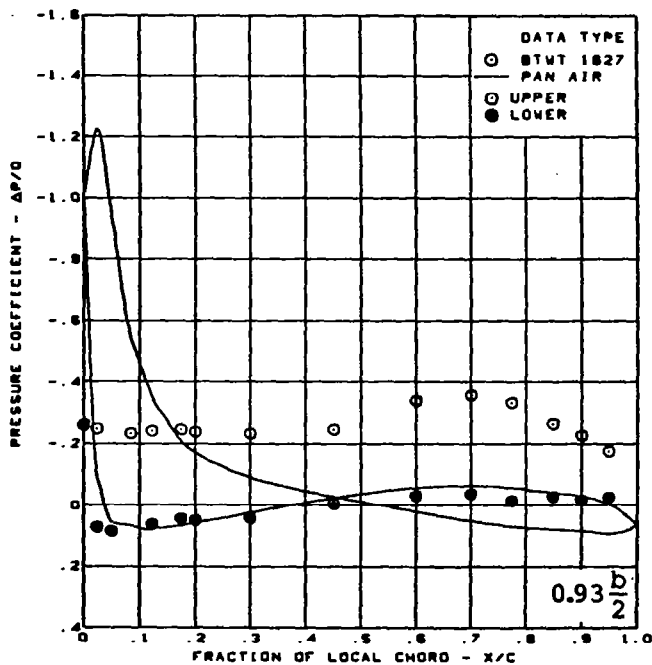
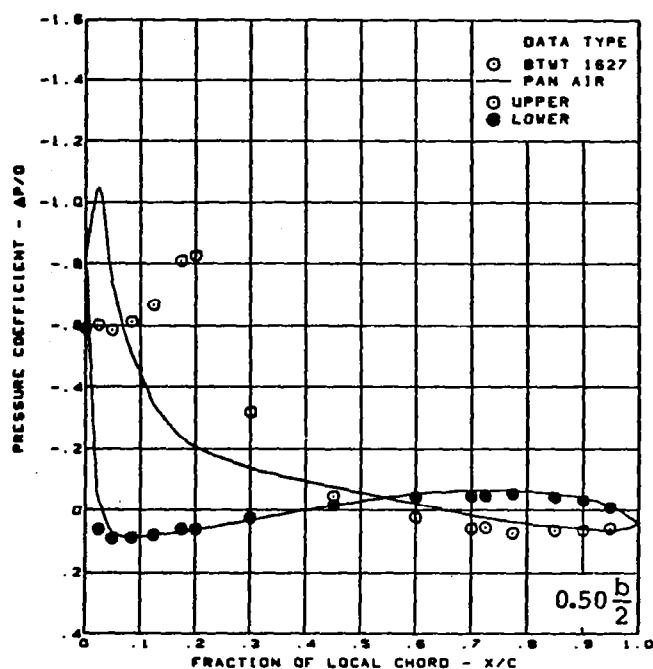
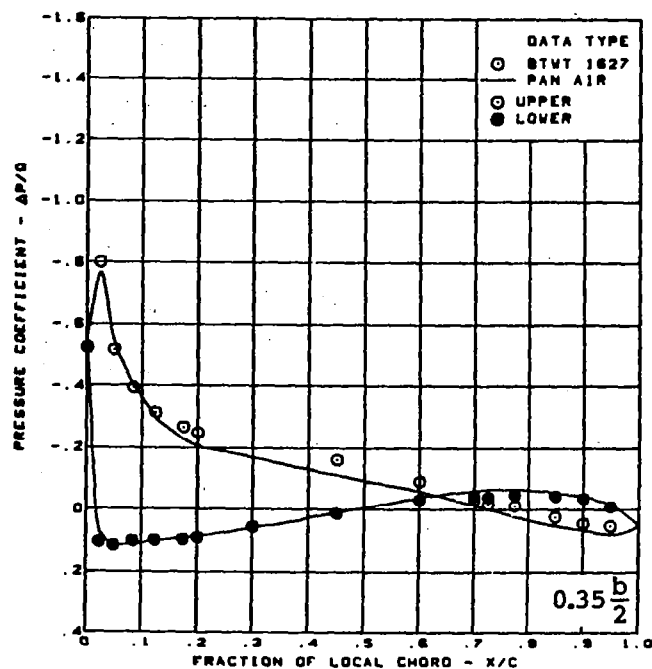
(b) (Concluded)

Figure 47. - (Continued)



(c) Surface Chordwise Pressure Distributions -  $\alpha = 8^\circ$

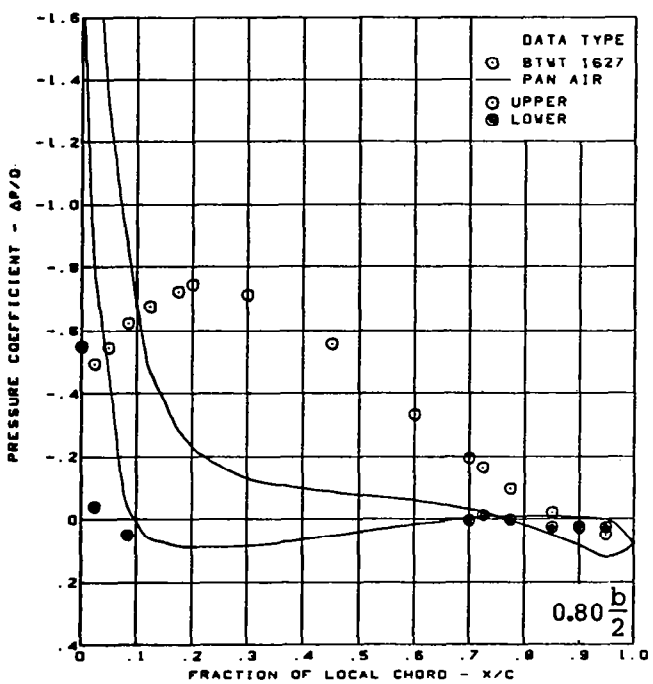
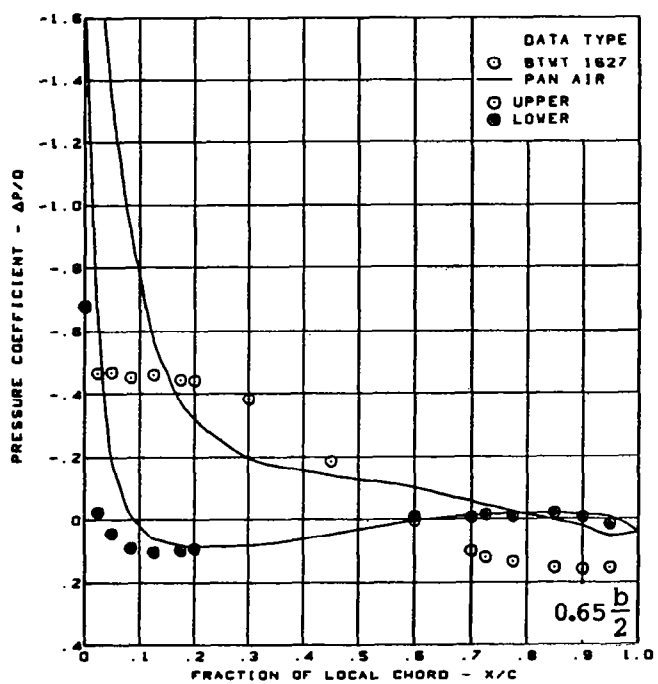
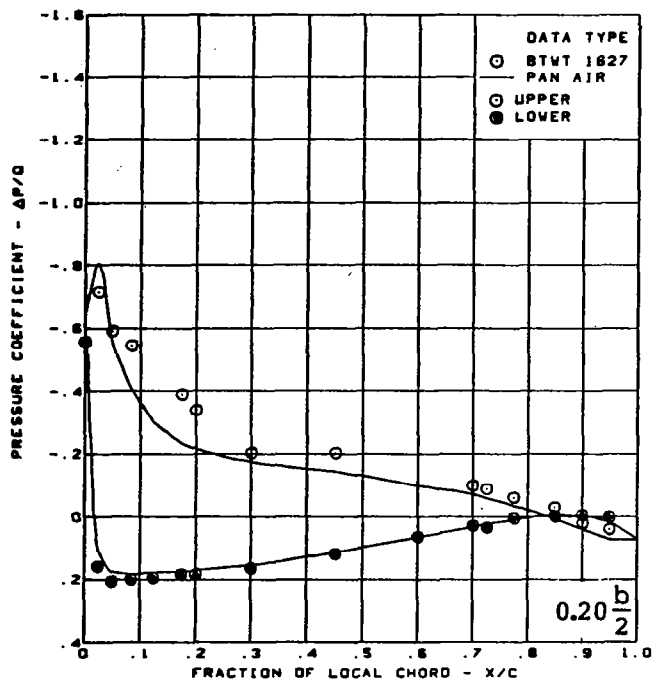
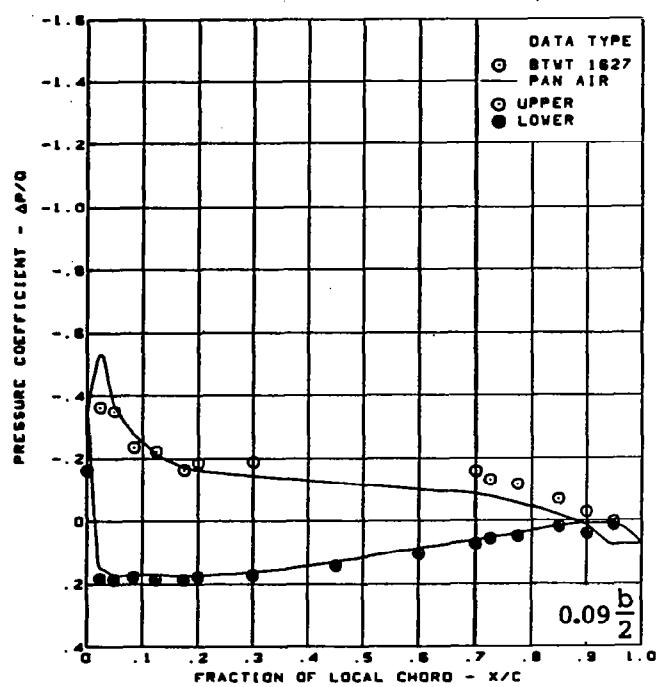
Figure 47. - (Continued)



$M = 0.85$  (run 48)  
 $\alpha = 8^\circ$   
 Cambered-twisted wing, rounded L.E.  
 Fin on  
 L.E. deflection, full span =  $0.0^\circ$   
 T.E. deflection, full span =  $0.0^\circ$

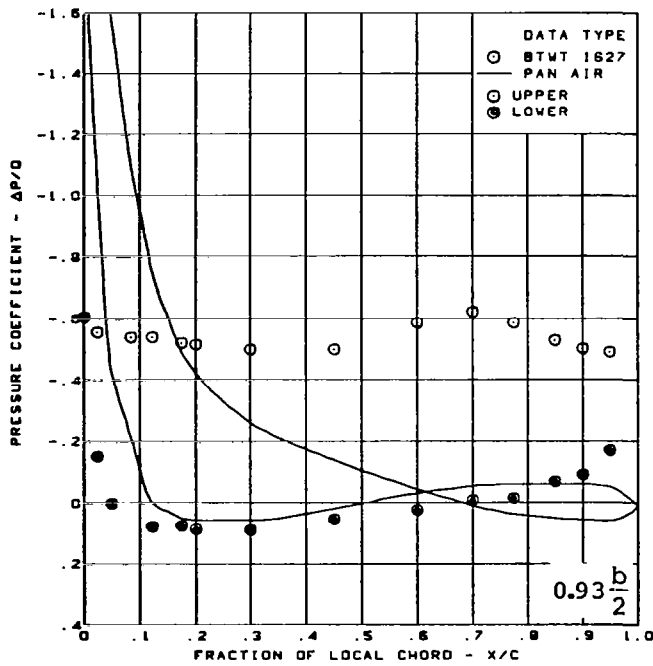
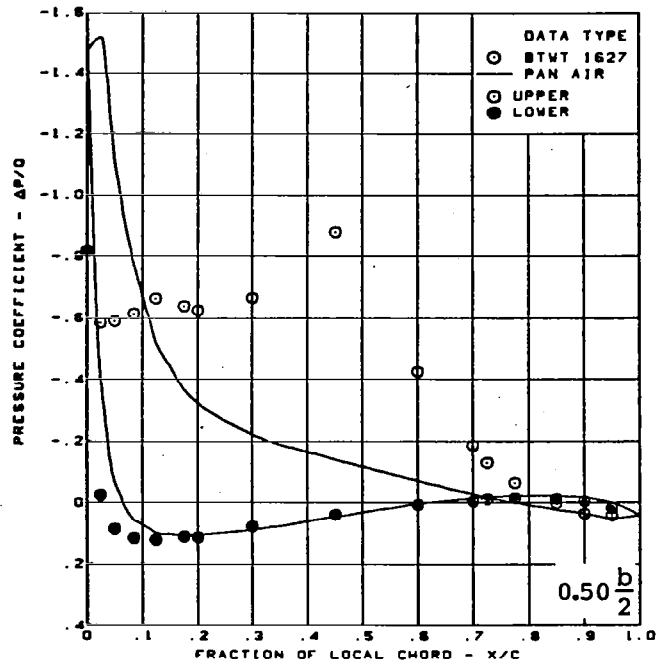
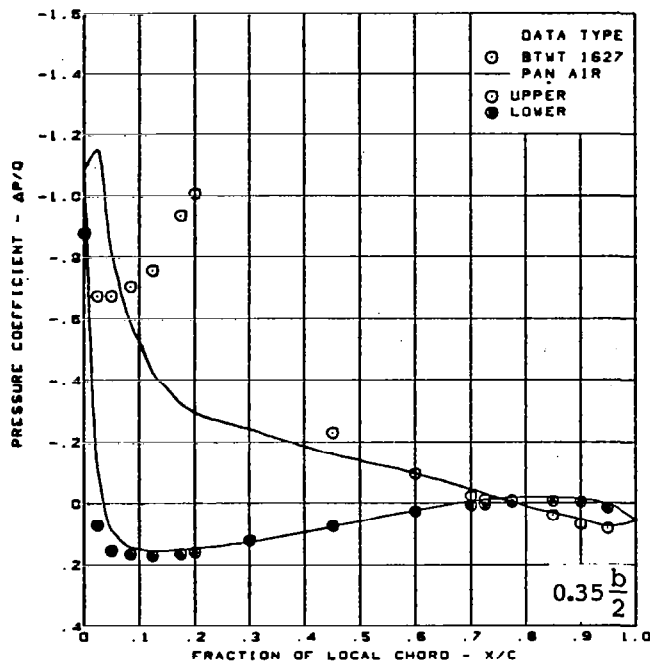
(c) (Concluded)

Figure 47. -- (Continued)



(d) Surface Chordwise Pressure Distributions -  $\alpha = 12^\circ$

Figure 47. - (Continued)

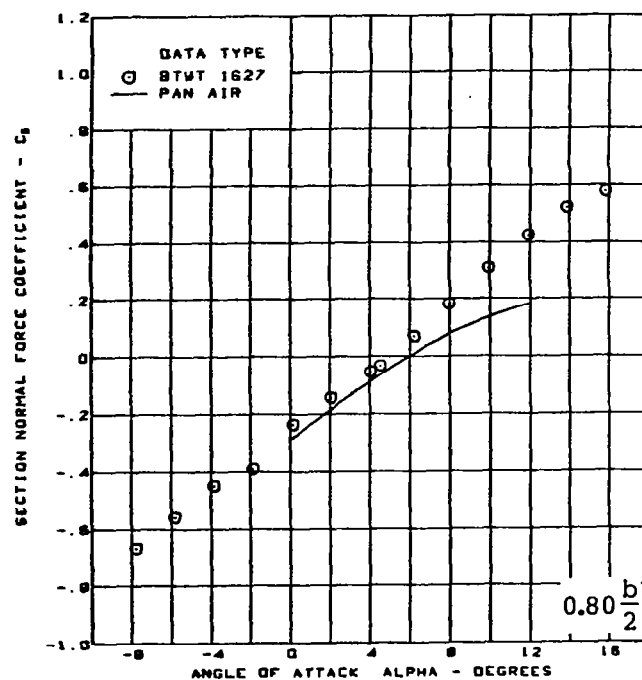
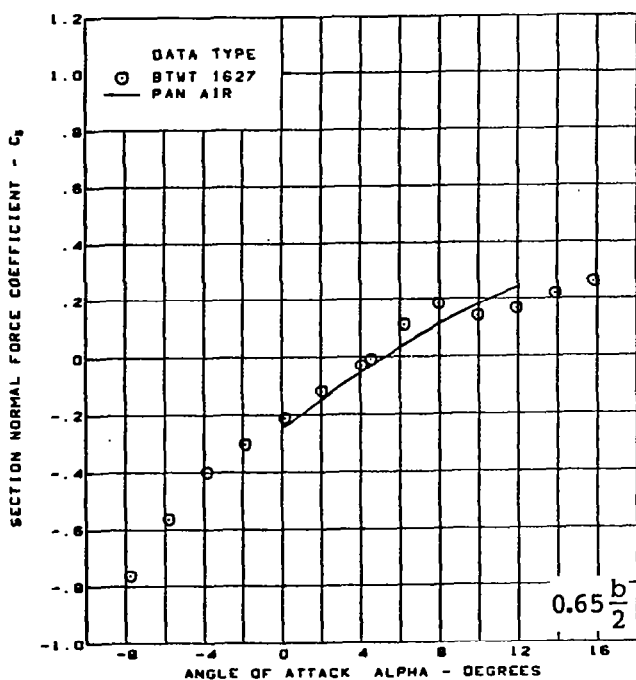
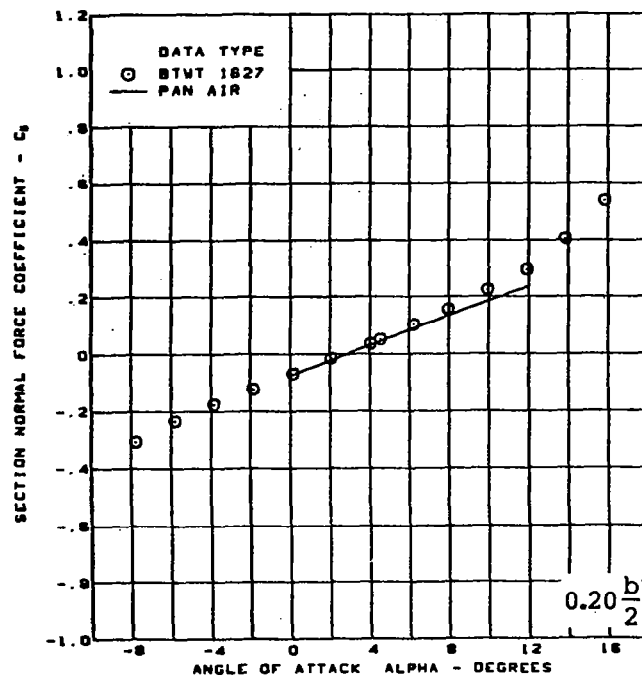
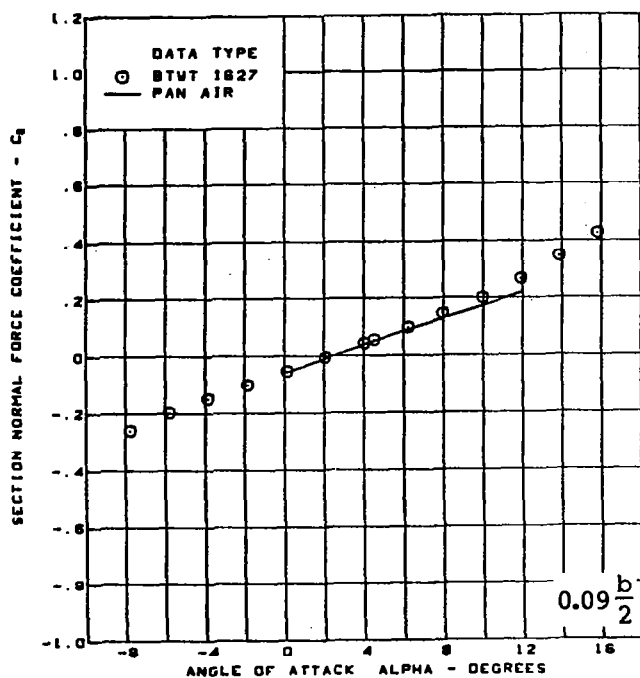


$M = 0.85$  (run 48)  
 $\alpha = 12^\circ$   
 Cambered-twisted wing, rounded L.E.  
 Fin on  
 L.E. deflection, full span =  $0.0^\circ$   
 T.E. deflection, full span =  $0.0^\circ$

(d) (Concluded)

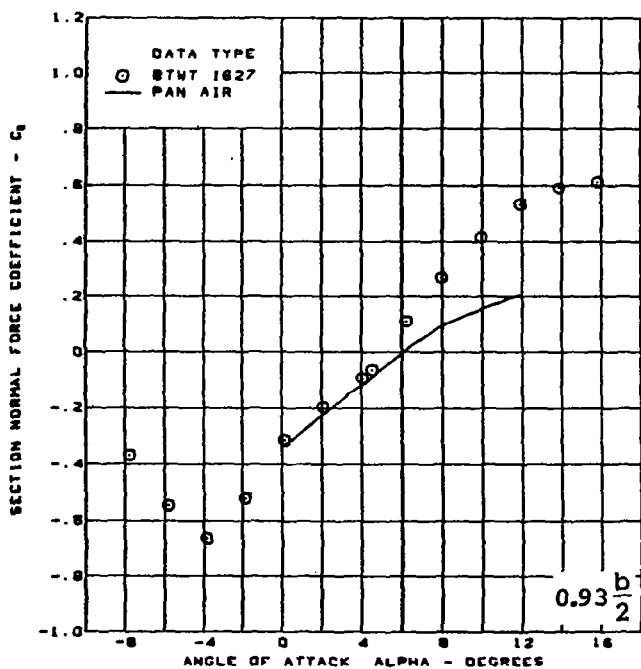
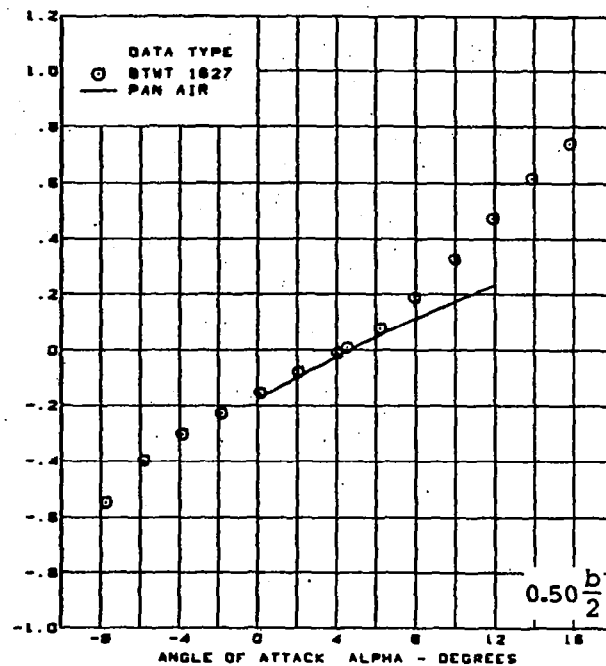
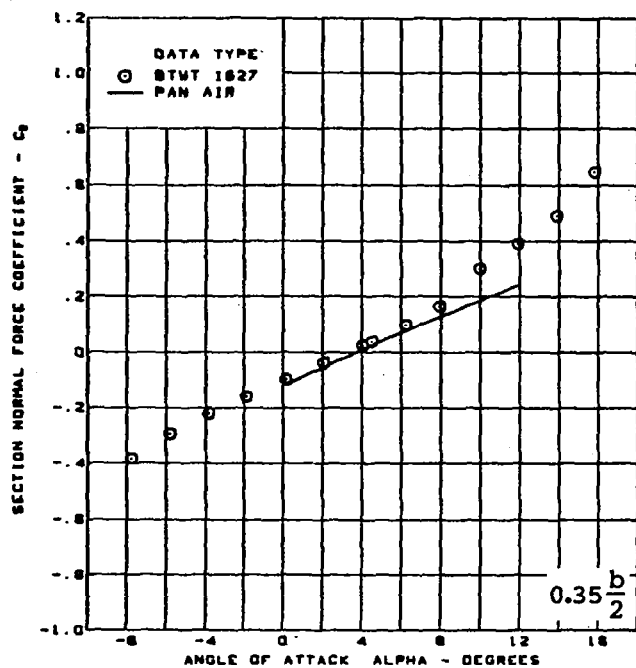
Figure 47. — (Continued)





(e) Section Aerodynamic Coefficients - Normal Force

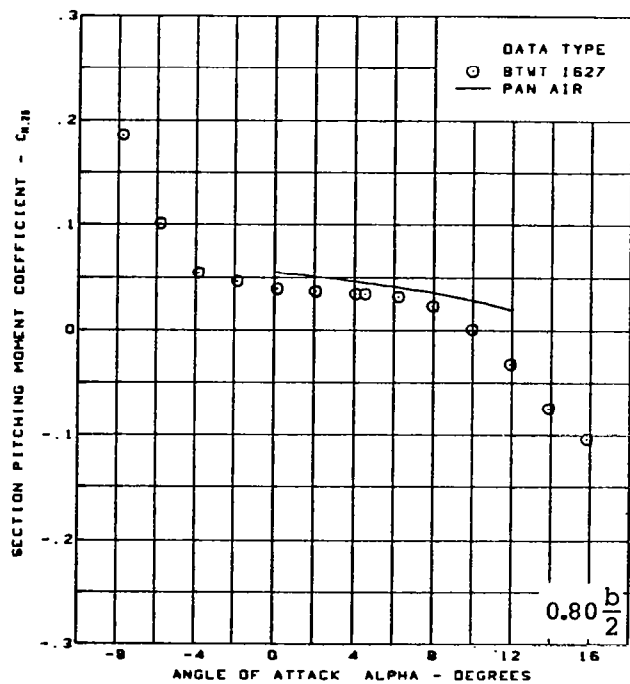
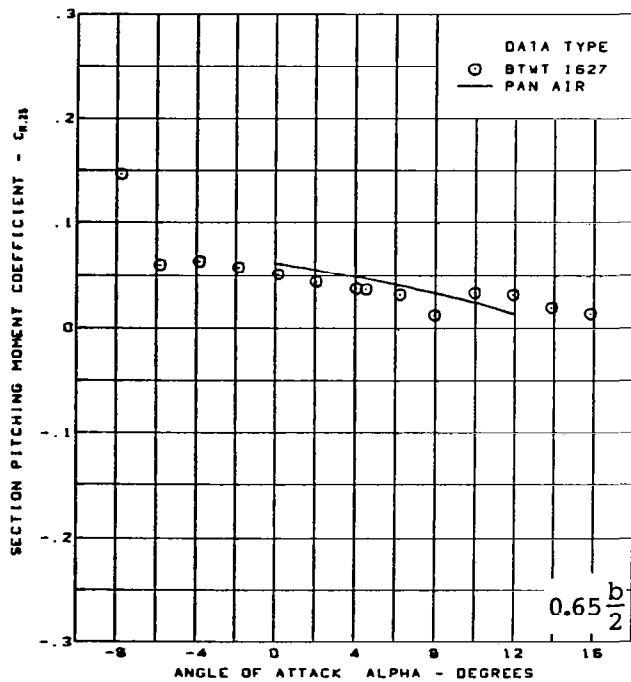
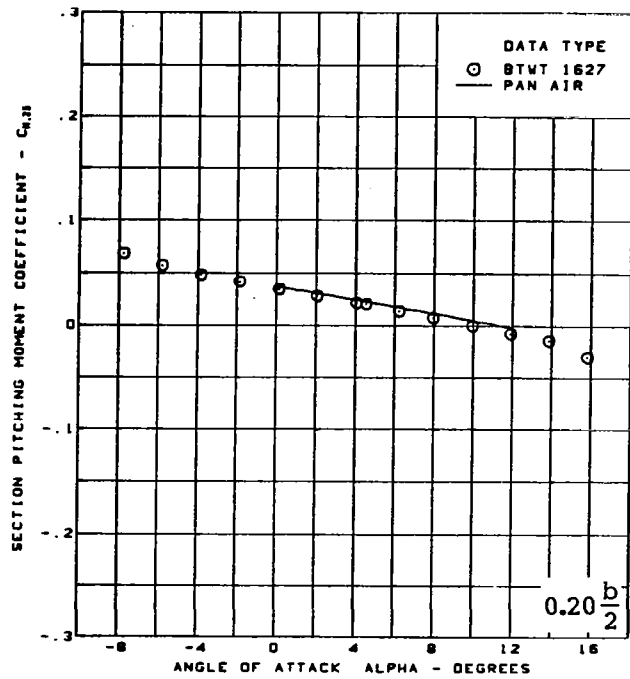
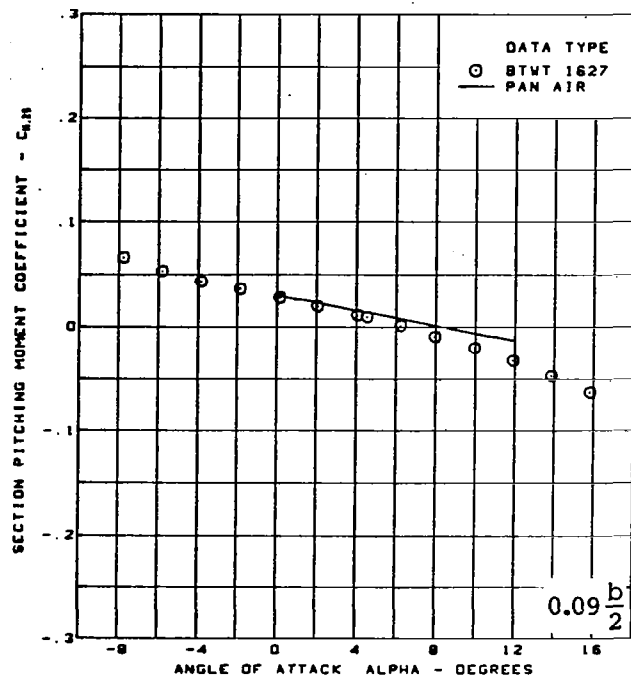
Figure 47. - (Continued)



M = 0.85 (run 48)  
 Cambered-twisted wing, rounded L.E.  
 Fin on  
 L.E. deflection, full span =  $0.0^\circ$   
 T.E. deflection, full span =  $0.0^\circ$

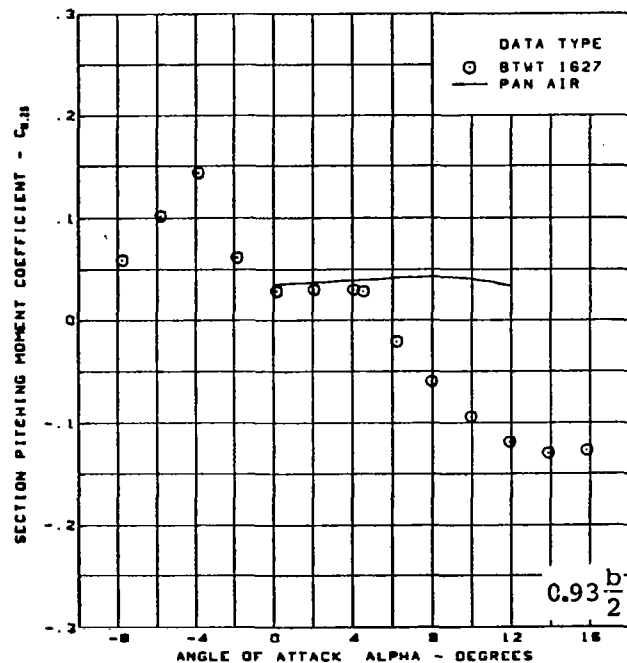
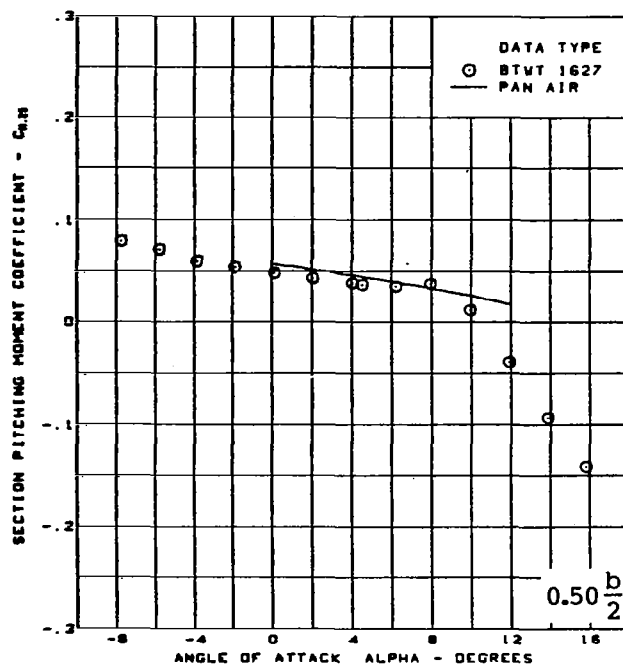
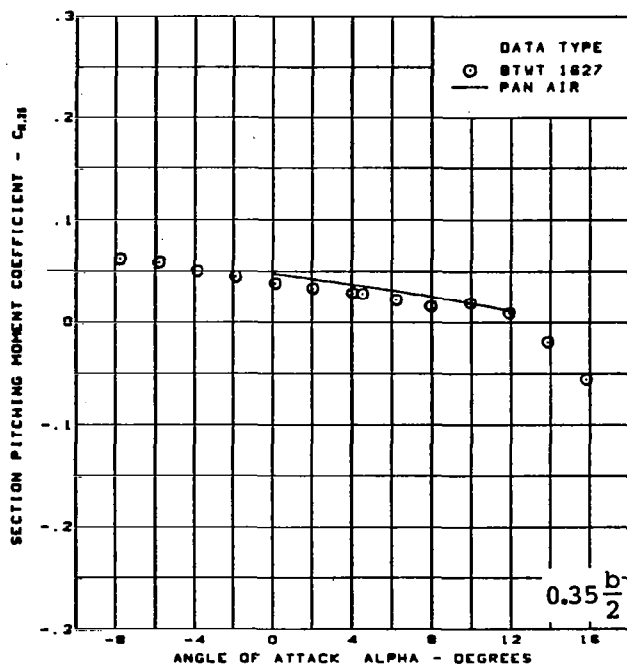
(e) (Concluded)

Figure 47. — (Continued)



(f) Section Aerodynamic Coefficients - Pitching Moment

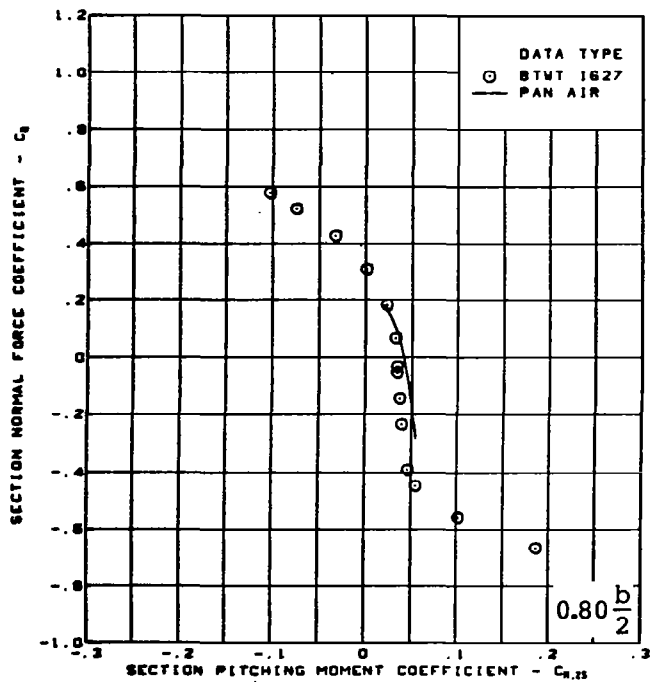
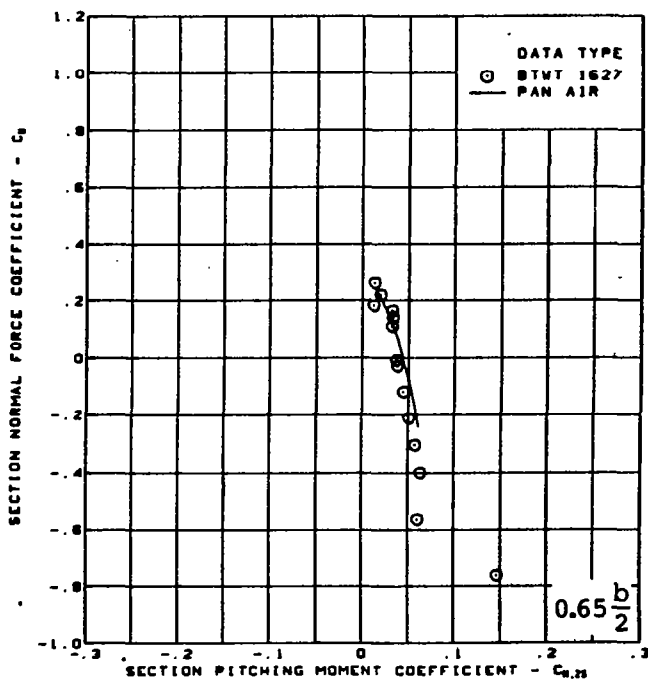
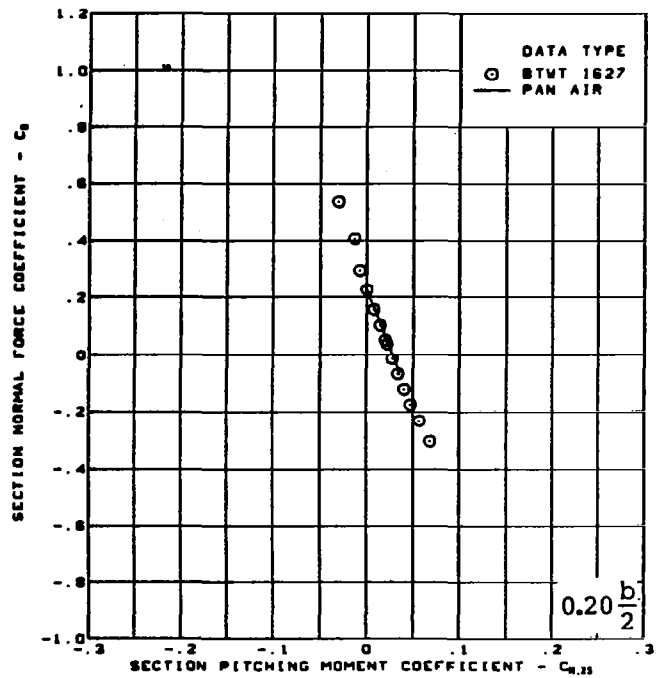
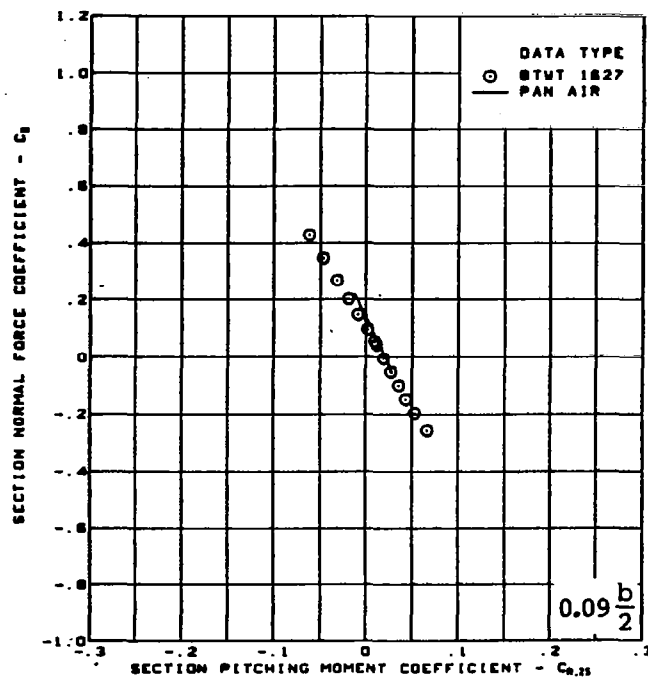
Figure 47. - (Continued)



$M = 0.85$  (run 48)  
 Cambered-twisted wing, rounded L.E.  
 Fin on  
 L.E. deflection, full span =  $0.0^\circ$   
 T.E. deflection, full span =  $0.0^\circ$

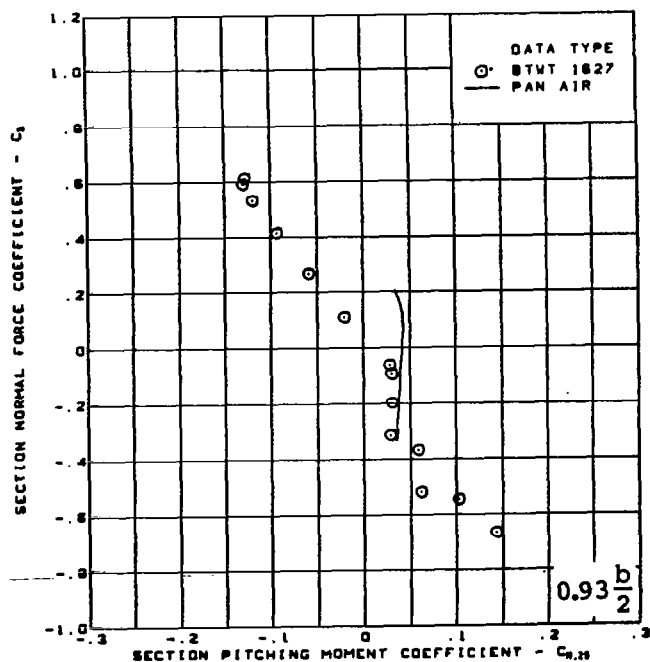
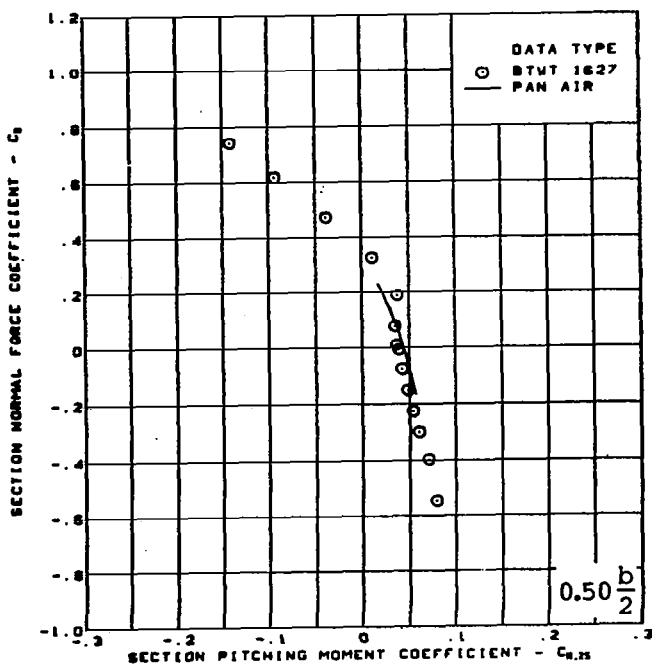
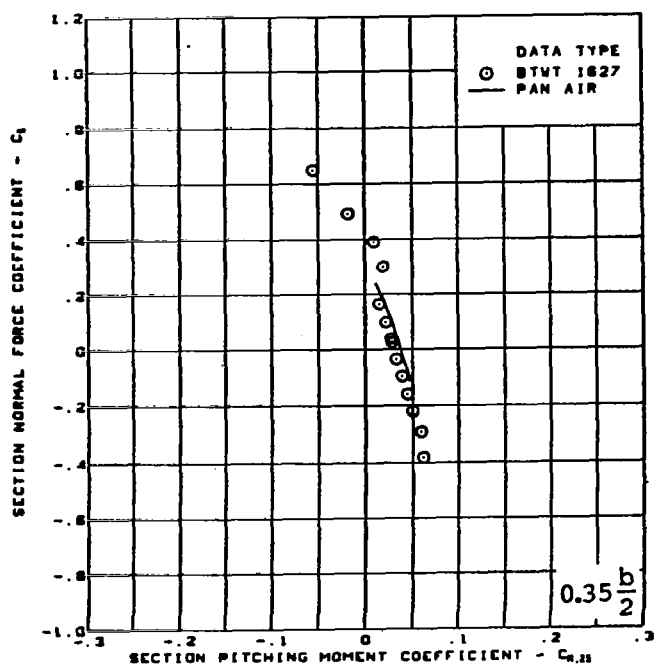
(f) (Concluded)

Figure 47. — (Continued)



(g) Section Aerodynamic Coefficients - Normal Force vs Pitching Moment

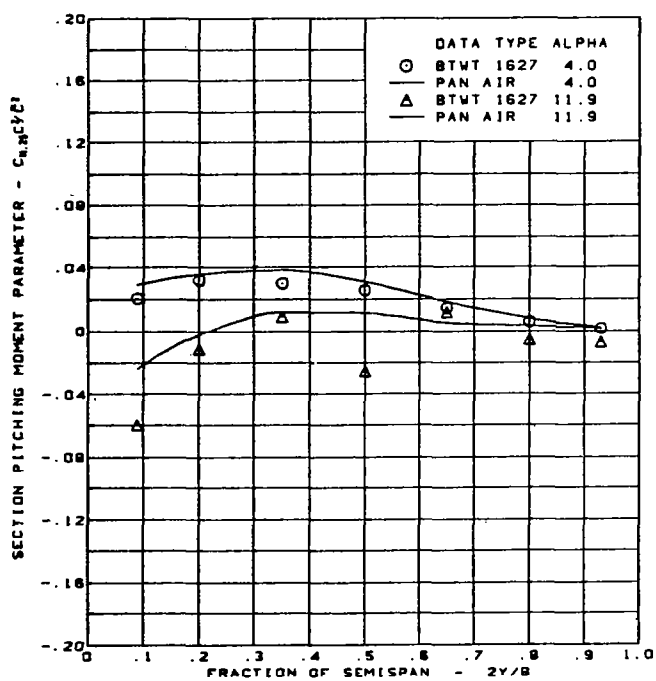
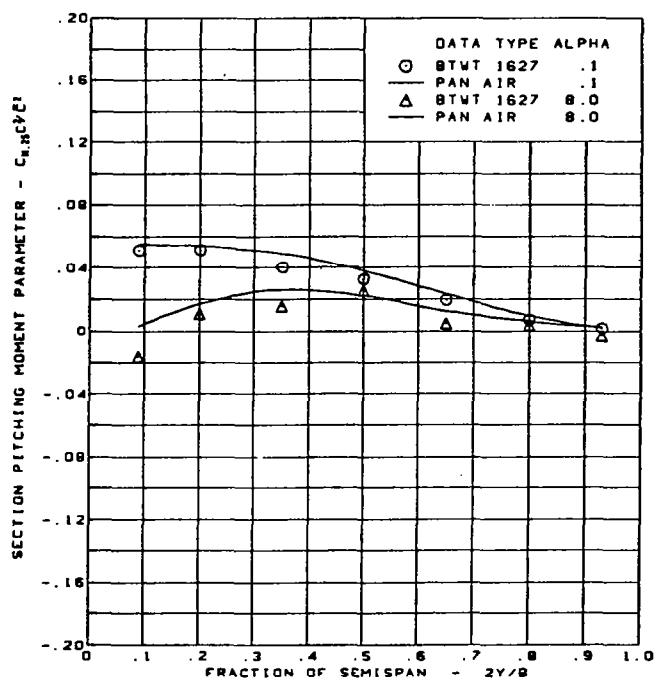
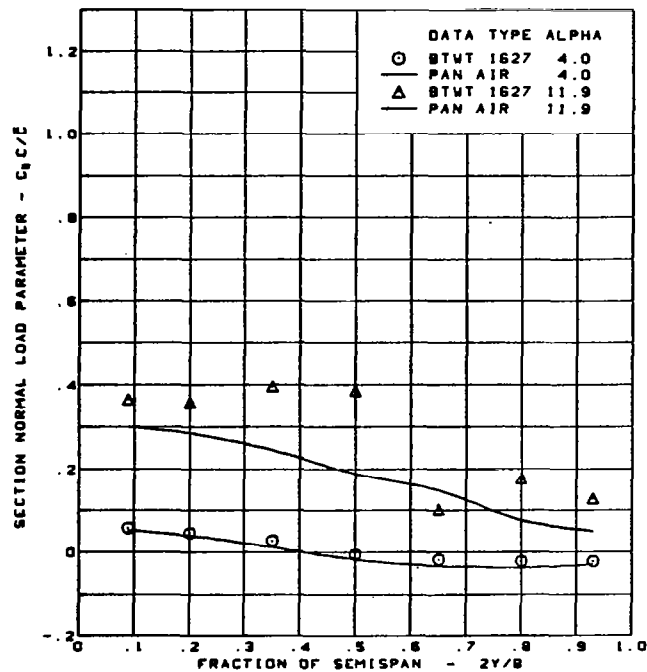
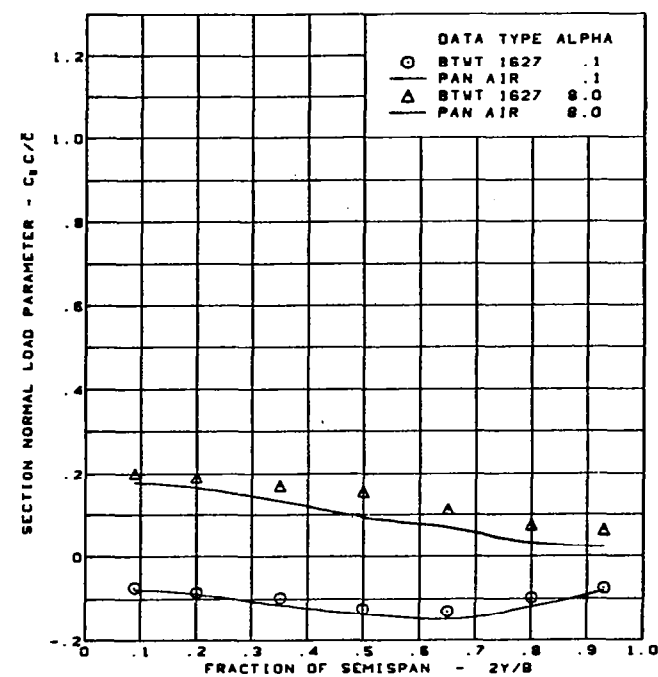
Figure 47. — (Continued)



$M = 0.85$  (run 48)  
 Cambered-twisted wing, rounded L.E.  
 Fin on  
 L.E. deflection, full span =  $0.0^\circ$   
 T.E. deflection, full span =  $0.0^\circ$

(g) (Concluded)

Figure 47. — (Continued)

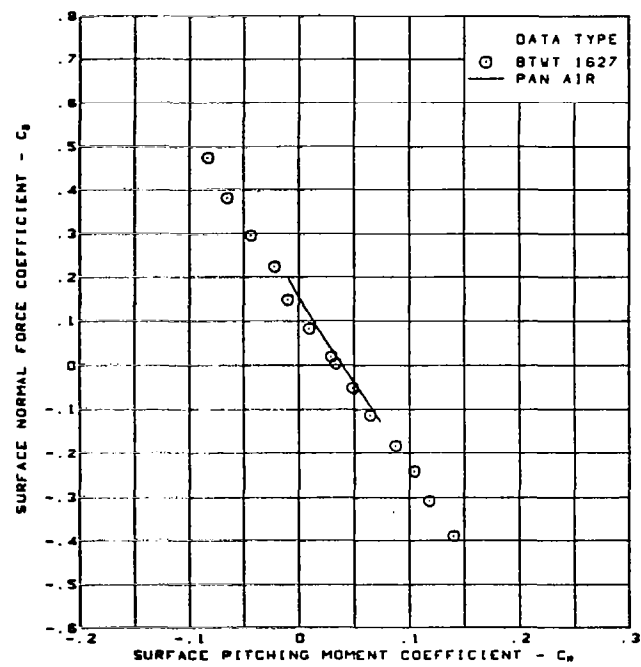
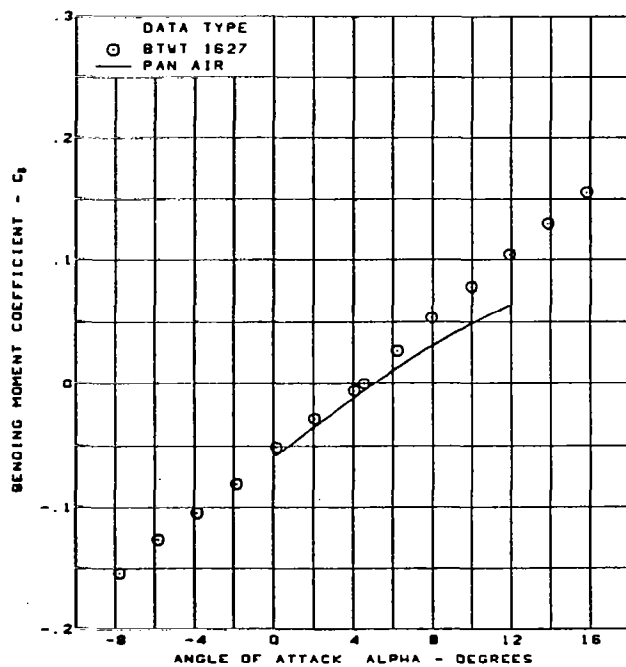
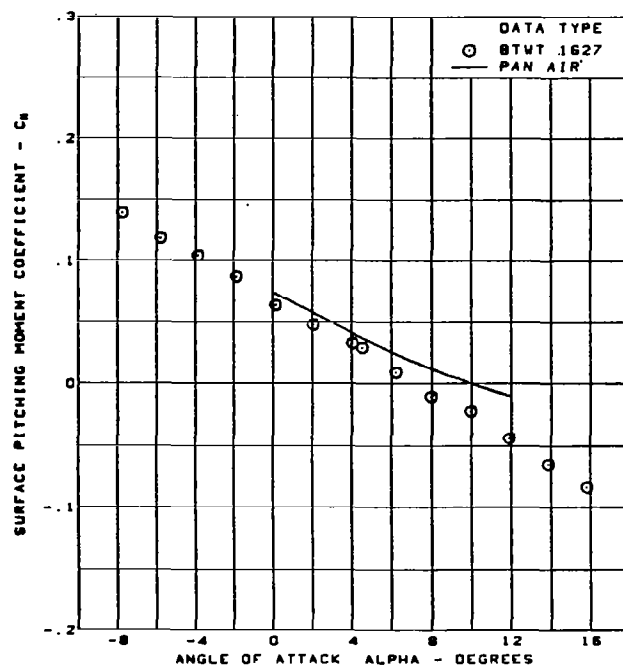
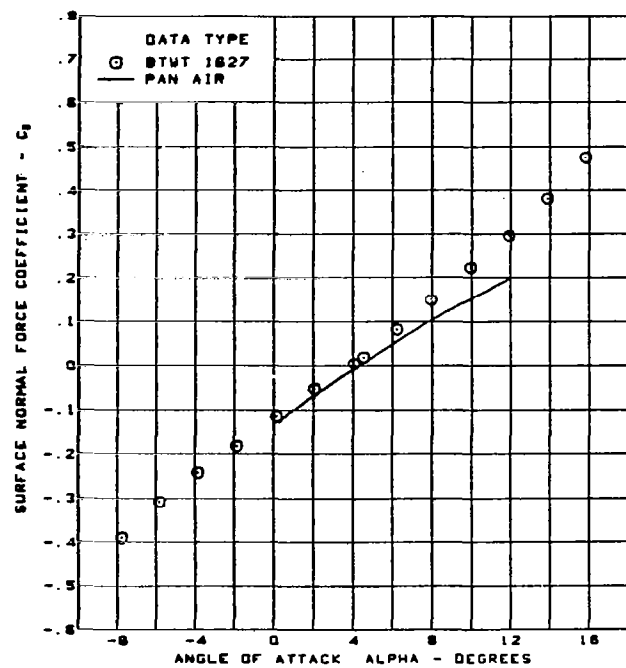


M = 0.85 (run 48)  
Cambered-twisted wing, rounded L.E.  
Fin on

L.E. deflection, full span =  $0.0^\circ$   
T.E. deflection, full span =  $0.0^\circ$

(h) Spanload Distributions

Figure 47. — (Continued)



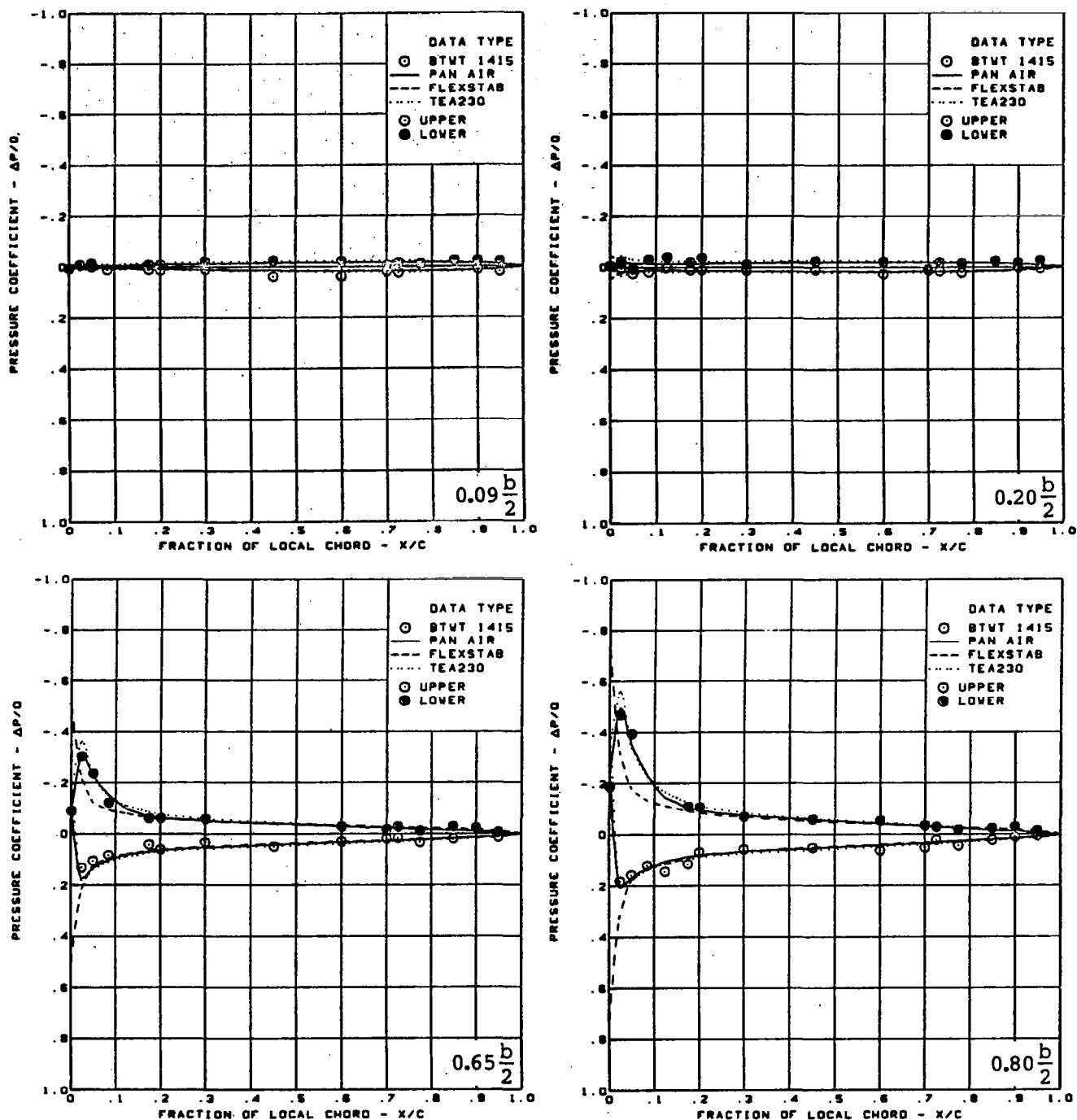
$M = 0.85$  (run 48)  
Cambered-twisted wing, rounded L.E.  
Fin on

L.E. deflection, full span  $\approx 0.0^\circ$   
T.E. deflection, full span  $\approx 0.0^\circ$

(i) Wing Aerodynamic Coefficients

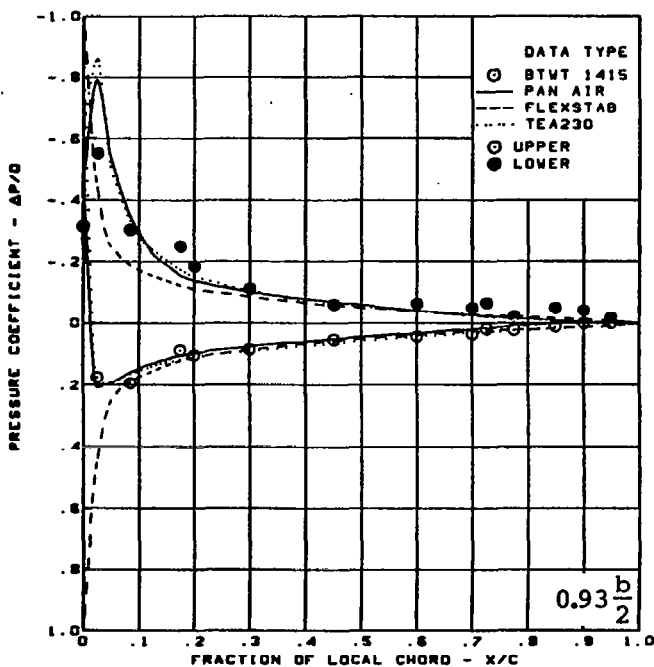
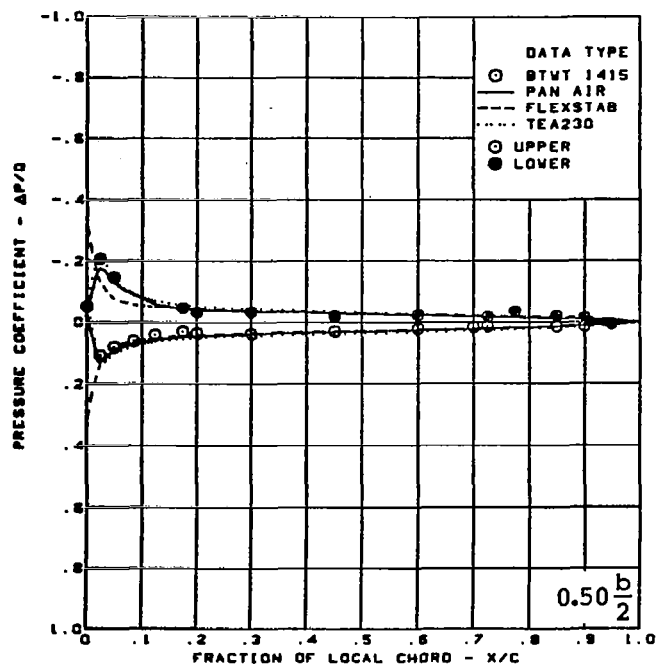
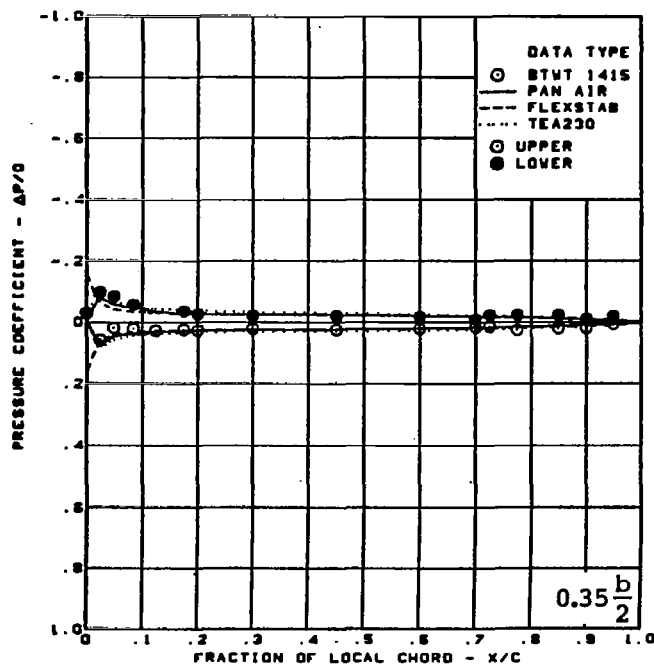
Figure 47. — (Concluded)





(a) Surface Chordwise Pressure Distributions,  $\alpha = 0^\circ$

Figure 48. — Wing Theory-to-Experiment Comparison—Effect of Incremental Twist;  
T.E. Deflection, Full Span =  $0.0^\circ$ ;  $M = 0.40$



$M = 0.40$

$\alpha = 0^\circ$

Twisted wing data minus flat wing data

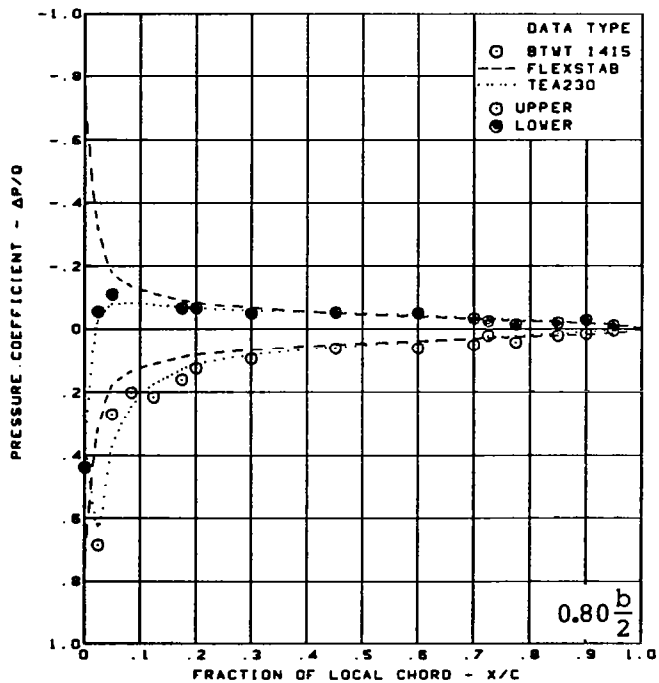
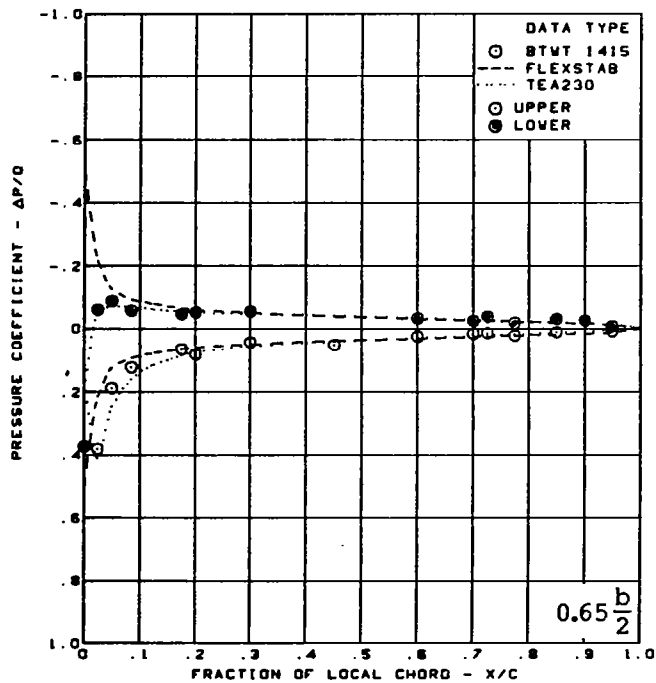
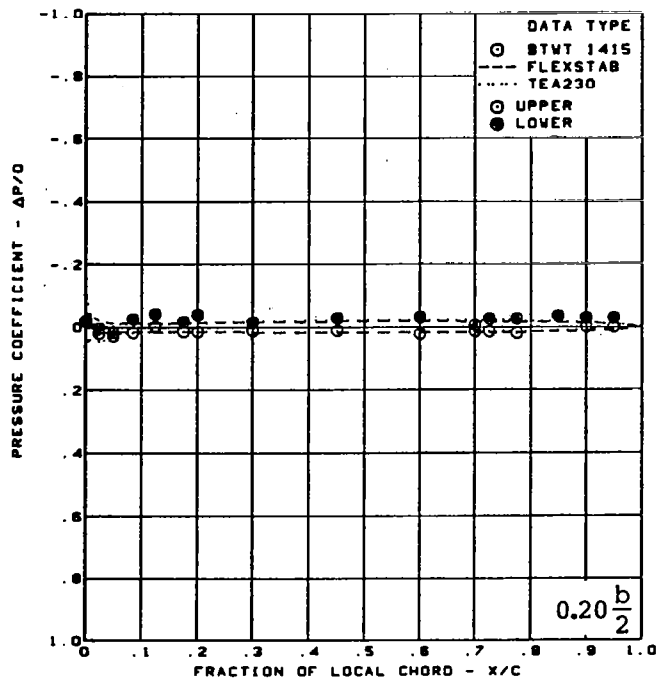
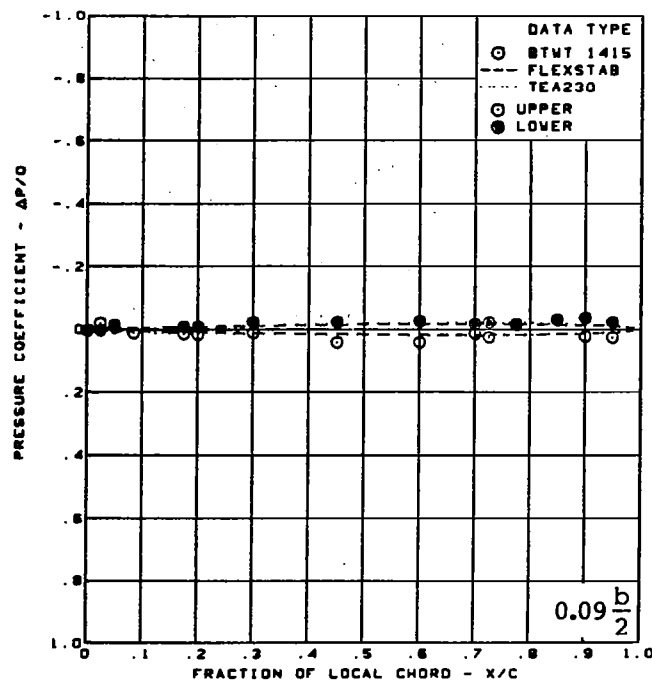
Rounded L.E.

L.E. deflection, full span =  $0.0^\circ$

T.E. deflection, full span =  $0.0^\circ$

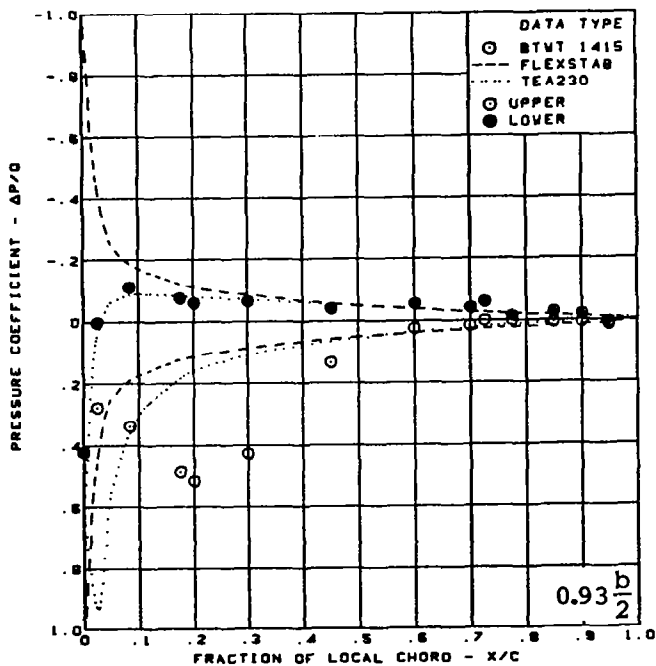
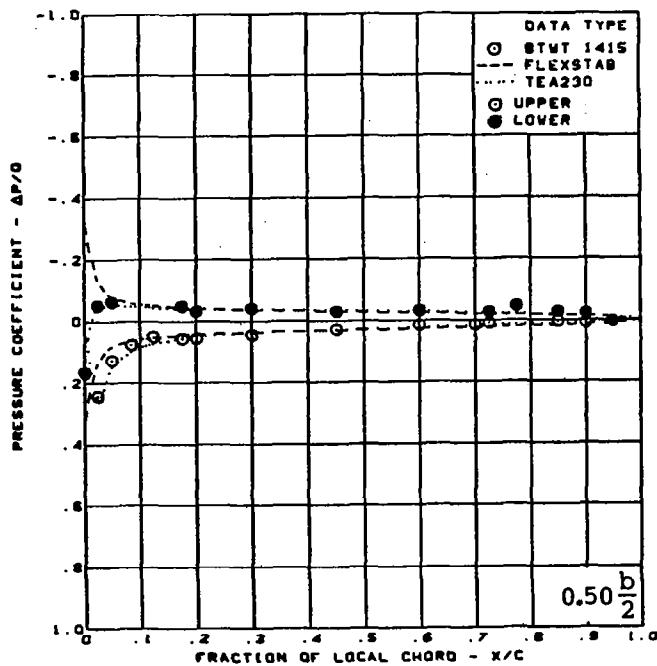
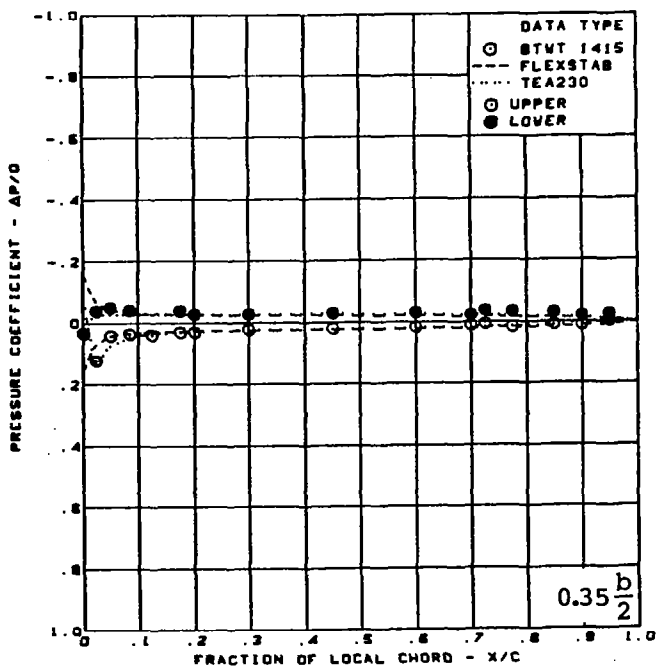
(a) (Concluded)

Figure 48. - (Continued)



(b) Surface Chordwise Pressure Distributions,  $\alpha = 4^\circ$

Figure 48. — (Continued)



$M = 0.40$

$\alpha = 4^\circ$

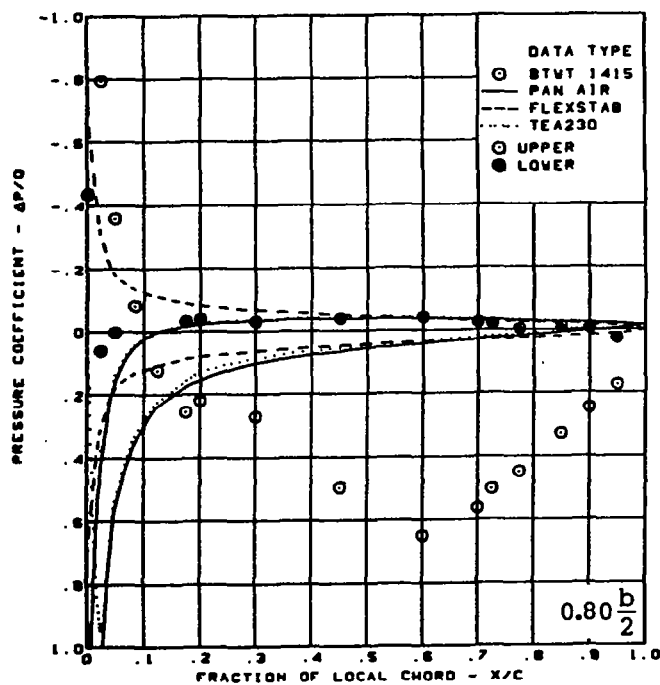
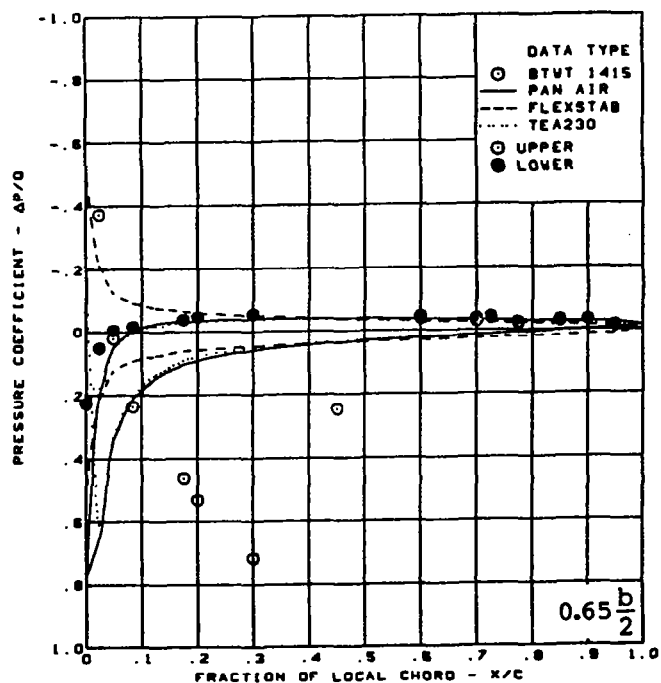
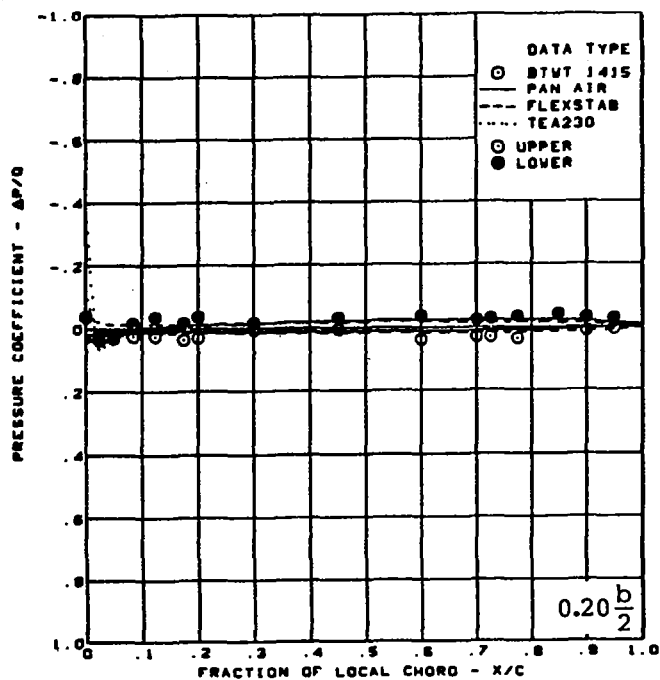
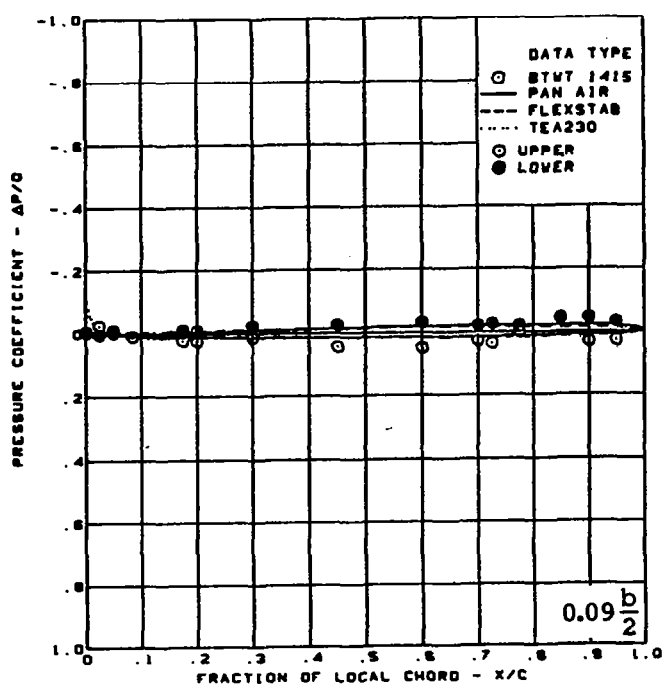
Twisted wing data minus flat wing data  
Rounded L.E.

L.E. deflection, full span =  $0.0^\circ$

T.E. deflection, full span =  $0.0^\circ$

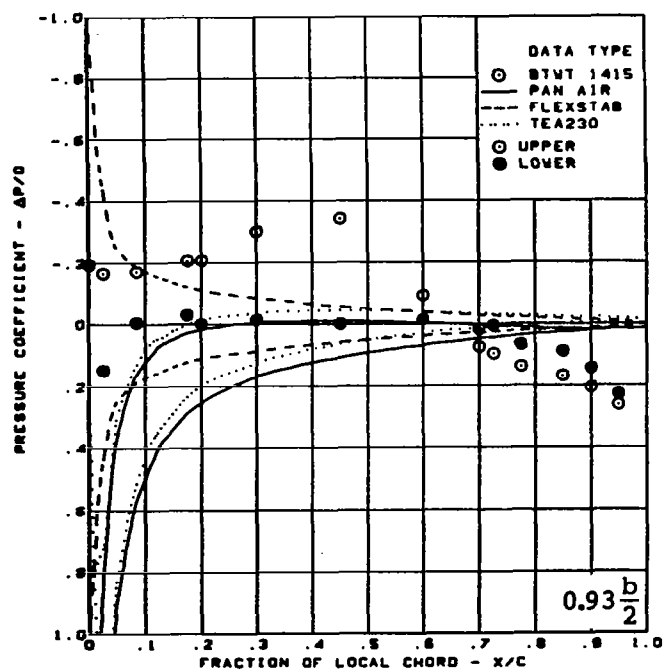
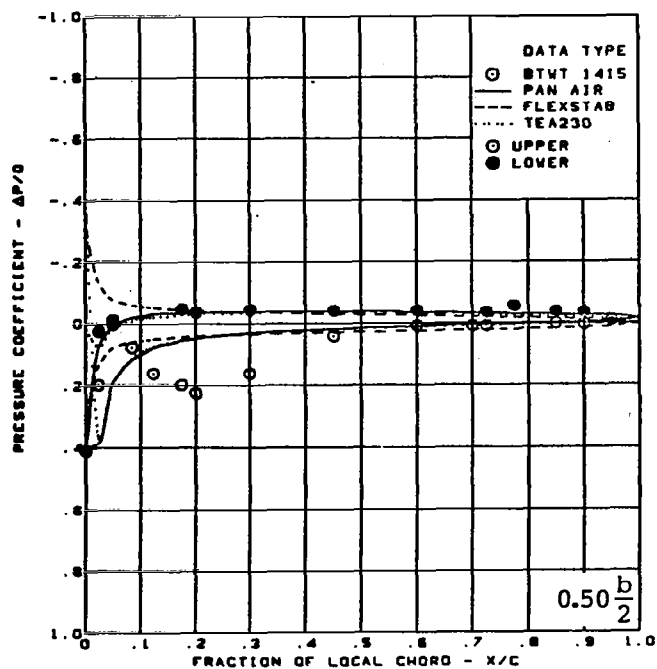
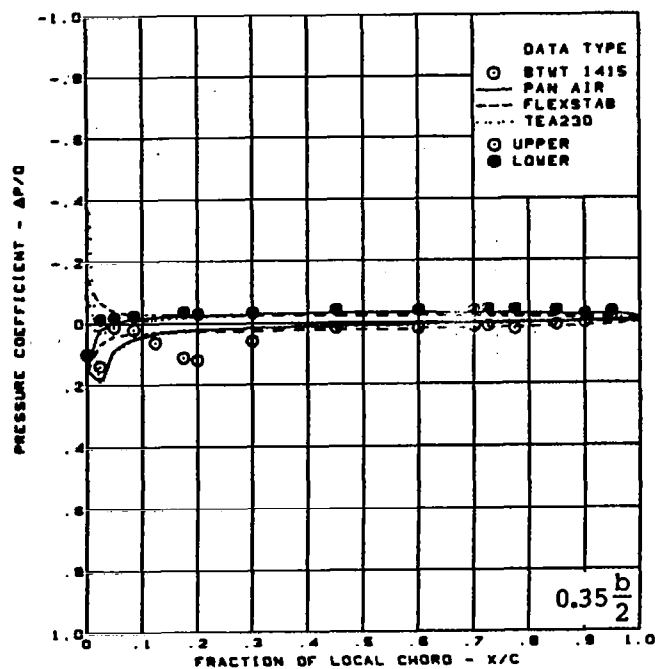
(b) (Concluded)

Figure 48. - (Continued)



(c) Surface Chordwise Pressure Distributions,  $\alpha = 8^\circ$

Figure 48. — (Continued)



$M = 0.40$

$\alpha = 8^\circ$

Twisted wing data minus flat wing data

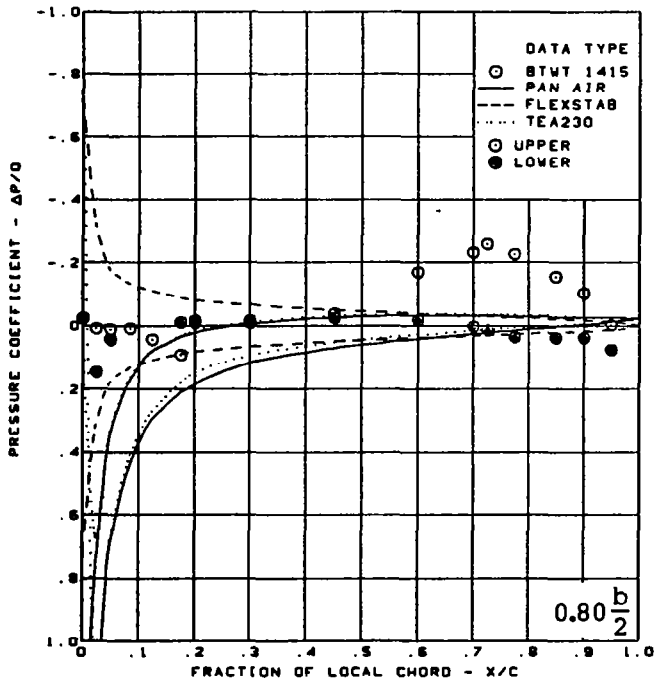
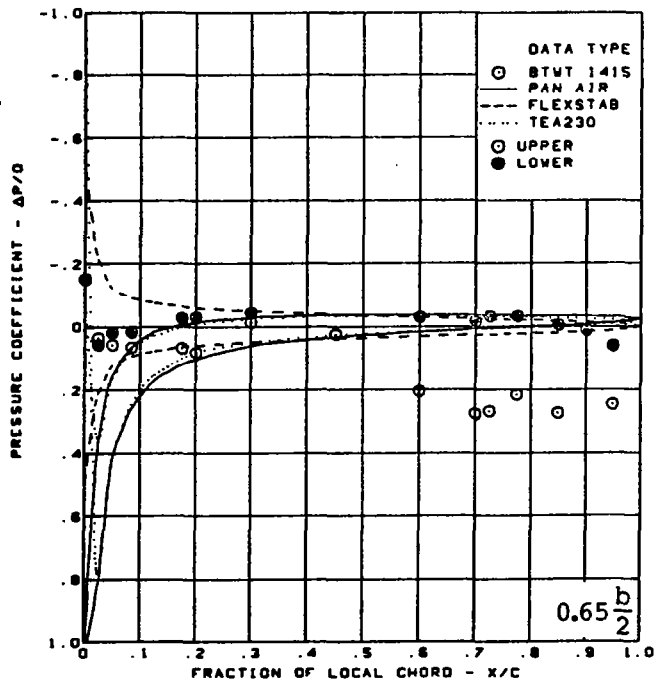
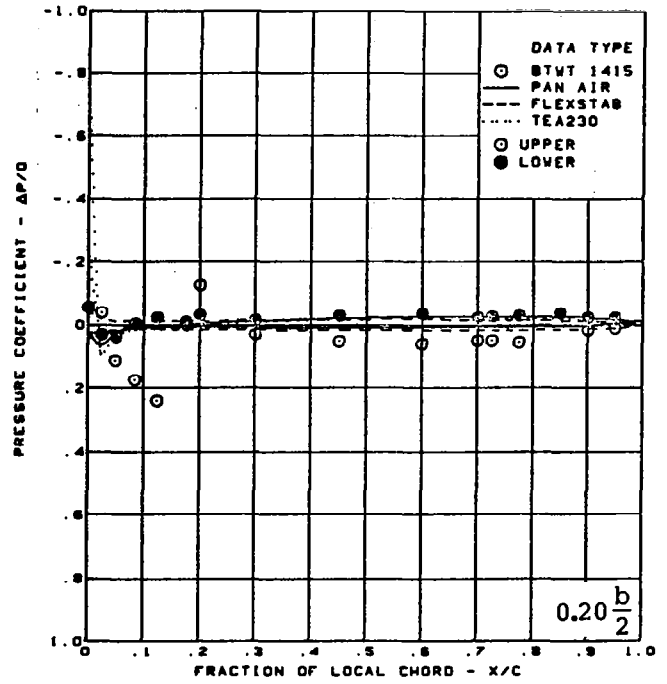
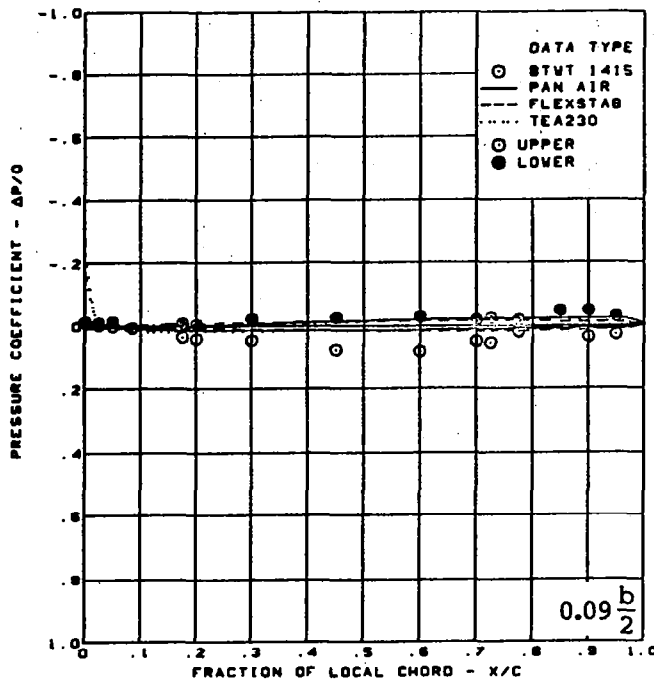
Rounded L.E.

L.E. deflection, full span =  $0.0^\circ$

T.E. deflection, full span =  $0.0^\circ$

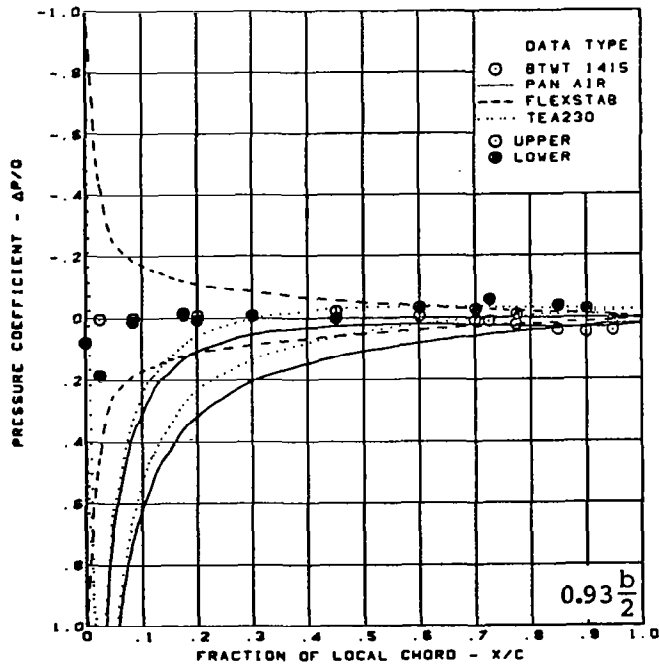
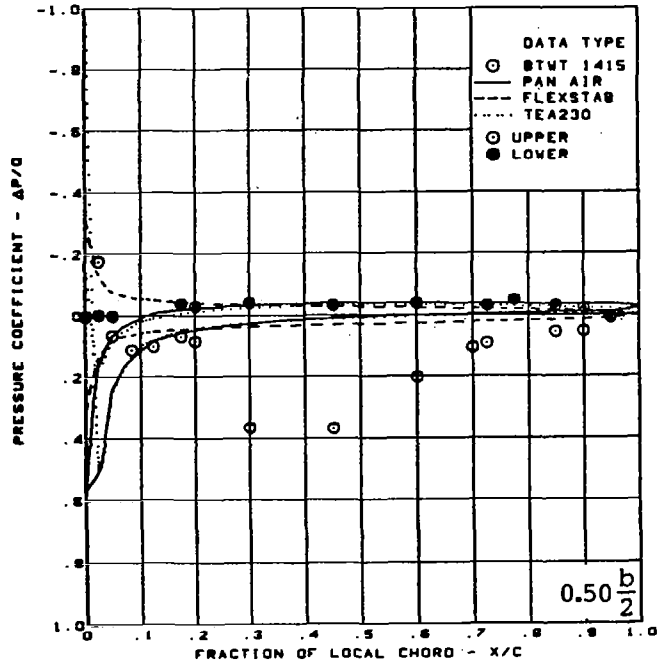
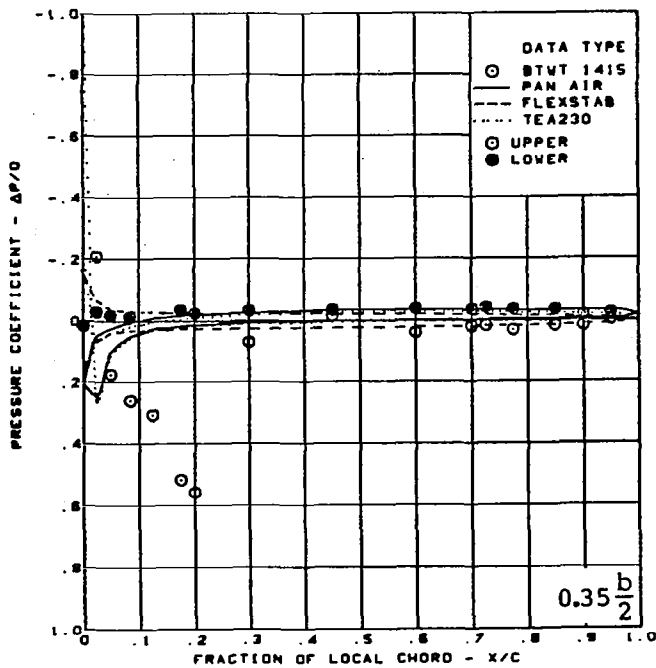
(c) (Concluded)

Figure 48. — (Continued)



(d) Surface Chordwise Pressure Distributions,  $\alpha = 12^\circ$

Figure 48. — (Continued)



$M = 0.40$

$\alpha = 12^\circ$

Twisted wing data minus flat wing data  
Rounded L.E.

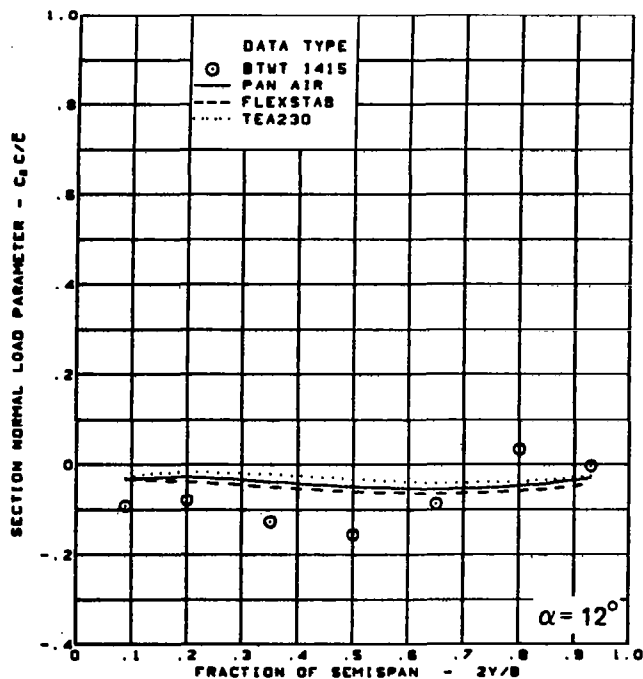
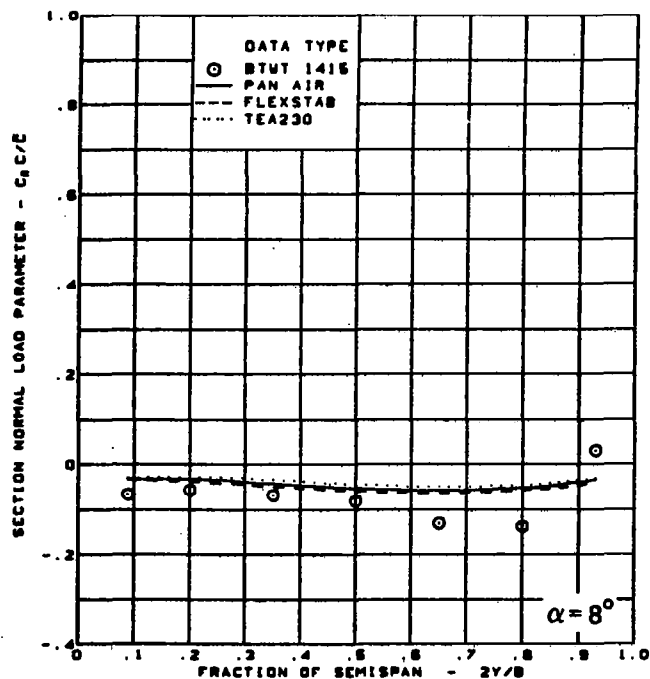
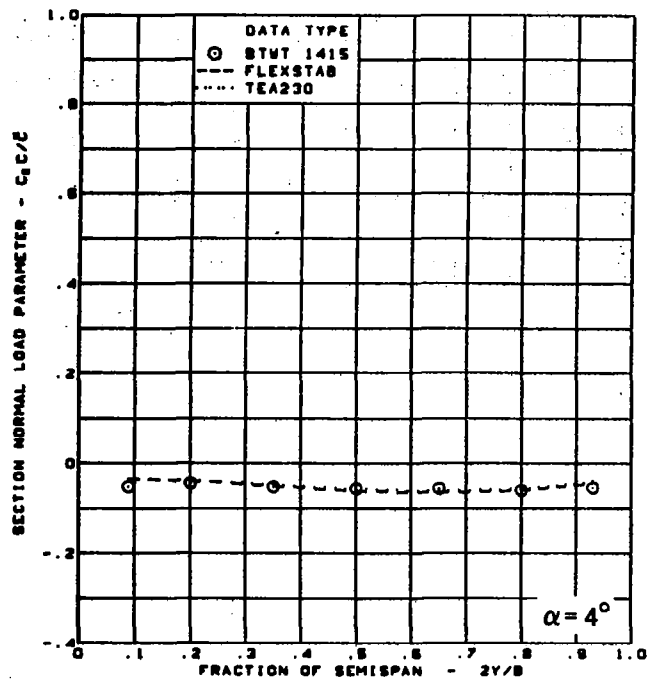
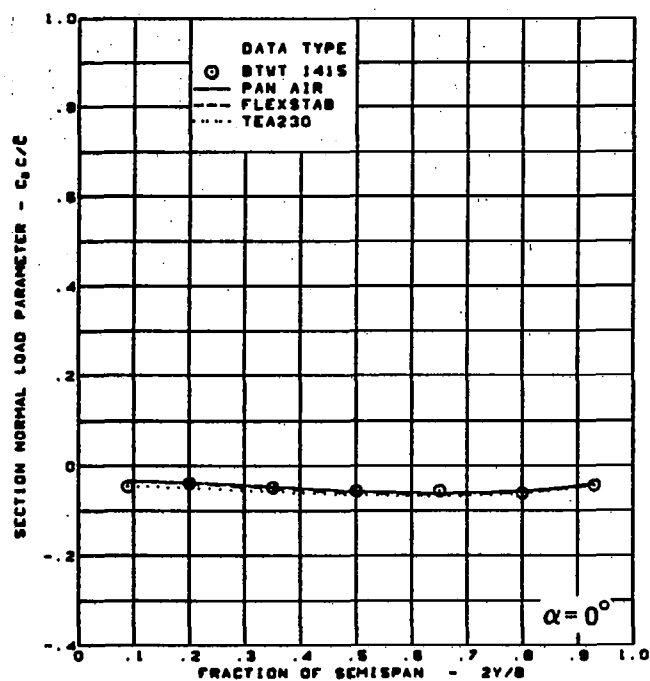
L.E. deflection, full span =  $0.0^\circ$

T.E. deflection, full span =  $0.0^\circ$

(d) (Concluded)

Figure 48. — (Continued)





$M = 0.40$

Twisted wing data minus flat wing data

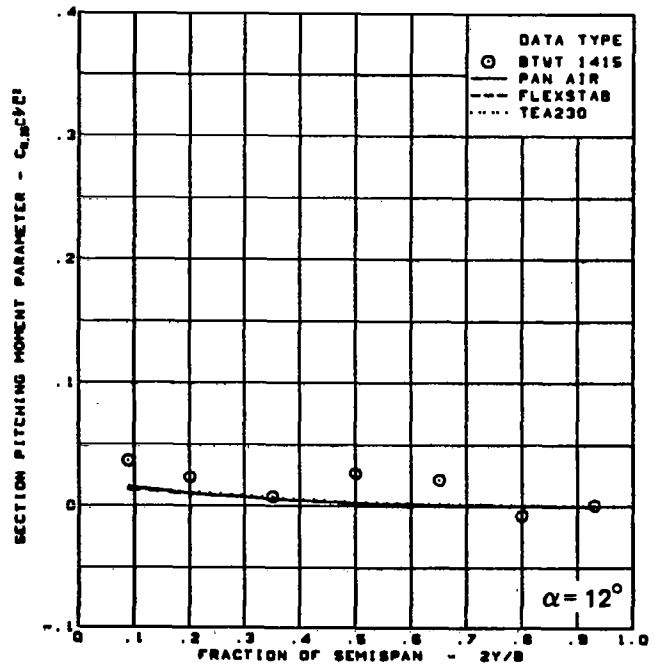
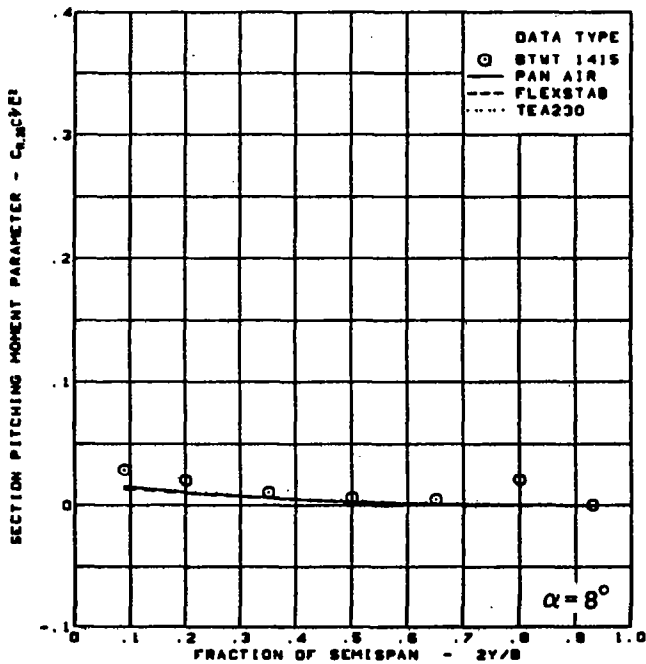
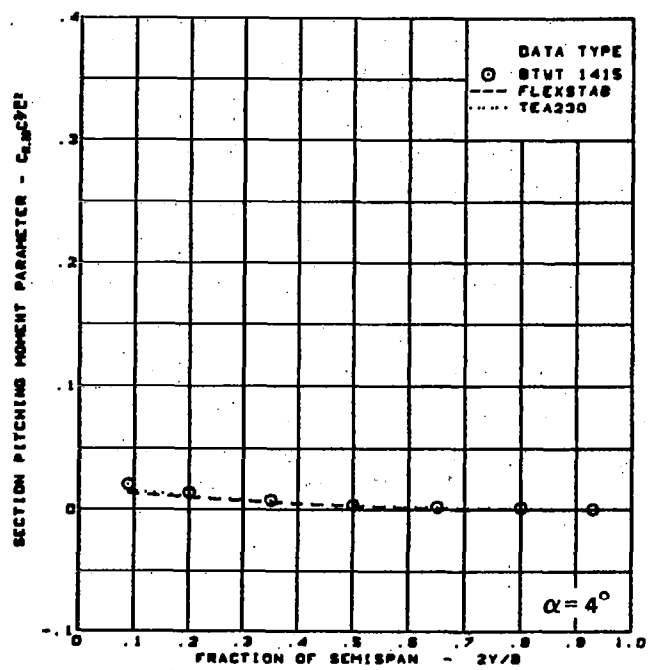
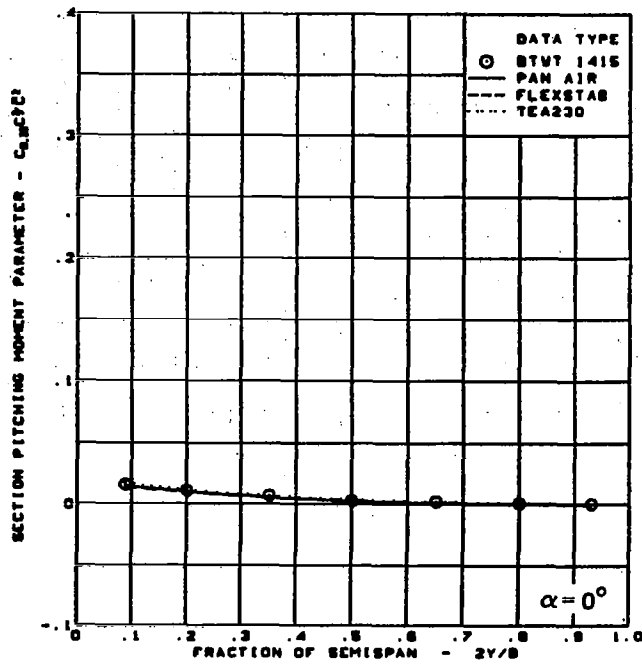
Rounded L.E.

L.E. deflection, full span  $= 0.0^\circ$

T.E. deflection, full span  $= 0.0^\circ$

(e) Spanload Distributions - Normal Force

Figure 48. - (Continued)



$M = 0.40$

Twisted wing data minus flat wing data

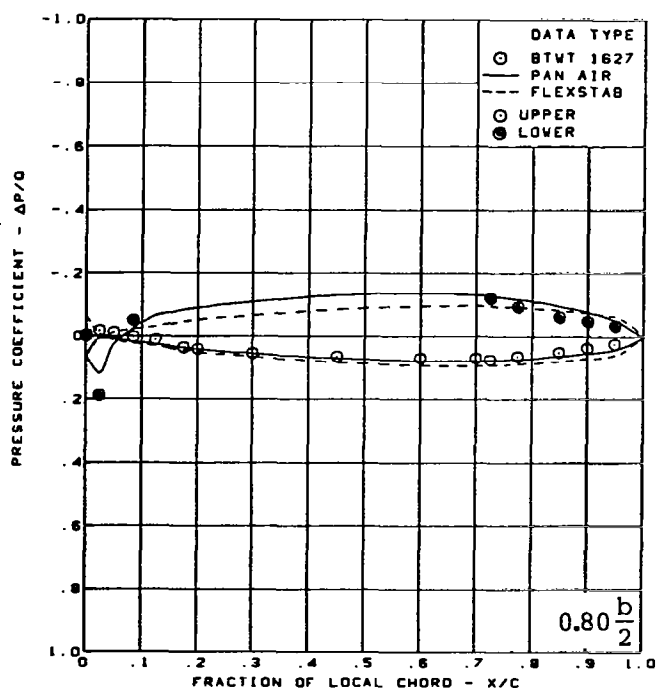
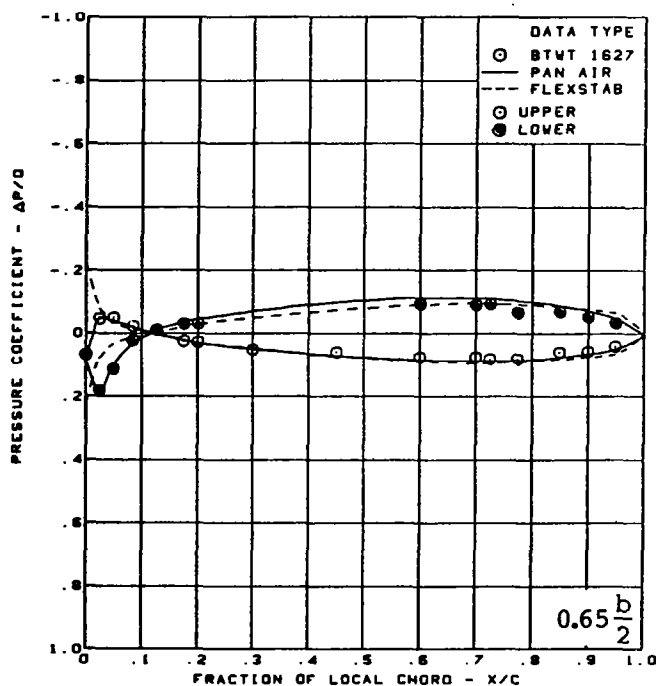
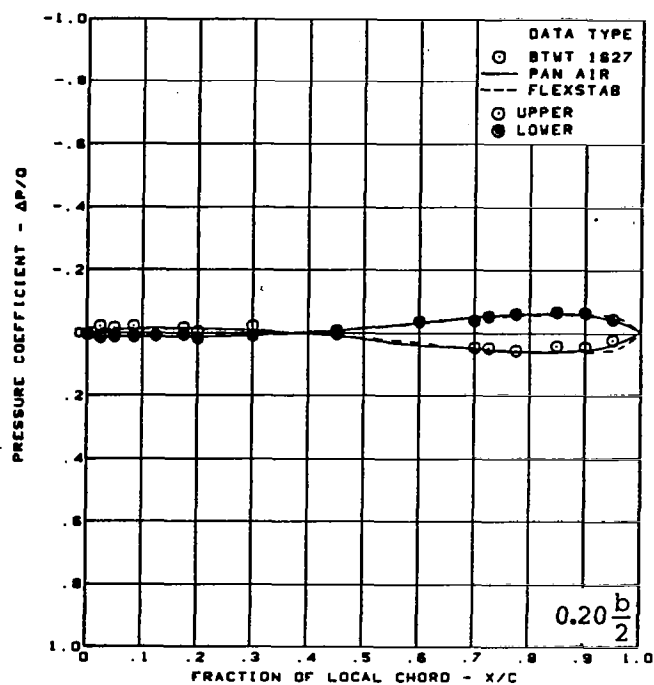
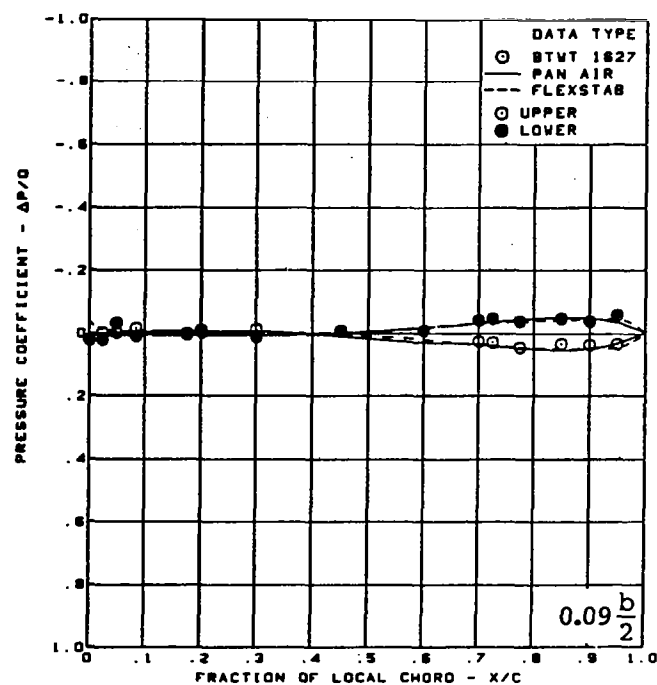
Rounded L.E.

L.E. deflection, full span  $\approx 0.0^\circ$

T.E. deflection, full span  $\approx 0.0^\circ$

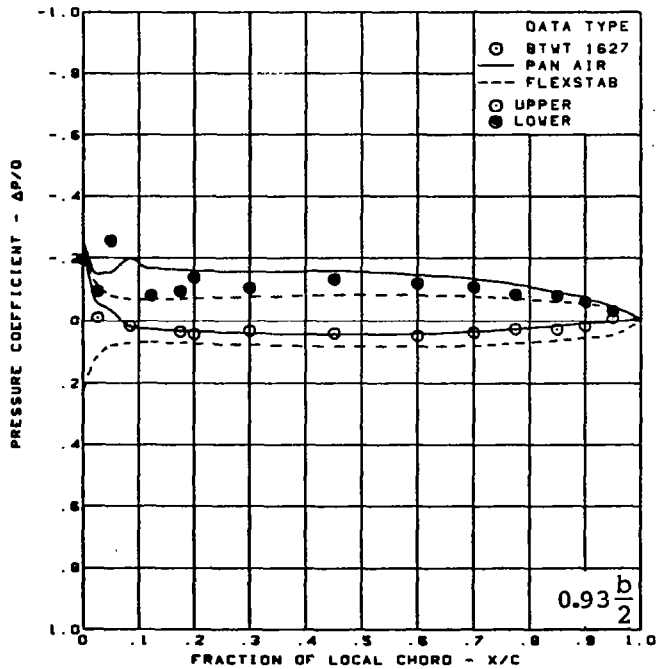
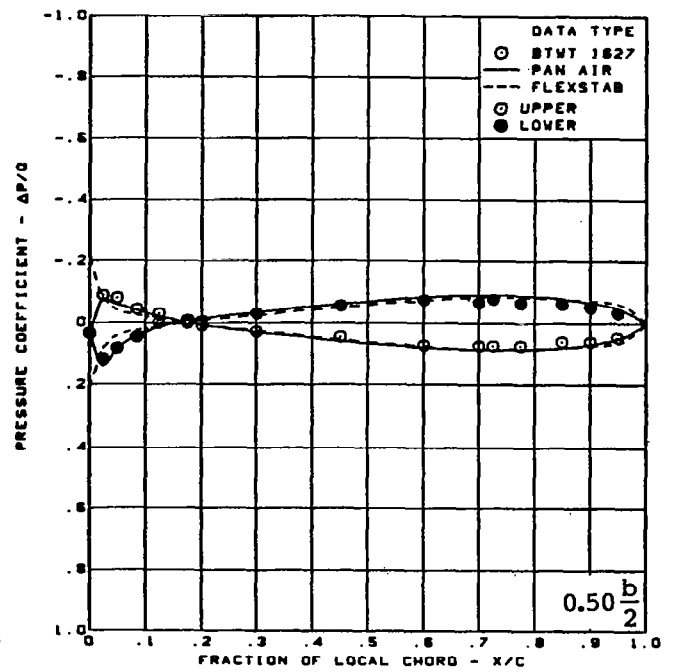
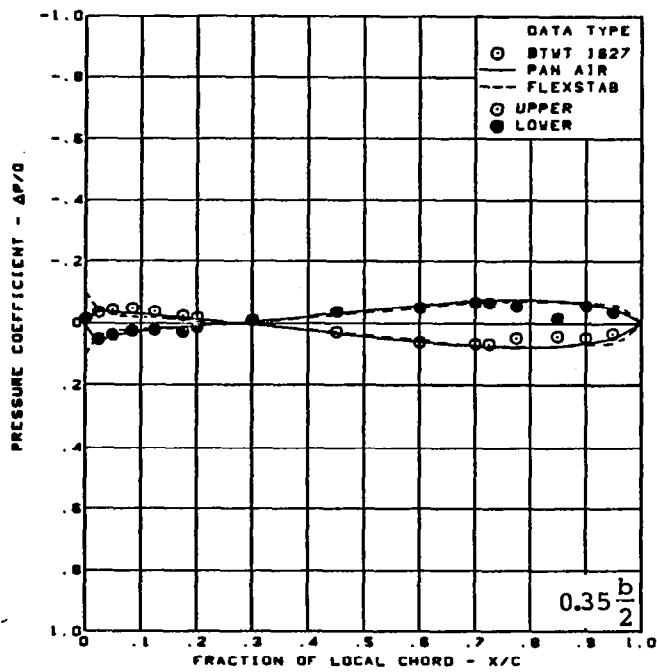
(f) Spanload Distributions - Pitching Moment

Figure 48. - (Concluded)



(a) Surface Chordwise Pressure Distributions,  $\alpha = 0^\circ$

Figure 49. — Wing Theory-to-Experiment Comparison—Effect of Incremental Camber;  
T.E. Deflection, Full Span =  $0.0^\circ$ ;  $M = 0.40$



$M = 0.40$

$\alpha = 0^\circ$

Cambered-twisted wing data

minus twisted wing data

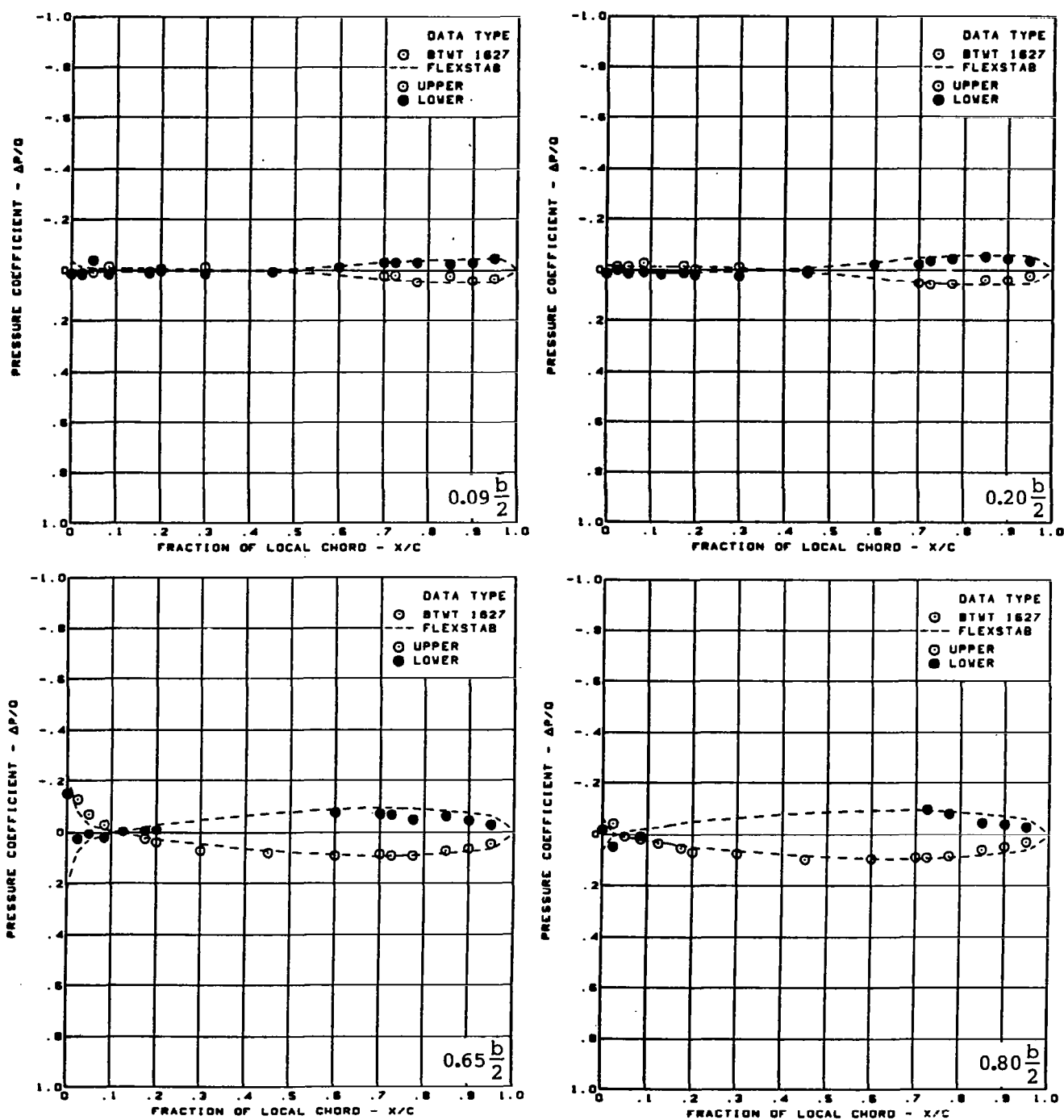
Rounded L.E.

L.E. deflection, full span =  $0.0^\circ$

T.E. deflection, full span =  $0.0^\circ$

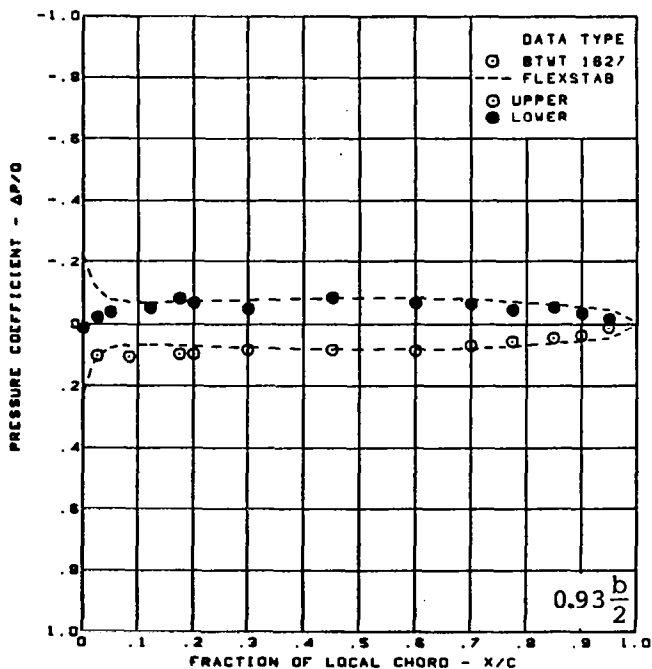
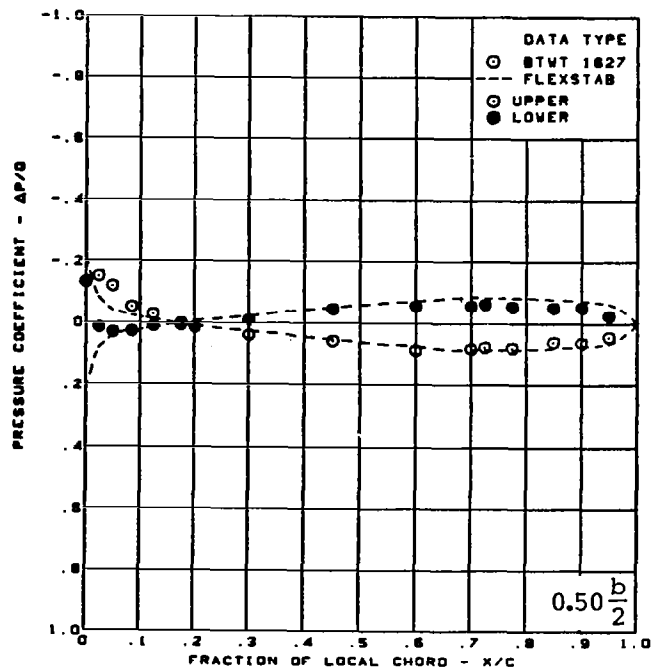
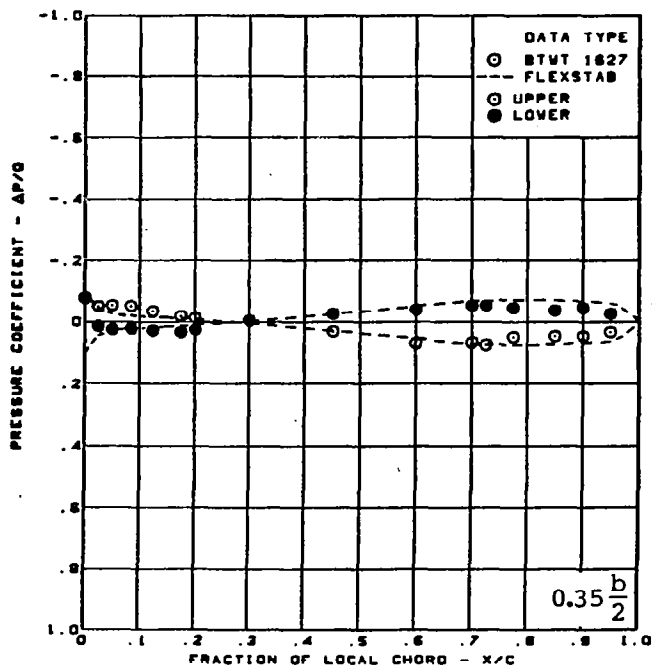
(a) (Concluded)

Figure 49. — (Continued)



(b) Surface Chordwise Pressure Distributions,  $\alpha = 4^\circ$

Figure 49. — (Continued)



$M = 0.40$

$\alpha = 4^\circ$

Cambered-twisted wing data

minus twisted wing data

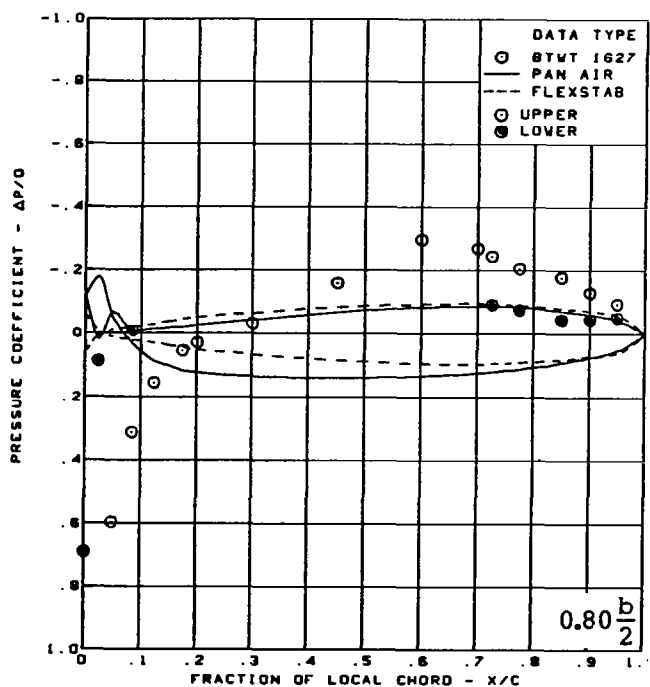
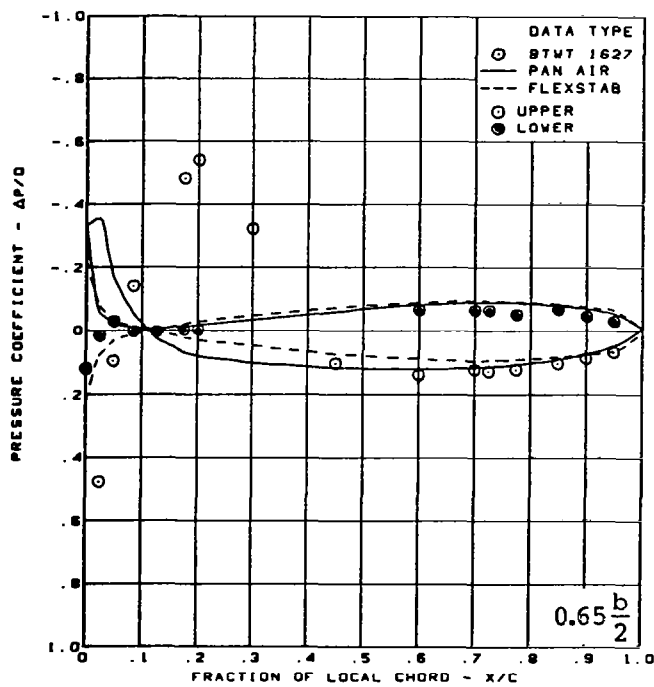
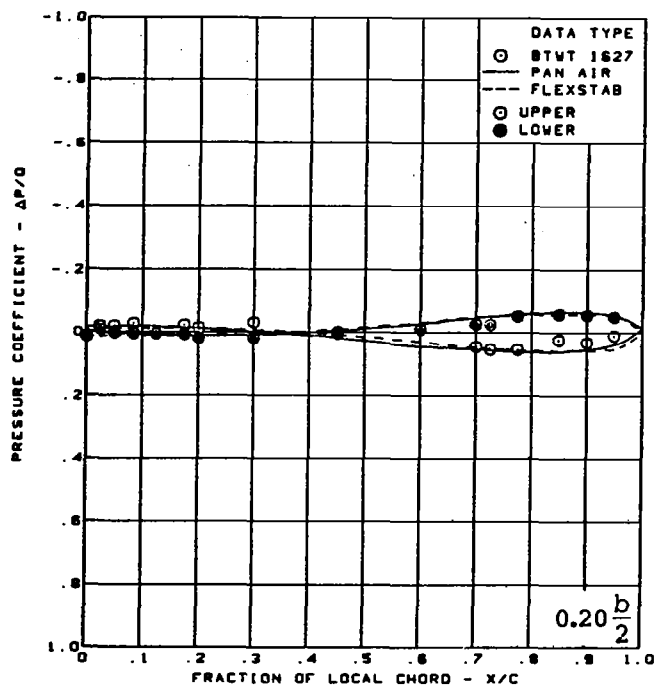
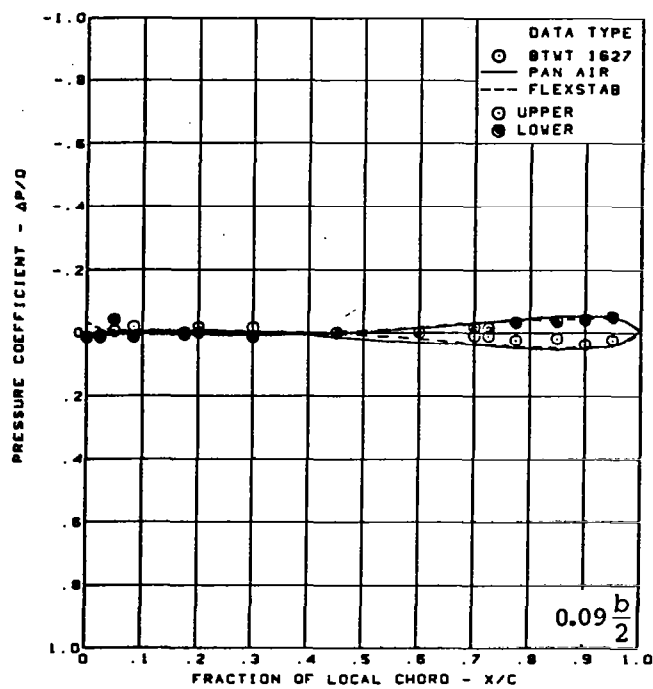
Rounded L.E.

L.E. deflection, full span =  $0.0^\circ$

T.E. deflection, full span =  $0.0^\circ$

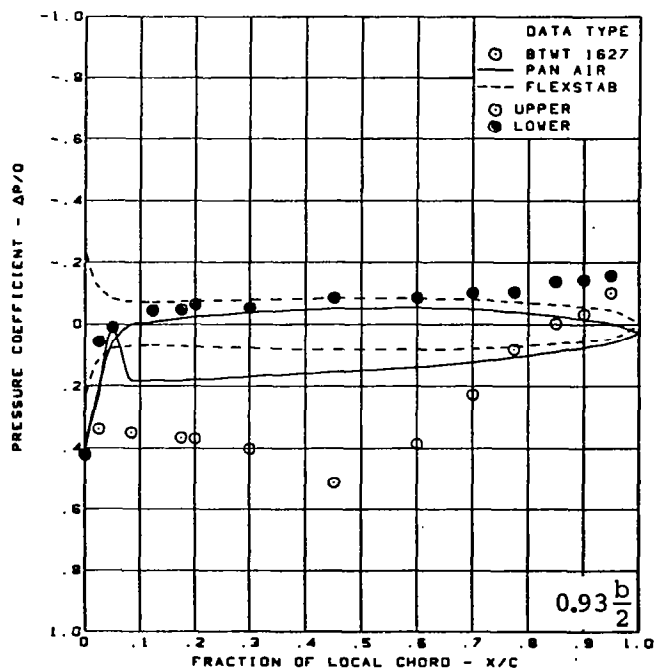
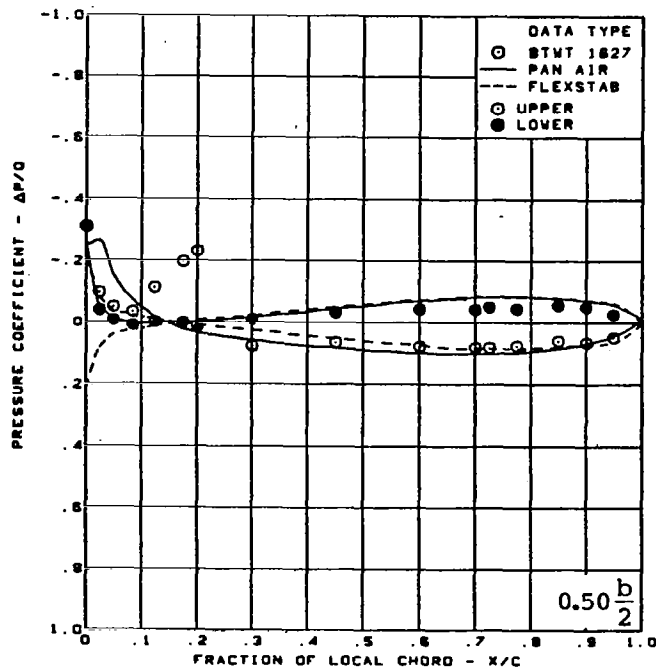
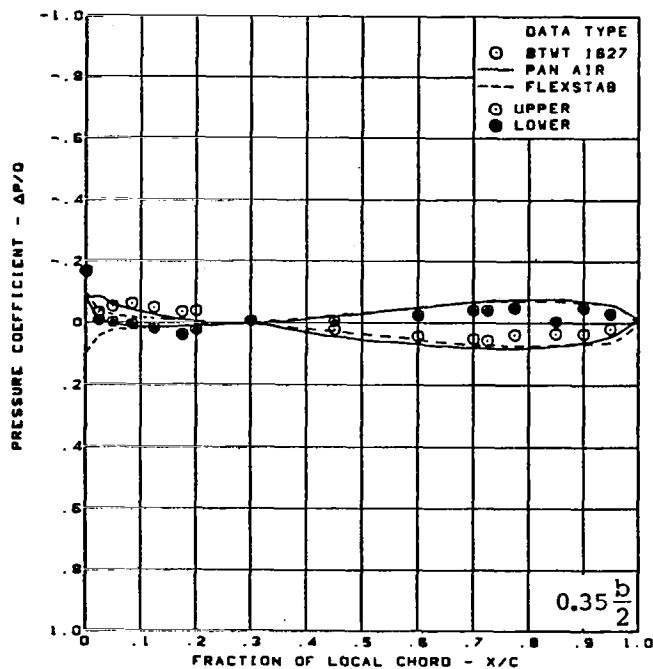
(b) (Concluded)

Figure 49. — (Continued)



(c) Surface Chordwise Pressure Distributions,  $\alpha = 8^\circ$

Figure 49. - (Continued)

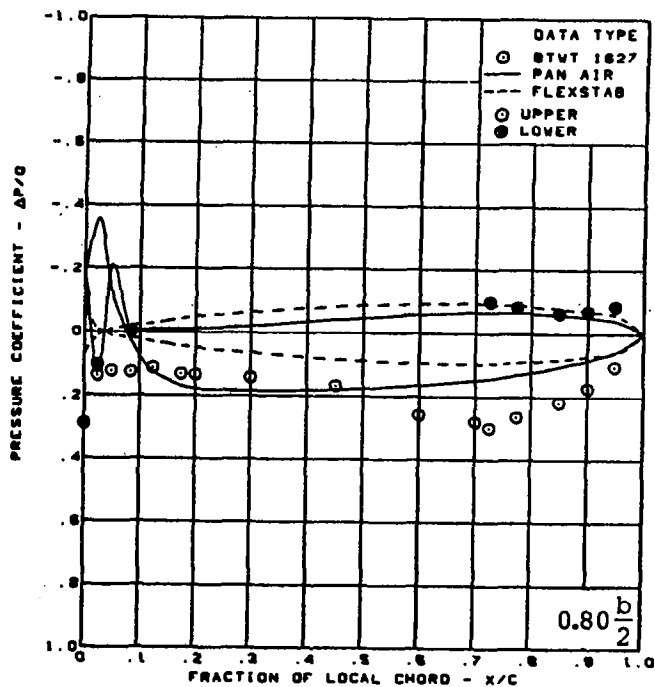
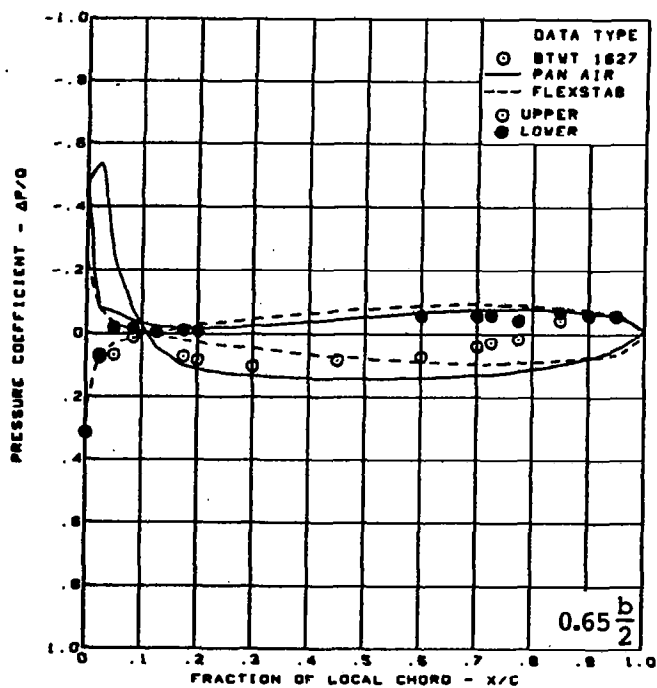
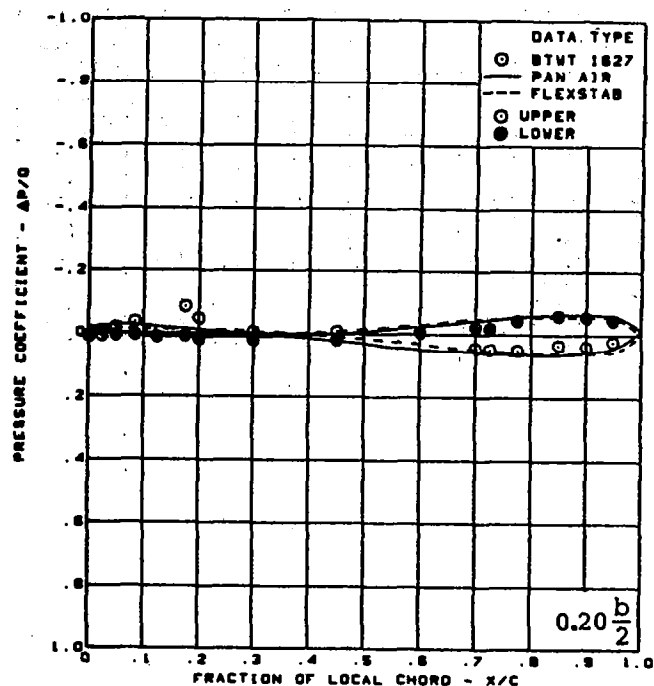
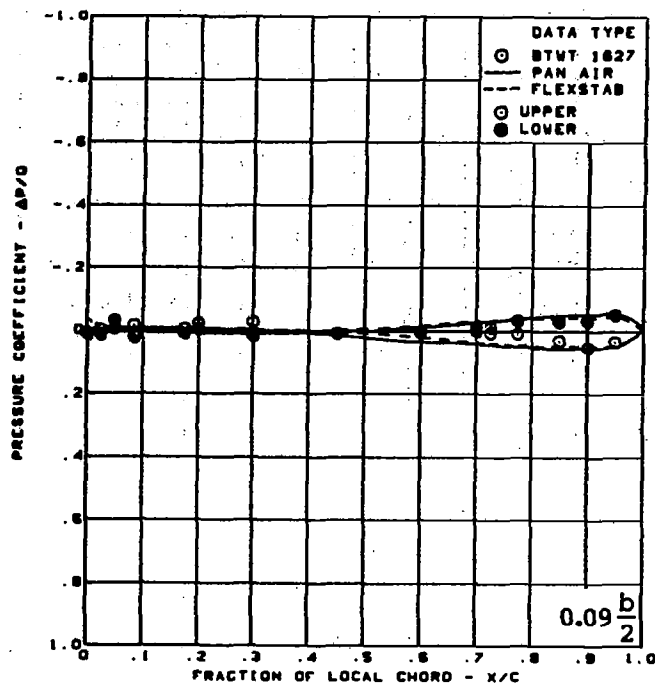


$M = 0.40$   
 $\alpha = 8^\circ$   
 Cambered-twisted wing data  
 minus twisted wing data  
 Rounded L.E.  
 L.E. deflection, full span =  $0.0^\circ$   
 T.E. deflection, full span =  $0.0^\circ$

(c) (Concluded)

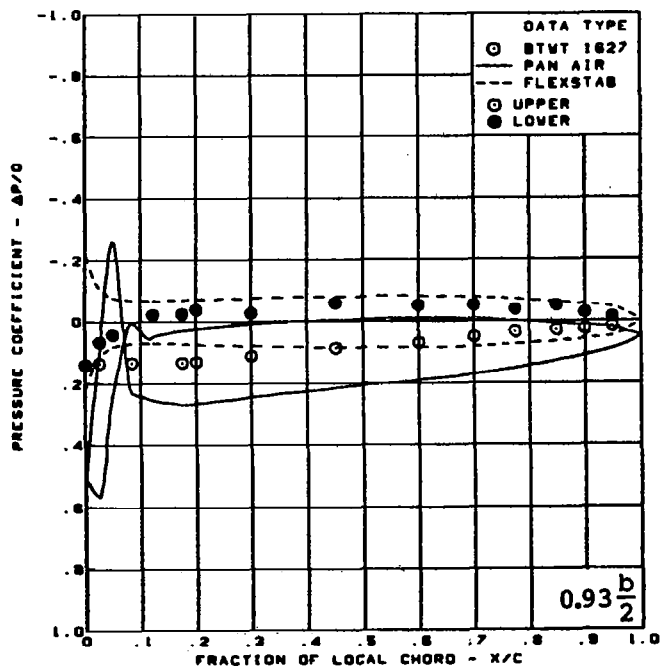
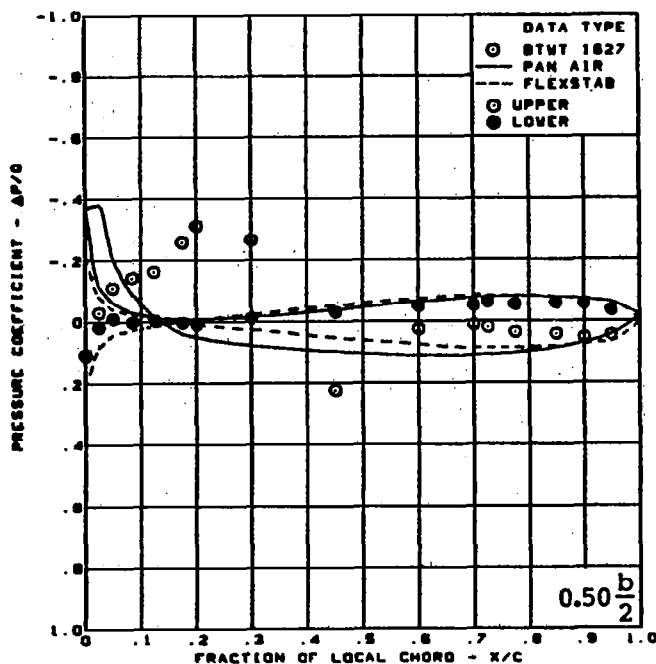
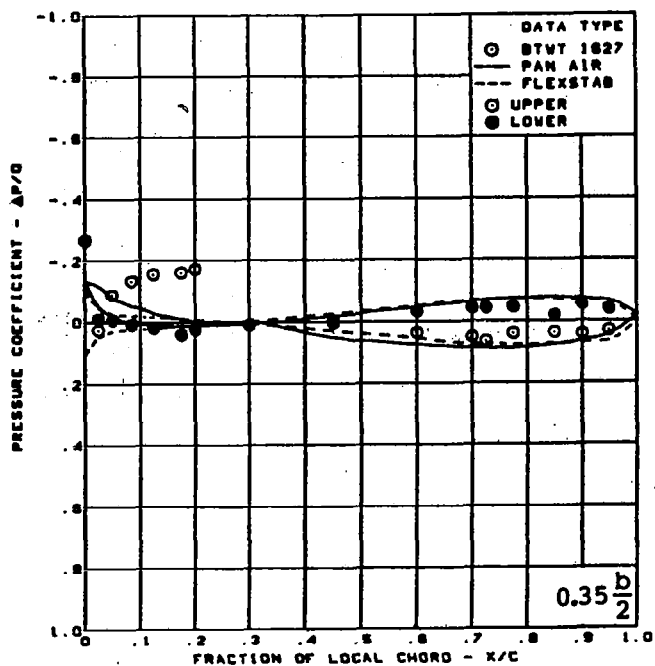
Figure 49. — (Continued)





(d) Surface Chordwise Pressure Distributions,  $\alpha = 12^\circ$

Figure 49. - (Continued)



$M = 0.40$

$\alpha = 12^\circ$

Cambered-twisted wing data

minus twisted wing data

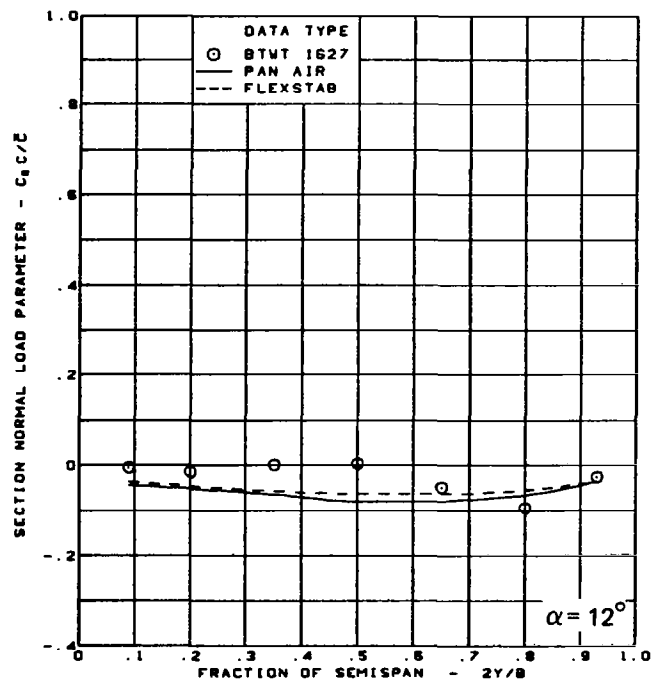
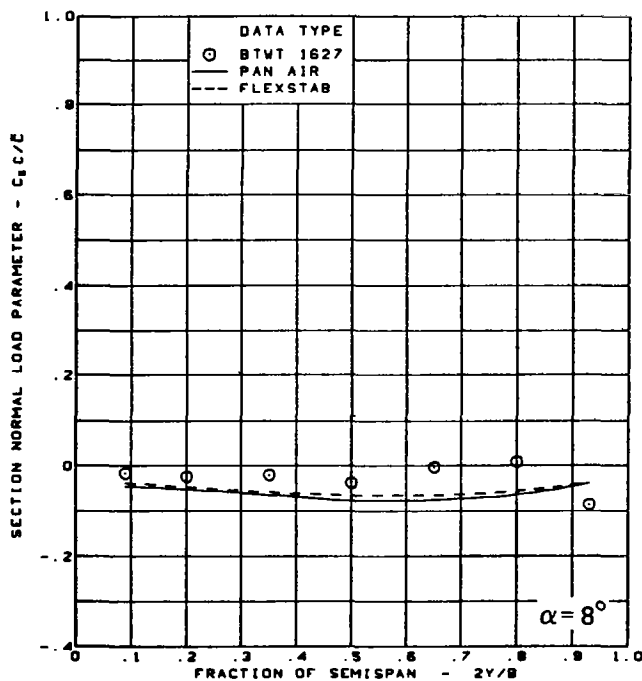
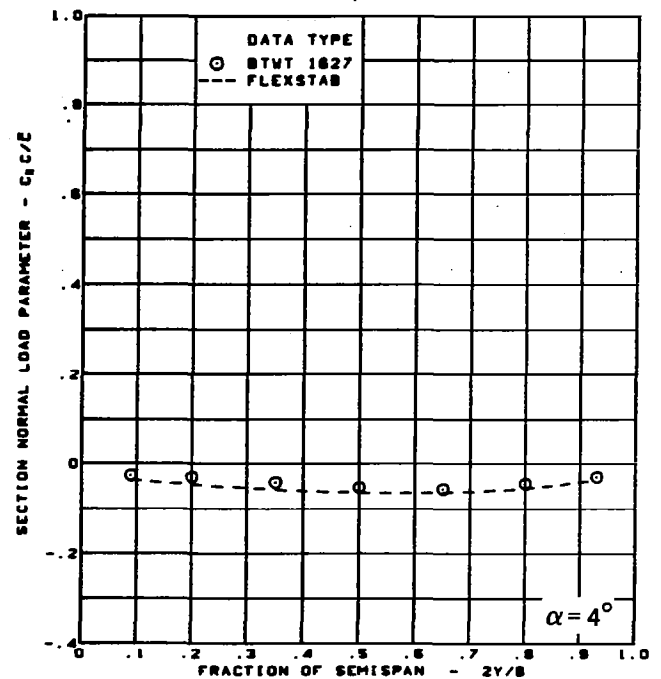
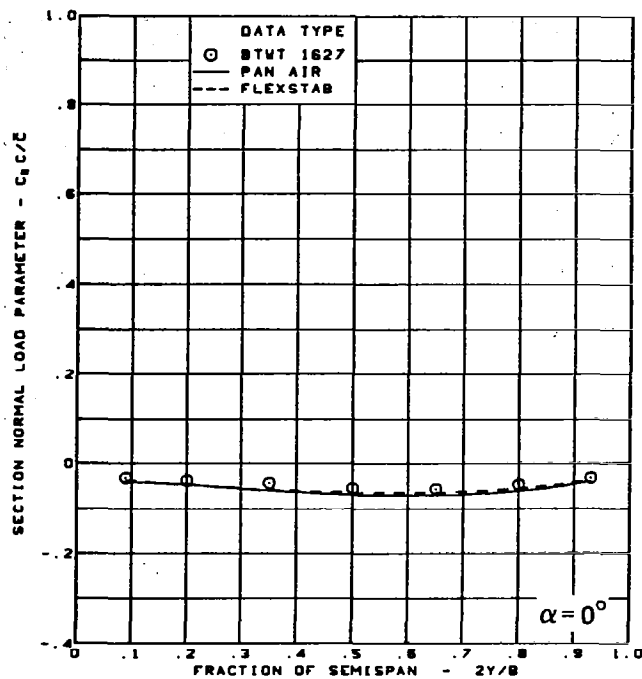
Rounded L.E.

L.E. deflection, full span =  $0.0^\circ$

T.E. deflection, full span =  $0.0^\circ$

(d) (Concluded)

Figure 49. - (Continued)



$M = 0.40$

Cambered-twisted wing data  
minus twisted wing data

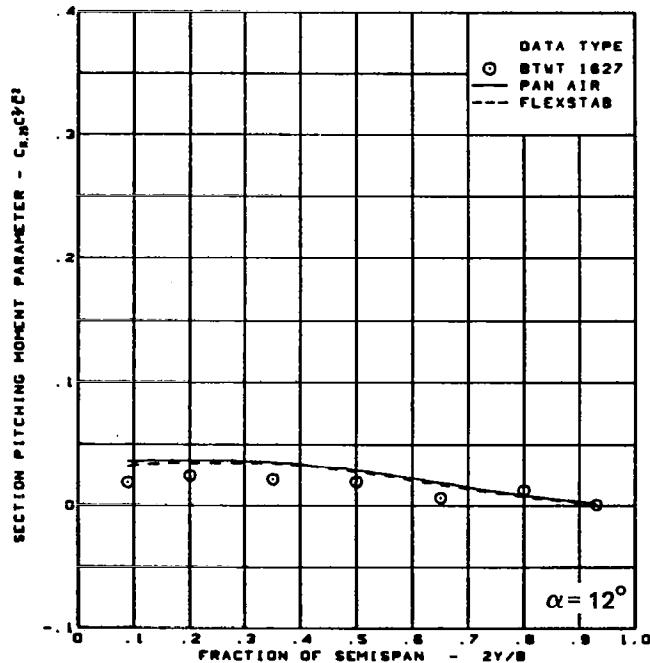
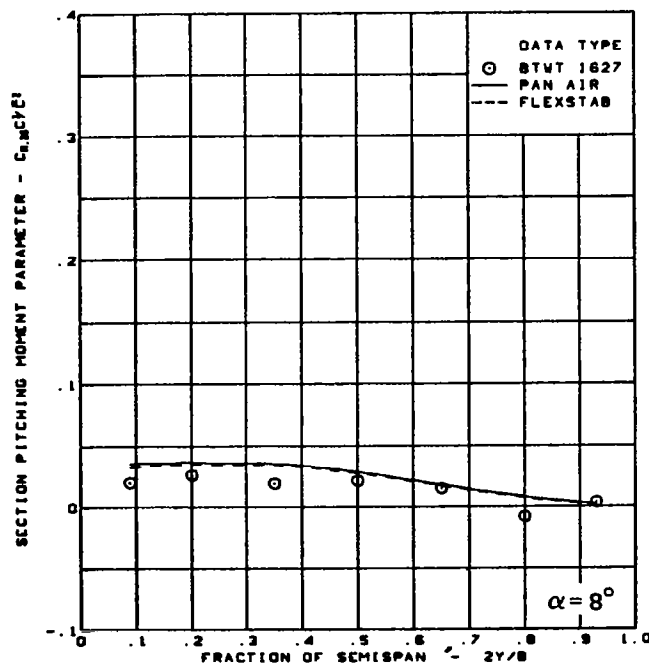
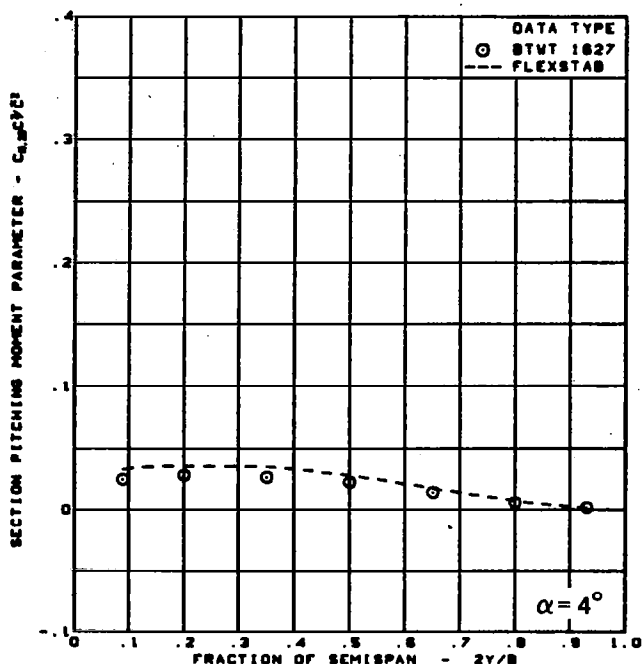
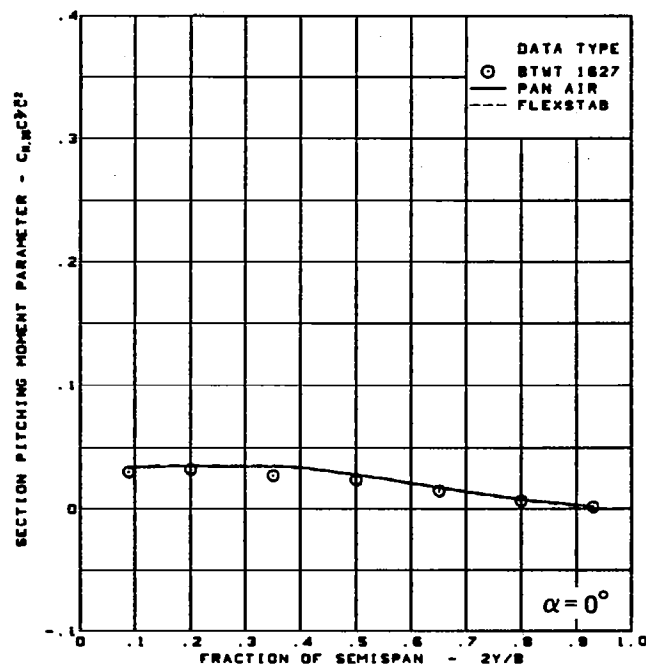
Rounded L.E.

L.E. deflection, full span =  $0.0^\circ$

T.E. deflection, full span =  $0.0^\circ$

(e) Spanload Distributions - Normal Force

Figure 49. - (Continued)

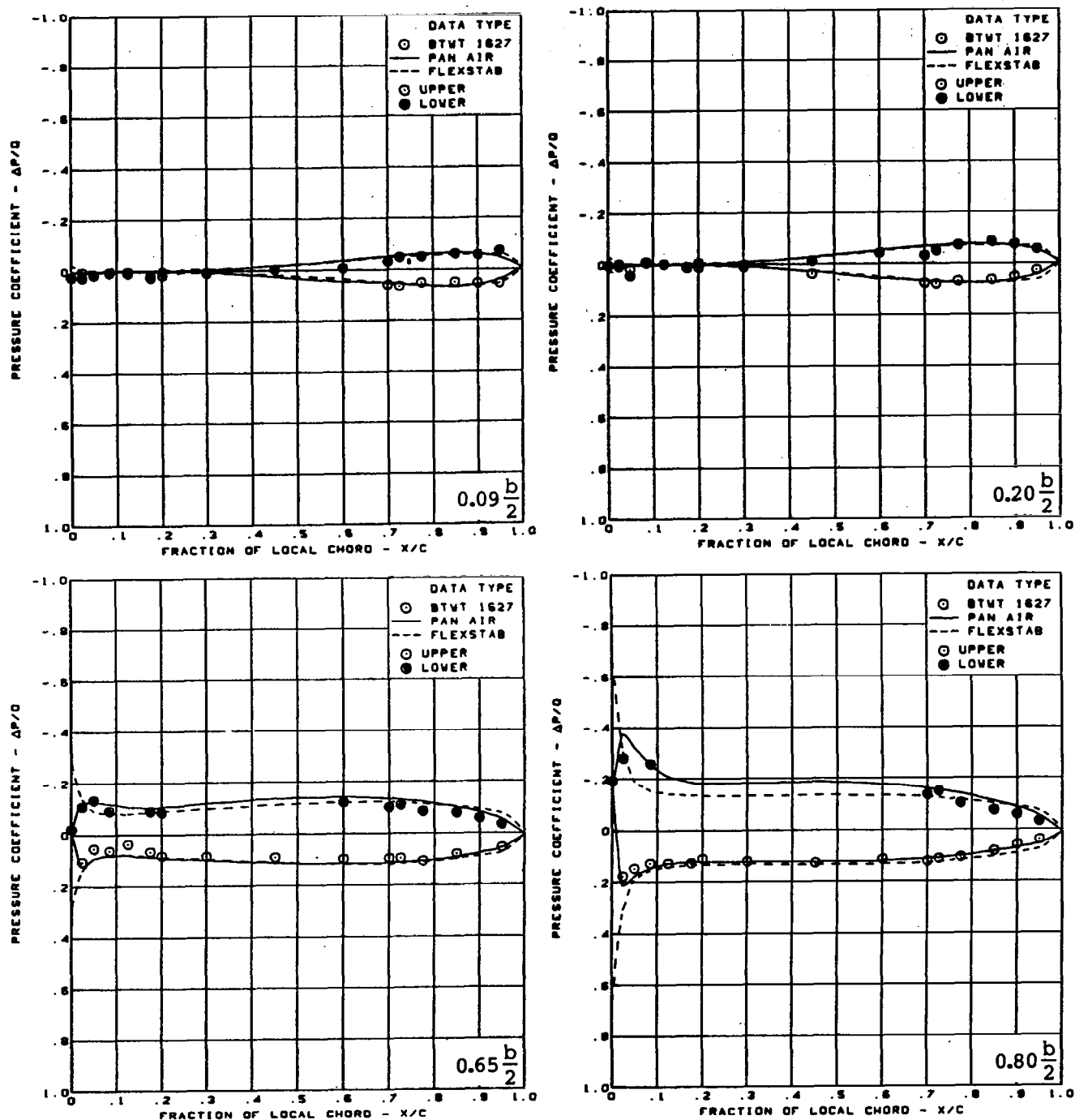


M = 0.40  
 Cambered-twisted wing data  
 minus twisted wing data

Rounded L.E.  
 L.E. deflection, full span =  $0.0^\circ$   
 T.E. deflection, full span =  $0.0^\circ$

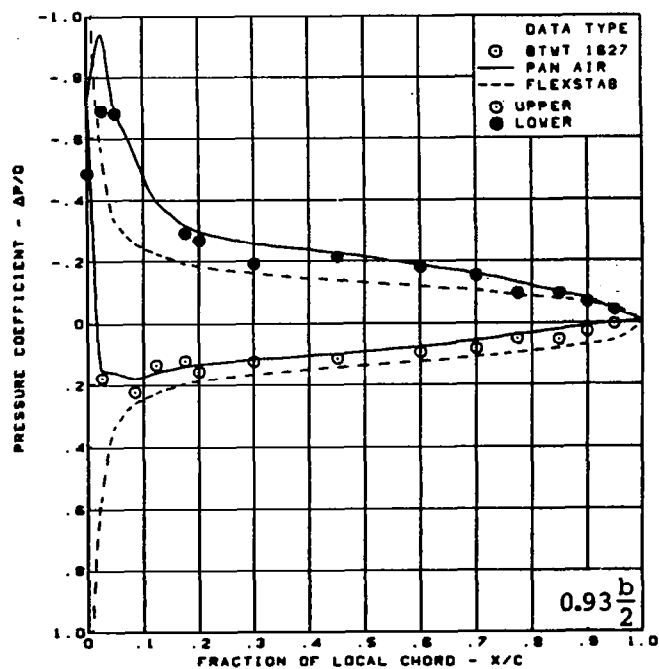
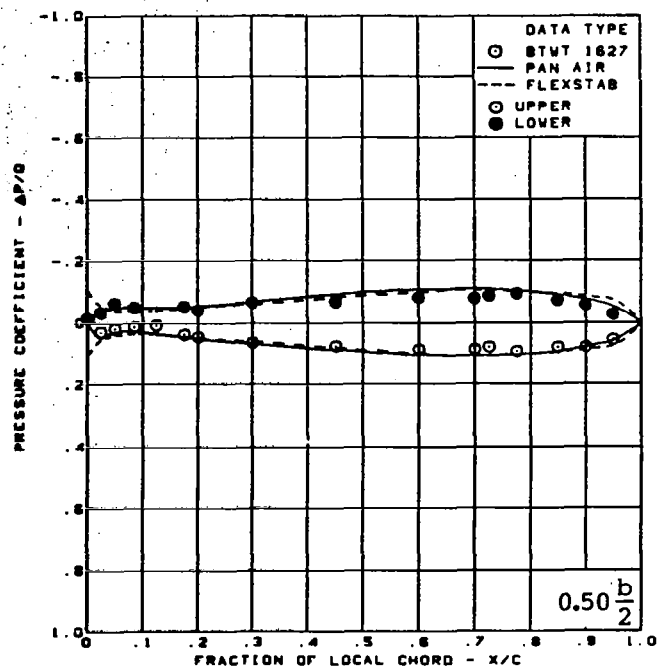
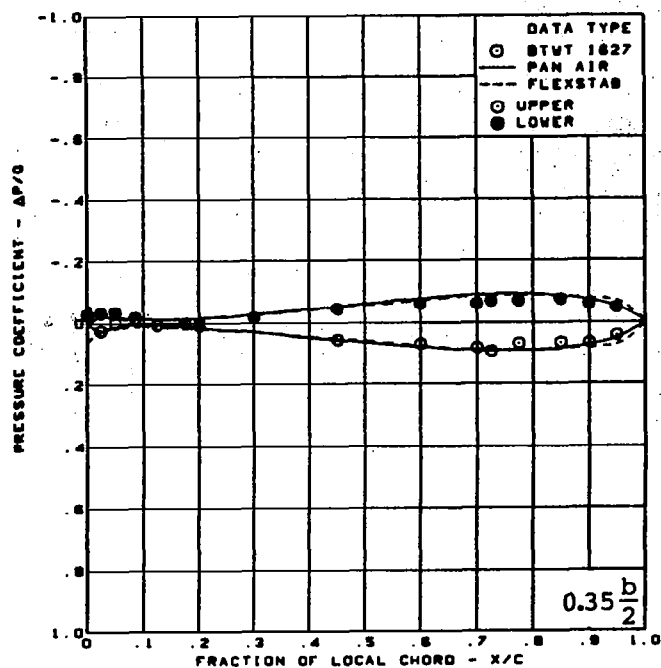
(f) Spanload Distributions - Pitching Moment

Figure 49. — (Concluded)



(a) Surface Chordwise Pressure Distributions,  $\alpha = 0^\circ$

Figure 50. — Wing Theory-to-Experiment Comparison—Effect of Incremental Camber and Twist;  
T.E. Deflection, Full Span =  $0.0^\circ$ ;  $M = 0.40$



$M = 0.40$

$\alpha = 0^\circ$

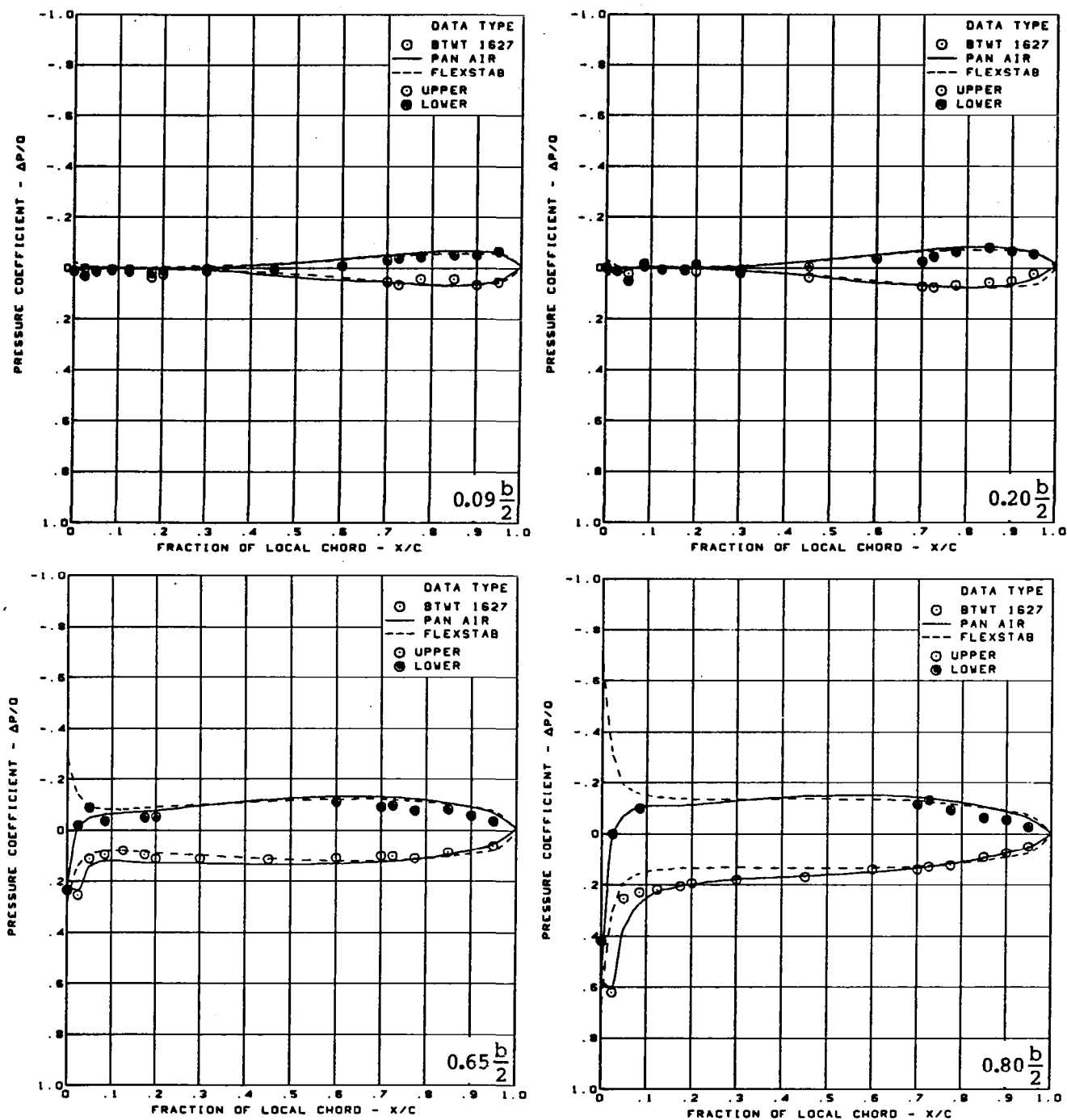
Cambered-twisted wing data minus flat wing data  
Rounded L.E.

L.E. deflection, full span =  $0.0^\circ$

T.E. deflection, full span =  $0.0^\circ$

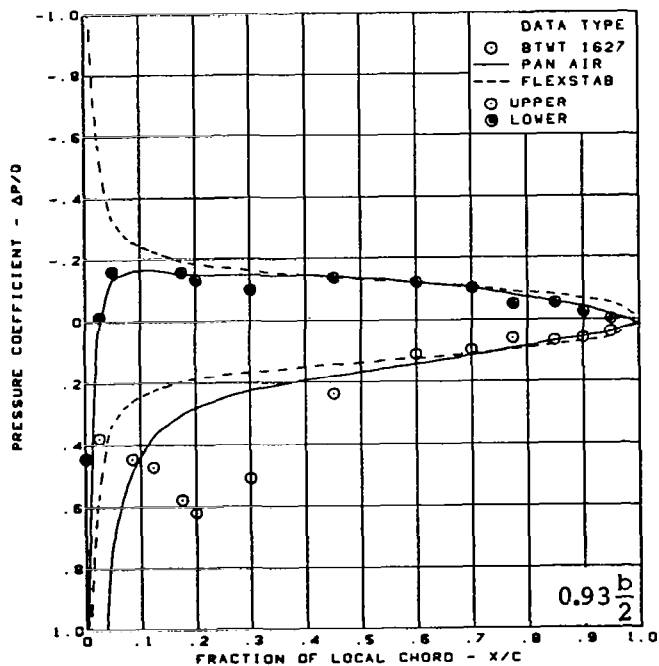
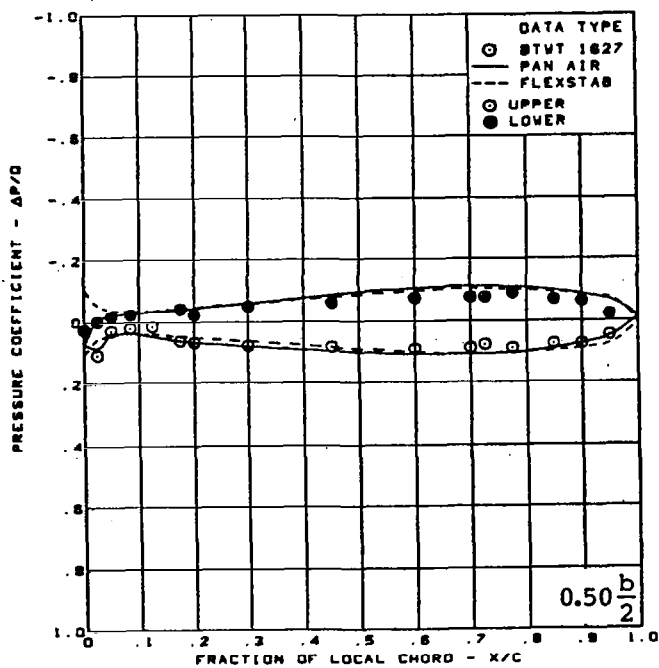
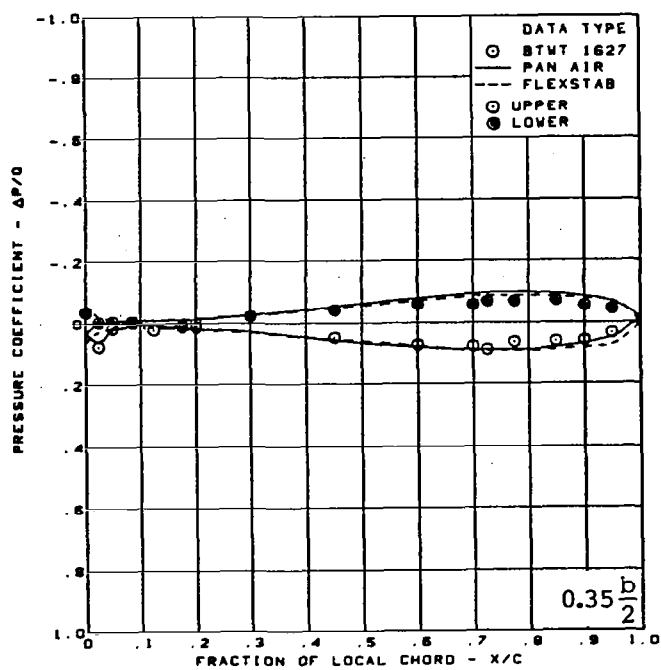
(a) (Concluded)

Figure 50. — (Continued)



(b) Surface Chordwise Pressure Distributions,  $\alpha = 4^\circ$

Figure 50. — (Continued)



$M = 0.40$

$\alpha = 4^\circ$

Cambered-twisted wing data minus flat wing data  
Rounded L.E.

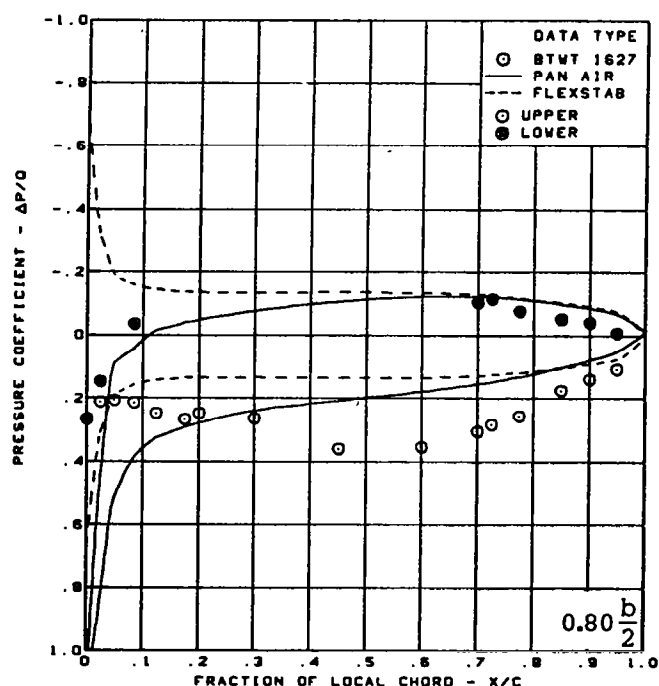
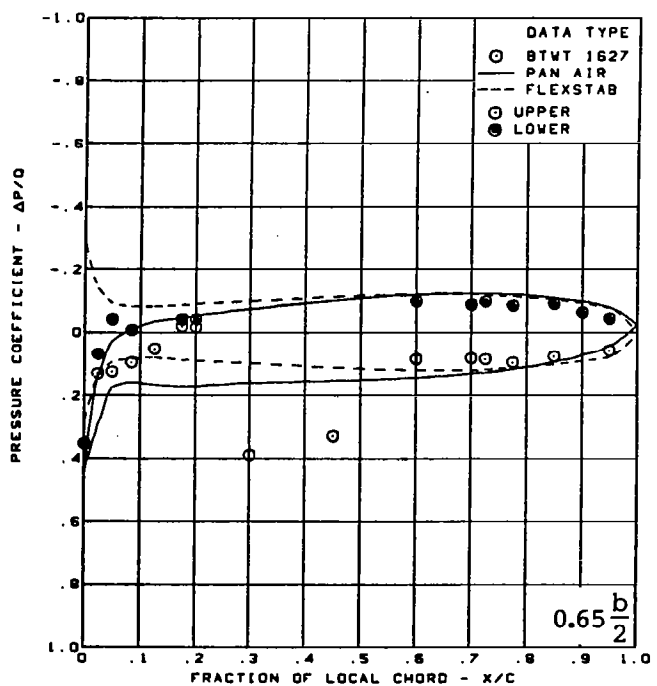
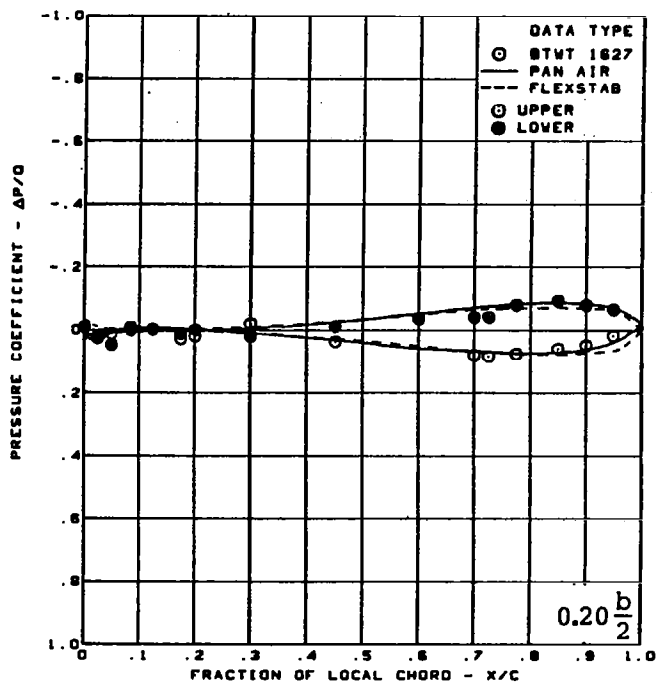
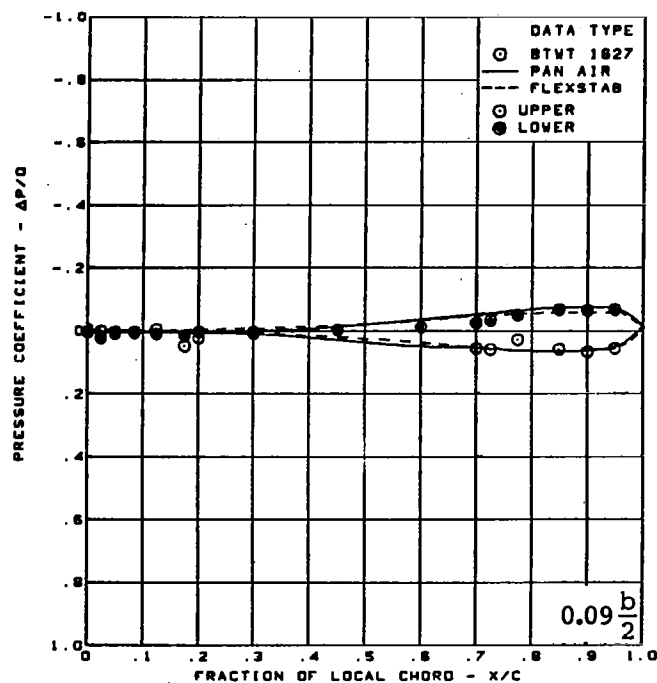
L.E. deflection, full span =  $0.0^\circ$

T.E. deflection, full span =  $0.0^\circ$

(b) (Concluded)

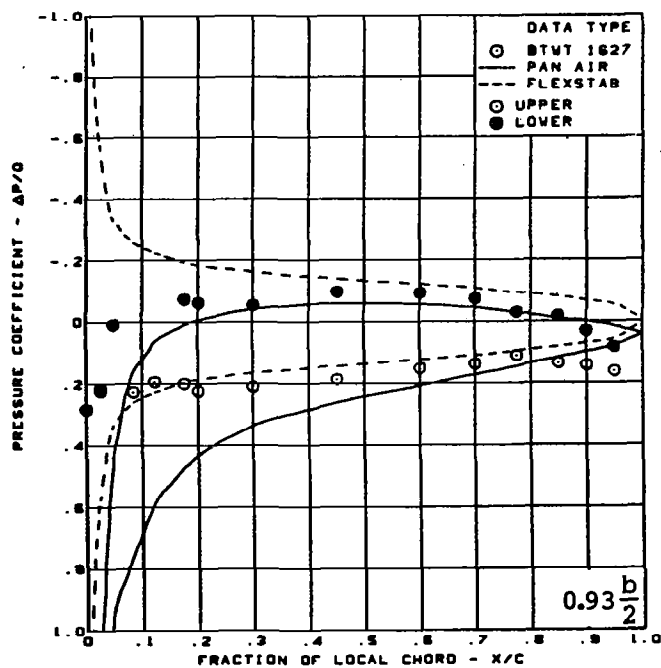
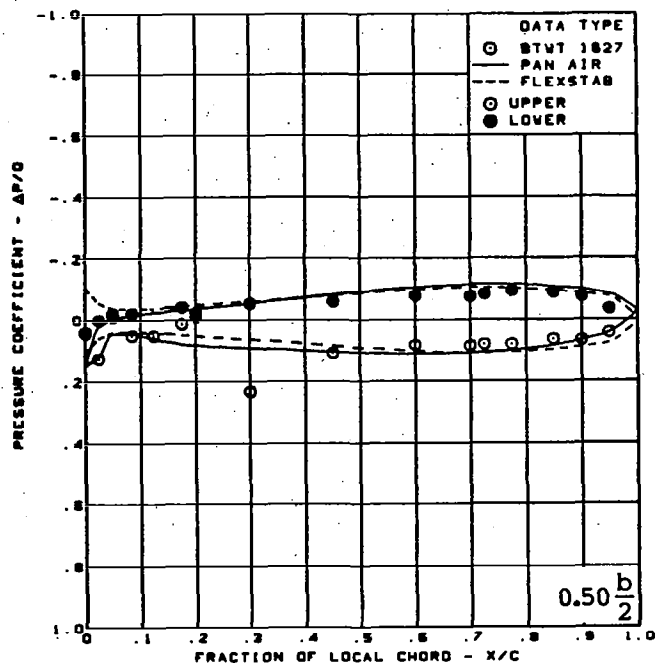
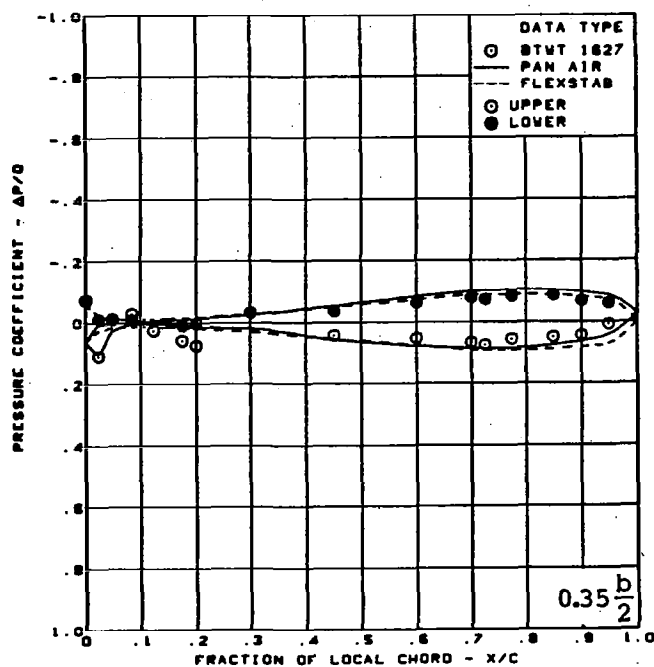
Figure 50. — (Continued)





(c) Surface Chordwise Pressure Distributions,  $\alpha = 8^\circ$

Figure 50. — (Continued)



$M = 0.40$

$\alpha = 8^\circ$

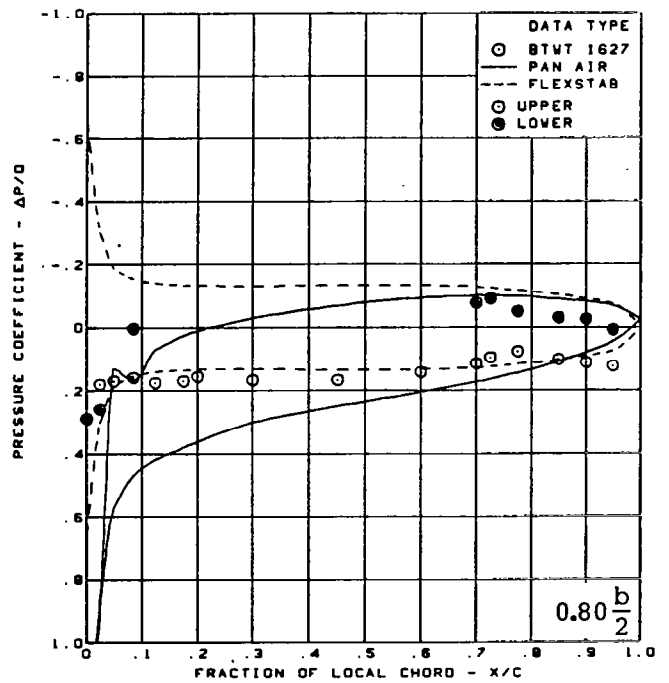
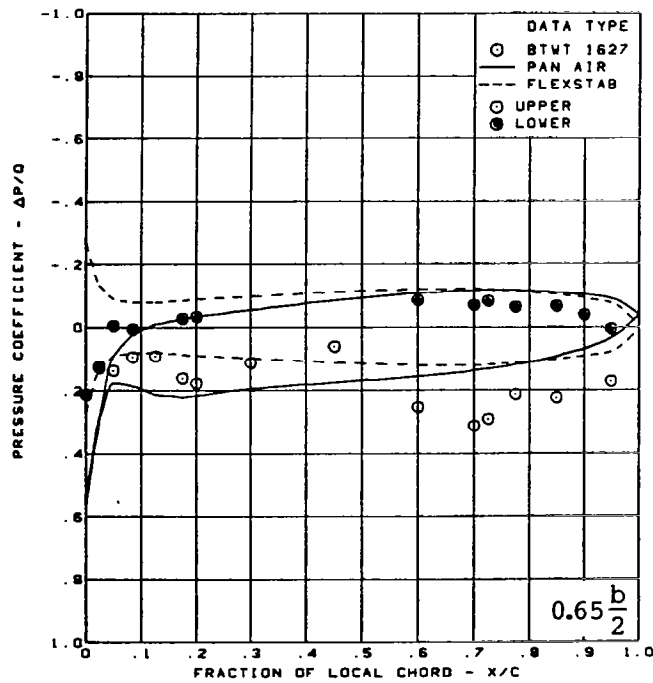
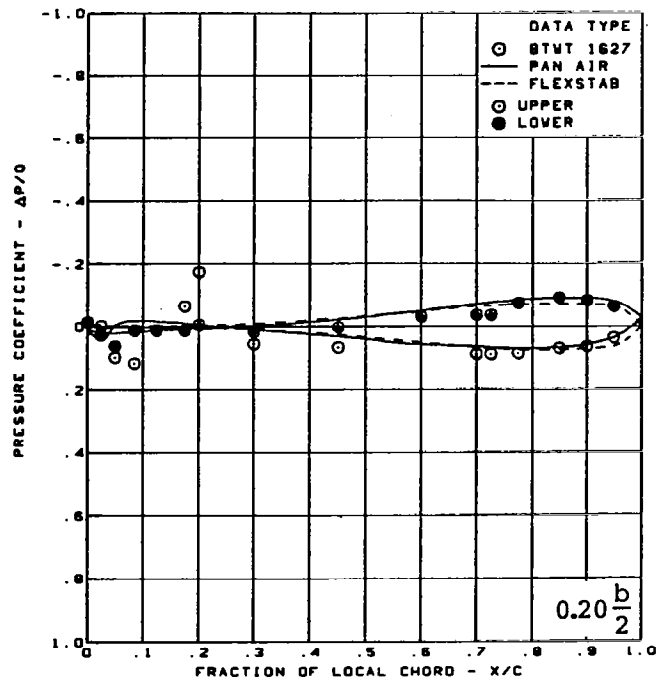
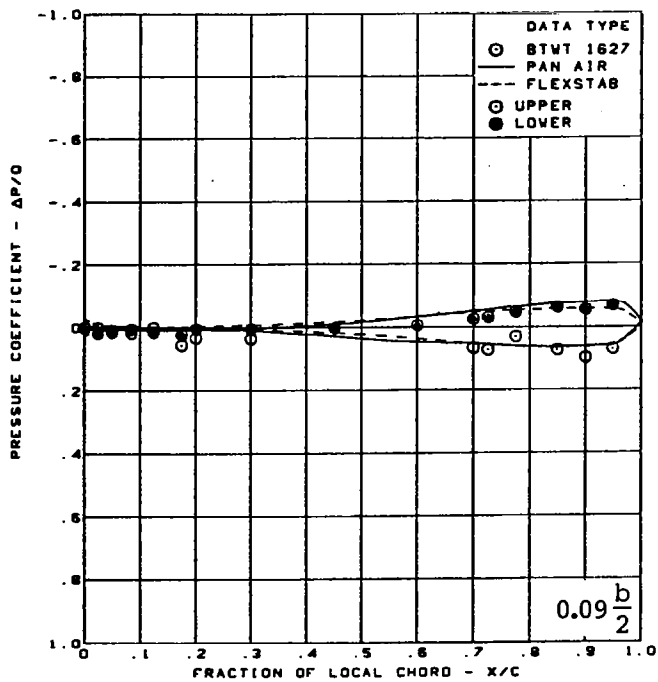
Cambered-twisted wing data minus flat wing data  
Rounded L.E.

L.E. deflection, full span =  $0.0^\circ$

T.E. deflection, full span =  $0.0^\circ$

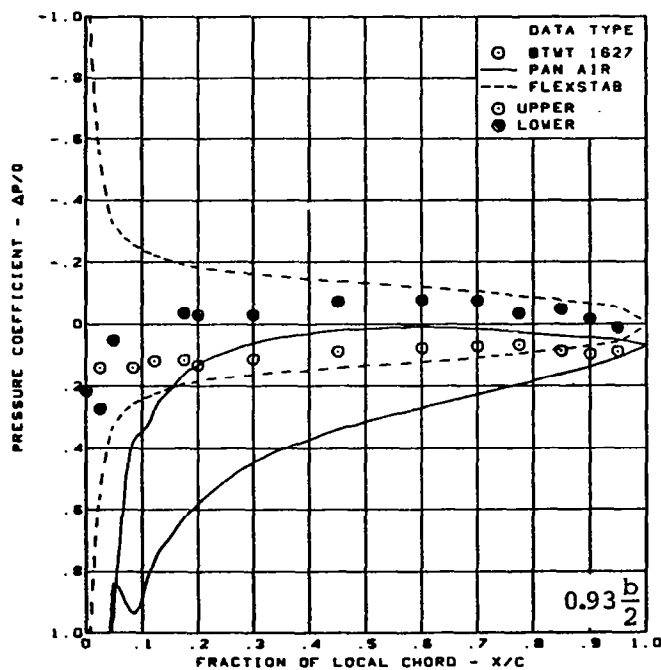
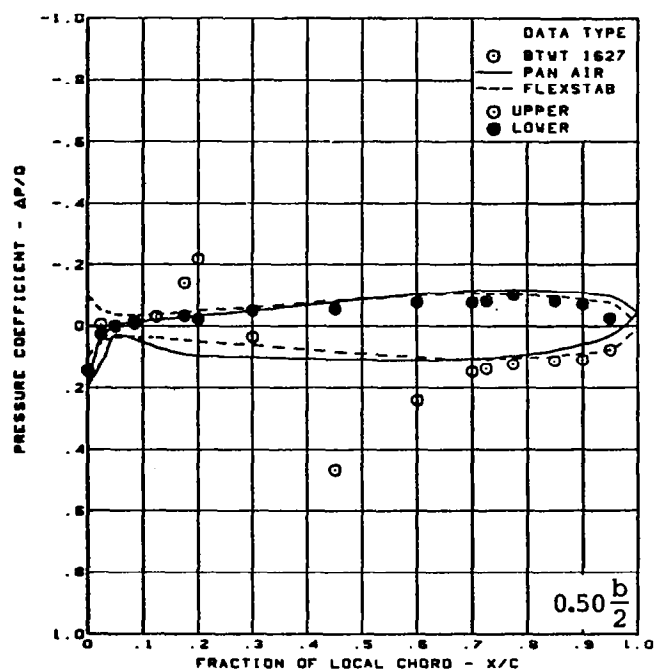
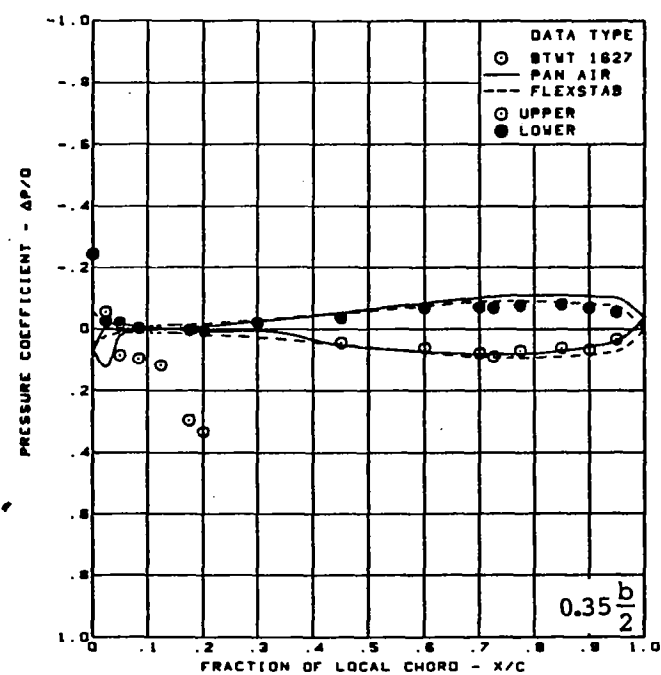
(c) (Concluded)

Figure 50. — (Continued)



(d) Surface Chordwise Pressure Distributions,  $\alpha = 12^\circ$

Figure 50. - (Continued)



$M = 0.40$

$\alpha = 12^\circ$

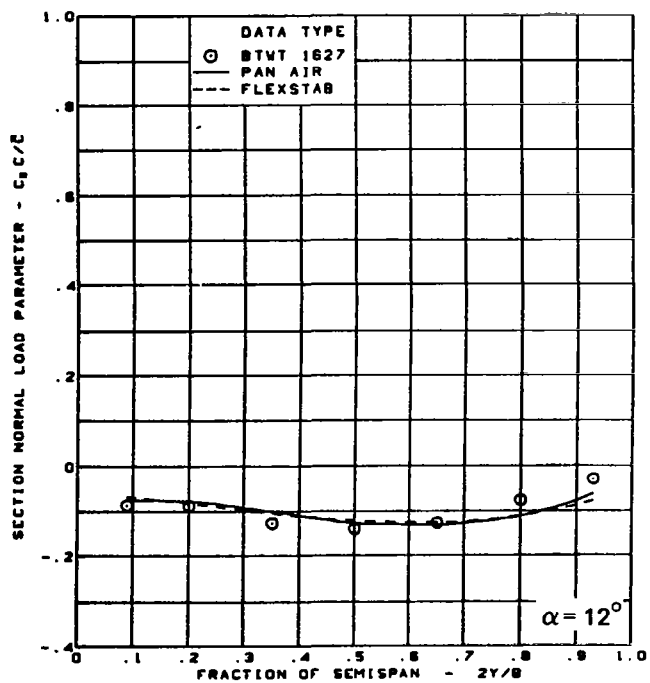
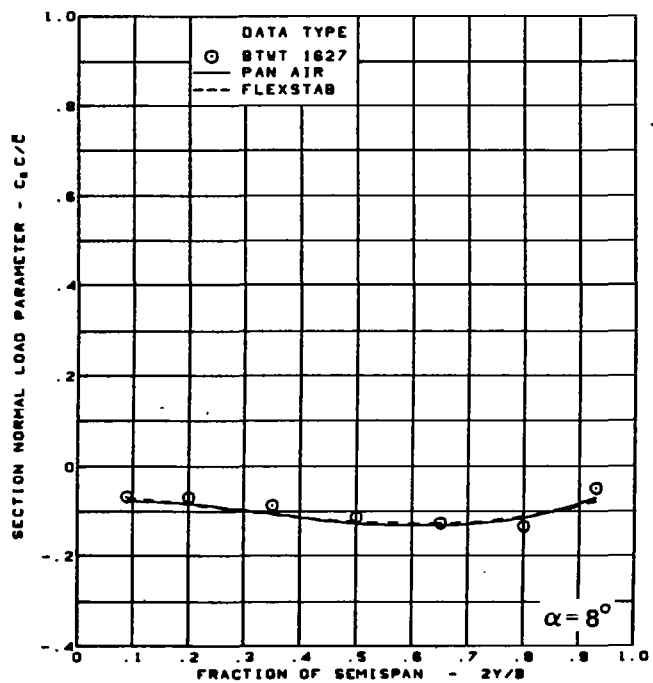
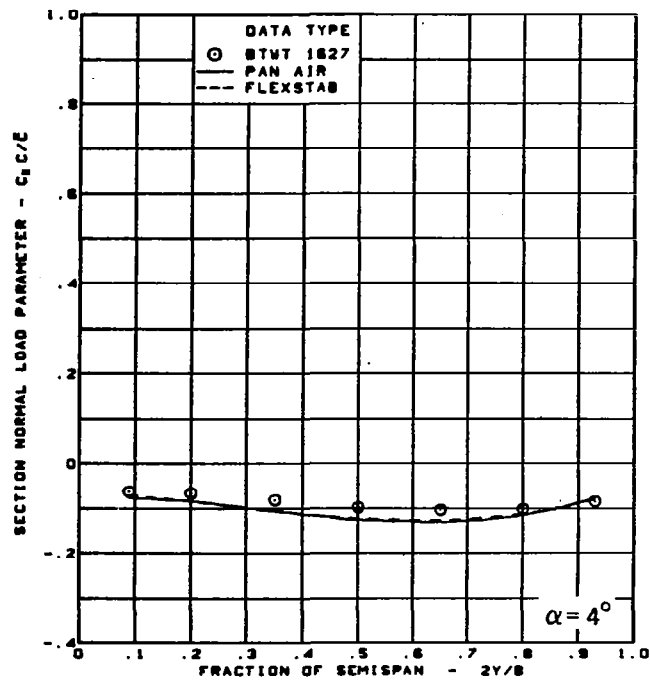
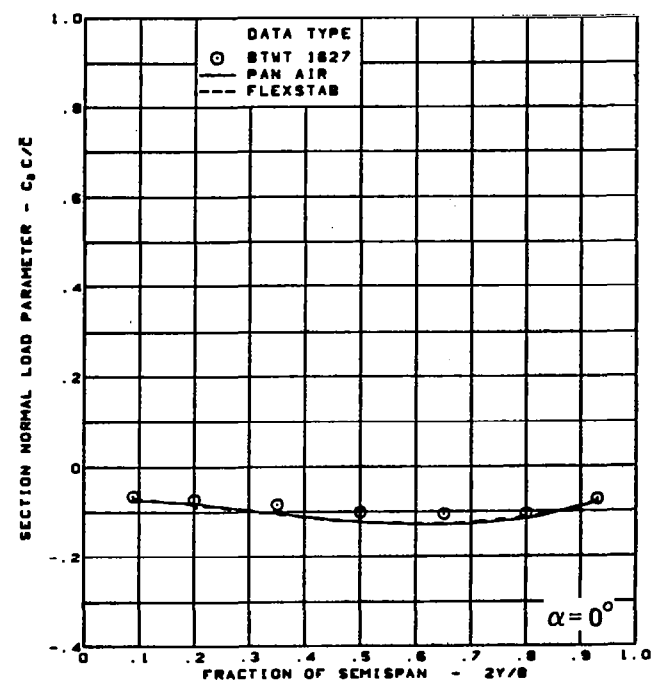
Cambered-twisted wing data minus flat wing data  
Rounded L.E.

L.E. deflection, full span =  $0.0^\circ$

T.E. deflection, full span =  $0.0^\circ$

(d) (Concluded)

Figure 50. - (Continued)

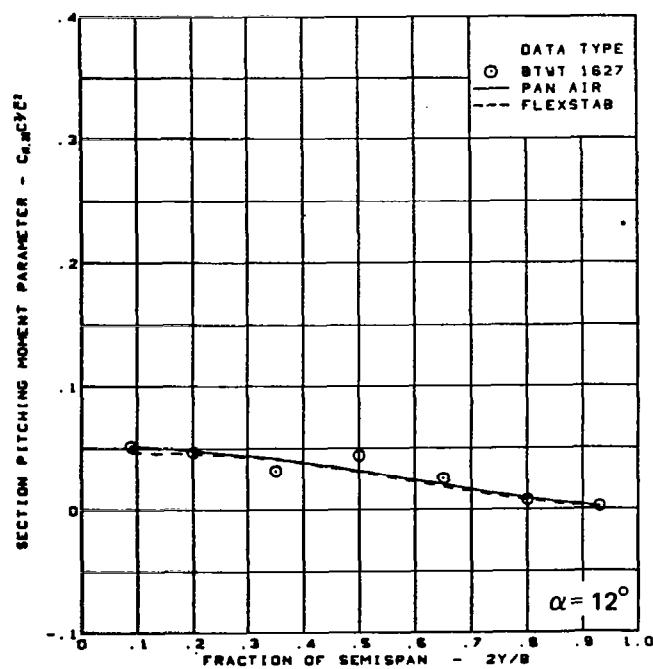
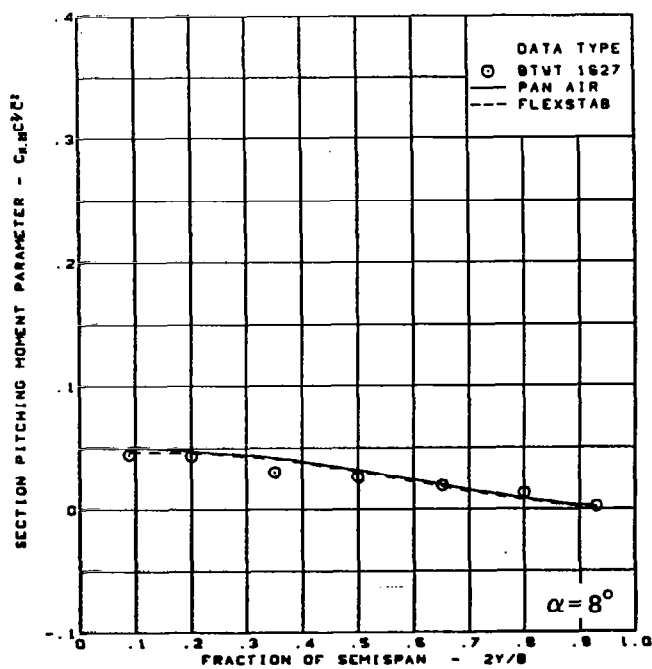
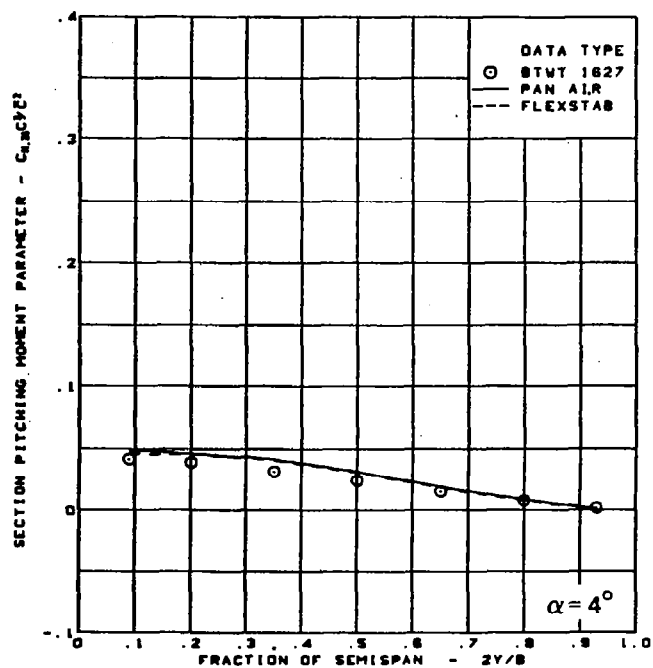
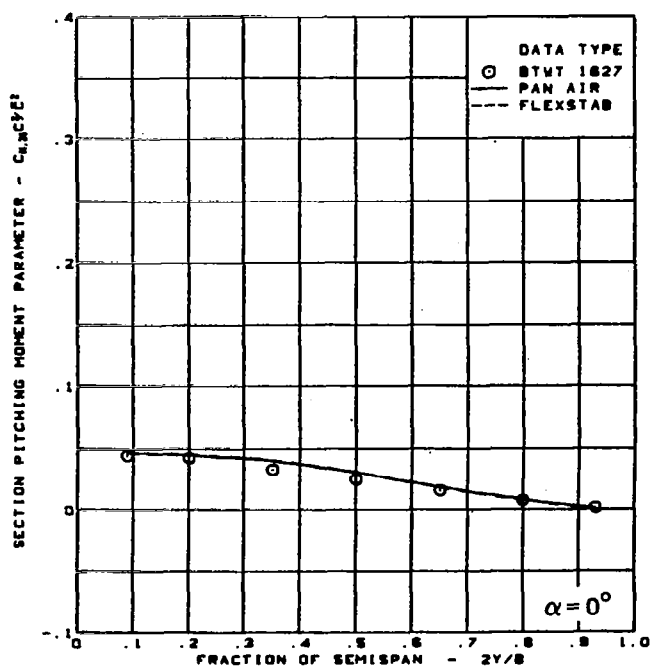


$M = 0.40$   
 Cambered-twisted wing data  
 minus flat wing data

Rounded L.E.  
 L.E. deflection, full span  $= 0.0^\circ$   
 T.E. deflection, full span  $= 0.0^\circ$

(e) Spanload Distributions - Normal Force

Figure 50. — (Continued)

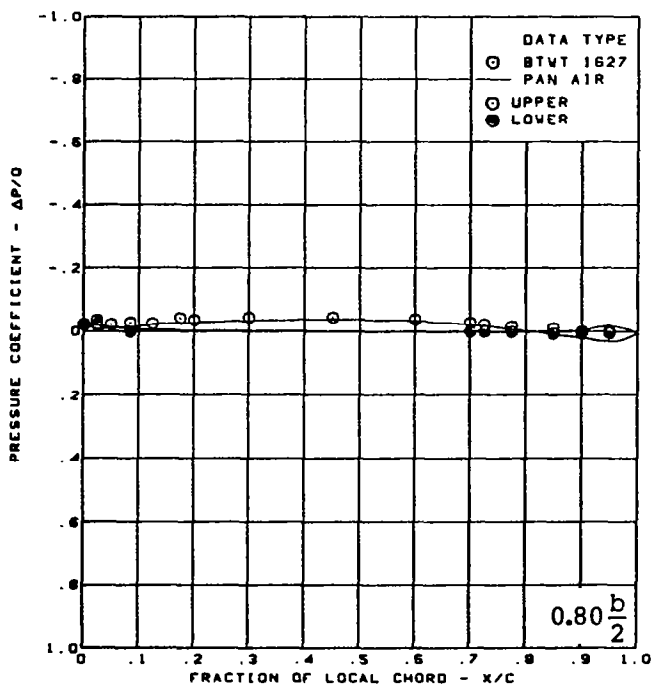
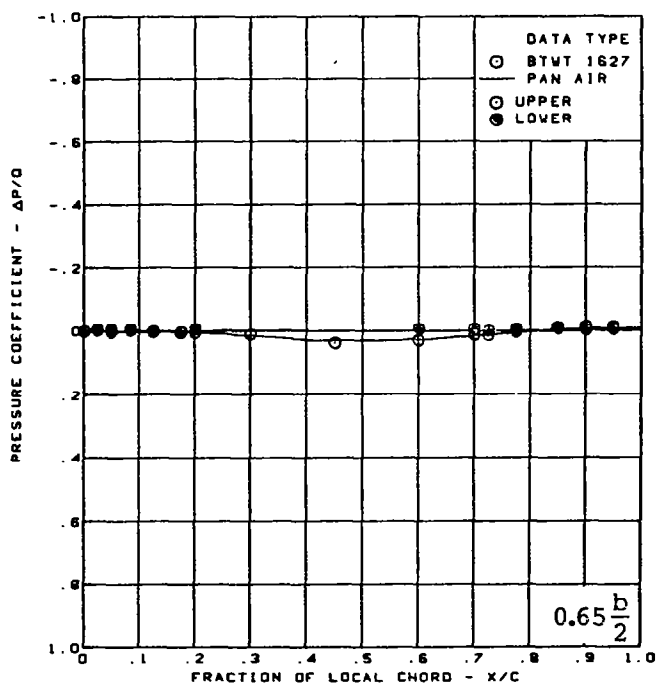
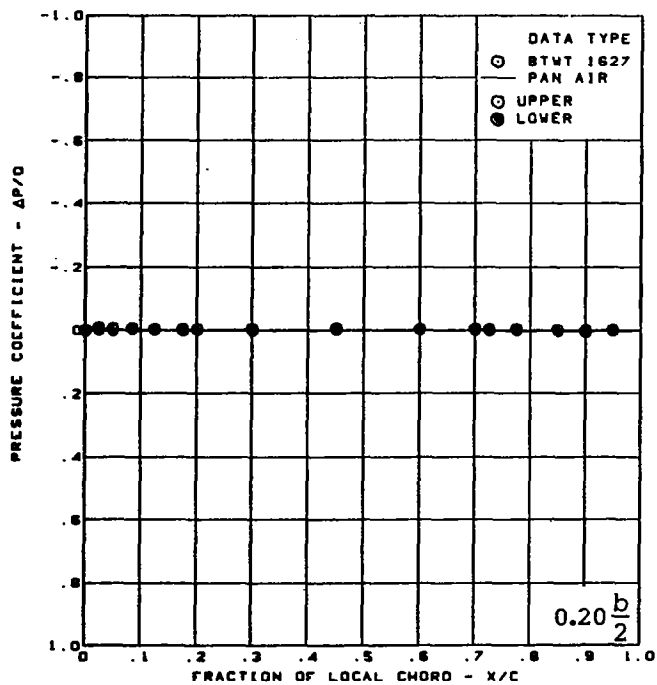
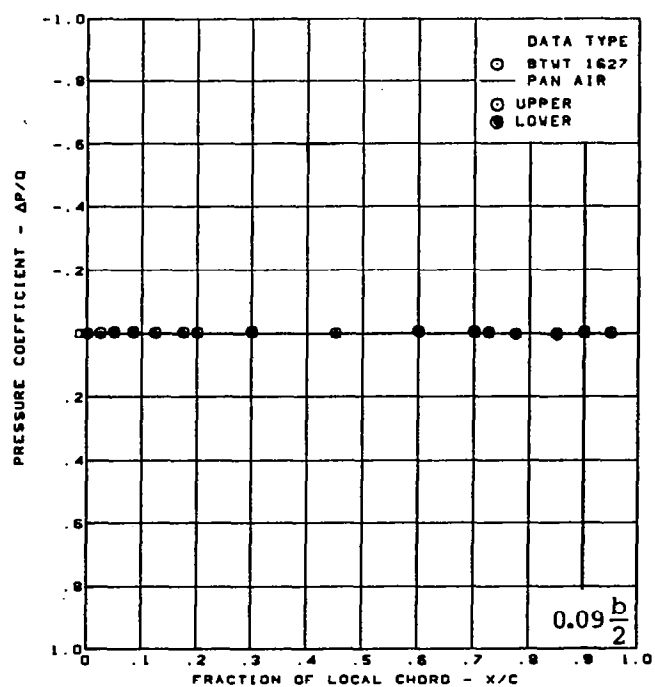


$M = 0.40$   
Cambered-twisted wing data  
minus flat wing data

Rounded L.E.  
L.E. deflection, full span =  $0.0^\circ$   
T.E. deflection, full span =  $0.0^\circ$

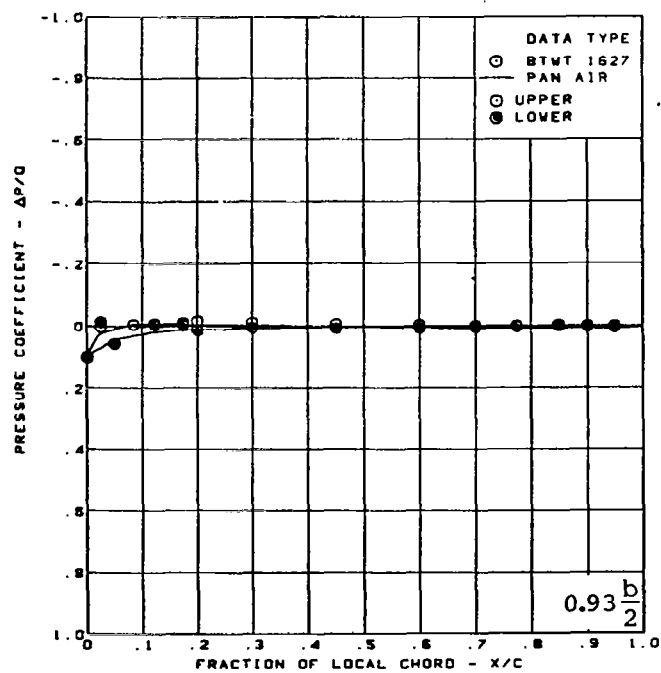
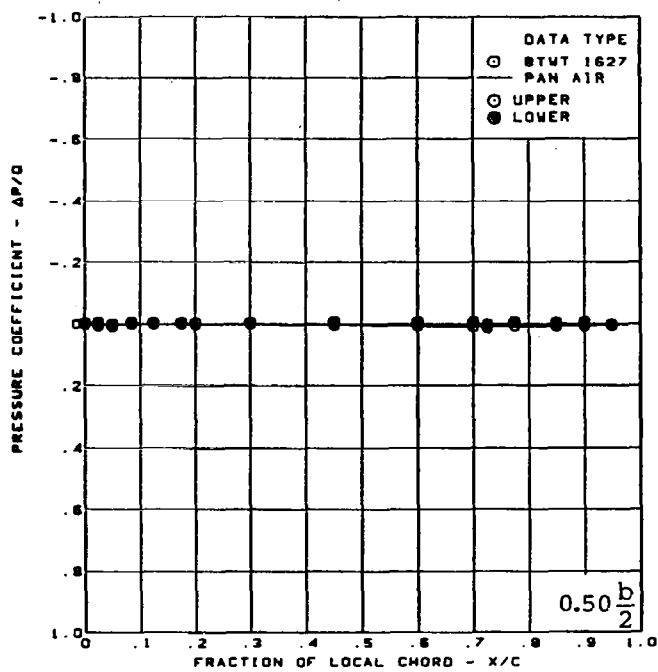
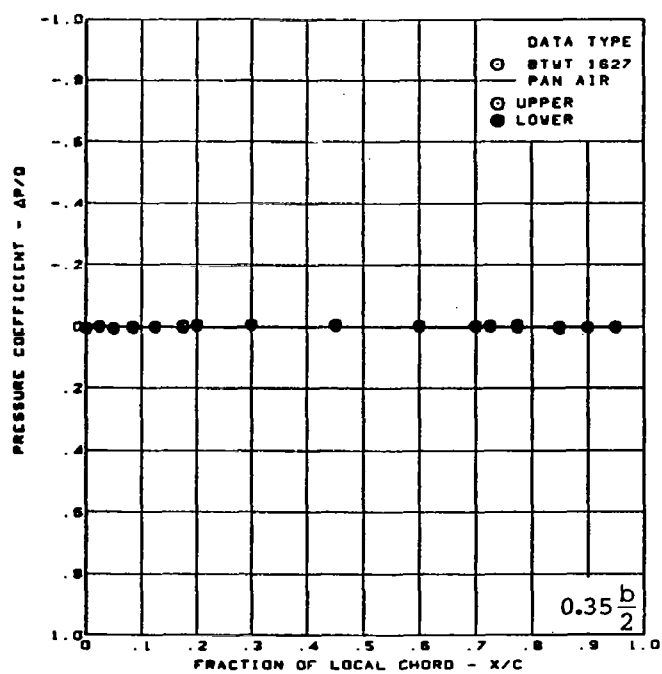
(f) Spanload Distributions - Pitching Moment

Figure 50. — (Concluded)



(a) Surface Chordwise Pressure Distributions,  $\alpha = 0^\circ$

Figure 51. — Wing Theory-to-Experiment Comparison—Incremental Effect of a Wing Fin; Cambered-Twisted Wing; T.E. Deflection, Full Span =  $0.0^\circ$ ;  $M = 0.40$



$M = 0.40$

$\alpha = 0^\circ$

Cambered-twisted wing, rounded L.E.

Fin on data minus fin off data

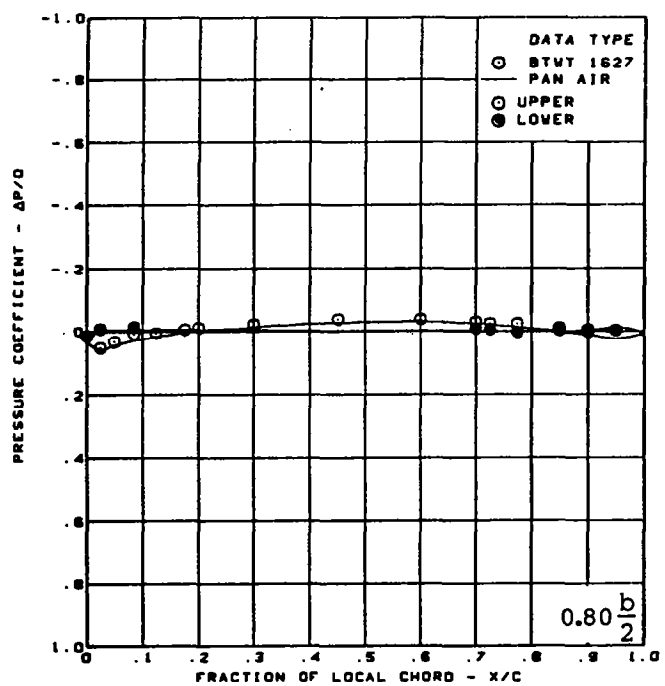
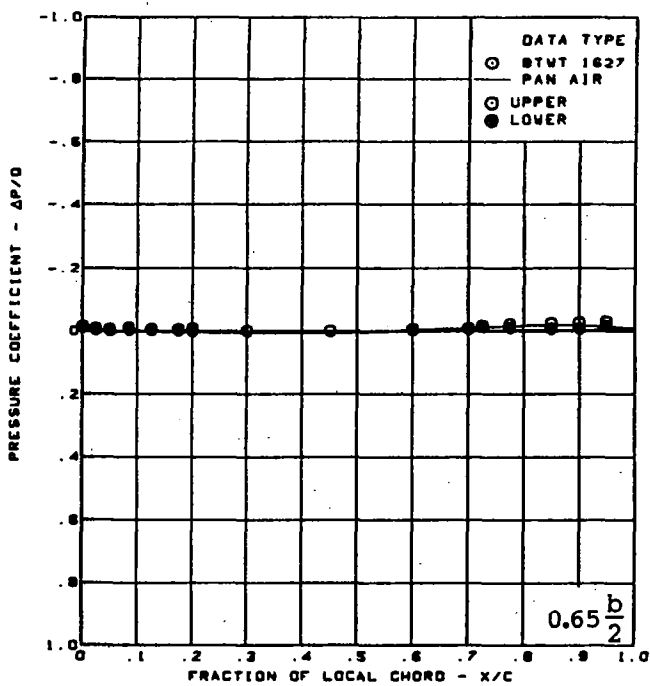
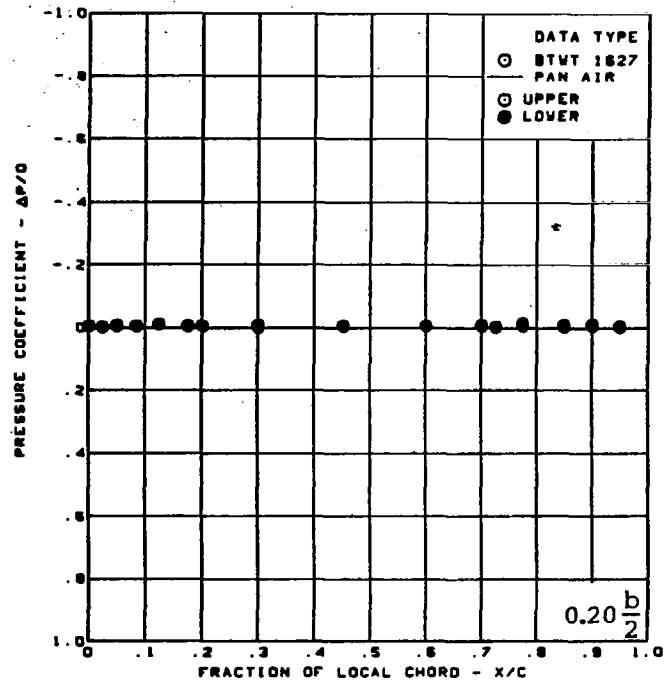
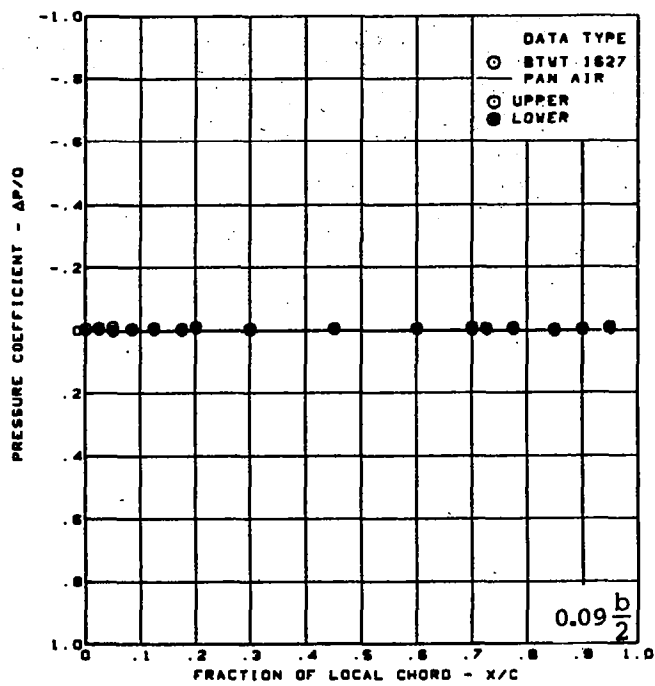
L.E. deflection, full span =  $0.0^\circ$

T.E. deflection, full span =  $0.0^\circ$

(a) (Concluded)

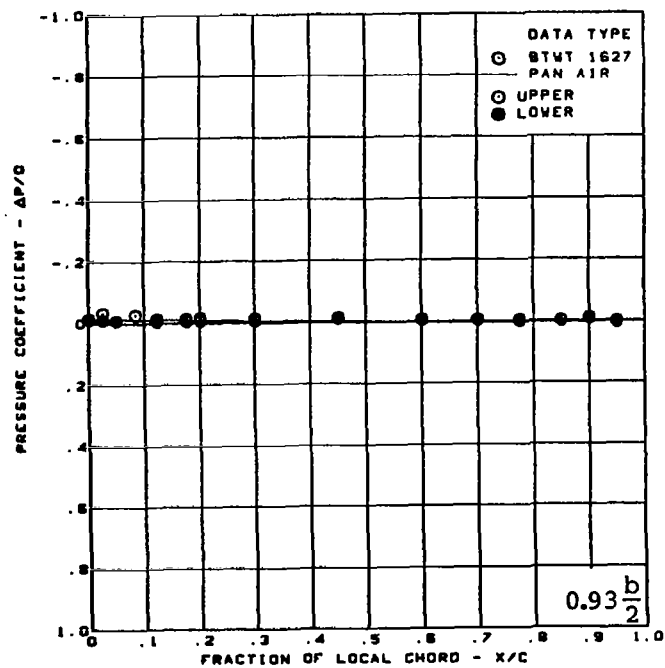
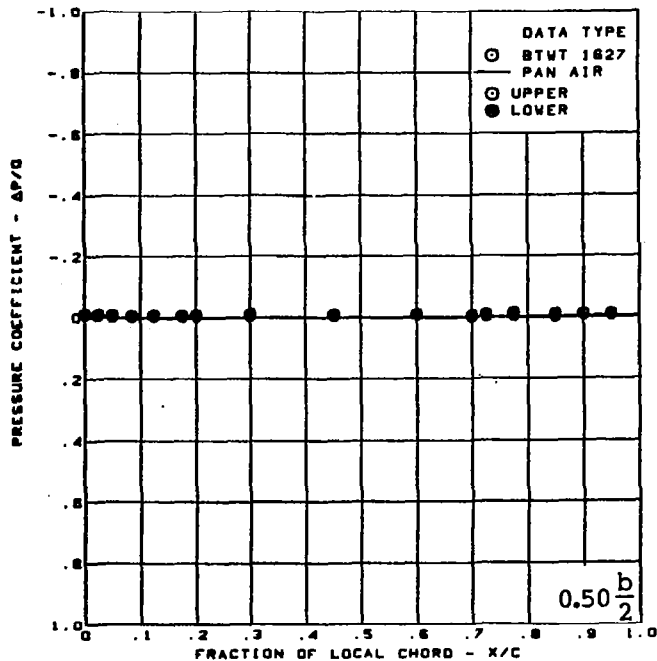
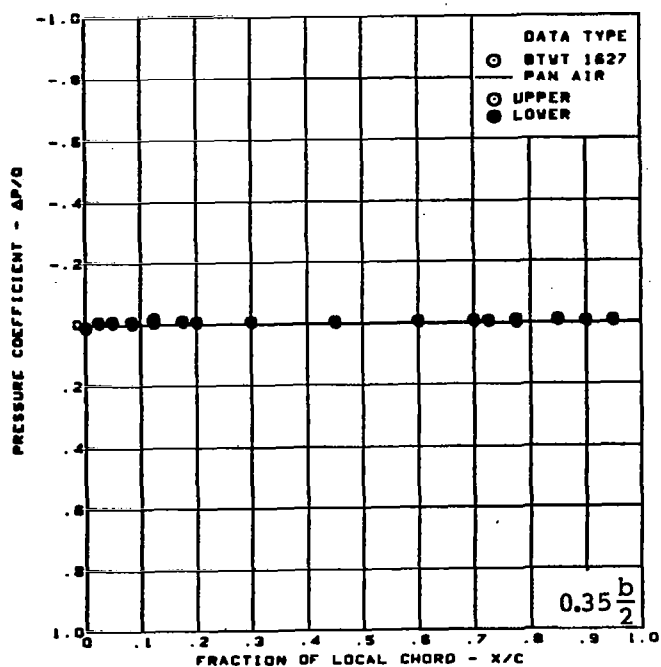
Figure 51. - (Continued)





(b) Surface Chordwise Pressure Distributions,  $\alpha = 4^\circ$

Figure 51. - (Continued)



$M = 0.40$

$\alpha = 4^\circ$

Cambered-twisted wing, rounded L.E.

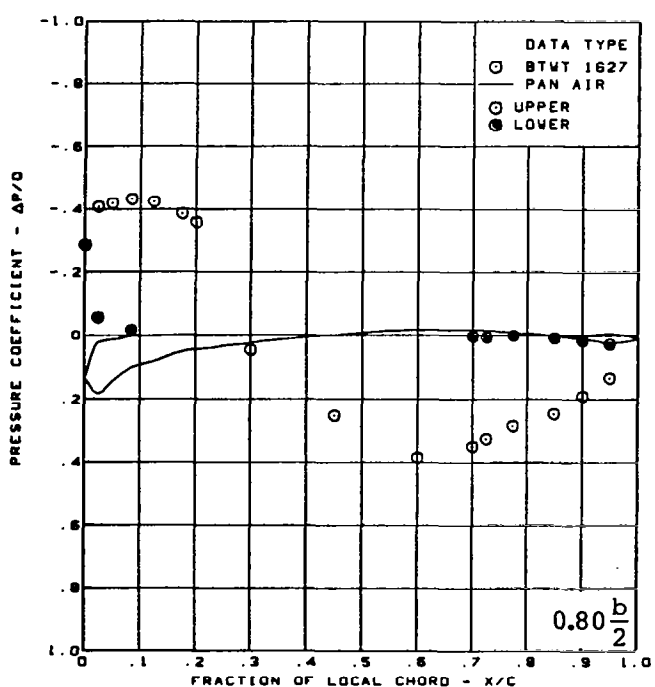
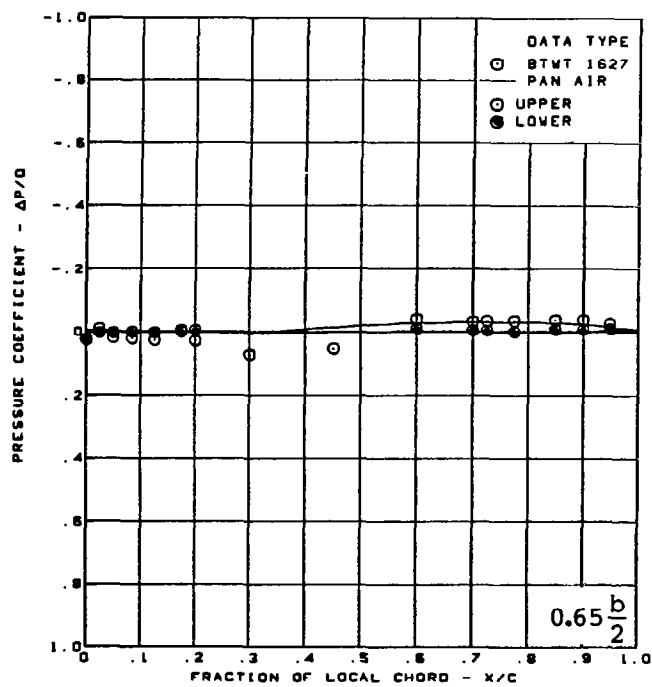
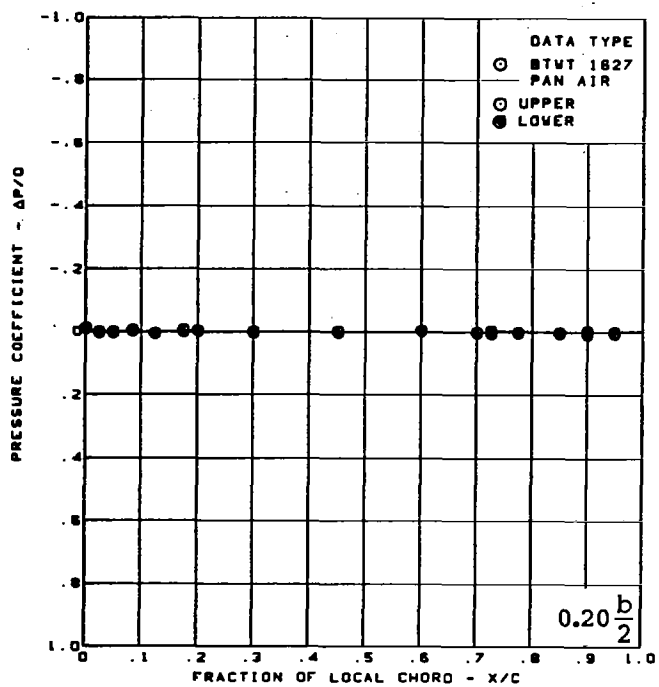
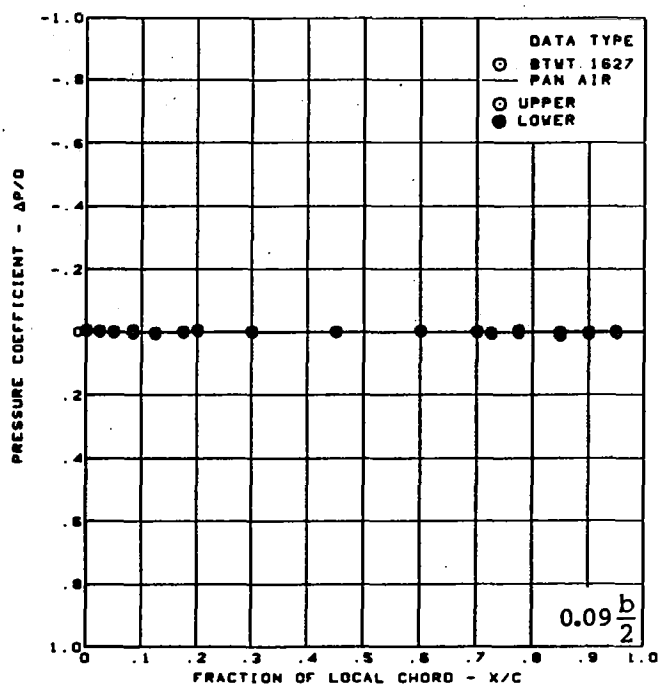
Fin on data minus fin off data

L.E. deflection, full span  $\approx 0.0^\circ$

T.E. deflection, full span  $\approx 0.0^\circ$

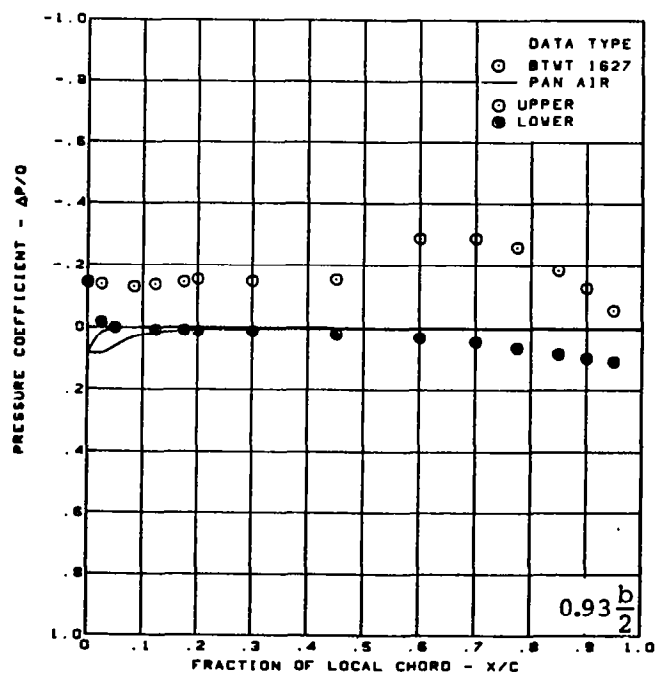
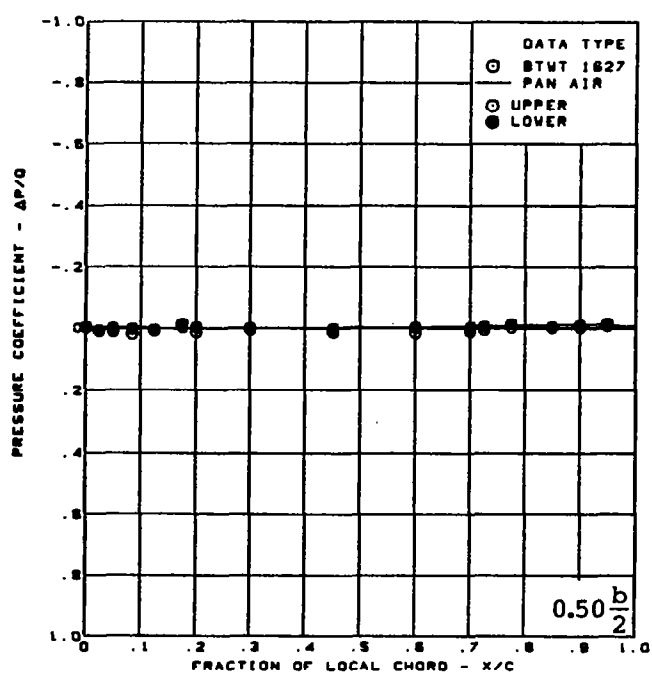
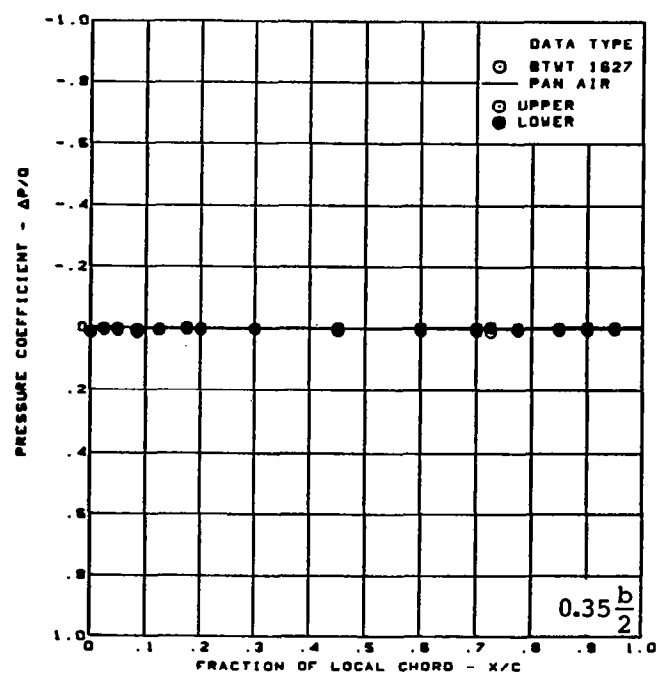
(b) (Concluded)

Figure 51. — (Continued)



(c) Surface Chordwise Pressure Distributions,  $\alpha = 8^\circ$

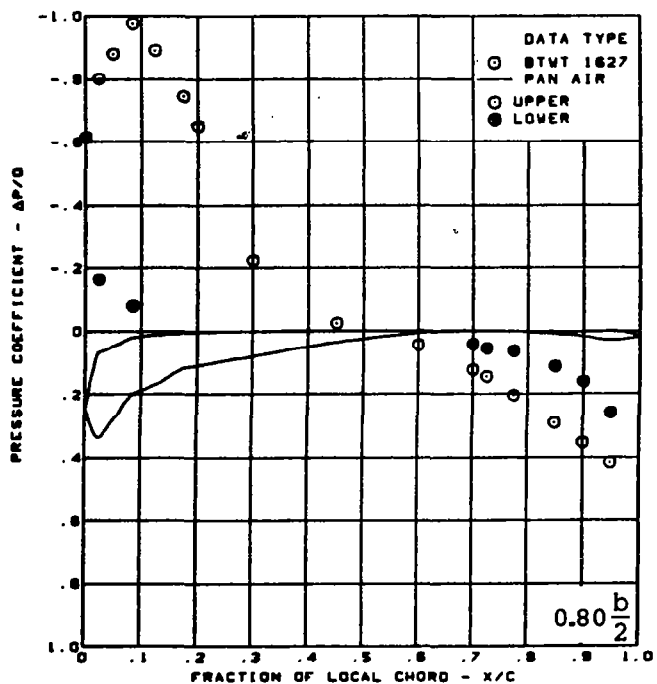
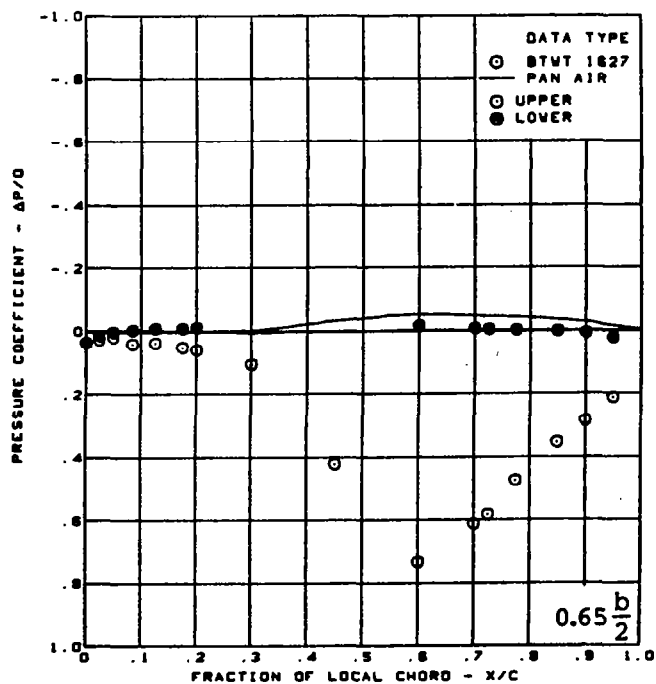
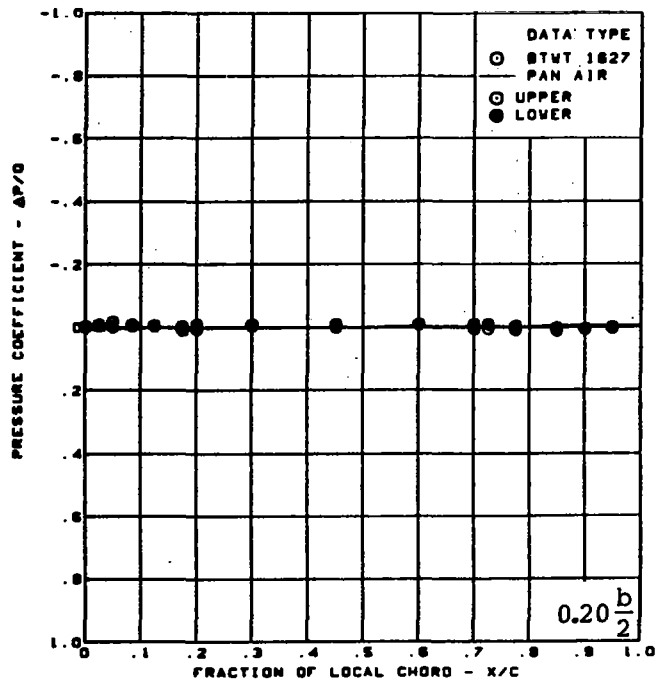
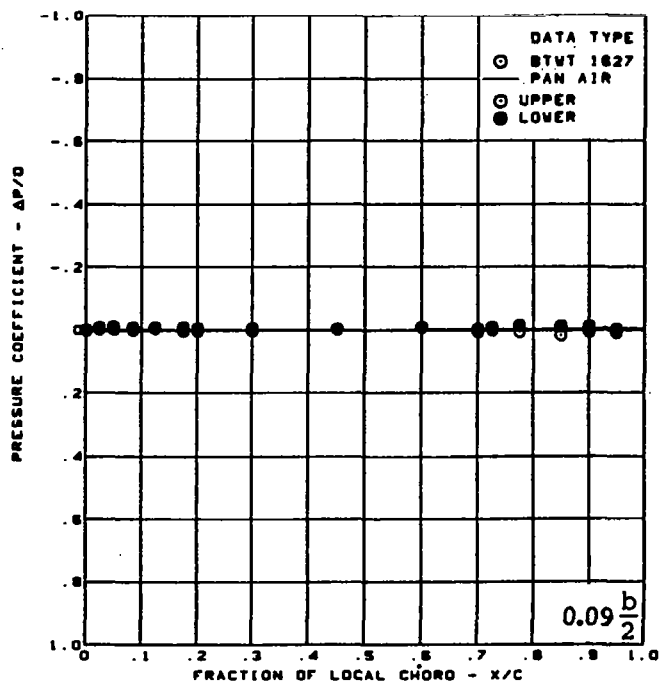
Figure 51. — (Continued)



$M = 0.40$   
 $\alpha = 8^\circ$   
 Cambered-twisted wing, rounded L.E.  
 Fin on data minus fin off data  
 L.E. deflection, full span =  $0.0^\circ$   
 T.E. deflection, full span =  $0.0^\circ$

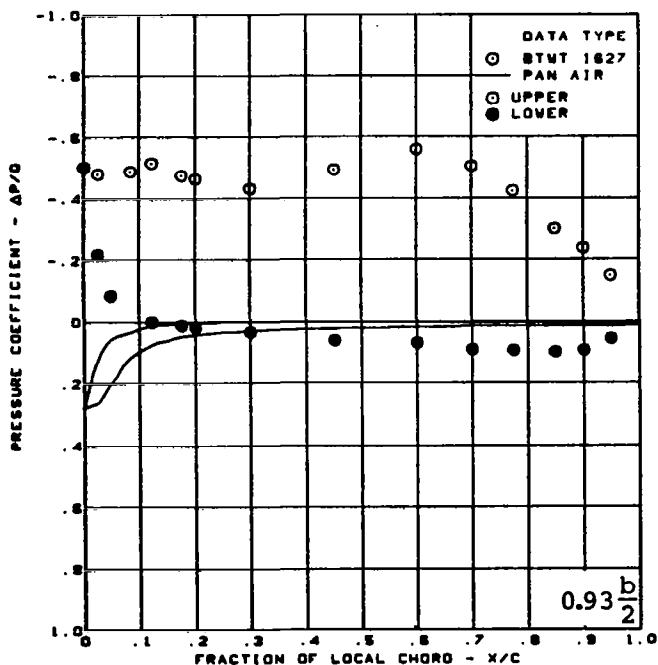
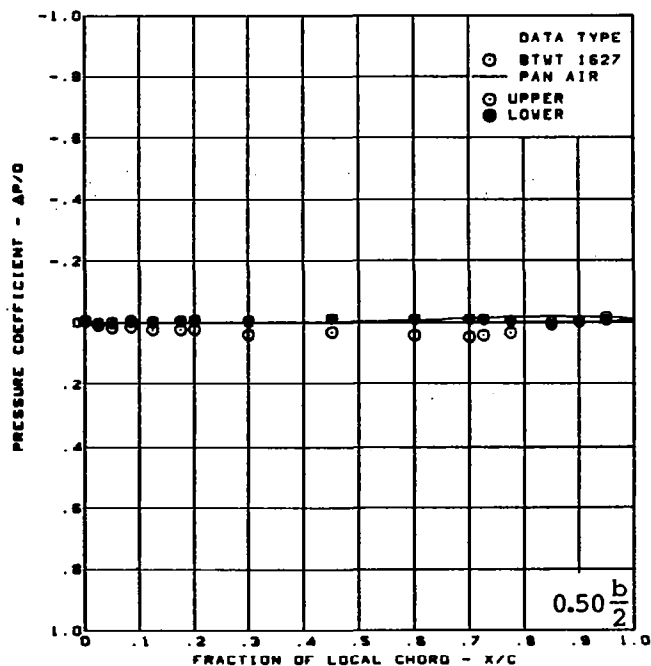
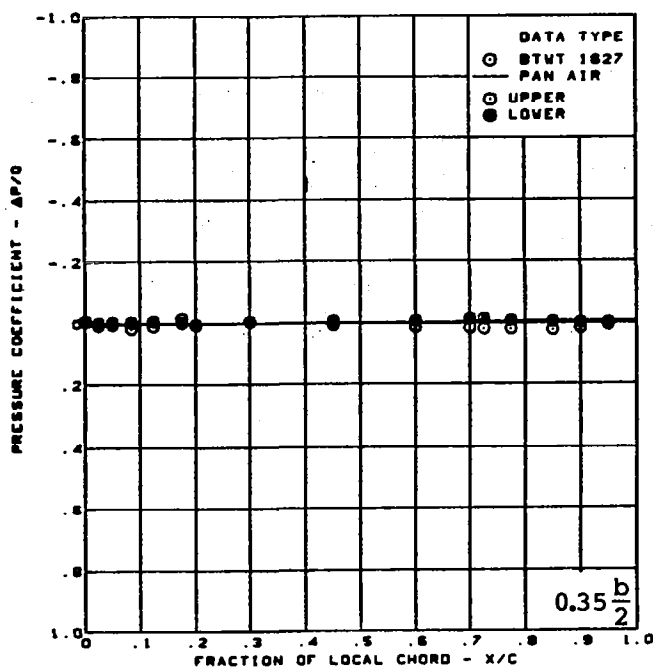
(c) (Concluded)

Figure 51. - (Continued)



(d) Surface Chordwise Pressure Distributions,  $\alpha = 12^\circ$

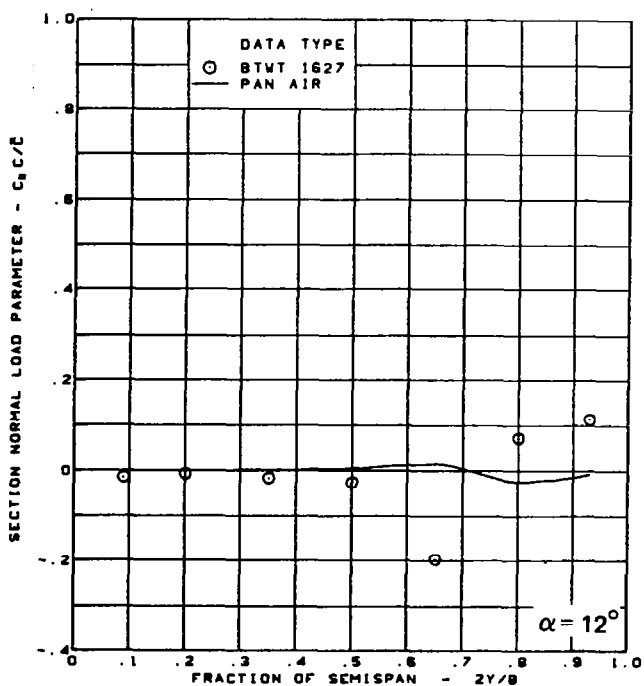
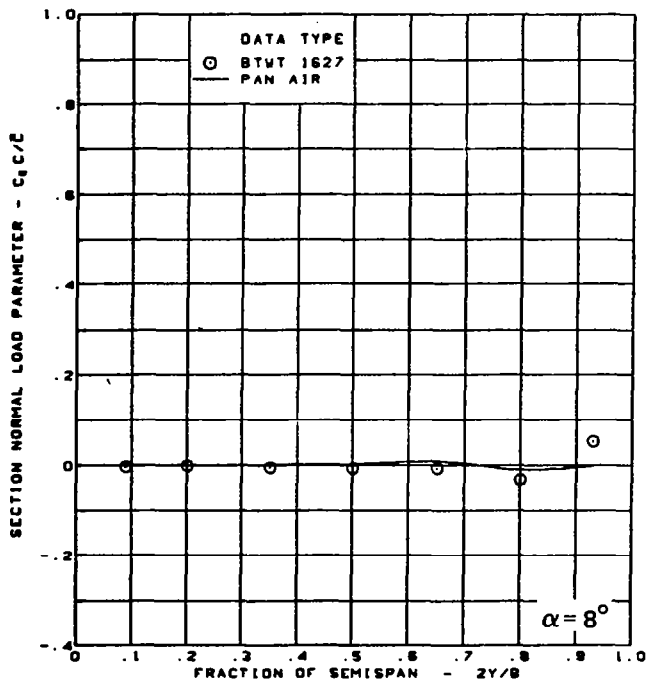
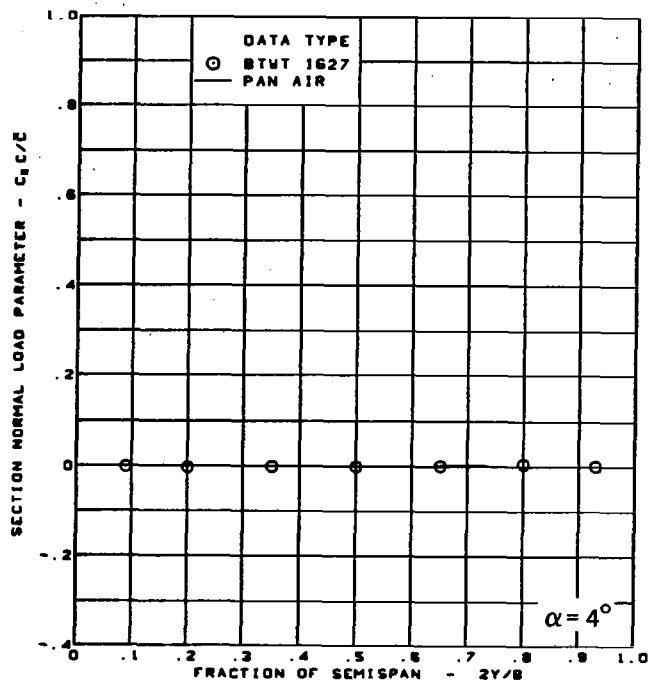
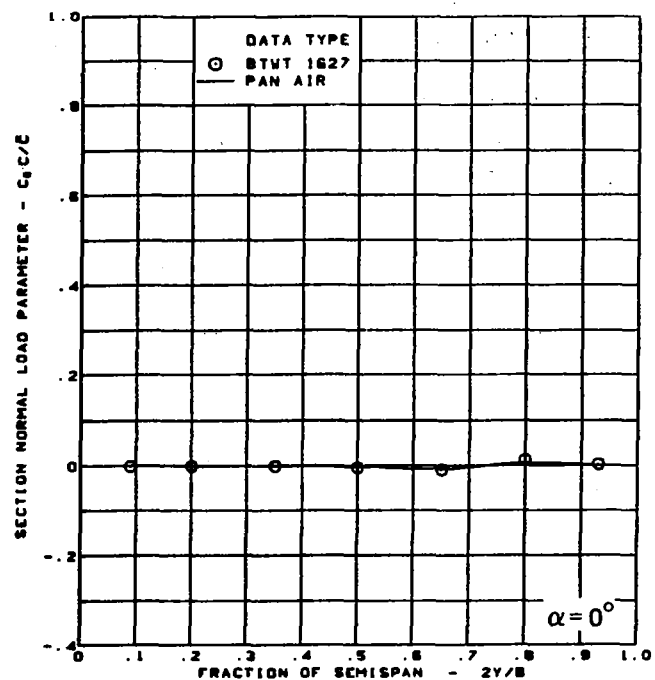
Figure 51. - (Continued)



$M = 0.40$   
 $\alpha = 12^\circ$   
 Cambered-twisted wing, rounded L.E.  
 Fin on data minus fin off data  
 L.E. deflection, full span =  $0.0^\circ$   
 T.E. deflection, full span =  $0.0^\circ$

(d) (Concluded)

Figure 51. — (Continued)



$M = 0.40$

Cambered-twisted wing, rounded L.E.

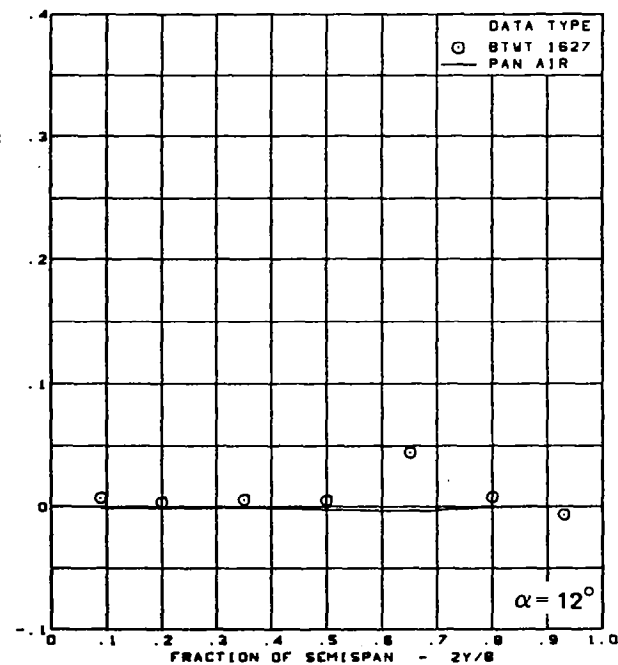
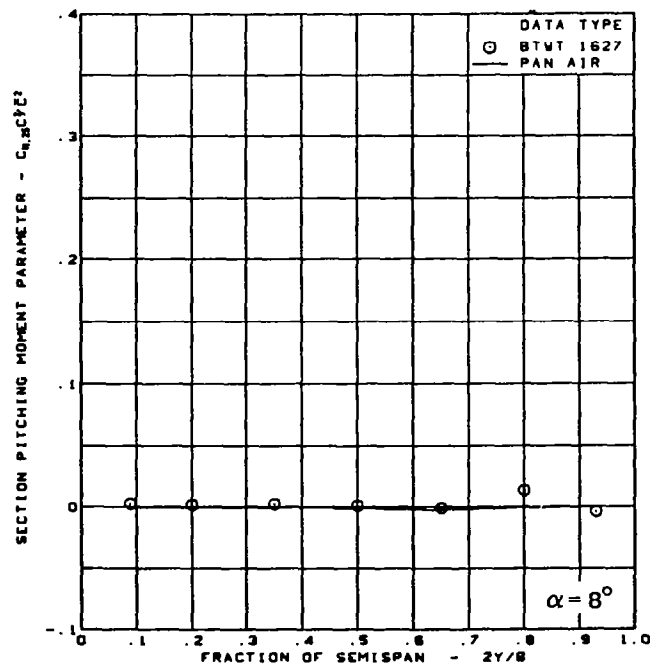
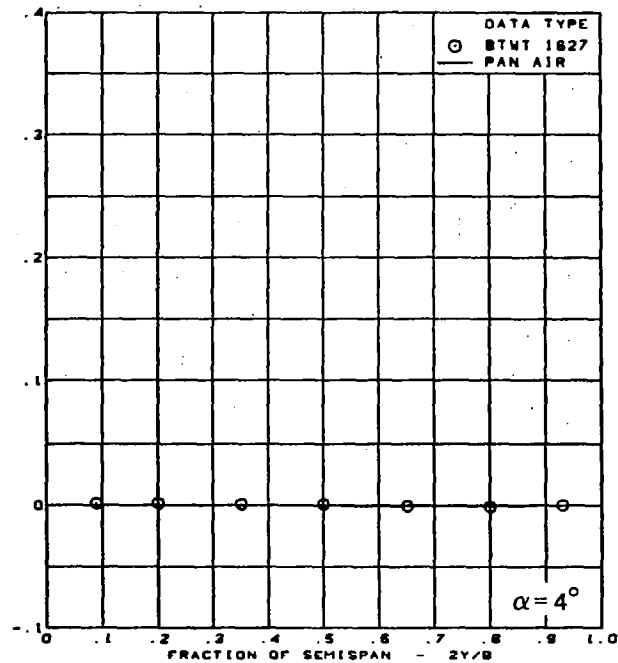
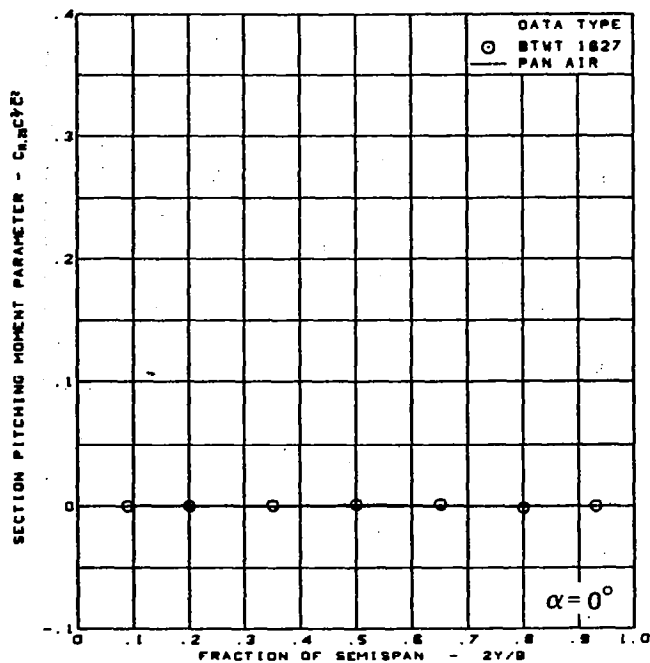
Fin on data minus fin off data

L.E. deflection, full span =  $0.0^\circ$

T.E. deflection, full span =  $0.0^\circ$

(e) Spanload Distributions - Normal Force

Figure 51. - (Continued)



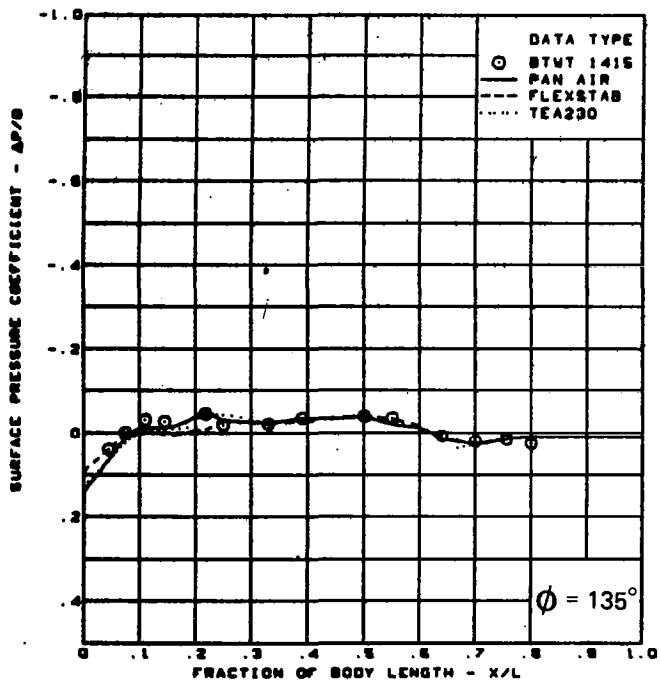
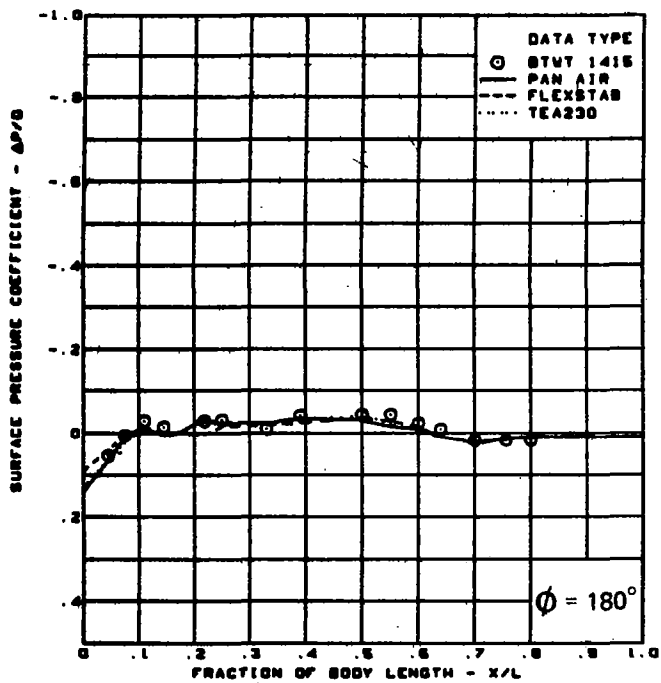
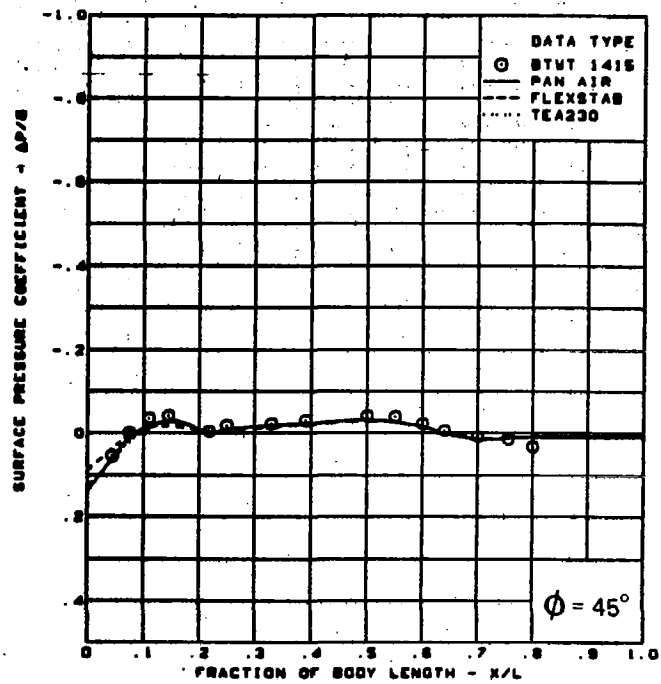
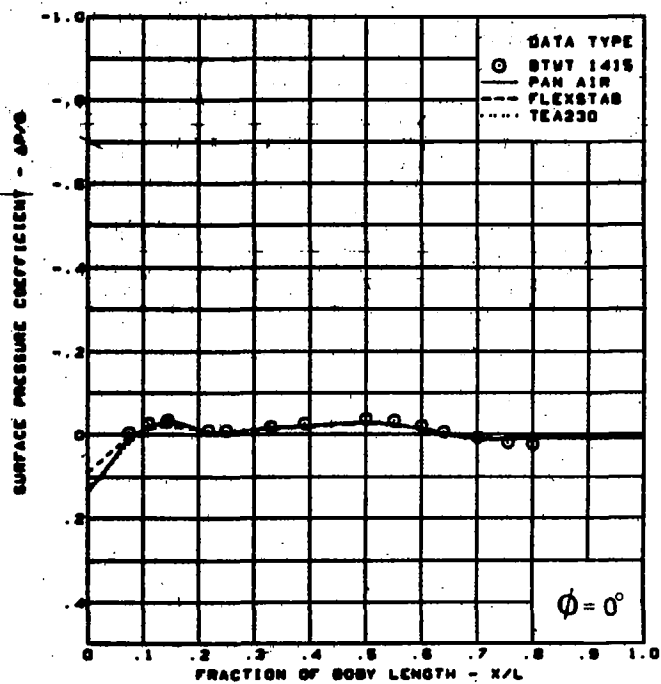
$M = 0.40$   
 Cambered-twisted wing, rounded L.E.  
 Fin on data minus fin off data

L.E. deflection, full span =  $0.0^\circ$   
 T.E. deflection, full span =  $0.0^\circ$

(f) Spanload Distributions - Pitching Moment

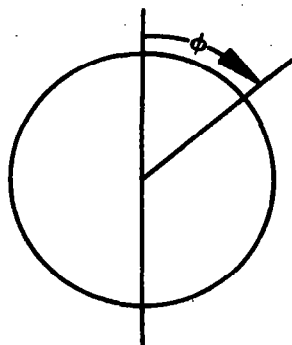
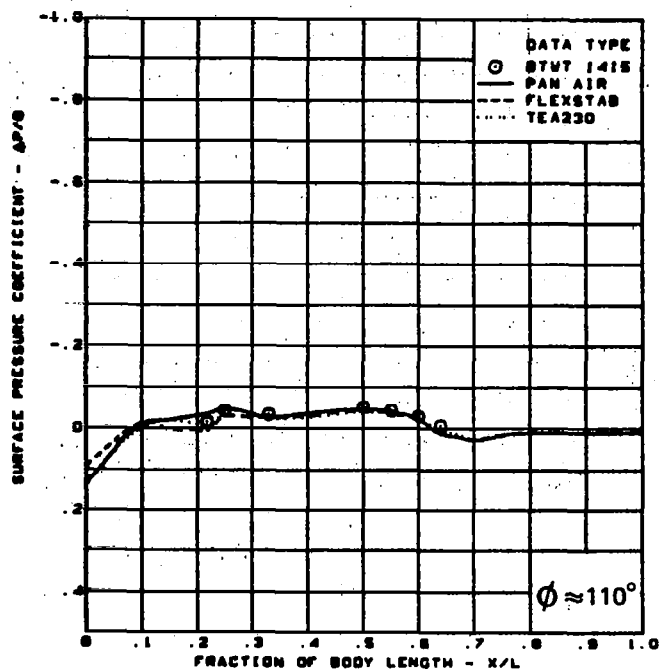
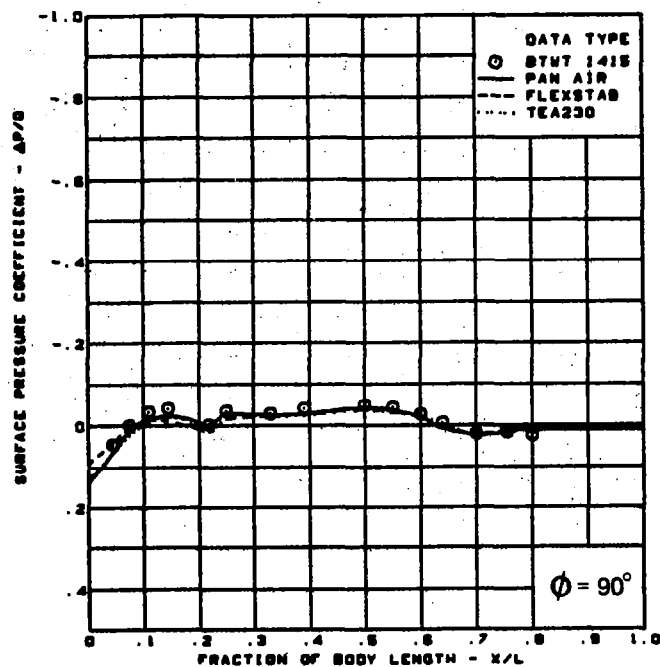
Figure 51. — (Concluded)





(a) Surface Longitudinal Pressure Distributions,  $\alpha = 0^\circ$

Figure 52.—Body Theory-to-Experiment Comparison; Flat Wing; T.E. Deflection, Full Span =  $0.0^\circ$ ;  $M = 0.40$



$M = 0.40$  (run 269)

$\alpha = 0^\circ$

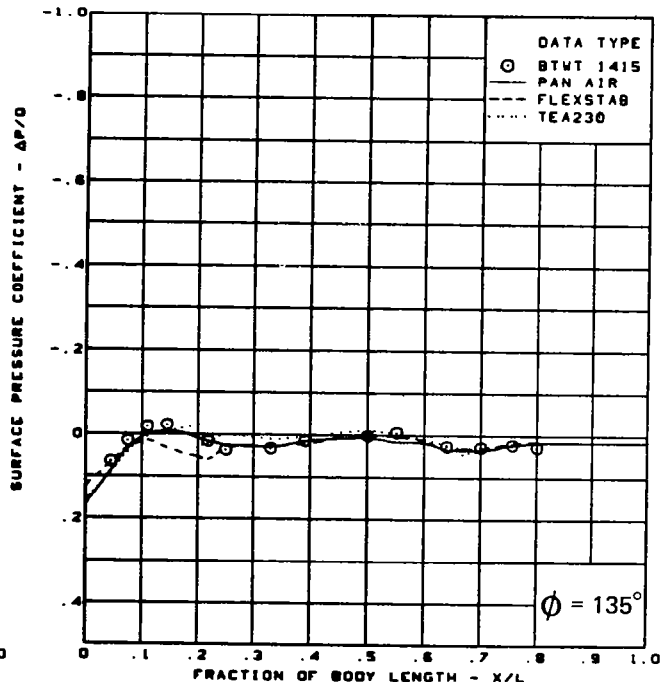
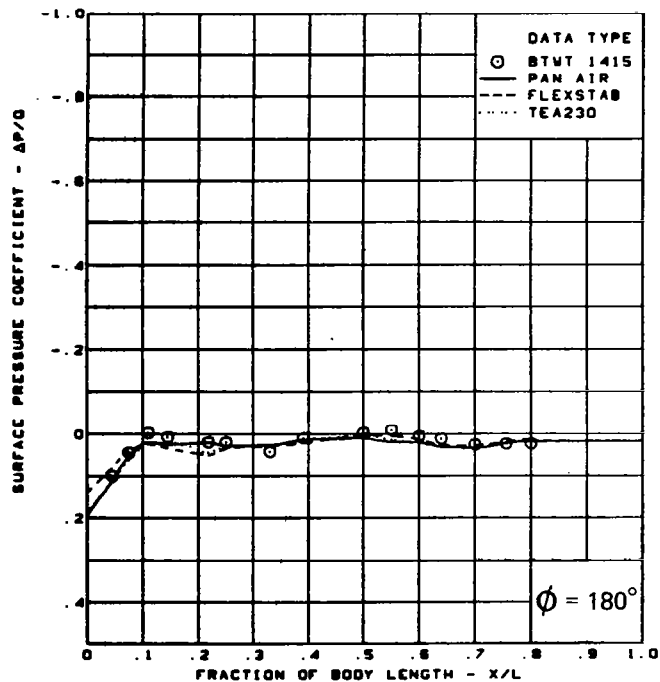
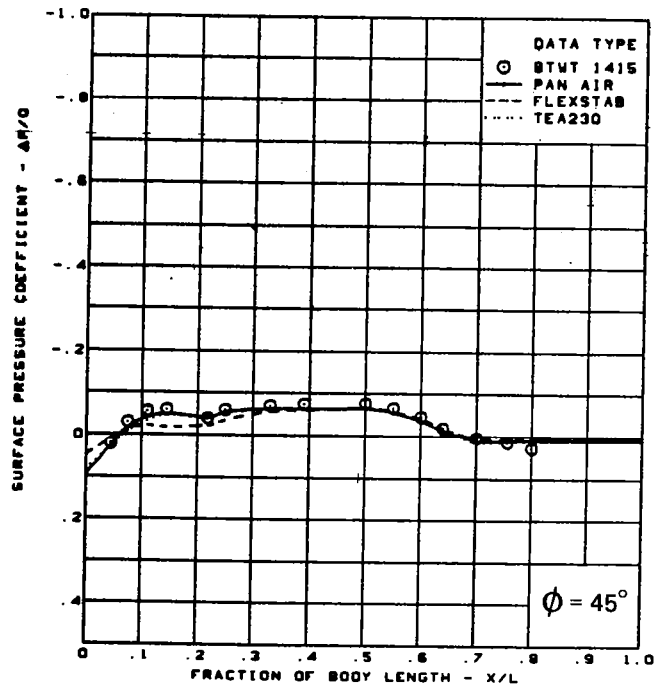
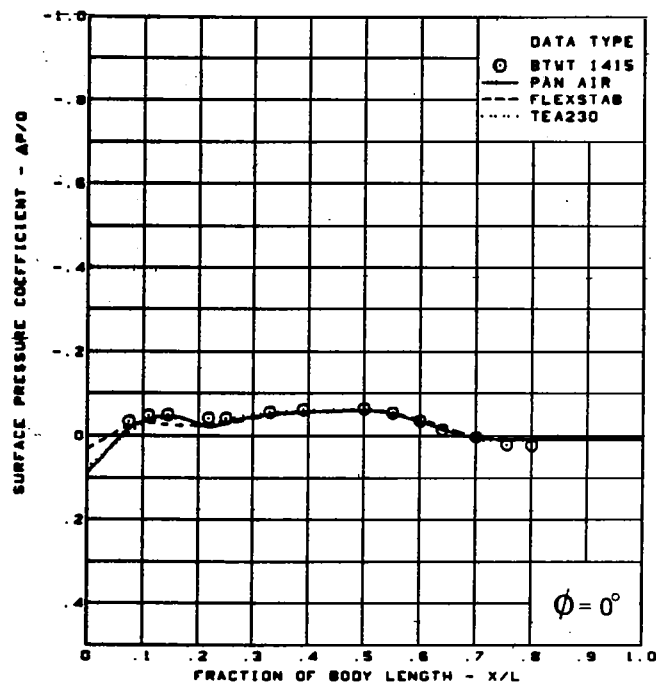
Flat wing, rounded L.E.

L.E. deflection, full span =  $0.0^\circ$

T.E. deflection, full span =  $0.0^\circ$

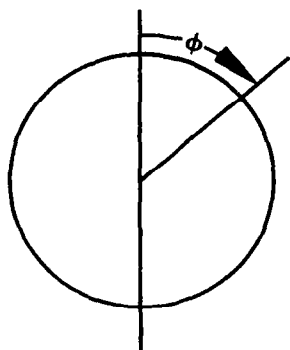
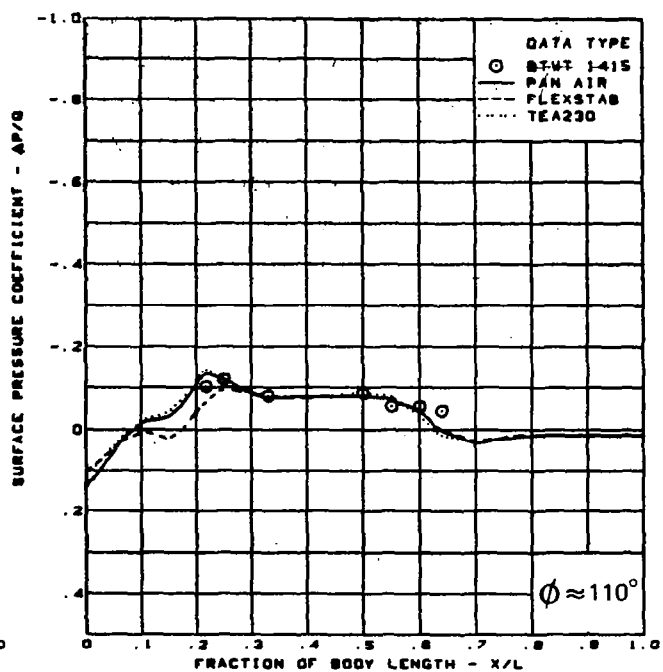
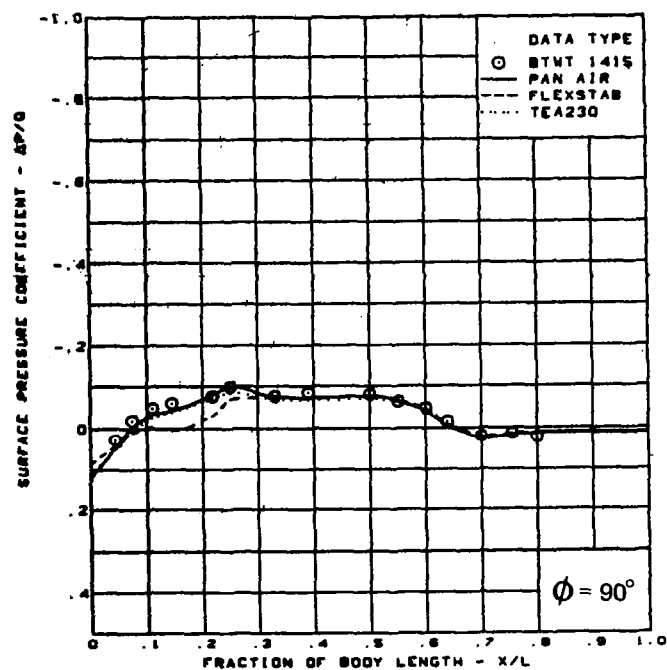
(a) (Concluded)

Figure 52. —(Continued)



(b) Surface Longitudinal Pressure Distributions,  $\alpha = 4^\circ$

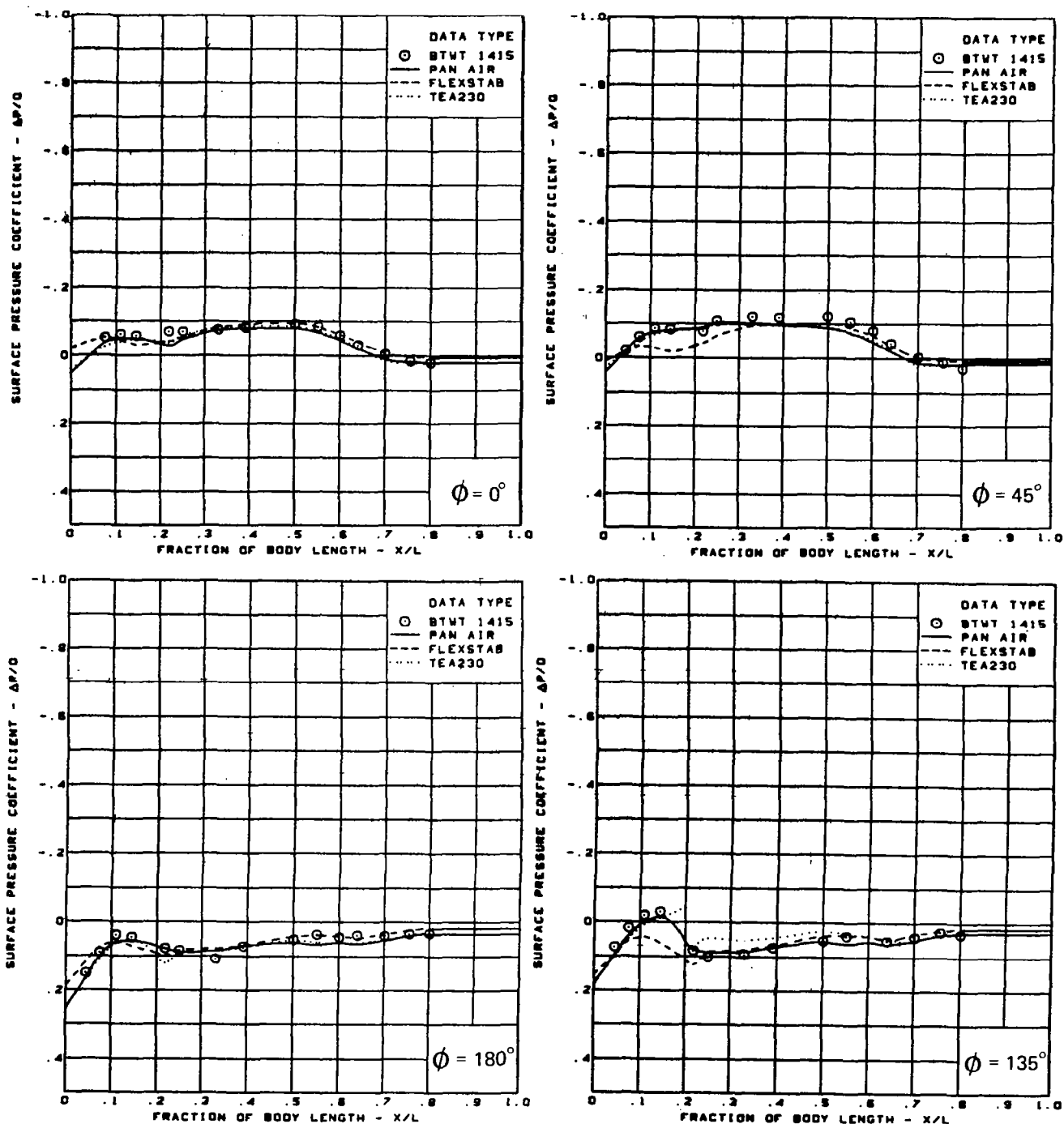
Figure 52.-(Continued)



$M = 0.40$  (run 269)  
 $\alpha = 4^\circ$   
 Flat wing, rounded L. E.  
 L.E. deflection, full span =  $0.0^\circ$   
 T.E. deflection, full span =  $0.0^\circ$

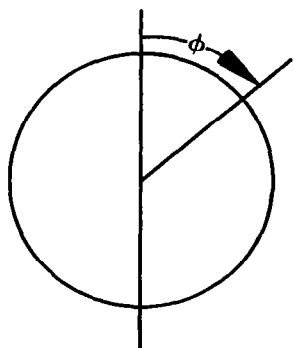
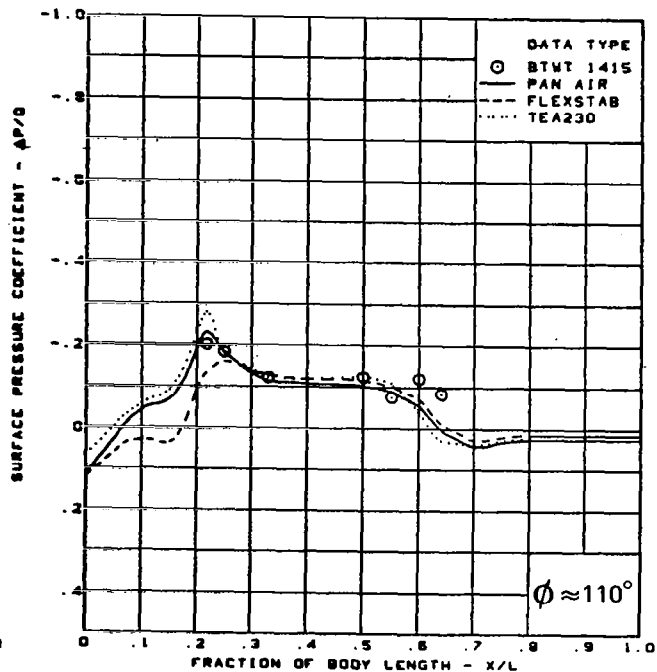
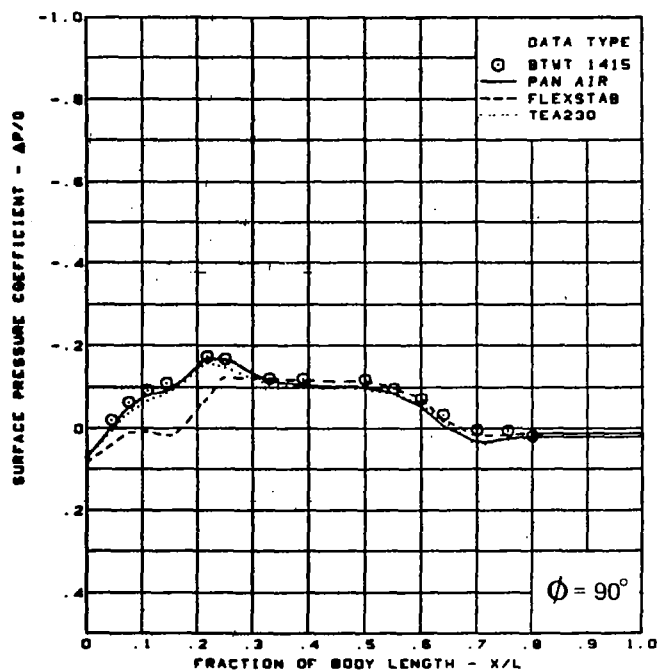
(b) (Concluded)

Figure 52. — (Continued)



(c) Surface Longitudinal Pressure Distributions,  $\alpha = 8^\circ$

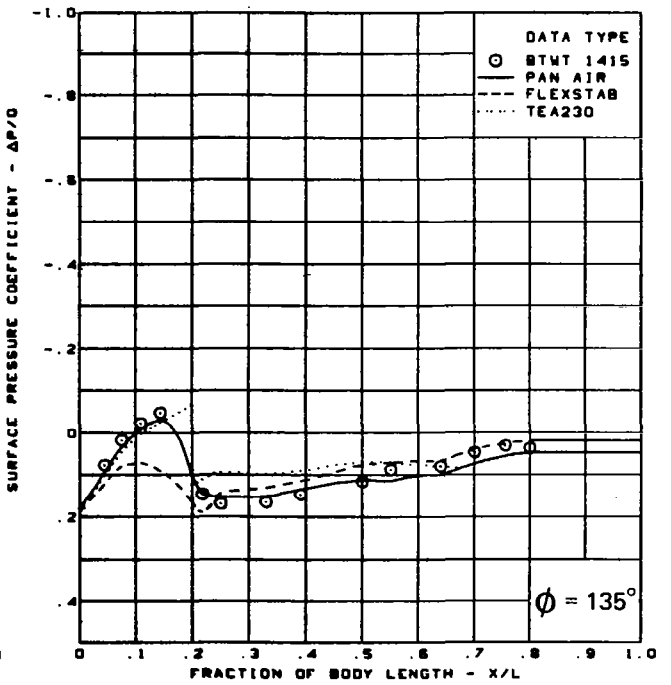
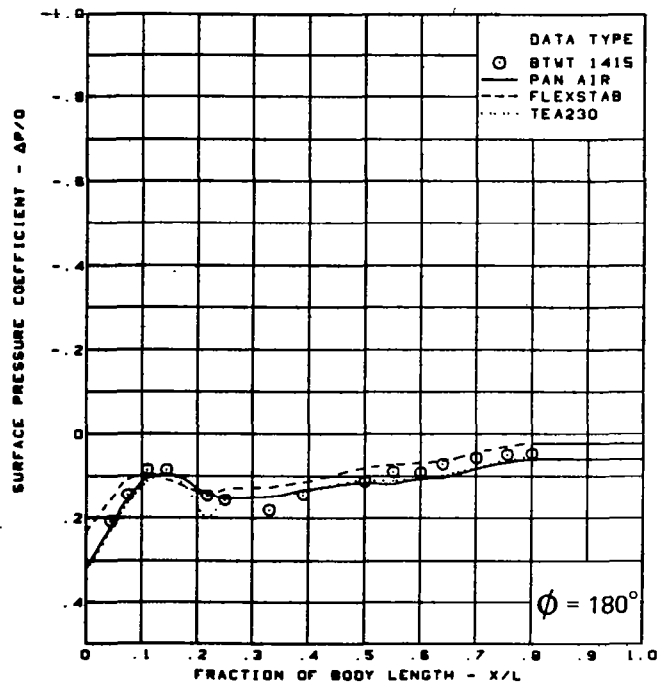
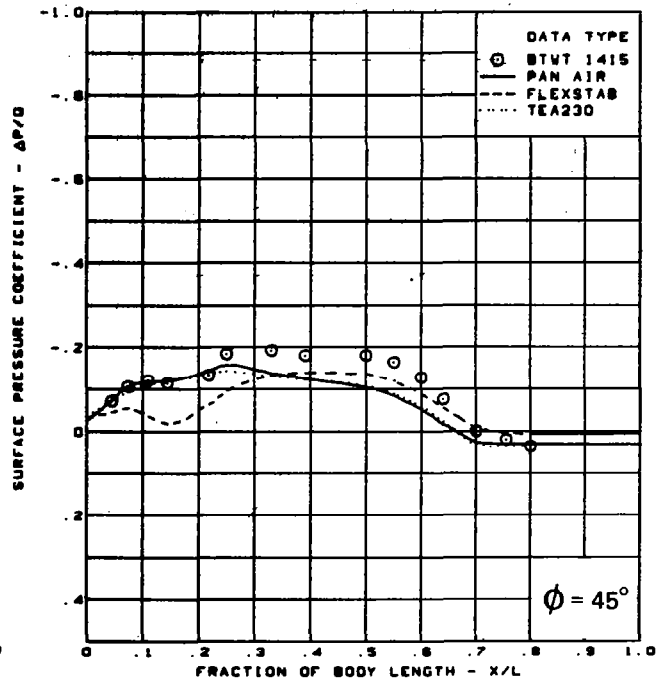
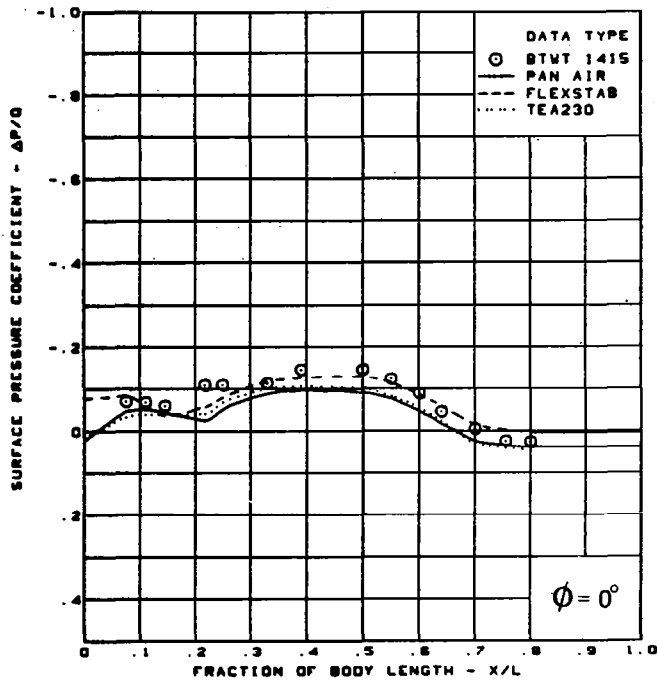
Figure 52. —(Continued)



$M = 0.40$  (run 269)  
 $\alpha = 8^\circ$   
 Flat wing, rounded L. E.  
 L.E. deflection, full span =  $0.0^\circ$   
 T.E. deflection, full span =  $0.0^\circ$

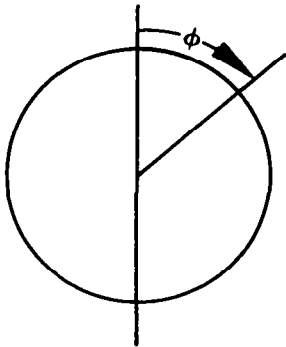
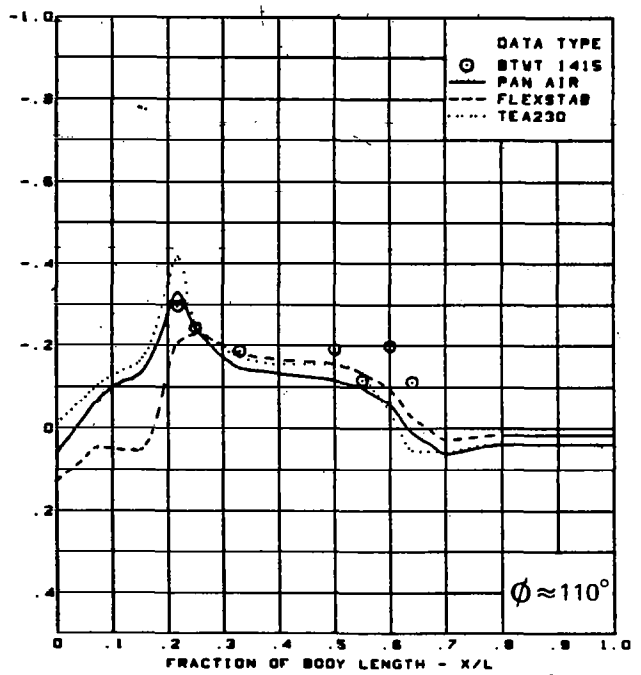
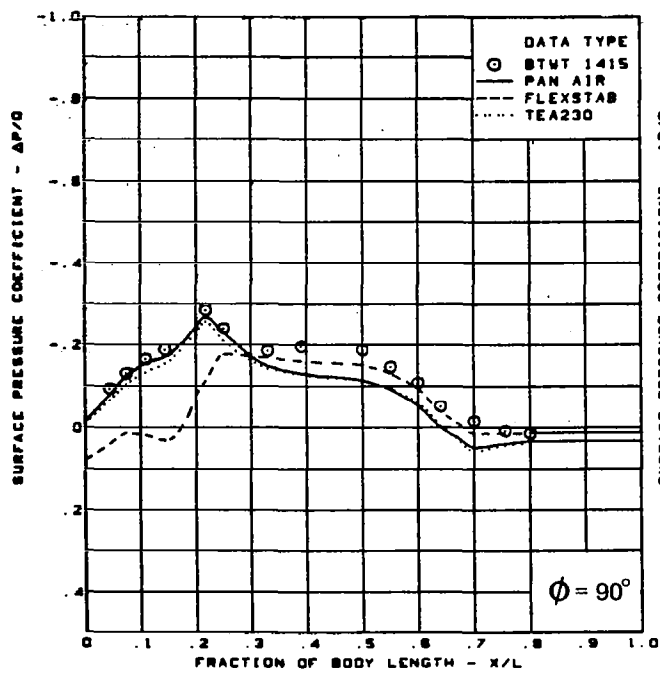
(c) (Concluded)

Figure 52. —(Continued)



(d) Surface Longitudinal Pressure Distributions,  $\alpha = 12^\circ$

Figure 52. —(Continued)

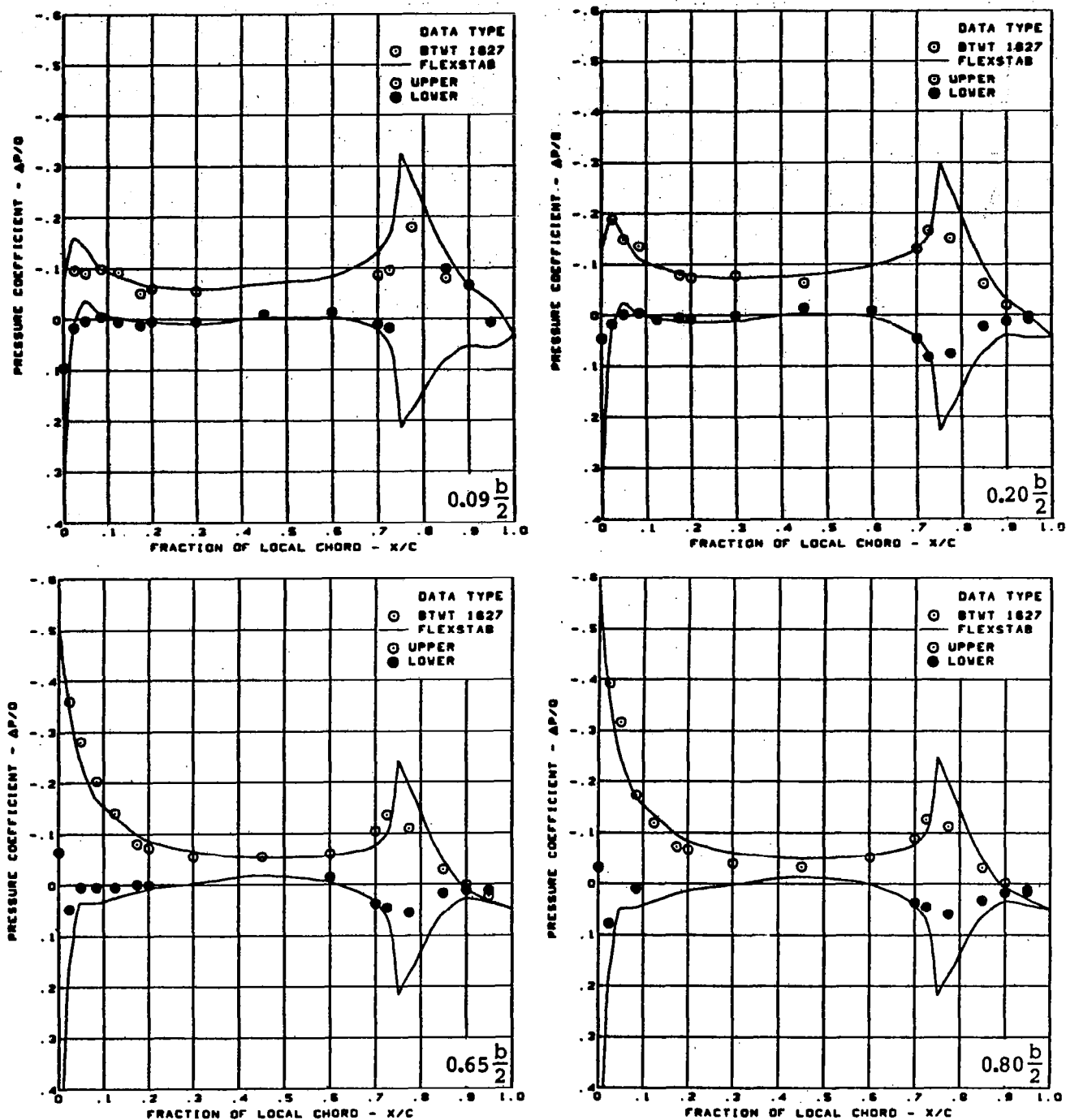


$M = 0.40$  (run 269)  
 $\alpha = 12^\circ$   
 Flat wing, rounded L. E.  
 L.E. deflection, full span =  $0.0^\circ$   
 T.E. deflection, full span =  $0.0^\circ$

(d) (Concluded)

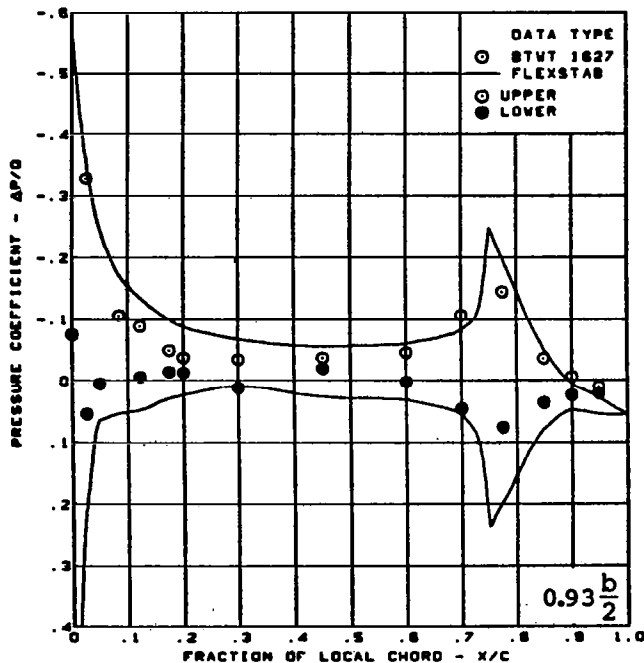
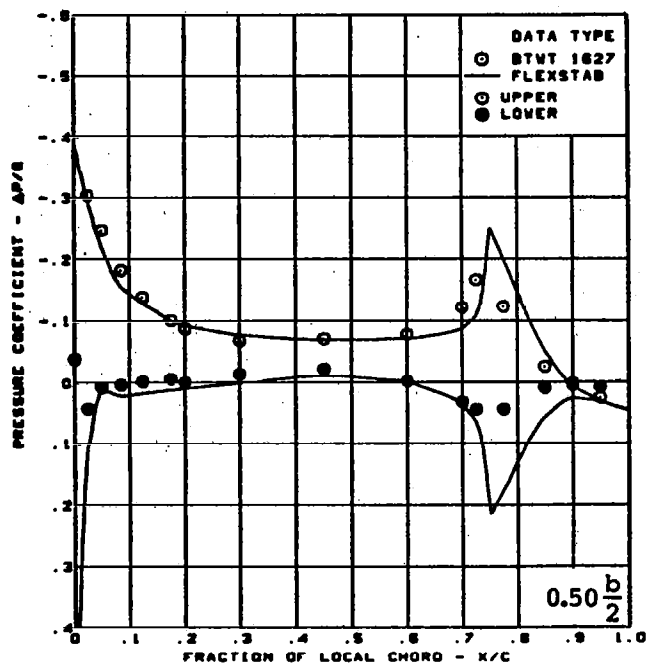
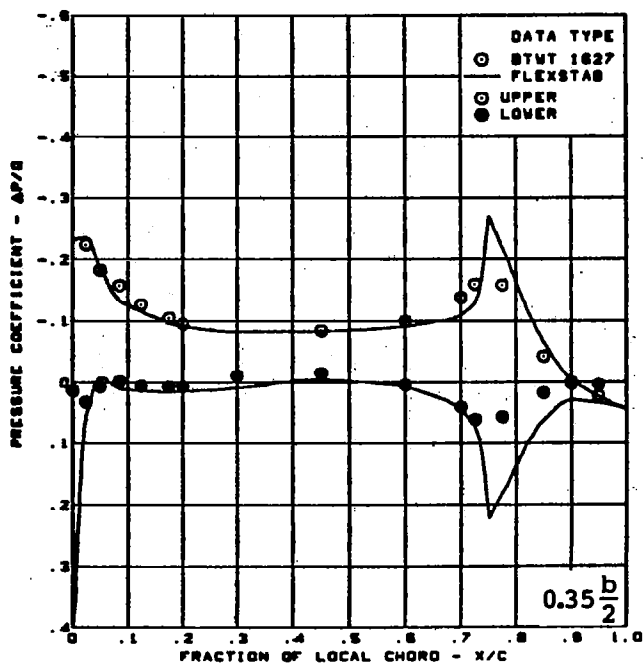
Figure 52. -(Concluded)





(a) Surface Chordwise Pressure Distributions -  $\alpha = 2^\circ$

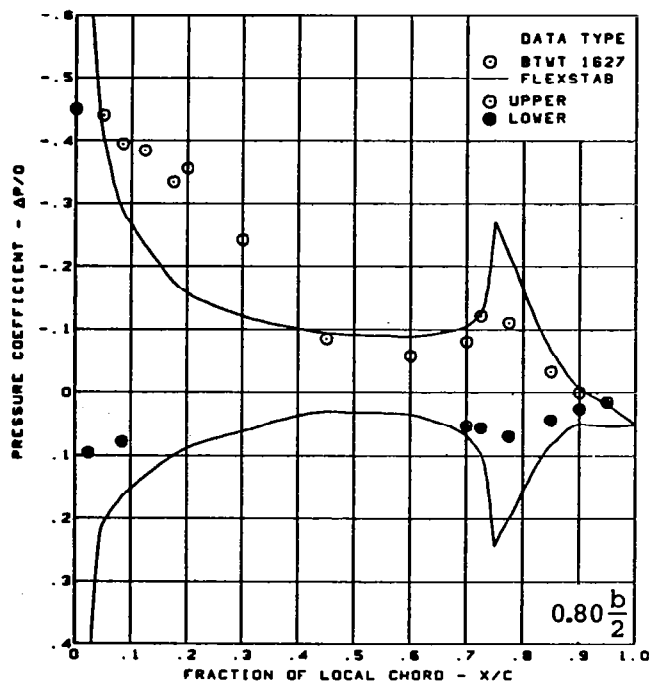
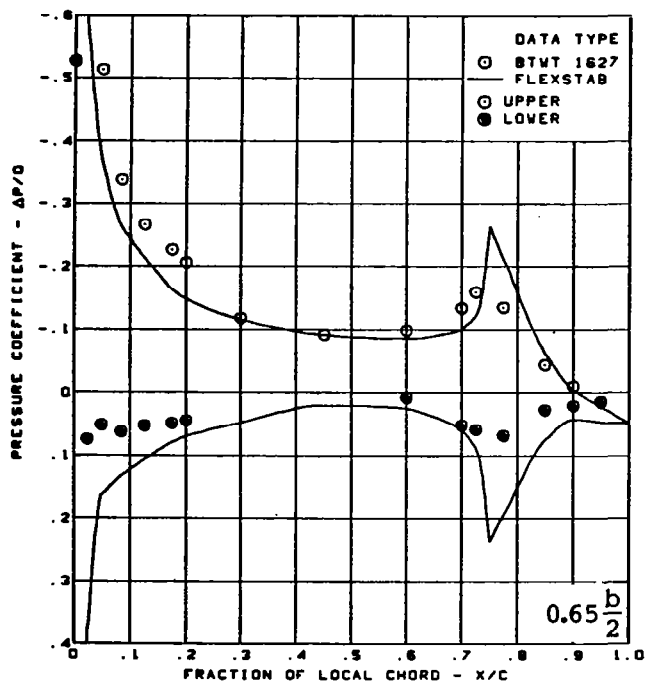
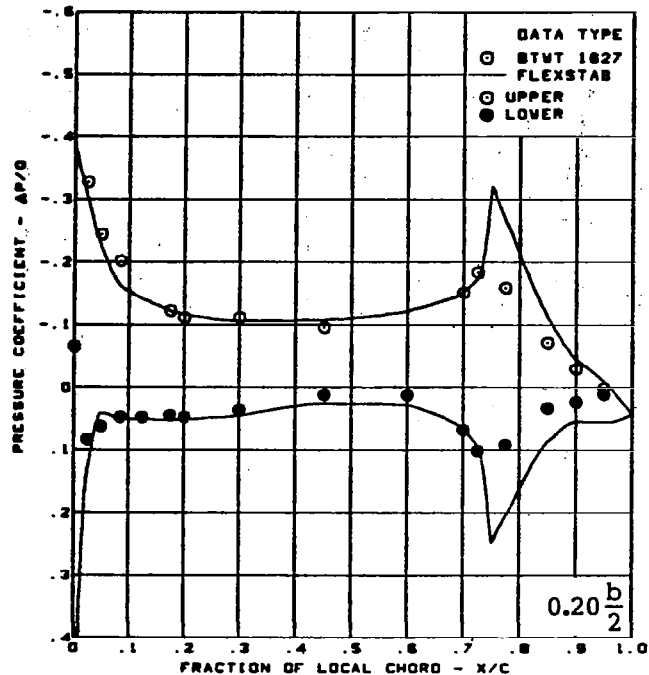
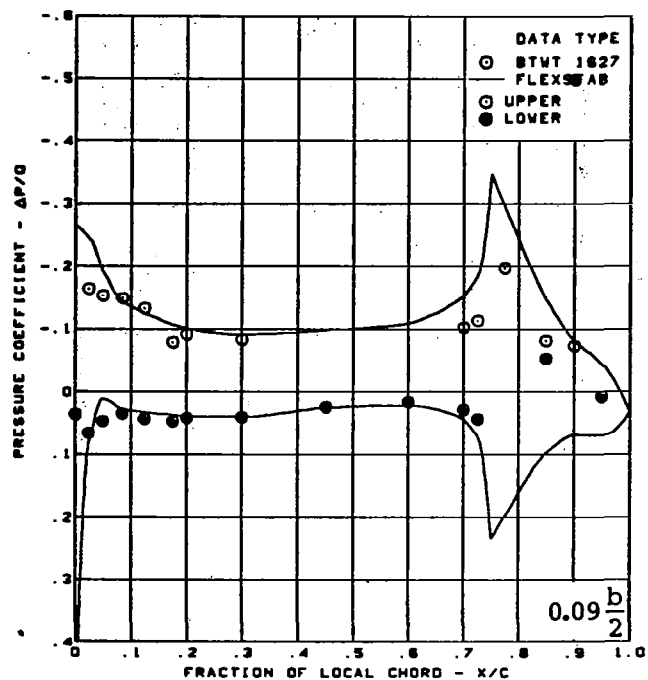
Figure 53. — Wing Theory-to-Experiment Comparison; Cambered-Twisted Wing;  
Fin Off; T.E. Deflection, Full Span =  $8.3^\circ$ ;  $M = 0.40$



$M = 0.40$  (run 65)  
 $\alpha = 2^\circ$   
 Cambered-twisted wing, rounded L.E.  
 Fin off  
 L.E. deflection, full span =  $0.0^\circ$   
 T.E. deflection, full span =  $8.3^\circ$

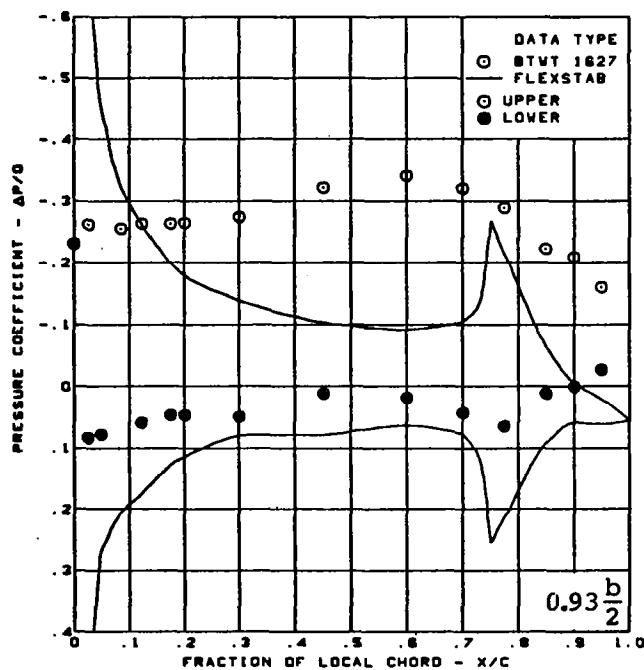
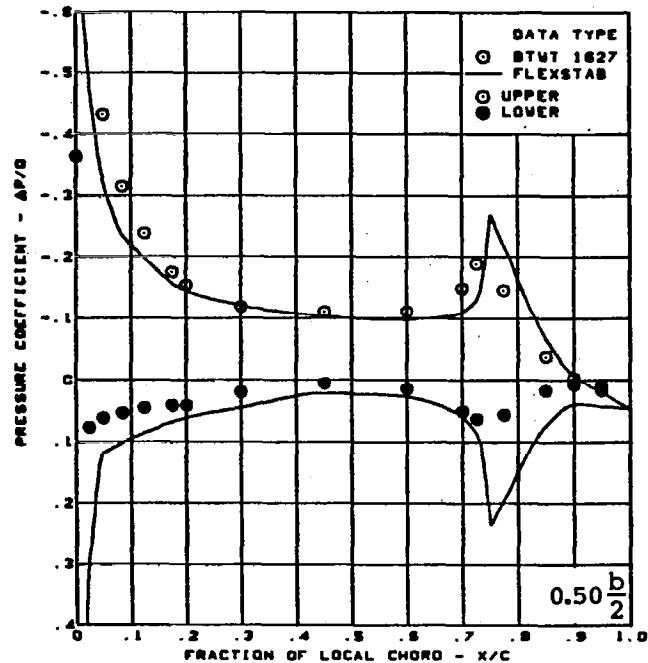
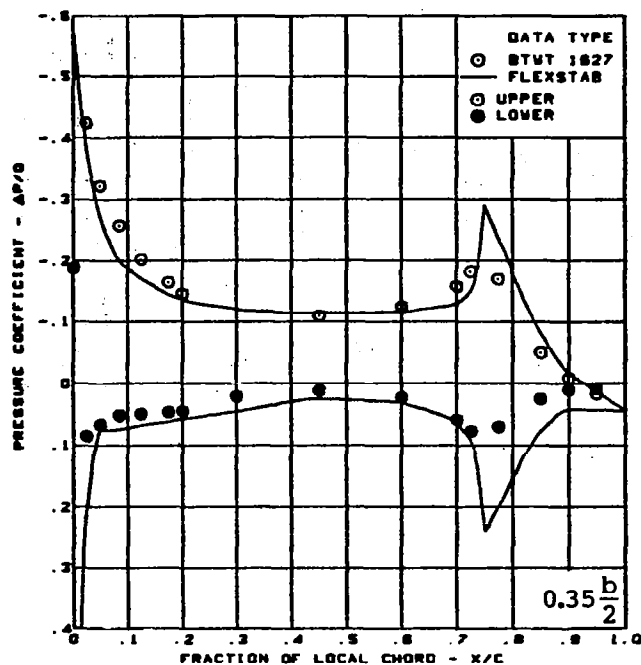
(a) (Concluded)

Figure 53. — (Continued)



(b) Surface Chordwise Pressure Distributions -  $\alpha = 4^\circ$

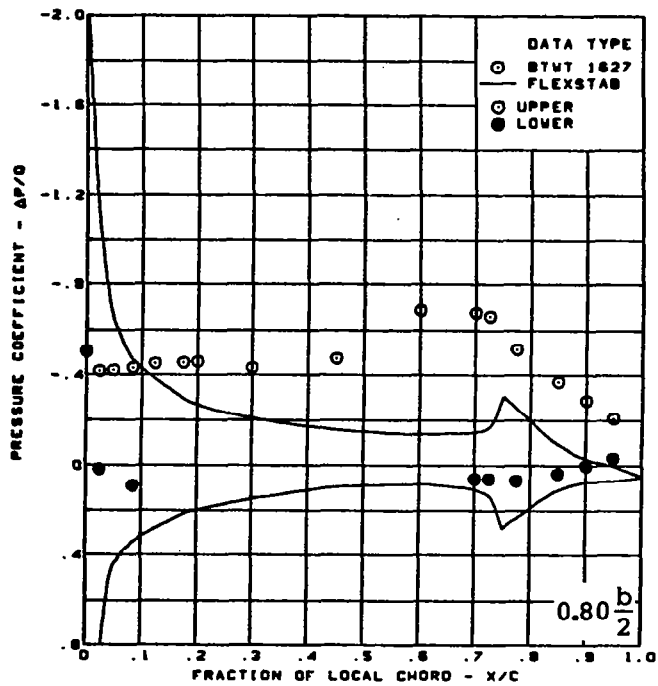
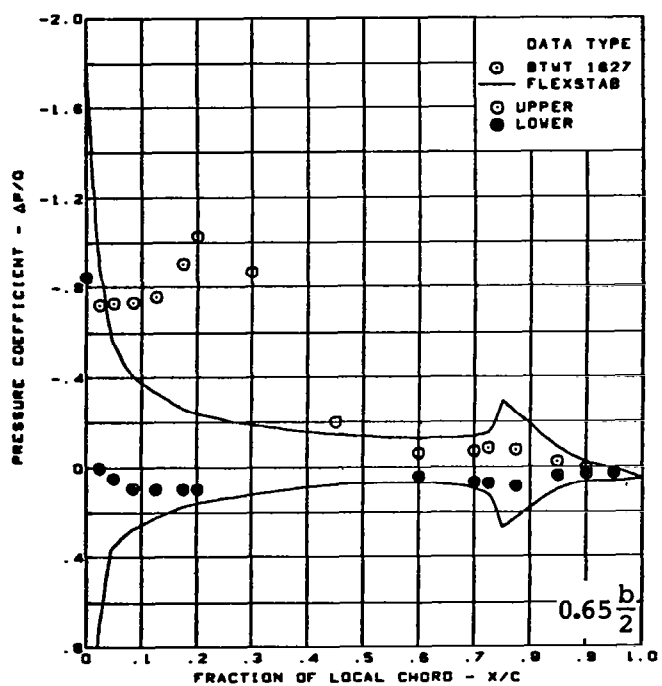
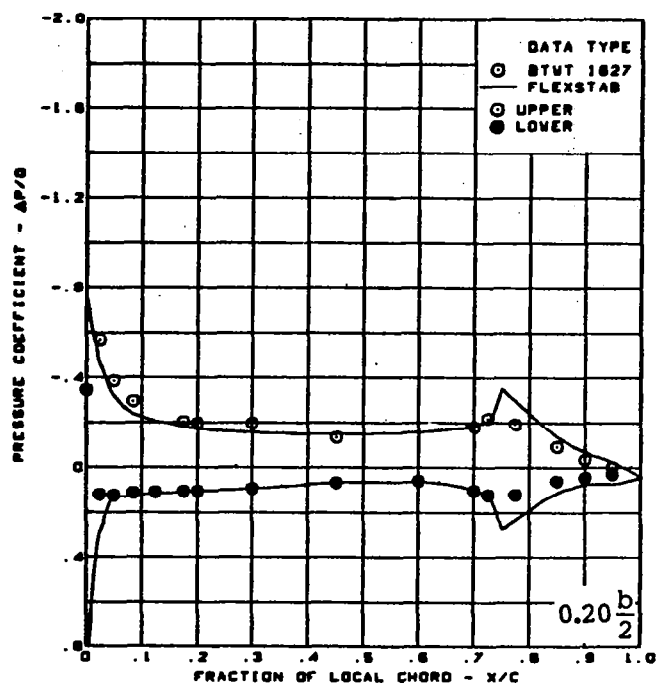
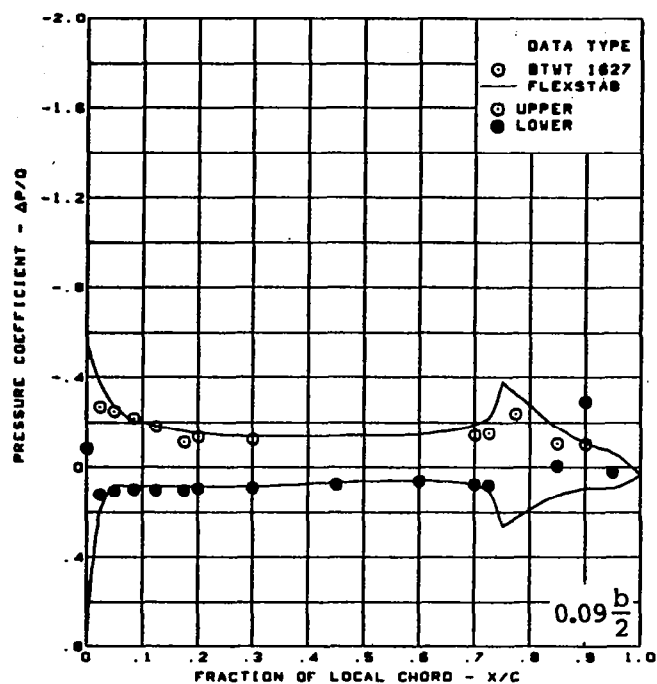
Figure 53. - (Continued)



$M = 0.40$  (run 65)  
 $\alpha = 4^\circ$   
 Cambered-twisted wing, rounded L.E.  
 Fin off  
 L.E. deflection, full span =  $0.0^\circ$   
 T.E. deflection, full span =  $8.3^\circ$

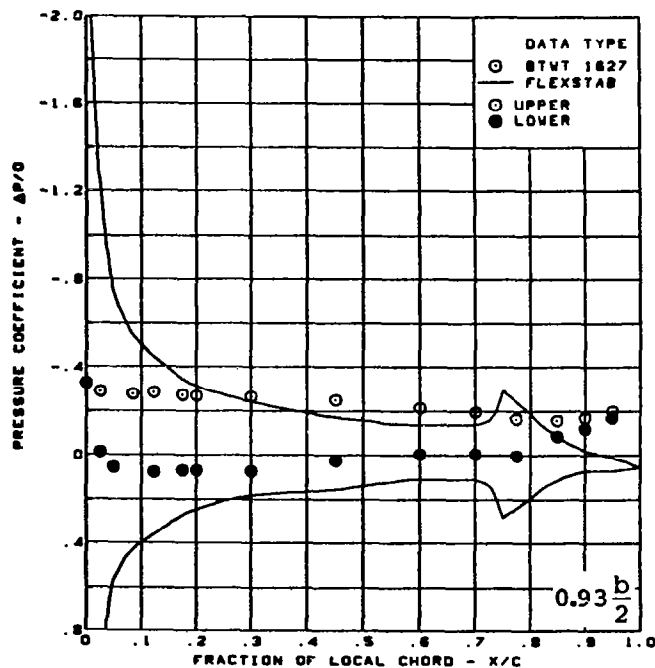
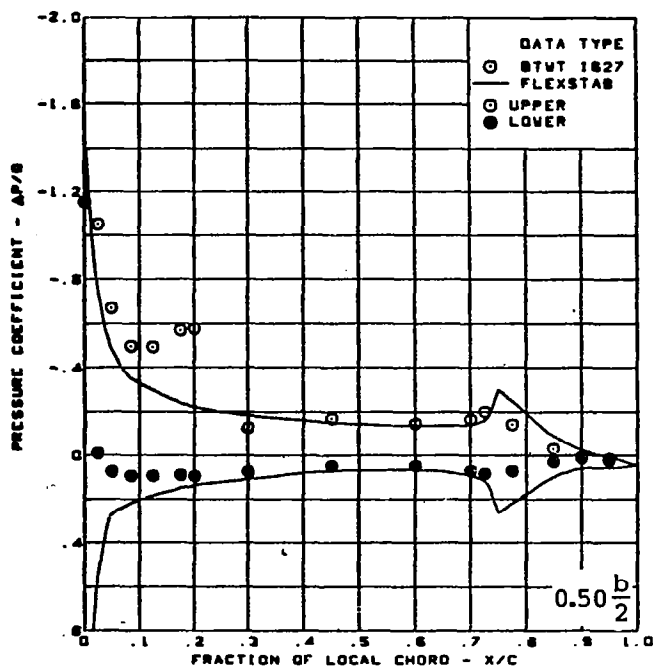
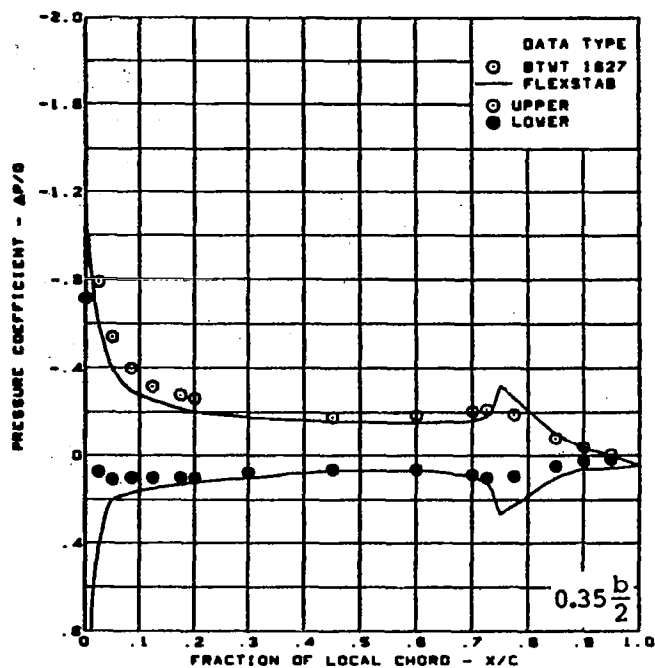
(b) (Concluded)

Figure 53. - (Continued)



(c) Surface Chordwise Pressure Distributions -  $\alpha = 8^\circ$

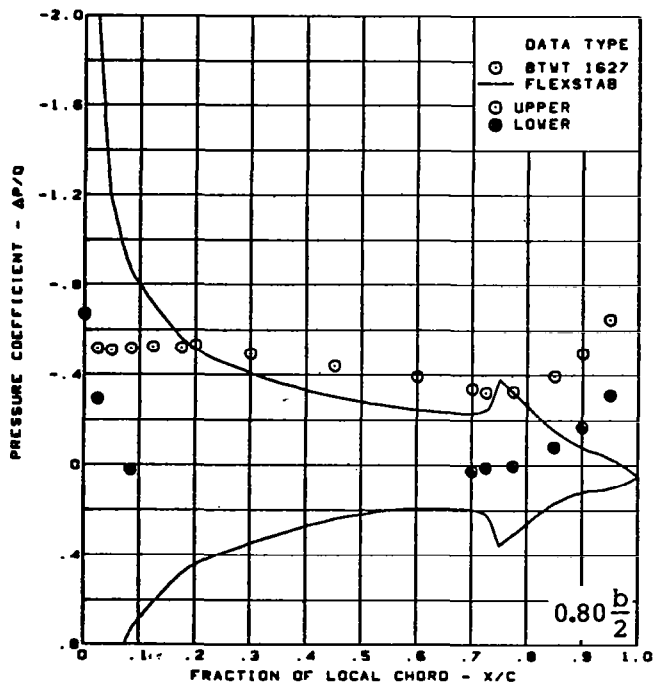
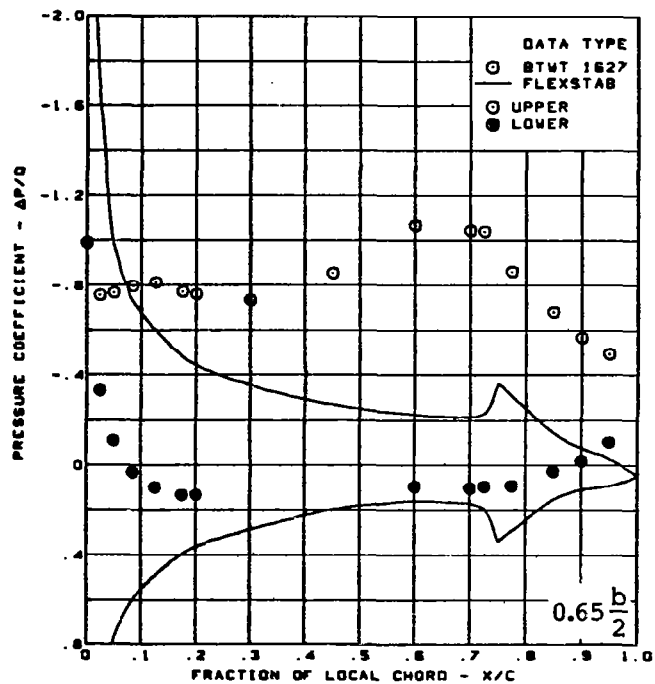
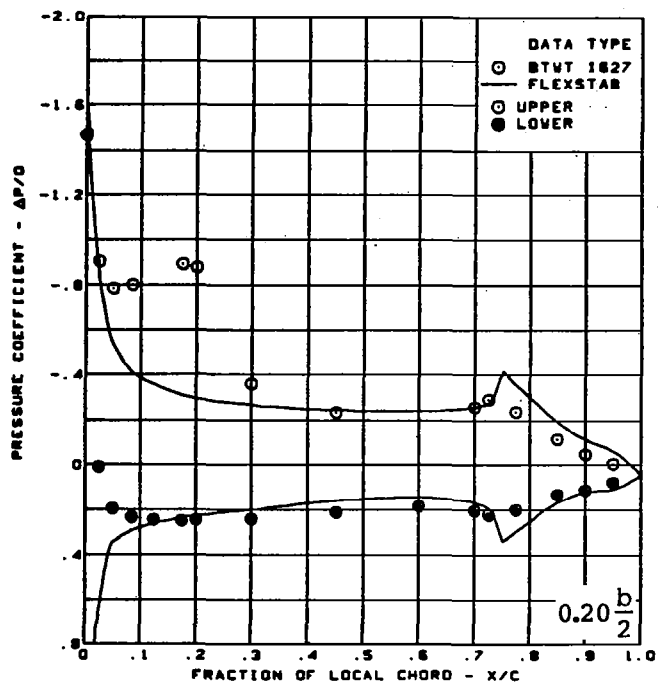
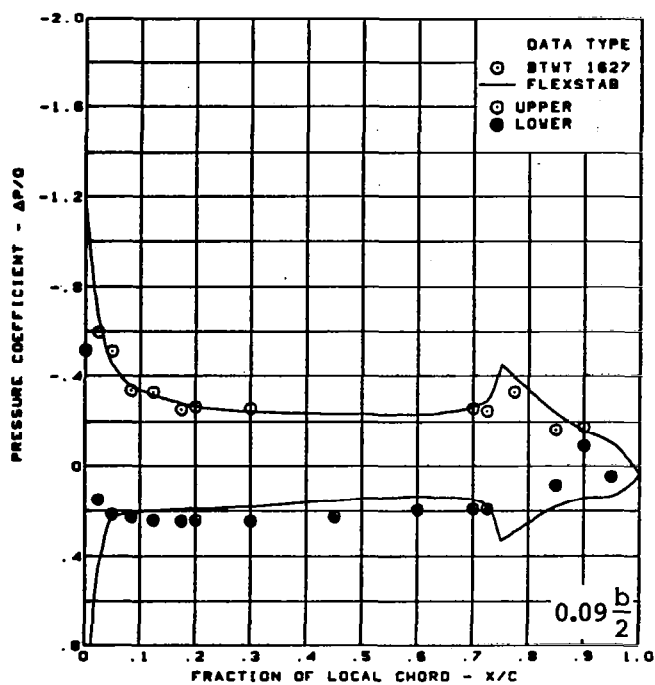
Figure 53. - (Continued)



$M = 0.40$  (run 65)  
 $\alpha = 8^\circ$   
 Cambered-twisted wing, rounded L.E.  
 Fin off  
 L.E. deflection, full span =  $0.0^\circ$   
 T.E. deflection, full span =  $8.3^\circ$

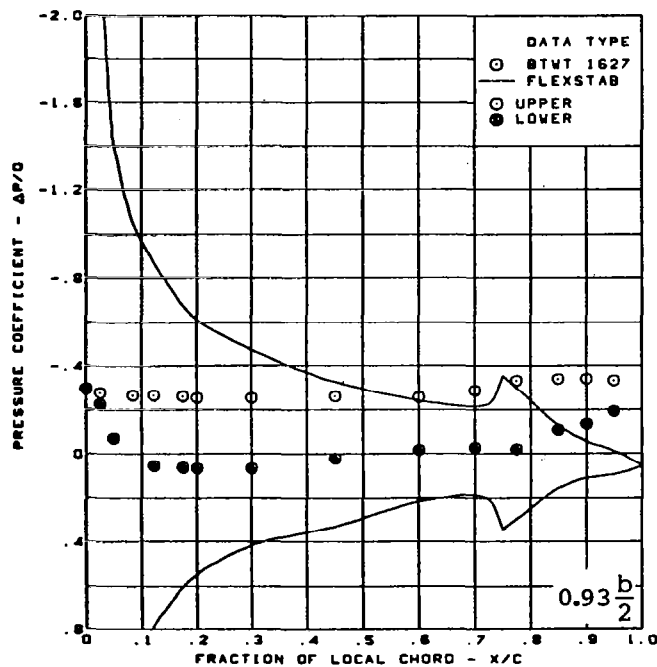
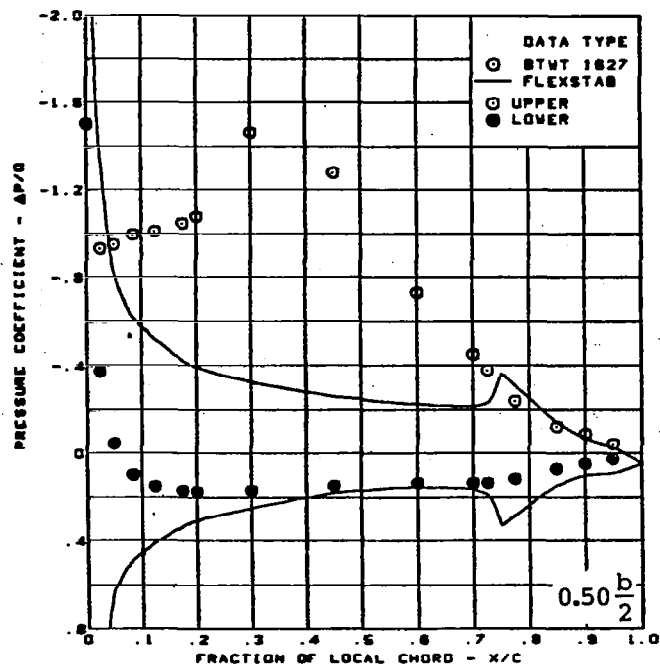
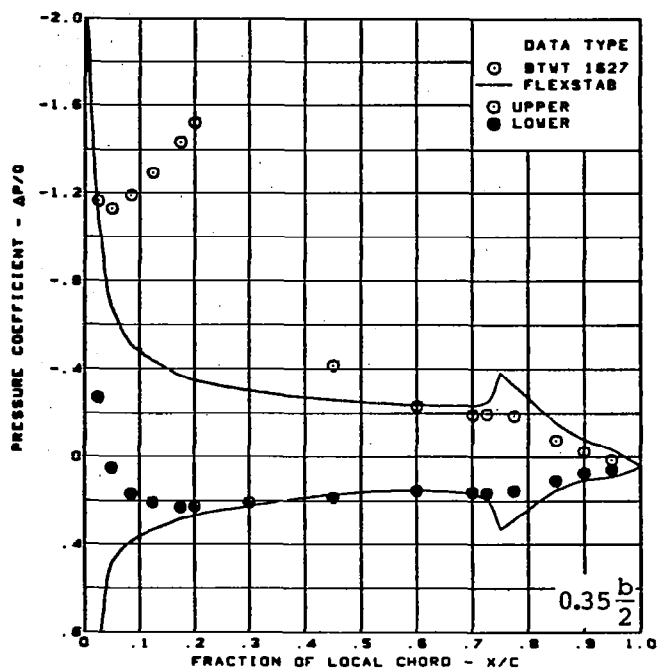
(c) (Concluded)

Figure 53. - (Continued)



(d) Surface Chordwise Pressure Distributions -  $\alpha = 16^\circ$

Figure 53. - (Continued)

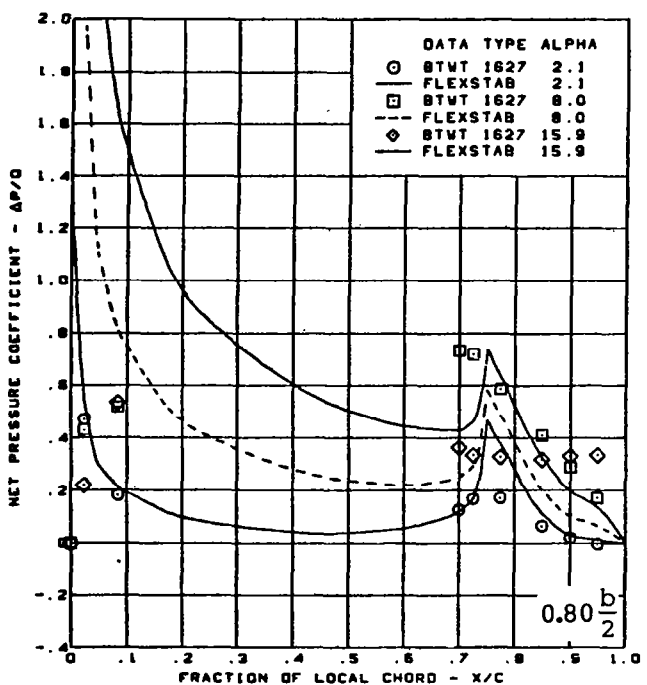
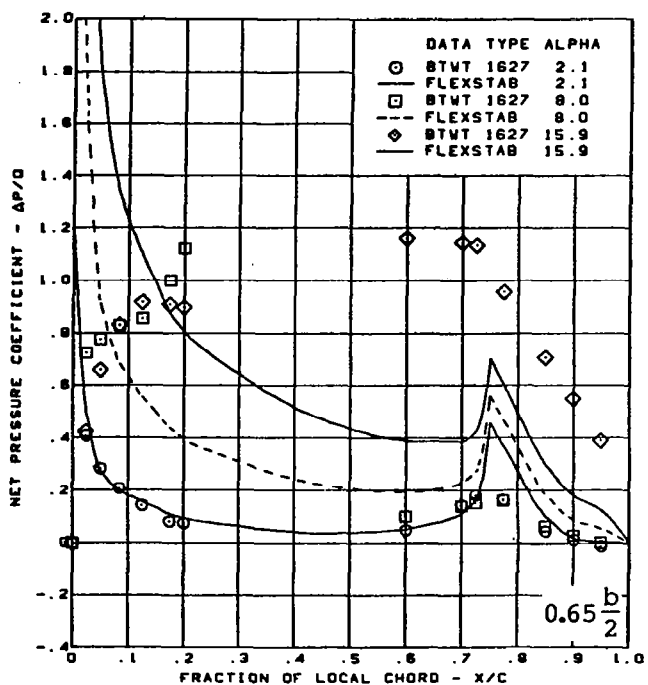
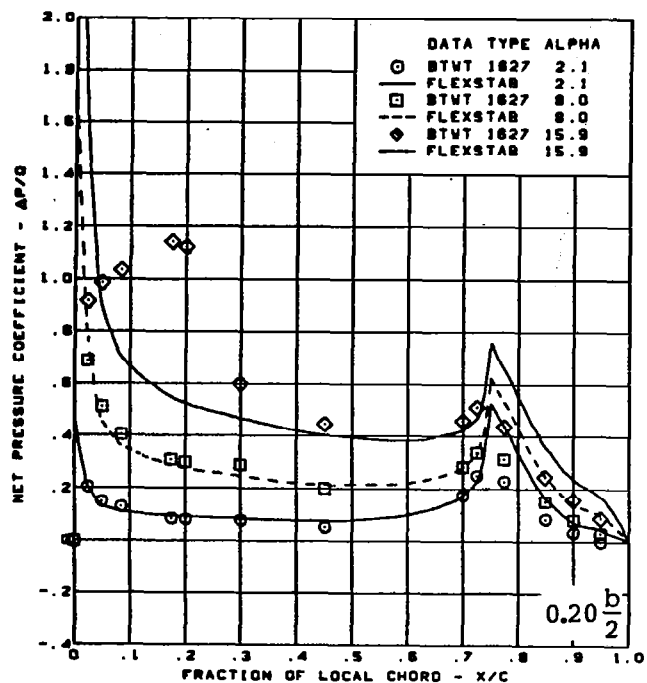
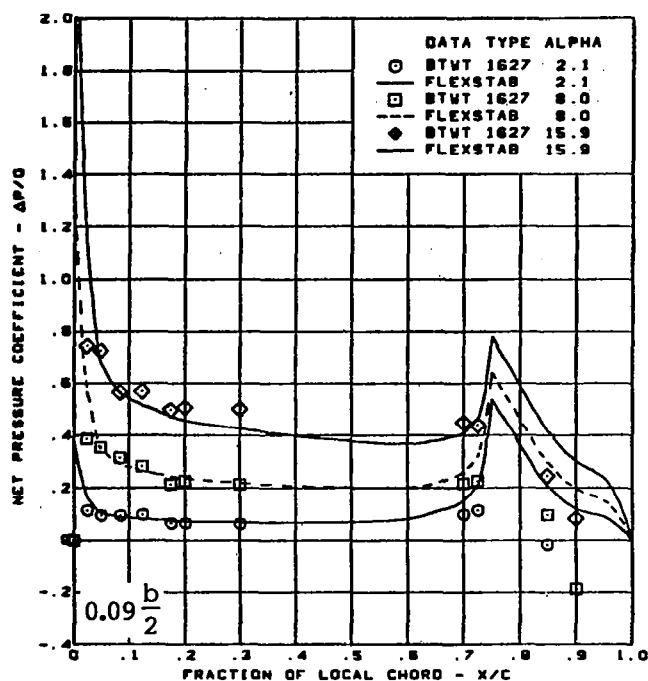


$M = 0.40$  (run 65)  
 $\alpha = 16^\circ$   
 Cambered-twisted wing, rounded L.E.  
 Fin off  
 L.E. deflection, full span =  $0.0^\circ$   
 T.E. deflection, full span =  $8.3^\circ$

(d) (Concluded)

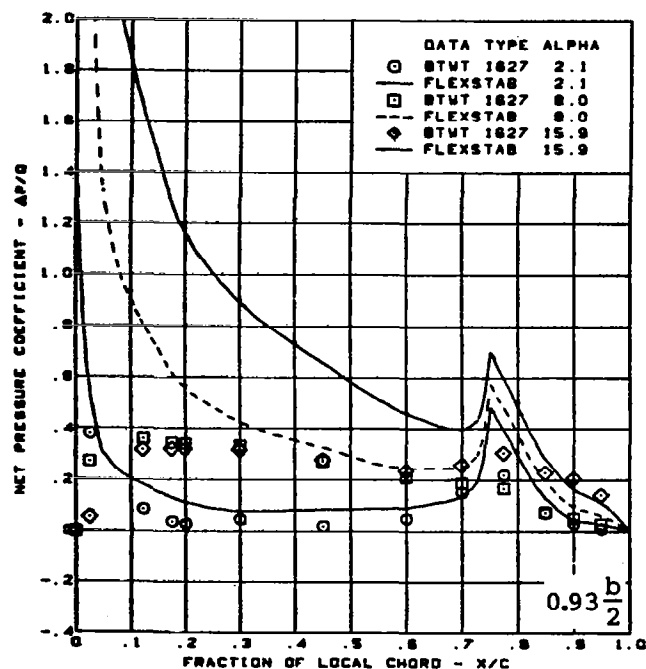
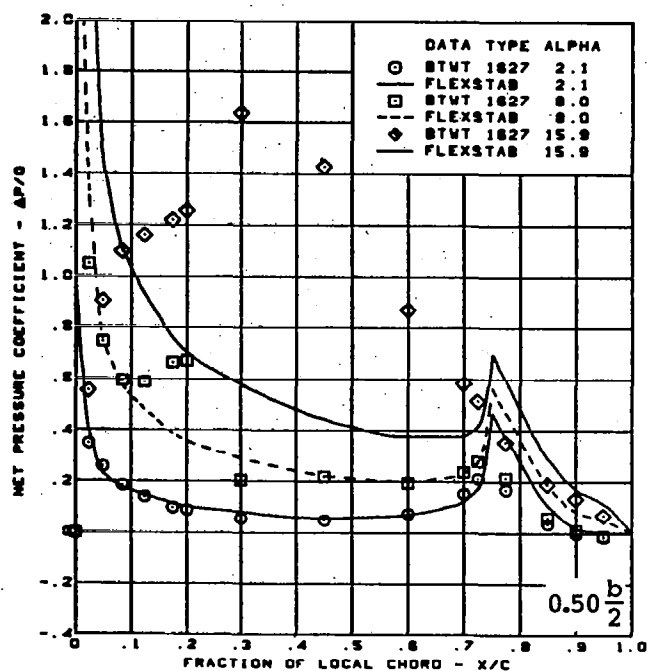
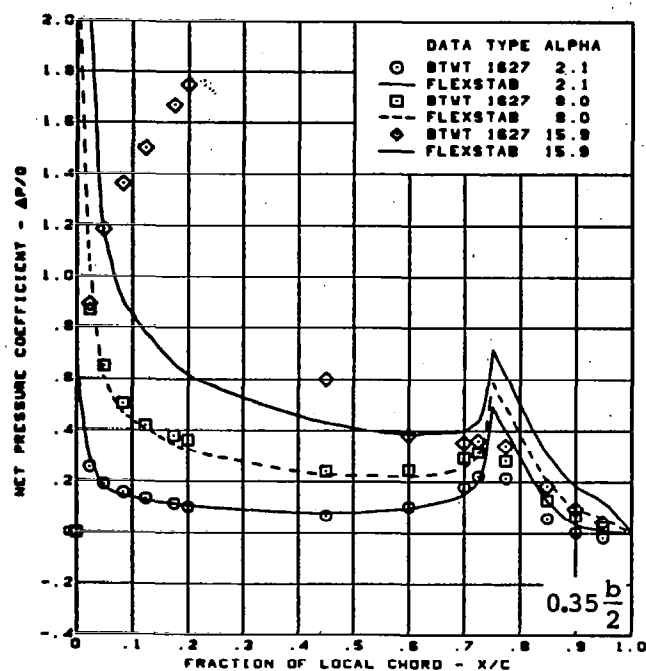
Figure 53. - (Continued)





(e) Net Chordwise Pressure Distributions

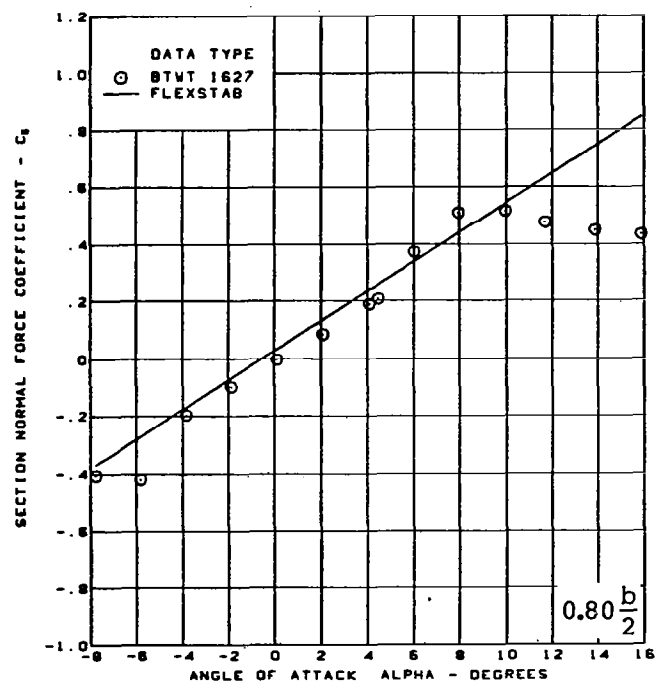
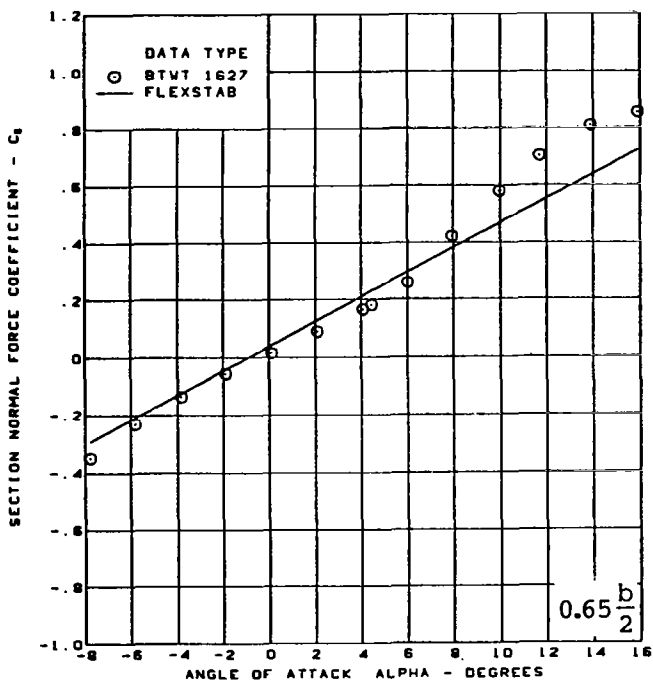
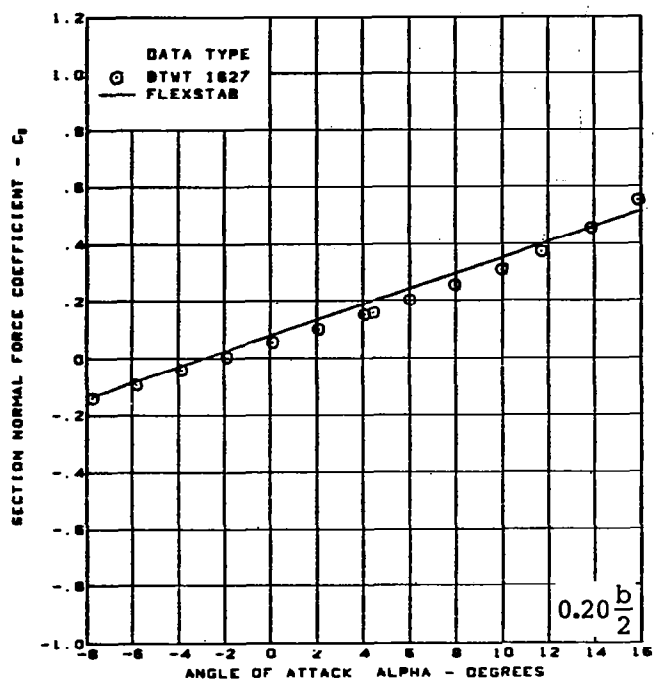
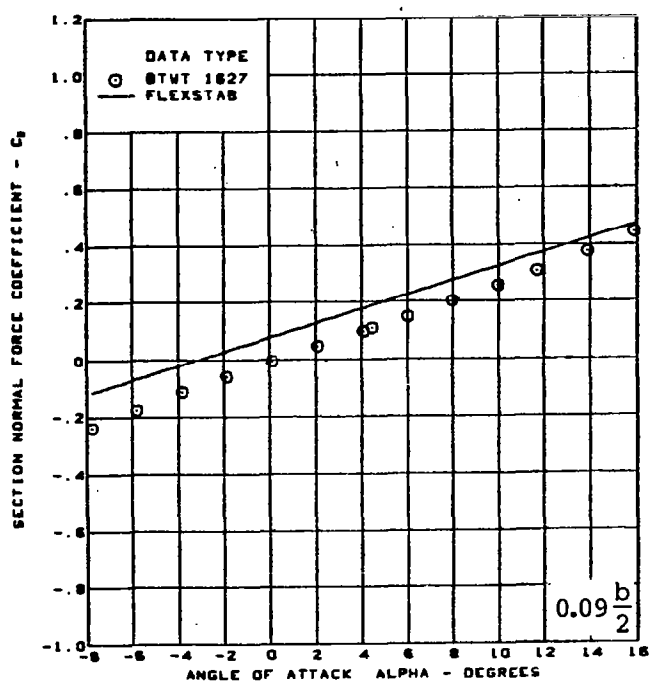
Figure 53. - (Continued)



$M = 0.40$  (run 65)  
 Cambered-twisted wing, rounded L.E.  
 Fin off  
 L.E. deflection, full span =  $0.0^\circ$   
 T.E. deflection, full span =  $8.3^\circ$

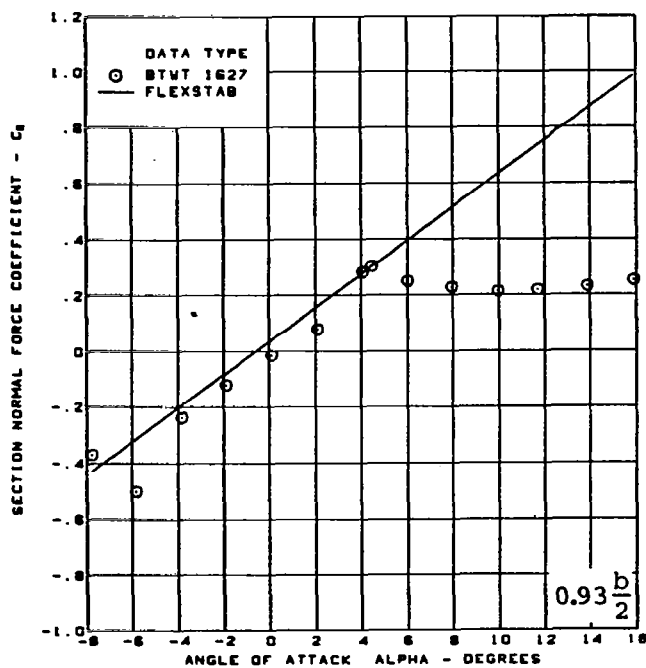
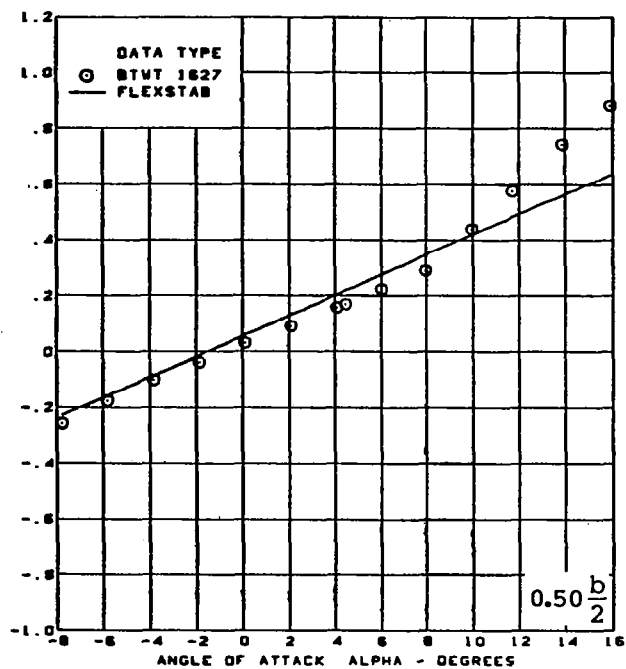
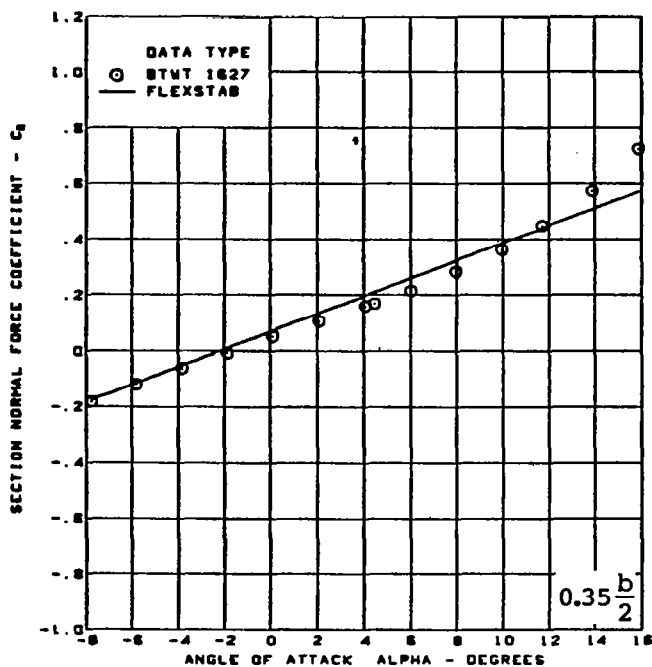
(e) (Concluded)

Figure 53. — (Continued)



(f) Section Aerodynamic Coefficients - Normal Force

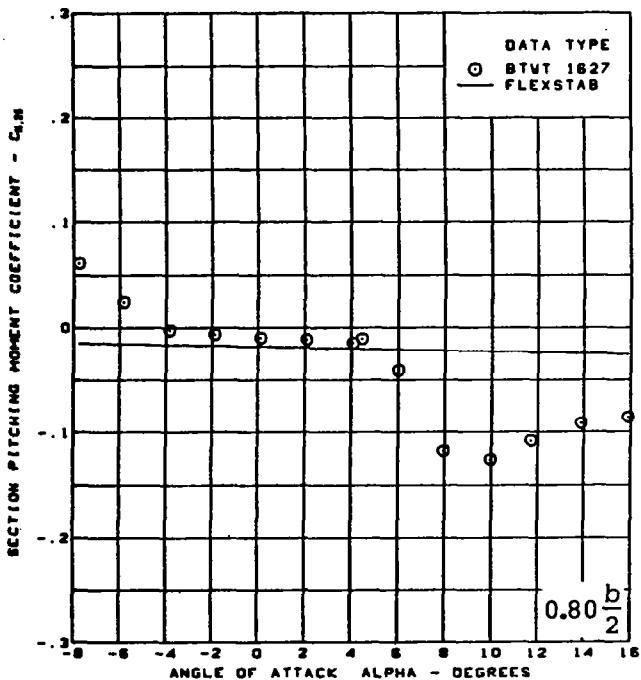
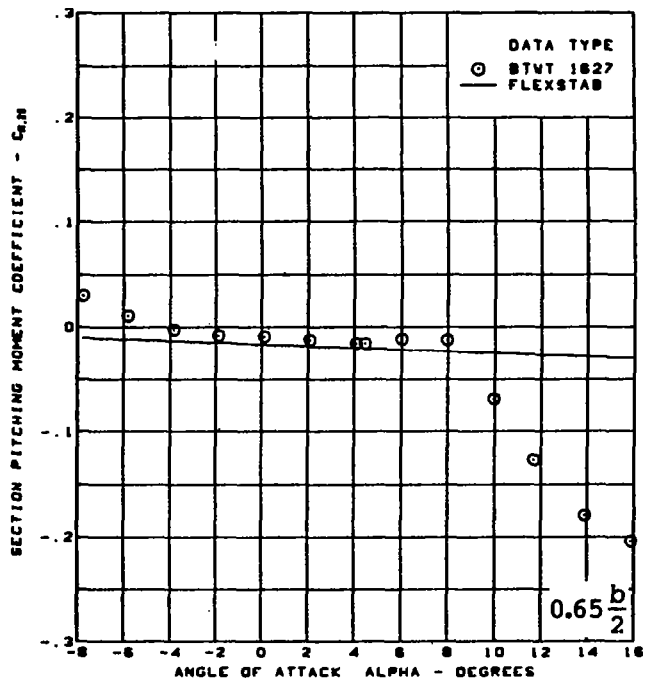
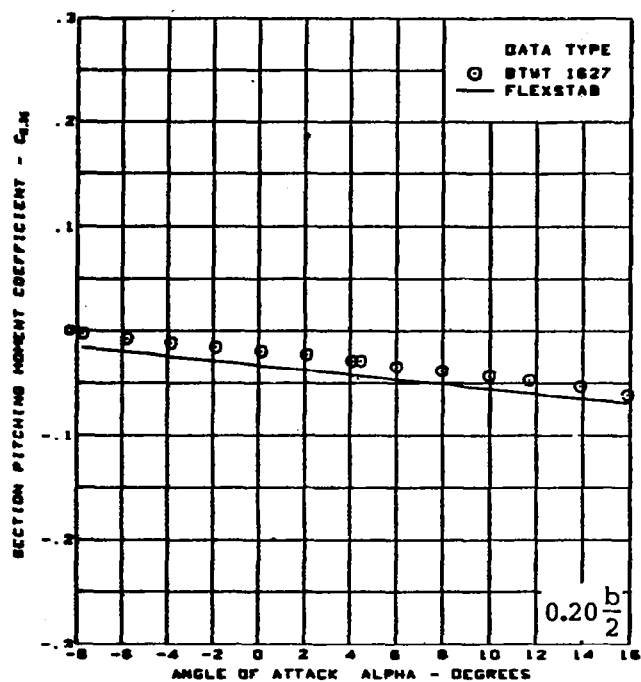
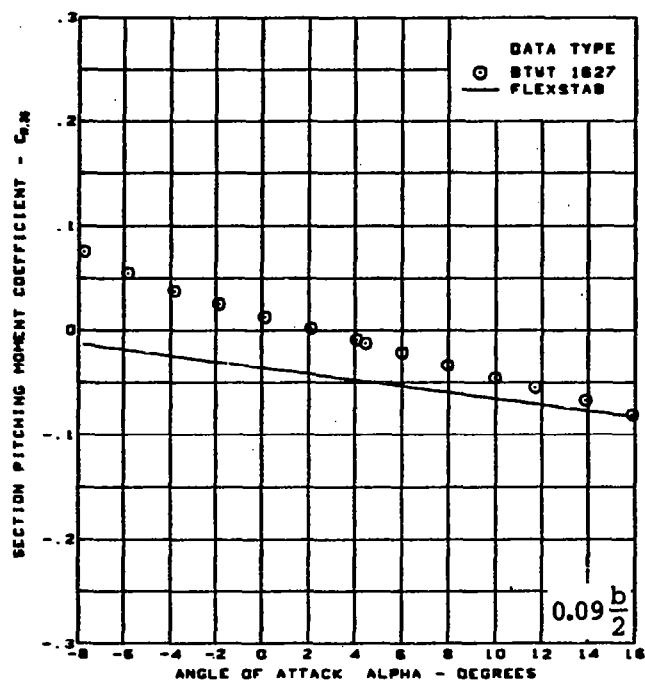
Figure 53. — (Continued)



$M = 0.40$  (run 65)  
 Cambered-twisted wing, rounded L.E.  
 Fin off  
 L.E. deflection, full span =  $0.0^\circ$   
 T.E. deflection, full span =  $8.3^\circ$

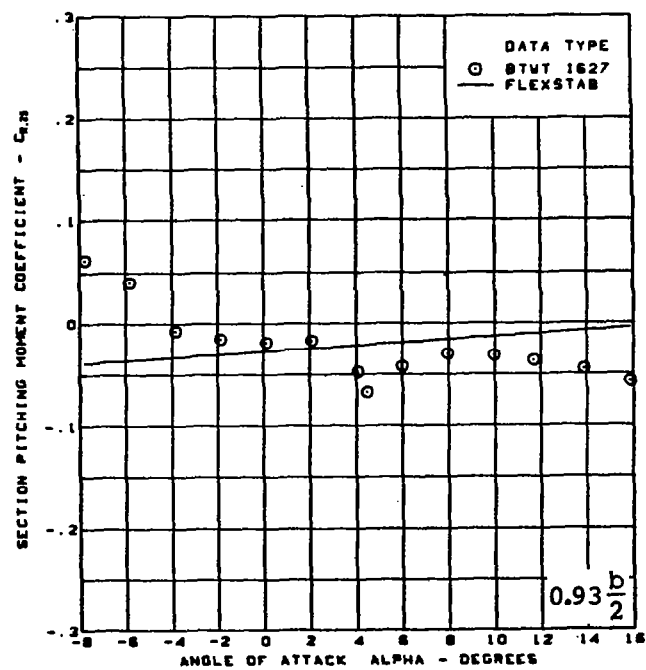
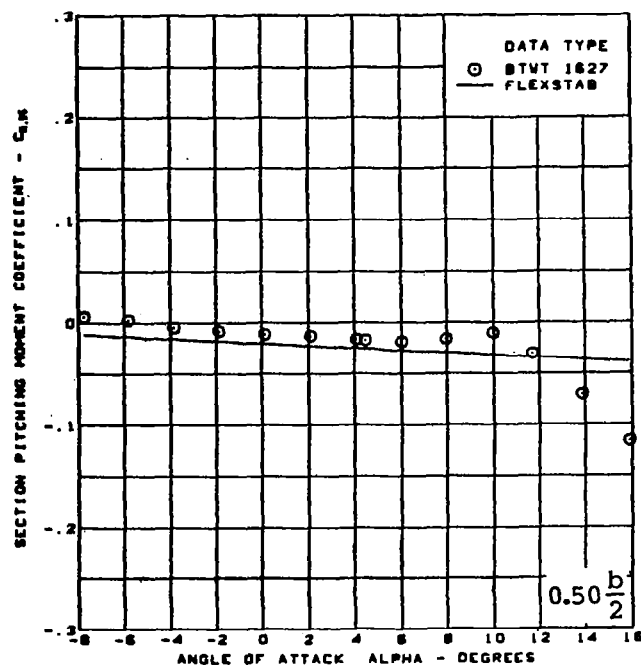
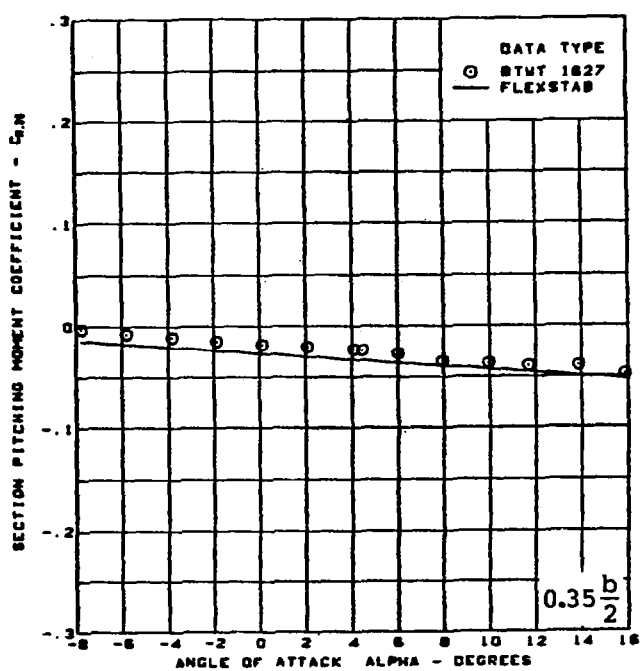
(f) (Concluded)

Figure 53. — (Continued)



(g) Section Aerodynamic Coefficients - Pitching Moment

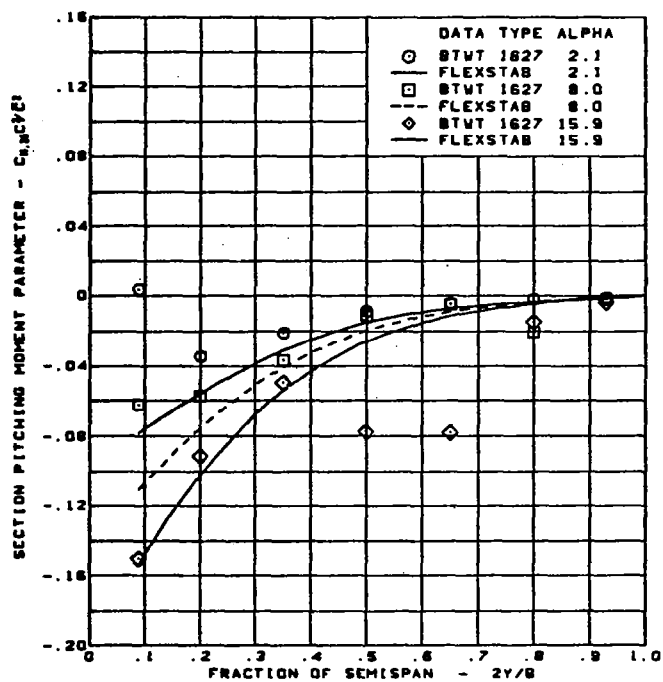
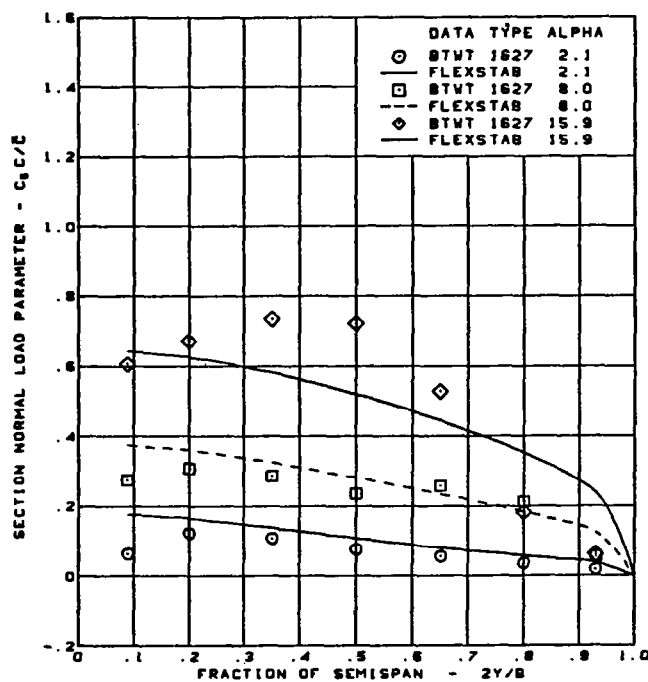
Figure 53. - (Continued)



M = 0.40 (run 65)  
 Cambered-twisted wing, rounded L.E.  
 Fin off  
 L.E. deflection, full span =  $0.0^\circ$   
 T.E. deflection, full span =  $8.3^\circ$

(g) (Concluded)

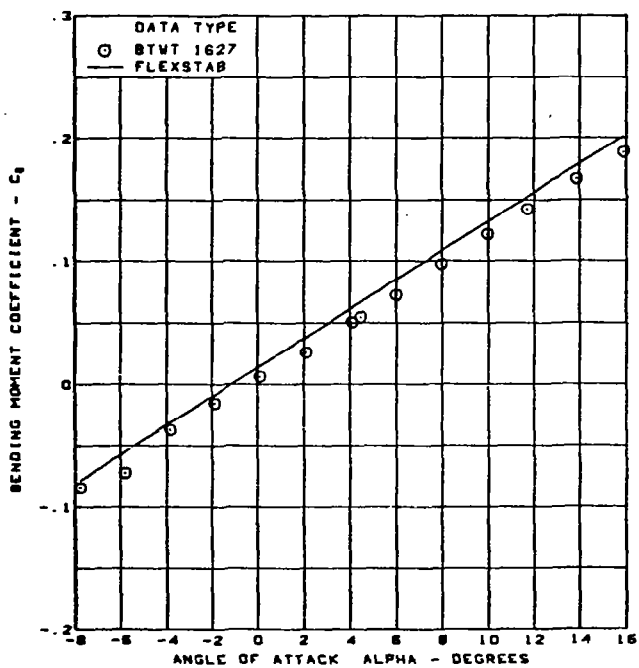
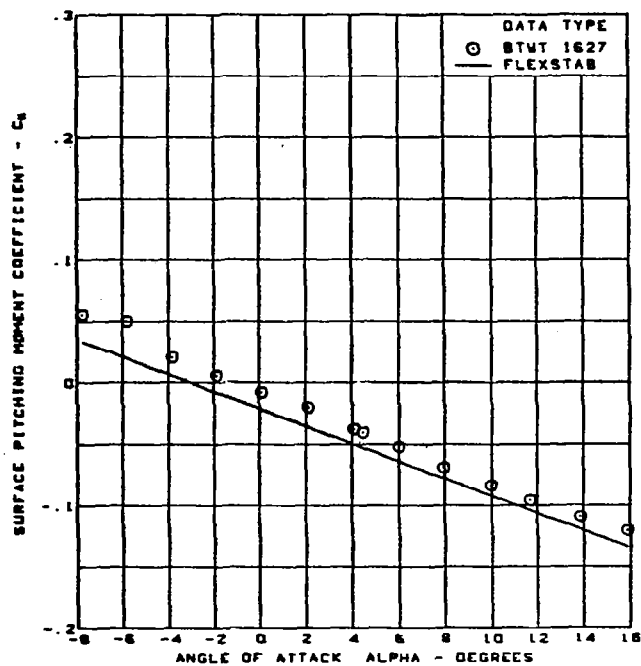
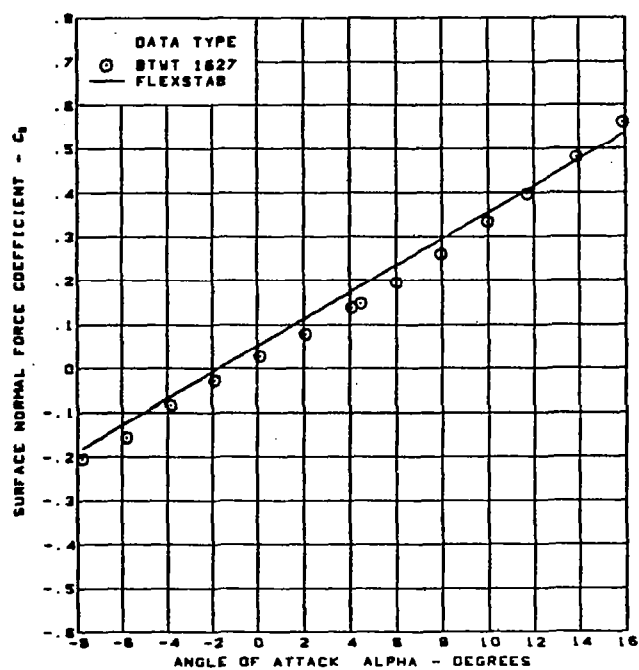
Figure 53. - (Continued)



$M = 0.40$  (run 65)  
 Cambered-twisted wing, rounded L.E.  
 Fin off  
 L.E. deflection, full span =  $0.0^\circ$   
 T.E. deflection, full span =  $8.3^\circ$

(h) Spanload Distributions

Figure 53. — (Continued)



$M = 0.40$  (run 65)  
 Cambered-twisted wing, rounded L.E.  
 Fin off  
 L.E. deflection, full span =  $0.0^\circ$   
 T.E. deflection, full span =  $8.3^\circ$

(i) Wing Aerodynamic Coefficients

Figure 53. — (Concluded)



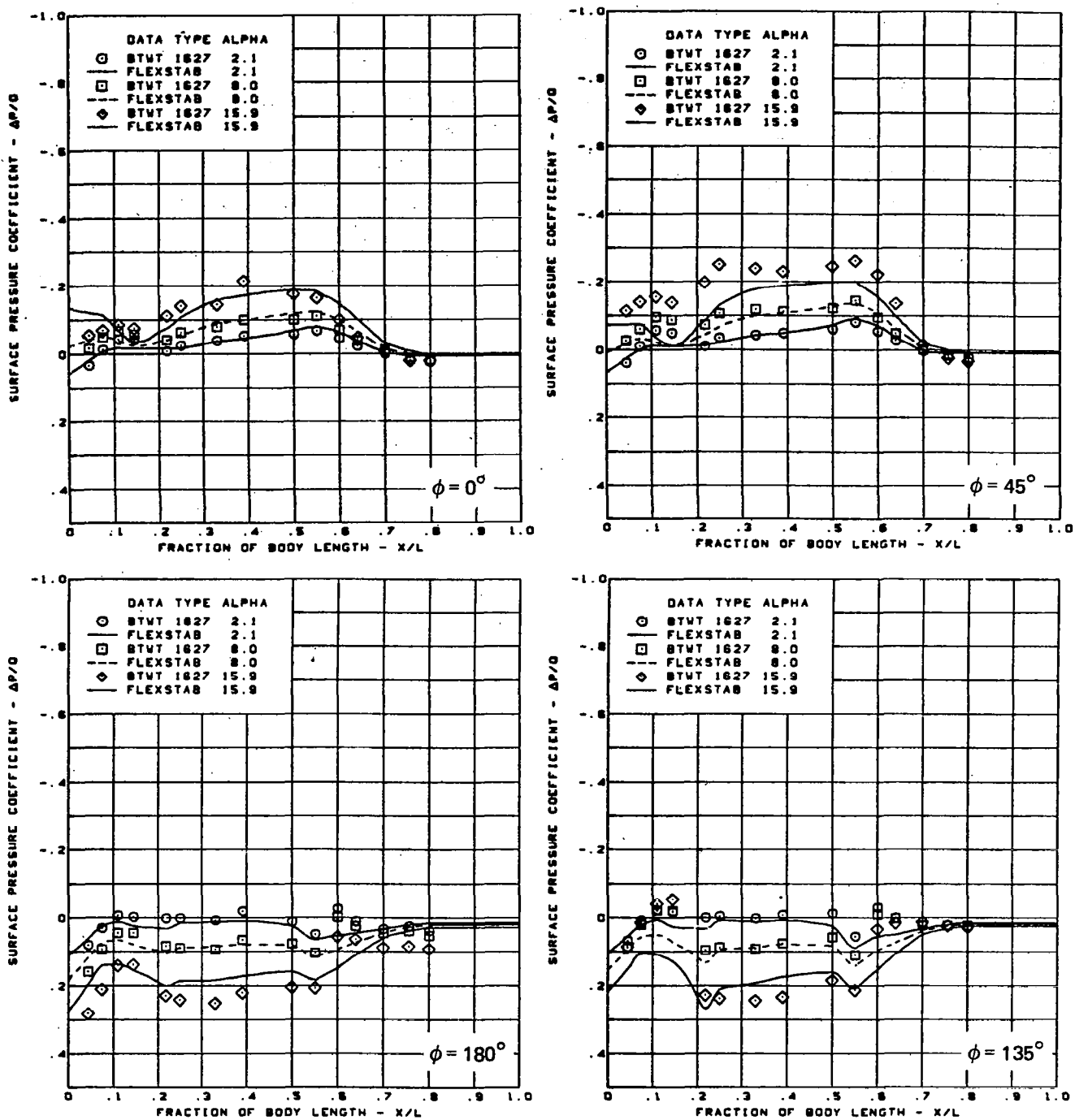
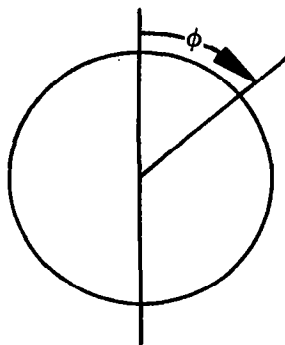
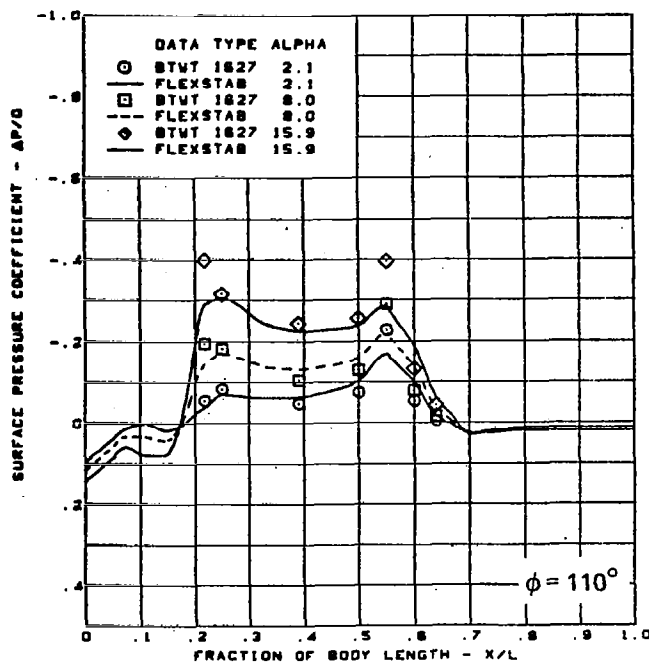
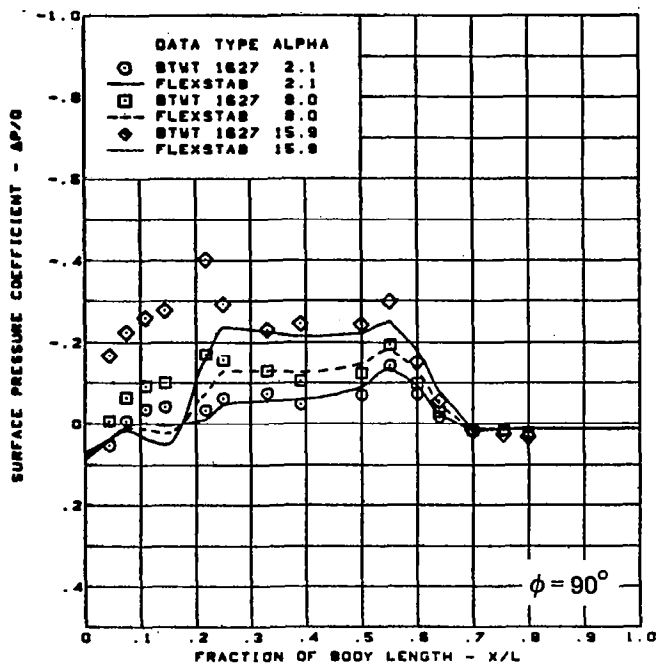


Figure 54. — Body Theory-to-Experiment Comparison; Cambered-Twisted Wing; Fin Off; T.E. Deflection, Full Span =  $8.3^\circ$ ;  $M = 0.40$



$M = 0.40$  (run 65)  
 Cambered-twisted wing, rounded L.E.  
 Fin off  
 L.E. deflection, full span =  $0.0^\circ$   
 T.E. deflection, full span =  $8.3^\circ$

Figure 54. — (Concluded)

1. Report No. <b>NASA CR-3434</b>	2. Government Accession No.	3. Recipient's Catalog No.	
4. Title and Subtitle <b>TRANSONIC PRESSURE MEASUREMENTS AND COMPARISON OF THEORY TO EXPERIMENT FOR THREE ARROW-WING CONFIGURATIONS, Summary Report</b>		5. Report Date <b>February 1982</b>	
		6. Performing Organization Code	
7. Author(s) <b>Marjorie E. Manro</b>		8. Performing Organization Report No. <b>D6-51079-1</b>	
9. Performing Organization Name and Address <b>Boeing Commercial Airplane Company P.O. Box 3707 Seattle, Washington 98124</b>		10. Work Unit No.	
		11. Contract or Grant No. <b>NAS1-14962</b>	
12. Sponsoring Agency Name and Address  <b>National Aeronautics and Space Administration Washington, D.C. 20546</b>		13. Type of Report and Period Covered  <b>Contractor Report</b>	
		14. Sponsoring Agency Code <b>743-01-12-02</b>	
15. Supplementary Notes <b>Technical monitor - Percy J. Bobbitt, Chief, Subsonic-Transonic Aerodynamics Division, NASA Langley Research Center, Hampton, Virginia. Experimental and attached flow theory pressure data are available on magnetic tape. Final report.</b>			
16. Abstract <p>Wind tunnel tests of arrow-wing body configurations consisting of flat, twisted, and cambered-twisted wings, as well as a variety of leading- and trailing-edge control surface deflections, have been conducted at Mach numbers from 0.4 to 1.05 to provide an experimental pressure data base for comparison with theoretical methods. Comparisons of the predictions of current state-of-the-art and advanced attached-flow methods to the detailed experimental pressure distributions have been made to delineate conditions under which these theories are valid for these wings.</p> <p>This report summarizes the results of the entire program. NASA CR-165701 presents more detailed results of the experimental phase of the program for the basic data and comparison of the effect of wing shape - twist, camber, and combined camber and twist. The effects of trailing-edge control surface deflection and of the wing fin are presented in NASA CR-165702. NASA CR-165703 presents in more detail the comparisons of the predictions of attached-flow theory to experimental data.</p> <p>These reports supplement those from earlier test programs using this model which cover a range of Mach numbers from 0.40 to 2.50. Only the flat wing and the twisted wing were available for these earlier test programs. These data have been reported in NASA CR-2610, NASA CR-132727, NASA CR-132728, NASA CR-132729, and NASA CR-145046.</p>			
17. Key Words <b>Aeroelasticity Experimental pressure distributions Aerodynamic theory Arrow-wing configuration Wind tunnel test</b>		18. Distribution Statement  <b>Unclassified-unlimited</b>  <b>Subject category 02</b>	
19. Security Classif. (of this report) <b>Unclassified</b>	20. Security Classif. (of this page) <b>Unclassified</b>	21. No. of Pages <b>548</b>	22. Price <b>A23</b>